Proceedings of the 58th International Convention of
Society of Wood Science and Technology
June 7-12, 2015 - Grand Teton National Park, Jackson, Wyoming, USA

58th SWST International Convention
June 7-12, 2015

Jackson Lake Lodge
Grand Teton National Park
Jackson, Wyoming, USA

Convention Theme: Renewable Materials and the Bio-Economy

Edited by: H. Michael Barnes and Victoria L. Herian

Overall General Co-Chair: *Eric Hansen, Oregon State University, USA*

Table of Contents

Biomass Energy: Innovations, Economic Realities, and Public Perception
Session Moderator: Nikki Brown, Pennsylvania State University, USA

Early Stage Researcher Full Oral Slot (8 minutes)
Session Moderators: David DeVallance, West Virginia University, USA and Tobias Keplinger, ETH Zurich, Switzerland

Early Stage Researcher Full Oral Slot (8 minutes)
Session Moderators: Dick Sandberg, Luleå University of Technology, Sweden and Bonnie Yang, Mississippi State University, USA

Early Stage Researcher Speed Slot (3 minutes)
Session Moderator: Michael Burnard, University of Primorska, Slovenia

Student Poster Competition
Session Moderator: Frederick Kamke, Oregon State University, USA

Proceedings of the 58th International Convention of
Society of Wood Science and Technology
June 7-12, 2015 - Grand Teton National Park, Jackson, Wyoming, USA

Biomass Chemistry for a Greener Environment Session
Moderator: Elisha Ncube, Copperbelt University, Zambia

Improving Water Resistance of Soybean Meal-Based Adhesive by a Polyepoxide and Post Heat Treated Process

Jing Luo, Qiang Gao, Jianzhang Li**

MOE Key Laboratory of Wooden Material Science and Application, Beijing Key Laboratory of Lignocellulosic Chemistry, MOE Engineering Research Centre of Forestry Biomass Materials and Bioenergy, Beijing Forestry University, Beijing, China

Contact information: MOE Key Laboratory of Wooden Material Science and Application, Beijing Forestry University, Beijing 100083, China.
luojing.rowe@gmail.com, +8615510155899
*Corresponding author: gao200482@163.com, +8601062336912,
lijianzhang126@126.com, +8601062338083

Abstract

The aim of this study was to improve the water resistance of the soybean meal-based bio-adhesive with a 5, 5 dimethyl hydantoin polyepoxide (DMHP). The DMHP could react with active groups on protein molecule to form a cross-linking network, which improved the water resistance of the resulting adhesive. In addition, adding DMHP increased wettability of the adhesive, improved the cross-linking degree of the cured adhesive, and created a smooth surface with less holes and cracks to prevent moisture intruding, which further enhanced the water resistance of the adhesive. Incorporating 13 wt% DMHP effectively improved the water resistance of the adhesive by 182.9% to 1.16 MPa, which met interior use plywood requirement. At the same time we examined the effects of four different heat treatment processes on plywood bonded with the adhesive. The surface and core layer wet shear strength improved by 56.3% and 102.3%, respectively, with 4 min low pressure heat treatment. Heat treatment could also improve the water resistance of the adhesive by improving the cross-linking density of the adhesive layer in plywood and releasing its interior force, according to a vertical density profile analysis. Therefore, 8 h oven drying heat treatment at 120°C, the surface and core layer wet shear strength improved by 60.0% and 175.0%, respectively.

***Keywords**:* Soybean meal-based bio-adhesive; 5, 5 dimethyl hydantoin polyepoxide; Plywood; Water resistance; Heat treatment

1. Introduction

With the increasing concerns over environmental threats and sustainable development, deployment of biodegradable and renewable biomass for the production of wood adhesives is not only inevitable but also responsive to suppressing the impact caused by formaldehyde-based adhesives (Sellers, 2001). Soy protein has been used as a wood adhesive for centuries because of its low cost and environmental friendliness (Kumar et al., 2002). However, soy protein-based bio-adhesives have disadvantages which limited their application, i.e., low bond strength and poor water resistance (Orr, 2007). Therefore, there is an urgent need to improve the water resistance of soy protein-based adhesive.

2. Materials and Methods

2.1 Materials

Soybean meal was obtained from Xiangchi Grain and Oil Company in Shandong Province of China, and then milled to 250 mesh flour (SM). Components of the soybean meal flour were tested as follows: 46.8% soy protein, 5.86% moisture, 6.46% ash, and 0.56% fat. Polyacrylamide (PAM), sodium dodecyl sulfate (SDS), epichlorohydrin (ECH), sodium hydroxide (NaOH) were obtained from Tianjin Chemical Reagent Co.. The 5, 5 dimethyl hydantoin (DMH) was obtain from Tianjin institute of synthetic materials industry. Poplar veneer (40 × 40 × 1.5 cm, 8% of moisture content) was provided from Hebei Province of China.

2.2 Preparation of the different adhesives

For the SM adhesive, soybean meal flour (28 g) was added into deionized water (72 g) and stirred for 10 min at 20 ^{o}C.

For the SM/PAM adhesive, soybean meal flour (28 g) was added to a polyacrylamide solution (72 g, 0.01%) and stirred for 10 min at 20 ^{o}C.

For the SM/PAM/SDS adhesive, sodium dodecyl Sulfate (1 g) was added into the SM/PAM adhesive and further stirred for 10 min at 20 ^{o}C.

For the SM/PAM/SDS/DMHP adhesive, various amounts of the DMHP were added to the SM/PAM/SDS adhesive and further stirred for 10 min at 20 ^{o}C. Additions of the DMHP were 5%, 9%, 13%, 17%, respectively.

2.3 Preparation of the plywood sample

Three-ply plywood samples were prepared under the following conditions: 180 g/m^2 glue spreading for a single surface, 70 s/mm hot pressing time, 120 °C hot pressing temperature, and 1.0 MPa hot pressing pressure (Luo et al., 2014). After hot pressing, the plywood samples were stored under ambient conditions for at least 12 h before testing.

Five-ply plywood samples were made under the following conditions: 180 g/m^2 glue spreading for a single surface, 120°C hot pressing temperature, and 1.0 MPa hot pressing pressure. After hot pressing, the plywood samples were stored under ambient conditions for 8 h before testing.

2.4 Heat treatment

HT2: After hot pressing at 60 s/mm hot press time with 1.0 MPa pressure, then the pressure decreased to 0.1-0.2 MPa and kept for 2, 4, 6, 8, and 10 min, respectively. The hot press and heat treatment process were finished in one time press.

HT4: After hot pressing for 60 s/mm hot press time, the five-ply plywood was taken out and placed in an oven at 120°C for 4, 8, 12, 16, and 20 h, respectively.

3. Results and Discussion

3.1. Water resistance measurement

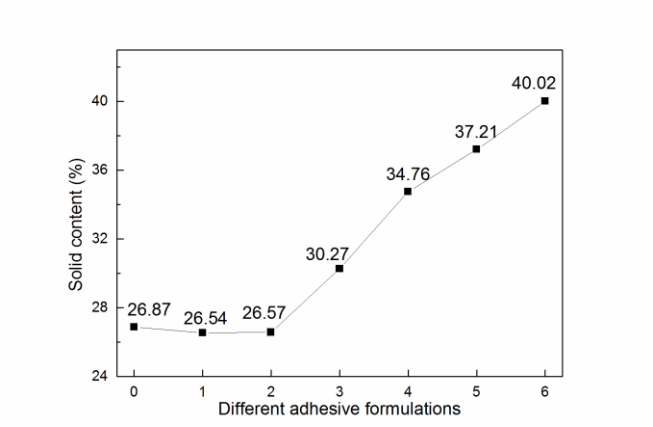

Fig. 1. The wet shear strength of the plywood bonded by different adhesive formulations: 0 (SM adhesive), 1 (SM/PAM adhesive), 2 (SM/PAM/SDS adhesive), 3 (SM/PAM/SDS/DMHP-5 wt% adhesive), 4 (SM/PAM/SDS/DMHP-9 wt% adhesive), 5 (SM/PAM/SDS/DMHP-13 wt% adhesive), 6 (SM/PAM/SDS/DMHP-17 wt% adhesive).

The wet shear strength of the plywood bonded by different adhesive formulations is shown in Fig. 2. The wet shear strength of the plywood bonded by the SM adhesive was 0.30 MPa, which failed to meet the interior use plywood requirement (≥0.7MPa). The wet shear strength of the plywood increased by 26.7% to 0.38 MPa upon PAM addition, which was due to the molecular lubrication effect of PAM. After further mixing with SDS, the wet shear strength was increased to 0.41 MPa, which was increased by 36.7% compared with the SM adhesive. SDS is a protein denature agent which unfolds soy protein molecule and exposes non-polar groups to enhance the water resistance of the resulting adhesive. From another aspect, SDS and PAM possessed electrical charges, which formed a mesh structure by electrostatic attraction with charged amino acids. This mesh structure benefited for a cross-linker cling and acted with soy protein molecules (Xu et al., 2014). The DMHP, used as a cross-linker, can link soy protein molecule by reacting with amino and hydroxyl groups to form three dimension cross-linked networks among the macromolecule to improve the water resistance.

The wet shear strength increased significantly upon 5 wt% DMHP additions, which was increased by 56.1% to 0.64 MPa compared with the SM/PAM/SDS adhesive. The wet shear strength of the plywood with addition of 9 wt% DMHP was 0.76MPa, which met the interior use panel requirement. However, from the standard deviation at formulation 4, the wet shear strength of the plywood specimens cannot be guaranteed over 0.70 MPa. As shown in Fig. 3, the wet shear strength of the plywood bonded with the adhesive upon 13 wt% DMHP additions increased by 52.6% and reached a maximum value of 1.16 MPa. By increasing the DMHP content to 17 wt%, the bond strength decreased to 0.69 MPa and could not meet the interior use plywood requirement (0.7 MPa). This was probably due to the over-low physical viscosity, which resulted in the adhesive over penetrating into the veneer. Therefore, based the above discussing, the optimum addition of the DMHP was selected at 13 wt% and the resulting adhesive was further characterized.

3.2. FTIR spectroscopic analysis

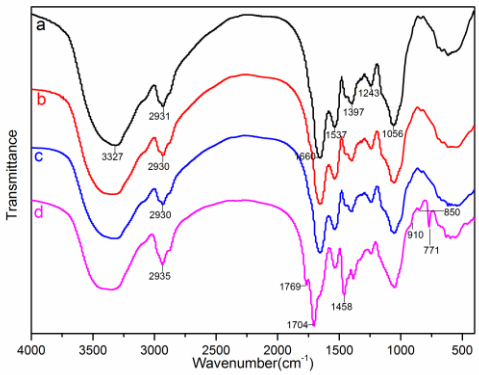

Fig. 2. FTIR spectra of the (a) SM adhesive and its hybrid adhesive (b) SM/PAM, (c) SM/PAM/SDS and (d) SM/PAM/SDS/DMHP adhesive.

Water readily associates with hydrophilic groups (e.g., hydroxyl groups) via hydrogen bonds, resulting in a poor water resistance of the adhesives. The FTIR spectra of the SM adhesive and its hybrid adhesives are presented in Fig. 3. A peak was observed at approximately 3327 cm^{-1} was related to the free and bound O-H and N-H bending vibrations, which could form hydrogen bonds with the carbonyl group of the peptide linkage in the protein. The peak observed at approximately 2930 cm^{-1} was attributed to the symmetric and asymmetric stretching vibrations of the $–CH_2$ group in different adhesives. The main absorption bands of the peptide were related to peaks approximately at 1660, 1537, and 1243 cm^{-1}, which were characteristic of amide I (C=O stretching), amide II (N-H bending) and amide III (C-N and N-H stretching), respectively (Chen and Subirade, 2009). The bands corresponding to COO– and $–C–NH_2$ bending were located at 1397, and 1056 cm^{-1}, respectively.

In the SM/PAM/SDS/DMHP adhesive, the absorption peak of COO– and $–C–NH_2$ (1397 cm^{-1} and 1056 cm^{-1}) decreased compared with the SM adhesive, which might be a result of the reaction between epoxy group of the DMHP and the –NH, –COOH groups of soy protein molecule, implying that the amount of hydrophilic groups in the adhesive decreased upon the DMHP addition (Lei et al., 2014). The amide I shifted from 1660 to 1704 cm^{-1} (blue shift) in the spectrum of the SM/PAM/SDS/DMHP adhesive, indicating that the soy protein molecule

had less random loose state in the SM/PAM/SDS/DMHP adhesive than that in the SM adhesive. A new peak appeared at 1769 cm^{-1}, which attributed to the stretching vibrations of the ester carbonyl bond. This band indicated that the formation of the ester linkage between the epoxy group and the hydroxyl group of soy protein (Schramm and Rinderer, 2006). The absorption peak at 910 cm^{-1} was assigned to the free epoxy group skeleton vibration (Yu, 1988). After incorporated the DMHP, there would be a strong absorption peak at 910 cm^{-1}. But in the Fig. 3, it exhibited a minor one (910 cm^{-1}) and even became neglectable in the spectrum of the SM/PAM/SDS/DMHP adhesive formulation, indicating that epoxy group of the resin reacted with active hydrogen on –OH and $–NH_2$ groups in the protein molecules during the curing process by a ring-opening reaction (Park et al., 2013). In addition, the peak at 910 cm^{-1} also showed the good dispersibility of the DMHP in a water soluble adhesive system. The above-mentioned absorption peak changes led to an improvement in the water resistance of the soybean meal-based bio-adhesive. On one hand, the mixing of the SDS, PAM and DMHP transferred the hydrophilic groups of soy protein to hydrophobic ones as much as possible. On the other hand, the DMHP addition increased the cross-linking density by a chemical reaction. The following reaction might take place in that process.

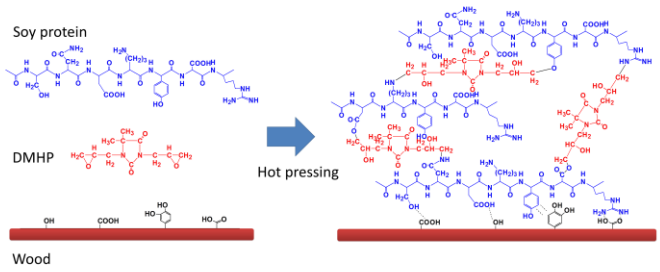

Fig. 3. The curing process of the SM/PAM/SDS/DMHP adhesive.

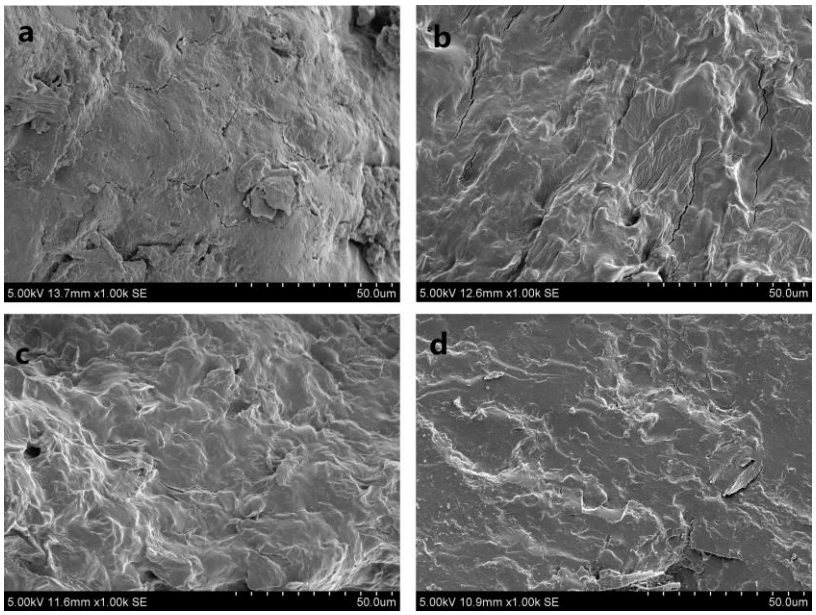

Fig. 4. The fracture surface micrograph of the cured (a) SM adhesive and its hybrid adhesive (b) SM/PAM, (c) SM/PAM/SDS and (d) SM/PAM/SDS/DMHP adhesive.

The fracture surface micrograph of the cured SM adhesive and its hybrid adhesives are shown in Fig. 4. A large number of holes and cracks were observed on the fracture surface of the SM adhesive. In addition, the whole fracture surface appeared very loose and disordered. These holes and cracks were formed by water evaporation in the adhesive during the hot press process, which led to a low water resistance of the SM adhesive (Zhang et al., 2014). After the DMHP was introduced, fewer holes and cracks were observed, and the fracture surface of the cured adhesive became smoother and more compact. This was caused reaction between the DMHP and soy protein molecule and a cross-linking network formed, which improved the water resistant of the adhesive.

3.3. Effects of heat treatment on wet shear strength of plywood

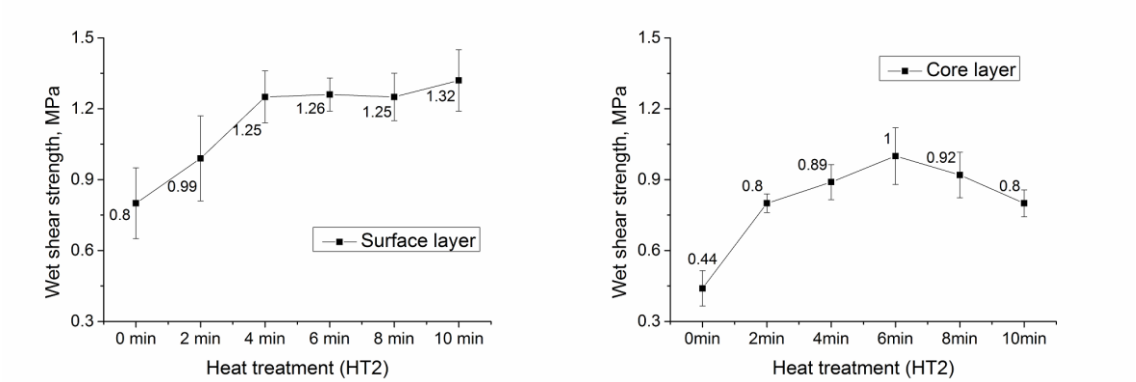

Fig. 5. Effect of HT2 on plywood surface and core layer wet shear strength.

Fig. 5 shows the effect of HT2 on the surface and core layer wet shear strength of plywood. The wet shear strength of the surface layer with 2 min heat treatment improved by 23.4% to 0.99 MPa competed with no treatment. In addition, the wet shear strength of all specimens met interior use plywood requirements. After 4 min heat treatment, the surface layer wet shear strength improved by 56.3% to 1.25 MPa. The increase in wet shear strength may occur for two reasons. One is that the water in the plywood may escape more easily during the low-pressure process. This process could make the adhesive cure quickly and completely. The other is that the interior plywood stress decreases with the low-pressure heat treatment process, which also could improve the wet shear strength of the resulting plywood. After 2 min heat treatment, the wet shear strength of the core layer improved by 81.8%, from 0.44 to 0.80 MPa. With 6 min of HT2, the wet shear strength of the core layer improved by 25.0% to a maximum value of 1.0 MPa. Compared with plywood without heat treatment, the wet shear strength of the core layer with 6 min of HT2 increased by 127.3%. Water could help heat conduction in the plywood, but too much water creates vapor, especially in the core layer. If these vapors are unable to escape during the hot press process, the core layer bonds break when hot pressing stops. The core layer will only achieve the designed temperature (120°C) after the water in the core layer is removed. Water vapor escaped during the hot press process for 0 to 2 min of HT2. Most of the water in the plywood was removed, which caused the wet shear strength to increase rapidly. The further increase in the wet shear strength on the core layer is attributed to an interior force reduction during the low-pressure heat treatment. From 6 to 10 min of HT2, the wet shear strength decreased by 20.0% from 1 to 0.8 MPa, which contributed to an increase in the interior forces caused by over-drying.

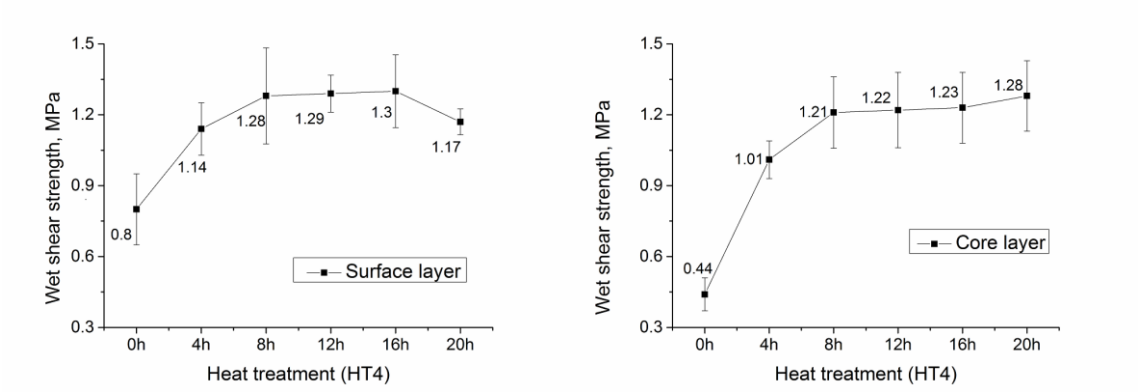

Fig. 6. Effect of HT4 on plywood surface and core layer wet shear strength.

Using a DMHP with soybean meal-based adhesives can further improve the wet shear strength of plywood by interacting with soy protein molecules and improving the degree of cross-linking of the cured adhesive. Therefore, the reaction process requires a high temperature. Up to 120°C oven drying was used to improve the wet shear strength of the plywood. Fig. 6 shows the effect of HT4 on the plywood surface and core layer wet shear strength. Results show that 4 h of heat treatment improved the surface layer wet shear strength by 42.4%, from 0.80 to 1.14 MPa. With 8 h heat treatment, the surface layer wet shear strength increased by 12.3% to 1.28 MPa, which is an increase of 60% compared with no heat treatment. The increase in wet shear strength of the surface layer occurred because the high temperature could accelerate the soy protein and DMHP reaction. Both of these factors could cure the adhesive more completely and improve the wet shear strength. The wet shear strength of the surface layer showed no obvious difference from 8 to 16 h. With 20 h heat treatment, the wet shear strength of the surface layer decreased to 1.17 MPa. This may occur because of thermal degradation of the adhesive, and an increase in interior forces because of the long heat treatment time. The heat treatment showed a significant effect on core layer wet shear strength from 0 to 8 h. With 4 h heat treatment, the core layer wet shear strength increased by 129.5%, from 0.44 to 1.01 MPa. With 8 h heat treatment, the wet strength of the core layer improved by a further 19.8% to 1.21 MPa. There was no obvious difference in wet shear strength from 8 to 20 h of heat treatment. The maximum wet shear strength with 120°C treatment improved by 30.6% and 28%, respectively. This was because the no-pressure heat treatment process released the interior force of the core layer, thus improving the wet shear strength.

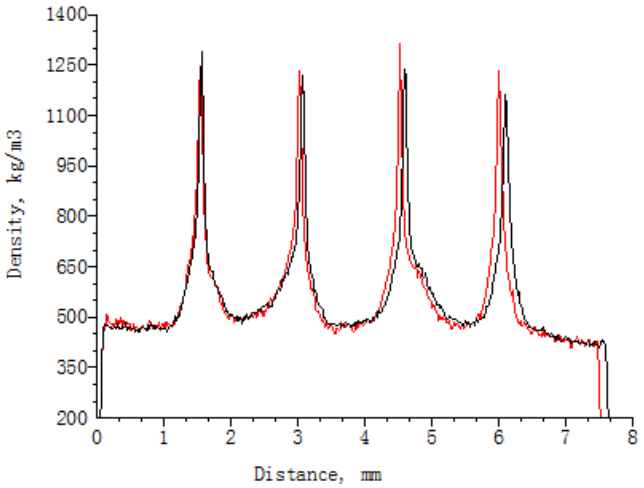

Fig. 7. Vertical density profile of plywood samples. (red line: vertical density profile of plywood with 120°C heat treatment for 8 h, black line: control.)

A vertical density profile was used to measure composite panel densities. It can also be used to detect density changes of the plywood. Fig. 8 shows the vertical density profile of the plywood. The black line (control) is plywood fabricated at 60 s/mm of hot press time. The red line is the control plywood sample that is heat treated for a further 8 h at 120°C after hot pressing. In Fig. 7, the peak is the adhesive layer in the plywood. For wood bonding, the adhesive permeates into wood gaps and cures to form an interlock between two veneers, which also increases the density near the adhesive layer. Therefore, the density between the veneers shows a wide peak. The peak on the red line was higher than that on the black line, which means that adhesive layer density increased after heat treatment. However, there was no difference in peak width, indicating no further permeation of adhesive in the veneer. The adhesive cured completely with heat treatment, thereby increasing the density of the adhesive layer and the wet shear strength. Fig. 7 shows that the second peak moved to the first peak, as did the third and fourth. This may be because of a decrease in moisture content or a change in interior force in the plywood after heat treatment. During heat treatment, the interior force is released and balanced, which may also improve the wet shear strength of the plywood.

Conclusions

Using 13 wt % the DMHP effectively improve the water resistance of the resulting adhesive by 182.9% to 1.16 MPa, which was attributed to a solid cross-linking network formation by the reaction between the epoxy groups and the active groups on soy protein molecule, and a smoother fracture surface formed to prevent moisture intruding.

With 4 min of low pressure heat treatment after 60 s/mm hot pressing, the wet shear strength of the surface layer and core layers of the resultant plywood increased by 56.3% to 1.25 MPa and 102.3% to 0.89 MPa, respectively. This is practical for the soybean meal-based adhesive application. With 8 h of no pressure heat treatment (120°C) following 60 s/mm hot pressing,

the wet shear strength of the surface and core layers of the resultant plywood increased by 60.0% to 1.28 MPa and 175.0% to 1.21 MPa, respectively. The results of the vertical density profile show that the density of the adhesive layer increased and that the interior forces in the plywood may be released and balanced during the heat treatment process, thereby improving wet shear strength.

References

Chen, L., Subirade, M., 2009. Elaboration and Characterization of Soy/Zein Protein Microspheres for Controlled Nutraceutical Delivery. Biomacromolecules 10, 3327-3334.

Kumar, R., Choudhary, V., Mishra, S., Varma, I., Mattiason, B., 2002. Adhesives and plastics based on soy protein products. Ind Crops Prod 16, 155-172.

Lei, H., Du, G., Wu, Z., Xi, X., Dong, Z., 2014. Cross-linked soy-based wood adhesives for plywood. Int. J. Adhes. Adhes. 50, 199-203.

Luo, J., Luo, J., Gao, Q., Li, J., 2014. Effects of heat treatment on wet shear strength of plywood bonded with soybean meal-based adhesive. Ind Crops Prod.

Orr, L., 2007. Wood Adhesives–A Market Opportunity Study. Omni Tech International, Ltd., Midland, MI.

Park, C.H., Lee, S.W., Park, J.W., Kim, H.J., 2013. Preparation and characterization of dual curable adhesives containing epoxy and acrylate functionalities. React. Funct. Polym. 73, 641-646.

Schramm, C., Rinderer, B., 2006. Application of polycarboxylic acids to cotton fabrics under mild curing conditions. Cell Chem. Technol. 40, 799-804.

Sellers, T.J., 2001. Wood adhesive innovations and applications in North America. Forest Prod. J. 51, 12-22.
Xu, H., Luo, J., Gao, Q., Zhang, S., Li, J., 2014. Improved water resistance of soybean meal-based adhesive with SDS and PAM. BioResources 9, 4667-4678.

Yu, L., 1988. Solitons & polarons in conducting polymers. World Scientific.

Zhang, Y.H., Zhu, W.Q., Lu, Y., Gao, Z.H., Gu, J.Y., 2014. Nano-scale blocking mechanism of MMT and its effects on the properties of polyisocyanate-modified soybean protein adhesive. Ind Crops Prod 57, 35-42.

Proceedings of the 58th International Convention of
Society of Wood Science and Technology
June 7-12, 2015 - Grand Teton National Park, Jackson, Wyoming, USA

Fractionation of the Liquefied Lignocellulosic Biomass for the Production of Platform Chemicals

Junming Xu, finechemistry@163.com
Xinfeng XIE,
Jingxin WANG,
Jianchun JIANG,

West Virginia University, 372 Gilmore Street, Morgantown, WV 26506 USA

Abstract

A facile and sustainable process was designed to intrigue a degradation reaction of biomass and produce biopolyols and phenolic compounds. Liquefaction of lignocellulosic materials was conducted in methanol at temperature of 180 ℃ for 15 minutes with the conversion of raw materials at about 75.0%. It was found that a majority of those hydrophobic phenolics could be separated from aqueous solution. The phenolic products that extracted from the aqueous phase were mainly composed of phenolic derivatives such as 2-methoxy-4-propyl-phenol and 4-hydroxy-3-methoxy-benzoic acid methyl ester. The aqueous solution was then distilled under vacuum to remove the water and formed a viscous liquid product named biopolyol. As evidenced by GC-MS, the biopolyols mainly contain methyl sugar derivatives, including methyl β-d-mannofuranoside, methyl α-D-Galactopyranoside, methyl α-D-Glucopyranoside and methyl β-D-Glucopyranoside. The production rate of phenolics and multi hydroxyl compounds (including glycerol and sugar derivatives) in phenolic products and biopolyols is 66.75% and 84.69%, respectively.

Proceedings of the 58th International Convention of
Society of Wood Science and Technology
June 7-12, 2015 - Grand Teton National Park, Jackson, Wyoming, USA

Concentrations of heavy metals in Eucalyptus and Pinus wood sawdust and smoke, Copperbelt province, Zambia

Ncube, enncube@yahoo.com
Benjamin Phiri, elisha.ncube@cbu.ac.zm

Copperbelt University, P O Box 21692, Jambo drive, Riverside, Kitwe Zambia

Abstract

Heavy metals assimilated by trees or adsorbed by sawdust from polluted air poses a health hazard. The amount of heavy metals in Eucalyptus and Pinus sawdust was evaluated to establish whether sawdust use for energy and surface amendments was safe. Wood sawdust and smoke from a burning test were analyzed for heavy metals by atomic adsorption spectrophotometetry. The heavy metal concentrations in Eucalyptus sawdust were 11.5-61.1 mg Pb/kg, 3.3-7.9 mg Cd/kg, 4.9-56.9 mg Cr/kg and 20.2-43.4 mg Ni/kg while that in Pinus sawdust were 17.1-32.8 mg Pb/kg, 5.1-8.6 mg Cd/kg, 9.9-28.2 mg Cr/kg and 18.7-67.4 mg Ni/kg. The concentrations of chromium and cadmium in both wood types from Kitwe exceeded the limit, and so the sawdust was deemed unsuitable for surface applications. This was the same for nickel in Pinus sawdust. The study showed that sawdust from both wood types was not safe for mulching, composting and animal bedding. The annual exposure limits of 0.2 μg Cr/m3, 180 μg Ni/m3 and 0.2 μg Cd/m3 set by the World Health Organization were not exceeded by the smoke from both wood types. This suggested that combustion emissions embedded on large particulate matter from Eucalyptus and Pinus sawdust which has been in storage for about two years in conditions found in Kitwe is unlikely to have adverse short-term health effects associated with heavy metals.

Proceedings of the 58th International Convention of
Society of Wood Science and Technology
June 7-12, 2015 - Grand Teton National Park, Jackson, Wyoming, USA

Synthesis and Characterization of Sucrose-Melamine-Formaldehyde Adhesives

Weixing Gan, gwxgxdx@126.com
Yifu Zhang,
Haibing Yang,
Licheng Pan,
Zhoufeng Huang,

Guangxi University, Wood Science Department , 100 University Road, Nanning, Guangxi

Abstract

Due to the limitation of the petroleum resources and the unstable fossil fuel prices, there is more demand on the development of bio-based adhesives synthesized from the renewable bio-resources. Sucrose, rich in hydroxyl groups, is a class of renewable and biodegradable biomaterials which can be used as a substitute for the synthetic polymers like lactose. In this work, sucrose–melamine-formaldehyde (SMF) resin was synthesized in a base condition. The shelf-life of the SMF resin was determined by a method of viscosity measurement. It was found that the shelf-life of SMF resin was increased as the sucrose content was increased. The effect of sucrose content on the bonding strength, formaldehyde emission of SMF bonded plywood were studied, and a sucrose to melamine mole ratio of 0.6:1 was determined. Fourier Transform-Infrared Spectroscopy (FT-IR) and Mass Spectrum (MS) were employed to analyze the chemical structure of the SMF resin. The spectrogram of FT-IR and MS revealed the structures of sucrose, melamine and formaldehyde in the SMF. The chemical reaction of SMF resins occurred between the three primary hydroxyl groups of sugarcane and the hydroxymethyl of melamine.

Proceedings of the 58th International Convention of
Society of Wood Science and Technology
June 7-12, 2015 - Grand Teton National Park, Jackson, Wyoming, USA

Preparation and Characterization of Activated Carbon Fibers from Liquefied Wood by KOH Activation

*Yuxiang Huang, Guangjie Zhao**

College of Materials Science and Technology, Beijing Forestry University, Tsinghua East Road 35, Haidian 100083, Beijing, China

Abstract

Activated carbon fibers (ACFs) have been prepared from liquefied wood by chemical activation with KOH, with a particular focus on the effect of KOH/fiber ratio in term of porous texture and surface chemistry. ACFs based on steam activation served as a blank for comparison. The properties of the ACFs were investigated by scanning electron microscope (SEM), X-ray diffraction (XRD), and nitrogen adsorption/desorption, FTIR spectroscopy, and X-ray photoelectron spectroscopy (XPS). The results show that the KOH-activated ACFs have rougher surfaces and more amorphous structure compared with the blank. The pore development was significant when the KOH/fiber ratio reached 3, and achieved a maximum Brunauer-Emmett-Teller (BET) surface area of 1371 $m^2 g^{-1}$ and total pore volume of 0.777 $cm^3 g^{-1}$, of which 45.3% belong to mesopores with diameters of 2-4 nm, while the blank activated at the same temperature had a BET surface of 1250 $m^2 g^{-1}$ and total pore volume of 0.644 $cm^3 g^{-1}$, which are mainly micropores. The surface functional groups are closely associated with the KOH/fiber ratios. KOH-activated ACFs with KOH/fiber ratio of 3 have more oxygenated surface functional groups (C-O, C=O, -COOH) than the blank.

Key words: activated carbon fibers (ACFs); liquefied wood; KOH activation; microstructure; surface properties

1. Introduction

Activated carbon fibers (ACFs), as a new type of activated carbon, have unique characteristics compared with granular or powdered activated carbons due to their abundantly developed pore structure and special surface reactivity. They have been widely applied in many fields as a result, such as adsorption and separation, electronic materials, catalyst support, and the storage of natural gas[1]. ACFs are currently prepared from polyacrylonitrile (PAN), pitch or phenolic resin fibers. Since environmental protection and resource conservation have attracted more and more attention in recent years, biomass resources such

* Correspondence to: Guangjie Zhao; E-mail: zhaows@bjfu.edu.cn. Tel/Fax: 86 010 62338358.

as bamboo[2], jute[3] and cotton waste[4] become popular as alternatives to petrochemical resources.

Wood, being a main component of biomass containing abundant cellulose and lignin[5], has been utilized as well in the preparation of wood-based ACFs by liquefaction with phenol. This way did not require the separation of chemical components in wood, giving a higher wood utilization ratio than other methods[6-7]. Lately, ACFs have been successively made from liquefied Chinese fir sawdust[8] and poplar bark[9] by physical activation with steam. Although the obtained ACFs had high specific surface area, their yield was relatively low and most of them were microporous with very narrow pore size distribution (PSDs). On the other hand, ACFs prepared by steam activation had very high C content, thereby possessing less oxygen-containing surface functionalities. In turn, previous literature has shown that chemical activation with KOH can widen the PSDs[10] and introduce oxygen-containing surface groups[11]. To date, one of the most extended utilization of activated carbon materials is electric double layer capacitors (EDLCs) [12]. From the point of view of this application not only the wide PSDs and more mesopores over high SSA are required [13], but the surface chemistry especially the O functionalities also has a significant effect on the capacity of EDLCs on account of their enhancement in pseudocapacitance[14]. Hence, it can be expected that chemical activation with KOH of liquefied wood-based fibers could deliver ACFs with added mesoporosity and surface chemical properties that may be advantageous for application in EDLCs.

The aim of this work was to control the porosity and surface chemical properties of W_{liq} based ACFs. To this end, ACFs should be prepared by KOH activation and the KOH/fiber ratio should be investigated in terms of the ACFs' porous structure and surface chemistry. The results will be compared with those obtained from ACFs based on steam activation (blank). The surface morphology of the prepared ACFs will be observed by SEM and XRD. The pore structure will be evaluated by N_2 adsorption/desorption. FTIR spectroscopy and X-ray photo-electron spectroscopy (XPS) should contribute to the characterization of the materials.

2. Experimental

2.1 Preparation of ACFs

Chinese fir (Cunninghamia lanceolata) was firstly ground and screened to particle size of 60-80 meshes for use in the experiments. The mixture of wood flour, phenols and H_3PO_4 at a mess ratio of 1:5:0.4 was heated in an oil bath at 160℃ for 2.5 hours with continuous stirring to obtain liquefied wood. After the liquefaction, 5 wt% (based on the weight of liquefied solution) hexamethylenetetramine as synthetic agent was added to the liquefied wood to prepare the spinning solution by heating the mixture from room temperature up to 170 ℃ in 40 minutes. The spun filaments were prepared by melt-spinning at 120℃ with a laboratory spinning apparatus. When the spinning was over, the resultant fibers were cured by soaking in a solution with HCHO and HCl (1:1 by volume) as the main components at 90 ℃ for 2 hours and then washed with distilled water and finally dried at 80℃ for 4 hours to obtain the precursor fibers. 20 g of the resultant precursors were then carbonized in a horizontal transparent tube furnace (Y02PB, Thermcraftinc U.S.A) at 500°C in N_2 flow for 1 h

carbonization. The carbonization yield (CY) was calculated by the weight ratio of the resultant carbon fibers (CFs) to precursor fibers.

About 6 g of CFs were put in the tube furnace after impregnation with KOH at KOH/fiber ratios of 1, 2 and 3 (w/w). About 2 g of each CFs was carbonized by heating the mixtures under N_2 flow (200 cm^3 min^{-1}) at a heating rate of 4°C min^{-1}. The activation temperature was 850°C and the holding time was 1 h. The obtained ACFs were washed with distilled water until neutral pH and dried at 103±2°C. The KOH-activated ACFs are labeled as ACF-1, -2, and -3, where the numbers represent the impregnation ratios KOH/fiber as indicated above. The activation yield (AY) was calculated by the weight ratio of ACFs to CFs, thereby the total yield was obtained by multiplying AY by CY.

For comparison, steam activation was also conducted, where 2 g of CFs were similarly heated from r.t. to 850°C and were held at this temperature for 1 h by introducing a steam flow and then cooled down to r.t. These products are labeled as ACF-S or simply as the blank.

2.2 Characterization of ACFs

Surface morphology

Surface morphology of the ACFs was examined with a scanning electron microscope (SEM, S-3400N, Hitach Company in Japan). Before observation, the samples were metalized with a thin layer of Pt.

XRD analysis

X-ray diffraction (SHIMADZU, XRD-6000) measurements were conducted with an X-ray diffractometer using CuKa radiation (wavelength 0.154nm) at 40 kV and 30 mA. The scanning rate was 2°/min with a scanning step of 0.02° from 5° to 60° (2θ).

Nitrogen adsorption measurement

Surface area and porosity of the ACFs were evaluated by N_2 adsorption-desorption isotherm measured at -196 ℃ by a surface area analyzer and a pore size analyzer: Autosorb-iQ. Before analysis, the samples were degassed at 300℃ for 3 h. The SSA (S_{BET}) was calculated by the Brunauer–Emmett–Teller (BET) method using N_2 adsorption isotherm data[15]. The total pore volume (V_{tot}) was evaluated by converting the amount of N_2 adsorbed at a relative pressure of 0.995 to the volume of liquid adsorbate. The micropore area (S_{micro}) and micropore volume (V_{micro}) were obtained by t-plot method[16]. PSDs were calculated using the Density Functional Theory (DFT) method[17], which based on calculated adsorption isotherms for pores of different sizes.

FTIR analysis

The chemical groups of the ACFs were examined using pressed potassium bromide (KBr) pellets containing 5% of samples by Fourier transform infrared spectrum analysis spectrometer (FTIR, BRUKER Tensor 27, German) in the scanning range of 4000-500 cm^{-1}. The samples were pulverized (100 mesh) and mixed with KBr before being pressed into a disk.

XPS analysis
XPS measurements were carried out on a spectrophotometer to determine the number of functional groups present on the surface of the ACFs with a monochromated Al Ka X-ray source (hv = 1486.6 eV). A current of 10 mA and a voltage of 13 kV were used. The survey scans were collected from the binding energy ranging of 0 to 1350eV. A nonlinear least squares curve-fitting program (XPSPEAK software, Version 4.1) was employed for XPS spectral deconvolution.

3. Results and Discussion

Surface morphological observation
SEM micrographs of the ACFs are presented in Fig .1. A very smooth surface is clearly identifiable for the ACFs-steam, as shown in Fig. 1a. However, the morphological features of the KOH-activated ACFs show distinct patterns (Fig.1 b~d) that their surface is rugged due to the ablative effect of KOH. As the KOH/fiber ratio increases, highly cracked and collapsed surfaces are obtained, indicating that the etching reactions between KOH and surface carbon became violent as the amount of KOH on the surface of the fibers increased as a result of the mass ratio rising, which led to the creation of pores and high surface areas. The even and clear distribution of the folds demonstrates a great impregnation effect that KOH was uniformly deposited.

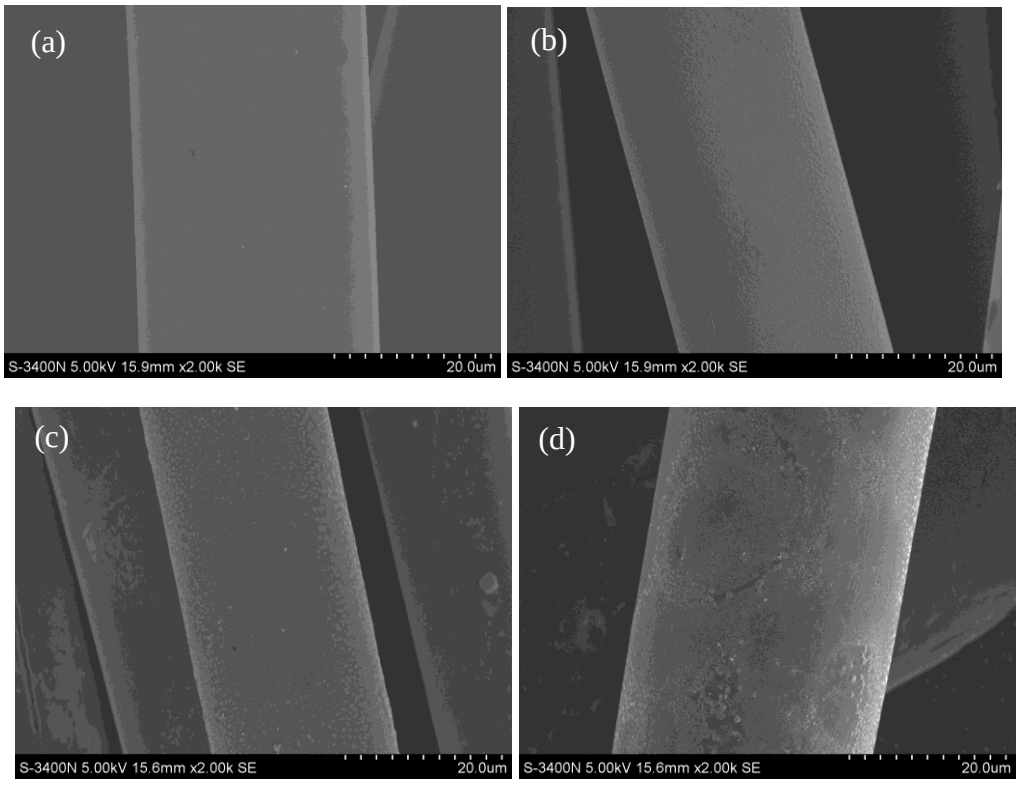

Fig.1 SEM photographs of surface of KOH-activated and steam-activated ACFs; (a) ACF-S; (b) ACF-1; (c) ACF-2; (d) ACF-3.

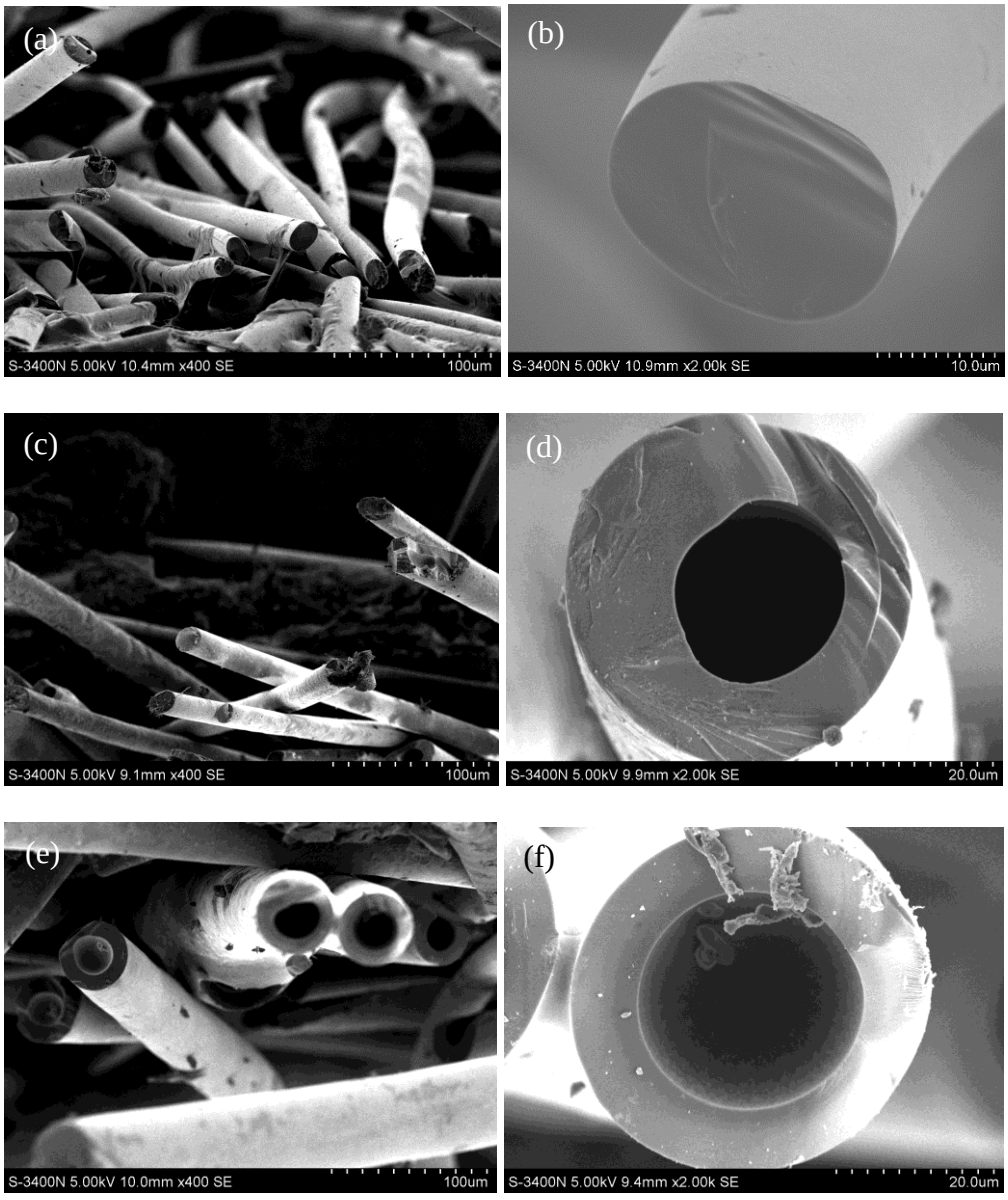

Fig.2 SEM photographs of cross section of KOH-activated ACFs; (a) ACF-1; (b) magnified ACF-1; (c) ACF-2; (d) magnified ACF-2; (e) ACF-3; (f) magnified ACF-3. The numerals 1-3 refer to the KOH/fiber ratios.

According to the Fig. 2, the cross section of ACFs appears to be oval rather than circular. The ACF-1 has a very flat section (in the inset of Fig.2 b), however, when the KOH/fiber ratio exceeds 1, holes appear at the core of the ACFs owing to the skin-core structure of the ACFs[18] that edge structure was tight while the core structure was relatively loose to form holes when the reaction of KOH and carbon took place. The holes become larger gradually by keep on increasing the KOH/fiber ratio (in the inset of Fig2. c-g), which could be related

to the fact that an increase in mass ratio resulted in more KOH penetration into the interior of the fibers, whose structures would be destroyed severely after the activation reaction.

XRD analysis

Fig. 3 shows the XRD patterns of the ACFs as a function of KOH/fiber ratio in comparison with the steam-activated ACFs. The latter displays a peak at approximately 24° and another at approximately 43°, which were assigned to the disordered graphitic 002 plane and 10 plane (overlapped 100 and 101), respectively[19], suggesting the ACFs prepared from liquefied wood were made of graphite-like microcrystallites[20]. Compared with the blank, the peaks at 24° shift to a low angle for the KOH-activated ACFs, meaning that their amorphous structures were strengthened. In other words, their graphitic microcrystallites were destroyed more severely, which may lead to widening of the pores because the pore walls in ACFs are made up of graphitic microcrystallites.

In addition, all the KOH-activated ACFs show peaks at about 30.7° (corresponding to the standard JCPDS card of K_2CO_3, the number is 71-1466) due to the residual K_2CO_3 particles in the fibers, which were the reaction products of KOH and carbon[21]. As the mass ratio increases, the peaks related to 002 plane moves to a lower angle and becomes broader while the peaks attributed to K_2CO_3 are better resolved. This is because, on the one hand, intenser reaction between KOH and carbon brought about more severely destructive crystal structure, which is consistent with the analysis of the SEM results. Relatively, the crystal diffraction peak of K_2CO_3 is clearer. On the other hand, high KOH/fiber ratio meant more KOH involved in the activation reaction, causing greater K_2CO_3 to be produced and remained after washing, which would also made the peak remarkable.

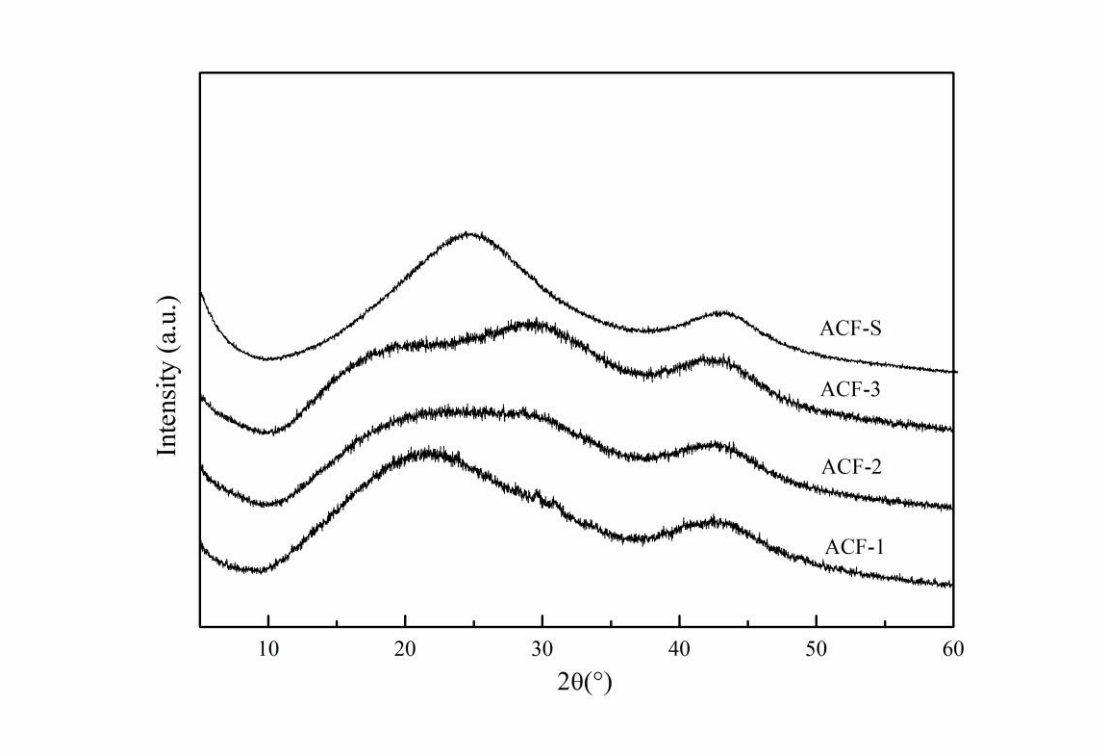

Fig.3 X-ray diffraction patterns of KOH-activated ACFs and steam-activated ACF.

N_2 adsorption/desorption isotherm

Fig. 4 shows the adsorption/desorption isotherms of N_2 for the ACFs. In the blank, the volume adsorbed increases quickly with increasing pressure at low pressure ranges but levels off when the relative pressure is above 0.1. This means that the isotherms belong to type I according to the IUPAC classification[22], where microporous adsorption is the prominent adsorption. As for the KOH-activated ACFs, however, the volume absorbed maintains an upward trend when the relative pressure exceeds 0.1, especially for the ACF-1 and ACF-2. It's worth noting that adsorption/desorption hysteresis can be found in the isotherms of the KOH-activated ACFs, while no hysteresis for the steam-activated ACFs. These results could probably be related to the difference in mesopores between the KOH-activated ACFs and the blank.

Pore properties of all the ACFs including S_{BET}, S_{mic}, S_{meso}, V_{tot}, and yield are listed in Table 1. S_{BET} and V_{tot} of the KOH-activated ACFs gradually increase with increasing KOH/fiber ratio while the yield decreases correspondingly. However, the S_{meso} of ACF-2 reaches the maximum of 525m^2/g and then reduces with increasing KOH/fiber ratios, while the S_{mic} keeps highly increasing, most likely because of the limited availability of KOH when KOH is attached on the surface, thus the activation only took place on the surface of the fibers and there was little generation of metallic K which can intercalate into carbon lattices of the carbon matrix to further develop the porosity[23]. With the prolongation of the activation, micropores were gradually enlarged to mesopores[24]. When the mass ratio exceeded 2, KOH was enough to penetrate into the interior of the fibers. On the one hand, the etching of the carbon framework was conducted from outer to inner and the metallic K generated by the redox reactions between various KOH and carbon further developed the micropores by efficiently intercalating into the carbon lattices. Moreover, the continuous activation on the surface would further etch the previously generated mesopores and even cause them to collapse so their quantities began to reduce. S_{BET}, S_{micro} and S_{meso} of steam-activated ACFs are 1240 m^2/g, 969m^2/g and 281m^2/g respectively, which are slightly less than those of ACF-3. However, the ACF-3 has a higher yield obviously and the ratio of mesopore volume to total pore volume is 45.3% while that of the ACFs-steam is only 9.3%, demonstrating ACFs by steam activation were mainly microporous and ACFs by KOH activation had abundant mesopores.

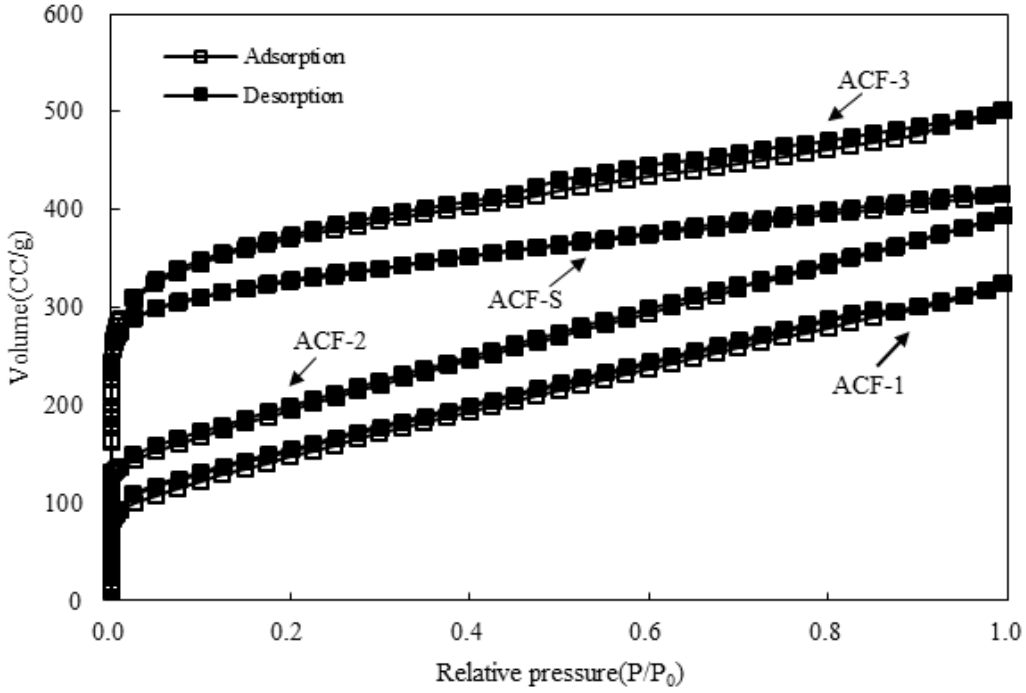

Fig.4 N_2 adsorption/desorption isotherms of KOH-activated and steam-activated ACFs.

Table 1 Pore properties of the KOH-activated and steam-activated ACF.

Sample	Pore structure parameters						
	$S_{BET}(m^2/g)$	$S_{micro}(m^2/g)$	$S_{meso}(m^2/g)$	$V_{tot}(cm^3/g)$	$V_{meso}(cm^3/g)$	$V_{meso}/V_{tot}(\%)$	Yield(%)
ACF-1	536	35	501	0.504	0.471	93.5%	66.8
ACF-2	700	175	525	0.611	0.516	84.5%	58.2
ACF-3	1371	1024	347	0.777	0.352	45.3%	35.6
ACF-S	1250	969	281	0.644	0.060	9.3%	29.7

PSDs based on DFT method are presented in Fig. 5. The PSDs in mesopore region for the KOH-activated ACFs exhibit a broad similarity in the range around 2-5 nm, while clear difference can be observed in micropore region that the micropores mainly accumulate in a narrow range below 1nm with low KOH/fiber ratios. In case of AFCs-3, the distribution range is widened to 1-2 nm, where two distinct peaks at 1.25 and 1.45 nm are visible. Accordingly, increasing KOH/fiber ratios leads to more micropores and enlarge the pore width. Though micropores of the blank at 0.65 nm are similar to that of the KOH-activated ACFs, the PSDs in the mesopore region can hardly be recognized in the blank.

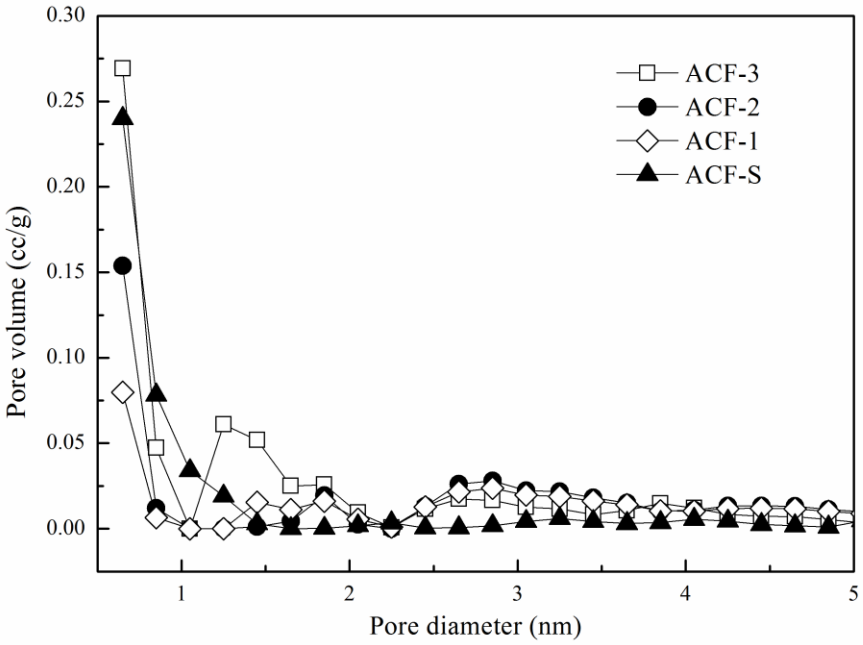

Fig.5 PSDs of KOH-activated and steam-activated ACFs.

FTIR analysis

FTIR, as a sensitive technique for surface analysis, was used to characterize the surface chemical structure of ACFs by different activation methods[25]. Fig. 6 shows the spectra of steam- and KOH-activated ACFs at different KOH/fiber ratios.

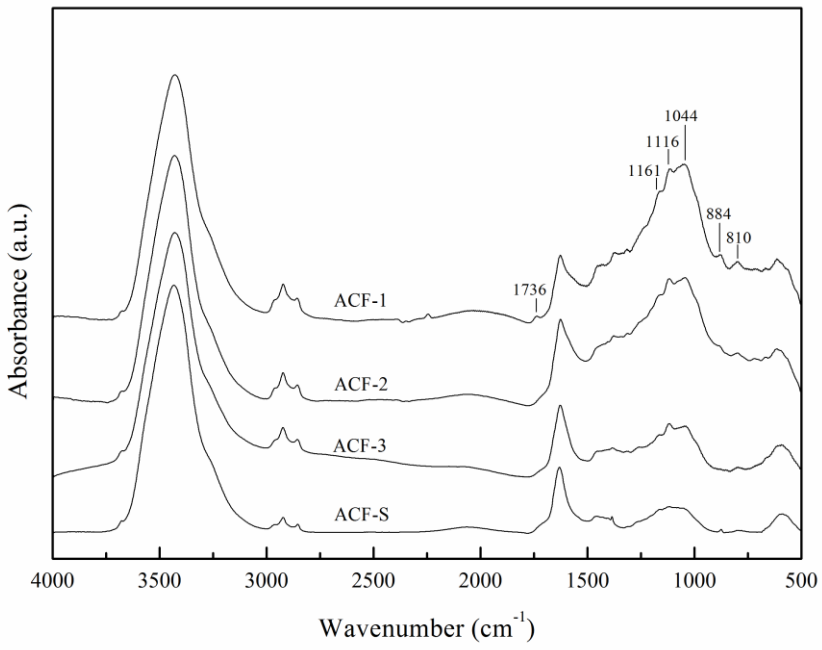

Fig. 6 FTIR spectra of KOH- and steam-activated ACFs.

For KOH-activated ACFs, All the spectra exhibit simlilar bands and shoulders which are assigned to various vibration modes in atomic groups and structures. The broad absorption band at 3600-3200cm^{-1} with a maximum at about 3428cm^{-1} is characteristic of the stretching vibration of hydroxyl[26], which is always accompanied by a band around 1630cm^{-1} assighned to H-O-H bending of absorbed water molecules[27]. The bands at 2923cm^{-1} and 2855cm^{-1} correspond to the symmetric and asymmetric streching vibration of -CH_2-. The weak band at 1736cm^{-1} is attributed to the stretching vibration of C=O[28]. The peak at 1468cm^{-1} is assigned to –CH_2- scissoring vibration, while the peak at 1384cm^{-1} is likey to be caused by bending vibration of –CH_3. The band at 1300-1000cm^{-1} region is quite difficult to be identified because it may be ascribed to C-O in acids, alcohols, phenols, ethers or ester groups[29]. At least three peaks at 1161cm^{-1}, 1116cm^{-1}, and 1044cm^{-1} are observed in this region, indicating that various types of C-O groups existed in KOH-activated ACFs. The peaks at 884cm^{-1} 810cm^{-1} are both characteristic of the out-of-plane bending vibration of C-H in the aromatic rings. As the mass ratio increases, the intensity of the peaks identified as oxygen-containing functional groups such as C=O and C-O decreases significantly, while that of other peaks remains unchanged fundamentally. This may be resulted from the reduction of O content during the activation process with increasing KOH/fiber ratios

As seen from the FTIR spectrum of ACF-S, no obvious peak can be found in the region at 1300-1000cm^{-1}, demonstrating that steam-activated ACFs had lower C-O groups than KOH-activated ACFs. Furthermore, there are few bands at 900-650cm^{-1}, suggesting that a multi-benzene fused ring structure formed. In other words, ACFs-steam had more graphitic structure, which is consistent with the results of XRD analysis. To sum up, the analysis of the FTIR spectra indicates that the KOH-activated ACFs had richer surface functional groups than the steam-activated ones.

XPS analysis

Fig. 7 expresses the XPS spectra of both steam-activated and KOH-activated ACFs. It's apparent that element C is the most dominant constituent in all samples and element O is the second. However, the peak of element K can be found in the KOH-activated samples, which verifies the existence of potassium complex. Atomic concentrations on the surface of the ACFs are summed up in Table 2. With the increasing KOH/fiber ratio, carbon content increases from 85.2% to 88.6%, while the oxygen content decreases from 13.8% to 9.8%, which gives an explanation for the decrease in O/C atomic ratio. This implies that although more carbon would consume by reacting with KOH when the KOH/fiber ratio increased, oxygen of the ACFs themselves was subjected to a greater loss. This further supports the findings of FTIR that intensity of oxygen-containing functional groups decreased as the mass ratio raises. However, O/C atomic ratio of the blank is only 9.4%, reflecting that KOH-activated ACFs had probably more oxygen-containing functional groups because of the different reaction mechanisms. This result was similar to that obtained by Babel and Jurewicz who used viscose fibers as precursors to prepare ACFs by KOH and steam activation[11]. Nevertheless, in their study, activation temperature rather than KOH/fiber ratio on O content had been discussed. The findings that KOH-activated ACFs had more O content that steam-activated ones were interpreted as the fact that O might be incorporated in the network during activation, due to C oxidation by KOH. Conversely, the present work revealed that O suffered a great loss which even intensified as the mass ratio grew up during the activation

process. And as a result, lower O content in steam-activated ACFs compared with KOH-activated ACFs was supposed to be the great loss of O merely instead of a lower O incorporation during steam activation.

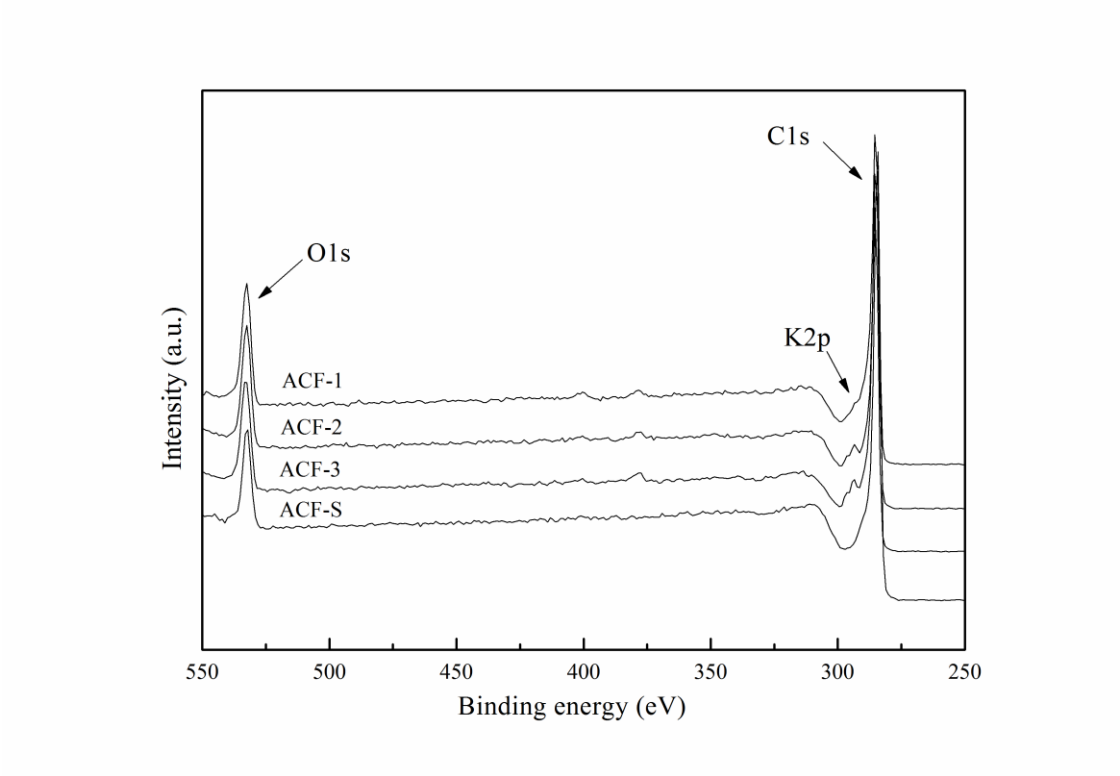

Fig. 7 XPS spectra of KOH-activated ACFs and steam-activated ACFs.

Table 2 Elemental composition on the surface of ACFs as determined by XPS.

Sample	C(at.%)	O(at.%)	K(at.%)	O/C(%)
ACF-1	85.2	13.9	1.0	16.3%
ACF-2	86.1	12.4	1.5	14.4%
ACF-3	88.6	9.8	1.6	11.1%
ACF-S	91.4	8.6	-	9.4%

To investigate the difference of specific surface functional groups between the ACFs prepared by KOH and steam activation, measurements of the XPS spectra of the C1s region were analyzed and the calculated percentages of graphitic and functional carbon atoms are further summarized in Table 3. The C1s spectra of all the samples were almost the same, therefore only the ACF-3 sample is provided in Fig.8 as an example. The C1s region exhibits an asymmetric tailing, which was partially due to the intrinsic asymmetry of the graphite peak or to the contribution of oxygen surface complexes. For the ACF-3, the C1s spectra can be divided and fitted into four components corresponding to the graphite (284.7eV), C-O (285.6eV), C=O (286.5eV) and -COOH (288.3eV)[30], with the relative percentages of 58.64%, 16.65%, 12.24% and 12.47%, respectively, compared to 68.05%, 15.05%, 7.69% and 9.20% for the ACF-S, confirming that more oxygen-containing functional groups were related to KOH activation. In addition, the graphite content of the KOH-activated ACFs gradually decreases from 66.36% to 58.64% with the increasing of KOH/fiber ratio, meaning

that the fiber matrix structure was disrupted due to the partially degradation of graphene layers by the reaction of KOH and carbon. Therefore, it was believed that KOH as an activating agent caused more unstable carbons in the matrix of ACFs during activation, which helped to form the mesopores.

Table 3 Results of the fits of the C1s Region. BE: binding energy; M: mole percentage. The numerals 1-3 in the context of ACFs refer to the KOH/fiber ratios.

	Graphite		C-OH		C=O		-COOH	
Sample	BE (eV)	M (%)	BE (eV)	M (%)	BE (eV)	M (%)	BE (eV)	M (%)
ACF-1	284.7	66.4	285.6	15.1	286.5	10.4	288.3	8.1
ACF-2	284.7	58.8	285.7	20.2	286.6	11.7	288.4	9.3
ACF-3	284.7	58.6	285.6	16.7	286.5	12.2	288.3	12.5
ACF-S	284.7	68.1	285.5	15.0	286.6	7.7	288.4	9.2

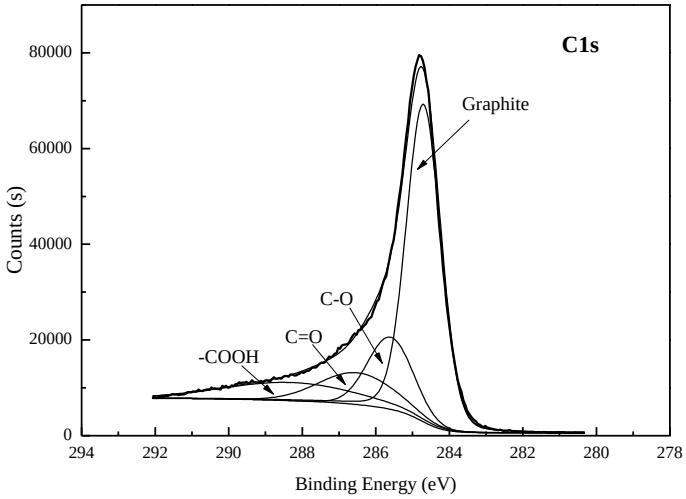

Fig.8 XPS spectra of C1s region of the ACF-3.

4. Conclusion

ACFs were prepared from liquefied wood by KOH activation. In case of KOH/fiber ratio 3, the BET surface area of ACFs could reach values up to 1371 $m^2 g^{-1}$. Compared with the ACFs activated by steam at same temperature, the samples ACF-3 have more small micropores (<0.7 nm) in addition to more mesopores in the range of 2-4 nm. The KOH-activated ACFs had more oxygenated functional groups on their surfaces than the steam-activated ACF-S, which would play an important role when the ACFs should be used in electric double-layer capacitors [14].

Acknowledgement

The research was financially supported by Specialized Research Fund for the Doctoral Program of Higher Education (No. 20130014130001).

References

[1] M. Suzuki, Activated carbon fiber: Fundamentals and applications, Carbon. 32(1994) 577-586.

[2] D. Li, X. Ma, X. Liu, Preparation and characterization of nano-TiO_2 loaded bamboo-based activated carbon fibers by H_2O Activation, Bioresources. 9(2014) 602-12.

[3] N.H. Phan, S. Rio, C. Faur, L. Le Coq, P. Le Cloirec, T.H. Nguyen, Production of fibrous activated carbons from natural cellulose (jute, coconut) fibers for water treatment applications, Carbon. 44(2006) 2569-77.

[4] J. Zheng, Q. Zhao, Z. Ye, Preparation and characterization of activated carbon fiber (ACF) from cotton woven waste, Appl Surf Sci. 299(2014) 86-91.

[5] M.J. John, R.D. Anandjiwala, Recent developments in chemical modification and characterization of natural fiber-reinforced composites, Polym Composite. 29(2008) 187-207.

[6] M.H. Alma, M.A. Basturk, Liquefaction of grapevine cane (Vitis vinisera L.) waste and its application to phenol–formaldehyde type adhesive, Ind Crop Prod. 24(2006) 136-171.

[7] S. Pu, N. Shiraishi, Liquefaction of Wood without a Catalyst I - Time course of wood liquefaction with phenols and effects of wood /phenol ratios, Mokuzai Gakkaishi 39(1993) 446-452.

[8] W. Liu, G. Zhao, Effect of temperature and time on microstructure and surface functional groups of activated carbon fibers prepared from liquefied wood, BioResources. 4(2012) 5552-5267.

[9] J. Zhang, W. Zhang, Preparation and characterization of activated carbon fibers from liquefied poplar bark, Mater Lett. 112(2013) 26-28.

[10] Ruiz-Fernández, M., Alexandre-Franco, M., Fernández-González, C., Gómez-Serrano, V., Development of activated carbon from vine shoots by physical and chemical activation methods. Some insight into activation mechanisms, Adsorption 17(2011), 621-629.

[11] K. Babel, K. Jurewicz, KOH activated carbon fabrics as supercapacitor material, Journal of Physics and Chemistry of Solids. 65(2004) 275-280.

[12] A. Castro-Muñiz, F. Suárez-García, A. Martínez-Alonso, J.M.D. Tascón, Activated carbon fibers with a high content of surface functional groups by phosphoric acid activation of PPTA, J Colloid Interf Sci 361(2011), 307-315.

[13] X. Ma, F. Zhang, J. Zhu, Preparation of highly developed mesoporous activated carbon fiber from liquefied wood using wood charcoal as additive and its adsorption of methylene blue from solution, Bioresource Technol. 164(2014) 1-6.

[14] H. Oda, A. Yamashita, S. Minoura, M. Okamoto, T. Morimoto, Modification of the oxygen-containing functional group on activated carbon fiber in electrodes of an electric double-layer capacitor, J Power Sources 158(2006), 1510-1516.
[15] S. Brunauer, P.H. Emmett, E. Teller, Adsorption of gases in multimolecular layers, J Am Chem Soc. 60(1938) 309-319.

[16] J.H. de Boer, B.C. Lippens, B.G. Linsen, J.C.P. Broekhoff, A. van den Heuvel, T.J. Osinga, The t-curve of multimolecular N2-adsorption, J Colloid Interf Sci. 21(1966) 405-414.

[17] C. Lastoskie, K.E. Gubbins, N. Quirke, Pore size distribution analysis of microporous carbons: a density functional theory approach, The Journal of Physical Chemistry. 97(1993) 4786-4796.

[18] X. Ma, H. Yang, L. Yu, Y. Chen, Y. Li, Preparation, Surface and Pore Structure of High Surface Area Activated Carbon Fibers from Bamboo by Steam Activation, Materials. (2014) 4431-4441.

[19] Z. Ryu, H. Rong, J. Zheng, M. Wang, B. Zhang, Microstructure and chemical analysis of PAN-based activated carbon fibers prepared by different activation methods, Carbon. 40(2002) 1131-1150.

[20] L. Wang, X. Wang, B. Zou, X. Ma, Y. Qu, C. Rong, Y. Li, Y. Su, Z. Wang, Preparation of carbon black from rice husk by hydrolysis, carbonization and pyrolysis, Bioresource Technol. 102(2011) 8220-24.

[21] D.W. McKee, Gasification of graphite in carbon dioxide and water vapor−the catalytic effects of alkali metal salts, Carbon. 20(1982) 59-66.

[22] Q. Qian, M. Machida, H. Tatsumoto, Preparation of activated carbons from cattle-manure compost by zinc chloride activation, Bioresource Technol. 98(2007) 353-360.

[23] E. Raymundo-Piñero, D. Cazorla-Amorós, A. Linares-Solano, S. Delpeux, E. Frackowiak, K. Szostak, F. Béguin, High surface area carbon nanotubes prepared by chemical activation, Carbon.40(2002) 1614-1617.

[24] X. Dai, X. Liu, L. Qian, Z. Yan, J. Zhang, A novel method to synthesize super-activated carbon for natural gas adsorptive storage, J Porous Mater. 13(2006) 399-405.

[25] S. Shin, J. Jang, S.H. Yoon, I. Mochida, A study on the effect of heat treatment on functional groups of pitch based activated carbon fiber using FTIR, Carbon 35(1997) 1739-1743.

[26] J. Xu, L. Chen, H. Qu, Y. Jiao, J. X. Preparation and characterization of activated carbon from reedy grass leaves by chemical activation with H_3PO_4, Appl. Surf. Sci. 320(2014) 674-680.

[27] P. Sathya, G. Velraj, S. Meyvel, Fourier transform infrared spectroscopic study of ancient brick samples from Salavankuppam Region, Tamilnadu, India, Advances in Applied Science Research, 3(2012) 776-779.

[28] X.D. Ma, F. Ouyang, Adsorption properties of biomass-based activation carbon prepared with spent coffee grounds and pomelo skin by phosphoric acid activation, Appl. Surf. Sci. 280(2013) 1-7.

[29] M. Benadjemia, L. Millière, L. Reinert, N. Benderdouche, Preparation, characterization and methylene blue adsorption of phosphoric acid activated carbons from globe artichoke leaves, Fuel Process. Technol. 92(2011) 1203-1212.

[30] I.V. Pavlidis, T. Vorhaben, T. Tsoufis, P. Rudolf, U.T. Bornscheuer, D. Gournis, H. Stamatis, Development of effective nanobiocatalytic systems through the immobilization of hydrolases on functionalized carbon-based nanomaterials, Bioresource Technol. 115(2012) 164-171.

Proceedings of the 58th International Convention of
Society of Wood Science and Technology
June 7-12, 2015 - Grand Teton National Park, Jackson, Wyoming, USA

Design for Environment: Use of Renewable Materials Session

Moderator: *Andreja Kutnar, University of Primorska, Slovenia*

Environmental Product Design of Wood-Plastic Composites

Philipp F. Sommerhuber

Research Associate, Thünen Institute of Wood Research, Hamburg, Germany
philipp.sommerhuber@ti.bund.de

Abstract

The European bio-economy is promoting wood for products and energy use in our society. Resource efficiency has become an important issue for the harvested timber products industry through increasing prices of wood particles and market competition. Production and use of wood-plastic composites (WPC) are projected to increase, alongside with a decreased availability of suitable wood particles. This conflict leads to considerations of using alternative resources, like secondary resources from the waste stream. Mechanical properties of WPC made from virgin and recycled high-density polyethylene (HDPE), virgin spruce and recycled wood are investigated. Flexural properties are not affected by the use of recycled content and are comparable to WPC made from virgin content. Impact strength of recycled composites is lower. A ratio of 30% recycled wood particles with 70% recycled HDPE and 3% maleic anhydride polyolefin (MaPE) is a promising WPC mixture in terms of resource efficiency when compared to the mechanical properties of virgin WPC.

Keywords

Wood-Plastic Composite; cascade use; circular economy; waste valorization; recycled wood and plastics; mechanical properties

Introduction

Wood resources are facing a strong competition between material and energy utilization through the promotion of wood-based products and an increased share of renewable biomass for the provision of energy in Europe. In Germany, 35% (25.4 Mio m^3) of harvested wood were directly used as energy carrier in 2011. The biggest share is used in households for heating (Junker et al. 2014, Seintsch and Weimar 2012). Based on market information of waste wood trade in Germany from Mantau et al. (2012), 78.3% of the waste wood is energetically used and 21% is used materially. Landfill is almost negligible (0.5%) due to the ban of organic waste on landfills fixed by the European *Waste Framework Directive* 2008/98/EC (European Commission 2008) and its implementation in Germany.

Post-consumer wood has become an important secondary raw material, i.e. for the particleboard industry. However, through the lack of a sophisticated material cascade chain in our society, more waste wood is burned than materially used. This issue has led to an increase in prices of wooden co-products and waste wood and has already negatively affected the economy of the wood panel industry.

About 30% of this energetically used waste wood can be classified as AI-AII according to the *German Recycled Wood Directive* AltholzV (AltholzV 2012). This classified waste wood could have been used as a raw material for wood-based products first, instead of being directly burned as an energy carrier. This leads to loosing valuable resources.
These secondary wood resources could have been used in Wood-Plastic Composites (WPC) products. On a global perspective, Europe is the third largest producer of WPC. The predominant thermoplastic polymers used for WPC are Polyethylene (PE) and Polypropylene (PP) – each polymers comprise a share of 37% – and Polyvinylchloride (PVC) with a share of 26% (Eder 2013). These resources are mostly derived from virgin fossil-based hydrocarbon sources, what implies significant environmental impacts.
This article focuses on the utilization of potential secondary resources for WPC. Research has been conducted by Kamdem et al. (2004). The authors compared mechanical properties of WPC made from chromated copper arsenate (CCA) treated wood particles blended with virgin and recycled high-density polyethylene (HDPE). Chaharmahali et al. (2008) studied the possibility of producing wood-plastic panels using a melt blend/hot press method from medium-density fiberboard and particleboard with 60 – 80% wood content as filler with recycled HDPE from milk bottles. Shalbafan et al. (2013) demonstrated flat pressed WPCs produced from residues of light-weight foam core particleboards which consisted of wood particles (with cured urea-formaldehyde resin) and expanded polystyrene.

These articles state that WPC can be produced from recycled resources but a broader perspective on the availability and price situation of the resources is missing. The aim of this research project is to develop a methodology for evaluating the use of resources for WPC, considering technical, economic, environmental and social aspects, and for contributing to an environmental product design of WPC. The first step is to identify alternative resources for WPC on a macro-economic level and to evaluate differences of mechanical properties of WPC produced from virgin and recycled resources. In the next step, Life Cycle Assessment (LCA) of WPC from virgin and recycled content will be conducted with a focus on mechanical properties. Multi Criteria Analysis (MCA) evaluates the different resource

alternatives based on their mechanical behavior, economic and socio-technical aspects in WPC. In this paper, first results of the mechanical properties of virgin and recycled content WPC are presented.

Materials & Methods

Materials

Virgin wood (spruce – *Picea abies*) and recycled wood are mixed in various fractions with virgin and recycled HDPE by adding Maleic anhydride polyolefin (MaPE).

Wood. The recycled wood was provided by a local recycling company in Hamburg, Germany, in October 2014 and is predominantly composed of used transport pallets and some post-consumer derived timber products. The waste wood category can be classified as A II according to the *German Recycled Wood Directive* (AltholzV 2012), although contaminations were not tested specifically. The transport pallets were chipped at the recycling site to a particle size of < 200 mm. The moisture content was calculated to 33% at delivery at the lab.

Kiln dried virgin spruce was chosen for the comparison. The dimension of the board was 2000 x 165 x 30 mm³ with an average density of 430 kg/m³ (Rüter and Diederichs 2012). The moisture content was estimated to 10 – 15%.

Plastics. The recycled HDPE granulate was provided by INTERSEROH Dienstleistungs GmbH, a recycling company which collects and recycles post-consumer packaging waste, besides other services. It is a licensed party of *Dual System*, which is the take-back system of sales packaging in Germany. According to the data sheet of ALBA recythen® HD 2, the recycled plastic is a mixture of various types of polyethylene with a predominant HDPE content. It can be used for injection molding and extrusion. The melt flow index (190/5) is 2 g/10min according to DIN ISO 1133 and the density is 940 kg/m³ according to DIN EN ISO 1183.

Virgin HDPE was chosen because of the mass flow index (MFI) properties of ALBA recythen® HD 2. Virgin HDPE is derived from a company situated in Saudi Arabia and has a MFI of 1.8 g/10min according to ISO 1133 and a density of 952 kg/m³ according to ISO 1183.

Additives. MaPE was used as the coupling agent. It has a MFI of 2 g/10 min and a density of 890 kg/m³, both specifications according to ISO 1133.

Experimental design is presented in Table 1. Wood and plastic content of the WPC formulas are calculated on the basis of 97% (100% WPC – 3% MaPE).

Wood content	0%		30%		60%	
	A	***B***	***C***	***D***	***E***	***F***
Specimen	*rPE*	*pPE*	*rWPC*	*pWPC*	*rWPC*	*pWPC*
	0/100	*0/100*	*30/70*	*30/70*	*60/30*	*60/30*

Waste wood A I-II	-	-	29%	-	58%	-
ALBA recythen® HD 2	100%	-	68%	-	39%	-
Virgin spruce	-	-	-	29%	-	58%
Virgin HDPE	-	100%	-	68%	-	39%
MaPE	-	-	3%	3%	3%	3%

Table 1. Experimental design. r… indicates recycling content; p… indicates virgin content.

Methods

***Experimental Processing*.** The recycled wood had to be manually sorted for nails and cut in two steps from < 200 mm to < 100 mm by a counter blade cutter to get a homogenous particle size distribution for the drying process. The waste wood chips were dried at 80°C for 30 min. until 4% equilibrium moisture content was reached. Moisture content of the dried wood chips was measured to 5.6% after 24h at 103°C.

The virgin wooden boards were sawn to smaller sticks and cut using the same counter blade cutter to < 100 mm. No sorting and drying was needed. The waste wood chips and virgin wood chips were milled with 1 mm mesh size in a *Retsch* laboratory mill. Moisture content of 9% for the virgin wood was measured after 24h at 103°C.

Virgin and recycled HDPE and MaPE were obtained as directly usable for compounding. The wood particles had to be oven-dried for 24h at 103°C to be compoundable with the plastic particles and MaPE in a laboratory internal mixer named *HAAKE Reomix 3000 OS.* The material was fed manually and compounded with tangential counter-rotating twin-screw extruder geometries. The process temperature was 170°C for 15 minutes compounding duration. After the WPC mixtures were cooled down, they were milled in the *Retsch* laboratory mill with 8 mm mesh size.

The milled WPC granulates were pressed to flat panels in a metal frame sized 250 x 170 x 4 mm³ using a *Siempelkamp* computerized hydraulic heating press. The process temperature was 180°C.

***Characterization*.** The specimens were conditioned in 20°C/65% atmosphere until constant mass < 0.1% after 24h was reached and tested in the same conditions. Rod-shaped specimens (80 x 10 x 4 mm³) were used for all tests. Flexural test was conducted according to DIN EN ISO 178. Charpy impact test (a_{cU}) was conducted according to DIN EN ISO 179-1 edgewise for flat pressed panel conditions ($1eU^b$).

Results and Discussion

Mechanical characterization

Results of material characterization are presented in Table 2.

	Flexural test				Charpy impact test	
	Modulus of elasticity (GPa)		**Strength (MPa)**		**Impact strength (kJ/m²)**	
Specimen	Mean value	Standard Deviation	Mean Value	Standard Deviation	Mean Value	Standard Deviation
A (rPE 0/100)	0.91	0.06	25.1	0.82	-	-
B (pPE 0/100)	0.99	0.04	25.4	0.62	-	-
C (rWPC 30/70)	1.58	0.14	31.4	1.99	7.61	1.48
D (pWPC 30/70)	1.54	0.16	33.6	2.13	8.35	1.52
E (rWPC 60/40)	2.62	0.20	31.6	2.51	5.42	1.07
F (pWPC) 60/40	2.77	0.42	42.3	4.30	7.97	2.36

Table 2. Results table.

Flexural properties. The addition of wood to the polymer matrix increases linearly the flexural modulus of elasticity (FoE) (Fig. 1). It is negligible if recycled or virgin wood and plastic resources are used at a significance level of $\alpha = 0.05$. By using wood content up to 60%, the FoE is more heterogonous dispersed than by adding 30%. Flexural strength properties (Fig. 2) reflect the same mechanical behavior as FoE with the exception that the flexural strength is not increased by using recycled resources at 60% wood content (specimen E). Flexural strength properties are almost equal at 30% wood content (C).

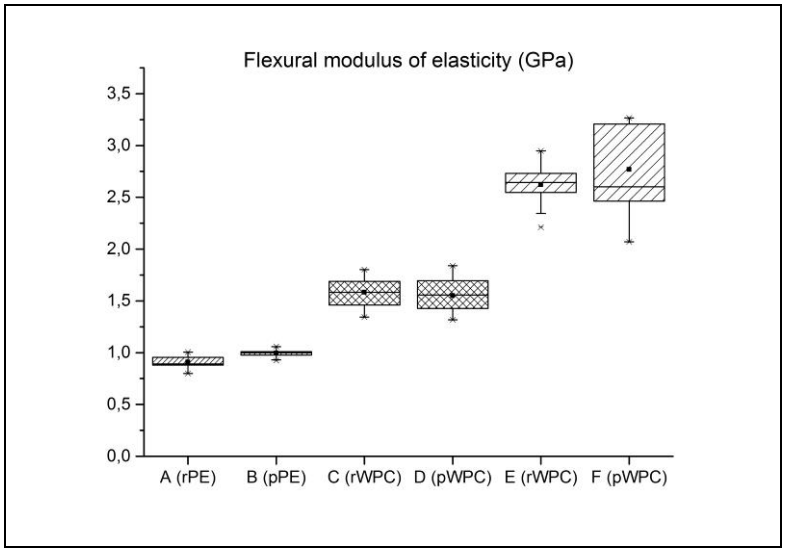

Figure 1. Flexural modulus of elasticity.

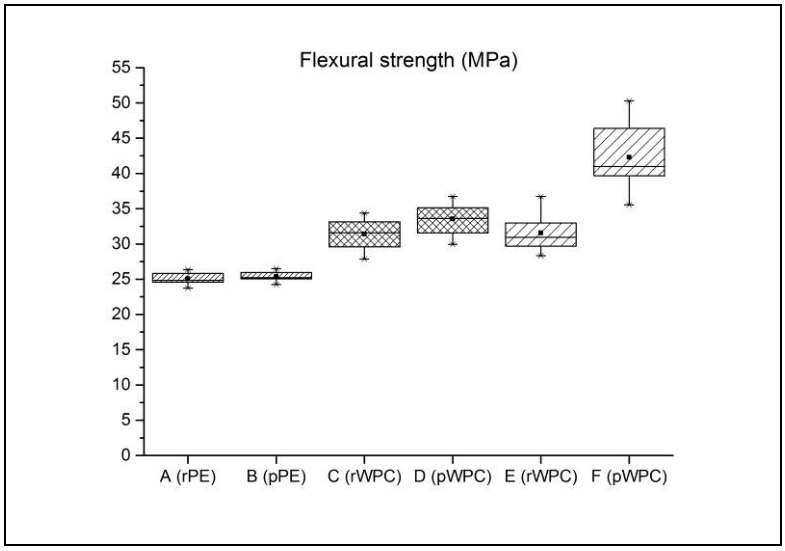

Figure 2. Flexural strength.

Charpy impact test. A pendulum of 1 Joule (J) was used for testing impact strength of the specimens. The specific impact strength of pure HDPE specimens (A and B) could not be determined by using a pendulum of this energy, so a pendulum of 6 J had to be used. Specimens of 0% wood content (A and B) were deformed but did not break. Therefore, the impact strength of those specimens was not evaluable.

With increasing wood content, the impact strength of WPC decreases due to the wood particles in the polymer matrix (Fig. 3). This can be observed on the recycled WPC specimens (C and E). In the case of virgin resources, the impact strength increases slightly by increasing the wood content (F). In addition, a very high outlier of 57% above the mean value could be observed in this specimen group.

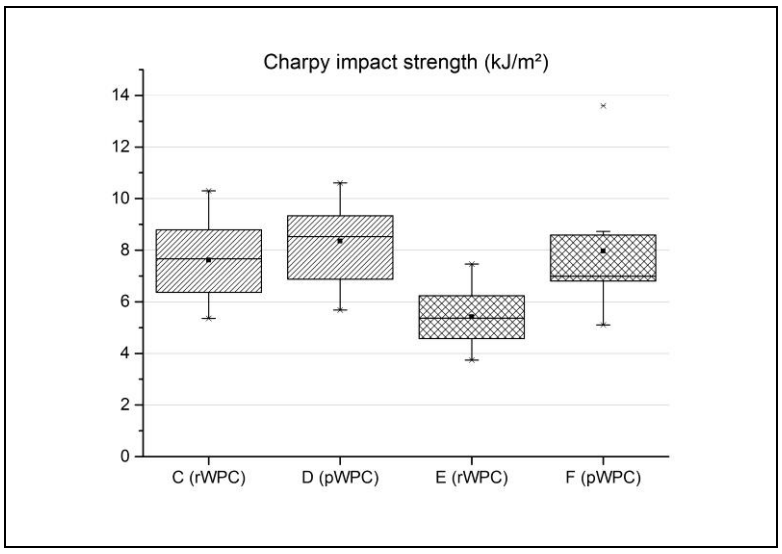

Figure 3. Charpy impact strength.

Summary and Conclusions

Resource efficiency has become an important issue for the wood processing industry in Europe and Germany. WPC products are prospected to increase. Reducing the amount of wood in wood-based panels and mobilization of secondary resources for material utilization are promising strategies.

In the first step, potential secondary resources are investigated for the production of WPC and compared to virgin resources. The increase of wood content improved the flexural properties of WPC. The differences are negligible if WPC is produced with recycled instead of virgin wood. However, the increase of wood content affects negatively the impact strength properties. A ratio of 30% recycled wood and 70% of ALBA recythen® HD 2 with the addition of 3% MaPE is a promising alternative to WPC made from virgin content. This ratio reflects a resource efficient supply chain for wood-based panels in addition.

On an environmental design perspective, further research will be done on investigating mechanical properties alongside the environmental differences through LCA of virgin and recycled resources by reflecting the technical properties of the composites.

Acknowledgements

The research has been supported by the EU through the Marie Curie Initial Training Network (ITN) action “CASTLE”, grant agreement no. 316020. The contents of this publication reflect only the author’s/authors’ views and the European Union is not liable for any use that may be made of the information contained therein.

References

AltholzV (2012) German Recycled Wood Directive (AltholzV) from 15 Aug 2002 (BGBl. I S. 3302), last modified by article 5 paragraph 26 of the law from 24 Feb 2012 (BGBl. I S. 212). Federal Ministry of Justice and Consumer Protection.

Chaharmahali M, Tajvidi M, Kazemi-Najafi S (2008) Mechanical properties of wood plastic composite panels made from waste fiberboard and particleboard. Polym Composite 29(6):606–610.

Eder A (2013) Markets and trends in biobased composites in Europe 2012. 5th German WPC-Kongress, 10 December 2013. Köln, Germany.

European Commission (2008) Directive 2008/98/EC of the European Parliament and of the Council of 19 November 2008 on waste and repealing certain Directives.

Junker F, Haß M, Hubold G, Kreins P, Salamon P, Seintsch B (2014) Potenziale einer biobasierten Wirtschaft. Thünen Institute, Braunschweig. 35 pp. In German with summary in English.

Kamdem P, Jiang H, Cui W, Freed J, Matuana LM (2004) Properties of wood plastic composites made of recycled HDPE and wood flour from CCA-treated wood removed from service. Compos Part A-APPL S 35(3):347–355.

Mantau U, Weimar H, Kloock T (2012) Standorte der Holzwirtschaft - Holzrohstoffmonitoring. Altholz im Entsorgungsmarkt - Aufkommens- und Vertriebsstruktur 2010. Universität Hamburg, Zentrum Holzwirtschaft; Johann Heinrich von Thünen-Institut, Hamburg. 65 pp.

Rüter S, Diederichs S (2012) Ökobilanz-Basisdaten für Bauprodukte aus Holz. Johann Heinrich von Thünen-Institut; Universität Hamburg, Zentrum Holzwirtschaft, Hamburg. 316 pp. In German with summary in English.

Seintsch B, Weimar H (2012) Actual sitation and future perspectives for supply and demand for hardwood in Germany *in* N Róbert and A Teischinger, eds The 5th conference on hardwood research and utilization in Europe. 6-7 September, Sopron, Hungary.

Shalbafan A, Benthien JT, Welling J, Barbu MC (2013) Flat pressed wood plastic composites made of milled foam core particleboard residues. Holz Roh Werkst 71(6):805–813.

Proceedings of the 58th International Convention of
Society of Wood Science and Technology
June 7-12, 2015 - Grand Teton National Park, Jackson, Wyoming, USA

Carbon Policy Failures and the Opportunity for Better Uses of Wood: If We Have Carbon Negative Technologies Why Aren't We Using Them?

*Bruce Lippke**
Professor Emeritus
College of Environment
University of Washington
Seattle, WA, 98195
blippke@uw.edu

Elaine Oneil
Executive Director: CORRIM &
University of Washington
Seattle, WA, 98195

Holly Fretwell
Research Fellow PERC &
Faculty Montana State University
Bozeman, MT, 59718

Abstract

The rate of global carbon emissions continues to increase. The objective is to stop the increase and even reduce atmospheric carbon. That requires using carbon negative technologies. Just increased efficiency in the use of fossil fuel to reduce emissions at best only slows down the rate of increase. Yet we have carbon negative technologies such as storing carbon taken from the atmosphere by forest growth in wood products while displacing the emissions from using fossil fuels. Some uses of wood store and displace 10 times the carbon as other uses. So why aren't these technologies being better used? There is no incentive to innovate for even better uses because there is no cost for emitting fossil carbon emissions. The problem is exacerbated because we subsidize the use of fossil fuels as well as other incentives that promote the lowest leverage use of wood products. We examine why policies are not working and how different approaches can be much more effective. Carbon cap and trade is not working and especially for uses of wood with thousands of different product carbon pools that are interacting with other pools that would require trading rules far beyond the capabilities of masses of regulators. We develop a hierarchy of displacement efficiencies for different product uses. Any significant value placed on fossil carbon emissions will motivate better uses of wood to displace fossil emissions along with new

innovations to improve the production process and the way we use wood. Integration of the analysis from forest to products to uses and their displacement is essential to understand best uses. Forest carbon by itself is inherently only useful for a one-time reduction in carbon before reaching the carrying capacity of the land. In contrast harvesting wood near its maximum growth rate and using that wood to store carbon in products while displacing fossil intensive products is a sustainable use carbon-negative technology.

Key Words: carbon mitigation, carbon emissions, carbon negative technologies, Life Cycle Inventory Assessment (LCI, LCA), carbon policies, sustainable forestry, carbon Cap & Trade, biofuels, wood products, carbon displacement.

Introduction

The rate of global carbon emissions continues to increase. If the objective is to stop the increase, or even reduce atmospheric carbon, it requires using *carbon negative technologies*. Increased efficiency in fossil fuel use to reduce emissions only slows the rate of increase at best. The carbon in the air continues to increase as the forcing function for climate change (Figure 1).

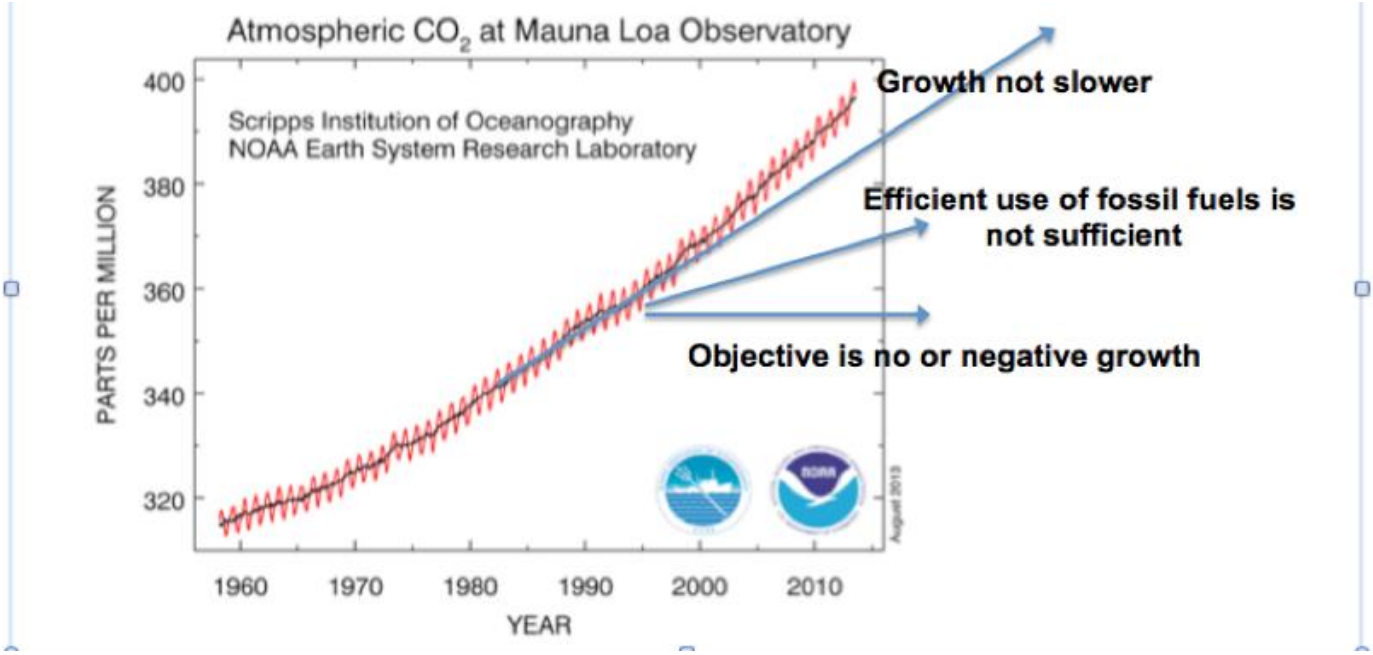

Figure 1. CO2 is still growing and will require carbon negative technologies to meet the objective

Carbon Negative Technologies

We have carbon neutral and carbon negative technologies. Harnessing solar radiation, as a source of energy, is essentially carbon neutral after the solar capturing mechanism is in place and carbon negative when it displaces fossil energy sources. The use of wood products can extend the storage of carbon in the forest to the products. Furthermore, the use of wood products displaces the emissions from otherwise using fossil-intensive products (Gustavsson and Sathre 2011). Such use of wood products provides a sustainable carbon negative technology (Oliver et al. 2013) as the carbon stores and displacement exceed the carbon emissions from processing (Figure 2).

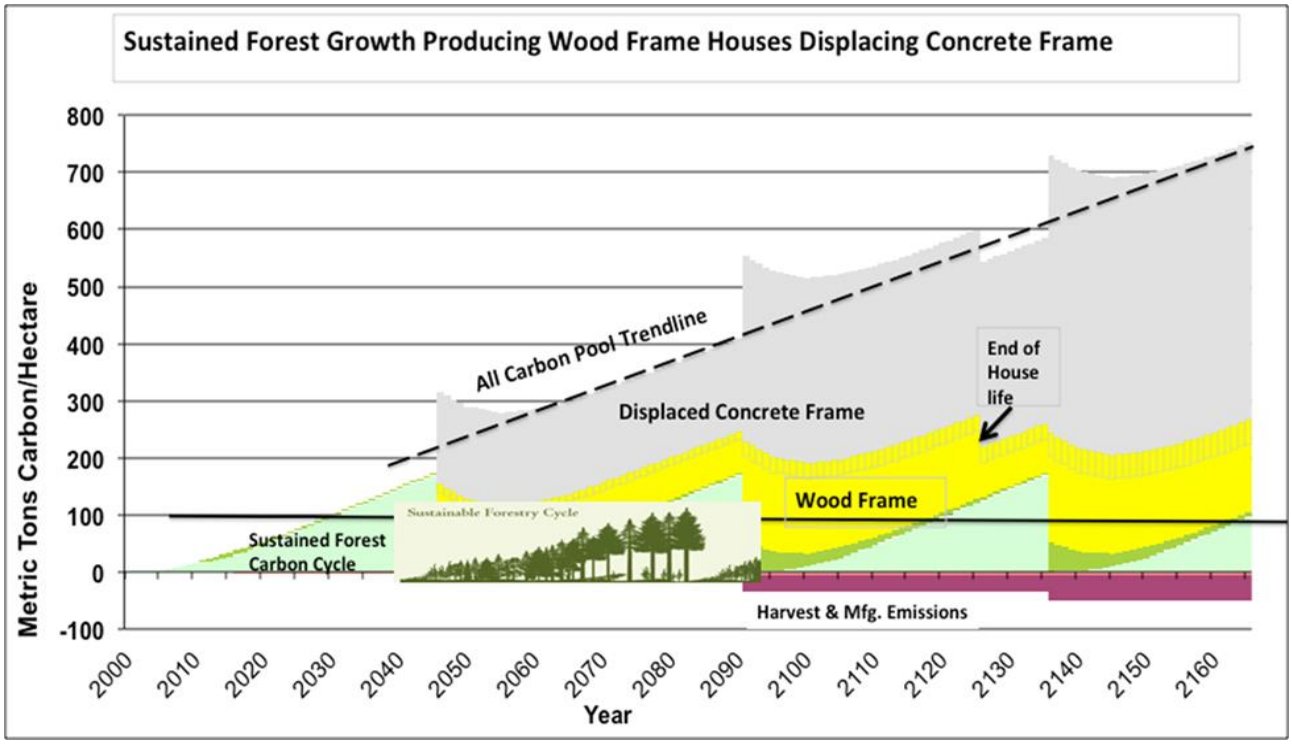

Figure 2. Harvesting to store carbon in products and displace fossil intensive products is sustainable
(Data from Perez-Garcia et al 2005, Wood Fiber Sci 37:18-29 and Lippke et al 2010, Wood Fiber Sci 42:12)

Understanding why policies are not succeeding in greater use of these technologies and how different policies can be made much more effective is essential for carbon mitigation.

Some uses of wood store and displace 10 times the carbon as other uses. How do we know that? Research measures the carbon impact across the full life cycle of growing trees, harvesting wood, transportation, manufacturing products and using them such as for buildings that store the carbon for a long time, and finally end of first life recycling or disposal (Figure 3).

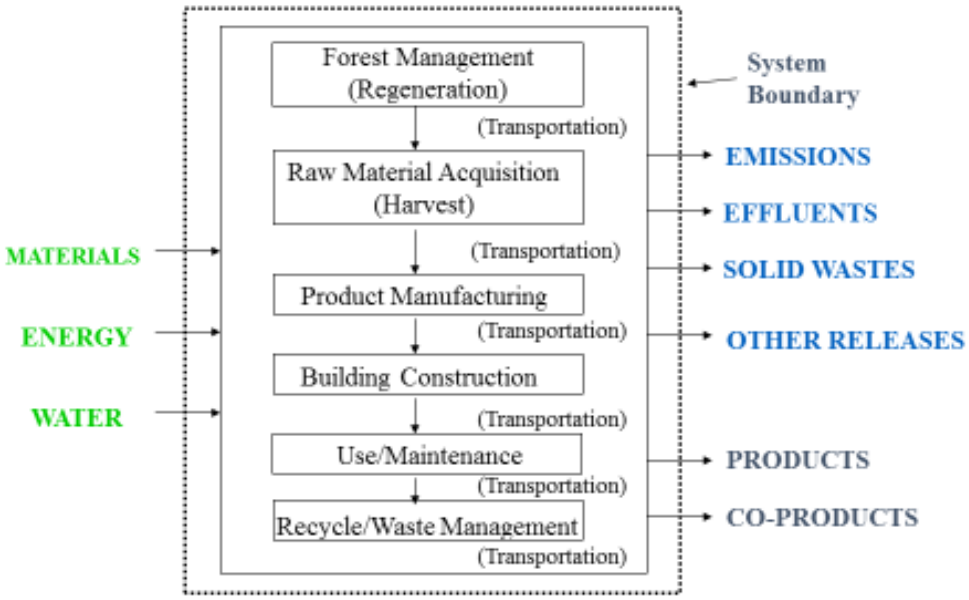

Figure 3. Life Cycle Inventories – 'cradle to grave' (adopted from Perez-Garcia et al 2005)

CORRIM[1] (the Consortium for Research on Renewable Industrial Products) used forest inventory data from the USFS Forest Inventory Analysis, collected primary survey data on all the life cycle inputs (resources & energy) for producing mills for each major wood species and product as well as all the outputs (products, co-products, water and air emissions, waste) to generate a full life cycle impact analysis of inputs and outputs across all stages of processing from cradle to grave. It enables the comparison of each wood use to non-wood alternatives such as wood products versus steel; wood frame versus concrete framing; wood versus glass, plastic, or metal tables and chairs (and many more products); each with different efficiencies in displacing carbon emissions.

Policy Failures

Why aren't carbon technologies in high demand? Under current policies there is no incentive to select better ways to mitigate carbon emissions. There is no cost penalty for producing fossil emissions into the atmosphere. The attempts to provide incentives for better uses of the wood do not consider the hierarchy in efficiency for displacing carbon by each different use of the wood (Figure 4). Similarly, there is no motive to innovate for even better products, designs, and uses.

[1] CORRIM is organized as a not for profit research corporation, a consortium of 19 Research Organizations (mostly universities) developing life cycle information on all wood uses. Funding has been provided largely by USFS and DOE research grants and private donors. www.CORRIM.org

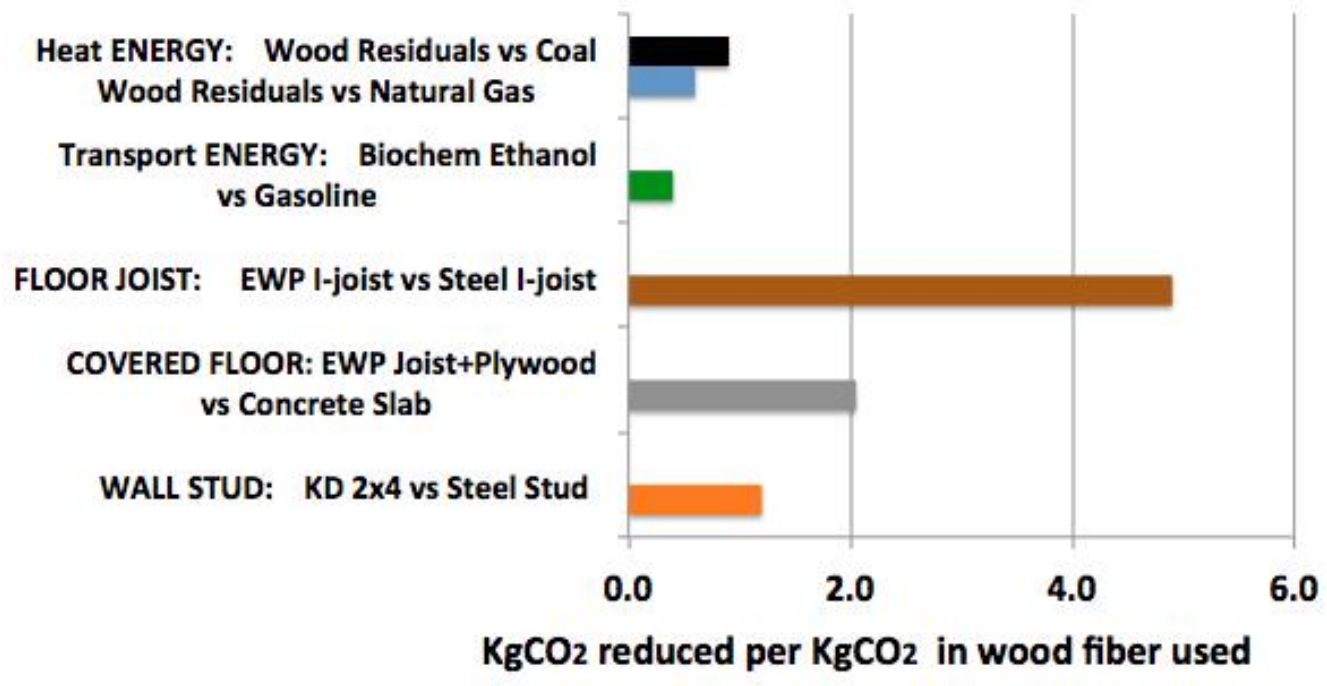

Figure 4. Carbon Emission Reductions by displacing Non-Wood Products & Fuels
(Data from Lippke et al. 2011)

There are major problems with current incentives for using wood because we subsidize the least effective uses of wood rather than the most effective. Each different use of wood has a different efficiency to displace fossil emissions. Ethanol is subsidized even though it is one of the least efficient uses of wood, and the subsidy motivates stealing the feedstock from other wood products such as panels that are more efficient in displacing fossil emissions.

When wood is used directly for its fuel value by making ethanol to displace gasoline, 0.4 units of carbon emissions are reduced per unit of carbon in the wood used. Compare that to 0.8 units of carbon emissions from natural gas per unit of wood used in boilers for heating or drying (Lippke & Puettmann 2013). When wood biomass is instead substituted for coal, the efficiency in wood for heating or drying increases to 1.0 units of carbon emissions reduced per unit of wood used.

Almost any use of wood products displaces more carbon than using wood to displace fossil fuels directly. Using wood framing instead of concrete floors and walls displaces about 2 units of carbon emissions for every unit of carbon in the wood used. Using Engineered Wood Product I-joists instead of steel joists displaces about 5 units of carbon. Any system to efficiently displace fossil carbon emission must acknowledge that there are many different uses of wood. Incentives for the lowest leverage wood use simply steal feedstock from better uses, a counterproductive impact on the goal to reduce carbon emissions.

Another common problem with current policy is that it leaves out important linkages in how wood is used. Timber owners are paid for carbon offsets if they do not harvest. The theory is that the carbon in the forest will keep growing or at least not decompose except through wind, fire, or disease disturbance. The biggest impact, however, is more direct because if

wood is not harvested to produce products it will be replaced by non-wood products that are fossil intensive resulting in far more fossil emissions than any savings in forest carbon.

Furthermore, forest carbon only removes carbon from the atmosphere until the carbon per unit of land has reached the carrying capacity of that land. Like a garden, forests do not keep on growing forever. Forest carbon unharvested results in a one-time reduction in CO2 not a sustainable reduction. It is the act of removing wood from the forest no faster than its growth rate and storing it in products, while also displacing the emissions from non-wood products that supports sustainable carbon reduction.

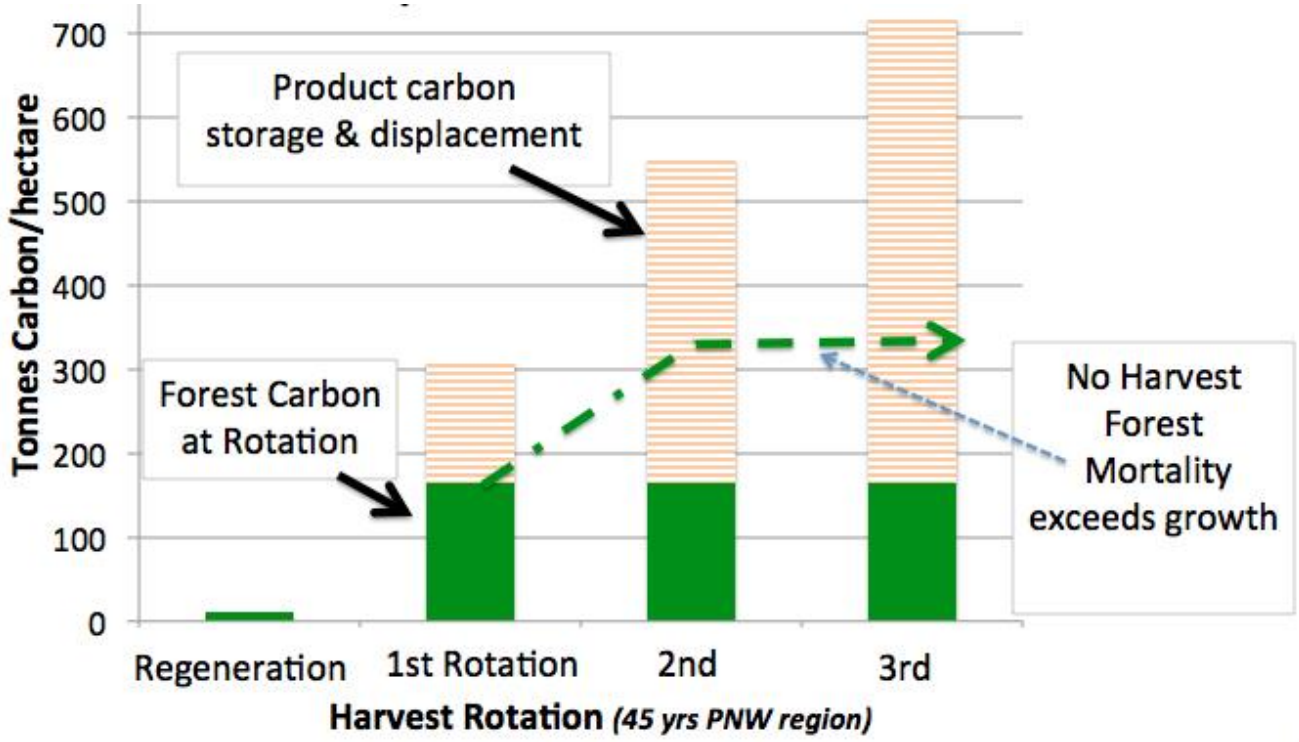

Figure 5. Forest carbon unharvested provides a one-time reduction in CO2 not a sustainable reduction

Perhaps the worst policy is the political acceptance that placing caps on big emitters and allowing trades with other carbon negative sources is working. Carbon Cap and Trade is not working and especially for those uses of wood with much higher leverage for displacing fossil emissions. There are hundreds if not thousands of different wood uses, each with a different efficiency in reducing carbon emissions and each with different interactions with other wood uses. Carbon negative technologies, such as storing carbon taken from the atmosphere by forest growth supports thousands of different product carbon pools that are interacting with other pools. For Cap and Trade to be effective requires accountability to trading rules for thousands of different products and uses, much more than can be handled by a regulatory system. Subsidizing the least effective uses of wood such as making ethanol, to meet renewable fuels standards, or to not harvest is considered a tradable offset even though it has a counterproductive impact in reaching the objective of reduced carbon emissions.

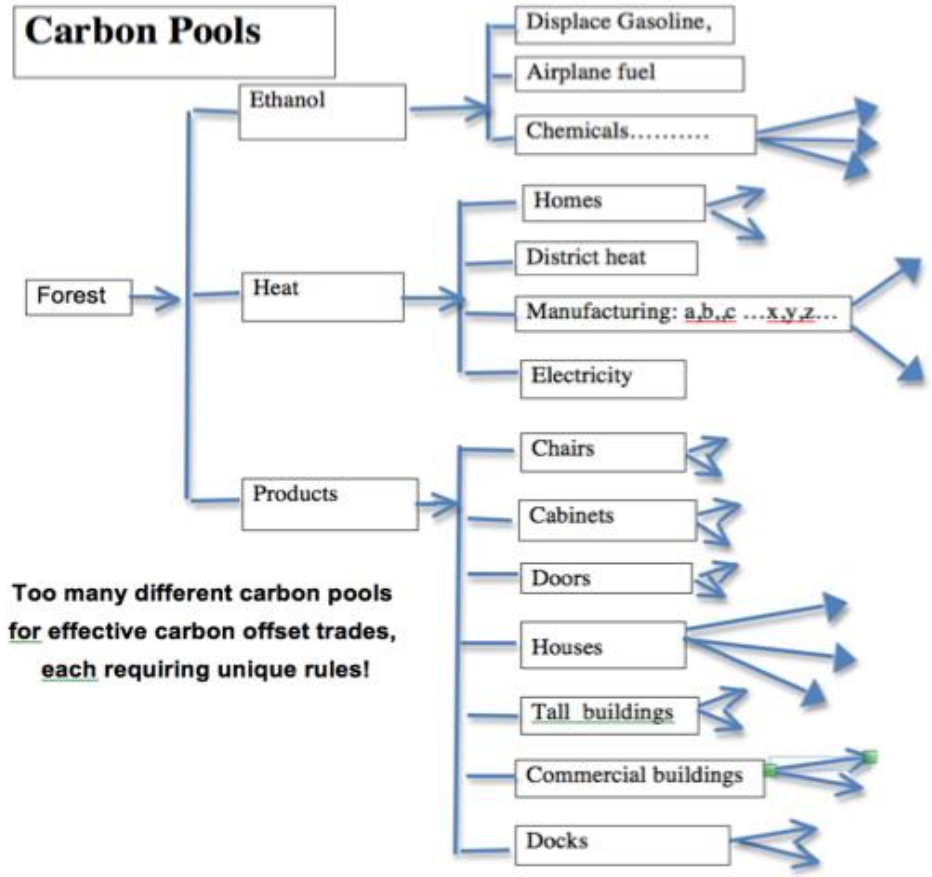

Figure 6. Every product and stage of processing alters carbon – too many for carbon trading

As evidence one needs only to look at the price history for the European carbon trading system (The Economist 2013). Prices are completely unstable with the most recent prices so low as to suggest no accountability in trade metrics, or worse yet fraudulent (Figure7).

Figure 7. Unstable carbon prices under Cap & Trade (European Trading System in Euros)

Better options than carbon trading: Taxing the emissions is one way to motivate the market to develop innovations that provide better ways to lower emissions. But the reduction in after tax income would become a drag on economic activity and jobs. Making the carbon tax income neutral by diverting all proceeds from the tax back to the consumers and producers offsets the negative growth aspects of such a tax. British Columbia has instituted a carbon tax that has increased to $30/ton of CO2, which has reduced the consumption of fossil intensive products by about 18% relative to the rest of Canada with no loss in growth relative to the rest of Canada (Elgie and McClay 2013). In effect, the major impacts of such a tax appear to be working (Figure 8).

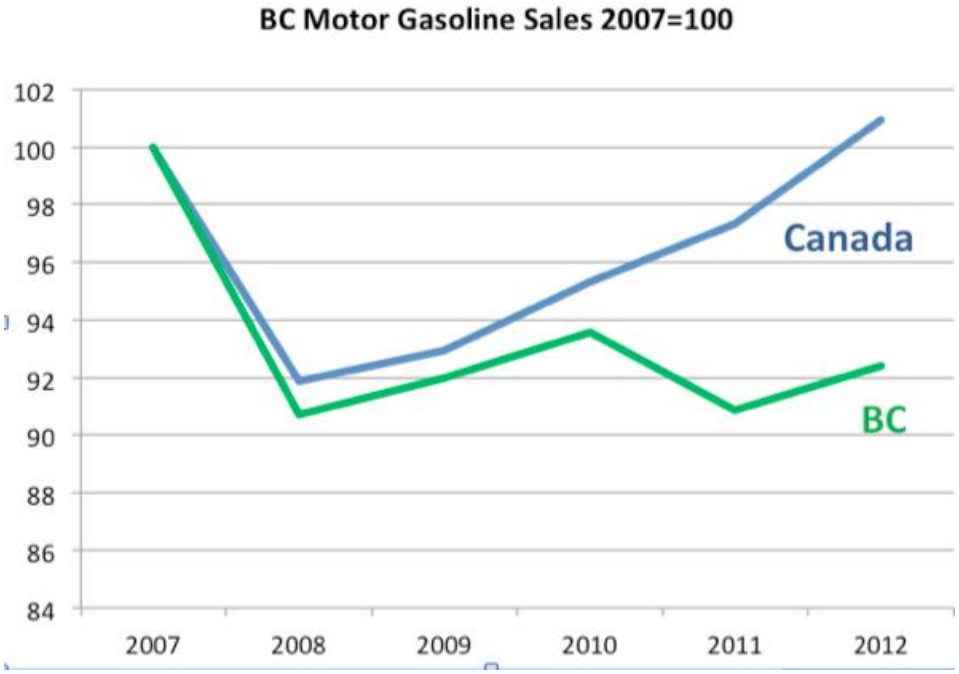

Figure 8. Per Capita Fossil Emissions reduced by 18% vs all other Canada

The more difficult problem facing a regional emission tax is what it does to competitiveness at the border. Producers within the region that compete with producers outside the region without such a tax will lose competitiveness unless a comparable tax offset is applied to such imports. The benefits of the broader regional use of such a tax eliminates the loss in competitiveness and allows the price spread for the more efficient low emission uses to be applied to innovative changes in the uses of wood.

Innovation from Carbon Taxes

So long as the cost of fossil fuels remains low and there is no tax on fossil emissions there will be no significant progress toward better uses of wood for reducing carbon in the atmosphere. With a carbon emission tax of $30/ton of CO2 ($110 per ton of C) there will be increased motivation to collect waste wood such as forest residuals or demolition wood for recycling or reprocessing or recapturing the demolition materials for their energy value. It

will likely require an increasing price on fossil emissions above$30/ton CO2 (Nordhaus 2010, EPA 2013) which will substantially change the motivation to innovate new uses of wood, upgrading the efficiency of wood use in terms of new products, new construction designs, and new manufacturing processes. Even a $30 per ton CO2 tax effectively raises the advantage of wood vs fossil intensive products by almost $55/ton of dry softwood; a substantial increase in competitiveness for products with a high leverage in displacing fossil intensive products ($250 per ton advantage for EWP I-joists over steel). The result would be increased forest management intensity producing more wood faster, increased innovation in new and better uses of wood, increased use of waste-wood including recycling and reprocessing, as well as increased recovery of demolition and other sources of waste-wood for reprocessing or at least their energy value. Increased use of wood in multi-storied buildings (Figure 9a) and greater use of wood in non-residential structures (Figure 9b) are obvious examples of increased innovation.

Hi rate of substituting wood for non-wood

Figure 9 (a) 14 floor modular construction, Bergen Norway; **(b)** Tacoma WA sports dome

Conclusions

For any system to work effectively to reduce fossil emissions, the cost of the emissions must be proportional to their volume. Cap and trade systems do not even keep track of the most important uses of wood. Getting any significant value placed on fossil carbon emissions will motivate better uses of wood to displace fossil emissions along with new innovations to improve the production process and the way we use wood. Integration of the analysis from forest to products to uses and their displacement is needed to understand best uses. Forest carbon by itself is inherently only useful for a one-time reduction in carbon before growth reaches the carrying capacity of the land. In contrast, harvesting wood near its maximum growth rate and using that wood to store carbon in products while displacing fossil intensive products is an effective and sustainable use of a carbon-negative technology.

References

The Economist. 2013. The failure to reform Europe's carbon market will reverberate around the world. *Economist* print edition April 20th.

Elgie, S., and Jessica McClay. 2013. BC's Carbon Tax Shift After Five Years: Results. *SP (Sustainable Properties) Research Report (published in Canadian Public Policy),* University of Ottawa. July 2013.

EPA 2013. Fact Sheet: Social Cost of Carbon *http://www.epa.gov/climatechange/download/EPActivities/SCC-fact-sheet.pdf* http://www.whitehouse.gov/sites/default/files/omb/assets/inforeg/technical-update-social-cost-of-carbon-for- regulator-impact-analysis.pdf

Gustavsson L, Sathre R. 2011. Energy and CO_2 analysis of wood substitution in construction. *Climate Change.* 105(1-2):129-153

Lippke, B., J. Wilson. J. Bowyer, J. Perez-Garcia, J. Bowyer, J. Meil, 2004. CORRIM: Life Cycle Environmental Performance of Renewable Building Materials. *Forest Products Journal.* June 2004. pages 8-19

Lippke, B., E. Oneil, R. Harrison, K Skog, L. Gustavsson, R. Sathre et al. 2011. Impacts of forest management on carbon in the forest and wood products: knowns and unknowns. *Carbon Management.* 2011 2(3): 303-333.

Lippke, B., M.E. Puettmann. 2013. Life-Cycle Carbon from Waste Wood Used in District Heating and Other Alternatives. *Forest Products Journal.* Vol 63(1/2):12-23

Nordhaus, William 2010. Economic aspects of global warming in a post-Copenhagen environment http://www.econ.yale.edu/~nordhaus/homepage/RICEmodels.htm.

Oliver C.D., N.T. Nassar, B.R. Lippke, and J.B. McCarter. 2013. Carbon, fossil fuel, and biodiversity mitigation with wood and forests. *Journal of Sustainable Forestry*. 33:3:248-275

Perez-Garcia J, B Lippke, D Briggs, J Wilson, J Bowyer, J Meil. 2005a. The environmental performance of renewable building materials in the context of residential construction. *Wood Fiber Sci* 37(1):3–17.

Perez-Garcia, J, B Lippke, J Comnick and C Manriquez. 2005b. An assessment of carbon pools, storage, and products market substitution using life-cycle analysis results. *Wood and Fiber Sci* Vol37, December 2005: 140-148.

Sathre, R., J. O'Connor. 2010. Meta-analysis of greenhouse gas displacement factors of wood product substitution. *Environ. Sci Policy* 13:104-114

Proceedings of the 58th International Convention of
Society of Wood Science and Technology
June 7-12, 2015 - Grand Teton National Park, Jackson, Wyoming, USA

Life-Cycle Inventory Analysis of Laminated Veneer Lumber Production in the United States

Richard D. Bergman [1*]

[1] Research Forest Product Technologist, U.S. Forest Service Forest Products Laboratory, Madison, Wisconsin, USA
* *Corresponding author*
rbergman@fs.fed.us

Abstract

Documenting the environmental performance of building products is becoming increasingly common. Developing environmental product declarations (EPDs) based on life-cycle assessment (LCA) data is one way to provide scientific documentation. Many U.S. structural wood products have LCA-based "eco-labels" using the ISO standard. However, the standard requires underlying life-cycle inventory (LCI) data to be of recent age. This study updates the gate-to-gate manufacturing LCI data for laminated veneer lumber (LVL) for Pacific Northwestern (PNW) and for southeastern (SE) United States. Modeling the primary industry data per 1.0 m^3 of LVL through LCI analysis provides the inputs and outputs from veneer logs to LVL starting at the forest landing. For PNW and SE, cumulative mass-allocated energy consumption associated with manufacturing 1.0 m^3 of LVL was found to be 5.64 and 6.87 GJ/m^3, respectively, with about 25% of the primary energy derived from wood residues. Emission data produced through modeling found that estimated biomass and fossil CO_2 emissions in kg/m^3 were 127 and 139 for the PNW and 108 and 169 for the SE. One m^3 (~535 OD kg wood potion) of LVL stores about 980 kg CO_2 equivalents. The amount of carbon stored in LVL thus exceeds total CO_2 emissions during manufacturing by about 350%. This study provides the necessary gate-to-gate LVL manufacturing LCI data for the cradle-to-gate LCA to develop an updated EPD.

***Keywords*:** environmental product declaration, life-cycle inventory, laminated veneer lumber, life-cycle analysis, LCA, wood.

Introduction

Documenting the environmental performance of building products is becoming widespread because green building programs and concerns that some green-marketing claims are misleading (i.e., green-washing). Developing environmental product declarations (EPDs) for building products is one way to provide scientific documentation and to counter green-washing (Bergman and Taylor 2011). Life-cycle inventory (LCI) data are the underlying data for subsequent development of life-cycle assessments (LCAs) and EPDs. EPDs are similar to

nutritional labels for food. The LCI was in conformance with the Product Category Rules (PCR) for North American Structural and Architectural Wood Products (FPInnovations 2013) and ISO 14040/14044 standards (ISO 2006a, b). This report follows data and reporting requirements as outlined in the PCR and contains the LCI components for producing a North American EPD (ISO 2006c; FPInnovations 2013). At present, there are many EPDs for structural wood products made in North America.

LCI compiles all raw material and energy inputs and outputs associated with the manufacture of a product on a per-unit basis within defined system boundaries. These boundaries can be limited to only one stage within the product lifecycle (e.g., gate-to-gate). Multiple sequential LCI stages are usually combined to produce an LCA. LCAs describe the total environmental impact for a particular product, referred to either as cradle-to-gate (raw material extraction to mill gate output) or as cradle-to-grave (raw material extraction to waste disposal) analysis.

Description of laminated veneer lumber

Many engineered structural wood products have been developed in the last several decades, e.g., laminated veneer lumber (LVL) in the early 1970s (Figure 1). LVL is comprised of many thin layers of dry wood veneers glued together with resins to form lumber-like products (USEPA 2002; Stark et al. 2010). The veneers are laid with their grain orientation in the same direction (Wilson and Dancer 2005). LVL is designed to be used in the same manner as solid wood products such as sawn lumber. The veneers are typically made from rotary peeling veneer logs.

Figure 1. Laminated veneer lumber.

Goal

The goal of this paper is to document the gate-to-gate LCI of LVL manufacturing for Pacific Northwest (PNW) and Southeast (SE) United States as part of a cradle-to-gate LCA. The paper documents material flow, energy type and use, emissions to air and water, solid waste production, and water impacts for the LVL manufacturing process on a per unit volume basis of 1.0 m^3. Primary mill survey data were collected through a structured questionnaire mailed

to LVL plants. This survey tracked raw material inputs (including energy), product and byproduct outputs, and pertinent emissions to water, air, and land.

An industry standard production unit (i.e., reference unit) was translated to a metric production unit. Secondary data, such as pre-mill gate processes (e.g., wood and electricity production), were from peer-reviewed literature per CORRIM guidelines (CORRIM 2010). Material and energy balances were calculated from primary and secondary data. Using these material and energy data, the environmental impact was estimated by modeling emissions using the software package SimaPro 8 (Pré Consultants 2015), which follows internationally accepted standards and uses the U.S. LCI Database (NREL 2012).

A large sample is required to attain results that are representative of the LVL industry. CORRIM (2010) protocol targets a minimum of 5% of total production with preferred percentage of 20% for an industry such as the LVL industry that has relatively few manufacturers.

Method

Scope

This study covered the manufacturing stage of LVL from veneer production and/or layup to the final product leaving the mill according to ISO 14040 and 14044 standards (ISO 2006a,b; ILCD 2010). Impacts from (offsite) veneer production were included in the analysis using secondary data from the U.S. LCI Database (NREL 2012). This manufacturing stage LCI provided a gate-to-gate analysis of cumulative energy of manufacturing and transportation of raw materials. Analyses included LVL production's cumulative energy consumption and environmental outputs like CO_2 emissions.

Selecting an allocation approach is a vital part of a LCI study. In the present study, all primary energy and environmental outputs were assigned by mass allocation. The decision was justified by the understanding that the wood residues are coproducts with a value rather than a waste material.

Six U.S. LVL plants representing 43.2% of 2012 U.S. LVL production, 0.456 million m^3 provided primary data for the PNW and SE (APA 2014). Total U.S. LVL production for 2012 was 1.31 million m^3. The PNW and the SE are the primary regions for producing structural wood products such as LVL (Smith et al. 2004). The surveyed plants provided detailed annual production data on their facilities, including on-site energy consumption, electrical usage, veneer volumes, and LVL production for 2012. Two of the six surveyed plants were in the PNW with the remaining four in the SE. Wilson and Dancer (2005) performed a 2000 U.S. LVL LCI study that covered 34% and 52% of production in the PNW and SE, respectively. LVL production data by region are no longer available.

Declared unit

The study used a declared unit of 1.0 m^3 of LVL. LCI flows including cumulative energy consumption were reported per 1.0 m^3 of the final product, LVL.

System boundary

Defining system boundaries determined the unit processes to include and standardized material flows, energy use, and emission data. The cumulative system boundary is shown by the solid line in Figure 2 and includes both on- and off-site emissions for all material and energy consumed. Three unit processes exist in manufacturing LVL: (1) lay-up, (2) hot pressing, and (3) sawing and trimming, with energy generation as an auxiliary process. All emissions (i.e., outputs to the environment) and energy consumed were assigned to the LVL and the co-products (i.e., sawdust) by mass.

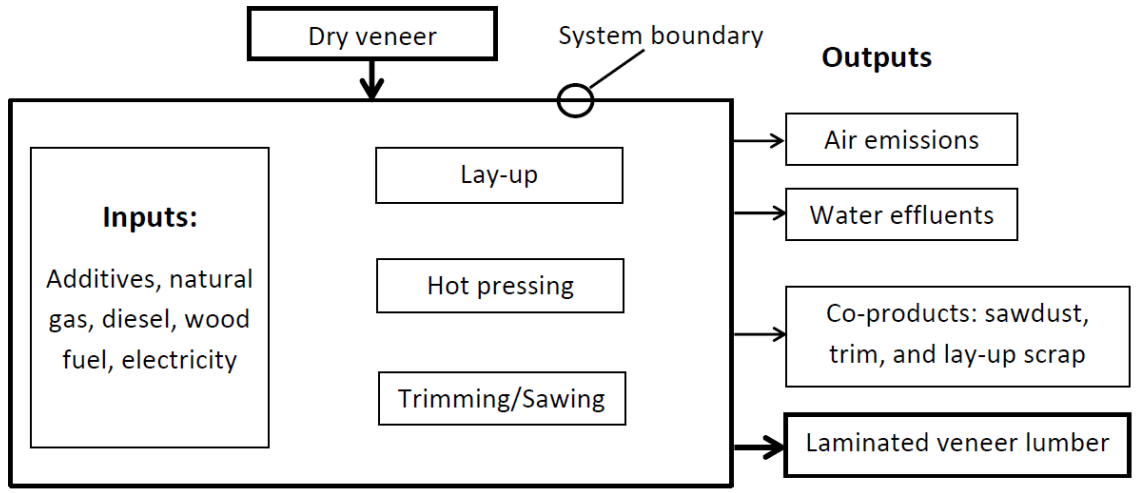

Figure 2. System boundary for laminated veneer lumber manufacturing life-cycle stage

Fuel resources used for the cradle-to-gate production of energy and electricity were included within the cumulative system boundary. Off-site emissions include those from grid electricity production, transportation of feedstock and additives to the plant, and fuels produced off-site but consumed on-site. Ancillary material data such as motor oil, paint, and hydraulic fluid were collected and were part of the analysis.

Results and Discussion

Six LVL plants provided detailed primary data on mass flow, energy consumption, fuel types and air emissions. Data were weight-averaged based on each mill's production volume and expressed on a per 1-m^3 unit basis.

Material

To evaluate data quality, a mass balance was performed (Table 1). In performing the mass balance for LVL, all unit processes located within the site system boundary were considered. Veneer usage was 585 and 612 oven-dry (OD) kg for PNW and SE mills, respectively, and 23 OD kg of binding agents (additives) produced 1.0 m^3 (553 OD kg on average) of LVL

along with some co-products (~70 OD kg on average). Phenol-formaldehyde (PF) resin made up most of the additives.

Table 1. Mass balance of LVL manufacturing per m^3

	Inputs	Mass	CoV[a]	Outputs	Mass	CoV[a]
	Pacific Northwest			Southeast		
	(OD kg)	Mass (%)	CoVw (%)	(OD kg)	Mass (%)	CoVw (%)
Feedstocks						
Produced veneer	0			254	32.1%	155%
Purchased veneer	585	96.3	4.1%	358	64.4%	73.0%
TOTAL, FEEDSTOCK	585	96.3	4.1%	612	96.4%	6.5%
Additives						
Phenol-formaldehyde resin	17.8	2.9%	8.3%	23	3.6%	30.2%
Sodium hydroxide	3.2	0.5%		0		
Catalyst #2	0.2	0.0%		0		
Melamine	1.6	0.3%		0		
TOTAL, ADDITIVES	23	3.7%		23	3.6%	30.2%
TOTAL, IN	608	100%		635	100.0%	
Products						
Laminated veneer lumber	543	89.3%	2.9%	563	88.7%	4.0%
Co-Products						
Sawdust, sold	53	8.7%	15%	44	6.9%	46%
Sawdust, wood fuel	0			9	1.5%	221%
Panel trim, sold	3.4	0.5%	126%	6	0.9%	101%
Lay-up scrap	2.9	0.5%	–	13	2.0%	–
Tested LVL, used	5.9	1.0%	–	0		
TOTAL, CO-PRODUCTS	65	10.7%	46%	72	11.3%	46%
TOTAL, OUTPUTS	608	100%		635	100%	

[a] Production weight-averaged coefficient of variation.

Energy inputs

Weighted-average energy inputs consumed at the LVL manufacturing site were developed from survey data (Table 2). Electricity and natural gas were the primary energy inputs at 77 kWh and 15 m^3 for the PNW and 112 kWh and 19 m^3 for the SE per m^3 of LVL. Thus, less electricity and natural gas was consumed in the PNW. The production-weighted coefficient of variation showed large variation for natural gas consumption for the SE at 53% although consumption was similar to the PNW.

Carbon

Carbon in wood products can be considered a long-term storage. Carbon content for wood products is assumed to be 50% by mass of OD wood. Therefore, the carbon stored in the wood portion of 1.0 m^3 (~535 OD kg) of LVL is equivalent to 980 kg CO_2[2] pulled from the atmosphere during forest growth. Basically, the CO_2 value is equivalent to the CO_2 removed from the atmosphere during tree growth that is now stored in the final product.

Table 2. Weighted-average on-site energy inputs for LVL manufacturing

	Pacific Northwest	Southeast

[2] 550 OD kg wood * (0.5 kg carbon/1.0 OD kg wood) * (44 kg CO_2/kmole/12 kg carbon/kmole) = 980 kg CO_2

	Quantity	Unit	CoVw[a] (%)	Quantity	Unit	CoVw[a] (%)
Energy inputs						
Electricity	77	kWh	61%	112	kWh	67%
Natural gas	15	m^3	9%	19	m^3	53%
Wood fuel	–	kg		32	kg	221%
Diesel	0.35	L	37%	0.74	L	69%
Propane	0.48	L	52%	0.78	L	10%
Gasoline	–	L		0.59	L	244%

[a] Production-weighted coefficient of variation.

Cumulative energy consumption

Cumulative energy consumption for manufacturing LVL was 5.64 and 6.87 GJ/m^3, with wood fuel accounting for about 25.7% and 26.9% for the PNW and SE, respectively (Table 3). Natural gas, wood residues, and coal were the three most important energy sources. Most of the wood fuel was consumed before the LVL manufacturing stage where drying the wood was accomplished via steam boilers fueled primarily by wood (residues) and not fossil fuels. In addition, most LVL facilities use natural gas as the heat source for hot pressing the veneer into billets. Furthermore, natural gas (and coal) are used to fuel the electricity grid. Therefore, natural gas is the largest fuel input for making LVL for both regions.

Table 3. Cumulative energy (higher heating values (HHV)) consumed during production of LVL—cumulative, allocated gate-to-gate LCI values[a]

	Pacific Northwest			Southeast		
Fuel[b,c]	(kg/m^3)	(MJ/m^3)	(%)	(kg/m^3)	(MJ/m^3)	(%)
Natural gas[d]	31.8	1,732	30.7	37.4	2,035	29.6
Wood residue	71	1,486	26.3	88	1,848	26.9
Coal[d]	44.6	1,167	20.7	62.3	1,630	23.7
Crude oil[d]	18.7	849	15.1	18.6	845	12.3
Uranium[d]	–	285	5.0	–	17	0.2
Hydro	0.00024	92	1.6	0.00130	497	7.2
Energy, other	–	33	0.6	–	0	0.0
Total		5,640	100		6,870	100

[a] Includes fuel used for electricity production and for log transportation.
[b] Values are allocated and cumulative and based on HHV.
[c] Energy values were found using their HHV in MJ/kg: 20.9 for wood oven-dry, 26.2 for coal, 54.4 for natural gas, 45.5 for crude oil, and 381,000 for uranium.
[d] Materials as they exist in nature and have neither emissions nor energy consumption associated with them.

Emissions

Emission data produced through modeling found that estimated biomass and fossil CO_2 emissions in kg/m^3 were 127 and 156 for PNW and 108 and 169 for SE (Table 4). Therefore, the amount of carbon stored in LVL, 980 kg is equivalent to about 350% of the total carbon emissions released (as CO_2) during manufacturing. For on-site, burning natural gas for hot pressing LVL was the main source of fossil CO_2. Most of the biogenic CO_2 emissions came from processing logs into dry veneer and was consistent with energy inputs of wood residues shown in Table 2. Other large sources of fossil CO_2 emissions were from generating electricity (off-site) and from manufacturing dry veneer. Surprisingly, most of nitrogen oxides (NOx) released, about 98% were derived from the production of PF resin. As for water effluents, chloride comes from three main sources: production of dry veneer and

natural gas and the combustion of electricity. More specifically, nitrous oxide comes from the extraction and processing of natural gas.

Table 4. Cumulative environmental outputs for producing 1 m^3 of LVL[a]

	Pacific Northwest	Southeast
Substance	(kg/m^3)	
Water effluents		
BOD5 (Biological oxygen demand)	1.25	1.05
Chloride	4.21	4.56
COD (Chemical oxygen demand)	6.13E-02	6.67E-02
DOC (Dissolved organic carbon)	2.86E-04	3.60E-04
Oils, unspecified	3.16E-03	3.49E-03
Suspended solids, unspecified	5.62	5.96
Industrial waste[b]		
Waste in inert landfill	0.77	3.05
Waste to recycling	0.36	58.36
Solid waste[c]	13.46	4.3
Air emissions		
Acetaldehyde	5.24E-02	4.75E-02
Acrolein	2.64E-01	2.13E-03
Benzene	2.68E-03	2.27E-03
CO	0.63	0.55
CO_2 (biomass (biogenic))	127	108
CO_2 (fossil)	156	169
CH_4	0.46	0.52
Formaldehyde	1.77E-02	5.02E-03
Mercury	4.73E-06	3.70E-06
Methanol	7.36E-02	5.58E-02
NOx	36.2	45.6
Non-methane VOC	2.21E-02	2.12E-02
Particulate (PM10)	7.99E-02	7.94E-02
Particulate (unspecified)	0.37	0.29
Phenol	1.51E-03	5.28E-04
Propanal	3.43E-03	3.41E-03
SOx	1.93E-03	1.91E-03
VOC	0.59	0.33

[a] Includes the impacts of manufacturing dry veneer.
[b] Includes solid materials not incorporated into the product or co-products but left the system boundary.
[c] Solid waste was boiler ash from burning wood. Wood ash is typically used a soil amendment or landfilled.

Wood products typically consume more energy during the manufacturing stage than any other stage (Puettmann and Wilson 2005; Winistorfer et al. 2005; Puettmann et al. 2010). To compare with an earlier CORRIM study on making 1.0 m^3 of LVL in the PNW and SE, cumulative allocated energy consumptions are 4.43 and 5.75 GJ/m^3 (Puettmann and Wilson 2005; Wilson and Dancer 2005). Like the present study, Wilson and Dancer (2005) used mass allocation. As stated previously, primary energy is energy embodied in the original resources such as crude oil and coal before conversion.

Conclusions

EPDs present life-cycle data in a concise and consistent format to enable industry to communicate with customers. This study provides the underlying gate-to-gate LCI data for updating the North American LVL EPD. Future efforts will work on incorporating the LCI data into a cradle-to-gate LCA and then eventually into an EPD for LVL.

Structural wood products such as LVL used in building construction can store carbon for long periods, which is typically greater or far greater than the carbon dioxide emissions released during manufacturing (Puettmann and Wilson 2005; Bergman and Bowe 2010; Puettmann et al. 2010). The amount of carbon stored in LVL if allowed to decay is equivalent to about 350% of the total carbon dioxide emissions released during manufacturing.

Acknowledgments

I gratefully acknowledge funding for this project was through a cooperative agreement between the USDA Forest Service Forest Products Laboratory and the Consortium for Research on Renewable Industrial Materials (13-CO-11111137-014). In addition, I appreciate the reviews provided by Scott Bowe (University of Wisconsin), Indroneil Ganguly (University of Washington), and Adam Taylor (University of Tennessee-Knoxville).

References

APA (2014) Engineered wood statistics: Third quarter 2014. APA—The Engineered Wood Association. Tacoma, WA. 9 p.

Bergman RD, Bowe SA (2010) Environmental impact of manufacturing softwood lumber in northeastern and north central United States. Wood Fiber Sci 42 (CORRIM Special Issue):67–78.

Bergman RD, Taylor A (2011) Environmental product declarations of wood products—An application of life cycle information about forest products. Forest Prod J 61(3):192–201.

CORRIM (2010) Research guidelines for life-cycle inventories. Consortium for Research on Renewable Industrial Materials (CORRIM), Inc., University of Washington, Seattle, WA. 40 p.

FPInnovations (2013) Product Category Rule (PCR): For preparing an Environmental Product Declaration (EPD) for North American Structural and Architectural Wood Products. UN CPC 31. NAICS 21. 17 pp. https://fpinnovations.ca/ResearchProgram/environment-sustainability/epd-program/Documents/wood-products-pcr-version-v1.1-may-2013-lastest-version.pdf. (March 30, 2015).

ILCD (2010) International Reference Life Cycle Data System (ILCD) Handbook - General guide for Life Cycle Assessment—Detailed guidance. EUR 24708 EN. European Commission–Joint Research Centre–Institute for Environment and Sustainability. Luxembourg. Publications Office of the European Union. 417 p.

ISO (2006a) Environmental management—life-cycle assessment—principles and framework. ISO 14040. International Organization for Standardization, Geneva, Switzerland. 20 p.

ISO (2006b) Environmental management—life-cycle assessment—requirements and guidelines. ISO 14044. International Organization for Standardization, Geneva, Switzerland. 46 p.

ISO (2006c) Environmental labels and declarations—Type III environmental declarations—Principles and procedures. ISO 14025. International Organization for Standardization, Geneva, Switzerland. 25 p.

NREL (2012) Life-cycle inventory database project. National Renewable Energy Laboratory. https://www.lcacommons.gov/nrel/search. (accessed March 3, 2015).

PRé Consultants (2015) SimaPro 8 Life-Cycle assessment software package. Amersfoort, The Netherlands. http://www.pre-sustainability.com/simapro/. (accessed February 27. 2015).

Puettmann ME, Wilson, JB (2005) Life-cycle analysis of wood products: Cradle-to-gate LCI of residential wood building materials. Wood Fiber Sci 37 (Special Issue):18–29.

Puettmann ME, Bergman RD, Hubbard SS, Johnson L, Lippke B, Wagner F (2010) Cradle-to-gate life-cycle inventories of US wood products production—CORRIM Phase I and Phase II Products. Wood Fiber Sci 42 (CORRIM Special Issue):15–28.

Stark NM, Cai Zi, Carll C. (2010) Wood-based composite materials: Panel products, glued-laminated timber, structural composite lumber, and wood–nonwood composite materials. In: Wood handbook—wood as an engineering material. Gen Tech Rep FPL–GTR–113. Madison, WI: U.S. Department of Agriculture, Forest Service, Forest Products Laboratory. pp. 11-1–11-28.

Smith WB, Miles PD, Vissage JS, Pugh SA (2004) Forest resources of the United States, 2002. Gen Tech Rep NC-241. USDA For Serv North Central Research Station, St. Paul, MN. 137 p.

USEPA (2002) AP 42 Section 10.9 Engineered wood products manufacturing. United States Environmental Protection Agency. pp. 10.9-1–24. http://www.epa.gov/ttnchie1/ap42/ch10/final/c10s09.pdf (accessed March 3, 2015)

Wilson JB, Dancer ER (2005) Gate-to-gate life-cycle inventory of laminated veneer lumber production. Wood Fiber Sci 37 (Special Issue):114–127.

Winistorfer P, Chen Z, Lippke B, Stevens N (2005) Energy consumption and greenhouse gas emissions related to use, maintenance, and disposal of a residential structure. Wood Fiber Sci 37 (Special Issue):128–139.

Proceedings of the 58th International Convention of
Society of Wood Science and Technology
June 7-12, 2015 - Grand Teton National Park, Jackson, Wyoming, USA

Modification, Product Properties, and Environmental Impacts in Thermal Wood Processing

Dick Sandberg[1] *- Andreja Kutnar*[2]

[1] Professor, Luleå University of Technology, Wood Science and Engineering
SE-931 87 SKELLEFTEÅ, Sweden
dick.sandberg@ltu.se

[2] Assistant Professor, University of Primorska, SI-6000 KOPER, Slovenia
andreja.kutnar@upr.si

Abstract

The world's political and economic decisions are increasingly determined by resource and energy scarcity and by climate change. In these circumstances, a balance must be achieved between economics, ecology and social welfare, which was put forward at the end of the 20th century and has been irrevocably linked to forestry ever since. It is essential that the forest sector is placed at the centre of the developing bio-based economy. The value of the forest for mankind and the environment is irrefutable, and the value of the multitude of products made of wood is of great importance, socially, economically and environmentally. Over the last fifty years, sawn timber in particular has largely disappeared from many technological applications diminishing its contribution to sustainability in the one area where it could be most significant: as a substitute for energy-intensive materials (e.g., in the built environment). However, there is currently a resurgence of interest in timber products due to the environmental benefits they provide, a phenomenon that other industrial sectors are well aware of. This paper discusses the role of thermal wood processing in a sustainability of resource utilization context and what thermal wood processing should achieve to contribute to the European low-carbon economy.

Keywords: EPD, LCA, low-carbon bio-economy, PCR, sustainability

Introduction

Forest-based industries are continually developing advanced processes, materials and wood-based solutions to meet evolving demands and increase competitiveness. One of the emerging treatments involves the combined use of temperature and moisture, where force can be applied, so that one speaks of thermo-hydro (TH) and thermo-hydro-mechanical (THM) processes. Figure 1 show a simplified synoptic diagram of the most common TH and THM processes based on what is achieved through the process. Thermal wood processing (thermal treatment) involves temperatures between 100 and 300°C and can have two distinctly

different purposes: a) softening the wood in steam or water to release internal stresses and making the wood easier to further processing, or b) controlled degradation of the wood involving temperatures between 150 and 260°C with the purpose to improve shape stability and decay resistance.

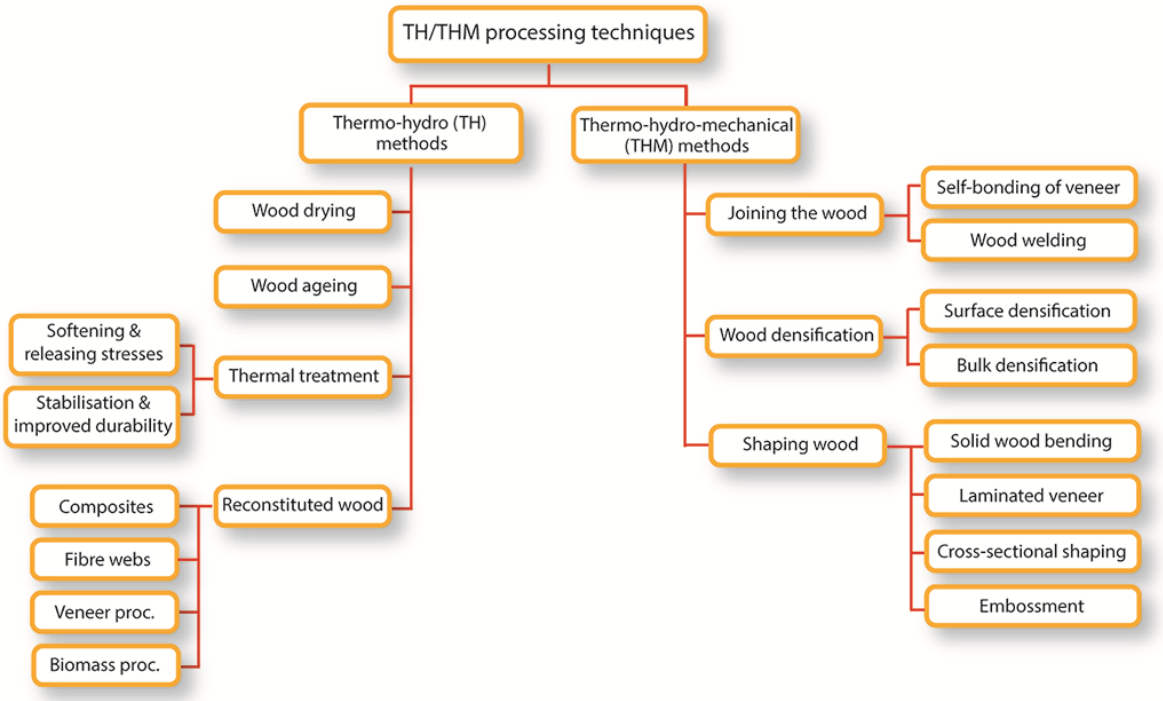

FIGURE 1. Classification of thermo-hydro (TH) and thermo-hydro-mechanical (THM) processes (Navi and Sandberg 2012).

The heat treatment of wood above 300°C is of limited practical value due to the severe degradation of the wood material. Wood ageing is a further development of the classical thermal-treatment processes currently used industrially. Wood ageing operates in a temperature range between wood drying and thermal treatment (100-150°C) and the negative effects that a classical thermal treatment normally has on the strength and brittleness of wood are therefore reduced. TH processing is also applied in many other processes that can be attributed to reconstituted wood products. The THM processes include three main areas of modification namely joining, densification and shaping of wood.

In the recent decades developments in the area of thermal treatment have accelerated considerably. During the 1980s, French and Japanese industries began to modify wood with help of heat in order to increase the resistance to microbial attack. Since then, the interest in thermal treatment has increased all over the world. Thermal treatment is wood modification in a strict sense, since the material undergoes chemical changes. The process essentially involves a controlled degradation of the wood primarily resulting in the destruction of hemicelluloses. The underlying reason for applying thermal treatment is the increasing demand for environment-friendly high-durability wood, i.e. to increase the service life of wood materials without the use of toxic chemicals.

The purpose of this paper is to present the role of thermal wood processing in a sustainability of resource utilization context and what thermal wood processing should achieve to contribute to the European low-carbon economy.

BioEconomy in Europe

For many years to come, the world's political and economic decisions will be determined by resource and energy scarcity and by climate change as a topic related to the consumption of fossil energy. In these circumstances, a balance has to be achieved between economics, ecology and social welfare that can be summed up as sustainability, which was put forward at the end of the 20th century and has been inseparably linked to forestry ever since.

The forest sector and wood-based industries are challenged by this change and feel that it is important to participate in the sustainability debate. This is for obvious reasons, as they themselves first put forward the concept of sustainability that is nowadays related to the global economy. Indeed, nobody questions the value of the forest for mankind and the environment, and nobody questions the value of the multitude of products made of wood. Wood, and especially sawn timber, has during the last fifty years to a large extent disappeared from technological applications (Radkau 2007) so that its contribution to sustainability fails to appear in the one area where it would be most significant, as a substitute for energy-intensive materials.

Wood is in volume the most important renewable material resource (Rowell 2002). The utilization of wood in all aspects of human existence appears to be the most effective way to optimize the use of resources and to reduce the environmental impact associated with mankind's activities. However, as timber possesses good but not outstanding properties, this is not an easy thing to achieve, and in view of the new materials emerging it becomes noticeably more difficult. The only properties it has that reign supreme are ecological fitness and, possibly, a low cost.

In the European Union (EU) measures are being discussed in economics and science that seek to improve the sustainability of resource utilization. European Policy is affecting and, indeed, directing current research, development and marketing in the EU. The main policies having a direct impact on the forest-based sector are the EU Sustainable Development Strategy "SDS" (European Commission 2009), which was published in 2006, and revised in 2009, the EU Roadmap 2050 (European Commission 2011), and the recycling society directive "Directive 2008/98/EC" (European Parliament Council 2008). The forest-based sector can considerably contribute to the European Commission's ambitious CO_2 emissions reduction goal of 80% reduction by 2050, i.e. Roadmap 2050, with innovative production technologies, reduced energy consumption, increased wood products recycling, and the reuse and refining of side-streams.

The need to reduce the whole-life energy consumption of buildings has highlighted the role that wood can play in construction. When buildings have net zero energy consumption, a major part of their overall environmental burden consists of their embodied energy and the associated greenhouse gas emissions. Compared with other construction materials the energy needed to

convert a tree into the final product is significantly lower, resulting in wood products having a low embodied energy.

It is vital that wood can be used effectively through the whole value chain, from forest management and multiple uses of forest resources through new wood and fiber-based materials and processing technologies to new end-use concepts. The fossil fuel consumption, potential contributions to the greenhouse effect and quantities of solid waste tend to be minor for wood products compared to competing products (Werner and Richter 2007). Impregnated wood products tend to be more critical than comparative products with respect to toxicological effects and/or photo-generated smog, depending on the type of preservative. Unfortunately, the number of Life Cycle Assessment (LCA) studies of wood–based composites and modified wood is relatively limited, they are geographically specific, and utilize of a variety of databases and impact assessment protocols. The aim of the "carbon economy" is to mitigate climate change and promote sustainable development in Europe by reducing energy consumption, pollution and emissions while increasing performance.

As a consequence of increased competition from traditional and new industries based on renewable resources, the forest resources must be considered to be limited. There are forecasts showing that, already in 2020, the European consumption of wood can be as large as the total European combined forest growth increment (Jonsson et al. 2011). According to the Communication "Innovating for Sustainable Growth: A Bio-economy for Europe" Europe needs radically change its production, consumption, processing, storage, recycling and disposal of resources. Thus, bio-economy is considered as one of the key elements for smart and green growth in Europe. The Strategic Research and Innovation Agenda for 2020 of the Forest-based Sector and the Horizons - Vision 2030 for the European Forest-based Sector see this sector as a key actor and enabler of the bio-based society.

Thermal Processing of Wood

Thermal treatments of wood have been investigated for many years and are now commercialized. In the beginning of the twentieth century, the use of heat and moisture in wood processing came into focus, and it was observed that wood dried at a high temperature changes colour, and has a greater dimensional stability and a lower hygroscopicity (Tiemann 1915; Koehler and Pillow 1925). After the First World War, comprehensive studies were made of the effect of the kiln drying temperature on the strength of wood for the aviation industry in the United States (Wilson 1920). Systematic research on how to improve wood properties by thermal treatment has been made of the US-based group around Alfred Stamm in the 1940th, and in Germany by Burmester (1973). The exact method of treatment can have a significant effect on the properties of the modified wood, and the most important process variables are: the treatment atmosphere, the choice of closed or open system, the choice of wet or dry systems, the use of a catalyst, the wood species, the time and temperature of treatment, and the dimensions of the material. Table 1 shows the processing conditions for the some well-known thermal processes in Europe.

One of the first commercial thermal-treatment units in Europe was based on Burmesters work and started in Germany around 1980, but was never industrialized in a great scale (Giebler

1983). It was not until 1990, when finish researchers together with industry developed the ThermoWood process, that thermal treatment got established as an industrial process for improvement of wood properties. This process is licensed to members of the Finish ThermoWood Association.

Table 1. Examples of thermal-treatment processes and their processing conditions.

Process	App. Year	Initial MC (%)	Temperature* (°C)	Process duration (h)	Pressure (MPa)	Media for heat transportation	Comments
FWD process	1970	10-30	120-180	Ca.15	0.5-0.6	Steam	Closed system
ThermoWood	1990	10 to green	130/185-215/80-90	20/5-8/5-15	Atmospheric	Steam	Continuous steam flow through the wood under processing that removes volatile degradation products
Plato	1980	14-18	150-180/170-190	4-5/70-120 up to 2 weeks	Super atmospheric pressure (partly)	Saturated steam/hot air	A two stage process
Retification process	1990	Ca. 12	160-240	9-24		Nitrogen	
OHT-process	2000	10 to green	180-220	2-4 up to ca. 20		Vegetable oils	Closed system
WTT process	2000	12	160-180	40	Up to 1	Steam + ev. oil	Closed system
Treatment temperature for different stages of the process is separated by "/"							

Physical changes in wood due to heat treatment

Thermal treatment significantly influences the properties of the wood, e.g. the hygroscopicity and dimensional stability, resistance against fungi and insects, mechanical properties, and also properties such as colour, odour, gluability and coating performance.
In general, most thermal treatments, even at mild temperatures, decrease the hygroscopicity of wood, i.e. its capacity for reabsorption of moisture from the air, although this effect may be eliminated upon saturation with water. Because of the loss of hygroscopic hemicellulose polymers during thermal treatment, the equilibrium moisture content (EMC) is reduced. Consequently, the swelling and shrinkage of thermal-treated wood were drastically reduced.

On average, the equilibrium moisture content is reduced to about half the value of the untreated wood. It is known that the hygroscopicity of thermal treated wood can vary considerably with varying process parameters. Table 2 shows a summary of the effect of thermal treatment on the EMC according to various authors.

Table 2. Reduction in equilibrium moisture content (EMC) in thermal treatment.

Wood species	Temperature	Time	Reduction in EMC	Reference
	(°C)	(hours)	(%)	
Fagus silvatica	180°C	4	40	Teichgräber (1966)
	190°C	2.5	60	Giebeler (1983)
Pinus pinaster	190°C	8–24	50	Esteves et al. (2006)
Pinus sylvestris	220°C	1–3	50	Anon. (2003)
Eucalyptus globulus	190°C	2–24	50	Esteves et al. (2006)
Pinus sylvestris	Plato		50–60	Tjeerdsma (2006)

Welzbacher and Rapp (2007) compared different types of industrially thermal-treated products using several different fungi in laboratory tests and in different field and compost conditions. Table 3 shows the weight loss during an EN 113 (1996) test using three different fungi. The thermal treatment in oil was the most effective, but the effect of the oil in the decay test is not known. Schwarze and Spycher (2005) reported that THM densified wood post treated at 180°C is more resistant to colonization and degradation by brown-rot fungi. In contrast, results obtained by Welzbacher et al. (2008) showed that a "very durable" to "durable" THM densified wood is produced only when the thermo-mechanical densification is used in the combination with oil-heat treatment. Additionally, Skyba et al. (2008) found that THM treatment increased the resistance of spruce but not of beech wood to degradation by soft-rot fungi. Furthermore, Kutnar and co-workers (2011) determined that viscoelastic thermal compression (VTC) of hybrid poplar did not change decay resistance to fungi like *Pleurotus ostreatus* and *Trametes versicolor*. Additionally, Ünsal and co-workers (2008) found that specimens that were subject to thermal compression had higher mass losses after 12 week decay resistance test than control wood specimens.

Table 3. Weight loss (%) of different woods after different thermal-treatment processes (Welzbacher and Rapp 2007).

Material		***Postia placenta***	***Coriolus versicolor***	***Coniophora puteana***
Control species				
Pinus sylvestris L.	1)	31.0	5.1	47.5

Pinus sylvestris L.	2)	26.2	35.7	60.3
Pseudotsuga menziesii F.		14.0	2.6	27.4
Quercus petrea Liebl.		0.8	14.3	3.9
Thermal treated wood	**Process**			
Pices abies (L.) Karst.	Plato	10.0	6.8	3.7
Pinus sylvestris L.	ThermoWood	16.0	9.0	1.9
Pinus maritima Mill.	Retification	13.3	7.8	12.2
Pinus sylvestris L.	OHT	7.4	5.6	3.4

1) including both sap- and heartwood
2) including only sapwood

Table 4 presents a summary of other data on strength changes in thermal-treated wood. In all cases, there was only a small decrease in MOE but major changes in MOR depending on temperature, time and atmosphere.

Table 4. Reduction in MOR in thermal treatment in relation to untreated wood (from Navi and Sandberg 2012)

Species	Treatment	Process	Reduction in MOR (%)
Birch *(Betula pendula)*	Vapour, 200°C 3 hours	ThermoWood	43
Spruce *(Picea orientalis)*	Air, 200°C 10 hours	Open system	40
Pine *(Pinus sylvestris)*	Oil, 220°C 4.5 hours	OHT	30
Eucalyptus *(Eucalyptus globulus)*	Vapour, 200°C 10 hours	Closed system	50

Discussion and Outlook

The awareness of climate change and its potentially disastrous consequences are stimulating a transformation towards sustainable development, with increasing economic efficiency, the protection and restoration of ecological systems, and the improvement of human welfare. Wood as a renewable biological raw material in numerous applications is therefore gaining in importance. This presents an opportunity for the forest-based sector to become a leader in achieving the European Commission's ambitious target of reduced CO_2 emissions with innovative production technologies, reduced energy consumption, increased wood products' recycling, and the reuse and refining of side-streams (e.g. by utilising by-products). The systematic evaluation of materials databases shows that, in spite of the major achievements made in material science, timber as a structural material can hardly be outperformed by any other materials, that it even remains the first choice as far as plate bending is concerned, even

outperforming carbon fibre composites, and that it is undisputedly unrivalled in terms of cost and environmental performance. These results show that timber is a high-performance material for structures, playing an essential role in construction and light weight design. Several of the species used by industry have deficiencies related to poor resistance to biological degradation and low shape stability that earlier could be reduced by e.g. preservation with more or less toxic substances that today is forbidden to use. Consequently, there has been a renewed interest in developing thermal processes in recent years.

Energy and material are inseparable. In this context it should be recalled that the first energy transition took place in the industrial revolution and that the unlimited, cheap coal available also brought about a material transition towards iron and steel. Today's energy transition is the reverse: It is at the expense of energy-intensive materials and would progress more quickly if savings on materials could be made or materials containing little embodied energy were be used. Forestry and the wood refining industry are stated to be capable of contributing considerably more to sustainable development if they managed to regain lost ground in technology. The forest can then contribute to environmental protection and sustainability in two ways: on the one hand, by extracting and retaining carbon from the atmosphere and at the same time limiting land erosion and, on the other hand, by replacing energy-intensive materials and construction techniques with innovative products. This would have the greatest impact.

Thermal processing will be implemented to improve the intrinsic properties of wood and to obtain the form and functionality desired by architects, designers and engineers. High performance at low weight and low price creates a considerable market potential for thermal treated timber products that can replace energy-intensive materials and methods of construction, and reveal a great potential in construction, architecture, light weight construction, and furniture manufacture. Different modification processes and parameters yield modified wood with different properties suitable for a variety of product lines. However, they also have different environmental impacts, which are consequently transferred into the materials and final products. **Interactive assessment of process parameters, product properties, and environmental impacts** should be used to aid development of innovative modification processes and manufacturing technologies. Recycling, up-cycling, the cradle to cradle (C2C) paradigm, and end-of-life disposal options need to be integrated in a fully developed industrial ecology for modified wood processes. New advances in wood-based material processing should support and promote **efficient product reuse, recycling and end-of-life use, and pave the way to a low-carbon economy**.

The low-carbon economy aims to mitigate climate change and promote sustainable development in Europe, by reducing energy consumption, pollution and emissions while increasing performance. Therefore, research into thermally based timber processing and the resultant products must place more emphasis on the interactive assessment of process parameters, developed product properties, and environmental impacts. Energy consumption contributes considerably to the environmental impact of thermally treated wood. However, the improved properties during the use phase might reduce the environmental impact of the thermally based timber processing. To achieve sustainable development, certain criteria within a framework of economic, environmental and social systems must also be followed. It is important to note that the effective use of wood throughout its whole value chain from forest management, through multiple use cycles, and end-of-life disposal can lead to a truly

sustainable development. Therefore, in order to contribute to the low-carbon economy, thermal wood processing should implement the following:

1. Establish a base line of environmental impacts. Identify and quantify the environmental loads involved, i.e. the energy and raw materials used, and the emissions and waste released. Then evaluate the potential environmental impacts of these loads, which should be followed by an assessment of the opportunities available to bring about environmental improvement.

2. Reduce emissions by redesigning of existing technologies.

3. Demonstrate a manufacturer's commitment to sustainability and showcase the manufacturer's willingness to go above and beyond. Therefore, Product Category Rules (PCRs), which include the requirements for Environmental Products Declarations (EPDs) for thermally processed wood, should be defined in an internationally accepted manner based on an open, transparent and participatory process. Furthermore, EPDs in which relevant, verified and comparable information about the environmental impact of products resulting from thermal processing of wood should be acquired. The EPDs can then be used as a proof of environmental claims in the public procurement arena.

4. Develop an "upgrading" concept for recovered products resulting from the thermal processing of wood as a source of clean and reliable secondary wooden products for the industry. This will further strengthen their market competitiveness and sustainability and mitigate climate change by longer storage of captured carbon in wooden materials.

References

Anon. (2003). ThermoWood handbook. Finnish ThermoWood Association, Helsinki.

Burmester A (1973) Effect of heat-pressure treatments of semi-dry wood on its dimensional stability. Holz Roh- Werkst 31(6):237-243.

EN-113, European Community for Standardization (1996) EN-113: Wood preservatives – Determination of toxic values of wood preservatives against wood destroying Basidiomycetes cultures on agar medium.

Esteves B, Domingos I, Velez Marques A, Nunes L, Pereira H (2006) Variation of dimensional stability and durability of eucalypt wood by heat treatment. In: *Proc. of ECOWOOD 2006,* Fernado, Pessoa University, Oporto, Portugal, pp. 185–194.

European Commission (2009) Mainstreaming sustainable development into EU policies: 2009 Review of the European Union Strategy for Sustainable Development, Commission of the European Communities.

European Commission (2011) A roadmap for moving to a competitive low carbon economy in 2050. Communication. Brussels: European Commission European Commission. http://eur-lex.europa.eu/LexUriServ/LexUriServ.do?uri=CELEX:52011DC0112:EN:NOT.

European Parliament Council (2008) Directive 2008/98/EC of the European Parliament and of the Council of 19 November 2008 on waste and repealing certain Directives. Directive. Brussels: European Parliament. http://eurlex.europa.eu /LexUriServ/LexUriServ.do?uri=CELEX:32008L0098:EN:NOT.

Giebler E (1983) Dimensionsstabilisierung von Holz durch eine Feuchte/Wärme/Druck-Behandlung (Dimensional stabilization of wood by moisture-heat-pressure-treatment). Holz Roh- Werkst 41(3):87-94.

Jonsson R, Egnell G, Baudin A. (2011) Swedish Forest Sector Outlook Study. United Nations, Geneva. http://www.unece.org/fileadmin/DAM/timber/publications/DP-58_hi_res.pdf, [March, 18 2014].

Koehler A, Pillow MY (1925) Effect of high temperatures on the mode of fracture of a softwood. Southern Lumberman 121:219-221.

Kutnar A, Humar M, Kamke FA, Šernek M (2011) Fungal decay of viscoelastic thermal compressed (VTC) wood. Holz Roh- Werkst 69(2): 325-328.

Navi P, Sandberg D (2012) Thermo-hydro-mechanical processing of wood. EPFL Press, Lausanne, Switzerland, 376 pp.

Radkau J (2007) Holz – Wie ein Naturstoff Geschichte schreibt, (Wood - how a natural material writes history.) Oekom Verlag, München.

Rowell RM (2002) Sustainable composites from natural resources. In: High performance structures and composites. C.A. Brebbia and W.P. de Wilde (Eds.). WIT Press, Boston, MA, pp. 183–192.

Skyba O, Niemz P, Schwarze FWMR (2008) Degradation of thermo-hygro-mechanically (THM)-densified wood by soft-rot fungi. Holzforschung, 62(3): 277-283.

Schwarze FWMR, Spycher M (2005) Resistance of thermo-hygro-mechanically densified wood to colonisation and degradation by brown-rot fungi. Holzforschung 59:358-363.

Teichgräber R (1966) Beitrag zur Kenntnis der Eigenschaftsänderungen des Holzes beim Dämpfen. (On the alteration of the properties of wood during steaming). Holz Roh-Werkst, 24(11):548-551.

Tiemann HD (1915) The effect of different methods of drying on the strength of wood. Lumber World Review, 28:19-20.

Tjeerdsma BF (2006) *Heat treatment of wood – thermal modification.* SHR Timber Research, Wageningen, The Netherlands.

Ünsal O, Kartal SN, Candan Z, Arango R, Clausen CA, Green F (2008) Preliminary investigation of biological resistance. Water absorption and swelling of thermally compressed pine wood panels. IRG/WP; 08-40396. Stockholm, IRG Secretariat, 11 p.

Welzbacher CR, Rapp A (2007) Durability of thermally modified timber from industrial-scale processes in different use classes: Results from laboratory and field tests. Wood Material Science and Engineering, 2(1):4–14.

Welzbacher CR, Wehsener J, Rapp AO, Haller P (2008) Thermo-mechanical densification combined with thermal modification of Norway spruce (Picea abies Karst) in industrial scale – dimensional stability and durability aspects. Holz Roh- Werkst 66: 39-49.

Werner F, Richter K (2007) Wood building products in comparative LCA. A literature review. Int. J. LCA 12(7):470–479.

Wilson TRC (1920) The effect of kiln drying on the strength of airplane woods. National Advisory Committee for Aeronautics, Washington DC, Report No. 68.

Proceedings of the 58th International Convention of
Society of Wood Science and Technology
June 7-12, 2015 - Grand Teton National Park, Jackson, Wyoming, USA

Tall Buildings – An Approach to Modeling Economic, Carbon, and Employment Effects

Pablo J. Crespell[1]

[1] Senior Scientist, Business Analysis –
FPInnovations. 2665 East Mall, Vancouver, Canada V6T 1Z4
pablo.crespell@fpinnovations.ca

Abstract

Trends continue to gear towards higher shares of mid- and high-rise construction, especially for apartments. There is much interest in pursuing this trend as a way to ensure further levels of penetration of wood-based systems. Europe has a lead over North America but a wealth of knowledge has been created over the last years and recent code changes may be the final steps needed to allow the inroad of wood into this market.

The proposed methodology relies on actual and conceptual buildings to calculate wood use factors for several building systems, including light wood frame, mass timbers and hybrid (beams, elevated slabs). A lower limit (low factor) and upper limit (high factor) bound is assigned to each story class based on feasibility by building system. For instance CLT is only used up to 15 stories. Past that point only post & beam and/or hybrid systems are used. Similarly, a central wood core is assumed for all non-platform frame solutions up to 20 stories to provide resistance to lateral forces. Over twenty stories a concrete central core is assumed.

Wood use factors (ft^3/sqft) are multiplied by the respective floor areas by story class to estimate potential demand for wood (lower and upper limit by story class). Alternatively these volumes can be inputted into any of the available carbon calculators to estimate sequestered CO_2 equivalent and/or the associated avoided GHG emissions by replacing non-wood buildings with a higher carbon footprint.

Building code limitations are not considered in the assessment of the maximum opportunity or size of the market. The actual opportunity for wood buildings will be dependent on: building systems, configurations, location, building code limits and market penetration. Reasonable levels of market penetration should consider current shares of wood by end-use and height class. For instance wood platform frame has over 50% share in the mid-rise class (5-7 stories). So it may be reasonable to simulate an additional 20% for the lower limit and a total no higher than 25-30% for the upper limit (mass timbers).

It is assumed that the lumber stock required to produce the needed engineered wood products is already available, therefore we propose quantifying the associated labor without including primary transformation. By estimating total demand of wood and average size of plants it is possible to estimate employment opportunities associated to the construction of tall wood buildings in North America. Such trend is expected to have enormous economic multipliers in the design and construction community and the associated trades.

Keywords: Tall wood buildings, wood use, nonresidential construction, residential construction, carbon economy, employment.

Acknowledgements

Forestry Investment Initiative
NRCAN
Wood Works BC
FPInnovations

Proceedings of the 58th International Convention of
Society of Wood Science and Technology
June 7-12, 2015 - Grand Teton National Park, Jackson, Wyoming, USA

Wood-based Green Fuels and Chemicals Session
Moderator: *Patricia Townsend, Washington State University, USA*

Beyond Biofuels: Shifting from Hardwood-Based Transportation fuels to Biochemicals

Kevin Zobrist, kevin.zobrist@wsu.edu
Patricia Townsend, patricia.townsend@wsu.edu
Nora Haider, nora.haider@wsu.edu
Marina Heppenstall, marina.heppenstall@wsu.edu
Orion Lekos, orion.lekos@wsu.edu

Washington State University, 600 128th St SE, Everett, WA 98208

Abstract

Advanced Hardwood Biofuels Northwest (AHB) is a Pacific Northwest-based, USDA-funded Project that is looking at hybrid poplar as a feedstock for renewable biofuels. Since this effort began, there have been profound changes in the bioenergy industry. Greater availability of domestic sources of petroleum and natural gas are contributing to lower fossil fuel prices. Future political support for renewable fuels is uncertain. Given these factors, poplar-based biofuels cannot compete economically with conventional fossil fuels in the near-term. The loss of expected near-term economic opportunities for both biorefinery operators and poplar growers to produce poplar-based biofuels has required significant changes in the scope and focus of the AHB project. In this presentation, we will discuss how we have responded to the changing bioeconomy by shifting our end product focus from liquid transportation fuels to an alternative product line of high-value biochemical such as acetic acid, ethylene, and ethanol. We will discuss potential economic opportunities for these biochemicals in the Pacific Northwest, the potential for poplar-based biochemical production in other regions, and the role of biochemical in establishing a foundation for future poplar-based fuel production. We will also discuss how we have shifted our Extension outreach efforts to focus on broader bioenergy themes and poplar production practices to better prepare the region for future biofuel opportunities.

Proceedings of the 58th International Convention of
Society of Wood Science and Technology
June 7-12, 2015 - Grand Teton National Park, Jackson, Wyoming, USA

Wood Residues as Feedstock for the 3G CIMV Biorefinery

Michel Delmas, m.delmas@cimv.fr
Bouchra Benjelloun Mlayah, b.benjelloun@cimv.fr

CIMV/ University of Toulouse, 6 allee des Amazones, 34432, Toulouse cedex 4

Abstract

Forestry and logging industries generate a lot of lignocellulosic residues like agriculture with: corn, wheat, rice, barley straws, sugarcane bagasse. This huge quantity of feedstock has been considered by people engaged since 20 years in the development of the 2G biofuels industry. There is not today a great interest for wood residues. This is due probably by the fact that the 2G biorefinery focus only on glucose to produce bioethanol in poor economic conditions requiring high subsidies. We are pleased to present here our 3G biorefinery which works with all kind of lignocellulosic residues, including timber, mainly hardwood. We shall develop here how biolignin™, cellulose and hemicelluloses and others compounds of wood are separated for industrial purpose. Glucose and xylose are produced without degradation with high purity and quantitative yields what opens the way to a 3G biofuels production, very profitable without subsidy. Cimv (www.cimv.fr) operates a pilot plant (2T/day of feedstock) since 6 years. We have during this time collect the requiring data for the demo and commercial plant construction and the validation of our products with our industrial partners in Europe. A part of these is public due to the final report of the European research program on biorefinery: Biocore (www.biocore-europe.org). The demo and commercial plants development in Europe and USA will be presented

Proceedings of the 58th International Convention of
Society of Wood Science and Technology
June 7-12, 2015 - Grand Teton National Park, Jackson, Wyoming, USA

Development of a New Nanocatalyst for Upgrading Wood Pyrolysis Bio-Oil to Green Fuels

Armando McDonald, armandm@uidaho.edu
Yinglei Han, han4115@vandals.uidaho.edu
David McIlroy, dmcilroy@uidaho.edu

University of Idaho, 875 Perimeter Drive, MSC1132, Moscow, ID 83844

Abstract

In order to reduce the greenhouse gas (GHG) emissions, woody biomass derived fuels have become an alternative to fossil fuels. Fast pyrolysis is a process can convert the woody biomass to a crude bio-oil which contains anhydro-sugars, alcohols, ketones, aldehydes, carboxylic acids and phenolics. Nevertheless, some of these compounds contribute to bio-oil shelf life instability and difficulty in refining. The bio-oil can be catalytically upgraded by a hydrodeoxygenation (HDO) treatment to stable hydrocarbons which can be refined into various fuel grades (such as gasoline and jet fuel). Therefore, developing new catalysts with enhanced performance and lowering costs for upgrading bio-oils is required. This study aims at developing and evaluating nickel (Ni) and ruthenium (Ru) decorated SiO2 nanosprings (Ni-NS and Ru-NS) as HDO catalysts for upgrading pyrolysis bio-oils. The Ni-NS, and conventional catalysts were characterized by H2-temperature program reduction (H2-TPR), transmission electron microscopy (TEM) and X-ray diffraction (XRD). Phenol was used as a representative model compound of bio-oil and used for catalyst optimization. The reactions were performed in a stirred reactor at 300oC at 4000 psi H2 pressure. The phenol and bio-oil HDO reaction products were characterized by GC-MS for volatile products and ESI-MS for oligomeric products. The results show that the Ru-NS based catalysts showed excellent conversion yields into hydrocarbons with good catalyst stability

Proceedings of the 58th International Convention of
Society of Wood Science and Technology
June 7-12, 2015 - Grand Teton National Park, Jackson, Wyoming, USA

Hydrothermal Processing Effects on Bioethanol Production from Lignocellulosic Material

Reza Hosseinpour, hosseinpourreza@gmail.com
Pedram Fatehi, pfatehi@lakeheadu.ca

Islamic Azad University, No. 19 Asadi Aly North, Satari Highway Noor SQ, Tehran

Abstract

The development of products derived from biomass is emerging as an important force component for economic development in the world. Rising oil prices and uncertainty over the security of existing fossil reserves, combined with concerns over global climate change, have created the need for new transportation fuels and for the manufacture of bioproducts to substitute for fossil-based materials. The concept of a biorefinery that integrates processes and technologies for biomass conversion demands an efficient utilization of all components. Hydrothermal processing is a potential clean technology to convert raw materials such as lignocellulosic materials into bioethanol and high added-value chemicals. In this technology, water at high temperatures and pressures is applied for hydrolysis, extraction and structural modification of materials. This paper is focused on providing an updated overview on the fundamentals of hydrothermal processing and its modelling, as well as separation and applications of the main components of lignocellulosic materials into bioethanol.

Proceedings of the 58th International Convention of
Society of Wood Science and Technology
June 7-12, 2015 - Grand Teton National Park, Jackson, Wyoming, USA

An Economic Analysis of Bagasse as a Bio-fuel Feedstock

Sun Joseph Chang, xp2610@lsu.edu

Louisiana State University Agricultural Center, School of Renewable Natural Resources, Baton Rouge, LA 70803

Abstract

Every year the sugar mills in Louisiana produce about 1 million green tons of bagasse with 505 moisture content as a by-product of sugar production. Over the years, it has been considered as a source of raw materials for pulp production and bagasse board production. With the current drive for bio-energy, this paper examines the feasibility of using such material as a competitor with wood for bio-energy production. More importantly, this paper examines the feasibility of using bagasse as the feedstock for biofuel - ethanol production. The results of the analyses suggest that when natural gas, the key competitor of biofuel, is expensive, bagasse is too valuable to the sugar mills to be sold as the feedstock of biofuel. On the other hand, when natural gas is inexpensive, sugar mills must pay the biofuel plants to take bagasse as the feed stock. Not surprisingly, sugar mills rationally choose to burn bagasse to power their plants.

Proceedings of the 58th International Convention of
Society of Wood Science and Technology
June 7-12, 2015 - Grand Teton National Park, Jackson, Wyoming, USA

Biomass Energy: Innovations, Economic Realities, and Public Perception Session

Moderator: *Nikki Brown, Pennsylvania State University, USA*

Overcoming Barriers to Biomass Cogeneration in the U.S. Wood Production Industry

Omar Espinoza. [1*] *– Maria Fernanda Laguarda Mallo*[2] *– Mariah Weitzenkamp*[3] *– Urs Buehlmann*[4]

[1] Assistant Professor, Department of Bioproducts and Biosystems Engineering – University of Minnesota. St. Paul, MN 55108
* *Corresponding author*
espinoza@umn.edu
[2,3] Graduate Student and Student, Department of Bioproducts and Biosystems Engineering – University of Minnesota. St. Paul, MN 55108
[4] Associate Professor, Department of Sustainable Biomaterials – Virignia Tech. Blacksburg, VA 24061

Abstract

Cogeneration, also known as Combined Heat and Power (CHP), is the simultaneous generation of electric and thermal energy from the same fuel source. Some of cogeneration's proven benefits are much higher efficiencies than conventional power generation and its ability to facilitate distributed energy and lower energy costs. However, only a small number of wood products manufacturers have adopted this technology. In this research project, drivers, perceptions and barriers for cogeneration were investigated to gain understanding on the reasons for the low adoption of this technology among wood products manufacturers. Interviews to experts and a non-probability, target survey of non-adopters was carried out to identify operational characteristics, perceptions about benefits of cogeneration and barriers to its implementation Findings show that economies of scale and coincidence between thermal and electric loads are some of the major factors for cogeneration feasibility. Main barriers identified are the initial investment and complexity, companies' return on investment requirements, utility tariff policies, and inadequate policies and incentives. Another major finding is a lack of awareness and knowledge about cogeneration, presenting organizations that support the industry with an opportunity to provide education and outreach to these industries.

Keywords: forest products industry, cogeneration, combined heat and power

Introduction

The U.S. wood products industry has faced many difficulties and significant downsizing during the last decade. Adding to this challenging environment has been the steady increase in energy prices (EIA, 2014; American Hardwood Export Council, 2006). The increased energy costs clearly threaten profitability and indicate a need to reduce energy expenditures. Another important development has been the increase in concerns about energy independence, climate change, and environmental sustainability. There has been a global push to increase the share of energy generated from renewable sources, since these types of fuels produce relatively low levels of greenhouse emissions. In the U.S., 29 states have now renewable energy portfolio standards and nine have renewable energy goals (DSIRE, 2014). These goals invariably consider a mix of renewable energy sources such as solar, wind, hydropower, geothermal, biomass. Among the latter, woody biomass has been gaining attention for its environmental advantages over fossil fuels: it is abundant, renewable, it has low carbon emissions, low metals and sulfur, and produces minimal amounts of ash (Bergman & Zerbe`, 2004; Bowyer et al., 2011). Additionally, wood biomass has cost advantages over other energy sources (EIA, 2014).

Cogeneration can be defined as the simultaneous generation of thermal and electrical energy from the same energy source (EPA, 2014c). Cogeneration plants typically have efficiencies that double those of conventional power plants. Within the U.S. wood products industry, cogeneration has the potential to cover a considerable part of its energy needs from wood residues. However, relatively few companies in the industry have adopted cogeneration technology. Possible reasons for this lack of widespread adoption are: high initial investment, not enough steam pressure generated on-site, low fossil fuel cost (i.e., natural gas), among others (Lamb, 2008). Moreover, there is a lack of current information about the benefits and drawbacks of cogeneration applied to the wood products industry. Research is needed to develop a sound, detailed scientific analysis to help understand the potential benefits of cogeneration operations for the wood products industry, and the major factors for technical and economic feasibility. Outcomes will facilitate decision making by companies interested in the technology.

The goal of this research project was to evaluate wood biomass-based cogeneration technologies for U.S. wood products manufacturers, and identify barriers to their adoption. The specific objectives were to: (1) investigate the status of biomass-based cogeneration in the wood products industry, (2) identify perceived and actual barriers to adoption of cogeneration, and (3) investigate economical and technical conditions under which cogeneration could become a viable option for wood products manufacturers.

Methods

To accomplish the study's objectives, a combination of literature review, expert and industry interviews, and a target survey of wood products manufacturers was used to accomplish the study's objectives. A detailed explanation of methods follows.

Interviews

After an extensive literature review, interviews with cogeneration experts and industry representatives were conducted to identify and learn about the critical topics of cogeneration as it applies to the wood products industry. A list of potential interviewees including, technology experts, industry adopters and non-adopters, was compiled. Topics included in the interviews were: (1) conditions/drivers for cogeneration, (2) barriers to cogeneration, (3) role of policies, and (4) the interviewee's outlook for cogeneration. The interviews were recorded, transcribed and then coded for analysis. Organization and analysis of the responses were carried out using Microsoft Excel spreadsheet software.

Target Survey of Non-Adopters

Using as major input the expert and industry interviews, a targeted web-based survey of U.S. wood products manufacturers was conducted. The targeted sampling approach used is a non-probability strategy, where the researchers do not have certainty of whether all potential respondents have the same chance of selection (Rea, 2005), thus generalizations from the results cannot be made to the entire population of interest. The reasons for selecting this sampling strategy were related to time and resource limitations, and availability of lists of current and valid e-mail addresses.

Sample Development

A sample of companies in the population of interest (NAICS codes 321: Wood Products, and 337: Furniture and Related Products) was developed using the Wood2Energy database (Wood2Energy, 2014). This database contains several fields, which can be used to sort companies. A list of 946 companies was compiled and used for the survey. Efforts were made to try to have a sample that reflects the regional distribution of the industry.

Questionnaire Development

The Tailored Design Method's recommendations by Dillman were followed (Dillman 2009) to design and conduct the survey. The survey instrument was developed in three steps: (1) A list of topics and initial draft were created based on results from interviews to experts conducted during the first stage of the research. The platform used for the web-based survey was Qualtrics survey software (Qualtrics, 2014). (2) The questionnaire was subject to review by four industry and experts and feedback was used to create a new and improved version. (3) A survey pre-test was conducted among a sample of 103 companies randomly selected from the distribution list. Changes were made based on response patterns and feedback received. A final version of the questionnaire was then ready for its final distribution.

Results and Discussion

Expert and Industry Interviews

Experts and industry representatives were interviewed during spring and summer of 2014. The major findings from the analysis are presented in this section.

Drivers for Cogeneration

- Energy costs: The most common response, when asked about the motivations and drivers for cogeneration, was the increasing costs of energy.
- Growing energy needs: All the companies interviewed for this study mentioned "growing energy needs," especially thermal energy, as a major driver for considering cogeneration.
- Wood residue utilization: Interviewees also mentioned the need for more profitable outlets for their wood residues as a major driver to consider cogeneration.
- Environmental driver: Of all the drivers mentioned during the interviews, environmental considerations did not seem to be regarded as a major motivation, especially for manufacturers. One manufacturer indicated that, purchasing electricity from a utility that in turn obtains a considerable part of its energy from wind, allowed the company to meet its environmental goals without resorting to cogeneration.

Factors for Cogeneration

- Scale of operation: This was a common theme in the interviews. Responses suggest that economies of scale make cogeneration more or less feasible for wood products manufacturers.
- Match between electric/thermal loads: According to our interviewees, along with economies of scale, a good coincidence between electric and thermal load was mentioned as one of the most important factors for economic feasibility of cogeneration. The importance of strategy for system design was also mentioned.
- Low seasonal variability in thermal loads: Cogeneration operations need constant thermal loads throughout the year to be economically feasible.
- Location (relative to utilities and fuel): Due to the low energy density of wood biomass, location relative to the fuel is especially important for bioenergy operations. Location relative to utilities is also an important factor.
- Age of thermal equipment: Companies that need considerable upgrading of their thermal equipment (boiler, steam lines) for the implementation of cogeneration may find it financially challenging to engage in such investment.
- Spark spread: Spark spread is the difference (in $ per kWh) between the price of delivered electric energy and the cost of generating power with a cogeneration system (EPA, 2014a). This metric was seen as an important consideration for the economic feasibility of a cogeneration project and the design strategy to be used.

Barriers to Cogeneration

- Initial investment: Economies of scale are important for the initial investment required for a cogeneration plant. For some operations, an important component of the initial investment is the acquisition of emissions control equipment.
- Company hurdle rate and required payback period: Although experts mentioned that, in general, cogeneration projects have relatively short payback periods, companies sometimes require even shorter payback period to consider implementing a project.
- Complexity of operation and maintenance. All of the adopters interviewed coincided that there is a need to hire personnel with specific qualifications to run and maintain the cogeneration facility.
- Adequate markets for wood residues: While looking for better utilization of wood residues was a major driver for considering cogeneration, having more profitable outlets for them can also be a barrier.
- Tariff policies by utilities and inadequate power purchase agreement: Since most cogeneration projects are designed to meet thermal loads, there is usually a discrepancy between a manufacturing facility's load and the cogeneration output, thus companies need to negotiate power purchasing agreements with utilities.
- Emissions regulations and permitting issues: Adopters interviewed for this study mentioned that for small operations emissions regulations are usually not a big hurdle, but as the size of the operation increases, emissions requirements become more stringent.
- Inadequate policies/incentives: The Environmental Protection Agency lists 349 policies related to cogeneration in its Cogeneration Policies and Incentives database (EPA, 2013). Some of our interviewees noted that the incentives from PURPA ("Public Utility Regulatory Policies Act of 1978 (PURPA)," 1978), which in large part facilitated important increases in cogeneration capacity, were rolled back with the passage of the Energy Policy Act of 2005 ("Energy Policy Act of 2005," 2005), mostly affecting the utilities' power buying obligations.
- Lack of education/awareness: Lastly, several interviewees mentioned that there is a lack of awareness and education about cogeneration technologies.

Survey of Wood Products Manufacturers

The survey was conducted in the summer of 2014, with one initial distribution and two reminders, lasting four weeks in total. The initial distribution list contained 946 companies. Accounting for bounced emails, surveys not fully completed and four companies that declined to participate, the adjusted response rate was of 8%. Given the sampling method used and the low response rate, it is important to state that the conclusions listed here apply only to the facilities that responded to the survey.

Most respondent were primary manufacturers (sawmills), architectural millwork manufacturers, wood components producers, and dimension lumber and planer mills. Companies in 30 U.S. states answered the survey, from which most indicated to be located in the Eastern U.S.

Familiarity with Cogeneration and Company Status Regarding Cogeneration

Companies were asked about their familiarity with cogeneration. Overall, 63.4% of respondents reported being "somewhat familiar" or "very familiar" with cogeneration, while 30.7% indicated being "not very familiar" or "not at all familiar" with cogeneration. Companies were also asked to report their status in regards to cogeneration. Of all respondents to this question, 36.5% indicated that they do not have enough information to consider cogeneration. This suggests that there is opportunity for education and outreach efforts in the industry, and confirms some of the interviewees responses in the first phase of the study.

Perceived Benefits of Cogeneration

As with any other technology, adoption of cogeneration depends on the perceptions about the technology benefits that the potential adopter may have. To evaluate this, companies were asked to rate their agreement with a number of statements. Most respondents agreed or strongly agreed that cogeneration makes efficient use of wood residues, has a good environmental performance, and has potential for energy cost reduction (70.2% 64.6%, and 60.4% "strongly agree" or "agree," respectively). Agreement was not as widespread with cogeneration's ability to provide a more reliable source of power (56.3%); and there was low level of agreement with the statement regarding cogeneration as revenue generator (35.4%).

Barriers for Cogeneration Adoption

Respondents were asked to rate their agreement with a number of statements about barriers to cogeneration adoption. Responses are shown in Figure 3.

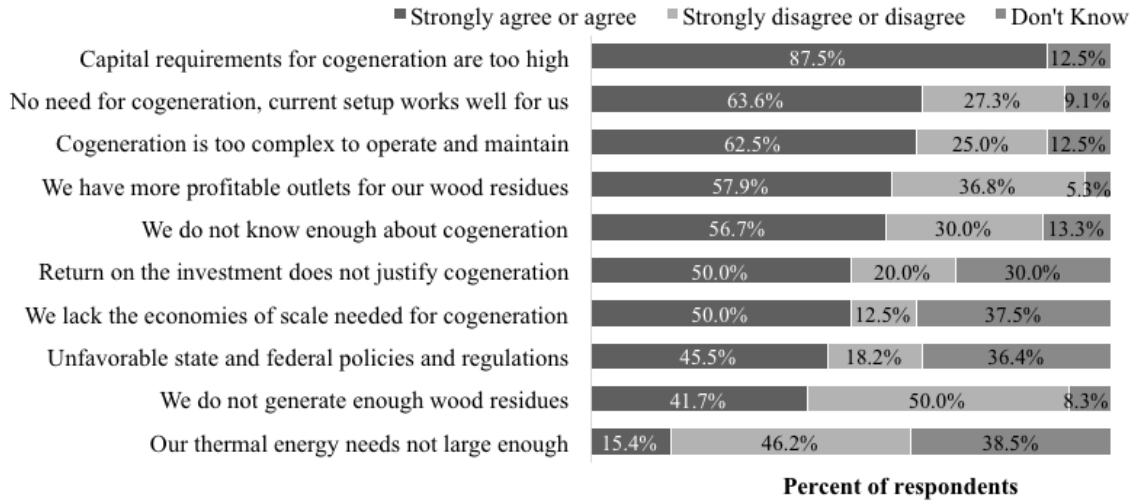

Figure 3. Barriers to cogeneration. N=variable.

Conditions for Cogeneration

Companies were also asked about what they thought would be an adequate payback period to make cogeneration an attractive investment. Two-thirds of companies indicated not having enough information about cogeneration to answer this question. Among those who specified a payback time, answers were at the two extremes: 15.6% of companies requiring 20 years or shorter payback and 13.3% of respondents requiring 5 years or shorter payback.

Summary and Conclusions

Research was conducted to understand the drivers, factors, and barriers to cogeneration adoption in the wood products industry Major findings from this study are listed below.

- From interviews with experts, it was found that the major drivers (in order of importance) for cogeneration implementation are: reduction of energy costs, growing energy needs by companies and desire to more effectively utilize wood residues.
- Among the most important factors considered when thinking about a cogeneration investment were: scale of the operation, good coincidence between electric and thermal loads and having a low seasonal variability in thermal loads.
- Most important barriers mentioned were: large investment required, companies' return of investment requirements, complexity of operating and maintaining a cogeneration unit, more profitable markets for wood residues, and lack of awareness about cogeneration among industries.
- Most survey respondents indicated being somewhat or very familiar with cogeneration (63.4%) while 30.7% were not very or not at all familiar with cogeneration. More than a third (36.5%) of respondents said they lack the information necessary to consider cogeneration.
- Among the perceived benefits from cogeneration were: efficient use of wood residues, environmental performance, and potential for cost reduction.
- Most important barriers perceived were: the capital requirements, followed by complexity of operation and maintenance.

Answers seemed to indicate a lack of knowledge and awareness about cogeneration. This represents an opportunity to provide education and outreach. The authors consider that further research is needed on feasibility of wood biomass cogeneration, including case studies of successful (and not so successful) implementations that could inform companies interested in cogeneration.

References

Alreck P L, Settle R B (2004) The survey research handbook. McGraw-Hill/Irwin, Boston, MA. 3rd Ed. Vol. xxv. 463 pp.

American Hardwood Export Council (2006) Understanding the North American Hardwood Industry: An Overview. Date accessed: April 22, 2008. http://www.ahec-europe.org/

Bergman R, Zerbe J (2004) Primer on Wood Biomass for Energy. Date accessed: June 2013. http://www.dof.virginia.gov/mgt/resources/pub-usda-fs-primer-on-wood-biomass-for-energy.pdf

Bowyer J, Bratkovich S, Frank M, Fernholz K, Howe J, Stai S (2011) Managing Forests for Carbon Mitigation. Dovetail Partners, Inc., Minneapolis, MN. 16 pp.

Dillman D A (2009) Internet, mail, and mixed-mode surveys : the tailored design method Wiley & Sons. Hoboken, N.J. 3rd Ed. Vol. xii. 499 pp.

DSIRE (2014) Database of State Incentives for Renewables & Efficiency (DSIRE). , http://www.dsireusa.org/ (October 3, 2014)

EIA (2014) Energy Information Administration. http://www.eia.gov/ (September 26, 2014)

Energy Policy Act of 2005 (2005).

EPA (2013) Database of CHP Policies and Incentives (dCHPP). http://www.epa.gov/chp/policies/database.html (February 9, 2013)

EPA (2014c) Combined Heat and Power Partnership - Basic Information. http://www.epa.gov/chp/basic/index.html (October 3, 2014)

Lamb F (2008, April 29, 2008). [Electronic mail communication].

Public Utility Regulatory Policies Act of 1978 (PURPA), H.R. 4018 C.F.R. (1978).

Qualtrics (2014) Qualtrics [computer software] Qualtrics, LLC. Provo, Utah http://www.qualtrics.com/

Rea L M (2005) Designing and conducting survey research : a comprehensive guide. Jossey-Bass. 3rd Ed. Vol. xvi, San Francisco, CA. 283 pp.

Wood2Energy (2014) Wood to Energy User Facility Database (Database). University of Tennessee Center for Renewable Carbon. Date accessed: July 2014. http://www.wood2energy.org

Acknowledgements

The author would like to acknowledge Dennis Becker, Ben Wallace, and Keith Landin for their help during the questionnaire development. Special thanks to the Office of the Vice President for Research, University of Minnesota, for providing financial support for this research. Lastly, we would like to acknowledge the companies that participated in this study, and who kindly provided their input and time.

Proceedings of the 58th International Convention of
Society of Wood Science and Technology
June 7-12, 2015 - Grand Teton National Park, Jackson, Wyoming, USA

Internal and External Barriers Impacting Non-food Lignocellulosic Biofuel Projects in the United States

Jeremy Withers, jeremyw7@vt.edu
Quesada Henry, quesada@vt.edu
Robert Smith, rsmith4@vt.edu

Virginia Tech, Brooks Center (0503), 1650 Research Center Dr., Blacksburg Virginia 24061

Abstract

This research identifies drivers and barriers impacting non-food cellulosic biofuel projects. Exploratory research on secondary sources was conducted. Different qualitative and quantitative tools were used to organize, classify and code the relevant data found. First phase results indicated that since the 2005 U.S. Epact, 54 known non-food cellulosic biofuel projects have attempted to reach economies of scale. Examined projects were classified by; company, type, location, current status, feedstock. Figures were created to display project status and percent within each category; pilot, demonstration, or commercial. Then the projects were mapped by dividing by the U.S. map vertical median and overlaying the five categories of; shutdown, cancelled, planning, under construction, operating. Of those, an average of 2/3 have shutdown, mothballed, or stalled in pilot and demonstration level status. Few have reached the full potential of biofuel production economies of scale. Results also indicated that little information is publicly known about factors determining project sustainability. This led to conducting an assessment of U.S. non-food based cellulosic bio-refinery projects that could be identified, and the factors affecting a sustainable undertaking. During a second phase, this research will conduct interviews, focus groups, and industry visits to collect information from primary sources in order to better understand the internal and external factors impacting these projects.

Proceedings of the 58th International Convention of
Society of Wood Science and Technology
June 7-12, 2015 - Grand Teton National Park, Jackson, Wyoming, USA

Self-Activation Process for Biomass Based Activated Carbon

Changlei Xia [1] *– Sheldon Q. Shi* [2]*

[1] PhD Candidate, Department of Mechanical and Energy Engineering, University of North Texas, Denton, TX 76203, USA.
Changlei.Xia@unt.edu

[2] Associate Professor, Department of Mechanical and Energy Engineering, University of North Texas, Denton, TX 76203, USA.
* *Corresponding Author*
Sheldon.Shi@unt.edu

Abstract

Self-activation takes the advantages of the gases emitted from the pyrolysis process of biomass to activate the converted carbon, so that a high performance activated carbon is obtained. Different biomass types were used for the self-activation processes into activated carbon, including kenaf bast fiber, kenaf core, sugarcane bagasse, sugarcane leaf, coconut fiber, peanut shell, and sawdust. A linear relationship was shown between the BET surface area (SA_{BET}) and the yield (ln(SA_{BET}) and yield) for the self-activation process. The study also showed that a yield of 9.0% gave the highest surface area by gram kenaf core (115.3 m^2 per gram kenaf core), and the yields between 5.5%-13.8% produced a surface area per gram kenaf core that higher than 90% of the maximum.

Keywords: Self-activation, activated carbon, biomass, kenaf core

Introduction

Activated carbon is a crude form of graphite with a random or amorphous structure, which is highly porous with large internal surface area. Activated carbon may exhibit a broad range of pore sizes from visible cracks or crevices to slits of molecular dimensions. Generally, activated carbon has a surface area of higher than 500 m^2/g as determined by the gas adsorption technique. In the adsorption analysis, non-polar gases, e.g. N_2, CO_2, Ar, CH_4, etc., are used, and the N_2 adsorption at 77 K is widely used (Mohan and Pittman Jr, 2006).

The use of carbon can be traced back to ancient times. The earliest known use of carbon in the form of wood chars (charcoal) was in 3750 BC by the Egyptians and Sumerians (Inglezakis and Poulopoulos, 2006). However, activated carbon was first produced on an industrial scale was in early twentieth century. The major development of the activated carbon was in Europe. In the early stage of development of activated carbon, they were only

available in the form of powdered activated carbon (PAC). Recently, many of the types of activated carbon, e.g. granular activated carbon (GAC), pelletized activated carbon, etc. have been developed. The Swedish chemist von Ostreijko obtained two patents, in 1900 and 1901, covering the basic concepts of chemical and physical/thermal activation of carbon, with metal chlorides and with carbon dioxide and steam, respectively (Sontheimer et al., 1988). In 1909, a plant named 'Chemische Werke' was built to manufacture, for the first time on a commercial scale, the PAC Eponit® from wood, adopting von Ostrejko's gasification approach (Dabrowski, 1999).

Activation methods can be divided into two categories: 1) physical/thermal activation and 2) chemical activation. The physical/thermal activation uses a mild oxidizing gas, e.g. CO_2, water steam, etc., to eliminate the bulk of the volatile matters, followed by partial gasification with thermal treatment. This method develops materials with higher porosity and more surface area. The chemical activations are chemicals employed methods to increase the surface area. Prior to activation, the raw materials are impregnated with certain chemicals. Then, the chemicals loaded raw materials are processed by the activation steps (may combine with carbonization).

The self-activation process of biomass described in this research takes advantages of the gases emitted from the biomass during the carbonization process to serve as the activation agent, so that the carbonization and activation are combined into one step (Shi and Xia, 2014). Compared to the conventional activated carbon manufacturing, the processing cost using the self-activation is reduced, since no activating gas or chemical is used. In addition, the self-activation process is more environmentally friendly. The exhausting gases (mainly CO and H_2) can be used as fuel or as feedstock for methanol production with further synthesis.

In this study, we investigated the self-activation process, the relationship between yield and BET surface area, and the best yield for the highest total surface area per gram kenaf core.

Materials and Methods

Materials.

Kenaf core was obtained from Biotech Mills Inc., USA, with sizes of 3–30 meshes according to the US standard sieve series and moisture content of 11.7% based on the ASTM D4442 standard. Other biomass, including kenaf bast fiber, sugarcane bagasse, sugarcane leaf, coconut fiber, peanut shell, and sawdust, were used as received.

Pyrolysis process. A high temperature versatile box furnace (STY-1600C, Sentro Tech Corp., USA) was used (Figure 1a), including a type-k thermocouple with a data logger (TC101A, MadgeTech, Inc., USA) used in the furnace to detect the internal temperature, and a digital pressure gauge (ADT680W-25-CP15-PSI-N, Additel Corp., USA) used to measure the pressure of the furnace chamber. The following procedure was used for the self-activation pyrolysis process: 1) placed the biomass feedstock into the box furnace chamber. 2) Apply vacuum to reach a pressure of -14.200 ± 0.005 psi (96.6% vacuum) and then keep a closed system. 3) Conducted pyrolysis process following the three steps: I) ramping with 10°C/min; II) dwelling, and III) cooling with no more than 10°C/min to room temperature (Figure 1b).

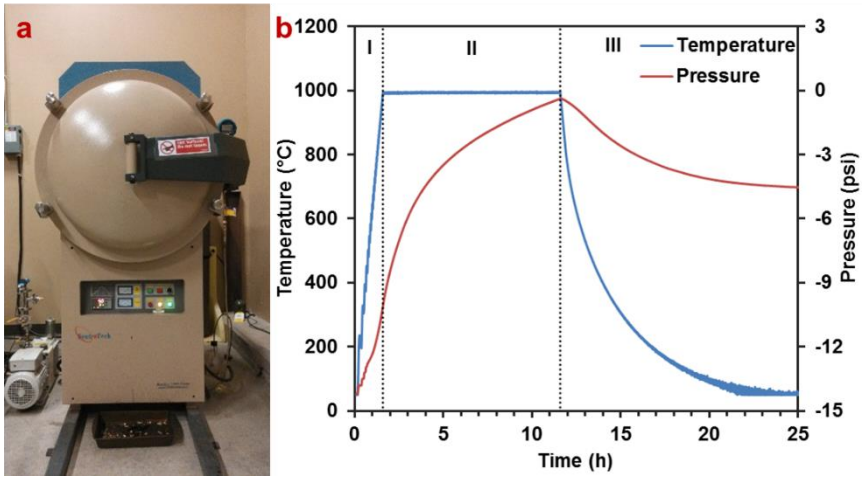

Figure 1. A box furnace (a) and (b) the internal pressure and temperature as a function of time in three pyrolysis periods: I) ramping of 10°C/min; II) dwelling for 10h; III) controlled cooling of 10°C/min and then self-cooling to room temperature.

Pulverizing.
The activated carbon products were pulverized by an ultra-fine pulverizing machine (RT-UF26, Rong Tsong Precision Technology Co., Taiwan). According to the ANSI/AWWA B600-10 standard, the requirements for the particle-size distribution of powdered activated carbon (PAC) are: not less than 99% of the activated carbon shall pass a No. 100 sieve, not less than 95% shall pass a No. 200 sieve, and not less than 90% shall pass a No. 325 sieve.

Characterization.
The adsorption capabilities of the PACs were determined by nitrogen adsorption at 77 K with a surface area and pore size analyzer (3Flex 3500, Micromeritics Instrument Corp., USA) (Figure 2). The samples were vacuum degassed at 350°C for 3–5 days using a degasser (VacPrep 061, Micromeritics Instrument Corp., USA) and then *in-situ* degassed at 350°C for 20h by a turbo molecular drag pump prior to the analyses. The specific surface areas were calculated from the isotherms through the instrumental software (3Flex Version 1.02, Micromeritics Instrument Corp., USA). Brunauer–Emmett–Teller (BET) method was used for the surface area analysis.

Figure 2. Micromeritics 3Flex surface area and pore size analyzer.

Results and Discussion

Self-activation vs. non-activation

Self-activation process was conducted on different biomass types, including kenaf bast fiber, kenaf core, sugarcane, sugarcane bagasse, sugarcane leaf, coconut fiber, peanut shell, and sawdust. Comparative experiments were conducted between the self-activation and non-activation. Table 1 shows the BET surface area (SA_{BET}) results for different biomass types pyrolyzed at 1,100°C for 2h that with or without self-activation process. The activated carbon fabricated from the self-activation process increase the SA_{BET} by 161% – 760%, and present surface areas greater than the minimum requirement of 500 m^2/g. The SEM observation of self-activation *vs.* non-activation was showed in Figure 3. It's clear seen that the pieces of carbon become thinner after the self-activation. The internal volume of the carbon becomes bigger.

Table 1. Comparisons of self-activation and non-activation.

Feedstock	SA_{BET} (m^2/g)		Increment (%)
	Non-activation	Self-activation	
Kenaf bast fiber	252	1280	408
Kenaf core	168	1148	583
Sugarcane bagasse	349	910	161
Sugarcane leaf	155	591	281
Coconut fiber	264	1413	435
Peanut shell	84	722	760
Sawdust	354	1199	239

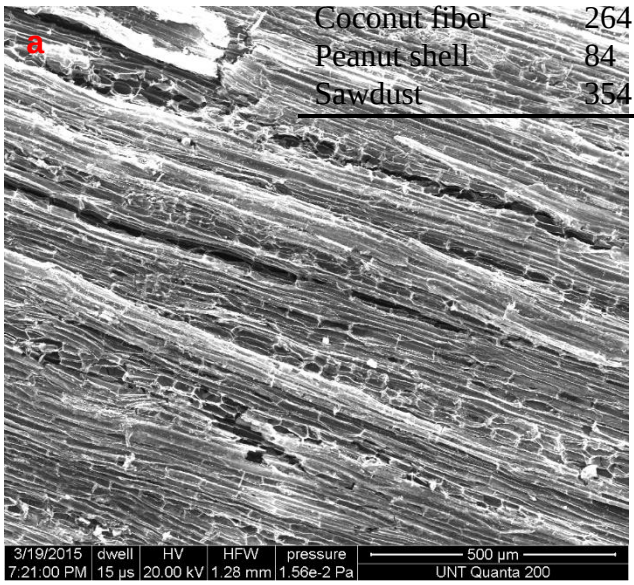

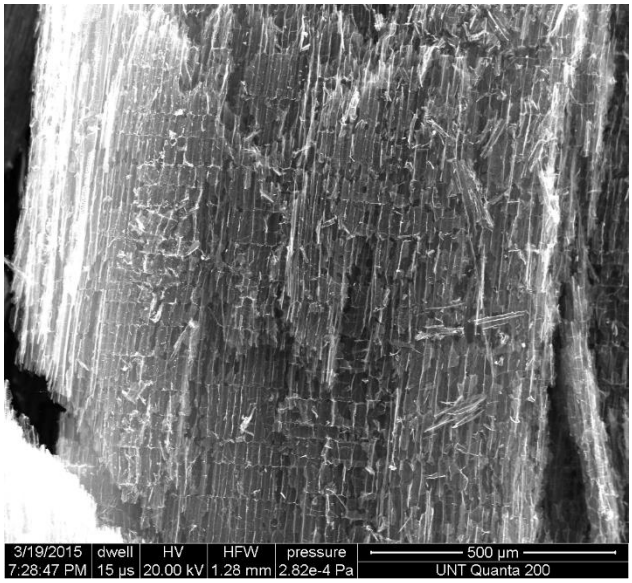

Figure 3. SEM photos of kenaf core based carbon by a) non-activation and b) self-activation.

Yield vs. SA_{BET}

Figure 3a shows the relationship between ln(SA_{BET}) and yield, where the activated carbon products are labeled as PACs (yields). The relationship is shown below with a very good R^2 of 0.98.

$$\ln(SA_{BET}) = -11.14 \times Yield + 8.16 \quad (1)$$

From Figure 4a, it's showed that PACs (1.97%, 17.54% – 20.73%), and Ash (1.74%) were excluded. PACs (17.54% – 20.73%) have a relatively lower SA_{BET} and higher yields compared to others. And the yield of PAC (1.97%) is very close to the Ash (1.74%), which is in the surface area reducing region.

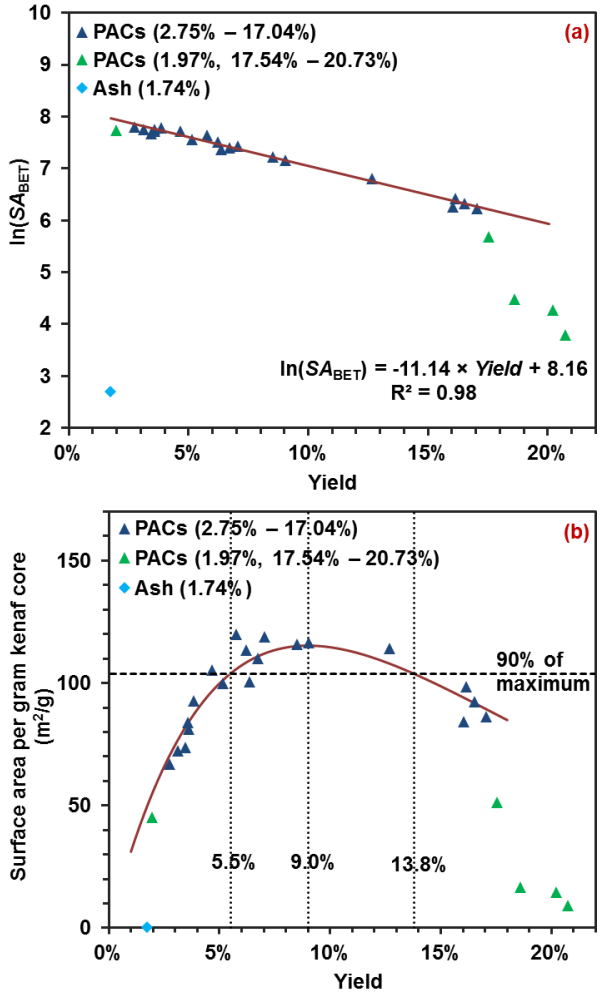

Figure 4. The relationships between yields of kenaf core based carbon and a) nature log of SA_{BET} and b) the total surface area produced by 1 g kenaf core.

Best yield investigation

Additionally, the efficiency of total surface area generation from kenaf core is analyzed (Figure 4b). The surface area per gram kenaf core is calculated by:

$$Surface\ area\ per\ gram\ kenaf\ core = SA_{BET} \times Yield \quad (2)$$

In terms of Eq. 1, SA_{BET} in Eq. 2 can be:

$$SA_{BET} = e^{-11.14 \times Yield + 8.16} \quad (3)$$

According to Eq. 2 and Eq. 3, the relationship between surface area per gram kenaf core and yield is shown below:

$$Surface\ area\ per\ gram\ kenaf\ core = e^{-11.14 \times Yield + 8.16} \times Yield \quad (4)$$

The red line in Figure 3b reflects the results of Eq. 4. In ideally, the PAC with a yield of 9.0% gives the highest surface area by gram kenaf core (115.3 m^2 per gram kenaf core), and the yields between 5.5% – 13.8% produce a surface area per gram kenaf core that higher than

90% of the maximum (103.8 m^2 per gram kenaf core). It provides a guide of taking the full advantage of kenaf core to making high total surface area by controlling the yields.

Conclusions

Self-activation is an effective activation process for activated carbon from biomass. The activated carbons were successfully produced without any additional activating gases or chemicals. The comparisons of self-activation and non-activation showed that the surface area of produced carbon can be dramatically increased. The relationships between yields and surface area (SA_{BET}) was investigated to have a lineal fitting between ln(SA_{BET}) and yields. In additional, the study of effective of kenaf core for producing highest total surface area showed that the yield of 9.0% received a maximum surface area per using gram kenaf core, and the yields between 5.5% and 13.8% were recommended for more than 90% of effectiveness.

Acknowledgements

This research was supported by National Science Foundation (NSF) CMMI 1247008. We acknowledge Dr. Liping Cai (Mechanical & Energy Engineering, University of North Texas).

References

Dabrowski, A., 1999. Adsorption-its development and application for practical purposes, Studies in Surface Science and Catalysis 123, 3-28.

Inglezakis, V.J., Poulopoulos S.G. 2006. Adsorption, ion exchange and catalysis: Design of operations and environmental applications. Elsevier Science & Technology.
Mohan, D., Pittman Jr, C.U., 2006. Activated carbons and low cost adsorbents for remediation of tri-and hexavalent chromium from water, Journal of hazardous materials 137, 762-811.

Shi, S.Q., Xia, C., 2014. Porositization process of carbon or carbonaceous materials, U.S. Patent Application 14/211,357.

Sontheimer, H., J. Crittenden, and R.S. Summers. 1988. Activated Carbon for Water Treatment, 2nd ed, Forschungstelle Engler-Bunte-Institute, Universität Karlsruhe, Karlsruhe, Germany.

Proceedings of the 58th International Convention of
Society of Wood Science and Technology
June 7-12, 2015 - Grand Teton National Park, Jackson, Wyoming, USA

Loss-on-Ignition Testing of Wood Ash

Robert Rice, Robert_rice@umit.maine.edu
J. Leah Jones, jlj3ua@virginia.edu

University of Maine, 119 Nutting Hall, , Orono, Maine 04469

Abstract

Loss on ignition (LOI) tests are used for determining the mass loss from solid combustion residues and ash that have been heated to prescribed temperatures. The mass loss can be from carbon, sulfur, potassium, sodium and other elements that volatilize and contribute to thermal energy or, possibly, to deleterious effects, such as sinter. When applied to coal and coke combustion, it is believed that the mass loss from the ash can be an estimate of the amount of carbon remaining in the residue. If substantial organic or inorganic carbon is found in the ash during the test, it is a clear indicator of combustion efficiency for a particular combustion system. Although loss on ignition testing is commonly applied to coal and coke, we have modified the testing protocols to better reflect elemental losses from wood ash. The details of testing along with an analysis of the chemistry changes that occur at various temperatures will be presented. The method appears to have substantial practical and theoretical use for the analysis of the bioenergy based combustion processes

Proceedings of the 58th International Convention of
Society of Wood Science and Technology
June 7-12, 2015 - Grand Teton National Park, Jackson, Wyoming, USA

Sustainable Development – International Framework – Overview and Analysis in the Context of Forests and Forest Products

Annika Hyytiä, annika.hyytia@helsinki.fi

University of Helsinki, Metsätieteiden laitos PL 27 , Voudintie 11, 00014 Helsingin Yliopisto

Abstract

Forests are a resource for Bio-based Economy. Strategies, technologies, policies and collaboration are important tools within the forest sector. Bio-based Economy is a challenge and a concept in a wider scope in the Green Economy. The goal is in combining the environmental goal with economic growth and in preventing dependency in fossil energy, poverty and ecosystem decrease to develop economic growth and employment with sustainable goals. There is international co-operation within the green initiatives. The investments and innovations are in a way to the sustained growth and give new opportunities.

Proceedings of the 58th International Convention of
Society of Wood Science and Technology
June 7-12, 2015 - Grand Teton National Park, Jackson, Wyoming, USA

Early Stage Researcher Full Oral Slot (8 minutes) Session
Moderators: *David DeVallance, West Virginia University, USA and Tobias Keplinger, ETH Zurich, Switzerland*

Development of a Sulfur-Free Delignification Process for Softwood Biorefineries

Claire Monot [1] - Christine Chirat [2]*

[1] PhD Student, Université Grenoble Alpes, Laboratory of Pulp and Paper Science and Graphic Arts (LGP2) – CNRS – Agefpi, F-38000 Grenoble, FRANCE.
* *Corresponding author*
claire.monot@lgp2.grenoble-inp.fr
[2] Associate Professor, Université Grenoble Alpes, Laboratory of Pulp and Paper Science and Graphic Arts (LGP2) – CNRS – Agefpi, F-38000 Grenoble, FRANCE.
christine.chirat@pagora.grenoble-inp.fr

Abstract

Nowadays, several pulp and paper biorefinery projects are under development. Particularly, the use of an autohydrolysis step prior to the production of cellulose fibers by wood delignification (cooking) is proposed to extract hemicelluloses. These could be a source of sugars, oligomers and polymers to produce bioproducts, biofuels and biomaterials. After cooking, the major part of lignin ends up in the effluent, the black liquor, which is currently burnt to recover the cooking reagents and to produce energy. Its gasification could produce more energy, however, traditional kraft cooking uses sulfur, which might be problematic in gasification processes. This is why sulfur-free cooking is studied, although it is usually less efficient than kraft cooking. Our study shows that autohydrolysis could improve the production of cellulosic fibers, by facilitating cooking as well as further oxygen delignification and bleaching, while using a sulfur-free process. Different types of cooking (kraft, soda, and soda/anthraquinone) on autohydrolysed and control softwood chips are compared. Autohydrolysis enables to apply a sulfur-free cooking on softwood chips, which is more difficult on control wood chips. Their kappa numbers (proportional to the lignin content) are lower than the ones of kraft pulp. Furthermore, the delignification during oxygen stage is better for those types of pulps.

Keywords: Prehydrolysis, sulfur-free cooking, pulp and paper biorefinery, anthraquinone, soda cooking, oxygen delignification

Introduction

Nowadays, pulp and paper biorefineries are under development. The principle of biorefineries is to valorize each component of wood in material or products and to produce energy to ensure the energetic autonomy of the mill.

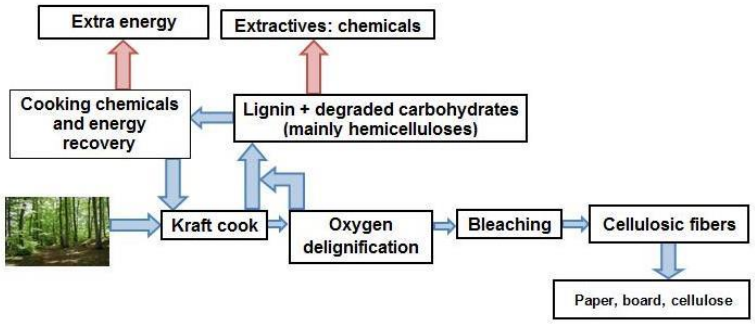

Figure 4: Today's kraft pulp mill

Figure 4 presents a kraft pulp mill producing bleached pulp as it operates today in most cases. Wood is fractionated during the kraft process (using NaOH and Na_2S, at 150-170°C during several hours): unbleached cellulose fibers are produced and are then bleached with oxygen bleaching and final bleaching (using chlorine dioxide and hydrogen peroxide in most cases) to end up with a fully bleached pulp used to produce paper and board. The effluent of the kraft cook called the black liquor, contains most of the lignin and degraded carbohydrates, and is burnt in a recovery boiler to produce enough energy for the mill. The chemical reagents for the cook are also recovered.
One aim of this project is to develop a gasification process of the black liquor to improve the energy yield. The problem of the black liquor produced in a kraft mill is that it contains sulfur, which is an inhibitor of gasification and is also corrosive for the gasifier. The development of a sulfur-free cooking could solve that problem. However it is known that sulfur-free cooking (soda cooking) is not as efficient as kraft cooking.

One of the most important projects in the development of pulp and paper biorefineries consists in the extraction of hemicelluloses using a prehydrolysis step before cooking (Gellerstedt 2008). Hemicelluloses could constitute a major source of sugars, oligomers and polymers to produce biomaterials, biofuel or bio-products (Ragauskas et al. 2006; Tunc and van Heiningen 2008; Chirat et al. 2010; Kämppi et al. 2010) (Figure 5).

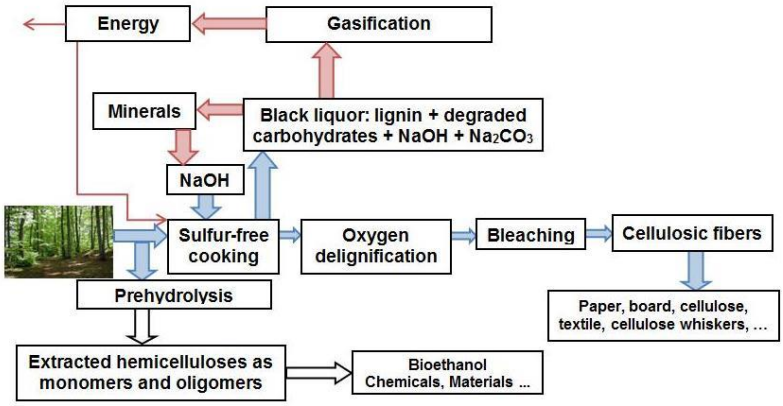

Figure 5: Tomorrow's kraft biorefinery mill

It has been shown that this prehydrolysis step could improve the manufacturing process of cellulosic fibres, by facilitating kraft cooking as well as oxygen delignification and bleaching (Colodette et al. 2011; Duarte et al. 2011; Chirat et al. 2011). It should then also facilitate the development of a sulfur-free cooking.

The first part of this study consisted in developing a sulfur-free cooking on prehydrolysed softwood chips. The second objective was to study the oxygen delignification of this type of pulp.

Materials and Methods

Wood Samples

Mixed softwood chips, kindly provided by the French kraft pulp mill, Fibre Excellence Tarascon, were used in this study. Their composition is 35 % Sylvestre Pine, 24 % Black Pine, 18 % Alep Pine, 16 % Spruce, 7 % Douglas fir. The average hemicellulose content was 28.0%.

Prehydrolysis

The prehydrolysis step (PH) was performed in stainless steel autoclaves placed in a rotating oil bath. The system is rotating. Autohydrolysis consisted in an acidic hydrolysis without addition of any external acid. Acetic acid released from the wood hemicelluloses when it is heated in water served as the acid source. The other operating conditions were: liquor to wood ratio of 4, time to T of 90 minutes, the time at temperature was 60 minutes and the temperature was 170°C.

Lignin Composition of Wood

The lignin composition of softwood is determined by Klason analysis on both types of wood. This analysis was performed as described in Tappi Standard (2011) T222 om-11.

Kraft and Soda-Anthraquinone Cooking

Control and hydrolysed wood chips were cooked by the kraft process according to the common industrial procedures. Cooking was performed in a stainless steel autoclaves placed in a rotating oil bath. The wood chips were processed under the following conditions: liquor

to wood ratio 4, the time to temperature 60 minutes, cooking temperature 170°C, time at temperature 110 minutes.

Soda-anthraquinone (Soda-AQ) cooking were performed using NaOH and a catalyst, anthraquinone (AQ), which is used to limit the degradation and solubilization of carbohydrates due to the peeling reaction. AQ percentages were 0.1 to 0.2% on wood. The temperature and time at temperature were the same as for the kraft cooking.
The amounts of NaOH and Na_2S are indicated in Table 2.

Table 2: Cooking and oxygen delignification stage conditions for each pulp

Cooking	PH	Cooking				NaOH % for oxygen delignification	
		Na_2S	NaOH	AQ	T (°C)	First O	Second O
Kraft	No	8.1%	18.9%	-	170	1%	-
Soda (27%)-AQ	No	-	27.0%	0.1%	170	1%	-
Soda (27%)	No	-	27.0%	-	170	2%	1.5%
PH-Kraft	Yes	8.1%	18.9%	-	170	1%	-
PH-Soda (27%)-AQ	Yes	-	27.0%	0.1%	170	1%	-
PH-Soda (19%)-AQ	Yes	-	19.0%	0.1%	160	2%	1.5%
PH-Soda (24%)	Yes	-	24.0%	-	170	2%	1.5%
PH-Soda (27%)	Yes	-	27.0%	-	170	1%	1%

Oxygen Delignification
Oxygen delignification was performed in the same stainless steel autoclaves placed in a rotating oil bath as for the cooking and the prehydrolysis. The temperature was 100°C and the oxygen pressure was set to 5 bars. The time at temperature was 60 minutes and the consistency was 10%. 0.3% of $MgSO_4$, $7H_2O$ was added to the pulp. Table 1 also shows the different conditions of oxygen delignification for each pulp.

Pulp Analyses
After cooking, the pulp obtained is characterized by its lignin content, the degree of polymerization and the pulp yield. Pulp makers are using the kappa number measurement to evaluate the performance of cooking. Kappa number is proportional to the lignin content. It is determined according to Tappi Standard (2013) T236 om-13. The degree of polymerization (DP) is relative to the length of the chains of cellulose. It gives information about the possible use of the cellulose obtained at the end of the process. DP is measured as described in Tappi Standard (2013) T230 om-13.

Results and Discussion

Previous studies on hardwood have shown that sulfur-free cooking is easier on prehydrolysed wood chips (Borrega et al. 2013; Sanglard et al. 2013). Three types of cooking (kraft (as the control cooking), soda and soda-anthraquinone) were performed on control and

prehydrolysed softwood chips in the present study. Anthraquinone (AQ) is used as a catalyst, enhancing delignification and limiting carbohydrate dissolution by peeling. It is also used in some kraft mills. However it is quite an expensive chemical, that cannot be recovered and its use in the industry is currently being questioned (Hart and Rudie 2014). This is why we decided to test soda-AQ cooking, but also simple soda cooking. Figure 6 shows kappa number versus global yield for each pulp. Kappa number is proportional to the residual lignin in pulp after cooking.

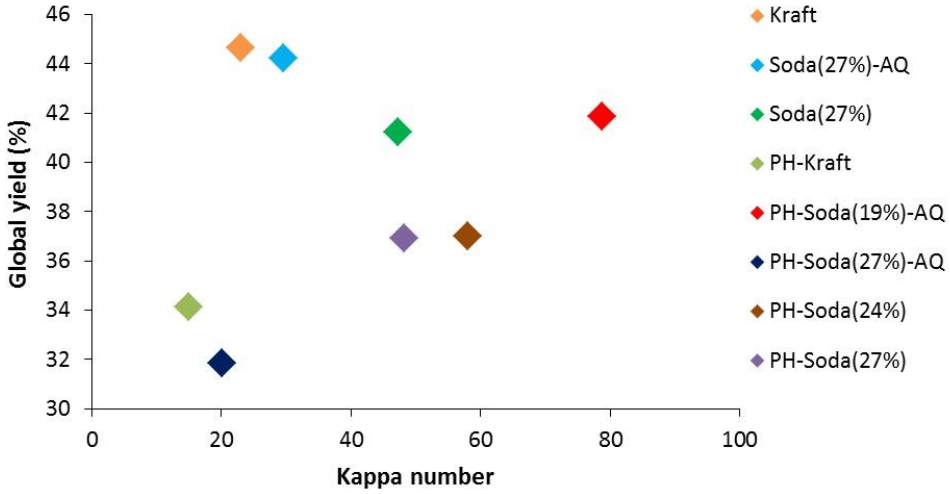

Figure 6: Kappa number versus global yield of each pulp (the number between parentheses represents the amount of NaOH applied to the wood during the cooking)

The global yield takes the prehydrolysis yield into account, which was of 80.2%. The global yield of prehydrolysed pulps are lower than the one of control pulps which is normal given the fact that a yield loss of almost 20% of wood components during this step was obtained. The aim is to obtain a pulp with the highest global yield and the lowest kappa number possible.

The main components eliminated during prehydrolysis are hemicelluloses which explains the proportionnal increase of lignin amount in wood (Table 3).

Table 3: Proportion of lignin in each type of wood

	Control softwood chips		Prehydrolysed softwood chips	
	Sample 1	Sample 2	Sample 1	Sample 2
Insoluble lignin content (%)	27.8	27.9	33.0	33.0

Despite the fact that prehydrolysed wood chips contain proportionnaly more lignin, control softwood chips gave higher kappa number than prehydrolysed softwood chips (comparison between Kraft and PH-Kraft and between Soda (27%)-AQ and PH-Soda (27%)-AQ). In the case of soda cook without any catalyst (Soda (27%) and PH-Soda (27%)) the kappa numbers were similar. It is thus confirmed that delignification is easier on prehydrolysed softwood chips for different types of cooking. One explanation could be that some ether type lignin-

hemicelluloses linkages were cut during the autohydrolysis, making then the lignin easier to be dissolved during the subsequent alkaline cooking (Monot et al. 2014).

In an attempt to increase the global yield after prehydrolysis and soda cooking, the amount of caustic soda applied was decreased (Fig. 3, PH-Soda (24%) and PH-Soda-AQ (19%)): the yield was increased but the kappa number also increased, logically, as the amount of caustic soda was decreased compared to the control cooks. The idea is then to apply an oxygen bleaching step, which is known to be more selective than the end of the cooking: this should lead to pulps with a higher yield and a higher polymerisation degree of cellulose. Oxygen bleaching was then applied to the different pulps, either in one (O) or two steps (OO). Table 3 presents the relative decrease of kappa number for each pulp after oxygen delignification.

Table 4: Relative decrease of kappa number after oxygen delignification

Cooking	Kraft	Soda (27%)-AQ	Soda (27%)	PH-kraft	PH Soda (19%)-AQ	PH Soda (27%)-AQ	PH-Soda (24%)	PH-Soda (27%)
Kappa number after cooking	23.0	29.6	47.2	15.0	78.8	20.1	58.1	51.1
Number of O stages	1	1	2	1	2	1	2	2
Relative decrease of kappa number (%)	45	40	62	64	63	53	78	61

The relative decrease of kappa number after oxygen delignification is either higher for prehydrolysed pulps (kraft cooking and soda-AQ cooking) or similar compared to the pulps produced from control wood.

To assess the quality of the pulps produced, degree of polymerisation (DP) was measured and plotted against kappa numbers for each pulp after cooking and one or two oxygen stages (Figure 7).

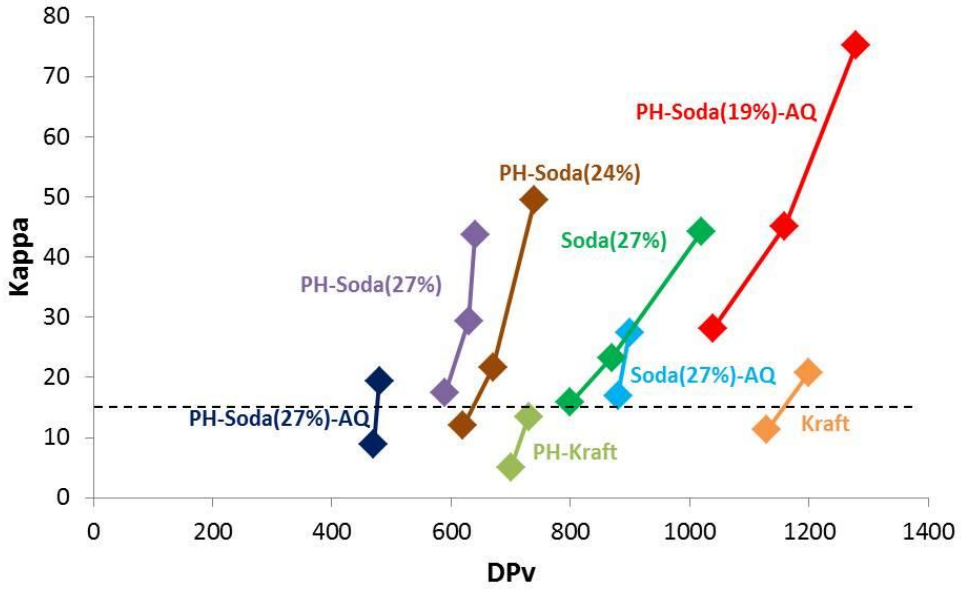

Figure 7: Degree of polymerization of pulp versus kappa number after one or two oxygen steps

For a similar type of cooking, and for a given lignin content (kappa number), DPs of prehydrolysed pulps are lower than the one of control pulps, which is due to the fact that the prehydrolysis step has already depolymerized cellulose. For the same type of wood (control or prehydrolysed), kraft cooking has a higher DP than soda or soda-anthraquinone cooking, which is the reason why the kraft cooking dominates at industrial scale.

The decrease in alkali (PH-Soda (27%) compared to PH-Soda (24%)) enabled to obtain better results after oxygen delignification: for a kappa number of 15 for example, the DP of PH-Soda (27%) after a double oxygen stage OO was 590, and it was of 640 for PH-Soda (24%) after OO. The result was even more pronounced when reducing the alkali to 19%.

A DP above 600 would be necessary to produce cellulose suitable for viscose application, so it has thus been shown that provided that the cooking is not too severe (reduction of the alkali) and that a strong oxygen delignification is applied after cooking to reduce the kappa number further, it will be possible to produce cellulose of adequate quality.
The next step will be to apply final bleaching to fully characterize the final pulps.

Conclusion

Results obtained on sulfur-free cooking of softwood chips seem promising. Cooking using caustic soda with or without anthraquinone will be possible after prehydrolysis, provided that the cooking conditions are not too severe to minimize cellulose depolymerisation. A strong oxygen delignification step should then be applied after cooking. The next step of this work will be to apply a bleaching sequence to confirm that a sulfur-free cooking could allow the production of cellulose suitable for viscose application.

Acknowledgments

Authors would like to thank Institut Carnot-Energie du Futur for the funding of this study.

References

Borrega M, Tolonen LK, Bardot F, et al (2013) Potential of hot water extraction of birch wood to produce high-purity dissolving pulp after alkaline pulping. Bioresour Technol 135:665–671. doi: 10.1016/j.biortech.2012.11.107

Chirat C, Boiron L, Lachenal D (2011) Bleaching ability of pre-hydrolyzed pulps in the context of a biorefinery mill. Pages 12-18 *in* Proceedings of the International Pulp Bleaching Conference, Tappi, Portland, USA.

Chirat C, Lachenal D, Dufresne A (2010) Biorefinery in a Kraft Pulp Mill: From Bioethanol to Cellulose Nanocrystals. Cellul Chem Technol 44:59–64.

Colodette JL, Longue D, Pedrazzi C, et al (2011) Pulpability and Bleachability of Xylan-Depleted Eucalyptus Wood Chips. Ind Eng Chem Res 50:1847–1852. doi: 10.1021/ie101799y

Duarte GV, Ramarao BV, Amidon TE, Ferreira PT (2011) Effect of Hot Water Extraction on Hardwood Kraft Pulp fibers (Acer saccharum, Sugar Maple). Ind Eng Chem Res 50:9949–9959. doi: 10.1021/ie200639u

Gellerstedt G (2008) Biorefinery solutions – The future of the forest based industry. Pages 1-4 *in* Proceedings of the European Workshop on Lignocellulosics and Pulp, Stockholm, Sweden.

Hart P, Rudie A (2014) Anthraquinone - A Review of the Rise and Fall of a Pulping Catalyst. Proceedings of the TAPPI PEERS Conference. TAPPI Press, Tacoma, WA.
Kämppi R, Hörhammer H, Leponiemi A, van Heiningen A (2010) Pre-extraction and PSAQ pulping of Siberian larch | NPPRJ. Nord PulpPaper 25:243–248.

Monot C, Evangelista B, Chirat C (2014) Relationship between lignin-carbohydrate complexes (LCC) from chips and pulps and their delignification and bleaching ability. Pages 259-265 *in* Proceedings of the International Pulp Bleaching Conference, Grenoble, France.
Ragauskas AJ, Nagy M, Kim DH, et al (2006) From wood to fuels: Integrating biofuels and pulp production. Ind Biotechnol 2:55–65. doi: 10.1089/ind.2006.2.55

Sanglard M, Chirat C, Jarman B, Lachenal D (2013) Biorefinery in a pulp mill: simultaneous production of cellulosic fibers from Eucalyptus globulus by soda-anthraquinone cooking and surface-active agents. Holzforschung 67:481–488.

Tappi Standard (2011) T 222 Om-11. Acid-insoluble lignin in wood and pulp. Technical Association of the Pulp and Paper Industry.

Tappi Standard (2013) T 236 Om-13. Kappa number of pulp. Technical Association of the Pulp and Paper Industry.

Tappi Standard (2013) T 230 Om-13. Viscosity of pulp (capillary viscometer method). Technical Association of the Pulp and Paper Industry.

Tunc MS, van Heiningen ARP (2008) Hydrothermal dissolution of mixed southern hardwoods. Holzforschung 62:539–545. doi: 10.1515/HF.2008.100

Proceedings of the 58th International Convention of
Society of Wood Science and Technology
June 7-12, 2015 - Grand Teton National Park, Jackson, Wyoming, USA

Effectiveness of *Gliricidia Sepium* Heart Wood Extractives as Preservatives Against Termite Attack

AGUDA L. O[1]., AJAYI B[2]., Owoyemi J[3]. Adejoba O.R[4] and Areo O.S[5].*
[1] Researcher, Department of Forest Products Development and Utilization, Forestry Research Institute of Nigeria, P.M.B. 5054, Ibadan, Oyo State, Nigeria.
[2] Professor, Head of Department of Forestry and Wood Tech., Federal University of Technology Akure, P.M.B. 704, Akure, Ondo state, Nigeria.
[3] Doctor, Senior Lecturer, Department of Forestry and Wood Tech., Federal University of Technology Akure, P.M.B. 704, Akure, Ondo state, Nigeria.
[4]Doctor, Assistant Director, Head of Department of Forest Products Development and Utilization, Forestry Research Institute of Nigeria, P.M.B. 5054, Ibadan, Oyo State, Nigeria.
[5]Researcher, Department of Forest Products Development and Utilization, Forestry Research Institute of Nigeria, P.M.B. 5054, Ibadan, Oyo State, Nigeria.
[*]E-Mail: larryall2000@yahoo.com. Phone No: +2348038724979

Abstract

Resistance of most wood species against termite attack is mainly as a result of their extractives components. The chemical compositions of extractives from matured *Gliricidia sepium* that are known to be very resistant against termite attack were studied to assess their role as wood preservatives. Ethanol-toluene and distilled water were used in the extraction of these compounds from the heartwood of this species. Chemical analysis of the extracts was done using Gas Chromatography-Mass Spectrometry (GC-MS) after derivatization using N,O bis (trimethyl silyl) acetamide.. More than One hundred and forty five compounds were identified from both extracts. Fatty acids, hydrocarbons, sterols, sterol ketones, phenolics, sterol esters and waxes were the main groups of compounds identified. The extracts obtained were used to treat four wood species that are known to be susceptible to termites attack. Treated samples were taken to a termitarium for a period of twelve weeks. It was observed that wood extracts used as preservatives improved the resistance of these susceptible wood species to termite attack more than 60% compared to the controls and also it was observed that removal of extractives decreased resistance of the durable samples significantly. It can be concluded that wood extractives contribute greatly to the protection of less durable wood against termite attack.

Keywords: Wood Extractives, bio-preservatives, termitarium, subterranean termites, Susceptible.

Introduction

Wood is a natural organic material that consists mainly of two groups of organic compounds: carbohydrates (hemicelluloses and cellulose) and phenols (lignin), which correspond to (65-75%) and (20-30%), respectively (Pettersen 1984). The wood is also constituted of minor amounts of extraneous materials, mostly in the form of organic extractives (usually 4–10%) and inorganic minerals (ash), mainly calcium, potassium, and magnesium, besides manganese and silica. Wood as a natural lingo-fibrous material produced by tree has been one of the earliest structural materials discovered by man. It is made from countless elongated hollow cells closely packed and joined end-to-end or overlapping. The cells are of different kinds and have special functions in the growing trees. As a result; its properties are subjected to wide variations brought about by the Physiology of trees and environmental factors affecting its growth.

Wood being a biological material is readily degraded by bacteria, fungi and termites (Walker, 1993; Schultz and Nicholas, 2002a). However, some wood species are resistant to these degrading agents while others are very susceptible to deterioration (Kityo and Plumptre, 1997). Natural resistance is the inherent ability of some wood species to resist the attack of bio-deteriorating agents without treatment with chemical preservatives (Owoyemi *et.al*, 2014). The natural resistance exhibited by some species is the resultant effect of the presence of extractives in the heartwood region. Milton, 1995 revealed that the sapwood of all known tree species is very susceptible to decay, regardless of any natural resistance of the heartwood. Unless sapwood is entirely removed or impregnated with preservatives, decay is likely to occur even in durable species (Adam, *et. Al*, 2002).

The term ‘natural durability’ therefore refers to the degree of resistance of untreated wood to bio-deteriorating agents. The natural durability of wood can only be appreciated through adequate knowledge of physiological processes of tree growth. As trees get older and larger, the storage cells in the center at the bottom begin to die resulting to a gradual transformation of the sapwood region to heartwood. Trees with more toxic natural chemicals deposited during the transformation have very durable heartwood that is highly resistant while some may be moderately resistant than others. Those that are susceptible must be treated with preservative chemicals to increase their service life.

The most common of these preservatives has been chromated copper arsenate (CCA) (Lebow, 2010). These synthetic chemicals are expensive and often harmful to the workers and the environment. Worse still, these preservatives are not readily degraded to harmless products and are not easy to detoxify. The copper based preservatives are also poor inhibitors of mould (Arango *et al.,* 2005) and are very costly. The dangers posed to wood treatment workers by most of the conventional proprietary wood preservatives, in addition to environmental degradation are becoming a matter of major concern worldwide (Barnes, 1992). Therefore, their application needs careful supervision to avoid polluting the environment.

In the recent times, the attention of researchers have been drawn to the problem of environmental pollutions, particularly contamination of soil and water resources is considered as a major risk for human communities throughout the world (Mohsen *et. al.*, 2011). Increase in the awareness on the negative impacts of these chemicals particularly on human health and environment has made this preservative unsuitable. Biological extracts are formulated from plants parts- such as fruits, leaves, seeds, bark, roots and so on. Research into the use of bio-extract has revealed that some bio-preservatives can serve as alternatives wood preservatives to the conventional ones. They are less expensive, readily available and environmentally friendly unlike the conventional preservative chemicals (Lebow, 2010; O'Callahan, 2012; Neemtreefarms, 2007; Burkill, 1985).

There are wood species that are naturally resistant to bio-deterioration agents. The resistance is mainly due to the accumulation of extractives in the heartwood some of which are decay inhibitors (Kityo and Plumptre, 1997). It is these extractives which render the heartwood poisonous to wood destroying organisms. Haygreen and Bowyer (1996) and Milton (1995) noted that the chemical composition and amount of extractives in wood is highly variable within and between tree species and can range from 2-15 % of wood weight.

Studies have shown that injecting wood extractives of durable species into non-durable specimen increases the wood samples' durability. It is therefore, pertinent to harness knowledge on the potent heartwood extractives of durable timbers for the development of environmental friendly wood protecting chemicals. Such intentions and pursuits not only have the ultimate aim of sustainable production of naturally durable species on the earth, but are also, reflective of growing concerns on the environmental impact of traditional wood preservatives. There is great potential in the use of extractives as natural preservatives, as many components of extractives are toxic to micro-organisms, imparting decay resistance to wood.

Gliricidia sepium is a leguminous tree and belongs to the family Fabaceae. Gliricidia, which originated in Central America, is used in many tropical and sub-tropical countries as live fencing. That is, it is planted along the side of fields, and the trunks are used as fence posts. During the dry season, when much of the forage is gone, the tree limbs are cut and the foliage is offered to livestock. It is an exotic species introduced into Nigeria as a source of fuelwood. However, its use has been mainly for fodder, life-fencing, manure and shades (Glover, 1989, Stewart and Simons, 1996). It can grow to a height of 15m if not pollarded, tolerate dry season and fire and can be propagated easily from seeds and branches (Lavini, 1996; Simons 1996). It has a distinctly dark brown heartwood and yellowish band of sapwood which could be mistakenly for *Milicia excelsa*, Afzelia africana planks.

The heartwood is resistant, very hard and heavy, strong, coarse-textured, within irregular grain. It seasons well and takes high polish (Elevitch and Francis, 2006). Oluwadare *et al* (2007) reports on the utilization potential of *Gliricidia sepium* revealed that the wood *Gliricidia sepium* is of high density and with strength superior to other hardwood species.

Materials and Methods

The heartwood of matured trees of *Gliricidia sepium* will be selected for this study based on its known natural durability. Two matured trees of the *Gliricidia sepium* were obtained from Forestry Research Institute of Nigeria (FRIN) staff quarters Ibadan, Nigeria. The wood specimen was divided into three groups; the first group was the sawdust of heartwood of *G.sepium* obtained during conversion of the wood species using circular saw. *G.sepium* extractives were obtained using distilled water and ethanol-toluene as solvents. The second group of twenty test samples (unground) of 20 x 20 x 60mm in dimension. The extractive in this group of wood blocks was extracted using distilled water and ethanol-toluene to obtain wood free from extractives. The leached wood samples were exposed to termites attack to test for the resistance of leached *G.sepium* to termites. This is to test for the effect of extractives on natural durability of *G. sepium*. The third group consisting ten samples of 20 x 20 x 60mm was used as controls for comparison. These samples were exposed to termite attack directly without treatment. The extraction was done using Soxlet extractors in the wood chemistry laboratory at Forest Products Development and Utilization Department in FRIN. The extracts obtained using ethanol-toluene was concentrated using Rotary Evaporator in the same department while the extracts from distilled water were used without concentration. Chemical composition of the extracts was done using Gas Chromatography-Mass Spectrometry (GC-MS) at Federal University of Technology Akure Central laboratory in Ondo State, Nigeria.

The sapwood of *Brachystegia eurycoma, Ceiba pentandra, Triplochyton scleroxylon* and *Nesogordonia papaverifera* were selected for this study because they are susceptible to deterioration. The wood species were cut into small test specimens of 20mm x 20mm x 60mm in accordance to ASTM D1413 (2003). One hundred and sixty (160) test blocks were dried for both species and labeled A1- 40 for *Brachystegia eurycoma*, B1- 40 for *Ceiba pentandra*, T1- 40 for *Triplochyton scleroxylon* and N1- 40 for *Nesogordonia papaverifera*. Each sample was labeled for ease of future identification. Five samples of 20 x 20 x 60mm were selected from A1-40, B1-40, T1-40 and N1-40 respectively. The samples were prepared for test by drying and sterilizing them in the oven for 18 hours at 103°C and weighed (W_1), the weight was recorded as initial dry weight for each of the blocks. This was used in the determination of the density of the wood and in the calculation of the percentage rate of absorption of the wood species. These samples were treated with a solution of 100ml of the extract from ethanol-toluene into 900ml of distilled water, 300ml of the same extract into 700ml of distilled water, pure solution of ethanol-toluene extract, 500ml of extract from distilled water in 500ml of distilled water, pure distilled water extract and CCA respectively. After the cold dipping preservatives treatment for 72hrs, the test samples were weighed (W_2), the weight was recorded and the percentage of absorption (AR) and retention of the preservative (kg/m^3) were calculated using `equation (1)

$$AR = \frac{W_2 - W_1}{W_1} \times 100 \text{ ---------- (1)}$$

The treated samples and the controls were oven dried at 60^{o}C for 48hrs, until a constant weight was achieved. The specimens were relabeled for easy identification, conditioned to equilibrium moisture content and weighed to determine their initial weight (W_3) before

exposed to termite attack in an active termitarium in the staff quarter of FRIN, Ibadan Oyo State, Nigeria for 12weeks. The effect of extractives on natural durability was tested by exposing *G. sepium* whose extracts had been removed to the same termite attack. Weekly visual assessment according to ASTM 2003 was carried out to determine the rate of attack and observations was noted. When is 12 weeks, the experiment was terminated and samples were removed, cleaned and oven dry for 18 hours at 60^0C. After conditioning to equilibrium moisture content (EMC), samples were again cleaned of all soil and weigh to determine their final weight (W_4). The percentage weight loss for individual test pieces was determined using equation;

$$WL = \frac{W_4 - W_3}{W_3} \times 100 \quad \text{---------- (2)}$$

Where: WL = Weight loss
W_3 = weight of samples after treatment but before exposure to termites.
W_4 = weight of samples after exposure to termites.

The data collected was computed and analyzed using 4 x 7 factorial experiments in Completely Randomized Design. Mean found to differ significantly was separated using Duncan Multiple Range Test.

Results and Discussions

Identification of compounds in wood extractives

Chemical analysis of the extracts using GC-MS revealed different individual components. More than One hundred and forty compounds were identified. Hydrocarbons, fatty acids, sterols, sterol esters, waxes and sterol ketones were the major groups of compounds detected and identified. Other compounds included phenolics and ethers. The main compounds detected included sitosterol, stigmasterol, squalene, pentadecanoic acid ester, linoleic acid, palmitic acid, heptadecanoic acid, decane, pentacosane oleic acid while the unique ones included 2-(3,7-dimtheyl-octa-2,6 dienyl) 1,4 dimethoxy benezene. 1-octadecanol, 1-tridecanol, hexacosane, squalene, pentacosane, 9 octadecanoic acid, heptadecanoic acid, palmitic acid, sitosterol, stigmasterol, vanillin, tetradecanone and docosanoic acid while the unique ones included benzestrol, dibutyl phthalate and diethyl phthalate as shown in table 1.

Field exposure to termites

Effect of treatment of less durable species with wood extractives

Weekly visual observation was conducted and the samples were rated as specified in ASTM D 3345-74 standards and a gravimetric method was used to assess weight loss due to termite damage after 12 weeks and the termites attack on the samples was rated 7 which indicate a moderate attack penetration within the first 6 weeks after which was rated 4 for the rest of the exposure duration because the samples were heavily attacked thereby leading to about 30 – 40% of the wood cross-section being eaten up by the termites. The average weight loss for *Brachystegia eurycoma, Ceiba pentandra*, *Triplochyton scleroxylon* and *Nesogordonia papaverifera* treated with CCA (a well-known effective wood preservative) were only 4.89, 4.94, 11.59 and 9 percent respectively after twelve weeks of exposure to termite attack. On the other hand, the untreated control samples have average weight loss of 66.07, 86.33, 65.77 and 65.29 percent respectively and 6.72, 14.15, 16.74 and 14.00 percent respectively were the

average weight loss of samples treated with *G. sepium* extractives which shows the best performance after filed exposure for the same period of exposure. This indicates that these four species are very susceptible to attack by termites. However their resistance to termite attack significantly improved after treatment with CCA and wood extractives preservative. The average weight loss for *Brachystegia eurycoma*, *Ceiba pentandra*, *Triplochyton scleroxylon* and *Nesogordonia papaverifera* when treated with wood extractives was 30.82, 36.16, 36.66 and 31.54 percent respectively after twelve weeks of exposure to termite attack. Table 1 shows that *Brachystegia eurycoma* treated with 4% concentrated CCA with average mean value of 4.89% is more effective than 100% ethanol-toluene extract with average mean value of 6.72% which performed better than other extractive solutions. Also from the table, *Triplochyton scleroxylon* treated with 100% ethanol-toluene extract with average mean of 16.74% is next in performance to 4% CCA with average mean of 11.59% while *Ceiba pentandra* with average mean of 14.15% when treated with 100% of distilled water extract and 4.94% average mean when treated with 4% CCA. When *Nesogordonia papaverifera* was treated with 300ml of distilled water extract into 700ml of distilled water solution with average mean value of 14% and 9% mean value when treated with 4% CCA concentration.

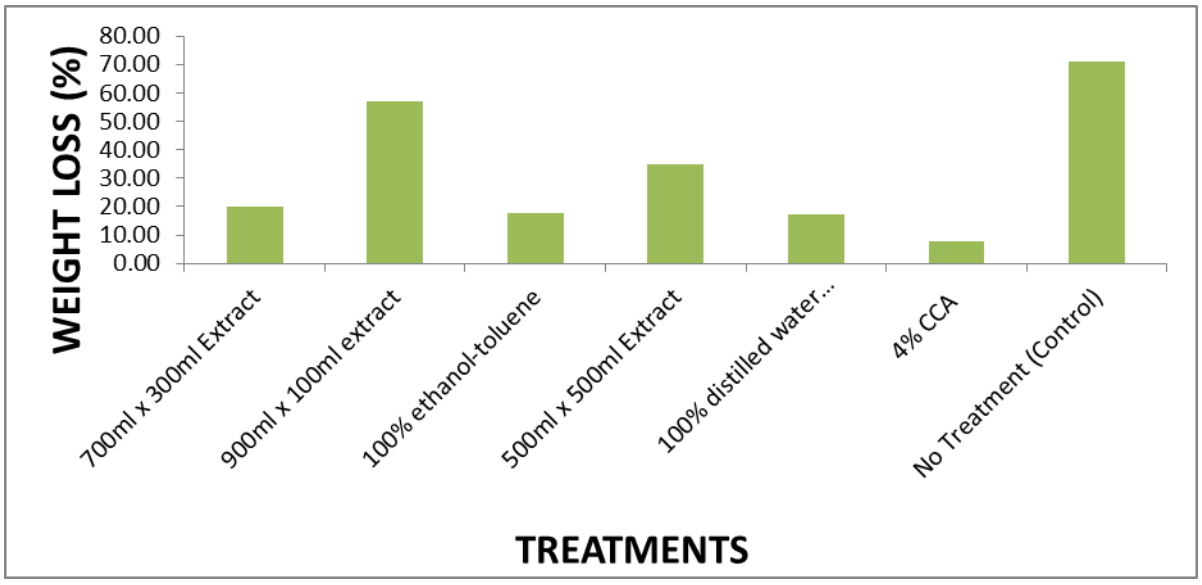

Figure 1: Effectiveness of the wood extractives

It was discovered that preservatives solutions with 500ml of distilled water extract into 500ml of distilled water solution and 100ml of ethanol-toluene extract into 900ml of distilled water solution recorded less resistant when used to treat the susceptible species after exposure to termite attack. This could be as a result of solvent (distilled water) used in extracting them and also the ratio of the extract to distilled water in the solution. Distilled water could have failed to extract some components compared to ethanol-toluene. So, different solvents remove different combinations of chemicals from the wood.

Table 1: Mean weight loss of species after exposure to termites attack

Treatment (Preservatives)	***Triplochyton***	***Ceiba***	***Nesogordonia***	***Brachystegia***	Mean
4% CCA	11.59	4.94	9.00	4.89	7.61
100% distilled H_20 extract	17.28	14.15	32.79	12.03	19.06

100% ethanol-toluene extract	16.74	20.57	27.77	6.72	17.95
700ml x 300ml distilled H_20 in ethanol-toluene solution	24.68	24.23	14.00	17.84	20.19
500ml x 500ml distilled H_20 in distilled H_20 extract solution	35.43	37.73	22.35	43.86	34.84
900 x 100 distilled water in distilled water extract	49.16	65.19	49.56	64.70	57.15
Without treatment (Control)	65.77	86.33	65.29	66.07	70.86
Mean	31.52	36.16	31.53	30.87	32.52

The analysis of variance shows that the resistance to termite attack increased significantly after treatment with wood extractives. However, the increase in resistance to termite attack was less effective than in CCA treatment. The analysis of variance also showed that the rate of weight loss within the species is not significantly different from each other. This may be attributed to the fact that the wood species are all susceptible to termite attack. And also there is no significant different in the rate of weight loss in the different species at 0.05 level of probability.

Wood extractives were found to increase resistance to termite attack in all *brachystegia eurycoma*, *ceiba pentandra*, *triplochyton scleroxylon* and *nesogordonia papaverifera* by 42%. Similar results were reported by goktas *et al*. (2007) who evaluated the wood preservative potentials of *sternbergia candidum* extracts and syofuna *et al*. (2012) who evaluates the efficiency of natural wood extractives as wood preservatives against termite attack where by weight losses for all treated samples decreased significantly confirming the effectiveness of extract solution in enhancing decay resistance. CCA which was a control was the most effective in increasing resistance to termite attack.

Conclusions and Recommendations

Conclusions

Wood resistance of less durable species significantly increased after treatment with hardwood extracts. However, wood extractives were not as effective as CCA in protecting the wood.

100% Ethanol-toluene extracts was the most effective in improving resistance of less durable wood samples against termite attack. Ethanol-toluene removed the highest number of chemicals from the wood when compared to distilled water and its extracts are more toxic to termites.

This is showed by the termite resistance of samples preserved with 100% ethanol-toluene extracts compared to those of 300ml x 700ml distilled water extract and distilled water, 100ml x 900ml ethanol-toluene extract and distilled water, 500ml x 500ml distilled water

extract and distilled water and finally 100% of distilled water extract which is the next to 100% ethanol-toluene extract in improving resistance of less durable species to termite attack. This is further revealed by the high number of chemical components identified in the extracts obtained from the different woods using ethanol-toluene and distilled water. *Gliricidia sepium* durability reduced after removal of its extractives but not significantly. It was concluded that extractives embedded in the cell walls were not readily removed by extraction.

There was also a tendency for treated less durable wood species to be consumed more by subterranean termites than the durable species whose extracts were removed. This was attributed to the fact that the introduced wood extractives could not 'enter' the cell wall but remained within the cell lumens. It was also concluded that density is another factor that enhances durability of this specie.

References

Adegeye, A. O., Ogunsanwo, O. Y. and Olajuyigbe, S. O. (2009). Antifungal Activities of Heart Wood Extract (HWE) of Teak *Tectona grandis* Against Two White Rots in Woods of *Gmelina arborea* and *Triplochiton scleroxylon. Academic Journal of Plant Sciences* 2 (4): 279-285, 2009

Amienyo. C. A and Ataga. A. E (2007). Use of Indigenous Plant Extracts for the Protection of Mechanically Injured Sweet Potato (*Ipomoea batatus*) tubers. Scientific Research and Essay Vol. 2(5), pp.167-170

Arango. A. R, Green, F. I., Hintz, K. , Lebow, P. K and Miller, B. R. (2005). Natural Durability of Tropical and Native Woods against Termite damage by *Reticulutermers Flavipes.* USDA. Forest service. International Biodeterioration and Biodegradation Vol 57(2006): pp 146-150

Asamoah, A., Atta-Boateng, A., Frimpong-Mensah, K. and Antwi-Boasiako, C. (2011). Efficacy of extractives from parts of Ghanaian pawpaw, avocado and neem on the durability of alstonia. *African Journal of Environmental Science and Technology* Vol. 5(2), pp. 131-135.

Balaban., M. (2004). Identification of the Main Phenolic Compounds in Wood of *Ceratonia siliqua* by GC-MC. Phytochemical Analysis 15, 385-388.

Bultman, J. D and Southwell, C. R (1976). Natural Resistance of Tropical American woods to Terrestrial Wood destroying Organisms. Biotropica. V ol 8, No.2, pp71-95.

Femi-Ola T. O. and Aderibigbe E. Y. (2008). Studies on the Effect of Some Wood Extracts on Growth and Cellulase Production by Strains of *Bacillus subtilis*. Asian Journal of Plant Sciences, Volume 7, Issue 4: 421-423

Goktas O., Mammandov. R., Duru. E. M., Ozen. E., Colak. M. A. and Yilmaz. F. (2007). Introduction and Evaluation of the Wood Preservative potentials of the Poisonous

Sternbergia canadidum extracts. African Journal of Biotechnology, Vol. 6 (8) pp. 982-986.

Milton, F. T. (1995). The Preservation of Wood. A self study manual for wood treaters. Minnesota extension service. University of Minnesota Collage of Natural resources.

Onuorah E.O. (2000). The Wood Preservative Potentials of Heartwood extracts of *Milicia excela* and *Erthrophleum suaveolens*. Bioresource Technology 75:171-173.

Owoyemi J. M.*, Olaniran O. S. (2014). Natural resistance of ten selected Nigerian wood species to subterranean termites attack. International Journal of Biological Sciences and Applications 2014; 1(2): 35-39

Peralta R.C.G, Menezes E. B, Carvalho A. G, Menezes E. L. A (2003). Feeding Preferences of Subterranean Termites for Forest Species associated or not to Wood Decaying Fungi. Floresta e Ambiente Vol. 10, No 2 pp 58-63.

Peralta, R. C. G, Menezes, E. B, Carvalho A. G, Menezes E. L. A (2004). Wood Consumption rates of Forest Species by Subterranean Termites (isoptera) under Field Conditions. Revista Arvore Vol. 28, No 2 pp 283-289.

Pereria D. M., Valentao P., Pereira J. A and Andrade P. B. (2009). Phenolics: From Chemistry to Biology. Molecules 14, 2202-2211.

Roll. D. (2003). Wood Preservation Category 4b, Commercial Wood Preservation Study Guide, Ohio Department of Agriculture. Publication for Pesticide Regulation 08/03

Schultz, T.P. and Nicholas, D.D. (2002b). Naturally durable heartwood: evidence for a proposed dual defensive function of the extractives. Phytochemistry 54, 47-52

Silverio F. O ., Barbosa L. C. A., Maltha.C. R. A., Silvestre.A. J. D., Veloso. D. P. and Gomide.J .L . (2007). Characterization of Lipophilic Wood Extractives from Clones of *Eucalyptus Urograndis* cultivate in Brazil. Bioresource 2(2) 157-168.

Syofuna A., A.Y. Banana1, G. Nakabonge (2012). Efficiency of Natural Wood Extractives as Wood Preservatives against Termite Attack. Maderas. Ciencia y tecnología, 14(2): 155-163.

Proceedings of the 58th International Convention of
Society of Wood Science and Technology
June 7-12, 2015 - Grand Teton National Park, Jackson, Wyoming, USA

Activated Carbon Monolith Derived From Bio-char

Lufei Li, lilufei1989@163.com
Wenliang Wang, growth_1989@sina.com
Liping Cai, liping.cai@unt.edu
Sheldon Shi, sheldon.shi@unt.edu
Jianmin Chang, cjianmin@bjfu.edu.cn

Beijing Forestry University, Haidian District, Beijing 100083

Abstract

Activated carbon monoliths were fabricated using powered bio-char as a raw material and bio-oil phenol-formaldehyde (PF) resin as a binder. The effect of the preparation condition on the physical and mechanical properties (compressive strength, bulk density, iodine adsorption value) of the resultant form was investigated. Using scanning electron microscopy (SEM) and N2 adsorption, the microstructure characteristics and adsorption performance under different conditions were observed. The results showed that the binder ratio and molding pressure had a significant effect on the pore size distribution and mechanical strength of activated carbon monoliths. It was found that an increase in the binder ratio would reduce the specific surface areas and strengthened the compressive strength of the carbon. The activated carbon monoliths prepared from the high molding pressures exhibited lower specific surface areas and total pore volume and higher compressive strength than those of the activated carbon monoliths prepared from low molding pressures. The optimum conditions to obtain the highest properties were the 30% content of the PF resin binder and 20 MPa of the molding pressure.

Proceedings of the 58th International Convention of
Society of Wood Science and Technology
June 7-12, 2015 - Grand Teton National Park, Jackson, Wyoming, USA

Reliability Analysis of Wood Floor Vibrations Considering Sheathing Discontinuities

Mubarak Adesina[1*] *and Arya Ebrahimpour*[2]
[1] Graduate Student, Department of Civil and Environmental Engineering, Idaho State University, Pocatello ID, USA.
**Corresponding author*
adesmuba@isu.edu

[2] Professor, Department of Civil and Environmental Engineering, Idaho State University, Pocatello ID, USA.
ebraarya@isu.edu

Abstract

Reliability analysis of wood floor vibrations under occupant induced loads is presented. The project adopts the finite element analysis approach using the Opensees simulation framework with Microsoft Excel used as the user interface. The Opensees results are imported into the user interface and compared against multiple vibration perception criteria. Analyses included the effect of sheathing continuity on the floor response. Extensive literature search was performed to obtain the relevant statistical data on sawn lumber joists. An automatic process was developed in which based on appropriate probability distribution functions, Excel interface simulated random values for the parameters considered. Limit state functions are developed based on the current vibration perception criteria. A combination of random and deterministic parameters is used in the limit state equations. Using Monte Carlo simulation, reliability index values were obtained for two floor systems of same dimensions. The first floor had discontinuous sheathing and the other had continuous sheathing. Results are discussed, followed by summary and conclusions. The results show a large range of reliability index values for the vibration serviceability criteria considered in this study.

Keywords: Reliability analysis, limit state, reliability index, wood floors, sawn lumber, wood floor sheathing, vibrations, OpenSees, finite element analysis.

Introduction

The prevalent use of wood floor systems has made it important to understand their behavior when subjected to occupant induced vibrations. A number of researchers have developed deterministic relations to quantify the vibration acceptability of floors under human-induced activities. Generally, the dynamic response of a wood floor system is a complex problem.

Each joist has a different modulus of elasticity and connections between joists and sheathing are non-rigid (Foschi and Gupta 1987). Also, the sheathing has significantly different properties compared to the joist properties. A reliability analysis will provide insight into the effect of uncertainties in material and geometric properties.

This research project has two goals: (1) to compare the reliability index values of current vibration acceptability criteria, and (2) to study the effect of sheathing continuity on structural reliability. The criteria used consider the natural frequency of the floor, the static deflection, and the root-mean-square value of response acceleration.

Review of Literature

Structural vibrations arise from normal human activity, operation of mechanical equipment within buildings, external traffic or wind storms and earthquakes. Methods of structural analysis and design are growing more refined, the systems are better integrated and use of high strength construction material is now common.

Serviceability requirements in current standards and specification which are little more than rules of thumb based on experience with traditional construction often are not sufficient for minimizing objectionable motion in modern structures (Ellingwood and Talin 1984). Detailed loading and resistance criteria have been developed for the ultimate or safety related limit states. However, serviceability requirements will determine the degree to which limit states design will lead to feasible and economical structure.

Numerous studies have been conducted in attempts to relate levels of floor vibration to human discomfort or tolerance levels. Specific findings in these studies are not always consistent due to diverse methods and purposes in the course of conducting the experiment or modeling the floor systems.

Ellingwood and Talin (1984) found that vibration is more likely to be a problem when caused by a single person walking than by a group of people. They concluded that a single person walking on the floor provides an appropriate dynamic model for developing serviceability criteria. A research by Foschi and Gupta (1987) used the finite strip method to study floor vibration induced by footfall impact loading. It was observed that the dynamic response analysis of wood floor was quite challenging due to variation in individual joist modulus of elasticity and connection between joists and sheathing are non-rigid. Similarly, Folz and Foschi (1991) used the finite-strip method for analyzing the dynamic response of very flexible floors. Humans were idealized as lumped oscillators that included masses, springs and dashpots in the vertical direction. They assumed that nails exhibit linear load-slip characteristics, allowing slip parallel to the joist, slip perpendicular to the joist and rotational slip.

The British standard (Guide to evaluation, 1992) states the general guidance on how to assess floor vibrations and how to predict human response to vibrations. Basic requirement for floor vibration assessment is that it must cover all important parameters affecting human response. The parameters include amplitude, damping and frequency of vibration. Frequency weighted

root mean square acceleration of vibration caused by a footfall impact satisfies this requirement (Chui 1986). Humans tend to tolerate higher vibration magnitude at higher frequencies than lower frequencies; thus, the calculated root-mean-square acceleration is frequency weighted. International Standards Organization states only frequencies between 8 and 80 Hz should be included scaled by a factor equal to $8/f_o$, where f_o is the floor fundamental natural frequency in Hertz (Hz). Smith and Chui (1988) introduced a design criterion based on the requirement that fundamental frequency of vibration for the floor be greater than 8 Hz and that the root mean square acceleration value for the first one-second of vibration be less than 0.45 m/s^2.

OpenSees Program and Excel Interface

Finite element modeling software can be a powerful tool for Engineers in all fields, but without proper calibration, comparison to real-world scenarios, and verification, finite element modeling software cannot be considered reliable. OpenSees, an open source software created and maintained by University of California, Berkeley, has not undergone the level of verification that is attained through the commercialization process. OpenSees does, however, receive constant verification at an academic level through ongoing peer-review and has even been adopted by the Pacific Earthquake Engineering Research Center.

The Excel user interface was designed to facilitate the use of OpenSees in estimation of vibration and deflection serviceability properties of wood floor systems. The interface allows the user to input values for various floor system properties which are then ported into OpenSees. Results from the OpenSees program are imported into the user interface and compared against multiple acceptance criteria which have been established by researchers to determine fitness of the floor system.

The synchrony between OpenSees and MS Excel was designed by Harvey Burch (2013) to examine the vibration analysis of wood floors considering sheathing discontinuities. His findings were measured against available thresholds published by previous researchers in the area of wood floor vibration. To ascertain if the program was working correctly, he verified it with an experimental result obtained by John Wolfe, a previous student.

Burch's program is a very useful tool as it is able to simulate various floor sizes, specify joists and sheathing sizes. It requires no knowledge of OpenSees, suitable for what-if situations including reliability analysis. When used for reliability analyses, the program can be modified to take advantage of Excel statistical functions.

Reliability Analysis of Wood Floor

The reliability analysis of a simple residential wood floor using regular lumber joist is presented. The floor is measured against set thresholds to derive the limit state equations to yield the reliability index (β), a measure of serviceability reliability. Table 1 gives the floor

dimensions and material properties. Also effects of continuous and discontinuous sheathing were taken into consideration in determining the reliability indices of the considered criteria.

Floor Property	**Dimension**
Floor width	3.6 m
Floor Span	3.72 m
Joist Size (Douglas Fir-Larch No 2)	38 mm x 235 mm
Joist Spacing	600 mm
Average Joist Modulus of Elasticity (E_j)	11032 N/mm^2
Joist Torsional Rigidity (GJ)	3,012 N.m^2
Sheathing Modulus of Elasticity (E_s)	3,190 N/mm^2
Sheathing Thickness	18 mm
Span rating	24 oc single floor
Fastener Type	Common 8d Nail
Fastener Spacing	254 mm
Fastener Horizontal Slip Stiffness	1,200 N/mm
Fastener Vertical Stiffness	17,513 N/mm
Fastener Rotational Stiffness	17,513 N/mm
Support Conditions	All four edges supported

Table 1: Properties and dimension of wood floor

The shear modulus G of the lumber joist is obtained from the wood handbook (2010).

$$\frac{G_j}{E_j} = 0.071 \qquad (1)$$

Limit State Equations

The following serviceability limit states were considered:

Static Deflection Criteria (Full Floor)
The first criterion considers only static deflection. The maximum allowable deflection for floor members with the application of the required live load of 1.92 kPa (40 psf) is L/360. The limit state equation is given as

$$g_1 = \frac{L}{360} - \delta_{1.92kPa} \qquad (2)$$

Where, $\delta_{1.92kPa}$ is the deflection under 1.92 kPa uniform load on the floor.

Bare Joist Static Deflection
Foschi and Gupta (1987) proposed that a bare joist loaded at mid-span with 1 kN (225 lb) concentrated should not deflect more than 1 mm (0.039 in.) independent of the length of the joist. Limit state equation is given as

$$g_2 = 1\ \text{mm} - \delta_{1kN} \qquad (3)$$

Where, δ_{1kN} is the deflection under 1 kN load.

Natural Frequency Criterion

In an effort to find a method of predicting acceptability of a floor during the design phase, Dolan, et al. (1999) created a vibration-limiting criterion that does not require any knowledge of the damping associated with a floor system. Their criterion is based solely on the calculated or predicted natural frequency of a floor system. The natural frequency of an unoccupied floor system must be higher than 15 Hz to be considered acceptable. Also, for an occupied floor system, the natural frequency must be higher than 14 Hz. The occupancy loads considered in the analysis of Dolan et al. range from 96 Pa (2 psf) to 192 Pa (4 psf). The limit state for an unoccupied floor system is

$$g_3 = f_u - 15 \text{ Hz} \quad (4)$$

Where, f_u is the unoccupied floor natural frequency. The limit state for an occupied floor system is

$$g_4 = f_o - 14 \text{ Hz} \quad (5)$$

Where, f_o is the occupied floor natural frequency.

Lin J. Hu Criterion

The criterion developed by Hu deals with a combination of natural frequency and static displacement. The criterion is designed for measurements on unoccupied floors without partitions, finishing, and furniture. The static deflection is measured after application of a 1 kN (225 lb.) load at mid-span of the entire floor system. Thus, the limit state equation is

$$g_5 = \left(\frac{f_u}{18.7}\right)^{2.27} - \delta_{1kN} \quad (6)$$

Where, f_u is the unoccupied floor natural frequency, δ_{1kN}- deflection under 1 kN load.

Smith and Chui Root Mean Square Acceleration Criterion

This criterion includes limitations on the natural frequency of the floor system as well as the root-mean-square (RMS) acceleration for a one second period of time. Smith and Chui state that the range of frequencies to which humans are most sensitive in terms of floor vibrations is from 4 to 8 Hz. In order to avoid excessive vibrations in this range, the natural frequency of the floor system must be greater than 8 Hz. Also, based on experimental work of Chui, an acceptable limit for the frequency-weighted root-mean-square acceleration should be less than 0.45 m/s^2 or 0.046g.

The limit state is given as

$$g_6 = 0.046g - A_{rms} \quad (7)$$

Where, A_{rms} is the frequency weighted RMS acceleration of the floor.

Discussion of Results

100 simulations were completed for the floor described in Table 1 with continuous sheathing and discontinuous sheathing to obtain the reliability index based on the limit state equations. For simplicity, only the variation in the modulus of elasticity of the joist E_j was considered. The mean E_j equals 11,032 N/mm^2 (1.6 x 10^6 psi) with a coefficient of variation of 9% (Al-Foqaha'a, 1997). Results obtained were plotted using a normalized limit state function for the above mentioned criteria. Figures 1 and 2 shows the simulated values of normalized limit states for discontinuous sheathing and continuous sheathing, respectively. The normalized limit state values (i.e., with values not to exceed 1 or not to be less than -1) were obtained by dividing the simulated limit state g values by the corresponding largest absolute value of g.

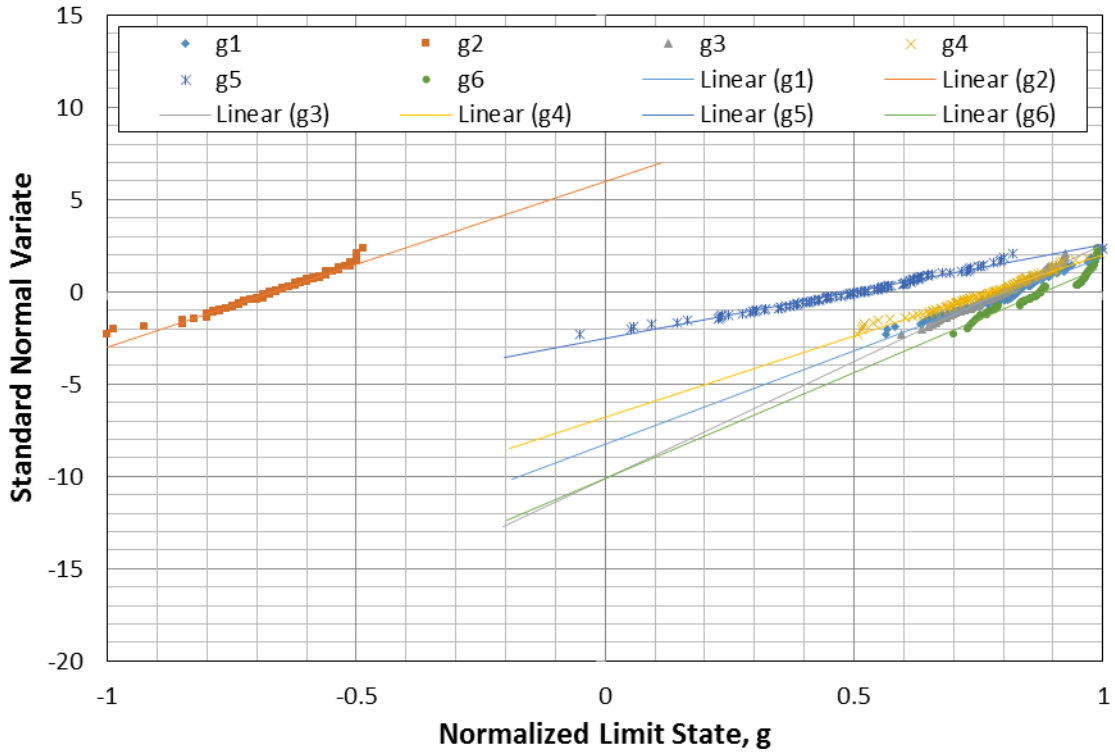

Figure 1: Normalized limit states for discontinuous sheathing.

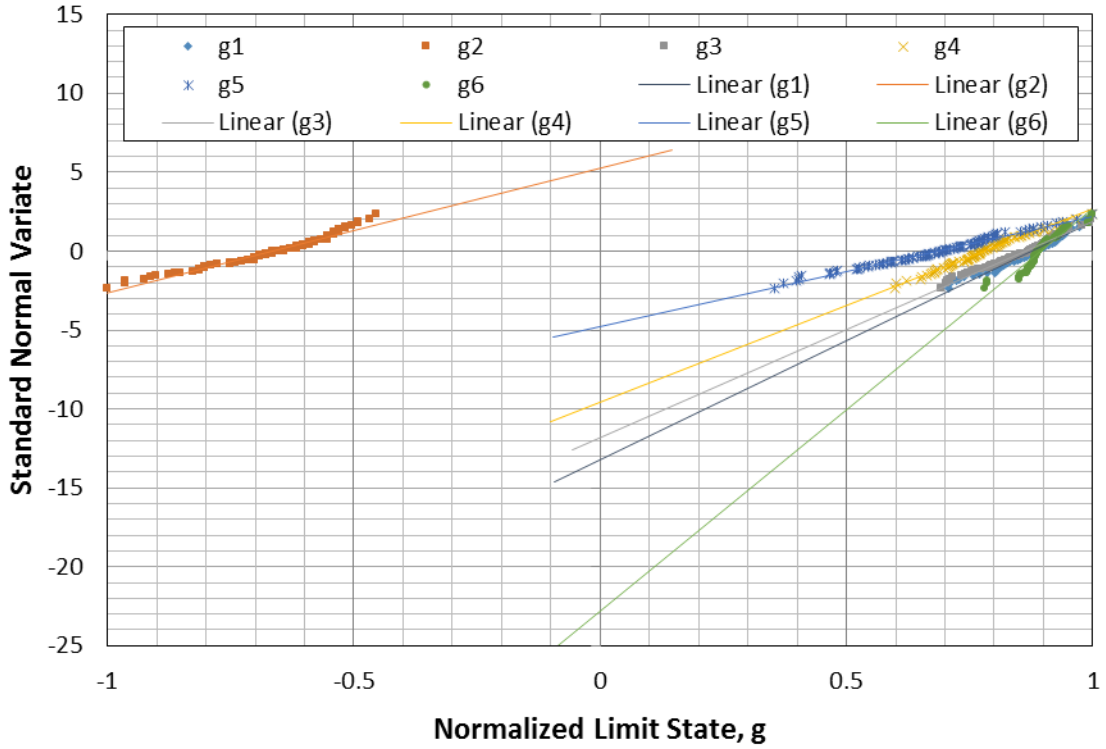

Figure 2: Normalized limit states for continuous sheathing.

Tabular comparison between reliability index and the corresponding probability of failure of the floor with discontinuous and continuous sheathing is shown in Table 2.

Limit State	Discontinuous Sheathing (β)	P(failure)	Continuous Sheathing (β)	P(failure)
g_1	8.2	1.2×10^{-16}	13.2	4.37×10^{-40}
g_2	-6	$\cong 1$	-5.2	$\cong 1$
g_3	10	7.62×10^{-24}	12	1.78×10^{-33}
g_4	6.8	5.23×10^{-12}	9.5	1.05×10^{-21}
g_5	2.5	6.21×10^{-3}	5	2.87×10^{-7}
g_6	10	7.62×10^{-24}	23	2.33×10^{-117}

Table 2: List of β values for discontinuous and continuous sheathing

Generally, the reliability index for a structure is around 3. Larger values are used for connections. For the above described floor only, the static deflection of the bare joist is not satisfied, all other criteria are satisfied for both the discontinuous and continuous sheathing. Although, individual comparison of each limit state with respect to sheathing discontinuities shows that the continuity of sheathing material increases the floor reliability index value.

Conclusion

Structural reliability considers the likelihood of structure reaching its limit state. The above results clearly show a large range of reliability index values for the serviceability criteria considered in this work. Amongst all criteria considered, the floor did not meet the Foschi and Gupta 1kN bare joist deflection requirement irrespective of the sheathing condition. However, comparison between reliability index values of same criterion with respect to sheathing shows continuous sheathing to have a higher reliability index over discontinuous sheathing. This means that for realistic wood floor vibration reliability analyses, sheathing discontinuities should not be ignored.

References

Al-Foqaha'a, A. A. (1997). Design criterion for wood floor vibrations via finite element and reliability analyses. Ph.D Dissertation, Washington State University, Pullman, Washington.

Burch H.R. (2013) Finite element vibration analysis of wood floors considering sheathing discontinuities. MS thesis, Idaho State University, Pocatello. ID. 254 pp.

Chui, Y.H. (1986) Vibrational performance of timber floors and the related human discomfort criteria. Journal of the Institute of Wood Science. 10(5): 183-188

Dolan, J.D., et al (1999) Preventing annoying wood floor vibrations. J. Structural Engineering. 125(1): 19-24

Ellingwood, B. and Talin, A. (1984) Structural Serviceability: Floor vibrations. J. Structural Engineering, ASCE 110(2): 401-418

Folz, B., and Foschi, R.O (1991) Coupled vibrational response of floor systems with occupants. J. Engineering Mechanics, ASCE 117(4): 872-892

Foschi, R.O., and Gupta, A. (1987) Reliability of floors under impact vibration. Canadian J. Civil Engrg. 14(5): 683-689

Guide to evaluation of human exposure to vibration in buildings (1992). British Standard Institution, London.

Hu, Lin J. (1997) Design guide for wood-framed floor systems. Canadian Forest Service No. 32.

Smith, I., and Chui, Y.H. (1988) Design of lightweight wooden floors to avoid human discomfort. Canadian J. Civil Engrg. 15(2): 254-262

Wood Handbook: Wood as an engineering material (2010) Forest product laboratory, United States Dept. of Agriculture forest service, Madison, WI.

Proceedings of the 58th International Convention of
Society of Wood Science and Technology
June 7-12, 2015 - Grand Teton National Park, Jackson, Wyoming, USA

Predicting Bending Properties of Stem and Branch Wood of a Tropical Hardwood Species from Density and Moisture Content

Peter Kessels Dadzie [1] - Martin Amoah [2]*

[1] Lecturer, Interior Architecture and Furniture Production Department, Kumasi Polytechnic, Box 854, Kumasi, Ghana.
**Corresponding author*
pkkdadzie@yahoo.com; peter.kdadzie@kpoly.edu.gh

[2]Senior Lecturer and Dean, Faculty of Technical Education, University of Education Winneba, Kumasi Campus, Kumasi, Ghana.
martamoah@yahoo.com

Abstract

Branchwood is being explored as supplements to stemwood in wood products manufacturing and bending properties are among those properties needed for wood for structural and nonstructural applications. However, non destructive methods are being adopted in determining wood properties, and wood density and moisture contents are some variables that can be applied. This study used density and moisture content to predict the MOE and MOR of branch and stem wood of *Entandrophragma cylindricum* (sapele) tested at two moisture levels (10±4%MC and 17±3MC). Density was determined in accordance with ISO 3131-1975. Bending properties determinations followed BS 373-1957 and using INSTRON TCM Machine with crosshead speed of 6.6mm/min. Results generally indicated that at each moisture level, branchwood had higher density than their stemwood counterparts. Generally at MOE and MOR at 10±4%MC were higher than at 17±3%MC but at 10±4%MC MOE and MOR of stemwood were higher than their branchwood counterparts. Whereas MC was found to have significant effect ($P < 0.05$), wood type and their interactions did not have significant effect on MOE and MOR of stem and branch wood. Moreover the predictive powers of MC and density as combined predictive variable for the bending properties were higher for branchwood than stemwood at both MC levels. It was concluded that for the species, branchwood had higher density than stemwood, and moisture content and density combined could predict MOE and MOR of both stem and branch wood of the species from 54.2% to 94.0% level of accuracy.

Keywords: Stem and branch wood, Bending properties of wood, Hardwood density, *Entandropharagma cylindricum*, Wood density and moisture relations.

Introduction

Among the reasons usually given for the non-extraction of timber from the crown area of tress is the lack of knowledge on the wood quality, including density and mechanical properties (Ayarkwa, 1998). Mechanical strength, especially bending strength is of much importance in measuring the stiffness (MOE) and the maximum load (MOR) of beams (Haygreeen & Bowyer, 1996; Tsoumis, 1991; Forest Products Laboratory, 2010). Furniture items like chairs and tables have parts that act like beams (e.g. seat slats, backrest slats, armrest, side rails and table tops) and are therefore subjected to bending stresses when loaded (Walton, 1974).

It is reported that decline in wood resource or forests influences a rise in the awareness of efficient use of wood and finger-jointing of wood for many lumber products (Gene, 2010). However, one step towards efficient wood utilization is the adaption of the whole tree utilization concept that advocate for the use of wood residues like branches and off-cuts (Haygreen and Bowyer 1996). Considering the rate of decline/depletion of Ghana's forest and their consequential effects on the economy and environment, forest depletion has become one major challenge facing the wood related entrepreneurs and the industries and has also resulted in a major rise in interest in wood residue utilization (Ministry of Lands and Natural Resources –MLNR, 2012). As a result of the alarming depletion rate (2%p.a) of forests in Ghana, the contribution of the forestry sector to national GDP has declined from 8% a decade ago to a current level of 4% in 2011 (MLNR, 2012). This state of affairs, among others, have caused some wood processing industries to either fold-up or not operating at full capacity due to lack of raw materials. What is most disturbing, in this turn of events, is the drastic extinction of the premium and commercial timber species which are used for furniture and other interior products. In the estimation of the International Institute for Environment and Development (IIED), the supplies of the traditional (premium and commercial) timber species such as *Entandrophragma cylindricum* (Sapele), among others, could fall by a further 50% within five years (Acquah & Whyte, 1998).

Due to the foreseen much threat of wood raw material extinction on the future of wood and construction industries, researchers are exploring the use of tree branches as supplements to tree stems. But studies on branchwoods have covered physical and mechanical properties/qualities as well as the workability of some Ghanaian hardwoods. Okai (2002) studied some physical and mechanical properties of *Terminalia ivorensis* (emire) and *Anigeria robusta* (asanfena), while Amoah *et. al.* (2012) have researched into the mechanical and physical characteristics of branchwood and rootwood of emire and *Milicia excelsa* (iroko/odum). Again Okine (2003), has also worked on the workability of emire and asanfena and has even used some to produce some furniture. However, there are no available studies on the natural durability qualities of branchwood of the "redwood species" especially Sapele.

Meanwhile Sapele tree has branches of about 25% of its extracted log volume which could be used as alternative or supplement to stemwood in new value-added products, like garden furniture, provided that their properties, specific to the intended application, are known (Dadzie 2013; Gurau *et. al.*, 2008) and bending properties are some of such properties. This study therefore seek to assess: 1) the variations in density of stem and branch wood of sapele at 2 moisture levels, 2) the bending strength properties between stem and branch woods at 2 moisture levels, and 3) use moisture levels and density to predict bending properties of stem and branch woods of sapele.

Materials and Methods

Samples collection and preparation

Four branch logs with diameters ranging from 26 cm to 48 cm and lengths from 1.5 m to 2 m were extracted for the study. A total of two branch and stem logs were extracted from a tree each from two natural forest reserves within two ecological zones of Ghana. Because samples were from natural forests the ages of the trees were unknown. However, the average diameter at breast height (dbh) was 120cm. All two reserves are concessions of Logs and Lumber Limited (LLL)- a timber processing firm in Kumasi, Ghana, and used for this study. Both through-and-through and quarter sawn methods were used for the conversion of the logs to lumber, using the same vertical bandmills that are being used for the conversion of logs in the factory. After the conversion, both branch and stem boards were re-sawn and crosscut into dimensions of 25 mm x 60 mm x 420 mm and grouped according to the two trees and the two reserves from which they were obtained and hence obtaining 4groups each (i.e. 1species x 2 trees x 2 reserves) for stem and branch woods. Clear heartwoods free of knots, fuzzy grains and any other visible defects were then sampled from each group. The stem and branch woods were regrouped into two each while ensuring that each group had samples of each tree and each reserve. One group each of the stem and branch wood was conditioned in the air-drying shed of LLL to average MC of 17±3% at same temperature and relative humidity used by the company to air-dry wood, whereas the other one group each were kiln-dried in the factory's kilns to average MC of 10±4% (average MC used for kiln-dried lumber products). After each drying process, 32 samples were finally prepared for stem and branch wood groups within each MC level in accordance with BS 373-1957 specifications for bending test.

Data Collection and Analysis

Wood density and bending properties

For each stem and branch wood group within each MC level, 30 samples were tested for density according to ISO 3131, whereas their modulus of elasticity (MOE) and modulus of rupture (MOR) were tested by a three-point flexural test in an INSTRON TCM universal testing machine model 4482 with crosshead speed of 6.6 mm/min. The INSTRON had a computerized data acquisition system that captured all relvant information on the test and test samples. Moisture contents of all tested samples were measured with moisture meter (model MO210 designed to measure MC of wood up to 44% as specified by the manufacturers) and which was found to have accuracy of ±2% upon validation with oven-dry method using 20 samples drawn from the stem and branch wood sample groups {i.e. (5 stem samples x 2 MC levels) + 5 branchwood samples x 2 MC levels) = 20 samples}. Determining MCs in wood properties studies with moisture meters has been acceptably used by some researchers, including Beaulieu *et al* (1987), Ayarkwa *et al* (2000), and Amoah *et al* (2012). Analysis of variance (ANOVA) and regression analysis were used to analyze the data obtained from both density and bending property tests using SPSS 17.0 version.

Results and Discussions

Wood density

Density of stem and branch wood of the *Entandrophragma cylindricum* (sapele) at the two moisture levels are as presented in Figure 1.

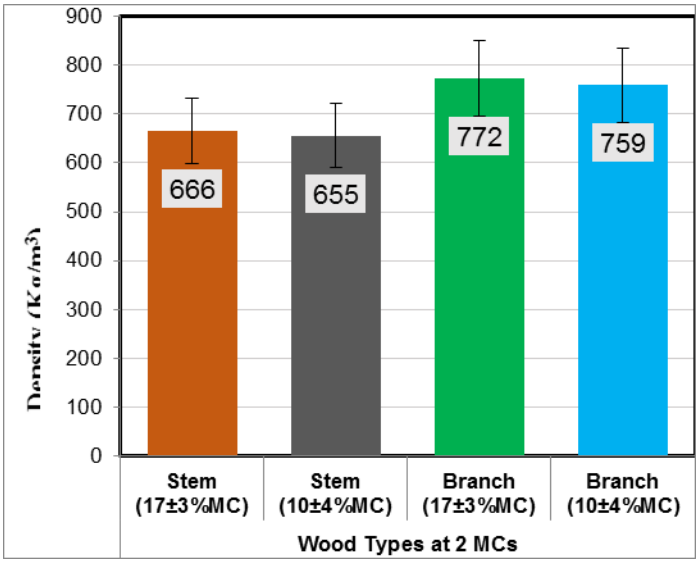

Figure 1: Density of stem and branch wood of Entandrophragma cylindricum (sapele) at 2 moisture levels. N= 30; Error bars are SE.

At the same MC level, density of branchwood was higher than that of stemwood. At 17±3%MC branchwood density was 772 kg/m^3 whereas stemwood density was 666kg/m^3 (resulting in a difference of 15.90%), and at 10±4%MC branchwood had density of 759kg/m^3 while stemwood recorded 655kg/m^3 (resulting in a difference of 15.88%). These agree with Okai (2002). Also same wood type (stem or branch) at different MC levels showed marginal density differences. Stem and branchwood dried to 17±3%MC respectively had 1.65% and 1.68% higher in density than their respective counterparts dried to 10±4%MC. These are on account of the moisture content differentials and they appear to be consistent with the findings of Lavers (1976) and Simpson and TenWorld (2010).

Bending Properties

The MOE (Figure 2a) and MOR (Figure 2b)of both stem and branch woods tested at the two moisture levels indicated that 10±4%MC were higher than those tested at 17±3%MC. However, at 17±3%MC MOE and MOR of branchwood were higher than those of stemwood but at 10±4%MC both MOE and MOR of stem were rather relatively higher than those of branchwood. MOE and MOR of stemwood at 17±3%MC were respectively lower by 82.89% and 52.39% than their counterparts tested at 10±4%MC. Also, MOE and MOR of branchwood tested at 17±3%MC were respectively lower by 42.43% and 40.14% than their counterparts tested at 10±4%MC level. These findings appear to corroborate those of Lavers

1974; Tsoumis 1991; Desch and Dinwoodie 1996 that both MOE and MOR of wood at relatively lower MC level are relatively higher than those at relatively higher MC level.

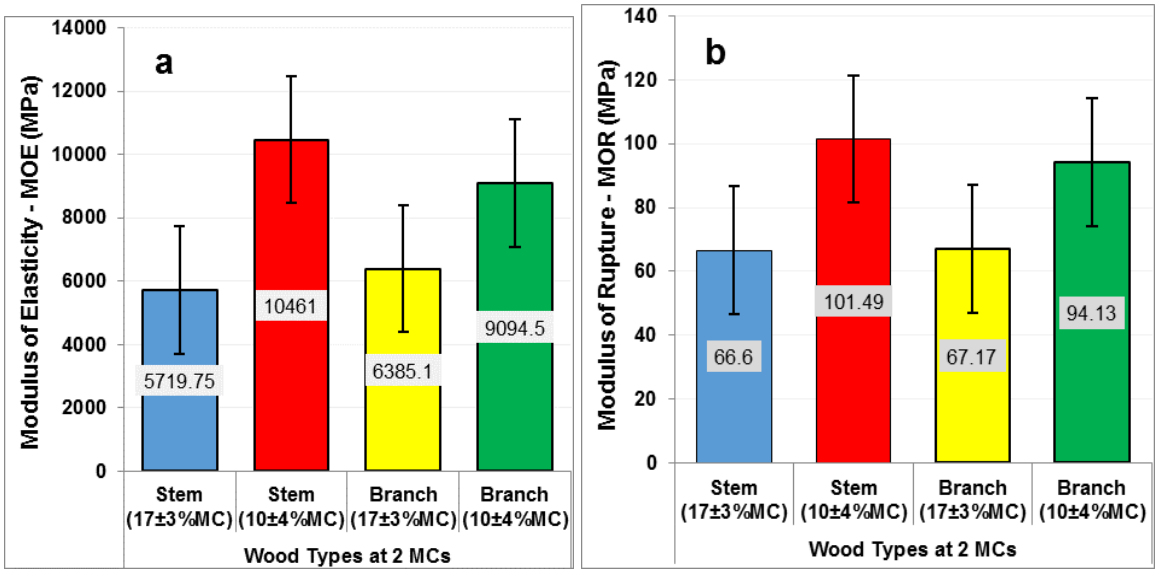

Figure 2: Bending properties of stem and branch woods of Entandrophragma cylindricum (sapele) tested at 2 moisture levels. **a** = MOE and **b** = MOR.

Again, MOE and MOR of stemwood the species tested at 17±3%MC were respectively lower by 11.63% and 0.86% compared to its branchwood tested at same MC level. However, MOE and MOR of stemwood tested at 10±4%MC were respectively higher by 13.06% and 7.25% than branchwood tested at same MC level. These findings also appear to support the findings of Okai 2002, 2003; Amoah et al. 2012 that at same MC level MOE or MOR of stem could be lower or higher than those of their branchwood counterparts.

The findings in Figure 2 appear to indicate that moisture level and wood type may have some effect on bending properties of sapele species. Hence, a Two-Way ANOVA was conducted for further explanations (Tables 1 and 2).

Source	Type III Sum of Squares	Df	Mean Square	F	Sig.
Corrected Model	2.992E8[a]	3	9.975E7	24.479	.000
Intercept	4.947E9	1	4.947E9	1.214E3	.000
Sapele_Wood_Types	2424913.770	1	2424913.770	.595	.443
Moisture_levels	2.739E8	1	2.739E8	67.230	.000
Sapele_wood_types * moisture_levels	2.037E7	1	2.037E7	4.999	.028
Error	3.056E8	75	4074790.542		
Total	5.535E9	79			
Corrected Total	6.048E8	78			

a. R Squared = .495 (Adjusted R Squared = .475)

Table 1: Two-Way ANOVA of the effect of moisture level and wood type on MOE of the wood types of sapele.

At 5% significance level, expectedly moisture level (F = 67.230; P = 0.000), and the interaction between moisture level and wood type (F = 4.999; P = 0.028) had significant effect on the stiffness (MOE) of stem and branch woods at the 2 moisture levels (Table 1). Also, as indicated by the adjusted R^2 value, moisture level and wood types explained about 47.5% of the variations in MOE among stem and branch woods at the two moisture levels.

Regarding bending strength (MOR) of stem and branch woods at the 2 moisture levels, at 5% significance level, only moisture level had significant effect (F = 44.584; P = 0.000) (Table 2). However, as indicated by the adjusted R^2 value, moisture level and wood types explained only about 35.6% of the variations in MOR among stem and branch woods at the two moisture levels. These findings appear consistent with reports that MC has significant effect on MOE and MOR of wood (Lavers 1974; Tsoumis 1991).

Source	Type III Sum of Squares	Df	Mean Square	F	Sig.
Corrected Model	19533.549[a]	3	6511.183	15.375	.000
Intercept	535419.424	1	535419.424	1.264E3	.000
Sapele_Wood_Types	227.220	1	227.220	.537	.466
Moisture_levels	18881.504	1	18881.504	44.584	.000
Sapele_wood_types * moisture_levels	309.983	1	309.983	.732	.395
Error	31762.544	75	423.501		
Total	585040.422	79			
Corrected Total	51296.093	78			

a. R Squared = .381 (Adjusted R Squared = .356)

Table 2: Two-Way ANOVA of the effect of moisture level and wood type on MOR of the wood types of sapele.

Predicting Bending Properties from Moisture Content and Density as Combined Predictors

Predicting MOE from Moisture Content and Density as Combined predictor

Table 3 presents the relationship between moisture content and density combined as prediction variable for MOE. Generally, wood density had significant relationships with MOE compared to the relationship of MC with MOE of sapele stem and branch woods. The only exception is the relationship found with MOE of sapele stemwood at 10±4%MC. Also from the R^2 (adjusted) values, MC and density had moderate (0.542) to very strong (0.940) predictive powers for MOEs of the sapele wood types but their influence in branchwood appeared to be higher than in stemwood. These mean that, MC and density can predict the MOE of stem and branch wood up to between 54% and 94% level of accuracy but they can predict MOE of branchwood better than as they can do for the stemwood.

Wood	N	Equation	Coefficients	t	P-Value	R^2 Adj.

			Symbol	Unstandardized B/Value	Std. Error	Standardized B/Value			
Sapele Stemwood 17±3%MC	20	MOE= c-αMC+βWD	c	-749.802	3988.499		-.188	.853ns	.769
			α	-181.920	124.656	-.244	-1.459	.163ns	
			β	14.092	3.397	.693	4.148	.001***	
10±4%MC	20	MOE= c-αMC+βWD	c	10024.605	21852.082		.459	.652ns	.542
			α	-1335.992	803.724	-.456	-1.662	.115ns	
			β	25.351	20.026	.347	1.266	.223ns	
Sapele Branchwood 17±3%MC	20	MOE= c-αMC+βWD	c	-9909.338	2595.244		-3.818	.001***	.909
			α	-14.191	49.327	-.033	-.288	.777ns	
			β	20.784	2.422	.985	8.580	.000***	
10±4%MC	19	MOE= c-αMC+βWD	c	-2681.350	1801.886		-1.488	.156ns	.940
			α	-239.033	76.896	-.206	-3.109	.007**	
			β	19.359	1.498	.855	12.926	.000***	

NOTE: The statistical analyses are significant at 95% confidence interval. ***p < 0.01; **p < 0.05; *p <0.1; and non-significant, nsP > 0.1; N; number of samples, WD: wood density (kg/m^3); MC: moisture content of wood (%).

Table 3: Relationship of wood density and moisture content combined (as predictor) for the MOE of stem and branch wood of sapele tested at two moisture levels.

Predicting MOR from Moisture Content and Density as Combined Predictor

Table 4 presents the relationship between moisture content and density combined and MOR that can be used as nondestructive prediction relations.

Wood Species/Type & MC	N	Equation	Coefficients: Symbol	Unstandardized B/Value	Std. Error	Standardized B/Value	t	P-Value	R^2 Adj.
Sapele Stemwood 17±3%MC	20	MOR= c-αMC+βWD		-7.839			-.230	.821ns	.801
			c		34.114				
			α	-1.263	1.066	-.184	-1.185	.252ns	
			β	.142	.029	.760	4.893	.000***	
10±4%MC	20	MOR= c-αMC+βWD	c	-252.043	174.309		-1.446	.166ns	.759
			α	-4.342	6.411	-.135	-.677	.507ns	
			β	.620	.160	.772	3.880	.001***	
Sapele Branchwood 17±3%MC	20	MOR= c-αMC+βWD	c	-16.550	21.635		-.765	.455ns	.911
			α	-.978	.411	-.270	-2.379	.029**	
			β	.130	.020	.730	6.441	.000***	
10±4%MC	19	MOR= c-αMC+βWD	c	-1.377	20.357		-.068	.947ns	.882
			α	-1.685	.869	-.181	-1.939	.070*	
			β	.153	.017	.843	9.038	.000***	

The statistical analyses are significant at 95% confidence interval. ***p < 0.01; **p < 0.05; *p <0.1; and non-significant, nsP> 0.1; N; number of samples, WD: wood density (kg/m^3); MC: moisture content of wood (%).

Table 4 : Relationship of wood densityand moisture content combined (as Predictor) for the MOR of stem and branch wood of sapele tested at 2 moisture levels.

Generally, wood density had significant relationships with MOR compared to the relationship of MC with MOR of sapele stem and branch woods. However, from the R^2 (adjusted) values, MC and density combined had very strong (from 0.759 to 0.911) relationships with MORs of

stem and branch woods of sapele but, as it occurred for the MOEs, the influence of MC and wood density combined appeared higher in branchwood than in stemwood (Table 4). These mean that, MC and density can predict the MOR of stem and branch wood up to between 75.9% and 91% accuracy but they can predict MOR of branchwood better than stemwood.

Conclusions and Recommendations

Based on the results the following conclusions were drawn;

1. Branchwood of sapele had higher density than its stemwood counterpart. However both stem and branch wood density increased with increase in moisture level.
2. Generally, bending properties of stemwood of sapele are relatively higher than those of its branchwood counterparts. Moisture content had significant effect on the variation in both MOE and MOR of sapele stem and branch woods.
3. Moisture content (MC) and wood density (WD) had moderate to strong relationship with MOE and MOR of both stem and branch woods of sapele. Subsequently, MC and WD combined can predict the bending properties of the wood types up to accuracies between 54% and 94%. However, the predictive strength of MC and WD appeared higher in branchwood than stemwood.
4. From the predictive strength of MC and WD as combined variables for MOE and MOR, the variables could be used nondestructively to predict the bending strength properties of stem and branch wood of sapele.

References

AFORNET- African Forest Research Network (2000) Wood Based Industries in Sub-Saharan Africa. www.afornet.org, (16 August 2005).

Alexander Rose Ltd. (2005) Fine quality traditional garden furniture, Alexander Rose Ltd, West Sussex. U.K.. 25pp.

Capito, Eugene (Hon.) (1993) Situation of African Forestry Policy. ATO, Information Bulletin No. 2 (1994) SGIT Impremerie de Louis, Gabon. pp.10-12.

Dadzie P.K (2013) The Potential Contribution of Branchwood Quantity, Left after Logging Operations, Towards Reducing Depletion Rate and Preserving Ghana's Forest Ecosystem, America Journal of Agriculture and Forestry, Vol. 1 No.2. PP. 32-39. http://www.sciencepublishinggroup.com/j/ajaf

Dadzie P K, Amoah M, Tekpetey S L (2014) Preliminary assessment of wealth creation in wood products' business in Ghana: The perspective of lumber and furniture production and implications for entrepreneurship, International Journal of Business and Economic Research,

3(6): 243-249. doi: 10.11648/j.ijber.20140306.15.
http://www.sciencepublishinggroup.com/j/ijber (20 December 2014)

Dadzie P K, Frimpong-Mensah K (2011) Value addition to wood resources, the case of Garden furniture production and export in Ghana; A case study of a local firm, conference paper presented at the 65th international convention of the Forest Products Society, 19th -21st June 2011, Portland, Oregon. U.S.A.
http://www.slideshare.net/julielang/session-8-ic2011dadzie (20 December 2014).

Doomson O, Vlosky R P (2007) A strategic overview of the forest sector in Ghana, Louisiana Forest Products Development Centre working paper #81, School of Renewable Natural Resources, Lousiana State University of Agricultural Centre, Baton Rouge. U.S.A. 17pp.

ITTO (International Timber Trade Organization) (2011) tropical timber market reports *in*; Bandara W A R T W, Vlosky R P (2012) An analysis of the U.S wood products import sector: prospects for tropical wood products exporters, Journal of Tropical Forestry and Environment 2 (02) 49-62.

Ratnasingam J (1998) The South-East Asian furniture industry siege, Southern African Wood and Timber Times 24 (1) 68-72.

The Ghanaian Times of January 23, 2015; www.ghanaiantimes.com.gh/. (3 February 2015)

TIDD.- Timber Industries Development Division (2001) Exporters performance/moving species/direction of trade-lumber (KD) and furniture parts; wood products export report, December, Data Processing Section, Takoradi. Ghana. 33pp.

TIDD (2002) Exporters performance/moving species/direction of trade-lumber (KD) and furniture parts; wood products export report, December, data processing section, Takoradi. Ghana. 36pp.

TIDD (2003) Exporters performance/moving species/direction of trade-lumber (KD) and furniture parts; wood products export report, December, data processing section, Takoradi. Ghana. 36pp.

TIDD (2004) Exporters performance/moving species/direction of trade-lumber (KD) and furniture parts; wood products export report, December, data processing section, Takoradi. Ghana. 42pp.

TIDD (2005a) The first 30 out of 126 exporters of all wood products, Jan-Feb 2005. wood products'export report for February 2005, data processing section of TIDD, Takoradi, Ghana. 32 pp.

TIDD (2005b) Exporters performance/moving species/direction of trade-lumber (KD), flooring and furniture parts. report on export of wood products for December 2005, data processing section of TIDD, Takoradi, Ghana. 54 pp.

TIDD (2006) Exporters performance/moving species/direction of trade-lumber (KD) and furniture parts; wood products export report, December, data processing section, Takoradi. Ghana. 36 pp..

TIDD (2007) Exporters performance/moving species/direction of trade-lumber (KD) and furniture parts; wood products export report, December, data processing section, Takoradi. Ghana. 31pp..

TIDD. (2008). exporters performance/moving species/direction of trade-lumber (KD) and furniture parts; wood products export report, December, data processing section, Takoradi. Ghana. 41 pp.
Waters M M (1970) Woodwork - A course for first exanimations, R & R Clark, Ltd. London. Great Britain. 136 pp.

Proceedings of the 58th International Convention of
Society of Wood Science and Technology
June 7-12, 2015 - Grand Teton National Park, Jackson, Wyoming, USA

Potential of Seed Oil of Hildegardia Barteri (mast.) Kosterm for Biodiesel Production

Abiodun Oluwafemi Oluwadare, femioluwadare@yahoo.com
Adenike Adeniyi, evelynadeniyi2004@yahoo.com

University of Ibadan, Department of Forest Resources Management, , Ibadan

Abstract

This study analysed seed oil of H. barteri as a source of biofuel. Mature fruits of H. barteri were collected from two mother trees and dehulled, oven and sun-dried and milled. Mechanical extractor and solvent extraction (N-Hexane) was used to obtain oil and analysed for presence of C, H, O, S, N, Pb, Cd, Ni, and Co; physicochemical properties, proximate analysis, calorific value and spectra analysis using FTIR. Oil yields ranged from 23.15-30.53% for mechanical and solvent methods. Moisture, crude protein and ash contents were 1.03-2.0, 1.02-1.79 and 0.05-0.12% respectively. Specific gravity, cloud point, conradson carbon, acid value and iodine values ranged from 0.83-0.85, 7.4-8.30C, 0.16-0.27%, 31.85-33.95 mgKOH and 57.3-61.8 respectively while C, O, H, N and S contents were generally higher in oil obtained by mechanical extraction. The Pb level was least (0.007%) in solvent extracted oil and highest (0.023%) in sun-dried mechanically extracted oil. Iodine values of solvent and mechanically extracted samples were 61.85 and 58.6 respectively. Calorific value of sun-dried solvent extracted oil was slightly higher (36,140kj/kg) than the oven-dried (35,690kj/kg).Identified functional groups were alcohol, esters, alkynes and alkanes. Results obtained showed promising indication that the seed oil of Hildegardia barteri could be used for production of biodiesel.

Proceedings of the 58th International Convention of
Society of Wood Science and Technology
June 7-12, 2015 - Grand Teton National Park, Jackson, Wyoming, USA

Assessment of Factors Affecting the Quality of Sliced Veneer from Four Timber Species

Kojo Afrifah A.[1*] *– Kwasi F. Mensah*[2]

[1]Lecturer, Department of Wood Science & Technology
Faculty of Renewable Natural Resource
Kwame Nkrumah University of Science and Technology, Kumasi, Ghana.
**Corresponding author*
kagyapong@gmail.com
[2]Associate Professor, Department of Wood Science & Technology
Faculty of Renewable Natural Resource
Kwame Nkrumah University of Science and Technology, Kumasi, Ghana.
frimpongmensah@hotmail.com

Abstract

The size and quality of timber for processing have reduced in recent times due to declining forest resource base. The most important price determinant of processed timber products however is the quality which is influenced by the raw material and other factors. This study therefore focused on assessing the factors that affect the quality of sliced veneer from *Pterygota macrocarpa*, *Aningeria species*, *Khaya species* and *Antiaris toxicaria* in an industrial setting in order to mitigate them. The study observed 17 defects as the commonest factors affecting the quality of sliced veneer from these species. These quality reducing factors were categorized as natural, material handling, and processing defects. Observations revealed that handling and processing defects could be reduced with the right production techniques. By contrast the effects of natural defects could not be eliminated but could be minimized with quality raw material with low inherent defects.

Keywords: Species, Defects, Sliced Veneer, Timber, Log, Flitch

Introduction

The production of veneer in Ghana is on the ascendancy due to the Government promoting the establishment of more timber industries. In 1990 – 1995 for instance there was an increase of about 29000 m^3 of veneer exported from the country (MFL 1996). Additionally, the increase in demand for veneer products such as plywood, laminated veneer lumber etc. locally mean higher requirements for both sliced and rotary veneer.

For the forest resource of Ghana to support the increases in demand for wood for various uses on sustainable basis, the supplies should be utilized efficiently to minimize waste and increase or improve recovery. Increase in recovery will ensure higher revenue from a unit volume of raw material (Afrifah and Mensah 2014). However, the most important price determinant is the quality or grade of the veneer. Thus a unit volume of sliced veneer of the same species but different in quality will attract different prices.

From the forgone reasoning, it is therefore necessary to conduct studies into the manufacturing processes of sliced veneer, a highly exported veneer from the country to find out how best the quality could be improved.

Four wood species were selected for this research based on their prevalent use for the production of sliced veneer exported in large quantities from Ghana (FPIB 1995). The species were *Pterygota macrocarpa*, *Aningeria species*, *Khaya species* and *Antiaris toxicaria*. They were assessed for factors influencing the quality of the sliced veneers produced from them.

Materials and Methods

The study was conducted at Logs and Lumber Limited (LLL), Kumasi – Ghana, a company that produces large quantities of veneer for export and plywood manufacture. The quality assessment was based on defects considered in the grading rules for grading sliced veneer in Ghana by the Timber Industry Development Division (TIDD) of the Forestry Commission. The defects were categorized as defects and characteristics inherent in wood, discolouration, other growth features, imperfections caused by wood destroying fungi, manufacturing defects, grain defects and defects due to borers.

Ten flitches selected at random for each species were studied. For each flitch ten sheets were randomly picked for observation. A total of hundred sheets were studied for each species.

The defects were further classified as countable and uncountable. Countable defects were graded according to the number and size of the defects as follows:

1. Defects with diameters between 1 and 20 mm.
- 1 to 5 of the defect - 1
- 6 to 10 of the defect - 2
- 11 and up of the defect -3

2. Defects with diameters greater than 21 mm.
- 1 to 3 of the defect - 1
- 4 to 6 of the defect - 2
- 7 and up of the defect - 3

The countable defects included knot, dead knot, mineral deposits, knife marks, shelling, pressure-bar marks, borer hole and inbark.

Uncountable defects were also scored according to the extent to which the defect covers the sheet (i.e. intensity) as follows:

- 1 to 20% of the sheet covered with the defect as 1

- 21 to 40% of the sheet covered with the defect as 2
- And more than 41% of the sheet covered with the defect was scored 3.

Some of these defects are angle grain, irregular grain, resin streak, sap stain, chemical stain, cracks/checks, coarse fiber, splits, buckling, blue-black stain, rot and blue stain.

The veneer sheets were inspected after drying at the drier to ensure that all the defects were present in order to determine their effect on the yield of the studied species. Normally, at the final processing stage (i.e. cutting to size and bundling) attempts were made to remove defects from defective sheets consequently the yield of veneer was reduced.

Results and Discussions

Grain defects

Grain defects found in the four species studied are presented in Table 1. They included angle grain and irregular grain. Angle grain occurred in all the species. This was because all the flitches studied were quarter sliced, therefore the expected orientation of the fibers in the veneer should have been in the general direction of the longer edge. Where possible portions of the sheets were clipped off to reduce the angle grain defect. Irregular grain defect only occurred in *Pterygota macrocarpa*, and *Khaya species*. This defect occurred mostly in the regions of the sheets where large knots and bumps caused deviation of the grains. Grain defects occurring at the end and edges of the sheets were clipped off reducing yield.
In grading, all types of grain patterns are accepted, but undesirable pattern downgrades the veneer (FPIB 1991).

Table 1 Classification of the grain defects in the veneer sheets of *Aningeria species, Antiaris toxicaria, Pterygota macrocarpa* and *Khaya species*

Species	Defect	% of the sheets with defect	% of the sheets with grade		
			1	2	3
Aningeria	Angle grain	56 (4.27)	94.64	5.36	
Antiaris	Angle grain	20 (2.53)	100		
African Pterygota	Angle grain	51 (2.38)	100		
	Irregular grain	19 (1.77)	100		
African Mahogany	Angle grain	88 (2.96)	100		
	Irregular grain	40. (1.78)	100		

The values in parentheses are the standard deviations.

Defects and characteristics inherent in the wood

Table 2 shows the proportion of dead knots and knots found in the studied veneer sheets for the four species. *Anigeria species* and *Pterygota macrocarpa* recorded the highest whilst *Khaya species* recorded the least (Table 2). The knots in *Khaya species* were observed in only one flitch as was the dead knots observed in *Aningeria* spp.

In grading sliced veneer, knots are allowed in the backing and occasionally in the interior but not in the face. Dead knots are not allowed in any of the grades (FPIB 1991). To obtain a higher grade, the knots are removed by trimming. If by virtue of the location of the knot, their removal could cause drastic reduction in yield, they were allowed in the sheets thus sacrificing quality. The knots observed occurred occasionally and were graded as 1 (Table 2). Their presence however downgraded the veneer sheets.

Table 2 Types and classes of the defects and characteristics inherent in the wood of *Aningeria species, Antiaris toxicaria, Pterygota macrocarpa* and *Khaya species*

Species	Defect	% of the sheets with defect	% of the sheets with grade		
			1	2	3
Aningeria	Knots	44(1.78)	100		
	Dead knot	5(1.5)	100		
Antiaris	Knots	27(1.95)	100		
African Pterygota	Knots	43(1.95)	100		
African Mahogany	Knots	4(1.32)	100		
	Dead knot	6(1.98)	100		

The values in parentheses are the standard deviations.

Defects due to other growth features

Table 3 shows the proportions and grades of inbark, resin streak and mineral deposits found in the veneer sheets of the species studied. The minerals and inbark were observed in only *Aningeria* spp. Mineral deposits were prevalent in *Aningeria* spp confirming what had been stated by Farmer (1972). Resin streak was also a prevalent defect associated with *Khaya* spp. and *P. macrocarpa*.

Generally except for Aningeria, the best logs were selected for sliced veneer production with the rejects mostly going for lumber manufacture. Because of the high demand for Aningeria veneer, almost all of Aningeria logs were processed for sliced veneer resulting in the incidence of the observed defects. Veneers, which contained a lot of minerals, were normally used for the production of plywood for the local market.

Table 3 Defects due to other growth features found on the veneer sheets of *Aningeria species, Pterygota macrocarpa* and *Khaya species*

Species	Defect	% of the sheets with defect	% of the sheet with grade		
			1	2	3
Aningeria	Inbark	38(4.69)	92.1	7.89	
	Minerals	74(3.59)	95.95	4.05	
African Pterygota	Resin streak	37(2.49)	100		
African Mahogany	Resin streak	100(0)	99	1	

The values in parentheses are the standard deviations.

Mineral deposits are not allowed in any of the grades of sliced veneer. They therefore had to be removed reducing recovery. There were also some buyers who specialised in buying Aningeria veneer with mineral deposits and graded such veneer as below backing. Inbark and resin streak were only allowed in the last grade. To achieve a higher grade the veneer should be free from these defects.

The resin streaks and mineral deposits caused formation of nicks on knives leading to knife marks on veneer sheets and blunting of knives. Knife marks were immediately corrected in *Aningeria spp* by honing the knives. This accounted for the low incidence of knife marks on their veneers in spite of the prevalence of mineral deposits in Aningeria.

Defects due to discolouration

The proportion of sapstain observed in Antiaris and African Mahogany are shown in Table 4. The stains might have occurred due to the poor storage practices used at the mill.

Antiaris is susceptible to insect and fungi attack and therefore, should ideally be used within hours after felling (TEDB 1994). By contrast, Mahogany is moderately resistant to agents of deterioration. However, both species developed discoloration because their logs were stored for long periods, under harsh conditions and exposed to agents of deterioration. Sapstain is a defect not allowed in high quality veneer and had to be removed resulting in a reduction in the yield.

Table 4 Proportion of discolouration defects found on the veneer sheets of *Antiaris toxicaria* and *Khaya species*

Species	Defect	% of the sheets with defect	% of the sheets with grade		
			1	2	3
Antiaris	Sapstain	22(1.83)	100		
African Mahogany	Sapstain	3(0.46)	66.67	33.33	

The values in parentheses are the standard deviations.

Imperfections caused by wood destroying fungi

Rot was the only defect considered under this category. Table 5 show the proportion of rot in African Pterygota and Antiaris. Rot is not allowed in any grade of sliced veneer (FPIB 1991). In humid weather conditions, rot require weeks or months to develop (Mahut and Nilsson 1992). The rot found in the sheets did not develop at the mill. They were remains of heart-rot in the logs which, were not removed during flitching.

Table 5 Proportion of imperfections caused by wood destroying fungi in the veneer sheets of *Pterygota macrocarpa* and *Antiaris toxicaria*

Species	Defect	% of the sheets with defect	% of the sheets with grade		
			1	2	3

African Pterygota	Rot	23(2.53)	100
Antiaris	Rot	8 (1.66)	100

The values in parentheses are the standard deviations.

Most of the logs of African Pterygota had heart-rot, this accounted for the high incidence of rot in the veneer of African Pterygota as shown in Table 5. Similarly, heart-rot was observed in the large diameter logs of Antiaris. Rots in the veneer sheets were clipped off at the guillotines before bundling and grading.

Manufacturing Defects

Table 6 presents the category of defects due to handling and manufacturing operations. Knife and pressure-bar marks occurred in all the species studied (Table 6). These defects occurred as a result of the formation of the nicks on the knife and pressure-bar. When this defect is not serious and does not affect strength of the veneer it is allowed in low grades of sliced veneer. However, veneer sheets with very serious scratches are rejected (Mahut and Nilsson 1992). During the study the knife marks observed were not many and deep enough to affect the strength of the sheets and therefore did not pose any serious problems to yield but considerably reduced the quality of veneer. It is very important that particular attention is given to the detection of this defect and immediately corrected by honing to ensure the production of high-grade veneer.

Table 6 Proportion of manufacturing defects found on the veneer sheets of *Aningeria species, Antiaris toxicaria, Pterygota macrocarpa* and *Khaya species*

Species	**Defect**	**% of the sheets with defect**	**% of the sheets with grade**		
			1	2	3
Aningeria	Knife marks	2(0.6)	100		
	Pressure-bar marks	1(0.3)	100		
	Cracks/checks	9(1.76)	100		
	Coarse fiber	2(0.4)	100		
	Splits	78(2.66)	88.46	11.54	
	Buckling	3(0.9)	100		
	Blue-black stain	3(0.46)	100		
Antiaris	Knife marks	30(1.56)	100		
	Pressure-bar marks	14(1.63)	100		
	Cracks/checks	20(1.67)	100		
	Coarse fiber	36(3.35)	100		
	Splits	71(2.64)	80.28	8.45	11.27
	Buckling	35(3.72)	100		
	Blue-black stain	19(1.45)	100		
African Pterygota	Knife marks	84(1.78)	100		
	Pressure-bar marks	38(2.27)	100		
	Cracks/checks	7(0.78)	100		
	Splits	48(2.35)	97.92	2.08	
	Buckling	83(2.45)	100		
	Blue-black stain	7(1.27)	100		

Mahogany	Knife marks	37(1.79)	100
	Pressure-bar marks	17(2.33)	100
	Cracks/checks	1(0.3)	100
	Splits	12(2.29)	100
	Buckling	93(0.95)	100
	Blue-black Stain	12(1.54)	100
	Shelling	20(4.0)	100

The values in parentheses are the standard deviation

Cracks on the side next to the knife were observed in all the species with Antiaris recording the highest occurrence. This defect was caused by splitting ahead of the knife or by bending of the sliced veneer as it passed the knife. It can be minimized by adequate heating of the wood and the use of correct pressure-bar pressure just ahead the tip of the knife. Antiaris was not steamed before processing, this might have contributed to the high occurrence of cracks in the sheets. Even though, Antiaris is relatively soft it should be heated to render it plastic and prevent cracking in the course of processing. All the other three species did not have serious cracks as shown in Table 6.

The splits in the veneer were generally related to splits already occurring in the flitches and rough handling. Splitting was highest in Anigeria and Antiaris (Table 6). According to Hawthorne (1990) Aningeria has a natural tendency to split. Consequently, most of the logs selected to be processed had splits at the end. New splits developed and old ones worsened during heating and slicing of the flitches due to poor handling practices. Antiaris, African mahogany, and pterygota developed the splits due to poor handling practices. Antiaris recorded high splitting because it was processed cold and therefore was not plastic enough. Cracks and splits are allowed only in the worse grades of sliced veneer (i.e. backing) so these were trimmed off. The trimming of some of the sheets resulted high reduction of yield.

Coarse fiber could arise from cutting thicker veneer, cutting unheated logs, poor adjustment of pressure-bar and the use of blunt knife (Mahut and Nilsson 1992). This defect was observed in Aningeria and Antiaris. The defect was serious in Antiaris because thicker sheets of 1.8 mm were being sliced compared to the 0.5 mm of Aningeria, 0.6 mm of African Pterygota, , and 1.5 mm of Mahogany. Slicing Antiaris without heating also compounded the problem. To minimize this defect proper heating of the wood and proper adjustment of the pressure-bar should be adopted.

Buckling was observed in all the species studied (Table 6). Buckling might have been caused by stresses in the wood, by irregular grain, irregular shrinkage, irregular drying rate or improper setting of slicer. Buckling was not a serious problem in Aningeria but African Pterygota, Antiaris and Mahogany recorded high incidence of this defect with the latter being the highest.

Mahogany recorded high incidence of grain defects in the form of angle and irregular grain. This coupled with irregular drying rates might have contributed to the buckling in the species. Knots which, contributed to irregular shrinkage were also observed as serious defects in Antiaris and African Pterygota. Stresses caused by the knots, grain defects and irregular drying rates might be the cause of buckling in Antiaris and African Pterygota. To reduce this

defect proper drying schedules should be adopted to dry the veneer to uniform moisture contents and maximum restraint should be used to hold the veneer flat when drying.

Blue-black stain was caused by the condensation of water on the knife and pressure-bar, which on contact with the wood containing tannins reacted to form a blue-black stain that stained the veneers. This defect imparts an unpleasant colour to the veneer and therefore should be controlled by cleaning and lacquering of the knife and pressure-bar.

Shelling was observed in Mahogany. The defect may be caused by overheating of the wood, too much pressure-bar pressure, too sharp a pressure-bar or dull knife (Mahut and Nilsson 1992). Observations revealed that steaming of flitches was not based on any proper schedule. For this reason the cause of this defect could not be easily ascertained. Shelling is not allowed in the high grades of sliced veneer. The portions with the defect were trimmed off reducing the yield.

Conclusions

This study assessed the factors affecting the quality of sliced veneer of *Aningeria spp, Antiaris toxicaria, Pterygota macrocarpa, and Khaya spp* in a factory setting.

The quality of produced sliced veneer were generally low due to the presence of preventable or manufacturing defects such as sapstain, knife marks, buckling, cracks, checks, splits, etc. The use of poor quality logs also resulted in veneer sheets with unpreventable natural defects such as knots, irregular grain, heart rot, etc. Implementation of proper processing techniques such as appropriate storage, heating, selection of good quality logs, proper handling practices, and etc. will mitigate the prevalence of defects and improve quality of sliced veneer and yield.

References

Afrifah KA, Mensah KF (2014) Assessment of the Effect of Log Diameter and Inherent Characteristics of Four Timber Species on the Yield of Sliced Veneer. Global Advanced Research Journal of Physical and Applied Sciences Vol. 3(2) pp. 017-024.

Farmer RH (1972) Handbook of hardwoods. Second ed. Department of Environmental Building Research Establishment, London. Pp22-91.

FPIB (1991) Decorative Veneer Grading Rules for Ghana. Forest Products Inspection Bureau, Takoradi, Ghana. 15pp.

FPIB (1995) Welcome to forest Products Inspection Bureau (FPIB). Fourth ed. Forest Products Inspection Bureau, Takoradi. 57pp.

Hawthorne WD (1990) Field guide to the forest trees of Ghana. Chatham: Natural resources institute for the overseas development administration, London, Ghana forestry series 1. 278pp.

Kollmann FFP, Kuenzi EW, Stamn UA (1975) Principles of wood Science and Technology. Springer-Velag, New York. 703pp.

Mahut J, Nilsson KG (1992) Decorative Veneer and Plywood Production. Technical University, Zvolen. 129pp.

MLF (1996) Forestry development master plan, 1996 – 2020. Ministry of Lands and Forestry, Accra, Ghana. 24pp.

TEDB (1994) The tropical timbers of Ghana. Timber Export Development Board, Takoradi, Ghana. 87pp.

Proceedings of the 58th International Convention of
Society of Wood Science and Technology
June 7-12, 2015 - Grand Teton National Park, Jackson, Wyoming, USA

Moisture Stability of Post-manufacture Thermally Modified Welded Birch (Betula pendula L.) Wood

Jussi Ruponen, jussi.ruponen@aalto.fi

Aalto University, Tekniikantie 3, Vuorimiehentie 1, Espoo FI-00076

Abstract

Welding of wood provides strong wood-to-wood bonding without adhesives. However, the bonds suffer from delamination when exposed to moist conditions. Therefore, this work studies if the delamination tendency of linear-friction welded wood bonds in birch (Betula pendula L.) could be reduced by post-manufacture thermal modification. According to the hypotheses, firstly, the bond line in birch wood has unsatisfactory water resistance and poor bond strength in moist conditions. Secondly, water resistance, or wet strength, could be maintained above certain level through thermal modification, yet below the level of non-modified welded wood, when immersed in water. The work included linear-friction welding of birch, thermal modification (at 200°C for 3 h and 5 h) under superheated steam in atmospheric pressure, determination of anti-swelling efficiency (ASE), internal bond (IB) strength testing, and water immersion to observe delamination behavior. Thermal modification improved the dimensional stability, resulting ASE values ranging from 25.9% to 38.0%. The IB strength in dry condition decreased as the thermal modification, yet yielding a value closer to wet. During water immersion, the non-modified specimens suffered from delamination more compared to thermally modified. Results indicate thermal modification could be applied to stabilize the welded bond lines, but the process needs optimization, for instance, to insure scalability and to minimize the loss in strength properties.

Proceedings of the 58th International Convention of
Society of Wood Science and Technology
June 7-12, 2015 - Grand Teton National Park, Jackson, Wyoming, USA

Early Stage Researcher Full Oral Slot (8 minutes) Session
Moderators: *Dick Sandberg, Luleå University of Technology, Sweden and Bonnie Yang, Mississippi State University, USA*

Dimensional Optimization of Beetle Kill Pine Interlocking Cross Laminated Timber (ICLT).

Massih Nilforoushan Hamedani, m.nilforoushan@utah.edu
Ryan Smith, rsmith@arch.utah.edu
Ben Hagenhofer-Daniell, ben.hagenhofer.daniell@utah.edu

University of Utah, 375 S. 1530 E. RM 236 , Salt Lake City, UT 84112

Abstract

Moisture content is a critical factor for dimensional stability in engineered wood products. This paper focuses on one such product: Interlocking Cross Laminated Timber fabricated with beetle killed pine from the intermountain west. This research engages in supply chain mapping, and the co-relational assessment of drying techniques that can lower moisture content to a consistent level for dimensional stability and performance of the product. The research will ultimately suggest a drying regime in-line with existing supply chains that is optimized for economy, schedule, and repeatability. While the focus is on a regionally specific timber resource and engineered timber product, the lessons learned should be applicable to engineered solid timber products generally. This research will also establish a framework for evaluating the management of moisture content in timber resources beyond beetle killed pine. In order to assess the drying phases in current supply chains, different intermountain supply chain strategies have been studied based on information from local sawmills and logging companies. Different approaches to dry solid timber products based on determined supply chains have been evaluated to develop efficient supply chain options to increase the opportunities for further commercialization of ICLT and other solid timber products in the USA.

Proceedings of the 58th International Convention of
Society of Wood Science and Technology
June 7-12, 2015 - Grand Teton National Park, Jackson, Wyoming, USA

Shearing Behavior of SIP Wall Shelled with Bamboo Scrimber Panel

Xuehua Wang[1,3]
Assistant professor, Email: xuehua3099@sina.com
Xiaohuan Wang[2]
Associate professor, Email: wxh811118@126.com
Zhihui Wu[1]*-
Professor, Email: wzh550@sina.com
Benhua Fei[3]*
Professor, Email: feibenhua@icbr.ac.cn

[1] Nanjing Forestry University
[2] Beijing Forestry Machinery Research Institute of the State Forestry Administration
[3] International Centre for Bamboo and Rattan
* *Corresponding Author*

Abstract

Shearing behavior of Structural Insulated Panel (SIP) wall, which was consisted of styrofoam core board, shell panel of bamboo scrimber and frame of Spruce-Pine-Fir (SPF) dimension lumber, was tested under monotonic and cyclic loads in this study. The results showed that SIP wall failed at similar positions under two loading modes, while more seriously destruction occurred under cyclic than monotonic load. There was a linear relationship between load and displacement at the initial loading stage, which indicated wall worked under elastic state; at later loading stage, bearing capacity and rigidity were reduced as result of wall slip. Shearing strength was 20.0 $kN \cdot m^{-1}$, 15.8 $kN \cdot m^{-1}$ respectively under monotonic and cyclic loads, which met the requirement of GB 50005 - 2003. Energy consumption of the SIP wall covered with bamboo scrimber was 11556.6 $J \cdot m^{-1}$.

Key words: bamboo scrimber panel, SIP wall, monotonic and cyclic loading, shearing behavior

Introduction

Structural Insulated Panel (SIP) is one of prefabricated building materials which has been the topic of interest among researchers in recent years (Ali et al. 2013). Compared with traditional light-frame wood structure, SIP building system has more advantages in insulation properties, acoustic performance, seismic performance and material utilization (Jared 1997; Michael 2000; Edward 2006; Kermani 2006).

Bamboo is a fast growing and resourceful biomass material in China. Given increasingly serious shortage of wood resources, bamboo would be an effective alternative resource of wood. There are various bamboo-based products, such as bamboo curtain plywood, bamboo mat plywood, bamboo glulam, and so on (Wang et al. 2003). Bamboo scrimber, which obtains by bamboo reorganization and remolding, is one of the new and more competitive products during the many bamboo products (Yu 2012).

There was a higher compression and tension strength of bamboo scrimber than that of larch and spruce (Zhang et al. 2012). While reports about bamboo scrimber used as structural component are only seen in exemplary buildings, there was few reports about bamboo scrimber used as SIP shell panel yet. In order to take full advantages of SIP system and bamboo scrimber, bamboo scrimber was expected to be used as shell panel of SIP wall. In this study, SIP wall shelled with bamboo scrimber was tested under monotonic and cyclic loads. Failure phenomenon was observed and shearing parameters were calculated to investigate the shearing performance to provide some information for bamboo scrimber used in SIP system.

Experimental Procedure

Materials and methods

Bamboo scrimber used for SIP shell was made of *Neosino calamus affinis*. SIP panel contains two shell panels and one core board. Size of bamboo scrimber shell panel was 2440×1220×6 mm (length ×width × thickness). Size of polystyrene core board was 2364×1144×89 mm (length × width ×thickness). Polyurethane adhesive was used to bond shell panel and core board according to ASTM D2559. Distance between shell edge to core edge was 38mm. Groove formed by shell panel and core board was filled with wooden dimension-lumber (Fig. 1).

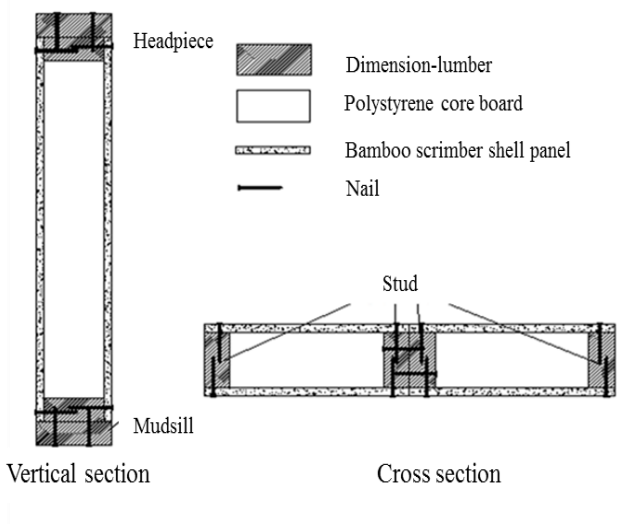

Fig. 1 Section of SIP wall

SIP wall sample was consisted of two SIP panels and eight wooden dimension-lumbers which composed headpiece, mudsill and studs of SIP wall. Headpiece and mudsill were consisted of two dimension-lumbers respectively. Mid-studs between two SIP panels were consisted of two dimension-lumbers, the right and left stud was consisted of one dimension-lumber respectively. Sizes of dimension-lumbers were listed in table 1. Dimension-lumbers and shell panels were connected by nails. The wall and load beam, the wall and groundsill were connected by screw bolts. Hold-downs were fixed between the left/right stud and mudsill (Fig. 2). Connectors between hold-down and left/right stud were tapping screws, and between hold-down and mudsill were screw bolts.

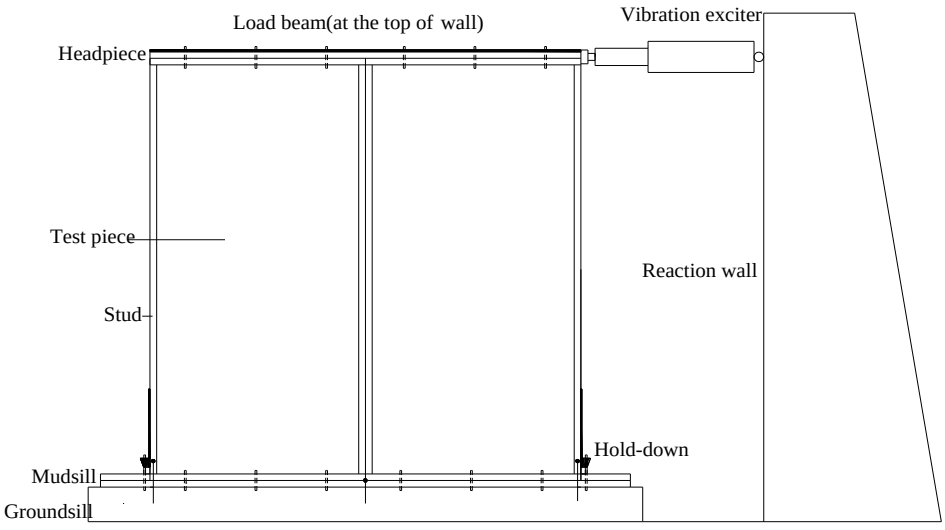

Fig. 2. Sketch for SIP wall installation and loading position

Loading method

Only horizontal load, no vertical load was applied during testing.

Monotonic load testing was loaded according to standard ISO 22452. Loading program was controlled by force; load increased sustainably until SIP wall wrecked. Loading speed was set at 6 kN/min.

Cyclic load testing was loaded according to standard ISO 21581. Loading program for cyclic load testing was controlled by displacement. The ultimate displacement obtained in monotonic load testing was used as control displacement. Taken 1.25%, 2.50%, 5.00%, 7.5%, and 10.00% of the ultimate displacements as target displacement and loaded in order, every displacement was repeated for one time. Then taken 20%, 40%, 60%, 80%, 100%, 120% of the ultimate displacements as target displacement and loaded in order, every displacement was repeated for three times. Loading speed was set at 100 mm/min.

Shearing behavior parameters

Skeleton curve under cyclic load gained according to the first cycle of different target displacements was showed in Fig. 3 (the curve with black box); displacement-load curve under monotonic load and its symmetrical curve about base point were also figured.

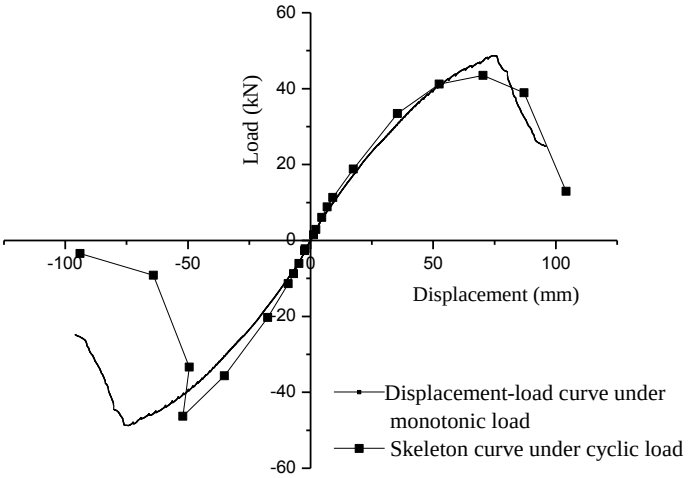

Fig. 3. Skeleton curve under cyclic load and displacement-load curve under monotonic load

Shearing behavior parameters were defined according to equivalent elastic-plastic curve (abbreviated as EEPC) (Dolan et al. 1996; Hu 2007; Guo et al. 2011).

Results and Discussions

Phenomenon of SIP wall damage

Failure phenomenon was similar under both monotonic and cyclic loads. There were three stages: elastic stage, plastic stage and failure stage (Fig. 4). At the initial stage, load-displacement curve shaped nearly linear. As load increased, wall displacement increased with slight sound. As increasing to maximum load, displacement increased rapidly, cracks turned up between hold-down and the wall, bamboo scrimber panel and the mudsill, bearing capacity of the wall dropped sharply.

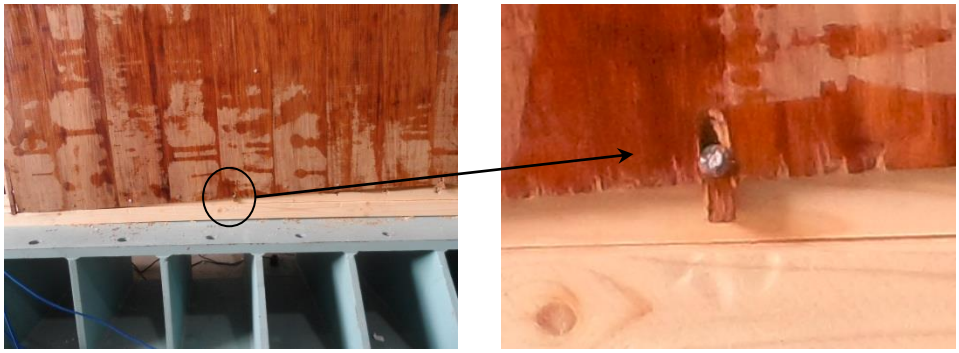

a. Under monotonic loading

b. Under cyclic loading

Fig. 4. Damage situation at bottom of SIP wall

Cracks were mainly distributed at bottom of SIP wall. Damage at mudsill was shown in Fig. 5. Shell panel where contacting with mudsill and tacked nails was destroyed under both monotonic and cyclic loads. Under monotonic load, nails connecting mudsill and bamboo scrimber panel stayed in mudsill and looked undamaged from the part exposed on panel surface (Fig. 5-a). Under cyclic load, nails connecting mudsill and bamboo scrimber panel were pulled out and bended from the pulling out part, stayed in bamboo scrimber panel. Mudsill was destroyed seriously (Fig. 5-b).

Fig 5a. Diagonal of vibration exciter under monotonic load b. Lower of vibration exciter under monotonic load

c. Diagonal of vibration exciter under cyclic load d. Lower of vibration exciter under cyclic load
Fig. 6. Damage at hold-downs

Damage of hold-downs at left (located at diagonal of vibration exciter) and right (located at lower of vibration exciter) side stud was different under monotonic load. The left one seemed no damage (Fig. 5-a) while the right was pulled out from side stud and bended (Fig. 5-b). Hold-downs at left and right were both pulled out (Fig. 6-c, d) and bended obviously under cyclic load.

Displacement-load curve

The displacement-load curve of SIP panel under monotonic and cyclic loads was showed in Fig. 7. The black line was displacement-load curve under monotonic load (in first quadrant); its symmetrical curve about base point was given (the black line in third quadrant). The colored line was the displacement-load curve under cyclic load, and the different colors meant different cycles with different control-displacements.

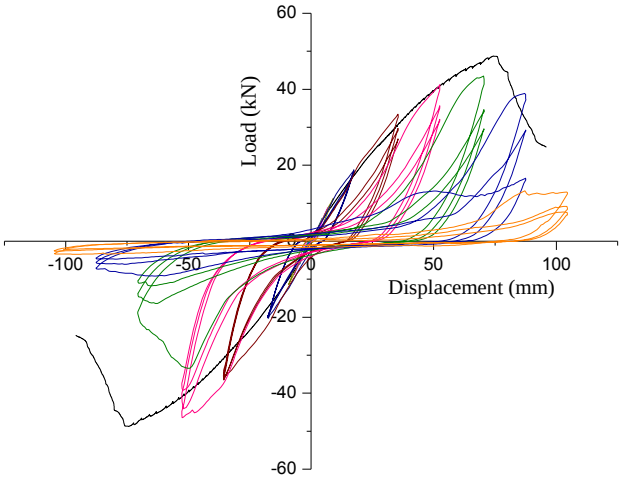

Fig. 7. Displacement-load curve under monotonic and cyclic load

Conclusions

Failures were mainly occured at bottom of wall. Under monotonic load, nails stayed in mudsill, looked undamaged from the part exposed on panel surface. Shell panel and mudsill was slightly damaged. Hold-down lower vibration exciter turned bended. Under cyclic load, nails were forced out and bended at the pulling out part, stayed in bamboo scrimber panel. Mudsill was destroyed seriously. Hold-downs at left and right were both bending deformation.

Displacement-load curve was almost linear at initial loading stage both under monotonic and cyclic loads. Area enclosed by hysteresis loop was small. Rheostriction phenomenon was obvious form the displacement- load curve. Wall members were damaged as repeated loading, and further lessened strength, load capacity and stiffness. At grades with different target displacement, hysteresis loop turned from S-shape to Z-shape as the displacement increased, wall slip effect appeared.

Ultimate load, shearing strength, ultimate displacement and elastic stiffness of the SIP wall shelled with 6 mm bamboo scrimber were 48.8 kN, 20.0 $kN \cdot m^{-1}$, 82.5 mm, 971.1 $kN \cdot m^{-1}$ under monotonic load, and 44.9 kN, 17.8 $kN \cdot m^{-1}$, 63.7 mm, 1140.7 $kN \cdot m^{-1}$ under cyclic load. Energy dissipation under cyclic load was 11556.6 44.9 kN.

References

ASTM (2004) D 2559-2004. Standard Specification for Adhesives for Structural Laminated Wood Products for Use under Exterior (Wet Use) Exposure Conditions, West Conshohocken, PA 19428-2959.

ASTM (2006) E564-06, Standard Practice for Static Load Test for Shear Resistance of Framed Walls for Buildings, West Conshohocken, PA 19428-2959.

Kermani A, Hairstans R (2006) Racking performance of structural insulated panels. Journal of structural Engineering, 132(11): 1806-1812.

Panjehpour M, Ali AAA, Voo YL (2013) Structural Insulated Panels: Past, Present, and Future. Journal of Engineering, Project, and Production Management, 3(1): 2-8.

GB (2003) 50005-2003, Code for design of timber structures, Beijing, PA 100000.

Dolan JD, Johnson AC (1996) Cyclic tests of long shear walls with openings. Virginia Polytechnic Institute and State University, Timber Engineering Report No. TE-1996-002. Blacksburg, Virginia: VPISU. 39 pp.

Du Min, XIE Bao-yuan, FEI Ben-hua, WANG Xiao-huan, LIU Yan (2013) Shear Performance of Wood-Frame Shear Walls Made of Domestic Material. Journal of Building Materials 16(3): 487-490 (in Chinese).

Du Min, Xie Baoyuan, Fei Benhua, Wang Xiaohuan, Liu Yan (2012) Shear performance of wood-frame shear walls with cross brace. Chinese Journal of Applied Mechanics 29(3): 314-320 (in Chinese).

Edward L Keith, P E (2006) Standardization testing of structural insulated panels (SIPs) for the structural insulated panel association, Gig Harbor, Washington. APA Report No. T2006P-33 for the Engineered Wood Association, Tacoma, WA. 40 pp.

Guo H, Hao J, Li F (2011) Cyclic test of simi-rigid composite steel frame with diagonally stiffened steel plate shear walls. Journal of Earthquake Engineering and Engineering Vibration, 31(1): 54-60.

Hu Guoxi (2007) Study about lateral force resisting performance of irregular wooden shear wall. MS thesis, Tongji University, Shanghai, 84 pp (in Chinese).

ISO (2011) 22452-2011, Timber structures - Structural insulated panel walls - Test methods, Geneva, Case postale 56 · CH-1211.

ISO (2010) 21581, Timber structures - Static and cyclic lateral load test methods for shear walls, Geneva, Case postale 56 · CH-1211.

Jared Bernard Jamison (1997). Monotonic and cyclic performance of structurally insulated panel shear walls. MS thesis, Faculty of the Virginia polytechnic institute and state university, Virginia, 177 pp.

Liu Yan, Ni Chun, Lu Wensheng, Lu Xilin, Zhou Dingguo (2008) Effect of variable upper stiffness on the performance of wood shear walls. China Civil Engineering Journal, 41(11):63-70 (in Chinese).

Morley, M. (2000). Building with structural insulated panels (Sips): strength and energy efficiency through structural panel construction. Taunton Press, 192 pp.

Shim KB, Park MJ, Hwang KH, Park JS, Park MJ(2010) Shear performance of hybrid post and beam wall system with structural insulation panel (SIP). Mokchae Konghak 38(5): 405-413.

Wang Zhao-hui, Jiang Ze-hui (2003) Status on standards for bamboo-based panels and its prospect. World Bamboo and Rattan, 1(3):5-10 (in Chinese).

Yu Wen-ji (2012). Current Status and Future Development of Bamboo Scrimber Industry in China. China Wood Industry, 26(1):11-14 (in Chinese).

ZHANG Jun-zhen, REN Hai-qing, ZHONG Yong, ZHAO Rong-jun (2012). Analysis of compressive and tensile mechanical properties. Journal of Nanjing Forestry University (Natural Sciences) 36(4):107-111 (in Chinese).

Proceedings of the 58th International Convention of
Society of Wood Science and Technology
June 7-12, 2015 - Grand Teton National Park, Jackson, Wyoming, USA

Life-Cycle Inventory Analysis of I-joist Production in the United States

Richard D. Bergman [1*]

[1] Research Forest Product Technologist
U.S. Forest Service Forest Products Laboratory, Madison, Wisconsin, USA
* *Corresponding author*
rbergman@fs.fed.us

Abstract

Documenting the environmental performance of building products is becoming increasingly common. Creating environmental product declarations (EPDs) based on life-cycle assessment (LCA) data is one approach to provide scientific documentation of the products' environmental performance. Many U.S. structural wood products have LCA-based "eco-labels" developed under the ISO standard 14025. In this study, the standard dictates underlying life-cycle inventory (LCI) data to be used reflect current practices in the industry. Therefore, gate-to-gate manufacturing LCI data for I-joist must be developed to construct updated cradle-to-gate LCAs for southeastern (SE) and for Pacific Northwestern (PNW) regions of the United States. Modeling the production weighted-average primary industry data per 1.0 km of I-joists with an assumed average depth of 4.8 cm through LCI analysis provides cumulative energy consumption and environmental outputs. For PNW and SE, cumulative mass allocated energy consumption associated with manufacturing 1.0 km of I-joist was found to be 65.7 and 71.0 GJ/km, respectively, with about 30% of the primary energy provided from wood residues. Emission data produced through modeling found that estimated biomass and fossil CO_2 emissions in kg/km were, respectively, 1,774 and 1,969 for the PNW and 1,808 and 2,042 for the SE. One km (5,240 oven-dry kg wood portion, on average) of I-joist stores about 9,610 kg CO_2 equivalents. The amount of carbon stored in I-joists thus exceeds total CO_2 emissions during manufacturing by about 200%. From this study, the gate-to-gate I-joist manufacturing LCI data can now be incorporated into the cradle-to-gate LCAs to develop an updated EPD.

***Keywords*:** environmental product declaration, life-cycle inventory, I-joists, life-cycle analysis, LCA, wood, structural composite lumber

Introduction

Documenting the environmental performance of building products is becoming widespread because green building programs and concerns that some green-marketing claims are misleading (i.e., green-washing). Developing environmental product declarations (EPDs) for building products is one way to provide scientific documentation and to counter green-washing (Bergman and Taylor 2011). In addition, EPDs are increasingly being required in green building rating systems and building codes. Life-cycle inventory (LCI) data are the underlying data for subsequent development of life-cycle assessments (LCAs) and EPDs. EPDs are similar to nutritional labels for food. The LCI was in conformance with the Product Category Rules (PCR) for North American Structural and Architectural Wood Products (FPInnovations 2013) and ISO 14040/14044 standards (ISO 2006a, b). This report follows data and reporting requirements as outlined in the PCR and contains the LCI components for producing a North American EPD (ISO 2006c; FPInnovations 2013).

LCI compiles all raw material and energy inputs and environmental outputs associated with the manufacture of a product on a per-unit basis within carefully defined system boundaries. These boundaries can be limited to only one stage within the product lifecycle (e.g., gate-to-gate). Multiple sequential LCI stages are usually combined in an LCA. LCAs describe the total environmental impact for a particular product, referred to either as cradle-to-gate (raw material extraction to mill gate output) or as cradle-to-grave (raw material extraction to waste disposal) analysis.

Description of I-joists

Many engineered structural wood products have been developed in the last several decades, eg, I-joists (Fig 1). An I-joist is comprised of a web made from structural wood panel, mostly oriented strandboard (OSB) and some plywood. The web is glued between two flanges made from solid-sawn or finger-jointed lumber, but mostly laminated veneer lumber (LVL) (USEPA 2002; Wilson and Dancer 2005; Stark et al. 2010; ASTM 2013). I-joists have an “I” shape form and are measured in linear feet in the United States. Production values and study results were reported per linear km with an assumed average depth of 4.8 cm. I-joist depth varies notably, but large quantities of I-joists made in the United States have a depth of 4.8 cm. These engineered structural wood products are designed to be used in the same manner as solid wood products such as sawn lumber but with different properties.

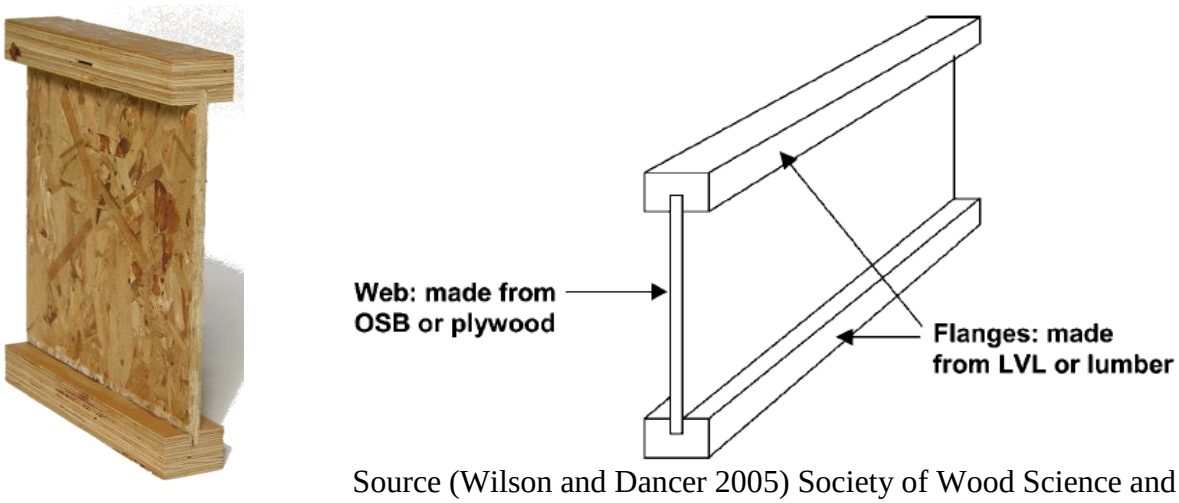

Source (Wilson and Dancer 2005) Society of Wood Science and Technology

Figure 8. I-joist.

Goal

The goal of this paper is to document the gate-to-gate LCI of I-joist manufacturing for Pacific Northwest (PNW) and Southeast (SE) United States as part of a cradle-to-gate LCA. The paper documents material flow, energy type and use, emissions to air and water, solid waste production, and water impacts for the I-joist manufacturing process per 1.0 km. Primary mill data were collected through a survey questionnaire mailed to I-joist plants. This survey tracked raw material inputs (including energy), product and byproduct outputs, and emissions within the cut-off rules and system boundary definition to water, air, and land. An industry-standard production unit (i.e., reference unit) was incorporated that can be translated to a metric production unit. Secondary data, such as pre-mill gate processes (e.g., wood and electricity production), were drawn from peer-reviewed literature per CORRIM guidelines (CORRIM 2010). Material and energy balances were calculated from primary and secondary data. Using these material and energy data, the environmental outputs were estimated by modeling using the software package SimaPro 8 (Pré Consultants 2015), which follows internationally accepted standards and uses the U.S. LCI Database (NREL 2012).

A large sample is required to attain results that are representative of the I-joist industry. CORRIM (2010) protocol targets a minimum of 5% of total production with preferred percentage of 20% for an industry such as the I-joist industry with relatively few manufacturers.

Method

Scope

This study covered the manufacturing stage of I-joist from web and flange components to final product leaving the mill according to ISO 14040 and 14044 standards (ISO 2006a,b; ILCD 2010; FPInnovations 2013). Impacts from (offsite) oriented strandboard (OSB), laminated veneer lumber (LVL), plywood, softwood plywood, and finger-jointed lumber production were included in the analysis (Kline 2005; Wilson and Sakimoto (2005); Bergman 2015; Milota et al. 2005). New data, once developed, will be incorporated into the cradle-to-gate I-joist LCA. OSB and plywood made up the web materials whereas LVL and finger-jointed lumber comprised the flange materials. Data for dry planed softwood lumber acted as a proxy for finger-jointed lumber. Because finger-jointed lumber has additional processing from cutting and gluing compared to solid-sawn lumber, the emission estimates shown in the present study will likely be lower than if finger-jointed lumber data were incorporated. The manufacturing stage LCI was the result of a gate-to-gate analysis of cumulative energy of manufacturing and transportation of raw materials.

Selecting an allocation approach is a vital part of a LCI study. In the present study, all primary energy and environmental outputs were assigned by mass allocation. The decision was justified by the understanding that the wood residues are coproducts with a value rather than a waste material.

Industry data

Five U.S. I-joist plants representing 57.7% of 2012 U.S. I-joist production (63,135 km) provided primary data for the PNW and SE (APA 2014). Total U.S. I-joist production for 2012 was 109,387 km. The surveyed plants provided detailed annual production data on their facilities, including on-site fuel consumption, electrical usage, web and flange volumes, and I-joist production for 2012. A previous 2000 U.S. I-joist LCI study was performed by Wilson and Sakimoto (2005) that covered 33% and 27% of production in the PNW and SE, respectively. Production data for I-joist by region are no longer available.

Declared unit

The present study selected a declared (reference) unit of 1.0 (linear) km of I-joist with an assumed average depth of 4.8 cm. For conversion from the U.S. industry measure, 1 km equals 3.281 thousand ft. Cumulative energy consumption and LCI flows were reported per 1.0 km of the final product, I-joist.

System boundary

The defined system boundary determined the unit processes to include and standardized material flows, energy use, and emission data. The cumulative system boundary is shown by the solid line in Fig 2 and includes both on- and off-site emissions for all material and energy consumed. Three main unit processes exist in manufacturing I-joist: (1) routing and shaping of web and flanges, (2) assembly of I-joists, and (3) sawing and curing with energy generation as an auxiliary process (USEPA 2002; Wilson and Dancer 2005). All emissions (i.e., environmental outputs) and energy consumed were assigned to the I-Joist and co-products (i.e., sawdust) by mass.

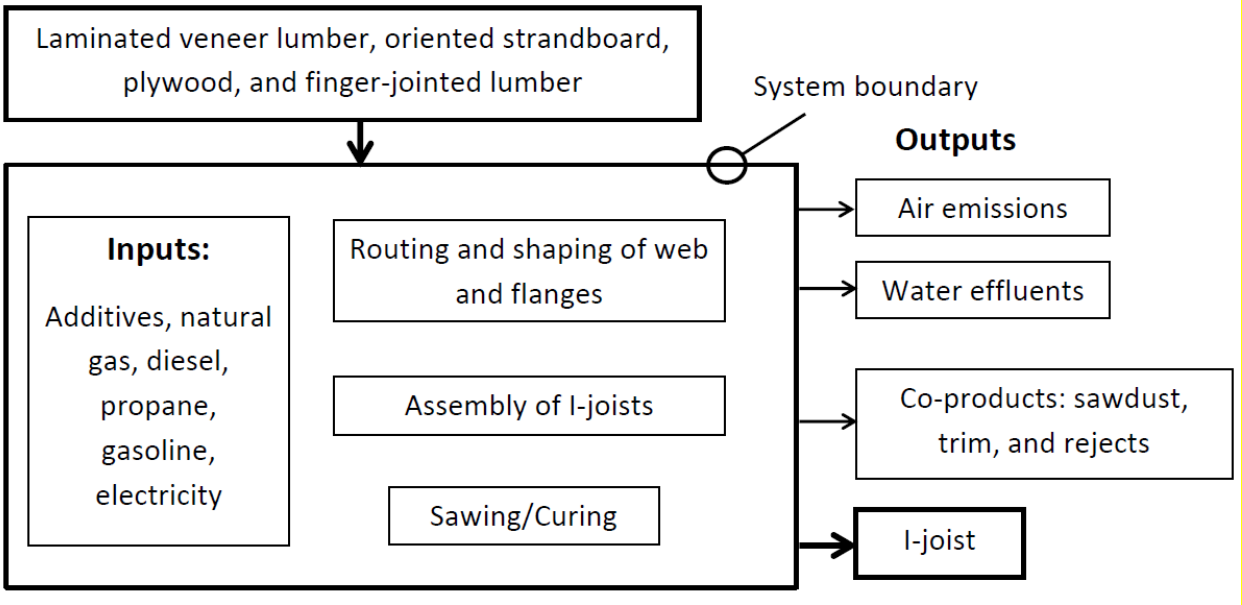

Figure 9. System boundary for I-joist manufacturing life-cycle stage

Fuel resources used for the cradle-to-gate production of energy and electricity were included within the cumulative system boundary. Off-site emissions include those from grid electricity production, transportation of feedstock and additives to the plant, and fuels produced off-site but consumed on-site. Ancillary material data such as motor oil, paint, and hydraulic fluid were collected and were part of the analysis.

Results and Discussion

Five I-joist plants provided detailed primary data on mass flow, energy consumption, fuel types, and air emissions. Primary data were weight-averaged based on each mill's production volume and modeled using LCA modeling software to estimate cumulative energy consumption and environmental outputs expressed on a per 1-km unit basis with an assumed depth of 4.8 cm.

Energy inputs

Weighted-average energy inputs consumed on-site at the I-joist manufacturing site were developed from survey data (Table 1). Electricity and natural gas were the primary energy inputs at 378 kWh and 36 m^3 for the PNW and 312 kWh and 41 m^3 for the SE per linear km of I-joist. Primary energy is energy embodied in the original resources such as crude oil and coal before conversion (e.g., combustion). Thus, PNW I-joist manufacturing consumed more electricity but less natural gas. The production-weighted coefficient of variation (CoVw) showed the large variation for natural gas consumption for the PNW with a value of 103%, although consumption per km of final product was somewhat similar to the SE value of 41 m^3.

Table 5. Weighted-average on-site energy inputs for I-joist manufacturing per km

	Pacific Northwest			Southeast		
	Quantity	Unit	CoVw[a] (%)	Quantity	Unit	CoVw[a] (%)
Energy inputs						
Electricity	378	kWh	35%	312	kWh	20%
Natural gas	36	m^3	103%	41	m^3	49%
Diesel	2.99	L	76%	4.77	L	16%
Propane	3.87	L	4.7%	4.73	L	5.3%
Gasoline	0.054	L	–	0.217	L	141%

[a] Production-weighted coefficient of variation.

Material

To evaluate data quality, a mass balance was performed (Table 2). For the material inputs, LVL, OSB, plywood, and finger-jointed lumber usage were 2,318, 1583, 1033, and 797 oven-dry (OD) kg for the PNW and 2,597, 2,212, 0, and 28 OD kg for the SE plants, respectively, to produce 1.0 km of I-joists. Final mass of the PNW I-joist was heavier at 5,760 OD kg compared to 4,840 OD kg for SE. The average mass of an I-joist is 5,270 OD kg/km. The mass balance also includes additives. Phenol-resorcinol-formaldehyde (PRF) resin was the largest component of the additives used to glue the I-joist together as a single unit followed by a hardener. Of special unit is the large difference in consumption between the regions and the large variance for additives in the SE region, up to 141%.

Table 6. Mass balance of I-joist manufacturing per km

	Pacific Northwest			Southeast		
	(OD kg)	Mass (%)	CoVw[a] (%)	(OD kg)	Mass (%)	CoVw[a] (%)
Feedstocks	INPUTS			INPUTS		
Laminated veneer lumber	2318	40.2%	58%	2597	53.7%	2.4%
Oriented strandboard	1583	27.5%	3.6%	2212	45.7%	7.0%
Plywood	1033	17.9%		0	0.0%	
Lumber, finger-jointed[b]	797	13.8%	162%	28	0.6%	
TOTAL, FEEDSTOCK	5731	99.5%	19.0%	4809	99.4%	2.2%
Additives						
Phenol-resorcinol-formaldehyde resin	13.8	0.2%	71.4%	33.5	0.7%	141%
Phenol-resorcinol resin	1.9	0.0%	245%	0.0	0.0%	
Aqueous emulsion polymer	0.0	0.0%		1.5	0.0%	141%
Polyurethane polymer	0.0	0.0%		0.3	0.0%	141%
Hardener	9.0	0.2%		0.5	0.0%	141%
Catalyst	2.0	0.0%	157%	0.0	0.0%	
TOTAL, ADDITIVES	25	0.4%	47.1%	36	0.7%	46.2%
TOTAL, IN	5760	100%		4840	100%	
Products	OUTPUTS			OUTPUTS		
I-joist	5381	93.4%	21.9%	4415	91.2%	4.6%
Co-Products						

Sawdust, sold	363	6.3%	99%	411	8.5%	18%
Sawdust, wood fuel	0	0.0%		1	0.0%	141%
Panel trim. Sold	2	0.0%		17	0.4%	141%
Rejects	10	0.2%		0	0.0%	
TOTAL, CO-PRODUCTS	374	6.5%	98%	428	8.8%	46%
TOTAL, OUTPUTS	5760	100%		4840	100%	

[a] Coefficient of variation, production-weighted.
[b] Used dry planed lumber as proxy.

Cumulative energy consumption

Cumulative energy consumption for manufacturing I-joist was 65.7 and 71.0 GJ/km for the PNW and SE, respectively, with wood fuel accounting for about 30% (Table 3). Listed values include impacts from manufacturing the wood components (i.e., flanges and web). Wood residues and natural gas were the two most important energy resources followed closely by crude oil and coal. Most of the wood fuel was consumed before the I-joist manufacturing stage where drying the wood was accomplished via steam boilers fueled primarily by wood and not fossil fuels. In addition, consumption of natural gas on-site at the I-joist manufacturing facilities was for curing the resins applied during assembly of the I-joist. Natural gas and coal are also the two primary sources of energy to fuel the U.S. electricity grid. Therefore, natural gas is the largest fossil fuel input for making I-joist for both regions.

Table 7. Cumulative energy (higher heating values (HHV)) consumed during production of I-joist—cumulative, mass allocated, gate-to-gate LCI values[a]

	Pacific Northwest			Southeast		
Fuel[b,c]	(kg/km)	(MJ/km)	(%)	(kg/km)	(MJ/km)	(%)
Wood fuel	995	20,809	31.7	1014	21,208	29.9
Natural gas[d]	300	16,330	24.9	345	18,786	26.5
Crude oil[d]	274	12,452	19.0	489	12,803	18.0
Coal[d]	427	11,183	17.0	285	12,972	18.3
Uranium[d]	0.00635	2,419	3.7	0.01332	5,075	7.1
Hydro	-	2,252	3.4	-	149	0.2
Energy, other	-	249	0.4	-	4	0.0
Total		65,690	100		70,990	100

[a] Includes fuel used for electricity production and for log transportation.
[b] Values are unallocated and cumulative and based on higher heating values.
[c] Energy values were found using their HHV in MJ/kg: 20.9 for wood oven-dry, 26.2 for coal, 54.4 for natural gas, 45.5 for crude oil, and 381,000 for uranium.
[d] Materials as they exist in nature and have neither emissions nor energy consumption associated with them.

Wood products typically consume more energy during the manufacturing life-cycle stage than any other stage (Puettmann and Wilson 2005; Winistorfer et al. 2005; Puettmann et al. 2010). To compare with an earlier CORRIM study on making 1.0 km of I-joist in the PNW and SE regions of the United States, cumulative allocated energy consumptions are 44.2 and

58.2 GJ/km (Wilson and Dancer 2005). The values listed in Wilson and Dancer (2005) use mass allocation. As stated previously, this study allocates by mass.

Carbon

Carbon content for wood products is assumed to be 50% by mass of OD wood. Therefore, the carbon stored in the wood portion of 1.0 km (5,240 OD kg) of I-joist when completely decomposed is equivalent to 9,610 kg of CO_2[3] released directly to the atmosphere. Stating it another way, the CO_2 value is equivalent to the CO_2 removed from the atmosphere during tree growth and now stored in the final product.

Emissions

Table 4 lists allocated environmental outputs for manufacturing 1.0 km of I-joist for the cumulative system boundaries for the PNW and SE, respectively. Emission data produced through modeling found that estimated biomass and fossil CO_2 emissions in kg/km were 1,774 and 1,969 for PNW and 1,808 and 2,042 for SE. Therefore, the amount of carbon stored in 1.0 km of I-joist, 9,610 kg is about 250% of the total CO_2 emissions released during manufacturing. For on-site energy use, burning natural gas to cure the I-joist was the main source of fossil CO_2. Major sources of air emissions were from hot pressing and from the energy generation auxiliary process that includes grid electricity (off-site) and boiler operations (on-site). Notable, most of nitrogen oxides (NOx) released, about 98% was derived from the production of PRF resin for I-joists and LVL manufacturing and the production of slack wax for OSB manufacturing.

Table 8. Cumulative environmental outputs for producing one km of I-joist—cumulative, mass allocated gate-to-gate

	Pacific Northwest	Southeast
Substance	(kg/km)	
Water effluents		
BOD5 (Biological oxygen demand)	0.412	0.440
Chloride	81.4	86.77
COD (Chemical oxygen demand)	0.772	0.852
DOC (Dissolved organic carbon)	3.54E-03	5.06E-03
Oils, unspecified	4.84E-02	5.20E-02
Suspended solids, unspecified	104	111
Industrial waste[a]		
Wood waste, to recycling	484	472
Solid waste[b]	74	26
Air emissions		
Acetaldehyde	0.184	0.199
Acrolein	1.54E+00	7.17E-02
Benzene	9.70E-04	8.56E-04
CO	5.96E+00	6.13E+00
CO_2 (biomass (biogenic))	1,774	1,808
CO_2 (fossil)	1,969	2,042
CH_4	5.99E+00	7.24E+00

[3] 2,540 OD kg wood * (0.5 kg carbon/1.0 OD kg wood) * (44 kg CO_2/kmole/12 kg carbon/kmole) = 9,610 kg CO_2

Formaldehyde	3.29E-01	3.23E-01
Mercury	1.97E-05	2.13E-05
Methanol	8.62E-01	8.01E-01
Nitrogen oxides	94.3	154.0
Non-methane VOC	5.23E-01	5.13E-01
Particulate (PM10)	4.69E-01	4.78E-01
Particulate (unspecified)	5.83E+00	8.27E+00
Phenol	1.54E-01	1.73E-01
Propanol	5.12E-05	5.22E-05
SO_x	2.24E-03	2.20E-03
VOC	5.83E+00	4.60E+00

[a] Includes solid materials not incorporated into the product or co-products but left the system boundary such as bark recycled into mulch.
[b] Solid waste was boiler ash from burning wood. Wood ash is typically used a soil amendment or landfilled.

Conclusions

EPDs provide life-cycle data in a concise and consistent format to enable industry to communicate with customers. This study provides the underlying gate-to-gate LCI data for updating the North American I-joist EPD. Future efforts will incorporate the LCI data into a cradle-to-gate LCA and eventually into an EPD for I-joist.

Structural wood products such as I-joist used in building construction can store carbon for long periods, which is typically greater than the carbon dioxide emissions released during manufacturing (Puettmann and Wilson 2005; Bergman and Bowe 2010; Puettmann et al. 2010). For instance, the present study showed that the amount of carbon stored in I-joists, 9,610 kg/km would be equivalent to more than 250% of the carbon dioxide emissions released during manufacturing if the carbon stored in the final product was released directly to the atmosphere. This approximation held true regardless of where the I-joists were made. In addition, the CO_2 value of 9,610 kg now stored in the final product as carbon is equivalent to the CO_2 removed from the atmosphere during tree growth.

Acknowledgement

I gratefully acknowledge the financial assistance provided by the USDA Forest Service Research and Development that funded this research through CORRIM, cooperative agreement #13-CO-11111137-014. In addition, I appreciate the reviews provided by James Salazar (Athena Sustainable Material Institute), Indroneil Ganguly (University of Washington), and Adam Robertson (Canadian Wood Council).

References

APA (2014) Engineered wood statistics: Third quarter 2014. APA—The Engineered Wood Association. Tacoma, WA. 9 p.

ASTM (2013) Standard specification for establishing and monitoring structural capacities of prefabricated wood I-joists. ASTM International. West Conshohocken, PA. 33 pp.

Bergman RD, Bowe SA (2010) Environmental impact of manufacturing softwood lumber in northeastern and north central United States. Wood Fiber Sci 42 (CORRIM Special Issue):67-78.

Bergman RD, Taylor A (2011) Environmental product declarations of wood products—An application of life cycle information about forest products. Forest Prod J 61(3):192–201.

Bergman RD (2015) Life-cycle inventory analysis of laminated veneer lumber production in the United States. In: Proceedings, Society of Wood Science and Technology 58th International Convention. June 7-12, 2015. Jackson Hole, Wyoming. (*In press).*

CORRIM (2010) Research guidelines for life-cycle inventories. Consortium for Research on Renewable Industrial Materials (CORRIM), Inc., University of Washington, Seattle, WA. 40 pp.

FPInnovations. (2013) Product Category Rule (PCR): For preparing an Environmental Product

Declaration (EPD) for North American Structural and Architectural Wood Products. UN CPC 31. NAICS 21. 17 pp. https://fpinnovations.ca/ResearchProgram/environment-sustainability/epd-program/Documents/wood-products-pcr-version-v1.1-may-2013-lastest-version.pdf. (22 April 2015).

ILCD (2010) International Reference Life Cycle Data System (ILCD) Handbook - General guide for Life Cycle Assessment—Detailed guidance. EUR 24708 EN. European Commission–Joint Research Centre–Institute for Environment and Sustainability. Luxembourg. Publications Office of the European Union. 417 pp.

ISO (2006a) Environmental management—life-cycle assessment—principles and framework. ISO 14040. International Organization for Standardization, Geneva, Switzerland. 20 pp.

ISO (2006b) Environmental management—life-cycle assessment—requirements and guidelines. ISO 14044. International Organization for Standardization, Geneva, Switzerland. 46 pp.

ISO (2006c) Environmental labels and declarations—Type III environmental declarations—Principles and procedures. ISO 14025. International Organization for Standardization, Geneva, Switzerland. 25 pp.

Kline ED (2005) Gate-to-gate life-cycle inventory of oriented strandboard production. Wood and Fiber Sci 37(CORRIM Special Issue):74–84.

Milota MR, West CD, Hartley ID (2005) Gate-to-gate life-cycle inventory of softwood lumber production. Wood Fiber Sci 42(Special Issue):47–57.

NREL (2012) Life-cycle inventory database project. National Renewable Energy Laboratory. https://www.lcacommons.gov/nrel/search. (22 April 2015).

PRé Consultants (2015) SimaPro 8 Life-cycle assessment software package. Amersfoort, The Netherlands. http://www.pre-sustainability.com/simapro/. (22 April 2015).

Puettmann ME, Wilson, JB (2005) Life-cycle analysis of wood products: Cradle-to-gate LCI of residential wood building materials. Wood Fiber Sci 37 (Special Issue):18–29.

Puettmann ME, Bergman RD, Hubbard SS, Johnson L, Lippke B, Wagner F (2010) Cradle-to-gate life-cycle inventories of US wood products production—CORRIM Phase I and Phase II Products. Wood Fiber Sci 42 (CORRIM Special Issue):15–28

Stark NM, Cai Zi, Carll C. (2010) Wood-based composite materials: Panel products, glued-laminated timber, structural composite lumber, and wood–nonwood composite materials. In: Wood handbook—wood as an engineering material. Gen Techn Rep FPL–GTR–113. USDA For Serv Forest Products Laboratory, Madison, WI. pp. 11-1–11–28.

USEPA (2002) AP 42 Section 10.9 Engineered wood products manufacturing. United States Environmental Protection Agency. pp. 10.9-1–24.

http://www.epa.gov/ttnchie1/ap42/ch10/final/c10s09.pdf. (22 April 2015)

Wilson JB, Sakimoto ET (2005) Gate-to-gate life-cycle inventory of softwood plywood production. Wood Fiber Sci 37 (Special Issue):58–73.

Wilson JB, Dancer ER (2005) Gate-to-gate life-cycle inventory of I-joist production. Wood Fiber Sci 37 (Special Issue):114–127.

Winistorfer P, Chen Z, Lippke B, Stevens N (2005) Energy consumption and greenhouse gas emissions related to use, maintenance, and disposal of a residential structure. Wood Fiber Sci 37 (Special Issue):128–139.

Proceedings of the 58th International Convention of
Society of Wood Science and Technology
June 7-12, 2015 - Grand Teton National Park, Jackson, Wyoming, USA

Multi-scale Investigation of Adhesive Bond Durability

Paige McKinley, paige.mckinley@oregonstate.edu

Oregon State University, 119 Richardson Hall , Wood Science and Engineering, Corvallis, OR 97331

Abstract

Moisture durability is essential for wood composite products, especially those used in building construction, where products are prone to weathering. The main focus of this research is to determine if adhesive penetration into the cell wall has a positive influence on bond durability. This study uses bonded Douglas-fir test specimens (6mmx14 mmx64 mm), varying in bonded surface cell type (earlywood vs. latewood), bonded surface orientation (longitudinal vs. tangential), and adhesive type. The adhesives of interest are a low and high molecular weight phenol-formaldehyde, along with a pre-polymeric diphenylmethane diiscoyanate. Half of each type of test specimen undergoes accelerated weathering and the rest remain dry. All samples are mechanically tested in lap shear. The maximum load is recorded along with the stress and strain around the bondline, using Digital Image Correlation (DIC). Smaller samples (2mmx2mmx10mm) are cut from the same previously tested samples and then scanned at the Advanced Photon Source using micro X-ray Computed Tomography (XCT). All adhesive types were previously tagged with iodine to increase contrast during scans. This technique gives high resolution (1.3μm^2/voxel), 3D images for which cell wall penetration can be analyzed at both the micrometer and nanometer scale. The mechanical test results, DIC results, and XCT images of the weathered vs. dry samples will be compared and used to quantitatively measure the effects of moisture on the bondline.

Proceedings of the 58th International Convention of
Society of Wood Science and Technology
June 7-12, 2015 - Grand Teton National Park, Jackson, Wyoming, USA

3D Visualisation of Spiral Grain and Compression Wood in *Pinus Radiata* with Fluorescence and Circular Polarised Light Imaging

Jimmy Thomas[1,2,†]*- David A. Collings*[2]

[1]Wood Technologist & Laboratory Manager
Central Wood Testing Laboratory,
The Rubber Board, INDIA
woodtechnologist@gmail.com

Senior Lecturer,
[2]School of Biological Sciences, University of Canterbury,
Christchurch, NEW ZEALAND
david.collings@canterbury.ac.nz

† Corresponding author & Society of Wood Science & Technology member

To visualise the development of spiral grain in young pine trees, a novel technique was developed that is based on tracking the orientation of axial resin canals. 60 µm-thick complete serial transverse sections covering a stem length of nearly 10 mm were imaged at high resolution with a professional flatbed scanner using circular-polarised transmitted light. Lignin autofluorescence from compression wood in these sections was also imaged with a stereo-fluorescence microscope, using blue excitation and green fluorescence. Images were aligned and canals detected with ImageJ macros. A series of image processing steps were applied to the image stack and only resin canals were identified as black dots in the resultant image stack which was used to generate a 3D view of spiral grain using a plug-in '*3D Viewer*' in ImageJ. The 3D visualisation showed the organisation of resin canals and spiral grain inside the wood. 3D reconstruction to show the compression wood was made from overlays of the fluorescence and the scanner images. Imaging confirmed the rapid onset of spiral grain, with a near vertical adjacent to the pith reorienting to a strong left-handed spiral within the first year of growth. There were fewer canals in the compression wood which appeared to be straighter than the twisted canals found elsewhere. This new method provides new insights in to our understanding on the formation of spiral grain and compression wood and a possible link between their occurrence.

Keywords: circular polarised light, compression wood, radiata pine, resin canals, spiral grain, 3D visualisation

Introduction

Spiral grain and compression wood in radiata pine

Presence of spiral grain and compression wood in radiata pine trees is common and these wood quality issues devalue the wood due to reduction in strength of sawn timber (Cown et al., 1991) and have negative effect on the surface smoothness (Sepúlveda, 2001) which may result in the downgrading in quality and the rejection of large proportions of sawn boards (Johansson et al., 2001). Majority of drying problems in *Pinus radiata* are related to twist which is related to both diameter and spiral grain Cown et al. (1996). (Tarvainen, 2005) estimated the annual loss caused by distortion due to spiral grain in dried timber in Europe to nearly €1 billion. Compression wood however believed to be contributed to the formation of warping. Their occurrence and influence on wood properties have been well documented and reviewed(Thomas and Collings, 2014). However, their inter-relationship in radiata pine and other species is only rarely been investigated and not understood. In this study resin canals, which are formed from the same cambial initials as the tracheids and align with the grain, were used as a proxy to demonstrate the grain changes. The new imaging and 3D visualisation techniques provide a better diagnostic tool to understand the real-time grain orientation at various positions inside the stem and the link between spiral grain and compression wood

Materials and Methods

Novel imaging approach

One year old radiata pine trees, up to 10 mm in diameter, were cut with a sliding microtome (HM400, Microm, Walldorf, Germany) to produce complete transverse sections (60 µm). The sections were carefully transferred to a microscope slide after washing in distilled water and mounted in glycerol. Imaging of these sections was done with a professional flatbed scanner (Epson Perfection V700 Photo) at 2400 dpi and in 24 bit colour, and saved as TIFF images. For this, slides were placed on a sheet of linear polarising film (polariser) (catalogue number NT38-491, Edmund Optics, Singapore) on the scanner bed and a second sheet of linear polarising film oriented at right angles (analyser) to the polariser to create linear polarised light (Fig. 1a) (Arpin et al., 2002). Two sheets of quarter wave-retarder films (catalogue number NT27-344, Edmund Optics) were added to the optical path on either side of the microscope slides, and at an angle of 45^0 to the linear polarising sheets. This meant that the wood sections were imaged with circularly polarised light (Fig. 1a) (Higgins, 2010). Lignin autofluorescence from compression wood was imaged in these transverse sections with a Leica DFC 310 FX digital camera connected to a stereo-fluorescence microscope (model MZ 10F Fluo, Leica Microsystems, Heerbrugg, Switzerland), using blue excitation and green fluorescence under constant imaging conditions.

Image processing to view spiral grain

To generate 3D reconstructions the background of each serial section image was filled with white (Fig. 1b) to enable a uniform thresholding and the images were aligned manually in Photoshop. Subsequent image processing was completed using ImageJ. The stack of images was fully aligned with the plug-ins 'StackReg' and 'Cumulative Rotation'. Uniform thresholding was applied, and the 'Analyse particles' function run to detect the resin canals with restrictions (size = 25 - 500 square pixels, circularity = 0.5 to 1.0), and recording specific measurements ('Area', 'Stack position' and 'Centroid', the location of the object's centre). An output file generated by the 'Show Masks' option showing the location of the canals (Fig. 1c) was used to generate a 3D image of spiral grain using the plug-in '3D Viewer'(Fig. 1d)(Thomas, 2014; Thomas and Collings, 2014).

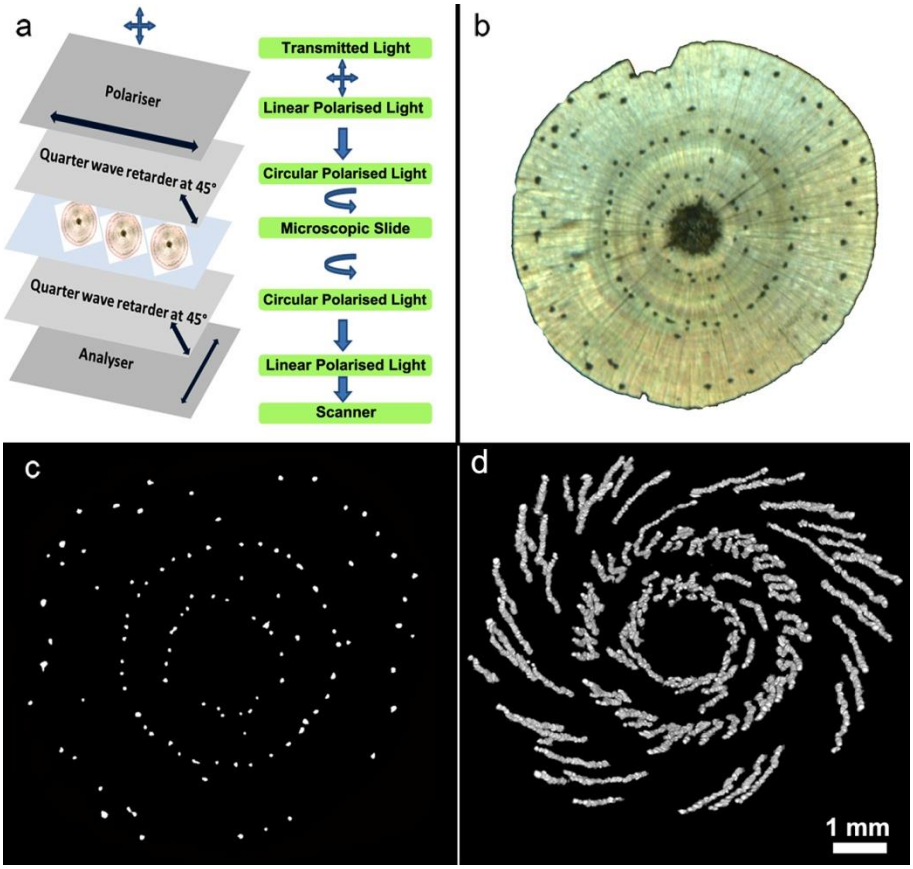

Figure 1 New imaging and resin canal detection method.

a. Imaging with circular polarised light.
b. A transverse section imaged with circular polarised transmitted light.
c. Resin canals, detected using ImageJ macros (white dots).
d. 3D visualisation of resin canals and spiral grain.

Another 3D image reconstruction was made to visualise both spiral grain (from scanned images) and compression wood (from fluorescence images). The stereo fluorescence microscope images had their background adjusted to black to enable uniform processing, and were partially aligned with Photoshop (Fig. 2a). Blue and green channels of these RGB images were removed by 'Curves' function. The brightness / contrast were adjusted such that only the compression wood parts were visible (Fig. 2b). The canvas size was made square, and the images were aligned using 'StackReg'. Overlay of these images was made by Photoshop (Fig. 2c) and saved as TIFF images with subsequent image processing completed in ImageJ. An image stack of the overlays was made, and a 3D projection of this image stack was made to visualise compression wood and spiral grain using 'Plugins' - '3D' - '3D Viewer' plugin (Fig. 2d) (Thomas, 2014; Thomas and Collings, 2014). Side (Fig. 2e) and bottom views (Fig. 2f) of the 3D visualisation also

clearly showed the organisation of compression wood and spiral grain in transverse section.

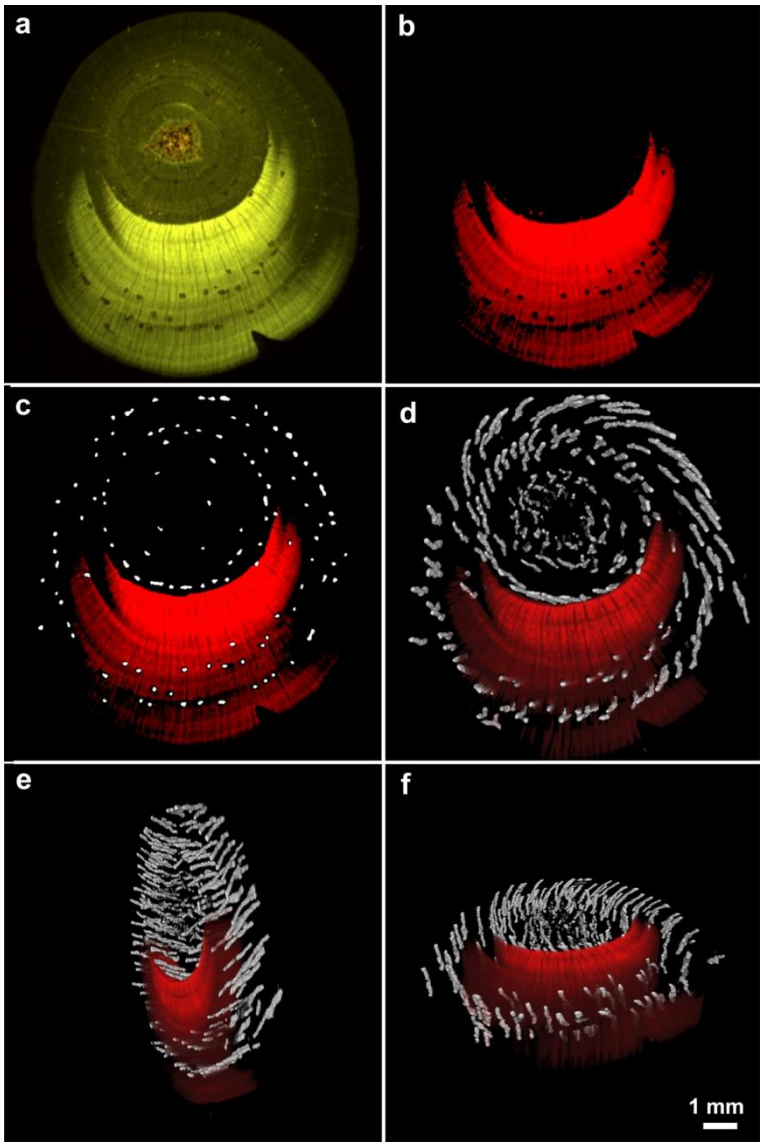

Figure 2 3D visualisation of the link between compression wood and spiral grain.

a. Fluorescence microscope image of the transverse section.
b. Compression wood segregated by thresholding.
c. Overlay stack of fluorescence images (a) whose blue and green channels were removed and corresponding scanner images in which resin canals were detected.
d. 3D visualisation of compression wood and spiral grain.
e. Side view of compression wood and spiral grain
f. Bottom view of compression wood and spiral grain.

Results and Discussion

Imaging stem transverse sections with a flatbed scanner

The new imaging technique, using a combination of the polariser (Arpin et al., 2002) and quarter wave-retarder film (Foster, 1997; Higgins, 2010), is a novel approach to create high-quality images suitable for any modern image analysis programme (Thomas, 2014; Thomas and Collings, 2014). It is an easy and economic way of replicating polarised light microscopy and is particularly useful for imaging large areas which is difficult with conventional microscopy. Circular polarised light has previously been suggested as a way to overcome image asymmetries such as Maltese cross effect (Higgins, 2010). However the use of circular polarised light with automatic image analysis is novel and this new imaging technique is simple to create, convenient to operate and provides better quality images. Moreover this new method is quick and easy to operate, and gives reproducible results.

3-dimensional image reconstructions and analysis of grain orientation

3D reconstruction of the circular polarised light images revealed the organisation of resin canals. The canals were arranged in concentric bands around the pith with the canals nearest to the pith nearly straight and those in the outer regions twisted leftwards (Fig. 1d). However there were fewer canals in the compression wood region and these were straighter than the twisted canals (Fig. 2d). This is consistent with Cown et al. (2003) who observed few or no canals in radiata pine compression wood. As the resin canals follow the tracheids in radiata pine, this twisting of the resin canals demonstrated the rapid and early onset of left-handed spiral grain in radiata pine trees, a pattern that is typical of pines.

The unknown link between compression wood and spiral grain

Fluorescence imaging demonstrated its capability to detect compression wood in wood cross section images. 3D reconstruction of serial sections collected over 4.5 mm revealed that the pattern of compression wood looked similar at different depths (Fig. 2d). By combining the polarised light and the stereo-fluorescence microscope images, both compression wood and spiral grain were visible for the first time. The low number of resin canals and their relatively straight orientation in compression wood areas are suggesting a possible link between the formation of compression wood and spiral grain in radiata pine. It is obvious that researchers have looked at the incidence of compression wood and spiral grain separately, and have made only very limited effort on approaching these issues together (Thomas, 2014). In this study, visualisation of the internal structure

of full cross section of young pine tree stems was successfully made for the first time. The orientation of the resin canals has shown the grain deviation along the length of the stem and hence this 3D reconstruction technique would give a great opportunity to study the generation and progression of spiral grain and compression wood in wood. Moreover this study is the first attempt to look at grain across an entire stem but considering events at a cellular level.

Acknowledgements

JT gratefully acknowledges funding for his PhD scholarship generously provided by Scion Ltd, Rotorua, New Zealand during this work.

References

Arpin TL, Mallol C, Goldberg P. Short Contribution: A new method of analyzing and documenting micromorphological thin sections using flatbed scanners: Applications in geoarchaeological studies. Geoarchaeology: An International Journal (2002) 17:305-313.

Cown DJ, Haslett AN, Kimberley MO, McConchie DL. The influence of wood quality on lumber drying distortion. Annals of Forestry Science (1996) 53:1177-1188.

Cown DJ, Ilic J, Butterfield B. Compression wood in New Zealand radiata pine (2003). Wood Quality Initiative Report No. STA 3, Rotorua, New Zealand.

Cown DJ, Young GD, Kimberley MO. Spiral grain patterns in plantation-grown Pinus radiata. New Zealand Journal of Forestry Science (1991) 21:206-216.

Higgins MD. Imaging birefringent minerals without extinction using circularly polarised light. The Canadian Mineralogist (2010) 48:231-235.

Johansson M, Perstorper M, Kliger R, Johansson G. Distortion of Norway spruce timber Part 2. Modelling twist. Holz als Roh- und Werkstoff (2001) 59:155-162.

Sepúlveda P. Measurement of spiral grain with computed tomography. Journal of Wood Science (2001) 47:289-293.

Tarvainen V. Measures for improving quality and shape stability of sawn softwood timber during drying and under service conditions - Best practice manual to improve straightness of sawn timber. (2005) VTT Publications Otamedia Oy, Espoo, Finland.

Thomas J. An investigation on the formation and occurrence of spiral grain and compression wood in radiata pine (*Pinus radiata* D. Don.). (2014) PhD Thesis, School of Biological Sciences, University of Canterbury, Christchurch, New Zealand.

Thomas J, Collings DA. Novel imaging and 3D rendering techniques to visualise spiral grain in *Pinus radiata*. In: 57th International Convention of Society of Wood Science and Technology, Barnes HM, Herian VL, eds. Technical University in Zvolen, Zvolen, SLOVAKIA. Society of Wood Science and Technology, USA (2014) 984-992.

Proceedings of the 58th International Convention of
Society of Wood Science and Technology
June 7-12, 2015 - Grand Teton National Park, Jackson, Wyoming, USA

Micro-compression of Solid Bamboo Fibers

Patrick Dixon, pdixon7@mit.edu
Lorna Gibson, ljgibson@mit.edu

Massachusetts Institute of Technology, 77 Massachusetts Avenue, Building 8-032, Cambridge, MA 02139

Abstract

Advances in micro- and nano-mechanical methods now allow for a direct measurement of the mechanical properties of plant cell walls. One emerging technique is micro-compression, in which micro-scale pillars are machined and compressed using a micro-mechanical tester. Although this method has been initially employed on wood, it has yet to be exploited for analysis of other plant materials such as bamboo. Bamboo has a fiber-reinforced structure, consisting of vascular bundles with vessels surrounded by dense longitudinal, sclerenchymatous fibers, embedded in a matrix of parenchyma cells. The fiber properties can serve as an effective estimate of the solid cell wall properties. In this study, micro-pillars are fabricated from high density fibers areas of Moso bamboo (Phyllostachys pubescens Mazel). Micro-pillars, 25 μm in diameter, with aspect ratios from 2 to 3, are created with a focused ion beam. The pillars are loaded in compression using a nano-indenter with a flat-end 80 μm diameter punch. Our initial results on micro-pillars compressed at a rate of 4 mN/s, give a compressive strength of 331.8 ± 31.0 MPa (mean ± standard deviation). For comparison, literature values for micro-pillar compression strengths of wood fiber cell wall lie in the range of 100 to 200 MPa. Further work is establishing if this difference is due to experimental conditions (e.g. loading rate control, loading rate) or truly points to the underlying reason for the extraordinary strength of bamboo itself.

Proceedings of the 58th International Convention of
Society of Wood Science and Technology
June 7-12, 2015 - Grand Teton National Park, Jackson, Wyoming, USA

Energy Use and Sensitivity Analysis of Energy Inputs ror Canola Production (Brassica Napus L.) in Iran

Payam Hooshmand, payam.hooshmand@yahoo.com
Adel Ranji, adelranji@yahoo.com
Hamid Khakrah, hrkhahrah@yahoo.com
Sohrab Chandaz, payam.hooshmand@yahoo.com
Milad Hosseinpoor, milad_hopr@yahoo.com

Sharif University of Technology, Azadi St, , Tehran

Abstract

The objectives of this study were to determine the energy consumption and evaluation of inputs sensitivity for Canola production (Brassica napus L.) in Mazandaran province, Iran. The sensitivity of energy inputs was estimated using the marginal physical productivity (MPP) method and partial regression coefficients on Canola yield. Data were collected from 62 Canola farms in September 2012. The sample volume was determined by random sampling method. The results revealed that total energy input for Canola production was 29531 MJ ha-1; the non-renewable energy shared about 99 % while the renewable energy did 1 %. Energy use efficiency, energy productivity, and net energy were 1.53, 0.07 kg MJ-1, and~15753 MJ ha-1, respectively. Econometric model evaluation showed that seed energy was the most significant input which affects the output level. Sensitivity analysis indicates that with an additional use of 1MJ of each of the seed, Toxin and machinery energy would lead to an increase in yield by 35.618, 1.031and 0.271 kg, respectively. Also, the MPP of human labor energy was calculated to be -16.886 implying that the use of human labor energy is in excess for canola production, causing an environmental risk problem in the region.

Proceedings of the 58th International Convention of
Society of Wood Science and Technology
June 7-12, 2015 - Grand Teton National Park, Jackson, Wyoming, USA

Particleboards from Reed Canary Grass

Johann Trischler[1] and Dick Sandberg[2]*

[1] PhD student, Department of Forestry and Wood Technology - Linnæus University, SE-351 95 Växjö, Sweden
* *Corresponding author*
johann.trischler@lnu.se
[2] Professor, Department of Engineering Sciences and Mathematics - Luleå University of Technology, SE-931 87 Skellefteå

Abstract

Particleboards are an important base for furniture production and interior use, and the production process is in general optimized for wood as the main raw material. Monocotyledons such as reed canary grass (*Phalaris arundinacea* L.) are an interesting raw-material resource for particleboards, especially since monocotyledons are less suitable than most wood species for thermal energy recovery and pulp and papermaking. In this work, the use of reed canary grass for single-layer particleboards was studied. A surface treatment with paper during pressing or a paper coating after pressing were also tested as a way to increase their mechanical properties. A waterborne acryl-based adhesive was used, and this allowed the reed canary grass to be used without any additional pre-treatment. The boards were tested according to the EN 312 standard. The results showed that the boards did not fulfil the requirements of the standard regarding mechanical properties and thickness swelling but that a surface treatment gave a considerable improvement in the mechanical properties. The low mechanical performance of the boards is due to problems related to the production process, where it appears that acrylic adhesive is not favourable for grass-based panel production.

***Keywords*:** Acrylic adhesive, Mechanical properties, Monocotyledons, Panels, Surface treatment.

Introduction

Reed canary grass (*Phalaris arundinacea* L.) is a perennial, rhizome-building C3 grass with high production of biomass in boreal zones (Xiong et al. 2008). The biomass production reaches 6-8 tons dry mass per hectare for spring (= delayed harvest) and 8-10 tons for autumn harvest (Finell 2003). Chipping of the grass during or after harvest results more or less in a mix of different parts of the plant, such as leaf, leaf sheath, and stem, that have different properties (Pahkala and Pihala 2000; Finell 2003).

Nowadays, reed canary grass is generally cultivated for use in thermal energy recovery, especially in Finland (Casler et al. 2009). The disadvantage of using monocotyledons for thermal energy recovery is, compared to wood, the relatively high ash content and low ash melting point (Diamantidis and Koukios 2000; Kim and Dale 2004; Greenhalf et al. 2012). Reed canary grass could also be a raw material for the pulp and paper industry, but it is not yet being considered for industrial use, at least not in Europe (Finell 2003). Another possible use of reed canary grass is in the production of particleboards as a substitute for wood. Table 1 shows that monocotyledons have a lower lignin content and a higher content of hemicelluloses than wood, and that the ash content is up to 10 times higher for monocotyledons. While the high content of hemicelluloses is problematic for particleboard production because of its greater water uptake, the ash is beneficial as this raw material is less favorable for e.g. thermal energy recovery.

Table 9: *Chemical composition in percentage of mass for different lignocellulosic materials. C: celluloses; L: lignin; HC: hemicelluloses; A: ash content*

Species	C	L	HC	A	References
Wheat straw	41	8	31	6.3	(Bridgeman et al. 2008)
Miscanthus	49	11	30	2.6	(Hodgson et al. 2011)
Reed canary grass	30-43	8-11	25-30	1.3 -6	(Dien et al. 2006; Bridgeman et al. 2008; Jansone et al. 2012)
Cup plant	36	12	18	9	(Wulfes 2012)
Softwoods	40-45	25-35	25-30	0.2-0.4	(Fengel and Grosser 1975) (Pettersen 1984)
Hardwoods	40-50	20-25	25-35	0.2-0.8	(Fengel and Grosser 1975; Pettersen 1984)

The tubular stalks of reed canary grass collapse during chipping and often break open in the longitudinal direction (parallel to the fibre direction), displaying two different surfaces, and resulting in a large variation in particle width. There are large differences between the external and internal surface of the particles (Wiśniewska et al. 2003), Figure 1.

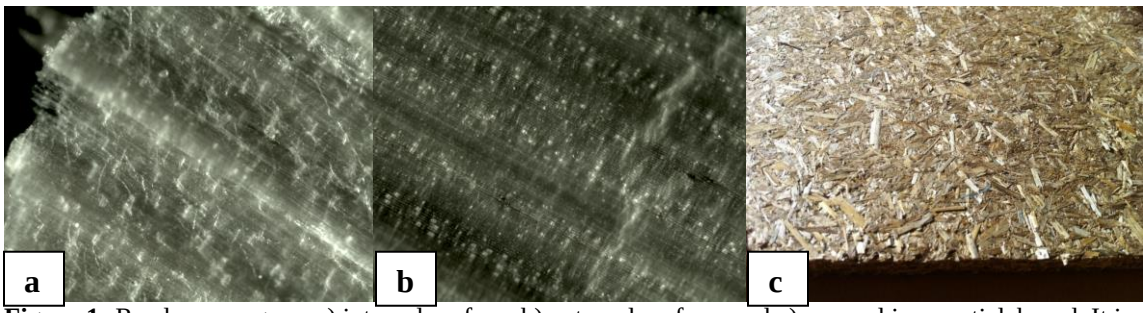

Figure 1: Reed canary grass a) internal surface, b) external surface, and c) pressed in a particleboard. It is easy to see the wide range of width and the shining (internal) and dull (external) surfaces of the grass particles

All monocotyledons have a special layer on their external surface consisting of cuticles and epicuticular waxes which are a protection against environmental impacts (Rentschler 1971; Barthlott and Neinhuis 1997). Figure 2 shows the structure of the external layer with epidermal cells followed by a layer of pectin on which there is a thick cutinised layer with embedded waxes, and finally the epicuticular wax layer (Wiśniewska et al. 2003; Buschhaus and Jetter 2011; Myung et al. 2013). This waxy layer makes it difficult to use the adhesives which are usually used in particleboard production, as they show low tack and poor adhesion on waxy surfaces.

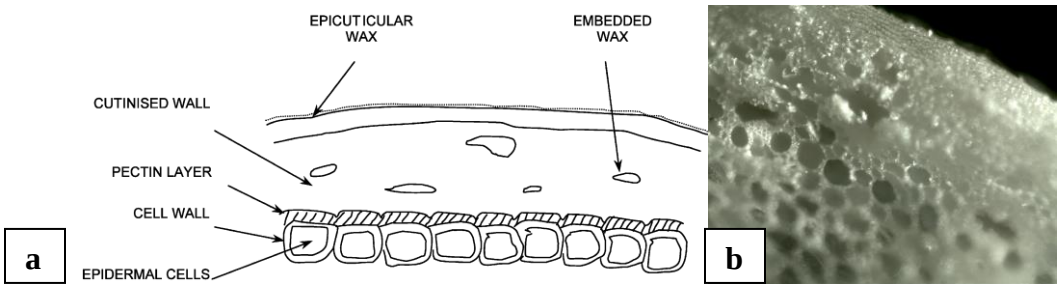

Figure 2: Basic structure of a monocotyledon surface layer (cross section) a) showing the cutinised layer with the embedded waxes on the layer of epidermal cells superposed by an epicuticular wax layer, after Wiśniewska et al. (2003) and b) a radial section of a reed canary grass stalk

Using monocotyledons in particleboard production may therefore cause problems if conventional adhesives are used (Boquillon et al. 2004). Either a pre-treatment of the waxy external surface or a different adhesive is necessary.

A pre-treatment should affect the waxy layer and lead to more similar surfaces of the monocotyledon particles by increasing the roughness and exposing more hydroxyl groups on the surface (Hua et al. 2009). The surface of the monocotyledon particles would then be more similar to the surface of wood particles and it would be possible to use the adhesives conventionally used in particleboard production.

Alternatively, isocyanate-based adhesives such as MDI (diphenylmethane diisocyanate), polymeric MDI (pMDI) or polyurethane (PUR) can be used due to their non-specific adhesive properties (Frazier 2003; Boquillon et al. 2004; Torkaman 2010). PVA

(polyvinyl alcohol) and PVAc (polyvinyl acetate) might also be suitable as these adhesives allow a large variety of modifications (Qiao et al. 2002). Other possibilities might be acryl-based adhesives or matrix-building epoxy adhesives (Trischler and Sandberg 2014).

Objectives

The purpose was to study the use of reed canary grass as raw material for particleboards, the use of an acrylic adhesive as binder and the effect of surface treatment on strength properties.

Materials and Methods

Delayed-harvest reed canary grass from northern Sweden was used. It was chipped to lengths of 1 to 50 mm and stored at a moisture content of 7.4%. The reed canary grass particles were used without any additional mechanical or chemical treatment.

Ten particleboards with dimensions of 250x250 mm and a thickness of 11 mm were produced and tested with regard to their modulus of elasticity (MoE), modulus of rupture in bending (MoR), thickness swelling (TS), and internal bond strength (IB) in accordance with EN 312. The target density for the boards was 400 to 600 kg/m^3. The amount of adhesive was 10 or 20% of the dry-weight of the particles. As adhesive, the acrylic adhesive 498 HV from Lascaux ®, which is generally used for relining and marouflages, was used.

A hydraulic press was used to manufacture the boards. The press-plate temperature was 100°C and the boards were taken out after the press had cooled to 20°C which was after approximately 4 hours. The pressure was adjusted according to the pre-calculated volume of the boards.

Half of the boards were surface laminated with paper. In some cased, the paper was placed without additional adhesive on the surface of the particle “cake” before the pressing of the board (lamination). In other cases, the paper was glued on the surface with acrylic adhesive after the board had been produced and dried (paper coating).

Results and Discussion

The three different types of particleboards, without surface treatment, with lamination, and with paper coating are shown in Figure 3.

Figure 3: Particleboards manufactured out of reed canary grass glued with an acrylic adhesive a) without surface treatment, b) with lamination, and c) with paper coating

The results of the mechanical tests are presented in Table 2. None of the boards reached the required values according to the standard P1 in EN 312. The lamination succeeded in only one case. In most cases, the high residual moisture content on the surface of the boards at the end of pressing time resulted in delamination of the lamination. The thickness swelling after 24 hours was proportional to the density of the boards, i.e. higher densities resulted in greater swelling. No relation could be found between the adhesive content in the panels and the internal bond strength (IB) or modulus of rupture (MoR). In all cases, the surface treatment gave an increase in MoR.

Table 10: *Results of the tests of modulus of elasticity (MoE), modulus of rupture in bending (MoR), thickness swelling (TS), and internal bond strength (IB) of each board according to EN 312*

#	Density	Surfacing	Adhesive content	Swelling 2 / 24 hours		IB	MoR	MoE
	(kg/m^3)		(%)	(vol%)		(N/mm^2)	(N/mm^2)	(N/mm^2)
1	430	-	10	12.7	18.6	0.01	1.4	373
2	430	Lamination	10				2.1	314
3	440	-	10	18.8	25.0	0.03	1.0	258
4	440	Paper coating	10				3.4	577
5	430	-	20	9.1	27.3	0.05	0.8	179
6	430	Paper coating	20				2.6	273
7	620	-	10	18.8	38.4	0.04	1.9	450
8	620	Paper coating	10				3.1	429
9	490	-	20	16.4	30.9	0.02	1.5	267
10	490	Paper coating	20				3.5	519
P1	-	-	-	(16	P4)	0.28	12.5	-

The acrylic adhesive cures by evaporation of water, and a high residual moisture content when the press had opened led to delamination of the whole cross-section of the panel as parts of the adhesive were still not cured. Especially at the surfaces of the boards, large amounts of condensation water were found. Nevertheless, it was decided not to increase the temperature or the pressing time as the adhesive has not been tested for high

temperature. Setting up the press at 100°C at the beginning of the pressing process should support the evaporation of the water.
The nature of the particles affects the low mechanical properties. Compared to wood, the particles of reed canary grass are flexible and have an internal surface of quite thin-walled brittle cells which relatively easily collapse or break. This explains why a larger amount of adhesive did not increase the mechanical strength of the board.

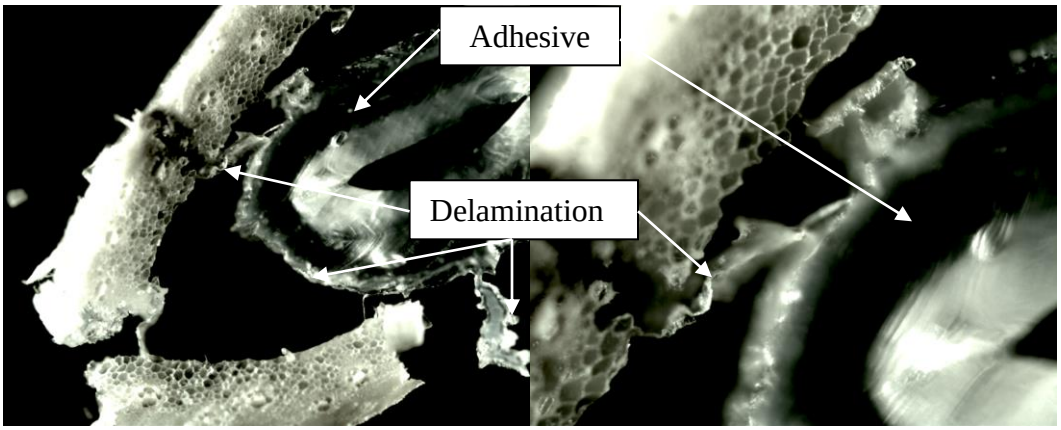

Figure 4: Reed canary grass glued on the internal layer and after mechanical stressing showing a tangential delamination by ruptures of the cell walls

The acrylic adhesive was chosen because it shows quite good tack to the external waxy surface, it is waterborne, and it is water-resistant after curing. Further, it is transparent after curing and handling during processing is much easier than with e.g. isocyanate-based adhesives. Disadvantages are that it is thermoplastic, it shows good tack to metal which led to problems in the press, and it has not been tested at higher temperatures, which led to inefficient mixing of the adhesive with the particles and inefficient pressing. The mixing was difficult as it was done with as little water as possible, and the pressing was inefficient as no higher temperatures could be used, which would have reduced pressing times and led to less residual moisture in the board. Higher temperatures would also lead to a thermo-mechanical treatment of the grass which can have a positive effect on the swelling, dimensional stability and delamination of the board by reducing the amount of hemicelluloses in the grass particles.

Even though the boards did not pass the minimum requirements according to the standard and there were problems relating to the mixing of the adhesive and the pressing, the mechanical properties and thickness swelling showed a strong improvement compared to earlier studies where reed canary grass was used as a core layer in particleboards glued with MUF (melamine-urea-formaldehyde) or protein (vital gluten) adhesive. The surface treatment by lamination or paper coating, similar to the concept of gypsum plaster boards, seems promising as the MoR values were approximately twice as high as those without surface treatment.

The problems relating to the efficiency of the pressing process and the curing of the acrylic adhesive mean that this type of adhesive is not interesting for grass-based panel production. An enzymatic pre-treatment of the particles under anaerobic conditions might be more promising. Such a treatment would not only lead to a reduction in fines and possibly eliminate the thin-walled, easy destructible cells, but it would also remove the waxy layer and decrease the silica content (Hua et al. 2009; Shen et al. 2011). Conventional adhesives such as MUF then give acceptable results.

Conclusions

Particleboards were manufactured out of reed canary grass (*Phalaris arundinacea* L.) glued with an acrylic adhesive. On some of the boards a surface treatment in the form of lamination or paper coating was applied. The boards were tested according to the standard EN 312. None of the boards met the minimum requirements with regard to mechanical properties, due not only to problems relating to the production process of the boards but probably also to the low density and the nature of the grass particles. Due the problems with the adhesive during the production process, acrylic adhesive cannot be recommended for the production of grass-based particleboards. A surface liner was shown to improve the mechanical properties of the boards, and lamination during the pressing was an especially promising way of strengthening this kind of panel.

References

Barthlott, W., and Neinhuis, C. 1997. Purity of the sacred lotus, or escape from contamination in biological surfaces. Planta 202(1): 1-8.

Boquillon, N., Elbez, G., and Schönfeld, U. 2004. Properties of wheat straw particleboards bounded with different types of resin. Journal of Wood Science 50(3): 230-235.

Bridgeman, T.G., Jones, J.M., Shield, I., and Williams, P.T. 2008. Torrefaction of reed canary grass, wheat straw and willow to enhance solid fuel qualities and combustion properties. Fuel 87(6): 844-856.

Buschhaus, C., and Jetter, R. 2011. Composition differences between epicuticular and intracuticular wax substructures: How do plants seal their epidermal surfaces? Journal of Experimental Botany 62(3): 841-853.

Casler, M., Cherney, J., and Brummer, E.C. 2009. Biomass yield of naturalized populations and cultivars of reed canary grass. BioEnergy Research 2(3): 165-173.

Diamantidis, N.D., and Koukios, E.G. 2000. Agricultural crops and residues as feedstocks for non-food products in Western Europe. Industrial Crops and Products 11(2–3): 97-106.

Dien, B.S., Jung, H.-J.G., Vogel, K.P., Casler, M.D., Lamb, J.F.S., Iten, L., Mitchell, R.B., and Sarath, G. 2006. Chemical composition and response to dilute-acid pretreatment and enzymatic saccharification of alfalfa, reed canarygrass, and switchgrass. Biomass and Bioenergy 30(10): 880-891.

Fengel, D., and Grosser, D. 1975. Chemische Zusammensetzung von Nadel- und Laubhölzern. Holz als Roh- und Werkstoff 33(1): 32-34.

Finell, M. 2003. The use of reed canary grass (*Phalaris arundinacea*) as a short fibre raw material for the pulp- and paper industry, Umeå, Sweden: Swedish University of Agricultural Sciences.

Frazier, C.E. 2003. Isocyanate Wood Binders In: Handbook of Adhesive Technology, Revised and Expanded, A. Pizzi and K.L. Mittal, eds. 2003. New York, NY: Taylor & Francis (Marcel Dekker Inc.).

Greenhalf, C.E., Nowakowski, D.J., Bridgwater, A.V., Titiloye, J., Yates, N., Riche, A., and Shield, I. 2012. Thermochemical characterisation of straws and high yielding perennial grasses. Industrial Crops and Products 36(1): 449-459.

Hodgson, E.M., Nowakowski, D.J., Shield, I., Riche, A., Bridgwater, A.V., Clifton-Brown, J.C., and Donnison, I.S. 2011. Variation in miscanthus chemical composition and implications for conversion by pyrolysis and thermo-chemical bio-refining for fuels and chemicals. Bioresource Technology 102(3): 3411-3418.

Hua, J., Yang, Z., and Xuefei, W. 2009. Effect of lipases on the surface properties of wheat straw. Industrial Crops & Products 30(2): 304-310.

Jansone, B., Rancane, S., Berzins, P., and Stesele, V. 2012. Reed canary grass (*Phalaris arundinacea* L.) in natural biocenosis of Latvia, research experiments and production fields. In: International Scientific Conference: Renewable Energy and Energy Efficiency, Jelgava (Latvia), 28-30 May 2012, J. Latvia University of Agriculture, ed. 2012. Jelgava, Latvia: Latvia University of Agriculture: 61-65.

Kim, S., and Dale, B.E. 2004. Global potential bioethanol production from wasted crops and crop residues. Biomass and Bioenergy 26(4): 361-375.

Myung, K., Parobek, A.P., Godbey, J.A., Bowling, A.J., and Pence, H.E. 2013. Interaction of organic solvents with the epicuticular wax layer of wheat leaves. Journal of Agricultural and Food Chemistry 61(37): 8737-8742.

Pahkala, K., and Pihala, M. 2000. Different plant parts as raw material for fuel and pulp production. Industrial Crops and Products 11(2–3): 119-128.

Pettersen, R.C. 1984. The chemical composition of wood. In: The chemistry of solid wood. Advances in chemistry series 207, R.M. Rowell, ed. 1984. Washington DC: American Chemical Society 57-126.

Qiao, L., Coveny, P.K., and Easteal, A.J. 2002. Modifications of poly(vinyl alcohol) for use in poly(vinyl acetate) emulsion wood adhesives. Pigment and Resin Technology 31(2): 88-95.

Rentschler, I. 1971. Die Wasserbenetzbarkeit von Blattoberflächen und ihre submikroskopische Wachsstruktur. Planta 96(2): 119-135.

Shen, J.-h., Liu, Z.-m., Li, J., and Niu, J. 2011. Wettability changes of wheat straw treated with chemicals and enzymes. Journal of Forestry Research 22(1): 107-110.

Torkaman, J. 2010. Improvement of Bondability in Rice Husk Particleboard Made With Sodium Silicate Ancona, Italy: Taylor & Francis/Balkema.

Trischler, J., and Sandberg, D. 2014. Monocotyledons in particleboard production : Adhesives, additives, and surface modification of reed canary grass. BioResources 9(3): 3919-3938.

Wiśniewska, S.K., Nalaskowski, J., Witka-Jeżewska, E., Hupka, J., and Miller, J.D. 2003. Surface properties of barley straw. Colloids and Surfaces B: Biointerfaces 29(2–3): 131-142.

Wulfes, R. 2012. Alternativen zu Mais – praktische Erfahrungen mit Produktion und Verarbeitung neuer Substrate –. Praxis der Biomassenutzung, Kompetenzzentrum_Biomassenutzung, ed., FH Kiel, FB Agrarwirtschaft, Rendsburg/Osterrönfeld.

Xiong, S., Lötjönen, T., and Knuuttila, K. 2008. Energiproduktion från rörflen: Handbok för el och värmeproduktion (Energy conversion with reed canary grass: a guide for electricity and heat production), Umeå, Sweden: Swedish University of Agricultures, Unit of Biomass Technology and Chemistry.

Proceedings of the 58th International Convention of
Society of Wood Science and Technology
June 7-12, 2015 - Grand Teton National Park, Jackson, Wyoming, USA

Tailoring the Addition of Moso Strands to Enhance the Properties of OSB but Reducing Board Density

Polo K. Zhang [1] – Kate E. Semple[2] - Greg D. Smith[3]*

[1] M.Sc. Student, Department of Wood Science, Faculty of Forestry, University of British Columbia, Vancouver BC, Canada.
polo.kq.zhang@gmail.com
[2] Research Scientist, Department of Wood Science, Faculty of Forestry, University of British Columbia, Vancouver BC, Canada.
kate.semple@ubc.ca
[3] Associate Professor, Department of Wood Science, Faculty of Forestry, University of British Columbia, Vancouver BC, Canada.
* *Corresponding author*
greg.smith@ubc.ca

Abstract

Moso bamboo (*Phyllostachys pubescens* Mazel) has great potential for improving the properties of wood-based strand composite building materials. In previous work we have shown that replacement of aspen surface strands with Moso bamboo strands significantly improves the strength and water resistance of oriented strand board (OSB) of the same density made from Aspen. However due to the greater density of bamboo, composite product density is an issue for development of building materials from bamboo. The aim of this work is to produce a low density bamboo–surface OSB that still meets CSA-O437.0 (2011) requirements for OSB. Three sets of six three-layer OSB were made with Moso bamboo strands in the surfaces and Aspen strands in the core. Board types are 1) MM: 50% bamboo (surfaces)/50% Aspen (core), target density = 760 kg/m^3, 2) MH: 25% bamboo (surface)/75% Aspen (core), target density = 720 kg/m^3, and 3) ML: same composition as Type 2, but pressed to a target density of 640 kg/m^3. Measured board strength properties include internal bond (IB), flexural properties (modulus of rupture, -MOR; and modulus of elasticity, -MOE), and water resistance (% thickness swell, TS; and % water absorption, WA). ML were fabricated to lowest density for structural products specified in CSA-O437.0 (2011). It was also the lowest in mechanical properties and the water resistance, but still met CSA-O437 minimum properties. This bamboo-substituted OSB therefore has good potential as a substitute for conventional wood OSB of similar density.

Keywords: Moso bamboo, OSB, density, mechanical properties, CSA-O437.0, structural materials

Introduction

Bamboo (*Poaceae*/*Graminaceae)* is a fast growing giant grass and can have better toughness and orientation properties than wood owing to its unique microscopic structure and chemical composition (Li 2004). Among over one thousand species of bamboo (Austin and Ueda 1971), Moso (*Phyllostachys pubescens* Mazel) is one of the few commercially used species. Lee et al. (1996) has proved the manufacture of strand boards from Moso bamboo is technically feasible. Although both physical and mechanical properties of bamboo oriented strand boards could meet industry-level standards (Lee et al.1996), the density of bamboo composites is often too high to be a practical direct substitute for commodity OSB manufactured from wood. However, the great concentration of vascular bundles makes the bamboo denser (Ghavami 2005). On the other hand, the strength of bamboo depends largely on the number of the vascular bundles (Lo et al. 2008). In our previous work (Semple et al. 2015) mixed Moso bamboo and Aspen (*Populus tremuloides* Michx.) wood strands together to produce a 3-layer Moso surfaces/Aspen core OSB with a density around 740 kg/m^3. However, according to CSA O437.0 (2011), the required density for OSB panels should be around 640 kg/m^3. The main objective of this study is to fabricate lower density Moso-Aspen hybrid OSBs which meet the CSA-O437.0 requirements for mechanical properties and water resistance.

Materials and Methods

Culm feedstock: 20 poles of 5-inch (12.7 cm) diameter Chinese Moso culm stock in 8 foot lengths were purchased from Canada's Bamboo World, located in Chilliwack, BC, who import Moso culms from Zhejiang Province in China. The Moso culms had an average diameter of 101.7 mm with an average weight of 6.6 kg. After cross-cutting, the volume of small specimens cut from the culms was measured using the water displacement method. With an average moisture content at 19.25±1.1%, the oven dry density of the culm is 744.8±21.4 kg/m³.

Stranding: Pre-saturated culm pieces measuring 130 mm long were converted to strands using a laboratory disk strander (CAE 6/36 single-blade disk) built by Carmanah Desigh and Manufacturing, Vancouver, BC. Disk rotational speed was set at 734 RPM, and knife projection was set at 0.675mm to give an average target strand thickness of 0.65 mm. Counter knife angle was 45° with a hydraulic piston-driven feed buffer rate of 0.37 m/min. Sheet metal shims measuring 0.002 inch in thickness are used to make tiny changes in the knife protrusion from its original block. A magnetic mounted dial gauge was used to measure the knife protrusion. From preliminary stranding trials (Smola 2013,

Semple et al. 2014), slicing longitudinally trough the culm wall produced narrower smoother strands that did not curl, than stranding the culm horizontally as is normally done for wood logs. In order to maximize the amount of material stranded per run and per culm round (Semple and Smith 2014), the bamboo culm rounds were cut into quarters, stacked and sliced through the radial-longitudinal plane (Figure 1). Strands were oven dried at 80°C over night and left to cool for at least 4 hours prior to sealing in plastic bags. The moisture content of the dried strands was approximately 2%.

Figure 10. Stranding culm pieces vertically.

Boar fabrication and Experiment design: Two strategies were used to reduce board density. First the weight ratio of Moso strands and Aspen strands was reduced. Second the overall amount of furnish used per board was reduced. Three types of 3-layer hybrid OSB were fabricated with six board replicates per type. Type 1 (MM) were 50% Moso bamboo strands in the surface layers and 50% Aspen strands in the core with a target density around 760 kg/m³. Type 2 (MH) were 25% Moso bamboo strands in the surface layers and 75% Aspen strands in the core with a target density around 720 kg/m³. Type 3 (ML) were 25% Moso bamboo strands in the surface layers and 75% Aspen strands in the core with a target density around 628 kg/m³. All boards were 740 mm x 740 mm, limited by the dimensions of the press platens. The target thickness was 7/16th inch (11.1 mm) which is a common thickness of general purpose OSB sheathing.

All 18 boards were fabricated under similar conditions during a continuous timeline. Moso and Aspen strands were blended separately with 6% w/w liquid Phenol Formaldehyde (PF) resin supplied by Momentive Specialty Chemicals Canada Inc., Edmonton, Alberta, Canada. The rotating drum blender (183 cm diameter by 61 cm depth) was equipped with small flights to lift and cascade strands. The required resin was applied via a compressed air-fed (30 psi) atomizer spray nozzle connected to a paint pot. The required amount of resin was sprayed based on monitoring the drop in weight of the tared pot. Resinated strands were left in the blender and tumbled for at least five minutes to ensure the resin was evenly mixed with the strands. After blending the required quantity of strands was weighed out in plastic tubs. Moso strands in the surface layers were oriented through 30 cm high 12-vane orienter, with 50 mm wide slots onto an oiled caul plate measuring 740 x 740 x 7.11 mm. After the bottom surface layer was laid down, Aspen strands were distributed randomly without the orienter, followed by oriented Moso

strands on the top surface. The mat was flattened with a plywood sheet and covered with a second oiled caul plate. The whole assembly was hot pressed at 150 °C for 15 minutes. During this process, maximum mat compaction pressure was 5.8 MPa for about 14 minutes. After pressing the board was removed, cooled, weighed and labeled with back RH(right hand) corner of press, board number (1-6) and Type (MM, MH or ML).

Specimen cutting: to reduce the influence of possible variability in temperature in the hot press platens, three different cutting patterns were used (two boards per type cut using each pattern) to redistribute the test specimens relative to location in press. In all the patterns, 30 IB specimens (51 x 51 mm) were located in different zones on the board. Four bending test specimens (290 x 76 mm) were located with two parallel-to-strands and two perpendicular-to-strands direction pieces for each board. One thickness swelling test specimen (152 x 152 mm) was cut per board. After cutting, each test specimen was labeled with board type, board (replicate) number, and test piece (observation) number. All specimens were conditioned at a relative humidity of 65±2% and a temperature of 20 ± 2°C to a constant average MC of 2% in accordance with ASTM D1037 (2012). Specimens were kept in the conditioning room till the weight change during 24hrs was less than 2%.

Results and Discussion

All results were analyzed using single-factor ANOVA (i.e. board type) in JMP 10 (SAS Institute, Inc. 2012), using the 5% probability level. Means were compared for all pairs of means using the Tukey-Kramer HSD evaluation. Board density and thickness were derived from measurements IB specimens and are given in Table 1. In CSA-O437.0 (2011), O-2 class OSB is recognized as being structurally equivalent to plywood when used as roof, wall and floor sheathing. Thus our results are compared to the requirements for O-2 class to determine whether low density bamboo hybrid OSB may be qualified to substitute for structural wood OSB.

Thickness and density: Due to the spring back of the board after the pressure was released after press opening, board thickness exceeded the target thickness of 11.1 mm by an average of 0.42 mm. Between the three board types, the differences in average thickness was statistically significant ($p<0.0001$). 50% w/w Moso hybrid boards (MM) showed the greatest springback, while 25% w/w Moso hybrid low density boards (ML) showed the lowest (Table 1). Note that the levels in the table not connected by same letter are significantly different (same meaning for all the tables following). Most board types were slightly higher in density than the target pressing density, despite the spring-back: MM boards exceeded the target density of 760 kg/m^3 by 0.60%; MH exceeded its target of 720 kg/m^3 by 1.15%; and ML exceeded its target of 628 kg/m^3 by 1.08%.

Group	Number	Thickness			Density		
		Mean (mm)	Std Dev	Levels	Mean (kg/m^3)	Std Dev	Levels
MH	180	11.4547	0.2622	B	728.306	82.2539	B
MM	180	11.5499	0.2744	A	764.525	64.8700	A
ML	180	11.2801	0.3084	C	634.803	73.7090	C

Table 11. Means and Standard deviations for thickness and density

Internal bonding strength: IB test is usually used to test the ultimate failure stress under a tensile load perpendicular to the plane of the board, which usually occurs in the weakest region of the core (Dai et al 2008, May 1983). As might be expected, the low density ML boards had the lowest IB strength (0.656 MPa), and the high density MH boards (0.799 MPa). Note no significant difference between MH and MM boards, whereas ML boards were significantly lower in density. MH and MM boards had approximately 20% better board consolidation than ML boards. And all groups satisfy CSA-O437.0 requirements for IB strength.

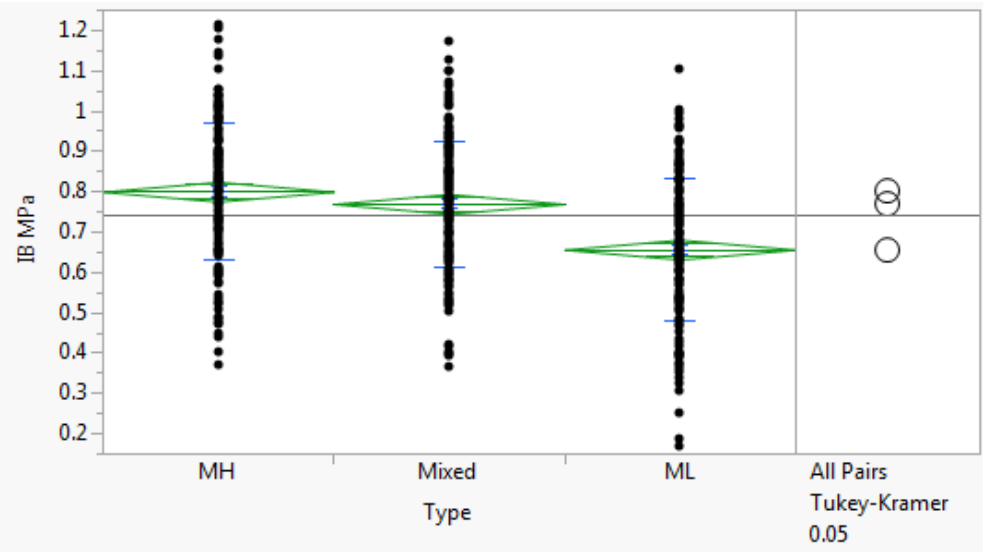

Figure 11. Oneway analysis of IB (MPa) by type

Flexural properties: For the specimens (290 mm x 76 mm) tested perpendicular-to-strand direction, no significant differences between the three different board types were found. Although both MOR and MOE of perpendicular specimens were much lower than the parallel specimens, all board types met the 12.4 MPa minimum perpendicular MOR and 1.5 GPa minimum perpendicular MOE required for O-2 class products by CSA O437.0 (2011).

Group	Number	Mean(MPa)	Std Dev	Levels
MH	12	24.380	6.1305	A
ML	12	20.386	2.2186	A
MM	12	20.246	6.8332	A

Table 12. Means and Standard deviations for MOR (perpendicular)

Group	Number	Mean(GPa)	Std Dev	Levels
MH	12	2.7233	0.4332	A
ML	12	2.4076	0.4342	A,B
MM	12	2.1410	0.4407	B

Table 13. Means and Standard deviations for MOE (perpendicular)

ML boards were significantly lower in parallel MOR and MOE than MH or MM types. Nevertheless they met the 29 MPa minimum parallel MOR and 5.5 GPa minimum parallel MOE required for O-2 class products by CSA O437.0 (2011).

Group	Number	Mean(MPa)	Std Dev	Levels
MH	12	59.090	11.2801	A
ML	12	44.233	8.6097	B
MM	12	64.925	10.0837	A

Table 14. Means and Standard deviations for MOR (parallel)

Group	Number	Mean(GPa)	Std Dev	Levels
MH	12	7.4350	0.7524	A
ML	12	6.0468	0.7290	B
MM	12	8.0058	0.7621	A

Table 15. Means and Standard deviations for MOE (parallel)

Water resistance: All three types of boards were fabricated without the addition of wax, which is normally added at about 1% w/w to wood-based OSB products (SBA 2010). Our previous study (Semple et al. 2015) found the all bamboo surface boards were below the maximum of 15% in 24 h TS required by CSA-O437.0 (2011) whereas pure Aspen boards made without wax were above 15% 24 h TS. There was no significant difference between ML and MM boards for 2 h or 24 h TS. Both types were at least 43.3% lower than ML for 2 h TS. However, this difference reduced to 24.7% for 24 h TS. Nevertheless ML boards still met the requirements of CSA-O437.0 for 24 h TS.

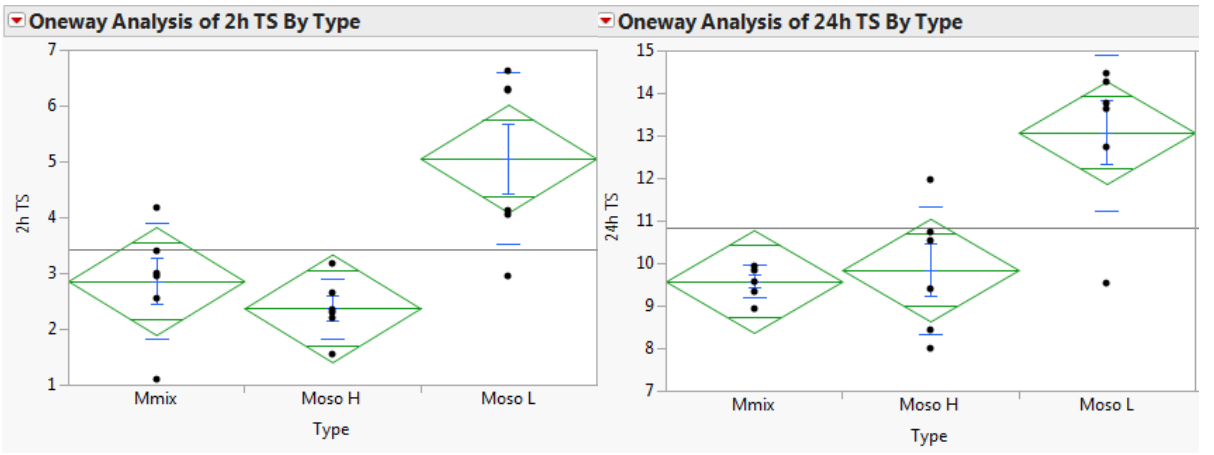

a ***b***

Figure 12. Oneway analysis of 2h and 24 h TS by type

Similarly, there was no significant between MH and MM for 2 h or 24 h WA. These absorbed 50.04% less water compared to ML at 2 hrs- and after 24 hrs, the difference was reduced to 38.2%. ML boards absorbed 43.43% of their weight in water after 24 hrs soaking, while MH absorbed 59.01% and MM absorbed 56.70%. Along with IB strength, TS and WA are possibly related to consolidation of the boards. Winistorfer and Xu (1996) have found that total thickness swelling has two components: the swelling of the wood due to MC change, and a combined effect of the compression stress release from the pressing and swelling potential variance between high and low density areas in the plane of the panel. With the similar size, low density boards have a larer space for water than the high density boards.

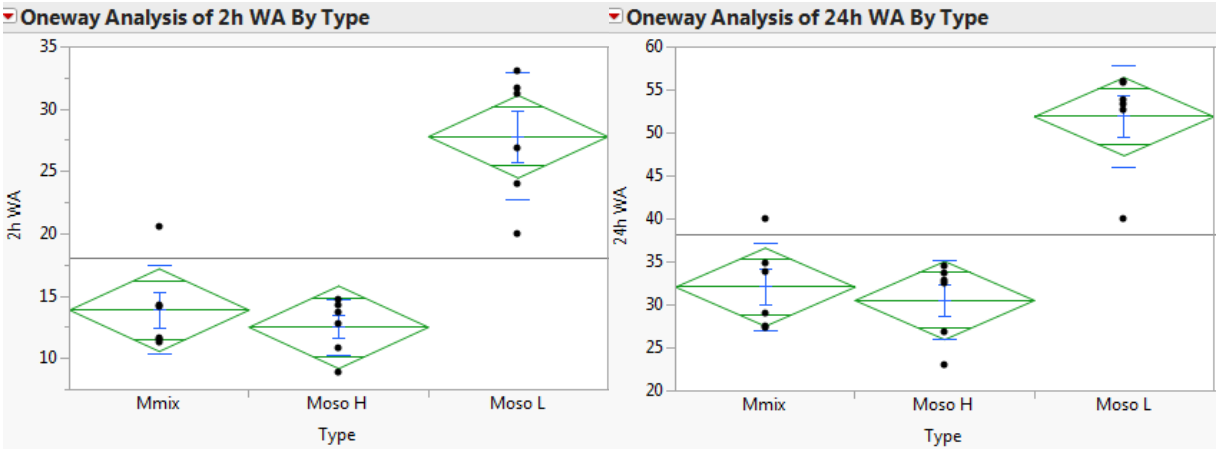

a ***b***

Figure 13. Oneway analysis of 2h and 24 h WA by type

Conclusion

The MM and MH group had a higher density than planned, while only ML group had a density met the target (Table 1). However, the ML group, which had the lowest density, showed a lower mechanical properties and worse water resistance ability.

Yet, all properties test proved that the 25% w/w low density bamboo hybrid board met the requirements by CSA-O437.0 with at least 95% of the results greater than the required limit. It is noticeable that with a low density (634.803 kg/m^3) and no wax addition in the fabrication, bamboo surface/Aspen core 3-layer hybrid boards still showed qualified properties to meet the requirements for the structure OSB materials. With these results, it is worth to carry on more research about how to retain the low density but improve the consolidation during the fabrication.

References

ASTM (2007) D 4442-07. Standard Test Methods for Direct Moisture Content Measurement of Wood and Wood-Base Materials American Society for Testing and Materials International, West Conshohocken, PA.

ASTM (2012) D 1037-12. Standard test method for evaluating properties of wood-base fiber and particle panel materials. American Society for Testing and Materials International, West Conshohocken, PA.

Austin R, Ueda K (1972) Bamboo. Weather Hill Publishing, New York. 211 pp.

CSA (2011) Standard O437.0-93R. Standards on OSB and waferboard. Canadian Standards Association, Toronto, ON. 88 pp.

Dai, C, Yu, C, Jin J (2008) Theoretical modelling of bonding characteristics and performance of wood composites. Part IV: Internal bond strength. Wood Fiber Sci 40: 146–160.

Ghavami K (2005) Bamboo as reinforcement in structural concrete elements. Cement & Concrete Composites 27: 637-649.

Lee A, Bai X, Peralta P (1996). Physical and Mechanical Properties of Strandboard Made From Moso Bamboo. Forest Products Journal 46: 84-88.

Li X (2004) Physical, Chemical, and Mechanical Properties of Bamboo and Its Utilization Potential for Fiberboard Manufacturing Anatomical. Doctoral thesis, Beijing Forestry University, Beijing, PRC. 68 pp.

Lo T, Cui H, Tang, P, Leung H (2008). Strength Analysis of Bamboo by Microscopic Investigation of Bamboo Fibre. Construction and Building Materials 22: 1532-1535.

May HA (1983) Relationship between properties, raw materials, and the density profile of particleboard. Part 4: effects of density differences and raw materials on the tensile strength perpendicular to the boards plane and the shear strength, . Holz als Roh-und Werkstoff 41: 271–275.

SAS Institute, Inc. (2012) JMP Version 10: Discovering JMP. SAS Institute Inc., Cary, NC. 154 pp

Semple KE, Smith GD (2014). Theoretical Models For Bamboo Strand Width Distribution. Pages 401-408 *in* Proceedings of the 3rd International Conf. on Processing Technologies for Forest and Bio-based Products Industries (PTF BPI 2014), 24-26 September 2014, Kuchl/Salzburg, Austria.

Semple KE, Smola M, Hoffman J, Smith GD (2014). Optimising the stranding of Moso bamboo (*Phyllostachys pubescens* Mazel) culms using a CAE 6/36 disk flaker. Pages 257 - 269 *in* M Barnes and V Herian (eds) Proceedings of the 57th International Convention of Society of Wood Science and Technology, 23-27 June, 2014, Zvolen, Slovakia.

Semple KE, Zhang PK, Smola M, Smith GD (2015) Uni-layer and three-layer Oriented Strand Boards made from mixtures of Moso bamboo (Phyllostachys pubescens Mazel) and Aspen (Populus tremuloides Michx.) strands. European Journal of Wood and Wood Products, accepted in 2015.

Smola M (2013). Producing Structural Elements from Moso Bamboo Culms. Unpublished Thesis.Fachhochscheule Rosenheim University, Rosenheim, German.

SBA – Structural Board Association (2010). Binders and waxes in OSB. Technical Bulletin. http://osbguide.tecotested.com/pdfs/en/tb114.pdf. (January 2013).

Winistorfer PM, Xu W (1996) Layer water absorption of medium density fiberboard and oriented strandboard. Forest Products Journal, 46(6), 69-72

Proceedings of the 58th International Convention of
Society of Wood Science and Technology
June 7-12, 2015 - Grand Teton National Park, Jackson, Wyoming, USA

Early Stage Researcher Speed Slot (3 minutes) Session
Moderator: *Michael Burnard, University of Primorska, Slovenia*

Determining Tension and Compression Strength and Basic Manufacturing Feasibility of CNC Router-cut Joints

Mesut Uysal, uysalm@purdue.edu
Cagatay Tasdemir, ctasdemi@purdue.edu
Eva Haviarova, ehaviar@purdue.edu
Rado Gazo, gazo@purdue.edu

Purdue University, 2491 Sycamore Ln., Apt 5, West Lafayette, IN 47906

Abstract

Joinery systems produced using advanced CNC equipment increasingly popular in wood products, could be manufactured faster, more accurately, requiring lower labor costs. These joints are used mainly in products made of engineered materials, processed by CNC machinery. The specific joint construction has self-locking character and variable strength related to manufacturing tolerance and joint design. In this respect, seven types of joints were evaluated for strength and manufacturing capacity. To understand better manufacturing feasibility of each joint type, calculation of material yield and processing time were determined. Yield percentages were calculated for samples and used to evaluate the manufacturing efficiency of CNC process for production of these joints. Moreover, recorded CNC manufacturing times for each sample have been averaged within its corresponding experimental group and employed to compare the burden created during the production of each joint in terms of efficient use of labor and machine time. Manufactured joint samples were then tested for strength in tensions and compression. Results of strength tests were compared to other CNC-made and also to traditional joint types. The results of this study are expected to provide information for furniture industry utilizing CNC manufacturing by providing a better understanding of manufacturing feasibility and strength capacity of different joint types.

Proceedings of the 58th International Convention of
Society of Wood Science and Technology
June 7-12, 2015 - Grand Teton National Park, Jackson, Wyoming, USA

Heat and Mass Transfer during Ultrasound-Assisted Vacuum Drying of Wood

Z.B. He[*], *Z.J. Zhao, Y. Zhang, Z.Y. Wang, S.L.* Yi

Beijing Key Laboratory of Wood Science and Engineering
College of Material Science and Technology
Beijing Forestry University
Beijing, 100083, P.R. China
E-mail: hzbbjfu@126.com

Abstract

Wood ultrasound drying is a kind of innovative approaches. In this paper, poplar with the dimensions of 450mm by 100mm by 40mm was taken as experimental material. The drying process was done under the conditions that the drying medium temperature was 60°C, the absolute pressure was 0.02 MPa, the ultrasound power was 100 W and the frequency was 20 kHz. The moisture distribution inner wood and water diffusion coefficient were studied, and the model among wood moisture content variation, drying time and water diffusion coefficient was established. Results indicated that the moisture gradient increases along with the increase of drying time during the drying process, free water and bound water are dried simultaneously when wood moisture content above the fiber saturation point; Wood moisture decreases almost linearly when moisture above the fiber saturation point while the descending rate decreases when the moisture content below the fiber saturation point. The water diffusion coefficient decreases along with the increase of drying time and increases exponentially along with the increase of moisture content. The moisture diffusion coefficient is $2.89\times10^{-4}cm^2.s^{-1}$ at the initial drying stage, it is $3.02\times10^{-6}cm^2.s^{-1}$ when the moisture content when the moisture content at the fiber saturation point, and it is $2.27\times10^{-7}cm^2.s^{-1}$ when the moisture content is 10%; The equation between the water diffusion coefficient and the moisture content was established and it could be used to predict the water diffusion coefficient during ultrasound-assited vacuum drying.

Key words: ultrasound; water distribution; water diffusion coefficient; vacuum drying

Introduction

All kinds of woods, which are the main raw materials in furniture, building and woodworking industry, must be dried after deforestation (Zhang *et al.* 2005). Thus, wood drying is one of the most important steps in wood product manufacturing. The drying process consumes roughly 40% to 70% of the total energy in the entire wood products manufacturing process (Zhang and Liu 2006). Compared with the traditional drying methods, wood vacuum drying has many advantages. For example, it could significantly shorten the drying time (particularly when the moisture content is below the wood fiber saturation point), it could increase suitability for drying large dimensions of timber, it has less risk of discoloration, and it has good energy efficiency (Ressel 1999; Welling 1994). However, vacuum drying methods are not suitable for timber with high initial moisture contents (Welling 1994), and surface checking and internal checking can be significant problems with wood vacuum drying, especially when the drying temperature is high; this is because of insufficient moisture movement from the center of the wood samples to the surface during the vacuum drying process which can cause steep moisture gradients from the core to wood surface layers, which could lead to checking (Kanagawa and Yasujima 1993; Avramidis *et al.* 1994). Therefore, exploring energy efficient new technologies for low temperature vacuum drying and improving product quality is an important goal in development of new drying technologies.

Ultrasound is an efficient non-thermal alternative to increasing the drying rate without significantly heating up the material (Cohen and Yang 1995). When ultrasound power is applied in liquid media, ultrasound waves cause rapid series of alternative compressions and expansions, in a way similar to a sponge when it is squeezed and released repeatedly. Also, ultrasound produces cavitation, which is beneficial for the removal of moisture that is strongly attached to the solid. Micro-deformation of porous solid materials, caused by ultrasonic waves, is likely responsible for the creation of microscopic channels that enhance diffusion and increase convective mass transfer (Fuente-Blanco *et al.* 2006; Gallego-Juárez *et al.* 1999; Soria and Villamiel 2010; Tarleton 1992).

In recent years, ultrasound has been implemented as an alternative method for drying, and the results have shown that ultrasound can greatly reduce the overall processing time (Aversa *et al.* 2011; Mothibe *et al.* 2011), increase the mass transfer rate (Cárcel *et al.* 2011; García-Pérez *et al.* 2011; Zhao and Chen 2011), and increase the effective water diffusivity (Bantle and Eikevik 2011). However, no reports so far have addressed the mass transfer during the ultrasound-vacuum combined drying process. In this work, poplar (*Populus spp.*), which is one kind of fast growing wood and planted in large area in China, was taken as material and the drying time and the water diffusion coefficient was studied during the ultrasound-assited vacuum drying process..

Materials and Methods

Material

Fast growing poplar (*Populus tomentosa*) provided by LANDBOND Furniture Co., Ltd, ShanDong, China, was taken as specimen. The dimension of the test specimens was 450 mm long by 100 mm wide by 40 mm thick with the initial moisture content of (130±5)% (according to GB/T 1931-2009) (Zhao *et al*. 2009). To simulate the real production process, all the faces of specimens, except one face with the dimension of 450 mm long by 100 mm wide, were blocked by covering them with epoxy resin.

Ultrasound-Vacuum Drying System

The scheme of the experimental set-up of the ultrasound-vacuum drying system is shown in Fig.1. The ultrasound-vacuum dryer is modified by applying a power ultrasound to a wood vacuum drying device (Shanghai Laboratory Instrumental Works Co., LTD, Shanghai, China). The pressure controller, vacuum pump, and pressure meter of this instrument could control the pressure with an accuracy of ±0.002 MPa automatically. The electronic generator driving the ultrasonic transducer is composed of an impedance matching unit, a power amplifier, and a resonant frequency control system. This system is specifically developed to keep constant power at the resonant frequency of the transducer during the drying process. The ultrasonic generator has a maximum power capacity of about 1200 W. The ultrasonic transducer (with a weight of 0.9 kg and a diameter of 0.066 m) is connected to the ultrasonic generator with corresponding power and frequency; it is also put on the wood specimen by its own weight to avoid ultrasonic energy attenuation. The gas valve is used to adjust the vacuum condition in the drying chamber. The air velocity is controlled by the pulse width modulation (PWM) at a constant rate of 1m/s and measured using a hot-wire anemometer. The temperature monitor is used to control the temperature according to the setting value, the heat generator consists of two sets of heat generators, and the highest temperature achievable is 200°C.

Methods

In this experimental test, the drying rates, wood moisture contents and water effective diffusion coefficient were examined at the drying conditions that the drying temperature was 60°C, the absolute pressure was 0.02 MPa, the ultrasound power was 100 W and the frequency was 20 kHz, and the air velocity was 2m/s, which was always used in wood drying (Zhang *et al.* 2005). The experimental steps were as follows,

(1) The ultrasound transducer with the power of 100 W and the frequency of 20 kHz was installed and connected to the ultrasonic generator. Then, the frequency of the ultrasonic generator was set to match the impedance of the ultrasonic transducer.

(2) Samples were put into the ultrasound-vacuum drying system and were attached with ultrasonic transducers to obtain ultrasonic waves, and the temperature inner vacuum dryer was set as 60°C.

(3) When temperature inner wood was constant, the absolute pressure inner vacuum dryer was set as 0.02MPa, and then the vacuum pump was started.

(4) The pressure inner vacuum dryer was recovered to normal pressure and cylindrical sample with the diameter of 3 centimeters was cut from wood sample at an interval of 4 hours, and the slice was cut from such cylindrical sample through the thickness direction, and then the weights of the slice were measured, which represent the wood layered moisture content at this moment.

(5) The sample was dried until its final moisture content was below 10%.

(6) All the slices were dried to oven dry, and their oven-dry weight were weighed.

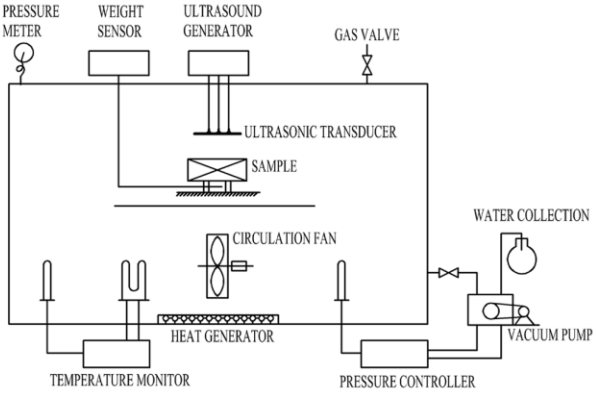

Fig. 1. Schematic of the experimental set-up of the ultrasound-vacuum dryer

Water Diffusion Coefficient Model

Both free water and boundary water are dried during wood drying process (Siau 1984), thus, a comprehensive water diffusion coefficient was used during the whole drying process in this paper. Making assumptions that water only moves from the thick direction during the ultrasound-assited vacuum drying process, the sample thickness is 2L, the length is a, the width is b, the initial moisture content is C_0 and the water concentration at wood surface is C_1, as showed in Fig.2.

Also, another assumptions were made during the drying process,

(1) The initial moisture content is uniform and the moisture content is C_0.

(2) The water evaporative rates at wood upper surface is equal to that at lower surface, and no water migration at wood central layer.

(3) Wood moisture content is C during the drying process.

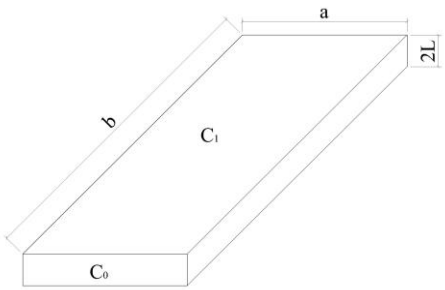

Fig. 2. The schematic diagram of specimen

Therefore, the water migration governing equation could be written as equation (1),

$$\begin{cases} \dfrac{\partial C}{\partial \tau} = \dfrac{\partial}{\partial x}(D\dfrac{\partial C}{\partial x}) \\ C(x,0) = C_0 \\ C(L,\tau) = C_1 \\ \dfrac{\partial C}{\partial x}\big|_{x=0} = 0 \\ \overline{C} = \dfrac{1}{L}\int_0^x C(x,\tau)dx \end{cases} \tag{1}$$

Combined with method of separation of variables, method of Laplace transformation and method given by crank(Crank 1975), equation (2) could be gotten,

$$Y = \frac{C - C_0}{C_1 - C_0} = 1 - \frac{4}{\pi}\sum_{n=1}^{\infty}\frac{(-1)^n}{2n+1}\cos\left(\frac{(2n+1)\pi x}{2L}\right)e^{-D(2n+1)^2\pi^2\tau/4L^2} \tag{2}$$

Wood moisture could be written as equation (3),

$$\begin{aligned} V_A &= abN_{Ax} = ab\left(-C_0 D\frac{\partial M(x,\tau)}{\partial x}\right) = ab\left(-C_0 D\frac{\partial Y(x,\tau)}{\partial x}\right) \\ &= ab(-C_0 D)\frac{\partial\left[1 - \dfrac{4}{\pi}\sum_{n=1}^{\infty}\dfrac{(-1)^n}{2n+1}\cos\left(\dfrac{(2n+1)\pi x}{2L}\right)e^{-D(2n+1)^2\pi^2\tau/4L^2}\right]}{\partial x} \\ &= ab(-C_0 D)\frac{2}{L}\sum_{n=1}^{\infty}(-1)^n\sin\left(\frac{(2n+1)\pi x}{2L}\right)e^{-D(2n+1)^2\pi^2\tau/4L^2} \end{aligned} \tag{3}$$

When the thickness of wood specimen is L, equation (3) could be written as (4),

$$V_A = ab(-C_0 D)\frac{2}{L}\sum_{n=1}^{\infty}(-1)^n\sin\left(\frac{(2n+1)\pi L}{2L}\right)e^{-D(2n+1)^2\pi^2\tau/4L^2} \tag{4}$$

Therefore,

$$V_A = ab(-C_0 D)\frac{2}{L}\sum_{n=1}^{\infty} e^{-D(2n+1)^2\pi^2\tau/4L^2} \quad (5)$$

The wood initial moisture content could be written as equation (6),

$$m_{A0} = C_0 abL \quad (6)$$

The decrease of wood moisture content in time τ could be written as equation (7),

$$m_A(\tau) = \int_0^{\tau} V_A d\tau = \frac{8abLC_0}{\pi^2}\sum_{n=1}^{\infty}\frac{1}{(2n+1)^2} e^{-D(2n+1)^2\pi^2\tau/4L^2} \quad (7)$$

Therefore, the ratio of moisture decrement and the whole moisture content could be written as equation (8),

$$\frac{m_A(\tau)}{m_{A0}} = \frac{8}{\pi^2}\sum_{n=1}^{\infty}\frac{1}{(2n+1)^2} e^{-D(2n+1)^2\pi^2\tau/4L^2} \quad (8)$$

Therefore,

$$\frac{m_A(\tau)}{m_{A0}} = \frac{8}{\pi^2}\frac{1}{(2n+1)^2}\sum_{n=1}^{\infty}\exp\left[-D(2n+1)^2\pi^2\tau/4L^2\right] \quad (9)$$

Results and Discussion

(1) Wood Moisture Content Variation along With the Drying Time

Wood moisture content distribution at different time and space along with the drying time was showed in Fig.3. It shows that wood moisture content is uniform before drying, and the initial moisture content is about 130%. The moisture gradient increases along with the increase of time, 6 h later, the moisture at wood surface layer is about 62.7%, while that at wood center does not change. 13 h later, moisture content at wood surface is below the fiber saturation point, it is about 12.0%, and 98 h later, moisture content for the whole wood is below the fiber saturation point. Therefore, wood is dried from surface to wood center during the ultrasound-vacuum combined drying process, and both free water and bound water are dried when wood moisture content above the fiber saturation point. For each wood layer, free water is dried at first, and then bound water begins to dry. It also indicates that wood moisture content from wood surface to the distance of 2 centimeters is constant after 50 h, this result is for the reason that wood moisture content is lower than the fiber saturation point at these areas while the moisture content at other wood place is above the fiber saturation point.

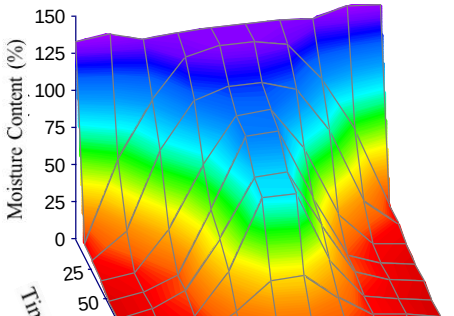

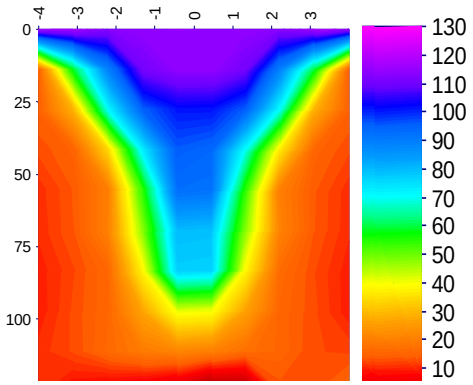

Fig. 3. The moisture content distribution diagram at different time and space during ultrasound-vacuum combined drying

What's more, for each wood layer, wood moisture content decrease along with the increase of drying time, and the drying rates is constant when wood surface is above fiber saturation point, the drying rates decrease when wood moisture content is below the fiber saturation point. Drying rates for the part which is near to wood surface are faster than that is far away from wood surface. The time for moisture content gets to the fiber saturation point are 98 h, 81 h, 53 h, 38 h, 25 h, 18 h and 10 h, respectively, for the wood parts, which are 1.0 centimeter, 1.5 centimeter, 2.0 centimeter, 2.5 centimeter, 3.0 centimeter, 3.5 centimeter, and 4.0 centimeter, respectively. Moreover, moisture content at wood surface decreases to 10% at a short time, this phenomenon is mainly because that the drying rates at wood surface is about 100 to 1000 times faster than that inner wood (Zhu *et al.* 1992), moisture inner wood could not get to wood surface immediately when moisture at wood surface is dried.

(2) Water Diffusion Coefficient at Different Moisture Content and Drying Time
Water diffusion coefficient is one of the most important parameters to measure wood drying rates and water migration rates. According to equation (9) and the drying parameters in this paper, the model among moisture content variation, drying time and water diffusion coefficient is showed in equation (10). Combined with wood moisture content at different drying time, the water diffusion coefficient at different drying time and moisture contents were got and showed in Fig.4.

$$\frac{m_A(\tau)}{m_{A0}} = \frac{0.811392}{(2n+1)^2}\sum_{n=0}^{\infty} e^{-0.154D(2n+1)^2\tau} \qquad (10)$$

Fig.4 shows that it took 53 h to dry wood from moisture content of 126% to the fiber saturation point, while 57 h was need to dry wood from the fiber saturation point to the moisture content of 10%, the drying rates above moisture content is 5.16 time faster than that below moisture content, so, ultrasound is beneficial to free water drying (He 2012). What's more, Fig.4 also indicates that water diffusion coefficient decrease along with the

increase of drying time, the water diffusion coefficient is 2.89×10^{-4} $cm^2\cdot s^{-1}$ at the beginning stage, it is 3.02×10^{-6} $cm^2\cdot s^{-1}$ when wood moisture content is at fiber saturation point and it is 2.27×10^{-7} $cm^2\cdot s^{-1}$ at the moisture content of 10%. Many exiting researches have the similar results(Siau 1984).

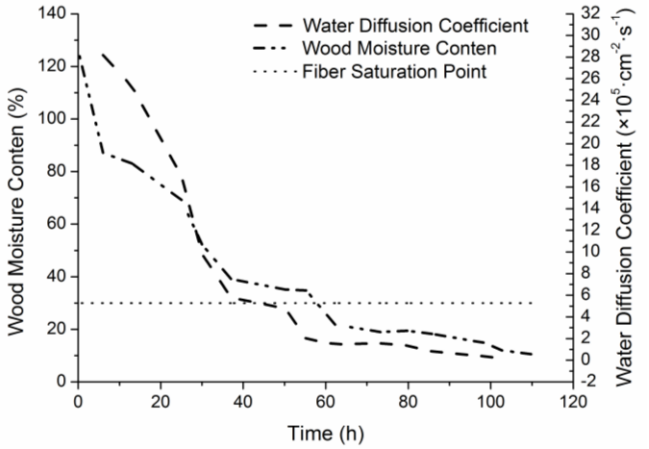

Fig.4 Water diffusion coefficient at different wood moisture content and drying time

(3) Relationship between Water Diffusion Coefficient and Wood Moisture Content

Wood moisture content has great effects on water diffusion coefficient (Siau, 1984). To study the influence of wood moisture content on the water diffusion coefficient, the relationship between wood moisture content and the water diffusion coefficient was established and showed in equation (11),

$$\overline{D} = -6.361 + 5.1841e^{0.0218M} \qquad (11)$$

Where, $\overline{D}$ is the average value of water diffusion coefficient when wood moisture content is above 8%, $10^{-5}cm^2\cdot s^{-1}$, M is the moisture content (%)

To measure the difference between the theoretical values, which calculate from equation (11), and the real value of water diffusion coefficients. Fig.5 shows the real value and the theoretical value of wood water diffusion coefficient at different moisture content. It indicates that the water diffusion coefficient increases exponentially along with the increase of moisture content, few differences between the real value and the theoretical value, and equation (11) could be used to simulate the water diffusion coefficient at different moisture content during the ultrasound-vacuum combined drying process.

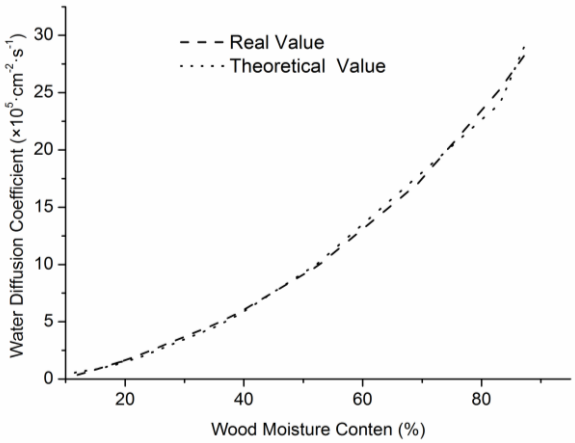

Fig.5 The theoretical and actual value of water diffusion coefficient during ultrasound-vacuum combined drying process

Conclusion

(1) The model among wood moisture content variation, drying time and water diffusion coefficient was established, and the water diffusion coefficient could be calculated by this model.

(2) The moisture gradient increases along with the increase of drying time during the drying process, 13 h later, moisture content at wood surface is below the fiber saturation point while that at wood center is much higher than the fiber saturation point. Wood is dried from surface to wood center during the ultrasound-vacuum combined drying process, and both free water and bound water are dried when wood moisture content above the fiber saturation point.

(3) For each wood layer, wood moisture content decrease along with the increase of drying time, and the drying rates is constant when wood surface is above fiber saturation point, and the drying rates decrease when wood moisture content is below the fiber saturation point.

(4) Water diffusion coefficient decrease along with the increase of drying time, the water diffusion coefficient is 2.89×10^{-4} $cm^2\cdot s^{-1}$ at the beginning stage, it is 3.02×10^{-6} $cm^2\cdot s^{-1}$ when wood moisture content is at fiber saturation point and it is 2.27×10^{-7} $cm^2\cdot s^{-1}$ at the moisture content of 10%.

(5) Water diffusion coefficient increases exponentially along with the increase of moisture content, and the equation between the water diffusion coefficient and the moisture content could be used to predict the water diffusion coefficient during ultrasound-assited vacuum drying.

Acknowledgments

This paper was supported by "the Fundamental Research Funds for the Central University (NO. BLX2014-41)" and "The National Science Foundation of China-Study on the Moisture Migration Mechanism during Ultrasonic-Assisted Wood Vacuum Superheated Steam Drying (31270604)".

Reference

Aversa, M., Van der Voort, A. J., De Heij, W., Tournois, B., and Curcio, S. (2011). An experimental analysis of acoustic drying of carrots: evaluation of heat transfer coefficients in different drying conditions, Dry Technol. 29, 239-244.

Avramidis, S., Liu, M., and Neilson, B. J. (1994). Radio-frequency/vacuum drying of softwoods: Drying of thick western red cedar with constant electrode voltage, Forest Prod J. 44(1), 41-47.

Bantle, M., and Eikevik, T. M. (2011). Parametric study of high-intensity ultrasound in the atmospheric freeze drying of peas, Dry Technol. 29, 1230-1239.

Cárcel, J. A., Garcia-Perez, J. V., Riera, E., and Mulet. A. (2011). Improvement of convective drying of carrot by applying power ultrasound-influence of mass load density, Dry Technol. 29, 174-182.

Cohen, J. S., and Yang, T. C. S. (1995). Progress in food dehydration, Trends Food Sci. Tech. 6(1), 20-25.

Crank, J. (1975), The mathematics of diffusion, second ed. Claredon press, oxford.

Fuente-Blanco, S., Sarabia, E. R. F., Acosta-Aparicio, V. M., Blanco-Blanco, A., and Gallego-Juárez, J. A. (2006). Food drying process by power ultrasound, Ultrasonics Sonochem. 44, 523-527.

Gallego-Juárez, J. A., Rodríguez-Corral, G., Gálvez-Moraleda, J. C., and Yang, T. S. (1999). A new high intensity ultrasonic technology for food dehydration, Dry Technol. 17, 597-608.

García-Pérez, J. V., Ozuna, C., Ortuño, C., Cárcel, J. A., and Mulet, A. (2011). Modeling ultrasonically assisted convective drying of eggplant, Dry Technol. 29, 1499-1509.

He, Z. B., Yang, F., Yi, S. L., and Gao, J. M. (2012). Effect of ultrasound pretreatment on vacuum drying of Chinese catalpa wood, Dry Technol. 30(15), 1750-1755.
Kanagawa, Y., and Yasujima, M. (1993). Effect of heat sources on drying time in vacuum drying of wood, Vacuum Drying of Wood'93, 292, Slovakia.

Mothibe, K. J., Zhang, M., Nsor-atindana, J., and Wang, Y. C. (2011). Use of ultrasound pretreatment in drying of fruits: Drying rates, quality attributes, and shelf life extension, Dry Technol. 29, 1611-1621.

Ressel, J.B. (1999). State of the art for vacuum drying in the wood working industry, cost action E15, workshop'. Edinburgh, UK.

Siau, J. F. (1984). Transport Process in Wood. Springer-Verlag, New York.

Soria, A. C., and Villamiel, M. (2010). Effect of ultrasound on the technological properties and bioactivity of food: a review, Trends Food Sci. Tech. 21, 323-331.

Tarleton, E.S. (1992). The role of field-assisted techniques in solid/liquid separation, Filtration Separation 3, 246-253.

Welling, J. (1994). Superheated steam vacuum drying of timber-range of application and advantages, The 4th IUFRO international wood drying conference. Rotorua, 460-461.

Zhao, F., and Chen, Z. Q. (2011). Numerical study on moisture transfer in ultrasound-assisted convective drying process of sludge, Dry Technol. 29, 1404-1415.

Zhang, B.G., and Liu, D.Y. (2006). Exploring a new developing way of wood drying technology in China, China Forest Prod. Ind. 33(4), 3-6.

Zhang, B. G., Gao, J. M., Yi, S. L., and Zhou, Y. D. (2005). Applied wood drying, Chemical Industry Press, Beijing.

Zhao, R.J., Fei, B.H., Lv, J.X., Yu, H.Q., Huang, R.F., Zhao, Y.Q., Huang, A.M., Cui, Y.Z. (2009) Wood moisture content measuring method.Wood-determination of moisture content for physical and mechanical test, MOD, CN-GB, GB/T 1931–2009.

Zhu Z.X. (1992). Wood Drying. China Forestry Publishing, Beijing.

Proceedings of the 58th International Convention of
Society of Wood Science and Technology
June 7-12, 2015 - Grand Teton National Park, Jackson, Wyoming, USA

Comparative Life Cycle Analysis of Fossil and Bio-based PET Bottles

Luyi Chen [1] – Rylie E.O. Pelton[2] – Timothy M. Smith[3]

[1] Graduate Research Assistant, Department of Bioproducts and Biosystems Engineering – University of Minnesota, Saint Paul MN, USA.
chen3461@umn.edu
[2] Graduate Research Assistant, Department of Bioproducts and Biosystems Engineering – University of Minnesota, Saint Paul MN, USA.
olso4235@umn.edu
[3] Associate Professor, Department of Bioproducts and Biosystems Engineering – University of Minnesota, Saint Paul MN, USA.
timsmith@umn.edu

Abstract

Both biofuels and bio-plastics are often regarded as sustainable solutions to current environmental problems such as climate change, fossil depletion and fine particulates emissions. However, both have been criticized for being economically costly, competing with other societally beneficial goods such as food, and offering limited environmental benefits compared to their fossil counterparts. Biorefinery, proposed as a sustainable counterpart to fossil refinery, provides the possibility of lowering production costs by producing and selling value-added co-products. This study provides a comparative environmental life cycle analysis for 100% bio-based PET bottles produced in a multi-output biorefinery system, versus fully fossil-based and partially fossil-based PET bottles. Results indicate that with consideration of displacement credits, some fully bio-based PET bottles have overall better environmental performance than any other scenarios. Results were found to be sensitive to data quality and allocation method. The study served as a building block for comprehensive analysis of optimized biorefineries.

Keywords
Comparative Life Cycle Assessment, Bio-PET, Bioplastics, Avoided Impacts, Biorefinery

Introduction

Growing concerns about fossil fuel depletion and global warming have driven scholars to seek for sustainable alternatives for crude oil refinery products. To address those issues, the biofuels and biochemicals were proposed as a solution. They were developed from non-food crops, agricultural residues and forest residues such as corn stover, wheat straw, switchgrass and woody biomass (Hsu et al., 2010a). However, the environmental excellence of a spectrum of bioproducts has yet to be decided (Borrion, McManus, & Hammond, 2012). To establish a both environmentally viable business mode for biomass based products, a novel manufacturing process co-producing biofuels and biochemicals has been proposed. Research have suggested that co-producing biofuels and biochemical would increase the economical viability of bioproducts industry (Cherubini, 2010). So far, nearly all bio-PET available only replace the petrochemical ethylene glycol with bio-ethylene glycol generated from corn or sugarcane ethanol, leaving PTA still coming from fossil resources. The aim of this study is to conduct a comparative Life Cycle Analysis for the traditional fossil-based PET bottle, partially bio-based PET bottles, and the aforementioned completely biomass derived PET bottles.

Materials & Methods

This study applied the Life Cycle Assessment (LCA) methodology, which is used for estimation and evaluation of environmental impacts attributable to the life cycle of a product (ISO, 2006; Rebitzer et al., 2004). Consider the data availability of pilot and demonstration biorefinery facilities, a traditional attributional life cycle assessment (aLCA) model was applied with sensitivity analysis of weak points in the system. The goal of this study is to quantify and compare environmental impacts of PET bottles produced through traditional fossil refinery facilities and through biomass processing facilities in the context of the United States, using a cradle-to-factory-gate approach.

Regarding the production of PET bottles, the two chemical precursors, purified terephthalate acid (PTA) and ethylene glycol (EG), are synthesized separately. In the traditional production of PET, PTA is produced from fossil refineries, whereas EG is produced from natural gas refineries. On the other hand, bio-based versions of PTA and EG can be produced from a variety of biomass materials, the environmental impacts of which are explored in different scenarios presented in Table 1. Softwood forest residues and corn stover were chosen as raw materials for bio-based purified terephthalic acid. Weighted average fuel consumption for forest regeneration, thining and harvesting operations was summarized by Puetmann et al. (Puettmann, Oneil, Milota, & Johnson, 2012).Upon harvesting, the woody biomass transportation scenario for equipment and distances was documented by Ganguly et al. (Ganguly, Eastin, Bowers, Huisenga, & Pierobon, 2014). Fig. 1 illustrates the system boundary of the study.

With regard to the functional unit (FU), the environmental impacts per 1 kg of PET bottles is investigated, which equals the weight of approximately 100 bottles with 0.5 liter capacity, and should be kept consistent for all compared scenarios in order to yield meaningful comparative results (Curran, 1996).

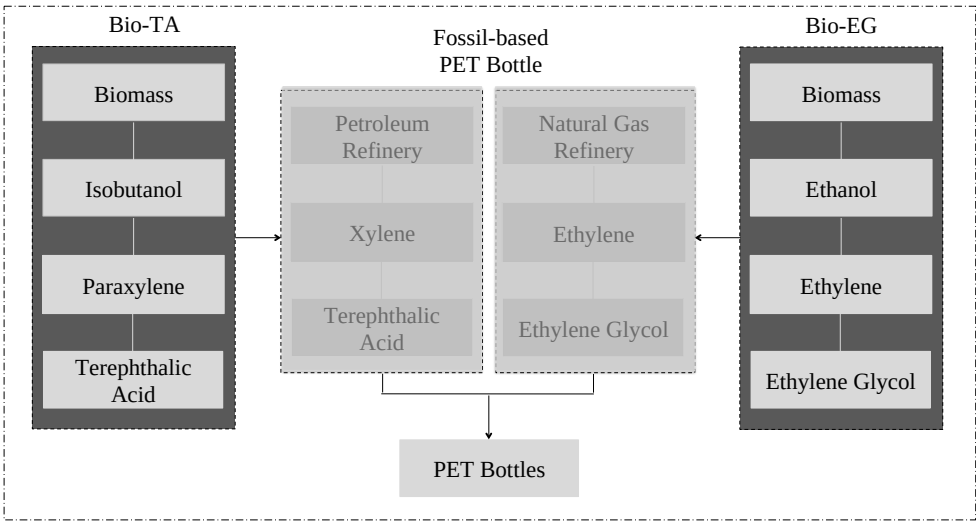

Figure 1. System boundary of life cycle for 100% bio-based PET bottles

Table 1. Scenarios of PET bottle production

PTA \ EG	Fossil	Corn	Switchgrass	Wheat Straw
Fossil	Scenario 1	Scenario 2	Scenario 3	Scenario 4
Wood	Scenario 5	Scenario 6	Scenario 7	Scenario 8
Corn Stover	Scenario 9	Scenario 10	Scenario 11	Scenario 12

Life cycle inventory were developed in the professional GaBi software. Ecoinvent (Frischknecht et al., 2005) was the primary database applied in this study, with supplementary information retrieved from literature (Hsu et al., 2010a; Tao et al., 2014) and other databases available in GaBi. Process datasets established on a European industry background were altered to fit the context of the U.S. industry. For biomass derived paraxylene production, each process was developed individually based on proprietary information provided by industry collaborators as well as literatures.

For a multi-output system, the main problem of LCA lies in how to attribute environmental debts or credits among them. According to ISO 14040 and 14044 standards, allocation should be avoided by expanding the investigated system boundary to include alternative production system of exported functions (ISO, 2006). In this study, three kinds of avoid impacts were accounted for:

a. Avoided impacts from slash pile burning (for forest residues). In Pacific Northwest area of the U.S., woody biomass residues left from harvesting would be collected and burned, and thereby increasing the CO_2 emissions by releasing carbon sequestered from atmosphere by photosynthesis (Stevens & Verhé, 2004). When bioenergy was harvested from residues, the avoided impacts from slash pile burning was qualified as a credit to the biofuel production system (Ganguly et al., 2014).
b. Avoided impacts from fossil-based electricity production (for forest residues, corn stover, switchgrass and wheat straw). Any excess energy produced was assumed to be sold to displace an equivalent amount of fossil derived energy. Impacts generated by depletion of a certain amount of fossil resources were thereby avoided and subtracted from bio-PET bottle systems. That assumption, though suggested by Cherubini and Jungmeier (Cherubini & Jungmeier, 2010), suffered from uncertainty and would later be evaluated in sensitivity analysis.
c. Avoided impacts from co-products (for corn). Corn grain, soybean meal and urea were listed as avoided products with ethanol produced from advance corn dry mill (Hsu et al., 2010b).

Results and Discussion

Midpoint impacts evaluation was applied given that endpoint impacts method was subjected to larger uncertainties (Finnveden et al., 2009; Pawelzik et al., 2013). Three impact categories were analyzed in this study, based on The Tool for the Reduction and Assessment of Chemical and Other Environmental Impacts (TRACI v2.1), which is designed by US EPA and normalized to reflect situations of the US industry (Bare & Gloria, 2006).

Comparative LCIA results were interpreted in Fig. 2. Global Warming Potential (GWP) of forest residues derived bottles (the second group of bars in the graph, where woody biomass PTA was paired with EG made from fossil resources, corn grains, switchgrass and wheat straw to make four different scenarios of PET bottles) were about 1.54 to 2.75 kg CO2 equivalent per kg PET. That is about 65% lower than GWP generated from fossil PTA derived bottle production (~5.04 to 6.19 kg CO2-eq/kg PET bottles) and 77% lower than those from producing corn stover PTA bottles (~7.97 to 9.18 kg CO2-eq/kg PET bottles) on average. However, note that the significant reduction of impacts primarily came from displacement credits of excess electricity, which decreased non-credit result by 66%. Without avoided impacts, wood based bottles had mediocre environmental performance with about 6.98 to 8.37 kg CO2-eq/kg PET bottles. That is about 36% higher than impacts of fossil PTA bottles, but 17% lower than that of corn stover PTA bottles.

Figure 3 presented the reasons why bio-based PET bottles have higher impacts than fossil-based ones. Extraction of biomass was found to be an impact significant phase. The establishment and cultivation of forest and cornfields, together with the harvest of forest residues and corn stover, made the raw material extraction phase a big emitter of greenhouse gases. Another primary impact contributor is the isobutanol (IBA) production process in wood PET scenarios. The process could be further broke down to pretreatment, enzymatic hydrolysis and fermentation, during which polysaccharides were destructed into fermentable sugars and then processed to IBA.

Comparing to non-woody biomass, woody biomass has higher lignin content. It tied cellulose and hemicellulose together and forms a structure called lignocellulose, which is very recalcitrant to microbial and enzymatic digestion (Zhu & Pan, 2010). Extra energy is required to digest woody biomass (Hendriks & Zeeman, 2009; Mosier et al., 2005), leading to higher environmental impacts comparing to petroleum refining process. It is also noticeable that switchgrass production yielded high impacts comparing to that of wheat straw and corn grain. Since switchgrass had not yet been produce in industrial scale, the uncertainty of data is relatively higher, which potentially led to its worse environmental profile (Hsu et al., 2010a).

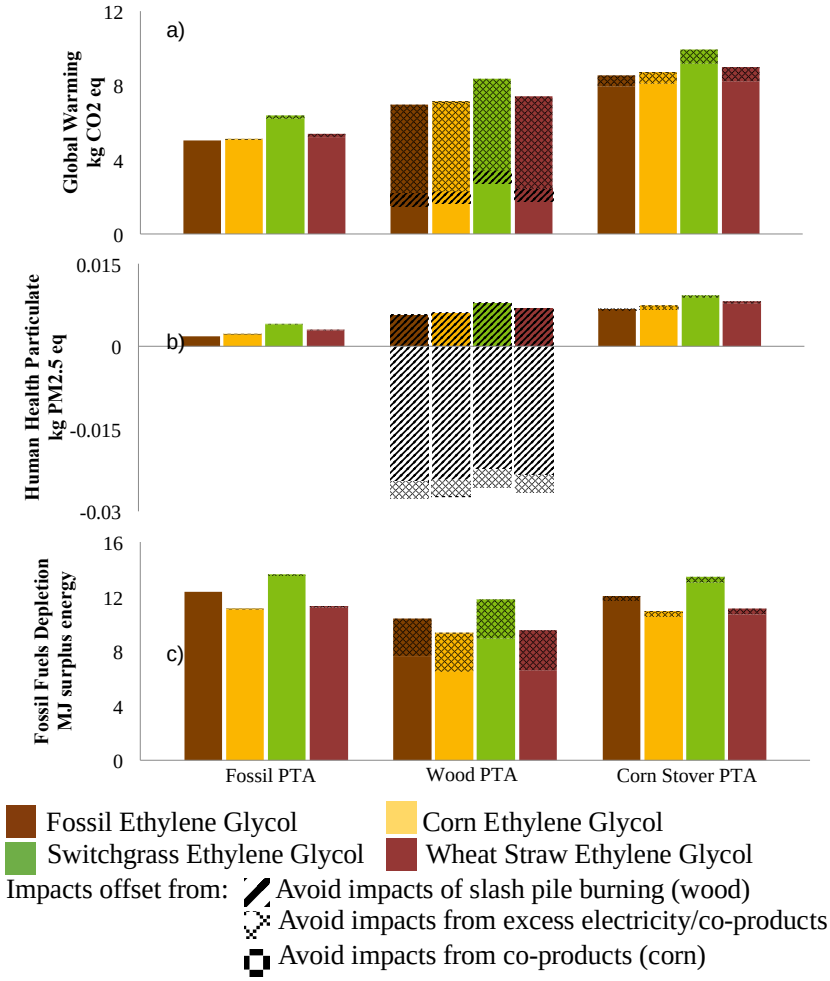

Figure 2. LCA results of 12 PET bottle production scenarios with Terephthalic Acid and Ethylene Glycol derived from different raw materials. a) Global Warming Potential, exclude biogenic carbon (kg CO2-Equiv.); b) Human Health Particulate Air (kg PM2,5-Equiv.); c) Resource Depletion, fossil fuels (MJ surplus energy).

Human Health Particulate (air) was measured in kg PM2.5 per kg PET bottles, shown in Figure 2b. The overall distribution of impacts across scenarios was similar to that of GWPs, where forest residues PTA has lowest impacts with displacement credits (~ -0.027 to -0.025 kg PM2.5/kg PET bottles) on average, but medium placement without avoided impacts incorporated (~ 0.006 to 0.008 kg PM2.5/kg PET bottles). While avoided particulate emissions from slash pile burning accounted for most of the credits (Ganguly et al., 2014), that assumption could be changed based on different selections of woody biomass feedstock, and will be discussed in sensitivity analysis.

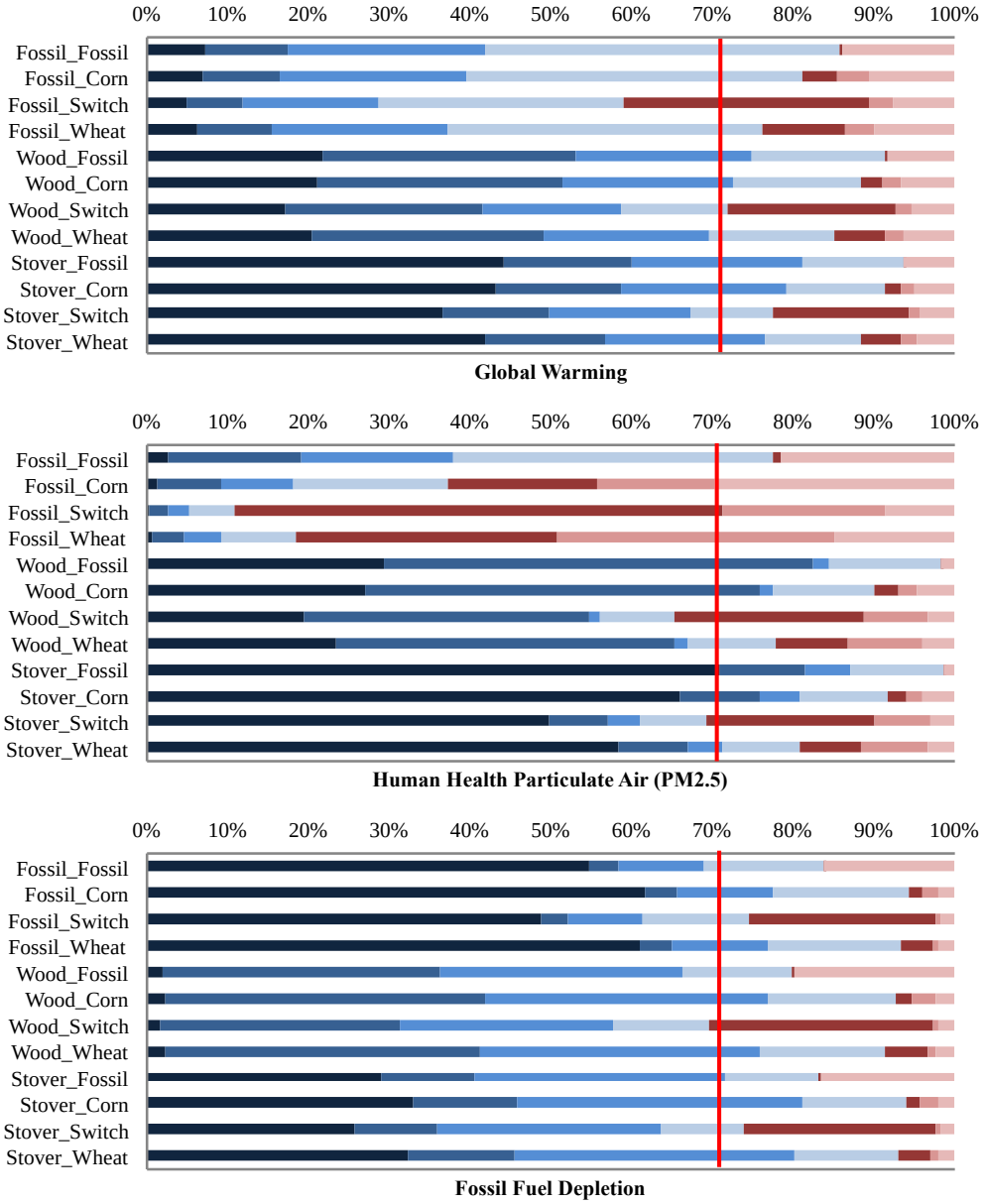

*For fossil based TA, no IBA is produced. PX are directly processed from a series of petroleum refinery co-products, so the IBA blocks for Fossil TA actually indicated impacts from petroleum refinery co-products.

Figure 3. Comparison of impacts generated from unit process for manufacturing terephthalic acid and ethylene glycol of 12 PET bottle production scenarios (scaled to 100%) . Scenarios are marked as '(Raw material for TA)_(Raw material for EG)' at the vertical axis. Functional unit is 1 kg PET bottle final product. Each color block implied the impacts caused by conversion processes to acquire a particular intermediate product.

Similarly, particulate emissions were significant in feedstock extraction phase as well as biomass pre-processing stage (see Figure 3). Note that impacts from fossil fuel extraction

were very trivial, which is questionable given that the major contributor to atmospheric particle emissions is transport fossil fuel combustion, especially coal combustion (Keuken et al., 2013; Zheng et al., 2005). It is possible that the more recent LCI datasets for biomass derived products had more detailed monitoring data for fine particles (PM2.5), which became a hotspot in academia only from the past decade. On the contrary, LCI for particulate emissions from fossil industry suffered from limited data availability (Liu, Paciorek, & Koutrakis, 2009), and thereby did not show significant impacts.

Results for fossil fuel consumption echoes the pre-assumption that bio-PET bottles consume less fossil energy than fossil PET bottles do, although the advantage was not obvious (Figure 2). Both credited wood PTA derived bottles (~6.48 to 8.94 MJ surplus energy/kg PET bottles) and non-credited ones (~9.34 to 11.82 MJ surplus energy/kg PET bottles) had lowest impacts on average, whereas corn stover PTA bottles and fossil PTA bottles consumed similar amounts of fossil energy. Figure 3 indicated that the leading fossil fuel consuming part of corn stover PTA was feedstock extraction. For forest residue bottles, aside from isobutanol (IBA) production, the unit process of converting IBA to paraxylene (PX) also required large fossil energy inputs. Life cycle inventory data for PX process was based on proprietary information and industrial patent (Peters, Taylor, Jenni, Manzer, & Henton, 2010), which will be evaluated in sensitivity analysis.

Results of sensitivity analysis were summarized in Table 2. It is clear that changes on excess electricity and energy consumption of paraxylene production would greatly alter the results of GWP, while the decisive factor for particle emissions was slash pile burning. The significant reliance of GWP results on excess energy (a 171% increase with 55% decrease of estimated excess electricity) requires further justification on data quality and assumptions.

Future Works

Other impact categories (ozone depletion, smog, eutrophication, acidification and ecotoxicity) will be incorporated to deliver a more comprehensive LCA study. Efforts will be continuously paid on seeking for more reliable data sources and assumptions will be justified. In the future, it is possible to merge the results of this study with other bio-refinery environmental profile for a complete sustainability analysis.

Table 2. Sensitivity analysis of weak points

Weak Point	**Paraxylene Process**			**Slash Pile Burning**			**Excess Electricity**		
% of Estimated Value*	45%	70%	110%	45%	70%	110%	45%	70%	110%

Global Warming Potential**	-43%	-23%	+8%	+23%	+12%	-4%	+171%	+93%	-31%
Human Health Particulate**	-0.33%	-0.18%	+0.06%	+74%	+41%	-14%	+6%	+3%	-1%
Fossil Fuel Depletion**	-19%	-10%	+3%	NA	NA	NA	+20%	+11%	-4%

*Percentage changes were imposed on estimated value of impacts for a specific process or avoided impacts

**Percentage changes were calculated based on impacts of wood terephthalic acid and fossil ethylene glycol PET bottle scenario.

References

(1) Bare, Jane C, & Gloria, Thomas P. (2006). Critical analysis of the mathematical relationships and comprehensiveness of life cycle impact assessment approaches. Environmental Science & Technology, 40(4), 1104-1113.

(2) Borrion, Aiduan Li, McManus, Marcelle C, & Hammond, Geoffrey P. (2012). Environmental life cycle assessment of lignocellulosic conversion to ethanol: A review. Renewable and Sustainable Energy Reviews, 16(7), 4638-4650.

(3) Cherubini, F., & Jungmeier, G. (2010). LCA of a biorefinery concept producing bioethanol, bioenergy, and chemicals from switchgrass. International Journal of Life Cycle Assessment, 15(1), 53-66. doi: 10.1007/s11367-009-0124-2

(4) Curran, Mary Ann. (1996). Environmental life-cycle assessment. The International Journal of Life Cycle Assessment, 1(3), 179-179.

(5) Finnveden, Göran, Hauschild, Michael Z, Ekvall, Tomas, Guinee, Jeroen, Heijungs, Reinout, Hellweg, Stefanie, . . . Suh, Sangwon. (2009). Recent developments in life cycle assessment. Journal of Environmental Management, 91(1), 1-21.

(6) Frischknecht, Rolf, Jungbluth, Niels, Althaus, Hans-Jörg, Doka, Gabor, Dones, Roberto, Heck, Thomas, . . . Rebitzer, Gerald. (2005). The ecoinvent database: Overview and methodological framework (7 pp). The International Journal of Life Cycle Assessment, 10(1), 3-9.

(7) Ganguly, I., Eastin, I. E. , Bowers, T., Huisenga, M., & Pierobon, F. (2014). Environmental Assessments of Woody Biomass-Based Jet Fuel. The Center for International Trade in Forest Products Newsletter, 3 - 10.

(8) Hendriks, ATWM, & Zeeman, G. (2009). Pretreatments to enhance the digestibility of lignocellulosic biomass. Bioresource Technology, 100(1), 10-18.

(9) Hsu, David D, Inman, Daniel, Heath, Garvin A, Wolfrum, Edward J, Mann, Margaret K, & Aden, Andy. (2010a). Life cycle environmental impacts of selected US ethanol production and use pathways in 2022. Environmental Science & Technology, 44(13), 5289-5297.

(10) Hsu, David D, Inman, Daniel, Heath, Garvin A, Wolfrum, Edward J, Mann, Margaret K, & Aden, Andy. (2010b). Support Information:
(11) Life cycle environmental impacts of selected US ethanol production and use pathways in 2022. Environmental Science & Technology, 44(13), 5289-5297.
(12) ISO, ISO14040. (2006). 14040: Environmental Management–Life Cycle Assessment–Principles and Framework. London: British Standards Institution.
(13) Keuken, MP, Moerman, M, Voogt, M, Blom, M, Weijers, EP, Röckmann, T, & Dusek, U. (2013). Source contributions to PM 2.5 and PM 10 at an urban background and a street location. Atmospheric Environment, 71, 26-35.
(14) Liu, Yang, Paciorek, Christopher Joseph, & Koutrakis, Petros. (2009). Estimating regional spatial and temporal variability of PM2. 5 concentrations using satellite data, meteorology, and land use information.
(15) Mosier, Nathan, Wyman, Charles, Dale, Bruce, Elander, Richard, Lee, YY, Holtzapple, Mark, & Ladisch, Michael. (2005). Features of promising technologies for pretreatment of lignocellulosic biomass. Bioresource Technology, 96(6), 673-686.
(16) Pawelzik, P, Carus, M, Hotchkiss, J, Narayan, R, Selke, S, Wellisch, M, . . . Patel, MK. (2013). Critical aspects in the life cycle assessment (LCA) of bio-based materials–Reviewing methodologies and deriving recommendations. Resources, Conservation and Recycling, 73, 211-228.
(17) Peters, Matthew W, Taylor, Joshua D, Jenni, Madeline, Manzer, Leo E, & Henton, David E. (2010). Integrated process to selectively convert renewable isobutanol to p-xylene: Google Patents.
(18) Puettmann, ME, Oneil, E, Milota, MR, & Johnson, LR. (2012). Cradle to Gate Life Cycle Assessment of Softwood Lumber Production from the Pacific Northwest. CORRIM Report Update.
(19) Rebitzer, G., Ekvall, T., Frischknecht, R., Hunkeler, D., Norris, G., Rydberg, T., . . . Pennington, D. W. (2004). Life cycle assessment part 1: framework, goal and scope definition, inventory analysis, and applications. Environ Int, 30(5), 701-720. doi: 10.1016/j.envint.2003.11.005
(20) Stevens, Christian, & Verhé, Roland. (2004). Renewable bioresources: scope and modification for non-food applications: John Wiley & Sons.
(21) Tao, Ling, Tan, Eric C. D., McCormick, Robert, Zhang, Min, Aden, Andy, He, Xin, & Zigler, Bradley T. (2014). Techno-economic analysis and life-cycle assessment of cellulosic isobutanol and comparison with cellulosic ethanol and n-butanol. Biofuels, Bioproducts and Biorefining, 8(1), 30-48. doi: 10.1002/bbb.1431
(22) Zheng, Mei, Salmon, Lynn G, Schauer, James J, Zeng, Limin, Kiang, CS, Zhang, Yuanhang, & Cass, Glen R. (2005). Seasonal trends in PM2. 5 source contributions in Beijing, China. Atmospheric Environment, 39(22), 3967-3976.
(23) Zhu, JY, & Pan, XJ. (2010). Woody biomass pretreatment for cellulosic ethanol production: technology and energy consumption evaluation. Bioresource Technology, 101(13), 4992-5002.

Proceedings of the 58th International Convention of
Society of Wood Science and Technology
June 7-12, 2015 - Grand Teton National Park, Jackson, Wyoming, USA

Development of Industrial Laminated Bridge Planks from Southern Pine Lumber

Bonnie Yang, bonnie.yang@cfr.msstate.edu
Rubin Shmulsky, rshmulsky@cfr.msstate.edu
Dan Seale, dseale@cfr.msstate.edu

Mississippi State University, Box 9820, Mississippi State, MS 39762

Abstract

Industrial southern pine laminated planks were proposed, manufactured and tested. This process sought to both develop high value construction bridge timbers and to improve the performance and utilization of low grade pine lumber. The laminated planks were made from No.3 grade southern pine dimension lumber with the cross section of 38 × 184 mm2, and the variable lengths of 2.45, 3.06, 3.68, 4.29, 4.90 m. Southern pine lumber was assembled with nonstructural square endjoints. Waterproof polyurethane adhesive was used to face-laminate the lumber into 192 mm × 319 mm × 4.29 m laminated planks. The planks were destructively tested in plank orientation by static bending. Beams were loaded by third-point configuration as specified in ASTM 5456. Modulus of rupture (MOR) and modulus of elasticity (MOE) were evaluated; bending design values for uniform load situations were also developed from the test results. The product of this research has applicability as member stock for bolt-laminating into construction bridges and mats.

Proceedings of the 58th International Convention of
Society of Wood Science and Technology
June 7-12, 2015 - Grand Teton National Park, Jackson, Wyoming, USA

Effect of Cross-Laminated Timber Floor Diaphragm Orientation on Shear Stiffness and Strength

Kyle Sullivan

CCE School and WSE Department, Oregon State University

Abstract

Cross-laminated timber (CLT) brings the forest industry to new heights with its ability to build taller wooden structures. Wood buildings in the US have typically and historically been light-frame wood construction under five stories. CLT provides the structural strengths and stiffnesses to potentially replace steel and reinforced concrete in more environmentally sustainable structural systems for mid-rise and possibly high-rise buildings. The "Toward Taller Wood Buildings" national symposium (November, 2014, Chicago, IL) brought together a group of leaders, firms, and organizations that are already deeply involved with the development of CLT in the US.

Two researchers who attended the symposium had a significant impact on the proposed direction of the research. Doug Rammer, Research General Engineer at the US Forest Service, and John van de Lindt, Professor at Colorado State University, both feel strongly that looking at how CLT floor diaphragms transfer lateral loads would lead to design provisions in the National Design Specification for Wood Construction and the IBC. CLT floor diaphragms experience lateral loading along both their strong and weak axes depending on the direction of earthquake ground motions or wind loadings and on the orientation of the panels. We will determine how lateral loads parallel to either axes are transferred through the diaphragm due to different strengths and stiffnesses in the two directions. The goal is also to develop preliminary estimates of design values for shear strength and stiffness based on ASTM E455, so that structural engineers will be able to confidently use CLT in lateral-force-resisting systems.

Proceedings of the 58th International Convention of
Society of Wood Science and Technology
June 7-12, 2015 - Grand Teton National Park, Jackson, Wyoming, USA

Trends in U.S Furniture Trade

Cagatay Tasdemir, ctasdemi@purdue.edu
Rado Gazo, gazo@purdue.edu

Purdue University, 2491 Sycamore Ln., Apt 6 , West Lafayette, IN 47906

Abstract

The US and global economy has experienced both a downturn and a recovery over the last decade. The objective of this study is to analyze trends in imports and exports of furniture in the US over this period of time. We evaluate top ten furniture exporting countries in terms of value and principal products. Main competitive strategies of countries exporting furniture to the U.S. are identified and briefly explained within the scope of this study by observing the changes in the values of last five years data. Taiwan was one of the most important furniture exporters to the US until 1994, when the country started to lose its power in the market due to the technological improvements made in other Asian countries. Decreasing trend of Taiwan export values continued in last ten years while Vietnam increased its share of the U.S. furniture market. Since 2004, China was the most important source of imported wood furniture and accounts for over 48.5% of total imports volume.

Overall, low-cost structure, government support and advanced technologies in Asia have provided the Asian countries with competitive advantage over their European and American competitors. Hence, lower price of imported products has been the main influential and decisive factor for furniture consumers in U.S. and set the benchmark for manufacturers in terms of competitive advantages.

Proceedings of the 58th International Convention of
Society of Wood Science and Technology
June 7-12, 2015 - Grand Teton National Park, Jackson, Wyoming, USA

Effect of Lignin as Additive on the Properties of Wood Flour/Polypropylene Composites

Shupin Luo[1] –Jinzhen Cao[2]*

[1] PhD Candidate, MOE Key Laboratory of Wooden Material Science and Application, Beijing Forestry University, Beijing, China.

[2] Professor, MOE Key Laboratory of Wooden Material Science and Application, Beijing Forestry University, Beijing, China.
* *Corresponding author*
caoj@bjfu.edu.cn

Abstract

This study was designed to investigate the effect of soda lignin incorporation on the physical, mechanical, and thermal properties of wood flour /polypropylene composites. Varying contents (1, 2, 4, and 8 wt%) of lignin was added to wood flour and polypropylene by direct mixing, then the composites were prepared by two-screw extrusion and compression molding. The performance of composites were evaluated via water absorption testing and mechanical testing. Results showed that lignin incorporation reduced the water absorption rates. Flexural properties and impact strength increased when 1 or 2 wt% of lignin was added; while these properties slightly decreased when lignin addition increased to 4 or 8 wt%. Dynamic mechanical analysis and Scanning electron micrographs also indicated improved interfacial bonding between wood flour and polypropylene by 1 and 2 wt% lignin addition.

Keywords: wood, lignin, mechanical properties, interfacial bonding

1. Introduction

Natural fiber reinforced polymer composites, as an important branch in the field of composite materials, have been intensively investigated in recent decades. Compared with conventional synthetic fibers like glass and carbon, natural fibers have several advantages. They are low cost, highly available and renewable, low density, high specific strength and biodegradable [1]. However, one of the main problems with using natural fibers as reinforcement is the poor compatibility between the inherently polar fibers and non-polar polymer matrices. The incompatibility caused ineffective stress transfer throughout the interface, resulting in low performance of composites. This means that the reinforcement potential of natural fibers cannot be exploited to the full extent, especially for short fibers and particles[2]. However, with the rising environmental concerns and depletion of petro-chemical resources currently, it is desirable to reduce the chemical input, energy cost and wastes during the production. An alternative to these methods are the use of natural materials as additives in the composites.

Lignin is the second most abundant biopolymer on our planet after cellulose, and it is one of the three main components found in the cell wall of natural lignocellulosic materials[3]. Large quantities of lignin are yearly available from numerous pulping processes such as paper and biorefinery industries. Most of them is burnt to produce energy although they can offer many other added value uses. Only approximately 2% of the lignin from pulp and paper industry has been commercialized [4,5]. The chemical structure of lignin is complex, largely depending on the origin, separation and fragmentation processes[6].

Some researchers incorporated commercial lignin into composites to ascertain if it was beneficial to the properties. Graupner[7] applied kraft lignin powder of eucalyptus as natural adhesion promoter in cotton fiber-PLA composites, resulting in improved tensile properties while decreased impact properties. Acha et al.[8] investigated the feasibility of using a commercial kraft lignin as a compatibilizer for jute fabric-PP composites, but found the improvement only obtained from impact behavior. Wood et al. [9] found the addition of 5 wt% Kraft lignin to hemp-epoxy composites generated a significant rise in the impact strength; both flexural and tensile modulus showed an increase when lignin was added up to 2.5 wt%. Previous studies on lignin as additive in natural fiber/polymer composites showed various results. Besides, there has been few studies about the lignin addition in WF/PP composite.

In this context, we applied the commercial soda lignin from alkaline pulping as additive in wood flour/PP composite, in order to ascertain if this kind of lignin was beneficial to the mechanical and physical properties of composites.

2. Materials and Methods

2.1. Materials

WF (WF) of poplar（Populustomentasa Carr.）with a size of 10-60 mesh was kindly supplied by Xingda Wood Flour Company, Gaocheng, China. Soda lignin with 3.96% ash content, in powder form, was commercially bought. PP (K8303) with a density of 0.9 g/cm^{3}was purchased from Beijing Yanshan petrochemical Co. Ltd., China. It has a melt point around 165 °C and a melt flow index of 1.5 to 2.0 g/10 min at 230 °C.

2.2. Characterization of wf and lignin

Chemical compositions of the WF were analyzed based on the following standards. The WF was firstly extracted with a benzene-ethanol solution according to ASTM D1105-96. Acid insoluble lignin content was analyzed according to ASTM D1106-96. Holocellulose and α-cellulose contents were analyzed according to Zhang et al.'s method[10]. Scanning electron micrographs of the WF and lignin were taken with a Hitachi (S-3400, Japan) scanning electron microscope (SEM) with an acceleration voltage of 5 kV. The samples were previously sputter-coated with gold. Particle size distribution of the WFs and lignin were measured by using a laser diffraction particle size analyzer (Mastersizer 2000, Malvern, UK).WF was suspended in water during measurement.

2.3. Fabrication of composites

Prior to manufacturing, WF and lignin was dried at 103±2 °C for 24 h. The WF and PP were weighed with the ratio of 1:1. Lignin was added at the following levels: 1, 2, 4, and 8 wt% (based on the total weight of WF and PP). Then WF, lignin and PP were dry-blended in a high speed mixer at a rotating speed of 2900 rpm for 4 min to achieve homogeneity. The mixture was then dried in an oven at 103±2 °C for 2 h and compounded using a 20 mm co-rotating twin-screw extruder (KESUN KS-20, Kunshan, China).The corresponding temperature profile along the extruder barrel was 165/170/175/180/175 °C, and the screw speed was set at 167 rpm. The extruded strands were cooled in air and pelletized. Then they were taken out for hand matting. The mat was pressed at 180 °C and 4 MPa for 6 min, then at 4 MPa for another 6 min at room temperature in a cold press.

2.4. Physical and mechanical tests of composites

Four specimens of each formulation with dimensions of 50×50×3mm3 were selected to determine the water absorption (WA) of the composites. They were dried in an oven for 48 h at 103±2ºC and then weighted to a precision of 0.001g. The specimens were subsequently immersed in distilled water and kept at 23ºC for 702h.Weight of the specimens was measured at different time intervals during the immersion. The flexural tests were determined according to the Chinese standard GB/T 9341-2000, which involves a three-point bending test at a crosshead speed of 1mm/min. Flexural testing were performed on a WDW-350A universal mechanical test machine (Jinan Shijin Group Ltd., Shandong, China). Charpy impact tests were performed for unnotched samples using a CEAST model 6957 impact tester according to Chinese standard GB/T 1843-1996.

2.5. Dynamic mechanical analysis

The dynamic mechanical properties of the specimens were measured with a dynamic mechanical analyzer (TA Q800) by a 3-point bending mode. Measurements were performed at a constant frequency of 1 Hz. The temperature scanning range was set from -40 to 140 ^{o}C at a heating rate of 3 ^{o}C /min.

2.6. Morphological analysis of the composites

Fracture surfaces of the impact test samples were taken and coated with a gold–palladium alloy and examined in a Hitachi (S-3400, Japan) scanning electron microscope with an acceleration voltage of 5 kV.

3. Results and Discussion

3.1. Characterization of WF and lignin

Chemical compositions of WF was determined for proper interpretation of the results obtained from the composites. The holocellulose, α-cellulose and acid insoluble lignin contents obtained were 73.56, 54.4 and 17.77%, respectively.

The morphologies of WF and lignin are shown in Fig. 1. WF particles exhibited a slender shape, while lignin particles were nearly spherical shape. Fig. 2 presents the size distributions of WF and lignin. The particle size of WF seemed to present a double distribution with a large portion centred on 80 μm and another one (smaller) on 400μm. Lignin average size was smaller than WF and also exhibited a double distribution.

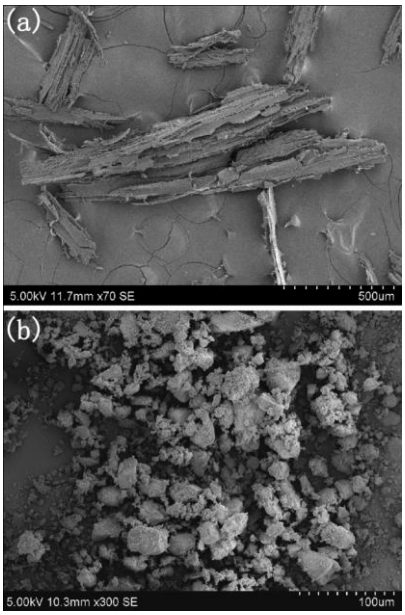

Fig.1 SEM images of WF (a) and lignin (b).

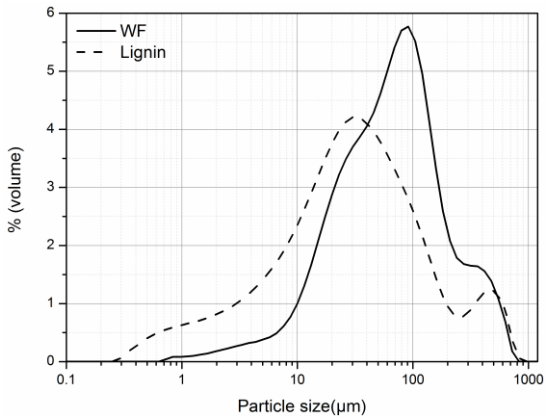

Fig.2 Distribution of particle size analysis of WF and lignin.

3.2.Water absorption analysis

WA values of composites are shown in Fig. 3. The WA increased continuously with the prolonging of time and reached a equilibrium after about 700 h immersion. Addition of lignin could reduce the WA of the composites. At the end of the measure, the WA of composites exhibited the following trend: C> 4L > 8L > 2L > 1L. The WA of 4L and 8L was very close to that of C group, and the difference between 1L and 2L was not obvious.

These results indicated that the lower loadings of lignin had better effect on the inhibition of WA compared with higher loadings.

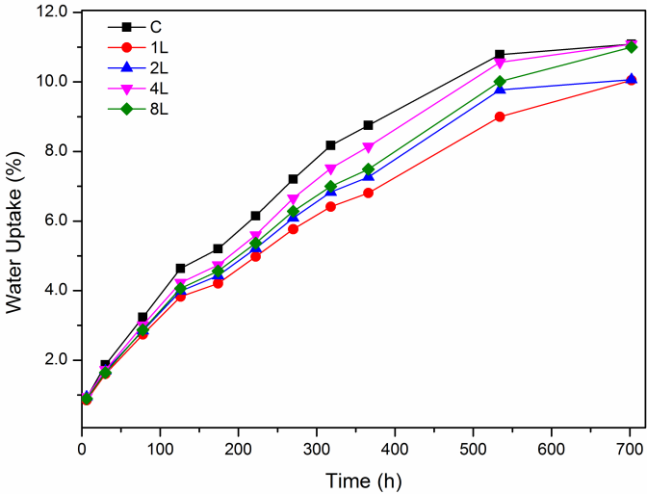

Fig.3 Water uptakes of WF/PP and WF/PP/lignin composites.

As WF possessed more hydrophilic nature than lignin, containing a large part (73%) of hollocellulose and only 17% of lignin, it was reasonable the WA of composites decreased when part of WF was replaced by lignin. It can be seen from SEM that 1% and 2% lignin addition caused composites with fewer voids and better adhesion at the interface than 4% and 8% (Fig. 7). This might be the reason that the lower loadings of lignin had better effect on the inhibition of WA compared with higher loadings

3.3.Mechanical properties

The results of the flexural testing are shown in Fig. 4. The maximum flexural strength was observed at 1L group with a value of 36.92 MPa, which increased approximately 30% compared with C group. With increasing lignin addition, there was no obvious improvement of the strength. Besides, the strength of 8L group (26.63 MPa) showed a slight decrease compared to control (28.56 MPa). The flexural modulus showed a similar pattern with flexural strength. The flexural modulus of 1L group showed an improvement compared with control, also indicating the positive effect of lignin on the flexural properties of WF/PP composite.

Fig. 5 shows the unnotched impact strength of the composites. The impact strength of control was 2.83 KJ/m^2, which increased to 3.5 KJ/m^2 at 1% lignin loading. Addition of 2% lignin showed no improvement compared with control. However, when the lignin content further increased to 4% or 8%, the impact strength even slightly declined. With increasing lignin addition, the agglomerates and non-uniform distribution of lignin might occur and generate local stress concentration, thus decreasing the crack initiation energy.

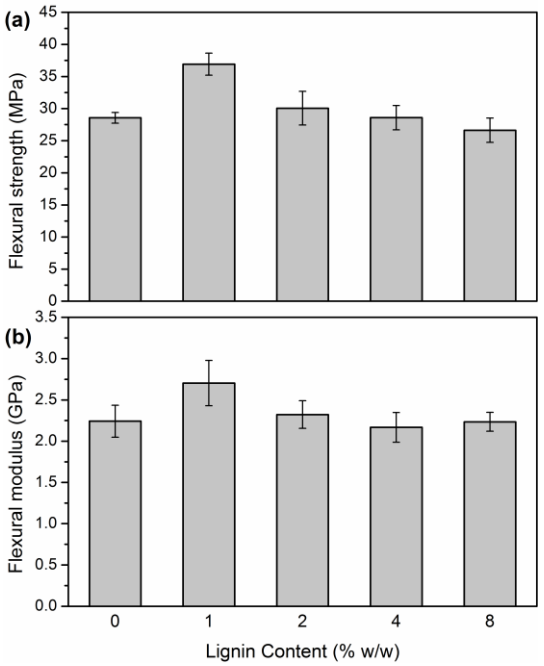

Fig.4 Flexural strength (a) and modulus (b) of WF/PP and WF/PP/lignin composites.

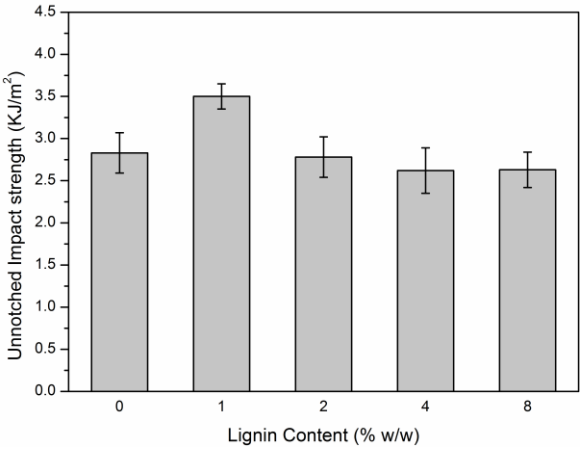

Fig.5 Unnotched impact strength of WF/PP and WF/PP/lignin composites.

3.4. Dynamic mechanical properties

The storage modulus and damping factor (tanδ) curves of the composites at a frequency of 1Hz are shown in Fig. 6. Storage modulus exhibited a downtrend within the entire temperature range, attributed to the increased molecular mobility of chain segments of PP at higher temperature. Incorporation of 1% lignin into the composites significantly increased the storage modulus. At room temperature, 1L group had the highest E', followed by 2L, 4L, control and 8L. It is to be noted that the storage modulus of 1L and 2L group were higher than control group within the whole measured temperature range. The storage modulus of 8L was below that of control, suggesting excessive lignin had a negative effect on the resistance to deformation.

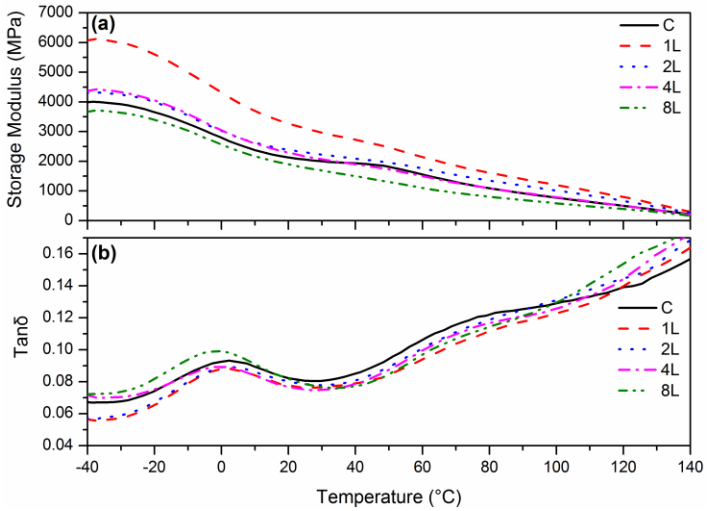

Fig.6 Storage modulus (E') and mechanical damping (tanδ) of the WF/PP and WF/PP/lignin composites.

As seen in Fig. 6b, one peak appeared around 0 ^{o}C in the tanδ curves for all samples. The primary damping peak can provide information about the interaction between the matrix and the fiber at molecular level. A composite with poorer interfacial bonding tends to dissipate more energy and need a lower temperature to initiate molecular motion, showing a higher tanδ magnitude and lower peak temperature than a composite with a strongly bonded interface. The tanδ peak amplitude of composites exhibited a decreasing order as: 8L > C > 4L > 2L >1L. This proved that the incorporation of a small quantity of lignin restrained the mobility of molecules. However, the damping peak of 8L and 4L group shifted to a lower temperature compared with C group, indicating excessive lignin had a negative effect on the interaction between the PP and WF.

3.5. Morphology of the composites

Fig. 7 shows the fractured surfaces of the composites after they were subjected to the Charpy impact testing. The sample with no lignin addition (Fig. 7a) shows evidence of apparent holes and gaps (as marked by arrows), indicating insufficient interfacial adhesion between WF and PP. At 1% lignin addition, composites had fewer holes and voids on the fracture surface compared to control group. Adding 2% lignin appeared to further increase the interfacial bonding, as the particle/matrix interface became obscure. However, when lignin addition increased to 4%, there were instances of fiber debonding (as indicated by arrows). And when addition increased to 8%, fiber breakage as well as fiber pull-out was observed (as indicated by arrows), indicating ineffective stress transfer from matrix to fiber.

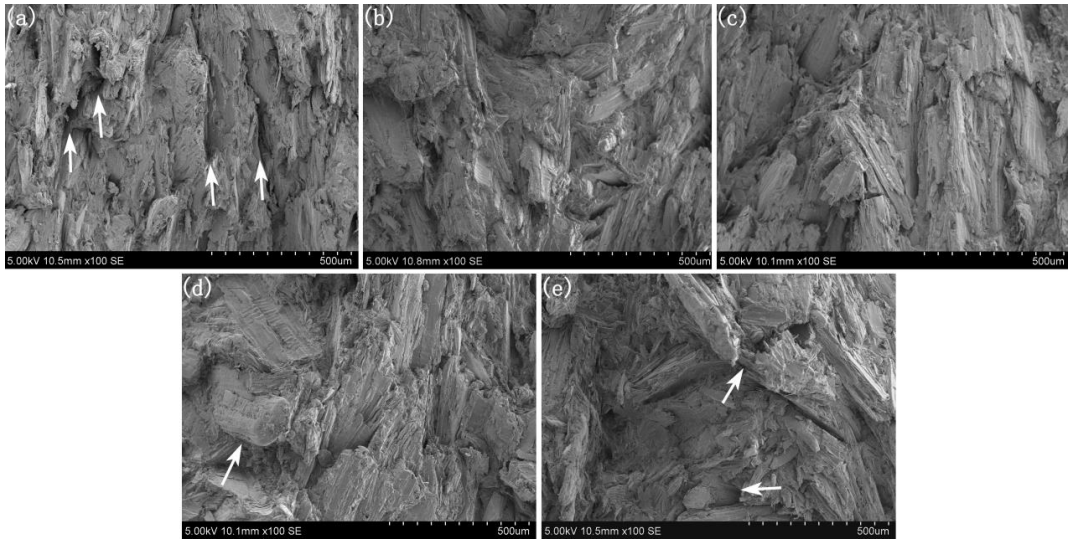

Fig.7 Micrographs of impact fractured surfaces of composites: (a) WF/PP, (b) WF/PP/1%L, (c) WF/PP/2%L, (d) WF/PP/4%L, (e) WF/PP/8%L.

In our study, the improved WF-PP bonding at lower lignin addition was observed, but the smooth coating of WF by lignin found by Morandim-Giannetti et al. [11] was not seen. The mechanism of the lignin effect might be that at large lignin loading, a large volumes of lignin particles preventing complete wet out of the fiber reinforcement. Also these lignin particles in fine powder form (average diameter: 68 μm) were prone to form agglomerates and became stress concentration point, resulting in ineffective stress transfer across the interface. So at low lignin loading level, the effect of improved fiber-

matrix interaction dominated; at high lignin loading level, the domination of improved interaction was replaced by negative effect of lignin aggregation. Besides, there was the possibility that the active groups of lignin were not highly effective, since it was used as received.

4. Conclusion

WF/PP composites were fabricated with incorporating varying amounts of soda lignin. Compared to control sample, addition of lignin to WF/PP composites resulted in reduced water absorption. Incorporation of a small quantity of lignin was shown to be beneficial towards improving the flexural properties and impact strength of the composites, although these properties remained unchanged or even reduced when lignin was added up to 4 and 8 wt%. DMA and SEM analysis also indicated that fiber-matrix adhesion could be improved at appropriate dosage. But the improvement was not enough to remarkably improve the physical and mechanical behavior of WF/PP composites, probably due to the aggregation of lignin particles and low reactivity with WF.

Acknowledgements

This study is financially supported by Fundamental Research Funds for the Central Universities in China (No. TD2011-14).

References

[1] Wambua P, Ivens J, Verpoest I (2003) Natural fibres: can they replace glass in fibre reinforced plastics? Compos Sci Technol 63(9):1259-64.

[2] Sobczak L, Brueggemann O, Putz RF (2013) Polyolefin composites with natural fibers and wood-modification of the fiber/filler-matrix interaction. J Appl Polym Sci 127(1):1-17.

[3] Thakur VK, Thakur MK, Raghavan P, Kessler MR (2014) Progress in Green Polymer Composites from Lignin for Multifunctional Applications: A Review. ACS Sustainable Chem Eng 2(5):1072-92.

[4] Gosselink RJA, de Jong E, Guran B, Abacherli A (2004) Co-ordination network for lignin-standardisation, production and applications adapted to market requirements (EURO LIGNIN). Ind Crop Prod 20(2):121-9.

[5] Laurichesse S, Averous L. Chemical modification of lignins: Towards biobased polymers. Prog Polym Sci 2014;39(7):1266-90.

[6] Chakar FS, Ragauskas AJ. Review of current and future softwood kraft lignin process chemistry. Ind Crop Prod 2004;20(2):131-41.

[7] Graupner N (2008) Application of lignin as natural adhesion promoter in cotton fibre-reinforced poly(lactic acid) (PLA) composites. J Mater Sci 43(15):5222-9.

[8] Acha BA, Marcovich NE, Reboredo MM (2009) Lignin in jute fabric-polypropylene composites. J Appl Polym Sci 113(3):1480-7.

[9] Wood BM, Coles SR, Maggs S, Meredith J, Kirwan K (2011) Use of lignin as a compatibiliser in hemp/epoxy composites. Compos Sci Technol 71(16):1804-10.

[10] Zhang H, Pang H, Shi J, Fu T, Liao B (2012) Investigation of liquefied wood residues based on cellulose, hemicellulose, and lignin. J Appl Polym Sci 123(2):850-6.

[11] Morandim-Giannetti AA, Agnelli JAM, Lanças BZ, Magnabosco R, Casarin SA, Bettini SHP (2012) Lignin as additive in polypropylene/coir composites: Thermal, mechanical and morphological properties. Carbohyd Polym 87(4):2563-8.

Proceedings of the 58th International Convention of Society of Wood Science and Technology
June 7-12, 2015 – Grand Teton National Park, Jackson, Wyoming, USA

Influence of Lignin Modification on Microfibril Angle in Young Transgenic Black Cottonwood Trees

Zachary Miller, zdmiller@ncsu.edu
Vincent Chiang, vchiang@ncsu.edu
Ilona Peszlen, impeszle@ncsu.edu
Perry Peralta, pperalta@ncsu.edu

North Carolina State University, 3911 Greenleaf Street, Raleigh, NC 27695

Abstract

Primary and secondary cell walls of plants contain a scaffold of cellulose microfibrils embedded in a hemicellulose and lignin matrix. Microfibril angle (MFA) refers to the angle between the long axis of the cell and the direction of helical windings of cellulose microfibrils in the secondary cell wall of fibers and tracheids. Wood in which the MFA is large has a low Young's modulus and not suitable for high-grade lumber, reducing its value as a raw material. This problem was not too serious in the past when trees were allowed to reach maturity before being harvested, however, the increase in demand for pulp and wood products is driving the forest industry towards short-rotation cropping of fast-growing species like Populus hybrids. In this study, genetically modified six-month-old black cottonwood (Populus trichocarpa) clones with modifications to genes located in the lignin biosynthesis pathway were investigated. Black cottonwood was chosen because of its sequenced genome, ease of propagation, fast growth and economic importance. Black cottonwood trees were propagated by rooted cuttings and grown in the Forest Biotechnology greenhouse at NCSU for approximately 6 months. These trees represent a wildtype for control and groups that received different genetic modifications based on the steps in the lignin biosynthesis pathway. The MFA was measured from bark-to-bark in samples using an X-ray diffraction technique. Significant variation in MFA from pith to bark was observed.

Proceedings of the 58th International Convention of Society of Wood Science and Technology
June 7-12, 2015 – Grand Teton National Park, Jackson, Wyoming, USA

Increasing Service Life of Wooden Chairs

Mesut Uysal, uysalm@purdue.edu
Eva Haviarova, ehaviar@purdue.edu
Carl Albert Eckelman, eckelmac@purdue.edu

Purdue University, 2491 Sycamore Ln., Apt 5, West Lafayette, IN 47906

Abstract

The goal of the study was to obtain background information concerning the effect of joint construction on the durability, reparability and parts reuse of wooded chair frames. Tests were conducted with simple chair frames with seven different types of joints grouped into two joinery systems. Namely, a) mechanical joinery – screw joints, bed bolts with dowel nut joints, pinned round mortise and tenon, and pinned rectangular mortise and tenon joints, and b) permanent (glued) joinery – dowel joints, glued round mortise and tenon, and glued rectangular mortise and tenon joints. Front to back load test was conducted to determine chair strength performance (moment capacity). Chair durability, reparability, and parts reusability were also evaluated. Mechanical joints were found to be the easiest to repair and resulted in largest reuse of parts. Glued round and rectangular mortise and tenon joints, however, provided high levels of strength which would potentially increase product service life (contributing to long lasting, more sustainable product). Joints constructed with large screws or lag screws produced about the same moment capacity as glued round and rectangular mortise and tenon joints. Screw joints are conceivably well suited for simple on-site repair of broken furniture with the advantage that broken furniture does not need to be disassembled prior to repair.

Proceedings of the 58th International Convention of Society of Wood Science and Technology
June 7-12, 2015 – Grand Teton National Park, Jackson, Wyoming, USA

Analysis of Mechanical Behavior of All-Wooden Joint Using FEM and DIC

Jaromír Milch[1] – Jan Tippner[1] – Václav Sebera[1] – Martin Brabec[1]*

[1] Department of Wood Science, Faculty of Forestry and Wood Technology, Mendel University in Brno. Zemědělská 3, 613 00 Brno.
** Corresponding author*
jaromir.milch@mendelu.cz

Abstract

The preservation of original material during reconstruction of valuable historical timber constructions results in higher attention on all-wooden joints that are necessary to implement into the trusses. This paper investigates a mechanical behavior of all-wooden joint with dowel connection using numerical modelling and full-field strain measurement. Numerical simulations of joints employ finite element analysis (FEA) in ANSYS software. Wood is considered as fully orthotropic elasto-plastic material (*Norway spruce* and *European beech*). Experimental testing employing optical evaluation of deformations based on optical methods based on digital image correlation (DIC) was used for verification of numerical models. During the measurements in testing machine, the area of interest focused on members of joints using the stereovision system. The first part of work dealt with assembling of fundamental anisotropic elasto-plastic material in simple finite-element (FE) 3D models and its verification. Sensitivity analysis was used for finding optimal characteristic of the material models, e.g. yield stress, tangent moduli. Subsequently, the verified anisotropic elasto-plastic material models were implemented into the simulation of whole 3D solid joints. The second part of work focused on a verification of the 3D numerical models using experimental data (displacements and forces). Last, an application of the verified anisotropic elasto-plastic material model of joints into complex structural analysis of truss will be demonstrated.

***Keywords*:** bilinear isotropic hardening, digital image correlation, dowel-type joints, elasto-plastic, finite element method.

Introduction

The assessment of historical timber monuments is currently paid a big attention from structural, architectural and safety point of view during restoration of damaged timber elements or connections in the structure (Abruzzese 2009). The missing information about global mechanical behavior of complex connections in the timber structures are reasons for evaluation of mechanical response when loaded using sophisticated methods. The numerical approaches based on finite element method (FEM) are one of several appropriate methods for virtual assessment and prediction of possible (points of fault) in the material, in the complex wood structure eventually. Many studies about construction joints with wooden dowels were investigated (Hill 1950, Kessel and Augustin 1996, Bulleit et al. 1999, Santos et al. 2009, etc.). Nowadays, considering the increasing interest about all-wooden joints with dowel connection many studies were performed by using approaches FEA and DIC for predict of mechanical behavior (Oudjene and Khelifa 2009, Dias et al. 2010, etc.). FEM may simplify the optimization of the timber connections according to various parameters in comparison with the experimental testing. Therefore, the numerical modeling is usually undertaken as an approach to study of timber connection in complex structures (Chen et al. 2003).

Wood is an anisotropic material, but under a certain set of conditions is usually considered as an elastic fully orthotropic material in the numerical analyses. However, this model is insufficient for prediction of ultimate strength in wood behavior (Moses and Prion 2002). Orthotropic plasticity theory based on Hill's formulation with hardening is utilized in describing the non-linear behavior up to and beyond the point of ultimate wood strength. The non-linear constitutive behavior of the wood strands is defined by four basic constitutive regimes: elastic, elasto-plastic and post-failure brittle or post-failure ductile (Clouston and Lam 2002). Therefore, the numerical simulations using elasto-plastic material model with hardening are more accurate and suitable for prediction of the mechanical behavior of other material, the wood eventually. Further, this model reflects a more realistic idea about the global behavior of numerical models of wood in comparison with experimental tests (Sohouli et al. 2011). Owing to crushing of wood cells and separation of the fibres, the stress-strain behavior is non-linear in the compression, meanwhile the tension and shear exhibit the linear stress-strain behavior until brittle failure occurs. The finding a suitable material model for the wood will allow to predicting “more realistic” behavior of the wooden elements under various loading conditions in numerous applications of structural engineering such as the connections behaviour, etc. (Moses and Prion 2002).

Materials and Methods

Experimental test

All tested joints were prepared from Norway spruce (*Picea abies* L. Karst.) with wooden dowels (nominal diameter d = 8 mm) that were made of European beech (*Fagus sylvatica* L.). Wood members of joints were cut parallel to grain with length and in the tangential

direction with the thickness (detail of grain orientation in Fig. 1c). The experimental tests consisted of a two series (each series had 10 tests). These series of joints with dowel: double-shear in tension – ds-T (Fig. 1a) and double-shear in compression – ds-C (Fig. 1b) were tested.

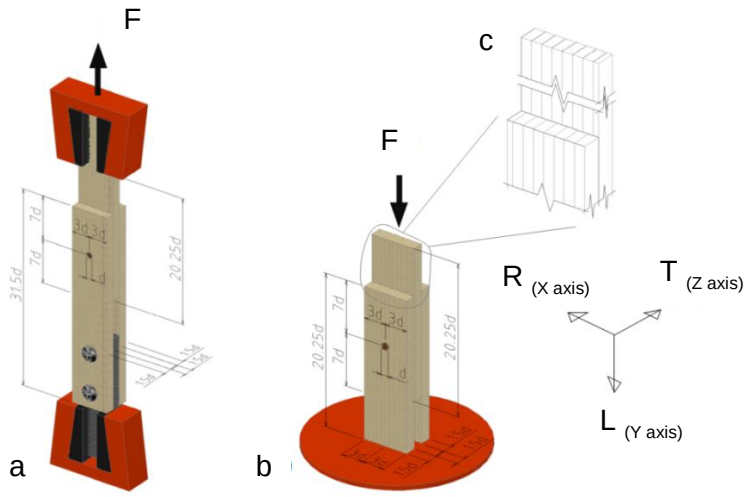

Figure 14 Experimental test configuration with geometry parameters of joints: a) ds-T, b) ds-T, and c) detail of grain orientation.

Figure 1 describes the experimental test configurations of joints with dowel including the geometric parameters that were derived from the nominal dowel diameter. The diameter of drill (8 mm) was used to bore the holes. Wooden dowels were inserted so that the grain on the cross section were oriented parallel to the load direction (tangential direction). Tests were performed on a universal testing machine Zwick Z050/TH 3A, (Roell AG, Ulm, Germany) with 50 kN load cell under crosshead displacement control. The displacement from crosshead was recorded in data acquisition interval of 0.25s = 4 Hz. Tests were carried out according to the standards EN 383 and EN 26891, in particularly, dimension of joints parameters. The specimens were loaded continually to abrupt failure (F_{max}); an automatic stop was triggered when the load decreased by 60% of the F_{max} or was reached time by 400s. Table 1 summarizes the average value of density and experimental conditions for each series of tested joints with dowel connection. All joints were assembled of wood members (side and centre) with similar density. The density of components with moisture content (MC) of ~12% varies from 412 to 614 kg·m^{-3}. The average density of dowels was 660 kg·m^{-3}.

Table 16 Summary of average density and experimental conditions during the tests.

Series	Number of samples	Density [kg·m^{-3}]		Load direction	Displacement rate [mm·s^{-1}]
		$\bar{x}$	VOC* [%]		
ds-T	10	527	12.4	parallel to grain	0.025
ds-C	10	529	12.3	parallel to grain	0.010
Diameter	Length	Density [kg·m^{-3}]		Load direction	

[mm]	[mm]	x̄	VOC* [%]		
dowel - 8	26 or 38	660	9.4	tangential	-

x̄ is mean value; *VOC is variation of coefficient

Validation of fundamental anisotropic elasto-plastic material models

A generalized 3D FE anisotropic plasticity material model with bilinear stress-strain behavior consists of 27 material constants was used. For the verification of anisotropic elasto-plastic material characteristics for wood models were computed simple 3D FEA of exams in compression (parallel to grain, perpendicular to grain in radial and tangential directions) and in bending. The anisotropic elasto-plastic material models developed here were verified using experimental data that were adopted from experimental measurements (Brabec et al. 2015) and from literature (Kollman and Côté 1968, Požgaj 1997). The yield stress of compression and tension were calculated from experiments (compression perpendicular to grain in radial and tangential direction). The tangent moduli of compression, tension and shear were firstly calculated by applying the multiplier 0.01 from the elastic moduli and then were corrected based on experimental data.

The total strain in compression parallel to grain in the load direction were calculated as the difference between two points and referenced to original distance of these points (10 mm). The calculation of total strain values corresponds with experimental measurement using "clip on" extensometers on the radial sample surfaces (R_s). The determining of the total strain in compression perpendicular to grain was calculated as deformation and referenced to original thickness of the samples in load direction. Subsequently, the verified anisotropic elasto-plastic material models were implemented into the simulation of 3D solid joints. The volumetric mesh for all members of joints was consisted of 3D 20-node structural solid element (SOLID95) with plasticity capabilities.

Finite element analyses of joints

The FE 3D solid models of joints were virtually assessment and parametrically built in ANSYS computational system using the Ansys Parametric Design Language (APDL, v.14.5). The volumetric mesh for all members of joints was consisted of 20-node structural solid element (SOLID95). The models of joints (both ds-T and ds-C) have two planes of symmetry and were modelled as the ¼ models for reduction of computation time. The displacements of the nodes located at the planes of symmetry were restrained along the normal direction to these planes. The models were virtually cut for create higher quality of mesh by sweeping technique. The FE models were locally refined at the joint elements' contact areas around the dowel (dowel's and hole's surfaces). The models of joints were consists of aprox. 7,615 and 7,598 FE's (ds-T and ds-C, respectively). The contact between the dowel and wood members, and contact between the central and side wood members was defined applying the contact elements available in ANSYS. The contact elements CONTA174 and TARGE170 were used to models, forming the so-called contact pairs. The contacts were defined as 3D surface-to-surface, symmetrical (each piece was target as well as contact); with an augmented Lagrange formulation where normal stiffness factor was kept for all analyses at 0.1. These contact surfaces were

set as flexible. Six contact pairs were considered: i) between the dowel and the surface of the hole of the side members; ii) between the dowel and the surface of the hole of the centre member; iii) between the centre and side members. The coefficient of friction (μ) was used 0.33 for wood for all analyses. Material characteristics of wood (*Norway spruce* and *European beech*) were based on the elasto-plastic fully orthotropic mechanic theory.

Results and Discussion

The objective of study was to propose and verify the anisotropic material model with non-linear behavior for wood based on the experimental and technical material characteristics with subsequent implementation into more complex FEA of wooden joints.

Fundamental anisotropic elasto-plastic material models

Figure 2 depict of comparison between the numerically and experimentally predicted stress-strain behavior of wood compressed parallel to grain and load-deflection behavior during bending (Figure 3) for both Norway spruce and European beech.

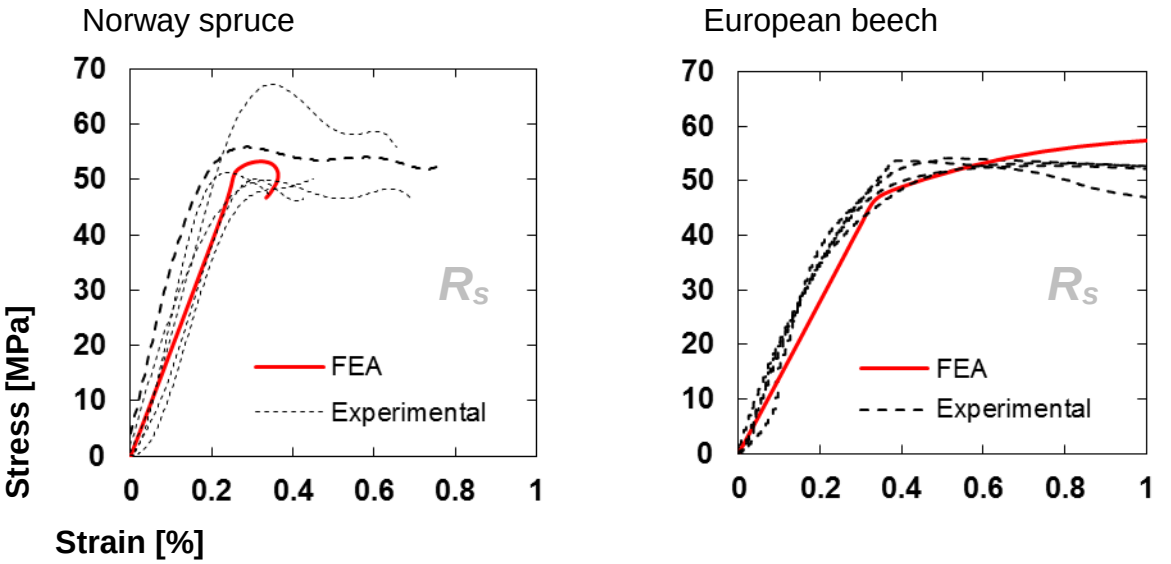

Figure 15 Stress-strain curves of compression parallel to grain. The red curves represent longitudinal strain measured using "clip on" extensometer on the radial sample surfaces (R_s).

Norway spruce European beech

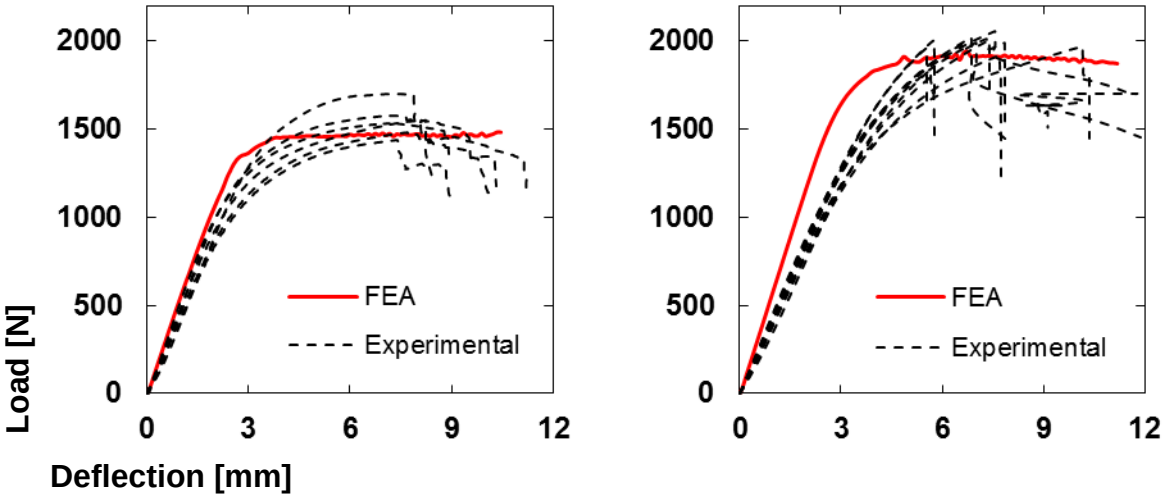

Figure 16 Bending load-deflection curves.

Based on determined material models can be observed very good agreement in the elastic and plastic behavior (Figure 2 and 3). In case of bending (Figure 3) there can be observed differences in the elastic range of behavior, in particular, for beech wood. These differences are given by the increasing longitudinal elastic moduli in compression (E_L), which is due to higher stiffness in compression zone inside the bending sample. This character of changes was detected during debugging of material characteristics. Furthermore, a verification of anisotropic elasto-plastic material models was carried out in compression perpendicular to grain in radial and tangential directions. Based on these results was found agreement with experiments, but will be omitted here.

Verification of global joints behavior

The verification of the numerical models was done using displacement obtained by DIC analysis. Displacement calculated using Vic-3D (Correlated Solutions, Inc.) is more accurate than displacement obtained by crosshead of testing machine. In the cases of joints loaded in tension, the differences can be justified by slip, especially of metal member of joints, in the clamping wedges. The displacement of double-shear in tension (ds-T) measured by crosshead was higher by 108% compared to results from DIC.
The objective was comparison and verification of numerical models of dowel type joints with anisotropic elasto-plastic material models. Figure 4 compares experimental and numerical behavior of joints under various loading. The numerical models were modelled using with elastic material model (blue curves in Figure 4) and anisotropic elasto-plastic material model with hardening (red curves in Figure 4). The load-displacement curves (Figure 4) exhibit the good agreement between the experiments and numerical results in the range of elastic and plastic deformation behavior of tested joints. The experimental and FEA results differences in the elastic range can be found due to different initial stiffness of dowel connection (owing to initial clearance and imperfect dowel hole).

ds-T in tension ds-C in compression

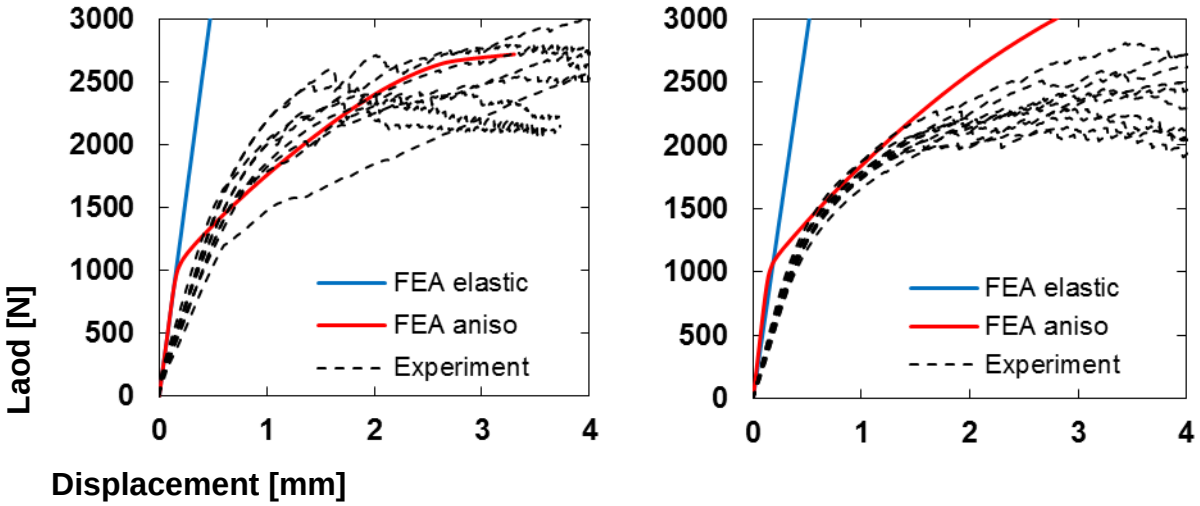

Figure 17 Comparison between experimental and numerical solution of load-displacement curves; left: ds-T; right ds-C.

Conclusion

The paper presents numerical-experimental approaches of anisotropic wood behavior during loading. The devised fundamental anisotropic elasto-plastic material models for both Norway spruce and European beech were verified based on the experimental results and sensitivity analyses of material characteristics of wood (changes of yield stress, tangent moduli etc.). The new anisotropic elasto-plastic material models for wood include fully orthotropic elasticity, anisotropic plasticity with hardening for the non-linear behavior of wood in compression and bending allowing the prediction of wood ultimate strength. The stress-strain behavior of FEA showed very good agreement with experimental multilinear curves for both anisotropic elasto-plastic material models. The numerical curves for all exams showed gradual elasto-plastic transitions which are similar with experimental stress-strain curves. Further, the verified fundamental anisotropic material models were implemented into the solver of more complex FEA of joints. These material models were compared and verified on the basis of experimental load-displacement behavior of tested double-shear joints under various load (compression and tension). The mechanical responds of numerical joints models showed good agreement with experimental behavior of wooden joints.

Acknowledgements

This paper was funded by the grant no. 21/2015 of Internal Grant Agency of Faculty of Forestry and Wood Technology at Mendel University in Brno and Ministry of Education, Youth and Sports of the Czech Republic (grant no. 6215648902) and by the project NAKI “Design and Assessment of Timber Joints of Historical Structures” reg. No, DF12P01OVV004, provided by the Ministry of Culture of the Czech Republic.

References

[1] Abruzzese D, Miccoli L, and Yuan J (2009) Mechanical behavior of leaning masonry Huzhu Pagoda, J Cult Herit 10:480–486.
[2] Brabec M, Tippner J, Sebera V, Milch J, Rademacher P (2015) Standard and non-standard deformation behaviour of European beech and Norway spruce during compression. Holzforschung. Online – 2015-01-23, vol. 0, issue 0, s. -. DOI: 10.1515/hf-2014-0231.
[3] Bulleit WM, Sandberg LB, Drewek MW, and O'Bryant TL (1999) Behavior and modeling of wood-pegged timber frames. J Struct Eng 125(1):3–9.
[4] Chen CJ, Lee TL, and Jeng DS (2003) Finite element modeling for the mechanical behavior of dowel-type timber joints. Comput Struct 81(30):2731–2738.
[5] Clouston PL, and Lam F (2002) A stochastic plasticity approach to strength modeling of strand-based wood composites. Compos Sci Technol 62(10):1381–1395.
[6] Dias AMPG, Van de Kuilen JW, Cruz HMP, and Lopes SMR (2010) Numerical Modeling of the Load-Deformation Behavior of Doweled Softwood and Hardwood Joints. Wood Fiber Sci 42(4):480–489.
[7] Hill R (1950) The Mathematical Theory of Plasticity, The Oxford Engineering Science Series, Oxford, pp. 97–114.
[8] Kessel MH, Augustin R (1996) Load behavior of connections with pegs II. Timber Framing. Journal of the Timber Framers Guild (39):8–10.
[9] Kollman FFP, Côté WA (1968) Principles of wood science and technology: solid wood. Allen & Unwin.
[10] Moses DM, and Prion, HG (2002) Anisotropic plasticity and failure prediction in wood composites. Research Report. University of British Columbia, Canada.
[11] Oudjene M, and Khelifa M (2009) Elasto-plastic constitutive law for wood behaviour under compressive loadings. Constr Build Mater 23(11):3359–3366.
[12] Požgaj A, Chovanec D, Kurjatko S, and Babiak M (1997) Štruktůra a vlastnosti dreva. Priroda, Bratislava. (in Slovak)
[13] Santos CL, De Jesus AM, Morais JJ, and Lousada JL (2009) Quasi-static mechanical behaviour of a double-shear single dowel wood connection. Constr Build Mater 23(1):171–182.
[14] Sohouli AR, Goudarzi AM, and Alashti RA (2011) Finite Element Analysis of Elastic-Plastic Contact Mechanic Considering the Effect of Contact Geometry and Material Properties. Journal of Surface Engineered Materials and Advanced Technology 1(03):125–129.

Proceedings of the 58th International Convention of Society of Wood Science and Technology
June 7-12, 2015 – Grand Teton National Park, Jackson, Wyoming, USA

Effects of Cement Strength Grade and Particle Content on the Compressive Strength of Bamboo-Cement Composites

Olayiwola H.O[1], Adesope A.S[2], Adefisan O.O[3]*

[1]Postgrad, Department of Agricultural and Environmental Engineering, Wood Products Engineering Unit, University of Ibadan, Nigeria
[*]*Corresponding author:*
olafiku@yahoo.com
[2]Research Officer, Forestry Research Institute of Nigeria, Forest Product Development and Utilization Unit
[3]Senior Lecturer, Department of Agricultural and Environmental Engineering, Wood Products Engineering Unit, University of Ibadan, Nigeria

Abstract

Escalating cost of conventional building materials and rapid population growth has led to acute shortage of housing units in developing nations; hence, the need for alternative low-cost and durable building materials. This study determined the influence of cement grade, particle content and chemical additive on the compressive strength of bamboo-cement composites.

Laboratory type 35mm-thick (cube) cement-bonded composites were made from particles derived from bamboo (*Bambusa vulgaris*). The proportion of cement, sand, stone-dust was done by weight in a nominal mix of 1:2:4. The particle content was substituted based on sand proportion. Two levels of the production variables were employed in the production. These are chemical additive (0% and 3%), particle content (10% and 20%), particle size (850µm and 1.18mm) and cement strength grade (32,5R and 42,5R).

Composites encapsulated with 42,5R cement had better strength from 1.16 to 3.02 N/mm^2 and 1.65 to 4.76 N/mm^2 at 0% and 3% chemical additive respectively. There was an inverse relationship between the particle content and compressive strength for both cement types and particle sizes.

The results indicated that composites produced with cement grade 42,5R at 3%$CaCl_2$, 10% particle content and 1.18mm particle size have higher compressive strength than those produced with cement grade 35,5R.

Keywords; Low-cost building material, bamboo-cement composites, cement grade, particle content and compressive strength

Introduction

Shelter is undoubtedly one of the most important requirements for human survival. This is why provision of rural housing and low-cost housing units top the list of government agenda in the developing nations. However, the use of conventional building materials are costly and highly energy intensive (Bharath et al; 2014). This has incapacitated the efforts of both governments and NGOs alike.The answer to the challenges of housing in the developing worlds lies in the encouragement of community participation in housing construction, small scale production of building components, use of non-skilled labour in the production and materials that are cheap and readily available.

Natural fibre composites are excellent low-cost alternative building materials that are claimed to offer environmental advantages such as reduced dependence on energy/material sources, lower pollutant emissions, lower greenhouse gas emission and enhanced energy recovery (Syed et al 2011). They have been reported to exhibit better electrical resistance, good thermal insulation and acoustic properties (Syed et al 2011; Manza et al 2010), high ductility and great crack resistance (Ali et al 2010). These render them well suited for use in structures exposed to cyclical and extreme live loads (Tsung-Chin Hou et at 2005; Ali et al 2010). Their superior tensile strength (Baruah and Talukdar 2007), ductility and crack resistance and ability to be moulded into any shape make them well sought-after materials in various engineering applications. Another positive side is the fact that the method of production can be adapted to suit the available local technology.

Natural fibres such as sisal, jute, coir, wood, kenaf, bamboo, rattan, baggasse, oil palm fibre have all been proved to be good reinforcement in thermoset, thermoplastic and cement matrices (Joseph et al .1996; Sreekala et al. 1997; Geethamma et al.1998; Badejo. 1988; Olorunnisola. 2005; Omoniyi. 2009). This work sought to find out the influence of strength grade of two commercially available cement types in Nigeria, on the compressive strength of bamboo reinforced cement composite- a prospective alternative low-cost building material.

Bamboo

Bamboo is a fast-growing minor forest product which is cheap and widely available. About 75 genera and 1250 species of this renewable resource grow in different parts of the world (Sattar 1995). The available species in Nigeria are *bambusa vulgaris,* Its role in poverty alleviation and economic development has been well studied. Bamboo products are excellent material for low-cost housing components
Bamboo possesses excellent strength properties, especially tensile strength. Most of these properties depend on the species and the climatic conditions under which they grow (

Sekhar and Gulati 1973). Strength varies along the culm height. Compressive strength increases with height while bending strength has the inverse trend (Kabir et al 1991;1993). These properties are expected to be carried over into composites when bamboo particles are mixed with cement.

Cement

Cements are made in a variety of compositions for a wide variety of uses. ASTM C150 defines Portland cement as "hydraulic cement(cement that not only hardens by reacting with water but also forms a water-resistant product) produced by pulverizing clinkers consisting essentially of hydraulic calcium silicates, usually containing one or more of the forms of calcium suphate as an inter ground addition." The low cost and widespread availability of the limestone, shales, and other naturally occurring materials make Portland cement one of the lowest cost materials widely used over the last century throughout the world.

Two brands of Ordinary Portland cement are common and popular in Nigerian markets. These brands have strength grades of 32,5R and 42,5R and carry the following tags respectively: CEM II/B-L 32.5N and CEM II/A-L42.5R.

Materials and Methods

Bamboo culms used in this study were procured within the University of Ibadan, Nigeria. Matured green culms were cut into pieces of average length of 4ft. and then air-dried to ensure breakdown of sugar and other extractives that could inhibit bonding with cement. The dried culms were then sliced and chipped with cutlass into average dimension of 1in. by 3in. to ensure easy milling. The chips were milled into flakes with hammer mill and screened into fines and particle sizes of 600µm, 850µm and 1.18mm.

The proportion of cement, sand, stone-dust was done by weight in a nominal mix of 1:2:4. A pre-determined quantity of cement, sand and stone-dust based on this formulation ratio was mixed with suitable amount of bamboo particles substituted at 10% and 20% of sand proportion in dry state until a homogenous mixture was achieved. This mixture was then blended with required quantity of water calculated using Equation 1, developed by Simatupang (1979), until a desired workability and consistency was attained. Two levels of $CaCl_2$ (0% and 3%) based on cement proportion was employed. This was dissolved in the water used for blending.

$$R_{H_2O} = 0.35\,W_{cement} + (0.30 - \alpha)W_{bamboo} \quad ----------1$$

Where:

R_{H_2O} = water required to blend the mixtures in (litres)

W_{cement} = weight of cement based on the formulation (kg)

α = moisture content of wood at time of use (%)

$$W_{bamboo} = \text{weight of bamboo required based on substitution (kg)}`$$

A quarter inch-thick plywood, 600mm × 600mm overlaid with polythene interface served as caul plate on which wooden moulds (6× 35mm^3) was positioned to produce BCCs of required geometry. A steel spoon was used to spread and level up the mortar evenly to the mould thickness of 35mm. It was then compacted with a tamping bar to eliminate air voids. The mould was then detached and resulting cubes left in the open air to dry.

To ensure complete hydration of cement to enable the composite products attain their full satisfactory strength, curing for this work took a total of 28 days. Initial setting took place in a dry cool place for a period of 24hr before the cubes were subjected to wetting for 7days to prepare them for 21 days curing in cold water. The compressive strength of the product was determined using Universal Testing Machine. The selected samples were put in-between the jaws of the machine, one after the other and loaded to failure at a rate of 1.2mm/min.

Results and Discussion

The results of the compressive strength of the bamboo-cement composites (bcc) bonded with cement Type I and II are shown in Tables 1 and 2 below. The mean compressive strength for the untreated bamboo fibres (@ 0% $CaCl_2$) encapsulated with Type I cement ranged from 1.33 – 2.64N/mm^2. The addition of 3%$CaCl_2$ resulted in increased compressive strength between 1.67 – 3.20N/mm^2. The same trend was noticed in composites made with cement Type II also. Untreated bamboo fibres bonded with type II cement had mean compressive strength ranging from 1.16 – 3.02N/mm^2. The range increased to 1.65 – 4.76N/mm^2 with the addition of 3%$CaCl_2$.

Table 1: Mean compressive strength of BCCs bonded with Type I cement

Bamboo content (%)	Compressive strength (N/mm^2) 0%$CaCl_2$		3%$CaCl_2$	
	850µm	1.18mm	850µm	1.18mm
10	1.88	2.64	3.20	2.89
20	1.33	1.56	1.67	1.97

Effect of cement strength grade on compressive strength

The mean compressive strength observed in BCCs bonded with Type II cement (grade 42,5R) was higher than encapsulated with Type I (grade 32,5N). This may be due to the differences in the compositions of the two cement types. Significant difference at ($p \leq 0.05$) existed between the two cement types with Type II having higher strength values.

Table 2: Mean compressive strength of BCCs bonded with Type II cement

Bamboo content (%)	Compressive strength (N/mm^2) 0%$CaCl_2$		3%$CaCl_2$	
	850µm	1.18mm	850µm	1.18mm
10	3.02	1.90	3.68	4.76
20	1.16	1.27	1.65	1.73

Effect of bamboo content and particle size on compressive strength

An inverse relationship was observed between the particle content and mean compressive strength for both cement types and particle sizes "Tables 1 and 2." This may be attributed to low bonding between the fibres and cement at high content. Huang and Cooper (2000) and Omoniyi (2009) also reported low mechanical properties in cement bonded particles at higher particles content.

From Tables 1 and 2, it is observed that a direct relationship existed between the compressive strength and particle sizes for all composites. BCCs made with particle size 1.18mm had higher strength values for both cement types than those made with 850µm particles. The only exceptions were seen in BCCs bonded with Type I cement at 10% particle content, 850µm size and 3%$CaCl_2$; and BCCs encapsulated with Type II cement at 10% particle content, 850µm size and 0%$CaCl_2$. They had slightly higher values. The general observation was in line with the findings of Badejo (1980) that the strength properties of hardwood-cement board increased as the flake dimensions increase while the exceptions follow the observation of Olorunnisola (2007) that an inverse relationship exist between the compressive strength and particle size of rattan-cement composites. This may imply that different lignocellulosics exhibit different mechanical behaviours when encapsulated in cement matrix.

Table 3: Duncan's multiple comparison of compressive strength for BCCs made with Type I cement

Factors	Variables	Mean Compressive strength (N/mm^2)
Particle size	850µm	2.03^B
	1.18mm	2.27^A
Bamboo content	10%	2.52^A
	20%	1.78^B
$CaCl_2$	0%	2.02^B
	3%	2.27^A

-means with same letters are not significantly different ($p \leq 0.05$)

Table 4: Duncan's multiple comparison of compressive strength for BCCs made with Type II cement

Factors	Variables	Mean Compressive strength (N/mm^2)
Particle size	850µm	2.38^A
	1.18mm	2.42^B
Bamboo content	10%	3.34^A
	20%	1.45^B

$CaCl_2$	0%	2.00^B
	3%	2.79^A

-means with same letters are not significantly different ($p \leq 0.05$)

Statistical analyses (Tables 3 and 4) revealed significant difference between the two levels of bamboo content with 10% having higher strength value. Significant difference also existed between the two particle sizes. Particle size 1.18mm had higher mean compressive strength.

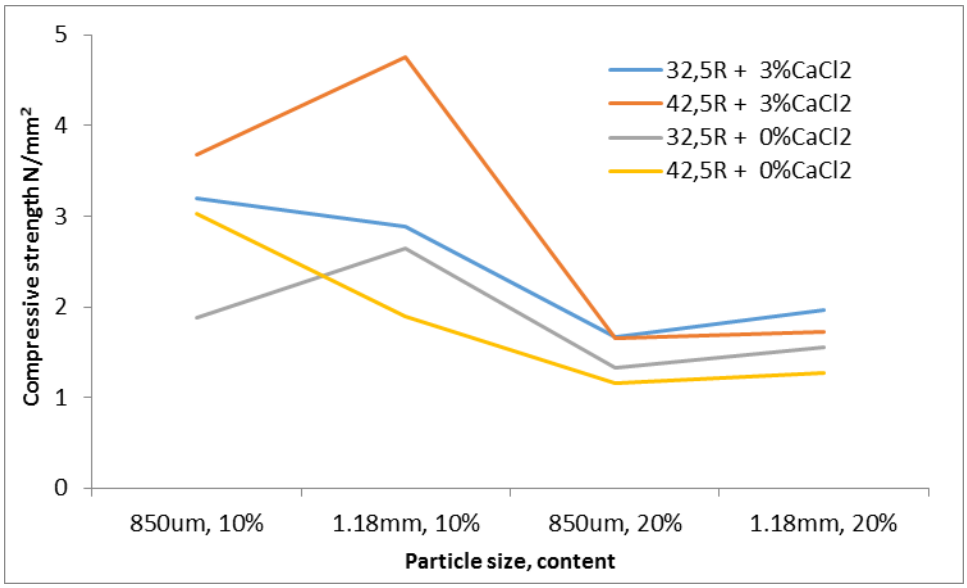

Fig. 1: Effects of particle size, particle content and cement type on compressive strength at 0 and 3%$CaCl_2$ levels.

Effect of chemical accelerator on mean compressive strength

Addition of 3%$CaCl_2$ resulted in increased compressive strength for both cement types (Fig.1). This was expected as $CaCl_2$ is a well-known inhibitory agent in cement composite production. Olorunnisola (2007) reported a similar observation. The addition rendered inhibitory substances contained in bamboo fibres inactive when encapsulated in cement matrix thereby enhancing better compatibility which resulted in improved strength property. Statistical analyses also revealed significant differences between the two levels of chemical addition (0 and 3%), with 3%$CaCl_2$ having higher mean compressive strength.

Conclusion

Based on the data collected and their statistical analyses, the following conclusions are drawn:

i. The compressive strength of bamboo-cement composites are affected by the strength grade of the Portland cement used in the production. 42,5R graded cement produced composites of higher strength values.
ii. Particle size and particle content exhibited an inverse and a direct relationship with compressive strength respectively.
iii. Addition of 3%$CaCl_2$ improved the compressive strength of the bamboo-cement composites.
iv. Bamboo-cement composites produced with cement grade 42,5R at 3%$CaCl_2$, 10% particle content and 1.18mm particle size have higher compressive strength than those produced with cement grade 35,5R.

References

Ali, M., Liu, A.,Sou, H. and Chouw N. 2010. Effect of fibre content on dynamic properties of coir fibre reinforced concrete beams. NZSEE Conference, 2010. Paper Id: 44.

ASTM C150-86. 1990. Standard Specification for Portland Cement. Annual book of ASTM Standards 4.02:89-93.

Badejo, S.O. 1988. Effect of flake geometry on properties of cement-bonded particleboard from mixed tropical hardwoods. Wood Science and Technology 22(4):357-370

Baruah, P., and Talukdar, S. 2007. A comparative study of compressive, flexural, tensile and shear strength of concrete with fibres of different origins. Indian Concrete Journal, 81(7):17-24

Bharath B, Maheshwar RL, Juberahmed P and Rahul RP (2014): " Studies on stabilised adobe blocks". International Journal of Research in Engineering and Technology, IJRET. Vol: 03 special issue: 06. Pp 259-264.

Geethamma, V.G., Mathew, K.T., Lakshmnarayanan, R. and Thomas, S. 1998. Composite of short coir fibers and natural rubber: effect of chemical modification, loading and orientation of fiber. Polymer, 39:1483

Joseph, K., Thomas, S. and Pavithran, C. 1996. Effect of chemical treatment on the tensile properties of short sisal fibre-reinforced polyethylene composites. Polymer, 37:5139^15

Kabir, M.F., Bhattacharjee, D.K., and Sattar, M.A. 1991. Physical and mechanical properties of four bamboo species. Bangladesh Journal of Forest Science, 20(1&2), 31-36

Kabir, M.F., Bhattacharjee, D.K., and Sattar, M.A. 1993. Effects of age and height on strength properties of dendrocalamus logispaths. Bamboo Information Centre, India. Bulletin 3(1), 11-15

Mahzan, S., Zaidi, A.M., Ahmad, Arsat N., Hatta, M.N.M, Ghazali, M.I. 2010. Study on sound absorption properties of coconut coir fibre composite with added recycled rubber. International Journal of Integrated Engineering, Vol. 2, No. 1. Pp. 29-34.

Olorunnisola, A.O. 2005. Dimensional stability of cement-bonded composite boards made from rattan cane particles. Journal of Bamboo and Rattan, Vol.4(2):173-182

Omoniyi, T.E. 2009. Development and evaluation of bagasse-reinforced cement composite roofing sheets. Ph.D Thesis submitted to the Department of Agricultural and Environmental Engineering, University of Ibadan.

Sattar, M.A. 1995. Traditional bamboo housing in Asia: Present status and future prospects. Proceedings of the Vth International Bamboo Workshop and the IVth International Bamboo Congress, Ubud, Bali, Indonesia. 19-22 June, 1995.

Sekhar, A.C and Gulati, A.S. 1973. A note on the physical and mechanical properties of Dendrocalamus strictus from different localities. Van Vigyan: 11(314), 17-22

Simatupang, M.H. 1979. The Water Requirement of Manufactured Cement-bonded Particleboard. Hole Roh-Werkst. 37;373-382

Sreekala, M.S., Kumaran, M.G. and Thomas, S. 1997. Oil palm fibers: morphology, chemical composition, surface modification and mechanical properties. Journal Applied Polymer Science, 66:8-821

Syed A.H, Pandurangadu V. and Palanikuamr K. 2011. Mechanical properties of green coconut fiber reinforced HDPE polymer composite. International Journal of Engineering Science and Technology (IJEST), Vol. 3. No. 11. Pp.7942-7952

Tsung-Chin Hou, Jerome P.L. 2005. Monitoring strain in ECC using wireless sensors. Proceeding of the International Conference on Fracture (ICFXI), Turin, Italy, March 20-25, 2005

Verma, D., Gope, P.C., Shandilya, A., Gupta, A., Maheshwari, M.K. 2013. Coir fibre reinforcement and application in polymer composites: a review. Journal of Material and Environmental Science. 4(2) (2013) 263-276

Proceedings of the 58th International Convention of Society of Wood Science and Technology
June 7-12, 2015 – Grand Teton National Park, Jackson, Wyoming, USA

Manufacturing and Mechanical Characterization of a 3D Molded Core Strand Panel

Daniel Way

Oregon State University, Corvallis, OR

Abstract

Three dimensionally (3D) molded core panels consist of two components: A core that is molded in a repeating structure that contains hollow areas and skins which make up the outer portion of the panel. These panels have been of interest to the wood composites community because of their ability to utilize low value materials, but have yet to enter the building construction materials market due to challenges in meeting necessary mechanical requirements for structural use.

The design of 3D molded core panels is unique compared to commercially available wood composite panels in that they behave more like a beam with the core acting as a load transfer mechanism between the high strength skins. Air space in the hollow core provides additional insulation but can also be designed to allow passage of hot air from attic spaces. Air space also lowers the thickness to weight ratio meaning that panels of greater depth may be produced without hindering jobsite handling. Unlike their solid composite panel counterparts, the two part core and skin system generally results in non-catastrophic failures.

This study investigates the use of wood strands for forming a molded core on the premise that wood strands typically have favorable mechanical properties opposed to their fiber and particle counterparts. Cores were molded using furnish typical of oriented strand board (OSB) and a proprietary core mold supplied by our industrial partner and commercially available OSB as skin material. Panels were tested for key mechanical properties to determine their adequacy for use as a structural sheathing material.

Keywords: 3D molded core panel, strand composites, structural sheathing, sandwich panels

Proceedings of the 58th International Convention of Society of Wood Science and Technology
June 7-12, 2015 – Grand Teton National Park, Jackson, Wyoming, USA

Multi-technique Characterization of Douglas-fir Cell Wall Deconstruction during Mechanical Milling Pretreatment

Jinxue Jiang [1] – Jinwu Wang[2] - Michael P. Wolcott[3]*

[1] Graduate student, Composite Materials & Engineering Center, Washington State University, Pullman WA, USA
[2] Research assistant professor, Composite Materials & Engineering Center, Washington State University, Pullman WA, USA
[3] Professor, Composite Materials & Engineering Center, Washington State University, Pullman WA, USA.
* *Corresponding author* wolcott@wsu.edu

Abstract

Overcoming recalcitrance of the wood cell wall to enzymatic degradation is believed to being crucial for effective biological conversion of polysaccharides to fermentable sugars. Mechanical milling has long been used to overcome the native structure barriers of cell wall for producing milled wood lignin. This process imparts macro/micro/nano morphological and physicochemical alternations that contribute to increased accessibility of cellulose without removal of chemical compositions. Multi-technique characterization of Douglas-fir cell wall disruption during mechanical milling were conducted using electronic microscopy (SEM, TEM), confocal laser scanning microscopy (CLSM), atomic force microscopy (AFM), and X-ray diffraction (XRD). Collectively, these techniques elucidate the evolution of cell wall changes. We propose that coincident with the particle size reduction of the wood material during the milling process includes tissue disintegration, cell wall fragmentation, disordering of layered cell wall fragment, and aggregation of disordered cell wall fragments. As evidenced by LSCM, the constituent cell wall polymers are redistributed following the ultrastructural disruption from the mechanical milling. XRD results demonstrated the amorphization of the semicrystalline polymers. Micro/nano porous structures were visualized by 3D-TEM tomography. The surface and ultrastructure alternation of cell wall contribute to enhancement of enzymatic digestibility by 4-14 folds over that of untreated cell walls depending on degree of milling pretreatment.

Key words: bioconversion, mechanical milling pretreatment, visualization, cell wall ultrastructure, accessible void

Introduction

Considerable interest has been emerged in converting sustainable lignocellulosic biomass into fossil fuel alternatives toward a diverse and economically viable renewable energy portfolio. The major challenge facing industrial-scale conversion of lignocellulosic biomass into biofuels are presented by the complex hetero matrix structure, which greatly impede chemical and microbial deconstruction of plant cell wall polysaccharides (Chiaramonti et al., 2012). Therefore, a pretreatment is recognized necessary to overcome the robust multi-scale recalcitrance and produce substrate highly susceptible to enzyme action for maximizing intermediate fermentable sugars release. Over the past decades, great efforts have been devoted on various thermochemical strategies, while the presence of chemicals and various solvents result in corrosion of processing equipment, formation of inhibitors to down stream process, and disposal/or recycle of the waste effluent, are responsible for the high cost and environmental impact of unsuccessful biorefinary(Barakat et al., 2014a, 2014b).

Mechanical milling pretreatment offers an attractive alternative to address these deficiencies and has a promising potential for implementation as a small scale facility, distributed sugar depot, to produce fermentable sugars. This process profoundly imparts multiple length scale structural alternations (i.e. tissue, cellular and molecular levels) by disrupting supramolecular cross-links of cellulose-hemicellulose-lignin matrix without removal of chemical compositions. Therefore, the versatile mechanical milling has recently attracted renascent interest in pretreatment arena for lignocellulose valorization due to its effectiveness to a variety of feedstock as well as great advantage of simple and green chemistry process(Takahashi et al., 2013). Particle size and cellulose crystallinity are the mostly characterized factors, which are correlated well with the improved enzymatic digestibility(Hoeger et al., 2013; Zakaria et al., 2014). The particle size reduction is believed to improve heat and mass transfer efficiency and increase enzyme accessibility with the increased specific surface area. It has been suggested that amorphogenesis of the highly ordered and tightly packed crystalline cellulose microfibrils also benefit in more hydrolytic enzyme accessible to cellulose substrate(Arantes and Saddler, 2010). Though such phenomenon description and elucidating deduction help to basically characterize milled biomass substrates, a comprehensive understanding of the ultrastructure change and redistribution of cell wall components would provide insight into fundamental mechanism of mechanical deconstruction of native cell wall recalcitrance and generating substrates susceptible to enzyme saccharification.

Microscopy methodologies help to determine the hierarchical architecture of plant cell wall as well as the macromolecular level distribution of components. Consequently, a variety of microscopy tools have been employed to probe the structure of plant cell wall with multi-scale resolution as well as the effectiveness of pretreatment on unlocking cell wall for cost effective biofuel production(Chundawat et al., 2011). However, there is currently no systematic, multi-scale, and integrated approach for comprehensive understanding of anatomical properties, such as visualization the morphological alternation and chemical composition distribution of cell wall correlating to the degree of mechanical milling wood. In the present study, we investigated the evolution of wood

cell wall deconstruction with multi-scale visualization and characterization to provide insight into fundamental mechanism of mechanical milling and native biomass recalcitrance.

2. Materials and methods

2.1 Material

Douglas-fir (*Pseudotsuga menziesii*) wood chips were obtained from Vaagen Brothers Lumber Inc. (Colville, WA). The original wood chips were passed through vibrating screen with an inch aperture and retained by No.4 mesh screen, and the screened chip had geometric mean diameter of 10.36mm. The screened wood chips were pre-ground into particles by a hammer mill fitted with a 1/8-inch screen, and stored at a conditioned room before using.

2.2 Mechanical milling pretreatment

Mechanical milling pretreatment of wood was conducted with a high-energy vibratory ring & puck mill (Standard mill, Rocklab Pty Ltd, New Zealand). The mill chamber had an inner diameter of 128 mm and height of 43 mm. The grinding mediums were a ring (inner diameter of 78mm, outside diameter of 100mm, and height of 41mm) and a puck (diameter of 52mm and height of 41 mm). Both milling chamber and grinding mediums were made of tungsten carbide. The sample (10 g) with moisture content of 5wt % (oven dry base) were loaded into the milling chamber and milling time was varied from 2-12 minutes at room temperature. The milling time chosen was dependent on our previous experiments about mechanical milling pretreatment of Douglas-fir with the same ring & puck mill.

2.3 Cellulose crystallinity index

X-ray diffractograms of the milled wood particles were obtained by a powder x-ray diffractometer (Rigaku, Miniflex 600, Japan) using Cu Kα (λ=0.154 nm) radiation generated at 40 kV and 15 mA. The instrument scanning range 2θ was from 10 to 40° with scanning rate of 1°/min. The relative degree of cellulose crystallinity, in terms of crystallinity index (CrI), was estimated as the height ratio between the intensity of crystalline peak and total intensity as described by Segal method(Segal et al., 1959.).

2.4 Scanning electron microscopy (SEM)

SEM imaging of samples were acquired typically at 20 kV accelerating voltage using FEI Quanta 200F, field emission gun with high vacuum ETD detectors (FEI Company, Hillsboro, Oregon, USA). Samples were mounted on aluminum stubs using carbon tape and sputter coated with 8 nm of gold for good conductivity prior to imaging.

2.5 Atomic force microscopy (AFM)

AFM imaging was conducted using a Dimension Nanoscope 3100 Scanning Probe Microscope (Digital Instruments) with a Nanoscope IIIa controller. Both amplitude and

phase images were collected simultaneously in tapping mode (in air) with an OTESPA7, etched silicon probe with a nominal frequency of 275 kHz and a nominal spring constant of 40 N/m. RMS roughness factors were estimated after image flattening and lane fitting of the height images using the software that came with the instrument.

2.6 Sample preparation for microtomy

Wood samples were processed using microwave electronic microscopy processing. Briefly, samples were fixed in 3% gluteraldehyde buffered in 0.05M Pipes buffer (Sigma, St Louis, MO) with 100% power of microwave. Dehydration was conducted in graded ethanol series for 40 seconds under microwave each (30%, 50%, 60%, 70%, 80%, 90%, and 3×100% ethanol). Samples were infiltrated with Spurr's low viscosity resin and incubated overnight at room temperature in a hood with increasing concentration of the resin (30%, 50%, 3×100% resin, diluted in isopropanol). Samples were then transferred to 1.5 mL microcentrifuge tubes with fresh Spurr's resin and then the resin was polymerized overnight in an oven with temperature of 70 °C. Spurr's resin embedded samples were sectioned to ~70-120nm using Leica Reichert Ultracut R microtome (Leica, Wetzlar, Germany). Glass knives were used to trim the block surface, and then a Diatome diamond knife was used to get the ultrathin sections.

2.7 Confocal laser scanning microscopy (CLSM)

Semi-thin (200 -500nm) sectioned samples were positioned on glass microscope slides and stained with saturated HPLC-grade acridine orange (AO; 3, 6-bis (dimethylamino) acridine hydrochloride, Sigma-Aldrich, St. Louis, MO) for 1 hour at room temperature(Yu et al., 2014). The images of stained samples were captured using a Leica TCS SP8 confocal scanning laser microscopy with a 20× dry objective lens. A white laser at λ=500 nm was used as the excitation light source. Flouorescence emission between λ=515 and 540 nm was collected as the green channel and emissions above λ=590 nm were collected as the red channel. Stacks of confocal optical sections were taken through the z-depth of the observed sections. Image analysis was performed using LAS AF Lite imaging analysis software. The images appear green in color were rich in carbohydrate and areas that are red in color are rich in lignin. When AO interacts with carbohydrates, it remains in a monomeric form that fluoresces and emits light primarily in the green region of the visible light spectrum. However, when AO interacts with the aromatic π electrons of lignin, the electron density of the molecule changes in such a way that causes other AO molecules to aggregate and this causes a fluorescence emission shift from green to red light spectrum.

2.8 Transmission electron microscopy (TEM) and 3D-TEM-tomography

The ultrathin sections were collected on Formvar coated copper or nickel slot grids (SPI Supplies, West Chester, PA). Grids were post-stained for 10 min with 1% aqueous KMnO4 to selectively stain for lignin. Images were captured with a 4 megapixel Gatan UltraScan 4K Eagle camera (Gatan, Pleasanton, CA) on a FEI Tecnai G2 20 Twin 200kV LaB6 TEM (FEI, Hilsboro, OR). Tomgrams were created by capturing dual-axis ±50-60°tilt series images. Tomograms were constructed using an R-weighted back projection algorithm within the Inspect 3D software (FEI, Hilsboro, OR). Single-axis tomograms

were then combined to yield dual-axis tomograms using Amira 3D software (FEI, Hilsboro, OR).

3. Results and Discussion

Scanning electron microscopy reveals particle size variability of milled wood

Fig. 1 shows the evolution of surface morphology of milled wood particles with increase of milling time, as demonstrating with scanning electron microscopy (SEM) images. At the primary stage of mechanical milling, fiber bundle breakage was initiated by development of either delamination between adjacent cell wall middle lamella or perpendicular rupture of individual fibers (Fig.1 A). With milling time of 4 minutes, total disintegration of fiber bundles were observed, and the fractured fibrous fibers was the main stream of particles. Individual fibers were perpendicularly cut off and formed plat-like particles. The cracks and splits along the fiber wall provided the initiations for further dissociation of fiber cellular structure. Thus, with the milling time continued increasing, the individual plat-like fibers underwent further breakage with complete disruption of the native hierarchical cell wall structure. Typical fiber cell wall structure was difficult to delineate. No noticeable particle size reduction was observed upon extended milling time from 6 to 12 minutes, except for much rounder and more uniform particle shape. These observations were consistent with the volume based particle size distribution profiles. It was found that there was significant particle size reduction to around 20 μm of median particle size when the milling time was 6 minitues. However, with milling time increased further, no significant particle size reduction was observed both from the median particle size and particle size distribution.

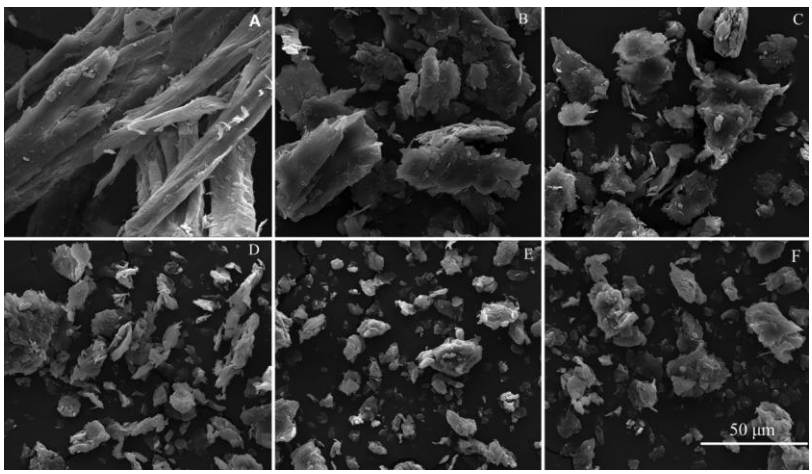

Fig. 1 SEM micrographs reveal fiber delamination and cellular fragmentation of milled wood under various mechanical milling time, 2 min (A), 4 min (B), 6min (C), 8min (D), 10min (E), 12 min (F).

Micro-scale evaluation of cellular fragmentation and chemical composition redistribution of milled wood

In order to investigate physical deconstruction phenomena of cell wall structure and redistribution of cell wall composition, confocal laser scanning microscopy (CLSM) with acridine orange-stained sections were used for direct visualization. As expected, the typical carbohydrates and lignin distribution were found tissues and locations variable. Lignin rich areas were found in ray parenchyma, cell wall corner and middle lamella. In contrast, strong green signal was found in carbohydrate-rich secondary cell wall layers. The results were consistent with previous results as reported by several authors(Sant'Anna et al., 2013). A series of time course images of wood particles with various degree of mechanical milling, showed remarkable fragmentation of cell wall structure and details of chemical composition redistribution as compared to the initial intact cell walls (Fig. 2). With milling time of 2 minutes, it was observed that fiber bundles were split off among middle lamella of adjacent cell walls, exposing large amount of lignin (Fig. 2A, a). With milling time of 4 minutes, more and more lignin was exposed on the surface of particles because of further dissociation of fiber bundles into individual fiber. There also existed fragments dissociated from individual fiber cell wall. Further milling process resulted in complete disintegration of discriminating cell wall with various size of fragments (Fig. 2 C, D, E, F). Simultaneously, lignin rich elements were dissociated and redistributed among fine particles along with the fracture of hierarchical cell wall structure. From Fig. 2 d, e, f, it was demonstrated that mechanical milling pretreatment was effective on destroying the highly ordered layer structure and cause microscale redistribution of lignin, which would contribute to improvement of digestibility of milled wood.

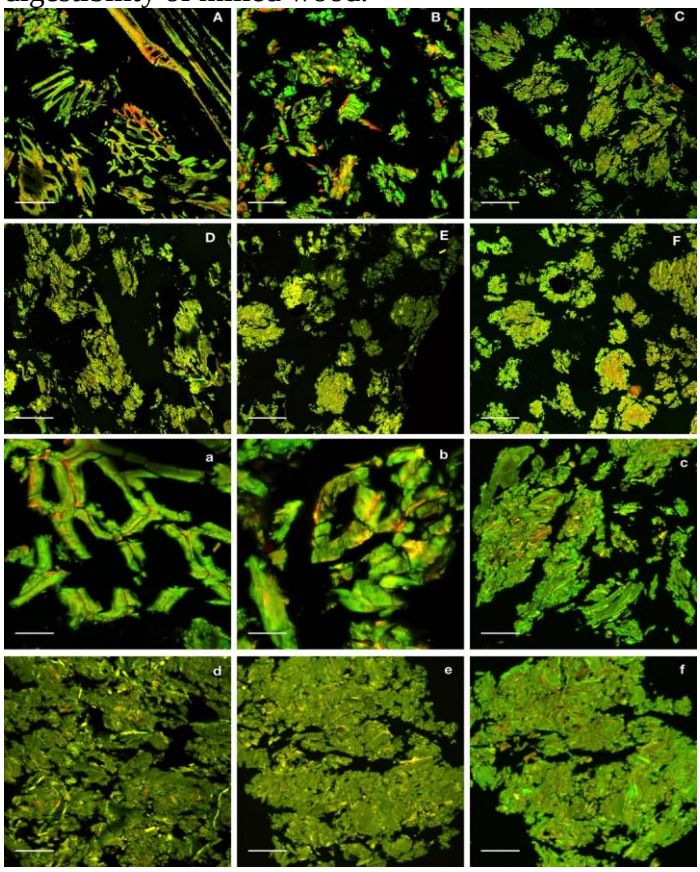

Fig. 2 CSLM micrographs reveal cellular fragmentation and chemical composition redistribution changes of milled wood under various mechanical milling time; 2 min (A, a), 4 min (B, b), 6min (C, c), 8min (D, d), 10min (E, e), 12min (F, f); scale bars = 100μm (A, B, C, D, E, F), 20μm (a, b, c, d, e, f).

Transmission Electron Microscopy Reveals Nanostructure alternation of milled wood

A series of micrographs of cell wall ultrastructure evolution after mechanical milling were presented in Fig. 3. It could be found that adjacent cell walls were separated through dislocation of middle lamella, as indicated in Fig. 2 A, B. Simultaneously, the secondary layer of cell wall was also fractured into fragments and delaminated into microfibril bundles. When wood particles were milled with 6 minutes (Fig.2C), the most resistant cell wall corner was also ruptured and some small particles were difficult to assign to specific cell wall location. With the prolongation of milling time, the ruptured cell wall fragments underwent further disruption and likely diffusion into each other to form homogeneous matrix (Fig.2 D, E, F). In Fig. 2 d, e, f, higher magnification TEM micrograhps delineated fibrous disordered microfibril network, which mainly due to intensive delamination and nanofibrillation. Inter-particle voids were clearly presented in the microfibrills network. It was also observed that the longer milling time, the higher degree of disordering of microfibril network. Correspondingly, the mechanical disruption and diffusion effect caused the rupture of intra- and intermolecular hydrogen bonds in the cellulose-hemicellulose-lignin matrix and a decrease in the crystallinity of cellulose. Additionally, it needs to note that serious disruption of cell wall ultrastructure also resulted in dissociation of cell wall matrix and redistribution of matrix components. The ultrathin sections were stained with $KMnO_4$ to selectively stain the lignin, which appeared to be black in TEM images. As seen in Fig. 2 e, f, nanoscale lignin agglomerations were found to randomly insert among disordered microfibrils network. As discussed above with CLSM micrographs, lignin migration from layered structure to agglomerated particles is also an important factor for activation of milled wood.

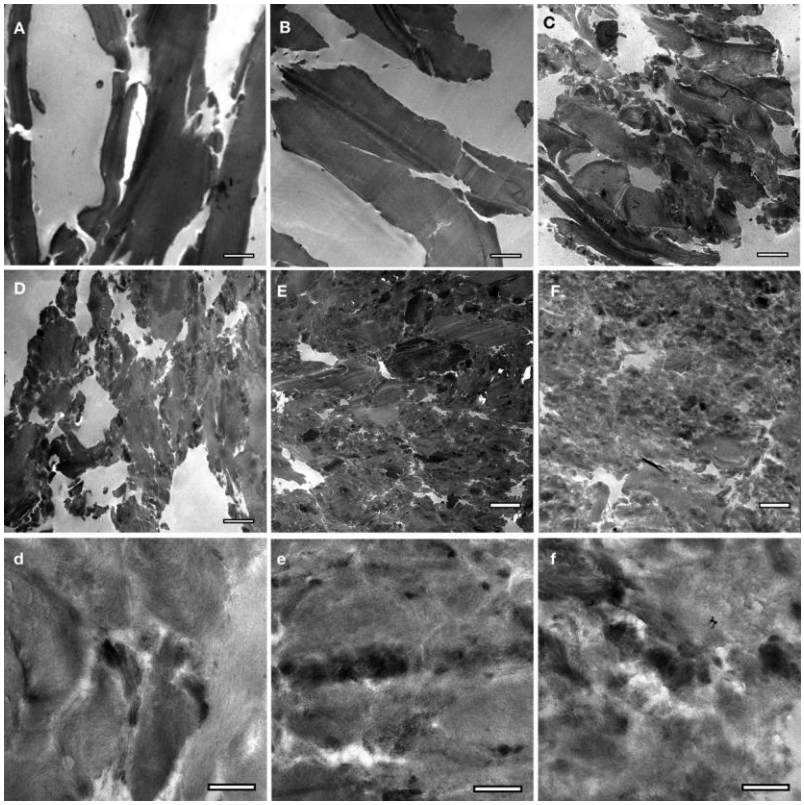

Fig. 2 Transimission electron microscopy of milled wood cell wall under various mechanical milling time, 2 min (A), 4 min (B), 6min (C), 8min (D, d), 10min (E, e), 12min (F, f); scale bars = 2μm (A, B, C, D, E, F), 500nm (d, e, f).

TEM Tomography Provides 3D Reconstructions of Nanoscale Morphology

Transmission electron 3D-tomograms assembled from tilt series TEM images were employed to quantitatively analyze the three dimensional nanoscale structure of milled wood using image segmentation and surface regeneration tools within Amira 3D software. Fig. 4A-F presented slices from tomographic reconstruction of evolution of milled wood cell walls with various milling time. Surface renditions of subvolumes from these tomograms shown in Fig. 4a-f provided a three-dimentional illustration of the nano-delaminated fibrous ruptured cell wall fragments. Delamination and crack propagation of cell wall structure shown in Fig. 4a-b, represented milled wood cell wall primary stage enzymes. There were no discernible pores or cracks within the relative intact cell wall layer fragments, which appeared to be relative smooth and nonporous with surface regeneration. With prolongation of milling process (Fig. 4c-f), the disintegrated cell fragments delineated increased porosity, cracks and fibrous channels, which could provide more accessible sites for reagents (i.e. catalyst, enzyme, etc.) to cellulosic substrates. To quantify the extent of fibrous structure disruption of milled wood particles, the intra-particle void fraction was calculated directly for each tomogram. The results were correlated strongly with the percentage of glucan released from milled wood as indicated in Table 1. The results highlighted the importance of improved accessible area of milled wood for enhancement of their subsequent digestibility. Similar conclusion was

attained with pretreated corn stover using different mechanical disruption reactor(Ciesielski et al., 2014).

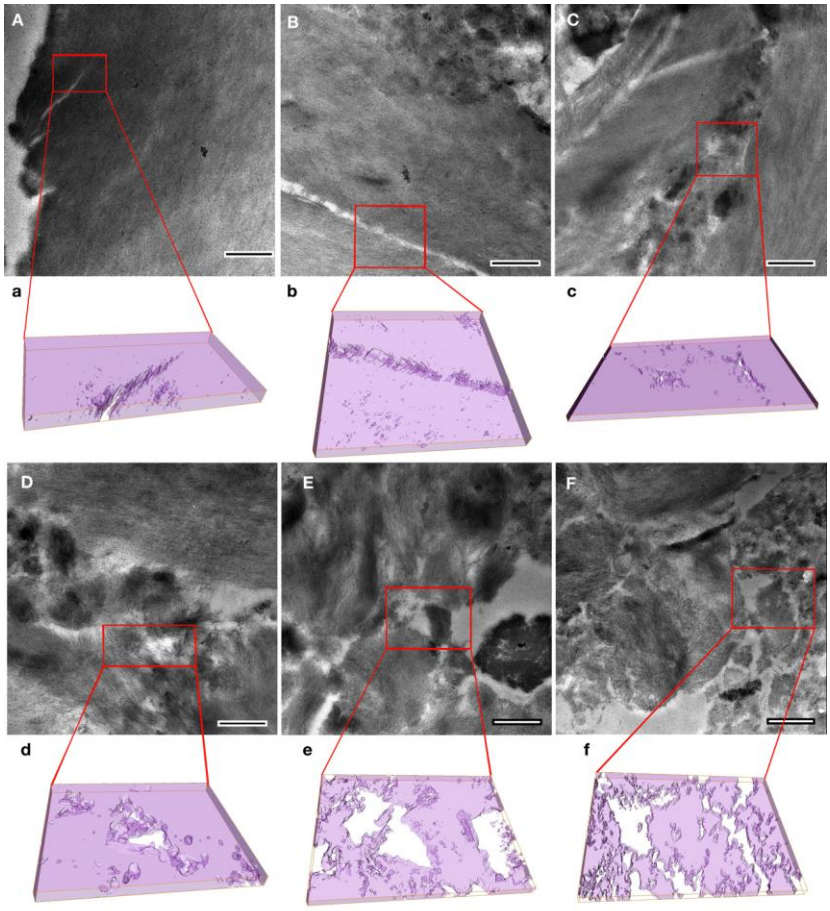

Fig. 4 TEM tomography of mechanical milled wood cell walls. Slices of tomographic volumes from 2minutes milling (A), 4 minutes (B), 6 minutes (C), 8 minutes (D), 10 minutes (E) and 12 minutes (F); scale bars 500 nm. Surface renditions (a-f) of subvolumes from the relative samples.

Table 1 Correlations between morphological/structural properties and digestibility

Sample	Glucan release %	Particle size µm	Aspect ratio	Inter-particle void %	Surface roughness /nm	Crystallinity index /%
Raw	6.23	1224	3.78	0.9	0.53	52.27
RM 2 min	23.73	115	2.050	3.6	0.67	47.9
RM 4 min	41.35	26.8	1.951	7.8	1.38	30.82
RM 6 min	62.06	21.7	1.831	15.7	2.76	22.64

RM 8 min	77.32	17.9	1.765	19.4	3.46	17.32
RM 10 min	81.77	15.5	1.729	32.5	4.34	11.92
RM 12 min	89.81	15.5	1.630	37.9	6.62	8.87
Correlation coefficient (R^2)		0.52	0.64	0.87	0.85	0.98

Surface analysis reveals changes in roughness of milled particles

Atomic force microscopy (AFM) analysis was employed to evaluate changes in particle surface after mechanical milling (Fig. 4). It was observed that the smooth surface of particle was obtained from milling time of 2 minutes. As discussed above, at the early stage of milling, mechanical action mainly resulted in dislocation of adjacent cell walls without any intensive disruption of fractured particles. Similar results of smooth surface of lignocellulosic biomass particles were also reported elsewhere(Chundawat et al., 2011). When milling process continued, the fractured cell wall fragments were activated with repeated mechanical force, resulting various degree of disruption of ultrastructure and surface depend with milling time. AFM micrographs revealed that the longer milling time, the more rough particle surface, suggesting increase in the disorder of microfibrils. For quantitative analysis, the surface roughness factors (RMS or root mean square) were measured and correlated strong with the enzymatic digestibility of milled wood particles, as indicated in Table 1. Therefore, the increased surface disruption of milled wood also contributed to enhancement of digestibility, as the increased substrate accessibility for enzyme.

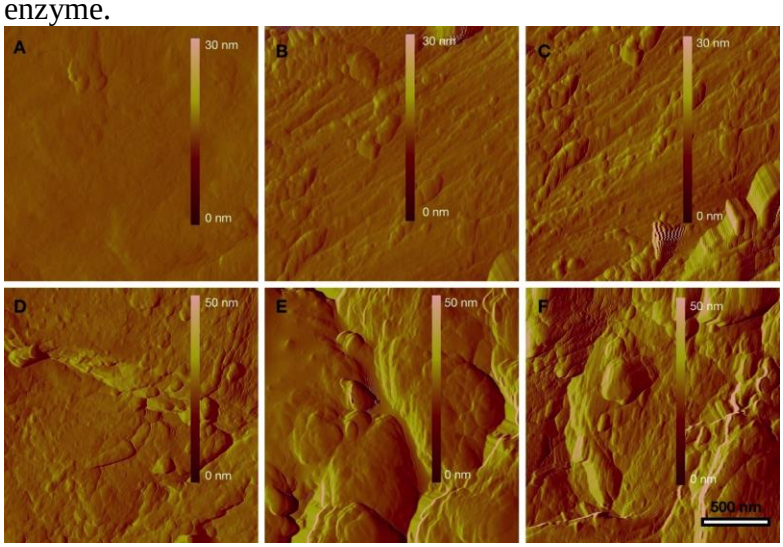

Fig. 4 AFM micrograph (amplitude) of mechanical milled wood from 2minutes milling (A), 4 minutes (B), 6 minutes (C), 8 minutes (D), 10 minutes (E) and 12 minutes (F).

Conclusions

Multi-scale disintegration and disruption of tissue bundles, intact fiber cell wall and cell wall fragments revealed by direct visualization of the micro- and nanoscale architecture

alteration in accessibility explains the increased enzyme susceptibility of milled wood. We proposed that enhanced degree of cell wall deconstruction was collectively achieved by particle size reduction, nanofibrillation of layered microfibrils and redistribution of chemical composition during mechanical milling process. The surface and ultrastructure alternation of cell wall contribute to enhancement of enzymatic digestibility by 4-14 folds over that of untreated cell walls depending on degree of milling pretreatment.

Acknowledgement

This research is supported by USDA National Institute of Food and Agriculture Coordinated Agricultural Research. The authours would also like to acknowledge the help of scanning electronic microscopy analysis from Franceschi Microscopy & Imaging Center (FMIC) at Washington State Univeristy, Pullman.

References

Arantes, V., Saddler, J.N., 2010. Access to cellulose limits the efficiency of enzymatic hydrolysis: the role of amorphogenesis. Biotechnol Biofuels 3.

Barakat, A., Chuetor, S., Monlau, F., Solhy, A., Rouau, X., 2014a. Eco-friendly dry chemo-mechanical pretreatments of lignocellulosic biomass: Impact on energy and yield of the enzymatic hydrolysis. Appl. Energy 113, 97–105. doi:10.1016/j.apenergy.2013.07.015

Barakat, A., Mayer-Laigle, C., Solhy, A., Arancon, R.A.D., de Vries, H., Luque, R., 2014b. Mechanical pretreatments of lignocellulosic biomass: towards facile and environmentally sound technologies for biofuels production. RSC Adv 4, 48109–48127. doi:10.1039/C4RA07568D

Chiaramonti, D., Prussi, M., Ferrero, S., Oriani, L., Ottonello, P., Torre, P., Cherchi, F., 2012. Review of pretreatment processes for lignocellulosic ethanol production, and development of an innovative method. Biomass Bioenergy 46, 25–35. doi:10.1016/j.biombioe.2012.04.020

Chundawat, S.P.S., Donohoe, B.S., da Costa Sousa, L., Elder, T., Agarwal, U.P., Lu, F., Ralph, J., Himmel, M.E., Balan, V., Dale, B.E., 2011. Multi-scale visualization and characterization of lignocellulosic plant cell wall deconstruction during thermochemical pretreatment. Energy Environ. Sci. 4, 973. doi:10.1039/c0ee00574f

Ciesielski, P.N., Wang, W., Chen, X., Vinzant, T.B., Tucker, M.P., Decker, S.R., Himmel, M.E., Johnson, D.K., Donohoe, B.S., 2014. Effect of mechanical disruption on the effectiveness of three reactors used for dilute acid pretreatment of corn stover Part 2: morphological and structural substrate analysis. Biotechnol. Biofuels 7, 1–12.

Hoeger, I.C., Nair, S.S., Ragauskas, A.J., Deng, Y., Rojas, O.J., Zhu, J.Y., 2013. Mechanical deconstruction of lignocellulose cell walls and their enzymatic saccharification. Cellulose 20, 807–818. doi:10.1007/s10570-013-9867-9

Sant'Anna, C., Costa, L.T., Abud, Y., Biancatto, L., Miguens, F.C., de Souza, W., 2013. Sugarcane cell wall structure and lignin distribution investigated by confocal and electron microscopy: Cell Wall Ultrastructure and Lignin Localization In Sugarcane. Microsc. Res. Tech. 76, 829–834. doi:10.1002/jemt.22235

Segal, L., Creely, J.J., Martin Jr, A.E., n.d. An Empirical Method for Estimating the Degree of Crystallinity of Native Cellulose Using the X-Ray Diffractometer. Text. Res. J.
Takahashi, T., Ito, K., Ito, A., Enda, Y., Gochi, M., Mori, H., Kobayashi, J., 2013. Tandem-ring mill pulverization benefits for enzymatic saccharification of biomass. Renew. Energy. doi:10.1016/j.renene.2013.07.046
Yu, Z., Gwak, K.-S., Treasure, T., Jameel, H., Chang, H., Park, S., 2014. Effect of Lignin Chemistry on the Enzymatic Hydrolysis of Woody Biomass. ChemSusChem 7, 1942–1950. doi:10.1002/cssc.201400042

Zakaria, M.R., Fujimoto, S., Hirata, S., Hassan, M.A., 2014. Ball Milling Pretreatment of Oil Palm Biomass for Enhancing Enzymatic Hydrolysis. Appl. Biochem. Biotechnol. doi:10.1007/s12010-014-0964-5

Preparation of Strips from *Bambusa Vulgaris* Schrad Culms from Recycled Scaffold for Intermediate Raw Materials Production

Adesope A.S [1] - Adewole N.A [2] - Olayiwola H.O [3]- Adejoba O.R[1]*

[1*]Researcher, Forestry Research Institute of Nigeria, Forest Products Development and utilization Dept
* Corresponding author
adeyinka_sope@yahoo.com.

[2]Senior Lecturer. Ph.D, Department of Agric and Environmental Engrg, University of Ibadan.
dabukyo@yahoo.com

[3]Postgrad, Department of Agric and Environmental Engrg, University of Ibadan.
olafiku@live.com

Abstract

In Nigeria, the main use of bamboo that attracts money is its use as scaffold and the massive number of bamboo used as scaffold always ended up as waste. But there are possibilities of recovering useful bamboo culms for the production of intermediate products like laminates among others particularly for semi-structural and non-structural purposes. The major constraint of using these recovered culms is the form in which bamboo occurs naturally (round). It is for this reason that this study is aimed at preparing strips from recovered bamboo culms to produce value added products. This study sourced and revealed the characteristics of bamboo reclaimed from scaffold use. From a total of 298 culms used as scaffold, only about 65% was good for re-use while others constituted a waste. The study was able to improvise treatment vat for the bamboo strips to enhance its durability. Intermediate products like bamboo wall clock, bamboo ply and bamboo boards were produced through lamination process. This study revealed the possibility of re-using bamboo from scaffold and was able to produce useful raw material and intermediate products from recovered bamboo waste.

Key-words: Bamboo culms, Scaffold, Intermediate Products, Bamboo Strips

Introduction

On account of the enforcement of our natural forest protection project in Nigeria, wood is becoming increasingly scarce. The realization that bamboo is the most potentially important non-timber resource and fast-growing woody biomass has evoked keen interest in the processing, preservation, utilization and the promotion of bamboo as an alternative to wood (Janssen, 2000). Its use as top grade building material and availability makes bamboo material always sought for in the field of construction. Its high valued utilization not only promotes the economic development, but also reduces pressure on our forest resources and protects the environment when used as wood substitute.

It has tremendous economic potential with its significant applications and innovative products. Also, its wide availability offers great opportunities to the micro, small and medium scale enterprises (Markus, 2008). Since the bamboo resource is widely available across the rural domains and industrial effort requires a lot of labour, bamboo has a great potential to offer job opportunity and income source to the rural masses. This can ultimately lead to the sustainable development of rural dwellers and hence contributing significantly to the economy (Sornai V, 2003; Suresh Moktan, 2007).

There are inherent variations in the bamboo culm features that limit its direct use for many valuable applications in round form (INBAR, 2006). Bamboo has hollow and come naturally with wall thickness which is not appreciable as compared with that of solid wood, hence the need for lamination to actualize its full potentials. Bamboo laminates have been of immense advantage because of the flexibility of standard sizes for use in the production of small to large structure (Pokhrel, 2008). Several other products have been made from bamboo laminates including furniture parts and novel items that are aesthetically pleasing. Despite the growing popularity of bamboo to meet several demands, it requires some level of technology and machinery for its processing before it can realize its full potential in meeting the demand (Janssen, 2000; Van, 2010).

African countries are yet to fully optimize the potentials of this valuable forest resource. In the case of Nigeria, the use of bamboo attracts commercial value in its use in construction industry for scaffold as observed by Adewole and Olayiwola (2011). After use as scaffold it becomes partially dried, and ended up as waste. Inadequate technological capacity and lack of processing facilities are major challenges to developing utilization schedule for the numerous bamboo resources and recovered bamboo from construction industries in Nigeria.

It is possible to create intermediate raw material from bamboo recovered from scaffold use in producing items that can be used interior decoration in building. The focus of this study is to explore ways of maximizing the potentials of bamboo resource through preparation of strips from *Bambusa vulgaris* Schrad culm for use in the production of intermediate raw materials.

Materials and Methods

Bamboo Laminates Production

The materials used in the production of bamboo-lam were; Bamboo culms; Moisture meter; Veneer calliper; Circular saw; Surface planner; Thicknesser; Preservative chemicals; Adhesive; Jig for glulam and brush. Used *Bambusa vulgaris* Shcrad (Plate 4.2) with large culms and thick walls were selected after sorting at the on-going building construction site within the premises of Veterinary Medicine Department, University of Ibadan. The selection of straight culms was given consideration to enhance ease of processing and to reduce wastage. The culms were cut to transportable lengths and transported to Forest Resources Management's (FRM) workshop at the University of Ibadan for further processing.

The culms were crosscut into short lengths (600mm) with the aid of cross-cutting machine and split on a circular saw machine with the internal nodes removed so as to get rid of external bulging and to get bamboo strips not having more than two nodes in a given length to facilitate further processing. The splits were rough planned on a planing machine to remove the epidermal layer and produce strips lengthwise with a rectangular transverse-section. The planed strips were soaked and boiled in a solution containing 1% concentration of boric acid for 24 hours in a treatment drum shown in Plate 1.1. This is necessary in order to improve the sections resistant to insect attack and fungal infestation thereby enhancing its durability in service. The strips were air-dried to a moisture content of about 12% as shown in Plate 1.2.

Production of Intermediate Raw Material from Bamboo Laminates

After preparation of the strips, the surface of the strips is cleaned to ensure they are free of dirt before the application of glue. Glue was then applied on the surfaces. The strips are loaded side-by-side on the base of the jig (the pressing device). The pressure applied through clamping ensures the strips are firmly bonded. The laminates were left in the jig for 24 hours to set and for the glue to cure. The laminates were later planed and shaped to required sizes, sanded with fine grit sandpaper to give a smooth outlook. The flow chat which describes the procedures involved in the production of bamboo-lam is shown in figure 1 and the procedure is shown next in the plate below

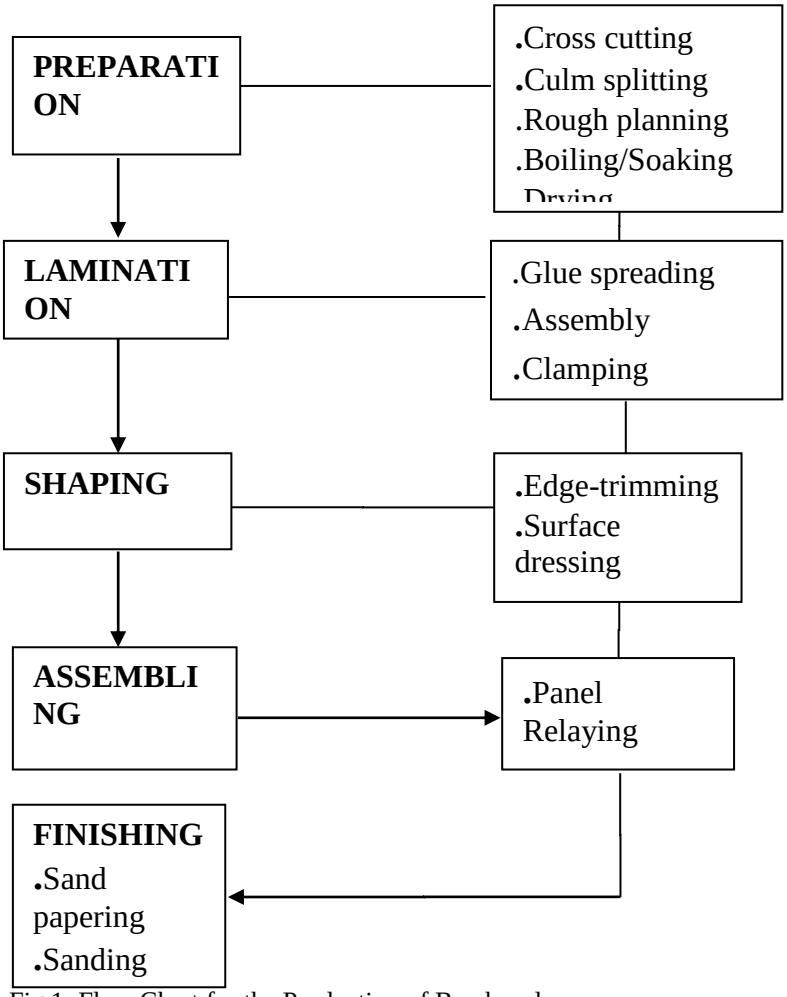

Fig 1: Flow Chart for the Production of Bamboo-lam

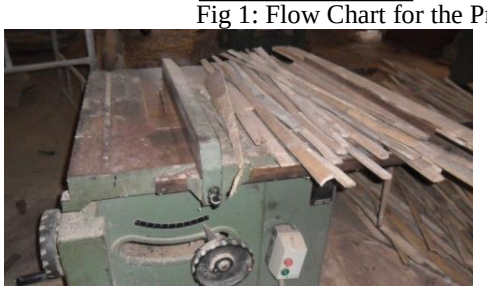

Plate 1: Surface Plainer

Plate 1.1: Treating Bamboo Strips Samples

Plate 1.2: Air-dr ti les in Progress

Plate 2: Edge Matching **Plate2.1: Pre-marking the Strips for Assembling**

Plate 2.2: Application of Glue and Assembling

Results and Discussions

Characteristics of Bamboo Reclaimed from Scaffold Use

The assessment of bamboo culms used for scaffold (Plate 3 and 3.1) at the construction site of the Veterinary Teaching Hospital Complex, Faculty of Veterinary, University of Ibadan showed that bamboo recovered from scaffold use was highly infested by vectors and fungi. Investigation revealed that the bamboo culms that are either harvested or bought for scaffold use is rarely deliberately selected. It is often a mixture in terms of maturity, dryness and is often lumped together.

The high sap content in the inner layer coupled with the current selection and handling practice appears to be largely responsible for the high infestation and staining of large number of bamboo culms from the stock that are reclaimed. The characteristics of the bamboo that were supplied to the construction site where the bamboo culms used for this study were got from is described in Figure 2. From a total of 298 bamboo culms that was available to be sorted for analysis after use, this includes those that were never used but brought to the site, only about 65% of the total culms can be processed into bamboo strips. The rest constitutes the immature, irregularly cracked ones, shrunk and insect infested ones. It is however revealed that prompt sorting has helped to reduce the percentages that were infested by the insect.

It was observed that recovered bamboo culm exhibited characteristic features that limit their use for making intermediate products. However, with careful sorting and selection, useful bamboo culms can be reclaimed from the lot used as scaffold. Thus this study presents how these challenges were surmounted in the sample retrieved from the study location.

Plate 3: Bamboo Culm Used as Scaffold at the Construction Site

Plate 3.1: Mode in which Recovered Bamboo Culms from Scaffold is Stored

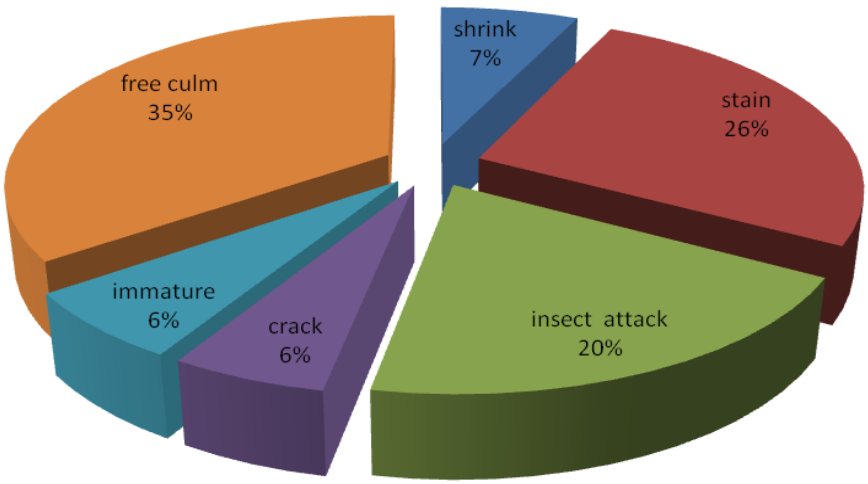

Figure 4.1: Characteristics of Bamboo Culm Recovered from Scaffold

Earlier studies by Allison *et al* (1978); Hing, (1982); Janssen, (1982); Liese, (1985); Anonymous. (1990); Hidalgo, (1992); Grewal et al; (1994) and Adewole and Olayiwola, 2011) have shown that machinery used for the production of bamboo laminates at various production stages contributed to the increased waste generated. Hence, there is need to develop a suitable jig for improved recovery from bamboo culm to be used for the production of bamboo laminate.

Intermediate Products from Recovered Bamboo Culm

The resulting materials from the lamination process can be used in the production of finished and semi-finished articles such as furniture, kitchen cabinet, kitchen coutertop, wall decoration and some other items among others. The process involved in the production of selected products such as Bamboo-Ply, Bamboo wall clock among others is as follows; Planed and treated bamboo strips were checked for moisture content (M.C). The M.C at this stage was ensured to range from 8-10%. The production procedure of the developed products is detailed here next.

Bamboo-Ply: an artificial board substrate of dimension 400mm x 600mm was prepared with the faces and backs cleaned of dirt. An adhesive was then applied on the upper and lower surfaces of the substrate. The strips were assembled horizontally on the substrate immediately having ensured that the adhesive has been applied on faces and edges of the strips to be laminated. Then, the laminate substrate is pressed in a cold press for 24 hours to cure the

Plate 4.1: Bamboo ply

adhesive. After the adhesive is cured, the press laminated substrate is removed from the press. The boards are then sanded smooth from both surfaces and edges, thereby forming a bamboo-ply as seen in Plate 4.10. This gives a board dimension of 590mm x 450mm x 20mm as shown below.

Bamboo Wall clock: this is made from the mixture of bamboo strips and wood strips laminated together with aid of a jig to form a single product. Bamboo and wood strips of 30mm wide were arranged vertically on a jig aftter adhesive has been applied on the surfaces. The laminates were press together for 24 hours for the adhesive to cure. After setting, the pressed laminates were removed from the press. The laminated products were cut to shape on a template with the aid of a jig saw and then machined on a wood lathe to obtain the desired picture of the intended end-product. Sanding and surface coating of the product was carried out to obtain a finished product as shown in Plate 4.2 below.

Plate 4.2: Bamboo Wall clock

The geometry and the appearance of the laminated product offer it an advantage for wide area of applications. It is especially interesting in those applications where the side of the plywood remain visible such as in kitchen work tops, example of which are kitchen cabinet and kitchen countertop.

Conclusion and Recommendations

Conclusions

The study has shown that bamboo strips from bamboo culms sorted from the recovered culms from the hitherto scaffold bamboo are suitable for laminate production. Intermediate raw materials and aesthetic appeal product was successfully produced from recovered *Bambusa vulgaris* Schrad culms.

Recommendations

Based on the study, the following recommendations are hereby put forward;

1. Processing equipment that can handle desirable thickness of bamboo strip should be made available to minimize waste due to conversion.
2. The process of making bamboo laminates is labour intensive and to increase the efficiency of the workers, proper training has to be given not only in the operation of the machine but also in handling of materials especially in the field of assembling, pressing and finishing, so that the product quality and finishing can be improved considerably.

References

Adewole, A.N and Olayiwola, H.O (2011*):* "Production of bamboo-lam from flat bamboo strip prepared from *Bambusa vulgaris* schrad" Accepted for presentation at The Annual Nigeria Materials Congress (*NIMACON 2011*). Theme: Materials Processing for Sustainable Environment and National Development. Venue: Engineering Materials Development Institute (EMDI), KM 4 Ondo Rd. Akure, Ondo State. Date: Nov 21st - 24th 2011

Janssen, J.J.A. (2000): *Designing and building with bamboo*, Beijing, China: INBAR Pp – 220

Markus, W (2008): Talking about the future within an SME? Corporate foresight and the potential contributions to sustainable development, Management of Environmental Quality: An International Journal, Vol. 19, No. 2, pp. 234-242.

Pokhrel, U.R. (2008): Bamboo in Nepal A Value Chain Upgrading Approach, Strategies and Interventions

Sorna, V.G and Mohini S., (2003): "Bamboo Composites--for sustainable rural development", *Journal of Rural Technology*, Vol. 1(1), pp. 6-10

Suresh, M (2007): Development of Small and Medium Enterprises In Bhutan: Analysing Constraints To Growth, South Asian Survey, Vol. 14 (2), pp. 251-282.

Van, H (2010): Method for manufacturing Bamboo-mats and Use thereof. Patent Application Publication. Feb, 4, 2010. Pp. 1-4.

Proceedings of the 58th International Convention of Society of Wood Science and Technology
June 7-12, 2015 – Grand Teton National Park, Jackson, Wyoming, USA

Gender Diversity Impacts on Firm Performance in Forest Sector Firms

Kendall Conroy

Oregon State University, Corvallis, OR

Abstract

The forest industry is predicted to lose a large percentage of its employees due to retirement in the coming decade. The industry also tends to lack diversity in its workforce, which makes this is an ideal time to move towards greater diversity. While many companies in the sector recognize the need for a more diverse workforce and have strategies in place to encourage diversity, there is little academic work evaluating the performance of such strategies. The existing research shows that greater diversity leads to increased creativity, openness to change, and innovation, all of which can contribute to increased financial performance. However, there is no information specific to forest sector firms. For that reason, we investigate the relationship between gender diversity and financial performance of large forest sector firms. We use the PricewaterhouseCoopers global 100 pulp, paper and packaging companies database and select those companies from Europe, North America and Oceania. Our data consists of the gender ratio of each of the 67 company's boards of directors and corporate executive teams. Preliminary regression analyses indicate a strong connection between greater female representation and firm performance. Consistent findings would provide further incentive for forest sector firms to strive for higher diversity in their workforces.

Investigating the Surface Quality of Tropical Hardwood Species: A Case of *Khaya ivorensis* from Ghana.

Stephen Tekpetey, nii9lartey@gmail.com

Forestry Research Institute of Ghana, Box 63 KNUST, Kumasi

Abstract

Tropical hardwood species are important commercial tree species for decorative veneer, cabinet work,canoe and boat construction. Surface quality of solid wood products is an important property which influence manufacturing such as strength of adhesive and finishing. Hence surface characterization and assessment of commercial hardwood species like Khaya ivorensis is relevant. There are, however, limited studies and information on the surface quality assessment of tropical African hardwood species such as Khaya ivorensis. In this study, surface roughness of plantation grown and naturally grown Khaya ivorensis harvested from Pra-Anum Forest reserve, Ghana were evaluated using the stylus profilometer. The assessment was made at three different height levels: Butt, middle and top portions. The average roughness (Ra), mean peak to valley height (Rz), core roughness depth (Rk), reduced peak height (Rpk), reduced valley depth (Rvk), total height of roughness (Rt), maximum surface roughness (Rmax) and maximum depth of roughness motif (Rx) were estimated on the tangential surfaces. Based on the results of statistical analysis, roughness parameters varied significantly at different portions of wood samples at p= 0.05 in both plantation and natural mahogany samples. Results also revealed that roughness parameters/values for plantation samples were relatively lower than the natural samples indicating smoother surfaces than natural ones.

Proceedings of the 58th International Convention of Society of Wood Science and Technology
June 7-12, 2015 – Grand Teton National Park, Jackson, Wyoming, USA

Poster Session and Student Poster Competition
Moderator: *Frederick Kamke, Oregon State University, USA*

Assessment of the Physical and Fiber Characteristics of *Alstonia boonei* for Pulp and Paper Production

Enoch ADJEI MENSAH [1] *- Kojo Agyapong AFRIFAH* [2*]

[1] Department of Wood Science & Technology
Faculty of Renewable Natural Resource
Kwame Nkrumah University of Science and Technology, Kumasi, Ghana.
+233-54-228-1936
menock03@gmail.com
[2] Department of Wood Science and Technology,
Faculty of Renewable Natural Resources
Kwame Nkrumah University of Science and Technology, Kumasi, Ghana,
+233-24-077-0941 Fax: +233-3220-60375
**Corresponding author*
kagyapong@gmail.com

Abstract

Timber resources have dwindled in the last few decades, resulting in the reduction of quality traditional wood species for the production of pulp and paper. This study therefore assessed the physical and fiber characteristics along the bole of *Alstonia boonei* an abundant lesser utilized timber species in order to ascertain its viability as an alternative material for pulp and paper production. The studied parameters were basic density, fiber length, fiber diameter, lumen diameter, cell wall thickness, flexibility ratio, slenderness ratio and runkel ratio. The results showed significant differences in basic density, fiber length, fiber diameter, lumen diameter and cell wall thickness between the butt, middle and top portions of the bole. Flexibility ratio, slenderness ratio, and runkel ratio were also significantly different for the various portions of the bole. The highest basic density (315 kg/m^3), fiber length (1421µm), flexibility ratio (68.5%), and runkel ratio (0.509) were recorded in the butt whereas the top had the lowest basic density (236 kg/m^3), fiber length (1185µm), flexibility ratio (61.4%), and runkel ratio (0.705). These ratings conform to the standards required for timbers used for pulp and paper production.

Thus, *A. boonei* was found to be suitable for pulp and paper production with the butt region offering the best biomass.

Key words: Biomass, Density, Fiber, Pulp, Paper, Species

Introduction

Paper is a versatile commodity that contributes to the growth and development of every country. The level of development of a country could be related to its paper consumption trends (Darkwa 1996). In recent times the global consumption of paper has been estimated to be around 400 million tons per annum and about 7.2 billion trees are felled to satisfy this need for purposes of writing, printing, wrapping, communication, education and packaging (Green tips 2010). This high demand for paper and its products is also observed in most developing countries such as Ghana. With the dwindling stands of traditional timber species, supply of paper to meet the increasing demand would require alternative sustainable raw materials to supplement the existing ones.

Wood quality affects the quality of pulp and ultimately the manufactured paper (Newel 1953). Thus most Softwood timbers are preferred over hardwoods because they have a preponderance of tracheid that reputedly produce strong paper. Nonetheless, Newel (1953) reported that hardwood pulps could have strength equal to or even greater than those from softwood. Therefore, it would be beneficial to assess the pulping characteristics of some lesser utilized hardwood species, including *Alstonia boonei* to augment the pulp form softwoods.

A. boonei, from the family Apocynaceae, is a pioneer tree very common on old farms and in swampy forest from Senegal through Ethiopia to Congo (Hawthorne and Gyakari 2006). This species provides firewood. As timber, its sapwood which is not differentiated from the heartwood, is very wide, up to 200 mm, soft, and light in weight when dried. The wood is nearly yellowish-white when freshly cut, the timber darkens on exposure. It has a low lustre and no characteristic odour or taste. The wood is also liable to staining. It works easily with hand and machine tools, but because of its softness, it is essential to use tools with sharp cutting edges. The wood can be glued, stained and polished satisfactorily. The well-known Asante stools of Ghana are made from it. It contains latex which gives an inferior resinous coagulate, and has been used to adulterate better rubbers (Orwa 2009).

The major determinants of the quality of any given pulp from a plant are its fiber length and chemical properties (Omotoso and Ogunsile 2009). Review of literature shows no documented information on these parameters for *A. boonei* despite the fact that this species is abundant. This study therefore, focused on analyzing the basic density and fibre characteristics of *A. boonei* in order to ascertain its potential for pulp and paper making.

Materials and Methods

Sample collection

A. boonei was collected from the demonstration farm of Faculty of Renewable Natural Resources, Kwame Nkrumah University of Science and Technology (KNUST), Kumasi - Ghana. The height of the tree was recorded and subsequently divided into butt, middle and top portions for sample collection and analysis.

Sample preparation

Basic density

Test samples were prepared to the dimensions of 20×20×20 mm according to TAPPI 258 om-11 (2011). A total of 54 samples were studied, with 18 samples each for the butt, middle and top portions. Dimensions of the samples were measured in the radial, tangential and longitudinal directions and weighed before soaking in water for 24 h.

Volume of saturated samples and wet weight were determined after 24 h. The samples were then oven-dried at 103±2°C. Dried weights and dimensions of the samples were measured and the basic density of *A. boonei* determined using Equation 1.

$$\text{Basic density} = \frac{\text{oven} - \text{dry weight of sample (kg)}}{\text{saturated volume } (m^3)} \ldots\ldots\ldots\ldots\ldots Eq.(1)$$

Maceration

Match-stick sized wood samples were taken from the top, middle and butt portions of the wood and placed in labelled test tubes. The samples were flooded with a mixture of Hydrogen Peroxide and Glacial Acetic Acid (1:1 v/v) in the test tubes and incubated at 65°C for 6 days. The fully macerated samples were then observed under microscope.

Determination of fiber dimensions and anatomical ratios

Slides of macerated wood were prepared and mounted. Images of the fibers were captured at a scale of ×200µm with a microscope that had a computer attachment using Micron (USB2) software. Determination of fiber length (FL), cell wall thickness (CWT), lumen diameter (LD) and fibre diameter (FD) was done on selected straight fibers using ImageJ software.

Determined fibre dimensions were used to calculate slenderness ratio (SR), runkel ratio (RR) and flexibility ratio (FR) as shown in Equations (3) to (5);

$$\text{SR} = \frac{\text{Fiber Length}}{\text{Fiber Diameter}} \text{(Varghese et al 2000)} \ldots\ldots\ldots\ldots\ldots\ldots\ldots\ldots\ldots \text{Eq. (3)}$$

$$RR = \frac{2 \times \text{Cell Wall Thickness}}{\text{Lumen Diameter}} \text{ (Hegde and Varghese 2008) ..... Eq. (4)}$$

$$FR = \frac{\text{Lumen Diameter}}{\text{Fiber Diameter}} \times 100 \text{ (Rana et al 2009) ..... Eq. (5)}$$

Results and Discussions

Basic density

Figure 1 shows the results on the mean basic density of the butt, middle and top portions of the tree. The butt portion produced the highest basic density (315.0 kg/m^3) while the top recorded the least (236.0 kg/m^3) (Fig 1).

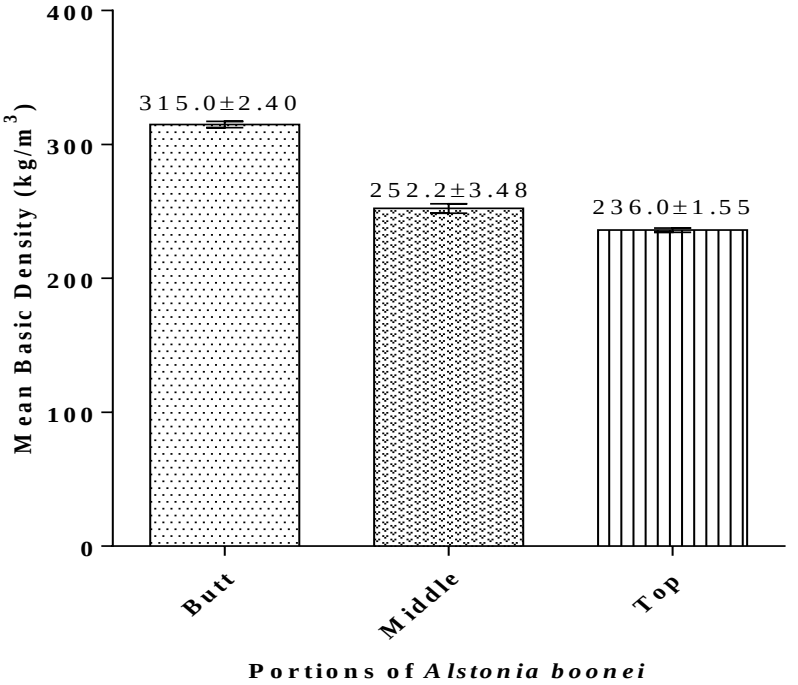

Fig 1: Mean basic density of the butt, middle and top portions of *A. boonei*

There were significant difference (p<0.05) between the mean basic densities of the butt, middle and top portions. The result is supported by studies by Zziwa et al (2012) who found that basic density of *Artocarpus heterophyllus* decreased along the trunk from the butt to the top.

Wood density allows prediction of the yield of pulp per unit volume of wood (Bowyer et al 2003). Higher density gives greater yield of pulp from a given volume of wood. This implies that, the butt portion that produced the highest basic density may transmit into higher pulp yield. Santos and co-workers (2008) reported that "*Eucalyptus globulus* with

the highest wood basic density exhibited a much higher pulp yield (58.7%) than the *E. globulus* with the lowest wood basic density (49%)".

Fiber dimensions and anatomical ratios

Fiber length and fiber anatomical ratios can be used to predict mechanical properties of the pulp and the suitability of the wood as pulp raw material. Table 1 presents the fiber dimensions and anatomical ratio for the various portions of the tree. The fiber dimensions decreased along the trunk of the tree from the base to the top of the stem. This is consistent with what has been reported by Dinwoodie (1961), Panshin and de Zeeuw (1970), Taylor and Wooten (1973) and Metcalfe and Chalk (1983). A comparison of the fiber dimensions indicated significant difference between them.

Table 1: Means morphological characteristics and anatomical ratios of *A. boonei* fibers

Portions	FL (µm)	FD (µm)	LD (µm)	CWT (µm)	SR	RR	FR (%)
Butt	1421^{ab}	48.97^{a}	33.18^{a}	7.90^{abc}	29.51	0.509	68.5
Middle	1339^{b}	42.27^{b}	27.71^{b}	7.28^{abc}	32.6	0.575	67.1
Top	1185^{c}	37.77^{c}	23^{c}	7.38^{abc}	31.92	0.705	61.4
Lsd (0.05)	101.4	3.752	2.996	2.029	3.44	0.2018	7.73
CV (%)	13.7	15.5	19	47.8	19.5	60.0	20.9
P-value	<0.001	<0.001	<0.001	0.812	0.149	0.151	0.155

Means with different alphabets implies no significant difference between them at $p<0.05$.

The RR, SR and FR influence the paper making properties of wood such as tensile strength, burst strength and resistance to tearing. High RR and low FR make poor quality pulp (Ververis et al 2004). Similarly, low value of SR can reduce tearing resistance. The implication is that, the low SR values obtained in this study (Table 1) would result in paper of low of tearing index.

Runkle ratio (RR) indicates fiber to fiber bonding (Biermann 1996, Bowyer et al 2003). The lower the value of RR, the higher the contact area between the fibers and the greater the burst and tensile strength. The RR values obtained for all the portions of the bole of *A. boonei* in this study are typical of the hardwoods and desirable. Consequently, it is expected that paper of high burst and tensile index would be produced, due to the anticipated large contact areas between the fibers.

Flexibility ratio (FR) is reported to influences the burst and tensile strength as well as folding endurance (Ververis et al 2004). Smook (1997) reported that hardwood species have flexibility index between 55 and 70, whereas softwood has an average of 75. Istas et al (1954) in their studies concluded that if the FR is between 50 and 70, fibers can be easily flattened to give good paper with high strength properties. From Table 1, the result shows FR of *A. boonei* is close to that of softwood. Due to the low value of RR and high value of FR of *A. boonei*, could be assumed that paper made from this species would have high burst and tearing index.

Conclusion

This study was conducted to analyse the basic density and fiber characteristics of the *Alstonia boonei* to identify its suitability for pulp and paper making.

The wood of *A. boonei* throughout this research has proven to have desirable potentials for quality pulp and paper production. Notwithstanding its low SR, the wood has desirable RR and FR to produce good paper with high strength properties. The mean fiber length, wall thickness, fiber diameter and lumen diameter of the wood of *A. boonei* meet the requirements for good pulp and paper production.

The butt portion of *A. boonei* was found to be denser and possessed the best fiber properties. This implies that the butt portion can yield higher pulp and would be the best portion for the pulp and paper industry.

References

Biermann CJ (1996) Hand Book of Pulping and Paper Making. Second Edition. California: Academic Press.

Bowyer JL, Haygreen JG, Schmulsky R (2003) Forest Products and Wood Science: An Introduction. Fourth edition. Iowa State Press.

Darkwa NA (1996) Pulp imports and consumption patterns in Ghana. *Ghana Journal of forestry*, Vol. 3, pp 55-60.

Dinwoodie JM (1961) Tracheid and fibre length in timber: A Review of Literature Forestry. 34: 73-118.

Green tips (2010) Paper Consumption Statistics. http://www.greenhomedesign.co.uk/paper-consumption-statistics-scary/. (15April 2014).

Hawthorne WD, Gyakari N (2006) Photo Guide for the Forest Trees of Ghana. A tree-spotters field guide for identifying the largest trees. Oxford, UK. pp 96-97.
Hegde RK, Varghese M (2008) Genetic analysis of wood traits in *Eucalyptus camaldulensis*. *J. Tree. Sci.* 27:1-13.

Istas JR, Heremans R, Roekelboom EL (1954) General Characteristics of Wood, Hardwood of Congo Belge in relationship with their utilization in industry paper pulp. Detailed Study of Some species. Gembloux: INEAC. Technical Series, No. 43.
Metcalfe CR, Chalk L (1983) Anatomy of the Dicotyledons. Vol. II. Clarendon Press. Oxford, UK.

Newel JS (1953) Pulping. In: Pulp and Paper Manufacture. 3rd ed. McGraw-Hill book Company Inc. USA. Vol. 3. pp 896-898.

Omotoso MA, Ogunsile BO (2009) Assessment of and potash production as options for management of wood waste. http://www.ncsu.edu. (18 October 2013).

Orwa C, Mutua A, Kindt R, Jamnadass R, Anthony S (2009) Agroforestree Database: a tree reference and selection guide version 4.0. World Agroforestry Centre, Kenya. Panshin AJ, de Zeeuw C (1980) Text Book of Wood Technology, Volume I. McGraw Hill, New York.

Rana R, Langenfeld-Heyser R, Finkeldey R, Polle A (2009) Functional anatomy of five endangered tropical timber wood species of the family Dipterocarpaceae. *Trees*. 23:512-529.

Santos A, Anjos O, Simoes R, Amaral ME, Vaz A (2008) Effect of *Eucalyptus globulus* wood density on papermaking potential. *Tappi Journal*. pp. 25-32.

Smook GA (1997) Handbook for Pulp & Paper Technologists. Vancouver: *Angus Wilde Publications.*

TAPPI (2011) T258 om-11. Basic Density of Wood and Pulp, *In: Tappi Test Methods*. Technical Association of the Pulp and Paper Industry, Atlanta, GA.

Taylor FW, Wooten TE (1973) Wood Property Variation of Mississippi delta hardwoods. Wood Fibre Sci 5: 2-13.

Ververis C, Georghiou K, Christodoulakis N, Santas P, Santas R (2004) Fibre dimensions, lignin and cellulose content of various plant materials and their suitability for paper production. *Industrial Crops and Products* 19(3): 245–254.

Zziwa A, Mugambwa R, Kizito S, Sseremba OE, Syofuna A (2012) Basic density, modulus of elasticity and modulus of rapture of *Artocarpus heterophyllus. Uganda Journal of Agricultural Sciences*, Uganda 13(1): 15-23.

Acknowledgements

We thank various people for their contribution to this project: Mr. Douglas Amoah, for his valuable technical support on this project; Mr. Kwadwo Boakye Boadu, for his assistance on the use of the software; Dr. Emmanuel Ebanyele and Mr. Govina, staff of Forest Research Institute of Ghana (FORIG), for their help in collecting the data on fiber dimensions and all the technicians who helped in handling the instruments.

Identification of the "Non-standard" Deformation Behaviour of European Beech and Norway Spruce During the Compression Loading

Martin [1] – Jan Tippner [1] – Václav Sebera [1]*

Jaromír Milch [1] – Peter Rademacher [1]

[1] Department of Wood Science, Faculty of Forestry and Wood Technology, Mendel University in Brno, Zemědělská 3, 613 00, Brno, Czech Republic
* *Corresponding author*
martin.brabec@mendelu.cz

Abstract

The purpose of paper was to analyze a negative increment of strain in the load direction observed in range of a plastic deformation during the compression parallel to the grain. The strain data for its description were obtained with use of different samples' lengths by means of two approaches: a) "clip on" extensometers and b) full-field optical technique based on digital image correlation (DIC). The samples were cut from the European beech (*Fagus sylvatica* L.) and Norway spruce (*Picea abies* L. Karst.) as clear special orthotropic blocks with a cross section radial (R) × tangential (T) = 20 × 20 mm^2 and the different lengths (h = 30, 40, 50 and 60 mm). Based on the strain analysis, it can be concluded that the deformation field consists of three sub-regions with different stiffnesses. The failure of less stiff zones located near the compression plates during loading reduced compression deformation of the stiffer middle zone to minimum or even leads to its expansion. The negative strain phenomenon of spruce and beech wood was most frequently occurred when h was 60 mm and 30 mm, respectively. The three-zone heterogeneity of deformation field induced a sharp difference of the displacement and strain (correlatively stiffness) when measured by mentioned approaches at various sample surface areas. Therefore, it should be of concern when wood is loaded in such mode.

Key words: compression test; damage zone; digital image correlation; strain; wood

Introduction

Wood anisotropy is often reduced to orthotropy, which makes the determination of reliable wood elastic constants easier, especially by using special orthotropic samples (Bodig and Jayne 1993). However, such samples do not exhibit the homogeneous deformation fields when loaded uniaxially because of wood's heterogeneity and problems of the representative volume element (RVE) determined by sample dimensions (Bodig and Goodmann 1973). In order to comprehensively explore the strain field heterogeneity the digital image correlation (DIC) is usually applied (Peters and Ranson 1982; Sutton et al. 2000).

When the wood samples are compressing parallel to grain, the strain field heterogeneity relates to the strain concentration in an area often called "damage zone" located near the compression plates (Choi et al. 1991; Zink et al. 1995; Dahl and Malo 2009). The zone between them is called "middle zone". Xavier et al. (2012) investigated the influence of the damage zones on the apparent Young's modulus (E), which they obtained from the displacement of the movable compression plate. The authors proposed the analytical model of sample as a series of three springs, in which two less stiff ones represent the damage zones and the stiff one is for the middle zone. The damage zones decrease the apparent E, meanwhile the friction that arises between the sample and the compression plates has a contrary effect. However, the damage zones have a much higher effect than the friction. Both phenomena become more crucial as the sample length decreases. Meanwhile, Bertolini et al. (2012) reported that the sample length in a range of 150–250 mm does not influence the E significantly when extensometers are used for measurements. An increase of the sample cross section near the compression plates causes lower strain magnitudes in the damage zones which results in higher apparent E. In this context, a dog-bone shape sample was investigated by André et al. (2013). The friction effects induce also the "barrel" deformation mode of the sample (Xavier et al. 2012). The "barrel", "buckling" or "shear" deformation modes complicate the determination of a passive strain needed for calculation the Poisson's ratios. The conditions for the maximal "homogeneous" deformation mode were proposed by Benabou (2008, 2010).

The motivation of this study is the decrease of strain as the load increases, i.e. a negative increment of strain in the loading direction (ε_L), which was detected by the extensometers during the compression of Norway spruce parallel to grain. The samples of European beech seldom exhibited described "non-standard" behaviour as well. In order to underlay our hypothesis, an analytical model of Xavier et al. (2012) introduced above was employed. It is hypothesized that, the negative increment of strain stems from the expansion of the middle stiffer spring in a series of three springs allowed by the failure of the two springs representing the less stiff damage zones within a sample. The objectives of this study are to elaborate this problem and to provide data for its

description. The amount of the samples behaving in the non-standard way should also be determined when sample length varies.

Materials and Methods

All source material was conditioned in a climate chamber at 20°C and 65% relative humidity (RH) until the equilibrium moisture content (EMC) was reached (~ 12%). The samples were cut as a clear special orthotropic blocks with a cross section radial (R) × tangential (T) = 20 × 20 mm^2 and different lengths (h = 30, 40, 50 and 60 mm) from the mature wood of European beech (*Fagus sylvatica* L.) and Norway spruce (*Picea abies* L. Karst.). The sample dimensions were derived from the BS 373 and ASTM D 143. Ten samples were prepared for each h and wood species. In order to improve the image matching during DIC computation, a basic matt white thin paint overlaid by a pigmented black paint was sprayed on the samples' side to be captured.

The loading of the samples parallel to the grain at a rate of 2 mm min^{-1} until the failure was carried out by the universal testing machine Zwick Z050/TH 3A equipped with the 50 kN load cell. In order to accommodate the sample between the compression plates, a preload of 10 N was applied. A detection of a negative increment of strain was performed by the "clip-on" extensometers equipped with two pairs of contact sensor arms separated by 10 mm, which were centered to a half of the sample length (Figure 18 – right). A full-field strain data for the description of that phenomenon were collected by the optical system consisting of two CCD cameras (cell size of 3.45 μm, resolution of 2452 × 2056 pixels) with the lenses (focal length of 25 mm) at stereovision configuration (Figure 18 – left).

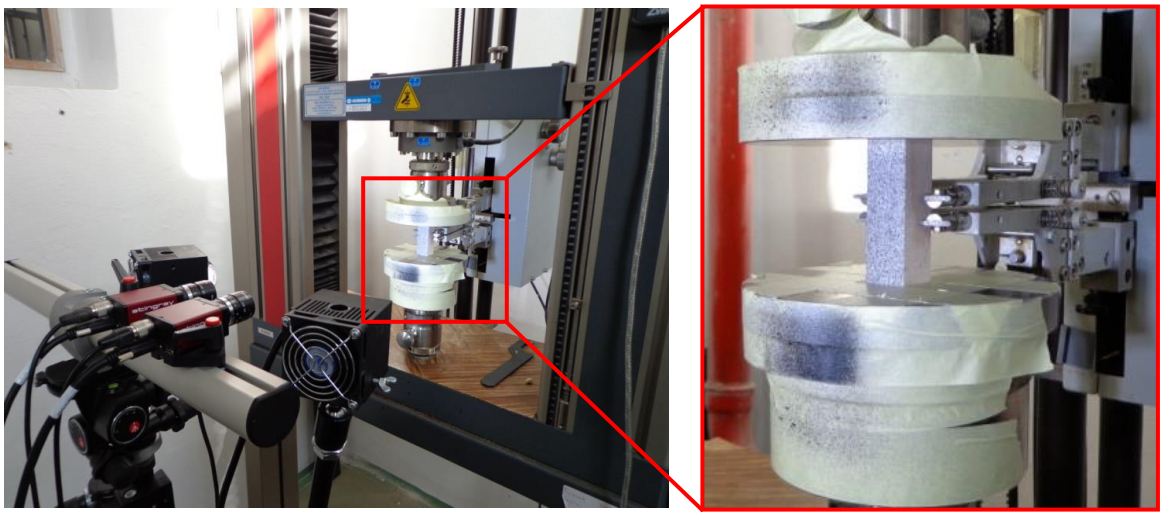

Figure 18: Experimental setup: left – the stereovision system; right – "clip-on" extensometers.

The contrast between the pattern components was enhanced by the cold light sources fitted by LED sensors. The system was focused to an area of interest (AOI) exactly

covering the patterned samples' surface and calibrated with help of the calibration images of a grid with 5.5 mm spacing at various geometric orientations. The appropriate measurement accuracy was adjusted by capturing the deformed sample surfaces with a scale of 12.5 px mm^{-1}. The calibrated system was placed in such a way that the centre of a captured area corresponded with the AOI centre.

Owing to the induced quasi-static loading rate, all experimental data such as the images, displacement and force was synchronically recorded with an acquisition interval of 0.25 s by a hardware trigger device. The calculation of the strain fields from the partial derivatives of the displacement using Lagrange notation was carried out in Vic-3D v. 2012 (Correlated Solutions Inc.). In order to obtain the appropriate spatial resolution of the measurement, the strains were calculated locally based on the lowest possible displacement field of 3 × 3 points and strain filter size of 5 × 5 points. A subset size of 25 × 25 pixels and subset step of 5 pixels were chosen based on the pre-study examining the optimal ratio between the density of the computed points (6 points mm^{-2}) and the efficiency of recognition the speckle pattern. The average accuracy of strain in the load direction equal to 89 micro strains was estimated with help of the noise detected on the five images while any loading force was not applying.

Results and Discussion

Strain field characterization

A full-field strain analysis proved the three sub-regions of a typical field of strain in the loading direction (ε_L) during compression (Figure 19). The deformation sub-regions are clearly distinguishable only across the sample length (h) which is in agreement with the observations made by André et al. (2013), Xavier et al. (2012), Benabou (2008), and Zink et al. (1995).

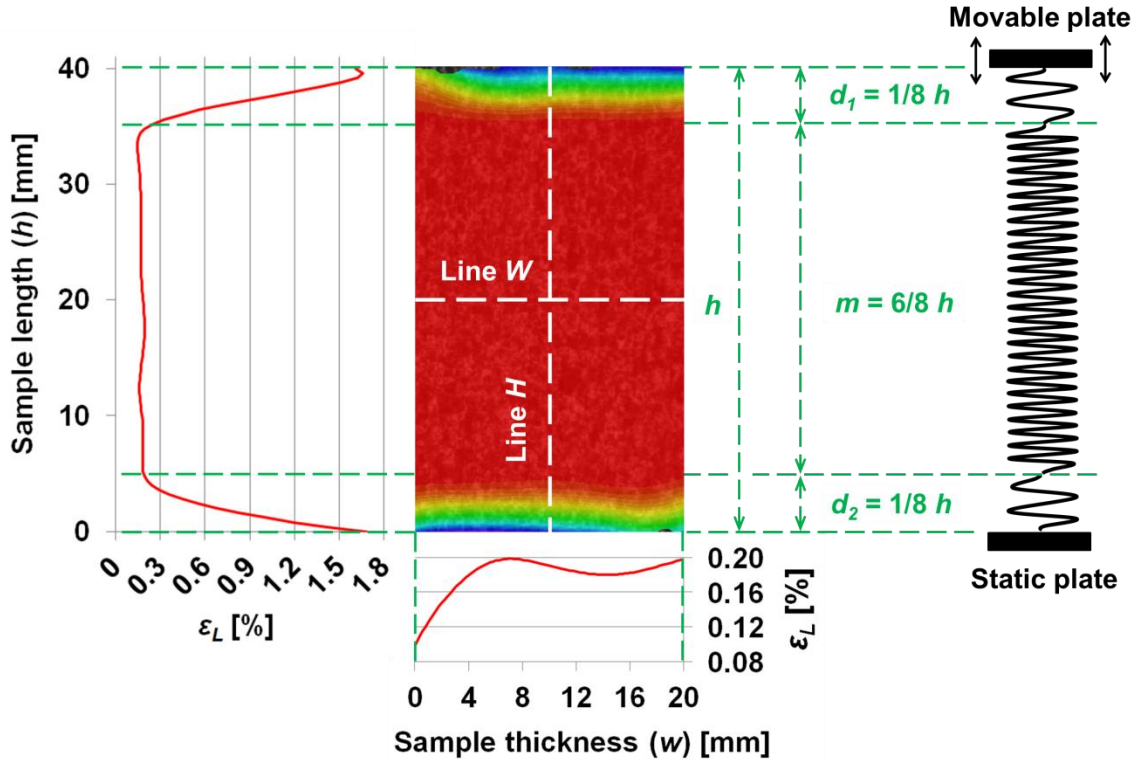

Figure 19: Typical deformation field of strain in the loading direction (ε_L) and its vertical and horizontal profiles at the $F_{50\%}$ of Norway spruce (20 × 20 × 40 mm^3) during compression parallel to grain.

The boundaries between the sub-regions are apparent on the vertical ε_L profile and on the ε_L plot as well (Figure 19). The sub-regions in contact with compression plates exhibited a high variation of ε_L (0.2 – 1.7%) and they are called as damage ($d_{1;\,2}$) zones, according to Xavier et al. (2012). The region between zones d_1 and d_2 (middle (m) zone) exhibited low variation of ε_L (0.1 – 0.2%). The ε_L value in zones $d_{1;\,2}$ exponentially increased as the distance from the compression plate decreased. The highest ε_L was concentrated on the interface of sample surface and compression plate.

It was proved that only the length of zone m increased as a function of h. The real length of zones $d_{1;\,2}$ varied by about 5 mm for all h, except h of 30 mm, where zones $d_{1;\,2}$ were about 4 mm. The relative constant length of zones $d_{1;\,2}$ was reflected in their decreasing proportion of h with an increasing h (Figure 20). This finding confirms the decreasing negative influence of zones $d_{1;\,2}$ on the apparent Young's modulus (E_L) as h increases, as reported by Xavier et al. (2012).

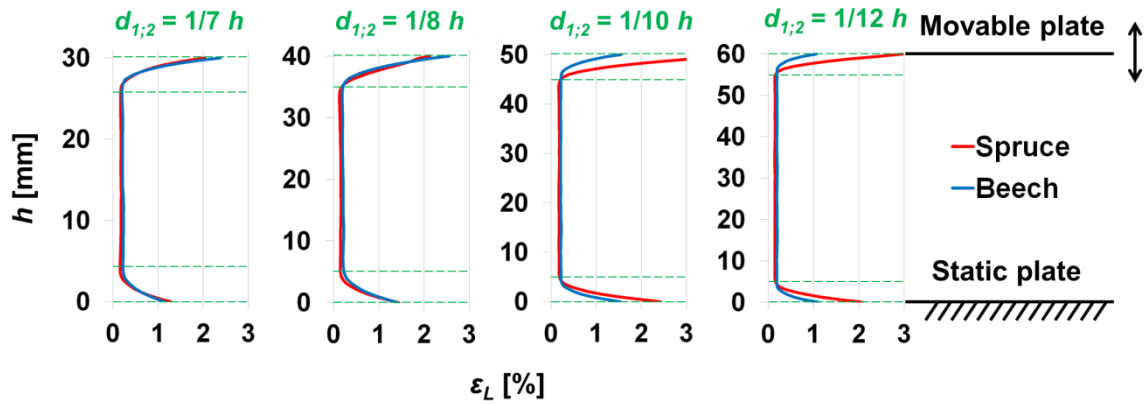

Figure 20: Influence of the sample length (h) and wood species on the length of the deformation sub-regions at the $F_{50\%}$.

The vertical dimensions of all sub-regions were almost the same for both spruce and beech. Such fact applied to all *h* throughout the elastic part of compression deformation. In conclusion, the length of zones $d_{1;2}$ was determined by the other issue, most likely such as the surface roughness of contact sample surface and compression plate, the degree of the surface fibre damage due to cutting tool during the sample preparation, etc. The more substantial changes occurred in the range of plastic deformation behaviour of samples. For a few samples, the expansion of zone *m* was indirectly confirmed by the successive disappearance of one or both zones $d_{1;2}$ from the computed ε_L plots due to compression and consequent stiffening of them.

Negative ε_L phenomenon investigated by various methods

A complex analysis of wood compression (stress-strain, displacement and velocity curves) showed that each sample deformed differently. Therefore, the curves depicted in Figure 21a to Figure 21h showed the most frequent cases of deformation behaviour of both beech and spruce samples.

"Clip on" extensometer

It turned out that the movement of the isolated points from each other causing the negative ε_L phenomenon can be successfully detected by the "clip-on" extensometer that is capable to mechanically track those points (Figure 21b). The crosshead also mechanically tracked isolated points but in contrast to extensometer located on the sample contact surfaces that moved throughout the compression test only relative to each other. The ε_L calculated by DIC and used for creating the stress-strain curves in Figure 21b are averaged over zone *m*, and therefore cannot capture the negative ε_L phenomenon as well. The sensitivity analysis (omitted here to save space) proved that this also applied to any size of averaged area within zone *m*. The negative increment of ε_L reported by the extensometer can be also caused by a "barrel" deformation mode of sample, which was reported by Benabou (2008, 2010). Nevertheless, the transverse displacement of edge points exhibited random spatial distribution along *h* in most of the samples.

Videoextensometer analyses

In order to better describe the negative ε_L phenomenon with help of the full-field data, the isolated points spaced with a constant initial distance (l_0) = 3 mm along *h* were virtually tracked. A higher ε_L within the zones $d_{1;2}$ and consequently their earlier collapse compared with zone *m* allowing the negative increment of ε_L was revealed (Figure 21d), which was in the contrast to samples behaving in the standard way (Figure 21c). In the second step, the isolated points symmetrically spaced with respect to the horizontal axis of AOI along *h* with the increasing l_0 were tracked. The curves (Figure 21e and Figure 21f) display the development of the difference (Δl) between l_0 and the actual distance (l_a) of the tracked points. Within the last section of the curve's courses it is possible to see the sharp increase of Δl attributable to an abrupt stiffness decrease in a plastic deformation range. However, such increase was reduced by the expansion of zone *m* when the samples exhibited negative ε_L phenomenon (Figure 21f). The shear crack plane originating in zone *m* within the samples behaving in the standard way had a similar effect but to a lesser degree (Figure 21e).

Velocity analysis

The negative ε_L phenomenon was also observable within the velocity of displacements in the loading direction obtained based on the full-field displacement data. The maximum velocity was observed where samples came into the contact with the movable compression plate. As the distance from that plate increased, the velocity decreased and its minimum equal to zero reached on the other contact zone at the static compression plate. However, this finding was not true throughout the compression test for samples exhibiting negative increment of ε_L (Figure 21h). It was proved by a higher velocity of point no. 3 compared with point no. 2 during the short time interval, in which the negative ε_L phenomenon was commonly measured by the extensometer.

Percentage of samples behaving in the non-standard way

The percentage of the negative ε_L phenomenon (P_n) was at its minimum when the *h* was 50 mm for both wood species, meanwhile the maximum was observed when *h* was 60 mm (P_n = 70%) for spruce and 30 mm (P_n = 10%) beech. These differences may be related to the failure modes of spruce and beech when compressed parallel to the grain.

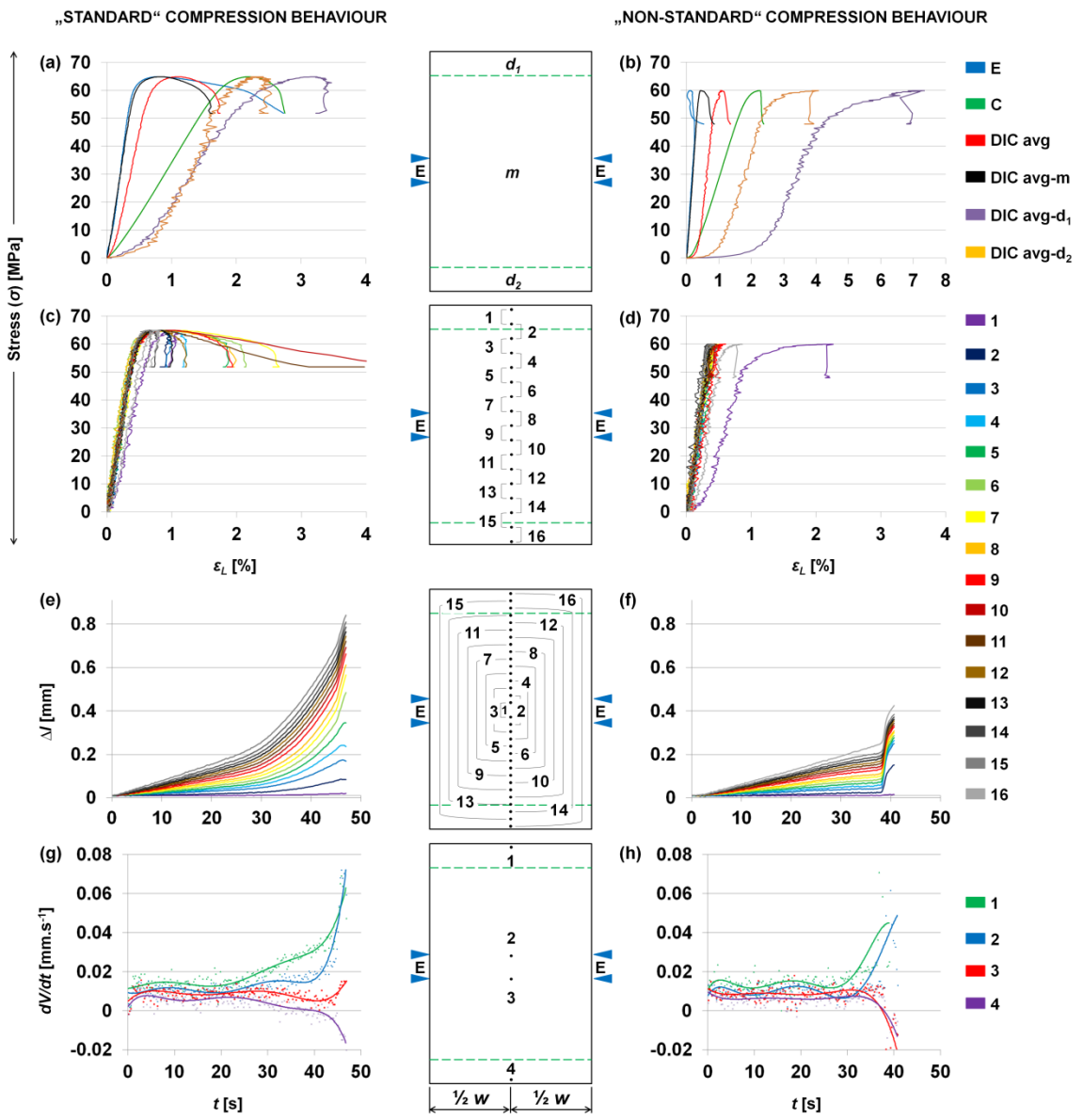

Figure 21: Comparison of "standard" (selected from beech samples) and "non-standard" (selected from spruce samples) compression behaviour from various perspectives.

a, b: Stress-strain curves obtained by crosshead (C), extensometer (E) and DIC

c, d: Stress-strain curves obtained from DIC between tracked points

e, f: Development of the differences (Δl) between the initial distance (l_0) and the actual distance (l) of the tracked points spaced along the sample length (h) with the increasing initial distance (l_0)

f, h: Development of displacement velocity (dV/dt) at selected points located near the compression plates (no. 1,4) and at the vertical position as the points tracked by the extensometers (no. 2,3)

Summary and Conclusions

This paper describes the negative increment of strain in the loading direction during the compression of Norway spruce (*Picea abies*, L. Karst) and European beech (*Fagus sylvatica*, L.) parallel to grain. We found that the deformation field of the samples consisted of two less stiff damage zones near the compression plates and one stiffer zone located between them. The full-field deformation analysis revealed that the negative increment of strain results in an expansion of the middle zone. We also found that the negative strain phenomenon occurred 7-10 times more often within the spruce than within the beech. The findings of this study can be helpful for the identification of weaknesses of standard compression tests, especially in the choice of the sample length and surface area for the deformation measurement.

Acknowledgements

This work was funded by the of Internal Grant Agency of Faculty of Forestry and Wood Technology at Mendel University in Brno (Grant No. 17/2015) and Ministry of Education, Youth and Sports of the Czech Republic (Grant No. 6215648902) and by the European Social Fund and the state budget of the Czech Republic, project "The Establishment of an International Research Team for the Development of New Wood-based Materials" Reg. No. CZ.1.07/2.3.00/20.0269.

References

André A, Kliger R, Olsson R (2013) Compression failure mechanism in small-scale wood specimens reinforced with CFRP: An experimental study. Construction and Buildings Materials 41:790-800.

ASTM D143 (1994) Standard test methods for small clear specimens of timber. American Society for Testing and Materials, Philadelphia, PA, USA.

Benabou L (2008) Kink band formation in wood species under compressive loading. Experimental Mechanics 48(5):647-656.

Benabou L (2010) Predictions of compressive strength and kink band orientation for wood species. Mechanics of Materials 42(3):335-343.

Bertolini MS, Silva DAL, Souza AM, Calil C, Lahr FAR (2012) Influência do Comprimento de Corpos-de-prova na Obtenção do Módulo de Elasticidade Ec0. Floresta e Ambiente 19(2):179-183.

Bodig J, Goodman JR (1973) Prediction of elastic parameters for wood. Wood Science and Technology 5(4):249-264.

Bodig J, Jayne BA (1993) Mechanics of wood and wood composites. Malabar: Krieger Publish. Company.

BS 373 (1957) Methods of testing small clear specimens of timber. British Standard Institution, London.

Dahl KB, Malo KA (2009) Planar Strain Measurements on Wood Specimens. Experimental of Mechanics 49(4):575-586.

Choi D, Thorpe JL, Hanna RB (1991) Image analysis to measure strain in wood and paper. Wood Science and Technology 25(4):251-262.

Peters WH, Ranson WF (1982) Digital Imaging Techniques In Experimental Stress Analysis. Optical Engineering 21(3):213-227.

Sutton MA, Mcneill SR, Helm JD, Chao YJ (2000) Advances in two-dimensional and three-dimensional computer vision. Photomechanics 77:323-372.

Xavier J, De Jesus AMP, Morais JJL, Pinto JMT (2012) Stereovision measurements on evaluating the modulus of elasticity of wood by compression tests parallel to the grain. Construction and Buildings Materials 26(1):207-215.

Zink AG, Davidson RW, Hanna RB (1995) Strain measurement in wood using a digital image correlation technique. Wood and Fiber Science 27(4):346-359.

Proceedings of the 58th International Convention of Society of Wood Science and Technology
June 7-12, 2015 – Grand Teton National Park, Jackson, Wyoming, USA

Dynamic Mechanical Analysis of Different Wood Species

Nicole Brown, nrb10@psu.edu
Timothy Gruver, timothy.gruver@mometive.com
Alex Storm, ajs6188@psu.edu

Pennsylvania State University, 209 Agricultural Engineering Bldg,
University Park, PA 16802

Abstract

This work explores results of dynamic mechanical analysis of several wood species, including aspen (Populus grandidenta), yellow-poplar (Liriodendron tulipifera), and southern yellow pine (Pinus spp.). Results suggested that at least one significant relaxation occurred in each species at different temperatures above 40C; for pine, two relaxations were observed. The energies associated with the relaxations are generally consistent with glass transitions. In this presentation we will discuss how these findings relate to the literature, and how we can further understand the underlying mechanism for the behavior.

Proceedings of the 58th International Convention of Society of Wood Science and Technology
June 7-12, 2015 – Grand Teton National Park, Jackson, Wyoming, USA

Fuel Bricks from Lignin and Coal Fines

Nicole Brown, nrb10@psu.edu
Leidy Peña Duque, lep16@psu.edu
Curtis Frantz, cwf125@psu.edu
Sridhar Komarneni, komarneni@psu.edu
Fred Cannon, fcannon@engr.psu.edu

Pennsylvania State University, 209 Agricultural Engineering Bldg, ,
University Park, PA 16802

Abstract

In this presentation, we will discuss the preparation of fuel bricks made from two key industrial wastes: lignin and coal fines. We will discuss how these bricks are a better environmental solution than coke, the main fuel source at metalcasting foundries. Our presentation will describe how the chemistry and morphology of the bricks change following different pyrolytic exposures; solid state NMR data suggests polyaromatic domains form from the lignin fraction, while SEM data indicates the formation of silicon carbide nanowires. Four tons of these bricks were successfully produced and piloted at each of two foundries, where up to 25% of the coke feed was replaced over a period of two days. The latest efforts to implement the technology will be discussed, as will our efforts to use lignin for other products.

Proceedings of the 58th International Convention of Society of Wood Science and Technology
June 7-12, 2015 – Grand Teton National Park, Jackson, Wyoming, USA

Characterizing Restoration Materials for Historic Buildings Using the Dynamic Vapor Sorption Technique

Manaswini Acharya, Majid Naderi, Daniel Burnett and Jurgen Dienstmaier

Surface Measurement Systems Ltd.
dburnett@surfacemeasurementsystems.com

Abstract

The moisture sorption properties are critical factors to building materials such as timber, bricks, stones, cement, mortar and fiber. Moisture damage brought upon building materials is significant in affecting and limiting the life of the building. In this context, investigating the moisture ingress properties of used building materials in a heritage structure is particularly important for selecting the restoration materials needed to carry out repairs and remedial measures. Proper selection of compatible repair materials is a core principle in conservation science and engineering of historical heritage structures. It is commonly accepted that compatibility of mechanical and physical properties is important (i.e. strength, thermal expansion capacity and porosity). However, moisture storage capacity has not been yet acknowledged as one of the parameters that should be considered when selecting repair/restoration materials. When compatible materials with near identical moisture holding capacity and thermal expansion properties are used it is likely that the combination will act well against hydration and humidification.
In this study, Dynamic Vapor Sorption (DVS) studies have been performed on building materials from Abbey Mill - an 18th century, grade II listed building (Tewkesbury, UK). Moisture sorption kinetics and isotherms were determined on wood, mortar, and brick samples. Comparisons in total sorption capacity and sorption/desorption hysteresis were used as a measure for selecting appropriate replacement/repair materials.

Proceedings of the 58th International Convention of Society of Wood Science and Technology
June 7-12, 2015 – Grand Teton National Park, Jackson, Wyoming, USA

How Wood Influences Well-being in Indoor Environments: Building Materials, Well-being and Perception of the Indoor Environment

Kristian Bysheim, kristian.bysheim@treteknisk.no
Anders Nyrud, anders.nyrud@treteknisk.no

Norwegian Institute of Wood Technology, Po Box 113, Blinder, , Oslo 0314

Abstract

Focus groups were carried out in several European countries to gain insight in how regular people view the correlation between building materials and the perception of indoor environment. The focus groups were carried out among regular people and bulding industry professionals. The participants discussed topics regarding choice of building materials, well-being in built environments, natural matierals, sustainability, and cleanability of building materials.

Preliminary analysis of the results indicate cultural differences being an important factor influencing perception of the built environment. Practical experience was also an important. Men tended to be more pragmatic regarding ethical and environmental issues, relying more on public approval and informatino from the distributor. Women tended to have a more active approach regarding the environment and other ethical issues.

Proceedings of the 58th International Convention of Society of Wood Science and Technology
June 7-12, 2015 – Grand Teton National Park, Jackson, Wyoming, USA

Anatomical Structures of Thermally Compressed Paulownia (*Paulownia* spp.) Wood

Ayse Dilek Dogu[1] – Kamile Tirak Hizal[2] – Davut Bakir[3] – Fatma Digdem Tuncer[1] – Zeki Candan[1] – Oner Unsal[1]*

[1] Department of Forest Products Engineering, Faculty of Foresty, Istanbul University, Sariyer, Istanbul, TURKEY
[2] Department of Forest Products Engineering, Faculty of Foresty, Duzce University, Duzce, TURKEY
[3] Department of Forest Products Engineering, Faculty of Foresty, Artvin Coruh University, Artvin, TURKEY
* *Corresponding author*
addogu@istanbul.edu.tr

Abstract

Various thermal modification techniques are used to improve some properties of wood materials which are getting more and more important. Thermal compression method is one of thermal modification techniques. In this study, the effects of thermal compression method on anatomical features of paulownia wood by microscopic methods were studied. Paulownia wood panels with dimensions of 150 mm by 500 mm by 18 mm were hot-pressed using a laboratory hot press at a temperature of either 150°C or 170°C and pressure of 1 MPa for 45 min. Anatomical investigations were also performed for untreated wood samples for comparison. All microscopic studies were carried out visually only on cross sections, radial sections, and tangential sections. Possible cracks, collapse, buckling, degradations, fractures, and ruptures on vessel walls, ray parenchyma cells, fibers, axial parenchymas, and pits were investigated.

Keywords: Thermal compression method; Paulownia wood; Anatomical features.

Proceedings of the 58th International Convention of Society of Wood Science and Technology
June 7-12, 2015 – Grand Teton National Park, Jackson, Wyoming, USA

Dynamic Mechanical Thermal Analysis (DMTA) of Hybrid Biocomposites

Zeki Candan[1] – Ahmed H. Hassanin[2] – Ali Kilic[3]*

[1] Department of Forest Products Engineering, Faculty of Foresty, Istanbul University, Sariyer, Istanbul, TURKEY
[2] Department of Textile Engineering, Alexandria University, Alexandria, EGYPT
[3] Temag Labs, Faculty of Textile Technology and Design, Istanbul Technical University, Istanbul, TURKEY
* *Corresponding author*
zekic@istanbul.edu.tr

Abstract

The main objective of this work was to evaluate dynamic mechanical thermal characteristics of hybrid biocomposites. Jute and glass fiber woven fabrics were used as reinforcement elements while unsaturated polyester resin was used as polymer matrix. Storage modulus, loss modulus, and tan delta values of the hybrid biocomposites were determined to evaluate DMTA performance. The results obtained in this study revealed that the storage modulus, loss modulus, and tan delta values of the hybrid biocomposites were affected by the reinforcement. The findings showed that the glass fiber reinforcement had a positive effect on the storage modulus values of the hybrid biocomposites. It could be concluded that the hybrid biocomposites having enhanced performance could be used as a novel green composite material for automotive, construction, and marine industry.

Keywords: Dynamic mechanical thermal analysis (DMTA); Hybrid biocomposites; Glass fiber; Jute; Polyester; Biomaterials

Introduction

In the last quarter of the previous century, due to the increasing of environmental consciousness, intensified efforts are being made to reduce the dependence on petroleum based materials. This led to grow the focusing on developing, discovering, creating and innovating eco-friendly, renewable, sustainable and bio-based materials (1) (2) (3). These materials eventually have to introduce several advantages such as low density, high

strength to weight ratio, corrosion resistance, low cost and, availability in many forms. So utilization of lignocellulosic fiber is a rapidly growing sector, not only for the production of commodities, such as textiles, but also for high-added-value products can be used in many fields such as home furniture, automotive industries, ships, wind turbine blades, and construction (4). So using lignocellulosic fiber as reinforcement in composite field to develop what can be called green composites is remarkably increasing trend. Depending on the nature of green composites constituents, green composites could be complete biodegradable or partial biodegradable. Partial biodegradable is the widest used one nowadays where the matrix is thermoset or thermoplastics petroleum based while the reinforcement is natural material. One of the most available and promising natural fiber is baste fibers such as flax, hemp, jute, ramie, sisal *etc.* these fibers are commonly used in many composite application (5) (6) (7).

In the present study, the main objective is to evaluate dynamic mechanical thermal characteristics of jute-glass hybrid biocomposites structure.

Materials and Methods

Yarn twisting

For the present experimental investigation, Jute yarns and E-glass roving were supplied form the local market then used for producing woven fabrics. Jute and glass yarn have been twisted together. Different twist levels have been carried out to figure out the optimum twist level which gives the maximum mechanical properties. Yarns twisting have been performed at AGTEKS Company of Istanbul Turkey as shown in Figure 1.

(a) (b)

Figure 1 AGTEKS Direct Twister machine (a), twisted hybrid jute/glass yarn (b)

Fabric manufacturing

Hybrid twisted yarn with optimum twist level has been chosen to be woven with the other jute and glass yarns. Fabrics were produced in hand loom located at Weaving Laboratory of College of Textile Technology and Design, Istanbul Technical University (ITU). Fabrics construction and specifications are given in Table 2. Warp yarns have been fixed

for the all samples as Jute, while weft yarns has been changed as can be seen from Table 2.

Table 2 Fabric Specifications and Constructions

Sample	**Structure**	**Warp Material**	**Weft Material**	**Warp (tex)**	**Weft (tex)**	**Warp density ends/cm**	**Weft density picks/cm**	**Areal Density (g/m^2)**
Group 1	Plain 1/1 Figure 3a	Jute	Jute	1000	1000	2.5	4	681.70
Group 2	Plain 1/1 Figure 3b	Jute	E-Glass	1000	1200	2.5	6	1022.51
Group 3	Plain 1/1 Figure 3c	Jute	Jute + glass [parallel/untwisted]	1000	1000/1200	2.5	4	725.16
Group 4	Plain 1/1 Figure 3d	Jute	Jute + glass [twisted/ 20 T/M]	1000	2200	2.5	3	929.34

Figure 2 Manual weaving loom at ITU

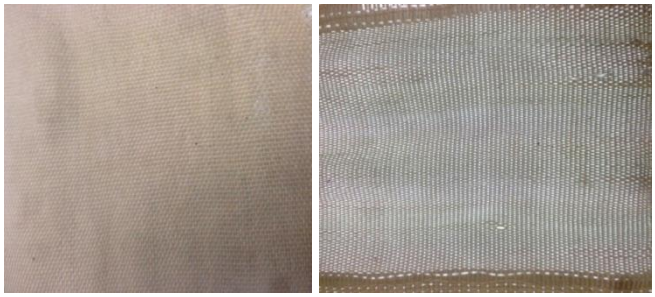

(a) (b)

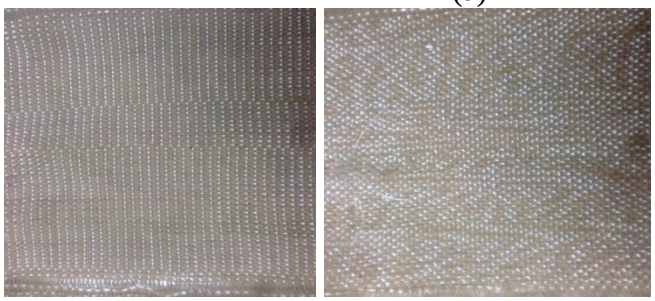

(c) (d)

Figure 3 woven fabric samples

Composite fabrication

In this study, Vacuum Assisted Resin Transfer Molding (VARTM) was used for preparing woven fabric /polyester composite samples. Resin was prepared by mixing the unsaturated polyester with 0.5 % wt Cobalt Octoate as an accelerator and 1% wt of MEKP as an initiator. To start the resin infusion process, infusion hose was placed into resin bucket and vacuum pump is turned on and resin was started to flow from the inlet to the outlet. Once the resin reach the out let, infusion hose was clamped and vacuum was turned off. Samples were set to consolidate for 24 hours (figure 3 d).

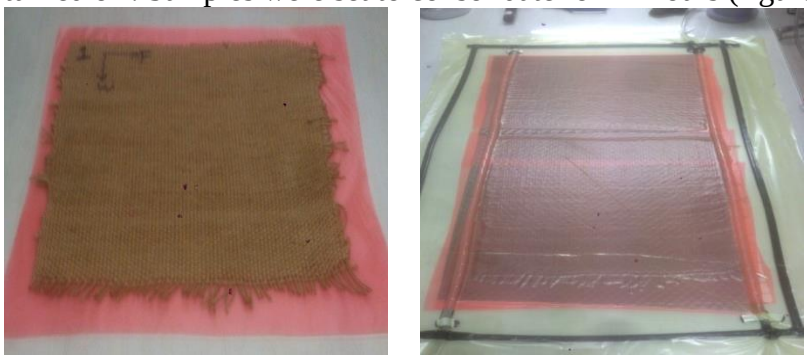

(a) (b)

Figure 4 VARTM process of woven jute/polyester composite sample

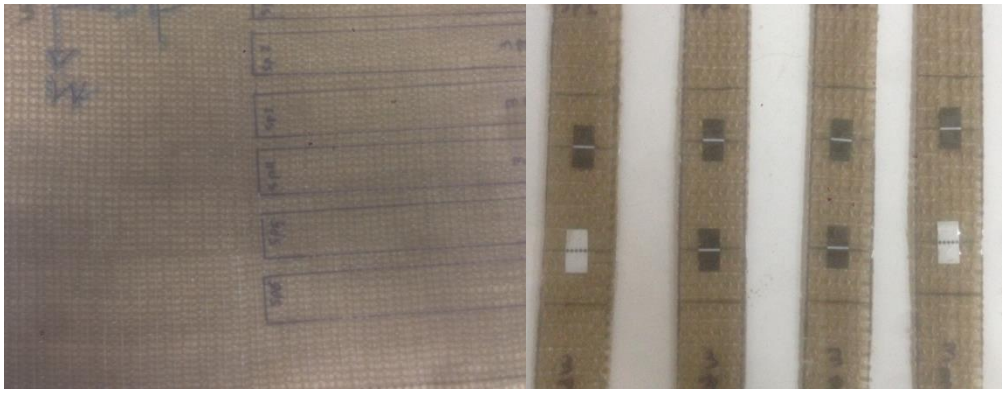

Figure 5 composites samples after VARTM process

Dynamic mechanical thermal analysis (dmta)

All hybrid biocomposite samples were performed in dual cantilever mode (3-point bending) at a controlled heating rate of 5°C/min from 20 °C to 250 °C at an oscillatory frequency of 1 Hz. Storage modulus, loss modulus, and tan delta values were calculated by the DMTA instrument (located in Nanotechnology Laboratory & Thermal Analysis Laboratory at Istanbul University) analysis software as a function of temperature. Three samples were analyzed for each composite group.

Results and Discussion

Storage modulus curves of the hybrid biocomposite samples are shown in Figure 6.

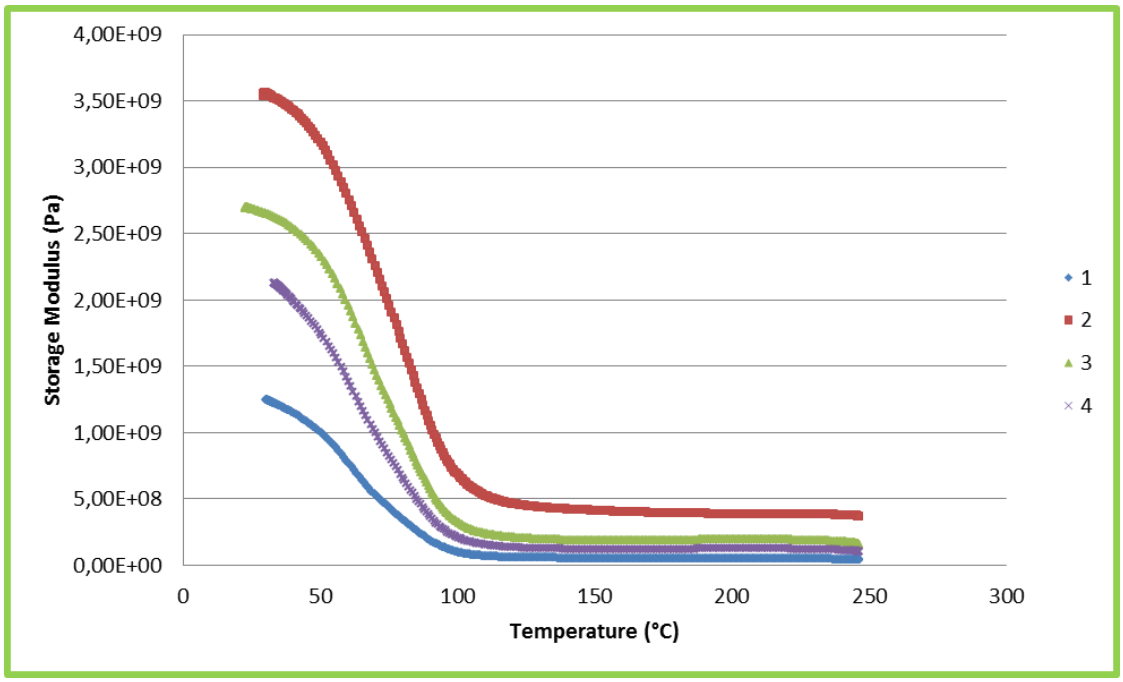

Figure 6 Storage modulus results of the hybrid biocomposites

The findings obtained in this research showed that the storage modulus values of all the hybrid biocomposite samples decrease with increasing temperature from 30°C to about 250°C. Sharp decrease observed in the storage modulus between 30°C and 100°C for all the hybrid biocomposite samples. After that point, a slight decrease was determined. All the storage modulus curves of the hybrid biocomposite samples were quite reproducible. The maximum initial storage modulus value was obtained from the Group 2 while the minimum storage modulus value was obtained from the Group 1. This was accepted because it is known that glass fiber has much more thermal resistant than jute fiber. It can be noticed clearly the significant enhancement in the storage modulus values that was achieved by Group 3 which was manufactured by hybrid yarns [glass + jute]. Whereas the storage modulus at room temperature increase from 1.3×10^9 Pa for Group 1 to 2.8×10^9 Pa for Group 3. 115% increasing in the storage modulus has been achieved just by replacing 50% of jute fiber by glass fiber. At 250°C, it can be noticed also a significant difference in storage modulus between Group1 and Group 3, whereas storage modulus values were 0.4×10^8 Pa and 1.5×10^8 Pa for Group1 and Group 3 respectively.

By comparing the results of storage modulus for Group 1 and Group 4, also a significant enhancement can be clearly noticed. Whereas the storage modulus at room temperature increased from 1.3×10^9 Pa for Group 1 to 2.2×10^9 Pa for Group 4. 70% increasing in the storage modulus has been achieved just by replacing 50% of jute fiber by glass fiber. The difference between the values of storage modulus of Group 3 and Group 4 can be attributed to the twist effect. Whereas in Group 4, jute fiber and glass fiber has been twisted and then inserted to the fabric to be woven while in Group 3 jute fiber and glass fiber inserted separately from each other then the fabrics were solidified by resin as it is shown in Table 1. This twist caused significant decrease in the storage modulus.

Conclusions

It is obvious that the glass fiber reinforcement affected the DMTA properties of the hybrid biocomposites. It was noticed huge difference between the DMTA properties of jute and glass fibers. Replacing just 50% of jute fiber by glass fiber caused 115% increasing in the storage modulus. Twisting jute and glass yarns causing decrease in the storage modulus values.

Acknowledgements

This work has been funded by Scientific and Technological Research Council of Turkey (TUBITAK) under grant number 21514107-216.01-237755. The authors would like to thank Istanbul University Research Fund for its financial support in this project (Project No: 51082).

References

1. **Ashori, Alireza.** Wood–plastic composites as promising green-composites for automotive industries. *Bioresource Technology.* 2008, Vol. 99, pp. 4661–4667.

2. **Shah, Darshil U.** Developing plant fibre composites for structural applications by optimising composite parameters: a critical review. *Journal of Material Science.* 2013, Vol. 48, pp. 6083–6107.

3. **Zhou, Yonghui, et al.** Lignocellulosic fibre mediated rubber composites: An overview. *Composites Part B.* 2015, Vol. 76, pp. 180-191.

4. **Cristaldi, Giuseppe, et al.** Composites Based on Natural Fibre Fabrics. [book auth.] Polona Dobnik Dubrovski. *Woven Fabric Engineering.* Rijeka : InTech, 2010.

5. **Zhu, Jinchun, et al.** Recent Development of Flax Fibres and Their Reinforced Composites Based on Different Polymeric Matrices. *Materials.* 2013, Vol. 6, pp. 5171-5198.

6. **Ku, H, et al.** A review on the tensile properties of natural fiber reinforced polymer composites. *Composites: Part B.* 2011, Vol. 42, 4, pp. 856–873.

7. **La Mantia, F.P. and Morreale, M.** Green composites: A brief review. *Composites: Part A.* 2011, Vol. 42, 6, pp. 579–588.

Proceedings of the 58th International Convention of Society of Wood Science and Technology
June 7-12, 2015 – Grand Teton National Park, Jackson, Wyoming, USA

Thermal Conductivity of Structural Plywood Panels Affected by Some Manufacturing Parameters and Aging Process

Cenk Demirkir[1] – Gursel Colakoglu[1] – Semra Colak[1]*

Ismail Aydin[1] – Zeki Candan[2]

[1] Department of Forest Products Engineering, Faculty of Foresty, Karadeniz Technical University, Trabzon TURKEY.
[2] Department of Forest Products Engineering, Faculty of Foresty, Istanbul University, Sariyer, Istanbul, TURKEY.
* *Corresponding author*
cenk@ktu.edu.tr

Abstract

Wood and wooden structure materials have been used in house, school, and office construction throughout the world. Wood composite materials are superior to other building materials in terms of thermal conductivity due to its porous structure. Thermal conductivity is one of the most important properties of composite panels used in construction. It was essential to determine the effect of aging process on the panel properties of used in structural applications. This study evaluates thermal conductivity of scots pine and black pine plywood panels manufactured from rotary cut veneers dried at three different temperatures: 110°C, 140°C, and 160°C. Phenol formaldehyde (PF) and melamine urea formaldehyde (MUF) adhesives were used for plywood panel manufacturing. The panels were exposed to aging process according to ASTM C 481-99 standard. The panels with five plies and 10 mm thickness were manufactured for each group. Thermal conductivity values of the plywood panels were determined. The thermal conductivity of the panels decreased with increasing the drying temperature. It was also found that the thermal conductivity of the panels decreased after the aging process.

Keywords: Thermal conductivity; Aging process; Structural plywood panels

Introduction

Wood and wooden structure materials have been used in house, school and office construction in many countries. Wood framed buildings are composed of framing studs or joists, sheathing materials (plywood, (OSB) oriented strand board), and fasteners (nails, screws) (Yan 1992). The most common materials used as sheathing are plywood and OSB (Breyer et al. 2003). Wood composite material is superior to other building materials in terms of thermal conductivity due to its porous structure (Gu and Zink-Sarp 2005; Krüger and Adriazola 2010). Plywood panels have well-balanced thermal insulation and warmth keeping properties (steady and non-steady-states), which is important for insulation performance in that they maintained temperature and relax severe temperature changes in residences exposed to diurnal and seasonal temperature changes (Kawasaki and Kawai 2006).

In plywood production, veneer drying is a different thermal process affecting veneer quality for bonding, durability and physical and mechanical properties of panels. The purpose of veneer drying is to reduce its moisture content to a suitable range for gluing. Mostly applied drying temperatures are between 90 - 160°C as called normal in plywood industry. Using high drying temperatures reduce the veneer drying time and increase the capacity. Reduction in drying time and energy consumption offers a great potential for economic benefit to the wood industries (Aydın and Colakoglu 2005). However, drying at very low moisture levels and at very high temperatures or at moderate temperatures for prolonged periods inactivates the veneer surfaces, causing poor wetting of veneer and hence poor bonding (Frihart and Hunt 2010). Drying temperature influences both physical and chemical surface properties of veneer and hence its thermal conductivity characteristics. However, the number of studies about the thermal conductivity of plywood panels related to the different drying temperatures was not enough level.

Sustaining to durability of wood-based panels is one of the most important features for structural products used in construction of houses (Norita et al. 2008). It is known that wood is deteriorated when it is exposed to outdoor conditions. Xie et al. (2005) stated that weathering of wood is caused by various factors such as solar radiation, heat, atmospheric pollutants and micro-organisms. Several studies have been researched about sustaining durability of wood and wood composite materials (Karlsson et al. 1996; Menezzi et al. 2008). The durability or moisture resistance of structural panels (plywood, OSB) is usually determined by standardized aging test methods that include various cycles of cold or hot water immersion, boiling, steaming, freezing, and drying (Norita et al. 2008). Variation of moisture content in wood can cause cracks and loss of mechanical and physical properties of wood. It has been thought that thermal conductivity could be affected by variation of moisture content in wood and wood based materials by weathering. It was stated that thermal conductivity of wood and wood composite materials such as plywood, OSB, medium density fiberboard (MDF), and particleboard has varied according to wood specie, direction of wood fiber, ratio of early and late wood, thickness of composite materials, density, moisture content, resin type and additives, temperature, and flow direction of heat in several studies (Bader at al. 2007;

Sonderegger and Niemz 2009; Kol et al. 2008). But there are few studies the effect of aging factors in using place on thermal conductivity of wood composite materials. In this study, it was studied that the effect of aging process and some manufacturing factors such as wood species, drying temperatures of veneer, adhesive types on the thermal conductivity of structural plywood panels.

Materials and Methods

Scots pine (*Pinus slyvestris*) and black pine (*Pinus nigra*) were used as wood species in this study. Densities of Scots pine and black pine (*Pinus nigra*) were 0.48 gr/cm^3 and 0.56 gr/cm^3, respectively. Logs for veneer manufacturing with an average diameter at breast height of 40 cm were obtained from Sinop, located at the most northern point of the Black Sea Region of Turkey. A rotary peeler with a maximum horizontal holding capacity of 80 cm was used for veneer manufacturing. The logs were steamed before the peeling process, and then veneer sheets with dimensions of 55 cm by 55 cm by 2 mm were clipped. The vertical opening was 0.5 mm and horizontal opening was 85% of the veneer thickness in the veneer manufacturing process. After rotary peeling, veneers were dried until moisture content of them reach to 4-6 % at three different temperatures: 110°C, 140°C, and 160 °C in a veneer dryer.

Five-ply-plywood panels with 10 mm thick were manufactured using PF glue resin with 47% solid content and MUF with 55% solid content. MUF resin solution used in the manufacturing was composed of 100 parts of MUF resin by weight, 30 parts of wheat flour by weight, and 10 parts of 15 % concentrated NH_4Cl by weight. Veneer sheets were conditioned to approximately 5-7% moisture content in a conditioning chamber before gluing. The glue was applied at a rate of 160 g/m^2 to the single surface of veneer using a four-roller spreader. Two replicate plywood panels were manufactured from each group. The experimental design of the panels is shown in Table 1.

Table 1. Experimental design

Glue Type	Veneer Drying Temperature (°C)	Wood Species	
		Scots Pine	Black Pine
PF	110	A1	C1
	140	A2	C2
	160	A3	C3
MUF	110	A4	C4
	140	A5	C5
	160	A6	C6

A quick thermal conductivity meter based on ASTM C 1113-99 (2009) hot-wire method was used. QTM 500 device, a product of Kyoto Electronics Manufacturing, Japan, was used for thermal conductivity measurement with PD-11 probe.

Measurement range is 0.0116 – 6 W/mK. Measurement precision is F5% of reading value per reference plate. Reproducibility is F3% of reading value per reference plate. Measurement temperature is -100 to 1000°C (external bath or electric furnace for temperature other than room). Sizes of the test specimens are 10x50x100 mm^3. Measuring time is standard 100–120 s. Five specimens were used for each group.

Results and Discussion

The average values of the thermal conductivity tests of the plywood panels are given in Table 2.

Table 2. Thermal conductivity results of the plywood panels

Wood Species	Glue Types	Veneer Drying Temperatures (°C)	Thermal Conductivity (W/mK)	
			Before Aging	After Aging
Scots Pine	PF	110	0.11 (0.008)	0.10 (0.006)
		140	0.11 (0.004)	0.09 (0.001)
		160	0.10 (0.004)	0.10 (0.001)
	MUF	110	0.11 (0.002)	0.09 (0.008)
		140	0.10 (0.003)	0.09 (0.002)
		160	0.10 (0.001)	0.09 (0.005)
Black Pine	PF	110	0.10 (0.001)	0.10 (0.010)
		140	0.11 (0.001)	0.10 (0.003)
		160	0.10 (0.001)	011 (0.003)
	MUF	110	0.11 (0.001)	0.10 (0.003)
		140	0.11 (0.005)	0.11 (0.003)
		160	0.11 (0.007)	0.11 (0.002)

*Values in parenthesis are standard deviations

Thermal conductivity of the plywood panels from black pine was higher than those of the panels from scots pine as seen from Table 2. It could be explained with plywood panels from black pine had higher density than panels from scots pine as shown in Table 2. It was reported that thermal conductivity mainly varied according to wood species due to their different density values (Baker 2002; Rice and Shepard 2004; Kol and Sefil 2011). Because, as wood having higher density, it is true that it has less space to in store air causing to increase in thermal conductivity (Suleiman et al. 1999). Urukami and Kukuyama (1981) also found that thermal conductivity increased with increasing wood density.

In this study, in general, thermal conductivity of scots pine panels decreased with increasing the veneer drying temperature, except for plywood manufactured with PF resin and veneers dried at 140°C and 160°C when thermal conductivity actually increased. The results of Student Newman-Keuls also proved that there was no significant difference between thermal conductivity of panels from veneers dried at 140°C and 160°C with respect to drying temperature with 0,001 error probabilities. This situation can be explained with decreasing in density of the plywood panels with increasing the veneer drying temperature.

According to the Newman-Keuls results with 0,001 error probabilities, in general, thermal conductivity values of test panels decreased with aging process. Considering the aging process steps, moisture content of the panels might have not reached the values they had before aging process because of hysteresis even if they were exposed to the conditions defined the concerning standard (Ors and Keskin 2001). Therefore, decreasing in the thermal conductivity after aging process may be due to decreasing the moisture content of the panels.

Conclusions

One of the most important properties of composite panels used in construction is thermal conductivity. It is essential to determine the effect of aging process on the properties of panels used in structural applications. In this study, the effect of some manufacturing factors and aging process on thermal conductivity of plywood panels was determined. It was concluded from the study that the effect of veneer drying temperatures and aging process on the thermal conductivity of test panels were significant.

Acknowledgements

The authors acknowledge the financial support of the Scientific and Technological Research Council of Turkey (TÜBİTAK).

References

APA (1998) Structural Adhesives for Plywood-Lumber Assemblies, Technical Note, Number Y391 C.

APA (2011) The Engineered Wood Association PS 2-10 Performance Standard for Wood-Based Structural-Use Panels. Form No. S350F/Revised June 2011/0400.

ASTM C 481-99 (2005) Standard Test Method for Laboratory Aging of Sandwich Constructions, United States.

ASTM C 1113/M 1113-09 (2009) Standard Test Method for Thermal Conductivity of Refractories by Hot Wire (Platinum Resistance Thermometer Technique). 2009, United States, March.

Aydin I (2004a) Effects of Some Manufacturing Conditions on Wettability and Bonding of Veneers Obtained from Various Wood Species. PhD Thesis. Karadeniz Technical University, Faculty of Forestry, Natural and Applied Sciences Institute, Trabzon, Turkey.

Aydın I (2004b) Surface Inactivation in Veneer Drying Process and Its Effects on Bonding Strength. Artvin Coruh University Journal of Forestry Faculty 1-2: 1-8.

Aydin I, Colakoglu G (2005a) Formaldehyde Emission, Surface Roughness, and Some Properties of Plywood as Function of Veneer Drying Temperature. Dry Technol 23: 1107-117.

Bader H, Niemz P, Sonderegger W (2007) Untersuchungen Zum Einfluss Des Plattenaufbaus Auf Ausgew¨Ahlte Eigenschaften Von Assivholzplatten. Holz Roh Werkst 65(3): 173–181.

Baker WA (2002) Wood Structural Panels, Chapter Two. APA Engineered Wood Handbook, Thomas G. Williamson, ISBN: 0-07-136029-8, page: 2.1-2.9.

Breyer DE, Fridley KJ, Pollock DG, Cobeen KE (2003) Design of Wood Structures – ASD: Fifth Edition. USA , New York.

Çolak S, Aydın İ, Demirkır C, Çolakoğlu G (2004) Some Technological Properties of Laminated Veneer Lumber Manufactured from Pine (Pinus sylvestris L.) Veneers with Melamine Added – UF Resins. Turkish Journal of Agricultural Forestry 28: 109-113.

EWPA (2010) Engineered Wood Products Association of Australasia, Structural Plywood & LVL Design Manual.

Gu HM and Zink-Sharp A (2005) Geometric Model for Softwood Transverse Thermal Conductivity. Part I. Wood Fiber Sci 37(4): 699-711.

He G, Yu C, Dai C (2007) Theoretical Modeling of Bonding Characteristics and Performance of Wood Composites. Part III. Bonding Strength Between Two Wood Elements. Wood Fiber Sci 39(4): 566-577.

Kamke FA, Kultikova E, Lenth CA (1996) OSB Properties As Affected By Resin Distribution. Pages 147– 154 in The Fourth International Panel and Engineered- Wood Technology Conference & Exposition, Atlanta, GA.

Karlsson POA, McNatt JD, Verrill SP (1996) Vacuum-Pressure Soak Plus Oven-Dry As An Accelerated-Aging Test For Wood-Based Panel Products. Forest Prod J 46: 84–88.

Kawasaki T and Kawai S (2006) Thermal Insulation Properties of Wood-Based Sandwich panel for use as structural insulated walls and floors. J Wood Sci 52: 75-83.

Kol HS, Özçifçi A, Altun S (2008) Effect of Some Chemicals on Thermal Conductivity of Laminated Veneer Lumbers Manufactured with Urea formaldehyde and Phenol formaldehyde Adhesives. Kastamonu University Journal of Forestry Faculty 8(2): 125-130.

Kol HS and Sefil Y (2011) The Thermal Conductivity of Fir and Beech Wood Heat Treated at 170, 180, 190, 200 and 212°C. J Appl Polym Sci 121: 2473-2480.

Krüger EL and Adriazola M (2010) Thermal Analysis of Wood-Based Test Cells. Constr Build Mater 24(6): 999-1007.

Menezzi CHS, Souza RQ, Thompson RM, Teixeira DE, Okino YA, Da Costa AF (2008) Properties After Weathering And Decay Resistance Of Thermally Modified Wood Structural Board. Int Biodeter Biodegr 62(4): 448-454.

Norita H, Kojima Y, Suzuki S (2008) The Aging Effects Of Water Immersion Treatments In Wet-Bending For Standardized Testing Of Wood Panels. J Wood Sci 54: 121-127.

Örs Y, and Keskin H (2001) Knowledge of Wood Materials (in Turkish). Atlas Publishing, ISBN: 975-6574-01-1, Turkey.

Pizzi A (1983) Wood Adhesives; Chemistry and Technology. Vol.1., Marcel Dekker, New York.

Rice RW and Shepard R (2004) The Thermal Conductivity of Plantation Grown White Pine (Pinus strobus) and Red Pine (Pinus resinosa) at Two Moisture Content Levels. Forest Prod J 54(1): 92-94.

Sonderegger W and Niemz P (2009) Thermal Conductivity and Water Vapor Transmission Properties of Wood Based Materials. Eur J Woo Woo Pro 67: 313-321.

Suleiman BM, Larfeldt J, Leckner B, Gustavsson M (1999) Thermal Conductivity and Diffusivity of Wood. Wood Sci Technol 33(6): 465–473.

Tan H (2011) Some Technological Properties of LVL and Plywood Produced from Logs of Spruce and Fir Growing in Distinct Regions, PhD Thesis. Karadeniz Technical University, Faculty of Forestry, Natural and Applied Sciences Institute, Trabzon, Turkey.

Urukami H and Kukuyama M (1981) The Influence Of Specific Gravity On Thermal Conductivity And Diffusivity Of Wood. Wood Sci Technol 33: 465-473.

Vick CB (1999) Adhesive Bonding of Wood Materials, Wood handbook – Wood as An Engineered Material Chapter 9. FPL-GTR-113.Department of Agriculture. Forest Service. Forest Product Laboratory, Madison, U.S.

Xie Y, Krause A, Mai C, Militz H, Richter K, Urban K, Evans PD (2005) Weathering of wood modified with the N-methylol compound 1,3-dimethylol-4,5-dihydroxyethyleneurea. Polym Degrad Stabil 89: 189-199.

Yan CC (1992) The reliability analysis of wood diaphragms under wind loading, PhD., Washington State University, Department of Civil and Environmental Engineering, Washington.

Youngquist JA, Myers GC, Murmanis LL (1987) Resin Distribution In Hardwood: Evaluated By Internal Bond Strength And Fluorescence Microscopy. Wood Fiber Sci 19(2): 215–224.

Proceedings of the 58th International Convention of Society of Wood Science and Technology
June 7-12, 2015 – Grand Teton National Park, Jackson, Wyoming, USA

The Effect of Alkaline Treatment on Tensile Properties of Single Bamboo Fiber

Hong Chen[1,2†], *Benhua Fei*[2*†]

[1]College of Furniture and Industrial Design, Nanjing Forest University, Nanjing, 210037, China
[2] International Centre for Bamboo and Rattan, Beijing, 100102, China
* Corresponding author: feibenhua@icbr.ac.cn
† SWST member

Abstract

The objective of this study was to investigate effect of alkaline treatment on the morphology of cellulose microfibril aggregates and tensile properties. Single bamboo fibers were treated by alkaline solution at five concentrations (6%, 8%, 10%, 15% and 25%) at room temperature for 2 hours. The morphology of cellulose microfibril aggregates were observed with AFM, and the tensile strength, tensile modulus and elongation at break were investigated. The results revealed that alkaline treatment affected the structure of cellulose microfibril aggregates and tensile properties significantly. Tinny pores appeared between cellulose microfibril aggregates in bamboo cell wall when treated by alkaline solution with concentration of 10% or more. Both the tensile strength and tensile modulus of single bamboo fiber decreased when treated with 6%, 8%, 10% alkaline solution, respectively. While when the concentration of alkaline solution increased to 15% and 25%, tensile modulus decreased sharply, but tensile strength changed little. The elongations at break were similar when the fiber treated by alkaline solution with concentration of 6% and 8%, respectively. When the concentration increased to 10%, the elongation began to increase obviously which increased sharply when the concentration went up to 15% and 25%. Besides, the fracture forms of bamboo cell wall were different with different alkali treatments. The fracture forms of fibers treated by 6% and 8% alkali solution liked the brush which represented tenacity. When the concentration increased to 10%, the fracture forms were like teeth, while the forms were orderly when the concentration increased to 15% and 25% which indicated the frangibility of fibers.

Proceedings of the 58th International Convention of Society of Wood Science and Technology
June 7-12, 2015 – Grand Teton National Park, Jackson, Wyoming, USA

Restoring the Mayflower II

Terry Conners[1†*]

[1] Associate Extension Professor, Department of Forestry, University of Kentucky, Lexington, KY 40546-0073, USA
† SWST member, Corresponding author*
E-mail: tconners@uky.edu

Abstract

The Mayflower II is a recreation of the ship that brought the Pilgrims to America in 1620, and it was given to the American people by the United Kingdom in 1957 as an expression of goodwill to celebrate our countries' alliance in WW II. After 60 years, however, the constant exposure to salt water and humidity, and the interaction of its iron fasteners with the English white oak that was used in the ship's construction have caused significant deterioration of the ship's planking and frame. Locating large high-quality white oak trees for repairs and restoration has been difficult, as most large white oaks are bucked and sold for more conventional products such as sawtimber, staves or veneer. This project has received a lot of favorable press aimed at the general public, and could be used to make the public more aware of forest management.

KEYWORDS: Forest management, white oak, Mayflower II, wooden ships

Introduction

The Mayflower II is a recreation of the original ship that sailed with the Pilgrims from England to Plymouth, Massachusetts in 1620. The original ship was lost long ago (though pieces of it may be incorporated into a barn in Jordans, Buckinghamshire, England), but a near-replica was constructed in England in the mid-1950s and given to the people of the United States as a token of the alliance that bound the U.S. and the United Kingdom during WW II. Owned and operated by Plimoth Plantation, a living history recreation of Plymouth as it was in 1627, the ship is docked at the Plymouth waterfront during tourist season (April through November), after which time it is towed to Fairhaven Shipyard on the south of Cape Cod for the winter. While at Fairhaven in 2013 the Mayflower II was inspected by the U.S. Coast Guard for seaworthiness. This is normally done on a biannual basis during the winter months, but that year the USCG removed the copper sheathing at the waterline (used to protect the hull from floating ice) and did a more thorough inspection. What they discovered wasn't encouraging: about sixty white oak planks

needed to be replaced, and a number of futtocks (frame sections) needed to be replaced as well (Figs. 1-3). At one time there had been nets filled with rock salt placed between the inner and outer hull (a traditional wooden ship practice) so that wetted salt would diffuse into the hull and act as a preservative, but it is unclear how long these were maintained (or indeed, whether they even had the desired effect).

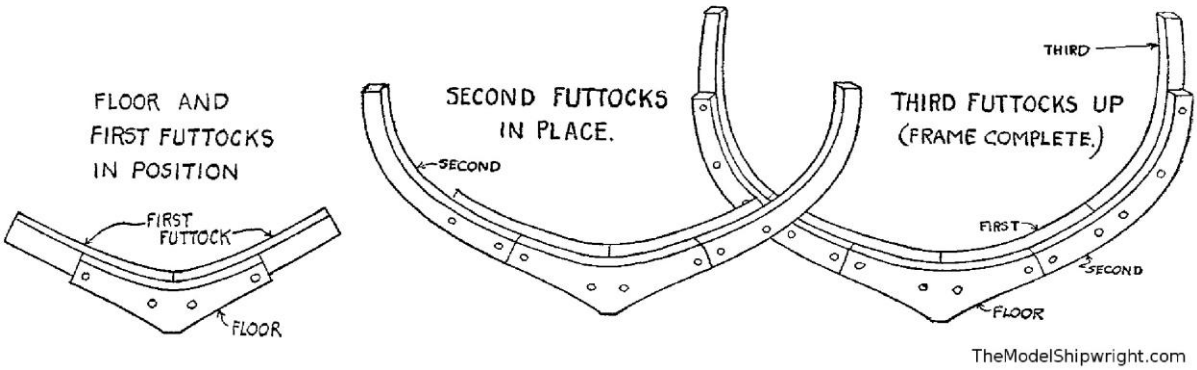

Figure 22. Futtocks are frame sections that define the shape of the hull. They are cut from naturally sweepy logs to preserve the strength of the wood. Diagram from Davis (1933), scan courtesy of TheModelShipwright.com.

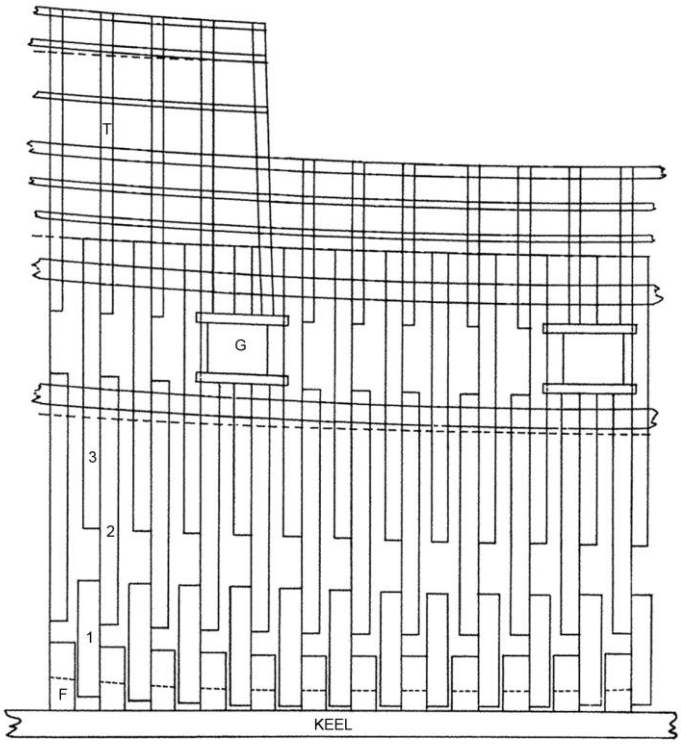

Figure 23. Framing plan for the side of the Mayflower II (Baker 1958). Identification of the timbers is as follows: F=floor (the piece of wood that bridges the keel; 1, 2 and 3: first futtock, second futtock, third futtock; G = gunport; T= toptimber

Figure 24. This sweepy piece of white oak is ready to be sawn into one or more futtocks.

2013: Repairs Begun

Tony Macedo, head shipwright for wooden ships at Fairhaven Shipyard, and I had a discussion about the white oak needed for the repairs. Wood for planking had to be white oak, preferably green, 24’ to 30’ long, 3-1/2” thick, with a minimum of 10” of heartwood, and flitch cut (sawn with a live edge) so that the shipyard could cut the plank as they liked. To complicate things, the water-side of the plank needed to be as clear as possible, with very few and very small defects. The back side didn’t have to be as defect-free, but any knots had to be small enough that they could be plugged. Through-knots were not permitted, as these would cause leaks. White oak wood intended for futtocks had to be naturally sweepy, as curved wood pieces are stronger when they are sawn with the grain rather than across the grain. Some wood was already at the shipyard, left over from previous work, but much more needed to be found.

Through the efforts of many people, some suitable wood was obtained from Georgia, Virginia and Massachusetts, but by mid-May 2013, the ship had been in dry dock for five months and repairs were far from complete. On the port side, the deteriorated futtocks had been replaced and replanking was underway (Fig. 3), while on the starboard side a number of planks had been removed to shorten the repair time once more oak arrived. It soon became apparent that there would not be enough white oak to commence the starboard side repairs, however, and this caused a huge problem. Time was of the essence: with the ship drying out more and more the longer it sat out of water, the USCG agreed to let the shipyard use red oak to replank the ship above the waterline on the starboard side temporarily. The ship finally was returned to Plymouth on August 7, 2013. The long delay in returning the ship caused considerable loss of summer tourist revenue,

not only to Plimoth Plantation, but also to the Plymouth shopkeepers and hoteliers who depend on the ship as a tourist attraction.

Figure 25. The orange paint is a protective marine coating used on the new futtocks installed on the port side of the Mayflower II at Fairhaven Shipyard. Note the new white oak planking.

2014: Kentucky White Oak Cut for Mayflower II

The ship returned to dry dock for further work during the winter of 2013–2014, but repair work was hindered by the lack of wood, and the search for large white oaks continued. A few large trees were found in a couple of locations, but the Kentucky connection turned out to be important. Many people were on the lookout throughout Kentucky and the Appalachian region for the size of trees that were needed and in early 2014 Clint Patterson, the Head Forester at Berea College (Berea, KY), found about ten large white oak trees on the college forest that would fit the specifications for Mayflower II planking. The Berea College administration generously agreed to donate the trees, but cutting the trees into planks was a complicated puzzle that ended up being a collaborative effort. We first had to secure a contract with Plimoth Plantation for the wood, and we gained a commitment to proceed from Ellie Donavan and Ivan Lipton (Executive Director and Chief Administrative Officer, respectively). Next, we had to consider that very few Appalachian hardwood sawmills are capable of sawing logs as long as 30', and the one established sawmill in KY that has the capability was quite a ways away. We contacted portable bandsaw mill manufacturers, but the mills that they had in the region weren't capable of sawing these logs either. We finally contacted Left Coast Supplies (Willits, CA) and they directed us to Ernie Tebeau, a sawyer from Toledo, OH who owns one of their sawmills. Ernie agreed to do the sawing, and Holger Groessler (Maple Log Farms LLC, Louisville, KY) agreed to fell the trees and arrange for them to be taken to a landing. Berea College provided several helpers to the effort as well, and Clint Patterson made the arrangements for the needed equipment. Left Coast Supplies further provided

extension rails at their cost so that the Lucas mill could cut up to 32’ logs. Tony Macedo flew down from Massachusetts to advise the sawyer for several days, and Whit Perry, the associate director for maritime preservation and operations, came out to inspect and supervise the loading on a snowy day in November when it was loaded onto a flatbed truck (Arnold M. Graton and Associates of Ashland, NH) for Massachusetts. Most of the wood will be used for replanking in 2015, but some of it will be used for other critical areas of the ship.

2015–2020: Further Work Needed on Mayflower II

All in all, about 2300 board feet were cut from the Berea trees, but much more is expected to be needed. In December 2014 the Mayflower II was taken to Mystic Seaport (CT) for the most extensive survey to date. Even the ballast (130 tons of cobblestones, pig iron and old railway ties) was removed for the first time since the ship was launched! Captain Paul Haley of G.W. Full and Associates (Orleans, MA) is conducting the survey and will send his report and recommendations to Plimoth Plantation in the spring of 2015. Plimoth Plantation already knows that more planking will be needed, and naturally bent sections of white oak trees will be needed to replace some knees (curved braces) which have failed or deteriorated (Fig. 4). Many wood sourcing issues and challenges remain. Plimoth Plantation plans to complete the restoration during the winter months over the course of the next several years so that Mayflower II can be completely restored by the quadricentennial of Plymouth’s founding in 2020.

Figure 26. This is one of the hanging knees (vertical braces) below decks which have to be replaced. These knees are strongest if their grain follows the naturally occurring grain of the wood, so they should come from the intersection of the stem with either branches or roots. Based on the direction of the grain where the wood has failed, it does not appear that this knee was cut properly.

During a quick tour of the Mayflower II in November 2014 (offered through the courtesy of Whit Perry), this author noted that most of the ship's structural components were made from white oak, and much original material remains from the 1955–1956 construction. Based on personal observations, there are likely going to be several types of wood deterioration noted in the expert's survey report. Some wood has deteriorated due to decay or "iron sickness" (a chemical interaction of the white oak with the original iron fasteners), some wharf beetles have been found, and there are numerous places where the wood feels noticeably soft to the touch as well as places where one can see the type of damage that is characteristic of salt damage (Figure 5). Water sometimes condenses on the wood surfaces at the lower levels of the ship, and this can only exacerbate several problems. Remarkably, the masts and spars were made of Douglas-fir imported into England from the Pacific Northwest. The masts are severely checked, and it will be interesting to find out whether they pass the marine surveyor's scrutiny.

Figure 27. Salt-damaged wood on Mayflower II. This photograph was taken from the underside of a porch (cubbridge head) where the people exit from between decks, at the middle level of the ship.

Future Demand for Large Timbers

Due to the well-known American history associated with the Mayflower, this project received a lot of favorable publicity (see Patton, 2014) for example, though it was posted elsewhere through the Associated Press). This project has also increased the awareness of the public about forestry. One thing that we all discovered while trying to find suitable wood for this project is that the white oak part of the U.S. forest industry is laser-focused on sawtimber, staves and veneer. There is very little awareness of alternative products,

and there is very little awareness of the needs of the wooden ship building industry. This isn't surprising, but it marks a huge change from the forest planning exercised by our forebears. For example, there are forests in in the Tronçais region in France that were deliberately planted with white oaks for shipbuilding in the late 1600s (Bouchard Cooperages 2015). The English had similar concerns, *e.g.*, as recognized by the 1542 Statute of Woods or Act for the Preservation of Woods (Thirgood 1971). With the interest in historic preservation and reenactment, there is still a need today for timbers to restore wooden ships. Besides the Mayflower II there are well-known survivors such as the whaler Charles W. Morgan (Mystic Seaport, CT) and the USS Constitution ("Old Ironsides") (Charlestown Navy Yard, Massachusetts); there are even newly-built ships such as the San Salvador, a replica of the flagship of the explorer Juan Rodríguez Cabrillo (berthed in San Diego, CA) and l'Hermione, a recreation of the ship on which Lafayette sailed to America in 1780 (berthed in Rochefort, France). All of these wooden ships will need continual upkeep and wood replacement. The large timbers needed for these ships are valuable, and the forest industry might do well to use the opportunity provided by these charismatic projects to talk about the importance of forest management to the general populace – and to grow larger white oak trees, with suitable signage to give the landowner (or National Forest) bragging rights for the next couple of hundred years!

References

Baker, William A. The New Mayflower. Her Design and Construction. Barre, MA: Barre Gazette, 1958. 164 pp., plus blueprints.

Bouchard Cooperages (2015). Forest Origin Comparison. http://www.bouchardcooperages.com/usa/news/forest_origin.html

Davis, Charles G. (1933). The Built-Up Ship Model. Publication Number 25 , Marine Research Society, Salem, Massachusetts. 206 pp.

Patton, J. (2014) Old oak trees from Berea provide timber for Mayflower II repair. Published on many websites because the story was distributed by the Associated Press, but the original was published here: http://www.kentucky.com/2014/12/25/3611291/special-wood-from-berea-college.html.

Thirgood, J.V. (1971). The historical significance of oak. *In:* Oak Symposium Proceedings. U.S. Department of Agriculture, Forest Service, Northeastern Forest Experiment Station: Upper Darby, PA. pp. 1–18.

Acknowledgements

The author gratefully acknowledges the work of the many people and groups mentioned in this article. It has truly been a group effort to get even this much accomplished! Holger Groessler, Clint Patterson and his staff and Ernie Tebeau did most of the organizing and all of the work, and it took them several weeks to do it. I also want to give special thanks to my father, Tom Conners, who alerted me to this problem, and to Berea College and Whit Perry, Ellie Donavan and Ivan Lipton of Plimoth Plantation.

Proceedings of the 58th International Convention of Society of Wood Science and Technology
June 7-12, 2015 – Grand Teton National Park, Jackson, Wyoming, USA

Furniture and Lumber Exports from Ghana: A Comparative Study of Some Market Trends

Peter Kessels Dadzie [1]

[1] Lecturer, Interior Architecture and Furniture Production Department, Kumasi Polytechnic, Box 854, Kumasi, Ghana.
pkkdadzie@yahoo.com; peter.kdadzie@kpoly.edu.gh

Abstract

Adding value to the dwindling timber resources in Ghana before export is an issue of much concern. However, it appears that wood products manufacturing firms in Ghana continue to produce and export lumber which have lower value relative to garden furniture. This study assessed values of wood species when used for garden furniture and kiln-dried (KD) lumber, and the destination and product type effect on these values. The study covered an eight year period (2001 to 2008). Reports on wood products export were reviewed to obtain data for analyses. Findings were that values/m^3 of all wood species were higher when used for garden furniture than when used to produce lumber for exports. Among the 15 most requested species for garden furniture, *Pericopsis elata* (afromosia) had the highest value for furniture (€3,308.844) and lumber (€869.00) whereas *Terminalia ivorensis* (emire) had the least furniture value (€1,336.936) while *Pycnanthus angolensis* (otie) had the least lumber value (€263.10). Generally, both products registered a decreasing trend in export volumes but lumber prices/m^3 appreciated whereas furniture prices fell. Sweden and U.S. A respectively offered the highest (€17,891.80) and lowest (€254.097) mean garden furniture value, while Cyprus and France respectively offered the highest (€644.80) and lowest (€314.97) lumber value. Direction of trade and product type had significant effect ($p<0.01$) on values of the products and they explained 92.3% of the variations. Conclusions were that the best destination for furniture export is Sweden and that for lumber is Cyprus. Based on monetary values, it was recommended that garden furniture production for exports should be encouraged than lumber, and furniture export to Sweden could yield higher values/m^3.

Key words: Furniture and lumber exports, Timber products from Ghana, Value addition to wood, Ghana's wood trading partners.

Introduction

Ghana's forest sector is a major contributor to the national economy. It is reported that the sector, which is dominated by timber industries, accounts for about 11% of the total export earnings of the country (Ghanaian Times 2015). The timber industry manufacture products like lumber, furniture parts, plywood, glulam etc for exports and these contribute about 6% to the Gross Domestic Product (GDP) and employ labour force of over 75,000 people, while providing direct livelihood to about two million people in total (Ghanaian Times 2015).

Furniture parts, which are one of Ghana's forest products for exports, is mainly garden furniture (Alexander Rose Ltd 2005). Such furniture are mostly used in open places where they are partly or wholly exposed to the weather and as such they are primarily produced from relatively durable and weather resistant wood species like iroko/odum (*Milicia excelsa*), mahogany (*Khaya spp.),* teak (*Tectona grandis*), utile (*Entandrophragma utile*), albizia (*Albizia ferrugenia*) etc. either alone or in combination with some metal components (Plow and heart 2006; TIDD 2003). In Ghana, 26 wood species have been identified as being used for the production of various garden furniture parts for exports (Dadzie et al 2014). However, wood has been the most favorite material for garden furniture globally due to its desirable attributes such as: easy to work on with both hand and machine tools; ability to be fastened satisfactorily with adhesive, nails and screws; natural beauty from variations in figure and colour that blends; and resistance to rust and corrosion (Ratnasingam 1998; Waters 1970). These same wood species in addition to others are being exploited for lumber production for exports and local consumption.

In the export market however, furniture parts have much higher value per unit volume than lumber. Trade statistics revealed that, while a cubic meter of kiln-dried lumber was €377.172, air-dried was €315.133 and overland was €68.578, the value of garden furniture parts stood at €1,677.850 per m^3 (TIDD 2005a). These show value differences between furniture and air-dried lumber per m^3 to be €1,362.717 (432.43%) and that between furniture and kiln-dried lumber to be €1,300.717 (344.85%). Additionally, individual wood species, when converted to garden furniture for exports could register appreciably higher values than when exported in the lumber forms. For instance, kiln-dried lumber of Mahogany (*Khaya Spp.*) and its furniture values registered an increase of 200.07%, whiles Odum (*Milicia excels*a) recorded a value increase of 178.10% (TIDD, 2005a). However, studies on market trends such as price variations over a considerable period of time, among importing countries/buyers and among wood species especially in relation to lumber or furniture produced in Ghana appear limited or unavailable.

This study therefore assessed the trend of; 1) Average value/m^3 for K.D lumber and garden furniture of the various wood species desired for garden furniture exports. 2) Average volume and value/m^3 of K.D lumber and garden furniture exports from Ghana over a period

3) Average value/m^3 of K.D lumber and garden furniture offered by importers of the two products from Ghana and 4) whether or not direction of trade and product type has significant effect on the value/m^3 of lumber and garden furniture.

Materials and Methods

Data collection

Average Value/m^3 (Free-on-Board FOB) and Volume (m^3) of Kiln-Dried Lumber and Garden Furniture exported from 2001 to 2008.

The average FOB values/m^3 of each specific wood species used for both garden furniture and kiln-dried lumber production were extracted from TIDD's export reports on wood products (TIDD 2001; 2002; 2003; 2004; 2005; 2006; 2007;2008). These average values were obtained by dividing each product's cumulative values by their respective cumulative volumes exported in each year. The mean of each wood species for either lumber or furniture for the 8 years were used as the average value of each species for the period. In estimating the average values/$m^3$of garden furniture and lumber, in general, the general cumulative values were also divided by their respective general cumulative volumes of each of the products exported in each year.

Average Value/M^3 of Kiln-Dried Lumber and Garden Furniture among Importers of the Two Products from Ghana.

The average FOB values/m^3 of garden furniture in general (i.e. without considering specific wood species) imported by each country were first extracted from TIDD's export reports on wood products for the period of study (i.e. 8 years). This was done by dividing their cumulative values by their respective cumulative volumes for each year from 2001 to 2008. The mean for the 8 years was used as the average purchased value/m^3 offered for the product in that country. After obtaining all the countries that import furniture products from Ghana, their kiln-dried lumber imports were also traced and their average values/m^3 for each year subsequently determined as was done in the case of garden furniture. All these estimates were done without considering any specific species but the products in general (i.e. kiln-dried lumber and garden furniture).

Data analyses

Data obtained on volumes and values of garden furniture exports across species, years and importing countries were analysed using Microsoft Excel 2003 and 2007 to determine their trends. SPSS 17.0 was also used to perform a Two-Way ANOVA to determine the influence of direction of trade and product type on the variations in values/m^3 of kiln-dried lumber and garden furniture in general (not for specific species).

Results and Discussions

Average value/m^3 for kiln-dried lumber and garden furniture of specific wood species

Figure 1 presents the trends of the values/m^3 (€) of kiln-dried lumber and garden furniture for the 26 identified wood species (Dadzie et. al. 2014) used in Ghana for the production and export of furniture parts. Among the 26 species, 15 were found to have made at least 50% appearances (i.e. ≥4 years of the 8 years of this study) in the international garden furniture market across the world. These were classified as most desired species for furniture production in Ghana for exports.

From figure 1, among the most desired wood species *Pericopsis elata* (afromosia) had the highest value for furniture (€3,308.844) and lumber (€869.00). This results in value difference of 2439.844 equivalent to 280.76% higher than the value of the species' lumber. However, *Terminalia ivorensis* (emire) had the least furniture value of €1,336.936 while *Pycnanthus angolensis* (otie) had the least kiln-dried lumber value of €263.10.

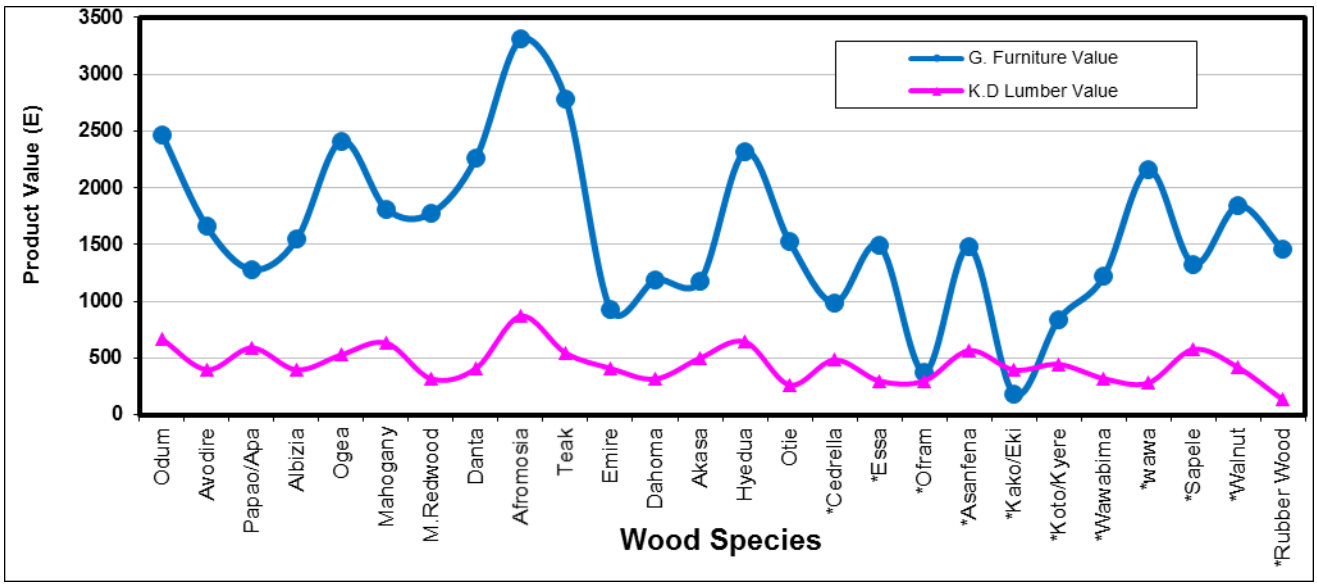

Figure 1. Average values/m^3 of specific wood species used in producing both kiln-dried (K.D) lumber and garden furniture (G.F) in Ghana from 2001 -2008. Note: *Species that had less than 50% appearances in the garden furniture market over the period (i.e between 1 and 3 years). Source: TIDD export reports 2001 to 2008.

Average volume (m^3) and value/m^3 (€) of kiln-dried lumber and garden furniture exports from Ghana over the period

Figures 2 and 3 respectively show the mean volumes (m^3) and values (€) of kiln-dried lumber and garden furniture exports from Ghana over the period of this study.

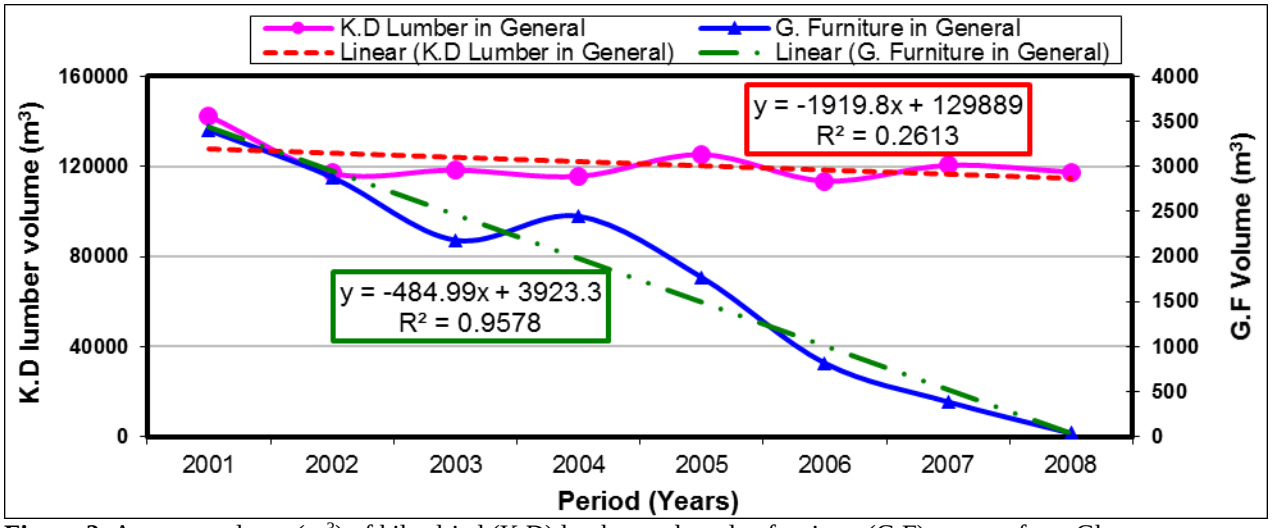

Figure 2. Average volume (m^3) of kiln-dried (K.D) lumber and garden furniture (G.F) exports from Ghana from 2001-2008. Source: TIDD export reports 2001 to 2008.

From figure 2, the quantity of both lumber and furniture exported from Ghana has generally declined from 2001 to 2008. However, the degree of decline appears higher for furniture than for lumber as indicated by the linear regression lines. However, it also appears clear that furniture exports from Ghana after 2008 is approaching zero but lumber exports are still around 3,000m^3 per annum. This appears to support report that firms in Africa, including Ghana appear to be exporters of raw or low value-added products whose prices are low and imports high value-added products whose prices are high (Capito 1993; AFORNET 2000).

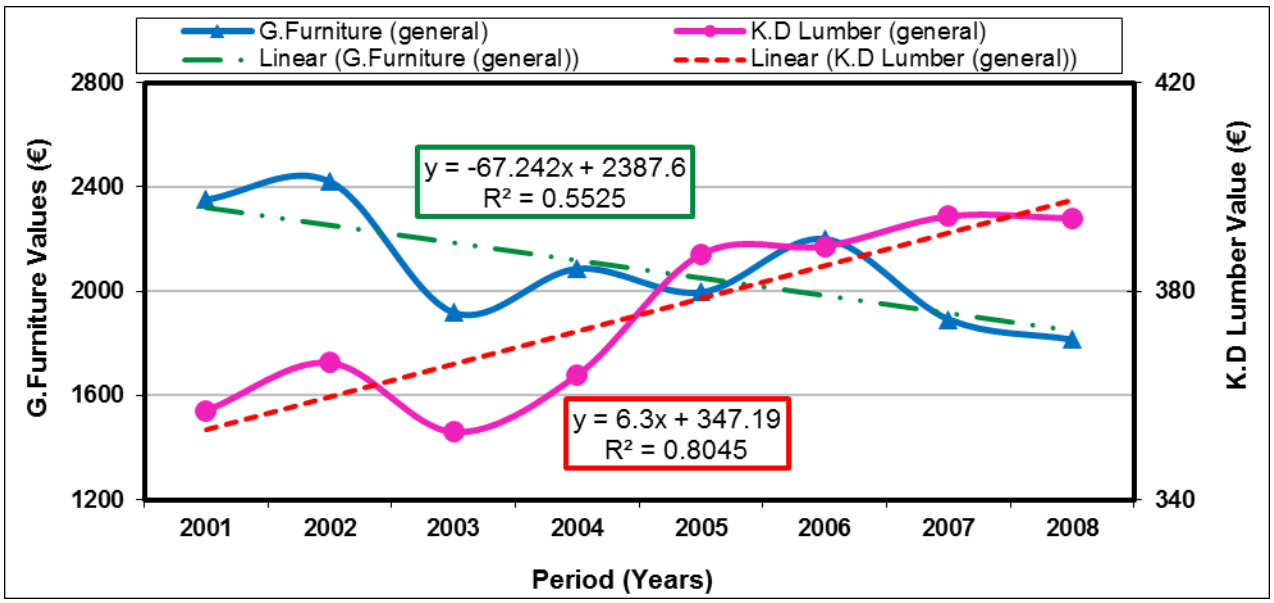

Figure 3. Average value/m^3 (€) of kiln-dried (K.D) lumber and garden furniture (G.F) exports from Ghana from 2001 to 2008. Source: TIDD export reports 2001 to 2008.

From figure 3, whereas the values/m^3 (€) of kiln-dried lumber generally appreciated over the period, those of garden furniture fell. This could be one reason accounting for the

seeming disinterest among Ghanaian wood products manufacturers to continue engaging in furniture production for exports. But despite the decline in value/m^3 of garden furniture over the years, it is reported that its production in Ghana for exports is generally profitable (Dadzie and Frimpong-Mensah 2011; Dadzie et. al. 2015).

Average value/m^3 (€) of kiln-dried lumber and garden furniture among importing countries.

Figures 4 and 5 respectively represent the average values/m^3 for kiln-dried lumber and furniture from 2001 to 2008 among importing countries. In all, a total of 14 countries were found to be importers of both two products from Ghana within the period of study. However, Canary Island was the only one that imported Ghanaian furniture but do not import Ghanaian kiln-dried lumber. Thus there are 13 countries, in effect, that imported both furniture and kiln-dried lumber from Ghana within the period of this study. However, among these countries, Sweden and U.S.A respectively offered the highest (€17,891.80) and lowest (€254.10) mean furniture value, whereas Cyprus and France respectively offered the highest (€644.80) and lowest (€314.97) lumber value.

The findings on U.S.A appear to support the finding that the country imports just about 4% of its wood products from Africa (mainly Ghana and Cameroon) (ITTO 2011 cited in Bandara and Vlosky 2012). The low value offered by U.S.A for Ghana's Furniture could be a contributory factor to this.

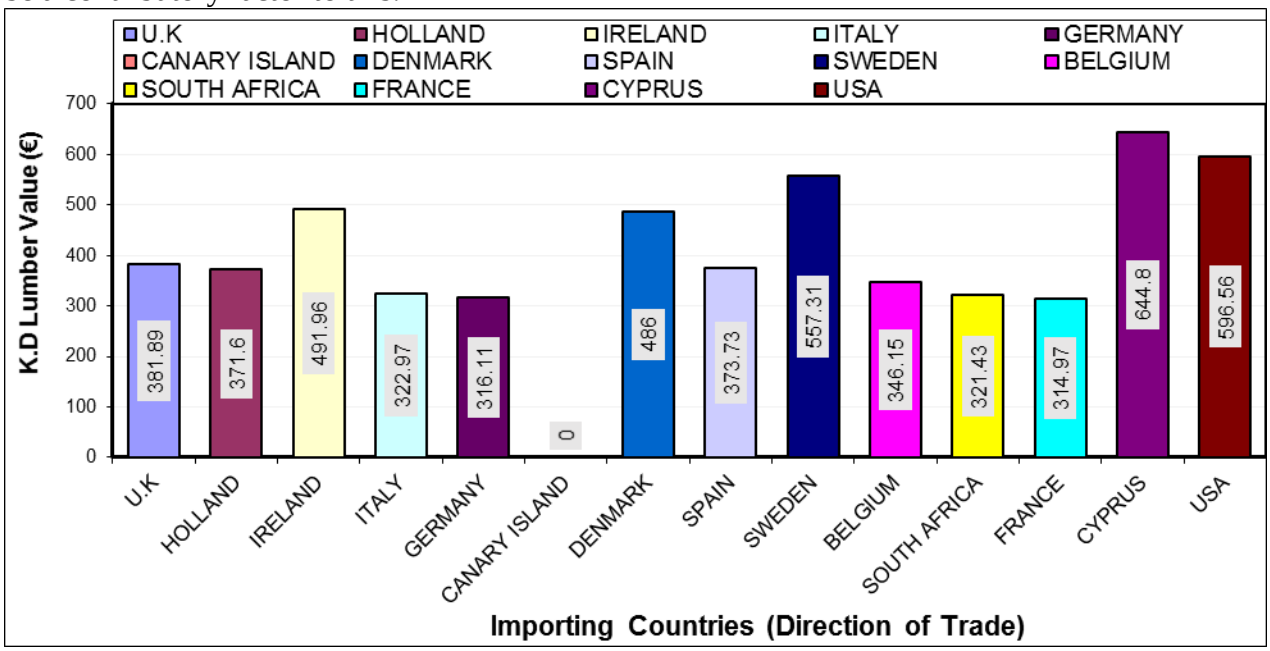

Figure 4: Average value/m^3(€) of kiln-dried lumber among importers of both furniture and kiln-dried lumber from Ghana from 2001-2008. Source: TIDD export report 2001 to 2008.

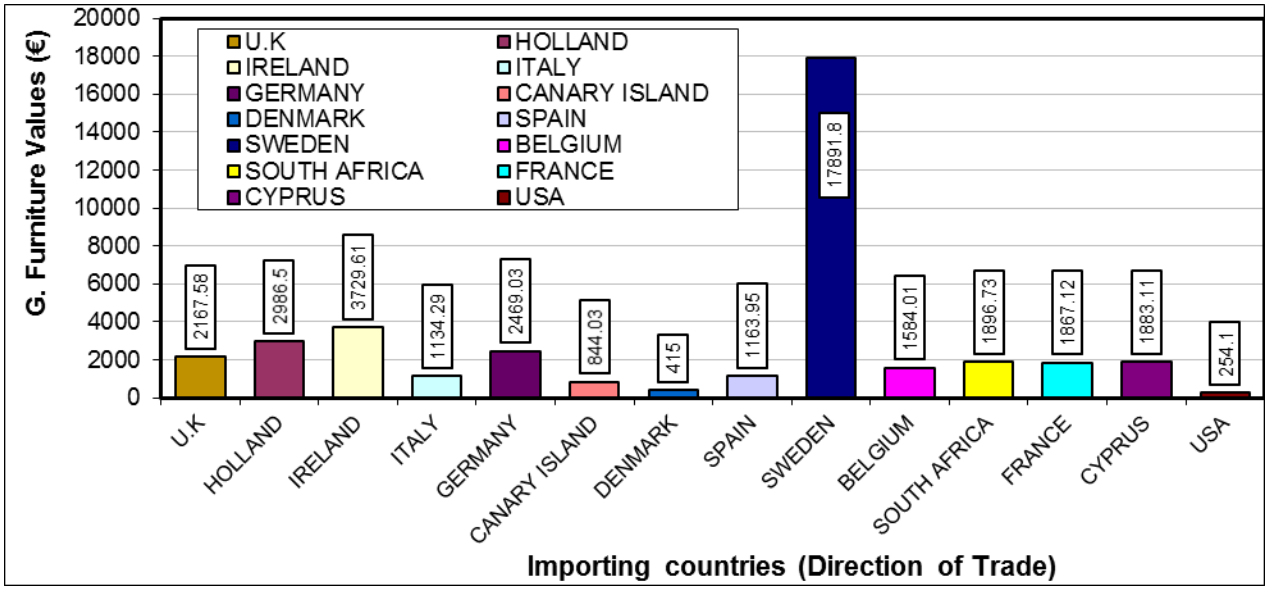

Figure 5: Average value/m^3 (€) of garden furniture (G.F) among importers of both kiln-dried (K.D) lumber and furniture from Ghana from 2001-2008. Source: TIDD 2001 to 2008.

Additionally, the finding on U.S.A also appear to contradict that of Doomson and Vlosky (2007) that U.S.A, India and Italy are among the 10 major importers of Ghana's wood products. But this could be due to the focus of this study being on only kiln-dried lumber and garden furniture and not on all wood products produced in Ghana for exports. These results (Figures 4 and 5) suggest that direction of trade (destinations) and the product type (either furniture or lumber) appeared to have some influence on the values of the products. However, the value/m^3 of furniture parts in Sweden appeared to be exceptionally higher than all the other trading partners since no country offered even up to €4000.00/m^3 for furniture in any of the years under review. This could be attributed to other factors other than destination or product type.

Effect of direction of trade (importing countries) and product type on the variations in the value/m^3 of lumber and garden furniture.

Two-Way ANOVA (Table 1) indicated that direction of trade or importing country *(F=82.500; p= 0.000)*, product type (furniture or lumber) *(F= 380.959; p = 0.000)* and the interactions between the two variables *(F= 84.758; p = 0.000)* had significant effects on the value/m^3 of the two products. Moreover, direction of trade and product type was found to have explained about 92.3% (as indicated by the adjusted R^2 value beneath Table 1) of the variations in the prices of the two products among the importing countries.

Table 1. *Two-Way ANOVA of the influence of direction of Trade (Importing Country) and Product type on the variations in Values/m^3 of lumber and furniture.*

Source	Type III Sum of Squares	df	Mean Square	F	Sig.
Corrected Model	6.933E8[a]	26	2.666E7	70.147	.000
Intercept	2.046E8	1	2.046E8	538.218	.000
Direction_of_Trade	4.077E8	13	3.136E7	82.500	.000
Product Type	1.448E8	1	1.448E8	380.959	.000
Direction_of_Trade * Product	3.866E8	12	3.222E7	84.758	.000
Error	4.676E7	123	380122.556		
Total	9.370E8	150			
Corrected Total	7.400E8	149			

a. R Squared = .937 (Adjusted R Squared = .923)

Conclusions and Recommendations

Based on the results, the following conclusions were drawn;

1. Garden furniture generally had higher values/m^3 for all species than kiln-dried lumber. However, furniture and lumber produced from *Pericopsis elata* (afromosia) wood are the most valued ones in the export markets whereas *Terminalia ivorensis* (emire) and *Pycnanthus angolensis* (otie) are the least valued species for furniture and lumber respectively.
2. Though the export volumes of both furniture and lumber have fallen over the period, unlike furniture, the price or value/m^3 of kiln-dried lumber have experienced some steady appreciation.
3. In terms of export value/m^3, Sweden and U.S. A were respectively the best and worst destinations for Ghanaian furniture whereas Cyprus and France were also respectively the best and worst destinations for lumber from Ghana.
4. Direction of trade (destination) and product type (furniture or lumber) had significant effect on the unit prices or values of both lumber and garden furniture.
5. It was recommended that garden furniture could result in higher incomes than lumber exports and much effort should be mad e to encourage its production and exports than lumber.

References

AFORNET- African Forest Research Network (2000) Wood Based Industries in Sub-Saharan Africa. www.afornet.org, (16 August 2005).

Alexander Rose Ltd. (2005) Fine quality traditional garden furniture, Alexander Rose Ltd, West Sussex. U.K.. 25pp.

Capito, Eugene (Hon.) (1993) Situation of African Forestry Policy. ATO, Information Bulletin No. 2 (1994) SGIT Impremerie de Louis, Gabon. pp.10-12.

Dadzie P. K, Frimpong-Mensah K, Amoah M, & Boampong E (2015) Scenario Analysis of Profits in Further Processing Lumber to Furniture in Ghana for Export: A Case Study of a Local Firm, *International Journal of Business and Economic Research, 4(2): 55-66. doi:10.11648/j.ijber.20150402.15* http://www.sciencepublishinggroup.com/j/ijber (20 March 2015)

Dadzie P K, Amoah M, Tekpetey S L (2014) Preliminary assessment of wealth creation in wood products' business in Ghana: The perspective of lumber and furniture production and implications for entrepreneurship, International Journal of Business and Economic Research, 3(6): 243-249. doi: 10.11648/j.ijber.20140306.15. http://www.sciencepublishinggroup.com/j/ijber (20 December 2014)

Dadzie P K, Frimpong-Mensah K (2011) Value addition to wood resources, the case of garden,furniture production and export in Ghana; A case study of a local firm, conference paper presented at the 65th international convention of the Forest Products Society, 19th - 21st June 2011, Portland, Oregon. U.S.A. http://www.slideshare.net/julielang/session-8-ic2011dadzie (20 December 2014).

Doomson O, Vlosky R P (2007) A strategic overview of the forest sector in Ghana, Louisiana Forest Products Development Centre working paper #81, School of Renewable Natural Resources, Lousiana State University of Agricultural Centre, Baton Rouge. U.S.A. 17pp.

ITTO (International Timber Trade Organization) (2011) tropical timber market reports *in*; Bandara W A R T W, Vlosky R P (2012) An analysis of the U.S wood products import sector: prospects for tropical wood products exporters, Journal of Tropical Forestry and Environment 2 (02) 49-62.

Plow**,** and Heart Inc. (2006). Furniture Buying Guide. www.plowhearth.com/ Outlet Store. Asp. (Accessed April 2006).

Ratnasingam J (1998) The South-East Asian furniture industry siege, Southern African Wood and Timber Times 24 (1) 68-72.

The Ghanaian Times of January 23, 2015; www.ghanaiantimes.com.gh/. (3 February 2015).

TIDD.- Timber Industries Development Division (2001) Exporters performance/moving species/direction of trade-lumber (KD) and furniture parts; wood products export report, December, Data Processing Section, Takoradi. Ghana. 33pp.

TIDD (2002) Exporters performance/moving species/direction of trade-lumber (KD) and furniture parts; wood products export report, December, data processing section, Takoradi. Ghana. 36pp.

TIDD (2003) Exporters performance/moving species/direction of trade-lumber (KD) and furniture parts; wood products export report, December, data processing section, Takoradi. Ghana. 36pp.

TIDD (2004) Exporters performance/moving species/direction of trade-lumber (KD) and furniture parts; wood products export report, December, data processing section, Takoradi. Ghana. 42pp.

TIDD (2005a) The first 30 out of 126 exporters of all wood products, jan-feb 2005. wood products'export report for February 2005, data processing section of TIDD, Takoradi, Ghana. 32 pp.

TIDD (2005b) Exporters performance/moving species/direction of trade-lumber (KD), flooring and furniture parts. Report on export of wood products for December 2005, data processing section of TIDD, Takoradi, Ghana. 54 pp.

TIDD (2006) Exporters performance/moving species/direction of trade-lumber (KD) and furniture parts; wood products export report, December, data processing section, Takoradi. Ghana. 36 pp.

TIDD (2007) Exporters performance/moving species/direction of trade-lumber (KD) and furniture parts; wood products export report, December, data processing section, Takoradi. Ghana. 31pp.

TIDD. (2008). exporters performance/moving species/direction of trade-lumber (KD) and furniture parts; wood products export report, December, data processing section, Takoradi. Ghana. 41 pp.

Waters M M (1970) Woodwork - A course for first exanimations, R & R Clark, Ltd. London. Great Britain. 136 pp.

Proceedings of the 58th International Convention of Society of Wood Science and Technology
June 7-12, 2015 – Grand Teton National Park, Jackson, Wyoming, USA

Natural Weathering Performance of Exterior UV Coating on Fast Growing Tropical Woods

Wayan Darmawan[(1)], Dodi Nandika[(1)], Rita Kartikasari[(2)], Helgadara[(2)], Douglas Gardner[(3)], Barbara Ozarska[(4)]

[(1)]Prof., Department of Forest Products, Faculty of Forestry,
Bogor Agricultural University (IPB), Bogor (16680), Indonesia.
Phone +62-251-8621285, Fax. +62-251-8621256
E-mail : wayandar@indo.net.id
* (Corresponding author)
[(2)]Research Assistant, Department of Forest Products, Faculty of Forestry,
Bogor Agricultural University (IPB), Bogor (16680), Indonesia.
[(3)] Professor, the University of Maine, USA
[(4)]Associate Professor, the University of Melbourne, Australia

Abstract

Wood products exposed outdoor could be weathered, especially in the tropical region with high in sun light intensity, rain intensity, and relative humidity. An effort that could be done to protect and enhance wood performance is finishing. The purpose of this research is to understand the durability of finishing layer of the finished wood exposed outdoor. The effects of surface condition of boards (planed and unplaned), sawing pattern (quarter sawn and plain sawn), and two water based wood finishes (Sayerlack and Ultran Politur P-03 UV) were studied.

The experimental results showed that finishing layer of pine was the lowest in durability. The results also indicated that durability of finishing layer depicted by flat sawn boards were lower than that of the quarter sawn board. The finishing layer was considered to provide a good protection to the surfaces of board against failures. The presence of failure due to microbial disfigurement and checking on the surfaces of the finished samples (in average) were 15% and 18% consecutively. On the other hand, the percentages of failure were observed to be 60% due to microbial disfigurement and 20 % due to checking for the unfinished wood. Comparing the two exterior water-based wood finishes used in this experiment, it was found that the two water based coating provided almost the same protection against microbial disfigurement and cracking.

Keywoord : Weathering, UV coating, tropical woods, checking, microbial disfigurement

Introduction

Wood is subject to degradation by biological (bacteria, fungi, and insect), mechanical, chemical, climatic, and thermal factors. Weathering is a general term used to define a slow degradation of wood materials exposed to the weather. Degradation mechanism depends on the type of wood material, but the cause is a combination of the factors. It is a well-known fact that the shorter wave lengths of the solar spectrum having higher photon energies are more deeply absorbed into polymeric materials such as wood, and the structure of chemical bonding within the cell wall is adversely influenced. The weathering initially causes the color of the wood surface to change, followed by the occurrence of surface checking and increased roughness of the samples. The discoloration of the surface is a direct indication of the chemical modification in the cell wall due to weathering. Most of the time, weathered wood would have a more pronounced yellow color than unexposed wood as a result of the modification of lignin and hemicelluloses. Such discoloration in the cell wall is influenced by photochemical reactions leading to the degradation of wood constituents, mainly lignin. A major part of solubilized lignin during degradation is washed out by rain. However, fiber-rich cellulose with a higher resistance against ultraviolet light degradation remains in the cell wall without significant modification and results in the wood acquiring a whitish to gray color (Feist and Hon 1984; Rowell and Barbour 1988).

Wood products, used for the outermost barrier to the weather are often wood siding, windows, decks, roofs, and garden furniture). If these wood products are to achieve a long service life, the weathering process and wood finishing (coating) treatments to retard this degradation should be understood. Surface coating of woods for exterior has two basic functions. One is to give an aesthetically acceptable surface appearance and color. The other is to provide protection against wood degradation by microbiological, chemical, physical or mechanical attack. For decorative purposes, the coating layer should be durable and retain its gloss and color for longer period of time, and either be unchanged by solar radiation. For protective purposes, the coating should be durable and retain its physical properties as long as possible in order to extend the interval between maintenance. These protective properties play an important role in the selection of proper coating materials for supreme durability. Assessment of these protective properties of coatings is a great importance. The durability of a coated exterior wood surface depends on its ability to resist the degradation processes that act on the coating and the wood substrate.

Wood products used under outdoor environmental conditions should be finished using different types of coatings with the purpose of protection so that the overall service life of the wood product is extended. Two basic types of treatment or coating methods are

commonly used to enhance resistance of wood surfaces against weathering. The first method is the applications of water repellents, and preservatives to protect wood against moisture and microbial activity. The second method is the application of wood finishes to the surface in the form of thin layers with limited penetration. In recent development, both water repellent, preservative treatment and finishing have been investigated for enhancing weathering resistance of wood (Williams 2005; Jacques 2000; Nejad and Cooper 2011).

Research works have investigated the application of inorganic chemicals to the surface of wood, including copper ethanolamine (Cu-MEA) to enhance its resistance against weathering (Zhang et al. 2009). It is determined that a Cu-MEA treatment delays the degradation of lignin due to weathering. It is also reported that the discoloration of wood decreases with increasing concentration of copper in the chemical (Williams 2005). According to findings of a past study, photo-stabilization of wood using chromated copper arsenate (CCA), ammonium copper quat (ACQ1900), linseed oil results in the decrease in delignification, and copper tebuconazole (CA-B) results in a reduction in wood discoloration (Temiz et al. 2007; Nejad and Cooper 2011). Treatment of solid wood with a melamine based resin is considered for possible protection of wood products against weathering, without changing their natural appearance (Hansmann et al. 2006). However, it has some limitation due to the formaldehyde emission. Another method is the application of clear-coats, which is the easiest and most common method for protecting wood against weathering degradation. Coating wood with water-borne transparent acrylic finishes is not very effective against photo-discoloration. However, wood products coated with semi-transparent acrylic is found effective against photo-degradation, which might be due to having a pigment content restricting transmittance of UV light to the wood surface (Schaller and Rogez 2007; Allen et al. 2002; Deka and Petric 2008). Therefore, it is important to reduce the light energy reaching the wood surface with use of a coating to prevent its photo-degradation.

Recently, organic and inorganic UV light absorbers have received great attention in transparent wood coatings because of their excellent properties as UV light blockers. Application of epoxidized triazine UV absorbers to wooden surfaces has realized increased photostability of surfaces with performance improvements (Kiguchi et al. 2001; Ozgenc et al. 2012). Though, there is no significant difference between acrylic clear-coats containing the organic and inorganic UV absorbers for stabilizing wood color and protecting the quality of the surface, however after exposure of the coated wood to weathering, the color stabilization and quality of both the acrylic clear-coat surfaces showed better quality than that of the control samples (Ozgenc et al. 2010; Schaller et al. 2008).

The previous results indicate that visible and UV radiation inevitably impacts the wooden surface when transparent varnishes are employed, even in the presence of various UV absorbers or free-radical scavengers in such coatings. The visible and UV radiation photodegrade the lignin in the wooden surface beneath the coating, leading to delamination and subsequent catastrophic coating failure due to the continued action of sun, rain, and biological factors. This coating failure leads to checking and cracking on

the wood surfaces. Checking may increase the uptake of water, thus accelerating the degradation on wood surfaces. Decay fungi, and mildew fungi often flourish when excessive water is present. Moisture also encourages the growth of lichens and other microorganisms that discolor the wood surface. Therefore, it is important to stabilize wooden surfaces prior to the application of transparent coatings to increase the exterior performance of clear coatings. This was the concept underlying our attempt to enhance exterior performance of clear coatings through stabilization of wood surfaces.

Since the main causes of wood surface degradation are UV irradiation, moisture uptake, and fungal activity, the approach taken in an attempt to enhance the weathering performance of clear-coated boards was pretreatment the surfaces of wooden boards and then apply clear coatings. Water repellent and water repellent preservative pretreatment were applied in this study. The clear coatings applied to the exposure surface of the pretreated boards were either UV acrylic and alkyd varnish. The clear-coated boards were exposed to exterior for 1 year. The purpose of this research work was to investigate the performance characteristics of UV clear coatings on fast growing woods under extended (3 years) natural weathering exposure.

Materials and Methods

Specimens preparation

Sample trees were obtained from a plantation forest planted by government at the West and East Java, Indonesia. Fast growing pine (*Pinus merkusii*) and teak (*Tectona grandis*) and slow growing teak (*Tectona grandis*) of 3 trees each were selected from the plantation site as representative specimens. The sample trees having straight stems, and with free external defects were chosen with the intent of minimizing tree-to-tree variation. The characteristics of the sample trees are shown in Table 1. After felling, the trees were cross cut in length of 2.0 m from the bottom part of the tree stem. The sample logs were kept cold, and maintained in the green condition, and they were transported to the wood workshop for preparation of test specimens. The sample logs were band sawed in flat cutting pattern to produce flat sawn (radial) and quarter sawn (tangential) flitches in thickness of 25 mm. The flitches were edged, and the boards produced were seasoned at 25 ^{o}C and relative humidity of 80% until moisture content of about 15% was reached. The boards were planed and cross cut to produce panels of 20 x 150 x 300 mm for specimens of natural weathering tests. Selection of 32 panels completely heartwood of each species for the test was done carefully to keep the defects free panels.

Coatings application

An industrial water-based coating was chosen. Ultran lasur transparent coating, representing a range of coating properties was used in the test set-up. Different wood/coating systems, consisting of a combination of wood substrate and coating, were included in this research. For each wood/coating system four replicates were produced resulting in 32 wood samples. The coating was professionally applied by brushing. All of the specimens were lightly wiped to remove any excess solution from their surface and

weighed at an accuracy of 0.01g to determine the retention value of the coating in the samples. These samples were retained in the laboratory for one additional week.

Outdoor exposure

Two replicate samples for each coating and for uncoated control samples were exposed outdoors, positioned vertically facing south west at the research field of the Bogor Agricultural University for 3 years. All samples were assessed visually each week for evaluating degree of checking, and degree of surface disfigurement by microbial (fungal or algal) growth using the rating scale developed in ASTM D 660-2000 and ASTM D 3274-2002, respectively. This rating scale is suitable to assess the weathering of coatings on tropical hardwood as it combines different features and includes specific degradation phenomena. The rating numbers have an increment of 2 allowing intermediate ratings. The photographic standards of the ASTM rate the checking and disfigurement of paint films from 0 to 10. A rating of 10 would indicate a film totally absent of checking or disfigurement by particulate matter. To analyze the development of surface appearance during the exposure, photographs on the surfaces of the uncoated and coated samples were made every week. Images were also made using digital video microscope to analyze the degree of checking, and disfigurement by microbial.

Results and Discussion

This study contains the data of 1 year of outdoor exposure, starting from October 2014 up to September 2015. One year outdoor exposure caused mainly aesthetical changes for the Ultran Lasur UV. Based on the microscopic evaluation, it was observed that the pine samples had a higher degree of microbial disfigurement (Figure 1 and 2). The uncoated teak and pine wood surfaces exposed to UV irradiation had several checks. Pine control samples had the highest numbers of checks identified as class 8, while teak control samples were within class 9. The coated teak and pine samples showed no checks after one year exposure, but had basic changes due to weathering.

The color change of both the uncoated pine and teak wood was higher than that of the coated pine and teak samples (Figure 3). It was observed from the micrographs that the depth of coating penetration was greater in the teak samples as compared to that of the pine specimens. The reason for the differences of the depth of the penetration in pine compared to teak could be due to the anatomical structure of the species.

Coating degradation gradually became more pronounced during weathering. At the beginning of the weathering, up to 1 year outdoor weathering, mainly aesthetical changes appeared. Therefore, the visual ratings up to 3 years would be considered for weathering assessment of the wood/coating systems under this study.

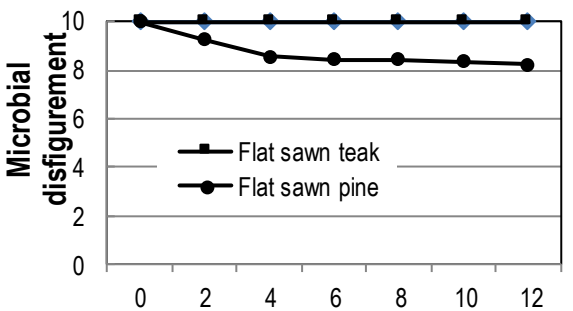

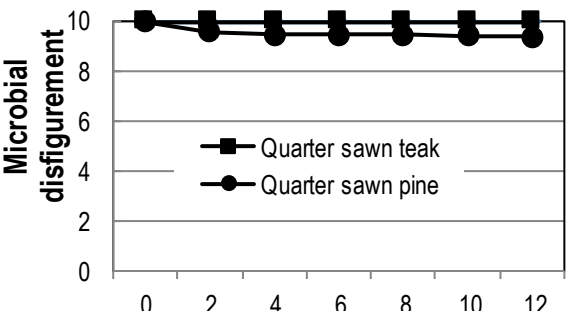

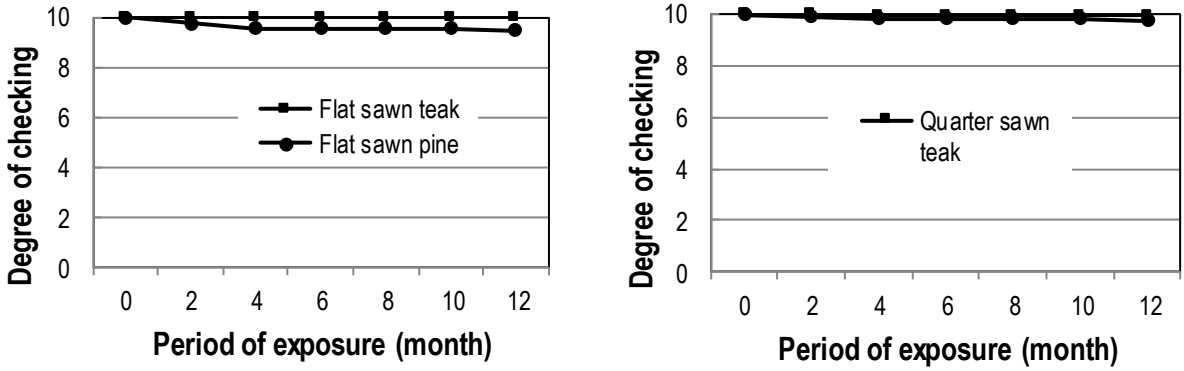

Figure 1. Degree of microbial disfigurement and checking for the flat and quarter sawn woods after one year of exposure

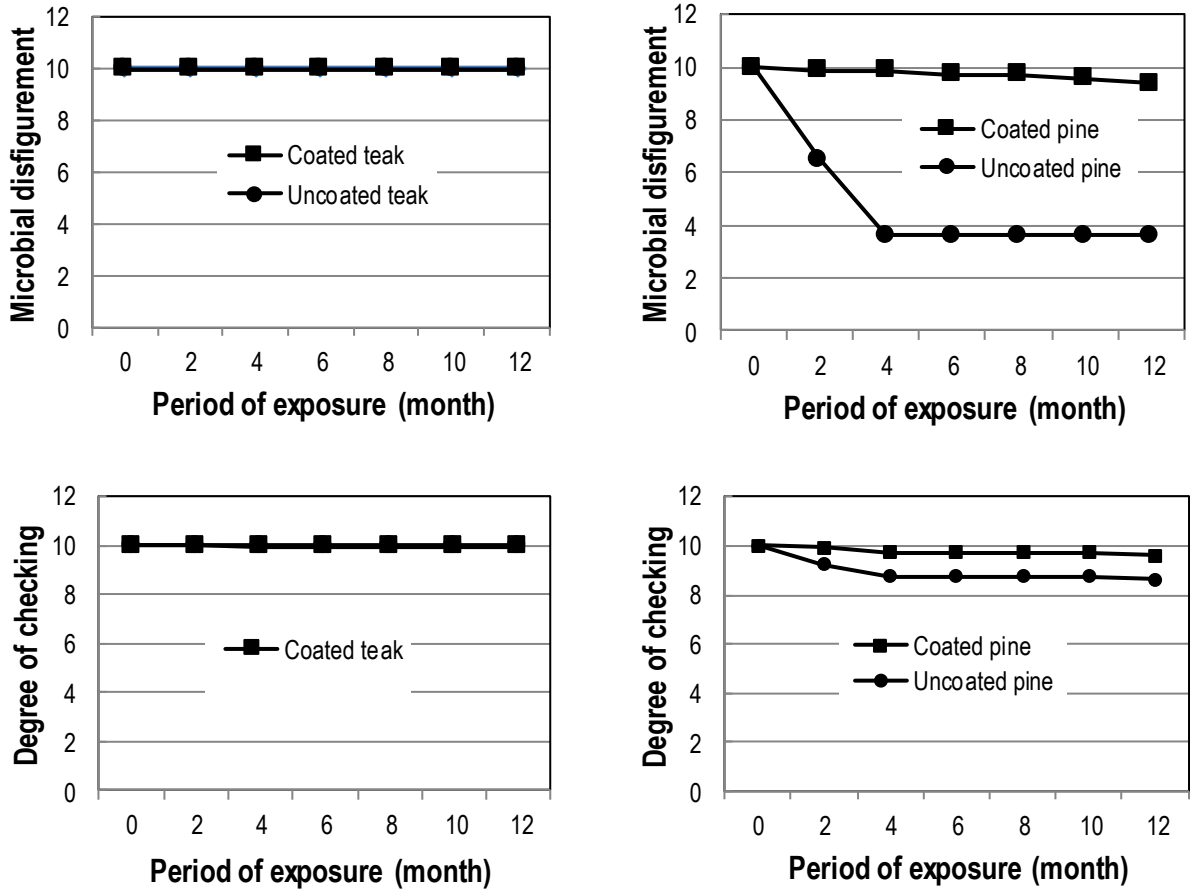

Figure 2. Degree of microbial disfigurement and checking for uncoated and coated sayerlack after one year of exposure

Figure 3. Uncoated and coated flat sawn teak and pine wood after one year weather exposure

Conclusion

Best performance was recorded for the water-based coatings used in this study. It was observed that aesthetical changes occur during the first year of outdoor exposure. Loss of gloss and discoloration were the first visible signs of degradation. During the first year of natural weathering the uncoated wood suffered a significant decrease on weathering performance. Teak wood retained better weathering performance than the pine wood.

Literature Cited

Allen, N. S., Edge, M., Ortega, A., Liauw, C.M., Stratton, J., and Mclntyre, R. B. **(2002)**. Behaviour of nanoparticle (ultrafine) titanium dioxide pigments and stabilizers on the photooxidative stability of water based acrylic and isocyanate based acrylic coatings. Polym. Degr. Stabil. Vol 7 (8) : 467 -478.

Deka M., and Petrid M. **(2008)**. Photo-degradation of water bome acrylic coated modified and non-modified wood during artihcial light exposure, BioResources Vol. 3 (2) : 346-362

Feist W. C., and Hon D. N. S. **(1984).** Chemistry of weathering and protection, In: Rowell, R. M. (ed.) The Chemistry of Solid Wood, Advances in Chemistry Series No. 207, American Chemical Society, Washington, DC, USA, Chapter 11, pp. 401-451.

Hansmann C., Deka M., Wimmer R., and Gindl W. **(2006)**. Artificial weathering of wood surfaces modified by melamine formaldehyde resins, Holz Roh Werkst. 64 (3) :168-203

Jacques L. F. E. **(2000)**. Accelerated and outdoor/natural exposure testing of coatings. Prog. Polym. Sci., Vol. 25 (9) : 1337 -1362.

Kiguchi M., Evans P. D., Ekstedt J., Williams R. S., Kataoka Y. **(2001)**. Improvement of the Durability of Clear Coatings by Grafting of UV-Absorbers on to Wood. Surf. Coat. Int. Part B: Coat. Trans., Vol. 84 (4) : 263–270 (2001)

Nejad M., and Cooper P. **(2011)**. Exterior wood coating : Performance of semitransparent stains on preservative treated wood. J. Coat. Technol. Res., Vol 8 (4) : 449-458

Ozgenc O., Hiziroglu S., and Yildiz U. C. **(2012)**. Weathering properties of wood species treated with different coating applications. BioResources Vol 7 (4) : 4875-4888

Rowell, M., and Barbour, R. J. **(1988)**. Archaeological wood: Properties, chemistry and preservation," In: Proceedings of 196th meeting of the American Chemical Society, Washington, Chapter 11.

Schaller C., and Rogez D. **(2007)**. New approaches in wood coating stabilization, J. Coat. Technol. Res. Vol. 4 (4) : 401-409

Schaller C., Rogez D., and Braig A. **(2008)**. Hydroxyphenyl-s-triazines: Advanced multipurpose UV-absorbers for coatings, J. Coat. Technol. Res. Vol. 5 (1) : 25-31.

Temiz, A., Terziev, N., Eikenes; M., and Hafren , J. **(2007)**. Effect of accelerated weathering on surface chemistry of modified wood, Appl. Surf. Sci. Vol. 253 (12) : 5355-5362.

Williams, R.S. **(2005)**. Handbook of wood chemistry and wood composites, In : Weathering of Wood, Forest Service, Forest Products Laboratory, USDA, Chapter 7.

Zhang, J., Kandem, D. P., and Temiz, A. **(2009)**. Weathering of copper-amine treated wood, Appl. Surf. Sci., Vol. 256 (3) : 842-846.

Proceedings of the 58th International Convention of Society of Wood Science and Technology
June 7-12, 2015 – Grand Teton National Park, Jackson, Wyoming, USA

Influence of Inherent Yellow-Poplar Characteristics on Adhesion Properties Needed for Cross-Laminated Timber Panels

David DeVallance, david.devallance@mail.wvu.edu
Daniel Hovanec, dhovanec@mix.wvu.edu

West Virginia University, PO Box 6125, Division of Forestry & Natural Resources, Morgantown, WV 26506

Abstract

Low-grade hardwood timber is an abundant resource in the Eastern United States. Hardwood timber species are not currently approved for manufacturing cross-laminated timber (CLT) panels under the ANSI/APA PRG-320, Standard for Performance-Rated Cross-Laminated Timber. However, many low-value, low-grade Appalachian hardwoods could be used for producing CLT products once the necessary research is performed. Specifically, it is necessary to determine which controllable factors affect adhesive bond quality, as the use of hardwoods in a bonding assembly can results in poor bond quality. For example, a greater presence of extractives can interfere with available bonding sites on the wood surface, and higher density can negatively affect bond quality as the dimensional changes resultant of moisture absorption and loss can create stress on the bond line. The objective of this research was to determine the characteristics of yellow-poplar lumber that affect adhesive bond quality for use in cross-laminated timbers (CLTs). Twelve different treatments were applied to yellow-poplar lumber to examine the interactions and main effects of adherend thickness, lamination orientation, and orthotropic orientation (saw pattern). Bond strength and durability was determined using shear-block and cyclic delamination tests. Results related to the inherent yellow-poplar characteristics that result in the best adhesion properties will be presented and compared to industrial-accepted softwood controls.

Proceedings of the 58th International Convention of Society of Wood Science and Technology
June 7-12, 2015 – Grand Teton National Park, Jackson, Wyoming, USA

Global Trends in Furniture Production and Trade and the Turkish Furniture Industry

Tuncer Dilik [1] – K. Hüseyin Koç[2] – E. Seda Erdinler[3]–Emel Öztürk[4]*

[1] Associate Professor, Department of Forest Industrial Engineering, Faculty of Forestry, Istanbul University, 34473,Istanbul, TURKEY.
** Corresponding author*
tuncerd@istanbul.edu.tr
[2] Professor Dr., Department of Forest Industrial Engineering, Faculty of Forestry, Istanbul University, 34473, Istanbul, TURKEY.
hkoc@istanbul.edu.tr
[3] Assistant Professor, Department of Forest Industrial Engineering, Faculty of Forestry, Istanbul University, 34473, Istanbul, TURKEY.
seda@istanbul.edu.tr
[4] Research Assistant Dr., Department of Forest Industrial Engineering, Faculty of Forestry, Istanbul University, 34473, Istanbul, TURKEY.
emelozt@istanbul.edu.tr

Abstract

New trends and their reflections show themselves also in furniture production and trade. The close relationship of furniture with fashion causes easier exposure of the trends in various fields from furniture design to production technology, procurement methods to renewal and changing interval. The study analyzes the impact of global furniture trends on the industries. For this purpose, status of the Turkish furniture industry, which has gained a fast development process, is being examined in terms of production capacity and trade volume, and it is tried to determine the impact of trends on development strategies. The priorities for ensuring sustainability in development are also discussed. In 2012, the global furniture production has been realized as US$ 450 billion, it's been clearly understood from the export figure of US$ 160 billion and import figure of US$ 154 billion that the international trade increases gradually. As mainly the first 25 countries in the list perform the global furniture trade, it can be said that 70 countries have an active role in the industry with roughly 200 companies. Although Turkey has more than 1% share in the global furniture production with its total production capacity and although new technologies and modern business practices have become common, it is possible to tell that the impact of global furniture trends is on top of the reasons why the market share is not at the desired level and there is no Turkish furniture image in the world yet.

Keywords: Turkish furniture industry, Global furniture trends, Furniture foreign trade, furniture production in Turkey, furniture export of Turkey, furniture import of Turkey.

Introduction

Trends and reflections rapidly developing with the impact of the globalization experienced in every area today also show themselves in furniture production and trade. Exposures arising from the trends are more apparent in the furniture industry compared to the other industries. The close relationship of furniture with fashion causes the impact of the trends to be seen easier in various areas from design to production technology of furniture, procurement methods to renewal and changing intervals. On the other hand, the developing technology and business administration practices oblige following up the trends [Kurtoglu and Dilik 2014]. The study analyzes the impacts of the trends developed in the world on the furniture industry. For this purpose, the status, production capacity and the trade volume of the Turkish furniture industry, which has gained a quick development process, are examined and the impact of the trends on development strategies is assessed. In addition to this, the priorities for ensuring sustainability in development and the trends are discussed.

When the development of the global furniture production during the last ten years is examined, it's seen that the production volume and its share in the international trade have grown apace. This can be seen from the export figure of 160 billion dollars and import figure of 154 billion dollars within the international trade part of the global furniture production of approximately 450 billion dollars, according to 2012 Turkish Statistical Institute (TUIK) and Trademap data. As the furniture industry is among the top five fastest growing industries of the country, it can easily be seen that this development in the world is also available in the Turkish furniture industry. Furthermore, the furniture industry appears on top of the industries with positive foreign trade balance while it continues to grow. With an estimated furniture production value of 11,6 billion liras, Turkey has a market share of more than two percent in the global furniture production. But this market share is not at the desired level considering the existing technological infrastructure of the industry [Trademap 2012, TUIK 2014, Turkey Furniture Products Assembly Industry Report 2013, Anonymous, 2012]. On the other hand, the Turkish furniture industry quickly discovers the new technologies and modern operational practices in the world and aims to increase its market share in the global furniture production. It can be argued that the impact of the global furniture trends is on top of the reasons why no Turkish furniture image is established and the desired level of development is obtained in the world yet. However, the Turkish furniture industry appears to have a remarkable effort in catching and discovering the trends in line with the developments in the world. As a matter of fact, it hosts trend works and innovation exhibitions (like ZOW on March 19-22, 2015 in Istanbul, Turkey Innovation Week on December 4-6, 2014 in Istanbul etc.) featuring the international furniture trends, which are held in the important centers of the furniture world during the recent years [DTM 2012, Imm Cologne 2014].

Materials and Methods

This study, using literature research and an observation based method, the impacts and reflections of the global trends in the field of furniture and decoration on the Turkish furniture industry are analyzed. For this purpose, the Industrial Commodity Statistics generated by the UNSD (United Nations Statistics Division), as well as national or international industry reports and market researches related to the furniture industry are used as a data source. With the data obtained within this scope, the development of the Turkish furniture industry in terms of production and foreign trade volume in line with the strategic targets, as well as the development status of the furniture industry in the world and in Turkey have been analyzed with production and foreign trade values. In addition to this, the status of the global trends and properties in furniture in the Turkish furniture industry has been discussed with sub-sector and product based assessments.

Results and Discussion

Place of furniture industry in the global economy and its development

The furniture industry is one of the most important economic industries in the world with a production value of 450 billion dollars in average together with primary and secondary components. Although half of this furniture produced is sold and consumed within the own production region, it's seen that a significant part (176 billion dollars) is sold outside the production region, in other words is subject to foreign trade. The global furniture industry features a significant number in terms of employment. The industry expands its area each passing day with an employment of 260.000 people, as well as with the furniture produced in the entire world [Trademap2012, Imm Cologne 2014]. In parallel to the economical and technological development, the furniture industry also strives for development and change against the changing demand levels and quantities. For this purpose, organizations and exhibitions with strategic themes, which were organized with a limited amount before, are now organized in great numbers in various countries. Through these exhibitions, both the furniture produced is evaluated in terms of design, diversity, innovation etc., and information related to the status of the industry is provided about the trends in every field from design to production, sales and marketing to after-sales service. Italy, hosting 10 of average 60 international exhibitions organized every year throughout the world, is on top of the exhibition organizations. Italy is followed by China organizing 9 exhibitions every year and Germany organizing 6 exhibitions every year [Gaggenau 2015, UNcomtrade, 2012]. Turkey strives for enabling its activities in this industry with 2 international and 4 national exhibitions organized every year.

Considering the global furniture production data for the last five years, it's seen that China directs the industry in various aspects. As it can be seen from Table 1, only China produces one fourth (25%) of the furniture produced in the entire world. China is followed by the USA (15%), Italy (8%) and Germany (7%) [Trademap, 2012, *CSIL 2011,*

CSIL 2013]. When the distribution rates in the furniture foreign trade are examined, it's seen that China is once again on top of the list with 30.9% and followed by Germany (9.6%), Italy (7.3%), Poland (5.2%), USA (5%), and Canada (2.3%). Turkey ranks 21st among the exporting countries with 1%. USA is on top of the list in import with 22.7%. Germany (10%), France (5.9%), UK (4.8%), Canada (4.3%), and Japan (3.9%) follow USA in the list of the highest furniture importing countries. Turkey ranks 25th in the global furniture import with 0.7%.

COUNTRIES	PRODUCTION (%)	EXPORT (%)	IMPORT (%)
China	25	30,9	1,5
USA	15	5	22,7
Italy	8	7,3	2
Germany	7	9,6	10
Poland	3	5,2	1
UK	3	1,5	4,8
France	3	2,2	5,9
Japan	3	0,9	3,9
Canada	3	2,3	4,3
Turkey	1	1	0,7
Other Countries	29	34	43,2

Table 1: Countries and their shares in Global Furniture Production, Export and Import [Trademap, 2012, CSIL 2011, CSIL 2013].

The effectiveness of the European Union countries compared to the other countries in the world is clearly observed. Their trend determining positions particularly in kitchen furniture and furnished furniture attracts notice. Germany and Italy are at the forefront compared to other European countries both in production, import and consumption. When the European furniture industry is examined within the scope of fields of activity, 35% of the industry is consisted of the producer companies that produce house furniture and furnishing, and furniture for office and outdoor. The associations and unions, fairs, offices and exhibitions operating in this field constitute a section of 30%. Lighting fixture and lighting material producers and household furniture producers have a share of 27% in the industry, while the auxiliary material, semi-finished product and accessory producers have a share of 6% in the industry [Imm Cologne 2014].

Development of the Turkish furniture industry

While listed as a sub-industry under the wooden works industry until 2009, the Turkish furniture industry is defined as a main industry by the Union of Chambers and Stock Exchanges of Turkey within the scope of the targets of the 9th Development Plan. It has become one of the industries without a foreign trade deficit with an increasing export value since 2001, exporting to 214 countries today with an export figure of 1.9 billion

dollars. The industry appears to have important strategic plan targets both for ensuring sustainability in this development, and achieving the targets for the development plans. For the foreign trade vision anticipated by Turkey for the year 2013, the furniture industry aims to be one of the furniture producers in the top 10 of the world and in the top 5 of the Europe with a production expectation of 25 billion dollars and export expectation of 10 billion dollars [Anonymous 2012]. While the per capita income in Turkey was 6.500 dollars in 2005, it has increased by 74% to 11.318 dollars in 2013. Accordingly, the share of the furniture industry has increased in the national income and it has allowed the industry to receive the investments required for the growth of the industry. Considering that the annual furniture consumption per person is 40 dollars in Turkey, 75-80 dollars in Europe, and more than 100 dollars in the USA, however, one can tell that the industry has lack of demand [Anonymous 2012, Turkey Furniture Products Assembly Industry Report 2013]. According to the export data based on the countries of TUIK, the Turkish furniture export has increased by 15% to approximately 1.9 billion dollars in 2012 and the Turkish companies exported to 209 countries. It is remarkable that approximately 84% of the export is made to the first 25 countries. While there is a significant increase in the furniture import of Turkey from 738 million dollars in 2010 to 941 million dollars in 2011, there has been a significant decrease in import with 817 million dollars in 2012. According to this data, the export rates of Turkey based on the product groups display a significant increase. It draws attention that there is no regular increase or decrease in import.

YEAR	2007	2008	2009	2010	2011	2012*
PRODUCTION (Million $)	7.800	9.000	10.500	12.500	14.000	16.300
DEMAND (Million $)	6.600	7.500	8.500	10.000	11.000	12.300
EXPORT (Million $)	1.020	1.316	1.138	1.344	1.583	1.819
IMPORT (Million $)	657	696	518	738	941	817

Table 2: Basic Data for the Turkish Furniture Industry (Million $) (2012 data is temporary) [Turkey Furniture Products Assembly Industry Report 2013, TUIK 2014]*.

Global trends and properties in furniture

The trend concept has a very broad extent and generally used for defining a behavior performed, action taken and technological development or a product expected by the majority of the society in fashion, technology or business fields during the last five to ten years, particularly during the last two years. For example, kitchen furniture trend, office furniture trend or mobile phone trend. The trend is mostly confused with fashion. One of the most fundamental reasons why this concept is confused with the word "fashion" is its impact on the masses. The most important difference between trend and fashion is time. While fashion covers events during a certain period of time, trend does not have such a limitation and even the changes in fashion are shaped with the influence of trends. In this case, fashion can be defined as an outcome of trend [Kurtoglu and Dilik 2014].

The use of vivid and striking colors and multi-purpose characteristics of the furniture can be listed as the most remarkable qualities of the trend determined in furniture during the recent years. It's also seen that the IT technology has an increasingly important place in the furniture world. In addition to their main intended purpose, the furniture has to have distinctive and remarkable properties. Actually, according to the visions of the furniture designers, almost everything in the house including seats, television and coffee table are now controlled remotely. Electronic parts placed inside the furniture, LED lighting technique saving energy and giving more light, and rubber derivative flexible construction materials are among the components frequently seen in this kind of furniture. Another current trend, quickly spreading as details that create a difference, is defined as "Global Style". This new trend, briefly meaning people transferring some designs they saw at the foreign countries during their holiday or in the media to their own living spaces, dominates the furniture and design industry, and also provides new opportunities to the industry [Kurtoglu and Dilik 2014, Imm Cologne 2014, Gaggenau 2015, Hafele 2011, Ergun et al. 2008]. In this context, the new trends expected to dominate the house furniture in 2015 with the impact of the global trends would integrate a single material to several different functions, feature environment-friendly designs, and decorate the walls, unusually big paintings and mirrors. It's also anticipated that integrating the multimedia systems into the decoration would become one of the outstanding applications. For example, designs covering the entire wall where the television is integrated into the wall board are expected to become popular over the usual television units on the wall (Picture 1).

*Picture 1: A house decoration example designed according to the global trends [*Blum 2015*]*

The solid wood, which was popular until the end of the 80s in furniture with the impact of global trend and then became less popular, is indicated to be used frequently with the impact of the ecological approach available in every field. Natural colors and natural finishes are preferred while adapting these furniture, which would create a rustic effect, from past to today. For the expected impact of the trends on the bedroom furniture, designing the bed together with the wall instead of bedrail appears as one of the most interesting approaches in the recent years with the use of materials in the entire design. As the retails customers increasingly look for more personal solutions, this naturally causes the furniture industry to generate innovative ideas. We particularly see a very rich

product variety for the kitchens. The collections now feature units with surface materials furnished with brand new patterns, as well as multisite and multiscope placement of Hi-Tech combining ease of use with energy efficiency. The life trends of the year 2014 indicate units with more flexibility and "smarter" functions, integrating modern flat screen televisions with interior architecture. For example, the target of the German kitchen industry appears applying these ideas, while determining good work flow, sufficient storage area and high movement comfort as three fundamental principles of a practical kitchen. Shortening the intervals between the purchases with easy replacement of the units when the designs become old fashioned also provides an advantage for the kitchen industry. As the new houses are mostly small and tight, they do not have a sufficient storage area. Therefore, several possible solutions such as better use of height and depth in the kitchens, where storage is required too much, are being developed [BLUM 2015, Gijs 2013]. About the impact of the global trends on the materials used in furniture; the effort on adapting the light materials, the indispensable material for the planes, ships and automobiles, into every field continues with full pace for a long time. However, it's been found out that this trend does not apply too much in the furniture industry, other than the exception of IKEA using light materials in high quantities. To date, the "lightness" factor did not trigger any industrial shift compelling the development of a new production technology. But this situation is expected to change with the furniture where materials with internal spaces, perfectly hiding the cables and connectors of lighting, home entertainment systems and electronic remote controls, are used. On the other hand, it's seen that the digital printing techniques, triggering innovation in every field with laser cut sidebands, are in forefront of the furniture industry with unlimited opportunities. But it's found out that this situation exposes the furniture industry to these questions: Who will carry out the printing job in the future? Decorators? Panel producers? Or furniture producers? Considering that all of them are investing to digital printing presses, one can say that the situation becomes increasingly unclear.

Summary and Conclusions

In our era where the needs such as quality and functionality stand out, the impact of global trends on the development of the furniture industry is clearly evident. The Turkish furniture industry has set the target of being the 10th biggest furniture producer in the world and 5th biggest furniture producer in Europe for the year 2023, 100th anniversary of the establishment of the Republic of Turkey. As in the development of the global furniture industry, following and anticipating the global trends appears to be important for the Turkish furniture industry in achieving the targeted development.

As a result, the impacts of the global trends observed on the development of the furniture industry can be summarized as follows:

- Emerging and spreading of modern electro-furniture equipped with technology as a requirement of the modern life.
- Reflection of smart house and green building on furniture. The increase in the importance of recycling and furniture wastes.

- Seeing smart furniture and environment-friendly furniture applications more.
- Quick increase of the human- and environment-friendly, light, functional, easily portable, modular furniture, which increase the life quality and provide ease of use in line with the urbanization and increasing housing understanding, in the global market.
- Suppliers attending to the design process more, stakeholders with specialties in different fields focusing more on joint design management works (furniture, electronic, IT technology, accessory etc.).
- Quicker development of advanced design skill, brand power, after-sales service quality effectiveness as the fields leading the growth in the industry.
- Developments in the fields of packing, packaging and transporting fields to increase the international action, facilitating the shipment of the products to distant regions, reducing the sales costs.
- Quickly increasing the use of dirt and stain free fabrics, leathers, environment-friendly sponges, paints and varnishes as a result of the reflections of nano-technology applications in the material.

References

Anonymous, 2012 Furniture Industry Report 2012/1 Science, Industry and Technology Ministry of Turkey, Directorate General of Industry, Ankara, Turkey, 2012.

BLUM, 2015 http://www.blum.com/tr/tr/03/10/ (23.02.2015).

CSIL, 2011 World Furniture Outlook 2010/2011 Annual Percentage Changes (Global Furniture Trade (Annual Trend)), Milan, Italy.

CSIL, 2013 World Furniture Outlook, 12th edition of the Seminar organized by CSIL, Wednesday, April 10, 2013, FIERA MILANO-RHO CONGRESS CENTRE. Italy.

DTM, 2012 Furniture import & export data. The Undersecretariat of Foreign Trade of Turkey, Ankara.

Ergun O, Koc K H, Erdinler E S, 2008 Ecologic Design and Turkish Furniture Industry. Furniture Decoration Magazine, Issue 87, 460-474, November-December 2008, Istanbul.

Gaggenau, 2015 http://www.gaggenau-press.com/TR/tr/press-releases.html?PHPSESSID=2vq69fu8mqlbm8irpblbejud35(27.01.2015).

Gijs van W, 2013 The Innovation Expedition, BIS Publishers, Amsterdam. ISBN:978-605-4789-07-8, TIM- Turkish Exporters' Assembly, December 2014, Istanbul.

Hafele, 2011 http://www.hafele.com.tr/documents/HTR_HAFELE_TREND_2011, (24.12.2014).

Imm Cologne 2014 Final report. http://news.imm-cologne.com/2013/01/final-report-imm-cologne-livingkitchen-2013/#more-484 (13.02.2015).

Kurtoglu A, Dilik T, 2014 Furniture Industry Coursebook Notes, Istanbul University, Faculty of Forestry, Department of Forest Industrial Engineering, Istanbul, Turkey, 2014.

Trademap, 2012 International Trade Center, Trade Statistics, Exports 2001-2011 International Trade in Goods Statistics by Product Group. List of exporters for the selected products 9401- 9404

TUIK, 2014 The Turkish Statistical Institute Database Annual Industrial Products Statistics. Ankara.

Turkey Furniture Products Assembly Industry Report 2013, ISBN: 978-605-137-339-3, TOBB Publication No: 2014/212 , Ankara, Turkey.

UNcomtrade, 2012 United Nations Commodity Trade Statistics Database. http://comtrade.un.org/db/default.aspx (11.02.2015).

Acknowledgement

This study is supported by Scientific Research Projects Coordination Unit of Istanbul University with project no. UDP-51869.

Proceedings of the 58th International Convention of Society of Wood Science and Technology
June 7-12, 2015 – Grand Teton National Park, Jackson, Wyoming, USA

Serviceability Sensitivity Analysis of Wood Floors Using OpenSees

Harvey Burch[1], Samuel Sanchez[2], Arya Ebrahimpour[3]*

[1] Structural Engineer, Engineering System Solutions, 4943 N 29th E, Suite A
Idaho Falls ID, USA
harveyburch@gmail.com
[2] Graduate Student, Dept. of Civil and Environmental Engineering,
Idaho State University, Pocatello ID, USA
sancsam2@isu.edu
[3] Professor, Dept. of Civil and Environmental Engineering
Idaho State University, Pocatello ID, USA
**Corresponding author*
ebraarya@isu.edu

Abstract

This paper reviews several design criteria for preventing unacceptable wood floor vibrations and presents the results of a sensitivity analysis on static and dynamic responses of wood floor systems under occupant-induced loads. To accomplish this task, a user interface for the OpenSees finite element analysis program was developed. The interface was created in Microsoft Excel and allows user input for various floor system properties which are used as input into OpenSees. Results from the OpenSees program are imported into the user interface and compared against multiple acceptance criteria which have been established by researchers to determine fitness of the floor system. It was determined that a system with a 1.92 kPa (40 psf) uniform load modeled as a floor with one continuous piece of sheathing covering the entire floor system produced deflections which averaged 32 percent to a maximum of 45 percent lower than a floor system modeled with jointed sheathing. For a 1 kN (225 lb) force applied at the center of the floor, floors with jointed sheathing had an average of 12 percent and a maximum of 15 percent larger displacements compared to the floors with continuous sheathing. Floors with jointed sheathing had an average of 8 percent and a maximum of 12 percent lower unoccupied natural frequencies compared to the floors with continuous sheathing. Floors with jointed sheathing had an average of 10 percent and a maximum of 13 percent lower occupied natural frequencies compared to the floors with continuous sheathing. Floors with jointed sheathing also achieved an average of 17 percent and a maximum of 38 percent larger frequency-weighted one-second root-mean-square acceleration values compared to the floors with continuous sheathing. The results show that great care must

be taken when simplifying the sheathing setup on a floor model since the results of the model create the illusion of better serviceability performance than actual installed floors will achieve.

Keywords: sensitivity analysis, wood floors, engineered joists, vibrations, OpenSees, finite element analysis, spreadsheet.

Introduction

Annoying floor vibrations in wood floor construction has become a major issue that needs to be considered at the time of design. The widespread use of engineered wood I-joist systems have allowed for longer spans and lighter construction. This advancement has come with many benefits but also with the increase of the vibrational response of floor systems. Footfall impact has been the most common source of annoying vibrations for wood floors. Over the years the design recommendation to limit deflection produced by a uniformly distributed static load of 1.9 kN/m^2 (40 psf) has been span/360. But, this requirement is insufficient in avoiding excessive vibrations. Researchers have presented other design criteria that limit vibrations in wood floors. However, some of the criteria need intensive calculations that require knowledge of structural dynamics.

The criteria studied were those of the International Building Code, Foschi and Gupta (1987), Onysko et al. (2001), Dolan et al. (1999), Lin J. Hu (2007), and Smith and Chui (1988). The first three criteria deal with static deflection. The International Building Code requires that the maximum allowable deflection for floor members with an applied live load be less than or equal to span/360. Foschi and Gupta's criterion requires that a "bare" joist loaded at the center with a concentrated load of 1 kN (225 lb) have a 1 mm (0.04 in.) or smaller defection. This deflection is found using Eq. (1).

$$\delta = PL^3/48EI \tag{1}$$

Onysko, et al. propose a criterion that limits floor vibration more accurately than the standard span/360. They proposed that to limit floor vibrations the following should be used:

a) $\Delta \leq 8.0/L^{1.3}$ for spans beyond approximately 3.0 m and 5.5 m
b) $\Delta \leq 2.55/L^{0.63}$ for span between 5.5 m and approximately 9.9 m
c) $\Delta \leq 0.6$ for spans beyond approximately 9.9 m
d) $\Delta \leq 2.0$ for spans under approximately 3.0 m
e) $\Delta_{udl} \leq L/360$ for all spans

Where, Δ = floor system deflection in mm under 1 kN (225 lb), L = span length in m, and Δ_{udl} = the maximum deflection of a floor member under the action of a uniformly distributed load of 1.9 kN/m^2 (40 psf).

The next three criteria predict acceptability of a floor by calculating the natural frequency of a floor system. Dolan, et al. provided a simple method of estimating the natural frequency. Their criterion proposes that the natural frequency be calculated using the following equation:

$$f = \frac{\pi}{2}\sqrt{\frac{gEI}{WL^3}} \tag{2}$$

Where, g = acceleration of gravity; E = joist modulus of elasticity; I = moment of inertia of joist alone; W = weight of floor system supported by joist; and L = span length.

Based on results of 180 floors tested the acceptability criterion states that for a floor to be adequate, the natural frequency of an unoccupied floor must be higher than 15 Hz, and 14 Hz for an occupied floor.

Hu's criterion deals with a combination of natural frequency and static displacement. This criterion was validated with a database of 160 floors. The floors were rated by occupants as to their vibration acceptability. Hu stated that the allowed deflection can be determined using the following equation:

$$d < \left(\frac{f}{18.7}\right)^{2.27} \tag{3}$$

Where, f = natural frequency (Hz); d = deflection (mm). The static deflection is measured after a load of 1-kN (225 lb) is applied at mid-span.

The last criterion is that proposed by Smith and Chui. Smith and Chui's research focuses on providing a method to predict the dynamic behavior of light-weight wood-joist floors. These floors are semi-rigid and are attached to wood based sheathing. Their method allows the user to predict the natural frequencies and the one-second root-mean-square acceleration under a simplified force function. Since humans are more sensitive to vibrations with natural frequencies between 4-8 Hz, Smith and Chui require that a floor system must have a natural frequency greater than 8 Hz. In addition, the criterion specifies that the frequency-weighted root-mean-square (rms) acceleration experienced by the observer must not exceed a threshold value. This value is a result of the heel-drop test impact where acceptable root-mean-square acceleration must be less than 0.45 m/s^2. Smith and Chui propose the following equation to estimate the floor natural:

$$f_o \cong \frac{\pi}{2a^2}\sqrt{\frac{E_j I_j (n-1)}{\rho_s h b + \rho_j c d (n-1)}} \tag{4}$$

Where, f_o = fundamental natural frequency; a = floor span; b = floor width; c = joist width; d = joist depth; h = sheathing thickness; E_j = modulus of elasticity of joist; I_j = area moment of inertia of joist; n = number of joist; ρ_s = density of sheathing; ρ_j = density of joist.

The objective of the current project is to provide a tool to designers in order for them to evaluate the floor systems at the design stage. The system is evaluated without requiring knowledge of structural dynamics and without the difficulties associated with modeling a complex system in a finite element analysis software. The Excel user interface works with OpenSees finite element package and returns results based on the above-mentioned acceptability criteria.

Program Calibration

Finite element modeling software has become a powerful tool for engineers. For this project OpenSees (2015) is used. OpenSees is an open software created and maintained by the University of California, Berkley. This program has received constant verification at an academic level through an ongoing peer-review process.

The program developed for this project was calibrated using the experimental work by John Wolfe (2007). Wolfe measured the deflections and/or vibrations of a single joist, a single joist and sheathing, and a full floor system composed of five joists and sheathing. Most material values found by Wolfe were used for comparison with the OpenSees model results. But, the effects of joist torsional properties were also included to better match the experimental results. Details of the program are provided in the M.S. thesis by Burch (2013).

Sensitivity Analysis

Using the program developed in this project, several sensitivity analyses were performed on a floor system. The objective was to see the relation between deflection, natural frequency, and the one-second root-mean-square acceleration response and the floor width for both continuous and jointed sheathing. For this study the floor system with parameters given in Table 1 was considered. The floor span was 4.93 m and the width was varied from 1.27 m to 5.33 m.

Joist Type	Engineered I-joist
Joist Center-to-Center Spacing	406 mm
Joist Depth	241 mm
Joist Model	110
Joist Torsional Rigidity (GJ)	574 N.m^2
Span Rating	24 o.c. Single floor
Sheathing Thickness	18.3 mm
Sheathing Modulus of Elasticity	3.19 GPa
Sheathing Poisson Ratio	0.092
Fastener Spacing	254 mm
Fastener Stiffness (Horizontal Plane)	5,318 N/mm

Fastener Stiffness (Vertical Plane – Pullout)	17,513 N/mm
Fastener Stiffness (Horizontal Axis)	17,513 N/mm
Fastener Stiffness (Vertical Axis)	0 N/mm
Occupancy Load	0.096 kPa
Floor Damping	3 %

Table 1. Constant parameters for a floor system with all edges simply supported.

Figure 1 shows the change in static deflection for the widths considered when floor model is loaded by a uniformly distributed load of 1.92 kPa (40 psf) for continuous and jointed sheathing.

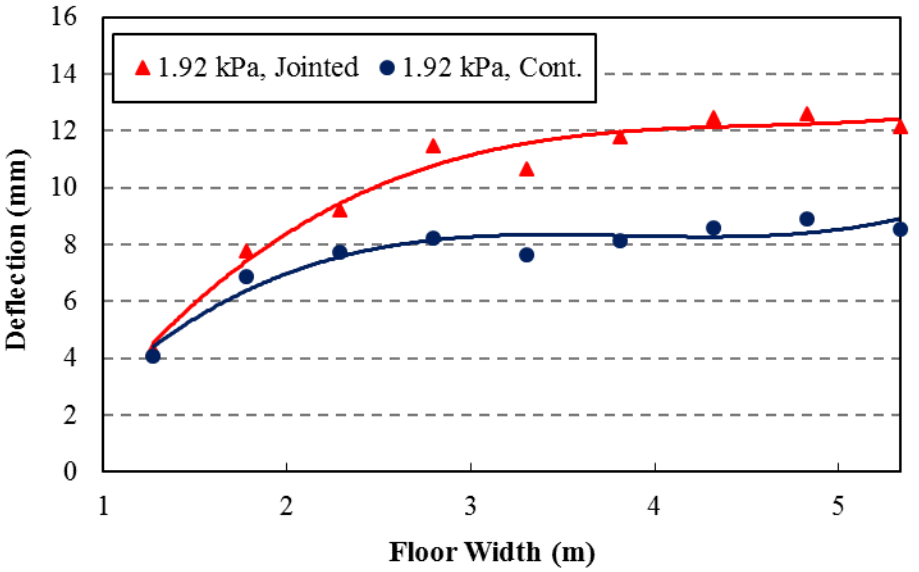

Figure 1. Floor displacement under a uniform load of 1.92 kPa.

Several researchers have noted that the assumption of continuous sheathing is acceptable when considering deflections and vibrations of floor systems. However, as it can be seen from Fig. 1, under a uniform load the jointed sheathing has considerably larger deflection, especially as the floor width increases. Floors with jointed sheathing had an average of 32 percent and a maximum of 45 percent larger displacements under a 1.92 kPa (40 psf) uniform compared to the floors with continuous sheathing.

Figure 2 shows the OpenSees deflections under a 1 kN (225 lb) force at the center of the floor and the allowable deflections based on Hu's recommended formula. See Eq. (3) in the previous section.

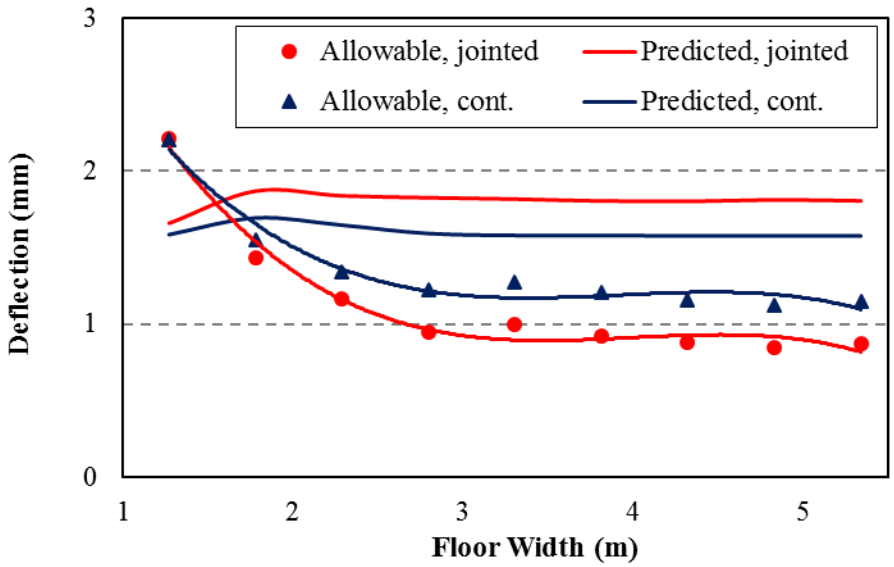

Figure 2. Displacement under 1 kN force.

As it can be seen from Fig. 2, the floor with jointed sheathing has larger deflection and yet, because of lower natural frequency, it is allowed to deflect less under the 1 kN force. For a 1 kN force applied at the center of the floor, floors with jointed sheathing had an average of 12 percent and a maximum of 15 percent larger displacements compared to the floors with continuous sheathing.

Figure 3 shows the occupied and unoccupied natural frequencies, obtained from OpenSees. Figure 3 also shows the calculated natural frequencies based on Dolan, et al. and Smith and Chui formulas which are both based on an unoccupied floor; see Eqs. (2) and (4), respectively. For both floors with jointed and continuous sheathing, the occupied and unoccupied natural frequencies decrease as the floor width increases.

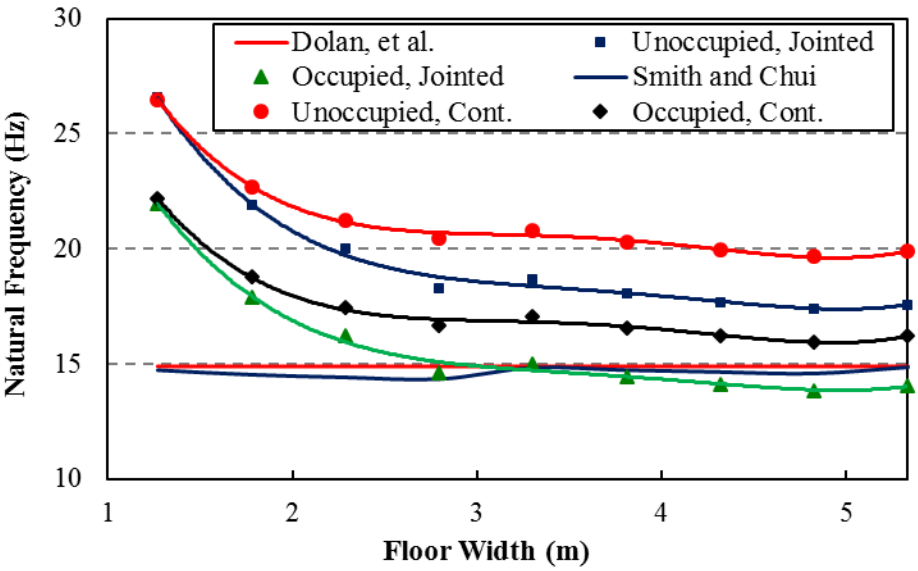

Figure 3. Natural frequency versus floor width.

In addition, for the system with jointed sheathing, both occupied and unoccupied frequencies are lower than the corresponding continuous sheathing floor. Floors with jointed sheathing had an average of 8 percent and a maximum of 12 percent lower unoccupied natural frequencies compared to the floors with continuous sheathing. Floors with jointed sheathing had an average of 10 percent and a maximum of 13 percent lower occupied natural frequencies compared to the floors with continuous sheathing.

Figure 4 shows the frequency-weighted root-mean-square acceleration values with respect to the floor width for both jointed and continuous sheathing. The root-mean-square of acceleration is initially the same for systems modeled with jointed sheathing and continuous sheathing. But, the value for jointed sheathing floor decreases at a slower rate as the floor width increases. Floors with jointed sheathing had an average of 17 percent and a maximum of 38 percent larger frequency-weighted root-mean-square acceleration values compared to the floors with continuous sheathing.

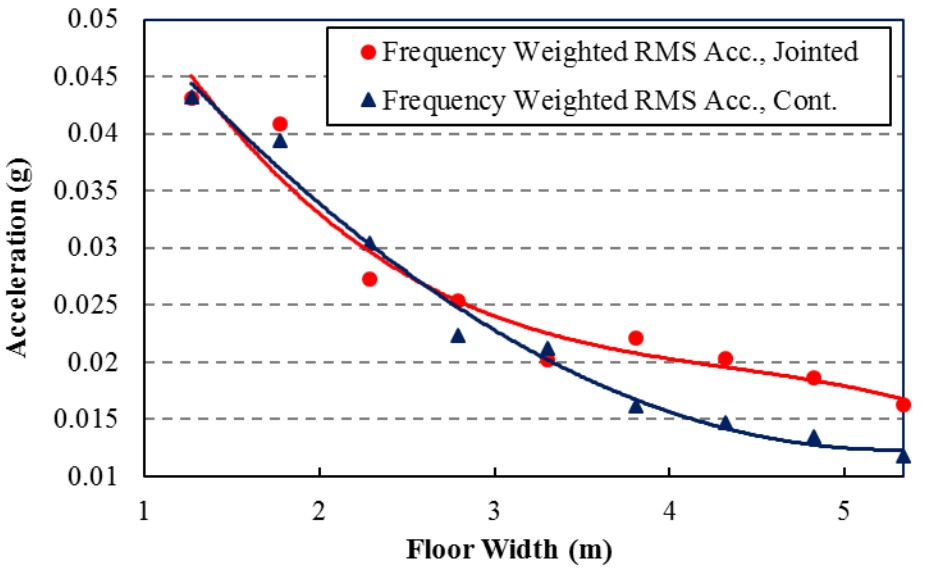

Figure 4. Frequency-weighted one-second root-mean-square acceleration responses.

Summary and Conclusion

Design criteria have been developed by researchers in order to help designers eliminate annoying floor vibrations. However, application of most of these criteria require knowledge of structural dynamics and involve complicated calculations. The program developed in this study requires no knowledge of dynamics and the OpenSees software. It only requires users to enter the design parameters in the Excel interface. In order to quantify the effects of jointed floor sheathing, a series of sensitivity analyses were performed.

Floors modeled with continuous sheathing had lower displacement values than the floors modeled with jointed sheathing. For a 1.92 kPa (40 psf) uniform load, floors with jointed sheathing had an average of 32 percent to a maximum of 45 percent larger displacement than floors with continuous sheathing. For a 1 kN (225 lb) force applied at the center of the floor, floors with jointed sheathing had an average of 12 percent and a maximum of 15 percent lager displacements compared to floors with continuous sheathing.

For unoccupied floors, floors with jointed sheathing had an average of 8 percent and maximum of 12 percent lower natural frequencies compared to the floors with continuous sheathing. Percentage decreased as the width of the floor increased. Floors with jointed sheathing had an average of 10 percent and a maximum of 13 percent lower occupied natural frequencies compared to the floors with continuous sheathing. For one-second root-mean square acceleration values, floors with jointed sheathing had an average of 17 percent and a maximum of 38 percent larger root-mean-square acceleration values compared to floors with continuous sheathing.

It can be concluded that modeling floor systems with once piece of continuous sheathing will give less conservative values than the actual values. In order to obtain more accurate results, floor systems should be modeled with jointed sheathing. Therefore, the program developed in this project is a useful tool as it allows users to examine the changes in displacement, natural frequencies, and root-mean-square accelerations with different system parameters, including the option of jointed sheathing.

References

Burch H R (2013) Finite Element Vibration Analysis of Wood Floors Considering Sheathing Discontinuities. MS thesis, Idaho State University, Pocatello, ID. 254 pp.

Dolan J D, Murray T M, Johnson J R, Runte D, and Shue B C (1999) Preventing Annoying Wood Floor Vibrations. J. Structural Engineering. 125(1): 19-24

Foschi R O, Gupta A (1987) Reliability of floors under impact vibration. Can. J. Civ. Engrg Ottawa 14: 683-689.

Hu L J (2007) Design Guide for Wood-Framed Floor Systems. Canadian Forest Service No. 32: 1-60.

ICC (2012) 333-335. International Building Code, Washington DC.

OpenSees (2015). http://opensees.berkeley.edu/OpenSees/home/about.php (12 Feb. 2015).

Onysko D M, Hu L J, Jones ED, Di LB (2001) Serviceability design of residential wood framed floors in Canada. Can. J. Civ. Engrg Ottawa: 1-8.

Smith I, Chui Y H (1988) Design of light-weight wooden floors to avoid human discomfort. Can. J. Civ. Engrg Ottawa 15: 254-262.

Wolfe J M (2007) Development of experimental data base for finite element vibration analysis of floor systems with rotated engineering wood I-Joist. MS thesis, Idaho State University, Pocatello, ID. 296 pp.

Proceedings of the 58th International Convention of Society of Wood Science and Technology
June 7-12, 2015 – Grand Teton National Park, Jackson, Wyoming, USA

Impact-Deformation Relation of Surface Treated Wood Material

E.Seda ERDINLER[1] K.Hüseyin KOÇ[2] -Tuncer DİLİK[3] - Ender HAZIR[4]*

[1] Assistant Professor, Faculty of Forestry, Department of Forest Industry Engineering, Istanbul University 34473 Istanbul – Turkey
* *Corresponding author*
seda@istanbul.edu.tr
[2] Professor Dr., Faculty of Forestry, Department of Forest Industry Engineering, Istanbul University, 34473 Istanbul – Turkey
hkoc@istanbul.edu.tr
[3] Associated Professor, Faculty of Forestry, Department of Forest Industry Engineering, Istanbul University, 34473 Istanbul – Turkey
tuncerd@istanbul.edu.tr
[4] Research Assistant, Faculty of Forestry, Department of Forest Industry Engineering, Istanbul University, 34473 Istanbul – Turkey
ender.hazir@istanbul.edu.tr[3]

Abstract

Wood and wood based material is used in various areas. Wood material is exposed to many external effects as it is used for furniture. Impact and drops have negative influence on these materials. Surface treatment is effective on wood material's durability. This may change due to layers of paint and the property of the paint used on the material. In this study, it's aimed to determine the differences by investigating the deformations occurring on wooden materials with various surface treatments due to impact and fall. MDF, intensively used in the furniture industry, was used. The impact-deformation relationship of the surfaces applied with wooden material, processed with surface treatment, together with cellulosic and polyurethane paint on various number of layer were examined. For surface hardness; impact tester was used for determining the effect of sudden impacts. Pendulum hardness tester was used to determine the layer hardness of the surfaces. Statistical assessment was performed for determining and revealing the impacts. At result of the study, for coating hardness, polyurethane paint provided better results in applications made with three layers, while cellulosic paint provided better results in applications with four layers, and cellulosic paint provided better results with five layers. Five-layer cellulosic application and three-layer polyurethane application provided similar results. Parameters effecting durability due to impact on different surface treatments and improvement of utilization quality have been determined which would be a base for a more effective application.

***Keywords*:** A. Wood material, B. Surface treatment, C. Impact, D. Deformation, E. Coating

Introduction

Wood is a material with an increasing importance in its use. It is one of the materials that the manufacturers have always used for centuries. Its characteristics and superiorities including the manufacturing stage play an important role in preferring the wood material. The economic life of the wood material should be prolonged and it should be used more effectively as it a valuable material. Protective surface treatments and impregnation applications are among the important procedures applied for prolonging the economic life of the wood material according to the place it is used for. Impregnation is the application related to the protection created by impregnating the chemical preservatives applied to the wooden material, used under atmospheric conditions, by the material. Protective surface treatments have a positive impact on the appearance of the product and also protect the material against external factors.

There are several studies related to different specifications of wood, and such studies still continue. In addition to light resistance and aging, the study carried out by Baysal (2011) examines the surface hardness performance in polyurethane varnish and alkyd based synthetic varnish applied to Fagus Orientalis wood impregnated with CCB. It's been stated that there is an increase in surface hardness in the samples varnished after CCB, and that an increase in surface hardening is observed on beech material as the concentration of CCB was increased.

In the study of Atar et al. (2004), it's been determined that bleaching agents reduce the surface hardness, and the surface hardness of the wood material did not affect the finishing varnish layer hardness.

In his study, Sönmez (1989) stated that the type of tree was not influential in the hardness of varnish layers, but the true impact depended on the type of varnish.

Çakıcıer et al. (2011) determined that surface hardness was very less in varnished samples after thermal treatment compared to the samples without varnish. They have stated that surface hardness value decreased with the increase in temperature and time. The same study also determined that the scraping resistance of the samples with thermal treatment was very lower than the ones without treatment.

In the study they examined the impact of boric acid solution on the hardness of water based varnish layer, Budakçı et al. (2009) suggested using beech material in the furniture and decoration components that were desired to have higher hardness value with the use of water based varnish, and 5% boric acid modification should be performed in the rate of 30% inside the water based varnish.

Oblak et al. (2006) stated that surface treatment statements should be analyzed in detail in order to completely reveal the physical, mechanical and chemical properties. As the surface treatment systems give different results with various application methods, it is important to determine the best method.

Similarly, Pavlic et al. (2004) stated that the systems should be tested and the best system should be selected according to the result of these tests in order to obtain a high quality surface treatment result. Resistance to impact is one of these test methods. It is used for determining the damages to be caused by the impacts during the use of impact test.

Impact tests evaluate the effects of accidental contact damage that may occur during use. They are usually carried out by the direct evaluation of the effect of a falling object, phere or dart of specified shape and hardness, onto the tested surface form different heights. During impact on coated surfaces, the deformation of the substrate can be relevant, significantly affecting the final results. It is of importance that the coating film is flexible enough to withstand, to a certain extent, the stretching at the fringes of the deformation without any cracking or cleavage.

Hardness can be defined as the ability of a coating film to resist indentation or penetration by a solid object. Hardness is also related to the dying state of the coating depending on solvents retention and, for chemical drying coatings, on the cross-linking effectiveness. The efficiency of the drying systems is then fundamental to achieve an adequate hardness. ISO 1522 is a damping method used to assess the hardness of a dry film of paint, varnish or related product by measuring how it reduces the oscillation amplitude of a pendulum (Bulian and Graystone 2009).

Persoz pendulum is used for this research as seen in Figure 1.

Figure 1. Pendulum Hardness Tester (TQC,2015)

The expectations from the wood surfaces vary according to the aim of their user. Resistance of the surface against wearing with different effects or maintaining its current structure against the impacts are among the important properties looked for, including the hardness value of the surface treatment material in several areas of use.

In this study, it's aimed to reveal the effect of different layer thicknesses, applied with different surface treatment materials on wooden panel, on the surface treatment performance.

Materials and Methods

In the study, MDF material is selected as the wooden panel due to its extensive usage in the furniture industry. Commercially manufactured MDF panels were supplied by a local manufacturer. Average density levels of MDF samples were 0.68 g/cm^3. Samples were cut into 1000 mm by 200 mm size having a thickness of 18 mm. Surface treatment was applied with cellulosic and polyurethane paint in different layer thicknesses. Samples were coated employing a spray gun using a pressure of 0.80 MPa. Sequential application of primer and top coat of the finishes were applied to the surface of each panels with an angle of 90 degrees. The layer thicknesses were set as three-layer, four-layer and five-layer. UV undercoat was used on the materials. The materials selected and their specifications are shown (Table 1).

Paint type		Density (g/cm^3)	Solid content (%)	Viscosity (DIN6. sn)
Cellulosic base	Primer coating	1.30	58	60
	Top coat	0.98	44	130
Polyurethane base	Primer coating	1.42	77	115
	Top coat	1.18	50	290

Table 1. *Specifications of the finishing materials used for the experiments.*

Surface treatment material and application method were determined as the main variables of the study. In this context, the relations of impact-deformation arising at different thicknesses were studied. Impact tester ISO4211-4 was used for impacts. Pendulum hardness tester was used for determining the layer thickness of the surfaces. The surface treatment application plan carried out is shown (Table 2). Minitab 17 software program and multiple variance analysis "ANOVA" test have been used for the statistical assessments of the results. The data was considered at the level of α=0,05 for determining the effect and significance levels of the factors examined.

Panel Type	Finish Type	No. of Sample	Reprication	Finishing Process
MDF	Cellulosic Paint	3	5	Application 1 (primer+primer+top coat)
		3	5	Application 2 (primer+primer+top coat+top coat)
		3	5	Application 3 (primer+primer+top coat+top coat+top coat)
	Polyurethane Paint	3	5	Application 1 (primer+primer+top coat)
		3	5	Application 2 (primer+primer+top coat+top coat)
		3	5	Application 3 (primer+primer+top coat+top coat+top coat)

Table 2. *Surface treatment application plan*

Results

Surface treatment applications carried out with different layer thicknesses and paint types are assessed with ANOVA analysis. The results are shown in Analyze of Variance Table (Table 3). The results are assessed statistically with 95% confidence level. As a result of the ANOVA analysis, it's been found out that the paint type is significant in terms of the appearing surface treatment hardness, the layer thickness is not significant alone, but paint type-layer thickness interaction is significant.

Source	DF	Adj SS	Adj MS	F-Value	P-Value
Paint Type	1	2538,7	2538,7	7,11	0,009
Application Type	2	929,1	464,5	1,30	0,278
Paint Type*Application Type	2	8591,3	4295,6	12,04	0,000

Error	84	29980,5	356,9		
Total	89	42039,6			

Table 3: *Analyze of Variance: Coating Hardness versus Paint Type; Application Type*

The main effects obtained according to the results appearing from the surface treatment applications carried out on the MDF panel are shown (Figure 2). Considered in terms of the paint types, the pendulum hardness values of the cellulosic paint are better than the polyurethane paint.

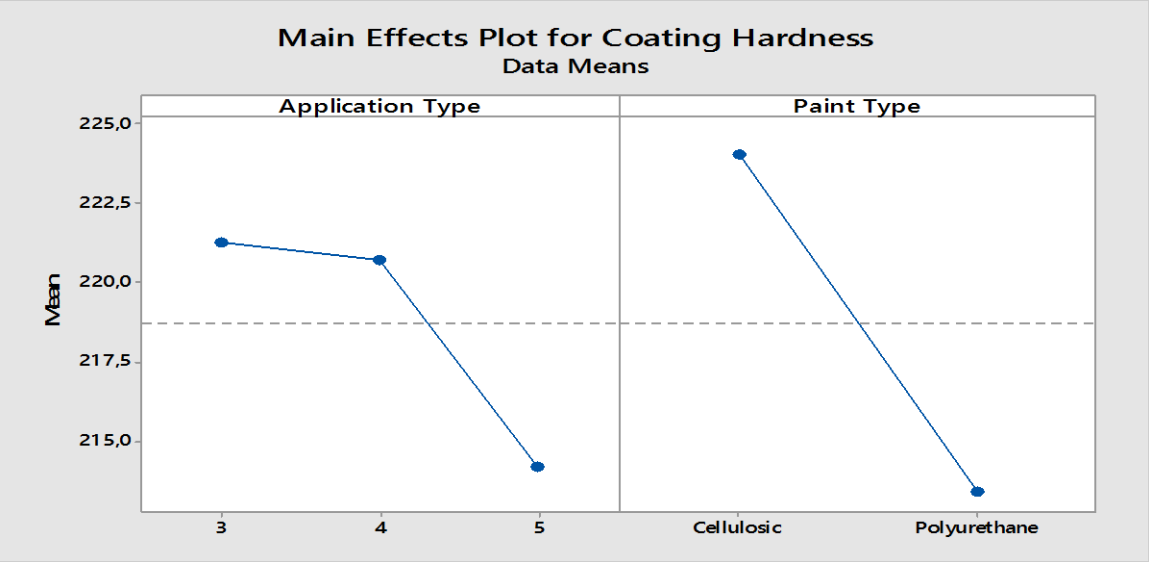

Figure 2: Main Effects for Coating Hardness

The results obtained when we assess the surface treatment parameters with interaction are as shown (Figure 3). Polyurethane paint provided better results compared to cellulosic paint in applications made with three layers. Cellulosic paint provided better results compared to polyurethane paint in applications made with four layers. For the applications made with five layers, cellulosic paint provided better results compared to polyurethane paint.

When the applications are compared with each other, five-layer cellulosic application and three-layer polyurethane application provided similar results.

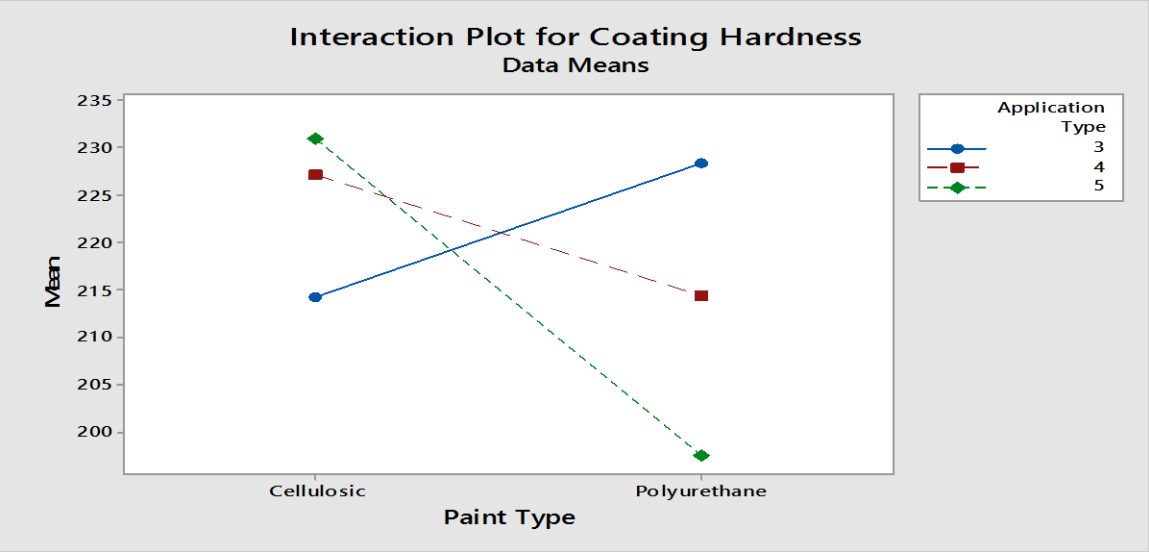

Figure 3: Interaction for Coating Hardness

Conclusions

It might be expected that the surface hardness values increase in general when the layer thickness is increased in surface treatment applications. According to the results of the study, however, there are significant differences when the interactions between the paint and number of layers are taken into account. Therefore, one can say that there is a need for determining different application thicknesses for different paint types for the properties expected from the surface treatment. Results of the studies performed by Oblak et al. (2006) suggest the need for right application methods at the right place for high quality surface treatment application. Waste values and cost arising in the surface treatment applications is another topic for discussion. Working with less layers would shorten the time of applications, as well as reduce the cost. Thus, the surface treatment parameters such as paint type, layer thickness etc. should be determined optimally for ensuring the targeted surface treatment performance.

References

Atar, M., Keskin, H., Yavuzcan, H.G., 2004, Varnish Layer Hardness of Oriental Beech (*Fagus orientalis* L.*)* Wood as Affected by Impregnation and Bleaching, JTC Research, 1(3):498-504.

Baysal, E., 2011, Surface Hardness of Oriental Beech Pre-Impregnated with CCB Before Varnish Coating After Accelerated Lightfastness and Accelerated Aging, *Wood Research,* 56(4):2011,489-498.

Budakci, M., Uysal, B., Esen, R., 2009, The effect of Boric Acid Modification on the Hardness Value of Water-Based Varnish, 5th International Advanced Technologies Symposium, 13-15,may, Karabuk, Turkey.

Bulian F, Graystone JA, 2009, Industrial Wood Coatings. Oxford, UK: Elsevier Publications.

Cakicier,N., Korkut,S. , Korkut Sevim, D., 2011, Varnish Layer Hardness, Scratch Resistance and Glossiness of Various Wood Species as Affected by Heat Treatment, *BioResorces*, 6(2), 1648-1658.

Oblak L, Krıcej B, Lipuscek I (2006) The Comparison of The coating Systems According to the Basis Criteria. Wood Research 51(4):77-86

Pavlic M, Kricej B, Tomazic M, Petric M () Selection of Proper Methods For Evaluation of Finished Interior Surface Quality. Copenhagen:COST E-18

Sonmez, A., Budakci, M., Yakin,,M. ,2004, Effect of Application Methods on the Hardness Gloss and Adhesion Strength of Waterborne Varnish Coating on the Wooden Surface, *Journal of Polytechnic*,(7)3, 229-235.

TQC (2015), http://www.tqc.eu/rsrc/artikel_downloads/pendulum-hardness-tester-sp0500-d44.pdf [10.04.2015]

Acknowledgement

This study is supported by Scientific Research Projects Coordination Unit of Istanbul University with project no. UDP-46844.

Proceedings of the 58th International Convention of Society of Wood Science and Technology
June 7-12, 2015 – Grand Teton National Park, Jackson, Wyoming, USA

The U.S. Hardwood Supply Chain

Urs Buehlmann, buehlmann@gmail.com
Omar Espinoza, espinoza@umn.edu

Abstract

This paper presents an overview of the U.S. hardwood value chain from harvest to lumber. Focus is given to log trade, sawmill log procurement, lumber production, and lumber distribution. This paper uses six earlier publications that individually describe segments of the U.S. hardwood markets to investigate effects of a changing customer base throughout the supply chain. Special focus is given on the role of intermediaries such as log and lumber brokers as these market participants have received scant attention from researchers so far.

Proceedings of the 58th International Convention of Society of Wood Science and Technology
June 7-12, 2015 – Grand Teton National Park, Jackson, Wyoming, USA

Effect of Silviculture on Loblolly Pine as Bioenergy Feedstock

Les Groom, lgroom@fs.fed.us
Thomas Elder, telder@fs.fed.us
Don Bragg, dbragg@fs.fed.us
Anurag Mandalika, anurag.mandalika@gmail.com
Jerry Spivey, jjspivey@lsu.edu

USDA Southern Research Station, 2500 Shreveport Hwy, Pineville, LA 71360

Abstract

Woody biomass is a broadly defined term that encompasses a wide variety of feedstocks ranging from clear bolewood to logging residues. However, the physical, chemical, and thermochemical properties can vary greatly depending on the origin and type of woody biomass feedstock. Furthermore, the majority of woody biomass to liquid transportation fuels plants under construction or being developed use a thermochemical conversion platform with a synthesis gas serving as an intermediate. This presentation will focus on the physical, thermal, and chemical composition of loblolly pine (Pinus taeda) grown under a variety of silvicultural regimes. In addition to the findings from laboratory analysis of physical, chemical, and thermochemical characterization of loblolly pine samples, results will also be shown for subsequent conversion to synthesis gas in a pilot-scale gasification unit. Efficacious conversion of the various woody biomass feedstocks into commercial liquid transportation fuels will be discussed based on the analyses presented.

Proceedings of the 58th International Convention of Society of Wood Science and Technology
June 7-12, 2015 – Grand Teton National Park, Jackson, Wyoming, USA

Life-Cycle GHG Emissions of Electricity from Syngas Produced by Pyrolyzing Woody Biomass

Hongmei Gu, Ph.D[1*]
Richard Bergman, Ph.D[1]

[1]U.S. Forest Service Forest Products Laboratory
Madison, Wisconsin, USA
**Corresponding author*
hongmeigu@fs.fed.us

Abstract

Low-value residues from forest restoration activities in the western United States intended to mitigate effects from wildfire, climate change, and pests and disease need a sustainable market to improve the economic viability of treatment. Converting biomass into bioenergy is a potential solution. Life-cycle assessment (LCA) as a sustainable metric tool can assess the impact of new bioenergy systems. Using the internationally accepted LCA method, this study evaluated the syngas electricity produced via a distributed-scale biomass pyrolysis system called the Tucker Renewable Natural Gas (RNG) system (pyrolysis system developed by Tucker Engineering Associates, Locust, NC). This system converts woody biomass in a high temperature and extremely low oxygen environment to a medium-energy synthesis gas (syngas) that is burned to generate electricity. The pyrolysis process also produces biochar as a byproduct and low-energy (unused) syngas as a waste. Results from the life-cycle impact assessment include an estimate of the global warming (GW) impact from the cradle-to-grave production of syngas for electricity. It showed a notably lower GW impact value (0.142 kg CO_2-eq /kWh) compared to electricity generated from bituminous coal (1.08 kg CO_2-eq /kWh) and conventional natural gas (0.72 kg CO_2-eq /kWh), when the carbon sequestration benefit from the biochar byproduct is included. In addition, the evaluation of the GW impact for Tucker syngas electricity showed the highest GHG emissions came from burning propane to maintain the endothermic reaction in the Tucker RNG unit. Using the previously unused low-energy (waste) syngas to supplement propane use would further reduce GHG emissions (ie fossil CO_2) associated with syngas electricity by 20%.
Keywords: Bioenergy, life-cycle assessment, GHG emission, syngas electricity, woody biomass.

Introduction

Restoration treatments on western U.S. forests produced large quantities of woody biomass that can be used as feedstock for production of biofuels and other bioproducts. Producing bioenergy and bioproducts from such forest thinning or timber harvest byproducts would contribute to achieving broad national energy objectives, including the nation's energy security and reduction of greenhouse gas emissions from fossil fuels. The U.S. Department of Energy and the U.S. Department of Agriculture are both strongly committed to expanding the role of biomass as an energy source and envision a 30% replacement of the current U.S. petroleum consumption with biofuels by 2030 (Perlack et al 2005). Biomass fuels and products are one way to reduce the need for oil and gasoline imports while supporting the growth of agriculture, forestry, and rural economies. Also, expanding biofuels and bioproducts production from biomass has the potential to reduce net greenhouse gas (GHG) emissions and improve local economies and energy security. The 2007 Energy Independence and Security Act (EISA) sets aggressive goals for moving biofuels into the marketplace to reduce the nation's dependence on foreign sources of energy and reduce GHG emissions by increasing the supply of renewable fuels from 4 billion gallons in 2006 to 36 billion by 2022 with 16 billion gallons cellulosic biofuel (EISA 2007). Schnepf and Yacobucci (2013) define cellulosic biofuel as renewable fuel derived from any cellulose, hemicellulose, or lignin sources that has life-cycle GHGs at least 60% less than the baseline life-cycle GHGs from gasoline or diesel as transportation fuel. Life-cycle assessment (LCA) is the pre-eminent and internationally accepted method for categorizing life-cycle GHGs.

LCA as a science-based tool is useful in assessing the claim that expanding bioenergy production from woody biomass has the potential to reduce net GHG emissions. Information provided by this analytical tool is essential for policy makers to make evidence-based judgments on expanding renewable energy production. LCA considers direct and related processes, flows of raw materials and intermediate inputs, waste, and other material and energy outputs associated with the entire product chain or system. Broadly, LCA can assess new products, new processes, or new technologies in an analytically thorough and environmentally holistic manner to guide more robust deployment decisions. LCA can calculate GHG and other emissions over a part or all of the whole life cycle of a product. One huge benefit is that LCA provides sustainability metrics for comparing competing products.

For our study, we applied LCA to the electricity generated from the synthesis gas (syngas) produced by a distributed-scale advanced biomass pyrolysis system, which will be referred to in this paper as the Tucker (developed by Tucker Engineer Associate, Locust, NC) renewable natural gas (RNG) unit. This study is part of a larger USDA project developing and evaluating the Tucker RNG unit that could generate bioenergy and bioproducts for higher value markets. The Tucker RNG unit uses high temperature conversion (>750 °C) in an extremely low oxygen environment to convert the feedstock from forest thinning and mill residues into the syngas that can be used for heat and electricity and into biochar for soil amendment or as a precursor in the manufacturing of

activated carbon and other industrial carbon products. Syngas-generated electricity is intended to substitute a portion (marginal part) of grid electricity generated from fossil fuels, most commonly natural gas and coal. The system was specifically designed to generate a high-quality biochar to become activated carbon and not as a soil amendment which sells at a lower price. However, LCA can focus on life-cycle stages that may not be considered once a process becomes commercialized but still in the development phase to evaluate what-if scenarios. In the present study, the what-if scenario was burning syngas to generate electricity with the biochar as a byproduct.

In this paper, LCA will estimate the GHG emission performance from the Tucker RNG technology in reference to established electricity technologies including fossil fuels. This is the first study to evaluate the production of syngas electricity from a distributed-scale thermochemical conversion system in the United States. We will answer the question of how much GHG emissions in kg CO_2-eq can be reduced by substituting fossil fuel electricity with forest residue-derived syngas electricity. Applying LCA can help to compare the processes or technologies for energy and environmental benefits and identify the hotspots (highest points) for energy consumption and GHG emissions.

Methods

The goal of this study was to estimate the GW impact of the electricity generated from the syngas produced by Tucker RNG unit with biomass residue as the feedstock and compare the results to a fossil fuel reference. To achieve this goal, the life-cycle inventory (LCI) for syngas electricity from cradle-to-grave including processes of raw material extraction, transportation, feedstock processing, pyrolysis conversion, and syngas electricity generation was modeled and conformed to the ISO 14040 and 14044 standards (ISO 2006a,b). LCI needs to be built before the impact analysis can be done. LCI is the data collection portion of a LCA. It tracks and quantifies inputs and outputs of a system including detailed resources, raw material, and energy flows.

Primary data were collected from a one-hour continuous run of the Tucker RNG unit for the pyrolysis converting process. The feedstock was wood chips processed from under-utilized small-diameter logs extracted from National Forests with a mix of conifer species dominated by lodgepole pine (*Pinus contorta*), Douglas fir (*Pseudotsuga menziesii*), and ponderosa pine (*P. ponderosa*). Before feeding into the Tucker RNG unit, the chips were dried to less than 10% moisture content (MC) to improve the performance in Tucker RNG unit. The LCI model was constructed in three parts 1) upstream model, including forest management, thinning material extraction, transportation, and feedstock processing; 2) pyrolysis thermal conversion model; 3) downstream model, including the generation of electricity from the primary product syngas and application of biochar as byproduct.

The focus of this study and the conversion technology is on syngas generation and burning to generate electricity. Therefore, the primary product from the Tucker RNG unit

is considered to be syngas, while biochar from the system is considered a byproduct. The environmental burdens were assigned 100% to the syngas as the product of interest. Since biochar is considered as byproduct in this study, it will not take any environmental burden from the LCA output, but its role for long-term carbon storage in the soil will be analyzed for carbon sequestration benefits in the LCA for syngas electricity environmental impacts. Secondary data were drawn from peer-reviewed literature according to CORRIM guidelines (CORRIM 2010). With the material and energy inputs and reported emissions, the cradle-to-grave LCI model for the Tucker RNG syngas electricity was built in SimaPro 8 to estimate the environmental outputs and cumulated energy consumption (PRé Consultants 2015). Within the SimaPro software, the inventory data were compiled into the impact category indicator of interest, global warming (GW).

Scope

This study covers the cradle-to-grave LCA of electricity generated from syngas produced by pyrolyzing woody biomass. LCI data for producing syngas from the Tucker RNG pyrolysis unit was already constructed by Bergman and Gu (2014) and was incorporated into the model. In addition to the LCA on syngas electricity from this study, data from LCI databases for electricity generated from other sources, such as coal, natural gas, and biomass were drawn and analyzed for a comparative partial LCA to examine the marginal effects on electricity grid. The electricity grid is comprised of many regions comprised of various energy sources (USEPA 2014a). The USEPA has broken the U.S. electricity grid into "eGrids" (USEPA 2014a).The eGrid system from the Northwest (NWPP) region included in the comparison to syngas electricity is referred to as NWPP. The eGrid NWPP is representative of year 2008 mix of fuels used for utility electricity generation in the northwestern United States. Fuels include coal, biomass, petroleum, geothermal, natural gas, nuclear, hydroelectric, wind, and other energy sources. NWPP electricity grid covers area including Washington, Oregon, Idaho, Utah, most of Montana, Wyoming, Nevada, and northern parts of California, Arizona, and New Mexico. It is intended that the Tucker RNG syngas provide marginal electricity for the grid because of its distributed-scale size.

Functional unit

Functional unit is the reference unit used to quantify the environmental performance of a product system. It is also a reference related to the inputs and outputs. Because the goal of this research is to compare the GHG performance of electricity generated from Tucker RNG syngas to that of electricity generated from other source, the functional unit is defined as production of 1 kWh of electricity. Material flows, energy use, and emission data are standardized based on this functional unit within the system boundaries described in the following section.

Unit processes

To do the life cycle impact assessment (LCIA), the syngas electricity system was built from unit processes. LCI databases contain large lists of unit processes. In the product system, starting from the functional unit, related processes are called on and built into the process tree with inputs and outputs matched to the delivery of the functional unit. For

the reference fossil fuel chains, the GHG performance was calculated using data from the USLCI Database (NREL 2012).

Processes for the upstream model of forest management and log extraction in the USLCI Database were used (NREL 2012). Chip processing was modeled with the specific operational data collected as part of this study. Then the pyrolysis conversion process was modeled using Tucker RNG unit specific operation data collected on the system for a 1-hour continuous run. The downstream electricity generation process was modified for Tucker syngas from the USLCI natural gas electricity generation process.
The mainstream model of this study was thermochemical conversion with the Tucker RNG unit. As mentioned previously, Bergman and Gu (2014) provided a detailed analysis of the Tucker RNG unit itself.

The process for electricity generation from the Tucker RNG syngas is similar to the process for natural gas electricity. Electricity is produced from burning the Tucker RNG syngas in a commercial 1.6 MWe Caterpillar generator derated to 1.2 MWe because the syngas has relatively low energy density compared to natural gas. Using wood, the Tucker RNG unit must produce about two times the volume of syngas to generate the same electricity as natural gas. The higher heating value (HHV) of the produced syngas is 19.5 MJ/m^3, one half of the natural gas HHV at 38.3 MJ/m^3. The main components by mass of the syngas are carbon monoxide (55.5%), carbon dioxide (20.1%), and methane (9.2%).

Compiling process data

Starting with the functional unit of 1 kWh electricity generated, fuels and equipment use, and transportation requirements were compiled in the SimaPro model to quantify the GHG emissions to the environment. The model then relates them to the 100-y GW impact according to the Tool for the Reduction and Assessment of Chemical and Other Environmental Impacts (TRACI) method (IPCC 2007; Bare 2011). TRACI 2.1 method is now incorporated in SimaPro software, version 8.

System boundary

Defining the system boundary selects the unit processes to be included in the system. Based on our goal to determine the environmental impacts of syngas electricity, we drew our system boundary to include the upstream of material handling, main conversion process with the Tucker RNG unit, and the downstream electricity product production. Figure 1 shows the system boundary defined for this cradle-to-grave LCA study. The Tucker thermochemical process includes feedstock conveyance, active reacting, passive reacting, condensing, tar cracking, cooling, collecting, and storing. The cumulative system boundary includes both on- and off-site emissions for all material and energy consumed. Fuel and electricity use for the upstream feedstock processing and Tucker pyrolysis converting process were included in the cumulative boundary (solid line) to calculate the total emissions. The on-site emissions include the processes within the dotted line (Fig 1). The off-site emissions include the grid electricity production, transportation, and fuels produced off-site but consumed onsite.

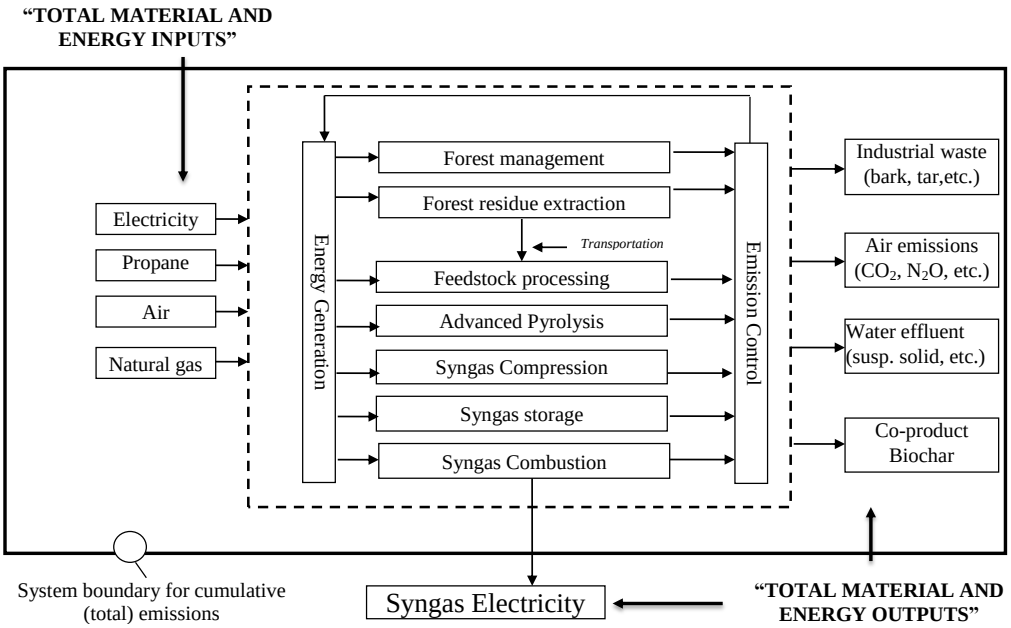

Figure 28. System boundary for the life cycle of generating synthesis gas electricity.

Project limitations

Human labor and the manufacturing LCA of the machinery and infrastructure were outside the system boundaries and therefore not modeled in this analysis.

Cut-off rules

If the mass/energy of a flow is less 1% of the cumulative mass/energy of the model flow it may be excluded, provided its environmental relevance is minor. This analysis included all energy and mass flows for primary data.

Results and Discussion

The environmental impact assessment for producing 1 kWh of bioelectricity from an advanced pyrolysis converting technology using wood residues was carried out using LCA and the results were described below.

LCIA of syngas electricity

The GW impact from cradle-to-gate LCA for syngas electricity was 0.525 kg CO_2-eq/kWh without considering biochar's potential for carbon sequestration. The GW impact results were divided into three stages: feedstock processing, syngas production, and syngas electricity, with syngas production releasing 72% (0.378/0.525) of the total. Feedstock processing is the second highest emission and includes extraction of forest thinning materials, transportation, and size reduction and pretreatment of the feedstock. About 27% of the total GHG emission was from this feedstock processing upstream

stage, which leaves only 1% of GHG emission associated with the syngas electricity generation process. The GW impacts were summarized from fossil CO_2, CH_4 (mainly fossil), and N_2O emissions. The fossil CO_2 emissions for the three stages calculated by SimaPro were 0.002, 0.334, and 0.095 kg/kWh, for syngas electricity generation, Tucker RNG gas, and feedstock processing, respectively. The fossil CH_4 emissions for the three stages were 1.23E-5, 0.0002, and 9.4E-5 kg/kWh, with N_2O emissions broken into 1.07E-5, 1.23E-7, and 3.55E-7 kg/kWh. N_2O emissions were much smaller in quantity but have a much larger GW impact by mass than fossil CO_2 (IPCC 2007).

In terms of the type of energy consumed in each of the three stages, more renewable biomass energy is consumed in the feedstock processing stage than both the syngas producing and electricity generation stage because it uses biomass heating for feedstock drying and some processing. CO_2 emissions from burning woody biomass are not considered in estimating the GW impact because the woody biomass consumption is equal to tree regrowth for a given period. Feedstock drying and processing took place at a sawmill with a wood boiler producing process heat for drying. The endothermic reaction of the Tucker RNG unit was sustained by propane combustion; therefore, pyrolysis conversion was identified as the major fossil fuel energy consumption (ie environmental hot spot) for the whole system. For a comparison, Steubing (2011) reports a GW impact of 0.103 kg CO_2-eq/kWh for a Swiss case where the syngas is primarily composed of CH_4 and very little fossil fuel (ie gas) is consumed in the production of syngas unlike the Tucker RNG unit (Steubing et al 2011).

Carbon sequestration effect from biochar

In this analysis, biochar was produced from Tucker RNG unit as a byproduct, thus taking no environmental burden from the process. However, in the case of biochar, the resultant product is highly stable and recalcitrant, with high carbon content, so that decomposition is delayed for hundreds to thousands of years, beyond current GHG accounting time frames (Cowie et al 2013). Thus, it is important to model this delay in emissions to demonstrate the direct climate change impacts from biochar in the system. As mentioned previously, all environmental burdens were assigned to syngas electricity because biochar was designated as a byproduct.

Biochar is characterized by stable aromatic C structures, low bulk density, and high ash content. The stable storage of biochar in soils represents a long-term removal of atmospheric C; ie C sequestration (Sohi et al 2010). There are two types of carbon movements. The movement of C from one reservoir in the ecosystem to another is called *carbon accumulation*. The movement of C from atmosphere into a reservoir is called *carbon sequestration*. According to IPCC (2007), *carbon sequestration* can be defined as the uptake of C-containing substances, and in particular CO_2, into another reservoir with a longer residence time.

If the biochar produced from the Tucker RNG unit as a byproduct is intended to be applied as a soil amendment, the benefit of C sequestration to slow or even reverse the increase in atmospheric concentration of CO_2 may apply to the GHG emission accounting. From the material ultimate chemical analysis, biochar from forest thinning

residue has a fixed carbon content as high as 90% on a dry weight basis. Based on Wang et al (2014), we calculated a Carbon Stable Factor for the biochar generated from the Tucker RNG unit of 85%. With this, the total C in the biochar produced as a byproduct for generating 1 kWh syngas electricity can be calculated and converted to CO_2-equivalent weight, as a reduction in the total GHG emission accounting for the entire process. The sequestration of the biochar C directly reduces the GW impact as shown in Fig 1. However, transportation of biochar, biochar spreading, and soil management practices and their associated environmental impacts were not included in this study. The GHG emissions from burning fossil fuels from these activities would likely reduce the benefits of applying biochar as a soil amendment (Gaunt and Lehmann 2008).

Comparing GHG emissions of syngas electricity to other electricity technologies

LCA for coal electricity, natural gas electricity, direct biomass combustion electricity, and the Northwest eGrid profile electricity were performed in the SimaPro software with the data from the built-in USLCI Database. Figure 2 shows the results of GHG emission data summarized from LCA. For 1 kWh electricity generated from the Tucker syngas converted from forest residue chips the GHG emissions were estimated to be 0.525 kg CO_2-eq/kWh without taking biochar carbon sequestration into consideration. This is close to the total GHG emission from the eGrid for Northwest region (0.499 kg CO_2-eq/kWh). However, coal and natural gas electricity has a substantially higher value than our studied syngas electricity (1.079 kg CO_2-eq/kWh and 0.72 kg CO_2-eq/kWh, respectively). Electricity generated from biomass direct combustion has a lower GW impact (0.087 kg CO_2-eq/kWh) because of less fossil fuel consumption and neutral impact to the environment from biogenic CO_2 emission, which is the major emission from the Tucker RNG unit technology. When including biochar carbon sequestration effect, the GHG emission value for our studied syngas electricity was reduced by more than 70% to 0.142 kg CO_2-eq. Thus, a notable influence was discovered from carbon sequestration by the byproduct biochar when included and should be emphasized in future analysis for biobased renewable electricity-generating technologies.

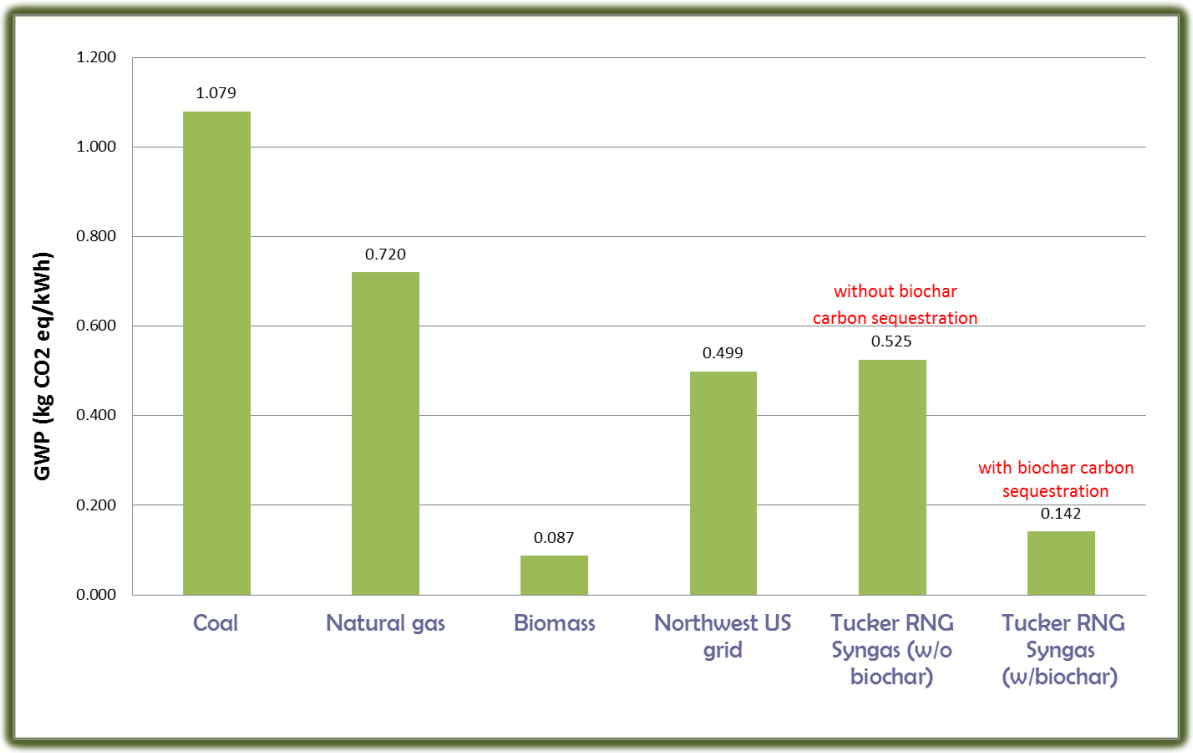

Figure 29. Global warming impacts for various electricity sources and technologies, and global warming potential (GWP) for Tucker syngas electricity with and without carbon sequestration accounting.

GHG performance indicator

To compare the GHG performance between the syngas electricity and fossil or other based electricity, the GHG performance indicator from Sebastian et al (2011) is used here and defined as the following:

$(GHG_{fossil\ or\ other} - GHG_{syngas})/GHG_{fossil\ or\ other}$ = GHG performance (in percentage)

This GHG performance indicator represents the GHG improvement of the syngas electricity over fossil or other source equivalent. The GHG emission for syngas electricity with biochar carbon sequestration is used in the calculations. The indicators are shown in Fig 3. The GHG performance of the studied syngas electricity demonstrated a greater than 80% improvement over the fossil fuel electricity (coal and natural gas), and about 71% improvement over the commercial NWPP eGrid electricity GHG performance. However, there is a negative improvement (–63%) for the syngas electricity over the biomass electricity because of less fossil fuel consumption in the direct biomass combustion to electricity system. Biomass-direct combustion process for electricity is simple and more straightforward than the biomass derived syngas electricity technology. In addition, no additional fossil fuel use is required to keep the reaction going during direct combustion, unlike the Tucker RNG unit. Therefore, it performs better in GHG emission than the studied syngas electricity system.

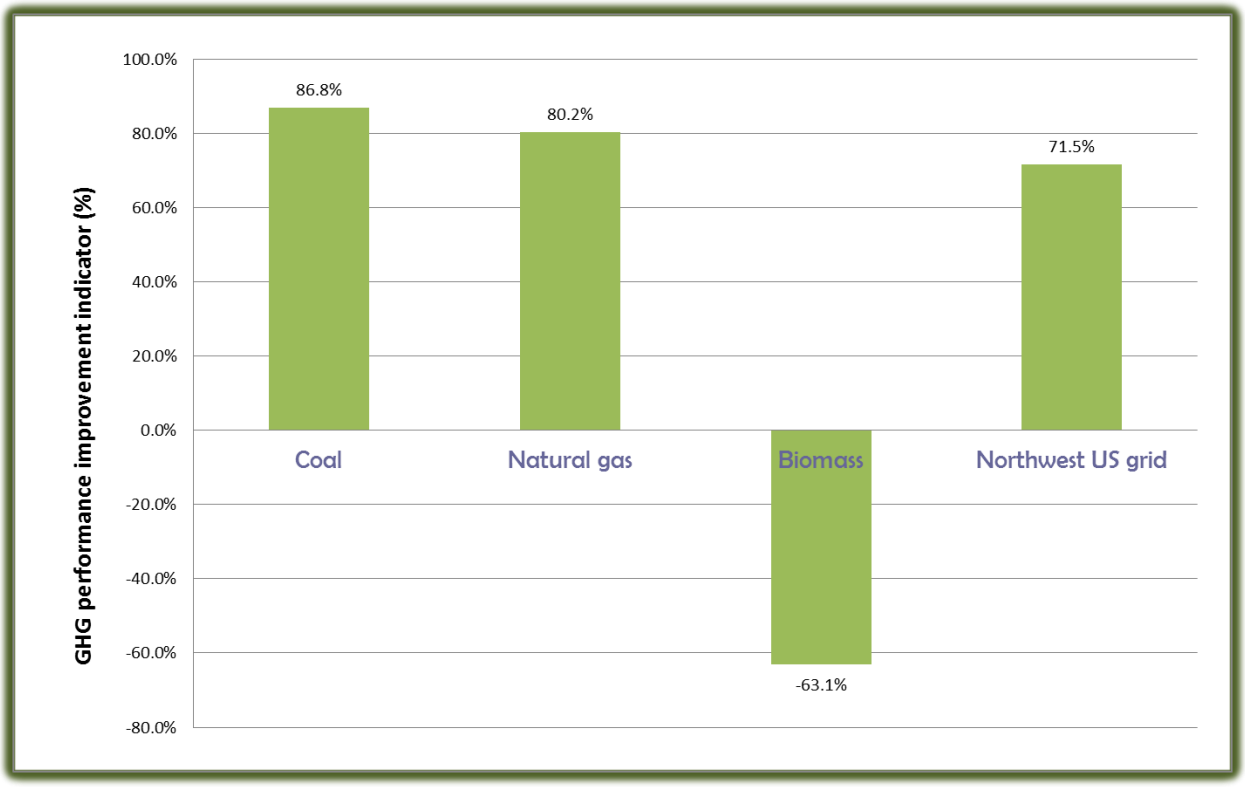

Figure 30. GHG performance indicator for the electricity generated from the Tucker RNG syngas compared to other electricity generation technologies.

In some cases, the process of producing bioelectricity from biomass feedstock is energy-intensive and therefore performs even worse for GHG emissions than fossil fuel electricity (Sebastian et al 2011). Turconi et al (2013) did a thorough review on LCA research for various electricity generation technologies and compare environmental impacts for these technologies. Figure 4 shows the range of data collected by Turconi et al's (2013) paper and our studied syngas electricity GW impact value. The Tucker syngas electricity GW is close or within the range of renewable energy generated electricity including biomass, hydropower, solar energy, and wind electricity. These are all significantly lower than the nonrenewable fossil fuel generated electricity, including hard coal, lignite, natural gas, and oil.

Scenario analysis

Quantifying GW showed both the carbon benefits (eg low GHG emissions) and the carbon "hotspots" such as from burning propane to maintain the endothermic reaction in the Tucker RNG unit. If reducing or substituting propane usage in the Tucker RNG unit is possible, the GW impact could be further reduced. During the pyrolysis conversion in the Tucker RNG system, low-energy (waste) syngas was produced without being collected for use. We anticipate collecting and using this low-energy (waste) syngas to supplement propane usage would further reduce GHG emissions (ie fossil CO_2) associated with syngas electricity. Therefore, we conducted a scenario analysis with 30% propane reduction with the substitute of now-unused low-energy syngas produced from

the Tucker RNG unit. The GWP improved by 20% in total for the cradle-to-grave syngas electricity.

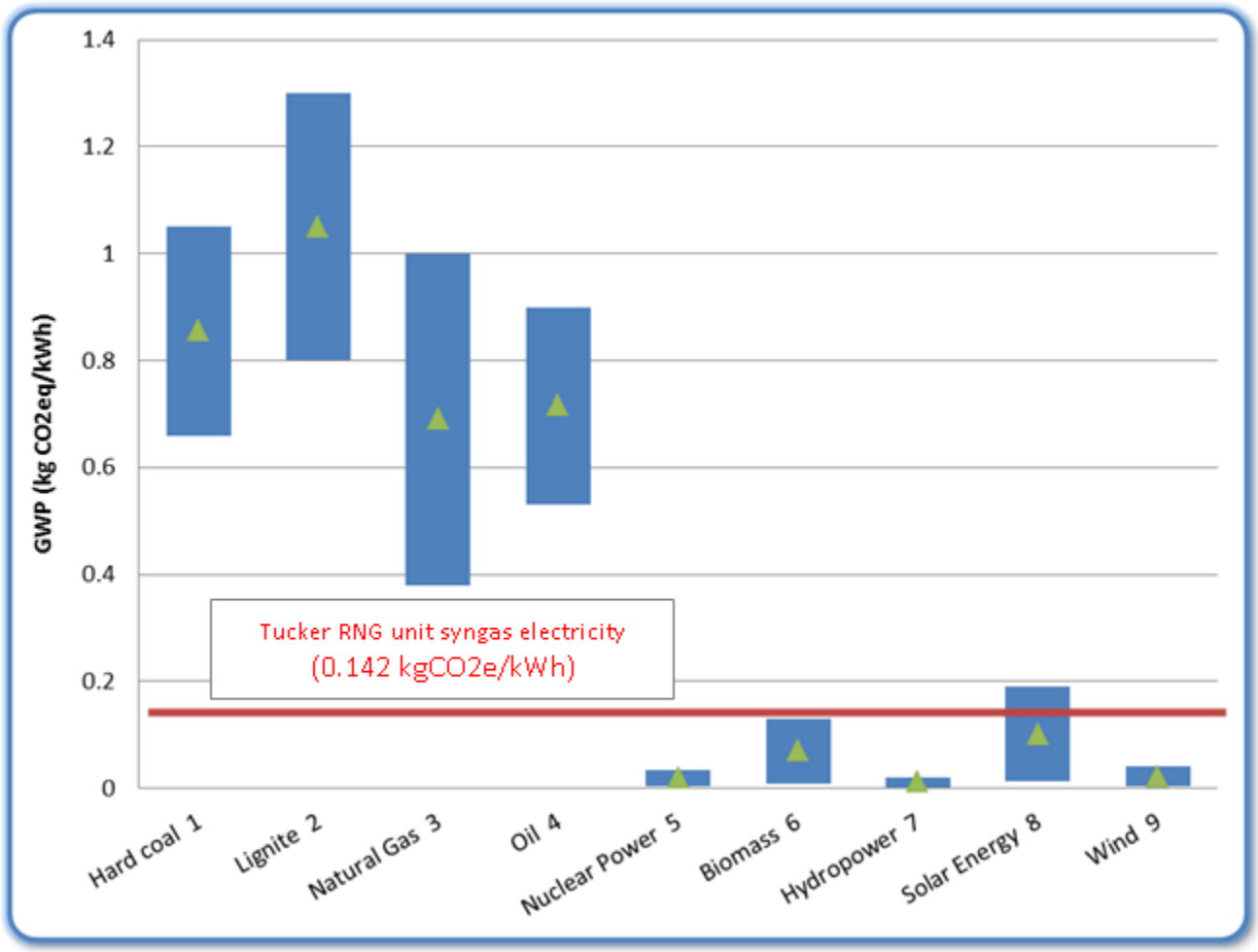

Figure 31. General range of global warming impact for various electricity generating technologies collected from literatures and the global warming impact of syngas electricity estimated in this study.

Conclusion

Generating electricity from wood-biomass sources such as the Tucker RNG unit can result in notable GHG reduction in comparison to fossil fuels. In addition, syngas electricity generated from Tucker RNG syngas is from a renewable energy as it consumes forest thinning or mill residues. Furthermore, systems like the Tucker RNG unit reduce energy dependency on fossil fuel or other non-renewable sources. Energy from biomass or its pyrolysis products used to substitute fossil fuel based energy leads to avoidance of CO_2 emissions associated with fossil fuels use.

Sequestering biochar when produced as a byproduct from thermochemical conversion processes such as the Tucker RNG unit can lower the GHG emissions associated with generating electricity. This occurs because the carbon stored in the biochar equates to CO_2 removed from the atmosphere because of its long-term stability.

The sum of these two effects associated with syngas electricity of using woody biomass as a feedstock and sequestering biochar lowers the GW impact (ie GHG emissions) substantially. It is known that electricity from burning fossil fuels is the main contributor to the GW impact (Hertwich et al 2013); thus, the consumption of biomass (directly combusted or indirectly derived) for bioelectricity is assumed as carbon neutral. Carbon neutrality for the biomass burned to generate electricity continues to be questioned (USEPA 2014b). Regardless, GHG emissions are generated that impact GW because the entire life cycle of the biomass is assessed so there are fossil CO_2 emissions in the cultivation, harvesting, processing, and transportation processes. The present study tracked these GHG emissions including fossil CO_2 and thus was included in our analysis. One additional point was added for wood harvested from sustainably managed forests. By doing so, substantial C benefits are gained by avoiding CH_4 emissions related to burning or natural decomposition of forest thinning residues but instead converting them into biomass-based electricity.

Future works for the broader project details utilizing the biochar as a co-product instead of a byproduct and then evaluating the additional life cycle of producing activated C. The reason is that biochar as activated C has a higher market value than as a soil amendment. However, it takes processing in tightly controlled environments such as the Tucker RNG unit to generate the physical properties required, which means additional energy and materials to make it so.

Acknowledgment

We thank Richard Tucker and David Barbee (Tucker Engineering Associates) for technical assistance. In addition, the authors especially thank Mark Knaebe (USDA Forest Service Forest Products Laboratory), Nathaniel Anderson (USDA Forest Service Rocky Mountain Research Station) and Prakash Nepal (U.S. Forest Service, Forestry Sciences Laboratory in Research Trainable Park, NC) for their peer review of this paper. We gratefully acknowledge financial assistance for this research project provided by the U.S. Department of Agriculture (USDA) National Institute of Food and Agriculture Biomass Research and Development Initiative (BRDI) award no. 2011-10006-30357. BRDI is a joint effort between the USDA and the U.S. Department of Energy.

References

Bare, J (2011) TRACI 2.0: the tool for the reduction and assessment of chemical and other environmental impacts 2.0. Clean Technologies and Environmental Policy, 13(5).
Bergman RD, Gu H (2014) Life-cycle inventory analysis of bio-products from a modular advanced biomass pyrolysis system. In: Proceedings, Society of Wood Science and Technology 57th International Convention. June 23-27, 2014. Zvolen, Slovakia: 405–415.
Cowie AL, Cowie AJ (2013) Case Study - Rural Climate Solutions (University of New England/ NSW Department of Primary Industries) Life cycle assessment of greenhouse gas mitigation benefits of biochar. http://www.ieabioenergy-task38.org/publications/T38_Biochar_case_study.pdf. (28 April 2015). CORRIM (2010) Research guidelines for life-cycle inventories. Consortium for Research on Renewable Industrial Materials. University of Washington, Seattle. 40 p.
EISA (2007) Legal Reference—Energy Independence and Security Act of 2007. GPO (Government Printing Office). Gaunt J Lehmann J (2008) Energy balance and emissions associated with biochar sequestration and pyrolysis bioenergy production. College of Agriculture and Life Sciences, Cornell University. Environmental Science & Technology 42: 4152–4158.
Hertwich, E.G., Gibon, T., Bouman, E.A., Arvesen, A., Suh, S., Heath, G.A., Bergesen, J.D., Ramirez, A., Vega, M.I., and L. Shi. (2013) Integraed life-cycle assessment of electricity-supply scenarios confirms global environmental benefit of low-carbon technologies. PNAS special feature.
http://www.pnas.org/cgi/doi/10.1073/pnas.1312753111. Pp. 6. (28 April 2015)
IPCC (2007) The physical scientific basis. Contribution of working group to the fourth assessment report of the intergovernmental panel on climate change, edited by S. Solomon et al, Cambridge Univ. Press, New York.
ISO (2006a) Environmental management—life-cycle assessment—principles and framework. ISO 14040. International Organization for Standardization, Geneva, Switzerland. 20 pp.
ISO (2006b) Environmental management—life-cycle assessment—requirements and guidelines. ISO 14044. International Organization for Standardization, Geneva, Switzerland. 46 pp.
NREL (2012) Life-cycle inventory database project. National Renewable Energy Laboratory. https://www.lcacommons.gov/nrel/search. (accessed March 3, 2015).
Perlack PD, Wright LL, Turhollow AF, Graham RL, Stokes RJ, Erbach DC (2005) Biomass as feedstock for a bioenergy and bioproducts industry: The technical feasibility of a billion-ton: Annual supply. April 2005. A joint study sponsored by U.S. Department of Energy and the U.S. Department of Agriculture.
http://www1.eere.energy.gov/bioenergy/pdfs/final_billionton_vision_report2.pdf (28 April 2015)
PRé Consultants (2015) Life-Cycle assessment software package SimaPro 8 Update Instructions. Stationsplein 121, 3818 LE Amersfoort, The Netherlands. http://www.pre-sustainability.com/ (28 April 2015).

Schnepf R, Yacobucci BD (2013) Renewable fuel standard: overview and issues. Congressional Research Service Report for Congress no. 7-5700 https://www.fas.org/sgp/crs/misc/R40155.pdf (28 April 2015).
Sebastian F, Royo J Gomez, M (2011) Cofiring versus biomass-fired power plants: GHG (Greenhouse Gases) emissions savings comparison by means of LCA (Life Cycle Assessment) methodology. Energy 36: 2029-2037.
Sohi SP, Krull E, Lopez-Capel E, Bol R (2010) Chapter 2 – A review of biochar and its use and function in soil. Advances in Agronomy 105:47–82.
Steubing B (2011) Analysis of the availability of bioenergy and assessment of its optimal use from an environmental perspective. PhD dissertation, École polytechnique fédérale de Lausanne, Lausanne, Switzerland. 181 pp.

Steubing B, Zah R, Ludwig C (2011) Life cycle assessment of SNG from wood for heating, electricity, and transportation. Biomass Bioenerg 35(7):2950–2960.

Turconi R, Boldrin A, Astrup T (2013) Life cycle assessment of electricity generation technologies: Overview, comparability and limitations. Renewable and Sustainable Energy Reviews 28: 555–565. USEPA (2014a) eGRID 9th edition version 1.0: Year 2010 summary tables. United States Environmental Protection Agency. Washington, D.C. 13 p. http://www.epa.gov/cleanenergy/documents/egridzips/eGRID_9th_edition_V1-0_year_2010_Summary_Tables.pdf (27 March 2015).
USEPA (2014b) Carbon dioxide emissions associated with bioenergy and other biogenic sources. United States Environmental Protection Agency. Washington, D.C. http://www.epa.gov/climatechange/ghgemissions/biogenic-emissions.html (28 April 2015).

Wang Z, Dunn JB, Han J, Wang MQ (2014) Effects of co-produced biochar on life cycle greenhouse gas emissions of pyrolysis-derived renewable fuels. Biofuels and Bioprod Bioref. 8:189–204.

Proceedings of the 58th International Convention of Society of Wood Science and Technology
June 7-12, 2015 – Grand Teton National Park, Jackson, Wyoming, USA

Viscoelastic Creep Behavior of Surface and Inner Layer of Sugi and Hinoki Boxed-Heart Timber under Various Temperatures

Andi Hermawan [1] – Noboru Fujimoto[2]*

[1] JSPS Postdoctoral Fellow, Department of Sustainable Bioresource Science, Laboratory of Wood Material Technology, Kyushu University, Fukuoka, Japan
** Corresponding author*
andi@agr.kyushu-u.ac.jp
[2] Associate Professor, Department of Sustainable Bioresource Science, Laboratory of Wood Material Technology, Kyushu University, Fukuoka, Japan

Abstract

This study was conducted to investigate the rheological behavior of Sugi and Hinoki boxed-heart timber at constant moisture content (MC) by using cantilever creep test. The focus of the study was on the effect of temperature on viscoelastic creep behavior of surface and inner layer specimen of Sugi and Hinoki boxed-heart timber. Surface and inner layer specimen of the timber with dimension of 75 mm in length, 25 mm in width, 3 mm in thickness and with an effective span of 40 mm was rigidly clamped at its fixed-end. Cantilever creep test of the specimen was conducted at temperature of 20, 65, 80 and 95°C with equilibrium moisture content (EMC) about 12%. A load of 20% from rupture load of the specimen at each temperature was applied at its free-end and strain gauges were bonded at fourth span (10 mm) on its upper and bottom faces. Loading and unloading duration was set for 300 and 180 min, respectively. Four-element burger model was used to model creep properties of the timber. It was found that temperature had significant effects on the creep properties of the timber. Creep compliance of surface and inner layer specimen of both Sugi and Hinoki boxed-heart timber tended to increase as temperature increased. Creep compliance of surface layer specimen of Sugi boxed-heart timber was larger than that of Hinoki boxed-heart timber at each temperature. However, creep compliance of inner layer specimen of Sugi and Hinoki boxed-heart timber was almost the same.

Keywords: Sugi, Hinoki, boxed-heart timber, viscoelastic creep, burger model, parameter identification

Introduction

Sugi (*Cryptomeria japonica*) and Hinoki (*Chamaecyparis obtusa*) are the most important commercial wood species in Japan. Generally, thinned Sugi and Hinoki trees are sawn into boxed-heart timber and used for structural purposes in Japanese traditional post-and-beam construction. In Japan, timber for structural purposes should be dried to the moisture content (MC) lower than 20% to prevent dimensional change in the future because of moisture fluctuation. However, to achieve high-quality dried boxed-heart timber is very difficult because surface checks often occur during drying the timber due to obvious anisotropic shrinkage.

In Japan, various pretreatments and drying methods have been developed to achieve a higher-quality dried boxed-heart timber with fewer surface checks as well as reduce its drying time (Ishiguri et al. 2001, Kobayashi et al. 2003). It was reported that high-temperature and low-humidity (HT-LH) pre-treatment is effective in preventing surface checks of Sugi boxed-heart timber (Katagiri et al. 2007). It is thought that during HT-LH pre-treatment, green Sugi boxed-heart timber was exposed to the dry heat at a temperature more than 100°C. Under this circumstances, thermal softening occurred at surface layer of the timber and contributed to the effective relaxation of tensile stress; thus a large drying set formed at the surface layer of the timber and resulting less surface check occurrence. On the other hand, it was reported also that excessive temperature and time of the pre-treatment conditions would give negative effect to the timber in term of internal check occurrence. However, an accurate understanding on the mechanism of HT-LH pretreatment affect checks occurrence of the timber is still unclear.

Very little research have been conducted to better understand the mechanism of HT-LH pretreatment on checks prevention of boxed-heart timber. Over a decade ago, rheological approach has been proposed to clarify the effect of temperature on checks development during drying of Sugi boxed-heart timber (Fujimoto et al. 2001). Tensile creep behavior of surface layer and compressive creep behavior of inner layer of the timber were investigated under various temperatures. Although tensile and compressive creep test is close analogy with the mechanical behavior of the timber during drying, however, in this experiment, tensile and compressive creep tests were conducted separately with different sample size and shape. On the other hand, Moutee et al. (2009) have developed cantilever creep test to model creep behavior of wood during drying. This test is simple and much closer analogy with the mechanical behavior of wood during drying because a cantilever beam when subjected to a load at its free-end, tension and compression stress occur on its upper and bottom faces, respectively at the same time.

This study was conducted as a part of effort to better understand the mechanism of HT-LH pretreatment on surface check prevention of Sugi and Hinoki boxed-heart timber. We believed that respond of the timber especially surface and inner layer of the timber on temperature and MC change under applied stress contributed to the checking occurrence of the timber. Therefore, in this study we investigated rheological behavior of the timber

at constant MC by using cantilever creep test. The focus of the study was on the effect of temperature on viscoelastic creep properties of surface and inner layer of Sugi and Hinoki boxed-heart timber. Four-element burger model was used to model creep properties of the timber. Creep and creep recovery parameters were obtained by fitting experimental data with the rheological model used in this study. Creep and creep recovery parameters of surface and inner layer specimen of Sugi and Hinoki boxed-heart timber was then identified under various temperature.

Materials and Methods

Materials

Sugi and Hinoki boxed-heart timber obtained from Fukuoka Prefecture, Japan were used as material in this study. The dimension of the timber was 133×133×3000 mm and 133×133×4000 mm for Sugi and Hinoki, respectively. The average initial MC and average air-dry density of Sugi boxed-hear timber were 47.1% and 0.43 g/cm^3, respectively. In case of Hinoki boxed-hear timber, the average initial MC and average air-dry density were 35.9% and 0.47 g/cm^3, respectively.

Specimen preparation

Sugi and Hinoki boxed-heart timbers were cut to a length of 500 mm by cross sectional cutting. The-500 mm-length timbers were cut parallel to the grain at its surface and inner layer to produce flat sawn and quarter sawn boards, respectively. The boards were then planned to a thickness of 3 mm and boards with dimension of 500 mm in length, 133 in width and 3 mm in thick were obtained. After conditioned at conditioning room to an equilibrium moister content (EMC) of 12%, the boards were cut perpendicular to the grain to a length of 25 mm. Finally, test specimens with dimension of 75 mm in length, 25 mm in width and 3 mm in thick were made and cantilever specimens with an effective span of 40 mm were used in this study. In addition, fixed-end position of the cantilever for the surface layer specimens were set at the middle of the flat sawn board. On the other hand, fixed-end of inner layer specimens of the timber were set at position little away from the pith. Figure 1 shows the specimen preparation and cantilever fixed-end position of each specimen.

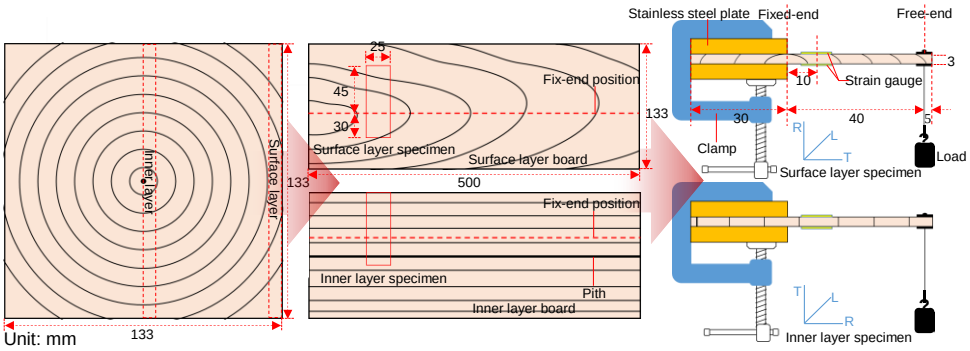

Figure 1. Schematic diagram of the specimens and the cantilever fixed-end position.

Rupture load and creep test

Rupture load and creep test were conducted in a laboratory temperature and humidity chamber at temperature of 20, 65, 80 and 95°C. EMC of the specimen was set to around 12% by adjusted the relative humidity (RH) inside the chamber. Table 1 shows the rupture load and creep test conditions. In rupture load test, a static load was set at the free-end of the cantilever using a jig which allow the static load connected to a load cell using a wire. The load cell was then connected using a wire through a pulley to the stepping motor so that the load was in static equilibrium condition as shown in Fig. 2. Load was applied and increased progressively until rupture occurred at the fixed-end of the cantilever by moving forward the stepping motor at a speed of 2 mm/min. Load increment data was recorded using data logger at interval of 1 s. In case of creep test, a load of 20% from rupture load at each temperature was applied at the free-end of the cantilever under constant EMC. Strain gauges were bonded at fourth span (10 mm) on the upper and bottom faces of the specimen. Load was applied using the same principle with that in rupture load test. A wire with a static load at the end was connected to the stepping motor through a pulley. Loading was conducted by moving the stepping motor forward until the static load hanged on a jig at free-end of the cantilever and vice versa for unloading. Loading duration was set for 300 min and recovery duration was set for 180 min after unloading. Surface strains was recorded using data logger at interval of 1 s. The specimen was conditioned for more than 6 and 9 h prior the rupture test and creep test, respectively. In addition, free-end deflection was measured only for rupture test and creep test conducted at temperature of 20°C.

Table 1. Rupture load and creep test conditions.

Temperature (°C)	RH (%)	EMC (%)	Replication
20	66	12.2	
65	78	12.3	6 (rupture load test)
80	80	11.6	3 (creep test)
95	86	12.0	

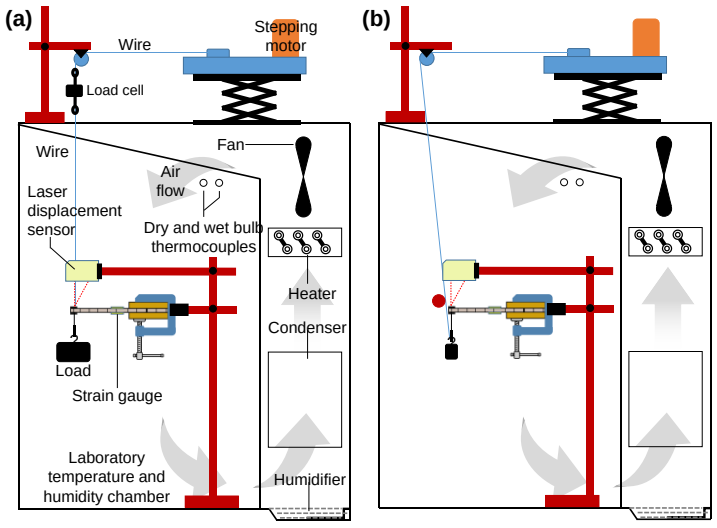

Figure 2. Schematic diagram of rupture load (a) and creep test (b).

Rheological model

Many rheological models have been proposed to describe creep behavior of wood. However, the four-element Burger model which consists of one Maxwell and Kelvin unit connected in a series has been widely used. Four-element Burger model including instantaneous, viscoelastic and viscous deformation resulting from Maxwell spring, Kelvin unit and Maxwell dashpot, respectively are presented in Fig. 3

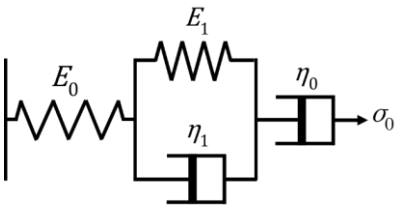

Figure 3. Schematic of four-element burger model.

The four-element burger model can be expressed by following equations:

$$\varepsilon(t) = \left[\frac{1}{E_0} + \frac{1}{E_1}\left(1 - e^{-t/\tau_1}\right) + \frac{t}{\eta_0}\right]\sigma_0, \tau_1 = \frac{\eta_1}{E_1} \quad (1)$$

In this study, the results were expressed by compliance function $J(t)$ as follows:

$$J(t) = \frac{\varepsilon(t)}{\sigma_0} \quad (2)$$

where $\varepsilon(t)$ is creep strain; E_0 and E_1 are instantaneous and delayed elastic modulus, respectively; $J(t)$ is creep compliance; σ_0 is applied stress; t is time; τ_1 is retardation time to produce 63.21% (or 1-1/e) of its total deformation; η_0 and η_1 are viscosities of dashpot in Maxwell and Kelvin unit, respectively.

From equations (1) and (2), $J(t)$ can be expressed as:

$$J(t) = J_0 + J_1\left(1 - e^{-t/\tau_1}\right) + \frac{t}{\eta_0}, J_i = \frac{1}{E_i} \quad (3)$$

where J_0 and J_1 are instantaneous and delayed elastic compliance, respectively.

When the constant load was removed at time t_0, the specimen starts to recover, which is the reverse of creep. According to Boltzmann superposition principle, creep strain at $t>t_0$ can be expressed as follow:

$$\varepsilon_r(t) = \sigma_0[J(t) - J(t - t_0)] \quad (4)$$

where $\varepsilon_r(t)$ is creep recovery strain and t_0 is unloading time.

Creep and creep recovery parameters were obtained by fitting experimental data with equation (3) and (4), respectively.

Results and Discussion

Rupture load

Modulus of rupture (MOR) and MC of the specimen before and after rupture load test is presented in Table 2. MOR of the specimen tended to decrease as temperature increased. It is well known that MOR is sensitive to the heat and many research have been reported that MOR of the timber decreased when exposed to a higher temperatures condition. On the other hand, MC of the specimen before rupture load test was lower than EMC at each temperature. This is probably because of unstable climate conditions inside the conditioning room. In addition, MC of the specimen after rupture load test was also different with EMC at each temperature and the difference become larger at higher temperatures.

Table 2. Average MOR and MC of the specimen before and after rupture load test.

Temperature (°C)	Sugi						Hinoki					
	Surface layer			Inner layer			Surface layer			Inner layer		
	MOR (MPa)	MC (%)		MOR (MPa)	MC (%)		MOR (MPa)	MC (%)		MOR (MPa)	MC (%)	
		Before	After		Before	After		Before	After		Before	After
20	9.76 (1.42)	11.9 (0.7)	13.6 (0.5)	13.28 (1.11)	10.8 (1.2)	12.9 (0.4)	13.51 (2.21)	10.9 (1.9)	12.5 (1.0)	17.25 (2.89)	10.5 (1.0)	12.9 (0.6)
65	7.53 (1.43)	10.5 (1.2)	13.5 (2.0)	12.53 (2.45)	10.7 (1.4)	12.5 (0.8)	11.98 (1.20)	9.9 (0.8)	11.8 (0.4)	14.86 (1.85)	9.3 (0.6)	12.1 (1.0)
80	7.48 (1.39)	10.0 (0.4)	10.7 (0.4)	11.36 (2.13)	9.6 (0.4)	10.2 (0.3)	10.55 (1.11)	9.5 (0.7)	9.9 (0.5)	14.09 (2.77)	10.8 (1.1)	10.0 (0.3)
95	4.55 (1.01)	10.3 (0.8)	9.9 (0.8)	9.14 (1.80)	9.5 (0.9)	9.4 (0.9)	6.15 (1.11)	9.7 (0.6)	9.7 (0.6)	10.00 (1.96)	9.4 (0.6)	9.6 (0.7)

Number in parentheses indicated standard deviations

Creep properties

Figure 4 shows typical of creep compliance of surface and inner layer specimen of Sugi and Hinoki boxed-heart timber at each temperature. Temperature had significant effect on creep compliance for all the specimens. Creep compliance of all the specimens tended to increase as temperature increased. Surface layer specimen both of Sugi and Hinoki boxed-heart timber has higher creep compliance than that of inner layer specimen. In addition, surface layer specimen of Hinoki boxed-heart timber has lower creep compliance than that of Sugi boxed-heart timber. However, creep compliance of inner layer specimen of Sugi and Hinoki boxed-heart timber was almost the same. Fitting experimental data with burger model used in this study shows a good agreement as seen in Fig. 4. Therefore, model parameters obtained in this study were applicable for

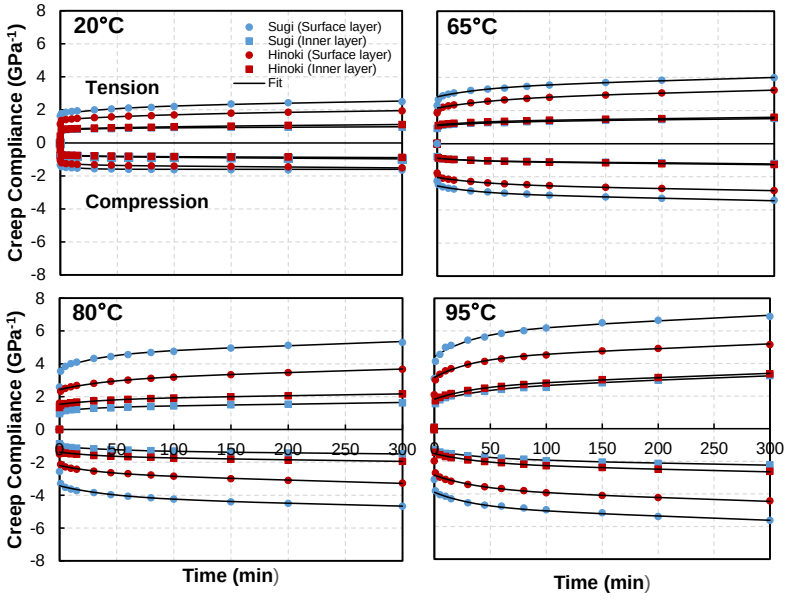

identification of creep properties of the timber.

Figure 4. Creep compliance of surface and inner layer specimen of Sugi and Hinoki boxed-heart timber at each temperature.

Figure 5 shows creep parameters of surface and inner layer specimen of Sugi and Hinoki boxed-heart timber at each temperature. Instantaneous (J_0) and delayed (J_1) elastic compliance of all the specimens tended to increase as temperature increased. According to equation (3), J_0 and J_1 are inverse of E_0 and E_1, respectively. Therefore, stiffness of all the specimen tended to decrease as temperature increased. In addition, J_0 and J_1 of inner layer specimen of both Sugi and Hinoki boxed-herat timber were lower than those of outer layer specimen. Moreover, surface layer specimen of Hinoki boxed-heart timber has lower J_0 and J_1 than that of Sugi boxed-heart timber. This behavior implied that inner layer specimen and Hinoki boxed-heart timber retained its elasticity better than outer layer specimen and Sugi boxed-heart timber as temperature increased. However, J_0 and J_1 of inner layer specimen of Sugi and Hinoki boxed-heart timber were almost the same.

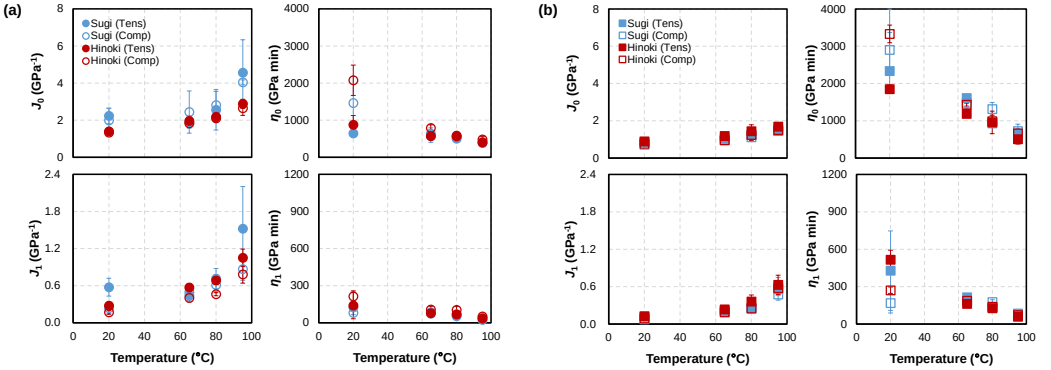

Figure 5. Creep parameter of surface (a) and inner (b) layer of Sugi and Hinoki at each temperature.

Figure 5 shows that viscosity of both Maxwell (η_0) and Kelvin (η_1) unit of all the specimens tended to decrease as temperature increased. η_0 represents the irrecoverable creep due to permanent deformation of the specimen while η_1 related to viscosity of Kelvin unit and as expressed in equation (1), the ratio between η_1 and E_1 is define as retardation time (τ_1). The results indicated an improvement in mobility of the molecular chains at a higher temperatures, thus decreasing retardation time and increasing permanent deformation of the specimen. η_0 and η_1 of surface layer specimen of both Sugi and Hinoki boxed-heart timber were lower than those of inner layer specimen. In addition, surface layer specimen of Sugi boxed-heart timber has lower η_0 and η_1 than that of Hinoki boxed-heart timber. However, inner layer specimen of Sugi boxed-heart timber has higher η_0 and η_1 than that of Hinoki boxed-heart timber.

Figure 6 shows creep recovery parameters of surface layer and inner layer specimen of Sugi and Hinoki boxed-heart timber at each temperature. Although difference in magnitude, creep recovery parameters have the same tendency with creep parameters. J_1 of all the specimens tended to increases as temperature increased. J_1 of inner layer specimen of both Sugi and Hinoki boxed-heart timber was lower than that of surface layer specimen. However, J_1 of surface layer specimen of Sugi and Hinoki boxed-heart

timber was almost the same. The same tendency was observed for inner layer specimens of the timber.

On the other hand, η_0 and η_1 of all the specimens tended to decrease as temperature increased. η_0 and η_1 of surface layer specimen of both Sugi and Hinoki boxed-heart timber was lower than that of inner layer specimen. In addition, η_0 of surface layer specimen of Hinoki boxed-heart timber was higher than that of Sugi boxed-heart timber. This finding implied that permanent deformation in surface layer specimen and Sugi boxed-heart timber was larger than that of inner layer specimen and Hinoki boxed-heart timber. Moreover, η_0 and η_1 of inner layer specimen of Sugi boxed-heart timber were higher than that of Hinoki boxed-heart timber.

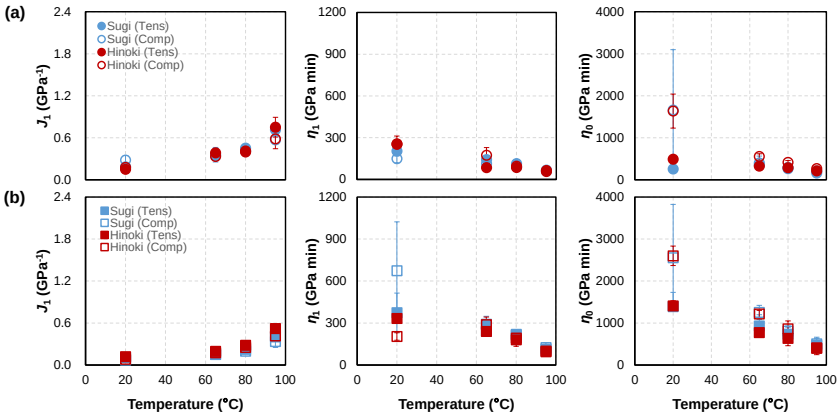

Figure 6. Creep recovery parameter of surface (a) and inner (b) layer of Sugi and Hinoki at each temperature.

Conclusion

Temperature had significant effects on the creep properties of Sugi and Hinoki boxed-heart timber. Creep compliance of surface and inner layer specimen of both Sugi and Hinoki boxed-heart timber tended to increase as temperature increased. Creep compliance of surface layer specimen of Sugi boxed-heart timber was larger than that of Hinoki boxed-heart timber at each temperature. However, creep compliance of inner layer specimen of Sugi and Hinoki boxed-heart timber was almost the same.

References

Fujimoto N, Tachiwana K, Oouchi K, Mataki Y (2001) Tension creep of surface layer and compression creep of inner layer perpendicular to the grain in Sugi boxed-heart square timber. Journal of the Society of Material Science Japan 50:914−919.

Ishiguri F, Andoh M, Yokota S, Yoshizawa N (2001) Effect of smoke heating on moisture content, surface checking and dynamic Young's modulus of Sugi (*Cryptomeria japonica*) boxed-heart timber. Mokuzaigakkaishi 47:350−357.

Katagiri Y, Fujimoto N, Murase Y (2007) Effect of the treatment temperature on the surface drying set of Sugi boxed-heart square timber. Drying Technology 25:507−510.

Kobayashi I, Kuroda N, Hisida T, Takahashi Y (2003) Superheated steam pre-treatment for the drying process of boxed-heart timber from Sugi (*Cryptomeria japonica* D. Don). Wood Industry 58:258−263.

Moutee M, Fortin Y, Laghdir A (2010) Cantilever experimental setup for rheological parameter identification in relation to wood drying. Wood Science and Technology 44:31−49.

Proceedings of the 58th International Convention of Society of Wood Science and Technology
June 7-12, 2015 – Grand Teton National Park, Jackson, Wyoming, USA

Preferences for Materials in City Buildings, Does Region of Origin Matter?

Olav Hoibo, olav.hoibo@nmbu.no
Eric Hansen, Eric.Hansen@oregonstate.edu
Erlend Nybakk, Erlend.Nybakk@bi.no

Norwegian University of Life Sciences, Box 5003, , Aas, NO-1432

Abstract

A fast-growing global population, increasing urbanization, and a focus on sustainable development brings into focus the housing sector and material use. Since carbon footprint is important for the environmental impact of buildings, wood based housing may be an attractive and sustainable option. Data in this study consists of responses from immigrants and native Norwegians. Norway is a country where wood has traditionally been a major building material in one and two story residential buildings (78% market share). The study revealed significant differences in preferences between building materials, and that the most preferred materials often were the same as the most common materials used in city buildings. Small differences were found between immigrants and native Norwegians. Still the difference in preference between types of materials was not consistent across different groups of people. Differences due to divergent attitudes, like concerns about material choice in general and where they wanted to live were found. The respondents that preferred city living preferred to a greater extent the commonly used city materials, like concrete and steel for structural use, compared to respondents that did not prefer city living. For cladding materials, stained or painted wood was one of the most preferred cladding materials even though it is not common on city buildings. Stone/bricks was the most preferred cladding.

Modeling and Design of a Disk-Type Furrow Opener's Coulter (Its Mechanical Analysis and Study for No-Till Machinery) (Combination and Bertini)

Payam Hooshmand, payam.hooshmand@yahoo.com
Jalaladdin Ghezavati, payam.hooshmand@yahoo.com
adel Ranji, adelranji@yahoo.com
Milad Hosseinpoor, milad_hopr@yahoo.com

Sharif University of Technology, Azadi St, , Tehran

Abstract

No-till practices play an important role in decreasing production costs, increasing soil organic matter content, improving soil structure and removing unwanted environmental impacts. However, due to a lack of access to proper machinery for direct seeding in unplowed lands, such practices have failed to produce successful results since they are incapable of providing sufficient contact between soil and seeds. This step can finally lead to the promotion of this practice in the potential areas. The total actual forces imposed to a furrow opener in practice are multiple times larger than a design's total. There are a number of factors contributing to this phenomenon including unknown environmental factors in soil, existence of fine and coarse gravels, and also different partial, unpredictable loads produced on impact with the soil. Empirically and practically, as well as based on results from agricultural projects on no-till machinery in Iranian arid and semi-arid regions, disk coulters of a furrow opener set sustain heavy damages during no-till farming. On the other hand, several parameters can influence the soil; as a result, the safety factor was also increased to improve the furrow opener's resistance against rocks, unknown soil factors, etc. Finally, the coulter's stress was determined using the von Mises criterion. The result showed that the minimum coulter stress was 1985.5Pa throughout the plane and its maximum belonged to the holes inside the hub with 1.0819*107 Pa.

Proceedings of the 58th International Convention of Society of Wood Science and Technology
June 7-12, 2015 – Grand Teton National Park, Jackson, Wyoming, USA

Optimization of Energy Required and Energy Analysis for Rice Production Using Data Envelopment Analysis Approach

Payam Hooshmand, payam.hooshmand@yahoo.com
Adel Ranji, adelranji@yahoo.com
Hamed Rajabzadeh, hamed.rajabzadeh67@yahoo.com
Hamid Atari, payam.hooshmand@yahoo.com
Milad Hosseinpoor, milad_hopr@yahoo.com

Sharif University of Technology, Azadi St, , Tehran

Abstract

The objective of this study was the application of non-parametric method of data envelopment analysis (DEA) to analyze the efficiency of farmers, discriminate efficient farmers from inefficient ones and to identify wasteful uses of energy for rice production in Mazandaran province, Iran. This method was used based on seven energy inputs including human labor, machinery, diesel fuel, fertilizers, biocide, Irrigation and seed energy and three output of rice(yield, straw and husk). Technical, pure technical, scale and cross efficiencies were calculated using CCR and BCC models for farmers. From this study the following results were obtained: from the total of 72 farmers, considered for the analysis, 9.7 % and 22.2 % were found to be technically and pure technically efficient, respectively. The average values of technical, pure technical and scale efficiency scores of farmers were found to be 0.78, 0.95 and 0.82, respectively. The energy saving target ratio for rice production was calculated as 7.47 %, indicating that by following the recommendations resulted from this study, about 4.57 GJ ha−1 of total input energy could be saved while holding the constant level of rice yield. The comparative results of energy indices revealed that by optimization of energy consumption, energy efficiency, energy productivity and net energy with respect to the actual energy use can be increased by 7.46 %, 7.46 % and 5.54 %, respectively.

Proceedings of the 58th International Convention of Society of Wood Science and Technology
June 7-12, 2015 – Grand Teton National Park, Jackson, Wyoming, USA

Practical Modeling of Lateral Load Paths in Light-Frame Classroom Structure

Thanh Huynh, huynhtha@onid.oregonstate.edu
Thomas Miller, thomas.miller@oregonstate.edu
Rakesh Gupta, rakesh.gupta@oregonstate.edu
Michael Lewis, mlewis@modernbuildingsystems.com

Oregon State University, WSE Department, Richardson Hall, Corvallis, OR, 97331

Abstract

The objective of this study is to use a validated modeling method to investigate lateral load paths and system behavior in an actual light-frame wood structure. The modeling methods were validated against full-scale tests on sub-assemblies and an L-shaped house by previous researchers. A model of a modular classroom structure is used to investigate the effects of stiffness distribution, torsion and uplift on system behavior and lateral load paths. ASCE 7-10 main lateral force resisting system and components and cladding wind loads are applied. The analysis is done for a series of foundation types. The modifications in the foundation change the locations where the structure is securely connected to the foundation, and therefore have significant effects on how the load will be distributed throughout the structure. Thousands of classrooms such as these are used throughout the United States. Consequently, accurate modeling techniques to validate the performance of these structures is integral to attesting that these structures are safe for occupancy under their designed loads.

Proceedings of the 58th International Convention of Society of Wood Science and Technology
June 7-12, 2015 – Grand Teton National Park, Jackson, Wyoming, USA

Versatile Strategies for the Modification and Functionalization of the Wood Structure

Tobias Keplinger, tkeplinger@ethz.ch
Etienne Cabane, cabanee@ethz.ch
Jana Segmehl, jsegmehl@ethz.ch
Ingo Burgert, iburgert@ethz.ch

ETH Zurich, Institute for Building Materials, Wood Materials Science,
Stefano-Franscini-Platz 3, Zürich 8093

Abstract

Wood has been used for thousands of years as a building material due to its superior properties such as high mechanical strength in view of its light weight. This is explained by the unique hierarchical structure. Additionally the porous structure offers potential for utilization in new application fields e.g. in membrane technologies or the wood inherent cellulose scaffold can be used for the development of new materials with a broad property profile. The development of such materials requires specific chemical modifications of the wood structure.

We report on a procedure which offers the possibility to insert new functionalities and to control the spatial distribution of the modifying substance in the wood structure. For the controlled spatial in-situ polymerization of monomers within the wood structure a modular 2 step process is presented. In addition we studied delignification procedures on bulk wood samples to obtain a cellulose scaffold while keeping the integrity of the hierarchical anisotropic structure intact. We then investigated the insertion of nanoparticles and polymeric components in order to implement new properties and functions. For both approaches it is important to visualize the chemical changes with high resolution in order to understand the modification at the cell wall level. For this purpose especially Raman spectroscopy in combination with multivariate data analysis is applied, yielding topo-chemical images with high chemical/spatial resolution.

Proceedings of the 58th International Convention of Society of Wood Science and Technology
June 7-12, 2015 – Grand Teton National Park, Jackson, Wyoming, USA

Natural Durability of Yellow-hearted Red Pine (Hwangjangmok)

Aehee Lee[1] - Namhun Kim[2] - Jaehyuk Jang[3] - Sewhi Park[4]*

[1]Master student, Division of Forest Materials Science & Engineering, Kangwon National University, Republic of Korea.
lah0818@kangwon.ac.kr
[2]Professor, Division of Forest Materials Science & Engineering, Kangwon National University, Republic of Korea.
**Corresponding author*
kimnh@kangwon.ac.kr
[3]Researcher, Division of Forest Materials Science & Engineering, Kangwon National University, Republic of Korea.
jhtojh@kangwon.ac.kr
[4]Master student, Division of Forest Materials Science & Engineering, Kangwon National University, Republic of Korea.
sehwi747@kangwon.ac.kr

Abstract

This study was carried out to investigate natural durability of Yellow-hearted red pine (YHRP, *Pinus densiflora* for. erecta Uyeki) grown in Korea. Anti-fungal and anti-termite properties at indoor conditions and color change at outdoor conditions were examined. Weight loss of the heartwood in YHRP after fungi test and termite was lower than that of the sapwood in YHRP. Furthermore, the highest mortality of termite was obtained from the heartwood of YHRP. Color indexes such as L*(brightness), a*(green-red), b*(cyan-yellow) decreased with time and then level off in all samples after 30 days of exposure time.

Keywords: Yellow-hearted red pine (YHRP), Red pine(RP), heartwood, annual ring, natural durability.

Introduction

YHRP (*Pinus densiflora* for. erecta Uyeki(Uyeki 1928)) with high ratio of yellow heartwood and extremely narrow ring width is one of the Korean red-pine species. Usually, it has longer life than one hundred year and ranged infrequently in some limited

area, such as in the east part of central region of South Korea. Since time immemorial, especially during Yi-dynasty, YHRP was used for various kinds of valuable wooden cultural assets such as Sungnyemun Gate (South Korea's No. 1 National treasure) and the oldest wooden building in Korea, Geukrakjeon Bongjeongsa Temple (National treasure No. 15). Ancestors loved YHRP's advantages such as straight grain and fine texture, high clear length and less knot, high dimensional stability when dry, light weight but high strength, and good fragrance and beautiful wood grain(Park 2006, Lee et al 2014). Unfortunately until now, there are not enough scientific basic information for significant identification between YHRP and Red pine. Moreover, it is difficult to identify the differences between both of them before harvesting or cutting. Therefore, this study was carried out to compare the macroscopic, anatomical, physical properties and natural durability of two different Red pine species for providing information for the wood identification and proving the excellence of YHRP.

Materials and Methods

Anatomical and physical properties

YHRP(*Pinus densiflora* for. erecta Uyeki) and Red pine(RP, *Pinus densiflora* S. et Z.) woods were obtained from Kumgang pine Forest in Southern Regional Korea Forest Service and Research Forest in Kangwon National University, respectively (Figure 1). We examined anatomical characteristics by naked-eye and microscope, and physical properties by usual methods(Korean Standards Association, 2004).

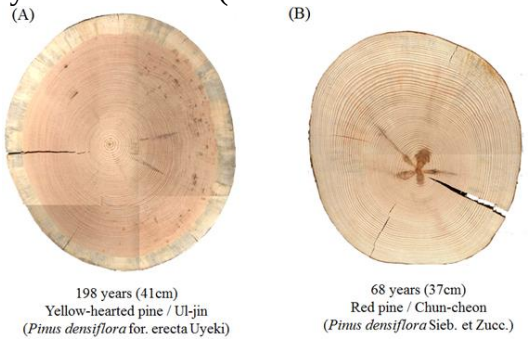

Figure 32. Appearance of YHRP and RP

Nature durability

Weathering operation

Weathering operation before termite and fungi test was conducted. Specimen were stirred in distilled water at R.T for 8H according to JIS K 1571, and dried for 16H at 60℃ in an oven-dryer.

Fungi test

Fomitopsis palustris(FOP, brown-rot fungi) and *Trametes versicolor*(TRV, white-rot fungi) were used for fungi resistance test. Shaking incubation of wood rot fungi in culture fluid(Distilled water 95mL, Glucose 2.5%, Malt extract 1.0%, Peptone 0.5%, KH2PO4

0.3%, MgSO4·7H2O 0.2%) was performed for 1week. Culture medium was prepared with quartz sand and culture fluid. And then put cultured wood rot fungi into culture medium and inoculated on wood samples. Inoculated wood samples were kept in darkroom at 26℃ and 70% RH for 12weeks and then calculated weight loss.

Termite test
Two hundred worker ants (*Reticulitermes speratus*) were selected and feed in the darkroom at 26℃ and 70% RH for 3weeks. And then weight loss and mortality were measured.

Extract analysis (Alcohol-benzene)
The amount of wood extractives was analyzed by alcohol-benzene method.

Color change
Color change of wood samples exposed to the outdoor during 120days was measured by color-difference meter (Minolta CR-410, Japan) every 2weeks.

Results and Discussion

Figure 2 shows the optical micrographs of cross section of YHRP and RP. Even though two different pine species had wide ring width in near pith, YHRP in near bark had extremely narrower and uniform annual ring width, compared to the RP. Figure 3 shows the radial variation of annual ring width of two different pine species. Table 1 shows the summary of macroscopic characteristics and density of two different pine species.

Average ring width in YHRP and RP was found to be 0.92mm and 2.58mm. Latewood percentage of YHRP was little bit greater than RP. The color of heartwood and sapwood in YHRP was deep-yellow to brown and creamy-white, respectively. On the other hand, RP showed light-brown and light-yellow in heartwood and sapwood, respectively. The air-dried density of YHRP was higher than RP.

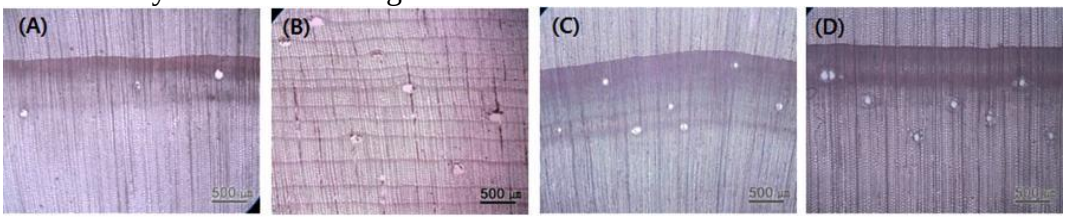

Figure 33. Cross sections of two different pine species

(A) *1st annual ring of YHRP, (B) 198th annual ring of YHTP,*

***(C)** 1st annual ring of RP, (D) 68th annual ring of RP*

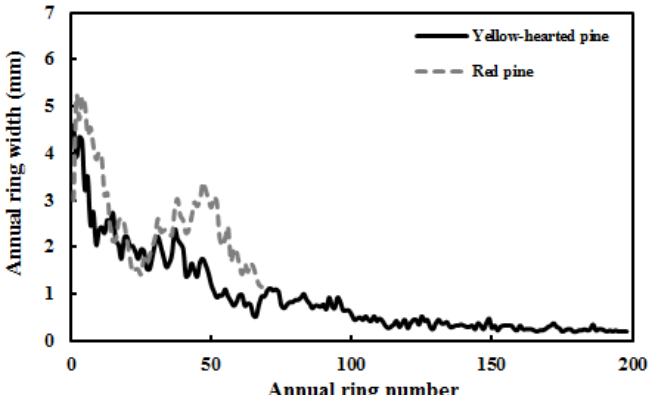

Figure 34. Radial variation of annual ring width in different pine species

Table 17. Macroscopic characteristics and density of two different pine species

Contents		Yellow-hearted pine	Red pine
Heartwood percentage (%)		80	43
Annual ring width (mm)	1~100 years	1.53 ± 0.14	-
	101~198 years	0.32 ± 0.09	-
	Average	0.92 ± 0.27	2.58 ± 0.99
Latewood percentage (%)	1~100 years	22 ± 5	-
	101~198 years	29 ± 7	-
	Average	26 ± 6	22 ± 5
Air-dried density (g/cm^3)	Heartwood	0.56±0.01	0.51±0.06
	Sapwood	0.45±0.04	0.43±0.04
Oven-dried density (g/cm^3)	Heartwood	0.54±0.04	0.46±0.06
	Sapwood	0.42±0.02	0.40±0.03

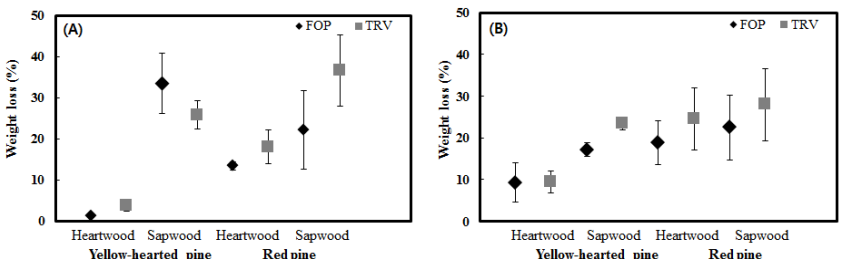

Figure 35. Weight loss of weathered samples(A) and non-weathered samples(B) exposed to F.palustris and T.versicolor for 12 weeks

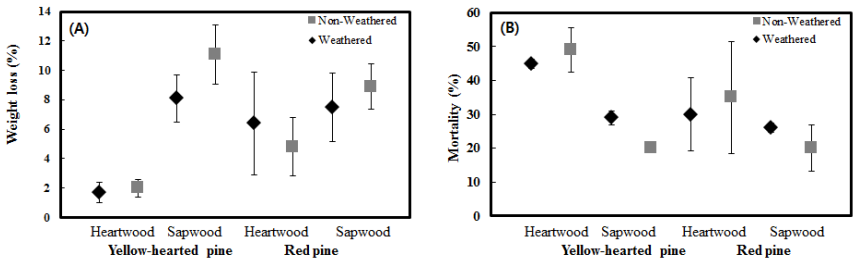

Figure 36. Weight loss(A) and mortality(B) of YHRP and RP by termite test

Figure 4 shows weight loss of weathered samples (A) and non-weathered samples(B) exposed to *F.palustris* and *T.versicolor* for 12 weeks. Weight loss of RP after fungi test was higher than that of YHRP in both of fungi types. It means fungi resistance of YHRP was higher than RP. Figure 5 shows the weight loss (A) and Mortality(B) of YHRP and RP by termite test. The termite resistance of YHRP was higher than RP. The lowest weight loss value after termite test was found to be less than 2% in heartwood part of YHRP. Furthermore, the highest mortality of termite was obtained from heartwood part of YHRP.

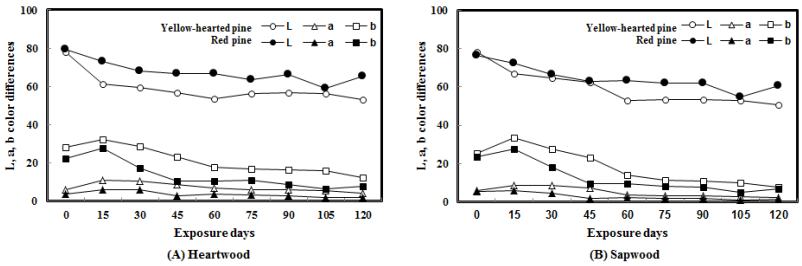

Figure 37. Color changes of YHRP and RP during weathering test for 120 days

Figure 6 show the color changes of YHRP and RP during weathering test for 120days. Color indexes such as L*(brightness), a*(green-red), b*(cyan-yellow) decreased with time and then level off in all samples after 30 days of exposure time. There were no significant differences of a* and b* values between YHRP and RP, however, brightness of YHRP was higher than that of RP.

Summary and Conclusions

Macroscopic structure as ring width, heartwood ratio and wood color might be able to be used as the indices of wood identification between YHRP and RP. The density of YHRP was higher than that RP. The weight loss of heartwood of YHRP was lowest by fungi and termite test. The extractives content and mortality of heartwood of YHRP was highest. It is considered that YHRP has better natural durability than RP.

References

[1] Uyeki H. (1928) On the physiognomy of *Pinus densiflora* growing in Korea and silicultural treatment for its improvement. Bulletin of Agriculture and Forestry College of Suwon pp.263.

[2] Park BW (2006) Pine and Hwangjangmok. Forestry Cooperative Federation. National Forestry Cooperative Federation 486: 28-33.

[3] Lee AH, Jang JH, Park BH, Kim NH (2014) Anatomical Characteristics of Yellow-hearted Pine (*Pinus densiflora* for. erecta Uyeki). Journal of Forest Science 30(1) : 56-61

[4] Korean Standards association (2004) KS F 2198

Acknowledgement

This research was supported by Basic Science Research Program through the National Research Foundation of Korea (NRF) funded by the Ministry of Education (2012R1A1A2009637).

Proceedings of the 58th International Convention of Society of Wood Science and Technology
June 7-12, 2015 – Grand Teton National Park, Jackson, Wyoming, USA

Effect of CNC Application Parameters on Wooden Surface Quality

K.Hüseyin Koç[1] –E.Seda Erdinler[2] –Ender Hazır[3] – Emel Öztürk[4]*

[1] Professor Dr., Faculty of Forestry, Department of Forest Industry Engineering, Istanbul University, 34473, İstanbul, TURKEY.
* *Corresponding author*
hkoc@istanbul.edu.tr
[2] Assistant Professor, Faculty of Forestry, Department of Forest Industry Engineering, Istanbul University, 34473, İstanbul, TURKEY.
seda@istanbul.edu.tr
[3]Research Assistant, Faculty of Forestry, Department of Forest Industry Engineering, Istanbul University, 34473, İstanbul, TURKEY.
ender.hazir@istanbul.edu.tr
[4] Research Assistant Dr., Faculty of Forestry, Department of Forest Industry Engineering, Istanbul University, 34473, İstanbul, TURKEY.
emelozt@istanbul.edu.tr

Abstract

Wood and wooden material are the materials that have increasing industrial importance with their wide usage area and comfort. Requirement for new data has occurred to determine the parameters and user expectations as advanced technology applications such as CNC machinery get to be used more in wood processing industry. Although wood is an easier material to process with respect to metal etc. its heterogeneous structure and variables due to process conditions make processing more complex. Research is on the effect of process parameters by CNC router on surface treatment quality. Two tree species and one wooden panel with intensive use in the furniture industry are selected for the study. The tree species are Beech and Ayous, and the wooden panel is MDF panel. The procedure parameters Spindle speed (rpm) and Feed rate (m/minute) are taken as variable, and the others are taken as fixed.

This study analyzes the impact of procedure parameters through CNC router on the surface treatment quality. In the analysis, cutter spindle speed, progress speed, cutting depth parameters and wooden material are taken as variable parameters. A two factorial experimental design is used. According to the results of the analysis, the surface structure significantly changes according to the material structure in CNC process. The surface structure becomes smoother as the spindle speed increases, and the surface structure gets worse as the feed rate is increased and a rougher structure appears.

***Keywords*:** A. CNC, B. Wood processing, C. Surface quality, D. Wood material, E. Surface roughness

Introduction

The majority of the problems arising the fields of use of the wooden materials is related to the failure in determining appropriate procedure parameters. The procedure speed varying from 0 to 60 meters per minute or processing thickness varying from 0 to 30 mm per minute and very variable speeds and other procedure parameters may have a wide range. Determining these parameters accurately is directly related with the expectation on the surface quality of the wooden material. It's been stated that applying CAD-CAM systems, which is based on CNC machinery, increases the efficiency up to 2,5 times [Kurtoglu et al. 1997, Kurtoglu et al. 1999].

The works on determining and defining the parameters for processing wooden material in CNC machinery increase by leaps. In a study, it's been suggested that the surface roughness has changed significantly depending to the parameters as a result of milling the material surfaces in CNC machinery and that these parameters can be defined with a suitable mathematical model [Nas et al.2012].

CNC applications become more popular in the forest industry. For example, 75% of the imported wood processing machines in Turkey are consisted of CNC machinery. Accurate selection and efficient use of CNC machinery depends of determining the procedure parameters [Aciyapamoglu 2013]. Procedure parameters in wood processing with CNC affect the surface quality [Karagoz 2010]. In addition to accurately determining the tool route and cutter movements in increasing the process efficiency, the structure of the cutter tool also directly affects the surface structure [Bozdogan 2012].

However, optimizing the process according to the expectation from the surface of the wooden material also brings some challenges. For this purpose, the sensor selection and surface estimations are studied in a study. The study states that it is possible to estimate the cutting depth with a regression analysis and artificial neural network as a result of low speed measurement procedures on the Paper Birch wood, and suggests a modeling for this purpose [Iskra and Hernandez, 2012]. In another study, it's been stated that the procedure time can be reduced by 54% in an optimization carried out with a fuzzy logic. The study particularly dwells on the feasible option of defining the relationship for the surface quality between the cutting force and the cutting direction [Gawronski 2013, Bajıc et al. 2008].

The readiness of the wood before use affects the expectations from the surface. The roughness values of a heat treated material is found out to be higher in radial directions with CNC process, and ideal application values differed for different tree species. It's been stated that the surface roughness after CNC process decreases when the heat

treatment temperature increases, but this does not apply for all cutting directions [Karagoz et al. 2011].

For the milling of beech wood with CNC, it's been found out that the cutting angle, feed rate and fiber direction affect the surface roughness, and cutting width does not have any impact on the surface roughness despite the increase in the sound intensity [Karagoz 2010, Karagoz et al.2011]

It's been stated that C++ and graphical interactive technologies can be used for increasing the efficiency and improving the quality in processing the wood with CNC [Lajie et al. 2011]. A study shows that the expectations related to the aging applications on wooden surfaces can be simulated with CNC machinery [Weg et al 2012].

It's been stated that cutting depth and cutting angle does not have an impact on surface roughness in processing the wood, but spindle speed and feed rate have an impact on surface roughness. The general information indicates that the roughness values would reduce when operated with lower feed rate and higher spindle speed [Rawangwong et al. 2011].

The cutting force is modeled with response surface method and box-behnken design and experiments methodology by using an experimental design in edge milling application on MDF [Norazmein et al. 2012].

In the CNC wood milling carried out on alder, a genetic algorithm was used and optimization results were obtained in a shorter time by optimizing it with CAM software [Krimpenis et al.2014].

Materials and Methods

Materials: Two tree species and one wooden panel with intensive use in the furniture industry are selected for the study. The tree species are Beech and Ayous, and the wooden panel is MDF panel. The samples are prepared as three samples with the dimension of 200 mm x 95 mm x 18 mm for each procedure parameter (Figure 1).

Figure 1: Examples for the Material Used

Methods: The study aims analyzing the impact of different surface treatment parameters on the surface quality in different wood materials. The samples are processed with 3-axis CNC router in an industrial environment for this purpose. A two factorial experimental design is used. The parameters selected and their levels are shown in Table 1.

Factors	High	Low
Spindle speed	18.000	15.000
Feed rate (m/minute)	10	8

Table 1: CNC Procedure Parameters and Levels

The assessment is carried out by taking 6.000 data on each sample, and 18.000 data in total. For this purpose, a robotic measurement system [Hazır 2012] consisted of a laser sensor and robot components is used. The results are subjected to statistical analyses with MINITAB software. The data is also processed with MATLAB software.

As the factors with an impact on surface quality in the study, cutting depth (2 mm), cutting angle, cutter type and diameter (10 mm) and cutting geometry (linear) are taken as fixed values.

Results

ANOVA analysis carried out related to the results arising with the wood treatment performed on different materials by using different surface treatment parameters with CNC is shown in Table 2. As it can be seen in Table 2, the results are assessed statistically with 95% confidence level. As a result of ANOVA analysis, the variables and their interactions are found out to be significant. The model explanation level of the variables used is R^2= 95,4%. This is considered as a very high level in the literature.

Source	DF	Adj SS	Adj MS	F-Value	P-Value
Material Type	2	2,957	1,4786	14097,95	0,000
Feed Rate	1	3,263	3,2632	31113,97	0,000
Spindle Speed	1	12,014	12,0142	114552,96	0,000
Material Type*Feed Rate	2	2,126	1,0630	10135,28	0,000
Material Type*Spindle Speed	2	5,284	2,6420	25190,78	0,000
Feed Rate*Spindle Speed	1	1,178	1,1776	11228,34	0,000
Material Type*Feed Rate*Spindle Speed	2	9,319	4,6596	44428,31	0,000
Error	17988	1,887	0,0001		
Total	17999	38,028			

Model Summary			
S	R-sq	R-sq(adj)	R-sq(pred)
0,0102410	95,04%	% 95,04	95,03%

Table 2: Analyze of Variance: Roughness versus Material Type; Feed Rate; Spindle

While there are significant changes in the surface structure according to the type of the material in CNC processing, the surface structure becomes smoother as the spindle speed increases, and the surface structure gets worse as the feed rate is increased and a rougher structure appears. Results of the main effects obtained are shown in Figure 2.

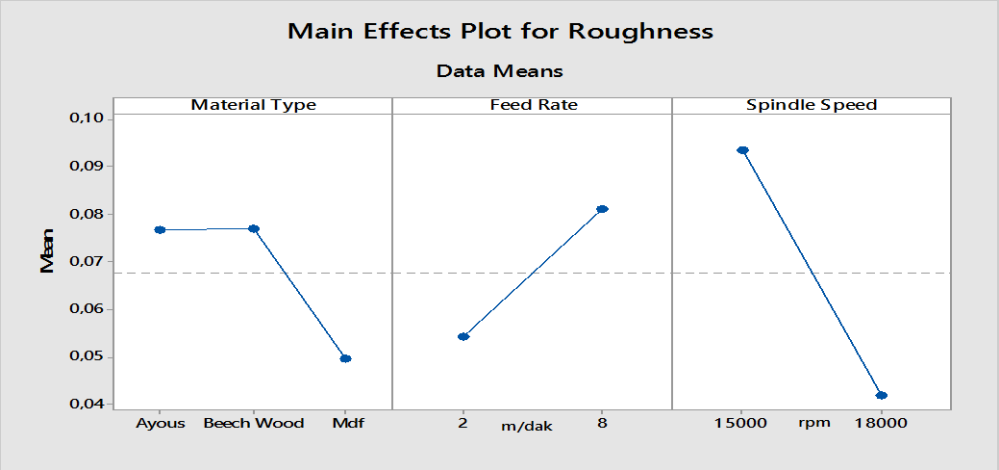

Figure 2: Results of Main Effects in Wood Processing

The results obtained when we interactively assess the surface treatment parameters used are as shown in Figure 3. According to these results, the surface structures obtained by applying the same parameters change when the material structure is changed. According to the findings of the study, approximately two times more surface structure differences are observed between each of three materials. When the feed rate changes, the surface structure also changes according to the material. Ayous has the less changing structure, while beech has the highest.

When the spindle speed increases, beech is the material with less surface structure impacts, while Ayous is affected the most.

The surface structure obtained with high spindle speed and low feed rate appears as the best structure.

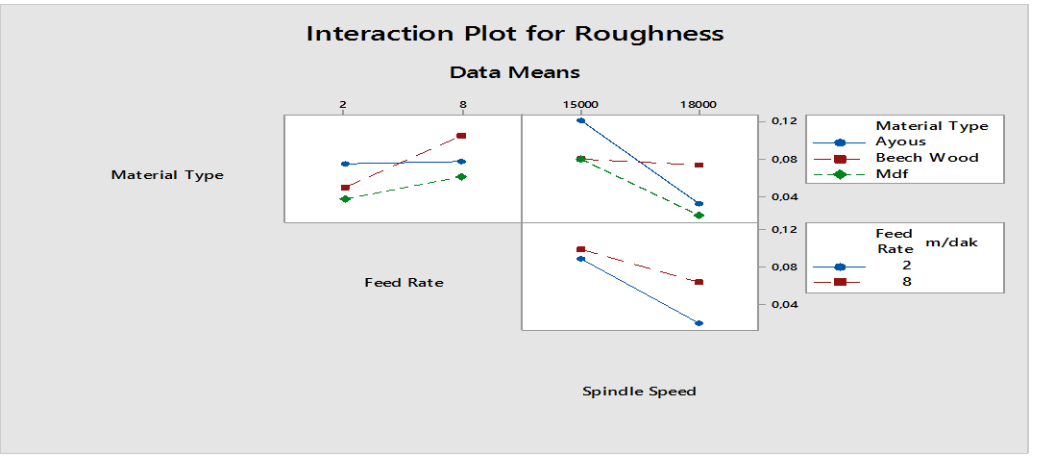

Figure 3: Interactive Results in Wood Processing

Conclusions

Surface structure in wood processing depends on to several factors. Material type, material structure, method for preparing the material to processing, feed rate, spindle speed, cutting angle, cutting depth (2 mm), cutter type, cutter diameter, cutting geometry (linear, curvilinear etc.) are basic factors that are effective on the surface quality. Assessing the surface structure generally based on surface roughness is a commonly used method. However, the limited number of data obtained and the limited number of actions in curvilinear surface structures necessitated the search for new measurements. In this study, the measurement is carried out by using a 2D laser displacement sensor. The results conform with the literature in general, but the results may differ when the interactions between the parameters are taken into account. It is an important field of argument to accurately determine the interaction between the parameters in processing with CNC.

References

Aciyapamoglu M, 2013 Multi Criteria Selection at CNC Wood Working Machinery. Istanbul Technical University, Graduate School of Science Engineering and Technology, MSc. Thesis

Bajıc D, Lela B, Zıvkovic D, 2008 Modeling of Machined Surface Roughness and Optimization of Cutting Parameters in Face Milling. Metalurgia 47(4):331-334.

Bozdogan M 2012 The Investigation Of Effects of Cutting Parameters and Cutting Tool Path of Surface Quality in CNC Milling Process. Marmara University, Institute of Pure and Applied Sciences, Mechanical Education Unit, MSc. Thesis

Gawronski T, 2013 Optimization of CNC Routing Operations of Wooden Furniture Parts. Int J Adv Manuf Technol (2013)67:2259-2267-DOI-10.1007/s00170-012-4647-5.

Hazir E, 2012 A Modeling Study on Evaluating the Quality of Wooden Surface. MSc. Thesis, Istanbul University Institute of Science, Istanbul, TURKEY

Iskra P, Tanaka C, 2005 The Influence of Wood Fiber Direction, Feed Rate and Cutting Width on Sound Intensity During Routing. Holz Als Roh-Und Werkstoff. 63(3),167-172.

Iskra P, Hernandez R, 2012 Toward a Process Monitoring of CNC Wood Router.Sensor Selection and Surface Roughness Prediction. Wood Sci Technol 46:115-128-DOI 10.1007/s00226-010-0378-7.

Karagoz U, 2010 Investigation of Machining Parameters on The Surface Quality in CNC Routing Wood and Wood-Based Materials, Suleyman Demirel University, Graduate School of Natural and Applied Sciences, MSc. Thesis

Karagöz U, Akyıldız M H, Isleyen O, 2011 Effect of Heat Treatment on Surface Roughness of Thermal Wood Machined by CNC, PRO LIGNO, Vol. 7, No.4, p. 50-58, ISSN 2069-7430

Krimpenis A A, Fountas N A, Tantziouras T, Vaxevanidis N M, 2014 Optimizing CNC Wood Milling Operations with The Use of Genetic Algorithms on CAM Software. Wood Material Science&Engineering, 2014, DOI 10.1080/17480272.2014.961959.

Kurtoglu A, Koc K H, Oner U, 1999, Edge Banding Application with CNC Machines and its Comparison with Conventional Machine. Furniture & Decoration Magazine,28,10-17.

Kurtoglu A, Koc K H, Oner U,1997, CAD-CAM Systems, CNC Machines and Turkish Furniture Industry, Machine-Metal Technology. 6(66), 114-120.

Lajie W U, Qiangbo Y E, Lijuan Y A O, Ruiwen H, Jing W, 2011 The Data Processing System of CNC Wood-Working Milling Machine. Second International Conference on Dijital Manufacturing &Automation, 2011 IEEE, DOI 10.1109/ıcdma.2011.306

Nas E, Samtas G, Demir H, 2012 Mathematical Modelling of Parameters Effecting Surface Roughness via CNC Routers. Pamukkale University, Journal of Engineering Sciences 18(1), 47-59.

Norazmein AR, Safian S, Sudin I, 2012 Mathematical Modeling of Cutting Force in Milling of Medium Density Fibreboard Using Response Surface Method. Advanced Materials Research 445(2012) 51-55.

Rawangwong S, Chatthong J, Rodjananugoon F, 2011 The Study of Proper Conditions in Face Coconut Wood by CNC Milling Machine,Proceedings of the 2011 IEE ICQR, 978-1-4577-0628-8/11.

Weg W, Chaun H, Xiang L, Feng M, Zang S, 2012 Antique Wood Flooring on the Feasibility Study for CNC Machining. International Conference on Biobase Material Science and Engineering, 978-1-4673-2383-3/12,2012 IEEE.

Acknowledgement

This study is supported by Scientific Research Projects Coordination Unit of Istanbul University with project no. UDP-46844.

Proceedings of the 58th International Convention of Society of Wood Science and Technology
June 7-12, 2015 – Grand Teton National Park, Jackson, Wyoming, USA

COST Action FP1407 - Understanding Wood Modification through an Integrated Scientific and Environmental Impact Approach

Andreja Kutnar[1]

[1]Assistant Professor, Andrej Marušič Institute, Faculty of Mathematics, Natural Sciences and Information Technologies, University of Primorska, Koper, Slovania.
Andreja.kutnar@upr.si

Abstract

Though many aspects of wood modification (chemical, thermal, impregnation) treatments are known, the fundamental influence of the process on product performance, the environment, and end of life scenarios remain unknown. To contribute to the low-carbon economy and sustainable development, it is essential to integrate interactive assessment of process parameters, developed product properties, and environmental impacts. Therefore, a group of researchers proposed a new COST Action FP1407 "Understanding wood modification through an integrated scientific and environmental impact approach", which was selected for funding in November 2014. The main objective of the Action FP1407 is to characterize the relationship between wood modification processing, product properties, and the associated environmental impacts in order to maximize sustainability and minimize environmental impacts. The Action will provide the critical mass of Europe-wide knowledge needed to achieve the future developments in the field. The networking, multi-disciplinary, exchange of knowledge, and scientific excellence, as well as the expertise of industrial members, will enable comprehensive research and development of modification processing and products design with emphasis on their environmental impacts. This presentation will briefly introduce the mechanism COST (European Cooperation in Science and Technology) and the key research areas, work plan and secondary objectives of this Action FP1407.

***Keywords*:** Modification, processing, LCA, EPD, cascading

Introduction

The Europeans Cooperation in Science and Technology (COST) is the longest-running European framework supporting trans-national cooperation among researchers, engineers and scholars across Europe. It was established in 1971 and covers 35 European member countries. Until 2015 it was structured into nine science and technology domains among which it is also Forest Products (FP) domain (for more details, see http://www.cost.esf.org/about_cost). New organization in place from 2015 has a single Scientific Committee, by which COST is aiming at guaranteeing a fully open and bottom-up approach.

COST provides funds for coordination of research through COST actions, while research remains funded on a national level. COST actions are thus networking activities based on predominantly nationally funded research projects on a research topic. There is a great emphasis on gender balance and inclusion of young scientists, as well as membership of researchers from COST Inclusiveness countries. It also allows all interested scientists from countries who sign the Memorandum of Understanding (MoU) to join the activities of the Action.

In the last call of past COST structure the COST Action FP1407 Understanding wood modification through an integrated scientific and environmental impact approach (ModWoodLife) was selected for funding. Its MoU is available on http://w3.cost.eu/fileadmin/domain_files/FPS/Action_FP1407/mou/FP1407-e.pdf. The Action started in March 2015 and will last until April 2019. The main aim of the Action is to characterize the relationship between modification processing, product properties, and the associated environmental impacts. This includes the development and optimization of modified processing and quantification of the impacts of emerging treatment technologies compared to traditional processing and alternative materials to maximize sustainability and minimize environmental impacts. The Action will provide the critical mass of Europe-wide knowledge needed to achieve the future developments in the wood modification processing with integrating assessment of process parameters, developed product properties, and environmental impacts.

The Action has members from 23 European countries (Figure 1) and 6 COST collaboration countries (Ukraine, Tunisia, USA, Canada, New Zealand, and Chile), while additional 3 expressed the intention to sign the MoU.

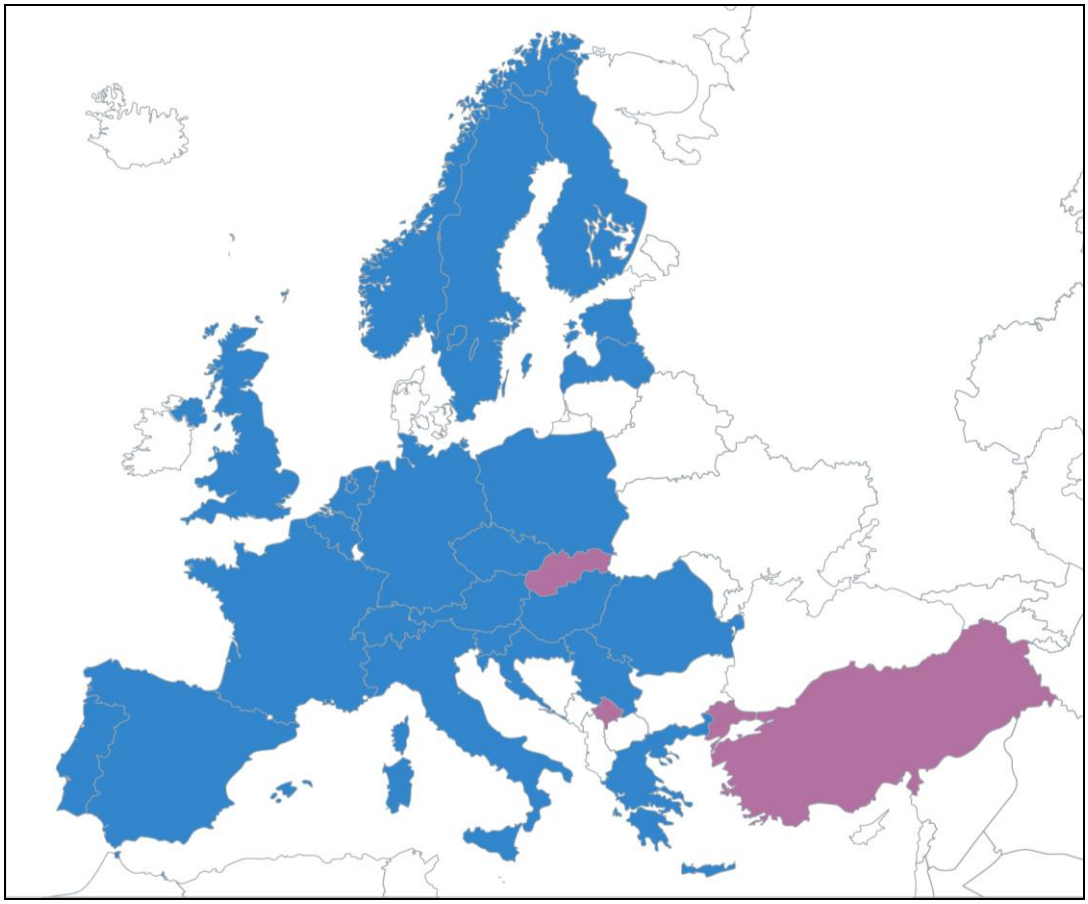

Figure 1: European countries involved in the Action FP1407 (blue – already members; violet intention to sign the MoU).

Reasons for the Action

The forest-based sector can become a leader in achieving the European Commission's ambitious CO_2 emissions reductions goal (Roadmap 2050) with innovative production technologies, reduced energy consumption, and increased wood products recycling. The use of forest products in long life products, such as in the built environment, allows for the possibility of extended storage of atmospheric carbon dioxide.

Forest-based industries are continually developing advanced processes, materials and wood-based solutions to meet evolving demands and increase competitiveness. Several emerging environmental-friendly processes of wood modification (chemical, thermal and impregnation/polymerization) have been developed, which can improve the intrinsic properties of wood, and provide desired form and functionality. However, a more detailed consideration reveals several issues which lead to the question: Is the global environmental impact of wood modification processing and further uses of the resulting products comparable with the impact of native, untreated wood? To address this question the Action FP1407 will apply the cradle to cradle (C2C) concept to the development of

products based on wood modification processes. This paradigm values new advanced wood-based materials with improved intrinsic properties that promote efficient product reuse, recycling and end-of-life use, and pave the way to a low-carbon economy.

Different modification processes, with possible variations in their parameters, yield modified wood with different properties, thusly enabling the creation of different product lines. However, they also have different environmental impacts, which are consequently transferred into materials, elements, and final products. Interactive assessment of process parameters, product properties, and environmental impact should be used to aid development of innovative modification processes and manufacturing technologies, existing and planned, which embrace the cradle to cradle paradigm. Recycling, up-cycling and end-of-life disposal options need to be integrated in a fully developed industrial ecology. Intelligent material reuse and up-cycling concepts could reduce the amount of waste destined for landfills or down-cycling. But in order to develop and/or optimize wood modification processing to minimize environmental impacts, much more information must be gathered about relevant process factors. This includes the development of chain of custody procedures throughout the entire life cycle.

Research into wood modification processing and the resultant products must place more emphasis on the interactive assessment of process parameters, developed product properties, and environmental impacts. Energy consumption contributes considerably to the environmental impact of modified wood. However, the improved properties during the use phase might reduce the environmental impact of the modified wood product overall. It is important to note that the effective use of wood throughout its whole value chain from forest management, through multiple use cycles, and end-of-life disposal can lead to truly sustainable development. Therefore, in order to contribute to the low-carbon economy, wood modification should implement: Establish baseline environmental impacts (Identify and quantify the environmental loads involved. Evaluate the potential environmental impacts of these loads followed by an assessment of the opportunities available to bring about environmental improvement); Demonstrate a manufacturer's commitment to sustainability and showcase the manufacturer's willingness to go above and beyond; (Product Category Rules (PCRs) should be defined in an internationally accepted manner based on an open, transparent and participatory process. EPDs should be acquired); Develop an "upgrading" concept for recovered products resulting from modified wood as a source of clean and reliable secondary wooden products for the industry that enable extended storage of captured carbon in wooden materials; Establish procedures for chain of custody value chain management for the whole life (tracking stored sequestered atmospheric carbon in timber products).

Organization of the Action

The Action FP1407 has 4 Working Groups (WG) that address the relevant key areas described in the MoU (http://www.cost.eu/COST_Actions/fps/Actions/FP1407):

WG1: Product Category Rules - Objectives: To develop product category rules for modified wood based on the scientific and industrial state-of-the-art of commercialized and developing modified wood products and technologies. Evaluation of current PCRs and adoption where appropriate.
Working Group 2: Life Cycle Assessments - Objectives: To perform objective environmental impact assessments of commercial modification processes and incorporate environmental impact assessments into wood modification processing and product development, including recycling and upgrading at the end of service life.
Working Group 3: Environmental products declarations - Objectives: To develop environmental product declarations based on WG1 and WG2 and force a harmonization of various national EPDs in the field of wood modification.
Working Group 4: Integration, dissemination and exploitation - Objectives: To ensure dissemination, evaluation, and exploitation of the Action's results together with establishing a strong network with the relevant industrial stakeholders.

The general organization (Figure 2) of the Action is as defined in organizational features common for all COST Actions "Rules and Procedures for Implementing COST Actions". The Action Chair, Vice Chair and WG Leaders together with the rest of Management Committee (MC) are in charge of the coordination, implementation and management of the Action. The Working Group (WG) Leaders report to the Action Chair and to the Management Committee (MC). The Action benefits from elected individuals serving on the MC and the Steering Committee (SC). The SC is comprised of the Chair and Vice-Chair of the Action, the Leaders and Vice-leaders of the Working Groups, a nominated manager for Short Term Scientific Missions. Given the direct relevance to commercial applications, industrial involvement is promoted through direct involvement within the MC/SC as a result of the creation of a dedicated industrial sub-committee, the Special Exploitation Committee (SEC). The SEC (comprised of industrial partners) promotes dissemination and commercialization of acquired knowledge.

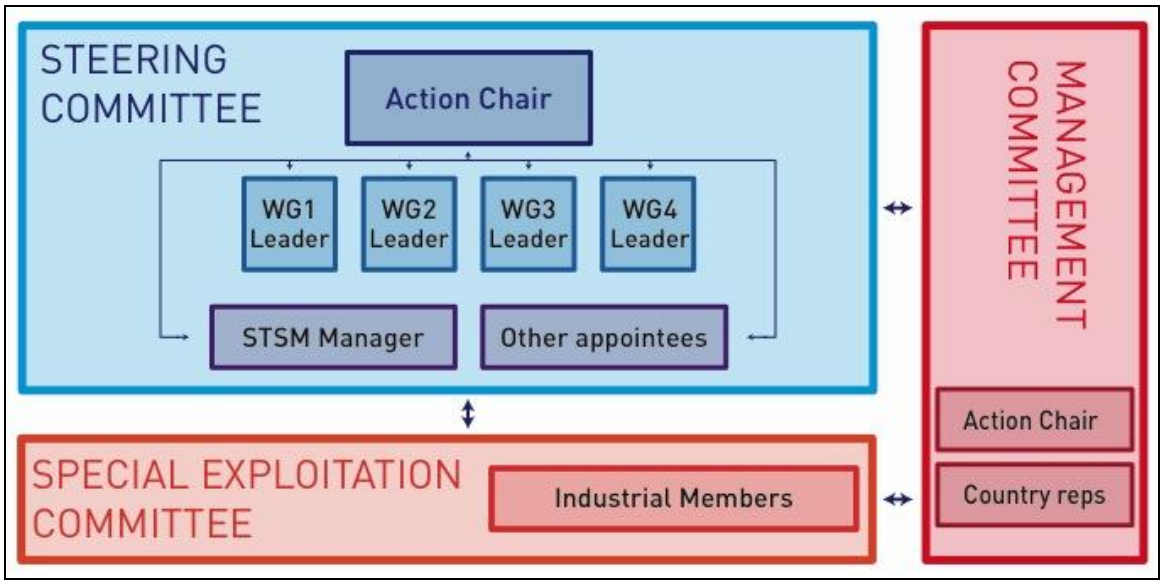

Figure 2: Management structure

Goals of the 1st Grant Period

The Action FP1407 defined 5 main goals of the 1st Grant Period (June 2015 – May 2016):

- Deliver state of the art of generic Life Cycle Assessments and Environmental Products Declarations of wood products in different Member States
- Perform systematic comparison of modification processes including their technical characteristics and environmental performance
- Deliver state of the art of life cycle analysis of different commercial modification processes ("cradle to gate" and "cradle to grave") and examine scenarios for the service life and end of life of wood products
- Explore possibilities to prepare a joint book to be suggested for publishing in Springer Series "Environmental Footprints and Eco-design of Products and Processes".
- Recruit industrial stakeholders to take part in a Special exploitation committee of the Action FP1407, which will promote dissemination and commercialization of knowledge acquired in Action FP1407.

Action created a Mendeley group, which is available on http://www.mendeley.com/groups/6789831/cost-action-fp1407-modwoodlife/, where a state of the art of the Action will be built.

Networking tools

The networking activities within the COST Action FP1407 include scientific and administrative meetings, short-term scientific missions and organization of training schools. Networking will yield the aims and objectives of the Action FP1407 by:

- M*aking* connections, facilitating collaboration and building enduring, mutually beneficial inter and intra disciplinary relationships between individuals, institutions and companies;
- *Creating* transnational, innovative interdisciplinary excellence to enhance the research and innovation performance of the sector;
- *Facilitate* collaboration between industry, SMEs, stakeholder associations, research organizations, leading-edge scientists from the wider range of disciplines covering wood materials, chemistry, construction, biology, polymer, environmental, and other relevant fields who will bring their broad expertise to this Action and enable the aims and objectives of this Action;
- *Scientific excellence*, interdisciplinary research and development leading to innovative and higher-value uses of renewable materials for technical applications;
- *Training and development* for professionals as well as under- and post-graduate students in COST countries, where special emphasis is given to exchange knowledge, especially between COST countries that traditionally have high levels

of participation to those who do not, like COST Inclusiveness countries and COST Near Neighboring countries.

-

These activities of the Action FP1407 will be enabled through Working Group meetings, Short Term Scientific Missions, Interaction with and visits to innovative companies, Training Schools for Early Stage Researchers, International seminars, and Workshops.

Impact of the Action

Networking, open discussion, planning and collaboration within the Action will provide the most productive, most proficient and most enduring tactic to build relationships among researcher from COST countries, COST Inclusiveness countries and COST Near Neighboring countries working on the topics of this Action and therefore leading to a positive transformation of the wood-based sector. Furthermore, strong emphasis on involvement of Early Stage Researchers and gender balance will have an impact on the future development of the sector in COST countries. High levels of participation will be encouraged to ensure these objectives are met, through the use of inclusive measures at meetings.

The expected scientific impacts will be the results of coordination and streamlining of profound scientific investigations on the basics of wood modification processing and modified wood, which will be used in industry for improvement and optimization of existing technologies and development of new modification processes, as well as development of Product Category Rules and life cycle models for modified wood. Besides the networking and collaboration based on current projects in the COST countries, this Action will result in new international and interdisciplinary project proposals, as well as the development of new standards.

Conclusion

The main aim and objectives of the Action FP1407 is to advance the research in the field of wood modification to allow significant contributions to the goals of European and global resource efficiency and a low carbon economy. These goals will be met by implementing excellent research in the area of wood modification, properties of modified wood, and environmental impacts. The interactive assessment of process parameters, product properties and environmental impacts performed in this Action will build on the previous scientific and technical research in environmental assessment and wood modification. The Action FP1407 will bring together knowledge, expertise, and infrastructure to achieve the Action’s aim. Current knowledge will be upgraded and known challenges overcome. The goals of sustainable development to increase economic efficiency, protect, and restore ecological systems and improve human well-being, or a combination of the three are expected to lead to new concepts, products, and processes

optimizing the multiple utilization/recycling of forest-based resources. Life cycle analysis, industrial ecology and the cradle-to-cradle concepts will be used as key tools also in economic developments leading to new business opportunities through innovative products with properties optimized to the end use requirements and the sustainable use of resources. It is emphasized that this work has to also extend to unmodified timber products, since baseline comparisons have to be made. This greatly extends the range and impact of the Action beyond the wood modification industries. Furthermore, the networking, multi-disciplinary collaboration, exchange of knowledge, and scientific excellence, as well as the expertise of industrial members, will lead to following indirect impacts:

- Low performing countries learning from advanced countries;
- Partners will become better equipped to seek competitive funding in national and international environment;
- Improved research and innovation culture of participants, especially SMEs;
- Participants write joint proposals for competitive funding and investment in RD&I within these;
- Dissemination activities enhance attitudes towards and perceived value of research and innovation in the general public and industry;
- Scientific discoveries, industrial developments and innovation achievements;
- Contributions to four "Europe 2020" flagship initiatives through innovation, resource efficiency, globalized industrial promotion and job creation.

Acknowledgments

The author would like to acknowledge the WoodWisdom-Net+ and the Ministry of Education, Science and Sport of Republic of Slovenia for financial support of the project CaReWood and W3B. Furthermore, the author would like to acknowledge the Slovenian Research Agency for financial support within the frame of the project Z4-5520.

More Information

COST Action FP1407 web page: http://costfp1407.iam.upr.si/en/

Proceedings of the 58th International Convention of Society of Wood Science and Technology
June 7-12, 2015 – Grand Teton National Park, Jackson, Wyoming, USA

Sustainability, Environmental Impact and LCA in Build Environment in Slovenia and Sweden

Andreja Kutnar, andreja.kutnar@upr.si
Dick Sandberg, dick.sandberg@ltu.se

University of Primorska, Andrej Marušič Institute, Muzejski trg 2, SI-6000 KOPER

Abstract

Forestry and forest-related industries have become more focused on the major challenges of the future, especially climate change and resource depletion. The forest-based sector can become a leader in achieving the European Commission's ambitious target of reducing CO2 emissions with innovative production technologies, reduced energy consumption, increased wood products recycling, and reuse. Apart from these undoubted environmental benefits, the use of forest products in long life products, such as built environment applications, allows for the possibility of extended storage of atmospheric carbon dioxide. Despite many sustainable and green building activities in recent years there is a lot of room for expansion and improvement in this area. In fact, a shift towards new building paradigms is just beginning. These paradigms shift the standard from minimal and zero environmental impact, towards positive impacts for both the environment and society.

In this paper the Slovenian and Swedish case is presented in relation to the current European and regional developments in the increased use of wood as a construction material for the future. Furthermore, the role of building and living with wood in sustainable development together with the topic of green buildings movements and the current trends of creating healthy living environments are introduced.

Proceedings of the 58th International Convention of Society of Wood Science and Technology
June 7-12, 2015 – Grand Teton National Park, Jackson, Wyoming, USA

Sustainable Built Environment in Canada and Europe

Alberto Cayuela, alberto.cayuela@ubc.ca
Angelique Pilon, angelique.pilon@ubc.ca
Andreja Kutnar, andreja.kutnar@upr.si

University of Primorska, Andrej Marušič Institute, Muzejski trg 2, SI-6000 KOPER

Abstract

Global political and economic decisions are increasingly determined by resource and energy availability and by climate change imperatives. Increasingly, balancing economic, ecological and social welfare objectives has become a key goal of development in many jurisdictions in Europe and North America. Because of their low embodied energy, their ability to displace carbon emissions and store atmospheric carbon, bio-based materials supplied through sustainable forest practices are becoming a cost-effective solution for urban sustainability. Concurrently, the focus on minimizing the impacts of development is shifting toward the idea that development can bring about net positive benefits to the environment and society. Despite the steady growth of green buildings in recent years and the transformative effect on the building industry of rating systems such as LEED and BREEAM, there still exists significant potential for increased adoption of sustainable practices by large sectors within the building industry. This presentation will introduce living laboratories (user-centred ecosystems that integrate research and systematic innovation processes within public-private-civil society partnerships) as catalyzers for sustainability in the built environment and describe the role that bio-based materials play. It will contrast European and Canadian case studies of projects focusing on wood and bio-based materials as integral elements of a sustainable built environment.

Proceedings of the 58th International Convention of Society of Wood Science and Technology
June 7-12, 2015 – Grand Teton National Park, Jackson, Wyoming, USA

Magnetic Resonance Investigation of Freezing and Thawing of Black Spruce Wood

Clevan Lamason[1], Bryce MacMillan[2], Bruce Balcom[2], Brigitte Leblon[1], and Zarin Pirouz[3]

[1]Faculty of Forestry and Environmental Management, University of New Brunswick (UNB), NB, CANADA
(clamason@unb.ca)
[2]Magnetic Resonance Imaging Center, Department of Physics, UNB, NB, CANADA
[3]Faculty of Forestry and Environmental Management, UNB, NB, CANADA
[4]Scientist, FPInnovations, Vancouver, CANADA

Abstract

This study examines the phase transitions of water in black spruce (*Picea mariana* Mill.) sapwood by unilateral magnetic resonance and magnetic resonance imaging. The goal is to observe and understand the behavior of water below 0°C in wood. The species studied presented one abrupt phase change that occurred around -3°C, which was attributed to the phase transition of free water. A more diffuse change occurred below -60°C which was attributed to a phase transition of bound water. A recently developed portable unilateral magnetic resonance instrument is demonstrated as a powerful tool in the study of water in wood. This portable magnet employed a bulk spin-spin relaxation time measurement that quantifies observable bound and free water in wood. Imaging is employed to verify the unilateral magnetic resonance results and to better understand realistic freeze/thaw behavior of log samples in the field. A ring boundary behavior during the thawing process was observed and likewise there are differences in the thawing behaviors of heartwood and sapwood samples.

Proceedings of the 58th International Convention of Society of Wood Science and Technology
June 7-12, 2015 – Grand Teton National Park, Jackson, Wyoming, USA

Carbon Policy Failures and the Opportunity for Better Uses of Wood: If We Have Carbon Negative Technologies Why Aren't We Using Them?

*Bruce Lippke**
Professor Emeritus
College of Environment
University of Washington
Seattle, WA, 98195
blippke@uw.edu

Elaine Oneil
Executive Director: CORRIM &
University of Washington
Seattle, WA, 98195

Holly Fretwell
Research Fellow PERC &
Faculty Montana State University
Bozeman, MT, 59718

Abstract

The rate of global carbon emissions continues to increase. The objective is to stop the increase and even reduce atmospheric carbon. That requires using carbon negative technologies. Just increased efficiency in the use of fossil fuel to reduce emissions at best only slows down the rate of increase. Yet we have carbon negative technologies such as storing carbon taken from the atmosphere by forest growth in wood products while displacing the emissions from using fossil fuels. Some uses of wood store and displace 10 times the carbon as other uses. So why aren't these technologies being better used? There is no incentive to innovate for even better uses because there is no cost for emitting fossil carbon emissions. The problem is exacerbated because we subsidize the use of fossil fuels as well as other incentives that promote the lowest leverage use of wood products. We examine why policies are not working and how different approaches can be much more effective. Carbon cap and trade is not working and especially for uses of wood with thousands of different product carbon pools that are interacting with other

pools that would require trading rules far beyond the capabilities of masses of regulators. We develop a hierarchy of displacement efficiencies for different product uses. Any significant value placed on fossil carbon emissions will motivate better uses of wood to displace fossil emissions along with new innovations to improve the production process and the way we use wood. Integration of the analysis from forest to products to uses and their displacement is essential to understand best uses. Forest carbon by itself is inherently only useful for a one-time reduction in carbon before reaching the carrying capacity of the land. In contrast harvesting wood near its maximum growth rate and using that wood to store carbon in products while displacing fossil intensive products is a sustainable use carbon-negative technology.

Key Words: carbon mitigation, carbon emissions, carbon negative technologies, Life Cycle Inventory Assessment (LCI, LCA), carbon policies, sustainable forestry, carbon Cap & Trade, biofuels, wood products, carbon displacement.

Proceedings of the 58th International Convention of Society of Wood Science and Technology
June 7-12, 2015 – Grand Teton National Park, Jackson, Wyoming, USA

Investigation of Hardwood Cross-Laminated Timber Design

Joseph , jloferski@vt.edu
Khris Beagley, beagleyk@vt.edu
Dan Hindman, dhindman@vt.edu
John Bouldin, woodyzz@vt.edu

Virginia Tech, 1650 Research Center Dr., Brooks Forest Products Center, Blacksburg, VA 24061-0503

Abstract

The objective of this paper is to investigate the feasibility of using various design methods for predicting the mechanical properties of hardwood cross laminated timber (CLT). A program was developed to compute the predicted stiffness properties using four different mechanics based methods: (1) the Shear Analogy Method, (2) the Gamma Method, (3) the k-Method and (4) classical transformed section analysis. The project compared predicted stiffness values to experimentally measured parameters. Yellow-poplar (Liriodendron tulipifera) lumber was used to create hardwood CLT beams that were non-destructively tested in bending in both flatwise and edgewise orientations with the face grains arranged either parallel or perpendicular to the span. Upon completion of non-destructive testing, the hardwood CLT beams were tested to failure in bending in either a flatwise or edgewise orientation. The tests emulated practical loading conditions and the experimental data collected was compared to analytically calculated deflections. The Modulus of Rupture (MOR) was calculated from each beam and used to determine the feasibility of utilizing CLT within each loading configuration. The experimental MOR was compared to predicted values.

The results support the conclusion that both the stiffness and strength of hardwood CLT can be predicted using the same design methods that were developed for softwood species. This finding opens the possibility of using hardwoods in CLT production.

Proceedings of the 58th International Convention of Society of Wood Science and Technology
June 7-12, 2015 – Grand Teton National Park, Jackson, Wyoming, USA

Cellulose Nano-Whiskers Dispersing Performance in Non-Polar Materials

Jing Luo, luojing.rowe@gmail.com
Gao Qiang, gao200482@163.com
Jianzhang Li, lijianzhang126@126.com
Sheldon Shi, Sheldon.shi@unt.edu

Beijing Forestry University, No.35 Qinghua East Road , Haidian District, Beijing 100083

Abstract

As a renewable functional materials, cellulose nano-whiskers(CNWs) were widely investigated in wood industry. The higher the cellulose content, the higher the percentage of the crystalline component, CNWs can present a higher mechanical property. CNWs are crystalline cellulose sticks with numbers of hydroxyl groups on their surface. Those hydroxyl groups can form hydrogen bond with water molecules, so that the CNWs could easily disperse in water or other polar solutions. Therefore, CNWs have been used to reinforce urea formaldehyde resin, soy protein-based adhesive, polyvinyl alcohol film in wood industry because of its water solubility. However, CNWs are difficult to be dispersed in non-polar liquid to form a stable and uniform solution, which has limited it applications. In this research, CNWs were first fabricated using acidolysis method. Then, CNWs was washed and dispersed into n-hexane or acetone by a physical method. The hybrid solution was introduced and dispersed into non-polar liquids in a high temperature, such as ethylene-co-vinyl acetate (EVA), polyvinyl chloride, and poly ethylene. The effect of the incorporation of cellulose nano-whiskers on tensile strength, modulus of rupture (MOR), light transmittance performance, cross section characteristic, thermostability of non-polar materials were investigated. Preliminary experiments showed CNWs was successfully dispersed into EVA and the MOR of the EVA was improved by at lest 20%

Proceedings of the 58th International Convention of Society of Wood Science and Technology
June 7-12, 2015 – Grand Teton National Park, Jackson, Wyoming, USA

Durability Assessment of Bamboo Slats

Arijit Sinha, arijit.sinha@oregonstate.edu
Byrne Miyamoto, miyamotb@onid.orst.edu
Jeff Morrell, jeff.morrell@oregonstate.edu

Oregon State University, 234 Richardson Hall, , Corvallis, OR 97331

Abstract

Bamboo is the most rapidly growing renewable material. In the western world, acceptance of bamboo has been limited to commodity products. Bamboo composites such as laminated bamboo lumber (LBL) can be used structurally in buildings, but a major challenge that limits acceptance of LBL is concern about long term performance under different climatic conditions. Bamboo culms are known to degrade rapidly after harvest when improperly processed. While LBL components are generally rapidly processed and often treated to provide long term protection, there are few data on the field performance of these materials. In this report, bamboo slats, which are the building blocks of LBL, along with Douglas-fir heartwood and hybrid poplar were exposed outdoors in a Ground Proximity test near Corvallis, OR. Douglas-fir is moderately durable while hybrid poplar has little resistance to biological degradation. The site has a Mediterranean climate with wet mild winters and dry summers and moderate above ground decay risk. Material properties and the degree of biological damage were assessed monthly over a 20 months. Flexural properties were increasingly variable with time for all three materials and the specimens began to experience stain and mold damage. No evidence of visible decay was noted. The results will be discussed in relation to the potential for using bamboo components where periodic wetting is possible and identify approaches for improving the durability of these materials.

The Effect of Urea-Formaldehyde Resin Adhesive on ohe Pyrolysis Mechanism of Poplar Particle Board with DAEM

Mu Jun[1], Zhang Yu[1], Yu Zhiming[1], Zhang Derong[1], Zhang Yang[1]*

[1] Associate Professor, MOE Key Laboratory of wooden Material Science and Application, Beijing Forestry University, Beijing, China.
* *Corresponding author*
mujun222@sina.com
[1] Graduate student, College of Material Science and Technology – Beijing Forestry University, Beijing, China.
zybjfu@126.com
[1] Professor, MOE Key Laboratory of wooden Material Science and Application, Beijing Forestry University, Beijing, China.
yuzhiming@bjfu.edu.cn
[1] Associate Professor, MOE Key Laboratory of wooden Material Science and Application, Beijing Forestry University, Beijing, China
zhdr666666@sina.com
[1] Assitant Professor, MOE Key Laboratory of wooden Material Science and Application, Beijing Forestry University, Beijing, China
zhangyang@bjfu.edu.cn

Abstract

In order to study the effect of urea-formaldehyde resin adhesive(UF) on the pyrolysis process of wood composites, the pyrolysis-related weight loss process of UF resin adhesive, poplar wood and poplar particle board was compared with temperature programming thermogravimetry analysis to test the adaptability of a DAEM (distributed activation energy model) to their kinetic analysis. With the Miura integration method, the activation energy distribution and the values of the frequency factor can be directly obtained from three weight loss curves at temperature rise of 5℃/min, 20℃/min and 50℃/min, requiring no prior assumption of the activation energy distribution of pyrolysis and the frequency factor assuming at a fixed value. The results obtained show that the activation energy of UF was higher than that of poplar and poplar particle board at the same conversion rate. The variation of activation energy curves was similar for the poplar and the poplar particle board. UF resin promoted the thermo degradation of poplar and

made the activation energy of particle board lower than that of the poplar during the main pyrolysis stage. The activation energy distribution of UF resin, poplar and poplar particle board was not a standard Gaussian curve, while the activation energy of poplar and particle board focused on 140~200 kJ/mol, however, the UF resin activation energy was concentrated at 150~300 kJ/mol. The activation energy and frequency factor of UF, poplar and particle board revealed a good kinetic compensation effect and the DAEM model can be used to describe a whole process of a non-isothermal pyrolysis of wood composites with resin. The distribution function of activation energy reveals changes of the reaction properties of mass in different stages of pyrolysis, which helps to investigate the pyrolysis mechanism of poplar particle board.

Key words: urea-formaldehyde resin adhesive, poplar particle board, pyrolysis kinetic, distributed activation energy model (DAEM)

Introduction

Wood composites, as a special bio-material, comprise the complicated and uneven characters when they are pyrolysis treated. The factors for pyrolysis of these waste wood composites include kinds and size of materials, pyrolysis air condition, temperature increasing speed, the final temperature, treatment time as well as pressure, all of which hinder the research on the pyrolysis mechanism of waste wood composites(Zhang and You, 2011). The dynamic analysis support an effective way for solving this problem. Nowadays, thermal dynamic analysis is generally applied in quantitative characterization of the pyrolysis reaction process.

Wood, as main component of wood composites, is a complicated natural polymer. It is difficult to monitor its pyrolysis process because the resin involved in the composites make the thermo degradation more complicated. Distributed Activation Energy Model can be used to study the pyrolysis process. Miura integration method is a quick and easy method to directly calculate the activity energy and frequency factor through step approximation function without a hypothesis of frequency factor (Chen, et al 2013). DEAM based on the assumption as the Fig.1, does not involve the concrete pyrolysis products, which can be used to describe the dynamic whole pyrolysis process adaptive for different materials and different temperature increasing rate(Wei, et al 2012).

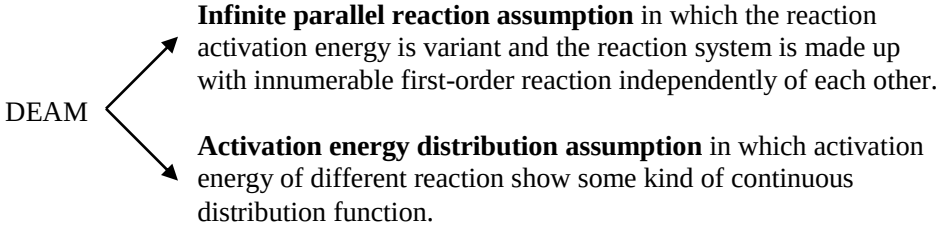

Fig.1 Distributed activation energy model assumptions

In this paper, the poplar particle board with UF resin adhesive was used as raw material to evaluate the applicability of DEAM to the thermal decomposition kinetics function of particle board with Miura integration method.

Materials and Method

Populus cathayana particle was purchased from Shandong Fumulin new energy equipment Co, Ltd with the size of 10~20 mm long and 0.1~0.5 mm thick. UF resin was got from Beijing keno wood company with 51.73% of solid content. The particle board was prepared in the lab with poplar particle and UF resin adhesive. The chemical composition was shown as in Tab.1.

Tab.1 Ultimate analysis and chemical composition of raw material

Sample	Ultimate analysis/%				chemical composition/%				
	C	H	N	O[a]	Holo cellulose	cellulose	hemi cellulose	lignin	Ash
P	48.44	5.49	0.13	45.95	77.19	48.76	28.43	21.54	4.4
UF	34.69	5.59	33.72	26.01	-	-	-	-	-
PB	48.04	5.78	2.00	44.18	-	-	-	-	-

[a]: Content of O was obtained by difference.

TG-DSC of simultaneous thermal analyzer (STA449F3) was sent from 50 to 900℃ under dynamic programmed temperature control at increasing rates of 5 ℃/min, 20 ℃/min and 50 ℃/min with high purity Argon as protecting gas at 20 mL/min of flow rate. All the data of reaction process was automatically recorded by the system.

Results and Discussion

According to the Miura integration method, equation (1) can be got as the following:

$$\ln\left(\frac{\beta}{T^2}\right) = \ln\left(\frac{k_0 R}{E}\right) + 0.6075 - \frac{E}{RT} \qquad (1)$$

Based on the TG data of UF, poplar and particle board at three different temperature increasing rates, the slope and intercept was obtained from the curve drawn with $\frac{1}{T}$ as horizontal axis and $\ln\left(\frac{\beta}{T^2}\right)$ as vertical coordinates at a conversion rate α, which represented activation energy E and frequency factor k_0 at conversion rate α, respectively. In the same way, the E and k0 at different conversion rate can be got. If the conversion

rate α was selected as horizontal axis and reactivation energy E as vertical coordinates, the variation tendency curve of activation energy can be drawn. Activation energy distribution curve $f(E)$ can be obtained by the activation energy for the conversion of differential.

Fig.2-4 showed the curve of $\frac{1}{T}-\ln\left(\frac{\beta}{T^2}\right)$ at the temperature increasing rate of 5 ℃/min, 20 ℃/min and 50 ℃/min, in which the data of three temperature increasing rates for UF, poplar, particle board can be connected to a line at a given conversion α.

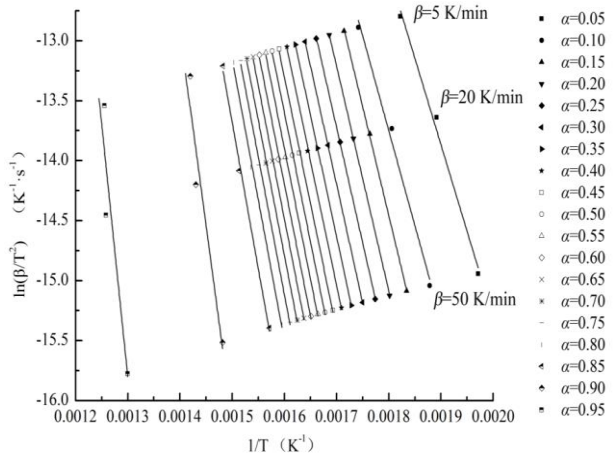

Fig2 The $\frac{1}{T}-\ln\left(\frac{\beta}{T^2}\right)$ curves of poplar

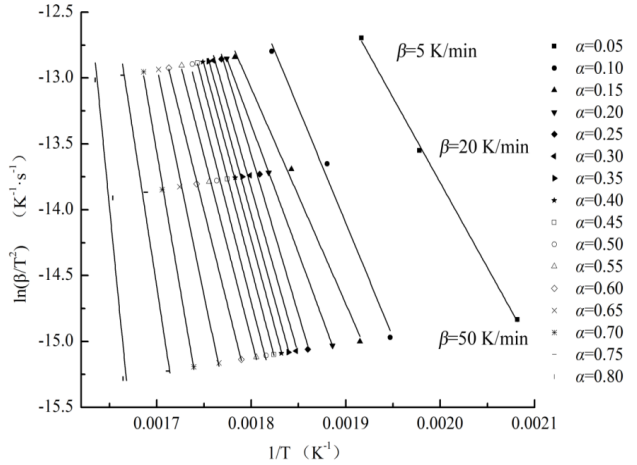

Fig3 The $\frac{1}{T}-\ln\left(\frac{\beta}{T^2}\right)$ curves of UF resin adhesive

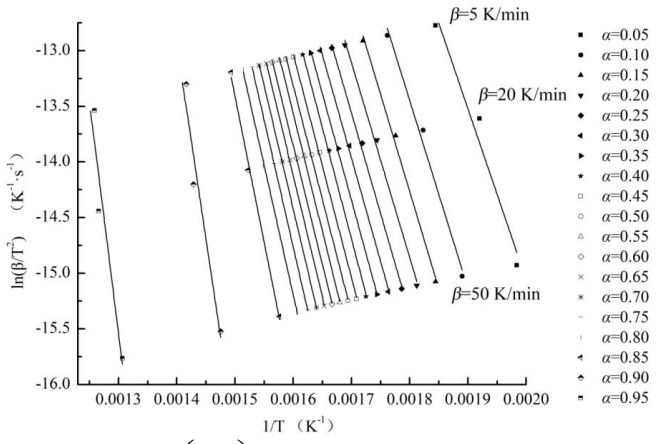

Fig4 The $\frac{1}{T}$ - $\ln\left(\frac{\beta}{T^2}\right)$ curves of particle board

The activation energy E and frequency factor k_0 were calculated from the slope and intercept base on the curves of Fig.2-4 and the values was showed in Tab.2. From Tab.2, the frequency factor k_0 of polar, UF resin and particle board was found to increase with the increasing of the activation energy E. The result accorded with the former research (Yang, et al 2010).

Tab.2 The activation energy and frequency factor of poplar, UF resin adhesive and particle board

α	Poplar			UF resin			Particle board		
%	E (kJ/mol)	k_0 (s^{-1})	R^2	E (kJ/mol)	k_0 (s^{-1})	R^2	E (kJ/mol)	k_0 (s^{-1})	R^2
0.05	119.87	5.87×10^{9}	0.992	107.31	1.17×10^{9}	0.9991	127.57	5.13×10^{10}	0.9695
0.10	131.44	2.10×10^{10}	0.9921	144.53	1.57×10^{12}	0.9927	140.29	2.06×10^{11}	0.9907
0.15	150.83	7.89×10^{11}	0.9997	135.88	1.11×10^{11}	0.9955	145.09	2.65×10^{11}	0.9961
0.20	155.56	1.21×10^{12}	1	162.02	2.88×10^{13}	1	145.45	1.59×10^{11}	0.9963
0.25	159.86	1.80×10^{12}	0.9999	201.52	1.48×10^{17}	0.9971	150.13	2.72×10^{11}	0.9978
0.30	163.90	2.62×10^{12}	1	210.26	7.93×10^{17}	0.9971	154.39	4.45×10^{11}	0.9982
0.35	168.41	4.38×10^{12}	1	216.90	2.81×10^{18}	0.9992	159.34	8.65×10^{11}	0.9992
0.40	172.84	7.42×10^{12}	0.9994	221.39	6.28×10^{18}	0.9997	165.89	2.43×10^{12}	0.9992
0.45	175.28	8.53×10^{12}	0.9993	227.47	1.93×10^{19}	0.9999	166.99	2.16×10^{12}	0.9994
0.50	179.12	1.36×10^{13}	0.9994	232.76	4.81×10^{19}	0.9945	169.91	2.91×10^{12}	0.9993
0.55	181.26	1.54×10^{13}	0.9992	231.47	2.73×10^{19}	0.9988	175.63	7.03×10^{12}	0.9995

0.60	182.83	1.56×10^{13}	0.999	239.04	9.16×10^{19}	0.9998	176.62	6.39×10^{12}	0.9997
0.65	184.91	1.76×10^{13}	0.9995	287.81	1.67×10^{24}	0.997	181.53	1.30×10^{13}	0.9999
0.70	187.26	2.07×10^{13}	0.9993	348.62	2.66×10^{29}	0.9984	184.45	1.71×10^{13}	0.9999
0.75	191.11	3.19×10^{13}	0.9984	387.25	2.88×10^{32}	0.9815	189.98	3.62×10^{13}	0.9998
0.80	195.04	4.73×10^{13}	0.997	615.03	3.46×10^{51}	0.9289	194.08	5.30×10^{13}	0.9991
0.85	202.87	1.19×10^{14}	0.9967	-	-		217.72	2.44×10^{15}	0.9971
0.90	270.30	2.54×10^{18}	0.9363	-	-		291.70	9.84×10^{19}	0.9541
0.95	350.31	1.92×10^{21}	0.8699	-	-		348.09	1.74×10^{21}	0.9265

Fig. 5 showed the variation of activation energy along with the conversion rate for the poplar, UF and particle board. The activation energy of poplar and particle board increased with the increasing of the conversion rate in a similar variation curve. When $0.15\leq\alpha\leq0.85$, the *E* of poplar increased gently, while the E increased obviously at $\alpha\geq0.85$. There might be more active sites for cellulose and hemicellulose which induced to react easily, active site of the wood decreased along with reaction development and need more energy for further reaction. At the final of the pyrolysis, lignin conversed into the charcoal and the activation energy increased because the activity lowed down (Li, en al 2007).

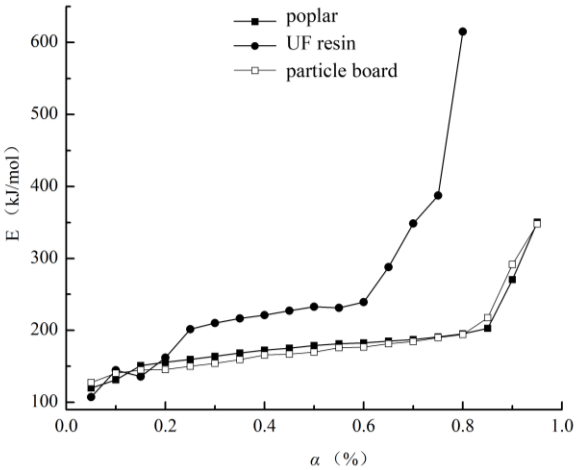

Fig.5 Activation energy E versus conversion rate α of poplar, UF resin and particle board

As shown in Fig.5, as $\alpha\geq0.20$, the activation energy of UF was obviously higher than that of the poplar and PB at the same conversion rate, which indicated that thermo degradation reactivity of UF was lower than the wood components. When conversion rate was between 0.15 and 0.80, the activation energy of PB was lower than that of poplar, which meant that the reaction of poplar and UF adhesive in the PB was not simply overlaid. UF resin promoted the decomposition of the PB during the main pyrolysis

process. However, as the conversion was over 0.8, the activation energy of PB turned to be higher than UF resin. UF resin might hinder the cross linking of thermo degradation product at the final stage.

Fig.6-8 showed the distribution curve of activation energy for poplar, UF resin and PB, respectively. The activation energy distribution of UF resin, poplar and poplar particle board was not a standard Gaussian curve, while the activation energy of poplar and particle board focused on 140~200 kJ/mol, however, the UF resin activation energy was concentrated at 150~300 kJ/mol. The distribution function of activation energy showed the maximum at E=182.83 kJ/mol for poplar, 221.39 kJ/mol for UF and 145.45 kJ/mol for PB. UF resin had a significant impact on the pyrolysis characteristics of PB.

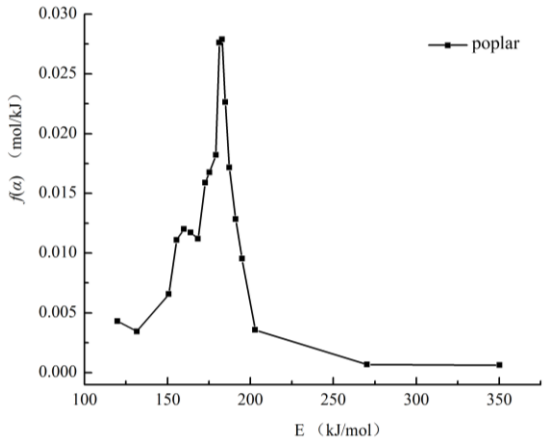

Fig.6 Activation energy distribution curve of poplar

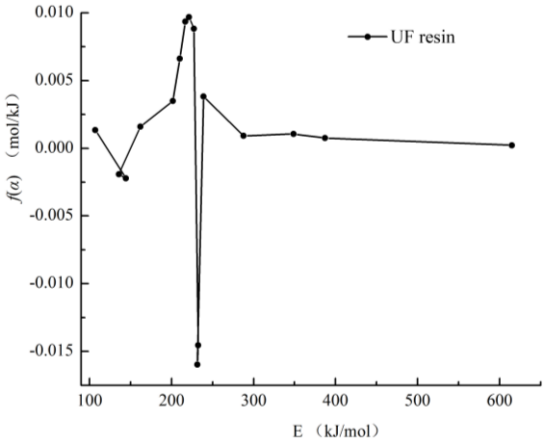

Fig.7 Activation energy distribution curve of UF resin

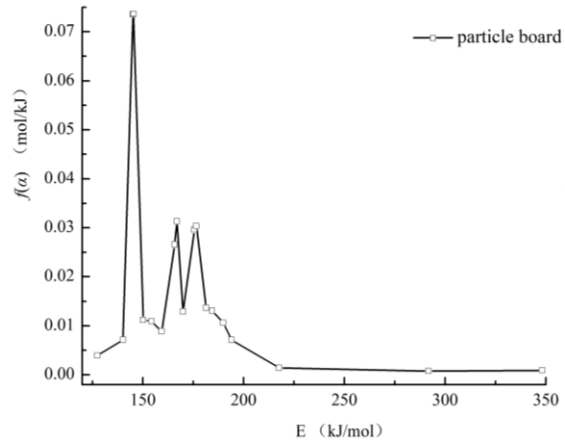

Fig.8 Activation energy distribution curve of PB

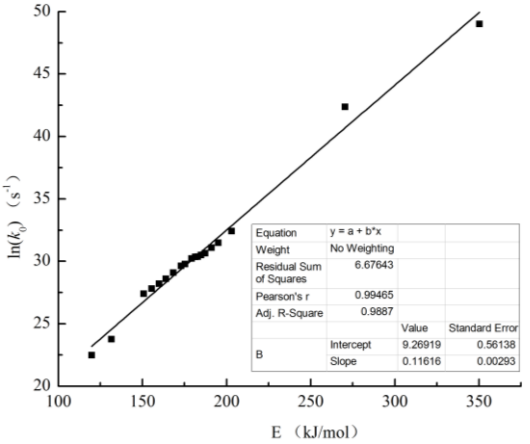

Fig.9 The *E*-ln(k_0) curve of poplar

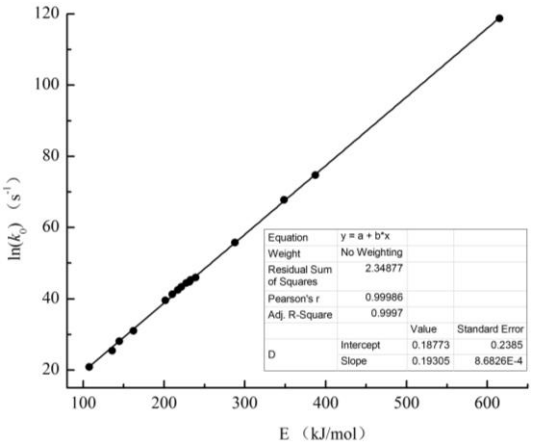

Fig.10 The *E*-ln(k_0) curve of UF resin adhesive

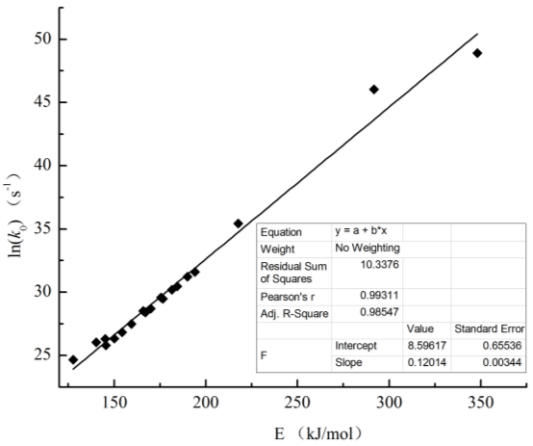

Fig.11 The *E*-ln(k_0) curve of particle board

From the *E*-ln(k_0) curve showed in Fig.9-11, there was a good liner relation between the *E* and ln(k_0), which indicated a compensation effect of dynamics(Hu and Shi, 2001). The *E*-ln(k_0) curve can be fitted into the equation as $\ln(k_0) = aE + b$, in which a and b were compensation factor. The relation factor R^2 of fitted curve was 0.9987, 0.9997 and 0.9855 for poplar, UF and PB. A good compensation effect of dynamics stated that DAEM was suitable to describe the pyrolysis process of wood, UF and wood composite because the calculation dynamic function was reasonable and practicable(Zhang and You, 2011).

Conclusion

Through the activation energy distribution method(AEDM),the result showed that the activation energy distribution of UF resin, poplar and poplar particle board was not a standard Gaussian curve, while the activation energy of poplar and particle board focused on 140~200 kJ/mol, however, the UF resin activation energy was concentrated at 150~300 kJ/mol. The activation energy of UF resin was higher than that of poplar and particle board at the same conversion rate. The UF resin induced to lower the activation energy of particle board and promoted the thermo degradation of wood during the main pyrolysis process. The activation energy and frequency factor of UF, poplar and particle board revealed a good kinetic compensation effect and the DAEM model can be used to describe a whole process of a non-isothermal pyrolysis of wood composites with resin.

Acknowledgements

This study was funded by National Natural Science Foundation of China (31170533).

Reference

Chen YX, Gan YP, Chang N (2013) The effect of Fe_2O_3 on the kinetic parameters of the Yulin coal pyrolysis. J. Xi'an Univ. of Arch. Tech. (Natural Science Edition) 44(5): 736-739. In Chinese with abstract in English.

Hu ZR, Shi QZ (2001) Thermal analysis kinetics. Science Press, Beijing.

Li SF, Fang MX, Shu LF, et al(2006) Pyrolysis and combustion mechanism of wood with distribution activation energy model. J. of Combustion Sci. and Tech. 12(6): 535-539.

Wei ZG, Huang YQ, Yin XL, et al (2012) Kinetics study on activating corncob hydrolysis residues char pyrolysis by ZnCl. Renewable Energy Resources 30(1): 62-66.

Yang JB, Zhang YW, Cai NS (2010) A comparison of a single reaction model with a distributed activation energy one based on coal pyrolysis kinetics. J. of Engineering for Thermal Energy & Power 25(3): 301-305.

Zhang K, You CF (2011) Research on the parallel reaction Kinetic Model of lignite pyrolysis. Proceedings of the CSEE 31(17): 26-31.

Proceedings of the 58th International Convention of Society of Wood Science and Technology
June 7-12, 2015 – Grand Teton National Park, Jackson, Wyoming, USA

CLT Served Any Way You Want It: n Overview of 19 Plants Toured in 2012-2014. Abridged

Lech Muszynski, Lech.Muszynski@oregonstate.edu

Oregon State University, 119 Richardson Hall, Corvallis, OR 97331

Abstract

Cross-laminated timber, or CLT, is a massive structural composite panel product usually consisting of 3 to 9 layers of dimensional timber (lamellas) arranged perpendicular to each other, much like layers of veneer in plywood, and can be used as prefabricated wall, floor and roofing elements in residential, public and commercial structures. This is not merely a new engineered composite panel product but an entirely new building technology revolutionizing the use of timber in construction. The CLT manufacturing process and the technology of erecting prefabricated houses based on this product has been developed in Europe over the last 16 years despite lack of the product standard. The output capacity of the industry worldwide has been growing exponentially. The organic development of the industry resulted in a surprising diversity in the manufacturing processes, products and market strategies. The author will present a brief overview of the profiles of 19 CLT manufacturing plants toured between 2012-14

Proceedings of the 58th International Convention of Society of Wood Science and Technology
June 7-12, 2015 – Grand Teton National Park, Jackson, Wyoming, USA

Characteristics of Densified Sengon Wood (*Paraserianthes falcataria (L) Nielsen*) by Compregnation Process

Dodi Nandika, dodina@ipb.ac.id

Bogor Agricultural University, Kampus IPB Darmaga, Bogor 16680

Abstract

Sengon (Paraserianthes falcataria (L) Nielsen). is a fast-growing tree species that widely planted in Indonesia. Low quality of the sengon wood mainly related to the strength and durability led to its limited use. A study was conducted to evaluate the effect of chitosan impregnation followed by thermal compression on the characteristics of densified sengon wood. Chitosan concentration used in this study was 0.5%. and compression level applied was 50%. Sengon boards was compressed under three different temperature (150°C. 170°C. and 190°C). The results of study showed that compregnation process improved its physical. mechanical properties. and its resistance against subterranean termite. Density of densified boards was 80.7 % larger than that of uncompregnated boards. The hardness. MOE. and MOR were investigated to be 54.6%. 53.2%. and 52.77%. respectively larger than the uncompregnated wood. In addition. the chitosan impregnated on the sengon wood could decrease spring back of the densified boards significantly. The optimum temperature for impregnation as well as compression process of the boards were 100°C and 150°C respectively.

Proceedings of the 58th International Convention of Society of Wood Science and Technology
June 7-12, 2015 – Grand Teton National Park, Jackson, Wyoming, USA

Local Production of Particle Board Using Ficus (SPP) Wood and Epoxy Resin Adhesive

Robert Ogbanje Okwori PhD & Adeogun Idris Olawale

Corresponding author: okworirobert@yahoo.com, Tel: +2348060966524
Department of Industrial and Technology education,
Federal University of Technology,
Minna, Nigeria

Abstract

Wood is utilized for providing shelter for man. Particle board (pb) was produced using ficus wood waste, epoxy resin adhesive, hardener (ammonium chloride), mould, hot presser, and intron testing machine. The wood was naturally seasoned and had 4% moisture content. The production of Pb was carried out using manual lay up technique. The Pb consisted of 20wt% of wood saw dust and 80wt% of epoxy resin. The mix was stirred manually. The cast of each Pb was cured under the load of 50kg for 24 hours before removing from the mould. The cast of each pb was post cured in the air for 24 hours after from removing the mould. The test result of mechanical properties given as follows: MOR values at the density of 700 kg/m3 at 25 °C and at the density of 800 kg/m3 at 25 and 40 °C, the IB values at the density of 600 kg/m3 at 40 °C and at the density of 800 kg/m3 at 55 °C. The SHP values had the test result according to the set standard except with the density of 600 kg/m3 at 40 and 55 °C. The density at 600kg/m^3 yields less MOE than at 700kg/m^3 at 800kg/m^3 respectively. The pb was finally treated with preservative. The pb is durable, resistant to insect and termites attack and it is affordable since is locally produced. Based on the above traits, it is recommended for cabinet makers and upholsterers for use.

Key words: Ficus wood, Particle board, Epoxy resin, Adhesive

Introduction

The demand for particle board and plywood has recently increased tremendously in Nigeria especially for domestic and industrial use. Particle board is a man made board produced from wood particles, such as wood chips, wood shavings or wood saw dust with the application of adhesive and press together. Particleboard is cheaper, denser and more uniform than solid wood. Particle board is cheap in price when compared to

plywood. Particle board is used for cabinet making and upholstered work. It can also be used for partitioning of walls, platform for chairs and stair treads. I can be combined with other materials to be used as inlaying and over laying for decorative purposes.

The strength and durability of particle board is a function of the mechanical characteristics of the component materials. Analysis of the mechanical characteristics is the investigation of the materials behaviour when subjected to loads. Material reactions under loads are the stress and strain generated within the materials and usually results in deformation.

A sufficient knowledge of the mechanical behaviour of wood enables a safe design for the materials service life. However, being a biological material like timber, it is subjected to greater variability and complexity due to various conditions as moisture. Wood is an orthotropic material which means it has particular mechanical characteristics in the three directions: longitudinal, radial and tangential (Youngquist, Myers & Muehl, 1993).

Particle boards are made from a wide range of materials such as fibers obtained from trees. It provides uniform and predictable in-service performance largely as a consequence of standards used to monitor and control their manufacture. The mechanical characteristics of particle board depends upon a variety of factors. This includes wood species, the type of adhesive used to bind the wood elements together, geometry of the wood elements (fibers, flakes, strands, particles, veneer, lumber) and density of the final product (Cai & Winandy,2006).

Model building codes in the United States stipulate that man made boards used for structural applications such as subflooring and sheathing must meet the requirements of certain U.S. Department of Commerce standards. Voluntary Product Standard PS 1–07 for construction and industrial plywood (NIST, 2007) and Performance Standard PS 2–04 for wood-based structural-use panels (NIST, 2004). It spells out the rules for manufacturing plywood (Halloran, 1980, APA, 1981). Particle boards are used for a number of structural and nonstructural applications. It is used for both interior and exterior construction in a house, furniture, flooring, paneling, partitioning, wall, ceiling panels and support structures in buildings and so on. Knowledge of the mechanical characteristics of these products is important to enhance its utilization.

Through out the world, sellers reported that the demand for wood composite products has increased substantially. Man made board as an alternative to solid wood has reduced the high demand for solid wood. The use of non-timber resources, wood wastes and agricultural residues are ways of saving solid wood. In order to overcome the wood shortage and to meet the future demand of wood products, studies have been conducted to utilize non-wood materials, agricultural residues, fast growing tree, low-grade wood species and underutilized wood species in the forest industry as raw material components for wood-based composite production in several countries. In developing countries most of these residues are mostly ploughed into the soil or burnt in the field, however, these residues can be used to produce particle board and medium density fiber board. (Youngquist, Myers & Muehi, 1993).

Statement of the Problem

The continuous increase in the cost of natural wood in Nigeria today has been a problem and this brought about other alternative wood materials (man-made board) that can serve as substitute for those materials that are scarce and expensive such as solid wood and metal. It is observed that particle boards imported are expensive therefore, woodworkers find it to afford. The researchers also observed that some particleboards produced do not meet the minimum mechanical property requirements specified (NIST, 2007). The mechanical properties of particleboard are indication of quality and suitability for use. In most cases the testing methods listed in the specific standards for determining these properties require sophisticated equipment. In fact, results are normally obtained several hours or even several days after the manufacture of the board (Cook *& Harten,* 2000).

Aim and Objectives of the Study

The aim of this study is to produce a single layer particle board locally using ficus (SPP) wood saw dust and epoxy resin adhesive. The objectives of the study include to:
1. Produce a single layer particle board using ficus (SPP) wood saw dust.
2. Determine the mechanical characteristics of ficus particle board.

Research Question

The following question was formulated to guide the study.
1. What are the procedures for producing ficus particle board?
2. What are mechanical characteristics of ficus particle board?

Materials and Methods

Materials used and methods of manufacturing particle board and the experimental procedures for the mechanical characterization is discussed in this section.

Research Design

Experimental research design was adopted for the study. Wood saw dust was collected and used for the production of the particle board. Specimens of suitable dimension were used for mechanical testing. It was aimed at testing the mechanical characteristics of the particleboard.

Materials
The raw materials used for the production of the particle board were;
Ficus wood saw dust, epoxy resin and hardener.

Wood sawdust
Sawdust was a by-product of cutting, drilling, sanding or otherwise pulverizing wood with a saw or other tools. It was composed of fine particles of ficus wood.
Wood sawdust was the main component of the particleboard.

Hardener
Hardener was added to epoxy resin to harden the surface of the particleboard.
Ammonium chloride (NH_4Cl) was used as hardener for this particle board.

Epoxy Resin
Epoxy rein adhesive was used for binding the particles (wood saw dust) together. The curing took some hours after its application.

Area of study
The practical was carried out at the Forestry and Wood Science Department Laboratory in University of Ibadan, Oyo state, Nigeria and Federal University of Technology, Minna, Niger state, Nigeria.

Apparatus
I. Intron testing machine.
II. Hot presser
III. Vacuum ovun dryer

Procedure for the production of particleboard
Wood sawdust of Ficus tree (Figure 1 & 2) were reinforced with epoxy resin used as the matrix material. Ficus wood sawdust was obtained from Apata saw mill, Ibadan, Oyo state. The maximum particle size was 500 (μm). The wood saw dust was dried before manufacturing in a vacuum oven for 24 h at 80^{o}C in order to remove moisture. The epoxy resin and hardener were used for the production. The fabrication of the particle board was carried out through the hand lay-up technique. Epoxy resin (Araldite and corresponding hardener were mixed in a ratio of 10:1 by weight as recommended). Particle board was fabricated from ficus wood dust. Each particle board consisting of 20wt.% of wood dust and 80wt.% of epoxy resin. The designations of this wood saw dust are given in Table 3.1. The mix was stirred manually to disperse the fibres in the matrix. Figure 2 shows the mixture of the specimens. The cast of each particleboard was cured under a load of about 50 kg for 24 hours before it was removed from the mould. It was low temperature curing. This cast was post cured in the air for another 24 hours after removing from the mould. Specimens of suitable dimension were used for mechanical testing. Utmost care was taken to maintain uniformity and homogeneity of the particleboard.

Figure 38. wood saw dust

Figure 39. Mixture of specimen

Table 1. Designation of Wood Dust

Composites	Composition
C	Epoxy (80wt%)+wood dust (20wt%)

Test Procedure

Finished boards were kept in an open space approximately for a week to remove the adhesive trapped inside. Then, all boards were cut to obtain 130 mm by 275 mm. It was in rectangular form. Specimens were conditioned to equilibrium at a temperature (25, 40 and 55 °C) for 24 hours before testing.

Mechanical Characteristics

After fabrication, the specimens were subjected to various mechanical testing. Three-point static bending, tensile perpendicular to board surfaces and screw withdrawal tests of the particle boards were carried out using Intron Testing Machine (Model 3382) with

some modifications due to the size of the boards. Modulus of rupture (MOR), modulus of elasticity (MOE), internal bond strength (IB) and screw holding power (SHP) were recorded. Figure 3 shows the tested specimen for flexural, tensile and hardness test respectively.

Figure 40 tested board

Results and Discussion

The procedure of processing these particleboards (pb) and the tests conducted on them have been described. The results of various characterization test were reported below. This includes evaluation of modulus of rupture, modulus of elasticity, internal bond and screw holding power. The interpretation of the results in relation to the mechanical properties is also presented in the figures below after the statistical analysis of the mechanical characteristics of pb using two way analysis of variance (ANOVA).When the ANOVA indicated a significant difference, a comparism of the mean was done employing scheffee's method of multiple comparism in identifying which group was significantly different from other groups at 0.05 confidence level.

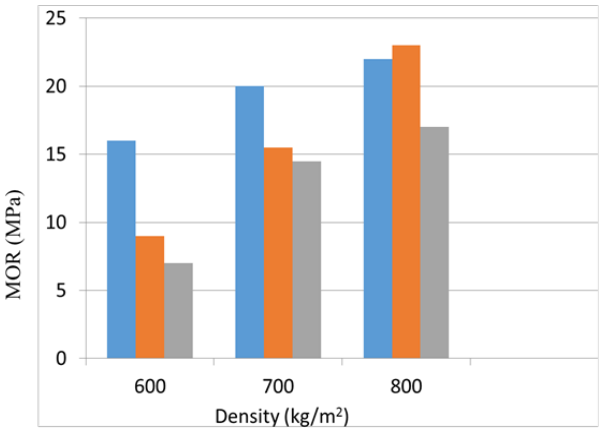

Figure 4 .Effect of density on MOR values of Panel

Figure 4 shows the effects of density on modulus of rupture (MOR), it indicated that effects of density was higher at 800kg/m^3 than that of 600kg/m^3 and 700kg/m^3.

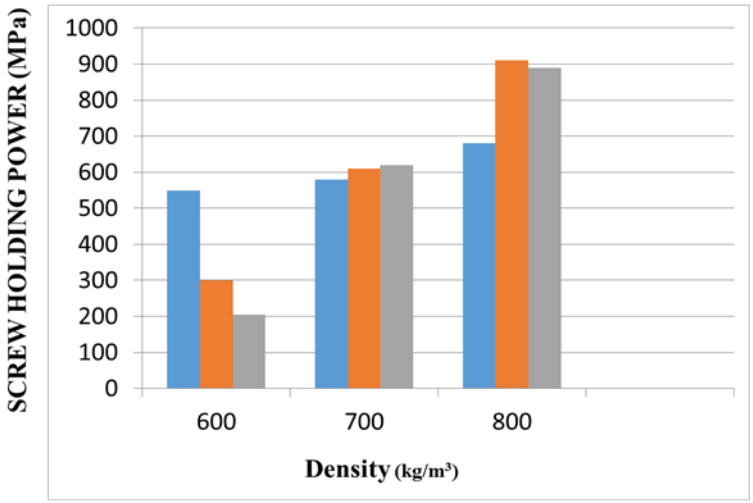

Figure 5. Effect of density on SHP.

Figure 5 showed that the screw holding strength (SHP) of particle boards manufactured at density 700 and 800 kg/m3 was higher. Moreover, the SHP values were found to be increased with increasing density ratio.

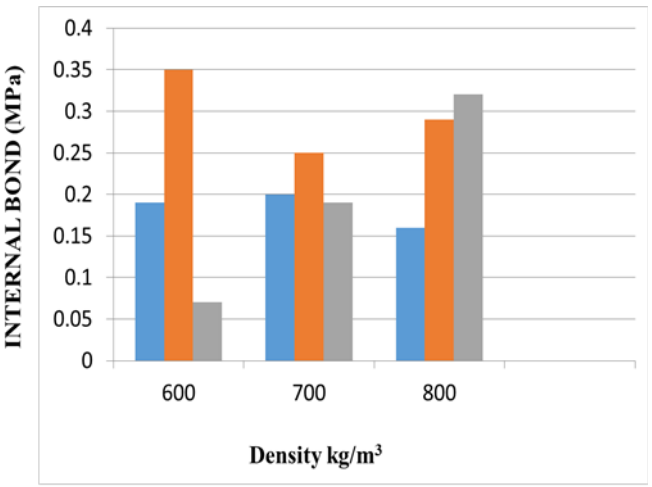

Figure 6. Effect of density on IB.

The effects of density on internal bond (IB) was showed in figure 6, it shows that the effects of density on IB is higher at 600kg/m^3 ,700kg/m^{3}and 800kg/m^3 . The effect of the density on IB is greater from 700kg/m^3.

The findings indicated that the mechanical properties of particleboard can be examined and tested. It also shows that the wood types also contribute or determine the mechanical

properties of particle board. A wide range of engineering properties are used to characterize the performance of wood-based composites. Mechanical properties are typically the most frequently used to evaluate wood-based composites for structural and nonstructural applications (Winandy, stark & Clemons, 2004).The minimum requirements for Modulus of rupture (MOR) and Modulus of elasticity (MOE) of particleboard panels for general uses and furniture manufacturing is between 18 and 3000 (MPa) respectively. The test result of mechanical properties showed that the MOR, MOE and IB values were not in the set criteria, except the MOR values at the density of 700 kg/m3 at 25 °C and at the density of 800 kg/m3 at 25 °C and 40 °C (Fig. 4), IB values at the density of 600 kg/m3 at 40 °C and at the density of 800 kg/m3 at 55 °C (Fig. 5). Figure 5 shows that the screw holding strength (SH) of particleboards manufactured at density 700 and 800 kg/m3 was higher. Moreover, the SH values were found to be increased with increasing density ratio.

The test results related that temperature has an effect on MOR and IB but density has impacts on all variables. It was also found that an interaction between temperature and density affects IB at (0.05) significant level. It was found that MOR at density 700 and 800 kg/m3 was higher than at 600 kg/m3. However, MOR at density 700 and 800 kg/m3 was not found to be different. It was showed that MOR at temperature 55 °C was less than at 40 °C and 25 °C. The density at 600 kg/m3 yields less MOE than at 700 kg/m3 and 800 kg/m3 respectively but MOE at density 700 kg/m3 and 800 kg/m3 was not different. As it can be seen, the temperature 40 °C yields the highest IB under the density 600 and 700 kg/m3. However, the density at 800 kg/m3, the IB at temperature 40 °C and 55 °C were not different. The mechanical properties of wood composites including particle board depend upon a variety of factors including wood species, the type of adhesive used to bind the wood elements together, geometry of the wood elements (fibers, flakes, strands, particles, veneer, lumber), and density of the final product (Cai & Winandy 2006).

Conclusion

Having carried out the production of ficus particle board and tested the mechanical characteristics of ficus particleboard, from the results of the test, it shows that temperatures has effects on modulus of rapture (MOR) and internal bond (IB) but density has impact on all the variables. Interaction between temperature and density have effects on IB at 0.05 level of significance.

Acknowledgements

The researchers thank University of Ibadan, Nigeria and Federal University of Technology, Minna, Nigeria for allowing them to their laboratories. For the production of the pb. They also wish to express their gratitudes to the mill workers for packaging the

ficus saw dust used for the fabrication of the pb. The efforts of the computer operator are highly appreciated for typing this manuscript.

Recommendations

The following are recommended based on the study:

1. When producing particle board, temperature should be considered so that the quality will not be affected since it has effect on MOR and IB.
2. Local production of particleboards should be encouraged by government since there are different species of trees in Nigeria and to reduce importation of such boards.
3. Wood workers in the saw mills should be educated using mass media to preserve wood dust for the production of particleboards e.t.c, instead of disposing them in the environment which causes environmental pollution.
4. Educational institutions offering woodwork technology should procure equipment that are essential for particle board production. This will encourage local production of particleboard by students and other woodworkers.

References

Cai, Z.; Muehl, J.H.& Winandy, J.E (2006). Effects of panel density and mat moisture content on processing medium density fiberboard. *Forest product Journal*. 56(10), 20–25.

Cook, T. & Harten, w. (2000). Lignocellulosic – Plastic Composites from Recycled Materials. *American Chemical Society*, 107, (40).

CPA. (1999). Particleboard standard. ANSI A 208.1-1999. Leesburg, VA: composite panel Association.

NIST. (2007). Voluntary product standard PS 1–07. Construction and industrial plywood. National Institute of Standards and Technology. Gaithersburg, MD: U.S. Department of Commerce.

Halloran, M.R. (1980). *The performance approach to acceptance of building products*. In: Proceedings of 14th Washinton state university particleboard symposium. Pullman, Pp.
77-84.

Winandy, J.E., N. M. Stark, & C. M. Clemons.(2004) .*Consideration In Recycling Of Wood-Plastic Composites.* 5th Global Wood and Natural Fiber Composites Symposium. Kassel- Germany.

Youngquist, J.A.; Myers, G.E.; Muehl, J.M.(1993). *Composites from recycled wood and plastics.* U.S. Environmental Protection Agency, Project IAG DW12934608–2. Madison, WI: U.S. Department of Agriculture, Forest Service, Forest Products Laboratory. 3 p.

Proceedings of the 58th International Convention of Society of Wood Science and Technology
June 7-12, 2015 – Grand Teton National Park, Jackson, Wyoming, USA

The Relationship Between Fibre Characteristics and Strength Properties of Three Lesser Utilized Ghanaian Hardwood Species.

Gladys Quartey, gladys.quartey@tpoly.edu.gh
Stephen Terpetey, niilartey@gmail.com

Takoradi Polytechnic, P. O. Box TD 372, , Takoradi, Western Region

Abstract

Wood exists as concentric bands of cells oriented for specific function and as softwood and hardwood. Hardwood fibers are generally shorter (1-1.5mm) than softwood fibers (3.5mm). Three hardwood species, Albizia ferruginea, Blighia sapida, and Sterculia rhinopetala were selected for anatomical investigations and mechanical strength tests. Maceration was done and structural size samples were tested for their mechanical properties according to EN 408 (2003). Results revealed that Sterculia rhinopetala had a bending strength of 61.4 N/mm2 at a moisture content of 29 % with an average density of 0.899 g/cm3. Albizia ferruginea had lowest bending strength of 50 N/mm2 at a lower average density of 0.740 g/cm3. Fiber lengths were measured using Leica DMLM light microscope with a Leica DFC 320 digital camera. Photomicrographs were then analyzed with Leica IM 1000 Version 4.0 Release 132. Sterculia rhinopetala had thick longest fibers with a fiber length ranging between 1479-1899µm. Albizia ferruginea had relatively short fibers which ranged from 1196 – 1274 µm. Whilst Blighia sapida had a fiber length of between 1127 – 1303 µm. This brings to the fore the fact that Sterculia rhinopetala with thick long fibers has a high bending strength whilst Albizia ferruginea with relatively short fibers has low bending strength.

Proceedings of the 58th International Convention of Society of Wood Science and Technology
June 7-12, 2015 – Grand Teton National Park, Jackson, Wyoming, USA

Assessing Geographic Information Systems (GIS) Use in Marketing Applications: A Case of Study in the Wood Products Industry

Henry Quesada-Pineda, quesada@vt.edu
Melissa Brenes-Bastos, mbrenes@vt.edu
Robert Smith, rsmith04@vt.edu

Virginia Tech, 1650 Research Tech Drive, Blacksburg, VA 24061

Abstract

Geographical Information Systems (GIS) is a worldwide growing technology, however it is not yet completely accepted. Of all of the business processes in an organization, marketing is perhaps one of the natural fitting-processes to apply GIS. Even though there is recent research regarding applications of GIS in the wood products industry, those applications are mostly related to biomass mapping and logistics issues. Little research has been conducted on the utilization of GIS as part of the marketing strategic plan in this industry. Thus, the main goal of this project is to understand GIS uses on marketing application in the wood products industry, specifically in the marketing mix strategic plan. The approach of this research consisted of the collection and analysis of data from secondary and primary wood products industries in the state of Virginia. A relational database was developed to organize the information and to create an industry directory for secondary wood products industries. Secondly, clustering techniques were used to test if wood products companies cluster around certain geographical regions. Confirmation of the clustering led to the construction of a GIS application to map wood products industries. Finally, guidelines were developed to describe how to use GIS in the marketing process of wood products firms.

Proceedings of the 58th International Convention of Society of Wood Science and Technology
June 7-12, 2015 – Grand Teton National Park, Jackson, Wyoming, USA

Firm Performance in the Swedish Industry for Off-Site Produced Wooden Single-Family Houses

Tobias Schauerte, tobias.schauerte@lnu.se
Fredrik Lindblad, fredrik.lindblad@lnu.se

Linnaeus University, Lückligsplats 1, Växjö 35195

Abstract

In the last years, the Swedish market for wooden single-family houses was characterized by an enormous downfall. Within five years, from 2007 to 2012, the number of produced wooden single-family houses declined from 12 100 to 4 800 units per year, equaling 60%. Yet, firms in the industry seem not to adjust their businesses or costs consequently, since the costs per m2 housing area increased by almost 20%. Looking back to 2001, costs even increased by ca 66%. These numbers supposably point on serious problems related to the firms' overall performances. Thus, the aim of this study is to map and analyze the overall performance of the firms producing wooden single-family houses in Sweden.
For 51 firms, balance sheets from 2010 to 2013 were collected and analyzed. Results show for example that the average turnover per firm decreased by ca 20%, whilst the average profit per employee in the industry increased by 75%. The relationship between these two numbers can be seen as mainly caused by the continuously rising housing prices due to severe national housing shortage. Further, looking at the operational risk of the firms, it can be seen that firms have a different sensitivity for short-term economic fluctuations and need to adjust their business activities accordingly.

Proceedings of the 58th International Convention of Society of Wood Science and Technology
June 7-12, 2015 – Grand Teton National Park, Jackson, Wyoming, USA

From Single-Family Houses to Multi-Family Houses - Resistance to Change and Perceived Hinders

Tobias Schauerte, tobias.schauerte@lnu.se
Fredrik Lindblad, fredrik.lindblad@lnu.se
Marie Johansson, marie.johansson@lnu.se

Linnaeus University, Lückligsplats 1, , Växjö 35195

Abstract

In the past decades, housing shortage in Sweden has accumulated to a level that has led to acute problems for many people in general, and combined with continuously rising housing prices, problems especially occur for younger people with relatively low income. On the market for single-family houses, where wood dominates with 85 – 90 % of market share, firms struggle with a low order intake and currently compete with very low margins, if any. Only few of these firms produce multi-family houses as well, even though production facilities often allow for that. One way to tackle the existing housing shortage could be to get more actors from the single-family house industry to produce multi-family houses. This would trigger competition, improve product quality and utilize economies of scale due to product relatedness, e.g. for prefabricated walls. In that way, profitability and the firms' margins could be improved.

This study is aiming at exploring potential hinders for Swedish firms producing wooden single-family houses to build multi-family houses. This will be done by deep interviews with decision makers in those firms and, based on that, a follow-up survey-study covering all listed firms in that industry segment. The results may show that resistance to change and perceived hinders mainly are related to management issues, lack of knowledge about the new segment and constructional requirements, firm size, risk taking or ownership model.

Proceedings of the 58th International Convention of Society of Wood Science and Technology
June 7-12, 2015 – Grand Teton National Park, Jackson, Wyoming, USA

Owning or Renting? Investigating Consumer Perceptions on Different Apartment Types in Wooden Multistory Houses in Sweden.

Tobias Schauerte, tobias.schauerte@lnu.se
Anders Ingwald, anders.ingwald@lnu.se

Linnaeus University, Lückligsplats 1, Växjö 35195

Abstract

In Sweden, housing shortage has become a serious problem. To overcome that shortage reasonably, the amount of new housing units per year should be around 60 000. However, not more than 25 000 housing units per year have been finalized the past years. As wood is regarded as a very suitable construction material to helping to overcome the shortage, an increase of wooden multistory houses on the market is expected in the near future. At the same time, discussions take place about an appropriate distribution of apartment types, i.e. rental apartments vs. condominiums. In Sweden, ca 25% of all apartments are rental apartments and ca 15% condominiums. More rental apartments are demanded from the publics, whilst firms on the construction market are very well aware of the higher profitability of condominiums. Yet, since prices for condominiums increased a lot in the past years, the attractiveness of condominiums seems only to be recognized from the seller part.

This study is aiming at investigating the perceptions of consumers on condominiums and rental apartments in wooden multistory houses. Thereby, we learn to understand how consumers link their personal values and needs to housing and different types of products' attributes; a crucial part of strategic segmenting of markets. Results show that there is a significant difference in consumers' perceptions on the type of apartments and that decisive arguments for consumers are linked to costs, security and quality of life.

Proceedings of the 58th International Convention of Society of Wood Science and Technology
June 7-12, 2015 – Grand Teton National Park, Jackson, Wyoming, USA

Hybrid Oriented Strand Boards from Moso Bamboo (*Phyllostachys pubescens* Mazel) and Aspen (*Populus tremuloides* Michx.): Bamboo Surfaces, Aspen Core

Kate E Semple[1], *Polo K Zhang*[2], *Gregory D Smith*[3*]

[1]Research Scientist, [2]Graduate Research Assistant, and [3]Associate Professor
**Corresponding author*
[1,2,3]Department of Wood Science-Composites Group, University of British Columbia, 2900-2424 Main Mall, Vancouver, BC, Canada, V6T 1Z4.
kate.semple@ubc.ca, polo.kq.zhang@gmail.com, greg.smith@ubc.ca.

Abstract

Five sets of six 3-layer strandboards were made in three configurations, (1) Moso bamboo in the surface and core layers, (2) Moso bamboo in the surface and Aspen in the core, and (3) Aspen in the surface and core layers. For the configurations containing bamboo strands in the surface layers, there were two sub groups: (a) all strands contain a node in the middle, and (b) strands are node free (internode). All 30 boards were comprised of 50% w/w surface furnish and 50% core furnish and fabricated to 737 mm x 737 mm x 11.1 mm. Standard mechanical (thickness, density, surface and core density) and strength properties (internal bond, flexure, lateral nail withdrawal resistance), and water resistance (2h and 24h thickness swell and water absorption) were assessed. Complete replacement of the Aspen in the surface layers with internode bamboo strands resulted in over 45% greater bending strength. Panels made with bamboo face layers met CSA O437.0 (1993) minimum requirement for water resistance without the need for wax addition, presumably because no densification of the surface material was observed. Due to high variance in nail resistance, effects of board type and core composition were not statistically significant, but values exceeded CSA O437.0 minimum requirements. Moso surface boards were low in stiffness which is consistent with unadulterated Moso bamboo tissue being high in bending strength and fracture toughness but low in specific stiffness. The presence of nodes in the bamboo strands significantly reduced the strength properties of boards, a problem which could be mitigated by minimising the frequency of nodes in the strands, particularly those used in the surface layers.

Keywords: Moso Bamboo, Aspen, Strands, Oriented Strand Board, Mechanical Properties.

Introduction

Used in a smart way in combination with commodity wood-based construction products, bamboo has the potential to significantly reduce costs and the carbon footprint of the construction industry in rapidly developing countries throughout the tropics and sub-tropics where bamboo is grown (Dagilis 1999, de Flander and Rovers 2010). Bamboo has some excellent material properties (for example tensile strength and fracture toughness) compared with wood but despite this relatively little progress has been made in developing and commercializing modern, engineered composite building materials from bamboo (Cai and Winnandy 2005, de Flander and Rovers 2010). Compared with most of the conventional bamboo panel products currently in production, the OSB process represents one of the best opportunities for automation, property control and consistency, mass production, and resin efficiency in manufacture of bamboo-based building materials, with minimal waste.

Intensive stand management makes bamboo culms and products costly to manufacturers and consumers and it is therefore logical to combine it with lower cost and grade wood resources for conversion into building products. Construction-grade OSB is made up of a three-layer mat with highly densified, uni-directionally oriented strands in the surface layers to enhance product strength and stiffness, and usually randomly oriented smaller strands and fines in the core to facilitate the release of core gas pressure and utilise finer material where it has less effect on board strength properties. Short cycle clonal Aspen (in this case *Populus* x *euramericana* cv. San Martine) has been widely cultivated in China for land reclamation and wood production for over 30 years (Su 2003), and the wood is very well suited for OSB production (Zhao 1990). Since the mid-1970's China has been developing and promoting the use of OSB as a renewable construction material to reduce demand for traditional bricks (Hua and Zhou 1996). By 2013 there were 104 OSB mills in China, the largest, Hubei Baoyuan Wood Industry Co. Ltd, having an annual output of 220, 000 m^3 (Anon 2013). The OSB manufacturing process has been adapted to bamboo in China (Fu 2007a,b; Anon. 2012), but economic production of products has been hampered by technical issues mainly associated with efficiently converting the culms to strands (Grossenbacher 2012).

The objective of this work is to produce a hybrid strandboard building product from bamboo and wood, locating the stronger, tougher bamboo strands in the surface layers of OSB and the weaker but more compactible aspen strands and fines in the core layer. Considerable attention has been focussed elsewhere on taking advantage of the high tensile strength of the fibre-rich outer zone of Moso bamboo culms in combination with lower density, lower grade woods to produce other kinds of high strength, low density hybrid composites. Examples include solid or hollow beams that place milled bamboo strips with the fibre-rich zone near the cortex on the top and bottom surfaces, i.e., the flanges, and solid or laminated strand lumber poplar as the web (Amino 2003, Lee et al.

1997). A hybrid OSB product that uses a similar principle but in the form of discrete layers of strands may be a good idea for manufacturers in a country like China that has large resources of both Moso bamboo and clonal poplars.

Materials and Methods

Details about the procurement of Moso bamboo culms and their conversion to strands using a disk flaker are given in Semple et al. (2014). Aspen was mill strands of face and core furnish used to make industrial OSB, supplied separately by Weyerhauser, Edson, AB. In order to recreate surface and core furnish from Moso bamboo that is similar in makeup (strands to fines ratio) to that of industrial Aspen furnish, size classification of the supplied Aspen face and core furnish was carried out using a 0.64- × 1.3-m mechanical shaker table into three size classes: >14.3-mm screen (strands), between 4.8- and 14.3-mm screens (intermediates), and <4.8-mm screen (fines and dust). The core furnish was comprised of 46% strands 105 mm long (average thickness 0.83 mm), 33% intermediates (average thickness 0.57 mm), and 21% fines (average thickness 0.47 mm), and the face furnish consisted of 73% strands, 13.5% intermediates, and 13.5% fines. The surface and core furnishes of bamboo was compiled based on these proportions. Moso core furnish was by weight 50% strands, 35% intermediates and 15% fines.

The required weights + 10 spillage of surface and core furnish of Moso and Aspen were blended separately with 6% (w/w furnish oven dry weight basis) of liquid PF resin (Cascophen EF47, 57.2% solids content, 140 cps viscosity, supplied by Momentive Specialty Chemicals Canada Inc). Blending was done in a rotating drum blender 180 cm diameter by 60 cm depth, equipped with small internal flights to lift and cascade strands. Blender rotational speed was 28 RPM. The resin was applied using a paint pot and compressed air-fed (30 psi) atomizer spray nozzle inserted through the front door of the blender. Resin dosage was controlled by weighing the mass loss from the paint pot during spraying and ceasing resin flow using a ball valve. After furnish removal and weighing into three batches of wet surface and core furnish, a three layer mat was assembled by using a 12-vane orienter to align the top and bottom layers of strands (50% of total furnish weight), but removing the orienter and randomly distributing the middle core layer. For comparative purposes all the boards including the Aspen controls were pressed to a common target density of 752.9 kg/m^3 (47 pcf). Six replicate boards each of five board types were fabricated and are outlined in Table 1, which also contains the properties tests and numbers of test specimens.

Board Types-surface and core composition

Board Type	Surfaces[a]	Core[b]	Replicates
1	Moso internode	Moso fines	6
2	Moso node	Moso fines	6
3	Moso internode	Aspen core	6

4	Moso node	Aspen core	6
5	Aspen face	Aspen core	6

Properties tests and specimen numbers

Sample type	Per Board	Per Treatment	Total
Thickness	30	180	900
Density	30	180	900
Internal Bond	30	180	900
MOR ∥	2	12	60
MOE ∥	2	12	60
MOR ⊥	2	12	60
MOR ⊥	2	12	60
LNR ∥	2-3	15	30
LNR ⊥	2-3	15	30
Thickness swell	1	6	30
Water absorption	1	6	30

[a]25% each by weight, oriented; [b]50% by weight, random.

Table1 Board types and properties tests.

All OSB were 720 x 720 x 11 mm with a three-layer sandwich structure of 50% by weight of total furnish in the randomly distributed core and 25% each in the two oriented surface layers. Types 1 to 4 had Moso strands in the surfaces; 1 and 2 with a Moso core, and 3 and 4 with an Aspen core. Type 5 was pure Aspen. For the bamboo surface boards, types 1 and 3 were made with node-free strands and 2 and 4 made with node strands. The effects of board type on physical and mechanical properties were assessed using single-factor ANOVA in JMP 10 (SAS Institute, Inc. 2012), using 5% probability level. Means were compared using the Tukey-Kramer HSD pairwise comparison test, and the significant differences between means for a particular property are indicated by the connecting letters report in Table 2. If there was no significant difference between two board types (for example node/internode strands in the surfaces for density, IB strength, and LNR) the data sets were pooled and the averages plotted for board composition (Pure Moso Hybrid, or Pure Aspen). To alter the locations from which test specimens were cut on a given board, three different cutting patterns were used; so only two boards per group of six had the same cutting pattern. From each board were cut 30 internal bond, IB (51 x 51 mm), 4 flexure (MOR/MOE) specimens (290 x 76 mm) - 2 perpendicular and 2 parallel-to-surface strand direction, and 1 Thickness Swell/Water Absorption, TS/WA, (152 x 152 mm). From the end of two the flexure specimens a 76 by 150 mm lateral nail Resistance (LNR) specimens was cut, one from the perpendicular and one from the parallel specimen. Specimens were conditioned to constant weight for three weeks at 20°C and 65% RH and mechanical properties tests were cut and carried out in accordance with ASTM D1037 (2006). A DX100 Olympus Digital Light Reflection Microscope (5x magnification) was used to examine polished cross-sections through the surface of bamboo OSB to examine the extent of tissue compression during hot pressing.

Results and Discussion

The averages for properties from the boards are given in Table 2. Although the mass of furnish was designed to achieve the same target density of almost 753 kg/m^3, average density ranged from 710 kg/m^3 for pure Moso boards to 737 kg/m^3 and 740 kg/m^3 for pure Aspen and Moso-Aspen hybrids, respectively. The lower density of the pure Moso boards was associated with the greater thickness (and by extension, volume) of the specimens. The average surface density for pure Aspen boards was 976.7 kg/m^3, and for bamboo surface boards, 878.3 kg/m^3; while average core density for pure Aspen boards was 648.5 kg/m^3 and for bamboo surface boards, 660.8 kg/m^3. Virtually all mechanical properties of OSB including IB are linked to board density and distribution of density through the thickness of the board (Andrews 1998, Dai et al. 2002).

Aspen is commonly used in the manufacture of OSB because it has a high compaction ratio, i.e. the board surface layers are very effectively densified during hot pressing to give a composite of small elements that is similar strength properties to undamaged solid parent material (Zhou et al. 2009). Given that the average dry density of Aspen is 380 kg/m^3 and Moso used here approximately 745 kg/m^3, the densification factor for Aspen was 2.57, and for Moso only 1.18. Light microscopy images (Fig. 1) of the transverse surface of an uncompressed Moso strand and the strands in the surface of hot pressed OSB show no visible compaction of the bamboo tissue under the hot pressing conditions used. The lateral (radial and tangential) compressive strength of Moso bamboo tissue is over 20 MPa (Dixon and Gibson 2014), almost 4 times the maximum ram pressure of 5.8 MPa experienced by the mat during hot pressing. The inability of the bamboo tissue to compress and collapse down during hot pressing likely lead to greater compaction stress and springback after press opening, explaining the higher final thickness of the pure bamboo boards. Surface strand type (aspen or bamboo) significantly affected IB, but the internode/node effect in bamoo strands was very small and not statistically significant. Mean IB of hybrid boards (0.73 MPa), and pure bamboo boards (0.77 MPa) were significantly higher than pure Aspen boards (0.65 MPa). This could have been due to the lack of conformability of bamboo surface strands increasing the compaction stress on the core of the board.

Test	Pure aspen	Moso-aspen-moso		Pure Moso	
		Internodes	Nodes	Internodes	Nodes
Thickness, mm	11.45a	11.39a	11.38a	11.7b	11.6c
Density, kg/m^3	737.1a	747.8a	735.3a	713.4b	706.0b
Surface density, kg/m^3	986.9a	913.8a	887.4a,b	856.5b	810.3c
Core density, kg/m^3	656.5a,b	684.8a	655.1a,b	640.7a,b	619.7b
Internal Bond, MPa	0.65a	0.72b	0.73b	0.76b	0.78b
MOR ∥, MPa	48.6a	70.5c	61.3b,c	69.07b,c	57.15a,b

MOE ∥, GPa	7.53a,b	7.75a,c	6.96a,b	8.09c	6.67a
MOR ⊥, MPa	20.2a	21.0a	17.3a	17.39a	17.15a
MOE ⊥, GPa	1.40a	1.96b	1.72a,b	1.58a,b	1.40a
LNR ∥, N	2238.1a	2345.1a	2364.1a	2338.5a	2869.0a
LNR ⊥, N	2658.2a	2460.4a	2868.7a	3058.9a	2849.0a
2h TS, %	10.93a	7.35b	5.29b,c	3.72d	1.85c,d
24h TS, %	21.21a	11.55b	10.92b	5.34c	6.79c
2h WA, %	33.85a	30.26a	23.18a,b	13.52b	23.70a,b
24h WA, %	58.83a	48.09a,b	41.77b	28.47c	38.37b,c

Table 2 Average values for measured physical and mechanical properties OSB. Values for a particular property followed by the same letter are not significantly different at $p \leq 0.05$.

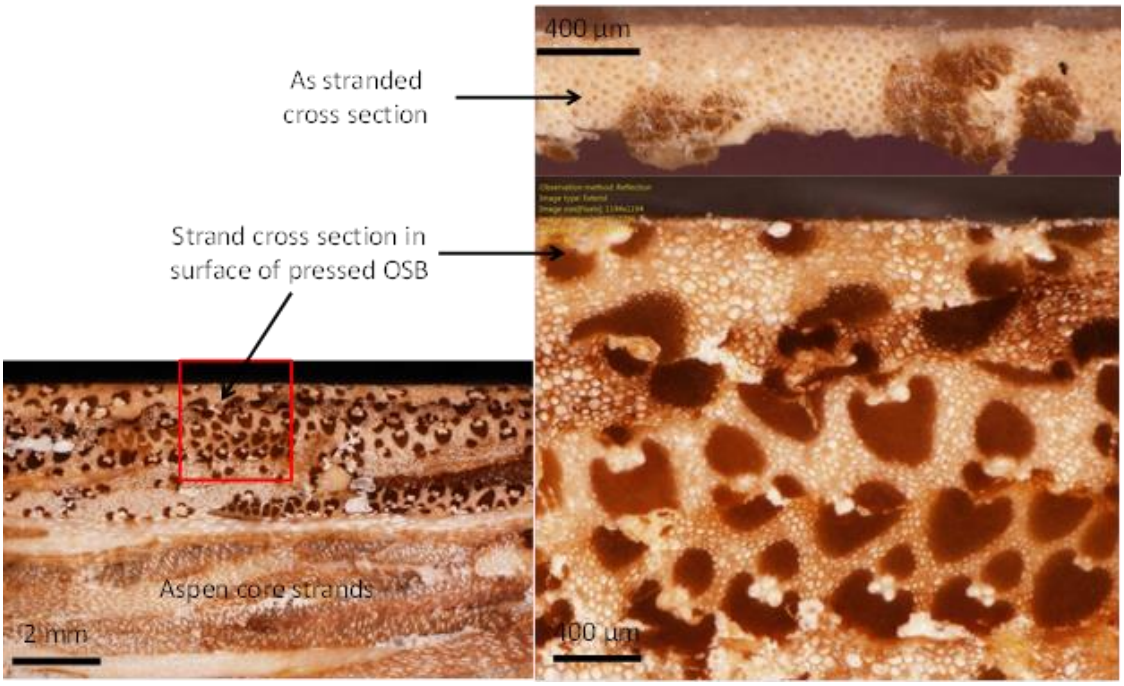

Figure 1 Appearance of Moso strands after (top) stranding, and (bottom) hot pressing boards.

Replacing the Aspen strands in the surface layers of OSB with Moso strands significantly increased ∥ MOR. Average ∥ MOR for boards made with internode strands was 70.5 MPa, over twice the 29 MPa required for industrial OSB products by CSA O437.0 (2011). Minimum ∥ MOE is 5.5 MPa. Moso surface boards were similar ∥ MOR and ∥ MOE regardless of whether the core was Aspen or Moso. Node tissue in the surface strands significantly reduced the flexural properties (∥ MOR = 61.3 MPa, and 57.15 MPa, and ∥ MOE = 6.96 MPa and 6.67 MPa for hybrid and pure Moso boards, respectively). Pure Aspen boards were 48.6 MPa in ∥ MOR and 7.53 in ∥ MOE. Values for ∥ MOE of bamboo-surface boards (hybrids or pure Moso) were similar to or lower than that of pure Aspen boards, but still above CSA O437.0 requirements. Minimum ⊥MOR and ⊥MOE for CSA O437.0 are 12.4 MPa and 1.5 GPa, respectively. Nodes in bamboo strands had

no effect on ⊥MOR and ⊥MOE. For boards with Aspen core the ⊥MOE values for bamboo-surface boards (1.72 GPa for internode and 1.96 GPa for node strands) were significantly higher than Aspen surfaces (1.40 GPa). The mean values of ⊥MOE for pure Moso boards were 1.58 GPa (internode) and 1.40 GPa (node), which are at or below the CSA O437.0 minimum requirements for ⊥MOE of OSB. Removing the influence of surface strand orientation, the flexural properties perpendicular to surface strand direction could be linked to the greater degree of compaction and densification observed in the core of boards made with bamboo strand surfaces. The resistance of the bamboo tissue softening and compaction during hot pressing means compaction stress from the platens is transferred through to the aspen core layer, which, in the case of the internode surface strands, was significantly higher in density than the pure aspen boards. Overall poor consolidation of the boards with noded strands meant the effect was not as apparent in this case.

When analysed as an aggregate model containing all 10 groups there was no statistically significant difference in ∥ or ⊥ LNR between any of the groups. COV values were between 25% and 35% indicating a high degree of variability in the LNR values within each group. The averages for LNR in all board types and strand orientations exceeded the CSA O437.0 minimum OSB of 70 x board thickness in N (i.e. 770 N for an average board thickness of 11.5 mm). It was observed however that lowest LNR values were for pure Aspen panels with stress parallel to surface strand direction (2238 N) and highest values were for pure bamboo boards (above 2800 N) suggesting that the bamboo tissue may be more resistant to localized damage from lateral stress on embedded nails. Of the numerous studies that have fabricated OSB from bamboo none provide any comparative data on LNR. Similar LNR tests done by Suzuki (2000) on 12-mm-thick OSB made from Sugi (*Cryptomeria japonica*) ranged 1600 N to 2300 N, for board densities ranging from 670 kg/m^3 to 720 kg/m^3, values which are slightly lower than ours.

A significant finding was that placing bamboo strands in the surface of OSB made without the necessary emulsified wax addition significantly reduces the 24 h thickness swelling and water absorption compared with boards containing pure Aspen. There were no differences in 24 h thickness swell and water absorption between boards made with internode or node strands in the surfaces. Note that after two hours soaking, the differences between Aspen and bamboo boards were not statistically significant, however the Aspen boards continued to absorb a greater amount of water, almost 60% of their initial weight, and swell more over the next 22 h. On the other hand, bamboo surface boards only absorbed an average of 45% of their initial weight in water. Average TS after 24 h for Aspen boards was 21.2% (exceeding the 15% maximum required for OSB in CSA O437.0 (2011), while the average for boards with bamboo surfaces was just 11.2%. Without wax addition thickness swelling in OSB is high due to the high degree of densification of the strands (Andrews 1998, Wolcott et al. 1990, Blomberg et al. 2006). A combination of lack of tissue compression and higher levels of naturally hydrophobic substances such as silica in the bamboo strands (Leise 1998) likely contributed to the much greater dimensional stability of the bamboo OSB.

It is relevant to try to compare our results for pure boards with Moso OSB made by other researchers using a similar resin type and dosage. Maximum physical and mechanical properties of 6% PF-bonded boards made without additives or wax by Zhang et al. (2007) were 45 MPa in ǁMOR, 5.5 GPa in ǁMOE, 0.55 MPa in IB, ≤12% TS, for boards with a density of 752 kg/m^3, figures that are not very different from ours. They found properties were reduced in boards compressed to a lower density. PF-bonded 11- mm-thick Moso bamboo OSB made by Lee et al. (1996) were 737 kg/m^3 in density, 37 MPa in ǁMOR and 6 GPa in ǁMOE, and 0.43 MPa in IB. 12-mm-thick PF bonded randomly aligned strand boards from Moso made by Sumardi et al. (2006) were 32 MPa in MOR, 3.7 GPa in MOE and 0.26 MPa in IB if compressed to a density of 730 kg/m^3. Another study on bamboo OSB by Fu (2007b) found that the following strand and board fabrication parameters led to optimum board properties: strand dimensions 110-120 mm in length, 9-15 mm in width and 0.6-0.8 mm in thickness; if using PF resin 6-8% solids content by oven dry bamboo strands is recommended; and pressing at 160°C platen temperature, 2.5 MPa pressure, with a pressing time of 70 s per mm of board thickness. Maximum board properties attained by Fu (2007b) were 36 MPa in ǁMOR, 5.3 GPa in ǁMOE, 0.40 MPa in IB. Information on board density or thickness swell/water absorption figures was not given.

The specific strength and stiffness of building materials (i.e. strength to weight ratio) is a key requirement for products handled manually on building sites. From our results the ǁMOE of bamboo surface OSB was not higher than that of pure Aspen OSB, when manufactured to a common density of 740 kg/m^3. Due to the high parent material density of bamboo, board densities here were high compared with commercial OSB commonly made from Aspen, which is usually between about 575 and 600 kg/m^3, but still exceeds the CSA O437.0 minimum parallel MOE of 5.5 MPa. Sumardi et al. (2006) found that MOR and MOE of pure Moso OSB were below about 7 MPa and 1.3 GPa respectively if board density was below 600 kg/m^3; these properties only increased with density once compaction ratio exceeded 1, i.e. densified to above the mean parent tissue density of 600 kg/m^3 for bamboo. Typical Douglas Fir plywood has even higher strength properties than OSB but is only 520 kg/m^3 in density and so for bamboo-based structural boards to be commercially viable they should have a density and properties that are at least comparable to or better than conventional wood-based building materials.

Further work should focus on why nodes in strands have such an adverse effect on board quality and find practical ways to mitigate the effect of nodes so that these do not need to be removed prior to stranding. Reducing the density of bamboo-Aspen OSB is also a priority; it may be possible to retain the beneficial effects of bamboo on board properties but reduce the ratio of bamboo strands in the surface layers, and achieve a reduction in overall board density.

Acknowledgements

This study was funded through an NSERC (National Science and Engineering Research Council) G8 Tri-Council grant. The authors gratefully acknowledge Mr John Hoffman, Forest Products Innovations (Western Division), for access to boil tank facilities and operation of the disk strander, and Mr Rick Fodor, Carmanah Design and Engineering, Inc., Surrey, BC for training and advice on setup and operation of the disk strander. Thank you very much also to Mr Jason Hutzkal, Momentive Specialty Chemicals, Inc, Edmonton, AB for supplying PF resin.

References

Amino Y (2003) Conception and feasibility of bamboo-precocious wood composite beams. Journal of Bamboo and Rattan 2(3): 261-279.

Andrews CK (1998) The influence of furnish moisture content and press closure rate on the formation of the vertical density profile in oriented strand board: relating the vertical density profile to bending properties, dimensional stability and bond performance. MSc Thesis, The University of Tennessee, Knoxville, TN.

Anon (2012) Aiming for domination. Wood Based Panels International Online,18 June 2012. http://www.wbpionline.com/features/aiming-for-domination/. Accessed 10 April 2013.

Anon (2013) OSB demand in China predicted to grow; new board capacities to appear in China and India. Global Trends Review, 24 May 2013.

ASTM (2006) Standard test method for evaluating properties of wood-base fiber and particle panel materials-D 1037-06a. American Society for Testing and Materials International, West Conshohocken, PA, 30 pp.

Blomberg J, Persson B, Bexell U (2006) Effects of semi-isotropic densification on anatomy and cell shape recovery on soaking. Holzforshung 60(3): 322-331.

Cai Z, Winandy JE (2005) Opportunity and development of bio-based composites. In: Proc. International Workshop on Pre-fabricated bamboo panel module housing, Nov. 24-25, 2005, Beijing, China.

CSA (2011) Standards on OSB and waferboard-O437.0-93R. Canadian Standards Association, Toronto, ON, 88 pp.

Dagilis TD (1999) Bamboo Composite Materials for Low-Cost Housing. PhD Thesis, Department of Civil Engineering, Queens University, Kingston, ON, 229 pp.

Dai CP, Mei C, Korai H (2002) Density and property relationships of wood strand composites. Proc 6th Pacific Rim Bio-Based Composites Symposium, Nov. 10-13, Portland, Oregon, pp. 458-466.

De Flander K, Rovers R (2009) One laminated bamboo-frame house per hectare per year. Constr & Bldg Mat 23(1): 210-2.

Dixon PG, Gibson LJ (2014) The structure and mechanics of Moso bamboo material. J Roy Soc Interface 11: 20140321. http://dx.doi.org/10.1098/rsif.2014.0321.

Fu W (2007a) Bamboo-A Potential Resource of Raw Material for OSB in China. China Forest Products Industry, 34: 21-24.

Fu W (2007b) A Study on Flaking Technique and Manufacture of Bamboo OSB. PhD Dissertation, Northeast Forestry University, Harbin, China, 86 pp.

Grossenbacher M (2012) Industrielle Herstellung von Bambus-OSB: Ein Erfahrungsbericht. In: 2nd Bieler Holzwerkstoff-Workshop, 28-29 November 2012, Biel, Switzerland.

Hua Y, Zhou D (1996) The development of oriented strand board in China. In H. Kajita and K. Tsunoda (eds) Proc 3rd Pacific Rim Bio-Based Composites Symposium, Dec 2-5, 1996, Kyoto, Japan, pp 64-71.

Lee AWC, Xuesong B, Peralta P (1996) Physical and mechanical properties of strandboard made from Moso bamboo. For Prod J 46(11/12): 84-88.

Lee AWC, Bai X, Bangi AP (1997) Flexural properties of bamboo-reinforced Southern pine OSB beams. For Prod J 47(6): 74-78.

Semple KE, Smola M, Hoffman J, Smith GD (2014) Optimising the stranding of Moso bamboo (*Phyllostachys pubescens* Mazel) culms using a CAE 6/36 disk flaker. Proceedings, 57th International Convention SWST, M Barnes, V Herian (eds), June 23-27, 2014, Zvolen, Slovakia, pp. 257-269.

Su X, Zhang B, Huang Q, Huang L, Zhang X (2003) Advances in tree genetic engineering in China. Proc XII World Forestry Congress, September 21-28, 2003, Quebec City, Quebec.

Sumardi I, Suzuki S, Ono K (2006) Some important properties of strandboard manufactured from bamboo. For Prod J 56(6): 59-63.

Suzuki S (2000) Effects of strand length and orientation of strength properties of OSB made from Japanese cedar. World Congress on Timber Engineering (WCTE) Vol. 1.3.8, July 31-August 3 2000, Whistler, BC, 8 pp.

Wolcott MP, Kamke FA, Dillard DA (1990) Fundamentals of flakeboard manufacture: Viscoelastic behavior of the wood component. Wood Fiber Sci 22(4):345-361.

Zhang H, Du F, Zhang F, Liao Z, Ye X, Zheng Z, Wang W (2007) Research and development of production technology of bamboo waferboard and oriented strand board based on biological characteristics and timber adaptability. J Bamboo Res 26(2): 43-48.

Zhou C, Smith GD, Dai C (2009) Characterizing hydro-thermal compression behavior of Aspen wood strands. Holzforschung 63(5):609 -617.

Zhou D (1990) A study of oriented structural board made from hybrid poplar - Physical and mechanical properties of OSB. Holz Roh- Werkst. 48(7-8): 293–296.

Proceedings of the 58th International Convention of Society of Wood Science and Technology
June 7-12, 2015 – Grand Teton National Park, Jackson, Wyoming, USA

Effects of Different Types of Housing Environment on Physiological Response

Shasha Song, songrui_1688@126.com
Fei Benhua

Beijing Forestry University, No.35 Qinghua East Road , Haidian District, Beijing 100083

Abstract

The aim of the present study was to promote the quality of living environment, working environment and create a healthy living environment through advocating the low carbon building and the green building. Physiological environment assessment of wood construction based on examined the physiological environment index of the participants in three different structure types of housing environment with CAPTIV synchronous test. The results of MANOVA revealed a significant main effect for log, glulam, reinforced concrete three different structures types of housing environment with skin temperature, ECG, respiration. In comparison, the influence of the physiological environment factors in log structure and glulam structure housing are better than the reinforced concrete structure housing, which is beneficial to the health of habitant. Participants are interested in the log structure and glulam structure housing environment, because the feeling of joy and comfortable. In this study, it provides the theoretical support and reference with the wooden constructure building living environment for the future of scientific and efficient use of product design, application.

Proceedings of the 58th International Convention of Society of Wood Science and Technology
June 7-12, 2015 – Grand Teton National Park, Jackson, Wyoming, USA

Bamboo for Furniture and Housing in Ghana: The Certification and Standard Issues.

Stephen Tekpetey, nii9lartey@gmail.com
Emmanuel Appiah-Kubi, appiahkemma@gmail.com
Francis Owusu, fwowusu3@yahoo.com
Charles Essien, cze0017@tigermail.com

Forestry Research Institute of Ghana, Box 63 KNUST, Kumasi

Abstract

Bamboo resources continue to gain greater recognition as a suitable construction material. With the rapid development of the global economy and constant increase in human population, the demand for green products like engineered-bamboo product (e-bamboo) will increase. In Ghana, engineered bamboo may soon become a more popular material for making housing components and furniture. In order to ensure the quality of e-bamboo products in Ghana and other emerging economies, manufacturing standards and certification will be vital for consumers' satisfaction and enhancement of international trade. This paper interrogates the issues around certification and standards for bamboo product for housing and furniture in Ghana. It further highlights the steps, challenges and concerted efforts required in the national standardization process of e-bamboo products in Ghana. It was recommended that a technical committee and testing laboratories for e-bamboo manufacture and bamboo products respectively should be set-up to boost confidence in the use e-bamboo for construction in Ghana and other countries where the resource abound.

Proceedings of the 58th International Convention of Society of Wood Science and Technology
June 7-12, 2015 – Grand Teton National Park, Jackson, Wyoming, USA

Identifying Stakeholder Interests and Concerns in the New Hardwood-based Bioeconomy

Patricia Townsend, patricia.townsend@wsu.edu
Nora Haider, nora.haider@wsu.edu
Marina Heppenstall, marina.heppenstall@wsu.edu
Stanely Asah, stasha@uw.edu
Kevin Zobrist, kevin.zobrist@wsu.edu

Washington State University, 728 134th St SW , Suite 213, Everett, WA 98204

Abstract

Across the United States, bioeconomy initiatives are paving the way for homegrown energy and biochemicals using sustainable and renewable biomass. In the Pacific Northwest, our project, Advanced Hardwood Biofuels Northwest (AHB), is researching and developing a supply chain using sustainably-grown poplar to support the bioeconomy by producing biochemicals and biofuels. For AHB and other bioeconomy initiatives to be successful, the concerns and interests of stakeholders across the supply chain must be addressed. As part of our outreach efforts, the AHB Extension Team has identified stakeholders essential for the success of hardwood bioeconomy. To further understand how we can support stakeholder needs, we are surveying three stakeholder groups: Extension professionals, environmental professionals, and landowners. Our goal is to understand the perceptions and concerns of these professionals and landowners regarding biofuels, the bioeconomy, and poplar as a feedstock. These assessments will assist us in determining how to best inform stakeholders on issues relevant to these new industries and use their input in addressing barriers to industry development. We will show how the initial survey results are being used to guide Extension and outreach activities that will assist in educating concerned stakeholders and landowners in supporting the emerging bioeconomy. We will share our experience in producing outreach materials and events tailored for these diverse stakeholders.

Proceedings of the 58th International Convention of Society of Wood Science and Technology
June 7-12, 2015 – Grand Teton National Park, Jackson, Wyoming, USA

Impacts on the Wood Properties under Changing Conditions of Environment and Industry

Johann Trischler[1] - Dick Sandberg[2] – Thomas Thörnqvist[3]*

[1] PhD student, Department of Forestry and Wood Technology - Linnæus University, SE-351 95 Växjö, Sweden
* *Corresponding author*
johann.trischler@lnu.se
[2] Professor, Department of Engineering Sciences and Mathematics - Luleå University of Technology, SE-931 87 Skellefteå
[3] Professor, Department of Forestry and Wood Technology - Linnæus University, SE-351 95 Växjö, Sweden

Abstract

Besides the traditional uses of wood in the construction, pulp- and papermaking and furniture industries, the energy recovery industry based on renewable resources such as wood has been growing strongly during recent years. Shortages in the supply affect the price of the raw material, and this affects its supply and leads to an oscillating raw material price because of permanently changing supply and demand. Forestry as the supplier of wood is trying to provide the most beneficial mix of raw materials to meet the market conditions.

In this study, parameters related to silvicultural operations which influence the wood as raw material for sawn timber are studied. By defining a strategic cube, it was possible to illustrate the impact of the different parameters on the type of available raw material. The method provides estimates of changes in the mix of raw materials caused by changing parameters. The results show that besides the climate conditions the demands of the different wood-using industries have a strong impact on the quality and quantity of available raw material. Climate change and innovation or trends in the construction and furniture industries, for example, influence silvicultural management, and this affects the raw material mix.

***Keywords*:** Silvicultural operations, Timber production, Wood properties.

Introduction

According to different scenarios published in the Forest Sector Outlook Study presented by FAO, the consumption of wood in Europe can become as large as Europe's total forest growth increment (Jonsson et al. 2011). For industries using wood as raw material, the increasing demand for this raw material leads to increasing competition. The promotion of wood for renewable energy, the preservation of biological diversity, and wood as a sustainable raw material in general may even tighten this effect.

Wood, like all other resources, is available only in limited amounts. A change in the demand within the wood-using industry affects not only the competitors within this industry but also forestry, which is the producer and main supplier of wood (Trømborg and Solberg 2010; Abt et al. 2012). The magnitude of such an impact depends on the shift in the levels of demand and supply. According to Schwarzbauer and Stern (2010), forestry and sawmills would profit from the greater demand and higher prices of wood for energy purposes while the wood-based panel industry and the pulp and paper industry would suffer. Nevertheless, sawmills might also be affected negatively if increasing prices make it more profitable for forest owners to provide wood for energy purposes in short rotation cycles than wood for timber in long cycles. The history of forest usage shows that using wood for energy purpose once had such a strong effect on the forests that the term "sustainability" had to be created (von Carlowitz 2013).

It is possible to increase the biomass production and to influence the wood properties in a positive way through selection of species and breeding (Hakmount 1948; Grattapaglia and Resende 2011). Plant properties which can be influenced are the volume and form of the stem, the crown shape, the wood properties such as density and fibre characteristics, the resin composition, and the biotic and abiotic resistance (Namkoong et al. 1980). The wood properties such as density, microfibril angle, fibre length, juvenile wood and knots, can further be influenced by silvicultural operations such as spacing, thinnings or stocking, pruning and fertilisation (Zobel 1992; Hart 2010).

An increased annual production of wood per area allows earlier harvests, as the required diameters are reached within a shorter time. The rate of growth of different species can be influenced by the availability of water and nutrients and by the temperature (Calder 1992; Soares and Almeida 2001; Stape et al. 2004) with conifers having in general higher growth rates under cool climate conditions than deciduous trees (Way and Oren 2010). If the work of Nylinder and Hägglund (1954) is considered in combination with that of Bergh et al. (1999), it can be supposed that temperature also has an indirect impact on the growth rate by influencing the mineralisation processes which in turn have an impact on the amount of available nutrients. For Norway spruce in Sweden, it was found that not only the width of the annual rings but also the amount of latewood and the mean fibre length decreased with increasing latitude. It was also shown that not only very wide but also very narrow annual rings lead to a decrease in wood density because of the greater amount of latewood with thicker cell walls (Nylinder and Hägglund 1954; Larson 1969; Thörnqvist 1993; Grahn et al. 1995).

Support of the growth rate of trees would lead to shorter harvesting cycles for required diameters. A negative effect reducing the harvesting cycles is the amount of juvenile wood, which differs from the mature wood especially in anatomical and physico-mechanical properties such as shrinking behaviour, lower wood density and shrinkage (Fight et al. 1989; Jozsa and Brix 1989; Kennedy 1995; Bao et al. 2001). These differences in wood properties can have a negative impact on the mechanical properties and quality of semi-finished products (Senft et al. 1985). For Norway spruce, for example, such fast-grown wood with a lower content of intermediate and mature wood is graded as having a lower quality at comparable diameters (Kyrkjeeide et al. 1994) and the lower density leads to lower values of the modulus of elasticity in bending (Eikenes and Lackner 1990).

Objectives

The purpose of this study was to illustrate different impacts of silvicultural operations including the effect of changes in silvicultural operations on the quality and quantity of wood raw material.

Materials and Methods

To illustrate the properties of wood as raw material for sawn timber under changing silvicultural operations the strategic cube developed by Steinmann and Schreyögg (2005) was used. For this method it was necessary to assume that intense silvicultural management leads to only one specific assortment of wood for which the output is maximized. This method illustrates also how climate conditions and silvicultural operations influence the properties and the amount of the wood as raw material and how future changes in wood quality and quantity would influence the wood-using industry.

Results and Discussion

The sides of the strategic cube (Figure 1) are defined by the rotation cycle, type of cultivation such as plantations or second growth forests, and the intensity of silvicultural operations such as intense thinnings, fertilisation and irrigation.

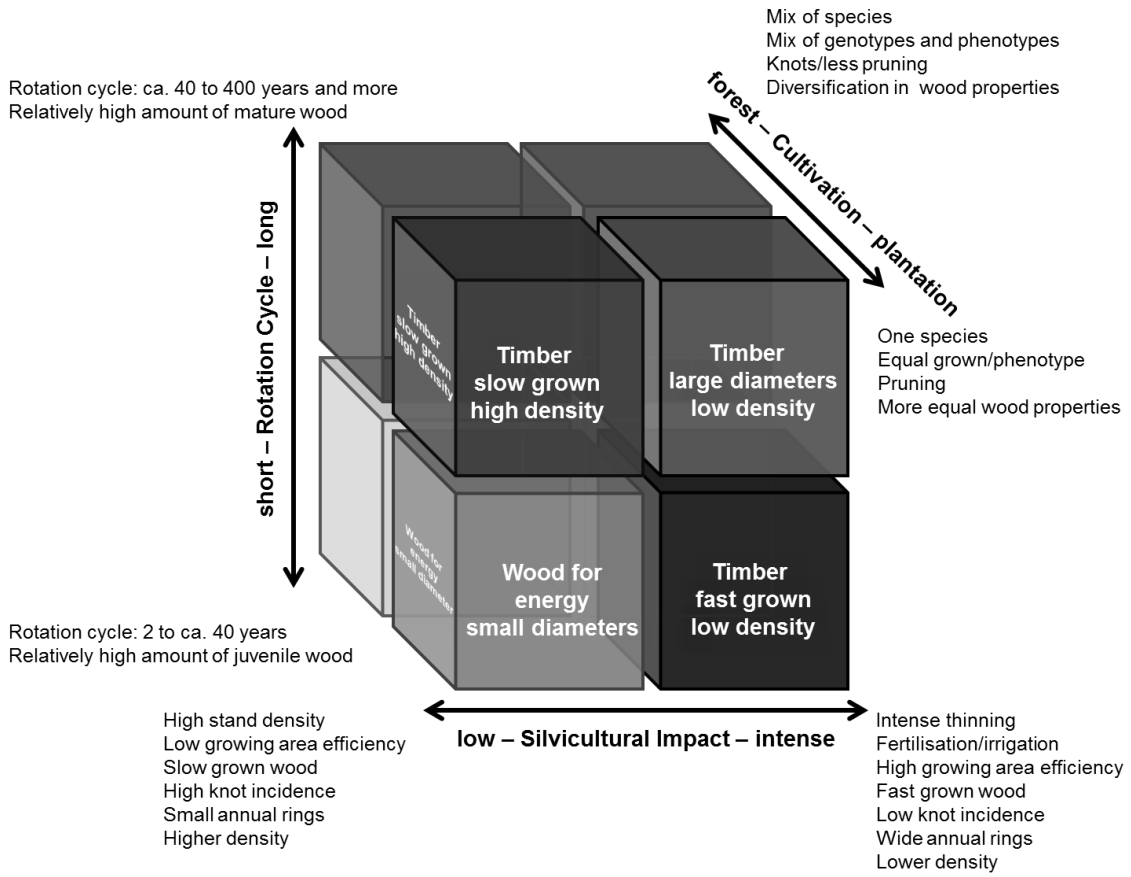

Figure 1: Strategic cube for the different assortments of wood as raw material for sawn timber to illustrate the impact of silvicultural operations on the quality and quantity of the raw material. The transparency of the cubes indicates the degree of relevance for one of these raw materials

Shift along the "cultivation" axis: The higher the level of cultivation of a forest for maximizing the production of one specific type of wood, the higher is the level of homogeneity in species and wood properties and the more the forest looks like a plantation. The benefit of a plantation is the greater effectiveness in producing a specific type of wood with only minor variations in its properties.

Shift along the "silvicultural impact" axis: The intensity of silvicultural practice gives the forests their typical characteristics and influences the wood properties. A low level of silvicultural impact results in a large number of trees on the site, high stand densities, high levels of self-thinning in higher age classes and low increments of the individual trees. The wood in such stands is in general slow-growing, of higher density, shows relative small annual rings and a high incidence of knots. Intensive silvicultural management can support the growth rate and development of selected trees.

Shift along the "rotation cycle" axis: The main wood assortment is defined by the length of the rotation cycle and the time to the final harvest, often in combination with other silvicultural operations. In long rotation cycles the influence of silvicultural operations is on the diameter and wood properties. In short rotation cycles, it is the crucial factor for the wood itself as too small diameters cannot be used for timber production.

Deduction: The manner of cultivation has an impact on the diversity of species, their genotype and phenotype, and silviculture can therefore react in various ways to the demands of the market. Besides the quantity, the quality of the wood can also be controlled. Intensive thinning in the early stages of the forest stand can reduce the rotation cycle, as the trees left on the site have a higher increment. Fertilisation, in combination with a very short rotation cycle, leads to high productivity of the stand over a short time period in the case of short rotation coppice. Higher stand densities and longer rotation cycles can increase the percentage of mature wood and the density of the stem. This method also indicates about how changing demands in the wood-using industry are changing the raw material mix of the forests and the forest type by silvicultural operations, and how this leads to a new raw material mix which in turn influences the wood-using industry. An increasing demand for one type of raw material on the market leads to increasing competition for the raw material which further stimulates additional supply, if possible, and this again affects the competitors, resulting in a new balance of supply and demand for the raw materials. Using the strategic cube, it becomes obvious that only one of the wood raw materials can be produced on a given site at one time when the production is maximized.

In general, advantageous wood properties and high growth rates of the species are appreciated. Faster growth in the young age classes combined with high stocking rates leads to a lower incidence of knots and earlier self-pruning which has a positive effect on the uniformity of wood properties. The lower wood density and the higher content of juvenile wood resulting from intensive thinning combined with a possible reduction in rotation time are critical for the timber production and related industries. While the wood-based panel production might compensate for these disadvantages by varying the density in the cross section of the board and specific adhesives, the pulp and paper industry might suffer from fibres with poor properties and the construction industry from sawn timber of lower quality.

Conclusions

In this study, the impact of climate, species and silvicultural operations on the quantity and quality of wood as raw material have been considered. It has been shown that these factors lead to different grades of wood with regard to wood properties. As forestry is the producer and main supplier of wood as raw material, it is strongly influenced by the shifts in supply and demand on the wood market.

Even if this concept is strongly simplified as it is based on the theory that each type of forest provides only one main type of raw material, it is shown that silvicultural operations have an impact on the quality and quantity of wood available on the market. Nevertheless, timber forests, for example, provide a mix of raw materials suitable for different purposes, and this has to be considered in a model illustrating the impact of silvicultural operations on the type of raw material.

References

Abt, K.L., Abt, R.C., and Galik, C. 2012. Effect of bioenergy demands and supply response on markets, carbon, and land use. Forest Science 58(5): 523-539.

Bao, F.C., Jiang, Z.H., Jiang, X.M., Lu, X.X., Luo, X.Q., and Zhang, S.Y. 2001. Differences in wood properties between juvenile wood and mature wood in 10 species grown in China. Wood Science and Technology 35(4): 363-375.

Bergh, J., Linder, S., Lundmark, T., and Elfving, B. 1999. The effect of water and nutrient availability on the productivity of Norway spruce in northern and southern Sweden. Forest Ecology and Management 119(1–3): 51-62.

Calder, I.R. 1992. A model of transpiration and growth of Eucalyptus plantation in water-limited conditions. Journal of Hydrology 130(1–4): 1-15.

Eikenes, B., and Lackner, R. 1990. Plantation grown Norway spruce (Picea abies (L.) Karst.) - Strength properties and grading of structural size timber. In: XIX World Congress: Montréal, Canada, 5-11/8/1990, I.U.o.F.R. Organizations, ed. 1990. Saint John, CA: Canadian IUFRO World Congress Organizing Committee: 12.

Fight, R.D., Fahey, T.D., and Briggs, D.G. 1989. Growing Douglas-fir for a "quality" market. Pacific Northwest Research Station, Forestry Sciences Laboratory, Portland, OR, [Unpublished document].

Grahn, T., Kubulnieks, E., and Lundqvist, S.-O. 1995. Vedråvarans egenskapsspridning. Fokus: Massa- och papperstillverkning. STFI Stockholm, Stockholm, Sweden.

Grattapaglia, D., and Resende, M.V. 2011. Genomic selection in forest tree breeding. Tree Genetics & Genomes 7(2): 241-255.

Hakmount, G.A. 1948. Forest-tree breeding. Economic Botany 2(3): 284-305.

Hart, J.F. 2010. A review of the effects of silviculture on wood quality. University of British Columbia, Faculty of Forestry, Vancouver, Canada, http://circle.ubc.ca/bitstream/handle/2429/30037/HartJamesFoster_WOOD_493_Graduating_Essay_2009.pdf?sequence=1, [September, 16 2014].

Jonsson, R., Egnell, G., and Baudin, A. 2011. Swedish forest sector outlook study. United Nations, Geneva, Switzerland, http://www.unece.org/fileadmin/DAM/timber/publications/DP-58_hi_res.pdf, [March, 18 2014].

Jozsa, L.A., and Brix, H. 1989. The effects of fertilization and thinning on wood quality of a 24-year-old Douglas-fir stand. Canadian Journal of Forest Research 19(9): 1137-1145.

Kennedy, R.W. 1995. Coniferous wood quality in the future: concerns and strategies. Wood Science and Technology 29(5): 321-338.

Kyrkjeeide, P.A., Lindström, H., and Thörnqvist, T. 1994. Konstruktionsvirke från grov gran: deformation och kvalitet hos reglar/ Building timber from large-dimension spruce - deformation and quality in wall studies -, Uppsala, Sweden: Sveriges lantbruksuniversitet.

Larson, P.R. 1969. Wood formation and the concept of wood quality, New Haven, CT: Yale University.

Namkoong, G., Barnes, R.D., and Burle, J. 1980. Screening for yield in forest tree breeding. Commonwealth Forestry Review 59(1): 61-68.

Nylinder, P., and Hägglund, E. 1954. Ståndorts- och trädegenskapers inverkan på utbyte och kvalitet vid framställning av sulfitmassa av gran /The influence of stand and tree properties on yield and quality of sulphite pulp of Swedish spruce (*Picea excelsa*). skogsforskningsinstitut, Stockholm, Sweden,
http://pub.epsilon.slu.se/9980/1/medd_statens_skogsforskningsinst_044_11.pdf, [June, 08 2014].

Schwarzbauer, P., and Stern, T. 2010. Energy vs. material: Economic impacts of a "wood-for-energy scenario" on the forest-based sector in Austria — A simulation approach. Forest Policy and Economics 12(1): 31-38.

Senft, J.F., Bendtsen, B.A., and Galligan, W.L. 1985. Weak wood: fast-grown trees make problem lumber. Journal of Forestry 83(8): 476-484.

Soares, J.V., and Almeida, A.C. 2001. Modeling the water balance and soil water fluxes in a fast growing Eucalyptus plantation in Brazil. Journal of Hydrology 253(1–4): 130-147.

Stape, J.L., Binkley, D., Ryan, M.G., and do Nascimento Gomes, A. 2004. Water use, water limitation, and water use efficiency in a Eucalyptus plantation. BOSQUE 25(2): 35-41.

Steinmann, H., and Schreyögg, G. 2005. Management. Grundlagen der Unternehmensführung. Konzepte - Funktionen - Fallstudien, Wiesbaden, Germany: Gabler Verlag.

Thörnqvist, T. 1993. Att utnyttja vedegenskaperna vid virkets förädling. In: Marknaden rår - skogen står, G. Lönner, ed. 1993. Umeå, Sweden: Sveriges lantbruksuniversitet: 107-119.

Trømborg, E., and Solberg, B. 2010. Forest sector impacts of the increased use of wood in energy production in Norway. Forest Policy and Economics 12(1): 39-47.

Way, D.A., and Oren, R. 2010. Differential responses to changes in growth temperature between trees from different functional groups and biomes: a review and synthesis of data. Tree Physiology 30(6): 669-688.

von Carlowitz, H.C. 2013. Sylvicultura oeconomica oder haußwirthliche Nachricht und naturmäßige Anweisung zur wilden Baum-Zucht, München, Germany: oekom Verlag GmbH.

Zobel, B. 1992. Silvicultural effects on wood properties. North Carolina State University, Piracicaba, Brazil, http://www.ipef.br/PUBLICACOES/international/nr02/cap05.pdf, [September, 16 2014].

Proceedings of the 58th International Convention of Society of Wood Science and Technology
June 7-12, 2015 – Grand Teton National Park, Jackson, Wyoming, USA

Comparing Load Caring Capacity of Different Joinery Systems for Remanufacturing of Wooden Furniture and Recycling its Parts

Mesut UYSAL[1], Eva Haviarova[2], Carl A. Eckelman[3]

[1] Graduate Student, Forestry and Natural Resources in Purdue University, 47906
[2] Assoc. Professor, Forestry and Natural Resources in Purdue University, 47906
[3] Professor, Forestry and Natural Resources in Purdue University, 47906

Abstract

The goal of the study was to obtain background information concerning the effect of joint construction on the durability, reparability and parts reuse of wooded chair frames. Tests were conducted with simple chair frames with seven different types of joints grouped into two joinery systems. Namely, a) mechanical joinery – screw joints, bed bolts with dowel nut joints, pinned round mortise and tenon, and pinned rectangular mortise and tenon joints, and b) permanent (glued) joinery – dowel joints, glued round mortise and tenon, and glued rectangular mortise and tenon joints. Front to back load test was conducted to determine chair strength performance (moment capacity). Chair durability, reparability, and parts reusability were also evaluated.

Mechanical joints were found to be the easiest to repair and resulted in largest reuse of parts. Glued round and rectangular mortise and tenon joints, however, provided high levels of strength which would potentially increase product service life (contributing to long lasting, more sustainable product). Joints constructed with large screws or lag screws produced about the same moment capacity as glued round and rectangular mortise and tenon joints. Screw joints are conceivably well suited for simple on-site repair of broken furniture with the advantage that broken furniture does not need to be disassembled prior to repair.

Key Words: Joints, Wooden chairs, Furniture, Reusing, Remanufacturing, Recycling and Cyclic load test

Proceedings of the 58th International Convention of Society of Wood Science and Technology
June 7-12, 2015 – Grand Teton National Park, Jackson, Wyoming, USA

Manufacturing Feasibility and Load Caring Capacity of CNC-Joinery Systems

Mesut Uysal[1], Cagatay Tasdemir[1], Eva Haviarova[2] and Rado Gazo[3]

[1] Graduate Student, Forestry and Natural Resources in Purdue University, 47906
[2] Assoc. Professor, Forestry and Natural Resources in Purdue University, 47906
[3] Professor, Forestry and Natural Resources in Purdue University, 47906

Abstract

Joinery systems produced using advanced CNC equipment increasingly popular in wood products, could be manufactured faster, more accurately, requiring lower labor costs. These joints are used mainly in products made of engineered materials, processed by CNC machinery. The specific joint construction has self-locking character and variable strength related to manufacturing tolerance and joint design. In this respect, seven types of joints were evaluated for strength and manufacturing capacity. To understand better manufacturing feasibility of each joint type, calculation of material yield and processing time were determined. Yield percentages were calculated for samples and used to evaluate the manufacturing efficiency of CNC process for production of these joints. Moreover, recorded CNC manufacturing times for each sample have been averaged within its corresponding experimental group and employed to compare the burden created during the production of each joint in terms of efficient use of labor and machine time. Manufactured joint samples were then tested for strength in tensions and compression. Results of strength tests were compared to other CNC-made and also to traditional joint types. The results of this study are expected to provide information for furniture industry utilizing CNC manufacturing by providing a better understanding of manufacturing feasibility and strength capacity of different joint types.

Keywords: CNC, Joints, Yield, Strength Design.

Proceedings of the 58th International Convention of Society of Wood Science and Technology
June 7-12, 2015 – Grand Teton National Park, Jackson, Wyoming, USA

Impact of Different Recycling Methods on Reconstituted Panel Performance

Hui Wan, hwan@cfr.msstate.edu
Xiangming Wang, xiangming.wang@fpinnovations.ca
Xioamei Liu, Mississippi State University
FPInnovations, Canada

Abstract

This paper presents the test results of panels with fibers come from different recycling methods: chemical impregnation together with thermal treatment, steam explosion, and hammer milling. It shows that different recycling methods affected the performance of panels made with recycled fibers. The main reason is that pH of recycled fibers changed a lot after the recycling processes.

Proceedings of the 58th International Convention of Society of Wood Science and Technology
June 7-12, 2015 – Grand Teton National Park, Jackson, Wyoming, USA

Compressive Failure Characterization of Embossed and TAD Features in Paper Towel

Guizhou Wang, gwang16@ncsu.edu
Steven Keller, kellerds@miamioh.edu

North Carolina State University, 2820 Faucette Dr., Raleigh, NC 27695

Abstract

The end use properties, including absorptivity, flexibility, softness, strength and others, of soft hygienic products such as tissues, napkins and towels, stem from the bulky fibrous structures. Features like creping, through air drying (TAD) patterning and embossing are intentionally used to bulk the structure and while maintaining strength between different layers. The goal of this research study was to measure and characterize a much lower range of compressive responses of towel which influence its end use properties mentioned above. The focus was on recording the compressive response curves that show the yield stress, limiting web thickness at 80 kPa and the Young's Modulus, characteristic of the collapse of TAD patterning and embossments found in paper towel samples. A modified micro compression instrument was developed to optimize the load sensitivity. The compressive responses with sensitivity to 1.0 kPa where specimen were compressed between a 2.37 mm diameter probe and a backing plate. The mass of the fibrous web within the test region was also determined so that apparent structural density could be accounted for. Video imaging of the web compression and collapse event was recorded to enhance the interpretation the compressive behaviors of the different towels. The results showed that conventional wet pressing embossment had a greater yield stress and Young's Modulus, while through air drying pattern had a larger web limiting thickness.

Proceedings of the 58th International Convention of Society of Wood Science and Technology
June 7-12, 2015 – Grand Teton National Park, Jackson, Wyoming, USA

Effects of Densification on Sugar Extraction from Woody Biomass

Amy Falcon, aeverman@mix.wvu.edu
Jingxin Wang, jxwang@wvu.edu

Abstract

Densified biomass is an ideal feedstock for biofuels because it can be stored for great lengths of time, is resistant to degradation over time, and can be transported more economically than chips or ground biomass. We tested whether densified material (pellets) could be used to produce the same quantity and quality sugars as ground wood. If the need for mechanical pretreatment is eliminated, then the time and energy necessary to pretreat the biomass at sugar facilities is greatly reduced. The effects of densification of biomass on sugar extraction was analyzed using three genotypes of hybrid willow biomass: Belleville SV1 Rep 1, Bellville SX61 Rep 2 and Belleville Owasco 99207-018 Rep 2 collected from Cornell University. Pelleted biomass was pretreated with hot water and urea, filtered, and a Nelson-Somogyi assay was used to determine the reducing sugar content of the liquid fraction of the biomass as an indication of total sugar content. The National Renewable Energy Laboratory, Laboratory Analytical Procedures (LAP) for the determination of structural carbohydrates and lignin were performed on the solid fraction, and the extracted sugars were quantified and qualified. Our preliminary results showed that pelleting the biomass had no observable effect on the extraction of sugar from woody biomass, thus allowing pellets and ground biomass to be used interchangeably for the removal of sugars from woody biomass for biofuels and bioproducts.

Proceedings of the 58th International Convention of Society of Wood Science and Technology
June 7-12, 2015 – Grand Teton National Park, Jackson, Wyoming, USA

Fractionation of the Liquefied Lignocellulosic Biomass for the Production of Platform Chemicals

*Junming XU[a], Xinfeng XIE[b], Jingxin WANG[b], *Jianchun JIANG[a]*

[a] Institute of Chemical Industry of Forestry Products, CAF; Key Lab. of Biomass Energy and Material, Jiangsu Province; National Engineering Lab. for Biomass Chemical Utilization; Key and Lab. on Forest Chemical Engineering, SFA, Nanjing 210042 China.
[b] Division of Forestry and Natural Resources, West Virginia University, Morgantown, WV 26506

Abstract

A facile and sustainable process was designed to intrigue a degradation reaction of biomass and produce biopolyols and phenolic compounds. Liquefaction of lignocellulosic materials was conducted in methanol at temperature of 180 ℃ for 15 minutes with the conversion of raw materials at about 75.0%. It was found that a majority of those hydrophobic phenolics could be separated from aqueous solution. The phenolic products that extracted from the aqueous phase were mainly composed of phenolic derivatives such as 2-methoxy-4-propyl-phenol and 4-hydroxy-3-methoxy-benzoic acid methyl ester. The aqueous solution was then distilled under vacuum to remove the water and formed a viscous liquid product named biopolyol. As evidenced by GC-MS, the biopolyols mainly contain methyl sugar derivatives, including methyl β-d-mannofuranoside, methyl α-D-Galactopyranoside, methyl α-D-Glucopyranoside and methyl β-D-Glucopyranoside. The production rate of phenolics and multi hydroxyl compounds (including glycerol and sugar derivatives) in phenolic products and biopolyols is 66.75% and 84.69%, respectively.

Proceedings of the 58th International Convention of Society of Wood Science and Technology
June 7-12, 2015 – Grand Teton National Park, Jackson, Wyoming, USA

Effects of Frequency and Processing Time on the Drying Course of Ultrasound-assisted Impregnated Wood

*Zijian Zhao Lv Huan Zhengbin He Songlin Yi**

Beijing Forestry University, China, 100083

Abstract

Impregnating wood assisted with ultrasound could promote the impregnation efficiency by improving the permeability and thus affect the subsequent drying course. Poplar lumber and phenolic resin were applied to investigate the influence of ultrasound-assisted impregnation on the wood drying process. The ultrasonic frequency and processing time were analyzed and correlated. The results indicated that average drying speed of impregnated group was slower than the control one throughout the whole course, especially below the fiber saturation point. At the earlier drying stage, the drying speed presented a decreasing tendency along with the increasing ultrasonic time when the frequency remained constant; while with the same processing time, a contrary trend was detected with the enlarging frequency. The frequency and time had irregular effect on the average speed at the later drying course. These findings could be applied to the impregnated wood drying industry to seek balance between the ultrasound-assisted performance and the following drying effectiveness.

Key words: wood drying, ultrasound, impregnation, frequency and time

Introduction

Impregnation modification is a kind of wood function-improving method. During the impregnating course, chemical additives are forced into the wood with special technology generally including two patterns— vacuum-press impregnation and atmospheric pressure impregnation (Luo, 2000). Impregnating at vacuum-press environment depends on certain equipment involving stirred tank, liquid accumulator, impregnating pot, vacuum pump, pressure pump and necessary controlling system. Although achieving higher impregnating depth and weight gain, this technology demands large capital, high power and complicated operation. Despite the weaker performance compared to the vacuum-press, impregnating at ordinary pressure needs simple device, small fund, low energy and

convenient handling (Li, 2005, Feng, 2006). Consequently, it is of great significance for the power reduction of wood manufacture to improve the impregnating performance at atmospheric pressure.

When ultrasound propagates in liquid media, there always appears cavitation phenomenon, generating numerous cavitation bubbles which immediately collapse and generate momentary high temperature and high pressure and strong local shock waves and microjets (Li, et al, 2006, He, et al, 2012, Gallego-Juarez, 1999, Muralidhara, et al, 1985, Mason, Peters, 2002). Based on this phenomenon, Li (Li, et al, 2006) demonstrates that when wood is impregnated assisted with ultrasound, the cavitation may cause pressure on the surface, promoting the modifier permeate into the wood. The previous studies of the author indicate that ultrasound-assisted impregnation at the ordinary pressure depends on the wood initial moisture content. When the content is around the green timber, the ultrasound could achieve a larger assistance, leading to a better impregnating performance. In addition, the impregnated wood needs to be dried only once, which is benefit to the decrease of energy and production cycle.

Wood drying is an important process during the producing course, however, there are few reports concerning the dewatering of the impregnated timber, particularly the ultrasound-assisted impregnated wood. This study focuses on the effects of frequency and processing time on the drying course of ultrasound-assisted impregnated wood, providing theoretical basis for the production practice.

Materials and Methods

Fast-growing poplar was obtained from Guangdong Landbond Furniture Co. Ltd in Guangdong Province, China. Poplar sapwood blocks with dimensions of 20mm×20mm×20mm (L×T×R) were prepared from defect free wood and with initial moisture content 150%～170%. The block samples were divided into 7 groups—A, B, C, D, E, F and G—with 30 replicates per group. The subsequent processing conditions of these groups are shown in Table.1, respectively.

Tab.1 processing condition of every group

	A	B	C	D	E	F	G
Frequency	28kHz	28kHz	28kHz	40kHz	40kHz	40kHz	--
Processing time	20min	40min	60min	20min	40min	60min	--

The impregnation was carried out in ultrasonic cleaning machine with an aqueous solution of 23% low molecular weight phenolic resin provided by Beijing Dynea Chemical Industry Co. Ltd in Beijing Province, China. After the impregnation finished, the impregnated specimens and the control ones were dried for 10h in the air and 9h at 70±2℃ and finally at103±2℃ until constant weight.

Before the impregnation, the initial weight of every sample was first recorded, then after the air-seasoning, the weight of samples was measured. During the 9h drying course at 70±2℃, the specimen weight was written down every 3h. When the weight of specimens became constant, they were finally recorded. The moisture content throughout the whole course and the final weight gain of every sample were calculated based on the measured data. The result of every group was the average of the 30 replicates.
Firstly, the initial moisture content of group G was determined according to equation (1),

$$MC_0 = \sum_{i=1}^{30} \frac{m_{0Gi} - m_{5Gi}}{m_{5Gi}} \times 100\% \qquad (1)$$

where MC_0 is the initial moisture content of group G, m_{0Gi} and m_{5Gi} is the initial and final weight of every sample of group G. This MC_0 was taken as the initial moisture of every block specimen. Secondly, according to MC_0 and the initial weight of the specimens of group A to F, the oven-dry weight of these specimens could be calculated with equation (2),

$$m_{od} = \frac{m_0}{1 + MC_0} \qquad (2)$$

where m_0 and m_{od} is the initial and oven-dry weight of these specimens of group A to F. Finally, the moisture content throughout the whole course and the ultimate weight gain of every group could be determined according to the above measured and calculated data.

Results and Discussion

Effects of frequency and processing time on the drying speed

The drying speed of group A to G at different period throughout the whole drying course is presented in Table 2.

Tab.2 Drying Speed at Different Period

	A	B	C	D	E	F	G
0～13h %/h	9.66	8.76	7.86	9.32	9.05	8.98	8.98
13～19h %/h	4.69	6.71	7.80	5.46	4.65	4.75	7.88
0～19h %/h	8.09	8.11	7.84	8.10	7.66	7.65	8.63

The speed of most impregnated groups is slower compared to that of control group G, especially at the period of 13h to 19h. In addition, the drying speed of the experimental groups differs from each other, indicating that the ultrasonic frequency and processing time have comprehensive effects on the dewatering speed of impregnated samples. In the previous 13h dewatering stage, when the treating time remains constant, in general, the higher is the frequency the faster is the drying course and the faster speed of the two frequency is not below that of the control group. While with the same frequency, the

drying speed presents a decreasing tendency along with the increasing ultrasonic time. During the drying period of 13h to 19h, when the processing time is the same, the groups of lower frequency generally has higher drying speed, while with the constant frequency, the speed of 28kHz groups increases along with the increasing of processing time and the speed of the 40kHz groups declines first and slightly rises subsequently.

Effects of frequency and processing time on the weight gain

The weight gain of phenolic resin of group A to F is shown in Figure 1.

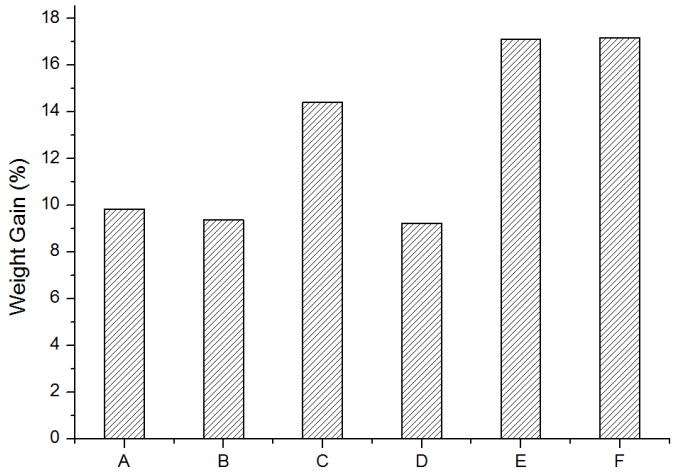

Fig.1 Weight Gain of Impregnated Groups

The wood absorption of resin is affected by both ultrasonic frequency and treating time. When the frequency is 28 kHz, the weight gain of group A and B is almost the same and both significantly smaller compared to that of group C, while with the frequency of 40 kHz, the almost identical resin absorption can be seen between group E and F whose resin gain is evidently higher compared with group D. When the treating time remains unchanged, the groups with higher frequency mainly reveal a larger resin gain compared with the lower groups and the largest variation appears between group B and E with processing time of 40 min.

Wood is a kind of porous material, having hundreds of thousands of holes in which fills with the free water when the timber is green. As a result, continuum liquid system consisting of the water in and around the wood could forms when the green timber is immersed into liquid medium generally constituted by chemical solution. Ultrasound spreads in this continuum system and generates cavitation which may split and even break down the pit membranes, thus improving the wood permeability. However, the wood absorption of the phenolic resin is accelerated because of the permeability improvement and the ultrasonic stirring, which reduces the permeability instead. In addition, the wood drying speed is closely associated with the permeability. Thus there exists a competition between the previous improvement and the following restraint of the

permeability, which comprehensively affected by the ultrasonic frequency and the processing time.

Normally, the permeability only influences the dewatering course of the free water which corresponds to the drying stage of the preceding 13h in this paper. The course of 13h to 19h could be seen as the dewatering of the bound water since the wood moisture content at 16h is already below the fiber saturation point.

The similar weight gain of group A, B and D indicates the identical restraint to permeability while the different drying speed of these groups reveals the various promotion. That is to say, the promoting effect of group A is the strongest while group B is the weakest because of the same tendency of their drying speed. However, the speed of both group A and D is larger than that of control group G, showing that the accelerating influence of A and D is stronger than their inhibiting effect. These analyses could be absolutely applied to the other groups. As a result, it could be concluded that with constant frequency, the shorter is the processing time the stronger and faster is the improving effect and the drying speed while the treating time remains unchanged, the lower is the frequency the higher is the possibility that the promoting effect is weaker, particularly with longer processing time.

With regard to the dewatering of bound water, the variation of drying speed between the groups may be attributed to the following. Firstly, the more is the resin gain the higher and slower is the dewatering resistance and drying speed. Secondly, the adulteration of some free water removal into the bound water drying course on this study condition makes it more complicated to identify the influence factor of bound water drying speed.

Conclusion

(1)Ultrasonic frequency and processing time comprehensively affect the drying course of impregnated wood whose dewatering speed is slower than that of the control group throughout the whole course, especially the bound water dewatering stage.
(2)In the previous 13h dewatering stage, when the treating time remains constant, in general, the higher is the frequency the faster is the drying course. While with the same frequency, the drying speed presents a decreasing tendency along with the increasing ultrasonic time.

(3)During the drying period of 13h to 19h, when the processing time is the same, the groups with lower frequency generally have higher drying speed, while with the constant frequency, the speed of 28 kHz groups increases and that of the 40kHz groups declines first and slightly rises subsequently along with the increasing of processing time.
(4)With constant frequency, the shorter is the processing time the stronger is the permeability improving effect while with the same treating time, the lower is the frequency the higher is the possibility that the permeability promoting effect is weaker, especially with longer processing time.

REFERENCES

FengNuo (2006) Ultrasound Handbook. Nanjing University Press, Nanjing. 90pp.

Gallego-Juarez J A, Rodriguez-Corral G, Gálvez Moraleda J C, et al. (1999) A new high-intensity ultrasonic technology for food dehydration. Drying Technology 17(3): 597-608.
HeZhengbin, GuoYuehong, et al (2012) Preliminary study of wood ultrasound-vacuum combined drying dynamics. Journal of Beijing Forestry University (34)2:133-136.

LiXiaodong (2005) Soaking Treatment of Wood Flame-proof and New Technology. Liaoning Chemical Industry 34(10):439-442.

LiXiaodong, HaoWanxin, QiXiangyang (2006) Application of Ultrasonic Wave in Soaking Methods of Wood Treated with Fire Retardant. Fujian Forestry Science and Technology, 33(1):64-66,79.

LuoJieshu (2000) A General Discussion on Flame Retardant Treatment of Wood. China Forest Products Industry 27(2):7-9.

Mason, T. J., & Peters, D. (2002). Practical sonochemistry: Power ultrasound uses and applications. Woodhead Publishing.

Muralidhara H S, Ensminger D, Putnam A. (1985) Acoustic dewatering and drying (low and high frequency): State of the art review. Drying Technology 3(4): 529-566.

Proceedings of the 58th International Convention of Society of Wood Science and Technology
June 7-12, 2015 – Grand Teton National Park, Jackson, Wyoming, USA

Effects of Boron-Containing Fire Retardants on the Fire Resistance of Bamboo Filament

Lili Yu[1,2] –Xianmiao Liu[1] - Fuqing Qiu[3]–Haiqing Ren[4] - Benhua Fei[1]*

[1,2] Ph. D, International Center for Bamboo and Rattan, Beijing 100102, China; Tianjin University of Science and Technology, Department of wood science and technology; Tianjin, 300222, China.
yulilucky@tust.edu.cn
[1] Associate Professor, International Center for Bamboo and Rattan, Beijing 100102, China;
[3] Senior Engineer, Hubei Chufeng bamboo CO. LTD, Wuhan 430000, Hubei, China.
[4] Professor, Research Institute of Wood Industry, Chinese Academy of Forestry, Beijing 100091, China;
[1] Professor, International Center for Bamboo and Rattan, Beijing 100102, China;
* *Corresponding author*

Abstract

As one of the indoor decoration materials, bamboo filament should be treated with the flame retardants for safe use. The effects of different treatment conditions on the retention of boron-containing flame retardants (boric acid: borax=1:1) in the bamboo filament have been investigated by the analysis of orthogonal and single factor tests in this study. Furthermore, the effects of boron-containing flame retardants on the combustibility of bamboo filament have been evaluated by Cone analysis. The results showed that the boring loading in the treated bamboo filament would increase distinctly as the treatment duration, temperature or solution concentration increased. Compared to the untreated and UV treated bamboo filaments, heat release reduced obviously in the treated bamboo filament with higher boron loading, heat rates were only 50 % and 30 % of untreated bamboo filament and UV bamboo filament, the total amount of the heat release were reduced by 39.7% and 56.5 %, respectively. During the combustion process, boron-containing flame retardants have excellent smoke suppression efficacy, and the total smoke release were reduced by 86.1 % and 91.1 %, respectively. Moreover, boron-containing flame retardants would promote the carbon residue production of the treated bamboo filament and reduce the mass loss during the fire.

Keywords: bamboo filament, boric acid; borax, heat release, smoke release

Introduction

Bamboo as a renewable and natural material of biological origin has been an essential material for human survival in the countries lack of timber resources, such as China. Compared to wood, bamboo has many advantages. For example, it has shorter growth period, higher production and mechanical strength, better dimensional stability, special visual enjoyment etc (Zhao et al. 2010). Nowadays, the idea material has several major features including environmental safety, natural, reused and low - carbon, bamboo just meet these demands. As the result, bamboo based material has been used much more widely in China and other regions (Yang et al. 2007, Zhang 2011, Lei et al. 2004). Among of them, bamboo filament not only has the special features of bamboo superior to other decorative material, but also has its own characteristics, such as the excellent flexibility and the smaller thickness, which make it curved arbitrarily and formed flexible and various shapes. The designers can express their thoughts and feelings directly and sufficiently. Moreover, as the indoor decorative material, bamboo filament material can be applied quickly, removed conveniently easily, recycled and reused easily, and is very environmental and natural. Therefore, bamboo filament is beginning to be applied into indoor decorative field to replace the traditional indoor decorative material, such as paint and wallpaper (Song et al. 2014), and has achieved favorable effects on decoration and beautifies the living environment.

However, bamboo based material burns easily when exposed to heat and air or strong heat radiation (Yang et al. 2014). Fire safety is an important concern in all types of constructions. Bamboo filament is exceptionally important in this regard, because its fire resistance is much poorer than wood based material. One of the reasons is the difference in their chemical compositions. The content of extracts are rather higher in the bamboo than in the wood, which results in the significant difference in the pyrolysis process (Uysal and Ozciftci 2004, Terzi et al. 2011, Blasi et al. 2007), and the poorer fire resistance of bamboo filament. The other reason is the thinner and smaller unit of bamboo filament. Some researches showed that the greater the material section, the greater the specific heat capacity, which needs more energy to reach the fire point; The greater the material section, the smaller the thermal expansion capacity, which means the internal stress caused by heat is also smaller; The surface of the materials with greater section is easier to form the charring layer, which could stop oxygen supply and consume a lot of heat; Also, the greater the material section, the lower the thermal conductivity.

However, the research on the bamboo based materials treated with boron based fire retardant are rather too few because of their lower loading and poor leaching performance, the aim of this study was to clarify the effects of immersed conditions (duration, temperature, solution concentration) on the drug loading and combustion performance, and the objective of the work reported here was to provide useful fire retardant treatment information for bamboo filament used as an indoor material.

Materials and Methods

Samples and treatment

Sapwood of moso bamboo (Phyllostachys edulis (Carr.) H.de Lehaie) filament were taken from a bamboo plantation located in Hubei Province,China. After air-drying, the moso bamboo filaments were stuck together with non - woven fabric and cut into small pieces with dimensions of 10.0 cm×10.0 cm×1.5 cm. Bamboo filament with similar weight were selected as test samples. The boron based fire retardant was made up of 50%

Influencing factor/No.	Conc. of Boron fire retardant (%)	Temp. (°C)	Duration (h)
1	5	20	0.5
2	10	40	1
3	20	60	2

Table 1 *Orthogonal experimental design.*

boric acid and 50% borax. The concentration used in this study was about 5%, 10% and 20% (w/w), respectively. The effects of immersed duration, solution temperature, and concentration on the boron loading were determined by orthogonal test, as shown in Table 1.

The optimal boron treatment conditions were investigated by range analysis of the OED method (Fisher 1922, Taguchi and Konishi 1987) and based on the treatment conditions, the single factor test was performed as shown in Table 2 to clarify different effects of these factors on the boron loading.

Table 2 *Single factor experimental design.*

Factor	Conc. of Boron fire retardant(%)	Temp. (°C)	Duration (h)
Temp.	20	20 40 60 100	2
Duration	20	60	0.5 1 2 4
Conc. of Boron fire retardant	5 10 20 25	60	2

Fire Test

After fire retardant immersion, the wood specimens were dried at room temperature. The fire performance of the specimens was evaluated by a cone calorimeter. Six specimens with the same treatment were prepared with dimensions of 100 mm (tangential) × 100 mm(longitudinal) × 1.5 mm (radial), and were placed horizontally under a cone heater with a heat flux of 50 kW/m^2. The data were recorded by a computer every second. Specimens with different treatments were selected for the cone calorimeter tests as shown in Table 3.

Thermo-gravimetric Analysis (TGA)

The treated and control specimens as shown in Table 3 were ground to pass through a

No.	Conc. of Boron fire retardant (%)	Temp. (°C)	Duration (h)	UVcoating （Y/N）	Boron loading /%
T1	5	20	2	N	2.02
T2	20	60	2	N	9.64
T3	20	100	2	N	11.25
T4	—	—	—	N	—
T5	—	—	—	Y	—

Table 3 Cone and TG experimental conditions

100-mesh sieve and then oven dried at 103±2 °C. TGA was performed using TGA 600; approximately 7 mg were weighted in aluminium-oxide crucibles. The TG curve was run under a dynamic nitrogen atmosphere flowing at 40 mL/min and at a scanning rate of 10.0 C/min from 0-800°C.

Results and Discussion

Influencing Factors of the Treatment Conditions Analysis

The influence of various factors and the optimal process parameters for the high boron loading can be obtained by means of range analysis (RA) based on OED method. As shown in Table 4, the optimal process is: Conc. of boron fire retardant=20%, Temp.=60°C, Duration= 2h and the order of the influence is: Conc. of boron fire retardant > treatment temp. = treatment duration. The results showed that higher treatment duration, temperature and concentration of boron fire retardant are the positive factors on the boron loading in the bamboo filament. Among of these three factors, the concentration of boron fire retardant plays more important role for the higher boron loading. However, the solubility of the boric acid and borax are rather too low at room temperature as proved by Zhang (2013). Although the solubility of the mixture of these two boron compound can be increased significantly, the highest solubility can only reach to 20% and the boron compound would be deposited when the concentration exceeds this point as observed from the single factor experiment (Fig.1).

Based on the results of RA (Table 4), the effects of different treatment conditions on boron loading in the treated bamboo filament was evaluated and the results were showed in Fig.1(a, b and c). It seems that the boron loading can be increased as the concentration, treatment temperature or treatment duration increased. Among of them, the trend of the boron loading in the treated bamboo filament changed much more obviously as the concentration changed compared to the other two factors, which is consistent with the results obtained from RA. 100°C is a promising key point treatment temperature for the bamboo filament, the boron loading can reach to more than 10% only for 2h, which is higher then the samples treated at 60°C for 4h. These results demonstrated that higher temperature just like a catalyst that can positively promote the chemical and physical reactions between boron compound acid and bamboo components. For the physical reactions, the higher treatment temperature increased the kinetic energy of the boron compound molecules and accelerated their penetration speed into the treated bamboo filament. At the same time, more extract in the treated bamboo filament has been dissolved in the hot water, as the result, the permeability of the treated bamboo filament has been improved greatly. For the chemical reactions, on one aspect, at 100°C, boric acid could be converted to metabolic acid with smaller molecular weight by dehydration reaction and reduce the permeability difficulty. On the others, the higher treatment temperature much be accelerated the chemical reaction between bamboo filament components and boron compounds molecules, although the formation products have not investigated clearly.

Table 4 Range analysis of boron loading in the orthogonal experiment.

Factor	Conc. of Boron fire retardant (%)	Temp. (°C)	Duration (h)
R_1	2.507	4.140	3.960
R_2	4.483	4.600	4.960
R_3	7.303	5.553	5.373
R	4.796	1.413	1.413

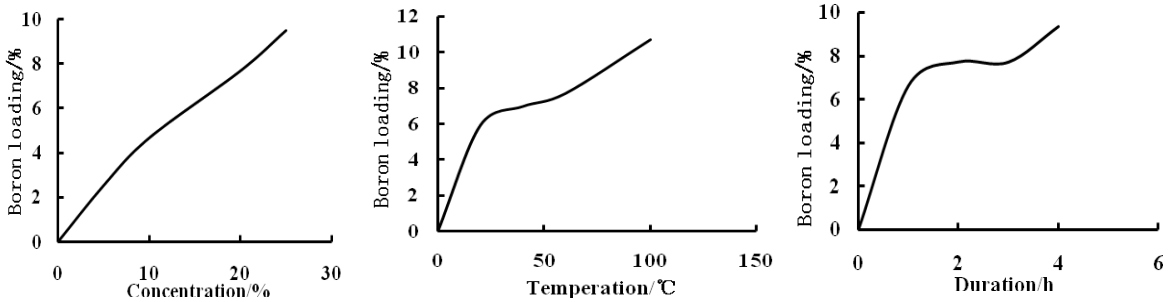

(a) solution concentration (b) solution temperature (c) treatment duration
Fig.1 Effects of different treatment conditions on boron loading in the treated bamboo filament

Heat Release Analysis

The rate of heat release (HRR) and the peak of HRR (pkHRR) are two of the most important parameters to characterize fire behavior. The greater the number the greater risk in the fire, and the faster pyrolysis of the material and the flame spread. From Fig.2(a), the highest HRR can be found in UV treated bamboo filament (T5), and the HRR is also much higher in the untreated bamboo filament (T4) than in other boron treated samples (T1-3). The most promissing result is observed in the samples with the highest boron loading (T3), which is treated with 20% boron compound fire retardant at 100°C for 2h. The similar result also can be observed in Table 5, the maximum pkHRR was also in the samples treated with UV paint (T5), and the pkHRR in the samples with the highest boron loading (T3) would be reduced by 40% compared to the untreated samples. This result demonstrated that boron compound could take efficient fire retardant on bamboo filament. The reason is attributed to the property of boron compound that could form molten B_2O_3 film at high temperature, which could spread on the surface of the samples, and isolate the oxygen effectively (Yang et al. 2014). Additionally, the boron compound could release the bound water that cool the material and absorb the heat during fire (Marosi et al. 2002, Enyu and Minxiu 1988, Silvo et al. 2007). Based on the result from Fig.2 (a) and Table 5, UV paint is more flammable and its treated bamboo filament which is widely used in the market nowadays conceal the huge fire danger.

The total amount of hear release (THR) is used to evaluate the amount of heat release during fire per unit of the material. The bigger the number the most the amount of the heat and the greater the fire risk. From Fig. 2(b), in the same fire period, the THR in the samples without boron treatment (T4 and T5) were much higher than these treated samples. The most promissing result is also observed in the samples with the highest boron loading (T3).From Fig. 2(b), the curves can be clarified into two different phases, first phase(0-200s) involves the fast thermal decomposition of the bamboo filament; and the second phase (200-800s) involves the slow thermal decomposition and the formation of the carbon film. From the results, it seems that different fire retardant treatment took obvious effects on the combustion phases. This is attributed to the fire retardant improvement in the samples with the higher boron loading; and another aspect, in the hot temperature, boron compound can combined much more stablely with the bamboo filament.

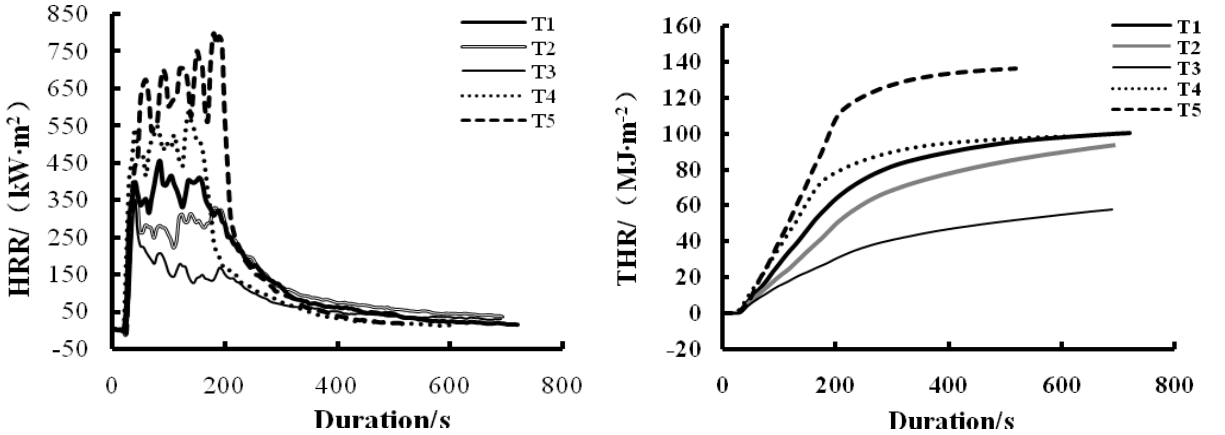

(a) the rate of heat release (HRR) (b) the total amount of heat release (THR)

Fig.2 Heat release from the treated bamboo filament with different treatments

Table 5 Peak of HRR from the treated bamboo filament with different treatments

Sample	T1	T2	T3	T4	T5
pkHRR / （kW·m^2）	455.5	395.5	352.0	585.2	796.7
Time to peak/s	85	40	40	135	138

Smoke Release Analysis

Smoke released from the fire is the most critical reason for the personal injury and death. TSP means the total amount of smoke release per unit of the material during the fire. It is very important to evaluate the smoke release from the fire as shown in Fig. 3. It can be seen that compared to the untreated and only UV treated samples, the figures of TSP were reduced dramatically in the boron treated bamboo filaments even in the samples with the lowest boron loading (T1). For the samples with the highest boron loading (T3), TSP could be reduced to only 0.08m^2, while the figures were 1.82 m^2. The high efficient smoke suppression of boron compound fire retardant has been proved by many researches (Mukherjee and Ansuman 2002, Wang 2000), in which boron compounds were chosen in order to reduce the smoke release of their fire retardants. The reason is that boron could rapidly form a film on the surface of the material to impede the smoke release.

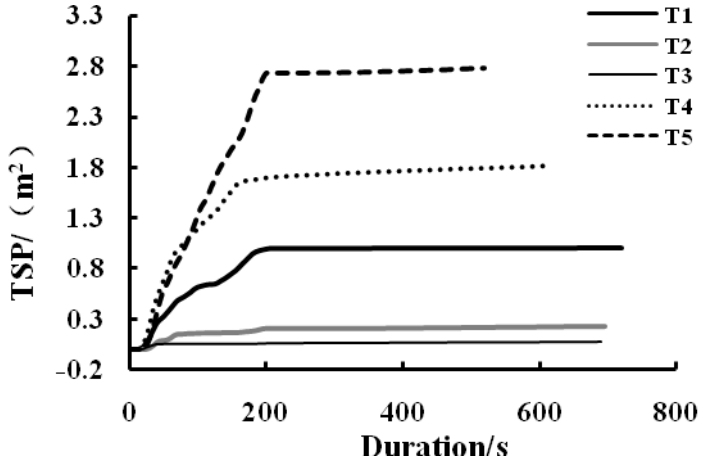

Fig.3 Smoke release of the treated bamboo filament with different treatments

Conclusions

Bamboo filament is easily destroyed by fire, and would produce abundant smoke and toxic gases. As the indoor decorative material, it is very efficient to be treated with boron containing compound for bamboo filament. The boron loading in the treated bamboo filament would increase distinctly as the treatment duration, temperature or solution concentration increased. In the future, more research will be performed to decrease the heat and smoke release furthermore.

References

AWPA (2006) Book of standards. American Wood Protection Association, Birmingham, AL, USA.

Baugh PJ, Hinojosa O, Arthur JC and Mares T (1968) ESR spectra of copper complexes of cellulose. J. Appl. Poly. Sci 18:249-265.

Bergervoet AJ, Marcinko JL, Walcheski PJ (1997) Fixation process for heat-fixable preservative treated wood. Appl. No.: 609087.

Zhao N, Lei D, Wu L (2010) Cultural and functional support in designing of bamboo products. Journal of Bamboo Research, 29(2):52-58.

Yang H, Chen G, Wang X (2007) Bamboo furniture and ecological design. Journal of Zhengzhou University of Light Industry, 8(4):73-75.

Zhang Y (2011) The research on artistic design-expression of the native bamboo. Master thesis, Hunan, China.

Lei D, Wu L, Chen D, et al. (2004) The modern furniture with raw bamboo：A blend of tradition form and modern aesthetics. Word Bamboo and Raton, 2(4):41-43.

Song S, Yang F, Sun Z, et al. (2014) The sliced bamboo winding technology and processing technology. China Forest Products Industry, 41(3):34-36.

Yang Y, Wu Y, Qing Y, et al. (2014) Effect of typical boron compounds on the thermal degradation and combustion properties of phyllostachys pubescen. Hunan Forestry Technology, 16(4):51-55.

Uysal B, Ozciftci A (2004) The effects of impregnation chemicals on combustion properties of laminated wood material. Combustion Science and Technology, 176 (1):117-133.

Terzi E, Kartal SN, Robert HW, et al. (2011) Fire performance and decay resistance of solid wood and plywood treated with quaternary ammonia compounds and common fire retardants. European Journal of Wood Products, 69:41-51.

Blasi CD, Branca C, Galgano A (2007) Flame retarding of wood by impregnation with boric acid-pyrolysis products and char oxida-tion rates. Polymer Degradation and Stability, 92: 752-764.

Fisher RA (1922) On the mathematical foundations of theoretical statistics. Philosophical Transactions of the Royal Society, A. 222: 309-368.

Taguchi G, Konishi S (1987) Taguchi methods orthogonal arrays and linear graphs: tools for quality engineering. American.

Zhang H (2013) Research progress of modificated zinc borate. Rubber and Science and Technology, 39:9-13.

Marosi G, Ma´rton A, Anna P, et al. (2002) Ceramic precursor in flame retardant systems. Polym Degrad Stab., 77:259–65.

Enyu X, Minxiu Z (1988) Flame retardant science and application. 1sted. Beijing: National Defence Industry Press; 1988.

Silvo H, Majda SS, Karin SK, et al. (2007) Flame retardant activity of SiO_2-coated regenerated cellulose fibres. Polym Degrad Stab., 92:1957–65.

Mukherjee GN, Ansuman D (2002) Mixed ligand complex formation of Fe with boric acid and typical N-donor multidentate ligands. Proc Indian Acad Sci (Chem Sci), 114(3):163–174.

Wang QW (2000) FRW fire retardant for wood. PhD dissertation, Northeast Forestry University, Harbin, China.

Proceedings of the 58th International Convention of Society of Wood Science and Technology
June 7-12, 2015 – Grand Teton National Park, Jackson, Wyoming, USA

Effect on Wood Mechanical Characteristics of Chinese Fur with High Temperature Drying Process

Derong Zhang, Xiaojuan Jin, Wei Pang

College of Materials Science and Technology, Beijing Forestry University, Beijing 100083, P R. China

Abstract

In order to improve the elasticity of table tennis racket bottom board through thermal treatment, in this research the effect of the drying temperature（130-190℃）and drying time on the character of Chinese fir（*Cunninghamia lanceolata*）were investigated, which indicated that dynamic modulus of elasticity and dynamic modulus of shearing show well relevance. The pulling force on wood, dynamic modulus of elasticity, static modulus of elasticity, dynamic modulus of shearing and storage modulus were all influenced by the drying treatment at high temperature, as well as the effect on dynamic modulus of shearing was stronger than that on dynamic modulus of elasticity. Besides, drying temperature had greatly affected the character of Chinese fir, but drying time caused little impact.

Keywords: drying temperature, drying time, dynamic modulus of elasticity, static modulus of elasticity, modulus of shearing, storage modulus.

Introduction

Wood is widely applied in the table tennis racket bottom board because of its low weight and good elasticity. A suitable table tennis racket can help athletes achieve good scores; however, used as the racket bottom board of table tennis, the same species wood with the same texture and the similar character cannot meet the demand of different athletes. It is a good method to improve the elasticity of table tennis racket bottom board by drying treatment at high-temperature to meet different athletes' demand.

The performance of tennis racquet depends on its wood features, while the striking force, resilience quality and feeling of the racquet are all affected by the dynamic mechanical properties of wood such as the storage modulus and loss modulus et al. Consequently, it has a great significance to investigate the relationship between wood's characteristics and properties of hitting. Meanwhile, different athletes have different requirements for the

racquet. It is meaningful on improving the technical level and achievements of athletes and promoting the development of table tennis that make the racquet meet the athletes' requirements by wood modification according to the dynamic mechanical properties of wood and the players' technical characteristics and requirements.

Materials and Methods

Selection of wood samples

Chinese fir, 350×200×5 mm; The thermal control box, Cantilever beam tester; The Chinese fir boards were treated in the thermal control box with different temperature and time. The treatment temperature were 130, 160, 190 ℃, and the treatment time were 30, 60, 90 min corresponding the treatment temperature, respectively. The characteristic of modified samples were tested after 48h at the room temperature.

Results and Discussion

The relationship between dynamic modulus of elasticity, static elastic modulus, dynamic shear modulus, storage modulus and density

The density of wood used in the experiment is mainly distributed in 350~370 kg/m^3. The difference of wood property can be seen depending on the varieties of trees. Besides, the different trees of the same species and even different parts of one tree also exit difference in wood properties because of the different site conditions. The density of wood has relevance with dynamic modulus of elasticity, static elastic modulus, dynamic shear modulus and storage modulus (Fig. 1-4). Besides, there were good correlations between dynamic modulus of elasticity and static elastic modulus as well as dynamic shear modulus and storage modulus (Fig. 5-6). These correlations provided theoretical basis for us to research the performance of table tennis board.

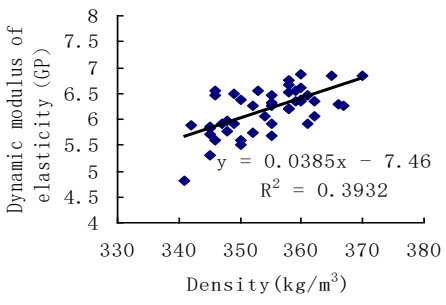

Fig.1
Relationship between dynamic modulus of elastic and density

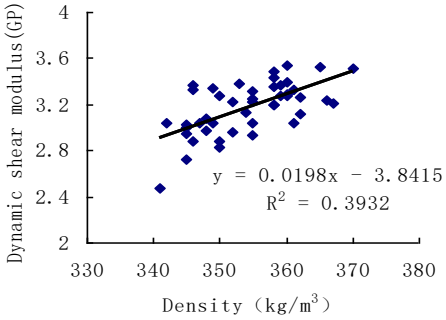

Fig.2
Relationship between dynamic shear modulus and density

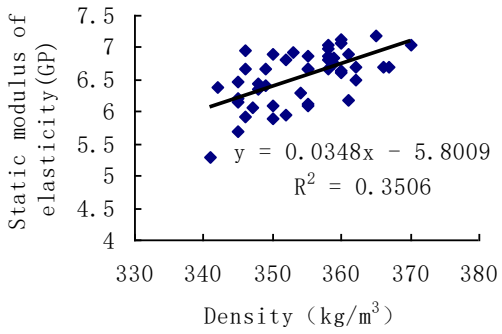

Fig.3 Relationship between static modulus of elasticity and density

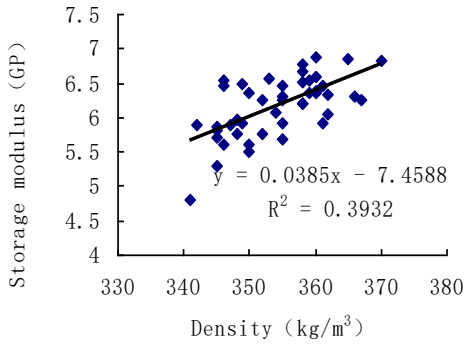

Fig.4 Relationship between storage modulus and density

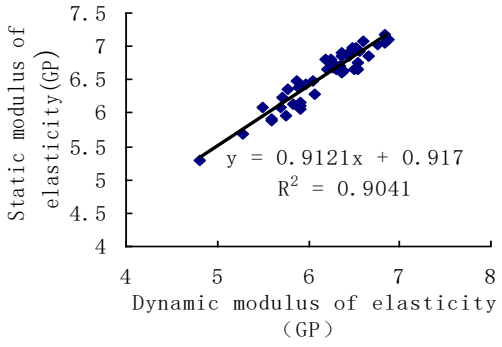

Fig.5 Relationship between dynamic and static modulus of elasticity

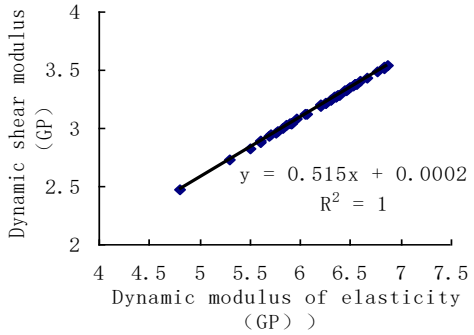

Fig.6 Relationship between dynamic modulus of elasticity and shear

Effects of high temperature treatment on the properties of wood

As a kind of natural polymer material, wood contains cellulose, hemicellulose, lignin and some volatile organic compounds (VOC) which had physical and chemical changes in the process of heat-treatment at high temperature. Moisture sorption site of wood inner decreased as the dehydration between -OH, which can improve the dimensional stability of wood. The research showed that the total volatile organic compounds (VOC) volume changed much more seriously during kiln drying at high temperature. The major components in VOC were methanol, acetic acid, formic acid, acetaldehyde, formaldehyde, acrolein acetone. The major terpine were α-pinene, D-limonene, camphene, β-pinene and β-phellandrene. The final moisture content of wood had a significant influence on emission amount of aldehydes and polar volatile compounds. The rate of formaldehyde emission increased gradually with the decreasing of moisture content (MC) for high temperature drying at 120℃(Longling et al.2008). With the treatment temperature increasing, the chemicals and volatile matters in the wood changed. When the treatment temperature exceeded 170 ℃, the properties of treated wood changed because of the transformation in chemical composition and structure and the degradation of hemicelluloses particularly. As the figure (Fig.7-8) shown, dynamic modulus of elasticity, static elastic modulus, dynamic shear modulus, storage modulus were all reduced after treatment. Consequently, for the wood using as table tennis board, changing the wood properties by high-temperature treatment to improve the hitting performance could make the board fit different players.

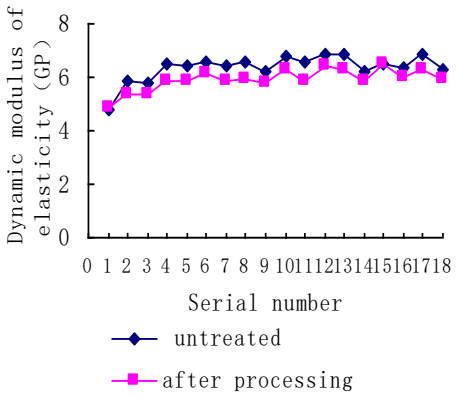

Fig.7 The effect on dynamic modulus of elasticity by high temperature drying

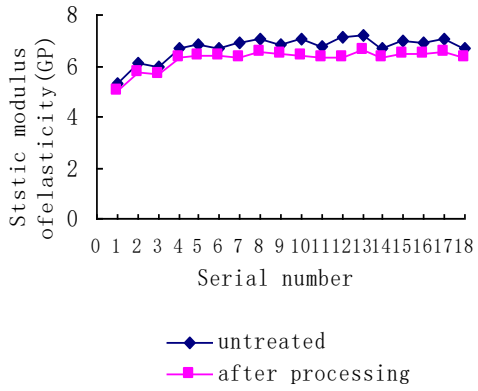

Fig.8 The effect on static modulus of elasticity by high temperature drying

Effects of treatment time and temperature on the properties of wood

The properties of wood changed with the increasing of temperature and treatment time. The effect of treatment time on the change was little than that of treatment temperature. Some matters in the wood and volatile matters could occur chemical changes at low temperature with the influence on wood properties. When the treatment temperature exceeds 170 ℃, the hemicellulose will be degraded and the degradation is severer as well as the changing of wood property is more obvious with the increase of the treatment temperature (Huachun Qi et al.2005). When the treatment temperature higher than 170 ℃, the degradation of hemicellulose raised with the increase of the treatment temperature that affects the wood properties more obviously. (Huachun Qi et al.2005). The appropriate treatment temperature should be confirmed firstly, and then the treatment time according to the treatment temperature (Fig.9-10).

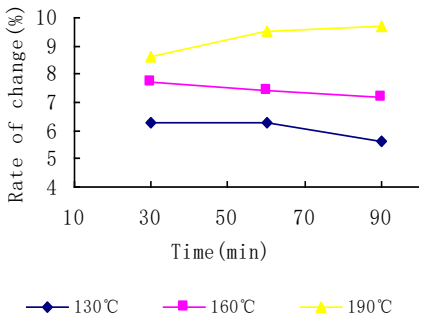

Fig9. The effect on dynamic modulus of elasticity by drying time

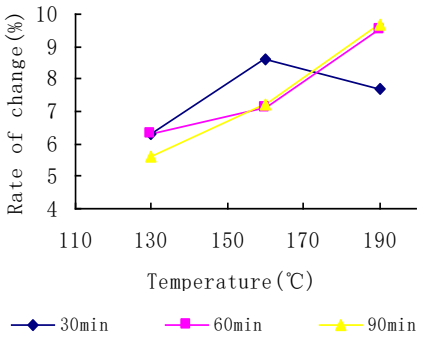

Fig.10 The effect on dynamic modulus of elasticity by drying temperature

Conclusion

The physical and mechanical properties of wood are highly related and it can be improved by high-temperature treatment. Moreover, treatment temperature has a greater effect on the properties of wood. Improving the properties of wood by high-temperature treatment make it possible to produce different texture of table tennis board to meet different requirements ,and then the athletes may improve their technical level and make greater achievements with the suitable and higher quality table tennis racket bottom board made by heat-treated wood.

Reference

Green W D, Gorman M T, Evans W J (2006).Mechanical grading of round timber beams. Journal of Material Civil Engineering (1):1-10.

Hakkou Mohammed, Petrissans Mathie, Gerardin Philippe, etc (2006).Investigations of the reasons for fungal durability of heat-treated beech wood. Polymer Degradation and Stability 91(2):393-397.

Huachun Qi, Wanli Cheng, Yixing Liu(2005).Mechanical Characteristics and Chemical Compositions of Superheated Steam-treated Wood under High Temperature and Pressure. Journal of Northeast Forestry University33(3):44-46.

Jianmin Gao (2008). Wood drying. Science press:15-19.

Longling,Xixian Lu(2008).VOC Emission from Chinese Fir (Cunninghamia lanceolata) Drying, Scientia Silvae Sinicae,44(1):108-116.

Yan Jie (2009). LabVIEW-based auto-timing counts virtual instrument system with ORTEC 974 Counter／Timer. Department of Modern Physics, University of Science and Technology of China. Nuclear Science and Techniques (20):307-311.

Zhongfu Tian,Yuehua Li, Xiurong Guo (2013). Wood drying principle and factors influencing drying speed. Journal of Anhui Agriculture Science, 4(33):12900-12904.

Student Poster Competition
Moderator: *Frederick Kamke, Oregon State University, USA*

Preparation of Strips from *Bambusa Vulgaris* Schrad Culms from Recycled Scaffold for Intermediate Raw Materials Production

Adesope A.S [1] - Adewole N.A [2] - Olayiwola H.O [3]- Adejoba O.R[1]*

[1*]Researcher, Forestry Research Institute of Nigeria, Forest Products Development and utilization Dept
* Corresponding author
adeyinka_sope@yahoo.com.

[2]Senior Lecturer. Ph.D, Department of Agric and Environmental Engrg, University of Ibadan.
dabukyo@yahoo.com

[3]Postgrad, Department of Agric and Environmental Engrg, University of Ibadan.
olafiku@live.com

Abstract

In Nigeria, the main use of bamboo that attracts money is its use as scaffold and the massive number of bamboo used as scaffold always ended up as waste. But there are possibilities of recovering useful bamboo culms for the production of intermediate products like laminates among others particularly for semi-structural and non-structural purposes. The major constraint of using these recovered culms is the form in which bamboo occurs naturally (round). It is for this reason that this study is aimed at preparing strips from recovered bamboo culms to produce value added products. This study sourced and revealed the characteristics of bamboo reclaimed from scaffold use. From a total of 298 culms used as scaffold, only about 65% was good for re-use while others constituted a waste. The study was able to improvise treatment vat for the bamboo strips to enhance its durability. Intermediate products like bamboo wall clock, bamboo ply and bamboo boards were produced through lamination process. This study revealed the possibility of

re-using bamboo from scaffold and was able to produce useful raw material and intermediate products from recovered bamboo waste.

Key-words: Bamboo culms, Scaffold, Intermediate Products, Bamboo Strips

Effectiveness of *Gliricidia Sepium* Heart Wood Extractives as Preservatives Against Termite Attack

AGUDA L. O[1]., AJAYI B[2]., Owoyemi J[3]. Adejoba O.R[4] and Areo O.S[5].*
[1] Researcher, Department of Forest Products Development and Utilization, Forestry Research Institute of Nigeria, P.M.B. 5054, Ibadan, Oyo State, Nigeria.
[2] Professor, Head of Department of Forestry and Wood Tech., Federal University of Technology Akure, P.M.B. 704, Akure, Ondo state, Nigeria.
[3] Doctor, Senior Lecturer, Department of Forestry and Wood Tech., Federal University of Technology Akure, P.M.B. 704, Akure, Ondo state, Nigeria.
[4]Doctor, Assistant Director, Head of Department of Forest Products Development and Utilization, Forestry Research Institute of Nigeria, P.M.B. 5054, Ibadan, Oyo State, Nigeria.
[5]Researcher, Department of Forest Products Development and Utilization, Forestry Research Institute of Nigeria, P.M.B. 5054, Ibadan, Oyo State, Nigeria.
[*]E-Mail: larryall2000@yahoo.com. Phone No: +2348038724979

Abstract

Resistance of most wood species against termite attack is mainly as a result of their extractives components. The chemical compositions of extractives from matured *Gliricidia sepium* that are known to be very resistant against termite attack were studied to assess their role as wood preservatives. Ethanol-toluene and distilled water were used in the extraction of these compounds from the heartwood of this species. Chemical analysis of the extracts was done using Gas Chromatography-Mass Spectrometry (GC-MS) after derivatization using N,O bis (trimethyl silyl) acetamide.. More than One hundred and forty five compounds were identified from both extracts. Fatty acids, hydrocarbons, sterols, sterol ketones, phenolics, sterol esters and waxes were the main groups of compounds identified. The extracts obtained were used to treat four wood species that are known to be susceptible to termites attack. Treated samples were taken to a termitarium for a period of twelve weeks. It was observed that wood extracts used as preservatives improved the resistance of these susceptible wood species to termite attack more than 60% compared to the controls and also it was observed that removal of extractives decreased resistance of the durable samples significantly. It can be concluded that wood extractives contribute greatly to the protection of less durable wood against termite attack.

Keywords: Wood Extractives, bio-preservatives, termitarium, subterranean termites, Susceptible.

Proceedings of the 58th International Convention of Society of Wood Science and Technology
June 7-12, 2015 – Grand Teton National Park, Jackson, Wyoming, USA

Comparative Life Cycle Analysis of PET Bottles Produced from Different Raw Materials

Luyi Chen, chen3461@umn.edu
Rylie Pelton, olso4235@umn.edu
Timothy Smith, timsmith@umn.edu

University of Minnesota Twin Cities, 1954 Buford Avenue, , St. Paul, MN 55108

Abstract

Growing concerns about fossil fuel depletion and global warming have driven scholars to seek sustainable substitutes for petroleum products. Generating energy and materials from biomass is no longer a novel approach, but how to extract economically profitable products from lignocellulosic biomass is still under debate, due to the high cost and technology barrier of breaking down ligno-cellulose fiber into simple sugars. Co-products, such as activated carbon and lignosulfonates, were studied to maximize the sustainability of the biorefinery industry. This work focuses on one value-added co-product, woody-biomass based PET bottles used in the soft drink industry. Study results contribute to market value/environmental impact analysis of the parameterized co-products model. In this study Life Cycle Analysis (LCA) was performed to investigate the environmental impacts of diverting a small portion of isobutanol from a projected bio-jet fuel production system to paraxylene, and further processing it to wood-based PET bottles. A comparative assessment was done for: 1), different industrial data; 2), different allocation methods; 3), different types of biomass.

Proceedings of the 58th International Convention of Society of Wood Science and Technology
June 7-12, 2015 – Grand Teton National Park, Jackson, Wyoming, USA

Gender Diversity Impacts on Firm Performance in Forest Sector Firms

Kendall Conroy

Oregon State University, Corvallis, OR

Abstract

The forest industry is predicted to lose a large percentage of its employees due to retirement in the coming decade. The industry also tends to lack diversity in its workforce, which makes this is an ideal time to move towards greater diversity. While many companies in the sector recognize the need for a more diverse workforce and have strategies in place to encourage diversity, there is little academic work evaluating the performance of such strategies. The existing research shows that greater diversity leads to increased creativity, openness to change, and innovation, all of which can contribute to increased financial performance. However, there is no information specific to forest sector firms. For that reason, we investigate the relationship between gender diversity and financial performance of large forest sector firms. We use the PricewaterhouseCoopers global 100 pulp, paper and packaging companies database and select those companies from Europe, North America and Oceania. Our data consists of the gender ratio of each of the 67 company's boards of directors and corporate executive teams. Preliminary regression analyses indicate a strong connection between greater female representation and firm performance. Consistent findings would provide further incentive for forest sector firms to strive for higher diversity in their workforces.

Proceedings of the 58th International Convention of Society of Wood Science and Technology
June 7-12, 2015 – Grand Teton National Park, Jackson, Wyoming, USA

Fungal Pretreatment Method Optimization for Small Wood Samples Degraded by Ceriporiopsis Subvermispora

Charles Edmunds, cwedmund@ncsu.edu
Vincent Chiang, vincent_chiang@ncsu.edu
Richard Giles, rgiles2@uncc.edu
Ilona Peszlen, impeszle@ncsu.edu
Perry Peralta, pperalta@ncsu.edu

North Carolina State University, 2820 Faucette Blvd, Raleigh, NC 27695

Abstract

Fungal pretreatment on genetically modified wood samples holds tremendous promise for a low-cost and environmentally-friendly method of increasing the reactivity of lignocellulosic biomass prior to bio-ethanol and bio-chemical conversion. One drawback of research in this area is the frequent requirement of testing young greenhouse-grown wood specimens. There is a lack of knowledge concerning the optimal technique for fungal pretreatment of small specimens from transgenic wood. This project explores testing different methods for fungal inoculation and incubation to study the utilization of a white-rot wood degrading fungus (Ceriporiopsis subvermispora) as a means to increase biomass reactivity. Sweetgum (Liquidambar styraciflua) wood is used as a representative fast growing hardwood species to develop methods that will be used for future testing of genetically modified Populus trichocarpa. Several variables regarding the inoculation and incubation of small hardwood (Liquidambar styraciflua) specimens were tested in order to optimize the procedure, as measured by a sufficient amount of biomass degradation (% weight loss) and low variation between replicates. The variables tested include: inoculation medium (liquid mycelium slurry or pre-colonized malt agar extract), wood particle size (ground 40-mesh vs. cylindrical stem shape); and incubation container (20 ml vial vs. large Petri dish). The results from this study are of great utility to fungal pretreatment research.

Proceedings of the 58th International Convention of Society of Wood Science and Technology
June 7-12, 2015 – Grand Teton National Park, Jackson, Wyoming, USA

Effect of TEMPO Nanofibrillated Cellulose Content on Copper Release from Antimicrobial Polyvinyl Alcohol Films

Changle Jiang [1] – Gloria S. Oporto[2] – Tuhua Zhong[1] – Jacek Jaczynski[3]*

[1] PhD student, Division of Forestry and Natural Resources,
West Virginia University, Morgantown WV, USA
[2] Assistant Professor, Division of Forestry and Natural Resources,
West Virginia University, Morgantown WV, USA
* *Corresponding author*
gloria.oporto@mail.wvu.edu
[3] Associate Professor, Division of Animal and Nutrition Science,
West Virginia University, Morgantown WV, USA

Abstract

The long-term goal of our research is to develop a novel antimicrobial film with controlled release of the active agent. In this work, copper nanoparticles (CuNPs) were synthesized on TEMPO nanofibrillated cellulose (TNFC) using a chemical reduction method. Polyvinyl alcohol (PVA) composite films were prepared by incorporating this TNFC-CuNPs hybrid material into the PVA matrices using a solvent casting process. Copper release from the final films was determined using Inductively Coupled Plasma Optical Emission Spectroscopy (ICP-OES). The final PVA/TNFC-CuNPs films with different TNFC concentration were investigated for copper release rate. The antimicrobial properties of PVA/TNFC-CuNPs film was conducted against nonpathogenic *Escherichia coli* (*E. coli*). The copper release measurement show that the release rate drops when TNFC concentration increases.

Keywords: TEMPO nanofibrillated cellulose, copper nanoparticles, copper release, antimicrobial films.

Proceedings of the 58th International Convention of Society of Wood Science and Technology
June 7-12, 2015 – Grand Teton National Park, Jackson, Wyoming, USA

Multi-technique Characterization of Douglas-fir Cell Wall Deconstruction during Mechanical Milling Pretreatment

Jinxue Jiang [1] *– Jinwu Wang*[2] *- Michael P. Wolcott*[3*]

[1] Graduate student, Composite Materials & Engineering Center, Washington State University, Pullman WA, USA
[2] Research assistant professor, Composite Materials & Engineering Center, Washington State University, Pullman WA, USA
[3] Professor, Composite Materials & Engineering Center, Washington State University, Pullman WA, USA.
* *Corresponding author* wolcott@wsu.edu

Abstract

Overcoming recalcitrance of the wood cell wall to enzymatic degradation is believed to being crucial for effective biological conversion of polysaccharides to fermentable sugars. Mechanical milling has long been used to overcome the native structure barriers of cell wall for producing milled wood lignin. This process imparts macro/micro/nano morphological and physicochemical alternations that contribute to increased accessibility of cellulose without removal of chemical compositions. Multi-technique characterization of Douglas-fir cell wall disruption during mechanical milling were conducted using electronic microscopy (SEM, TEM), confocal laser scanning microscopy (CLSM), atomic force microscopy (AFM), and X-ray diffraction (XRD). Collectively, these techniques elucidate the evolution of cell wall changes. We propose that coincident with the particle size reduction of the wood material during the milling process includes tissue disintegration, cell wall fragmentation, disordering of layered cell wall fragment, and aggregation of disordered cell wall fragments. As evidenced by LSCM, the constituent cell wall polymers are redistributed following the ultrastructural disruption from the mechanical milling. XRD results demonstrated the amorphization of the semicrystalline polymers. Micro/nano porous structures were visualized by 3D-TEM tomography. The surface and ultrastructure alternation of cell wall contribute to enhancement of enzymatic digestibility by 4-14 folds over that of untreated cell walls depending on degree of milling pretreatment.

Key words: bioconversion, mechanical milling pretreatment, visualization, cell wall ultrastructure, accessible void

Proceedings of the 58th International Convention of Society of Wood Science and Technology
June 7-12, 2015 – Grand Teton National Park, Jackson, Wyoming, USA

Optimization Study on Yield of CNC Cutting Wood-based Composite Panels for Upholstery Furniture Frames

Arif Caglar Konukcu, ak1047@msstate.edu
Jilei Zhang, jzhang@cfr.msstate.edu

Mississippi State University, Department of Sustainable Bioproducts , 201 Locksley Way, Starkville, MS 39759

Abstract

In today's competitive world, many furniture manufacturers are improving the efficiency of their process, eliminating unnecessary costs, and improving quality by using wood-based composite panels in their frames. Upholstery furniture frames, today, are made by using over 70 percent wood-based composite panels. Material utilization becomes the most important area of improvement. Many furniture manufacturers have realized increased design and production efficiencies using wood-based panel products as their frame stocks together with CNC technology, but they are continuously looking for alternatives for improvement of their bottom line such as cutting yield optimization. In this case study, effects of full panel size of wood-based composites, number of frames cut, and frame part shape and size on the cutting yield of a upholstery company were evaluated using computer simulation software with optimization capacity. Results indicated that the cutting yield is affected by full panel sizes and number of frames cut. Curve-shaped and small size parts can also lower the material cutting yield. The current company cutting yield of 79.80% can be improved up to the range of 80 to 84% through optimization of considering full panel size, number of frames cuts, etc.

Proceedings of the 58th International Convention of Society of Wood Science and Technology
June 7-12, 2015 – Grand Teton National Park, Jackson, Wyoming, USA

Water States in Black Spruce and Aspen during Drying Studied by Time-Domain Magnetic Resonance Devices

Clevan Lamason[1], Bryce MacMillan[2], Bruce Balcom[2], Brigitte Leblon[1], and Zarin Pirouz[3]

[1]Faculty of Forestry and Environmental Management, University of New Brunswick (UNB), NB, CANADA
(clamason@unb.ca)
[2]Magnetic Resonance Imaging Center, Department of Physics, UNB, NB, CANADA
[3]Faculty of Forestry and Environmental Management, UNB, NB, CANADA
[4]Scientist, FPInnovations, Vancouver, CANADA

Abstract

In this study, water content in black spruce (*Picea mariana Mill.*) and aspen (*Populus tremuloides Michx.*) sapwood samples was investigated with time-domain magnetic resonance (MR). Time-domain MR measurements easily distinguish water in different environments in wood according to the spin-spin relaxation time and provide quantitative information on water content. The MR techniques employed can distinguish and quantify the individual signal components. Both black spruce and aspen have two signal components at moisture contents above the fiber saturation point. These two signal components correspond to motionally restricted water, often referred to as bound water, and unrestricted, or free water. Bound water content is constant above 40% moisture content. No signal from free water was detected at or below 20% moisture content in either species. We also demonstrate the use of a recently developed portable unilateral magnet that can be employed as a powerful tool in the study and measurement of water content in wood.

Proceedings of the 58th International Convention of Society of Wood Science and Technology
June 7-12, 2015 – Grand Teton National Park, Jackson, Wyoming, USA

Evaluate Soil Parent Material and Nitrogen Fertilization Impact on Whole Tree Wood Quality of Douglas-fir in the Pacific Northwest

*Luyi Li, Eric C. Turnblom**

School of Environmental and Forest Sciences, College of the Environment, University of Washington, Seattle WA, USA.
**Corresponding author*

Abstract

The influence of two soil parent material types and a nitrogen fertilization treatment (224 kg N ha-1) on Douglas-fir (*Pseudotsuga menziesii* (*Mirb.*) plantation wood quality along the whole tree trunk was studied in western Oregon. Four aspects regarding wood quality were assessed and analyzed, (1) tree sonic acoustic velocity, (2) log resonance acoustic velocity, (3) specific gravity, and (4) latewood percentage. Higher quality wood can be found in the segment from stump to the live crown base. A variety of fertilization effects upon wood quality attributes were detected. A strong correlation ($R^2 = 0.92$) between tree sonic acoustic velocity and log resonance acoustic velocity was observed, and tree sonic acoustic velocity was 8% higher than log resonance acoustic velocity.

Key words: Douglas-fir, wood quality, soil parent material, nondestructive evaluation, specific gravity, latewood percentage

Introduction

Costal Douglas-fir (*Pseudotsuga menziesii (Mirb.) Franco*) is the predominant plantation species native to the western Pacific Northwest. Douglas-fir is widely valued as an important tree species in forest management because of its high volume timber production and the rapid growth rates on established stands. In addition, it is a premium timber resource for structural applications and its appearance is appreciated in both domestic and international markets. Nitrogen is consistently the most limiting factor to the growth of forests in the Pacific Northwest as well as the rest of the world (Hanson and Weltzin 2000, LeBauer and Treseder 2008). Decades of observations in the Pacific Northwest in detecting soil nitrogen and tree growth response to fertilization practices indicate that soil nitrogen tends to be limiting, and is therefore predictive of inherent forest productivity (Littke et al. 2011). Fertilization practices have been developed to

cope with insufficient nitrogen availability and stimulate tree growth (Keeney 1980). Research has shown coastal Douglas-fir will respond to 224 kg N ha-1 applications about 2/3 of the time.

The impacts of site attributes and management on Douglas-fir wood quality are unclear. This study focuses on evaluating the influence of two soil parent material types (SPM) and two fertilization treatment levels on four characteristics of wood quality along the entire tree trunk of middle-aged (23 and 28 years old) Douglas-fir in the Pacific Northwest.

Method

The study sites cover latitudes from 44°29'N to 45°52'N, and longitudes from 122°39'W to 123°17'W. Selected dominant and co-dominant Douglas-fir trees were chosen in 2007 before the growing season (Table 1). The SPM type was determined based on USGS geologic maps (USGS 2010). At the time of site set up, selected trees were measured for diameter at breast height (DBH), total height, and height to the live crown base. Trees with similar DBHs were paired up. Selected trees within a pair were randomly assigned to be treated either with nitrogen fertilization (urea 224 kg ha-1) or to be control trees (i.e. no fertilization). Upon the final measurement nitrogen applications have had enough time to act on wood quality at each site for its effects to be detected and analyzed.

Table 1. Stand attributes at the time of establishment.

Site Location	Soil Parent Material	Breast Height Age (year)	Site Index[+] (m)	Density (tree/ha)
Vernonia	Sedimentary	28	37.18	707.41
Sweet Home	Mixed (Sedimentary and Igneous)	23	43.02	976.64

[+]Site index, determined from King 1996.

For the two sites, 12 trees were measured with Fakopp TreeSonic, the cost-effective nondestructive evaluation instrument (Carter et al. 2005, Chauhan and Walker 2006, Thienel 2008). Three measurements were obtained and averaged to produce the single result of tree sonic acoustic velocity (TSAV). Trees were then felled, and the following segments along the tree trunk were determined: breast height (BH, 1.3 m above ground), height up to 4.88 m (TF16, or top of the first 16 foot log, including trim), the live crown base (LCB), and the top with diameter of 10 cm (TOP). Felled trees were bucked sequentially, stump to TOP, stump to LCB, and stump to the TF16. After each segment was cut, and prior to the next cut, segments were measured for length to the nearest meter and tested using the Director® Hitman-200, resonance acoustic instrument, to obtain log resonance acoustic velocity (LRAV, Carter et al. 2005, Chauhan and Walker 2006). Disks with 5 cm thickness were cut from each felled tree at each predetermined segment (Stump, BH, TF16, and TOP). In total, 56 disks, half from control trees and half from nitrogen fertilized trees, were obtained and transported to the laboratory.

Specific gravity (SG) is one of the single most important physical properties of wood, closely correlated with strength and stiffness, shrinking and swelling (Bowyer et al. 2007, Desch and Dinwoodie 1996, Shmulsky and Jones, 2011). Two woody blocks containing the treatment response period were sampled out of each disk to obtain green mass. Blocks were submerged in water for a certain period to absorb moisture at its maximum capacity; volume was then measured by applying Archimedes' principle. Woody blocks were oven-dried 48 hour at 105 degree Celsius.

Latewood percentage (LWP) is one of the most widely used wood quality characteristics for its ease in detection. Based on growth ring density and color changes, LWP provides a visual index of strength and structural properties and is highly correlated with wood SG (Zobel 1972, Kubo and Jyodo 1996). The tree ring measuring software ProjectJ2X (VoorTech Consulting 2014) and a microscope were used in determining the width of each annual ring component, earlywood and latewood (LW) for sample blocks. LWP was calculated thereafter.

Result and Discussion

Tree Sonic Acoustic Velocity (TSAV) and Log Resonance Acoustic Velocity (LRAV)

For both SPM types, TSAV was detected within the range of 4.09 to 4.13 m/s. Fertilized trees had greater values than unfertilized trees, and this gap between two treatment regimes was 0.04 km/s on the Mixed SPM site, and 0.02 km/s on the Sedimentary SPM (FER > Non.FER). It seems plausible that fertilizing Douglas-fir stands at age 23 and 28 slightly improves wood stiffness (Fig. 1).

Acoustic velocity magnitudes detected with resonance measurements were compared to log segments according to SPM types and nitrogen treatment regimes. As indicated by Figure 2, the highest LRAV was found in the segment of stump to the live crown base; followed closely by the butt log segment, i.e. stump to the top of the first 16 foot (4.88 m) log. Both segments of stump to live crown base and butt log had LRAV in the range of 3.7 - 3.9 km/s. LRAV sensed within the live crown had the lowest value. The overall tree LRAV was between these two extremes, which can be simply explained by reasoning the single log of stump to top contained about 50% live crown on both SPM sites. In Figure 3, the sequence of LRAV measurements was rearranged to look at variations for the same log segment according to SPM types and nitrogen treatment regimes. From the whole tree perspective (stump to top), fertilized Douglas-fir, on average, had higher LRAV than control trees for all segments corroborating TSAV results in Figure 1. LRAV from butt logs had very small changes through SPM types and nitrogen treatments. Fertilized Douglas-fir had a slightly higher LRAV, but it is not significant. As the log segment length increased, from stump to live crown base and stump to the 10 cm top, the contrast brought about by fertilization becomes increasingly obvious. The very top subdivision, abrupt changes from unfertilized to fertilized trees were quite clear with a difference of 0.26 km/s on the Mixed SPM site and 0.50 km/s on the Sedimentary SPM site.

The correlation between standing tree acoustic velocity measure and felled tree log resonance acoustic velocity was one of the principle interests in previous research. Wang (1999) found on red pine that TSAV was strongly correlated with LRAV (R^2=0.88). On average, TSAV was about 10% higher than LRAV (the age of wood was not reported). Mora et al (2009), tested loblolly pine with the age range of 14-19 year in the Southeastern United States using the same tool in this research, reported a good correlation (R^2 = 0.81) and a 32% higher TSAV than LRAV. Similar examinations were performed on radiata pine in New Zealand. Grabianowski et al (2006) found young stands (age 8 and 11) had TSAV 12% higher than LRAV. Chauhan and Walker (2006) used the Fakopp TreeSonic and Hitman and gained a positive correlation (R^2 = 0.75-0.91) between TSAV and LRAV.

To date, there is no publicly available, peer reviewed publication that reports on the correlation between TSAV and LRAV for Douglas-fir. On average, TSAV obtained in the butt log segment was 8.12% greater than the LRAV. A strong correlation (R^2 = 0.92) was identified between TSAV and LRAV for stands aged 23 and 28. Results are consistent with previous studies involving other species.

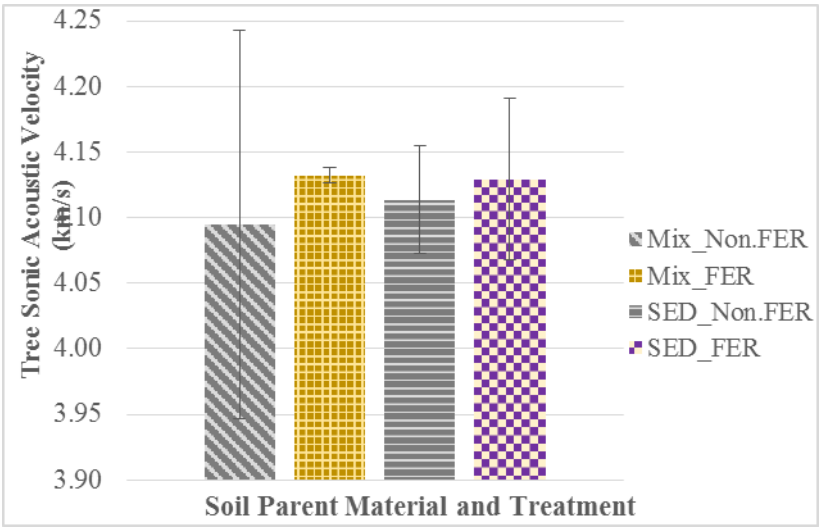

Figure 1. Tree sonic acoustic velocity on the Sedimentary and Mixed (Sedimentary and Igneous) stands, vertical bars represent the standard errors.

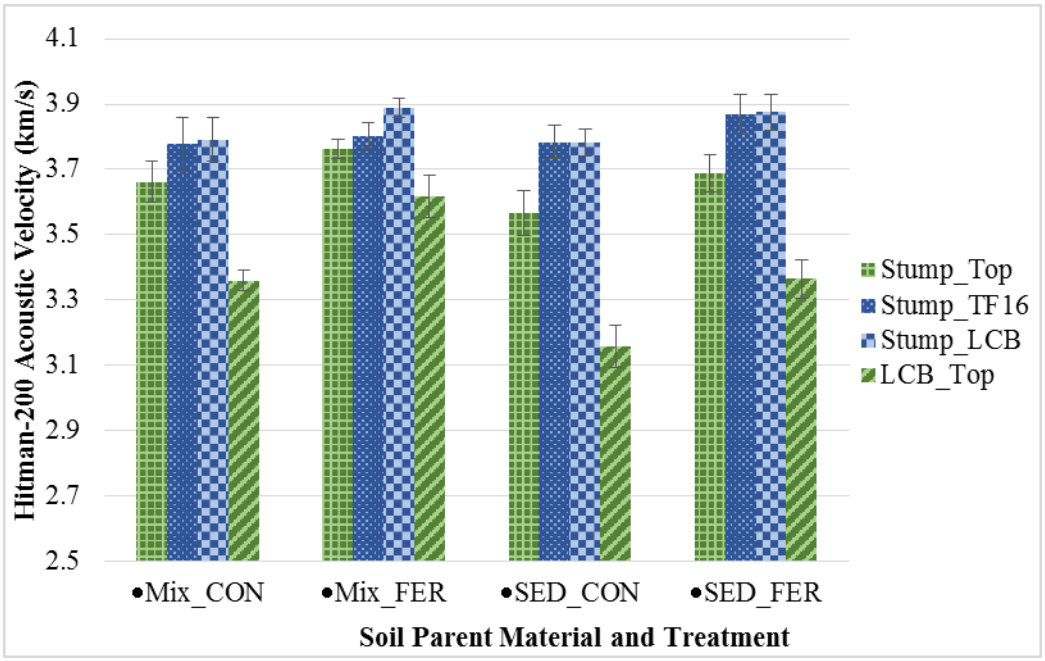

Figure 2. Log resonance acoustic velocity sorted by log position with the combination of soil parent material and fertilization regimes, vertical bars represent the standard errors.

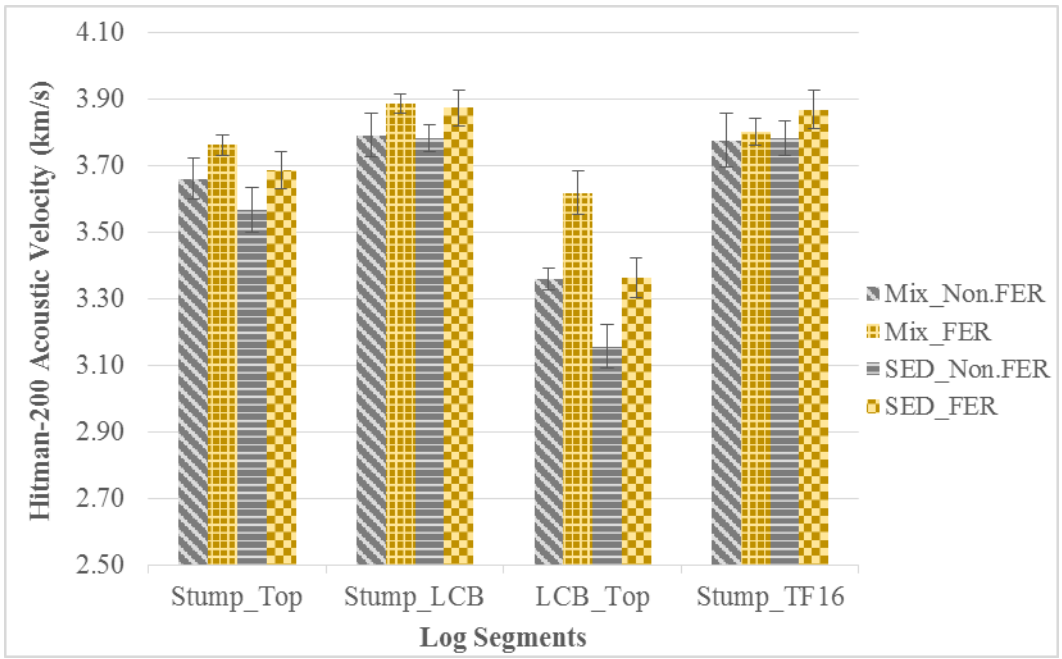

Figure 3. Log resonance acoustic velocity for Soil Parent Material and fertilization treatment combinations according to log position, vertical bars represent the standard errors.

Specific Gravity (SG) and Latewood Percentage (LWP)

Specific gravity, and latewood percentage for the treated period were measured through wood blocks obtained from 56 disks from sample trees.

Figure 4 shows the specific gravity (SG) over the entire tree trunk on the two sites. For the Mixed SPM, unfertilized trees had higher SG than the fertilized trees consistently. Though for the lower, close to the stump section, such differences were not obvious; while at the top of the first 16 foot log and live crown base, control trees maintained higher SG than those that were fertilized. A quite different trend was seen on the Sedimentary site. At lower tree segments, control trees had a slightly higher SG value, but the upper segments of the nitrogen treated group presented greater SGs.

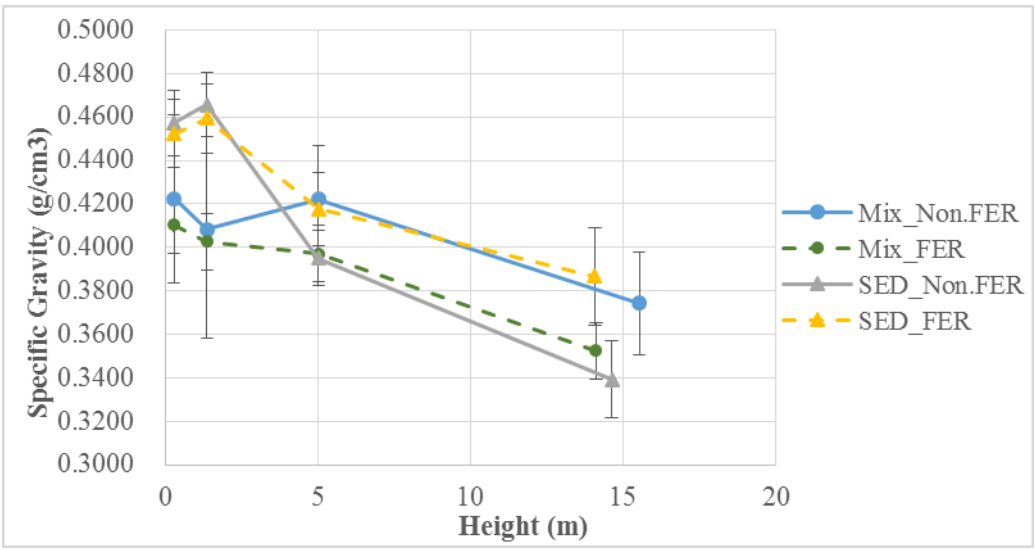

Figure 4. Specific gravity along height as related to Soil Parent Material and fertilization treatment, vertical bars represent the standard errors.

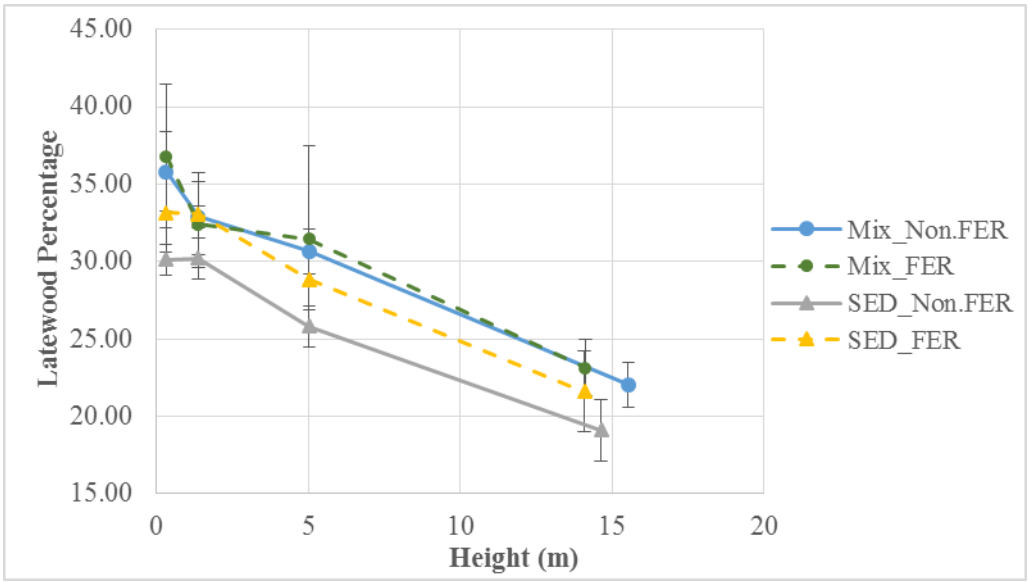

Figure 5. Latewood percentage along height as related to Soil Parent Material and fertilization treatment, vertical bars represent the standard errors.

For latewood percentage, the nitrogen treatment had a positive effect on sampled trees from a whole tree perspective. Almost all segments along the trunk of fertilized trees contained more latewood for the growth ring. The only exception came from the Mixed SPM site at breast height, where control trees had LWP 0.48% higher than the fertilized trees. Besides, fertilized trees on the Sedimentary site benefitted more from the added resource than trees from the Mixed SPM site, as indicated by the gaps between dashed and solid lines in Figure 5.

The fertilization treatment increased the magnitude of TSAV and LRAV, with the higher quality wood in the section from stump to the live crown base. By contrast, live crown segments were sensed having smaller LRAV values, because low stiffness juvenile wood is produced within this area. For the same log segment, in general, the fertilized trees had a 2%-3% increase in LRAV, while moving into the live crown, this value jumped to 8% and 6% for the Mixed SPM and Sedimentary SPM sites. Fertilization had various impacts in SG along the tree trunk, and there were conflicting results from the two sites. Trees on Sedimentary SPM site benefited from nitrogen application with improved SG. But woody blocks sawn from fertilized trees exhibited decreased SG at the Mixed SPM site. Such a difference was not great in the lower tree trunk.

Conclusion

Different SPM types had various inherent abilities to support Douglas-fir plantation. They also differently interacted with nitrogen treatment in reshaping wood quality of growing Douglas-fir. From a whole tree standpoint, fertilization increased planted Douglas-fir LWP, but only positively enhanced SG in the upper segments of trees on Sedimentary SPM site. In general, higher quality wood can be found in the segment from stump to the live crown base; the live crown region had the lowest quality in every assessed aspect. A strong correlation ($R^2 = 0.92$) between TSAV and LRAV indicated that 92% of destructive resonance based measurement can be explained by nondestructive evaluation with acoustic tree sonic method. Last, TSAV was generally 8% higher than LRAV.

Site and environmental variables were not regulated nor targeted in this research. Additional research is desirable using a greater replication of study sites with other factors (such as stand age, elevation, site index, etc.) to better understand their impact.

References

Bowyer JL, Schmulsky R, Haygreen JG (2007) Forest Product and Wood Science 5th ED. Blackwell Publishing. 558p.

Carter P, Briggs D, Ross RJ, Wang X (2005) Acoustic testing to enhance western forest values and meet customer wood quality needs. PNW-GTR-642. IN: Harrington, C.A., Schoenholtz, S.H. (eds.). Productivity of western forests: A forest products focus. USDA Forest Service, Pacific Northwest Research Station, Portland, pp 121-129.

Chauhan SS, Walker JCF (2006) Variation in acoustic velocity and density with age, and their interrelationships in radiata pine. Forest Ecology and Management. 229: 388-394.
Desch HE, Dinwoodie JM (1996) Timber: structure, properties, conversion and use. 7th ED. Macmillan Press LTD., London. 306p.

Grabianowski M, Manley B, Walker JCF (2006) Acoustic measurements on standing trees, logs and green lumber. Wood Science and Technology. 40: 205-216.

Hanson PJ, Weltzin JF (2000) Drought disturbance from climate change: response of United States forests. The Science of the Total Environment. 262 (2000) 205-220.

Keeney DR (1980) Prediction of soil nitrogen availability in forest ecosystems: a literature review. Forest Science. 26: 159-171.

King JE (1966) Site index curves for Douglas-fir in the Pacific Northwest. Weyerhaeuser Forestry Paper, No. 8, Weyerhaeuser Co., Forestry Research Center, Centralia, WA.

Kubo T, Jyodo S (1996) Characteristics of the annual ring structure related to wood density variation in sugi (Cryptomerica japonica). Mokuzai Gakkaishi, 42: 1156-1162.

LeBauer DS, Treseder KK (2008) Nitrogen limitation of net primary productivity in terrestrial ecosystems is globally distributed. Ecology. 89: 371-379.
Littke KM, Harrison RB, Briggs DG, Grider AR (2011) Understanding soil nutrients and characteristics in the Pacific Northwest through parent material origin and soil nutrient regimes. Canadian Journal of Forest Research. Vol.41: 2001-2008.

Mora CR, Schimleck LR, Isik F, Mahon JM Jr, Clark III, A, Daniels RF (2009) Relationships between acoustic variables and different measures of stiffness in standing Pinus taeda trees. Canadian Journal of Forest Research 39: 1421-1429.

Shmulsky R, Jones PD (2011) Forest Products and Wood Science. 6th ED. 576p.

Thienel GAC (2008) Nondestructive evaluation of wood quality in standing Douglas-fir trees in western Washington and western Oregon. Master thesis. College of Forest Resources, University of Washington, Seattle, WA.

The National Geological Map Database. 2010. U.S. Geological Survey: http://ngmdb.usgs.gov/ngmdb/ngmdb_home.html

Wang X (1999) Stress wave-based nondestructive evaluation (NDE) methods for wood quality of standing trees. Doctor dissertation. School of Forest Resources and Environmental Science, Michigan Technological University, Houghton, MI.

Zobel BJ (1972) Three rings-per-inch dense southern pine-can it be developed. Journal of Forestry. 70: 333-335.

Acknowledgement

The authors would like to thank Bob Gonyea, Bert Hasselberg, Randy Collier, Kim Littke, Monica Seeley and Armin Farahmandnia for their great assistance. Special thanks to the Stand Management Cooperative, Center for Intensive Planted-forest Silviculture, and USDA Forest Service PNW Research Station for resource support.

Proceedings of the 58th International Convention of Society of Wood Science and Technology
June 7-12, 2015 – Grand Teton National Park, Jackson, Wyoming, USA

Multi-scale Investigation of Adhesive Bond Durability

Paige McKinley, paige.mckinley@oregonstate.edu

Oregon State University, 119 Richardson Hall , Wood Science and Engineering, Corvallis, OR 97331

Abstract

Moisture durability is essential for wood composite products, especially those used in building construction, where products are prone to weathering. The main focus of this research is to determine if adhesive penetration into the cell wall has a positive influence on bond durability. This study uses bonded Douglas-fir test specimens (6mmx14 mmx64 mm), varying in bonded surface cell type (earlywood vs. latewood), bonded surface orientation (longitudinal vs. tangential), and adhesive type. The adhesives of interest are a low and high molecular weight phenol-formaldehyde, along with a pre-polymeric diphenylmethane diiscoyanate. Half of each type of test specimen undergoes accelerated weathering and the rest remain dry. All samples are mechanically tested in lap shear. The maximum load is recorded along with the stress and strain around the bondline, using Digital Image Correlation (DIC). Smaller samples (2mmx2mmx10mm) are cut from the same previously tested samples and then scanned at the Advanced Photon Source using micro X-ray Computed Tomography (XCT). All adhesive types were previously tagged with iodine to increase contrast during scans. This technique gives high resolution (1.3μm^2/voxel), 3D images for which cell wall penetration can be analyzed at both the micrometer and nanometer scale. The mechanical test results, DIC results, and XCT images of the weathered vs. dry samples will be compared and used to quantitatively measure the effects of moisture on the bondline.

Proceedings of the 58th International Convention of Society of Wood Science and Technology
June 7-12, 2015 – Grand Teton National Park, Jackson, Wyoming, USA

Dimensional Optimization of Beetle Kill Pine Interlocking Cross Laminated Timber (ICLT).

Massih Nilforoushan Hamedani, m.nilforoushan@utah.edu
Ryan Smith, rsmith@arch.utah.edu
Ben Hagenhofer-Daniell, ben.hagenhofer.daniell@utah.edu

University of Utah, 375 S. 1530 E. RM 236 , Salt Lake City, UT 84112

Abstract

Moisture content is a critical factor for dimensional stability in engineered wood products. This paper focuses on one such product: Interlocking Cross Laminated Timber fabricated with beetle killed pine from the intermountain west. This research engages in supply chain mapping, and the co-relational assessment of drying techniques that can lower moisture content to a consistent level for dimensional stability and performance of the product. The research will ultimately suggest a drying regime in-line with existing supply chains that is optimized for economy, schedule, and repeatability. While the focus is on a regionally specific timber resource and engineered timber product, the lessons learned should be applicable to engineered solid timber products generally. This research will also establish a framework for evaluating the management of moisture content in timber resources beyond beetle killed pine. In order to assess the drying phases in current supply chains, different intermountain supply chain strategies have been studied based on information from local sawmills and logging companies. Different approaches to dry solid timber products based on determined supply chains have been evaluated to develop efficient supply chain options to increase the opportunities for further commercialization of ICLT and other solid timber products in the USA.

Proceedings of the 58th International Convention of Society of Wood Science and Technology
June 7-12, 2015 – Grand Teton National Park, Jackson, Wyoming, USA

Effects of Cement Strength Grade and Particle Content on the Compressive Strength of Bamboo-Cement Composites

Olayiwola H.O[1], Adesope A.S[2], Adefisan O.O[3]*

[1]Postgrad, Department of Agricultural and Environmental Engineering, Wood Products Engineering Unit, University of Ibadan, Nigeria
[*]*Corresponding author:*
olafiku@yahoo.com
[2]Research Officer, Forestry Research Institute of Nigeria, Forest Product Development and Utilization Unit
[3]Senior Lecturer, Department of Agricultural and Environmental Engineering, Wood Products Engineering Unit, University of Ibadan, Nigeria

Abstract

Escalating cost of conventional building materials and rapid population growth has led to acute shortage of housing units in developing nations; hence, the need for alternative low-cost and durable building materials. This study determined the influence of cement grade, particle content and chemical additive on the compressive strength of bamboo-cement composites.

Laboratory type 35mm-thick (cube) cement-bonded composites were made from particles derived from bamboo (*Bambusa vulgaris*). The proportion of cement, sand, stone-dust was done by weight in a nominal mix of 1:2:4. The particle content was substituted based on sand proportion. Two levels of the production variables were employed in the production. These are chemical additive (0% and 3%), particle content (10% and 20%), particle size (850µm and 1.18mm) and cement strength grade (32,5R and 42,5R).

Composites encapsulated with 42,5R cement had better strength from 1.16 to 3.02 N/mm^2 and 1.65 to 4.76 N/mm^2 at 0% and 3% chemical additive respectively. There was an inverse relationship between the particle content and compressive strength for both cement types and particle sizes.

The results indicated that composites produced with cement grade 42,5R at 3%$CaCl_2$, 10% particle content and 1.18mm particle size have higher compressive strength than those produced with cement grade 35,5R.

Keywords; Low-cost building material, bamboo-cement composites, cement grade, particle content and compressive strength

Proceedings of the 58th International Convention of Society of Wood Science and Technology
June 7-12, 2015 – Grand Teton National Park, Jackson, Wyoming, USA

Moisture Stability of Post-manufacture Thermally Modified Welded Birch (Betula pendula L.) Wood

Jussi Ruponen, jussi.ruponen@aalto.fi

Aalto University, Tekniikantie 3, Vuorimiehentie 1, Espoo FI-00076

Abstract

Welding of wood provides strong wood-to-wood bonding without adhesives. However, the bonds suffer from delamination when exposed to moist conditions. Therefore, this work studies if the delamination tendency of linear-friction welded wood bonds in birch (Betula pendula L.) could be reduced by post-manufacture thermal modification. According to the hypotheses, firstly, the bond line in birch wood has unsatisfactory water resistance and poor bond strength in moist conditions. Secondly, water resistance, or wet strength, could be maintained above certain level through thermal modification, yet below the level of non-modified welded wood, when immersed in water. The work included linear-friction welding of birch, thermal modification (at 200°C for 3 h and 5 h) under superheated steam in atmospheric pressure, determination of anti-swelling efficiency (ASE), internal bond (IB) strength testing, and water immersion to observe delamination behavior. Thermal modification improved the dimensional stability, resulting ASE values ranging from 25.9% to 38.0%. The IB strength in dry condition decreased as the thermal modification, yet yielding a value closer to wet. During water immersion, the non-modified specimens suffered from delamination more compared to thermally modified. Results indicate thermal modification could be applied to stabilize the welded bond lines, but the process needs optimization, for instance, to insure scalability and to minimize the loss in strength properties.

Proceedings of the 58th International Convention of Society of Wood Science and Technology
June 7-12, 2015 – Grand Teton National Park, Jackson, Wyoming, USA

Effect of Cross-Laminated Timber Floor Diaphragm Orientation on Shear Stiffness and Strength

Kyle Sullivan

CCE School and WSE Department, Oregon State University

Abstract

Cross-laminated timber (CLT) brings the forest industry to new heights with its ability to build taller wooden structures. Wood buildings in the US have typically and historically been light-frame wood construction under five stories. CLT provides the structural strengths and stiffnesses to potentially replace steel and reinforced concrete in more environmentally sustainable structural systems for mid-rise and possibly high-rise buildings. The "Toward Taller Wood Buildings" national symposium (November, 2014, Chicago, IL) brought together a group of leaders, firms, and organizations that are already deeply involved with the development of CLT in the US.

Two researchers who attended the symposium had a significant impact on the proposed direction of the research. Doug Rammer, Research General Engineer at the US Forest Service, and John van de Lindt, Professor at Colorado State University, both feel strongly that looking at how CLT floor diaphragms transfer lateral loads would lead to design provisions in the National Design Specification for Wood Construction and the IBC. CLT floor diaphragms experience lateral loading along both their strong and weak axes depending on the direction of earthquake ground motions or wind loadings and on the orientation of the panels. We will determine how lateral loads parallel to either axes are transferred through the diaphragm due to different strengths and stiffnesses in the two directions. The goal is also to develop preliminary estimates of design values for shear strength and stiffness based on ASTM E455, so that structural engineers will be able to confidently use CLT in lateral-force-resisting systems.

Proceedings of the 58th International Convention of Society of Wood Science and Technology
June 7-12, 2015 – Grand Teton National Park, Jackson, Wyoming, USA

Trends in U.S Furniture Trade

Cagatay Tasdemir, ctasdemi@purdue.edu
Rado Gazo, gazo@purdue.edu

Purdue University, 2491 Sycamore Ln., Apt 6, West Lafayette, IN 47906

Abstract

The US and global economy has experienced both a downturn and a recovery over the last decade. The objective of this study is to analyze trends in imports and exports of furniture in the US over this period of time. We evaluate top ten furniture exporting countries in terms of value and principal products. Main competitive strategies of countries exporting furniture to the U.S. are identified and briefly explained within the scope of this study by observing the changes in the values of last five years data. Taiwan was one of the most important furniture exporters to the US until 1994, when the country started to lose its power in the market due to the technological improvements made in other Asian countries. Decreasing trend of Taiwan export values continued in last ten years while Vietnam increased its share of the U.S. furniture market. Since 2004, China was the most important source of imported wood furniture and accounts for over 48.5% of total imports volume.

Overall, low-cost structure, government support and advanced technologies in Asia have provided the Asian countries with competitive advantage over their European and American competitors. Hence, lower price of imported products has been the main influential and decisive factor for furniture consumers in U.S. and set the benchmark for manufacturers in terms of competitive advantages

Proceedings of the 58th International Convention of Society of Wood Science and Technology
June 7-12, 2015 – Grand Teton National Park, Jackson, Wyoming, USA

Manufacturing and Mechanical Characterization of a 3D Molded Core Strand Panel

Daniel Way

Oregon State University, Corvallis, OR

Abstract

Three dimensionally (3D) molded core panels consist of two components: A core that is molded in a repeating structure that contains hollow areas and skins which make up the outer portion of the panel. These panels have been of interest to the wood composites community because of their ability to utilize low value materials, but have yet to enter the building construction materials market due to challenges in meeting necessary mechanical requirements for structural use.

The design of 3D molded core panels is unique compared to commercially available wood composite panels in that they behave more like a beam with the core acting as a load transfer mechanism between the high strength skins. Air space in the hollow core provides additional insulation but can also be designed to allow passage of hot air from attic spaces. Air space also lowers the thickness to weight ratio meaning that panels of greater depth may be produced without hindering jobsite handling. Unlike their solid composite panel counterparts, the two part core and skin system generally results in non-catastrophic failures.

This study investigates the use of wood strands for forming a molded core on the premise that wood strands typically have favorable mechanical properties opposed to their fiber and particle counterparts. Cores were molded using furnish typical of oriented strand board (OSB) and a proprietary core mold supplied by our industrial partner and commercially available OSB as skin material. Panels were tested for key mechanical properties to determine their adequacy for use as a structural sheathing material.

Keywords: 3D molded core panel, strand composites, structural sheathing, sandwich panels

Proceedings of the 58th International Convention of Society of Wood Science and Technology
June 7-12, 2015 – Grand Teton National Park, Jackson, Wyoming, USA

Self-Activation Process for Biomass Based Activated Carbon

Changlei Xia [1] *– Sheldon Q. Shi* [2]*

[1] PhD Candidate, Department of Mechanical and Energy Engineering, University of North Texas, Denton, TX 76203, USA.
Changlei.Xia@unt.edu

[2] Associate Professor, Department of Mechanical and Energy Engineering, University of North Texas, Denton, TX 76203, USA.
* *Corresponding Author*
Sheldon.Shi@unt.edu

Abstract

Self-activation takes the advantages of the gases emitted from the pyrolysis process of biomass to activate the converted carbon, so that a high performance activated carbon is obtained. Different biomass types were used for the self-activation processes into activated carbon, including kenaf bast fiber, kenaf core, sugarcane bagasse, sugarcane leaf, coconut fiber, peanut shell, and sawdust. A linear relationship was shown between the BET surface area (SA_{BET}) and the yield ($\ln(SA_{BET})$ and yield) for the self-activation process. The study also showed that a yield of 9.0% gave the highest surface area by gram kenaf core (115.3 m^2 per gram kenaf core), and the yields between 5.5%-13.8% produced a surface area per gram kenaf core that higher than 90% of the maximum.

Keywords: Self-activation, activated carbon, biomass, kenaf core

Proceedings of the 58th International Convention of Society of Wood Science and Technology
June 7-12, 2015 – Grand Teton National Park, Jackson, Wyoming, USA

Hybrid Cellulose-Copper Nanoparticles Embedded in Polyvinyl Alcohol for Antimicrobial Applications

Tuhua Zhong[1] *- Gloria S. Oporto*[2*] *- Jacek Jaczynski*[3] *- Changle Jiang*[1]

[1] PhD student, Division of Forestry and Natural Resources,
West Virginia University, Morgantown, WV 26506.

[2] Assistant Professor, Division of Forestry and Natural Resources,
West Virginia University, Morgantown, WV 26506.
* *Corresponding author*
Gloria.oporto@mail.wvu.edu

[3] Associate Professor, Division of Animal and Nutritional Sciences,
West Virginia University, Morgantown, WV 26506.

Abstract. Copper nanoparticles on TEMPO nanofibrillated cellulose (TNFC) and on carboxymethyl cellulose (CMC) templates were successfully synthesized. Polyvinyl alcohol (PVA) films embedded with the resulting hybrids of cellulose-copper nanoparticles were prepared by solvent casting method. Antimicrobial testing demonstrated that both PVA composite films have excellent antimicrobial properties against *E.coli* DH 5α. Approximately 90% less cellulosic material was required when using TNFC as template compared to CMC template to get similar films antimicrobial performance. The maximum thermal decomposition temperature of the films increased 18℃ and 25℃, when TNFC-copper nanoparticles and CMC-copper nanoparticles were incorporated into the films. Likely, compared to pure PVA, the storage modulus at 48℃ resulted enhanced up to 164% and 217% after the incorporation of the hybrid materials. The results shows that both hybrid cellulose-copper nanoparticles materials have potentiality to be used as advanced antimicrobial and reinforcing materials for thermoplastic composite applications.

Keywords: TEMPO nanofibrillated cellulose, Carboxymethyl cellulose, Polyvinyl alcohol, copper nanoparticles, antimicrobial properties, reinforcement material.

Proceedings of the 58th International Convention of Society of Wood Science and Technology
June 7-12, 2015 – Grand Teton National Park, Jackson, Wyoming, USA

Nano to Macro Scale Wooden Composites Session
Moderator: *Levente Dénes, University of West Hungary, Hungary*

Grafted A-Cellulose - Poly(3-Hydroxybutyrate-Co-3-Hydroxyvalerate) Biocomposites

Armando McDonald, armandm@uidaho.edu
Wei Liqing, wei3095@vandals.uidaho.edu

University of Idaho, 875 Perimeter Drive , MSC1132, Moscow, ID 83844

Abstract

In this study, a green biocomposite from the bacterial bioplastic, poly(3-hydroxybutyrate-co-3-hydroxyvalerate) (PHBV), and α-cellulose fibers was prepared. The α-cellulose fibers were isolated from at-risk intermountain lodgepole pine wood by successive removing of extractives, lignin and hemicellulose. Grafting of PHBV onto cellulose was carried out by reactive extrusion using dicumyl peroxide free radical initiation at 175°C. The biocomposites were characterized by scanning electron microscopy (SEM) and dynamic mechanical analysis (DMA) and showed good interfacial bonding and compatibility between the two phases. The crystallinity of PHBV and cellulose in the biocomposite were reduced as determined by X-ray diffraction (XRD), differential scanning calorimetry (DSC) and Fourier transform infrared spectroscopy (FTIR) analyses. The mechanical properties of the biocomposites were improved by cross-linking due to better stress transfer between the two interphases as compared to the blend control composite without adding peroxide. This inline process offers an effective approach to improve biocomposite materials by reactive extrusion.

Proceedings of the 58th International Convention of Society of Wood Science and Technology
June 7-12, 2015 – Grand Teton National Park, Jackson, Wyoming, USA

Effect of TEMPO Nanofibrillated Cellulose Content on Copper Release from Antimicrobial Polyvinyl Alcohol Films

Changle Jiang [1] – Gloria S. Oporto[2] – Tuhua Zhong[1] – Jacek Jaczynski[3]*

[1] PhD student, Division of Forestry and Natural Resources,
West Virginia University, Morgantown WV, USA
[2] Assistant Professor, Division of Forestry and Natural Resources,
West Virginia University, Morgantown WV, USA
* *Corresponding author*
gloria.oporto@mail.wvu.edu
[3] Associate Professor, Division of Animal and Nutrition Science,
West Virginia University, Morgantown WV, USA

Abstract

The long-term goal of our research is to develop a novel antimicrobial film with controlled release of the active agent. In this work, copper nanoparticles (CuNPs) were synthesized on TEMPO nanofibrillated cellulose (TNFC) using a chemical reduction method. Polyvinyl alcohol (PVA) composite films were prepared by incorporating this TNFC-CuNPs hybrid material into the PVA matrices using a solvent casting process. Copper release from the final films was determined using Inductively Coupled Plasma Optical Emission Spectroscopy (ICP-OES). The final PVA/TNFC-CuNPs films with different TNFC concentration were investigated for copper release rate. The antimicrobial properties of PVA/TNFC-CuNPs film was conducted against nonpathogenic *Escherichia coli* (*E. coli*). The copper release measurement show that the release rate drops when TNFC concentration increases.

Keywords: TEMPO nanofibrillated cellulose, copper nanoparticles, copper release, antimicrobial films.

Introduction

Copper is considered a broad spectrum antimicrobial agent capable of inhibiting bacteria (Jia et al 2012; Ruparelia et al 2008) and fungi (Cioffi et al 2005). Currently, there is a growing interest to synthesize copper nanoparticles (CuNPs) due to their higher specific area and improved antimicrobial performance (Usman et al 2013; Palza 2015). Although, there are many ways to get nanoscale copper, synthesizing it on a biopolymer became

more and more attractive because it is expected to distribute the metal nanoparticles in an evener way (Qi et al 2004; Cai et al 2009).

Cellulose is the most abundant biopolymer on earth (Klemm et al 2005). Chemically modified cellulose fiber has been successfully demonstrated being a stabilizer for copper nanoparticles and improve the distribution of copper nanoparticles in a colloidal copper solution (Zhong et al 2013). In present work, CuNPs were prepared using TNFC as template, resulting a hybrid material TNFC-CuNPs. Copper release has been investigated upon forming polyvinyl alcohol (PVA) films which contain this hybrid material. Hybrid material TNFC-CuNPs with different TNFC concentrations were prepared before adding them to the PVA matrices. In addition, antimicrobial tests were performed in order to evaluate the film antimicrobial activity.

Materials and Method

Materials

TEMPO nanofibrillated cellulose (TNFC) (0.96 wt.%) from the Forest Product Laboratory, Madison. Technical-crystal Cupric sulfate pentahydrate ($CuSO_4 \cdot 5H_2O$) from fisher Scientific, USA; Sodium borohydride ($NaBH_4$) (0.5 M) from Acros Organics, USA. Polyvinyl alcohol (PVA) (99-100% hydrolyzed, approx. M.W. 86000) from Acros Organics, USA. Copper nanoparticles (Cu 99.9%, 40nm, metal basis) from US Research Nanomaterials Incorporation.

Preparation of TNFC-CuNPs hybrid material and PVA/TNFC-CuNPs film

The TNFC-CuNPs were prepared using a slight modification to the chemical reduction procedure presented by Zhong et al. (2013). PVA/TNFC-CuNPs films were prepared by the solvent casting method. The formulations evaluated are presented in Table 1.

Table 18. Formulation of PVA/TNFC-Cu films

Sample	TNFC ratio in TNFC-Cu (wt %)	Cu content in PVA/TNFC-Cu film (wt/wt)
PVA/TNFC-CuNPs0	0	0.7%
PVA/TNFC-CuNPs1	50	0.7%
PVA/TNFC-CuNPs2	60	0.7%
PVA/TNFC-CuNPs3	65	0.7%
PVA/TNFC-CuNPs4	70	0.7%
PVA/TNFC-CuNPs5	80	0.7%

Measurement of copper release

Square films with size of 2cm×2cm were cut from prepared PVA/TNFC-Cu films. These film were directly immersed into 10 ml deionized water in a sample bottle. The immersed films were digested in 1 ml nitric acid until the solution is clear. This digesting solution

was diluted by deionized water in 100 ml volumetric flask. 10 ml of this solution were tested in order to get the remaining copper content in the film. Copper release was characterized by Inductively Coupled Plasma Optical Emission Spectroscopy (ICP-OES). The copper release rate was calculated using the formula $\alpha=C_1/(C_1+C_2)$, where α is the copper release rate; C_1 is the copper content released into media; C_2 is the copper content still in the film. Three duplications were conducted regarding to each PVA composite film.

Antimicrobial Test

The *E.coli* DH5α (Invitrogen Inc., Carlsbad, CA) culture, with appropriately 108 colony forming units per milliliter (CFU/mL), was used as target microorganism to characterize antimicrobial activities of PVA/TNFC-Cu film. A 2-mL aliquot of such culture was transferred to a surface of PVA/TNFC-Cu film and incubated at room temperature for 1 week. The dilution and enumeration producers developed by (AOAC 1995, method 991.14; Black et al 2006; Levanduski et al2008) were followed to enumerate the *E.coli.* All bacterial enumerations were performed in triplicate. Mean values are reported as CFU/mL.

Results and Discussion

Effect of different TNFC concentration on copper release

PVA films containing TNFC-CuNPs with TNFC content of 50 wt.%, 60 wt.%, 70 wt.% and 80 wt.% were studied. Copper release rate of these films were determined upon 5 days releasing. As displayed in Figure 1, the copper release rate reduced from 0.08 to around 0.03 when TNFC content increased from 50 wt.% to 80 wt.%. In order to study the effect of TNFC on copper release from PVA film, PVA film only containing copper nanoparticles were prepared and compared with PVA film containing TNFC-CuNPs with 65% TNFC. As shown in Figure 2, TNFC film shows 49.7% reduction of total copper release rate when comparing to non-TNFC after 2 days immersion in deionized water, 44.8% after 4 days and 45.1% after 6 days. The average reduction of copper release rate after applying TNFC is 46.5%.

The results indicate that TNFC stabilized CuNPs can effectively control the copper release from PVA film. In addition, this effect can last over time. Since the total amount of copper in both films are the same, it can be inferred that TNFC can give longer period of effective copper release. Obviously, TNFC shows a delaying effect on copper release. This is due to that Cu was fixed onto TNFC chains. After the film contacting water, water penetrates into film. Cu were attracted by water and dissociated with TNFC chains and then transported to the media by water molecules. This process increased the difficulty of copper dispersion from film to water.

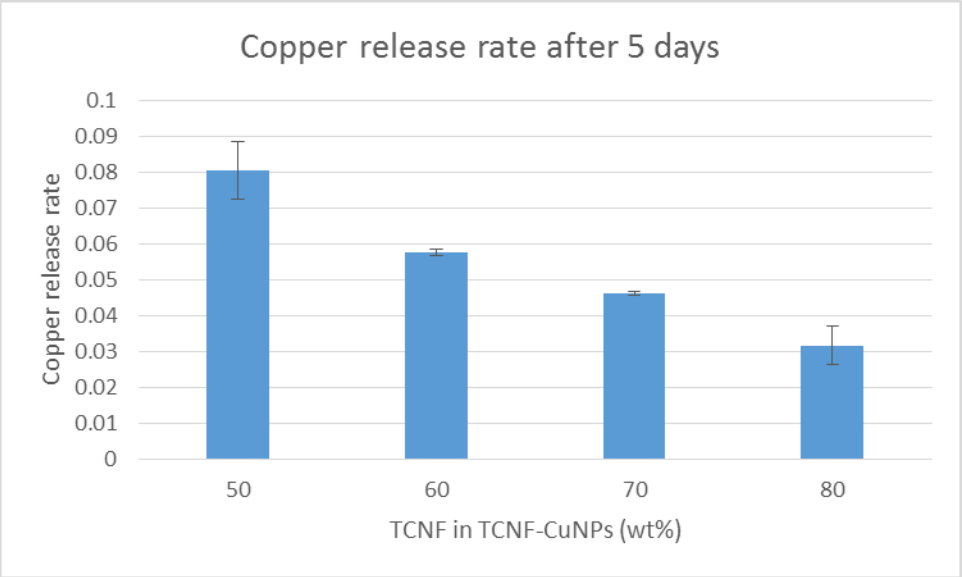

Figure 1. Copper release rate of different TNFC concentration after 5 days

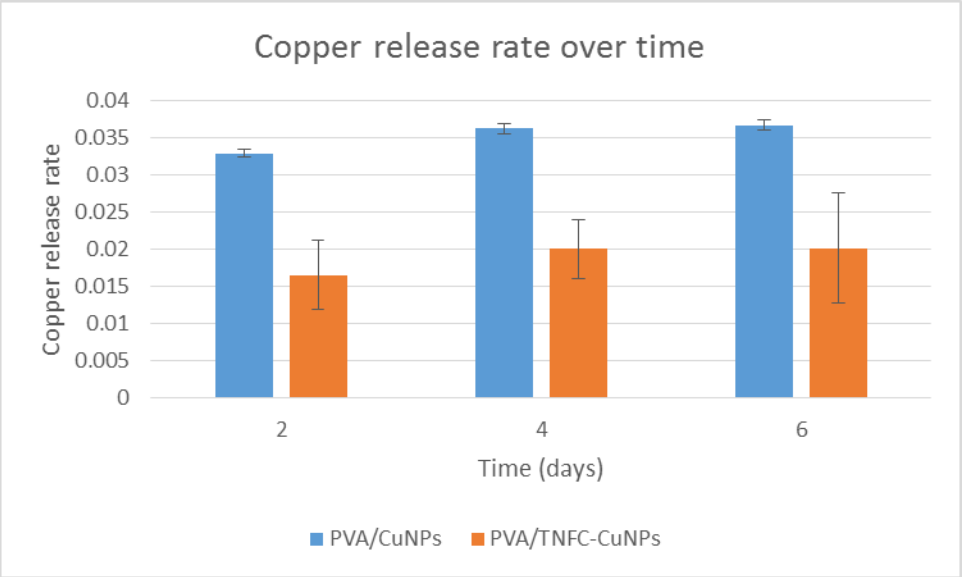

Figure 2. Time profile of copper release rate of PVA/CuNPs film and PVA/TNFC-CuNPs film

Antimicrobial property of PVA/TNFC-CuNPs film

Figure 3 displays bacterial enumeration of the 24-h *E.coli* culture which has exposed 7 days to (a) pristine PVA film and (b) PVA/TNFC-CuNPs film containing 0.7 wt.% copper. Figure 3a has adopted 10^7 times serial dilution, while the Figure 3b has adopted 10^2 times serial dilution. In Figure 3a, 5 colonies were observed on the count plate after 7 days exposure, which means the concentration of *E. coli* is 5×10^7 CFU/ml in original culture. Figure 3b displays non-detectable which means no colony of *E. coli* has been

observed in this situation. It indicates that at least 5-log microbial reduction has been obtained.

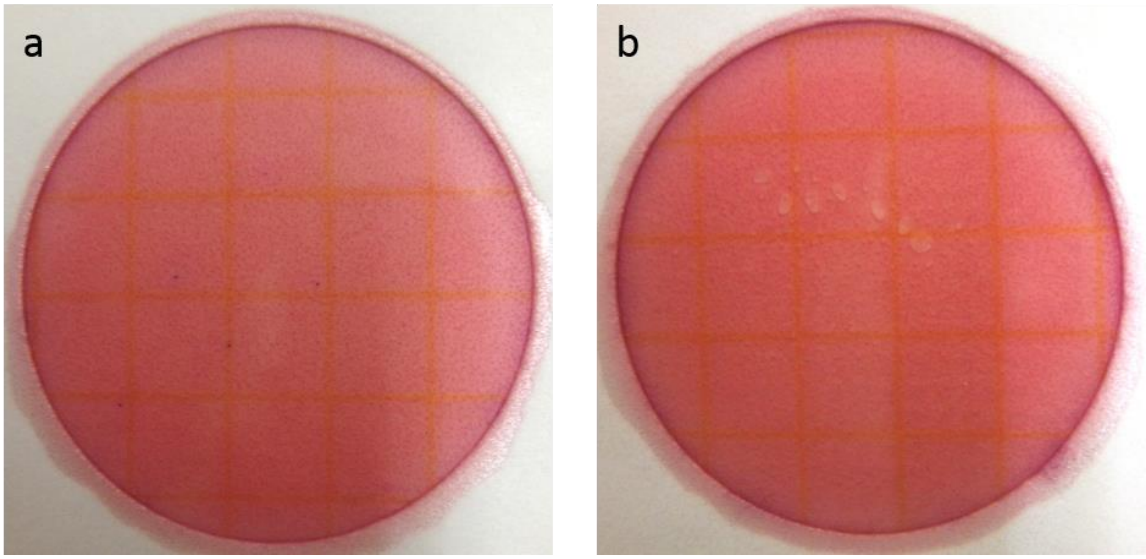

Figure 3. Antimicrobial results of *E.coli* in broth exposed 7 days to (a) pristine PVA film and (b) PVA/TNFC-CuNPs film containing 0.7% Cu.

Conclusion

- TEMPO nanofibrillated cellulose (TNFC) can be effectively used as a bio-based template for the synthesis of copper nanoparticles (CuNPs).
- TNFC can control the copper release rate from PVA films. The copper release rate reduced from 0.08 to around 0.03 when TNFC content increased from 50 wt.% to 80 wt.%.
- TNFC-CuNPs demonstrated effective performance against nonpathogenic *E. coli* when embedded in PVA films.
- TNFC-CuNPs is a promising material for controlled delivery of copper agent for antimicrobial applications.

References

AOAC (1995). Official methods of analysis. 16th ed. Association of Official Analytical Chemists International, Gaithersburg, MD.

Black JL, Jaczynski J (2006) Temperature effect on inactivation kinetics of Escherichia coli O157: H7 by electron beam in ground beef, chicken breast meat, and trout fillets. J Food Sci 71(6): M221-M227.

Levanduski L, Jaczynski J (2008) Increased resistance of Escherichia coli O157: H7 to electron beam following repetitive irradiation at sub-lethal doses. Int J Food Microbiol 121(3): 328-334.

Cioffi N, Torsi L, Ditaranto N, Tantillo G, Ghibelli L, Sabbatini L, Bleve-Zacheo T, D'Alessio M, Zambonin PG, Traversa E (2005) Copper nanoparticle/polymer composites with antifungal and bacteriostatic properties. Chem Mater 17 (21): 5255–5262

Cai J, Kimura S, Wada M, Kuga S (2009) Nanoporous cellulose as metal nanoparticles support. Biomacromolecules 10 (1): 87–94

Palza H (2015) Antimicrobial Polymers with Metal Nanoparticles. Int. J Mol Sci 16: 2099-2116

Isogai A, Saito T, Fukuzumi H (2011) TEMPO-oxidized cellulose nanofibers. Nanoscale 3: 71-85

Jia B, Mei Y, Cheng L, Zhou J, Zhang L (2012) Preparation of copper nanoparticles coated cellulose films with antibacterial properties through one-step reduction. ACS Appl Mater Inter 4 (6): 2897–2902

Klemm D, Heublein B, Fink HP, Bohn A (2005) Cellulose: fascinating biopolymer and sustainable raw material. Angew Chem Int Ed 44: 3358 – 3393

Qi L, Xu Z, Jiang X, Hu C and Zou X (2004) Preparation and antibacterial activity of chitosan nanoparticles. Carbohydr Polym 339 (16): 2693–2700

Ruparelia JP, Chatterjee AK, Duttagupta SP, Mukherji S (2008) Strain specificity in antimicrobial activity of silver and copper nanoparticles. Acta Biomater 4 (3): 707–716

Usman MS, Zowalaty MEE, Shameli K, Zainuddin N, Salama M, Ibrahim NA (2013) Synthesis, characterization, and antimicrobial properties of copper nanoparticles. Int J Nanomed 8: 4467–4479

Wang MS, Jiang F, Hsieh YL and Nitin N (2014) Nanofibrillated celluloseimprove dispersibility and stability of silver nanoparticles and induce production of bacterial extracellular polysaccharides. J. Mater Chem B 2: 6226-6235

Zhong T, Oporto GS, Jaczynski J, Tesfai AT, Armstrong J (2013) Antimicrobial properties of the hybrid copper nanoparticles-carboxymethyl cellulose. Wood Fiber Sci 45(2): 215-222

Proceedings of the 58th International Convention of Society of Wood Science and Technology
June 7-12, 2015 – Grand Teton National Park, Jackson, Wyoming, USA

Hierarchical PLA Structures Used for Wooden Sandwich Panel's Core Fortification

Levente Dénes, levente.denes@skk.nyme.hu

University of West Hungary, 4 Bajcsy Zs. St., Charles Simonyi Faculty of Engineering, Wood Science and Applied Arts, 9400 Sopron

Abstract

Hierarchical structures as organized assemblies of units are capable to confer unique properties to a structure via optimization over a large range of length scales. The architecture of cellulose chains in wood, cellular structure in an avian wing bone or in the human trabecular bone provides excellent examples of this. The ability to design and fabricate synthetic structures with similar characteristics would lead to components with remarkable properties for example outstanding strength and stiffness could be combined with excellent fracture toughness. Research studies on hierarchical and fractal geometries has shown that the scaling of material required for stability against loading can be altered by changing the hierarchical order of a structure. With the increased use of novel fabrication methods, a material's architecture can be controlled over an ever increasing set of length scales. Manipulation of a material's properties can then be achieved by design parameters settings. This paper details the design, manufacture and testing of regular hierarchical structures made of polylactic acid (PLA) rods. The structures were manufactured using the Fuse Deposition type rapid prototyping technology. A number of uni-axial compression tests were carried out to assess the effect of different geometries and rod sizes on sandwich panels' performance. Analytical estimates for the strength and stiffness are compared with the numerical simulations and experimental results

Proceedings of the 58th International Convention of Society of Wood Science and Technology
June 7-12, 2015 – Grand Teton National Park, Jackson, Wyoming, USA

Development of Wood Fiber-Polypropylene Laminates with Layer-By-Layer Assembly of Kraft Pulp Hand-Sheets and Polypropylene Films

Todd Shupe, tshupe@lsu.edu
Chung Hse, chse@fs.fed.us

Louisiana State University, Louisiana Forest Products Development Center, Baton Rouge, LA 70803

Abstract

This study examined the effects of polypropylene (PP) film thickness, hand-sheet fiber content (FC) in layer, and weight ratio of total fiber content (TFC) on tensile properties and dimensional stability of wood-plastic laminates. Wet-formed Kraft pulp hand-sheets were interleaved with polypropylene films to fabricate laminates of 1/8 in. thick. Experimental results showed that laminates of 0.75-mil film yielded better tensile strength (MORt) than those of 2.25-mil, due to better interpenetration of plastic, as evidenced in SEM observation. The effect of TFC and film thickness on percent elongation at break (ELONG) were not consistent at two higher TFC levels; however, TFC=50 showed the lowest ELONG at all film thickness levels. The interaction between TFC and film thickness had a varying effect on MOEt. At 0.75-mil, better interfacial adhesion in thin hand-sheets contributed to the increase of MOEt with TFC. At 2.25-mil, constitutive hand-sheets were too thick for plastic penetration and poor interfacial adhesion contributed to the reverse relationship in MOEt with nominal fiber content (NOMFC). With proper control of film thickness, wood fiber-polypropylene laminated with fiber loading as high as 70% can be fabricated with favorable mechanical properties.

Proceedings of the 58th International Convention of Society of Wood Science and Technology
June 7-12, 2015 – Grand Teton National Park, Jackson, Wyoming, USA

Effective Adhesive Systems and Optimal Bonding Parameters for Hybrid CLT

Blake Larkin, blake.larkin@oregonstate.edu
Lech Muszyński, lech.muszynski@oregonstate.edu
Arijit Sinha, arijit .sinha@oregonstate.edu
Andre Barbosa, andre.barbosa
Rakesh Gupta, rakesh.gupta@oregonstate.edu;

Oregon State University, 119 Richardson Hall, Corvallis, OR 97331

Abstract

The objective of this project is to determine effective adhesive systems and bonding parameters (adhesive spread rates and bonding pressures) for the hybrid Cross laminated timber (CLT) combinations. The Hybrid CLT combinations include both structural grade lumber and underutilized, low-grade lumber. For a reference species, we selected structural-grade beetle-killed pine (BKP), since lodgepole pine is a member of the US-SPF group closely related to the European species commonly used for CLT construction. The structural-grade, local species will be represented by Douglas-fir (DF), while the low-grade species will be represented by stud-grade BKP, DF, and Western Hemlock. The two adhesive systems investigated are: PUR, an adhesive currently used by the CLT industry that will serve as a reference, and phenol-resorcinol formaldehyde (PRF), a cold setting adhesive commonly used by the engineered wood products industry in North America that will represent a potential domestic alternative. The variables will include species combinations (6), adhesive types (2), clamping pressures (3), and, in some cases, spread rates (3), with repetition of 10 specimens per combination

Proceedings of the 58th International Convention of Society of Wood Science and Technology
June 7-12, 2015 – Grand Teton National Park, Jackson, Wyoming, USA

Micro X-Ray Computed Tomography Study of Adhesive Bonds in Wood

Fred Kamke, fred.kamke@oregonstate.edu
John Nairn, john.nairn@oregonstate.edu
Arijit Sinha, arijit.sinha@oregonstate.edu
Paige McKinley, paige.mckinley@oregonstate.edu
Daniel Ching, daniel.ching@oregonstate.edu

Oregon State University, 119 Richardson Hall, Corvallis, OR 97331

Abstract

Micro x-Ray computed tomography (XCT) is an emerging technology that has found many applications in biology and the study of materials. Although synchrotron-based XCT is still considered the best in regard to spatial resolution, scanning speed, and signal to noise ratio, point source XCT devices are now very capable of producing excellent tomography data with sub-micron resolution. The equipment is expensive, access to a synchrotron device is limited, and the technique generates large quantity of data for analysis. Several groups around the world have adapted XCT to the study of wood. This presentation will provide an overview of micro XCT research at Oregon State University, with a particular focus on adhesive bonds in wood. The research includes study of: anatomical features of several important wood species, penetration of three adhesive types into wood, moisture effects on bonding, and mechanical performance of bonds during XCT scanning.

Proceedings of the 58th International Convention of Society of Wood Science and Technology
June 7-12, 2015 – Grand Teton National Park, Jackson, Wyoming, USA

Continued Research into Fire Performance of Varying Adhesives in CLT Panels Constructed from Southern Yellow Pine

Bryan Dick, Perry Peralta, Miklos Horvath, Phil Mitchell, Ilona Peszlen, Weichiang Pang, Scott Schiff, Robert White

Abstract

Cross-Laminated Timber (CLT) is a construction system that has continued to gain popularity as a "green" alternative to traditional concrete and steel construction . A collaborative CLT project involving NC State, Clemson University, and the US Forest Products Laboratory was initiated to foster the use of southern pine in the manufacture of CLT panels. Fire tests following PS-1 procedures have been conducted to evaluate the fire performance of emulsion polymer isocyanate, 2 types of polyurethane, phenol resorcinol formaldehyde, and melamine formaldehyde adhesives. Since originally presenting the baseline research at SWST in 2014, the research team has furthered the research into the subject and has obtained informative data about the fire resistance of multiple adhesives that may be used in production. Results from the fire performance testing have been evaluated by both non-destructive and destructive means in an attempt to consistently evaluate and quantify the response of the adhesive to the laboratory scale and full scale fire performance tests. Product performance data will feed into efforts to gain building code approval and eventual public acceptance of southern pine CLT. Preliminary results indicate that there are substantial differences in the type of adhesive used for CLT production with southern yellow pine, to the extent that some adhesives may be deemed inappropriate for CLT production in SYP by the research team. This presentation provides an in depth look at the CLT fire testing performance project results so far.

Proceedings of the 58th International Convention of Society of Wood Science and Technology
June 7-12, 2015 – Grand Teton National Park, Jackson, Wyoming, USA

Gas Permeability and Porosity of Fiberboard Mats as a Function of Density

Pamela Rebolledo V. [1] *– Alain Cloutier*[2*] *– Martin Claude Yemele*[3]

[1] PhD candidate, Centre de recherche sur les matériaux renouvelables (CRMR), Département des sciences du bois et de la forêt, Université Laval, 2425 rue de la Terrasse, Québec, QC, Canada, G1V 0A6.
pamela.rebolledo-valenzuela.1@ulaval.ca
[2] Professor and director, Centre de recherche sur les matériaux renouvelables (CRMR), Université Laval, 2425 rue de la Terrasse, Québec, QC, Canada, G1V 0A6.
* *Corresponding author*
alain.cloutier@sbf.ulaval.ca
[3]Industry Advisor, Direction de la modernisation de l'industrie des produits forestiers, Ministère des forêts, de la faune et des parcs, 5700, 4e avenue Ouest, bureau A-202, Québec, QC, Canada, G1H 6R1.
martin-claude.yemele@mffp.gouv.qc.ca

Abstract

The properties and structure of fiberboard mats including density depend on the level of densification. The relationship between gas permeability, porosity and density needs to be investigated because these properties determine the mechanisms of heat and mass transfer in the mat as well as its rheology during the hot pressing process. Gas permeability determines the rate of convective heat transfer and is highly dependent on mat porosity which is changing during the hot pressing process. Mat porosity also impacts the mechanical behavior of the fiber assembly during consolidation. The aim of this study is to characterize the relationship between mat porosity, gas permeability and density. Panels of 560 x 460 x 16 mm without vertical density profiles were produced in a 862 x 862 mm laboratory hot press. Gas permeability was measured with an in-house built apparatus. Porosity was measured by X-ray microtomography, mercury porosimetry and thin microtomed section image analysis. The porosimetry measured by X-ray microtomography and image analysis have shown similar porosity results of about 55% void volume. Mercury porosimetry has shown a lower porosity of about 31% void volume. This difference may be due to the tortuosity of the porous network. Permeability measurement has shown slip flow. Cross-plane intrinsic permeability results were between 3.6 x 10^{-14} and 7.2 x 10^{-14} m^2 for panel densities between 808 and 910 kg m^{-3}, in

agreement with values published for fiberboards in other studies in the same range of density.

Keywords: wood fiber mats, image analysis, X-ray microtomography, mercury porosimetry, hot pressing modeling

Introduction

Medium density fiberboard (MDF) is made from fiber, adhesive, wax and void spaces. This system changes with time and space during hot pressing when consolidation progresses. The void space or porosity in the mat is reduced, the steam flow capacity or permeability of the mat decreases and its density increases. Gas permeability and porosity of the mat are fundamental properties because they are involved in the processes of heat and mass transfer by convection and conduction occurring during hot pressing (Dai and Yu 2004, Thömen *et al.* 2006, Kavazović et *al*. 2012).

The porosity of the mat is directly related to its microstructure. The porous system inside the mat is determined by the morphology of fibers and the consolidation level. With small size particles and low densities, the porosity of the material is relatively homogeneous. Particle size could have an effect on the mechanical behavior of mat because porosity is higher in areas with larger particles (Tran, 2012) and there are larger deformations in high porosity locations of the mat (Sackey and Smith, 2010). This latter study showed that for a high efficiency of compaction during pressing, it is necessary to mix small and large fibers. Previous works on the modeling of void formation in OSB have shown that inter-fiber and intra-fiber voids exhibit different behavior (Dai *et al.* 2005). Benthien *et al.* (2014) and NguehoYemele *et al.* (2008) found that particle size has an effect on panel mechanical performance. Nonetheless, experimental studies about microstructural characterization of thermal insulation of wood-based panels with X-ray micro-tomography have highlighted that during the compression process the decrease of inter-fiber porosity has a greater effect on the decrease of the total volume than the intra-fiber porosity (Delisée *et al.* 2008).

Permeability is defined by the ease with which fluids are transported through a porous material under the influence of a pressure gradient (Siau 1984). The most practical way to measure permeability in both solid wood and composite materials is by using air because there are no problems due to the clogging of the pores that occurs when using liquids (Comstock 1968). Gas permeability can be written as (Siau 1984):

$$k_g^* = \frac{QLP}{A\Delta P\bar{P}} \quad (1)$$

where:

k_g^* : apparent gas permeability ($m^3_{gas}\, m^{-1}_{wood}\, s^{-1}\, Pa^{-1}$)
Q : volumetric gas flow rate ($m^3_{gas}\, s^{-1}$)
L : length in the flow direction (m_{wood})
P : pressure at which Q is measured (Pa)
A : cross-sectional area of the specimen (m^2_{wood})
ΔP : pressure differential across the specimen (Pa)

$\overline{P}$: average pressure across the specimen (Pa)

The apparent permeability (k_g^*) must be corrected for slip flow. This corresponds to the intersect of the straight line of the graph k_g^* against $1/\overline{P}$ with the y axis. It corresponds to the gas permeability corrected for slip flow (k_g). The intrinsic permeability corresponding to the permeability independent of the fluid can be calculated as:

$$K = k_g \mu \quad (2)$$

where

K : intrinsic permeability ($m_{gas}^3 m_{wood}^{-1}$)

k_g : gas permeability corrected for slip flow ($m_{gas}^3 m_{wood}^{-1} s^{-1} Pa^{-1}$)

μ : viscosity of the fluid (Pa s)

Gas permeability is a parameter determined by the structure of the porous material. It plays an important role because it controls the mechanisms of heat and mass transfer inside the mat during hot pressing. Because the mat is made of particles of variable size and shape and due to the presence of a density profile across thickness, mat gas permeability is generally not isotropic (Bolton and Humphrey 1994). The in-plane permeability coefficient K_{pxy} (for gas flow perpendicular to the axis of mat compression) impacts heat and moisture transfer rate from the core to the edges of the mat. The cross-sectional permeability coefficient K_{pz} (for gas flow parallel to the axis of mat compression) impacts heat and moisture transfer from press platens to mat core. Many studies have shown that the in-plane permeability of the mat is higher than the cross-sectional permeability of the mat apparently due to the tendency of the fibers to lay in a direction parallel to the press platens thus facilitating steam flow in the plane of the mat. (Hata *et al.* 1993, von Haas 1998, Haselein 1998, Thömen *et al.* 2006). Mat permeability impacts panel densification during hot-pressing and is a necessary input for hot pressing simulation. A few studies demonstrated that fiber mat permeability is dependent on mat structure and density level. However, the effect of particle morphology is not clear yet (Thömen and Klueppel 2008, Belley 2009, Tran 2012). Nevertheless, a combined effect of particle morphology and mat density on permeability can be expected (Bolton and Humphrey 1994).

Previous work has shown that the relationship between permeability and density is logarithmic (Hata 1993, Bolton and Humphrey 1994, Haselein 1998, von Haas 1998, Garcia and Cloutier 2005, Belley 2009). Von Haas (1998) and Haselein (1998) proposed the following equation for in-plane permeability coefficient and cross-plane permeability coefficient (K_{pxy} and K_{pz} respectively) as a function of density:

$$K = e^{\frac{1}{a+b\rho+\frac{c}{\ln\rho}}} \quad (3)$$

where a, b and c are regression coefficients depending on flow direction and ρ (kg m^{-3}) is the density. Belley (2009) proposed a third degree polynomial relationship for intrinsic transverse permeability of wood fiber mats (in m^2):

$$K_{pz} = e^{0.3351+0.02108*\rho-0.00005\rho^2+2.24*10^{-8}\rho^3} \quad (4)$$

During hot-pressing, both permeability and porosity change with time because density increases due to consolidation. These two properties are sensitive parameters in models

of the thermo-mechanical behavior of the mat during the hot pressing process. The objective of this study is to investigate the relationship between density, permeability and porosity in fiberboard mats.

Material and Methods

Material

Wood fibers containing about 80% softwood and 20% hardwood obtained from an MDF manufacturer were used to produce panels for preliminary gas permeability and porosity measurements (Figure 1). The moisture content of the fibers was about 2% to 3%.

Figure 1. Wood fibers used to produce panels.

Figure 2. Hot-press used to produce panels and fiber mat.

Methods

Manufacture of Panels: Fibers at 2% to 3% moisture content and urea formaldehyde resin were used to produce panels at a resin content of 14% (oven-dry wood basis). A wax emulsion at 1% (oven-dry wood basis) was also used. The hot pressing was performed with a Dieffenbacher hot press with dimensions 862 x 862 mm (Figure 2). The dry wood fibers, wax and resin were mixed in a rotary drum-blender. Blended fibers mats of 560 x 460 mm were formed by hand and pressed (Figure 2) with the press platen temperature set at only 80°C in order to obtain flat vertical density profiles. The mat was pressed to the target thickness of 16 mm in about 171 s. Once the target thickness was reached, the temperature was increased by 5°C every 5 minutes until 100°C was reached in the core of the panel. The panel was then kept into the hot press for two minutes. Using this procedure we obtained panels with homogeneous density (Figure 3) across thickness in order to remove the effect of the density profile in the measurement of the properties.

Sample Preparation: In each panel, eight sample disks were cut for the measurement of gas permeability. Moreover, three cubes of 1 cm^3 were cut at the vicinity of each gas permeability sample (Figure 4).

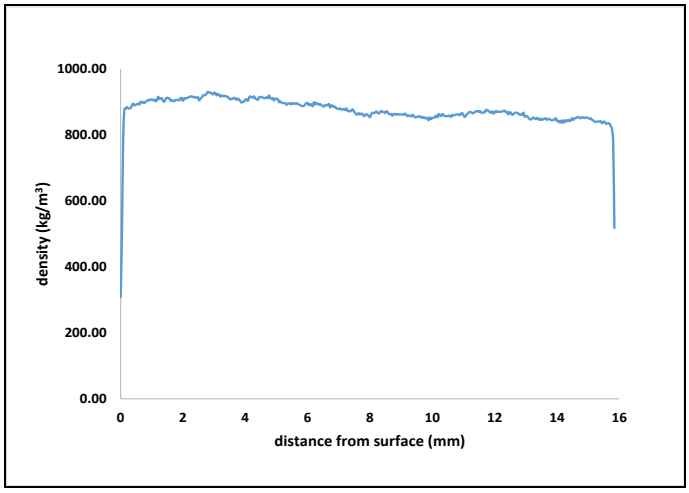

Figure 3. Typical vertical density profile of the panels produced.

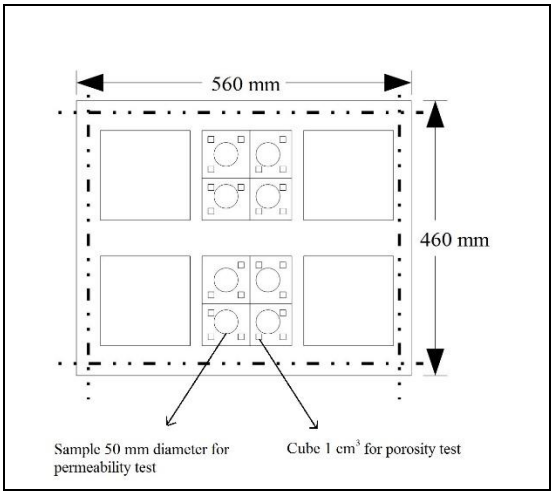

Figure 4. Sampling for permeability and porosity measurements.

Gas Permeability Measurement: Gas permeability was measured with air using an apparatus developed by Lihra *et al.* (2000) (Figure 5). The measurements were performed on panels of five different densities (200, 400, 600, 800 and 1000 kg m^{-3}) with 9 replicates for a total of 45 panels. Eight disks of 50 mm in diameter and 16 mm in thickness were cut from each panel for a total of 360 disks. Silicon seal was applied on the edge of the disks to provide a tight seal with the sample holder (Figure 5b). The apparent gas permeability k^*_g was measured at four pressure levels (50, 100, 150 and 200 kPa). A correction was applied for slip flow as described in Garcia and Cloutier (2005).

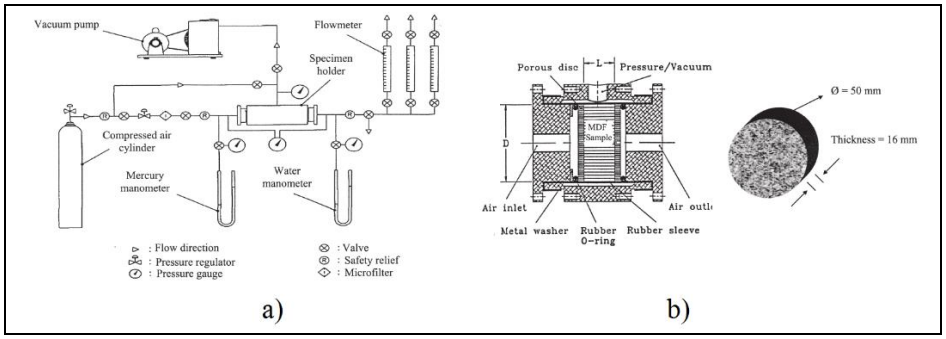

Figure 5. Permeability measurement apparatus (adapted from Lihra *et al. 2000*): a) schematic diagram of the apparatus b) specimen holder.

Porosity Measurement: We are considering three techniques for porosity measurement: Image analysis, X-ray microtomography and mercury porosimetry. For image analysis, a board sample was impregnated with LR White resin and cut in thin slices of 1.5, 2.0 and 3.0 µm using an ultramicrotom. Microphotographs were made using an optical microscope and analyzed with the WinCELL software to calculate the void space in the image. The X-ray microtomography uses an X-ray beam transmitted through the material. Different X-ray absorption patterns are obtained for the different phases of the material. The resolution of the equipment used was 8 µm. Mercury porosimetry is based

on the introduction of mercury into the material. The porosity is calculated from the volume of mercury required to fill the void spaces inside the sample.

Results and Discussion

Porosity

Preliminary measurements of porosity by X-ray microtomography have shown an average porosity of 55% with a standard deviation of 0.5% for panels of 850 kg m^{-3}. Microphotographs of the thin slices used for the measurement of porosity by image analysis are shown in Figure 6. The porosity measured by this technique is between 45% and 55% with an average of 50% and a standard deviation of 4% for panels of 850 kg m^{-3} average density. This is consistent with the results obtained by X-ray microtomography for the same panel density. However mercury porosimetry resulted in an average porosity of 31 % with a standard deviation of 2% for the same panel density. The porosity results obtained by X-ray densitometry and image analysis are close to those found by Belley (2009) for MDF. The lower porosity values obtained by mercury porosimetry can be due to an effect of tortuosity of the porous structure impacting the penetration of mercury.

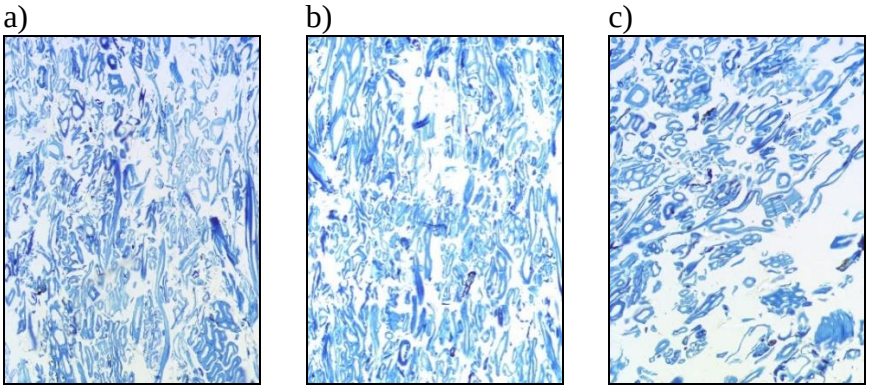

Figure 6. Typical images used for porosity measurement on panels with density of 850 kg m^{-3}. Microtom slices thicknesses are: a) 1.5 μm, b) 2.0 μm and c) 3.0 μm.

Permeability

As in other studies on solid wood and wood-based fiberboards (Lihra et al 2000, Salvo 2004, Garcia and Cloutier 2005, Leandro 2010, Rebolledo 2013) we found slip flow in the gas permeability measurement of the panels (Figure 7). Preliminary results of gas cross-plane permeability of panels of an average density of about 850 kg m^{-3} are shown in Table 1. These values are close to those reported by Belley (2009), von Haas (1998) and Haselein (1998) for density values close to 850 kg m^{-3}.

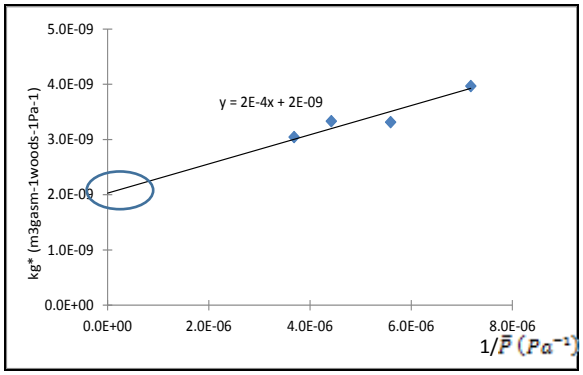

Figure 7. Results of gas permeability at 4 gas pressures showing slip flow effect.

Table 1. Preliminary results of gas permeability.

Sample	Density (kg m^{-3})	K (m^2)
1	874	7.2×10^{-14}
2	850	5.4×10^{-14}
3	869	3.6×10^{-14}
4	910	3.6×10^{-14}
5	851	5.4×10^{-14}
6	808	5.4×10^{-14}

Conclusions

The results obtained for porosity measurements by X-ray microtomography and image analysis are about 55% for a panel with a density of about 850 kg m^{-3} which corresponds to results found in other studies. The measurements of gas permeability have shown the presence of slip flow as for other studies on solid wood and fiberboard. The intrinsic gas permeability found so far of 3.6×10^{-14} to 7.2×10^{-14} m^2 is in the range of results found in previous works for panels with a density of about 700 to 900 kg m^{-3}. We currently pursue the measurement of porosity and gas permeability at different densities. We intend to consider fiber morphology as a factor that could impact both porosity and gas permeability.

Acknowledgements

The authors are grateful to the Natural Sciences and Research Council of Canada (NSERC) for funding this research under Discovery Grant #121954-2012.

References

Belley, D. 2009. Détermination des propriétés de transfert de chaleur et de masse des panneaux de fibres de bois MDF. M.Sc. Thesis, Université Laval, Québec, Canada. 70 p. [in French]

Benthien, J. T., Bähnisch, C., Heldner, S., Ohlmeyer, M. 2014. Effect of fiber size distribution on medium-density fiberboard properties caused by varied steaming time and temperature of defribation process. Wood Fiber Sci. 46(2): 175-185.

Bolton, A. J., Humphrey. P. E. 1994. The permeability of wood-based composite materials. Holzforschung 48: 95–100.

Comstock, G. L. 1968. Relationship between permeability of green and dry Eastern hemlock. For. Prod. J. 18: 20-23.

Dai, C., Yu, C., 2004. Heat and mass transfer in wood composite panels during hot-pressing: Part 1 A Physical-mathematical model. Wood Fiber Sci. 36(4):585-597.

Dai, C., Yu, C., Zhou, X. 2005. Heat and mass transfer in wood composite panels during hot-pressing: Part 1I Modeling void formation and mat permeability. Wood Fiber Sci. 37(2): 242-257.

Delisée, C., Badel, E., Lux, J., Malvestio, J. 2008. Caractérisation microstructurale 3D et densification locale d`isolants fibreux cellulosiques sollicites en compression. XXVI Rencontres universitaires de génie civil. Nancy, France. June 4-6. 8 p. [in French]

Garcia, R.A. Cloutier, A. 2005. Characterisation of heat and mass transfert in the mat during hot pressing of MDF panels. Wood Fiber Sci. 37 (1): 23-41.

Haselein, C.R. 1998. Numerical simulation of pressing wood-fiber composites. PhD Thesis, Oregon State Univ. Corvalis, U.S.A. 244 p.

Hata, T., S. Kawai, T. Ebihara, and H. Sasaki. 1993. Production of particleboards with a steam-injection press V. Effects of particle geometry on temperature behaviors in particle mats and on air permeabilities of boards. Mokuzai Gakkaishi 39(2):161–168.

Kavazović, Z., Deteix, J., Fortin, A., Cloutier, A. 2012. Numerical modeling of the medium-density fiberboard hot pressing process. Part 2. Coupled mechanical and heat and mass transfer models. . Wood Fiber Sci. 44(2): 243-262.

Leandro, L 2010. Propiedades de familias de *Eucalyptus nitens* relacionadas con el secado. (In Spanish). Tesis de Doctorado en Ciencias e Industrias de la Madera. Depto. Ingeniería en Maderas, Facultad de Ingeniería, Universidad del Bío-Bío, Concepciòn, Chile. 126 p. [in Spanish]

Lihra T. Cloutier A, Zhang S-Y. 2000. Longitudinal and transverse permeability of balsam fir wetwood and normal heartwood. Wood Fiber Sci. 32(2): 64-178.

Ngueho Yemele, M.C., Cloutier, A., Diouf, P. N., Koubaa, A., Blanchet, P., Stevanovic, T. 2008. Physical and mechanical properties of particleboard made from extracted black spruce and trembling aspen bark. Forest Prod. J. 58(10): 38-46.

Rebolledo, P. 2013. Interrelación entre las propiedades anatómicas y físicas con la permeabilidad gaseosa y estudio de la difusión del agua en *Eucalyptus nitens*. Tesis Magister en ciencia y tecnologia de la madera. Departamento de Ingeniería en Maderas. Facultad de Ingeniería, Universidad del Bío-Bío. Concepción, Chile. 157 p. [in Spanish]

Siau, F. 1984. Transport process in wood. Springer-Verlag. New York, U.S.A. 245 p.

Sackey, E., Smith, G. 2010. Characterizing macro-voids of uncompressed mats and finished particleboard panels using response surface methodology and X-ray CT. Holzforschung 64(1): 343–352.

Salvo, L. 2004. Relación de la estructura anatómica con la permeabilidad y tasa de secado de la madera de Pinus radiata D.Don. Tesis Magister en ciencia y tecnologia de la madera. Departamento Ingeniería en Maderas. Facultad de Ingeniería, Universidad del Bío-Bío. Concepción, Chile. 79 p. [in Spanish]

Tran, T. N. H. 2012. Study de compression behavior of wood-based fiberboard: characterization from non-destructive image techniques. PhD. Thesis, Université de Bordeaux, Bordeaux, France. 223 p.

Thömen, H., Klueppel, A. 2008. An investigation on the permeability of different wood furnish materials. Holzforschung 62(1): 215-222.

Thömen, H., Haselein, C.R., Humphrey, P.E. 2006. Modeling the physical process relevant during hot pressing of wood-based composites. Part 2. Rheology. Holz als Roh-und Werkstoff 64: 125- 133.

Von Haas, G. 1998. Investigation of the hot pressing of wood composite-mats under special consideration of the compression behaviour, the permeability, the temperature conductivity and sorption-speed. Ph.D. Thesis Hamburg University, Germany. 264 p. [in German]

Proceedings of the 58th International Convention of Society of Wood Science and Technology
June 7-12, 2015 – Grand Teton National Park, Jackson, Wyoming, USA

Pyrolysis of Si-Al compounds and Fibers in Burned Ultra-low Density Fiberboards

Min Niu[1] – Xiaodong (Alice) Wang[2] – Olle Hagman[3]– Olov Karlsson[4] – Yongqun Xie[5]*

[1] Lecture (also a Postdoc. at LTU in Skellefteå), Division of Wood Science and Technology, College of Materials Engineering, Fujian Agriculture and Forestry University,
350002, Fuzhou, Fujian, China
min.niu@ltu.se, *niumin521@163.com*
[2] Assistant Professor, Division of Wood Science and Engineering, Department of Engineering Sciences and Mathmatics,
Luleå University of Technology,
93162, Skellefteå, Sweden
alice.wang@ltu.se
[3] Professor, Division of Wood Science and Engineering, Department of Engineering Sciences and Mathmatics,
Luleå University of Technology,
93162, Skellefteå, Sweden
olle.hagman@ltu.se
[4] Associate Professor, Division of Wood Science and Engineering, Department of Engineering Sciences and Mathmatics,
Luleå University of Technology,
93162, Skellefteå, Sweden
olov.karlsson@ltu.se
[5] Professor, Division of Wood Science and Technology, College of Materials Engineering, Fujian Agriculture and Forestry University,
350002, Fuzhou, Fujian, China
* *Corresponding author*
fafuxieyq@aliyun.com

Abstract

Si-Al compounds significantly decreases release amount of heat, smoke and off-gases during combustion of ultra-low density fiberboards (ULDFs). Under the protection of Si-Al compounds, whether plant fiber (the matrix of ULDFs) was burned up at high temperature is the purpose of this study. Pyrolysis of Si-Al compounds themselves will be also analyzed in this paper. SEM with an EDS, XRD and FTIR was used to

characterize morphology and the microstructure of burned ULDFs, respectively. The results suggested that weight loss ratio of the specimen reached 63.89 % after combustion. Framework built by fibers was still visible in the bottom ash. But plant fibers were almost completely carbonized according to absence of hydroxyl radical and higher weight ratio of C. Weight ratios of Si and Al probably also increased in two ashes especially in upper ash. Infrared absorbance and X-ray diffraction intensity of Si-Al compounds became stronger. Judged by weight ratio of Cl, residual chlorinated paraffin in burned specimen was less. So combustion process results in pyrolysis of chlorinated paraffin and plant fiber, probably not Si-Al compounds.

***Keywords*:** Burned ultra-low density fiberboards, Pyrolysis, Si-Al compounds, Morphology, Microstructure

Introduction

Building energy consumption accounts for around 40% of total energy consumption. To reduce building energy consumption, scientists have designed passive houses (en.wikipedia.org), and developed several kinds of insulation materials. Those insulation materials can be used everywhere in the building and save building energy consumption of 70 to 90% (www.euroace.org). Nowadays, plastic foams and mineral-based insulation materials are the two most popular insulation materials in our market. They almost occupied market share of 95% in all insulation materials. Plastic foams mainly include polystyrene foam, polyurethane foam, polyisocyanurate foam, urea-formaldehyde foam and phenolic foam. Mineral-based insulation materials mainly contain rockwool (RockWool Co.) and glassfiber (Isover Co.). However, there are some problems for them on environmental sustainability and renewability of raw materials. So scientists have been looking for the substitute for insulation materials in recent years.

Cellulose fibers (Cervin et al. 2013), hemp (hempflax.com), wood chips (www.foxmaple.com), wood fibers (Kawasaki et al. 1998), and kenaf (Xu et al. 2004; Xie et al. 2015) was used as the raw material to produce bio-based insulation materials with different properties, respectively. Ultra-low density fiberboards (ULDFs) are one type of bio-based insulation materials and developed under requirement of this situation. Chemical pulp, mechanical pulp, recycled newspaper and carton box is used as the raw material, respectively. Inorganic substances are used as enhancement agents of physical and mechanical properties. Mixture of PVAc and starch is regarded as the glue. Sodium dodecyl benzene sulfonate (SDBS) is used as surfactant to dispersive the fibers and get lightweight material. Under a controlled manufacturing condition, ULDFs have ultra-low density of 10 to 90 kg/m^3 and low thermal conductivity of 0.026 to 0.038 W/m•K, sound absorption coefficient of 0.61 to 0.73, as well as good fire properties (Xie et al. 2012). This project developing ULDFs has been studied for more than 10 years. Manufacturing process, foaming mechanism and application of ULDFs had been reported in Xie et al. (2008). The studies on mechanical properties had also been done through verifying addition amount and types of inorganic fillers (Chen et al. 2015b). In addition, Liu (2013)

has studied fire properties of ULDFs in his doctoral thesis, and indicated chlorinated paraffin and Si-Al compounds had a synergistic effect on fire resistance. Under the synergistic effect, the released amount of heat, smoke and off-gases such as CO and CO2 significantly decreased.

However, past studies mainly concentrated on changes of processing parameters and improvement of physical and mechanical properties. Fire resistance mechanism of plant fiber or cellulose fiber under the synergistic effect of Si-Al compounds and chlorinated paraffin has been not yet reported. So the goal of this paper is to provide a foundation to further understand improvement mechanism of fire properties of ULDFs. In this paper, the morphology and microstructure of unburned and burned ULDFs will be analyzed by applying a SEM-EDS, XRD and FTIR.

Materials and Methods

Materials

Waste newspaper (collected in China) was used as raw material to prepare ULDFs. 500 and 900 mL Si-Al compounds, as the two levels, were added into the foaming system and mixed together with fibers to improve the fire properties of ULDFs. Manufacturing process of ULDFs was described in previous study (Niu et al. 2014). ULDFs were burned by Cone Calarimeter (FTT Co., England) at 780 ^{o}C in accordance with ISO 5660-1/2002. Then fly ash (upper ash) caused by complete combustion and bottom ash caused by incomplete combustion were obtained. The two types of ash along with unburned ULDFs were used as the specimens for next characterization.

Morphology

A scanning electron microscope (SEM, Jeol JSM-6460) with an energy dispersive spectroscopy (EDS, Oxford Instruments) was used to display micromorphology of the specimens, distribution and weight ratios of main elements, but not including fly ash with 500 mL Si-Al compounds (labelled 1-fly ash). The mapping was performed using an acceleration voltage of 25 kV, a current of 8 μA, and a working distance of 12 mm. Because JSM-6460 was broken in our office, 1-fly ash was tested by an extreme high resolution scanning electron microscope (XHR-SEM, FEI Magellan-400) with an EDS (equipped with X-Max 80 silicon drift detector) under the conditions: acceleration voltage of 10 kV, a current of 0.2 nA, and a working distance of 5.1 mm.

Crystallization

An X-ray diffractometer (XRD, PANalytical Empyrean with a PIXcel3D detector) was employed to identify crystalline substances with the conditions: 2θ range of 5 to 60^{o}, a voltage of 45 kV and current of 40 mA, and Cu LFF HR X-ray tube.

Functional groups

Infrared spectroscopy (IR, IFS 66V/S, Bruker) was used to determine the change in functional groups at room temperature of 22 ^{o}C, over a spectral range of 400 to 4000 cm^{-1}.

Results and Discussion

Morphology of burned ULDFs by a cone calorimeter

Morphology of burned specimens and elemental distribution of C, O, Al and Si, are shown in Figure 1.

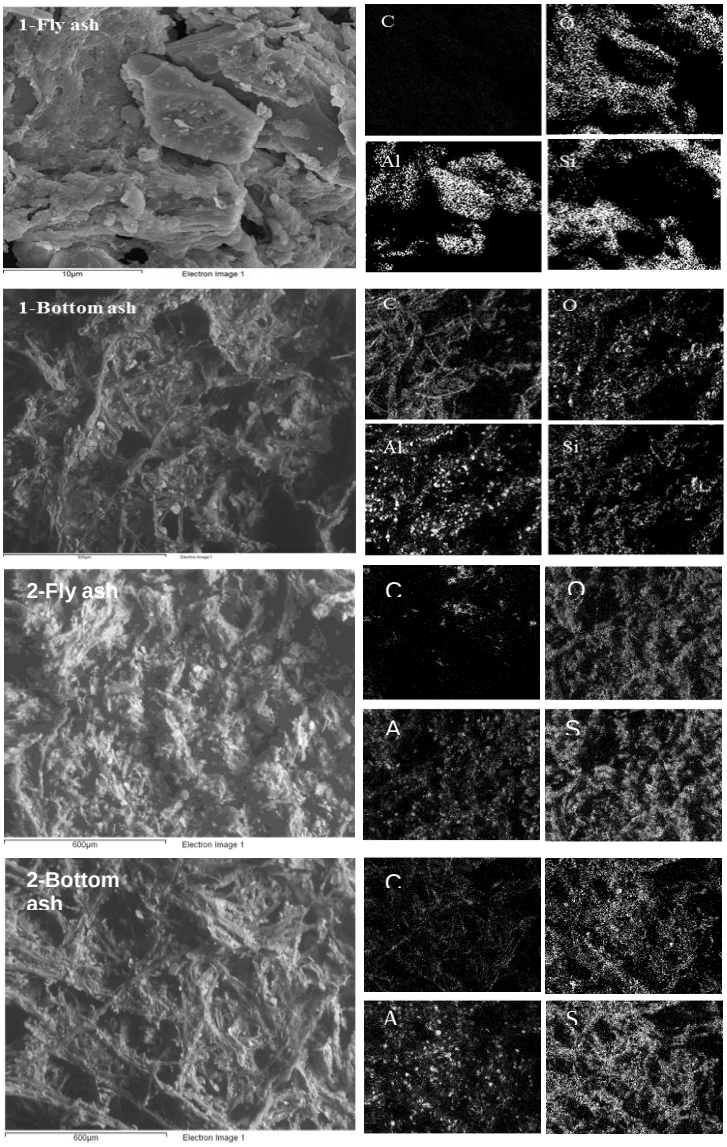

Fig. 1 Micromorphology and element distribution of fly ash and bottom ash from SEM-EDS (Jeol JSM-6460), except for 1-fly ash that was tested by FEI Magellan-400. 1-500 mL Si-Al compounds; 2- 900 mL Si-Al compounds.

From Fig. 1, fly ashes were fragmented, lamellar and lightweight; bottom ashes were integral, reticular and similar to the original structure of fibers. The element C in fly ashes especially in 1-fly ash with less Si-Al compounds was almost invisible. This was possibly because it reacted with O in the air and mainly generated the gas CO_2 on the surface of specimens, while the C in bottom ashes was visible and well-regulated. It was still retained in the fibers after combustion. Judged by weight loss of 62 to 71% (Niu et al. 2014) and brittleness of burned samples, fibers from bottom ashes were carbonized, and their molecular structure was destroyed, even if bottom ash had more Si-Al compounds. But if without fire retardants, ULDFs as porous ultra-low density materials will transform into fly ashes of 100% or less bottom ashes left after combustion. So carbonization of ULDFs was attributed to Si-Al compounds. On the other hand, glue, AKD and surfactant as other sources of C, all were decomposed into oxides of carbon and hydroxides when they suffered from high temperature. Morphology of O was more similar to the morphology of Si and Al. This suggested it existed in the form of the oxides of Si and Al, and the structures of Si and Al oxides were stable at high temperature of 780 ^{o}C. According to the sources of Si and Al, the two types of oxides were from hydrolysis products of Si-Al compounds charged into acidic foaming mixture. Compared with Si, Al spots were bigger and more concentrated especially in EDS profiles of bottom ashes. It was perhaps caused by agglomeration of Al oxides or Si-Al oxides (Al_2O_3-SiO_2) (Chen et al. 2015a). Weight ratio of the elements is listed in Table 1.

Table 1 Weight ratios of main elements in ULDFs before and after combustion

Elements	Weight ratio (%)					
	1-Fly Ash	1-Bottom Ash	1-Before Combustion	2-Fly Ash	2-Bottom Ash	2-Before Combustion
C	—	55.52	8.21	—	43.19	6.16
O	59.93	29.48	52.43	52.11	38.09	57.57
Al	23.85	8.35	11.04	20.09	7.77	14.95
Si	12.79	4.81	4.33	22.92	9.78	6.75
Cl	0.29	0.59	22.16	0.98	0.32	13.52
Total	96.87	98.75	98.17	96.10	99.15	98.95

1-500 mL Si-Al compounds; 2-900 mL Si-Al compounds. "—" means no data given.

C, O, Al, Si and Cl were five main elements in ULDFs. The sum of their weight ratio was more than 96% in total weight ratio of all elements. Combustion brought several elements significant changes. After combustion, weight ratio of Cl sharply decreased less than 1%, and C almost disappeared in fly ash and was up to the maximum in bottom ash. Weight ratios of Si and Al in bottom ashes were apparently lower than those of fly ashes. Actually, weight ratios of Si and Al will not be changed too much because Si-Al compounds have good high-temperature resistance and stable chemical structure (Liu 2010, Lu et al. 2008), Here, the decreases of their weight ratios were mainly caused by the increases of other elements. When Si-Al compounds increased from 500 to 900 mL, weight ratio of Si increased and Al decreased, especially for fly ash. But the sum of Si and Al probably increased in the two ashes with the increase of Si-Al compounds in spite of the effects of other elements.

Crystallization

XRD profiles of the specimens with 500 and 900 mL Si-Al compounds are given in Fig. 2.

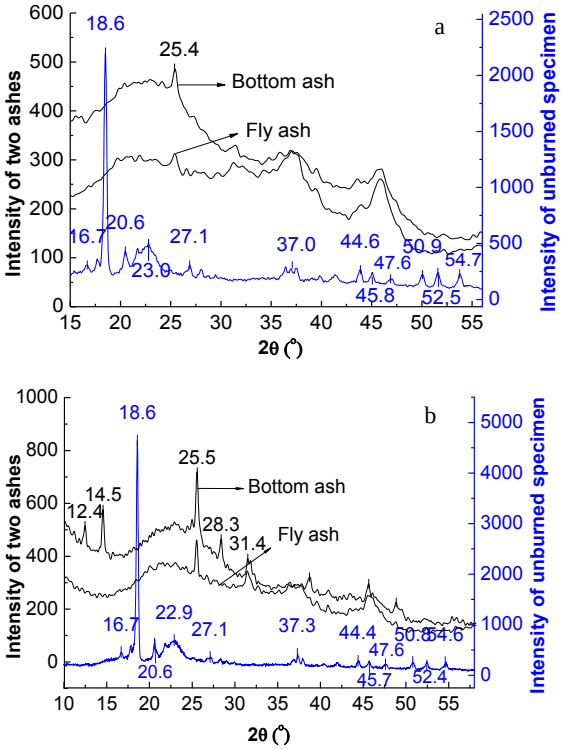

Fig. 2 Diffraction intensity of unburned and burned ultra-low-density fiberboards. a-500 mL Si-Al compounds; b-900 mL Si-Al compounds

Because unburned specimens contained both fibers and Si-Al compounds, their diffraction peaks were complicated and interesting. The peaks were from corporate contributions of fibers with crystalline cellulose at around $2\theta = 22^{o}$ (Lionetto et al. 2012) and Si-Al compounds with a crystalline phase at $2\theta = 18.6^{o}$ and a range from 25^{o} to 60^{o}, similar to crystalline zeolite (Kokotailo and Fyfe 1995, Kosanović et al. 2008). After combustion at 780 ^{o}C by cone calorimeter, carbohydrate components were pyrolyzed and the crystalline structure of Si-Al compounds was destroyed or reorganized (Kokotailo and Fyfe 1995). Therefore, the diffraction peak from crystalline cellulose and the maximum peak at 18.6^{o} (2θ) noticeably disappeared. Meanwhile, other sharp peaks became smaller and broader. The most significant broad diffraction pattern emerged at 2θ from 17^{o} to 30^{o} in the XRD profiles of fly ash and bottom ash, reflecting amorphous substances.

The change from a narrow and sharp crystalline phase to a broad and blunt amorphous phase was also attributed to smaller crystalline size and lower amount of crystalline substances in the specimens (Gajović et al. 2008) caused by pyrolysis. Amorphous carbon, amorphous silicon oxide, and amorphous aluminum oxide might remain in the ashes. These substances are very important to decrease heat released amount during

pyrolysis of carbohydrates. At the same time, some new crystalline substances were also detected from the XRD profiles of ash, especially in Fig. 2 (b), *e.g.*, diffraction angles located at 12.4°, 14.5°, 25.5°, 28.3°, and 31.4°. These may have been the results of the interaction among amorphous substances or caused by re-arrangement of the crystalline structure at high temperatures. Furthermore, because the crystalline structure was subjected to less damage because of a lack of oxygen, the diffraction intensity of bottom ash was higher than that of fly ash.

Functional Groups

Functional group changes caused by combustion were analyzed through the IR spectra shown in Fig. 3.

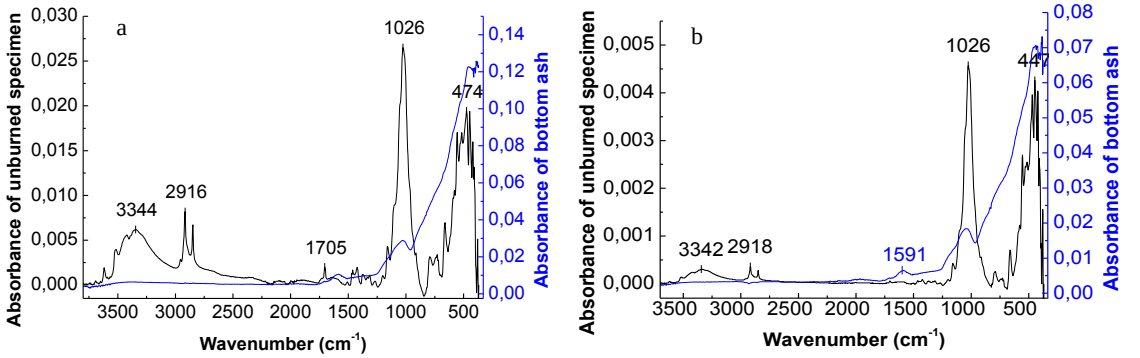

Fig. 3 IR spectra of unburned and burned specimens. a-500 mL Si-Al compounds; b-900 mL Si-Al compounds

Several main peaks, at roughly 3342, 2916, 1726, 1022, and 478 (447) cm^{-1}, can be seen for the unburned specimens. An absorbance peak between 3660 and 3060 cm^{-1}, with a maximum near 3342 cm^{-1}, is characteristic of a hydroxyl group typical of carbohydrates from fibers (Nishimiya et al. 1998). A band at 2916 cm^{-1} can be attributed to the CH stretching mode of methyl and methylene groups in carbohydrates. A band from 1200 to 950 cm^{-1}, with a maximum near 1026 cm^{-1}, resulted from the stretching vibration of Si-O and Si-O-Si (Nayak and Singh 2007, Prado et al. 2010). A broad absorption from 1000 to 400 cm^{-1} was due to the stretching vibration of Si-O-Al, Al-O, and Si-O (Nayak and Singh 2007). Compared to the specimens with label a, the specimens with label b had stronger absorbance at 1000 to 400 cm^{-1} because of a higher dose of Si-Al compounds. After the specimens were burned at 780 °C, their absorption peaks at 3342, 2916, and 1726 cm^{-1} disappeared. Three broad peaks were detected at 1591, 1022, and 478 (474) cm^{-1}. One absorption band at 1591 cm^{-1} was caused by the vibration of aromatic C-C bonds from bio-char (Părpăriţă et al. 2014). Meanwhile, two other bands ranging from 1200 to 400 cm^{-1} were induced by the vibration of the Si-Al compounds. They became broader and higher than those of unburned specimens. The results suggest that carbohydrate was almost completely pyrolyzed. Si-O and Al-O compounds formed after the crystalline structure was rearranged, and made a noticeable contribution to the suppression of heat and volatiles released during combustion of ULDFs.

Conclusions

Fibers, chlorinated paraffin, AKD, glue and surfactant are pyrolyzed to volatile Cl compounds like HCl, volatile C oxides (CO, CO_2) and lightweight C in bottom ashes after combustion. More Si-Al compounds still exist in the ashes in the form of amorphous oxides of Si and Al, even suffering from high temperature.

Acknowledgments

The authors are grateful for the support of ÅForsk in Stockholm, Grant. No. 239124.

References

Cervin NT, Andersson L, Sing Ng JB, et al. (2013). Lightweight and strong cellulose materials made from aqueous foams stabilized by nanofibrillated cellulose. Biomacromolecules 14(2): 503-511.

Chen TJ, Niu M, Xie YQ, et al. (2015a). Modification of ultra-low density fiberboards by an inorganic film formed by Si-Al deposition and their mechanical properties. BioResources 10(1): 538-547.

Chen TJ, Niu M, Wu ZZ, et al. (2015b). Effect of silica sol content on thermostability and mechanical properties of ultra-low density fiberboards. BioResources 10(1):1519-1527.

Gajović A, Gracin D, Djerdj I, et al. (2008). Nanostructure of thin silicon films by combining HRTEM, XRD and Raman spectroscopy measurements and the implication to the optical properties. Applied Surface Science 254(9): 2748-2754.

Kawasaki T, Zhang M, Kawai S (1998). Manufacture and properties of ultra-low-density fiberboard. Journal of Wood Science 44(5): 354-360.

Kokotailo GT, Fyfe CA (1995). Zeolite structure analysis with powder X-ray diffraction and solid-state NMR techniques. The Rigaku Journal 12(1): 3-10.

Kosanović C, Bosnar S, Subotić B, et al. (2008). Study of the microstructure of amorphous aluminosilicate gel before and after its hydrothermal treatment. Microporous and Mesoporous Materials 110(2-3): 177-185.

Lionetto F, Sole DR, Cannoletta D, et al. (2012). Monitoring wood degradation during weathering by cellulose crystallinity. Materials 5(10): 1910-1922.

Liu CH (2010). Wood fire retardant-Sodium silicate. Education in Chemistry 32(12): 71-72. (http://www.cnki.com.cn/Article/CJFDTotal-HXJX201012030.htm)
Liu JH (2013). Fire Retardant Properties and Mechanism of Ultra-Low Density Wood Fiber-Based Material, Ph.D. dissertation, Fujian Agriculture and Forestry University, China.

Nayak SP, Singh BK (2007). Instrumental characterization of clay by XRF, XRD and FTIR. Bulletin of Materials Science 30(3): 235-238.

Nishimiya K, Hata T, Imamura Y, et al. (1998). Analysis of chemical structure of wood charcoal by X-ray photo electron spectroscopy. Journal of Wood Science 44(1): 56-61.

Niu M, Hagman O, Wang XD, et al. (2014). Effect of Si-Al compounds on fire properties of ultra-low density fiberboard. BioResources 9(2): 2415-2430.

Părpăriţă E, Brebu M, Uddin M, et al.(2014). Pyrolysis behaviors of various biomasses. Polymer Degradation and Stability 100(2): 1-9.

Prado L, Sriyal M, Ghislandi M, et al. (2010). Surface modification of alumina nanoparticles with silane coupling agents. Journal of the Brazilian Chemical Society 21(12): 2238-2245.

Xie YQ, Chen, Y, Wei QH (2008). Study on forming a truss-like reticular structure made from nature fiber under the effect of liquid frothing. Journal of Fujian College of Forestry 28(3): 299-303.

Xie YQ, Liu JH, Lin M, et al. (2012). Reinforcement of plant fiber-based ultra low density material with sodium silicate. Journal of Beijing Forestry University 34(1): 115-118.

Xie YQ, Wei W, Wei QH, et al. (2015). A preparation method of insulation cotton using kenaf bark. Chinese patent CN103274637.

Xu JY, Sugawara R, Widyorini R, et al. (2004). Manufacture and properties of low-density binderless particleboard from kenaf core. Journal of Wood Science 50(1): 62-67.

Proceedings of the 58th International Convention of Society of Wood Science and Technology
June 7-12, 2015 – Grand Teton National Park, Jackson, Wyoming, USA

Characterization of Polymerization of Isocyanate Resin and Phenolic Resins of Different Molecular Weights. Part I: Morphology and Structure Analysis

XM Liu, Yan Luo, X.F. Zhang, H. Wan

Department of Sustainable Bioproducts
Mississippi State University
Mississippi State, MS 39762-9820
E-mail: xl257@msstate.edu

Abstract

The reaction of isocyanate resin and phenol-formaldehyde (PF) resins with different molecular weights was characterized by infrared spectroscopy (FTIR), scanning electron microscopy (SEM), X-ray diffraction (XRD), thermos gravimetric Analysis (TGA). FTIR and TG/DTG results showed that higher molecular weights of PF resins can not only promote the reaction of MDI and PF co-polymer system, but also result in the best thermal property of co-polymer. XRD results showed that the higher the molecular weight, the better the crystal structure would be. This kind of co-polymer system provides a great way to recycle isocyanate based polyurethane wastes and has the potential to improve the thermal resistance property of phenolic resins.

Proceedings of the 58th International Convention of Society of Wood Science and Technology
June 7-12, 2015 – Grand Teton National Park, Jackson, Wyoming, USA

Timber Physics from 1 µm to 10 m Session
Moderator: Samuel Zelinka, US Forest Products Laboratory, USA

Subcellular Electrical Measurements as a Function of Wood Moisture Content

Samuel L. Zelinka [1] – José L. Colon Quintana[2] – Samuel V. Glass[3]*
Joseph E. Jakes[3] – Alex C. Wiedenhoeft[5]

[1] Project Leader, Building and Fire Sciences, USDA Forest Service, Forest Products Laboratory, Madison, WI, USA
* *Corresponding author*
szelinka@fs.fed.us

[2] Student, University of Puerto Rico Mayaguez, Mayaguez, Puerto Rico
jose.colon68@upr.edu

[3] Research Physical Scientist, Building and Fire Sciences, USDA Forest Service, Forest Products Laboratory, Madison, WI, USA
svglass@fs.fed.us

[4] Research Materials Engineer, Forest Biopolymers Science and Engineering, USDA Forest Service, Forest Products Laboratory, Madison, WI, USA
jjakes@fs.fed.us

[5] Research Botanist, Center for Wood Anatomy Research, USDA Forest Service, Forest Products Laboratory, Madison, WI, USA
awiedenhoeft@fs.fed.us

Abstract

Recent work has highlighted the importance of movement of chemicals and ions through the wood cell wall. Movement depends strongly on moisture content and is necessary for structural damage mechanisms such as fastener corrosion and wood decay. Here, we present the first measurements of electrical resistance at the subcellular level as a function of wood moisture content by using a 1µm diameter probe. Measurements were taken with the probe contacting the S2 layer and the compound corner middle lamella of the cell wall within the latewood, and the compound corner middle lamella in the

earlywood. The resistance decreased with increasing relative humidity in all locations. The resistance decreased more rapidly with relative humidity in the S2 layer than in the middle lamella. These results give insight into how some moisture-dependent wood properties affecting ion movement may be partitioned across cell wall layers.

Keywords: wood-moisture relations, electrical properties of wood, timber physics, percolation theory, wood damage mechanisms

Introduction

Wood-moisture relations have long been studied using electrical measurements at the macroscopic level (Stamm 1929). Recently, Zelinka et al. (2008) proposed a new mechanism for electrical conduction in wood based upon percolation theory. The theory describes the rapid increase in conductivity of wood as a function of moisture content (MC) between roughly 15-30% moisture content in terms of a percolating network through which ion movement occurs. One key feature of the model is that there is a percolation threshold, the MC at which the percolating network first forms and below which ionic conduction cannot occur. Above the percolation threshold, the conductivity increases with a power-law behavior. Because the percolation threshold represents the lower bound for ionic conduction, it also represents the moisture content below which wood damage mechanisms that rely on ion transport cannot occur (Jakes et al. 2013). Jakes et al. (2013) developed a model for chemical movement in cell walls that is consistent with the percolation model for ionic conduction. In this model chemical movement occurs in regions of the cell where the hemicelluloses have softened through a moisture induced glass transition. Under dry conditions, the hemicelluloses in wood have a glass transition between 150 and 220°C, however, the glass transition temperature decreases with moisture content and eventually crosses room temperature when in equilibrium with a relative humidity (RH) of somewhere between 60% to 80% RH (Cousins 1976, 1978; Kelley et al. 1987; Olsson and Salmen 2004). Above the glass transition temperature, the hemicellulose backbones twist and bend facilitating movement of ions and other chemicals between energetically favorable sites. Just below the percolation threshold, some of the hemicelluloses have adsorbed enough moisture to soften at room temperature. As the relative humidity increases, the number and size of softened regions grows until there is a continuous pathway of softened regions through which chemicals and ions can have long range diffusion.

The percolation model developed by Zelinka et al. was based upon macroscale measurements of the electrical conductivity and implicitly treats the wood material as homogenous. The transport mechanism proposed by Jakes et al. depends upon a moisture induced glass transition occurring in the hemicelluloses. This theory suggests that there are likely differences in the threshold moisture content for moisture transport between different regions in the cell wall. For instance, the secondary cell wall contains cellulose microfibrils, amorphous cellulose, hemicelluloses, and lignin, where hemicelluloses are preferentially oriented along the microfibrils (Hafren et al. 2000;

Åkerholm and Salmén 2001; Stevanic and Salmén 2009). In contrast, in the middle lamella hemicelluloses exist in an irregular network of lignin (Hafren et al. 2000). Because of the differences in the arrangement and amount of hemicelluloses between these two cell wall regions, it is likely that these regions might exhibit differences in how the conductivity increases with moisture content. Since there are differences in the orientation and amount of the hemicelluloses between the secondary cell wall and middle lamella, it's possible that transport occurs differently between these two cell wall layers, and these differences may give further insight into moisture induced changes in wood.

Materials and Methods

Tests were conducted on microtome-cut transverse sections of Southern pine (*Pinus* sp.) wood. Although the exact species could not be determined, the tree was harvested from a plantation where over 90% of the trees were slash pine (*Pinus elliottii)*. Section thickness was examined as an experimental variable and was controlled with the microtome thickness settings: measurements were taken on 20, 40, and 60 µm sections. Sections were stored in ethanol to prevent microbial degradation. Immediately prior to testing, the sections were rinsed with water, placed in the sample holder, and conditioned at 50% RH and 22°C. Additionally, measurements were attempted on 500 µm sections cut by a fine saw; however, the surface roughness of these samples was too high to get reproducible results.

Making good electrical contact with the wood sample was challenging since the sections were prone to curling. To ensure good electrical contact, a sample holder was developed to press the section onto a conductive metal plate while still allowing the top to be accessed with the tungsten probe and exchange moisture with the environment. The sample holder consisted of an acrylic plate with a hole in the center (Figure 1). The section sat between the acrylic plate and an aluminum plate which was used as one of the electrodes. Bolts were used to tighten the acrylic plate to the aluminum plate and an extra bolt was attached to the aluminum so that a wire could be connected to it for the electrical measurements. The second electrode in the measurement was a tungsten probe with a 1 µm tip diameter (Electron Microscopy Sciences, Hartfield, PA).

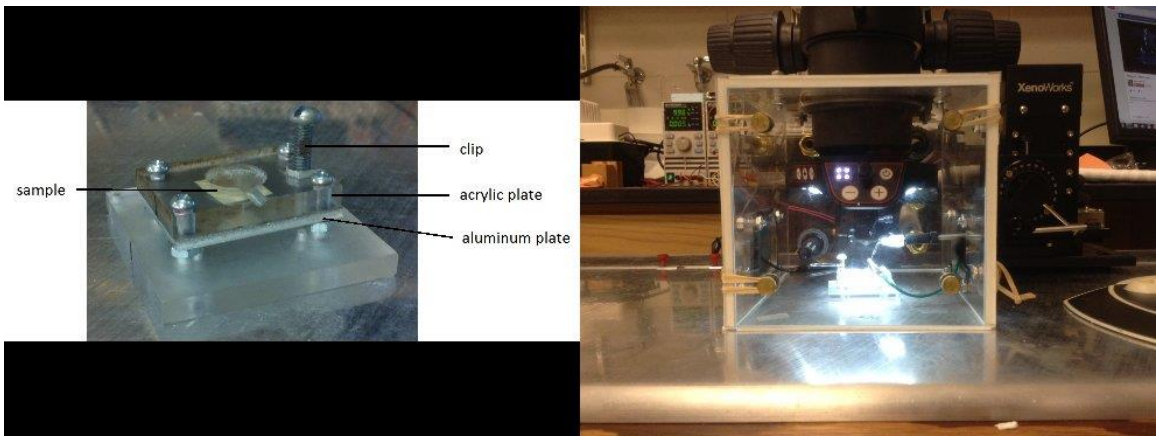

Figure 1: Left: Sample holder used to hold the sections against the aluminum electrode. Right: Chamber built around the stereomicroscope to control the relative humidity conditions.

Measurements were taken in a custom chamber built around a S8APO stereomicroscope (Leica, Wetzlar, Germany) (Figure 1). The chamber was built to house the tungsten probe and the objective of the stereomicroscope. The probe was positioned with a Xenoworks micromanipulator (Sutter, Novato, CA) with a minimum step size of 62.5 nm. Constant RH was maintained by a 2 L min^{-1} flow of conditioned air into the chamber from a HumiSys RH generator (InstruQuest, Coconut Creek, FL) that relied on an RH sensor placed inside the chamber.

For each relative humidity condition, the probe was placed in contact with a cell and the electrical resistance was measured. The RH was then increased, and the section was allowed to condition for 25 minutes at the new RH, this time allowed these thin specimens to get fairly close to equilibrium conditions. Then the measurements were repeated on the same ten cells that had been measured at the previous RH condition. Measurements were taken at seven different relative humidity conditions starting at 50% RH (50%, 57%, 64%, 71%, 78%, 85%, 95%).

Measurements in the earlywood could only be taken at the compound corner middle lamella at the intersection of four cells (Figure 2). Because the cell walls in the earlywood are so thin, the cell wall away from the middle lamella could not be individually measured with the probe we used. In the latewood, the cell wall thickness permitted measurements in both the S2 layer of the cell wall and in the compound corner middle lamella.

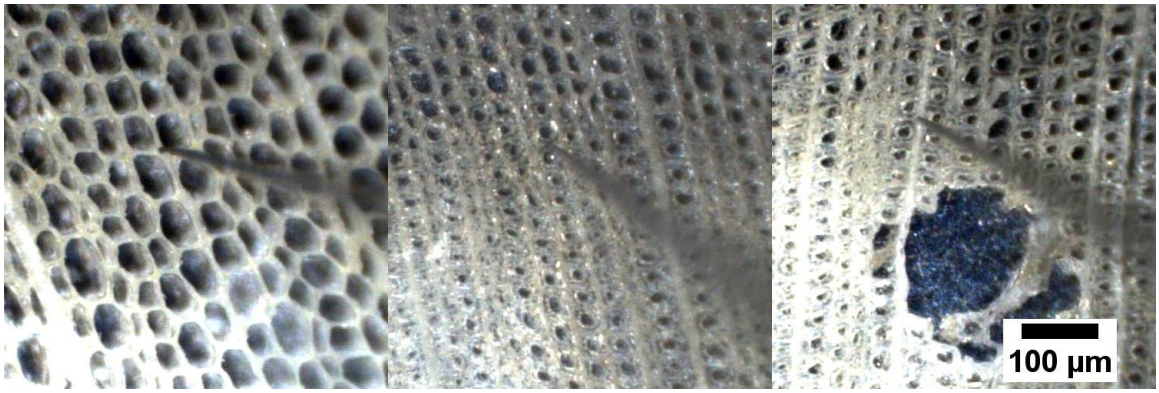

Figure 2: From left to right: example images showing probe placement in earlywood cells, in the S2 layer of latewood cells, and in the middle lamella in the latewood cells.

The resistance measurements were performed with an apparatus designed to minimize polarization effects and to allow for consistent and repeatable measurements (Boardman et al. (2012). The system applies 10 V across a 10 MΩ precision resistor in series with the specimen; polarization is prevented by switching the polarity of the bias voltage at a frequency of 1 Hz and averaging four measurements. The resistance of the wood is determined from measuring the voltage drop across the precision resistor, resulting in uncertainty of less than 6 % at 100 GΩ.

Results

The results of the measurements taken in the earlywood for the three different thicknesses are shown in Figure 3. The resistances range from nearly 50 GΩ at 50% RH to less than 5 GΩ at 95% RH. There is no apparent trend of resistance with section thickness. At the lowest RH conditions, the 60 µm thick sections have the highest resistance but between 70-90% RH, the 20 µm thick sections have the highest resistance. The data appear to have a nearly linear decrease in resistance as the relative humidity increases.

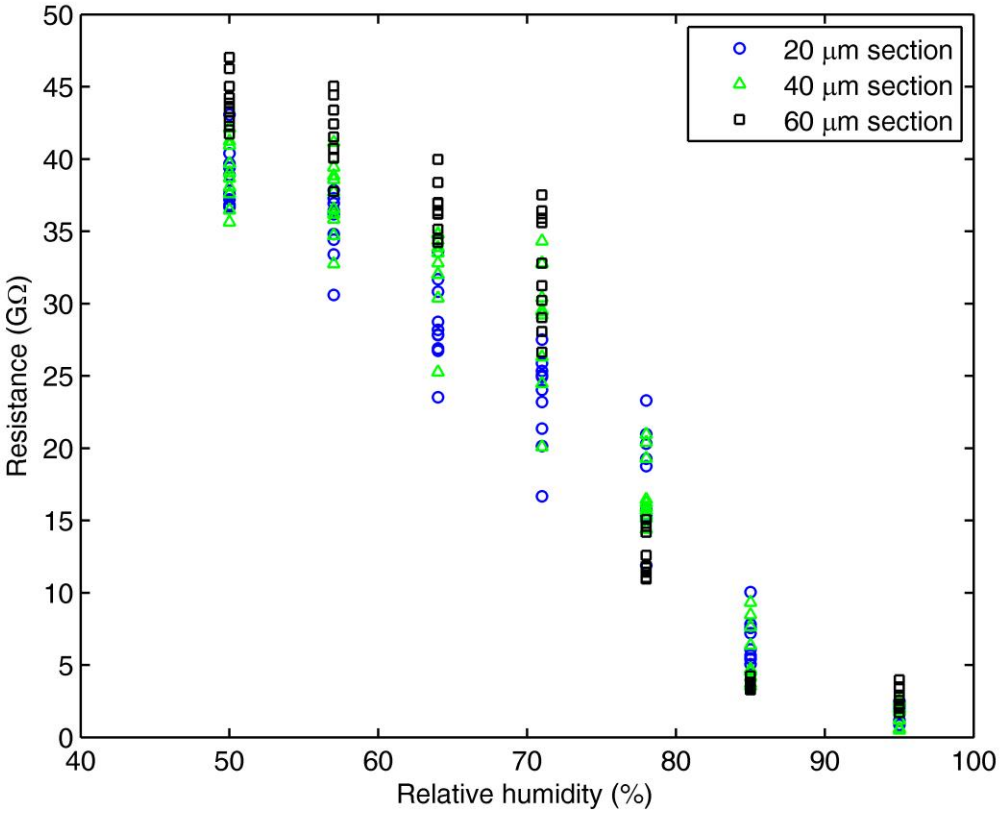

Figure 3: Resistance measurements taken in the compound corner middle lamella of the earlywood as a function of relative humidity.

The results of the latewood measurements taken from the 20 µm thick section are shown in Figure 4. Clear differences are visible in the behavior of the cell wall layers. At the 50% RH condition, the resistance of both layers is approximately equal. However, in the S2 layer, the resistance exhibits a steep drop between 50% and 70% RH. The measurements taken in the middle lamella appear similar to those taken in the earlywood, where the resistance decreased nearly linearly with increasing relative humidity.

Discussion

The measured resistances were independent of the section thickness. This is not surprising as the measurements were taken with a probe with a very sharp radius of curvature. Zelinka et al. (in press) used finite element models to show that for pin-type electrical measurements in wood, the resistance was independent of electrode spacing. Furthermore, when one of the electrodes is a point source, the resistance (R) depends upon only the resistivity of the material (ρ) and the radius of curvature (r)

$$\rho = 4\pi r R \quad \text{(Eq 1)}.$$

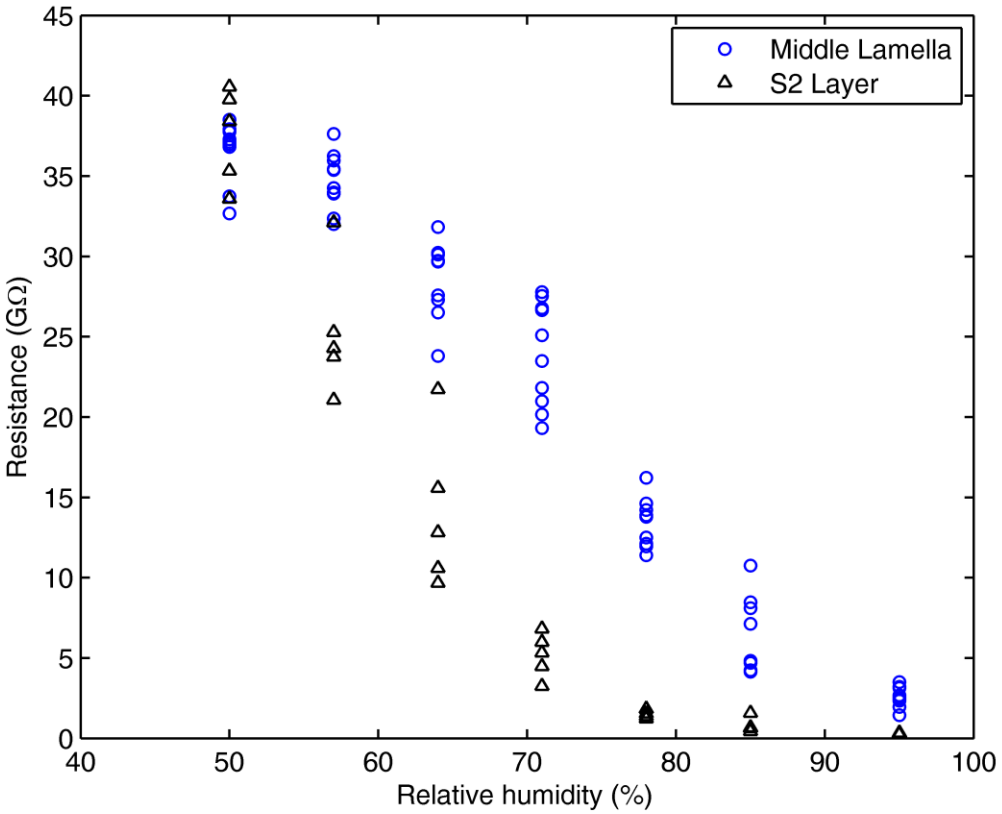

Figure 4: Resistance measurements taken in the compound corner middle lamella and S2 layers of the cell wall in the latewood as a function of relative humidity.

(Telford et al. 1990). Therefore, it is not surprising that there was no trend in the measurements with increasing thickness, and the measurements taken at different thicknesses help define the range of expected values for these measurements.
The resistance measurements taken in the compound corner middle lamella in the earlywood are almost identical to those taken in the same location in the latewood.

It is worthwhile to compare these data to those collected at the macroscale. Traditionally, electrical measurements in wood have plotted conductivity (σ, the reciprocal of the resistivity) as a function of the wood moisture content. Using Eq. 1, the conductivity ranges from 10^{-6} $\Omega^{-1}m^{-1}$ at 50% RH for both the S2 and middle lamella to 10^{-4} $\Omega^{-1}m^{-1}$ and $5 \cdot 10^{-5}$ $\Omega^{-1}m^{-1}$ at 95% RH for the S2 layer and the middle lamella, respectively. From sorption measurements previously taken on material from the same parent board (Zelinka et al. 2014), these RH conditions correspond with wood moisture contents of 7.8% and 22.4% MC, respectively. The macroscopic measurements of Stamm (1929) used to develop the percolation model ranged from 10^{-7} $\Omega^{-1}m^{-1}$ at 9% MC to $4 \cdot 10^{-5}$ $\Omega^{-1}m^{-1}$ at 22% MC; and are within an order of magnitude of the range of values found at the subcellular level. Furthermore, the relative change in the resistivity of the macroscopic measurements is similar to the relative change in resistivity of the measurements taken in the S2 layer.

The increase in conductivity with moisture content is important as it is a way to measure the mobility of ions at different moisture contents. Jakes et al. (2013) hypothesized that several wood damage mechanisms require chemical diffusion within the cell wall and that a better understanding of the diffusion of ions and other chemicals through the cell wall may lead to new ways of protecting wood from moisture-induced damage. In these measurements, it appears that there are clear differences in conductivity between the S2 layer and the middle lamella, and that movement increases more rapidly in the S2 layer than in the middle lamella as wood moisture content increases.

These measurements may give insight into where a percolating network first occurs in wood and how it may be related to mechanical softening. Specifically, the conductivity increases most rapidly in the S2 layer where the hemicelluloses are more regularly oriented, whereas in the middle lamella, there does not appear to be a sharp increase in the conductivity with moisture content. If a rapid increase in conductivity is indeed controlled by the hemicelluloses passing through a moisture induced glass transition, then these measurements suggest that the moisture content at which the glass transition occurs is different in the S2 layer and middle lamella and that the S2 layer is the first to soften. These measurements suggest treatments that preferentially affect the S2 layer may be more beneficial in reducing chemical movement in wood at moisture contents below fiber saturation, thereby protecting wood from moisture-induced damage.

Conclusions

Electrical resistance was measured across microtomed wood sections as a function of relative humidity using a 1 µm diameter probe contacting the secondary cell wall and compound corner middle lamella of southern pine. Several conclusions can be drawn from these measurements:

- The measured resistances were independent of section thickness between 20-60 µm. A smooth, microtomed surface was necessary to make good electrical contact and obtain reproducible results.

- Measurements could only be taken in the compound corner middle lamella in the earlywood. Measurements taken in the earlywood in the middle lamella were almost identical to those taken in the latewood in the middle lamella.
- The resistance decreased as the relative humidity of the chamber increased. The resistance of the S2 layer decreased more rapidly than the middle lamella.

Acknowledgements

Funding for J.L.C.Q. was provided through the Summer Research Experience for Undergraduates (SURE) program as administered by the University of Wisconsin, Madison. The authors acknowledge experimental assistance of Keith Bourne and the contributions of David Eustice of the Forest Products Laboratory machine shop.

References

Åkerholm M, Salmén L (2001) Interactions between wood polymers studied by dynamic FT-IR spectroscopy. *Polymer* 42(3):963-969.

Boardman C, Glass SV, Carll CG (2012) Moisture meter calibrations for untreated and ACQ-treated southern yellow pine lumber and plywood. *Journal of Testing and Evaluation* 40(1):1.

Cousins W (1976) Elastic modulus of lignin as related to moisture content. *Wood Science and Technology* 10(1):9-17.

Cousins W (1978) Young's modulus of hemicellulose as related to moisture content. *Wood Science and Technology* 12(3):161-167.

Hafren J, Fujino T, Itoh T, Westermark U, Terashima N (2000) Ultrastructural changes in the compound middle lamella of Pinus thunbergii during lignification and lignin removal. *Holzforschung* 54(3):234-240.

Jakes JE, Plaza N, Stone DS, Hunt CG, Glass SV, Zelinka SL (2013) Mechanism of transport through wood cell wall polymers. *Journal of Forest Products and Industries* 2(6):10-13.

Kelley SS, Rials TG, Glasser WG (1987) Relaxation behaviour of the amorphous components of wood. *Journal of Materials Science* 22(2):617-624.

Olsson A-m, Salmen L (2004) The softening behavior of hemicelluloses related to moisture. *In*: *ACS symposium series*: Washington, DC; American Chemical Society; 1999.

Stamm AJ (1929) The fiber-saturation point of wood as obtained from electrical conductivity measurements. *Industrial and Engineering Chemistry, Analytical Edition* 1(2):94-97.

Stevanic JS, Salmén L (2009) Orientation of the wood polymers in the cell wall of spruce wood fibres. *Holzforschung* 63(5):497-503.

Telford WM, Geldard LP, Sheriff RE (1990) Chapter 8. Resistivity Methods. *In*: *Applied geophysics*. Cambridge: Cambridge University Press.

Zelinka S, Glass S, Stone D (2008) A Percolation Model for Electrical Conduction in Wood with Implications for Wood-Water Relations. *Wood and Fiber Science* 40(4):544-552.

Zelinka SL, Glass SV, Boardman CR, Derome D (2014) Moisture storage and transport properties of preservative treated and untreated southern pine wood. *Wood Material Science & Engineering*:1-11.

Zelinka SL, Wiedenhoeft AC, Glass SV, Ruffinatto F (in press) Anatomically-informed mesoscale impedance specotroscopy in souther pine and the electric field distribution for pin-type electric moisture meters. *Wood Material Science and Engineering*.

Proceedings of the 58th International Convention of Society of Wood Science and Technology
June 7-12, 2015 – Grand Teton National Park, Jackson, Wyoming, USA

Thermal Conduction Behavior of Wood at Macroscopic and at Cell Wall Level

Oliver Vay [1] – Michael Obersriebnig [2] – Karin de Borst [3] – Wolfgang Gindl-Altmutter [4]*

[1] Senior Researcher, Wood K plus – Competence Centre for Wood Composites and Wood Chemistry, Linz, Austria.
* *Corresponding author*
o.vay@kplus-wood.at
[2] Junior Researcher, Institute of Wood Technology and Renewable Materials, BOKU – University of Natural Ressources and Life Sciences, Vienna, Austria.
[3] Professor, School of Engineering, University of Glasgow, Scotland.
[4] Professor, Institute of Wood Technology and Renewable Materials, BOKU – University of Natural Ressources and Life Sciences, Vienna, Austria.

Abstract

For an orthotropic material, the thermal conductivity in arbitrary directions follows from the conductivities in the principal material directions by rotation of the thermal conductivity tensor. Thus, if wood behaves othotropically, three analytical relations describe the thermal conductivity of wood between the principal anatomical directions depending on the rotation angle. Experiments were made at macroscopic level to prove if these functions hold for wood. Experimental data for thermal conductivity at angles to the grain were compared with values predicted from the conductivities in the principal anatomical directions using the relations for rotation of the thermal conductivity tensor. Excellent agreement between the experimental data and the theoretical curve was obtained. It is concluded that thermal conductivity of wood at angles to the principal anatomical directions can be described by transformation equations derived by the respective rotation of the thermal conductivity tensor.

At cell wall level, thermal conduction behavior was studied by means of scanning thermal microscopy. As a result of the deviating substructures of the cell wall layers, in particular the orientation of cellulose microfibrils, variations in thermal conductivity are observed. The assumption of high anisotropy of the thermal conductivity of crystalline cellulose, having a comparable higher conductivity in parallel to the orientation of the cellulose chains, explains well the observed behavior.

***Keywords*:** Anatomical direction, Grain angle, Scanning thermal microscopy, Thermal conductivity, Wood cell wall

Introduction

Due to the morphological structure wood exhibits a distinctive anisotropic material behavior. The anisotropy of thermal conductivity, as an important property in the field of building physics as well as for timber processing like wood drying and wood modification processes is discussed by several authors (e.g. Griffiths and Kaye 1923; Schneider and Engelhardt 1977; Bučar and Straže 2008, Sonderegger et al. 2011). Thermal conductivity at the macroscopic level is usually determined by means of a steady-state hot-plate method.

The heat transport property of wood along the grain is approximately 2–3 times as high as transverse to the grain, while differences between radial and tangential thermal conductivities are less pronounced. The higher conductivity along the grain compared to transverse conductivities can be explained by a higher conductivity of the cell wall in longitudinal direction of the cell and the orientation of the cells in the stem. As a result, for hardwoods with a high amount of ray cells, which are forming pathways for the heat transport in radial direction, the radial thermal conductivity is significant higher compared to tangential thermal conductivity while for softwood with a small amount of ray cells there is almost no difference between tangential and radial conductivities (Rowley 1933, Waangard 1940; Kühlmann 1962).

The anisotropic material behavior can be expressed by the following structure of the thermal conductivity tensor *K* (Frandsen 2005; Eitelberger and Hofstetter 2011)

$$K = \begin{bmatrix} \lambda_L & 0 & 0 \\ 0 & \lambda_R & 0 \\ 0 & 0 & \lambda_T \end{bmatrix} \tag{1}$$

with λ_L as longitudinal thermal conductivity, λ_R the radial thermal conductivity and λ_T the tangential thermal conductivity.

Thus, assuming reference axis coincide with the principal material axis, off-axis thermal conductivities can be implemented by the respective rotation of the conductivity tensor *K*. If wood behaves othotropically, three analytical relations describe the thermal conductivity of wood between the principal anatomical directions depending on the rotation angle (Vay et al. 2015).

An objective of the present study was to show the validity of these functions and, thus, to show orthotropic symmetry of the thermal conduction behavior of wood. Experimental verification was done in the longitudinal – radial plane. Thus, the respective relation describing the thermal conductivity can be implemented by rotation of the conductivity tensor *K* (equation 1) in the x_1-x_2 plane, about the x_3 axis, by an angle α from the x_1 towards the x_2 axis. Transformed thermal conductivity is given by:

$$\lambda_{(\alpha)} = \lambda_L \cdot \cos^2 \alpha + \lambda_R \cdot \sin^2 \alpha \quad (2)$$

Measurements were made in longitudinal and radial direction of wood and additionally at angles to the grain of 22.5, 45 and 67.5 degrees by means of a steady-state hot-plate method. To prove the validity of the function, experimental data for thermal conductivity at angles to the grain were compared with predicted values obtained by equation 2.

A structural reason for the higher conductivity along the grain compared to transverse conductivities could be a higher conductivity of the cell wall in longitudinal direction of the cell.

To study the thermal conduction behavior of the cell wall, scanning thermal microscopy (SThM) was used. SThM detects the thermal properties of a sample with a resolution of tens of nanometres. To this purpose, a standard AFM probe is substituted with an electrically heated one. The probe replaces one of the resistors in a Wheatstone bridge (Figure 1, see also Vay et al. 2013). This allows monitoring thermal changes in the probe via a feedback mechanism while at the same time topographical data are collected. Depending on the applied voltage, the probe can either act as a resistive thermometer for mapping the temperature distribution on the surface, or as a resistive heater. To act as a resistive heater, a relatively high voltage is applied, which elevates the tip temperature well above the sample temperature.

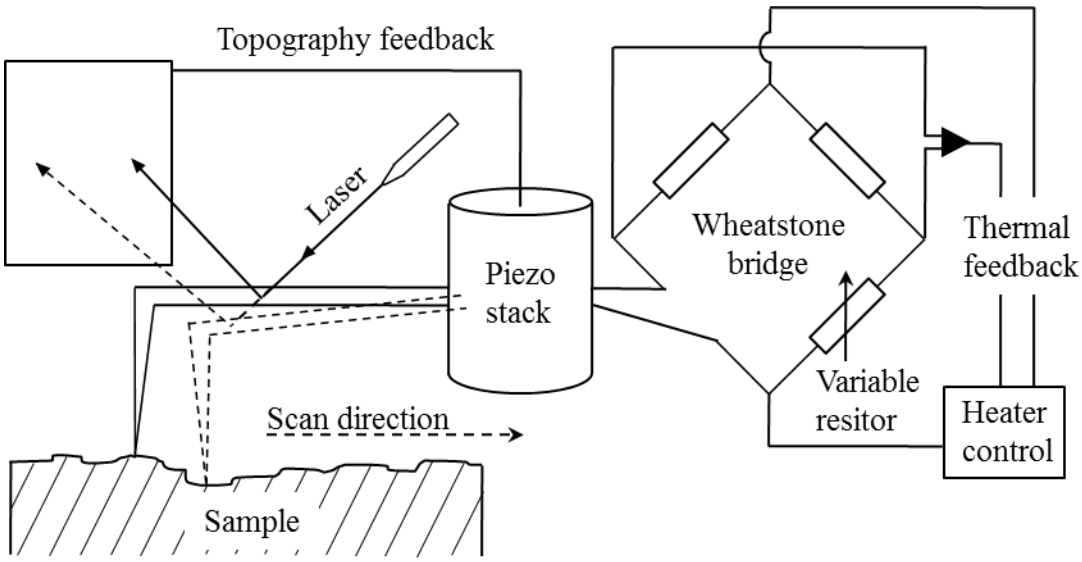

Figure 41. Schematic representation of SThM setup. The SThM-probe constitutes one of the resistors in a Wheatstone bridge, which allows gathering thermal data via a feedback loop. The variable resistor is necessary to zero the output voltage prior to the measurements. At the same time, the standard AFM setup collects the topographic data of the surface. (Vay et al. 2013).

Upon contact, the probe temperature diminishes as a function of the thermal conductivity of the sample. Via the feedback mechanism, the probe temperature is restored to its

original value while at the same time the thermal data is collected, thus providing a measure of thermal conductivity.

Material & Methods

Experiments were made with European beech (*Fagus sylvatica*) and Norway spruce (*Picea abies*).

To determine thermal conductivity by use of a guarded hot plate apparatus, flawless center boards were selected. For sample preparation, strips were cut from wood boards considering the respective angle between the fiber and the cutting direction, the strips were rotated about the axis aligned with the cutting direction about 90 degrees and adhesively bonded to a panel. Specimens were cut out of the panel. The size of the specimens was 150 x 150 x 25 mm³ with the grain at angles α of 0, 22.5, 45, 67.5 and 90 degrees, respectively, to the direction of heat flow, the angles referring to rotation in the longitudinal-radial plane (figure 2, see also Vay et al. 2015 for a more detailed description of sample preparation procedure).

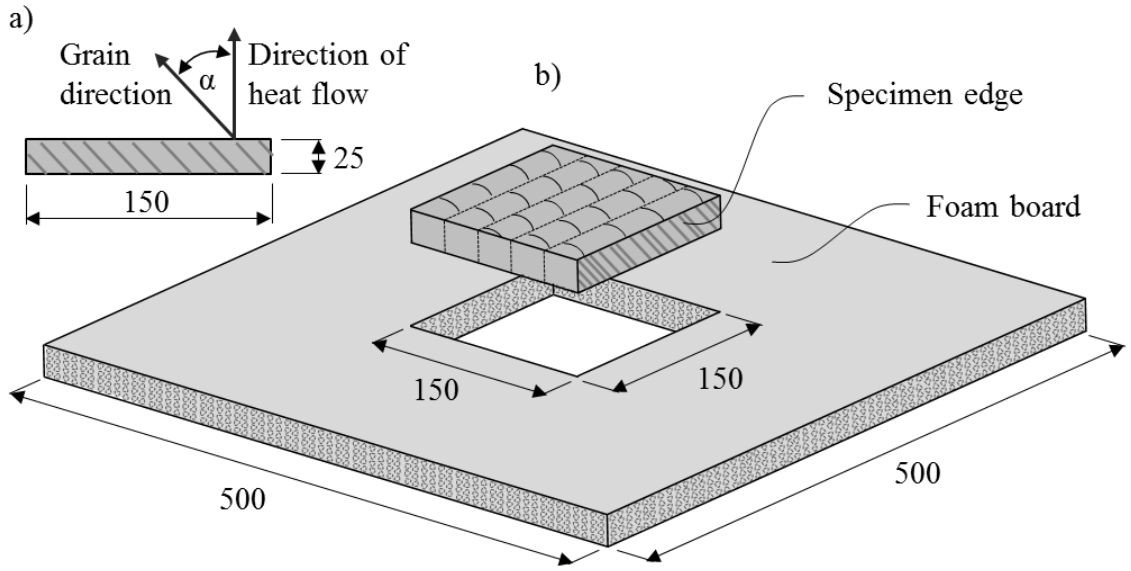

Figure 42. Representation of specimen for thermal conductivity test and experimental setup. (a) View at specimen edge with the grain at an angle α to the direction of heat flow, the angle referring to rotation in the longitudinal-radial plane. Specimen with the grain at angles of 0, 22.5, 45, 67.5 and 90 degrees were used. (b) Exploded view of specimen arrangement for thermal conductivity measurement by means of a guarded hot plate apparatus. Foam board in dimension of 500 x 500 x 25 mm³ with centrally located aperture in dimension of the specimens size (150 x 150 x 25 mm³) was used to bring about thermal conditions so that temperature field in the specimen is one-dimensional and stationary. Specimen was inserted in the aperture of the foam board. Foam board including the specimen was placed centrally at the sensor plates of the test tool (not shown).

temperature difference of the sensor plates of 10 K. All measurements were performed under steady state conditions.

18 specimens each with the grain at angles of 0, 22.5, 45 and 67.5 degrees, respectively and 9 specimens with the grain at an angle of 90 degrees were tested. Thermal conductivity tests were made according to the method given in ISO 8302. Test instrument was single-specimen guarded hot plate apparatus (Lambda Meter EP 500, Lambda Messtechnik, Dresden, Germany). For measurement, the specimen was inserted in an aperture located right in the center of a foam board (Plastazote LD 29, Zotefoam, England), which is needed to bring about thermal conditions so that temperature field in the specimen is one-dimensional and stationary. Foam as adjacent outer material will be not considered for the test result (figure 2). Measurements were made with mean sample temperature of 10°C at a temperature difference of the sensor plates of 10K. All measurements were performed under steady state conditions.

To analyse the influence of grain orientation, measured thermal conductivity values were standardised on mean density of all specimens at angles to the grain. Experimental points as the mean values of standardised data at angles to the grain of 0, 22.5, 45, 67.5 and 90 degrees are compared with predicted values obtained by equation 2. Therefore, equation 2 was used as the model for a least squares fit of the experimental points.
To study the conductivity of the cell wall along and transverse to the grain, small cubes of both wood species were prepared and smoothed with an ultra-microtome (Leica). Test instrument was a Bruker Dimension Icon (Bruker, Santa Barbara, CA, US) equipped with a standard SThM probe of the same manufacturer (VITA-DM-GLA 1, nominal tip radius <100 nm). For all scans a heating voltage of 2 V at a scan rate of 0.3 Hz with constant gain factors was applied and the scan size was 6 µm * 6 µm (see also Vay et al. 2013).

Results & Discussion

Figure 3 shows experimental data at angles to the grain and the respective curve fit for European beech and Norway spruce.

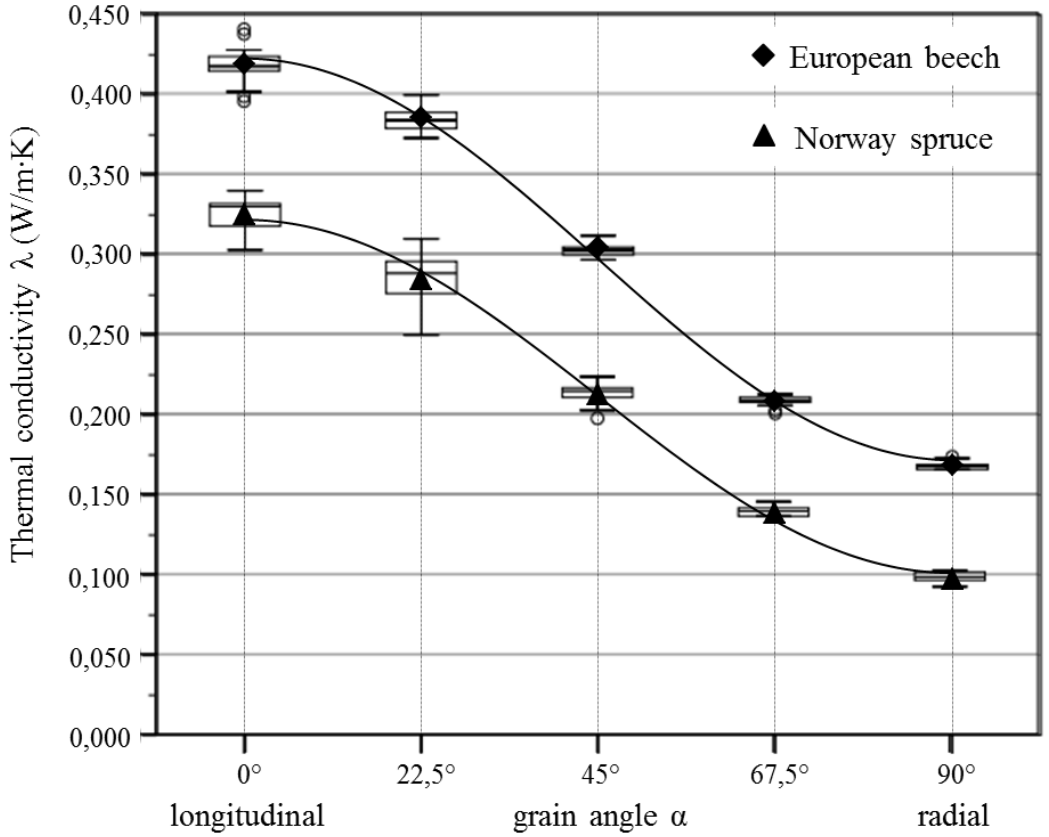

Figure 43. Thermal conductivity versus grain angle in the longitudinal–radial plane. Curve fit yields values of λ_L = 0.422 W/m·K and λ_R = 0.172 W/m·K. R^2 = 0.998 for European beech and values of λ_L = 0.321 W/m·K and λ_R = 0.102 W/m·K. R^2 = 0.998 for Norway spruce.

750 kg/m³ for beech and 484 kg/m³ for spruce. For both wood species highest thermal conductivity was evaluated in longitudinal direction while radial thermal conductivity was lowest. For European beech, curve fitting yields values of 0.422 W/m·K for longitudinal thermal conductivity and of 0.172 W/m·K for radial thermal conductivity. For Norway spruce, λ_L = 0.321 W/m·K and λ_R = 0.102 W/m·K are derived by curve fitting.

There is excellent agreement between experimental data and the respective curve as indicated by the coefficients of determination R^2. It follows that thermal conductivity of wood at angles to the grain in the longitudinal–radial plane is perfectly represented by the transformation equation for orthotropic materials implemented by the respective rotation of the thermal conductivity tensor (equation 2).

Results of the thermal scanning of the cell wall are shown in figure 4 and 5.
Figure 4 shows the microscopic images of the position of the scan on a cross section and a longitudinal section and the respective scanning probe images from European beech.

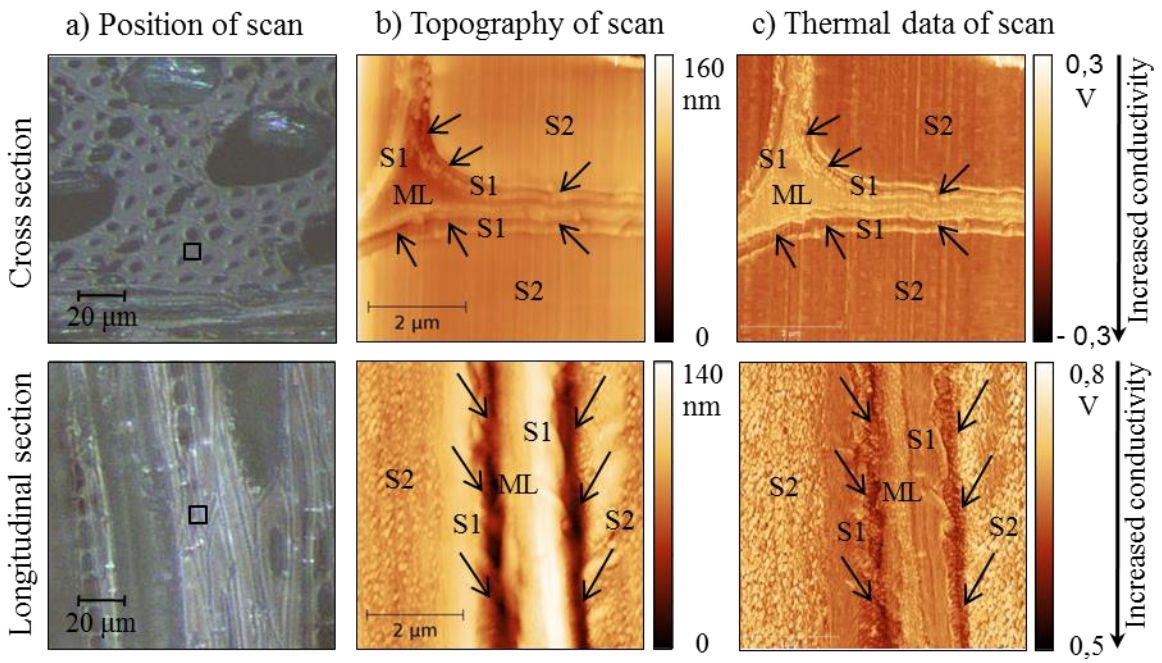

Figure 44. Microscopic and scanning probe images from European beech. (a) Microscopic images, position of the scan is marked (□) on cross section and longitudinal section, respectively. (b) Topography image of the scans on the cell wall of a fiber. On the cross section, the image shows a good flatness on the S2 layer and the middle lamella, while minimal dents in the S1 layer, marked with arrows, are apparent. Topography image on the longitudinal section shows flatness with the exception of two grooves, indicated by arrows, which influence the conductivity contrast image. (c) Conductivity contrast images of the scans. The cross section image shows a clear difference in conductivity between the S2 layer and the middle lamella with higher conductivity of the S2 layer. Observed conductivity of the S1 layer is influenced by the topographical features. On the longitudinal section a seemingly increased conductivity is observed along the grooves. Apart from that, the highest conductivity is observed for the S1 layer, followed by the middle lamella and the S2 layer.

Scanned surface of a cross section of a fiber from European beech is almost smooth with minimal depressions on the S1 layer (see respective contrast image for topography in figure 4b). Conductivity contrast image of the scan (figure 4c, with lighter colors in the latter corresponding to a lower conductivity) shows a higher conductivity of the S2 layer compared to the middle lamella. No clear difference in conductivity between the S2 layer and the S1 layer is apparent, as thermal data of the S1 layer could be influenced by the topography, possibly leading to an increase in the tip-sample contact area and thus, to an increase in conductivity. Topography image on the longitudinal section (figure 4b) show grooves along the interface S1/ML and S1/S2 and apart from that a rather flat surface. Here, a seemingly increase in conductivity is observed along the grooves as shown in figure 4c. Moreover, conductivity contrast image show a minimal higher conductivity of the S1 layer compared to the S2 layer and the middle lamella. Note that a different color scale is applied for the images from both planes to show variations within one image.

Images of the scans on a tracheid from Norway spruce are shown in figure 5.

As visible in the topography images of the cross section scan and the longitudinal section scan, respectively (figure 5b), the collected thermal data (figure 5c) is less influenced by topographical features compared to the scan on a fiber of European beech (see figure 4).

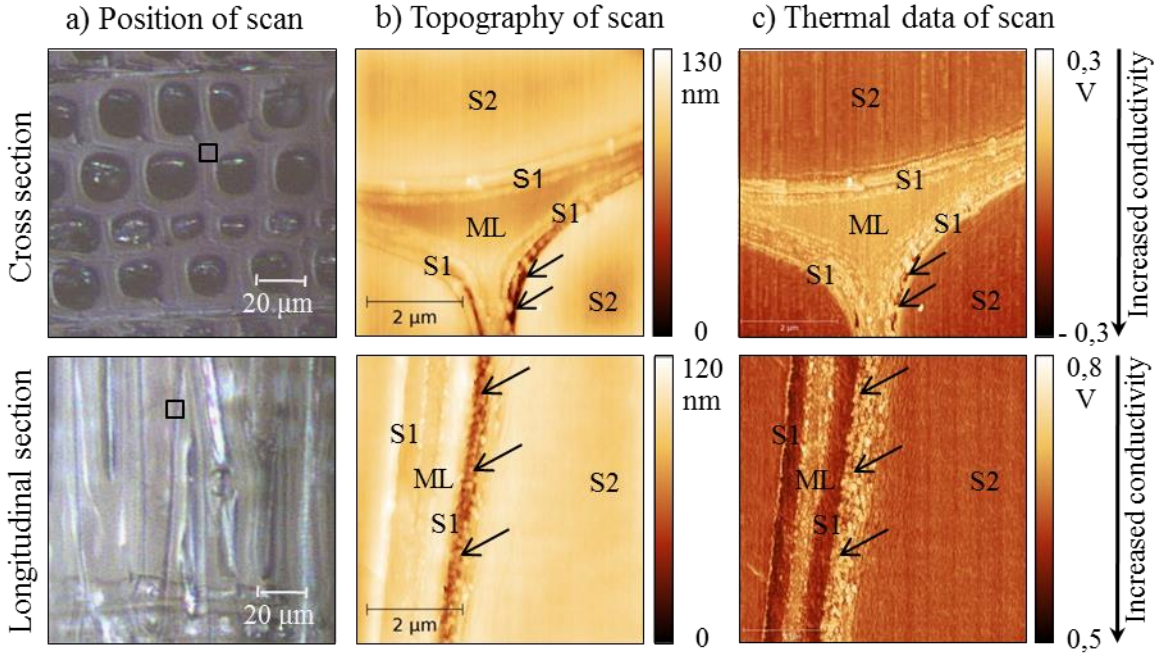

Figure 45. Microscopic and scanning probe images from Norway spruce. (a) Microscopic images, position of the scan on the cell wall of a tracheid are marked (□) on cross section and longitudinal section, respectively. (b) Topography images on the cross section as well as on the longitudinal section show overall good flatness with the exception of one groove in each image, marked with the arrows along one interface S1/S2. (c) Conductivity contrast images from the same scans. Apart from effects of topographical features (arrows) on the observed conductivity, on the cross section image, the S2 layers shows the greatest conductivity, followed by the middle lamella and the S1 layer while contrary on the image on the longitudinal section the S1 layer shows higher conductivity than the S2 layer and the middle lamella.

Variations in conductivity (see figure 5c) which are seemingly caused by variations in topography are marked with arrows. Apart from that, the cross section scan on the cell wall of the tracheid of Norway spruce (figure 5c) reveals a higher conductivity of the S2 layer compared to the S1 layer and the middle lamella. The S1 layer and middle lamella show approximately the same conductivity.
In contrast, the respective image from the longitudinal section scan shows highest conductivity of the S1 layer, followed by the S2 layer and the middle lamella.
The assumption of anisotropic thermal behavior of crystalline cellulose, with significant higher thermal conductivity along the cellulose chains compared to conductivity normal to the chains as well as the conductivity of the other cell wall materials could explain the conductivity contrast images. Almost vertically oriented cellulose fibrils increase the conductivity of the cell wall layer, as visible for the S2 layer in the cross section as well as for the S1 layer on the image of a longitudinal section scan.

Summary & Conclusions

The guarded hot plate experiment showed that thermal conductivity of wood between two principal anatomical directions are perfectly represented by the theoretical curve derived from the respective rotation of the thermal conductivity tensor. It follows that wood shows orthotropic symmetry regarding the thermal conduction behavior. It is concluded that thermal conductivity of wood in arbitrary directions can be calculated by this method.

The SThM experiment images thermal conductivity of the wood cell wall. The results show differences in conductivity between the individual cell wall layers. In cross sections, the S2 layer shows a higher conductivity compared to the S1 layer and the middle lamella. In contrast, in longitudinal sections thermal conductivity of the S1 layer is apparently higher than conductivity of the S2 layer and the middle lamella. The observed conduction behavior could be attributed to a clear higher conductivity of cellulose along the cellulose chains compared to the conductivity of cellulose normal to the cellulose chains as well as to hemicelluloses and lignin, respectively.

References

Bučar B., Straže A. (2008): Determination of the thermal conductivity of wood by the hot plate method: The influence of morphological properties of fir wood (Abies alba Mill.) to the contact thermal resistance. Holzforschung, 62: 362-367.

Eitelberger J., Hofstetter K. (2011): Prediction of transport properties of wood below the fiber saturation point – A multiscale homogenization approach and its experimental validation Part 1: Thermal conductivity. Composites Science and Technology, 71: 134-144.

Griffiths E., Kaye G. (1923): The measurement of thermal conductivity. Proc Roy Soc Lond Ser A, 104 (724): 71-98.

ISO 8302 (1991): Thermal insulation – Determination of steady-state thermal resistance and related properties – Guarded hot plate apparatus.

Kühlmann G. (1962): Untersuchung der thermischen Eigenschaft von Holz und Spanplatten in Abhängigkeit von Feuchtigkeit und Temperatur im hygroskopischen Bereich. Holz Roh Werkst 20(7): 259-270.

Schneider A., Engelhardt F. (1977): Vergleichende Untersuchungen über die Wärmeleitfähigkeit von Holzspan- und Rindenplatten. Holz als Roh- und Werkstoff, 35(7): 273-278.

Sonderegger W., Hering S., Niemz P. (2011): Thermal behaviour of Norway spruce and European beech in and between the principal anatomical directions. Holzforschung 65: 369-375.

Vay O., Obersriebnig M., Müller U., Konnerth J., Gindl-Altmutter W. (2013): Studying thermal conductivity of wood at cell wall level by scanning thermal microscopy (SThM). Holzforschung 67 (2): 155-159.

Vay O., De Borst K., Hansmann C., Teischinger A., Müller U. (2015): Thermal conductivity of wood at angles to the principal anatomical directions. Wood Science and Technology. DOI 10.1007/s00226-015-0716-x.

Wangaard F. (1940): Transverse heat conductivity of wood. Heating Piping Air Condition 12: 459-464.

Proceedings of the 58th International Convention of Society of Wood Science and Technology
June 7-12, 2015 – Grand Teton National Park, Jackson, Wyoming, USA

Mechanism and Regularity of Bending Creep Behavior of Solid Wood Beam in Varying Humidity *

Hong Jian Zhang[1], Ying Hei Chui[2]*
Chun Lei Dong, Yu Xiang Huang and Tong Li

[1] Professor, Faculty of Material Science and Technology
Southwest Forestry University, Kunming, China
[*]*Corresponding author*
hjzhang008@qq.com
[2] Professor, Wood Science and Technology Centre
University of New Brunswick, Fredericton, Canada
yhc@unb.ca

Abstract

In order to make the mechanism and regularity clear of the creep behavior of the solid wood beam in varying humidity (V-creep), a series of experiments were carefully done with the sample from poplar and sets of the accurately controllable system of temperature and humidity and the on line detecting system of the deformation. Results from the analyses indicated that: it was the mechanism of "**Stress coupling - loading – Moisture content – Varying mutual actions**" that regulated the behavior of the bending V-creep, in which the stress coupling was aroused by the hygro-stresses including swelling stress and shrinking stress excited by adsorption or desorption, whose varying state could be represented by the difference of stepping moisture content (**±*D***), and the loading stress; 2) the inner mechanism of the essentially negative creep in absorbing (ad-creep) was that a part of the compressive deformation and bucked and crumbed fibre under compression were transferred by the swelling - loading stress coupling into compression recovery, stretching of the fibre and then tensile deformation; the inner mechanism of the positive creep in desorbing (de-creep), whose deflection might huge, was that a part of the tensile deformation was transferred by the shrinking - loading stress coupling into tensile recovery, compressive deformation and fibre bulking and crumbling; 3) the appearing orientation, either negative or positive, of ad-creep including that of the first ad-creep, and the quantity of all kinds deflections occurred during V-creep were determined by **±*D***, loading, moisture content and their varying mutual actions; 4) the mechanism of the absolute deflection of the negative ad-creep becoming larger and larger and almost

* Supported by the National Nature Science Fund of China, 31170534

reaching the equalization of the positive deflection of de-creep was the smaller and smaller obstruction made by loading to the negative creep. The above mechanism and regularity concluded by this study could be a train or reference for the quantitative analyzing or modeling of the results from V-creep.

Keywords: Solid wood beam; Creep in varying humidity; Mechanism; Regularity; Difference of stepping moisture content; Stress coupling

1 Introduction

Great many efforts have being made to approach the mechanism and regularity of the creep of wood in varying humidity (abridged as V-creep) since the first publication of V-creep's behavior by Armstrong L. D. and Christensen G. N. (1961) [1]. However, few complete or convincible solutions have been got and widely acknowledged up to now, as indicated by Montero C. and Grill J. (2012) [2] and *et al*. Beginning from Armstrong L. D. (1961) [1] up to Hunt D. G. (1999)[3], Takahashi C. and Ishimaru Y. (2004)[4], Hassani M.M. and Wittle F. K. (2015)[5], and *et al*, almost all the researchers have being taken the "Moisture content" or "Range of moisture content" as an independent variable to study or model the behavior and result of V- creep, but it was not felt satisfied due to the lacking of reasonable mechanism. Beginning from Armstrong L. D. (1961) [1] too, Houška M. and Koc P. (2000)[6], Hanhijärvi A. (2000)[7], Srpčič S. and Srpčič J. (2009)[8], Svensson S. and Köhler J. (2010)[9], Li T. and Zhang H. J. (2013)[10], and *et al*. tried to explore the behavior in view of the moisture gradient, swelling or shrinking stress, transient stress and etc., there was still few fundamental equations have been made without the sufficient and necessary support by the mechanism, too.

In order to answer such puzzling questions exposed by Fig. 1 as that how the V-creep behavior was effected by changing moisture content, what orientation of and how large the creep deflection during adsorbing including the first adsorption should be exactly true, why the creep deflection during desorbing was much more than that at high but constant moisture content and could it possible that the deflection in desorbing to be counteracted by that in adsorbing, a series of bending creep experiments were carefully done with the sample of poplar (*Populous euramevicana*) and sets of the accurately controllable system of temperature and humidity and the on line detecting and recording system of the deflection in Southwest Forestry University of China. It was hoped that the expected solution of the mechanism and regularity of V-

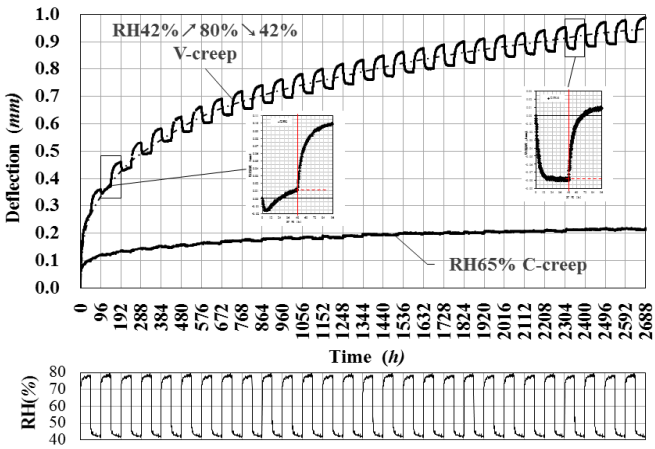

Fig. 1: 28 cycles of V-creep
Within RH42%-80% and C-creep in RH65%

creep from this study could be a train for the quantitative analyzing or modeling of the V-creep result.

2 Materials and Methods

2.1 Raw material and samples

The solid wood samples were cut semi-radially from the poplar, which was planted in Jiangsu province in China for LVL. 36 formal samples with almost the same density and MOE were carefully selected from the pre-selected 197 ones, whose average air-dried density was 0.540g/cm^3 (CV=3.47%), modulus of elasticity (MOE) was 14 730MPa (CV=2.90%) and modulus of rupture (MOR) was 0.33kN (CV=2.60%). The size of the symmetric beam samples was 110*10*5mm (L*W*H), whose 2 sides and 2 ends were sealed by paint and gluable plastic sheet. The asymmetric beam samples were 110*10*2.5mm with the extra seal of 1 plane. There were 2 samples for each creep condition with 6 for moisture control. All the samples except that for the creep in constant humidity (abridged as C-creep) were conditioned into constant weight prior to testing under 20±0.5℃ and relative humidity (RH) 42±2%.

2.2 Indexes valued and their testing methods

1) Moisture content (MC, %). This was an absolute MC by the interval weighting of the moment moisture content of the samples accompanying with creeping ones in varying humidity. 2) Difference of stepping moisture content (±D, %/mm). D= ($MC_{core\ or\ sealed} - MC_{surface}$)/2.5 (%/$mm$), which was calculated with reference of Yu C. M. (2011) [11]. D was to reflect the perpendicular state of moisture distribution in adsorbing, and -D to reflect that in desorbing. 3) Creep deflection (±Δ, mm). Δ was the average displacement of upper and down planes in the middle of the beam sample under 2-point loading (Fig. 2) and detected on line by a Linear Variable Differential Transformer (LVDT) system. Δ was defined for downward deflection as usual, but $-\Delta$ for the upward.

2.3 Methods and conditions for the experiments

When the creep during absorbing and desorbing were abridged separately as ad-creep and de-creep, and the creep at constant moisture lever as C-creep, the one cycle of 96h or 4d creep was supposed to be: [48h (ad-creep + C-creep) + 48h (de-creep + C-creep)] in constant temperature 20±0.5℃. There were 3 main experiments. Expr. 1: Long term creep, including: 1) Test of V-creep: 5mm thick symmetric beam; load P=25% Fr and 55% Fr (rupture force); range of varying humidity, RH42%↗80%↘42%; creeping duration, 96h(4d)/cycle * 28cycles = 2688h (112d); started on RH42% and P=0; 2) Test of C-creep: the symmetric beam samples were conditioned under 20±0.5℃ and RH65±2% till to EMC, fully sealed and then went to creeping together with the V-creep samples for the same period. Expr. 2: Short term deformation of 2.5mm thick asymmetric beam in varying humidity without loading: varying humidity

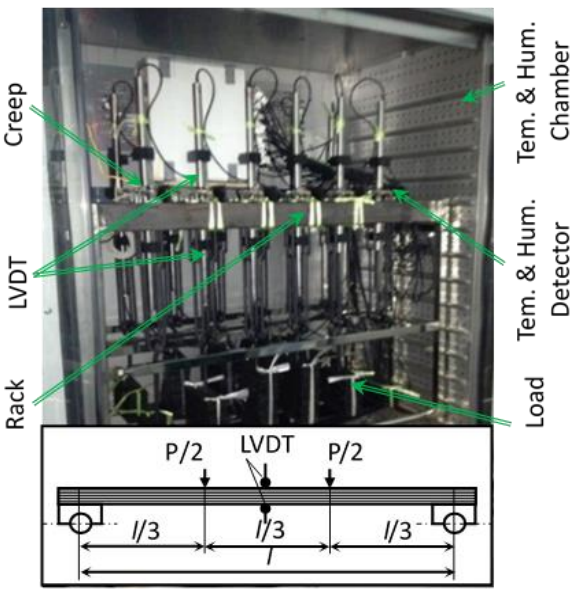

Fig. 2: Apparatus for test of creep

range, RH42%↗89%↘42%. Expr. 3: Orthogonal experiment $L_9(3^4)$ to tell the effects of mutual actions by *D* and *P*: 3 level *P*, 15%Fr, 25%Fr, 35%Fr;3 level humidity varying range (meant 3 level *D*), RH42%↗(65%, 80%, 89%)↘42%; duration, 2.5 cycles; started after 48h C-creep under RH42%.

2.4 Equipment

A conditioned room (20±2℃, RH 65±3 %); a Binder KMF720 temperature and humidity chamber (±0.5℃, RH±2%) which was put in the conditioned room; an on line LVDT system; 5 Testo174H temperature and humidity detectors and recorders (±1℃, ±3%RH); 2 specially designed racks for creep in the chamber; a Shimadzu AG-1 universal testing machine of mechanics, ±1N; and etc., as shown in Fig. 2.

3 Results and Analyses

3.1 Regularity of the birth and development of varying hygro-stresses

Fig. 3 was out of the Expr. 2, in which point a was the time of transferring increasing $|\pm D|$ into decreasing, b was the end time of the full recovery from the prior deformation, c was the time of $|\pm D|=0$ and T was the time of transferring deforming into recovering of the beam. By the deformation curve of the 2.5 mm thick asymmetric beam, it can be seen that: 1) there were hygro-stresses (σ_{hygro}) being excited by $\pm D$ including the swelling stress (σ_{sw}) by $-D$ leading to convex deforming against the sealed plane (Fig. 3A), and the shrinking stress ($-\sigma_{sh}$) by D leading to concave deforming (Fig. 3B); 2) trajectory of the changing deformation looked similar with that of the developing $|\pm D|$ from starting till increasing, transferring, decreasing and reaching towards zero; 3) quantity of the deformation appeared positive with $|\pm D|$, i.e. positive with $|\pm\sigma_{hygro}|$. However, the regularity of the deformation of the 5mm thick symmetric beam was completely different from that of the 2.5mm thick asymmetric one.

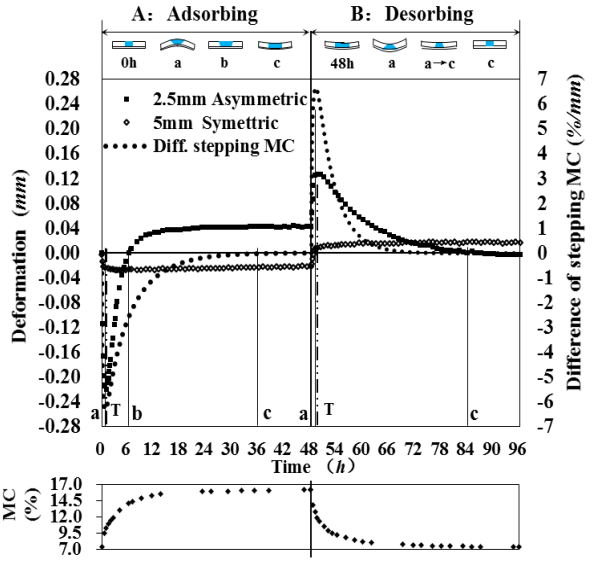

Fig. 3: Difference of the stepping MC and deformation of wood beam in varying humidity without loading

3.2 Coupling of the hygro-loading stress and its effectiveness

As shown in (Fig. 4-1 and Fig. 4-5, there are stepping compressive stress ($-\sigma_c$) and tensile stress (σ_t) separately distributing in the up and down part of the bending symmetric beam under load *P* according to the mechanic theory. Since the deformation of wood under compression happens much easily, esp. during adsorbing, than that under tension, the

mechanical neutral layer of the symmetric beam locates always below the center layer. Usually, the compressive deformation includes elas-plastic deformation and bucking of fibre, and the crumpling of fibre like the "slip plane" summarized by Hoffmeyer P. and Davidson R.W. (1989) [12].

Because the swelling stress σ_{sw} is opposite to $-\sigma_c$ but parallel to σ_t when adsorbing, the neutral layer of the beam must go upwards, as transferred the original compressed fiber between the original neural layer and the new layer into tensing (Fig. 4-2) after the recovering of compression and stretching of the bucked and crumpled fiber. As a result, the upward part of the beam was becoming longer, while the length of downward part kept unchanging since the moving of the neutral layer should not change the stress level. In this case, the upward creep happened. This upward creep was considered by this paper as a "negative creep" against the usual positive, i.e. downward creep, because it happened still under loading, unlike the true recovery of the asymmetric beam without loading in Fig. 3. *This was the coupling between the swelling stress σ_{sw} and loading stress $\pm\sigma_p$ (abridged as C_{sw*p}) and its effectiveness; and also was the mechanism for the ad-creep whose essential deflection orientation must be negative*.

When desorbing, since $-\sigma_{sh}$ is parallel to $-\sigma_c$ but opposite to σ_t, the neutral layer must go downwards, which transferred the original tensed fiber between the neural layer after adsorbing and the new one into recovering of tension and compressing (Fig. 4-6) including the easy bucking and crumpling of fibre. And then, the shortening of the up part of the beam should aggravated the positive creep. *This was the coupling between $-\sigma_{sh}$ and $\pm\sigma_p$ (abridged as C_{sh*p}) and its effectiveness; and also was the mechanism for the larger positive deflection during de-creep than that during C-creep*.

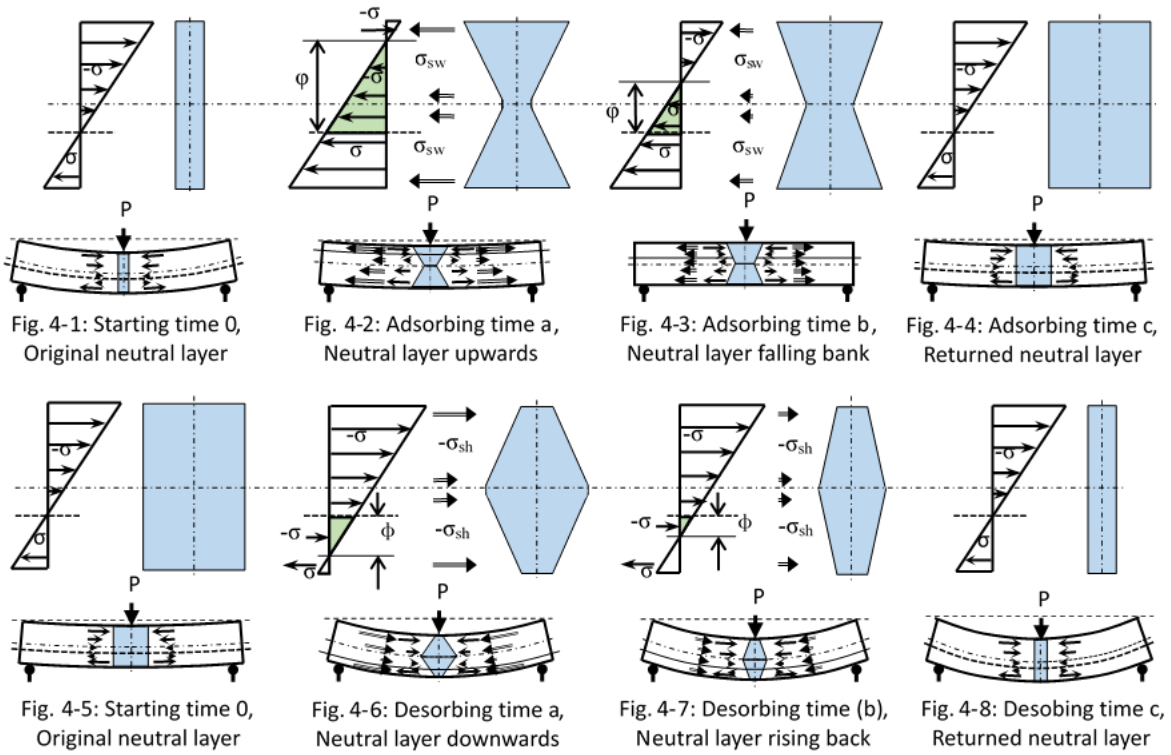

Fig. 4: Changing of MC and stress distribution, neutral layer and creep behavior

Accordingly, the negative deflection induced by C_{sw*p} could be named as "the deflection by coupling of swelling-loading stress (abridged as $-\Delta_{sw*p}$), and the positive deflection induced by C_{sh*p} could be named as "the deflection by coupling of shrinking-loading stress (Δ_{sh*p}).

3.3 Mutual actions between the stress coupling and the loading

Fig. 5 was the curve of the 2nd cycle V-creep under 25%Fr enlarged from Fig. 1 (out of Expr. 1), the measured *MC* and the calculated *D*. The T in Fig. 5a was the transferring time from the negative creep into the positive, which was quite different from that in Fig. 3.

As was mentioned above, adsorption may not change the stress level and the direction of bending moment, there must exist the positive deflection by load *P* (Δ_p). However, since Δ_p is opposite to $-\Delta_{sw*p}$ when adsorbing, there must be such an mutual anti-action as an obstruction for one to weaken and even suppress the deflection of the other. This meant one deformation appeared might embody the other's. Meanwhile, since -*D*, C_{sw*p} and the location of the neutral layer were varying (Fig. 4-1~4-4), this mutual obstruction might be varying, too. As shown in Fig. 5a, before time a, the sharp increasing of |-*D*| made $|-\Delta_{sw*p}|$ large enough to overcome the obstruction by Δ_p, so that the negative deflection $-\Delta_{ad}$ of ad-creep appeared ($-\Delta_{ad} = -\Delta_{sw*p} + \Delta_p$|); but after time a, since |-*D*| had changed from increasing into decreasing, $|-\Delta_{sw*p}|$ became smaller and smaller and finally was overcome by Δ_p at time T, the positive deflection Δ_{ad} of ad-creep appeared instead ($\Delta_{ad}=\Delta_p + -\Delta_{sw*p}$). However, before time T, though the obstruction by Δ_p was not strong enough, it could make the rate of developing $-\Delta_{ad}$ slowing and the transferring time T lagging behind the transferring time a of |-*D*|. Thus, it can be seen that, though *the essential orientation in the period of ad-creep must be negative* due to the effectiveness of C_{sw*p}, the appearing orientation, either negative or positive, would be determined by the mutual actions between Δ_{sw*p} and Δ_p. When $|-\Delta_{sw*p}| > \Delta_p$, $-\Delta_{ad}$ would appear; and when $|-\Delta_{sw*p}| < \Delta_p$, Δ_{ad} would appear instead. This is *the mechanism to explain why the orientation of ad-creep under loading could be negative or positive sometimes and the negative deflection would appear prior to the positive one all the time*.

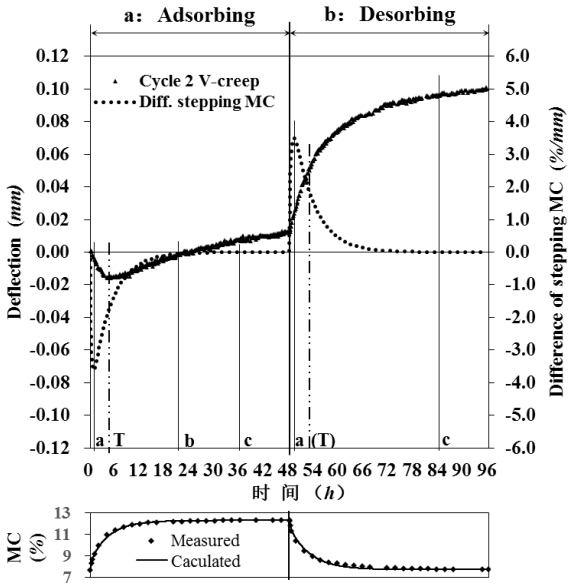

Fig. 5: Difference of stepping MC and deflection of V-creep under loading

This mechanism could be seen in the symmetric beam in Fig. 3. Since the only load by the proportional dead weight of the beam itself was too small to obstruct the $-\Delta_{sw*p}$, the negative deflection was certainly appeared, and the time T and the following positive deflection which should occur were not obvious. Oppositely, if the load was heavy, the $-\Delta_{sw*p}$ would look suppressed totally by Δ_p; but in fact, the struggling $-\Delta_{sw*p}$ could still appear even though it was so small (Fig. 6). Fig. 6 revealed that so large the σ_{sw} excited by the sharp increasing $|-D|$ that could produce so large the $-\Delta_{sw*p}$, when coupling with $\pm\sigma_p$, as to suppress the obstruction by Δ_p produced by a heavy load, though it appeared shortly.

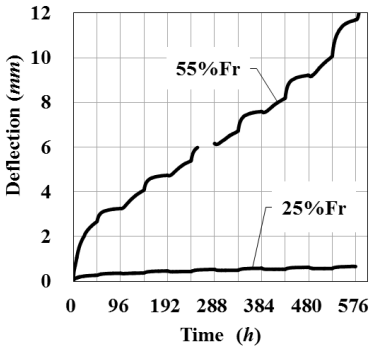

Fig. 6: V-creep under load of 55% rupture force

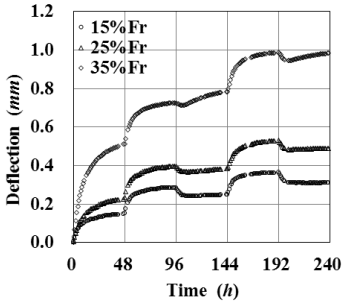

Fig. 7-1: Effcet by *P*

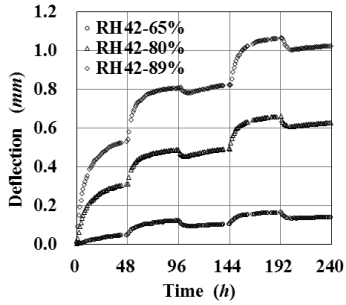

Fig. 7-2: Effect by *D*

Fig. 7: Effect of mutual actions by D & P on V-creep behavior by orthogonal expr. $L_9(3^4)$

During desorbing, since Δ_p is parallel to Δ_{sh*p}, there could be mutual promoting to produce large positive deflection Δ_{de} ($\Delta_{de}=\Delta_{sh*p}+\Delta_p$). But, of cause, there were no time *b* and T, and no orientation transferring in de-creep (Fig. 5b and Fig. 4-5~4-8).
Fig. 7 (out of Expr. 3) displayed the relationship of the mutual actions generally. When *P* was heavy, $|-\Delta_{ad}|$ was small, but Δ_{ad} was large. When $|-\Delta_{sw*p}|$ (i.e. $|-D|$) was large, $|-\Delta_{ad}|$ was large, but Δ_{ad} was small. And it was certain that Δ_{de} has a positive relationship with both *D* and *P*.

3.4 Influence by the changing moisture content on V-creep's behavior

Though the trajectory of the changing MC was not identical with that of V-creep (Fig. 3 and Fig. 5), the changing MC might increase or decrease the creep deflection during adsorbing or desorbing, as could not only change the quantity of Δ_p (Dong C. L., 2014) [13], but also increase or decrease the obstruction by Δ_p to $-\Delta_{sw*p}$ or Δ_{sh*p}.
On the other hand, though changing MC will arouse the swelling and shrinkage of the beam during V-creep, their quantity might be omitted. The experimental results pointed out that the swollen and shrined thickness under the humidity RH42%~80% for 2.5 cycles occupied only -0.63% and 1.27% separately of the total deflection of V-creep. Meanwhile, MC could hardly to change the trajectory of V-creep (Huang Y. X. and Zhang H. J., 2013).[14]

Conclusively, the physical influence by changing MC was only on changing a part of the quantity of the deflection, but D, P and their coupling and mutual actions determined not only the trajectories of V-creep, but also the most part of the deflection of V-creep.

3.5 Long term behavior of V-creep

Fig. 8 and Fig. 1 showed that $|-\Delta_{ad}|$ increased cycle by cycle during a long term v-creep, which was named by Hunt D. G. (1999)[3] as a "creep limit" (but still in argue). In view of the above mechanism, this phenomena could be explained that it was the result of the decreasing quantity of Δ_p with the developing of the creep, which always happens esp. in the early stage of either C-creep or V-creep, that made the obstruction by Δ_p to $-\Delta_{sw*p}$ reducing. It was this mechanism that led to the certain tendency of the equality between $|-\Delta_{ad}|$ and Δ_{de} which might happen at the end of elas-plastic creep.

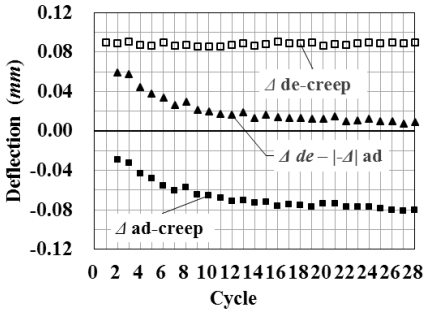

Fig. 8: Max. quantity of ad- and de-creep deflection of each cycle

3.6 The explanation for the creep behavior in the first adsorption

In general, the samples for testing of V-creep were always those that had been conditioned before. However, such condition would have made the most of prior produced deflection recovered and the bucked and crumpled fibre stretched, so that there left little compressed fibre to be transferred by the stress coupling into recovering and stretching. As a result, the positive creep of the softened beam with large deflection could always happened in the first adsorption, which usually situated in the very early stage of elas-plastic creep where the large deflection should happen originally and certainly. i.e. the mechanism of the positive creep always happened was the lacking of the object to be effected by stress coupling. However, more orientation of some other first ad-creeps could be determined by *D*, *P* and the location in the creeping period; and no more examples could be shown in this limited page.

4 Summary

It was the hygro-stresses (σ_{hygro}) including swelling stress (σ_{sw}) and shrinking stress (σ_{sh}) excited by adsorption or desorption, whose varying state could be represented by the difference of stepping moisture content ($\pm D$), and the load that aroused the bending creep behavior of solid wood beam in varying humidity. It was varying coupling of hygro-loading stress and the mutual actions between the stress coupling and loading that ruled such regularities as the trajectories, the essential and appearing orientation of the creep esp. those when adsorbing including the first one, the quantity of the appeared deflection, the tendency for the absolute deflection by adsorbing creep to be equal to that by desorbing creep due to the increasing of the absolute deflection cycle by cycle. The inner mechanism of this bending creep were: 1) either a part of the compressive deformation and bucked and crumbled fibre being compressed were transferred by the swelling-loading stress coupling into recovery of compression, stretching of the fibre and then tensing, or a part of the wood being tensed was transferred by the shrinking-loading stress coupling into the compressing; 2) the mutual negative obstructing or parallel promoting

created by both the stress coupling and loading which were affected by the changing moisture content.

Acknowledgments

Sincere thanks to all the supporters and helpers for this study.

References

[1] Armstrong L. D. and Christensen G. N. (1961) Influence of moisture changes on deformation of wood under stress [J]. Nature, 191(4791): 869-870.

[2] Montero C., Gril J. *et al*. (2012) Influence of hygromechanical history on the longitudinal mechanosorptive creep of wood [J]. Holzforschung, 66: 757-764.

[3] Hunt D. G. (1999) A unified approach to creep of wood [C]. Proc. R. Soc. Lond. The royal society, 455: 4077-4095.

[4] Takahashi C. Ishimaru Y., *et al*. (2004) The creep of wood destabilized by change in moisture content: Part 1: The creep behavior of wood during and immediately after adsorption [J]. Holzforschung, 58: 261-267.

[5] Hassani M. M., Wittle F. K., *et al*. (2015) Rheological model for wood [J]. Comput. methods appl. mech. engrg., 283: 1032-1060.

[6] Houška M., Koc P. (2000) Sorptive stress estimation: An important key to the mechano-sorptive effect in wood [J]. Mechanics of time-dependent materials, 4: 81-98.

[7] Hanhijärvi A. (2000) Advances in the knowledge of the influence of moisture changes on the long-term mechanical performance of timber structures [J]. Materials and Structures, 33: 43-49.

[8] Srpčič S., Srpčič S., *et al*. (2009) Mechanical analysis of glulam beams exposed to changing humidity [J].Wood Sci Technology, 43: 9-22.

[9] Svensson S., Köhler J. (2010) Including moisture induced stresses in the safety format of timber structure [C]. World conference on timber engineering (WCTE).

[10] Li T., Zhang H. J., *et al*. (2013) Static bending creep of solid wood beam under different moisture conditions [J]. Journal of southwest forestry university, 33(6): 82-85.

[11] Yu C. M. Numerical analysis of heat and mass transfer for porous materials: A theory of drying [M]. Beijing: Tsing Hua University Press, 2011.

[12] Hoffmeyer P., Davidson R. W. (1989) Mechano-sorptive creep mechanism of wood in compression and bending [J]. Wood sci. technol., 23:215-217

[13] Dong C. L. Quantitative analysis and design for bending modulus of elasticity of wood beams with gradient moisture content [D]. Ph.D. thesis (supervised by Zhang H.J. and Liu Y.X.). Hrbin, Northeast Forestry University, 2014.

[14] Huang Y. X., Zhang H. J., *et a*l. (2013) Creep of wood beams and its relationship with hygroscopic expansion in varying humidity. China wood industry, 27(3):9-12,24.

Proceedings of the 58th International Convention of Society of Wood Science and Technology
June 7-12, 2015 – Grand Teton National Park, Jackson, Wyoming, USA

Moisture and Heat Transfer in Cross Laminated Timber

Guizhou Wang, gwang16@ncsu.edu
Perry Peralta, pperalta@ncsu.edu
Phil Mitchell, pmitchel@ncsu.edu

North Carolina State University, 2820 Faucette Dr., Raleigh, NC 27695

Abstract

Due to the advantages such as superior fire, seismic, acoustic and thermal performance, excellent strength and stiffness properties and light weight, cross laminated timber (CLT) has been widely utilized in Europe and expected to have the potential to replace concrete, steel and masonry in low and middle rise residential and commercial constructions since its introduction in Switzerland in 1970s. Plenty of works have been conducted with regard to its design strategy, mechanical strength, fire resistance and other properties, while there are only limited studies of its diffusion properties, especially when considering the adhesive layers applied in the CLT panel. The goal of this study was to characterize the overall and adhesive layer's diffusion coefficient of moisture and heat transfer in 3-layer southern pine CLT panels. The influences of four commonly used adhesives, phenol formaldehyde resin (PFR), polyurethane (PU), emulsion polymer isocyanate (EPI) and melamine formaldehyde (MF), on the diffusion process had been studied here using the diffusion cup method. Nuclear Magnetic Resonance (NMR) was utilize to measure the moisture content dynamically and non-destructively in CLT panels with higher spatial resolution and lower system error. Diffusion coefficient was calculated based on the diffusion resistance model and inverse method.

Proceedings of the 58th International Convention of Society of Wood Science and Technology
June 7-12, 2015 – Grand Teton National Park, Jackson, Wyoming, USA

Analysis of Dimensional Stability of Thermally Modified Wood Affected by Wetting-Drying Cycles

Čermák, P. [1*] *– Rautkari, L.* [2] *– Rademacher, P.* [3]

[1] Postdoctoral Researcher, Department of Wood Science, Mendel University in Brno, Zemedelska 3, 613 00, Brno, Czech Republic.
* *Corresponding author*
xcerma24@mendelu.cz
[2] Assistant Professor, Department of Forest Products Technology, Aalto University, Tekniikantie 3, 164 00, Espoo, Finland.
lauri.rautkari@aalto.fi
[3] Research Director, Department of Wood Science, Mendel University in Brno, Zemedelska 3, 613 00, Brno, Czech Republic.
peter.rademcaher@hnee.de

Abstract

The dimensional stability of thermally modified wood exposed to several wetting-drying cycles was analyzed. Specimens of dimensions 15×15 ×15 mm^3 were thermally modified at 180 and 200 °C. The mass loss and chemical composition of the wood were determined in order to evaluate the effect and degree of modification. Afterwards, the radial, tangential, and volumetric swelling, anti-swelling efficiency and mass loss due to wetting-drying cycles were determined and compared. The specimen's mass tended to decrease with each additional rewetting cycle. Additional extractives that were formed via thermal decomposition leached out during wetting cycles. Thermal modification positively affected the dimensional stability of all investigated species. The wood's swelling was reduced, a result attributed to hemicellulose degradation. Dimensional stability was improved by 24 to 30% following mild treatment and by 26 to 54% following more severe treatment. When specimens were exposed to six consecutive rewetting cycles, the swelling of the modified wood increased, whereas it slightly decreased for the control (hornification). The effective dimensional stability of thermally modified wood was reduced by 34 and 28.4% for beech, 47 and 19.6% for poplar, and 19.3 and 24.5% for spruce compared to the initial anti-swelling efficiency following the first wetting cycle.

***Keywords*:** Thermal modification; Anti-swelling efficiency; Dimensional stability; Wetting-drying cycle; Chemical composition; Shape stability; Heat treatment

Introduction

Wood is a biodegradable, dimensionally unstable material. These fundamental properties of wood can cause problems when using certain wood products. Wood that is subjected to outdoor conditions, or even to humidity changes indoors, shrinks and swells, causing issues. Several common wood modification techniques are applied to fundamentally change the properties of wood (its bio-durability, dimensional stability, and others). Thermal modification of wood has long been recognized as a potential method to improve the natural properties of the wood and has been one of the most successful methods of modification for many years (Viitanen et al. 1994; Viitaniemi et al. 1997; Militz 2002; Hill 2006 and 2011; Čermák et al. 2014).

Heating wood to a relatively high temperature (160 to 260 °C) results in degradation associated with chemical changes in its structure (Esteves and Pereira 2009). If the process is controlled carefully, the properties obtained following thermal modification can be tailored for further use of the wood in specific applications. One of the most important characteristics of thermally modified wood is a decrease in its equilibrium moisture content (EMC) and, consequently, greater dimensional stability. Such reduction in the EMC has already been reported by Tiemann (1920), who showed that drying at high temperatures decreased the EMC of wood, inhibiting swelling and shrinking. The principal driver of the enhanced dimensional stability and reduced water absorption is likely a reduction in the number of hydroxyl groups of the hemicelluloses, as well as decreased accessibility of water molecules to cellulose hydroxyl groups due to the increase in cellulose crystallinity and cross-linking in lignin (Weiland and Guyonnet 2003; Hakkou et al. 2005). According to Militz (2002) and Tjeerdsma (1998), the dimensional stability of wood depends on the species, conditions of use, and the anatomical direction. Yildiz (2002) reported that the ASE reached 50% for beech wood treated at 200 °C. Tjeerdsma (1998) and Sailer et al. (2000) reported ASE values of about 40% for spruce and pine. Similar results were presented by Militz (2002) and Giebeler (1983), in which the ASE was determined to be 35 to 40% for pine and beech and 50% for poplar. Sailer et al. (2000) and Esteves et al. (2008) stated that the dimensional stability was greater in the tangential direction (by about 2.5%).

Nearly all of the thermally modified timber commercially available today is used for outdoor applications (i.e., cladding, decking, flooring, garden furniture, and others). These products are commonly exposed to cyclic moisture conditions during seasonal changes and the issue of dimensional stability of modified wood in these types of environments is of fundamental importance. Unfortunately, studies of the dimensional stability of thermally modified wood exposed to cyclic moisture conditions are scarce. The present study is therefore focused on the basic analysis of the dimensional stability of modified wood as affected by several wetting-drying cycles. The present study was conducted in order to evaluate material performance in such conditions.

Materials and Methods

Materials

Beech (*Fagus sylvatica* L., 0.72 g/cm3), poplar (*Populus alba* L., 0.39 g/cm3), and spruce (*Picea abies* L. Karst., 0.41 g/cm3) wood obtained from Czech forest enterprises were studied. Specimens of dimensions 15×15×15 mm were cut from a single log with the growth rings parallel to two edges. Afterwards, the specimens were sorted into three groups (control, modified at 180 °C, and modified at 200 °C). Each group consisted of 6 specimens. Prior to treatment, the specimens were conditioned in a climate-controlled chamber at 65% relative humidity and 20 °C, resulting in initial moisture content (MC) of 12±2%.

Methods

Thermal modification

Thermal modification (TM) was carried out using a small-scale laboratory heat-treatment chamber (Katres spol. s r.o., CZ) at 180 or 200 °C. The schedule of the five-stage thermal modification process throughout 50 h was achieved with a temperature control system as shown in Figure 1. In additional Figure 1 shows information about wet-and-dry-bulb thermometer, consists of two thermometers, one that is dry and one that is kept moist with water on a sock. Values gives an indication of atmospheric humidity i.e. psychrometer difference.

The maximum temperatures (180 or 200 °C) were maintained for 3 h. The mass loss (ML) of thermally modified specimens was determined immediately after the end of the modification process in order to evaluate the degree of the modification. The ML of the modified specimens was calculated as follows,

$$ML\ (\%) = (m_{u,O.D.} - m_{m,O.D.})/m_0 \cdot 100 \quad (1)$$

where $m_{m.O.D.}$ is the oven-dry mass of the specimens following thermal modification and $m_{u,O.D.}$ is the oven-dry mass of the specimens prior to thermal modification.

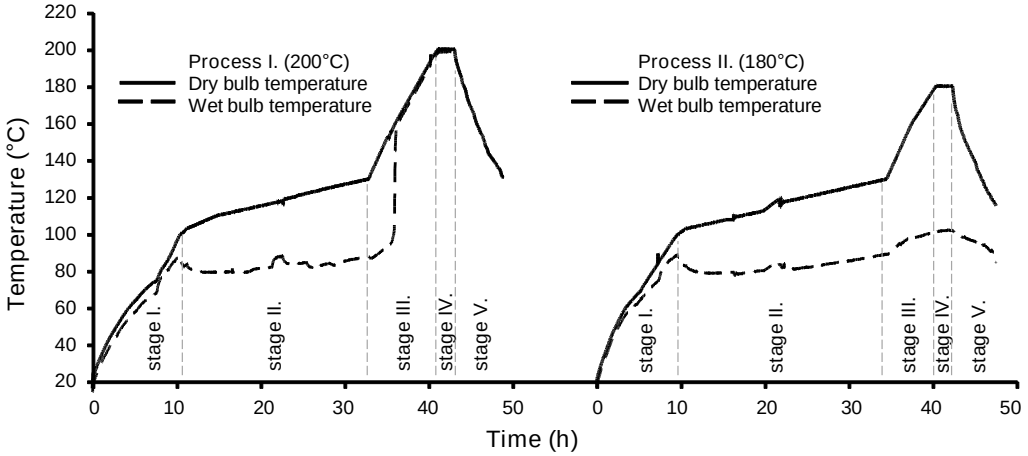

Fig. 1. Thermal modification processes at 200 and 180°C, including the dry-bulb and wet-bulb temperatures and stages

Wetting-drying cycles and dimensional stability

The dimensional stability was evaluated using a wetting-drying test until the difference between the previous two measurements was less than 1% (6 cycles). Selected specimens were submerged in water at 20 °C for 24 h for each cycle. The radial, tangential, and longitudinal dimensions and weights of the saturated specimens were determined. After wetting, the specimens were oven-dried to 0% MC in three phases (to prevent cracks from occurring). Phase (1) involved heating at 40°C for 24 h; Phase (2), at 60 °C for 12 h; and Phase (3), at 103 °C for 12 h. When 0% MC was reached, the specimen dimensions (to within 0.01 mm) and weights (to within 0.001 g) were determined. The entire wetting-drying cycle was repeated 6 times.

The radial (S_R), tangential (S_T), and volumetric (S_V) swelling, anti-swelling efficiency (ASE) and mass loss due to wetting-drying cycles were determined and compared

Results and Discussion

Mass Loss and Dimensional Stability after Re-wetting Cycles

An average mass loss during rewetting cycles was determined after each cycle, as shown in Figure 2, based on oven-dry weights. The specimens tended to decrease in mass with each incremental cycle. After six wetting-drying cycles, the initial mass decreased differently for each of the species studied. The highest mass losses were 1.5 and 2% for beech and poplar, respectively, and only 0.5 to 0.7% for spruce.
Thermal modification led to an increase in extractives content, which can leach out during wetting-drying cycles, resulting in decreased dry mass. The extractives content increased with treatment temperature, so the leachable content was expected to be higher at higher temperatures. The highest mass losses occurred following mild treatment.

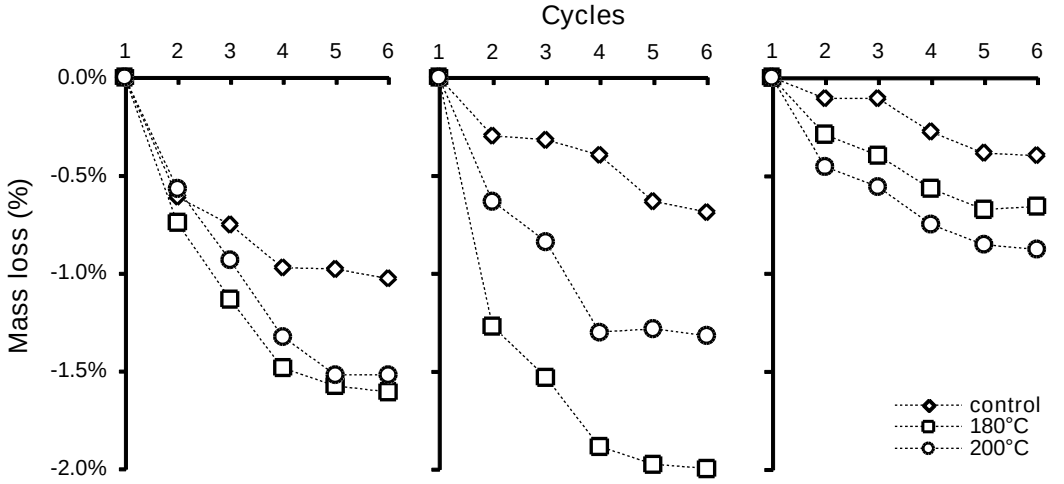

Fig. 2. Mass loss due to wetting-drying cycles exposure for control and thermally modified wood

Furthermore, the radial, tangential, and volumetric swelling of the investigated species, exposed to six wetting-drying cycles, are shown in Figure 3. The control (untreated) specimens had greater radial, tangential, and volumetric swelling than the thermally

modified specimens. Certain thermal modification processes decreased swelling via the degradation of the hemicelluloses with the -OH groups primarily responsible for the highly hygroscopic behaviour of wood. Burmester (1975) concluded that thermal modification of wood results in significant reduction of hemicelluloses content, thus improving the dimensional stability of the wood.

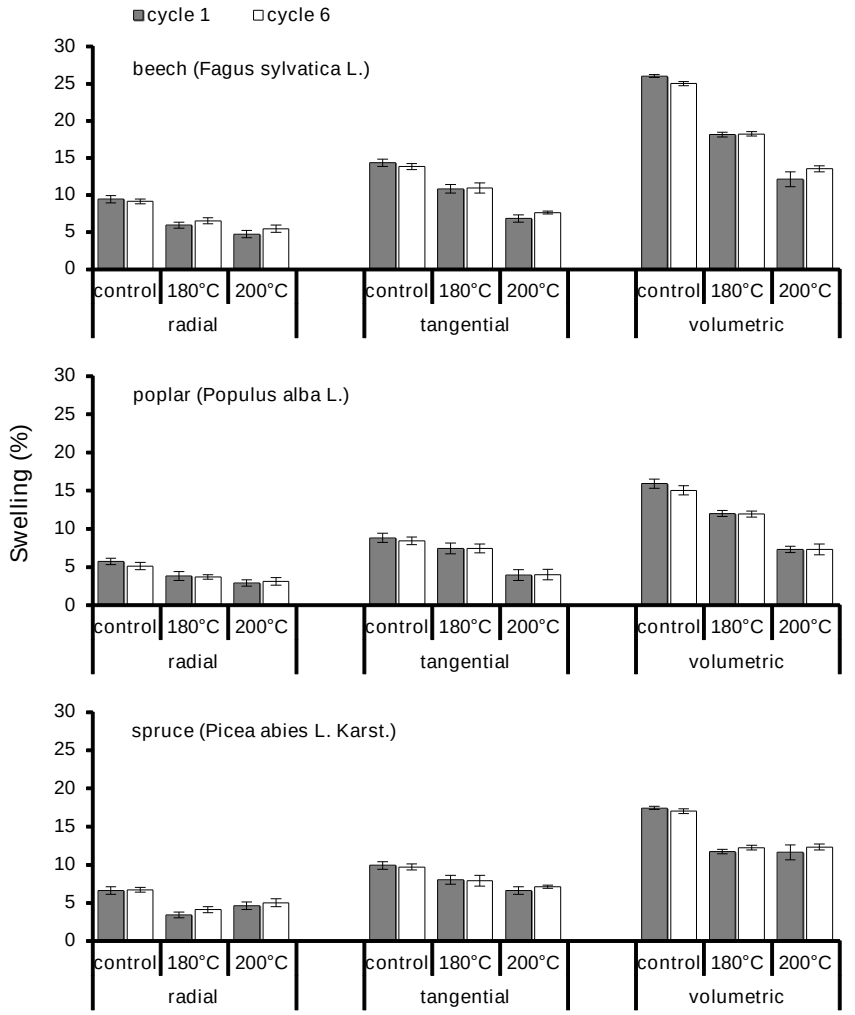

Fig. 3. The changes in the radial, tangential, and volumetric swelling of investigated species after first and sixth wetting cycle

After exposure to 6 wetting-drying cycles, the swelling of control specimens decreased slightly (2.1 to 3%), whereas that of thermally modified specimens increased (3.6 and 7.9% for 180 and 200 °C, respectively). The reduction of swelling in the control specimens was likely due to hornification (Matsuda et al. 1994; Park et al. 2006; Rautkari et al. 2013). According to Weise (1998) and Crawshaw and Cameron (2000), hornification occurs more readily with additional drying cycles. The higher swelling values after several rewetting cycles can be explained by the formation of extractives, which can leach out during soaking cycles, during thermal decomposition.

Even though several authors (Tjeerdsma et al. 1998; Esteves et al. 2007; Esteves et al. 2008) mentioned that swelling values are superior in the tangential direction, the present study did not reach such a conclusion. The severe treatment at 200 °C confirmed such results: the ratio of tangential-to-radial swelling was 1.52, 1.66, and 1.45 for the control specimens and 1.42, 1.30, and 1.43 for thermally modified beech, poplar, and spruce specimens, respectively. On the other hand, the mild treatment yielded ratios of 1.69, 2.03, and 1.95. Despite the more substantial dimensional changes following treatment at 200 °C, swelling anisotropy still remained in the thermally modified species investigated (Sailer et al. 2000; Esteves et al. 2008).

The anti-swelling efficiency (ASE) is the most common method used to evaluate the dimensional stability of modified wood. For each specimen, ASE values were calculated for each wetting-drying cycle, as shown in Figure 4. The dimensional stability improved in the species studied. The ASE was approximately of 24 to 30% following the milder treatment and 36 to 54% following the more severe treatment. The differences between the applied treatment temperatures were determined to be approximately 23 to 30% of the ASE, except in the case of spruce wood, for which the treatment temperature did not noticeably affect the ASE (only a 9.5% improvement). There were only slight variations in mass loss after both treatments. According to Fengel and Wegener (1989), hardwoods are less thermally stable than softwoods, which may explain why the ASE values of beech and poplar increased to greater levels than that of spruce.

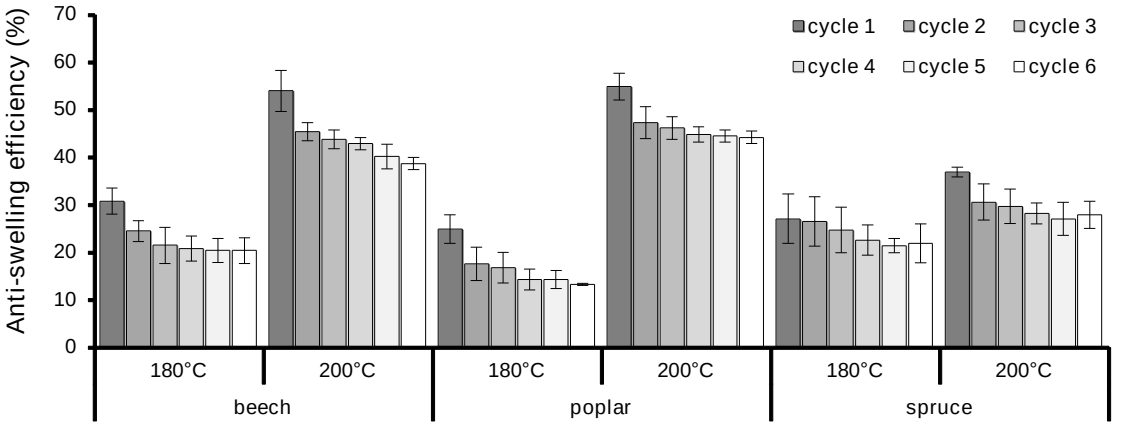

Fig. 4. Changes in the anti-swelling efficiency (ASE) of investigated species after six wetting-drying cycles

The ASE values declined as the specimens were exposed to six consecutive soaking cycles. The effective dimensional stability of the thermally modified wood was reduced by 34 and 28.4% for beech, 47 and 19.6% for poplar, and 19.3 and 24.5% for spruce, respectively, after pretreatments at 180 and 200 °C, compared to the initial ASE after the first soaking cycle. The highest decrease was observed after the first soaking cycle (an average of 17%). Moreover, the ASE decreased slowly and stabilized after five cycles. This decline was because some of the newly formed extractives leached out from the wood during rewetting, making more cell wall spaces accessible to water.

Conclusions

Thermal modification led to significant chemical changes, resulting in 2.8 to 10.4% of mass loss (species depended). Hemicelluloses were the most degraded wood component, while amount of extractives increased. Thermal modification significantly improved the dimensional stability of the wood. The radial, tangential, and volumetric swelling of modified wood decreased, resulting in 24 to 30% ASE following mild treatment (180 °C) and 36 to 54% following severe treatment (200 °C). When specimens were exposed to several rewetting cycles, the initial dimensional stability of the thermally modified wood was reduced by 34 and 28.4% for beech, 47 and 19.6% for poplar, and 19.3 and 24.5% for spruce for 180 °C and 200 °C respectively. Dimensional stability reduction following numerous soaking cycles can be partly attributed to the formation of leachable extractives within the thermally modified wood as a result of thermal degradation. This leaching rendered new regions within the cell wall accessible to water molecules. The control specimens underwent lesser swelling during rewetting cycles, which is likely due to hornification. This resulted in a reduction of -OH group accessibility after repeated soaking cycles. Although some of the phenomena observed in this study were explained, more detailed analysis of the -OH group accessibility of thermally modified wood exposed to cyclic conditioning should be done in the future.

Acknowledgements

This work was supported by the OP Education for Competitiveness European Social Fund and the state budget of the Czech Republic CZ.1.07/2.3.00/30.0031 Postdocs in Technical and Economical Sciences at MENDELU

References

Burmester, A. (1975). "Zur Dimensionsstabilisierung von Holz," *Holz Roh-Werkst* 33(9), 333-335. DOI: 10.1007/BF02612789

Čermák, P., Horáček, P., and Rademacher, P. (2014). "Measured temperature and moisture profiles during thermal modification of beech (*Fagus sylvatica* L.) and spruce (*Picea abies* L. Karst.) wood," *Holzforschung* 68(2), 175-183. DOI:10.1515/hf-2013-0047

Crawshaw, J., and Cameron, R. E. (2000). "A small angle X-ray scattering study of pore structure in Tencel® cellulose fibres and the effects of physical treatments," *Polymer* 41(12), 4691-4698.

Esteves, B., Domingos, I., and Pereira, H. (2008). "Pine wood modification by heat treatment in air," *BioResources* 3(1), 142-154.

Esteves, B., and Pereira, H. (2009). "Wood modification by heat treatment: a review," *BioResources* 4(1), 370-404.

Fengel, D., and Wegener, G. (1989). *Wood: Chemistry, Ultrastructure, Reactions*, Walter de Gruyter.

Giebeler, E. (1983). "Dimensionsstabilisierung von Holz durch eine Feuchte/Wärme/ Druck-Behandlung," *Holz Roh-Werkst.* 41, 87-94.

Hakkou, M., Pétrissans, M., Zoulalian, A., and Gérardin, P. (2005). "Investigation of wood wettability changes during heat treatment on the basis of chemical analysis," *Polym. Degrad. Stab.* 89(1), 1-5. DOI:10.1016/j.polymdegradstab.2004.10.017

Hill, C. (2006). *Wood Modification: Chemical, Thermal and Other Processes*, Wiley Series in: Renewable Resources, John Wiley & Sons.

Hill, C. (2011). "Wood modification: An update," *BioResources* 6(2), 918-919.

Matsuda, Y., Isogai, A., and Onabe, F. (1994). "Effects of thermal and hydrothermal treatments on the reswelling capabilities of pulps and paper sheets," *Journal Pulp Pap. Sci.* 20, 323-327.

Militz, H. (2002). "Heat treatment of wood: European processes and their background," in: Proceedings of conference on "Enhancing the durability of lumber and engineered wood products", February 11-13, Kissimmee, Orlando.

Park, S., Venditti, R. A., Jameel, H., and Pawlak, J. J. (2006). "Changes in pore size distribution during the drying of cellulose fibers as measured by differential scanning calorimetry," *Carbohyd. Polym.* 66(1), 97-103.

Rapp, A., and Sailer, M. (2004). "Oil heat treatment of wood in Germany - State of the art. Review on heat treatment of wood," Cost Action E 22, Proceeding of Special Seminar Held in Antibes, February 2004, France, 47-62.

Rautkari, L., Hill, C. Curling, S., Jalaludin, Z., and Ormondroyd, G. (2013). "What is the role of the accessibility of wood hydroxyl groups in controlling moisture content?" *J. Mater. Sci.* 48(18), 6352-6356.

Sailer, M., Rapp, A., and Leithoff, H. (2000). "Improved resistance of Scots pine and spruce by application of an oil-heat treatment," in: International Research Group Wood Pre, Section 4-Processes, NºIRG/WP 00-40162.

Sinner, M., and Puls, J. (1978). "Non-corrosive dye reagent for detection of reducing sugars in borate complex ion-exchange chromatography," *J. Chromatogr. A.* 156(1), 197-204.

Sinner, M., Simatupang, H., and Dietrichs, H. (1975). "Automatic quantitative analysis of wood carbohydrates by borate complexation chromatography," *Wood Sci. Technol.* 9(4), 307-322.

Tiemann, H. (1920). "Effect of different methods of drying on the strength and hygroscopicity of wood," in: *The Kiln Drying of Lumber*, 3rd Ed., Chap. 11, J. P. Lippincott Co.

Tjeerdsma, B., Boonstra, M., and Militz, H. (1998). "Thermal modification of nondurable wood species. Part 2. Improved wood properties of thermally treated wood," International Research Group on Wood Pre., Document no. IRG/WP 98- 40124.

Viitanen, H., Jamsa, S., Paajanen, L., Nurmi, A., and Viitaniemi, P. (1994). "The effect of heat treatment on the properties of spruce – A preliminary report*," International Research Group on Wood Preservation*. Document No. IRG/WP 94-40032.

Viitaniemi, P., Jämsä, S., and Viitanen, H. (1997). "Method for improving biodegradation resistance and dimensional stability of cellulosic products," United States Patent N° 5678324 (US005678324).

Weiland, J., and Guyonnet, R. (2003). "Study of chemical modifications and fungi degradation of thermally modified wood using DRIFT spectroscopy," *Holz Roh-Werkst* 61(3), 216-220.

Weiland, J. J., and Guyonnet, R. (2003). "Study of chemical modifications and fungi degradation of thermally modified wood using DRIFT spectroscopy," *Holz Roh-Werkst* 61(3), 216-220.

Weise, U. (1998). "Hornification: mechanisms and terminology," *Paperi ja Puu* 80(2), 110-115.

Yildiz, S. (2002). "Effects of heat treatment on water repellence and anti-swelling efficiency of beech wood," In: International Research Group Wood Pre, Section 4- Processes, NºIRG/WP 02-40223.

Zaman, A., Alen, R., and Kotilainen, R. (2000). "Thermal behavior of Scots pine (*Pinus sylvestris*) and silver birch (*Betula pendula*) at 200-230°C," *Wood Fiber Sci.* 32(2), 138-143.

Proceedings of the 58th International Convention of Society of Wood Science and Technology
June 7-12, 2015 – Grand Teton National Park, Jackson, Wyoming, USA

Analysis and Development of Green Roof Structures

Jerome E. Johnson

Professor, Engineering and Technology Department,
University of Wisconsin-Stout, Menomonie, WI USA.
johnsonj@uwstout.edu

Abstract

Green roofs, living roofs, and vegetative roofs are all synonymous with Norwegian torvtak, which translates to turf roof. The Scandinavian torvtak dwellings implemented two layers of turf (bottom layer green side down and top layer green side up) placed over multiple layers of birch bark. While some traditional torvtak construction methods are still used today, contemporary methods utilize membranes made of various synthetic materials. The depth of growth mediums delineates the difference between "extensive" and "intensive" green roof structures. Extensive roofs are usually less than 15 cm deep; intensive roofs range from 15-60cm. Vegetation for extensive roofs have typically been made of succulents, which tend to be drought resistant but do not add to the biodiversity of the roof. Alternatives such as native prairie grasses and mosses are investigated for their resilience and added-value. Costs for roofing materials and installation range from $110 to $134 per m^2 more for extensive green roofs compared to a conventional black roof made of Ethylene Propylene Diene Monomer. Vegetative roofs have a higher rate of evapotranspiration than conventional roofs made of impervious materials, thus reducing the temperature near the roof and the energy consumption for cooling a structure in the summer months. Experimental construction models initially showed effectiveness of the membrane, growth medium, and vegetation, as well as attractiveness to birds.

Keywords: vegetative roof, green roof, membrane

Introduction

Initial investigations into green roof structures by the researcher occurred while traveling throughout Norway in 2011 for a sabbatical visit. Throughout the countryside, vegetative roofs were seen on many residences, storehouses, and commercial structures. While tile and rock replaced sod as the dominate roof covering in the 19^{th} and 20^{th} centuries, romantics have revived the older tradition.

Classroom research related to green roof structures was directed by the researcher for undergraduate students in the fall semester of 2014. Students were expected to review the literature and standards for vernacular architecture and contemporary installations, calculate loads, evaluate various growing substrate, drainage, water proofing membranes and plant materials, and develop well-crafted, purposeful prototypes in order to conduct longitudinal tests. This research established a foundation for on-going investigation into the construction methods for various vegetative roofs.

Materials and Methods

During the Middle Ages and Renaissance, green roofs were used by royalty, especially in castles to provide insulation and retention of heat in the winter months. Long before this time, Norwegians had begun to use soil on their roofs and had found that planting green material such as grass and small shrubs would hold the soil in place and provide adequate insulation during the winter season. The earliest settlers of the Faroe Islands, who landed from Scandinavia in about 400AD, took this technology with them, creating a key part of the islands' distinctive architectural vernacular (Wilson, 2014). Brennan (2010) indicated that a traditional Scandinavian sod roof was built with sloping wood boards, overlaid with several layers of birch bark, and then covered with two layers of sod. The birch bark acted as a water- and soil-resistant layer, lasting an average of 30 years before needing to be replaced. The bottom layer of sod was installed grass-side-down, allowing the wilted grass to act as a drainage layer. The second layer of sod was installed green-side-up, and thus allowed the roots to eventually permeate the bottom layer to create one solid structure. The combined thickness of the two layers was approximately 15cm.

Maihaugen in Lillehammer, Norway is an open air museum with 200 old and new buildings, exhibitions, and authentic crafts (Maihaugen, 2015). Volunteers continue the tradition of roofing many of the buildings using birch bark and sod.

Membranes

Birch bark was used as the waterproofing membrane in Scandinavia since it was readily available and the bark was easily stripped from the trunk in spring or early summer. Care was exercised with the lengthwise incision so only the outer bark was pried loose. Removing the phloem would cause the tree to die, but removing the outer bark would leave only a scar. The sheets of bark were stored flat under pressure to prevent curling. The bark was laid white side down directly onto the roof boards without any means of fastening. The coarseness of the outer bark helped it adhere to the roof boards through friction. The inner brown side of the bark is smooth and impervious to water, thus it was placed facing up (Hennessey, 2007). Bark sheets were laid from the eaves upward, overlapping like shingles, and straddling the ridge. Six to eight layers of birch bark were considered adequate. The first layers projected about 8 cm along the eaves, where they curved down around the edge of the outer board to form a throating suitable for mitigating fast runoff. Methods in the latter 20th century of Norwegian storehouses included construction of log structures with board decking and a plastic, dimpled

drainage sheet that also served as a weatherproofing membrane and root barrier (Stugaard, 2015).

The weather-protection membranes used in contemporary installations in the United States may contain chemically organic materials such as bitumen or asphalt, which is the case with built-up roofs and some fluid-applied membranes. A root-protection barrier is necessary as the roots of the growing medium penetrate the organic bitumen. Polyethylene sheeting has been used for this purpose. A more robust membrane, promoted by Firestone Building Products, is Ethylene Propylene Diene Monomer (EPDM) (Firestone, 2015a). This single-ply, synthetic rubber roofing membrane has been used extensively for commercial flat roof installations due to its durability, flexibility, cost, and ultra violet light (UV) resistance. In non-vegetative installations, however, the traditional color of black has raised the sunlight and heat absorption of the roof. Thermoplastic polyolefin (TPO), or polyvinyl chloride (PVC), which are white, have been installed to help cool buildings by reflecting the sunlight. A multi-ply EPDM, which is black on the underside and white on the top, has also gain acceptance. TPO and PVC, like all polymers, are subject to UV and heat degradation and PVC leaches toxins. PVC plasticizers, which are required to make the material flexible, can break down by attracting mold or microbes, causing it to revert to its original solid state (Mendoza, 2015). For green roof installations, 60 mil EPDM has been recommended by professional installers (Biermeier, 2015) as it is made from inorganic material and cannot be broken down by bacteria. It must be adhered to the roof structure with a low volatile organic compound adhesive. The drawback to using EPDM, though, is that the common seam adhesion product is petroleum based bitumen adhesive. Another narrow sheet of EPDM is usually placed over each seam, therefore making it more difficult for roots to penetrate the membrane. Firestone also offers a polyurethane-based pourable adhesive, Sealer S-10, which contains no organic material.

Drainage

Aggregate was used as a drainage layer on roof pitches less than 2/12. Contemporary installation use a geotextile mat for separating the growing medium from the drainage area. Most mats are made from polypropylene or a polypropylene/acrylic blend. Some retain water at a storage capacity of 6 l/m2 (0.15 gal/ft2). This material was ideal for use on extensive roofs with slopes from 1:12 to 3:12. Other drainage methods include 1" thick waffled plastic sheet made of recycled polypropylene. The waffles, or dimples, rest on the membrane so the upper side of the sheet stores 7 l/m2 water (0.17 gal/ft2) and the lower space serves as a high-volume drainage passageway (Conservation Technology, 2015). Aggregate is not required under the waffled sheets and thus a significant reduction in dead load is achieved. The geosynthetic waffled sheet drain should have polypropylene non-woven separation fabric on its top side.

Growth Medium

Since 1995, the German professional association Forschungsgesellschaft Landschaftsbau Landschaftsentwicklung (FLL) (English: The Landscaping and Landscape Development and Research Society) has highly researched various areas concerning green roof design, including the "Vegetation Support Course" (FLL, 2002). Green roofs have usually been

categorized as either "extensive" or "intensive" roofs. The terms have been used to describe the depth of growing medium. Extensive roof generally have between 7.5cm and 15cm of medium. Intensive roofs are >15cm deep. The United States General Service Administration classifies four types of green roofs commonly found around the world. These are: single-course and multi-course extensive, semi-intensive and intensive. They vary in terms of the type of plant grown, their need for irrigation, the type of drainage layer used to carry away excess water, and the composition of the growth medium, or the soil in which the plants are grown (GSA, 2011). It is common practice to use the term extensive to describe green roofs that are very thin and will only support hardy, drought-resistant vegetation such as sedums, herbs, and perennials. Intensive is used to describe green roofs that are thick enough to support a wider range of vegetation including grasses, shrubs, and small trees.

While the primary considerations for substrate composition are largely concerned with sustaining plant growth, the allowable weight of the green roof system can often govern the composition and thickness of the substrate. This is especially pertinent for retrofit applications (Claridge, 2012). Typical extensive green roof growing media is comprised of 70% (by volume) 4–10 mm pumice, 10% 1–3 mm zeolite, and 20% organic matter at a 100-mm depth is recommended minimum to maintain plants without irrigation (excluding drought conditions) and minimize weeds while preventing runoff from storms with less than 25 mm of rainfall (Fassman et al., 2012).

Inclusion of polyacrymide gel into the growing material of crushed waste red brick 2-5mm in size and 20% organic material (composted garden waste mixed with conifer bark mulch),was suggested by Young, et. al. (2014) as a means to retain water, and thus increase root biomass and shoot growth. Plant biomass was substantially increased when green waste compost was used in higher concentration of the organic matter component instead of bark. These factors affected the evapotranspiration rates of the vegetative roofs under study. A higher rate of evapotranspiration led to greater cooling effect. Young (2014) cautioned, though, that when designing green roof substrate to promote greater plant growth in order to increase cooling from evapotranspiration, there may be a negative effect that higher evapotranspiration rates have upon the substrate water reservoir during times of drought. If this is depleted too quickly, leading to water stress and stomatal closure, plants no longer transpire at the same rate, mortality may occur and the net cooling effect of the green roof could be reduced.

Vegetation

The most prominent vegetative cover for green roof structures has been succulents including sempervivums, sedums, sempervivum arachnoideum and jovibarbas. Succulent plants have evolved special water-storage tissues in thickened or swollen leaves, stems or roots as an adaptation to the arid climates of deserts and semi-deserts. Many of these habitats are associated with high day-time temperatures and special mechanisms have evolved to collect and conserve the limited moisture that is available. Examples of leaf succulents include aloe, haworthia, and sempervivum. Stem succulents, which have fleshy stems and contain water storage cells overlaid by photosynthetic tissue include

most cacti, euphorbia, and obesa. Root succulents have swollen fleshy roots that store water underground and have stems and leaves that are often deciduous and shed during prolonged dry seasons. These include calibanus hookeri, fockea capensis, and pterocactus kunzei (Simply Succulents, 2015).

While sedums and other succulents are drought, heat, and wind tolerant, Kraf (2013) suggested that one of the plant's biggest failings is that it does not encourage biodiversity of plant species on the roof. Low-diversity mix of Sedum species often focused on ornament and minimized the potential for wider environmental benefits. Biodiversity is a measure of the variety of plants and animals in an area. Green roofs provide new habitat for beneficial plants and animals in helping to increase biodiversity. Increased biodiversity can help ecosystems continue to function even when they are disturbed by development or in other ways.

The GSA (2011) reported that prairie grassland was one of the few specific landscapes that have been recreated successfully on green roofs in North America. Extensive green roofs can mimic dry meadow grassland through their minimal supply of nutrients, quick drainage and sun exposure. Importantly, western short-grass prairies, like green roofs, have functionally shallow growing medium depths and restricted root space because annual precipitation rarely permeates deeply (Sutton, et. al. 2012). Gill et al. (2002) found root production in the short-grass prairie greatest in the top 20 centimeters of soil. Coffin and Lauenroth (1991) noted that the majority of blue grama (Bouteloua gracilis) roots grew within five centimeters of the soil surface and no deeper than ten centimeters. Skabelund (2011) observed some hairy grama (Bouteloua hirsuta), sideoats grama (Bouteloua curtipendula), and little bluestem (Schizachyrium scoparium) did not completely brown out on the west side of the Kansas State University Seaton Hall Green Roof even though they were not supplemented with water during July-October 2011.

Mosses have been found to survive quite well as a plant type for shallow growing medium, extensive green roofs. They require little soil and virtually no maintenance once they have been established. Mosses grow quickly and are cost-effective to install. They don't produce flowers and don't have actual roots that draw up any nutrients or water. Mosses have minute ducts that open when moistened and become dormant with the lack of moisture and then become active when moistened. Mosses do have chlorophyll and do photosynthesize regardless of the temperature, hence they remain green in color even in winter (Dwyer, 2009). The majority of mosses prefer no direct sunlight and prefer an acidic soil (pH between 5.0 and 5.5), which is why they are often found under and near pinus species. As they have no true roots, mosses will grow on logs, rocks and even on concrete or clay planters. This is accomplished by rhizoids that attach the gametophyte to the substratum and facilitate the absorption of minerals and water (Britannica, 2015). While the literature asserted that the primary role of rhizoids is in attachment to the substrate, the rhizoids of the endohydric moss Polytrichum have been shown to take up water from the substrate, though the importance of this route of water uptake is probably minor compared with uptake across aerial surfaces of the plant (Jones et. al., 2012). Many types of mosses will tolerate sun, however, all mosses do require humidity to thrive.

Structure

The dead load of a green roof assembly is based on the saturated soil weight and determined on a project-specific basis, because growth medium composition varies from job to job. ASTM E2397 is the established standard procedure for determining the dead and live loads associated with green roof systems. Roofmeadow® green roofs engineered to be both lightweight and efficient, generally weigh about 4,746 kg/m^2 (6.75 pounds per square foot) for each 2.54cm (1 inch) of media depth. Thus, the saturated weight of a 7.6 cm (3-inch) deep system is about 14,060 kg/m^2 (20 pounds per square foot), including a mature plant cover. Mid-range, 12.7 cm (5-inch), systems weigh approximately 166 kg/m^2 (34 pounds per square foot) and are compatible with wood or steel decks (Roofmeadow, 2015). Heavier intensive green roofs generally require a concrete supporting deck. The modular Firestone SkyScape Vegetative Roof System under full wet conditions. Maximum system weight after installation is slightly less at 156.2 kg/m^2 (32lbs/sqft) (Firestone, 2015b).

If people are not meant to walk on the roof then it is considered a landscaped roof and should be designed for a live load of 97.65kg/m^2 (20lbs/sqft). If people access the roof then it is a garden and designed for a live load of 488.2 kg/m^2 (100lbs/sqft). For more in-depth information, the ASTM (Standards E2397 and E2399) has published specific protocols for determining the weight and dead load of green roofs.

Extensive roof designs may be installed on roofs that are pitched to a maximum of 3/12 (3 units of rise per 12 units of run). While the rafters or trusses, ceiling joists, and wall studs of the superstructure for sloped roofs should be sized according to job-specific conditions, crucial components to the roof structure are the peat holder, commonly referred to as eave beam, and peat holder hooks or jacks (Norwegian:torvholdstokk og Torvholderkroker). The jacks are usually forged or bent steel at 90 degrees and are fastened directly to the roof deck and the outside of the eave beam. The membrane is placed over the jacks. A small gap between the eave beam and the membrane, equal in thickness to that of the jack minus the membrane thickness, is sufficient for water drainage under the beam. Typical Norwegian installations used gutter hooks (takrennekroker) to hang a birch log beneath the eave. This log slowed the water flow from underneath the beam. The logs were often slanted in one direction to direct the flow as well. Modern installations utilize various gutters.

Results

Experimental models were created to assess membrane, growing mediums, water runoff, and vegetative effectiveness. The researcher produced a stabbur (store house) for later use as a bird feeder. Construction details included redwood post and beam construction, ¼” exterior grade plywood roof sheathing, GAF StormGuard® self-adhering ice and water shield, sand and gravel substrate, and Dicranium flagellare and Dicranella heteromalla moss for vegetation. While the ice and water shield is a bitumen-based product, it was anticipated that the rhizoids would not penetrate during the feeders life

expectancy. Most all of the moss continued to grow through the first winter into the spring. Bare spots were a result of birds disrupting the moss before it had a substantial hold on the substrate. Leaks were not detected below the plywood deck.

Students developed an experimental model with rafters, eave beam, and spacers all constructed of redwood. On the peak of the roof acrylic was used for observation of the various layers. Ice and water shield was used on half of the structure as a membrane and birch bark was used on the other half. On top of the membrane boards were secured to the fascia boards with ½" holes drilled every six inches to act as a spacer for water to be able to flow under the growing medium. Gravel was placed on top of the membrane and held in place by the eave beam and spacers. A polypropylene sheet was placed above the gravel and organic growing matter with assorted seed was placed above the separation mat. The seed had not germinated at the time of writing and leaks had not been detected.

At the time of writing a shed with a 2/12 slope was being structurally retrofitted to accommodate an extensive roof. Additional rafters, ceiling joists and studs were spaced between the existing members. The oriented-strand-board (OSB) roof sheathing was replaced with 19mm (3/4") exterior grade plywood. New fascia was added and the eave beam was installed. The membrane of EPDM was adhered to the roof deck and fascia. There were no seams as the width of the EPDM extended from eave to ridge to eave. Polypropylene drainage mats were purchased and are awaiting installation. Growing medium and vegetation are to be transplanted from on-site.

Conclusions

One of the most significant benefits of a vegetative roof is extending the number of years typically needed before a roof must be replaced, as compared with conventional black rubber, asphalt shingle, and white roofs (GSA 2011). This is due to a green roof's vegetation layer and growing medium protect the roofing membrane from damaging UV radiation and from fluctuations in temperature extremes. Temperature fluctuations cause daily expansion and contraction in the membrane, wearing it out over time. The GSA (2011) study puts the average life expectancy of a green roof at 40 years versus 17 years for a black roof. The lifetimes of green roofs are difficult to predict because some do not need to be replaced even more than 50 years after installation.

Green roof installation costs per unit area decrease as size increases. The installed cost premium for multi-course extensive green roofs ranged from $110 to $134 per m^2 ($10.30 to $12.50 per square foot) more compared to a conventional black roof. The installed cost premium for semi-intensive green roofs ranged from $174 to $212 per m^2 ($16.20 to $19.70 per square foot) more compared to a conventional, black roof. Annual maintenance for a green roof is typically higher than for a black roof, by $2.26 to $3.33 per m^2 ($0.21 to $0.31 per square foot) (GSA, 2011).

During the summer, green roofs have a higher rate of evapotranspiration than conventional roofs made of impervious materials, creating a cooling effect on and around buildings. In both summer and winter, green roofs have an insulating effect on buildings, reducing peak heating and cooling demands in hot and cold seasons. This makes a smaller contribution to energy savings than the evapotranspiration effect.

Variations in growing medium can affect the ability of a green roof to promote biodiversity. Deeper growing medium provides a potential habitat for a greater number of plants and animals because of its increased ability to hold water and nutrients and its ability to accommodate plants with deeper roots. The shallow growth medium commonly used in extensive green roofs is less effective, as it intensifies the already extreme rooftop environment.

Intensive roofs require a professional roofing contractor, professional engineer, a large crew, and extensive material handling equipment for proper and lawful installation. The results of this research suggest that individual home owners can begin their own green roofs by starting with small bird feeders, pergolas, outhouses, and sheds, and then evaluate the aesthetic qualities and membrane effectiveness, before considering adding a green roof to a dwelling.

Structural wood components must be sized appropriately for extensive roof systems. If extensive green roofs become more prevalent on outbuildings, store houses, and even bird houses, there may be an increased demand for substantially larger framing, skeletal, and trim members.

The type of vegetation used is the most important factor in a green roof's ability to encourage biodiversity. Intensive roofs typically support a greater diversity of rare spider and bird species than extensive roofs, which are generally visited by more common bird species. Both types of roof attract a similar number of insect species (GSA, 2011). As succulents are most commonly used for extensive roofs and are quite ornamental, but do not contribute to the biodiversity of the roof system, additional research must be made in the United States into which native prairie grasses with small root depth and which mosses are most tolerant of threatening roof conditions and contribute to the biodiversity on extensive roofs.

Through proper planting schemes, the aesthetic value of structures with green roofs (Norwegian: Torvtak) can be greatly enhanced. Vegetative roofs can create exciting, visual and olfactory effects, which are intrinsic to human health and happiness.

References

Biermeier M (2015) TEK Roofing Company, Inc., Eau Claire, WI, Personal Communication.

Brennan A (2010) Green Building, old school: Scandinavian sod http://www.justmeans.com/blogs/green-building-old-school-scandinavian-sod. (2 November 1998).

Britannica (2015) http://www.britannica.com/EBchecked/topic/501471/rhizoid . (1 April 2015).

Claridge N, Edwards L (2012) Green Roof Technology – Research, Design and Implementation of a Green Roof at The University Of Canterbury. University of Canterbury Sustainability Office and the Department of Civil and Natural Resources Engineering http://www.sustain.canterbury.ac.nz/summer/Green_Roof_Technology.pdf . (31 March 2015).

Coffin D, Lauenroth W (1991) Effects of Competition on Spatial Distribution of Roots of blue grama, Bouteloua gracilis . Journal of Range Management 44:68–71.

Conservation Technology (2015) Green Roof Components http://www.conservationtechnology.com/greenroof_components.html . (31 March 2015).

Dwyer M (2009) Moss Gardening: A Low-Maintenance Option for Shade http://www.gardensmart.tv/?p=articles&title=Moss_Gardening. (11 December 2014).

Fassman E, Simcock R (2012) Moisture Measurements as Performance Criteria for Extensive Living Roof Substrates. Journal of Environ. Engineering, 138(8), 841–851.

FLL (2002) Guideline for the Planning, Execution and Upkeep of Green Roof Sites, Forschungsgesellschaft Landschaftsentwicklung Landschaftsbau .

Firestone (2015a) EPDM Roofing Systems, Firestone Building Products http://firestonebpco.com/roofing/epdm-roofing-systems/ . (1 April 2015).

Firestone (2015b) Skyscape™ Vegetative Roof Systems: Design & Installation Guide, Firestone Building Products. http://firestonebpco.com/assets/2014/07/skyscape-design-and-installation-guide.pdf . (1 April 2015).

Gill R, Burke I, Lauenroth W, Milchunas D (2002). Longevity and Turnover of Roots in the Shortgrass Steppe: Influence of Diameter and Depth". Plant Ecology 159:241.

GSA (2011) The Benefits and Challenges of Green Roofs on Public and Commercial Buildings: A Report of the United States General Services Administration. http://www.gsa.gov/portal/mediaId/158783/fileName/The_Benefits_and_Challenges_of_Green_Roofs_on_Public_and_Commercial_Buildings.action . (9 March 2015).

Hennessey T (2007) Entirely by hand ... From the ground up. Penobscot River Restoration Trust, http://www.penobscotriver.org/content/4060/birch-bark-canoe . (27 March 2015).

Jones V, Dolan L (2012) The evolution of root hairs and rhizoids. Annals of Botany, 110 (2):205-212 http://aob.oxfordjournals.org/content/early/2012/06/23/aob.mcs136.full . (12 April 2015).

Kraft A (2013) Why Manhattan's Green Roofs Don't Work--and How to Fix Them Scientific American, a division of Nature America, Inc. http://www.scientificamerican.com/article/why-manhattans-green-roofs-dont-work-how-to-fix-them/ . (31 March 2015).

Mendoza (2014) TPO: Getting Better With Age, TPO product manager, Firestone Building Products http://firestonebpco.com/content/uploads/2012/07/FINAL-2014-TPO-Technical-Paper.pdf . (4 April 2015).

Roofmeadow (2015) Details & Specs, Roofmeadow, Inc. Philadelphia, PA http://www.roofmeadow.com/details-specs-services/details-specs/ . (10 April 2015).

Simply Succulents (2015) Simply Succulents Nursery, Cable, WI https://www.simplysucculents.com/ . (10 March 2015).

Skabelund, L. 2011. Observations on the Kansas State University Seaton Hall Green Roof. Personal Communication.

Stugaard K (2015) Observations on the construction of the Stabbur in Hedalen, Norway Personal Communication.

Sutton R, Harrington J, Skabelund L, MacDonagh P, Coffman R, Koch G (2012) Prairie-Based Green Roofs: Literature, Templates, and Analogs, Journal of Green Building. 7 (1) https://agronomy.unl.edu/c/document_library/get_file?p_l_id=4128278&folderId=5114339&name=DLFE-65734.pdf . (10 April 2015).

Wilson M (2014) Why a rooftop garden makes environmental and economic sense. House and Home. http://www.ft.com/cms/s/0/76672710-5dd9-11e4-b7a2-00144feabdc0.html#axzz3XQTpnl5E (15 April 2015).

Young T, Cameron D, Sorrill J, Edwards T, Phoenix G, (2014) Importance of different components of green roof substrate on plant growth and physiological performance. Urban Forestry & Urban Greening, 13, (3) 507–516.

Proceedings of the 58th International Convention of Society of Wood Science and Technology
June 7-12, 2015 – Grand Teton National Park, Jackson, Wyoming, USA

Wood Solutions to Satisfy Energy Codes in Building Construction

Robert M. Knudson, bob.knudson@fpinnovations.ca
Jieying Wang, jieying.wang@fpinnovations.ca
Jean-Frederic Grandmont, jean-frederic.grandmont@fpinnovations.ca

FPInnovations, 2665 East Mall, Vancouver BC V6T 1Z4

Abstract

Buildings account for approximately 40% of energy use in most developed countries. In North America, the requirements for new buildings constructed after 2012 are expected to yield approximately 30% increases in energy efficiency. Targets will continue to ramp upward into the future. Developing wood-based solutions to meet the changing energy codes is an opportunity for the forest industry. FPInnovations, in collaboration with numerous partners, is working actively to meet these challenges. FPInnovations responded to the rapidly changing energy efficiency requirements for buildings across Canada and the United States by publishing guides to extend the building industry's existing design and construction practices. New wood-based insulation materials are also being investigated. An assessment of European dry process wood fibre insulation products for manufacture and use in North America has been carried out. Other research is exploring a new process for manufacturing rigid insulation products from pulp fiber. FPInnovations has been working on development of multi-functional, wood-based panel systems combining both structural and thermal insulation attributes. Short term work has focused on fabricating multi-functional panels from existing products. Longer term work will evolve to explore entirely new panel and other engineered wood products. To be successful, any new wood or wood-based products must function as part of building systems and at the same time be cost competitive.

Proceedings of the 58th International Convention of Society of Wood Science and Technology
June 7-12, 2015 – Grand Teton National Park, Jackson, Wyoming, USA

Easy Assembly Systems- Integration of Post-Tensioned Heavy Timber and Smart Architecture in Construction Practices

Zahra Ghorbani [1], Ben Hagenhofer-Daniell [2], Ryan E Smith[3]

[1] Research Assistant, College of Architecture + Planning, School of Architecture, University of Utah, SLC UT,USA
z.ghorbani@utah.edu
[2] Research Assistant Professor, College of Architecture + Planning, School of Architecture, University of Utah, SLC UT, USA
[3] Associate Professor, College of Architecture + Planning, School of Architecture, University of Utah, SLC UT, USA
rsmith@arch.utah.edu

Abstract

Digital modeling and manufacturing techniques in timber construction have matured in recent years. This computation has increased the potential for geometrically complex forms. Despite this advances, *assembly methods* for wood structures remain cumbersome with too much inefficiency in cost, materials, and scheduling. The environmental benefits of wood as a sustainable building material are well documented, yet sub-trades are often unfamiliar with heavy timber construction.
This project develops a new and easy method of Timber Assembly System. This Timber Assembly System (TAS) will be established through the confluence of two primary domains of research: 1) Structural system development including post-tensioned timber system development and assessment of wood properties and behavior. 2) Geometric system development including smart geometry, sequencing, and joinery detailing.
This project utilizes techniques from masonry and concrete construction, applied to the planar frame, wall, roof and floor systems in buildings, to presents new and innovative possibilities for timber assemblies. This system relies on smart geometry, the tendon to material location, and smart joinery. Furthermore, the structural system enables the use of demolition waste wood, small diameter logs, and beetle killed pine. This intelligent system of assembly will reduce labor and material costs while increasing the demand for timber specified in building construction.

Key Words: Easy Assembly of architecture, Post – Tension Timber, Smart Architecture, Digital Fabrication, Assembly System for Wood Building Material, Integration of Architecture and Structure and construction, Bio structural morphology.

Introduction

The increasing power of parametric modeling for a possibility of geometrically complex forms and digital fabrication in line with built environment are a milestone in the world of architecture and engineering. Design engineering has been developed as an interactive medium for collaboration between architects and structural engineers to innovate effective, sustainable method of construction. Thanks to design engineering, inefficiency in construction, the negative impact of site construction activities on the environment, cost of construction and schedule can be moderated. This approach leads to study on assembly system that is even recommended by National Research Council (NRC) to exploit the greatest potential, and advance the competitiveness and productivity of the U.S. construction industry in the next 20 years. (National Academies Press, 2009)

Theory of Easy Assembly System (EAS) with smart components through the post-tensioned structure can provide a new vision of flexible method to build complex geometries, and control construction issues. This research offers more controlled conditions, fewer job-sites environmental impacts, compressed project schedules, and reduce construction waste material. It focuses on how wood members could be assembled by post-tension or compression forces depending on its geometries. In the other words, it tries to create innovative architectural and structural techniques to build an immense structure efficiently depending on the eco-friendly material. In order to Integration of Post-Tensioned and Smart Architecture in wood structure, structure and smart geometries must be simultaneously considered.

Structure

Traditional Cordwood House and Log Construction are interesting a precedent to shape the foundation of this research, but it is matured by Post-Tensioned Laminated Veneer Lumber technology. Log building can be defined as stacking the logs horizontally to make walls. There are two different types of log house;

- Handcrafted: Handcrafted homes were usually built of large logs and chinking to fill and seal the spaces between logs. Skills of handcrafted can guarantee the quality of the structure. The cost for this sort of log house is almost high.
- Manufactured or machine milled: it is based on shaped and milled logs that make more opportunity to build a house with different types of profile, including interlocking tongues and grooves in the length of the logs and precise corner notches.

The point is finding proper notching technique for a corner of log in both types of log house to join member together accurately. The stability of the house is just related to the

type of corner joint. As much as the joints are accurate and precise, the walls will be fortified. The existing corner system;

- Butt & Pass: it is very simple and widely prevalent such that one log of a corner pair butts against the other log of the pair. And second logs are usually overhung outside the corner of the house to create a different pattern. Mortise & tenon detail improves corners to firmer and enough tight.
- Dovetail: precise cutting is required for fixed and stable model. Full Dovetail Notch, Half-Dovetail Notch, Square Notch, V-Notch, and Saddle-notch are different types of a dovetail joint.

Cordwood construction or cordwood masonry is a kind of stack wall construction, which cordwood or short pieces of logs are laid up crosswise with masonry or cob mixtures to build walls. The strangeness of cordwood walls is related to wood mortar adhesion. The depth of the grooves, the thickness of bumps or sharp edges will improve solidity and strength in the walls and eventually building. Same as traditional building, in transversely post-tensioned heavy timber, woods serve as mass, volume, and structure. So construction detail analysis, building performance, resource utilization, and manufacturing processes will all be relevant, but a system of threaded through rods is set up for shear wall to put members together and fix them. It performs like a synthetic tendon material, making it more flexible to utilize a far greater range of log sizes, shapes, and grades for most parametric curvilinear forms.

On the other exploration, many old traditional wood frame buildings have been found which still standing in the world, and it is hard to find much damage as a result of timber structural behavior. In the past, multi-stories timber structures have been used in the buildings that designed by bearing wall leading short span floors and beams, but new modern architecture required large open floor plans. Subsequently concrete composite flooring systems or alternative pre-stressed concrete slabs have emerged to span large lengths that needed larger section sizes to support beams and withstand floor loads. One point of Post-tensioned timber frames is capability of achieving long spans with thinner members in a firm, light and bearable structure.

The significant benefit of timber structure is Environmental Preservation. Wood structure offers the opportunity to provide sustainable building through its eco-friendly features and life cycle recyclability. Wood structures postpone releasing stored carbon in woods for decades or longer. New kind of timber products like laminated veneered timber is made from thin veneers of wood, which are glued together. Because LVL products are manufactured under controlled specifications, they much less likely than conventional lumber to warp, bend, bow, or shrink due to its composite nature. It proves how much they are stronger, straighter and more uniform than ordinary wood.

Post-tensioning techniques used to assemble structural engineered wood like LVL products for both frame and wall systems. College of Creative Arts (CoCA) at Massey University in Wellington is the preeminent building with post-tensioned LVL timber

frames, and Carterton Community Centre is another building that utilizing post-tensioned timber with LVL shears walls.

Additionally, assembly of post-tensioned heavy timber tries to exploit the real potential of an integrated CAD/CAM design/manufacture process in front of modern log construction that already exists. Post-tensioned heavy timber, when coupled with an integrated CAD/CAM approach can respond to contemporary architectural issues.

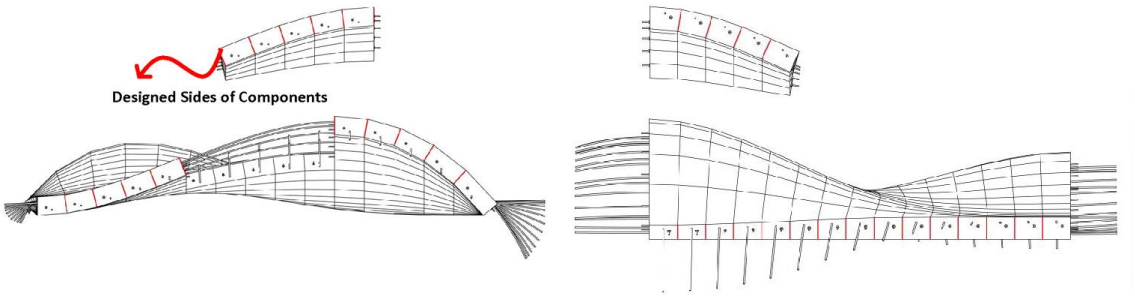

Figure 46, Models Generate based on Section of Components through External Post- tension Forces

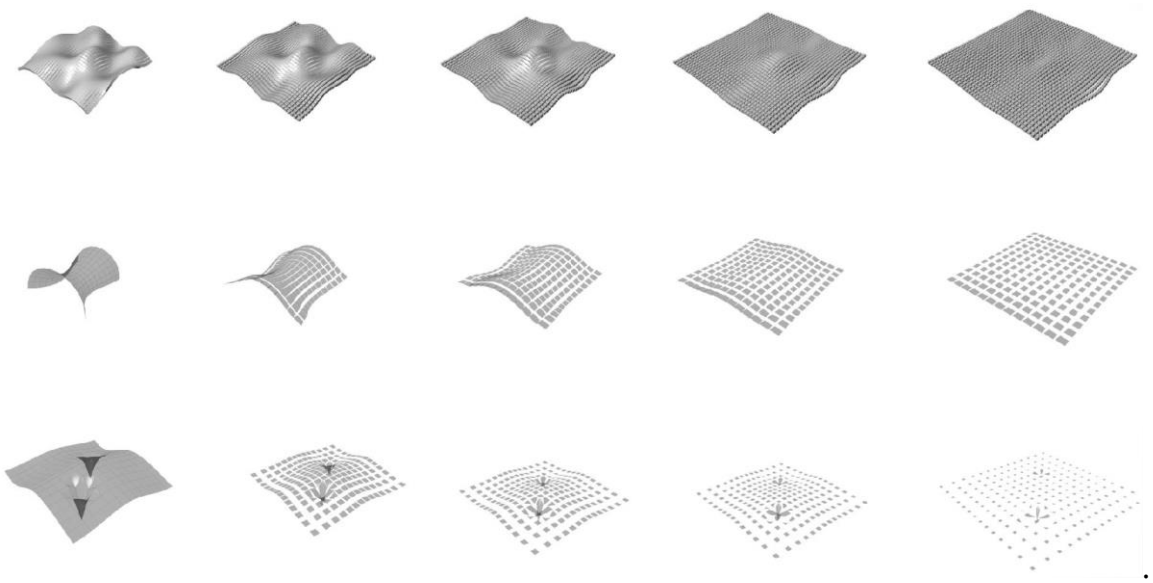

Figure 2, Models Generate based on Section of Components through External Post- tension Forces

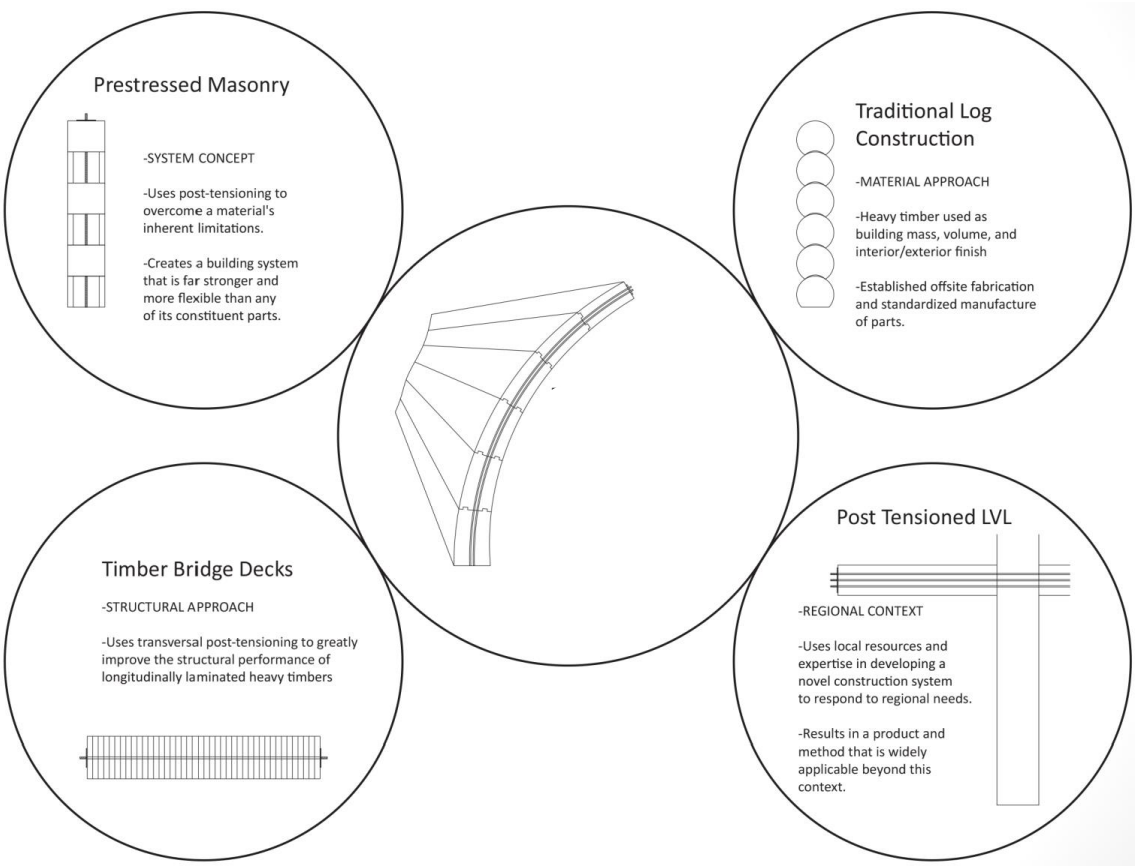

Figure 3, Transversally Post-tensioned Heavy Timber

Smart Geometries and Assembly

Study of self-assembly system and assembly sequence must be considered to support the aspect of the geometry and assembly sequence. Most of the self-assembly system research have done on the nature manufactures things. MIT's Self-Assembly Lab, directed by Skylar Tibbits, focuses on self-assembly and programmable material technologies for novel manufacturing, products, and construction processes. They believe that Self-Assembly is a method that ordered structure is built from disordered parts and local interaction. In this sort of aspect, they are exploring in the design and characterization of DNA tetrahedral, which can serve as rigid building blocks. It can act as molecular glue, as the fuel for molecular engines, and as a structural material in self-assembling nanostructures. Skylar Tibbits explains that the essential ingredient embedded within these natural systems is self-assembly, and he has applied same simulation in some interesting prototype modeling. It is an alternative vision for the future of construction, one that scales from the minutest of biological structures to the largest of infrastructures. This assembly system imagines what we have learned from the Industrial Revolution by slamming together the digital and physical worlds. This research is not

exploring in DNA or self-assembly system, but Tibbis's approach about design geometries, joints, and sequence of assembly was like guidance to rethinking about the geometry of components and appropriate force to provide easy assembly sequence that can be integrated with timber structure.

Human Body with its skeleton as an internal structure can be a good example of design in dynamic balance through tension forces. Vertebrae are the 33 individual bones that interlock with each other to form the spinal column. The Shape of the backbone and the geometry of the lumbar spine can be explained by the integration of all structural systems hard and soft, rigid and flexible in thin and thick geometries, those that tolerate pressure and those that resist it. The connection between vertebras can be studied as an outstanding designed joint. Spinal column joints are called facet joints linking the vertebrae together and give them the flexibility to move against each other. Between each vertebra is soft to absorb pressure and keeps the bones from rubbing against each other. Each vertebra is held to the others by groups of ligaments. Ligaments connect bones to bones. There are also tendons in the spine, which connecting muscles to the vertebrae. The whole structure is held together and moved by the muscular system; ligaments, membranes, tendon, and muscles, the whole network is in tension. A group of muscle that is in tension can keep extending and straightening limbs or joints.

So it might be said the post-tensioned model has some definition of extended and straight spine under the tension of muscles spine. The geometry of components based on designed side shaped final model and had a unique identity while their variations will be optimized like the bones of the vertebrae. Internal post-tension cable divides the components into different groups and works like Ligaments. So closest components are in the same situation are tied together. The benefit of this dividing is an easier way to assemble groups of component instead of some individual part. And then external post-tensioning system connects all together and shape steady model that is done by muscle in the spine.

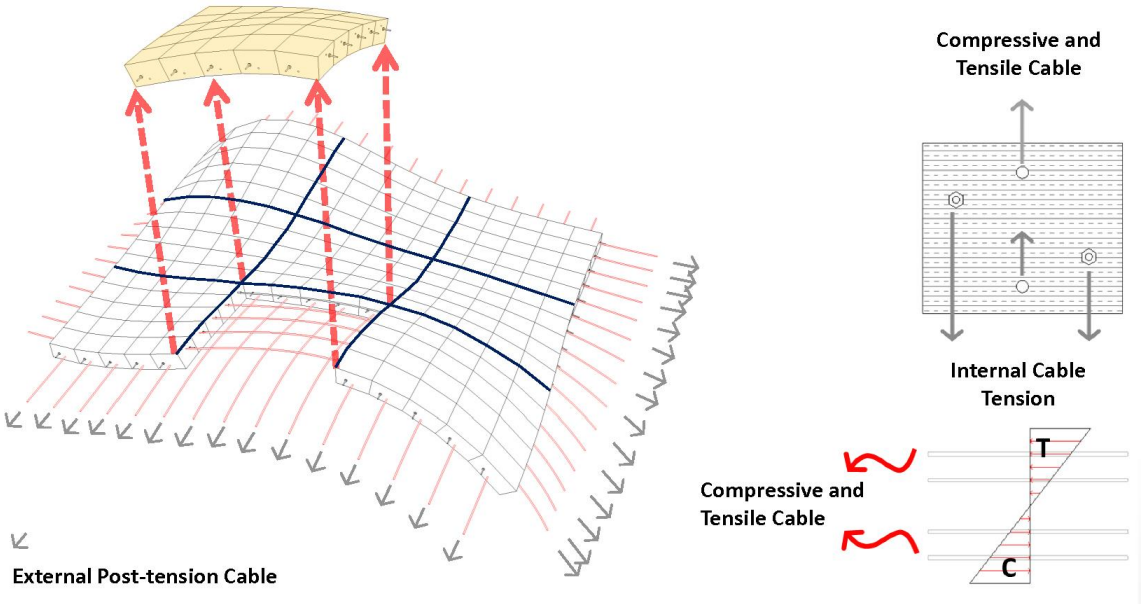

Figure 4, Internal and External Post- tension Forces

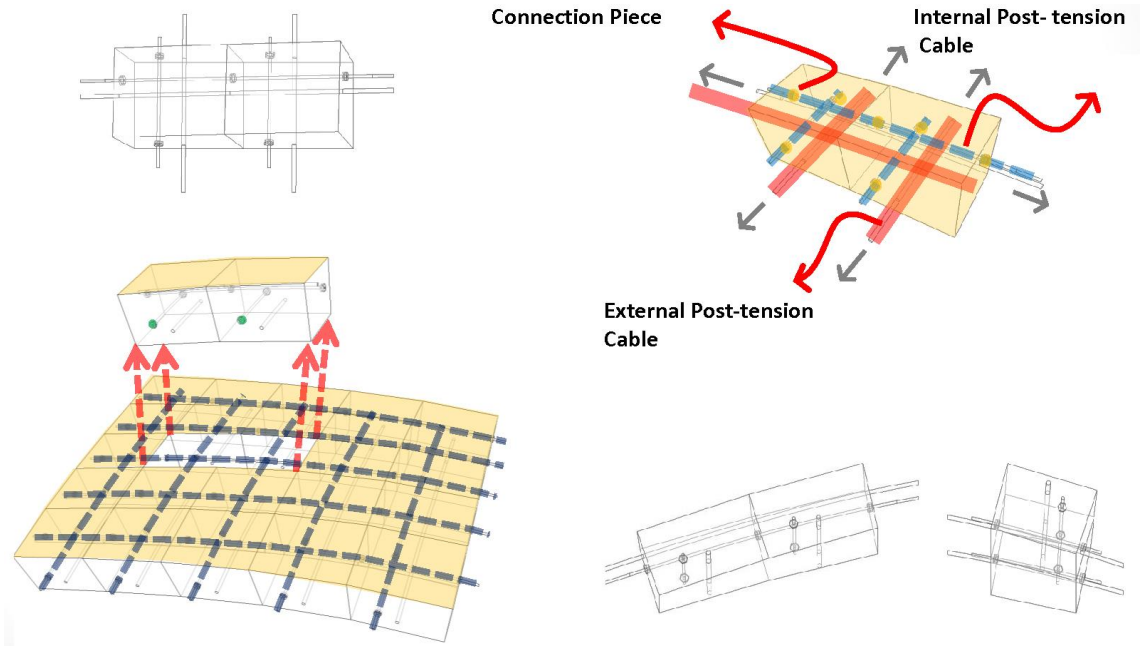

Figure 5, Internal Post- tension Forces and components

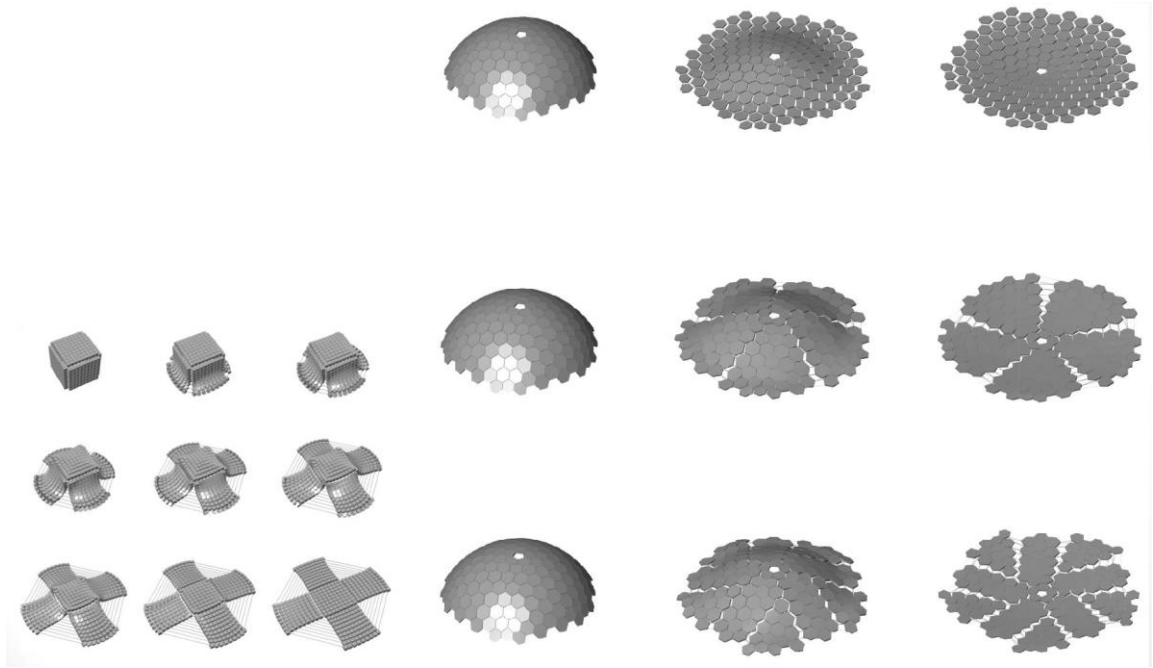

Figure 6, Easy Assembly, Figure out Different size for Group of Components by Internal Post- tension Forces, Activate Internal Post-tension Forces, Activate External Post- tension Forces

Design Challenge

The important point of the digital design- fabrication is providing more accuracy in the design model, details, and manufacturing.

- In case of elements to be connected to each other, any geometry can be corrected.
- The tolerances of production in construction are controlled accurately.

To design components, the points and surfaces where connections are made have to be adaptable and have to be designed in an easy assembly way. The detail of connections has to be accurately characterized, and the geometry and physical properties of all parts have to be well defined. It allows classifying components to optimize the different types. The best approach is to set a few basic parts and determine all other components by means of those few basic parts. Finding differentiation of these elements has to be done to group them only according to a specific principle and unnecessary differentiation is also avoided. Therefore, families of components can be assembled in an easier and faster sequence with similar tools.

It is possible to add a specifically designed element into the connection zone to assemble complex structures with minimum types of the group while having different connection elements. Moreover, it must be tried to control the number of element connections, and non-parallel the connection work. Since these flexible technologies have emerged, it is possible to assemble complex structures prior to the start of the construction work. Thus, by bringing the pre-assembled parts of the site, the huge cost of positioning, adjusting and fixing of small parts is diminished. On the other words, model optimization provides a low cost and quick construction with low environmental impact. So, in digital fabrication, components are designed clearly, simply and precisely. Then, Proper assembly sequence in one direction is considered to provide the easiest alignment instead of several orientations. It leads to finding minimum issues over handling, orientation and identification.
This paper has been written based on the basic idea that is under study and design. To reach our goal, applying this system in real construction, we must carefully monitor our methodology.

Phase 1

- Develop baseline structural performance criteria. Review existing log construction ICC code and previous empirical log wall research to determine what will constitute equivalent performance in a fully post-tensioned system utilizing regionally sourced beetle kill pine.
- Work with forestry, manufactured log home builders, and advanced timber fabricators to determine the range log lengths and thicknesses, as well as any geometric limitations. This would be based on the timber harvested, but more on the specific capabilities of timber milling and machining equipment and processes.
- Outline a digital workflow from design through to manufacture. Work through issues of interoperability. Determine what work is best done at what stage of

design/fabrication and with what software packages. The emphasis here will be on defining inputs and outputs that are native to, or compatible with, widely adopted and industry standard software.

Phase 2

- Build a full-scale prototype of an entirely post-tensioned wall system and analyze its performance relative to established baseline metrics for loads, creep, the necessity of re-tensioning, etc. Use this prototype to work through specific details of tendon materials and hardware.
- Develop necessary software tools (scripts, plug-ins, custom or off the shelf) to move from generalized 3D modeled forms to fabrication ready CAM files. The emphasis here is on variable geometry, both at the level of global form and at the level of individual components, which operates within the parameters determined in phase 1.

Phase 3

- Use the previously developed software tools to design and fabricate multiple full-scale prototypes that exercise the full range of formal possibilities. This includes walls of varying thickness, angle, curvature, etc. New structural issues (e.g. overturning) may come to the fore in some cases.
- Incorporate these empirically determined limits into established design software tools.

Phase 4

- Design and build a full-scale prototype transversally post-tensioned heavy timber shell structure. This should work through a set of by now very well defined constraints and attitudes of this novel structural system and attendant CAD/CAM tools.

Conclusion

Now the new theory of Easy assembly with smart wood components through the post tension system can combine existing methods of easy assembly system and post tension timber to bring a solution for practical constraint, and cover the lack of efficiency. Efficiency improvements are ways to cut waste in time, costs, materials, energy, skills, and labor while the building has the complexity and beauty of Architecture. Easy assembling system moderates between the enhancement of the architectural concepts and the optimization of structural designs to change the traditional construction approach and build our environment through creative academic solution and efficient, practical method.

References

1. Bonwetsch, Tobias. "Robotic Assembly Processes as a Driver in Architectural Design."*Nexus Network Journal*: 483-94.

2. Enns, Jonathan. "Intelligent Wood Assemblies: Incorporating Found Geometry and Natural Material Complexity." *Architectural Design*: 116-21.
3. Graham, D.A. Carradine, D.M. Bender, D.A. Dolan, J.D. (2010) "Performance of Log Shear Walls Subjected to Monotonic and Reverse-Cyclic Loading". *Journal of Structural Engineering* 136(1):37-45
4. Mora, Rodrigo, Claude Bédard, and Hugues Rivard. "A Geometric Modelling Framework for Conceptual Structural Design from Early Digital Architectural Models." *Advanced Engineering Informatics*: 254-70.
5. National Academies Press (2009) *Advancing the Competitiveness and Efficiency of the U.S, Construction Industry*. Washington, D.C.
6. Oxman, Rivka. "Informed Tectonics in Material-based Design." *Design Studies*: 427-55.
7. Roy, Robert L (1980) *Cordwood Masonry Houses: A Practical Guide for the Owner-builder*. New York, Sterling.
8. Roy, Robert L. *Stoneview (*2008) *How to Build an Eco-friendly Little Guesthouse*. Gabriola: New Society Publishers
9. space lab by kohki hiranuma architect & associates - designboom | architecture & design magazine (designboom architecture design magazine space lab by kohki hiranuma architect associates Comments)
10. Sarti, F., Palermo, A., Pampanin, S. (2012) "Simplified Design Procedures for Post-Tensioned Seismic Resistant Timber Walls." *Proceedings 15th WCEE, Lisbon*.
11. Seismic design: engineering wood | ArchitectureAU, http://architectureau.com/articles/seismic-design-engineering-wood/ (accessed April 16, 2015).
12. Tibbits, Skylar(2012) "Design to Self-Assembly." *Architectural Design*: 68-73.
13. Zhang, J.y., M. Ohsaki, and Y. Kanno. "A Direct Approach to Design of Geometry and Forces of Tensegrity Systems." *International Journal of Solids and Structures*: 2260-278.
14. Anatomy of the Spine: vertebrae, sacroiliac joints, cervical .., http://www.allaboutbackandneckpain.com/understand/anatomy.asp (accessed April 16, 2015).

Proceedings of the 58th International Convention of Society of Wood Science and Technology
June 7-12, 2015 – Grand Teton National Park, Jackson, Wyoming, USA

Design and Performance of Steel Energy Dissipators to be used in Cross-Laminated Timber Self-Centering Systems

Arijit Sinha, arijit.sinha@oregonstate.edu
Andre Barbosa, andre.barbosa@oregonstate.edu
Anthonie Kramer, anthoniekramer@gmail.com

Oregon State University, 234 Richardson Hall, , Corvallis, OR 97331

Abstract

A new alternative energy dissipation solution to be used with cross-laminated timber (CLT) self-centering walls is presented. CLT could potentially be used for high-rise construction. The development of high performance seismic design solutions is necessary to encourage innovative structures. The objective of this study is to investigate a connection system that is easy to install and replace (structural fuse), which is designed to be used with a self-centering CLT rocking wall. The proposed energy dissipators are fabricated following concepts used in developing steel Buckling Restrained Braces, having a milled portion which is designed to yield and is enclosed within a grouted steel pipe. The connection system is investigated experimentally through a unique test sequence of displacement controlled cycles based on a modified version of the test method developed by the American Concrete Institute to facilitate development of special precast systems. Digital Image Correlation was used to analyze strain behavior of the milled portion, as well as track movement of the panels during quasi-static uniaxial and cyclic testing. The results show the energy dissipation properties of the connection system. Damage was focused primarily in the energy dissipators, with negligible deformation and damage to the CLT panels and connections. These tests demonstrate the ability of these systems to be used as a viable energy dissipating solution in self-centering rocking or hybrid systems.

Proceedings of the 58th International Convention of Society of Wood Science and Technology
June 7-12, 2015 – Grand Teton National Park, Jackson, Wyoming, USA

Use of Virtual Visual Sensors in Obtaining Natural Frequencies of Timber Structures

Kristopher Walker, Kris.Walker@oregonstate.edu
Thomas Miller, Thomas.Miller@oregonstate.edu
Rakesh Gupta, Rakesh.Gupta@oregonstate.edu

Oregon State University, 900 SE Centerpointe Dr., Apt A303, Corvallis, OR 97333

Abstract

Many nondestructive methods of structural health monitoring are subjective in nature and largely based on visual observations of damage. Most current methods of objective data collection are limited to localized damage on the structure, rather than global response. Recent research involves the use of commercially available digital video cameras, or virtual visual sensors, to obtain structural dynamic behavior. This project focuses on the determination of natural vibration frequencies by monitoring the intensity value of a single pixel coordinate over the course of a few seconds of video of structural vibration and applying a fast Fourier transform to extract signal frequencies. Natural frequencies are used to calculate stiffness properties of materials and structural systems. The focus here is primarily on the application of the virtual visual sensor technique to timber structures. Experimentation focuses on verification of the method to extract vibrational frequencies in various scenarios, using naturally occurring color gradients in wood structures to achieve this analysis. Applications are made to in-use structures such as a US Forest Service pedestrian bridge to examine the potential usefulness of the technique to objectively infer structural health. Preliminary results show high accuracy in determining vibrational frequencies, and good use of naturally occurring color gradients in both lab and field tests.

Proceedings of the 58th International Convention of Society of Wood Science and Technology
June 7-12, 2015 – Grand Teton National Park, Jackson, Wyoming, USA

Treatments and Durability Session
Moderator: *Dodi Nandika, Bogor Agricultural University, Indonesia*

Non-Destructive Detection and Monitoring of Durability Issues in Full-Scale Wall Envelopes under Accelerated Weathering

Paul Frederik Laleicke, paul.laleicke@oregonstate.edu
Fred Kamke, fred.kamke@oregonstate.edu

Oregon State University, 119 Richardson Hall, Corvallis, OR 97331

Abstract

Many wood composites are known to poorly resist the effects of moisture and temperature extremes over time. Long-term experiments on small specimens are required to evaluate the durability and weather resistance of wood composites. Duration of testing and efforts to assess the performance of wood composites in full scale assemblies constrain the development of new products and applications. Accelerated weathering technologies have the potential to shorten the process of time-dependent effects of natural weather exposure and can be applied to simulate regional weather characteristic. The multi-chamber modular environmental conditioning (MCMEC) system at Oregon State University is capable of exposing full-scale wall elements to specific patterns of temperature, moisture and ultraviolet-radiation. Degradation and excessive shrinking and swelling alter the interfacial boundaries, a critical performance factor. Non-destructive approaches to detect and monitor weather related chemical and structural changes of the interfacial boundaries are acousto-ultrasonics and dielectric analysis. Based on the data and findings multi-scale models that allow the prediction of wood composite specific and climate related deterioration and alteration phenomena shall be developed.

The outcome of this study can drastically shorten the process of durability testing and clear the way for the development and placement of new wood composites.

Proceedings of the 58th International Convention of Society of Wood Science and Technology
June 7-12, 2015 – Grand Teton National Park, Jackson, Wyoming, USA

What is Fire-Retardant-Treated Wood?

David G. Bueche. [1*]

[1] Marketing Representative, Hoover Treated Wood Products,
Thomson, GA, USA.
* *Corresponding author*
dbueche@frtw.com

Introduction

August 2013, marked the 120th anniversary of the granting of US Patent 502,867 to Lina Schuler for a 'Fireproofing Compound.' Max Bachert, widely acknowledged as the father of the fire-retardant-treated wood (FRTW) industry, started pressure treating wood with Schuler's formula at the Electric Fireproofed Wood Company in New York during the early 1890's. The first commercial use of FRTW in buildings was reportedly made in 1895. From that time until the beginning of World War II, the industry was more or less localized in the New York – New Jersey area. The tremendous military demand for FRTW during the war expanded production nationwide.

Interest and demand for FRTW began to grow after the war as the insurance underwriting industry started rating FRTW equivalent to steel for fire insurance nationally. This was the result of tests conducted to emulate and evaluate the cause of the Hydra-Matic plant fire. These full scale tests changed the perception of fire performance of building materials by demonstrating to insurance underwriters and building and fire officials that no building material was immune to fire damage. The outcome was the promulgation of provisions for FRTW for use in lieu of noncombustible materials in the model codes.

As the success and demand for FRTW has grown, so have the number of products which would like to be regarded as FRTW. This paper will serve as an aid, answering the question *"What is fire-retardant-treated wood?"*

Fire, Treatment and Performance

Fire has been described as uncontrolled combustion. Combustion is defined as "a self-sustained, high-temperature oxidation reaction." Note that combustion does not require flames to be present. Non-flaming combustion includes glowing and smoldering combustion. The overall effect of combustion is an exothermic reaction. Reaction rates increase with increasing temperature, so the energy given off in an exothermic reaction can increase the reaction rate, resulting in the release of even more energy (heat).

The primary effect of heat on solid fuel is to decompose or pyrolyze the solid mass into molecules simple enough to combine directly with oxygen in a flame. Pyrolysis is the chemical degradation of a substance by the action of heat. The gases and vapors generated diffuse into the surrounding air, and can form a flammable mixture that can ignite and burn. Pyrolysis does not signify ignition which is the initiation of combustion.

While most solids must be pyrolyzed to burn, exceptions are the chemical elements. Since, by definition, an element is the simplest chemical substance, it cannot be broken down further. Charcoal is mostly carbon with smaller proportion of hydrogen and other elements. Elements including charcoal burn primarily by glowing combustion. In this type of combustion, chemical reactions occur directly at the surface, resulting in a glow.

Combustion in the absence of flame is referred to as either glowing or smoldering, depending on whether or not light is emitted. Continuous glowing is a property allowing a product to glow after the fire exposure has been removed. Smoldering refers to fire development in a product caused as the result of a long-term, low intensity heat exposure.

Flaming occurs earlier than glowing, progresses more rapidly, and is mainly responsible for the rapid spread of fire. Glowing assists in maintaining the production of flames and is the main factor contributing to the resistance of fire to extinction. Smoldering is the heart of the fire hazard problem due to its potential for transition to flaming combustion. There usually is a clear distinction between materials which may char under the influence of the ignition source, but which do not propagate further (non-progressive combustion) and those where smoldering develops in extent and spreads (progressive combustion).

How Wood Burns

As wood is heated, its temperature rises steadily according to the amount of heat applied to the wood and its own specific heat. At approximately 100º C, there is a pause in the temperature rise due to the rapid evaporation of the free water in the wood. Once the water has evaporated, the temperature rises steadily and a gradual chemical change begins, resulting in the decomposition of wood into volatile and solid constituents. This change is slight at first and below 200º C is indicated by a slight darkening of the wood.

Around 270 to 300º C, however, the action becomes very rapid, and because it is exothermic, the temperature rise accelerates causing the pyrolysis of wood. This process results in burnable gases such as methane, volatile liquids such as methanol in the form of vapors, combustible oils and resins, and a great deal of water vapor, ultimately leaving behind a charred residue, which is primarily carbon or charcoal.

When exposed to the air and a small ignition source, the vapors ignite and the wood begins to burn with the familiar flaming. This flaming liberates considerable quantities of heat so that continued distillation may be independent of the external heat source, and the fire begins to spread. The burning gases continue to heat the charcoal, and when the flame retreats it exposes the charcoal and the air, causing it to ignite and glow, furthering the release of large quantities of heat.

Wood cannot ignite unless it has pyrolyzed. This can be demonstrated by heating a small stick of wood. It has to discolor and turn dark before ignition is possible; however, the converse is not necessarily true. A piece of wood which has pyrolyzed so much as to turn into a black char may still never reach the right conditions for ignition. The process of combustion of charcoal, the solid phase in the pyrolysis products of wood, is essentially independent of the process of flaming combustion of the gaseous and liquid phases. At temperatures of approximately 230° C, wood can be reduced to charcoal without either flame or glow; between 230° and 465° C, wood chars and then is consumed by glow without flame; above 465° C, wood flames until the evolution of volatile combustibles ceases, and then glows until the charcoal is consumed.

Once heat is obtained from the burning wood, combustion may proceed without the addition of supplemental heat. Combustion is the mechanism of the transfer of the heat from the burning material to preheat the unburnt material which determines at what rate, if at all, the spread of burning will proceed. Wood by nature has a low thermal conductivity, which means the surface of a piece of wood can be heated until it bursts into flame, but there is a limiting rate at which the heat can be transferred to the interior of the wood. If the source of external heat is removed, the rate at which heat is radiated and conducted from the flame through the char to the unburnt wood is dependent on local exposure of the wood in the vicinity of the flame. Only a portion of the flame is transmitted back to the wood, and if this portion is insufficient to heat enough wood to maintain the supply of flammable vapors, flaming will gradually die down.

The burning of wood can occur in a primary mode, where visible flames are present from the combustion of flammable gasses, or in a secondary mode, where flames are absent. Flameless combustion is referred to as glowing or smoldering, depending on if light is emitted. Smoldering combustion may occur in the charred area or consume the entire specimen, proceeding as a front in the solid state rather than a flame in the gas phase.

Fire-Retardants

Wood cannot be treated so that it will be unaffected by heat; however, it can be treated so that it will not flame or glow, but merely char under the influence of heat, and therefore not assist the spread of fire. As the action is a chemical one, intimate contact of the fire retardants with the wood is necessary; meaning the wood must be impregnated.

Given flaming combustion and glowing combustion occur at different times and by distinctly different mechanisms, they may be expected to differ in the means by which they are controlled. Treatments may prevent flaming but fail to retard glow and vice versa. They must, therefore, be considered separately and are broadly classified as either flame retardants or smoldering retardants. Flame retardants refer to chemicals added so that the treated material will not support flaming combustion after the igniting flame is removed. Smoldering retardants refer to chemicals which effectively prevent smoldering combustion, which occurs after the igniting flame is removed.

Effective treatments influence the decomposition of wood under heat, increasing the yield of water and solid charcoal at the expense of the volatile hydrocarbons responsible for

flame. In fact, the yield of flammable volatiles is insufficient to give combustible mixtures in air and fire-retardant-treated wood consequently does not flame. Moreover, retardants raise the temperature at which the decomposition becomes exothermic. In addition, the denser charcoal is so modified that it will not glow under normal conditions. Various tests (ASTM 1993; ASTM 2007) consistently demonstrate that FRTW will be self-extinguishing of both flaming and glowing once the primary source of heat and fire is removed or exhausted. FRTW alone will not continue to burn unaided.

Performance of Materials in Fire

All building materials have their own peculiar properties when exposed to conditions of severe heat: wood burns, metals melt, and concrete crumbles. Heavy timber members burn slowly because of their size and can be exposed to a prolonged fire and still support their load. In the case of smaller members, structural failure is gradual as cross sectional areas are reduced in size.

Metal building materials are not combustible, yet they are subject to collapse in the early stages of a fire. As temperatures rise, steel loses strength rapidly and begins to weaken between 320º and 425º C. It does not take long to reach these moderate temperatures in a fire. Additionally, steel readily expands under the influence of heat. Often, this expansion pulls the building walls, floors, and roof down without warning.

At one time, roof assemblies were assumed to be fire safe if the deck and supports were constructed of metal, particularly when the fire hazard of the building's contents were considered low to moderate. This type of roof construction was classed as "non-combustible" even though the vapor barrier, insulation and roofing were combustible.

These assumptions were challenged on August 12, 1953, when a flash fire at the General Motors Hydra-Matic Transmission Plant in Livonia, MI, swept with lightning speed through the entire factory. The fire started at the floor level. The heat from the fire rose to the underside of the roof, heating the steel deck. The roofing materials began pyrolyzing, releasing combustible vapors that flowed under the roof covering entering the building through the seams in the steel deck. These vapors ignited and, within half an hour, began propagating an intense fire under the roof deck and inside the building. In only a few minutes, this 34-acre building, constructed entirely of noncombustible materials, collapsed completely, destroying both the building, and all of its contents.

By contrast, only 2 years later in the summer of 1955, a fire started in an exhaust duct of a plywood mill in Tillamook, OR. The fire swept both upward and downward over the roofing material on the outside of the building, stimulated by a strong wind (Anon 1956). This structure was one of the 17 large wood hangars constructed during World War II by the US Navy to house blimps used to patrol both coasts against attack by submarines. These 1,000 feet long, 170 feet high, by 296 feet wide structures were constructed of FRTW heavy timber wood arch trusses (Anon 1943; Smith 1944).

Altogether, this fire burned over 40,000 square feet of roofing, or about one-tenth of the roof area. Approximately 3,000 square feet of 2-inch roof planking was charred through,

and eventually about 15,000 square feet of the planking was replaced. No structural damage occurred to the rafters, purlins, bracing, or other parts, despite the fact that the flames swept through a charred hole in the roof (Anon 1956).

Realizing they weren't protected against major loss, even though noncombustible construction materials cannot burn, many fire insurance companies sought a performance standard for all types of materials. Companies supporting Factory Mutual Engineering Services asked for full-scale testing of materials.

Full-Scale Testing

Beginning in 1953, Factory Mutual Engineering Division (FMED 1955) developed what is referred to as the 'White House' test, a full-scale procedure developed to replicate the disastrous Hydra-Matic fire. Engineers designed the test to determine why the fire progressed so quickly below the roof assembly that had a noncombustible surface. Original testing evaluated similar, if not identical, materials to the Hydra-Matic building. The test structure was a 100 feet long by 20 feet wide, and subjected the exposed underside of a roof construction to a standard ignition source duplicating the ASTM E119 time temperature curve in the first 20 feet of the structure. The edges of the roof were sealed tightly to prevent pyrolysis vapors from venting prematurely. This made it possible to replicate a real-world fire exposure for most large commercial and industrial buildings, revealing more information about how fires grow and propagate.

The fire tests were divided into two parallel tests using identical test samples each time. A full-scale test was made to provide information indicative of the performance of the flat steel roof deck construction with various combustible materials on the upper surface. The principle purposes of this test were to determine the extent these combustible materials contributed to the spread of the fire, the smoke inside the building, and the building collapse. These large scale tests used a structure designed and constructed to be representative of a portion of a steel frame metal roof deck type of building incorporating the extent of restraint of structural members as in actual buildings. Tests (Thompson and Cousins 1959) were also made with identical samples in the small-scale FM Construction Material Calorimeter in order to correlate full-scale tests with the small-scale tests.

Based on the performance of fire retardant treated wood in the Tillamook fire, Thomson (1957) conducted a full-scale test at Factory Mutual Engineering to determine if "fire retardant type" lumber on the large roof deck structure would qualify as Class I. Class I, by definition, is a metal roof deck construction with no greater rate of heat contribution within a building than would be obtained from a deck consisting of plain vegetable fiber insulation, mechanically fastened to a steel deck, with no asphalt or other combustible adhesive between. Constructions of greater heat contribution are considered as Class II and generally require protection by automatic sprinklers.

Results demonstrated that fire-retardant-treated lumber performed equivalent to Class I decks for exposures not exceeding 30 minutes (Figure 1 and Table 1) with respect to heat contribution. The test also showed that "fire retardant type lumber does have other qualities of merit. The time delay afforded over unprotected lumber, the elimination of glowing combustion after withdrawal of exposure, the absence of obscuring smoke, and the prevention of structural collapse over the exposure fire for more than one hour are commendable factors."

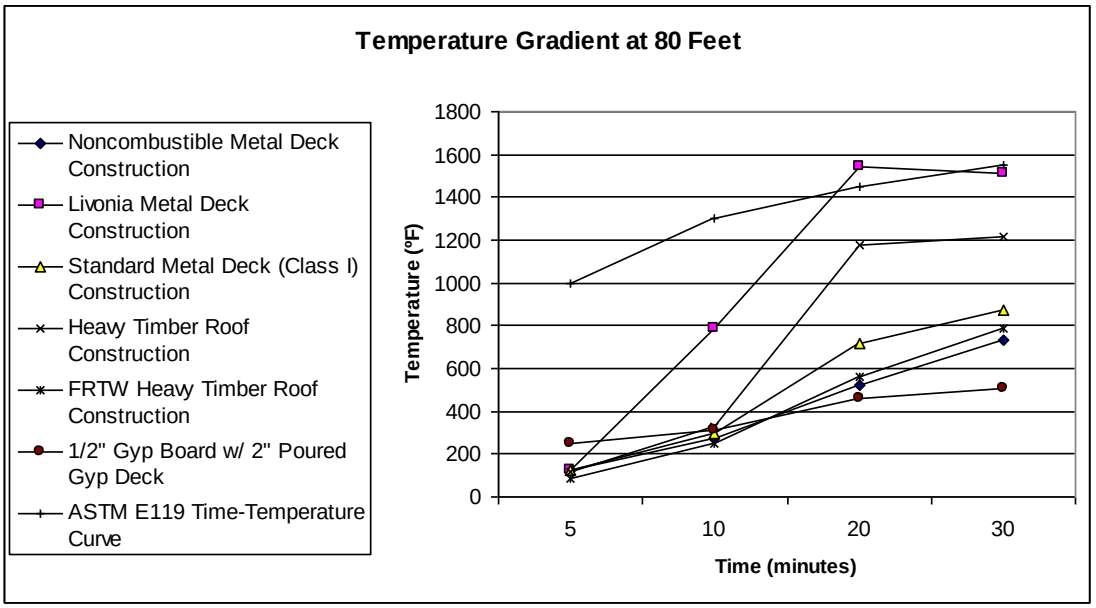

Figure 1. 'White House' test results (FMED 1955; Steiner 1955; Thomson 1957).

The method was so successful that other laboratories have used it for testing certain types of roofing material and decks, including Underwriters' Laboratories, Southwest Research Institute, and Omega Point Laboratories.

Table 1. Structural Roof Deck Assemblies Evaluated with FM Construction Materials Calorimeter (Wilson 1966)

	Maximum Average Rate of Heat Contribution (BTU/Ft^2/Min) For Various Time Intervals			
Structural Roof Deck Description	3 min	5 min	10 min	30 min
Treated 2" Douglas fir (Tillamook Hangar)	323	318	299	246
Untreated 2" Douglas fir	474	447	381	358
¾" Treated Plywood	325	293	275	245
Standard for FM Class I Insulated Metal Deck	385	365	340	270
Unclassified Insulated Metal Deck (Livonia)	1583	1531	1203	701

Steiner (1936) at Underwriters' Laboratories, first utilized a tunnel as part of his fire protection engineering thesis titled, "Investigation of Effectiveness of Fireproofed Red

Oak and Maple Lumber." Later Steiner (1943; 1944) adapted his tunnel for measuring and classifying the fire hazard of building materials including the classification of chemically impregnated lumber and plywood to reduce fire hazard. This tunnel has become the best known and most widely used large-scale test for classifying the burning characteristics of building materials with a 10 minute test duration (ASTM 2015).

Steiner (1955), again at Underwriters' Laboratories, utilized the full-scale 'White House' test structure to evaluate roof deck constructions. Steiner found that the results of tests in the full-scale structure conducted at UL, in addition to the full-scale tests conducted at Factory Mutual, correlated well with performance in the tunnel. As a result, UL began listing 'Fire Investigated,' UL's version of Class I roof constructions, in 1957 using the Steiner Tunnel. Two of the first listings were for chemically impregnated wood, i.e. NM501 for ¾ in. fire-retardant-treated plywood roof decks and NM502 for 1 inch fire-retardant treated lumber roof decks. The test method was later standardized and published by Underwriters' Laboratories as UL 1256 (2013) and ULC S126 (2014).

These tests at Underwriters' and Associated Factory Mutual Laboratories conducted for their affiliated fire insurance organizations assisted in setting insurance rates for the use of wood in construction. At the request of several insurance rating bureaus, UL wrote a performance standard for FRTW with required test method and conditions of acceptance. It covers wood products that are impregnated (filled or permeated thoroughly) by either pressure treating after the product has been manufactured or mixing intimately with the wood during manufacture of the product as discussed by McDonald (1970).

This new performance standard for FRTW prompted the testing of two full-scale 'White House, tests in 1963 to validate performance of ¾ inch fire-retardant-treated plywood and 1 inch fire-retardant-treated lumber roof decks in the 20-ft wide by100-ft long test structure (Malcomson 1964). Performance in the full-scale 'White House' test once again substantiated the results in the tunnel, and as a result, the 30-minute ASTM E84 test is now referenced for FRTW in all the current model building codes. This increase in exposure to 30 minutes for FRTW in the ASTM E84 apparatus and labeling by UL (Malcomson and Bono 1967), enabled it to be differentiated from other building materials that obtain only a 'flame spread rating' in the 10 minute test.

Summary

For more than 120 years the wood preserving industry has produced wood pressure impregnated with fire retardant salts to enhance its performance in fire. FRTW does not support combustion and there is no significant glowing after flames are removed. Also, fire-retardant treatments substantially reduce the combustion rate of wood while limiting flame spread. One of the most important aspects to remember is this: Pressure impregnated fire-retardant-treated plywood was developed as an alternative to metal roof decks and has demonstrated equivalency to steel in fire tests based on fire experience under actual fire conditions; it is given comparable insurance rates, and FRTW roof

systems are suitable for the same uses. Conversely, products which claim to be the same as fire-retardant-treated plywood have not been tested in the full scale test and their performance has not been evaluated in comparison to the Fire Classified unprotected metal deck.

References

Anon (1943) Fireproof lumber construction by U.S. Navy (1943). Wood Preserving News, May, 54-57.

Anon (1956) Everybody said: 'There she goes!' But she didn't. Wood Preserving News, May, 6-9.

ASTM (1993) E60-80 Test method for combustible properties of treated wood by the crib test. American Society for Testing and Materials, West Conshohocken, PA.

ASTM (2007) E69-02 Standard test method for combustible properties of treated wood by the fire-tube apparatus. American Society for Testing and Materials, West Conshohocken, PA.

ASTM (2014) E119-14 Standard test methods for fire tests of building construction and materials. American Society for Testing and Materials, West Conshohocken, PA.

ASTM (2015) E84-15 Standard test method for surface burning characteristics of building materials. American Society for Testing and Materials, West Conshohocken, PA.

FMED (1955) Insulated metal roof deck fire tests. Factory Mutual Engineering Division, Associated Factory Mutual Fire Insurance Companies, Norwood, MA.

McDonald CE (1970) Fire retardant hardwood plywood. Wood Preserving News, April, 6- 9, 12, 14 & 15.

Malcomson RW (1964) Report on roof deck construction NM-501 (File R4859, Assignment 63K3955). Underwriters' Laboratories, Chicago, IL.

Malcomson RW Bono JA (1967) Underwriters' Laboratories, Inc. Issues new labels for FRTW. Wood Preserving News, September, 24-25 & 27.

Smith WH (1944) Fireproofed wood for airship hangars. Proceedings of the American Wood Preservers Association, 40, 17-24.

Steiner AJ (1936) Investigation of effectiveness of fireproofed red oak and maple lumber. MS Thesis, Armour Institute of Technology, Chicago, IL.

Steiner AJ (1943) Report on fire hazard classification of Douglas fir and southern yellow pine impregnated with chromated zinc chloride *(CZC)* (Retardant 2755, Application No. 41C1373). Underwriters' Laboratories, Chicago, IL.

Steiner, A. J. (1944) Fire hazard classification of building materials. UL Bulletin of Research Number 32. Underwriters' Laboratories, Chicago, IL.

Steiner AJ (1955) Summary of comparative fire performance of two types of roof deck constructions (File R3796, Assignment 54C6305). Underwriters' Laboratories, Chicago, IL..

Thompson NJ (1957) Examination of Protexol fire retardant lumber on 100 ft x 20 ft test structure (Laboratory Report No. 13159-924). Norwood, MA: Factory Mutual Engineering Division Factory Mutual Laboratories.

Thompson NJ Cousins EW (1959) The FM construction materials calorimeter. NFPA Quarterly, 52(3), 186-192.

UL (2013) 1256 Standard for fire test of roof deck constructions. UL, Northbrook, IL.

ULC (2014) S126 Standard method of test for fire spread under roof-deck assemblies. Underwriters' Laboratories of Canada, Toronto, Ontario Canada.

Wilson JA (1966) Fire retardant treated lumber and the FM construction materials calorimeter. Proceedings of the American Wood Preservers Association, 62, 205-212.

Proceedings of the 58th International Convention of Society of Wood Science and Technology
June 7-12, 2015 – Grand Teton National Park, Jackson, Wyoming, USA

Fungal Pretreatment of Genetically Modified Black Cottonwood - Merging Novel Low-Input Fungal Pretreatment with Next-Generation Lignocellulosic Feedstocks

Charles Edmunds, cwedmund@ncsu.edu
Vincent Chiang, vincent_chiang@ncsu.edu
Ratna Sharma-Shivappa, rsharm2@ncsu.edu
Perry Peralta, pperalta@ncsu.edu
Ilona Peszlen, impeszle

North Carolina State University, 2820 Faucette Blvd, Raleigh, NC 27695

Abstract

Rising demands for liquid fuels and the finite supply of petroleum resources drives research for biofuels and biochemicals. Pretreatment steps are required to open the structure of lignocellulosic biomass and reduce its recalcitrance prior to further processing. Fungal pretreatment has the potential to become a low-cost and environmentally-friendly method of pretreatment that can displace current pretreatment methods which utilize high temperatures, harsh chemical, and high energy input. Under investigation is wood specimens from the species Populus trichocarpa which have undergone several modification to individual and groups of genes regulating lignin biosynthesis, yielding wood with unique properties. Little is known about how genetic modifications to the lignin biosynthetic pathway will influence fungal degradation. Wood with reduced or altered lignin could enhance the effectiveness of fungal pretreatment and benefit the biofuels/biochemicals and pulping industries by reducing chemical and energy requirements, thus increasing processing efficiency and decreasing the environmental impact. In this study, genetically modified P. trichocarpa was subjected to the white-rot fungus Ceriporiopsis subvermispora for 30 days. After the pretreatment period, the weight loss, changes to cell wall carbohydrates, lignin content and structure, and enzymatic hydrolysis were measured.

Proceedings of the 58th International Convention of Society of Wood Science and Technology
June 7-12, 2015 – Grand Teton National Park, Jackson, Wyoming, USA

Understanding Decay Resistance, Dimensional Stability and Strength Changes Acetylated Wood

Roger M. Rowell

Professor Emeritus, University of Wisconsin, Madison, WI, USA and Guest Professor, EcoBuild, Stockholm, Sweden rmrowell@wiisc.edu

Abstract

The reaction of wood with acetic anhydride has been studies since the late 1920's. The acetylated wood is known to have greatly reduces hygroscopicity,improved dimensional stability and decay resistance due to the esterification of the accessible hydroxyl groups in the cell wall polymers. The bonded acetyl reduce hydrogen bonding with water and bulk the cell wall back to its original green volume. Both the sorption of primary and secondary water are reduced. Dimensional stability is not 100% since the water molecule is smaller than the acetyl group so water can access hydroxyl sites even when the wood is fully acetylated. The equilibrium moisture content is reduced in a linear relationship to the level of acetyl content. This means that the reduction in moisture content is not dependent on where the acetylation reaction takes place in the cell wall. The reduction of moisture sorption reduces the sorption and desorption of environmental gasses such as formaldehyde. There is a greater difference in the sorption-desorption isotherm (hysteresis) in acetylated wood as compared to non-acetylated wood. This may be due to the increased time it takes for moisture to sorb into the acetylated cell wall. Resistance to fungal attack increases as the level of acetylation increases. The level of acetyl needed to stop white-rot fungal attack (7 – 10%) is much lower than that needed to stop brown-rot fungal attack (17 – 19%). The mechanism of brown-rot fungal attack is not completely understood but it may be that the cell wall moisture content is too low at high levels of acetylation to support fungal growth so the initial colonization does not take place. The increase in fungal resistance, however, is not linear with the increase in acetyl content indicating that fungal resistance is due to more than one type of hydroxyl substitution. Strength properties are not significantly changed in acetylated wood and acetylation results in greatly improved wet strength and wet stiffness properties. Wet stiffness in non-acetylated wood is greatly reduced due to the low Tg of the cell wall hemicelluloses.

Key Words: Acetylation, acetyl content, brown-rot fungus, white-rot fungus, equilibrium moisture content, sorption isotherm, dimensional stability, sugar analysis, Tg, wet and dry strength and stiffness, wood.

Introduction

Wood acetylation can trace its history to the late 1920's when it was used to isolate both lignin and hemicelluloses (Rowell 2006). The first patent was in 1930 in Austria. All woods contain acetyl groups: softwoods, 0.5 – 1.7% and hardwoods, 2 – 4.5%. Increasing acetyl groups to the cell wall results in major changes to the properties and performance of the acetylated wood.

The reaction of wood with acetic anhydride starts in the S_2 layer and moves to the middle lamella. Lignin is the fastest to react but since there is much higher percentage of hemicelluloses in wood as compared to lignin, the hemicellulose react to a higher

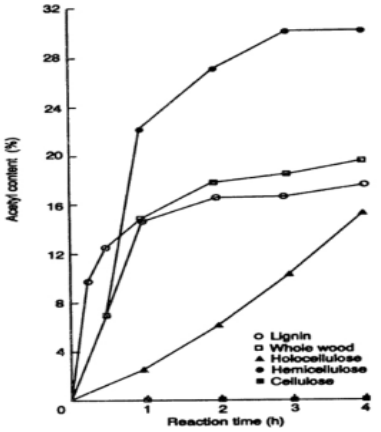

Figure 1 – Reaction of wood and cell wall polymers with acetic anhydride.

degree (Figure 1). The reaction rate is based on the rate of chemical penetration to the reactive site. The hydroxyl groups substituted with an acetyl weight gain of 16-19%: 89% of lignin, 25% of holocelluloses, 100% accessible hemicelluloses and no cellulose hydroxyl are substituted.

Acetylation and Sorption and Movement of Moisture

Moisture enters wood in one of two ways: by capillary action as liquid water in end grain or as moisture from the surrounding atmosphere. It is the end grain capillary uptake of liquid water that is the problem in the corners of windows and doors. Since wood is hygroscopic, it attracts moisture which bonds to the cell wall polymers through hydrogen bonding. The most hygroscopic cell wall polymers are the hemicelluloses and moisture moves in the cell wall through the hemicelluloses (Figure 2). Jakes et al. 2013 have reports that the glass transition temperature for hemicelluloses at 65% RH is 25°C. This means that at room temperature and 65% RH, the hemicelluloses are softened and moisture is starting to percolate in the hemicellulose interconnecting matrix. The cell wall model shown in Figure 2 by Henriksson does not show a connecting network in the hemicelluloses so this model needs to be updated.

At 90% RH, the equilibrium moisture content (EMC) in the hemicelluloses is well over the moisture level needed for fungal colonization. As the level of acetylation goes up, the equilibrium moisture content goes down (Table 1). The bonded acetyl groups are less hygroscopic then the unreacted hydroxyls. More evidence of the increase in hydrophobicity of acetylated wood is in contact angle measurements. Using the Wilhelmy method for acetylated scots pine sapwood at 20% weight gain the contact angle was found to be 81.5 while the control was 59.7 (Wålinder et al. 2010). Also, as the acetyl weight goes up, the wood increases in volume (Table 2). At a level of about 22 percent acetyl weight gain, the volume of the dry acetylated wood is the same as the starting wood green volume.

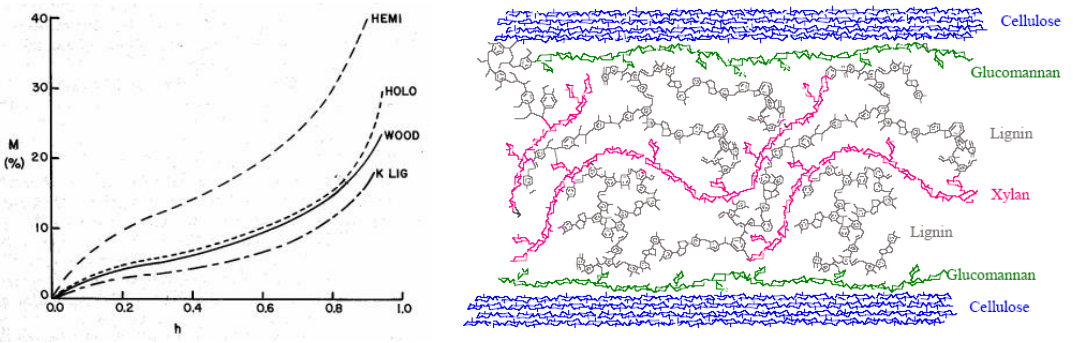

Henriksson in Ek et al., Ljungberg Textbook 1, pg. 143 (2006)

Figure 2 – Sorption of moisture of cell wall polymers (left), Wood cell wall showing the interconnecting network of hemicelluloses and lignin (right).

Table 1 – Equilibrium moisture content of pine at different levels of acetyl weight gain.

Weight Percent Gain	Equilibrium Moisture Content at 27C		
	30%RH	65%RH	90%RH
0	5.8	12.0	21.7
6.0	4.1	9.2	17.5
10.4	3.3	7.5	14.4
14.8	2.8	6.0	11.6
18.4	2.3	5.0	9.2
20.4	2.4	4.3	8.4
22.9	1.9	3.6	4.8

Figure 3 shows the sorption-desorption isotherms for control and acetylated spruce fibers (Stromdahl 2000). The 10 minute acetylation curve represents an acetyl weight gain of 13.2% and the 4 hour curve represents a weight gain of 19.2%. The untreated spruce reaches an adsorption/desorption maximum at about 35 - 40% moisture content, the 13.2 sample, a maximum of about 30%, and the 19.2 a maximum of about 10%. These results support experimental laboratory values for fiber saturation point for pine (Table 2, Rowell 1991).

Table 2 – Fiber saturation point for control and acetylated pine.

Acetyl weight gain	FSP (%)
0	45
6	24
10.4	16
18.4	14
21.1	10

There is a very large difference between the adsorption and desorption curves for both the control and the 13.2 WPG fibers but much less difference in the 19.2 WPG fibers (Figure 3). The sorption of moisture is presumed to be sorbed either as primary water or secondary water. Primary water is the water that is sorbed on primary sites with high binding energies such as hydroxyl groups. Secondary water is that water sorbed to less binding energy sites which is water molecules sorbed on top of the primary layer or sites with less binding eneregies. Since some of the hydroxyl sites are esterified with acetyl groups, there are fewer primary sites to sorb water. And since the fiber is less hydrophilic due to acetylation, there may also be less secondary binding sites.

There is a greater difference (hysteresis) in the adsorption and desorption in the acetylated samples (Figure 3). Since this is a time-sensitive relationship, equilibrium at a given relative humidity is based on the time it takes to sorb or desorb a water molecule (Hill et al. 2010). In the adsorption part of the acetylation curve, a water molecule is added to the cell wall and the cell wall must expand to accomodate it. Because of the high level of accessible hydrozyl with bonded acetys, any primary or secondary sites that might be available will be hindered by the bonded acetyl. In the case of desorption, a swolen cell wall loses a water molecule and shrinks which is faster than adsorbing one.

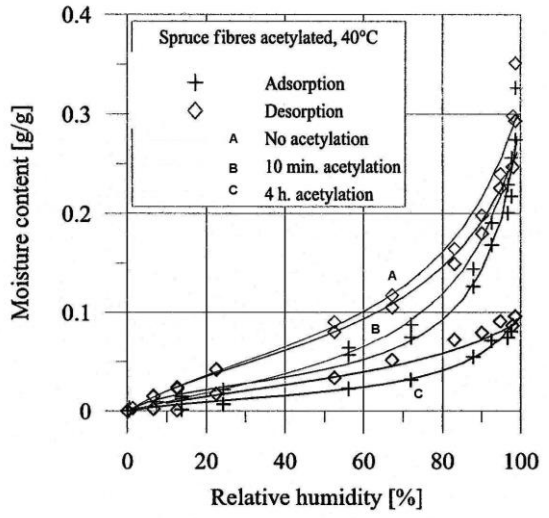

Figure 3 – Sorption isotherms for control and acetylated spruce fiber.

Table 3 – Change in volume in wood from oven dry to acetylated

Green Vol (cm^3)	OD Vol (cm^3)	Change Vol (%)	Ac (%)	OD (cm^3)	Change (%)
38.84	34.90	-10.1	22.8	38.84	+10.1

There is a correlation between the EMC wood and many properties of acetylated wood (Rowell 2013). For example, as the level of acetyl weight gain increases, the EMC decreases proportionally (Rowell 2006, Figure 4). As the level EMC decreases, dimensional stability increases proportionally (Rowell 1984, Figure 5). This is logical since the mechanism of dimensional stability is based on bulking of a less hydroscopic group on the cell wall hydroxyls.

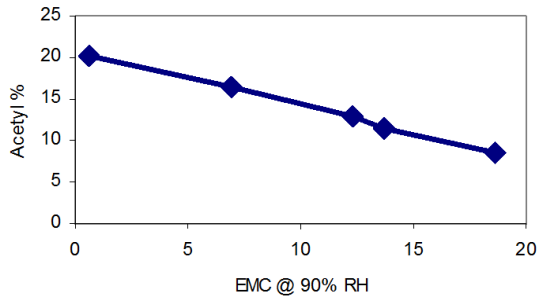

Figure 4 – Relationship between EMC and acetyl weight gain

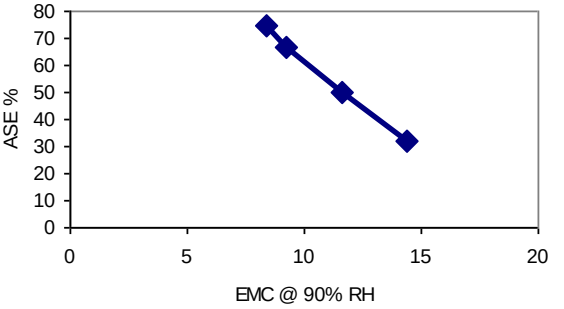

Figure 5 - Relationship between EMC and antishrink efficiency.

Acetylation and Decay Resistance

As the level of bonded acetyl goes up, resistance to attack by both brown- and white-rot fungi goes down. Table 4 shows the results of an ASTM standard 12-week soil block test using the brown-rot fungus *Gloeophyllum trabeum* or the white-rot fungus *Trametes versicolor*. At an acetyl weight gain of only 6%, the weight loss is almost cut in half in both the the brown- and white-rot fungal tests. At an acetyl level of about 10%, weight loss due to brown-rot attack is cut to less than 7% and white-rot to less than 3%. At an acetyl level of about 15%, weight loss due to brown-rot attack is less than 4% and white-rot is within experimental error for zero. Complete protection against brown-rot fungus is achieved at an acetyl level of about 18%.

Table 4 – Weight loss in an ASTM standard test using a brown- and a white-rot fungus.

Acetyl Weight Gain (%)	Weight Loss After 12 Weeks Brown-rot Fungus (%)	White-rot Fungus (%)
0	61.3	7.8
6.0	34.6	4.2
10.4	6.7	2.6
14.8	3.4	<2
17.8	<2	<2

The relationship between EMC and decay resistance is not linear or proportional (Figure 6). At an EMC under about 13%, the weight loss due to attack by a brown-rot fungi is less than 5 percent. The reported EMC where no attack occurs is about 8% (Rowell 2006). This data shows that the first hydroxyls to react have the most impact on reducing EMC and increasing decay resistance. It has been shown that the lignin phenolic hydroxyl groups are the first to react with acetic anhydride in wood followed by the hemicelluloses (Rowell et al.1991). The hydroxyls on lignin are almost completely substituted at a weight gain approximately 20 percent acetyl (Rowell et al.1982) while only about 25% of the hydroxyls are substituted on the hemicelluloses.

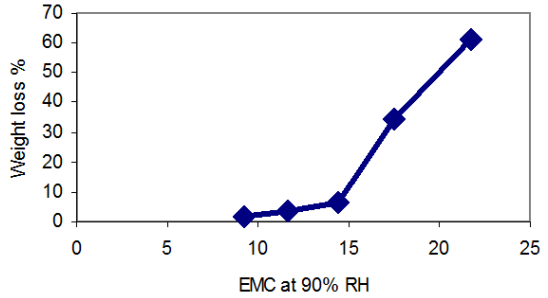

Figure 6 – Relationship between EMC and weight loss due to attack by a brown-rot fungus.

Based on Figure 4, an EMC of about 13% represents an acetyl weight gain of approximately 12%. The EMC's of the different cell wall polymers at 65% RH and 90% RH are shown in Table 5. At 65% RH, the EMC of the hemicelluloses are close to the level needed to support fungal colonization. At 90% RH, the hemicellulses are well above the moisture level needed to support fungal colonization.

Table 5 – EMC of cell wall polymers at 65% RH and 90% RH

Cell wall polymer	EMC @ 65% RH	EMC@ 90% RH
Hemicellulose	22	38
Lignin	7	16
Wood	11	21
Cellulose	5	12

Figure 7 shows electron micrographs of control and acetylated pine. The control sample before the test (A) and the control after the 12 week test with a brown-rot fungus Figure B and C. The control sample after test is almost completely covered with fungal hypha (Figure 7B) with a destroyed cell wall (Figure 7C). The acetylated sample shows a few hypha growing on the inner cell wall but no weight loss is detected.

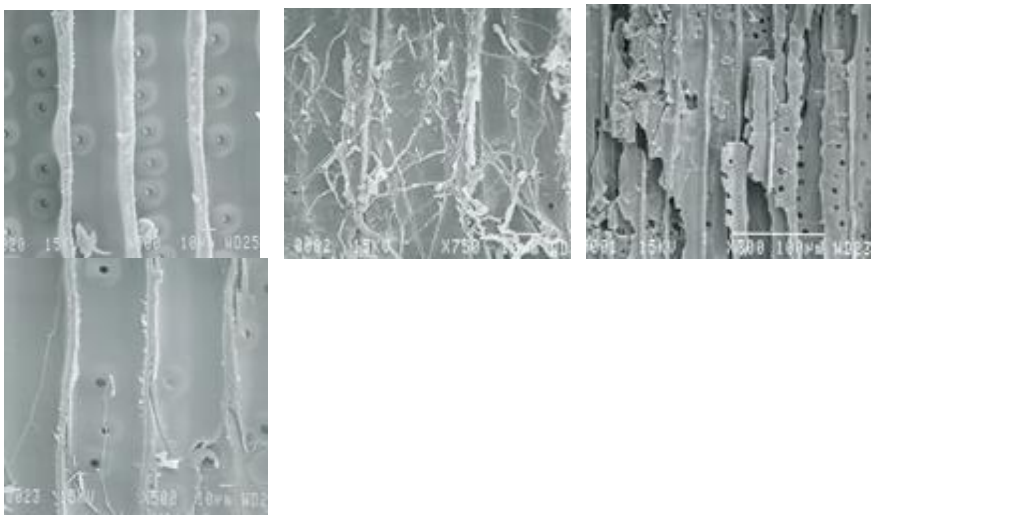

A B C D

Figure 7 - Electron micrographs of pine control before test,(A), (B) and (C) control after 12 weeks with a brown-rot fungus, control and acetylated (D) after the 12 week test.

Table 6 shows the carbohydrate analysis before and after the 12 week soil block test using the brown-rot fungi. There was no loss of lignin or cellulose in the sample containing 15% acetyl but some degradation did take place. There was a weight loss of only 1.4% but a major loss in arabinose with lessor losses in galactose, mannose, rhamnose and xylose. Arabinose is the only pentose sugar in the hemicelluloses that contains a strained five-membered ring. This could be significant in the study on the mechanism of brown-rot attack on softwoods.

Table 6 – Carbohydrate analysis of pine before and after attack by a brown-rot fungus.

WPG	Weight Loss %	Total Carbo Lost %	Arab Lost %	Gala Lost %	Rham Lost %	Glu Lost %	Xyl Lost %	Man Lost (%)
0	51.7	85.8	87.9	71.9	90.0	83.8	90.6	92.5
15	1.4	13.2	89.0	55.2	70.0	0	38.3	42.0

There are many theories on the mechanism of the attack of brown-rot fungi on softwoods. Many researchers have tried to explain the mechanism as being one or two steps. However, I think that is too simple and the actual mechanism involves many steps as I theorize as follows:

Step 1 – A favorable environment

Fungi need an environment that is conducive to their survival: temperature, moisture, pH, and toxicity. If the temperature is too high or too low, the fungi cannot survive. If the wood is too wet or too dry, the fungi cannot survive. If the pH is too high or too low, the fungi cannot survive. And, if there are toxic chemicals in the wood, the fungi cannot survive. If the environment is favorable, then the degradation mechanism progresses to Step 2. Resistance to attack by acetylation might function at this level with a moisture content too low for colonization (Rowell 2013).

Step 2 – Recognition

Since Nature does not waste energy, the pH of the wood starts to drop as the fungus starts to colonize. The hyphae of a brown-rot fungus must detect a source of nutrition in the wood it has come into contact with in order to survive. The first attack is thought to be in a oxidation and rearrangement of lignin by an enzymatic reaction. No lignin is lost but it is known to be somewhat oxidized and condensed. If the colonization takes place, then the mechanism progresses to Step 3. At this stage, the fungus is undergoing gene expression to start the production of cellulosic enzymes. (Alfredsen et al.2013, 2015, Ringwood et al. 2014). It is possible that the fungal enzymes cannot recognize the modified cell wall polymer substrates since this enzyme reaction is very specific.

Step 3 – First attack

Since the result of brown-rot degradation is mainly a loss of cell wall carbohydrate polymers, it is logical to assume the first degrading reaction is an enzymatic attack on some very easily hydrolysable carbohydrate sugar that is probably located in the side chain of an accessible hemicellulose structure. The hypha grows in the inside of a cell wall so it is in contact with the S_3 layer which is rich in hemicelluloses. The products of this attack provide the energy to proceed to a major chemical reaction in Step 4.

Step 4 – Fenton chemistry

The first enzyme reaction then leads to the generation of a peroxide/ferrous ion and a hydroxyl radical chemical system (Fenton 1894) that depolymerizes the structural polysaccharides in the cell wall matrix resulting in strength losses (Goodell 2006). The hemicelluloses and the cellulose polymers start to degrade and major strength losses are observed.

Step 5 – Weight loss

As this Fenton chemistry progresses, new enzyme reaction take place in other accessible regions of the cell wall polysaccharides resulting in significant weight losses. Very little lignin is lost in the final stages of attack.

Acetylation and Strength Properties

Dry and wet strength and stiffness properties of acetylated pine are shown in Table 5. Modulus of rupture and modulus of elasticity are about the same for dry control and acetylated wood with the acetylated vales slightly higher than control. The real difference between control and acetylated pine are in the values for wet modulus. Control pine strength is greatly decreased upon wetting while the acetylated pine retains much of its dry strength. Wet stiffness is greatly decreased upon wetting in the control pine while the acetylated pine retains much of its dry stiffness.

While both the control and acetylated samples were cut from the same species, they differ in percentage of springwood and summerwood, number of annual rings, sample size in testing and moisture content. A standard ASTM test for MOR and MOE are run at 65% RH. The control sample has a moisture content of about 12% at this RH while the acetylated sample has a moisture content of about 4% (Table 7). It is well known that strength and stiffness properties are very dependent of moisture content. For MOR, there is a 4% different for each 1% change in moisture content and for MOE, there is a 2% difference for each 1% change in moisture content. Because the pine samples are measured at different moisture contents, it is hard to compare the values derived from these tests.

Table 7 – Dry and wet strength and stiffness for control and acetylated pine.

Sample	Dry Strength MOR N/mm^2	Wet Strength MOR N/mm^2	Dry Stiffness MOE N/mm^2	Wet Stiffness MOE N/mm^2	EMC 65% RH
Radiata Pine	63.6	39.4	10,540	6760	12
Acetylated Radiata Pine	64.4	58.0	10,602	9690	4

Conclusions

Wood acetylated to approximately 20% acetyl weight gain show a large reduction in cell wall moisture content due to the bonding of a much less hygroscopic acetyl group replacing a hydroxyl group. The increase in dimensional stability is due to the cell wall bulking of the dry bonded acetyl groups and bulking the cell wall back to its original green volume. Since the elastic limit of the cell is not exceeded during the acetylation process, no cell was structural damage is done. The mechanism of decay resistance of acetylated wood is not clear but several possible mechanisms have been suggested. It may be that the cell wall polymers have such a low moisture content, the first specific enzyme reaction does not take place. A water molecule is necessary at a glyosidic bond for it to be hydrolyzed. There is very difference in dry strength and stillness in both control and acetylated pine, however, there are major differences in wet strength and stiffness with the acetylated pine retaining much of its dry strength and stiffness. The difference in moisture content of the test specimens under the test conditions make it difficult to compare the test values

References

Alfredsen, G., Flæte, P. O. and Militz, H. (2013). Decay resistance of acetic anhydride modified wood – a review. Int. Wood Prod. J., 4, 137–43.

Alfredsen, G., Ringman, R., Pilga, A. and Fossdal, C.G. (2015). New insight regarding mode of action of brown rot decay of modified wood based on DNA and gene expression studies: a review. International Wood Products Journal 6 (1) 5-7.

Fenton, H. J. H. (1894). Oxidation of tartaric acid in the presence of iron.
J. Chem. Soc. Trans., 65, pp.899–911.

Goodell, B., Daniel, G., Jellison, J. and Qian, Y. (2006). Iron-reducing capacity of low molecular-weight compounds produced in wood by fungi. Holzforschung, 60, pp.630–36.

Hill, C.A.S., Norton, A.J. and Newman, G. (2010). The water vapour sorption properties of Sitka spruce determined using a dynamic vapour sorption apparatus. Wood Sci and Tech. 44: 497-514.

Jakes, J.E., Plaza, N., Stone, D.S., Hunt, C.G., Glass, S.V. and Zeliinka, S.L. (2013). Mechanism of transport through wood cell wall polymers. K. Forest products and industries, 2(6) 10-13.

Ringman, R., Pilgard, A. and Richter, K. (2014). Effect of wood modification on gene expression during incipient *Postia placenta* decay. Int. Biodeter. Biodegr., 86, 86–91.

Rowell, R.M. (1982). Distribution of reacted chemicals in southern pine modified with acetic anhydride, Wood Sci. 15(2): 172-182.

Rowell, R.M. (Ed.). (1984). The Chemistry of Solid Wood. Advances in Chemistry Series 207, American Chemical Society, Washington DC, USA.

Rowell, R. M. (1991). Chemical modification of wood, Handbook on Wood and Cellulosic Materials, Hon, D. N.-S., and Shiraishi, N.,eds., Marcel Dekker, Inc., New York, NY, Chapter 15, 703-756.

Rowell, R.M. (2006). Acetylation of wood: A journey from analytical technique to commercial reality, Forest Products Journal, 56(9): 4-12.

Rowell, R.M. (2013). Moisture properties, Handbook of wood chemistry and wood composites, Second Edition, Rowell, R.M., Ed, CRC Press, Boca Raton, FL, Chapter 4, 75-98.

Rowell, R. M., Simonson, R. Hess, S., Plackett, D.V., Cronshaw, D. and Dunningham, E.(1991). Acetyl distribution in acetylated whole wood and reactivity of isolated wood cell wall components to acetic anhydride. Wood and Fiber Sci. 26(1): 11-18.

Stromdahl, K. (2000). Water sorption in wood and plant fibers, PhD thesis, The Technical University of Demark, Department of Structural Engineering and Materials, Copenhagen, Denmark.

Wålinder, M., Segerholm, K., Larsson-Brelid, P., and Westin, M. (2010). Liquids and coatings wettability and penetrability of acetylated scots pine sapwood. In: Proceedings 5th European Conference on Wood Modification, Riga, Latvia, 381-388.

Proceedings of the 58th International Convention of Society of Wood Science and Technology
June 7-12, 2015 – Grand Teton National Park, Jackson, Wyoming, USA

Effect of Preservative Treatment on I-joist Bending Stiffness

H. Michael Barnes, mike.barnes@msstate.edu
MG Sanders, msanders@cfr.msstate.edu
GB Lindsey, blindsey@naturalwoodsolutions.com

Mississippi State University, Box 9820, Department of Sustainable Bioproducts, Mississippi State, MS 39762-9820

Abstract

A series of I-joists were treated with a new preservative system and tested full-sized in bending. Statistical analysis indicated that no changes in the bending stiffness were attributable to the treatment. This indicates that no change is design values are needed for treated I-joists.

Wood Quality and Improvement Session
Moderator: Wayan Darmawan, Bogor Agricultural University, Indonesia

Optimization of the Thermo-Hygromechanical Densification Process of Sugar Maple Wood

Qi Lan Fu[1] – Alain Cloutier [2] – Aziz Laghdir[3]*

[1] PhD candidate, Centre de recherche sur les matériaux renouvelables (CRMR), Département des sciences du bois et de la forêt, Université Laval, 2425 rue de la Terrasse, Québec, QC, Canada, G1V 0A6.
qilan.fu.1@ulaval.ca
[2] Professor and director, Centre de recherche sur les matériaux renouvelables (CRMR), Département des sciences du bois et de la forêt, Université Laval, 2425 rue de la Terrasse, Québec, QC, Canada, G1V 0A6.
* *Corresponding author*
alain.cloutier@sbf.ulaval.ca
[3] Research scientist and co-director, Service de recherche et d'expertise en transformation des produits forestiers (Serex), 25 Armand-Sinclair, porte 5, Amqui, QC, Canada, G5J 1K3.
aziz.laghdir@serex.qc.ca

Abstract

Densified wood is a promising engineered wood product, especially for heavy-duty applications. However process temperature, steaming, and duration impact the characteristics of densified wood. The objective of the current study was to optimize thermo-hygromechanical (THM) densification process temperature and duration for sugar maple wood. The response variables studied were compression set recovery and hardness. The THM densification process was performed at three different temperatures (180°C, 200°C, 220°C), densification times (450 s, 900 s, 1350 s) and post-treatment times (900 s, 1350 s, 1800 s). The response surface methodology was used to analyze the impact of the parameters studied. The effect of temperature on wood density through the thickness was also determined. The results suggest that the density of densified samples across the thickness was above two times that of the control and was fairly constant but

decreased sharply near the surface. Density did not increase proportionally with temperature. Wood densified at 200°C reached the maximum density and the higher surface to core density gradient. A higher weight loss occurred at 220°C, resulting in a significant decrease in density and hardness of wood. On the other hand, almost no compression set recovery was observed for sugar maple densified at 220°C.

Keywords: Density, hardness, compression set recovery, response surface methodology.

Introduction

Wood densification is a modification method, aiming at compressing wood to obtain a higher density material. It has been known since 1900, when the first patented densification process appeared (Kollman et al 1975). It is well known that most mechanical properties of wood are proportional to its density. The main purpose of densification is to enhance wood density, hence to improve its mechanical performance and commercial value.

Compression set recovery (CSR) is an important issue in wood densification and has been studied rather extensively (Laine et al 2013; Ito et al 1998; Popescu et al 2014; Kutnar and Kamke 2012 a), because it is an indication of its dimensional stability and defines its potential end-uses. The release of elastic strain energy stored in amorphous and semi-crystalline cellulose and microfibrils is considered as the main reason to cause the set recovery (Laine et al 2013). Three fundamental mechanisms were proposed to prevent set-recovery (Norimoto et al 1993): Relaxation of internal stresses, formation of cross-linkages between matrix components, and isolation of wood polymers under the effect of moisture and heat to prevent re-softening. Navi and Heger (2004) reported that the hemicelluloses hydrolysis occurring during the thermo-hygromechanical (THM) densification process have an important role to relax wood internal stresses. In the presence of heat and steam, the hemicelluloses which are the least stable to withstand heat among the three major components of wood, degrade and the bonds connecting the molecules of the matrix can be broken and reformed. In addition, thermal degradation of the hemicelluloses reduces the hygroscopicity of wood and weakens the connection between microfibrils and lignin (Navi and Heger 2004), providing additional void space to rearrange the microfibrils and release the internal stresses (Inoue et al 1993).

The objective of this study was to investigate the effects of THM densification temperature and time on the compression set recovery and hardness of densified wood. The impacts of temperature and treatment time on the density profile of densified wood were also investigated. The overall objective of this larger initiative was to optimize the THM densification process for sugar maple wood to obtain high quality densified wood products.

Materials and Methods

Materials

Thin strips of sugar maple wood with an original average oven dry density of 582 kg/m^3 was used. The dimensions of the strips were 5.7 mm (radial) x 700 mm (longitudinal) x 83.6 mm (tangential). Samples were placed in an environment-controlled room (20°C, 65% relative humidity) until an equilibrium moisture content of approximately 12% was achieved before densification.

Thermo-hygromechanical densification process

A steam injection press with dimensions 862 mm x 862 mm was used for the densification process (Fig.1). Steam injection holes (diameter =1.5 mm) are distributed uniformly at 32 mm intervals on both the upper and lower platens of the press. The press platens were preheated to the target temperature before treatment. The densification process was composed of three main steps: wood softening, wood compression and post-treatment. Eight strips per test were softened with steam at a pressure of 550 kPa with an increasing mechanical stress up to 3.0 MPa. The strips were then compressed to the target thickness corresponding to a compression set of 50%. Steam was continuously injected during the whole densification process. After post-treatment, steam injection was stopped and steam released through the holes in the platens.

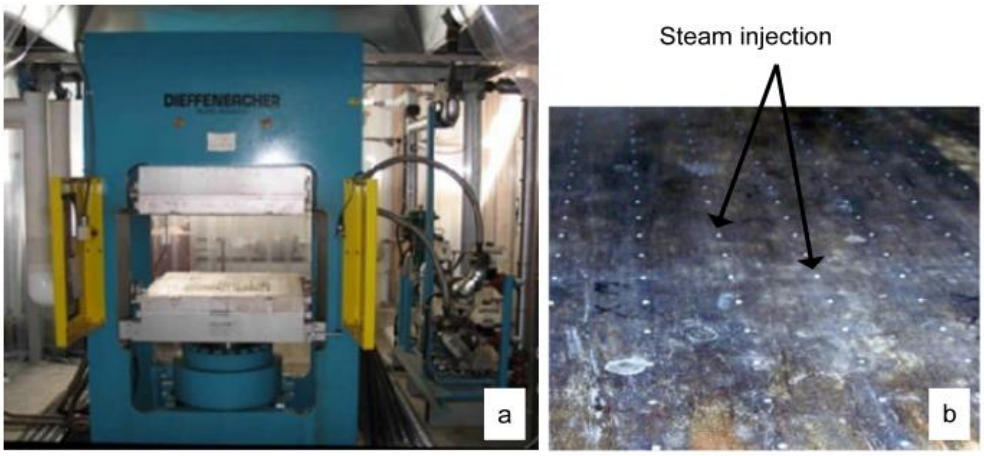

Figure 1. Steam injection hot press used for the densification treatment. a) 862 mm x 862 mm hot press, b) Press platen with steam injection holes.

Optimization of the Densification Process

A Box-Behnken experimental design with 3 factors, 3 levels and 15 runs was used to optimize the THM densification process. This design efficiently selects points located on a hypersphere equidistant from center points as experimental arrangements (Bezerra et al 2008). Compression set recovery (CSR) and hardness (H) were chosen as selection criteria. The three independent variables and their coded levels are listed in Table 1.

Table 1. Code and factor levels chosen for the trials.

Factor	Code and Level

	-1	0	+1
Temperature (°C)	180	200	220
Densification time (s)	450	900	1350
Post-treatment time (s)	900	1350	1800

Properties Determination

Brinell Hardness

Brinell hardness tests were conducted according to the European standard EN 1534 (2000).

Compression Set Recovery

After densification, specimens (50 mm longitudinal x 50 mm tangential) were first dried in an oven to determine oven-dry thickness before swelling. Then oven-dried samples were immersed into water at room temperature for 24 h and oven-dried again for 24 h. The compression set recovery TC (%) was calculated as follows:

$$TC= [(T_s-T_o) / (T_u-T_o)] \times 100$$

Where T_s is the oven-dry thickness after swelling (mm), T_o is the oven-dry thickness before swelling (mm) and T_u is the initial oven-dry uncompressed thickness (mm).

Density Profile

The density profiles of control (not densified) and densified samples at 180°C, 190°C and 200°C, respectively were measured using an X-ray densitometer (Quintek Measurements Systems model QDP-01X) at intervals of 0.02 mm through the thickness.

Results and Discussion

Compression set recovery and hardness

Average compression set recovery and hardness obtained for each treatment are presented in Table 2. The CSR of densified samples was in the range of 1.1% to 19.2%. The maximum value of CSR was approximately 17 times that of the minimum CSR. The hardness of densified samples varied from 25.2 N/mm^2 to 51.4 N/mm^2. The maximum value of hardness was approximately twice as much as the minimum value. Furthermore, lower CSR values and higher hardness values were not obtained under the same experimental conditions. Therefore, it is necessary to analyze the effects of process parameters on CSR and hardness and further optimize the densification process to obtain high quality products. In this study, relatively higher hardness values and lower compression set recovery values were obtained simultaneously for treatments No. 11, 12 and 15.

Table 2. Average compression set recovery and hardness obtained for the treatments applied

(standard deviation given in parenthesis).

No.	Temperature (°C)	Densification time (s)	Post-treatment time (s)	Compression set recovery (%) (n=5)	Hardness (N/mm^2) (n=8)
1	200	450	900	13.0 (4.5)	35.7 (7.1)
2	200	1350	1800	14.4 (4.5)	33.5 (5.0)
3	220	900	900	3.7 (1.2)	33.3 (10.1)
4	220	1350	1350	2.3 (1.5)	31.2 (12.3)
5	180	900	900	10.6 (1.3)	39.3 (6.1)
6	200	450	1800	10.4 (2.9)	50.4 (4.6)
7	200	900	1350	12.3 (4.4)	46.9 (5.9)
8	180	450	1350	15.5 (3.1)	49.4 (3.2)
9	220	450	1350	4.6 (2.9)	36.3 (14.1)
10	200	1350	900	19.2 (3.0)	39.0 (5.7)
11	180	900	1800	8.6 (2.0)	46.2 (3.2)
12	180	1350	1350	5.7 (4.5)	51.4 (4.7)
13	220	900	1800	1.1 (0.7)	25.2 (6.3)
14	200	900	1350	7.9 (3.4)	46.8 (5.0)
15	200	900	1350	8.9 (2.3)	46.9 (6.0)

Effect of temperature, densification time and post-treatment time on compression set recovery

The main and interaction effects of temperature, densification time and post-treatment time on CSR are presented in Fig. 2 by the response surface plots of CSR against two of the three parameters considered. The third parameter was set at the intermediate level. As shown in Fig. 2a, CSR decreased with increasing temperature. Samples treated at low temperature and short densification time showed a higher CSR. These results are in agreement with the literature (Fang et al 2012; Popescu et al 2014; Kutnar and Kamke 2012 a). The lowest CSR (1.1%) was obtained for specimens densified at 220°C for a post-treatment of 1800 s, suggesting a permanent fixation of the compression set. This might be due to the hydrolysis of the hemicelluloses.

Effect of temperature, densification time and post-treatment time on hardness

The main and interaction effects of temperature, densification time and post-treatment time on hardness are shown in Fig. 3. It can be seen that hardness decreased with increasing temperature. Samples treated at higher temperature and longer densification time or post-treatment time exhibited a lower hardness. This result is in agreement with the results reported by Fang et al (2012) and Li et al (2013). The decrease in hardness as temperature increases could be explained by advanced degradation of the matrix (lignin and hemicelluloses) (Fang et al 2012).

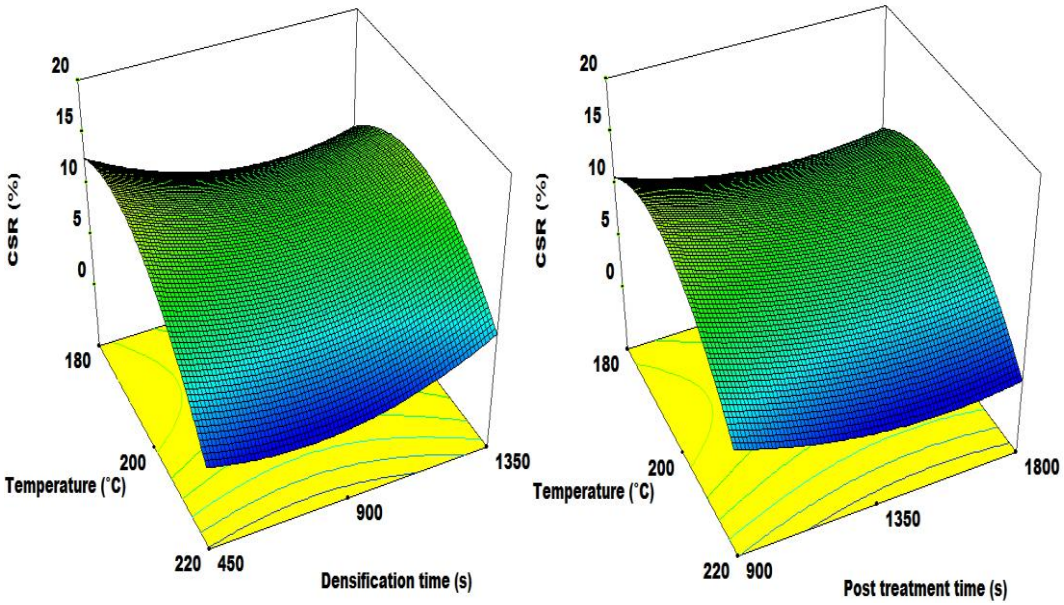

a) b)

Figure 2. Response surface plots of CSR against a) temperature and densification time, b) temperature and post-treatment time.

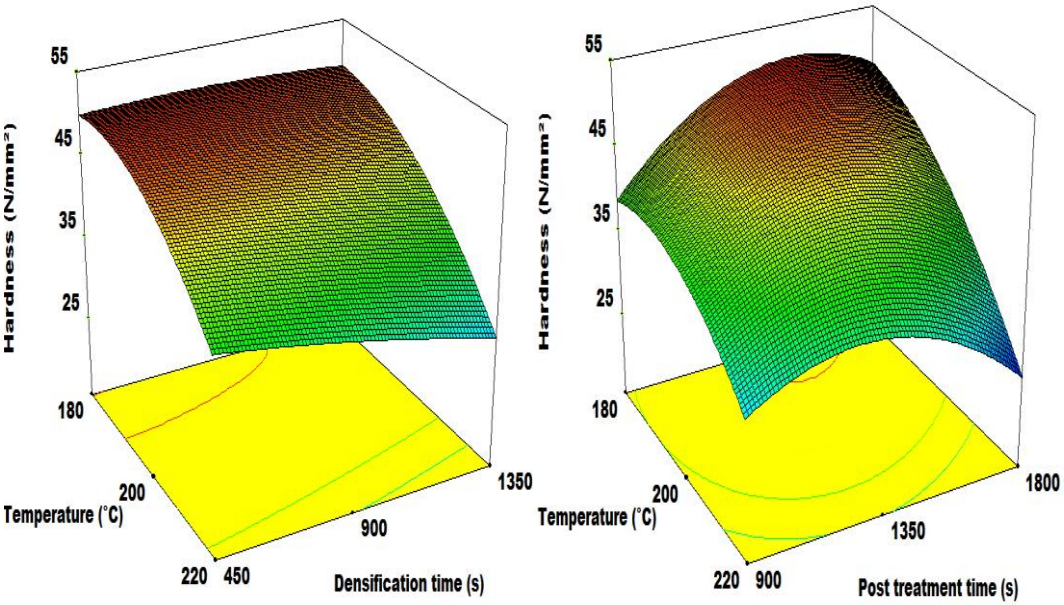

a) b)

Figure 3. Response surface plots of hardness against a) temperature and densification time, b) temperature and post-treatment time.

Density Profiles

Figure 4 presents the density profiles obtained for control and densified samples at 180°C, 200°C and 220°C. The density of the control sample is almost constant throughout the thickness, to the exception of lower density values observed on both surfaces. The underlying reasons for this variation occurring only for about 0.2 mm on

each surface are not entirely clear. This may be a measurement artifact due to the imperfect alignment of the sample in the densitometer. Kutnar and Kamke (2012 b) explained that lower density on both surfaces of densified samples was owing to heterogeneous thickness recovery. Additionally, it can be observed that the density of THM densified samples was above two times that of the control sample and was fairly constant across the thickness but decreased sharply near the surface. Furthermore, different densification temperatures resulted in different density profiles. Density did not increase proportionally with the increase in temperature. Wood densified at 200°C reached the highest density compared with samples densified at 180°C and 220°C. A higher weight loss occurred at 220°C which might be induced by the degradation of wood components, resulting in a decrease of wood density.

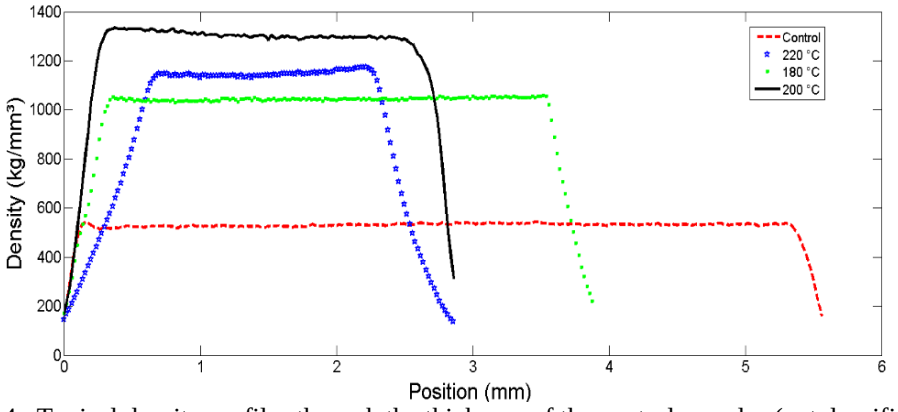

Figure 4. Typical density profiles through the thickness of the control samples (not densified) and samples densified at different temperatures.

Conclusions

Temperature was the most dominant parameter on compression set recovery and hardness of densified wood. The density of densified samples was more than twice that of the control and was fairly constant across the thickness but decreased sharply near the surface. A higher percentage of weight loss occurred at 220°C, resulting in an important decrease in density and hardness of wood. Simultaneously, almost no compression set recovery was observed for sugar maple densified at 220°C.

Acknowledgements

The authors are grateful to the Natural Sciences and Research Council of Canada (NSERC) for funding this research under Discovery Grant #121954-2012.

References

Bezerra MA, Santelli RE, Oliveira EP, Villar LS, Escaleira LA (2008) Response surface methodology (RSM) as a tool for optimization in analytical chemistry. Talanta 76(5):965-977.

EN 1534 (2000) Wood and parquet flooring-determination of resistance to indentation (Brinell)-test method. CEN-European Committee for Standardization, Brussels.

Fang CH, Mariotti N, Cloutier A, Koubaa A, Blanchet P (2012) Densification of wood veneers by compression combined with heat and steam. Eur. J. Wood Prod 70(1-3):155-163.

Inoue M, Norimoto M, Tanahashi M, Rowell RM (1993) Steam or heat fixation of compressed wood. Wood Fiber Sci 25(3):224-235.

Ito Y, Tanahashi M, Shigematsu M and Shinoda Y (1998) Compressive-molding of wood by high-pressure steam-treatment: Part 2. Mechanism of permanent fixation. Holzforschung 52(2):217-221.

Kutnar A, Kamke FA (2012 a) Influence of temperature and steam environment on set recovery of compressive deformation of wood. Wood Sci Technol 46(5):953-964.

Kutnar A, Kamke FA (2012 b) Compression of wood under saturated steam, superheated steam, and transient conditions at 150°C, 160°C and 170°C. Wood Sci Technol 46(1-3):73-88.

Kollman FP, Kuenzi EW and Stamm AJ (1975) Principles of wood science and technology. V 2, Wood Based Materials. Springer, Berlin, 116-139.

Laine K, Belt T, Rautkari L, Ramsay J, Hill CAS, Hughes M (2013) Measuring the thickness swelling and set-recovery of densified and thermally modified Scots pine solid wood. J Master Sci 48(24):8530-8538.

Li T, Cai JB and Zhou DG (2013) Optimization of the combined modification process of thermo- mechanical densification and heat treatment on Chinese fir wood. Bioresources 8(4):5279-5288.

Navi P, Heger F (2004) Combined densification and thermo-hydromechanical processing of wood. Mater Res Soc Bull 29(5):332–336.

Norimoto M, Ota C, Akitsu H,Yamada T (1993) Permanent fixation of bending deformation in wood by heat treatment.Wood Res 79:23-33.

Popescu MC, Lisa G, Navi P, Froidevaux J, Popescu CM (2014) Evaluation of the thermal stablility and set recovery of thermo-hydro-mechanically treated lime (Tilia cordata) wood. Wood Sci Technol 48(1):85-97.

Proceedings of the 58th International Convention of Society of Wood Science and Technology
June 7-12, 2015 – Grand Teton National Park, Jackson, Wyoming, USA

Non-Destructive Pre-Harvest Measurement of Diameter Profiles of Standing Mature Pine Trees by Terrestrial Laser Scanning (TLS)

Per Otto Flæte [1*]

[1] Senior researcher, Norwegian Institute of Wood Technology - PO Box 113 Blindern - NO-0314 Oslo - Norway.
* *Corresponding author*
per.otto.flate@treteknisk.no

Abstract

The conversion of forest resources to solid wood products is a chain of closely related activities. Decisions taken at one stage will have consequences for the following ones. At an early stage, the bucking operation occurs. Tree bucking performed by harvesters in cut-to-length harvesting systems is an important part of the forestry supply chain. Modern harvesters are equipped with tools to measure stem dimensions (diameter, length) and to predict the stem profile during processing. If the stem diameter profiles of the trees in a stand are available prior to harvesting, this information can be utilized for tailoring log supply. The information can be used for allocating logs from specific stands to different purchasers and by using the stem profiles for optimal bucking of the trees.
This paper discusses Terrestrial Laser Scanning (TLS) as potential technique for non-destructive prediction of diameter profiles of standing mature Scots pine trees. TLS has been developed to capture detailed and highly accurate information relating to an object's dimensions, spatial positioning, texture and colour in both two and three dimensions. It is now a widely used technology in architectural, engineering and industrial measurement applications, for example to digitize the external surface of buildings and archaeological sites. For forest monitoring purposes, the use of TLS is in an early stage. The reported results are based on measurements of Scots pines scanned with TLS in Norway.

Keywords: Terrestrial laser scanning, diameter, stem profiles, Scots pin

Introduction

Terrestrial laser scanning (TLS) has been developed to capture detailed and highly accurate information relating to an object's dimensions, spatial positioning, texture and colour in both two and three dimensions. It is now a widely used technology in

architectural, engineering and industrial measurement applications, for example to digitize the external surface of buildings and archaeological sites.

For forest monitoring purposes, the use of terrestrial 3D-laser scanners is in an early stage. While airborne laser scanners can easily be used for large scale monitoring as they are able to cover large regions (Næsset 2007), terrestrial scanners are to be carried around on the ground. TLS has been applied to forest inventory measurements (plot cartography, species recognition, diameter at breast height, tree height, stem density, basal area and plot-level wood volume estimates) and canopy characterizations. The technique also provides potential support as a non-destructive tool for pre-harvest stand value and wood quality assessment (Keane 2007).

The conversion of forest resources to solid wood products is a chain of closely related activities. Decisions taken at one stage will have consequences for the following ones. At an early stage, the bucking operation occurs. Tree bucking performed by harvesters in cut-to-length harvesting systems is an important part of the forestry supply chain. Modern harvesters are equipped with tools to measure stem dimensions (diameter, length) and to predict the stem profile during processing (Koskela 2007). If the stem diameter profiles of the trees in a stand are available prior to harvesting, this information can be utilized for tailoring log supply. The information can be used for allocating logs from specific stands to different purchasers and by using the stem profiles for optimal bucking of the trees.

The objective of this study was to evaluate TLS as a potential technique for non-destructive prediction of diameter profiles of standing mature Scots pine trees.

Material and Methods

The data are based on measurements of 27 mature Scots pines from three plots scanned with TLS in a stand located in eastern Norway. Diameter at breast height (Dbh) was callipered manually on each tree. Mean Dbh was 244 mm, ranging from 278 mm to 353 mm.

Each plot was scanned with a TLS (Fig. 1.)

Figure 1. 3D-laser scanner acquiring data from a Scots pine stand in eastern Norway surrounded by members of the BALABU project team. The BALABU (Bakkemontert laser som verktøy for bedre utnyttelse av skogressursene) project is investigating TLS based inventory methodology in forestry.

The basic principle of laser scan measurement involves the emission of laser light pulses towards an object. A pulse hits the object and is reflected back to a sensor. The angle of laser pulse emission and reflection, together with the time between laser pulse emission and return, are used to record highly accurate X, Y and Z co-ordinates for each point of reflection. Several million reflection points can be collected per scan, collectively referred to as a point cloud (Fig. 2.).

Figure 2. TLS generated images of a Scots pine forest stand in Eastern Norway.

The TLS data were processed by Treemetrics Ltd., Cork, Ireland (project partner in the BALABU project) and converted to StanForD stem files. A stem file comprises stem diameters recorded in 10 cm intervals from the base towards the top for a tree. This is the same file format as used in harvesters.

The pine trees were harvested by a single grip harvester and the stem files produced by the harvester were collected. Modern harvesters are equipped with tools to measure stem dimensions (diameter, length) and to predict the stem profile during processing. This information is part of the bucking control system of a harvester.

To evaluate the potential of using TLS for producing diameter profiles of standing trees the TLS based data were compared with the manually callipered diameters on each tree and with the diameters measured along each stem by the harvester.

Results and Discussion

Diameter at breast height (Dbh)

Data for measured Dbh are shown in Table 1. Dbh measured by conventional caliper was used as a measure of the true Dbh (reference). The difference between reference Dbh and corresponding Dbh measured by harvester or by TLS was on average 2 mm for both methods. However, the higher standard deviation for the difference calculated for the TLS based Dbh estimates indicate a poorer accuracy compared with the harvester.

Table 1. Diameter at breast height (Dbh) measured by conventional calliper (reference), by harvester and by TLS. Statistics for the difference between reference and harvester and between reference and TLS are shown in right column. N = 27

	Dbh (mm)			**Difference**	
	Reference (R)	Harvester (H)	TLS	R - H	R - TLS
Mean	244	242	246	2	-2
St. dev.	45	49	55	11	19
Min	178	151	150	-20	-51
Max	353	355	390	50	50

Stem diameter profiles

The stem diameter profiles of the 27 pine trees comprised 3 871-diameter recordings in total (in 10 cm steps along the stem of each tree from base to upper cross cut made by the harvester). The stem diameter profiles of two of the trees are displayed in Fig. 3.

The difference between each stem diameter measured by the harvester and the corresponding stem diameter measured by TLS was calculated. Mean difference was - 1 mm, ranging from – 83 mm to 63 mm, and with a standard deviation of 20 mm.

By plotting the stem diameter profiles tree by tree, it was noticed that the largest differences between harvester and TLS were found in the upper part of the stems. This is shown in Fig. 3 B). One possible explanation can be that the canopy tends to cover a larger part of the stem in the upper part of a mature Scots pine tree and thereby impedes the TLS reflecting the true stem profile. Since the upper part of a stem consists of small diameter logs, often of low value, this part of the stem profile is normally of less interest to model accurately.

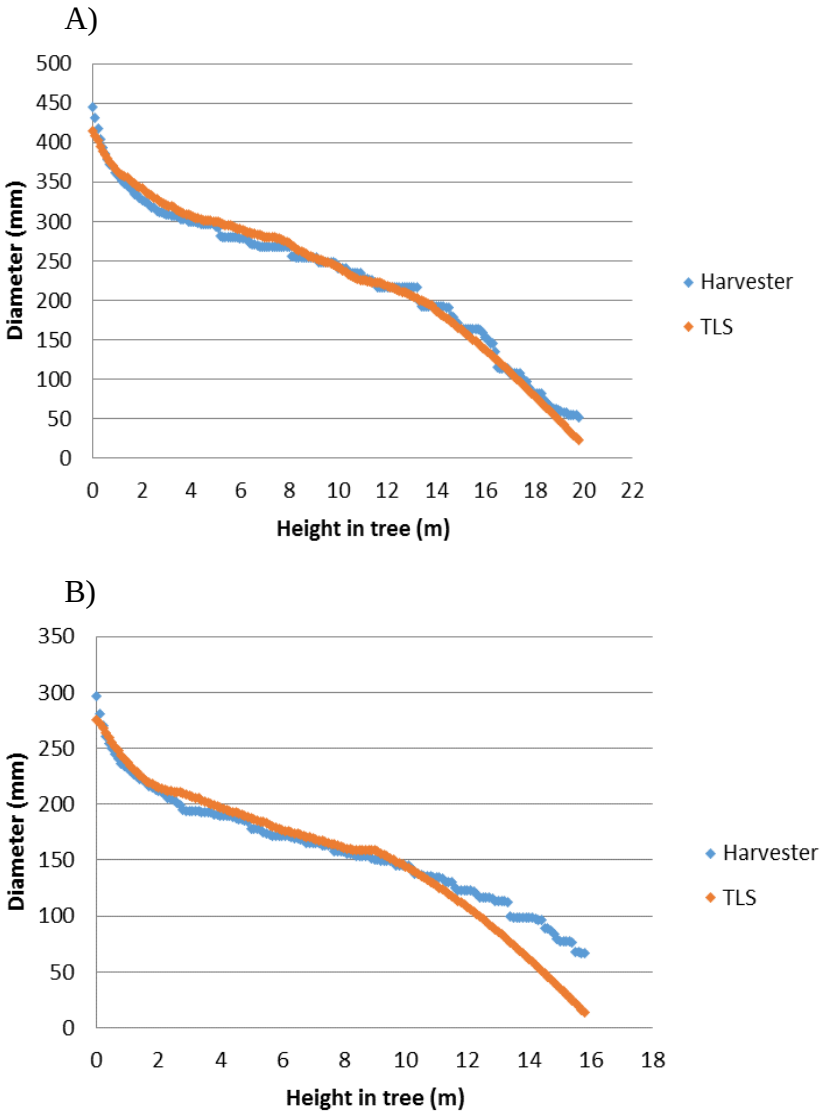

Figure 3. Diameter profiles of two trees measured by harvester and TLS. A) Good fit between harvester and TLS along the stem. B) Difference between harvester and TLS in the upper part of the stem.

Conclusion

This study shows that the stem diameter profiles of standing mature Scots pine can be non-destructive predicted by means of TLS. This can be a useful tool in pre-harvest bucking simulations for optimal utilization of the wood resources. The accuracy of the predictions should be explored more in detail based on a larger material than used in the present study.

References

Keane, E (2007) The potential of terrestrial laser scanning technology in pre-harvest timber measurement operations. COFORD connects. Harvesting/Transportation No. 7. 4 pp.

Koskela, L (2007) Contributions to Statistical Aspects of Computerized Forest Harvesting. Academic dissertation. Acta Universitatis Tamperensis 1237. University of Tampere, Department of Mathematics, Statistics and Philosophy, Finland. ISBN 978-951-6982-4.

Næsset, E (2007) Airborne laser scanning as a method in operational forest inventory: Status of accuracy assessments accomplished in Scandinavia. Scandinavian Journal of Forest Research 22: 433-442.

Proceedings of the 58th International Convention of Society of Wood Science and Technology
June 7-12, 2015 – Grand Teton National Park, Jackson, Wyoming, USA

Properties of Plantation Grown KOA

Brian Bond, bbond@vt.edu
Ian Wilton, iaw17@vt.edu
Nick Dudley, ndudley@harc-hspa.com

Virginia Tech, 1650 Research Center Dr, Blacksburg, VA 24061

Abstract

Acacia koa (koa), endemic to Hawaii, is used in furniture, cabinetry, musical instruments, and a wide variety of other decorative and craft products. It is sold for average prices of 5.00 - $15.00 U.S. per board foot. Premium instrument grade Koa with vertical grain and heavy figured material can sell for over $100 U.S. per board foot. No harvesting of koa is currently permitted on state owned land in Hawaii and sources of koa are diminishing. Koa has been identified as adaptable to plantation management and planted koa could theoretically become a substitute source. Presently little is known about the properties of plantation-grown koa. The research presented describes several wood properties, (color, specific gravity, hardness, heartwood/sapwood ratios and anatomical structure) of Hawaiian plantation-grown koa and compares them to published data from natural grown material.

Proceedings of the 58th International Convention of Society of Wood Science and Technology
June 7-12, 2015 – Grand Teton National Park, Jackson, Wyoming, USA

Wear Characteristics of Newly Coated Cutting Tools in Milling Wood and Wood-Based Composites

Wayan DARMAWAN[(1)], Dodi NANDIKA[(1)], Fauzan FAHRUSSIAM[(2)]
Hiroshi USUKI[(3)], Masahiro YOSHINOBU[(3)], Shuhou KOSEKI[(4)]

(1) Professor at Bogor Agricultural University, Indonesia / wayandar@indo.net.id
(2) Research Assistance at Bogor Agricultural University, Indonesia/fuzan@yahoo.com
(3) Professor at Shimane University, Japan/usuki@riko.shimane-u.ac.jp
(4) Hitachi Tool Engineering Ltd.Japan

Abstract

This article presents the characteristics of wear on the clearance face of newly multilayer-coated K10 cutting tools when milling mersawa wood and particleboard. The K10 cutting tools were coated with monolayer titanium aluminum nitride (TiAlN), multilayer TiAlN/titanium silicon nitride (TiSiN), and TiAlN/titanium boron nitride (TiBN). Mersawa wood with density of 0.80 g/cm^3 and particleboard with a density of 0.61 g/cm^3 were cut using the coated tools and uncoated K10. Cutting tests were performed at a high cutting speed of 17 m/s and a feed rate of 0.1 mm/rev to investigate the wear characteristics on the clearance face of these coated tools. Experimental results showed that the coated tools experienced a smaller amount of wear than the uncoated tool when milling the mersawa and particleboard. The best coating was multilayer TiAlN/TiBN. The high hardness, low coefficient of friction, high resistance to oxidation, and high resistance to delamination wear of the multilayer-coated TiAlN/TiBN tool indicate a very promising applicability of this coating for high-speed cutting of abrasive woods and wood based materials.

Keywords : particleboard, abrasive wood, silica, multilayer coated tools, clearance wear

Introduction

Recently, the use of abrasive wood (wood with high silica) and wood-based material has been known for building construction and decorative purposes. In the secondary wood manufacturing industry, where the abrasive wood and wood-based material are machined extensively, tool wear would be an important economic parameter. Therefore, investigating wear characteristics will lead to making better choices of cutting tool materials used to cut the abrasive wood and the wood-based material.

Machining of the abrasive materials causes cutting tools to wear out much faster than machining of solid woods. Rapid dulling of steel cutting edge of blades, saw teeth, or other knives when machining abrasive materials is a well-known phenomenon. The use of tungsten carbide tools for cutting particleboard has been limited because of the relatively high rate of wear caused by high-temperature oxidation and abrasion (Sheikh-Ahmad and Bailey 1999, Darmawan et. al 2012). Thus, an effort to coat the surfaces of the carbide cutting tool with newly hard materials has been made to increase the wear resistance of the carbide tool.

In a previous study (Salje and Stuehmeier 1988, Darmawan et. al 2001), K10 tungsten carbide inserts were coated with TiN and TiC films by the chemical vapor deposition method and then used for cutting particleboard. Those authors noted that the TiN coating brought no advantages in the milling of particleboard; in other words, the edge life attained or the total tool paths were not longer than those attained using uncoated cutting edges. The TiC-coated tungsten carbide tools were also reported to show large edge fractures after a short time of operation. In a study by Sheikh-Ahmad and Stewart (1995), K grades of tungsten carbide tools were coated with TiN, TiN/TiCN, and TiAlN by the physical vapor deposition (PVD) method for continuous milling of particleboard, and those authors noted that a slight improvement in wear resistance was provided by coatings that were synthesized to carbide grade with fine grain size (0.8 μm) and low cobalt content (3%). In contrast, coatings applied to carbide grade with higher cobalt content and coarse grain size decreased the wear resistance of the tools. The primary failure mode for the PVD coatings tested in that work was chipping of coatings on the rake face. This was caused by inadequate adhesion of coating over the tool surfaces because of improper substrate and coating combination.

In a study by Fuch and Raatz (1997), TiN, Titanium Aluminum Oxide Nitride TiAlON, and TiC coatings were synthesized on the surface of tungsten carbide (93.5% Tungsten Carbide WC, 5% Co, 1.5% Tantalum Carbide and Niobium Carbide (TaC/NbC)) by plasma-assisted chemical vapor deposition for milling laminated particleboard. Those authors noted that TiN- and TiAlON-coated carbide tools did not provide any improvement in wear resistance compared with the uncoated carbide tool and that the TiC-coated carbide tool provided only a slight improvement. Darmawan et al. (2001) reported that the wear of TiN, CrN, CrC, TiCN, and TiAlN coatings when cutting wood-chip cement board resulted from delamination of the coating film at both low- and high-cutting speeds. Among the coatings tested in that study, TiAlN exhibited the lowest occurrence of delamination. For high-speed cutting, delamination of these coating films was caused by oxidation, which was accelerated by an increase in cutting temperature.

The findings of the studies discussed above indicate that the monolayer coatings did not provide significant improvement in the cutting tool life for high-speed cutting of wood-based materials. Therefore, ongoing research is proposed to achieve better performance of the coated carbide tools when cutting these materials. Multilayer coatings would be a promising technique to improve the performance of monolayer coatings. Therefore, TiAlN coating, which is high in hardness, good in oxidation resistance, and better in wear

resistance than the other monolayer coatings, was multilayered in the present study with the newest-generation coatings of titanium boron nitride (TiBN), and titanium silicon nitride (TiSiN), which have been noted to keep excellent properties (high hardness, low friction coefficient, and high oxidation and corrosion resistances; Ding et al. 2006, Chang et al. 2007). Multilayer coatings of TiAlN/TiBN, and TiAlN/TiSiN were synthesized onto the surface of K10 tungsten carbide using the arc-ion plating method, and the multilayer-coated tools were experimentally investigated for their possible use in machining mersawa wood and particleboard. The purpose of this study was to investigate the clearance wear characteristics of these tools in the high-speed cutting of mersawa wood and particleboard.

Materials and Method

Multilayer-coated cutting tools and work materials

General specifications of the multilayer-coated cutting tools tested and the materials machined are shown in Tables 1 and 2, respectively. The K10 carbide tool (90% WC, 10% Co) that was selected as a substrate was 7 mm long, 4 mm width, and 2 mm thick. The hardness of the K10 was measured to be 1450 HV. The 13° rake and 5° clearance angles used in this experiment is now being commercially produced especially for cutting wood and wood-based materials. The K10 carbides were coated with a monolayer coating of TiAlN and multilayer coatings of TiAlN/TiBN, and TiAlN/TiSiN by the arc-ion plating method on both rake and clearance faces. The multilayer coatings were deposited onto the surface of K10 in a thickness of 3 μm (1.5 μm of TiAlN coating above the substrate and 1.5 μm of TiBN, or TiSiN above the TiAlN layer).

Table 1.—Specifications of the coated carbide tools tested.[a]

Coating material	Film thickness (μm)	Hardness (HV)	Oxidation temperature	Friction coefficient
Uncoated K10		1450		
TiAlN	3	2800	Start at 800°C	0.8
TiAlN/TiBN	3	2700	Start at 800°C	0.6
TiAlN/TiSiN	3	3600	Start at 1100°C	0.9

[a]Film thickness was targeted. Hardness, oxidation temperature, and friction coefficient values were measured according to ASTM E2546 (ASTM International 2009a), ASTM G111 (ASTM International 2006), and ASTM G99 (ASTM International 2010), respectively

Table 2.—Specifications of the particleboard machined.

Characteristic[a]	Particleboard	Mersawa
Thickness (mm)	15	50
Moisture content (%)	8	12
Density (g/cm^3)	0.61	0.80
Silicate content (%)	1.86	1.00

[a]Silicate contents were measured according to TAPPI T211 om-85 (TAPPI 1991).

Experimental setup
Cutting test was set up on the numerical controlled (NC) router. The board samples were prepared in rectangular form. A piece of sample was placed on the table of the NC router and locked by screws. A cutting tool edge was held rigidly in a tool holder with a cutting circle diameter of 12 mm. Cutting was performed along the edge of the board and with spindle rotation set in the clockwise direction. The movement of the board during cutting was controlled by feeding directions of the NC table in such away that caused the board to be edged in a down-milling action, and then to be edged in an up-milling action.

Measurements
The coated tools were inspected with an optical video microscope before testing to ensure that no surface cracks and defects of coating film were on the rake and clearance faces. The cutting was stopped at every specified length of cut (100 m), at which abrasion wear was measured along the clearance faces of the tools. Measurements of wear on the clearance faces were made using an optical video microscope. The tools were also inspected after the final cut using scanning electron microscopy/energy dispersive spectroscopy (SEM/EDS) for identification of the mode of cutting-edge failure and occurrence of oxidation.

Results and Discussion

Wear behaviors on clearance faces of the coated tools are provided in Figure 1. The results indicate that the amount of clearance wear increased with increasing cutting length. The coated tools provided better performance, especially in reducing the progression of clearance wear, than the uncoated tool when cutting both mersawa wood and particleboard. Though the monolayer and multilayer-coated tools showed almost the same wear progress near the beginning of cutting, the clearance wear of the monolayer-coated tool increased markedly and exceeded the clearance wear of the multilayer-coated tools, which showed only gradual progression of wear during cutting of the mersawa and particleboard. The uncoated cutting tool suffered clearance wear of about 68 μm for cutting the mersawa and about 78 μm for cutting the particleboard at the 1-km cutting length. The monolayer-coated TiAlN suffered clearance wear larger than 50 μm, on the other hand, the clearance wear of the multilayer-coated tools was less than 50 μm at the 1-km cutting length. The lower hardness, lower oxidation resistance, and higher friction coefficient of the uncoated tool compared with the coated tools (Table 1) would be the reason for this phenomenon.

It also appears from the results shown in Figure 1 that the particleboard caused a higher amount of clearance wear compared with the mersawa wood. The SEM micrograph of mersawa wood in Figure 2a reveales a few round crystals. It appears under high magnification that the surface of the silica crystals in the mersawa wood was corrugated, which abraded the surfaces of the cutting tools during the cutting. The SEM photomicrographs of particleboard revealed cured thermosetting resin (Figure 2b). EDS analysis on the round crystals of the mersawa wood and particleboard revealed the

presence of Si and O (Figure 2 right), which indicated the presence of silica. This is one of the main reasons for the increased tool wear when milling the high silicate wood and the particleboard. The higher silicate content (Table 2) in the particleboard imposed more severe mechanical abrasion during the cutting compared with the mersawa wood.

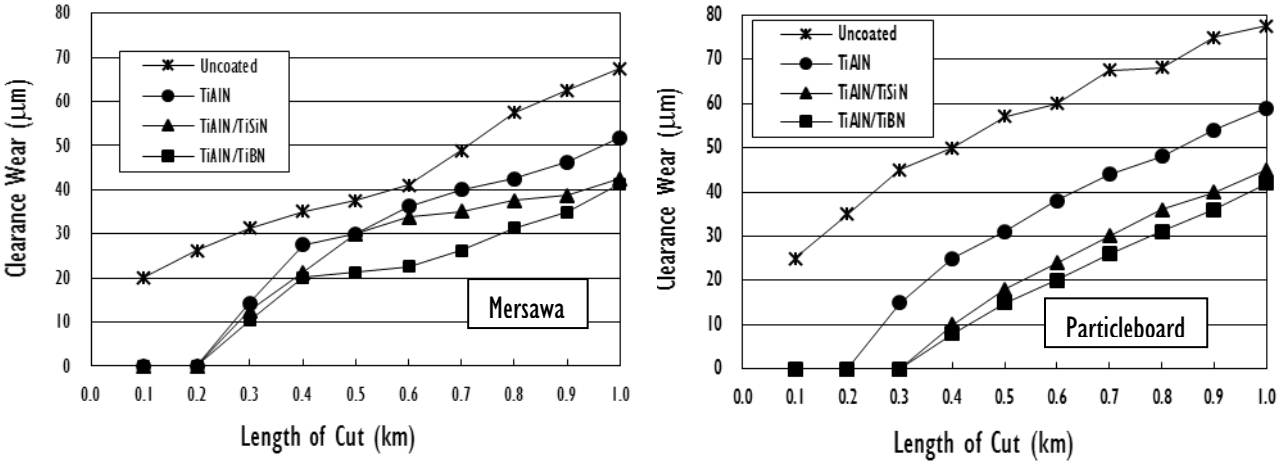

Figure 1. Clearance wear behaviors of the uncoated and coated tools with cutting length when milling the mersawa wood and the particleboard.

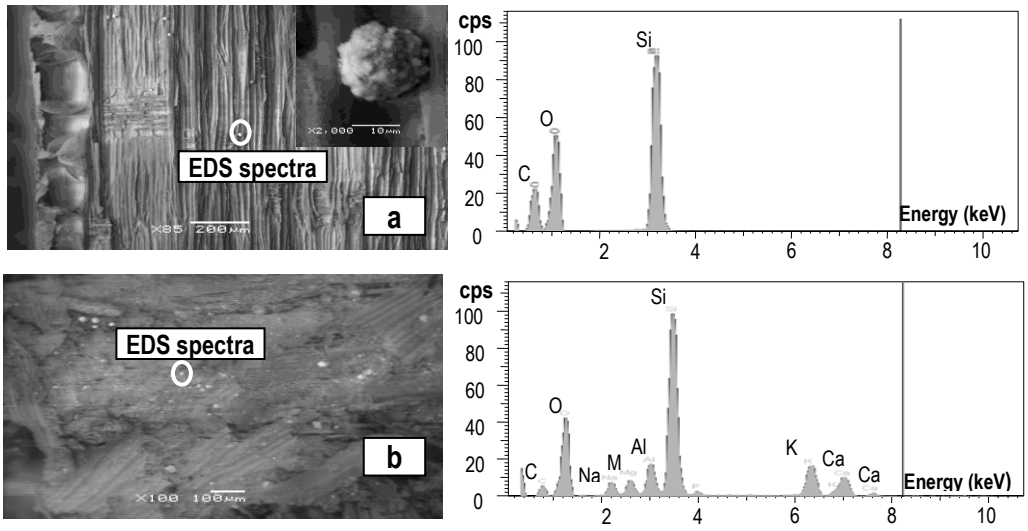

Figure 2. SEM micrograph (left) and EDS profile (right) of the wood materials showing the abrasives for mersawa wood (a) and particleboard (b)

The results shown in Figures 1 indicate that the multilayer-coated TiAlN/TiBN tool had the highest resistance to clearance wear compared with the multilayer-coated TiAlN/TiSiN and monolayer-coated TiAlN tools when cutting the mersawa and

particleboard. The high wear resistance of the TiAlN/TiBN tool is considered as a result from the following reasons. First, the friction coefficient of the multilayered TiAlN/TiBN coating was lower than that of TiAlN, and TiAlN/TiSiN coatings, which led to less abrasion against the hard abrasive materials contained in the mersawa wood and particleboard. Second, it was reported in another study (Usuki et al 2013) that the TiBN film provides lubrication effect at high temperatures.

The worn edges of the coated tools under an optical video microscope showed similar delamination mechanisms of coating films in cutting the mersawa wood and the particleboard. Figure 3 depicts the mechanism of delamination of the TiAlN/TiBN coating, which is selected for discussion in this article. Delamination of the TiAlN/TiBN coating was preceded by premature chipping of the coating film at the cutting edge. The extent of chipping was found to increase at a cutting length of 200 m. As the cutting continued up to a length of 300 m, the cutting edge underwent more prominent chipping of the coating film. Chipping of the coating film occurred on the whole cutting edge as the cutting length reached 400 m. Furthermore, the TiAlN/TiBN coating gradually delaminated in proportion along the cutting edge as the cutting action continued beyond 400 m. We consider that the wear of the K10 substrate occurred as the TiAlN/TiBN films were removed from the substrate.

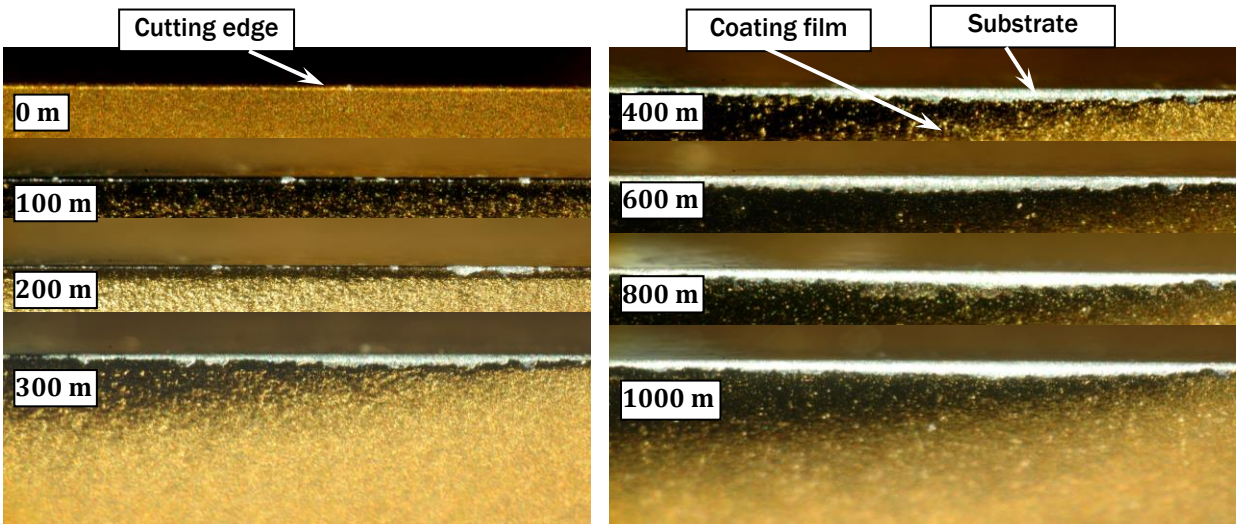

Figure 3. Wear mechanism of the TiAlN/TiBN multilayer coating when cutting particleboard.

The SEM micrographs of the worn edges of the TiAlN/TiBiN-coated tool in cutting the mersawa wood and particleboard for a 1-km cutting length are shown in Figure 4. These micrographs reveal that the patterns of edge wear generated by TiAlN/TiBiN in the two materials were relatively the same. Delaminations of coating film were generated by the TiAlN/TiBiN-coated carbide tools. This suggests that the substrate of the TiAlN/TiBiN-coated tools would be exposed to any possible mechanical abrasion, which caused retraction of tungsten carbide grains from the substrate during

cutting. Retraction of carbide grains was reported to cause a corrugated cutting edge, which tends to produce rough board surfaces during cutting (Darmawan et al. 2008).

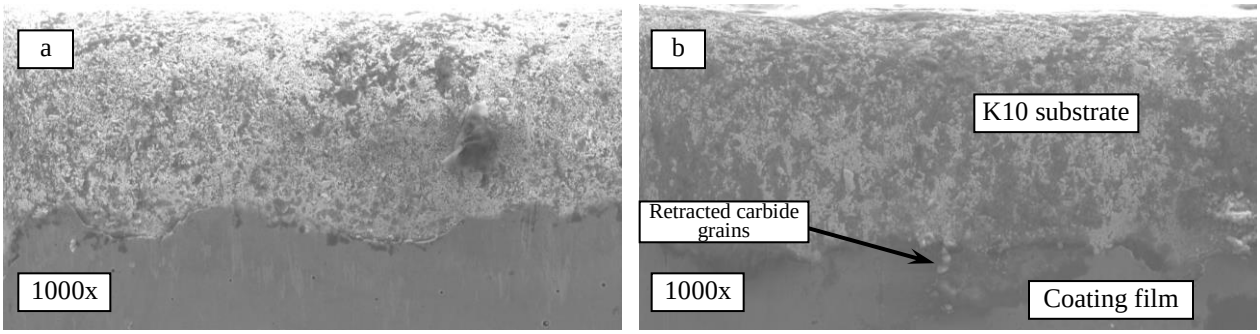

Figure 4. Scanning electron micrographs of the worn edges of the newly coated cutting tools when cutting particleboard at the final cutting length of 1 km: (a) TiAlN, (b) TiAlN/TiBN, (c) TiAlN/TiSiN, and (d) TiAlN/CrAlN.

Conclusions

1. The following conclusions can be made based on the findings of this study.
2. Delamination of the TiAlN, TiAlN/TiSiN, and TiAlN/TiBiN coating films is preceded by chipping of the coating films, which is caused mainly by mechanical abrasion.
3. The wear patterns of the coated carbide tools when cutting mersawa wood and particleboard are almost the same; the wear of the carbide substrate occurs after the coating films have disappeared from the carbide substrate.
4. The multilayer coated tools, which are better in reducing the progression of delamination wear, indicate a very promising applicability for high-speed cutting of abrasive wood and wood-based materials.

Literature Cited

ASTM International (2006) Standard guide for corrosion tests in high temperature or high pressure environment. ASTM G111-97. *In:* Annual Book of ASTM Standards. Vol. 03.02. ASTM International, Philadelphia.

ASTM International (2009) Standard practice for instrumented indentation testing. ASTM E2546-07. *In:* Annual Book of ASTM Standards. Vol. 03.01. ASTM International, Philadelphia.

ASTM International (2010) Standard test method for wear testing with a pin-on-disk apparatus. ASTM G99-05. *In:* Annual Book of ASTM Standards. Vol. 03.02. ASTM International, Philadelphia.

Banh T L, Phan QT, and Nguyen DB (2004) Wear mechanisms of PVD coated HSS end-mills used to machine 1045 hardened steel. *Adv. Technol. Mater. Mater. Process.* 6(2):244–249.

Chang CL, Chen WC, Tsai PC, Ho WY, and Wang DY (2007) Characteristics and performance of TiSiN/TiAlN multilayer coatings synthesized by cathodic arc plasma evaporation. *Surf. Coat. Technol.* 202(7):987–992.

Darmawan W, Tanaka C, Usuki H, Ohtani T (2001) Performance of coated carbide tools when grooving wood-based materials : Effect of work materials and coating materials on the wear resistance of coated carbide tools. J. Wood Science. Vol. 47 (2) : 94 - 101

Darmawan W, Rahayu I, Nandika D, Marchal R (2012) The Importance of Extractives and Abrasives in Wood Materials on the Wearing of Wood Cutting Tools. Journal of BioResources. Vol 7 (4) : 4715 – 4729

Ding XZ, Tan ALK, Zeng XT, Wang C, Yue T, and Sun CQ (2006) Corrosion resistance of CrAlN and TiAlN coatings deposited by lateral rotating cathode arc. *Thin Solid Films* 516:987–992.

Fuch I and Raatz C (1997) Study of wear behavior of specially coated (CVD, PACVD) cemented carbide tools while milling of wood-based materials. *In:* Proceedings of the 13th International Wood Machining Seminar. University of British Columbia, Vancouver, B.C., Canada, June 17-19, pp 709–715.

Salje E and Stuehmeier W (1988) Milling particleboard with high hard cutting materials. *In:* Proceedings of the Ninth International Wood Machining Seminar. University of California Forest Products Laboratory, Richmond, California, October 10-12, pp 211–228.

Sheikh-Ahmad JY and Bailey JA (1999) High-temperature wear of cemented tungsten carbide tools while machining particleboard and fiberboard. *J. Wood Sci.* 45(6):445–455.

Sheikh-Ahmad JY and Stewart JS (1995) Performance of different PVD coated tungsten carbide tools in the continuous machining of particleboard. *In:* Proceedings of the 12th International Wood Machining Seminar. Kyoto University, Kyoto, Japan, October 2 – 4, pp 282–291.

Stewart HA (1992) High-temperature halogenation of tungsten carbide cobalt tool material when machining medium density fiberboard. *Forest Prod. J.* 42(10):27–31.

TAPPI (1991) TAPPI Test Methods: Ash in Wood and Pulp (T211 om-85), Vol. 1. TAPPI Press, Atlanta.

Usuki H, Uehara K, Isaka M, and Kubota K (2013) Machining of Inconel 718 with Lubricant-Coated Tool. Int. J. of Automation Technology, 7 (3) : 306-312

Acknowledgments

The authors thank the Directorate of Research and Community Service of the Ministry of Research and Technology for the Republic of Indonesia for the research grant, and Hitachi Tool Engineering Ltd. Japan for preparing the coated cutting tools

Proceedings of the 58th International Convention of Society of Wood Science and Technology
June 7-12, 2015 – Grand Teton National Park, Jackson, Wyoming, USA

Influence of Wetting on Surface Quality during Scots Pine Planing

Victor Grubîi [1] – Micael Öhman [2] – Mats Ekevad [3]*

[1] Master student Luleå University of Technology, Skellefteå, Sweden
* *Corresponding author*
vicgru-3@student.ltu.se
[2] Lecturer Luleå University of Technology, Skellefteå, Sweden
micael.ohman@ltu.se
[3] Professor Luleå University of Technology, Skellefteå, Sweden
mats.ekevad@ltu.se

Abstract

Planing of timber in the sawmill industry are decisive for the quality of the final products. An important issue represents the torn grain defect while planing dried Scots pine timber. The defect is characterized by a splintered wood surface occurring usually around knots, where the fibers orientation is nearly perpendicular to the cutting direction.

The aim of this study was to establish how wood wetting processes influenced the occurrence of planing defects, especially the torn grain defect. For surface quality characterization, 120 surfaces were analyzed when dry and wet planing using a qualitative method and graded based on ASTM D1666-11 standard procedures. Due to its limitations, a separate quantitative assessment method was proposed for application and compared with the qualitative method. The quantitative assessment was based on a *mechanical measurement* of the torn grain parameters and grading classes based on quantification of the qualitative assessment grades.

Both assessment methods showed slight improvements in surface quality assessment after the wetting processes mainly because of positive impact of wetting on planing of the disturbances zones in wood. Results have shown that with increasing of the wetting time there is an increase in moisture penetration depth too which affects negatively the surface quality after planing. Overall, the qualitative assessment tends to be more accurate for general surface quality assessment while the quantitative method has the main focus on torn grain defect characterization.

Key words: torn grain, fuzzy grain, surface quality, planing defects, moisture content

1. Introduction

During wood machining and especially during planing, surface defects may occur. The possibility of the wood to be integrated in finished products like furniture depends on the degree of the defects. Accordingly, methods to reduce defects on wood surface are in much demand.

The present study is focused on *torn grain* occurrence while planing kiln dried Scots pine *(Pinus sylvestris* L.*)* wood. The defect is characterized by a splintered wood surface where small particles have been broken or lifted from the surface. This happens when the knives are working against the grain, usually around knots (Davim, 2011). The main factor in torn grain occurrence, the grain orientation, was confirmed by Goli et al. (2008) which refers to different chips types formation by cutting at different grain angles, worst chip formation being represented by cutting at 90^o grain orientation with increased depth of cut. A specific cause for torn grain occurrence represents the typically increased timber feed speeds in modern sawmill lines, 50-150 m/min (Jackson et al. 2006).

Another reason for torn grain occurrence which makes the problem statement of the current study, is the material low moisture content, 6-8%, at which the material could be too brittle and sudden changes in the grain orientation cause the surface fibers avulsion – torn grain defect. On the other hand, if the material has too high moisture content, other defects of planing might occur (Davim 2011 such as fuzzy and raised grain. Fuzzy grain is characterized by a group of fibers that have not been cleanly cut and still remains lifted. Raised grain is a defect that appears afterwards the planing process and occurs because of density variation in the growth rings where denser latewood cells compress the lower density earlywood cells that will expand to their original shape because of moisture variations after planing. These defects occur because of improper machining conditions like worn knives, insufficient clearance angle, excessive pressure on the feeding rolls and/or high moisture content of wood, 20% or more (Davim, 2011).

According to Aguilera and Martin (2001), the most important input parameters in the planing process are the wood species, grain orientation, cutting depth, feed rate and cutting speed. According to Dinwoodie (2000), increasing moisture content from zero up to fiber saturation point, result in a linear loss in stiffness, further increase in moisture content having no influence in stiffness.

The aim of this study, is to ascertain if a wetting process can reduce torn grain and improve the quality of the wood surface.

In order to characterize wood surface quality there are several methods such as: *Mechanical contact* (Kirsch et al. 1999), *Artificial vision* (Garrido et al. 2007), *Pneumatic* (Mothe 1985), *Friction* (Davim 2011) and *Visio-Touch* (Triboulot 1984) but due to wood anisotropy none of them seems to be perfectly suitable (Davim 2011), each one having its advantages and disadvantages (Lemaster 1995). In both planing industry and for clients,

the most common method is the visual-tactile assessment which consists in simply viewing and touching the surface by rotating the finger. Although it is a simple method it has a main disadvantage, it relies on the subjectivity of the operator. This is why, surface grading based on precise measurement of the defects will have a positive impact on planing mills by means of saving manual labor and increasing product's reliability towards customers.

2. Materials and Methods

2.1 Material and machining properties

For the testing procedures, 60 samples with the nominal dimensions 500x120x19 mm were manufactured from Scots pine *(Pinus sylvestris L.)* sideboards, of quality C (EN 1310:1997) from north of Sweden. Quality selection decision was based on presence of knots as the main theoretical reason for torn grain occurrence. Samples were used for planing in length direction (500 mm) on the flatside (120 mm). 120 surfaces were prepared and divided randomly into 4 different wetting treatment groups (table 1). The *oven-dry* method point out that the initial moisture content (MC) for one representative specimen was 7%.

By wetting for different wetting times, different moisture penetration depths were observed. From results of initial tests, it was decided the treatment with 4 different wetting times might have different influence on surface quality after planing: *0 min., 30 min., 60 min.* and *120 min*. Specimens were divided into 2 groups, first group being wetted on one face for *0 min*. and for *60 min.* on the opposite surface. Respectively, second group was wetted for *30 min*. and *120 min*.

Table 1. Material properties per treatment group

Material Proprieties	0 min.	30 min.	60 min.	120 min.
Annual ring thickness [mm]	1.42	1.45	1.42	1.45
Knots per sample	2.16	2.36	2.2	2.4
Percentage of knots area of the surface [%]	1.58	1.59	1.65	1.64

The machining of specimens was performed on a *Jonsereds PH-MB* planer, equipped with 2 cutting knives with 30^{o} rake angle, using a feed speed of 15 m/min, 6000 cutter-head RPM and depth of cut (DoC) of 1.5 mm. These parameters were selected in order to get an aggressive machining condition since this is a pre-requirement for torn grain occurrence. Specimens had the same feeding direction for all the planing operations.

2.2 Surface wetting

After jointing and dry planing, the surfaces of the samples were wetted, by keeping them in contact with water saturated sponge cloths, made of cotton and cellulose. Water saturated wetting cloths were used in order to reduce the excess of water and the water

movement in the longitudinal direction of the specimens. Specimens from the *0 min.* wetting time group were tap sprayed until the whole surface become covered with water.

The aim of the wetting process was to increase the wood surface moisture content up to the fibre saturation point, 28% MC, as a requirement for wood softening. According to Dinwoodie (2000), the density of a piece of timber is a function not only of the amount of wood substance present, but also of the presence of both extractives and moisture. Thus, moisture intake could be measured using the vertical density profile represented as the surface layer with increased density both in latewood and earlywood portions.

2.3 Surface quality assessment methods

2.3.1 Qualitative grading. Visio-Touch method

Using the *Visio-Touch* (VT) method (Triboulot, 1984), samples were graded according to planing defects (torn, fuzzy and raised grain) before and after planing. Planed wood surfaces were analyzed visually and tactile and classified into 5 quality grades (ASTM D1666-11): 1-excellent, 2-good, 3-fair, 4-poor, 5-very poor. *Excellent* grade stands for defect-free specimens. *Good* quality represents specimens with defects that are hardly detected with naked eye, small rips around knots. *Fair* grade is described by small to medium torn grain spread over limited areas, few and medium fuzzy and lifted grain which is possible to eliminate by sanding or finishing. *Poor* grade is a surface with extended medium to big torn grain occurrence that requires an extra sanding and finishing passage. A *very poor* grade is abusive torn grain represented by deep and large, usually few surface rips. These rips are not possible to eliminate by further processing and they are usually covered with a filler.

2.3.2 Quantitative grading. Mechanical Measurement

Quantitative grading is based on *mechanical measurement* (MM) of the defects. Boards were visually inspected and measured according to the most evident torn grain defects (Fig.1). The most important features considered for torn grain characterization are: *max. torn depth*, *max. torn diameter* and *torn area*. *Max. torn depth* is the deepest hollow in the wood surface due to torn grain occurrence and was measured with a dial depth gage with 0.2 mm ball tip and 0.01 mm accuracy. *Max. torn diameter* is measured on the largest visually detected torn pit while *torn area* is the wood surface on which torn grain is spread. Both *max. torn diameter* and *torn area* were measured with a caliper with a 0.05 mm accuracy. *Torn area* represents the percentage of total area covered by torn grain rips and was calculated from the sum of estimated outer tangential rectangles areas of the torn rips divided by the whole surface area.

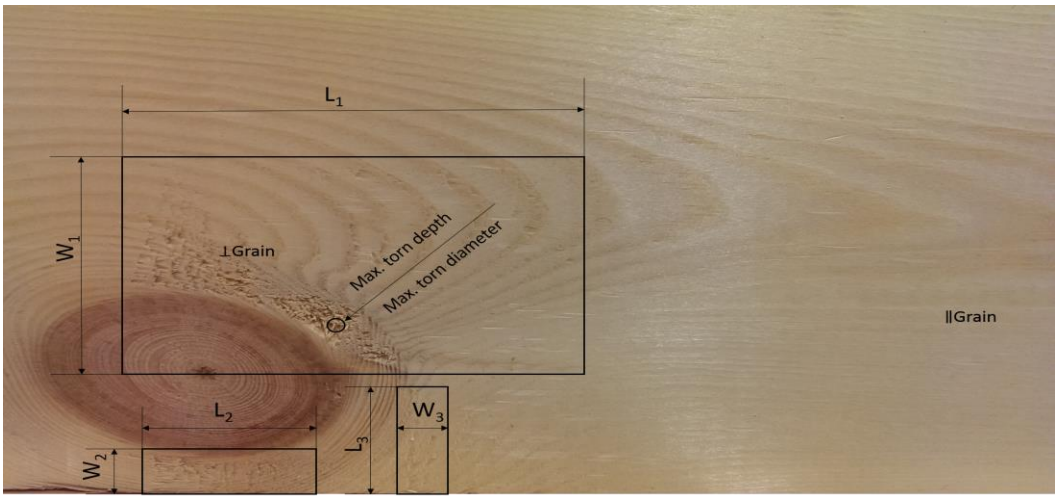

Fig.1 Appearance of torn grain occurrence on dry planed specimen and it's measurement procedure. The specimen surface has area with both parallel grain, defect free surface (∥Grain) and disturbances areas where grain is almost perpendicular to the surface (⊥ Grain). Selected areas represent the torn grain occurrence areas, identified and measured (Torn area= ∑W*L).

In *Table 2* it is fixed grading criteria for surface quality assessment in relation to torn grain defect. Grading boundaries are established in relation with the qualitative grading assessment but also with respect to possible further utilization after planing e.g. joinery. For instance, a *torn depth* of 0.5 mm can be removed by sanding, and even though it is a visible defect, the surface can be assessed as *fair*. The final grade was determined by the lowest parameter's grade.

Table 2. Surface quality grades according to torn grain defect

Grade	Quality	Torn depth [mm]	Torn diameter [mm]	Torn area [% of total surface]
1	Excellent	0	0	0
2	Good	<0.2	<0.5	<3
3	Fair	0.2-0.5	0.5-1	3-7
4	Poor	0.5-1	1-2	7-10
5	Very poor	>1	>2	>10

3. Results

3.1 Qualitative vs. Quantitative grading

Cumulative results of quality variation before and after water treatment using *Visio-Touch* assessment method are presented in the Figure 2. The quantitative grading results are presented in the Figure 3.

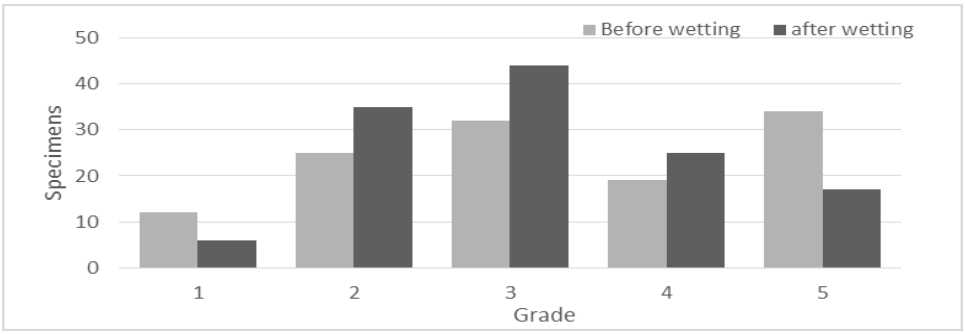

Fig.7 Summarized values of grading variation before and after the wetting processes using the Visio-Touch method

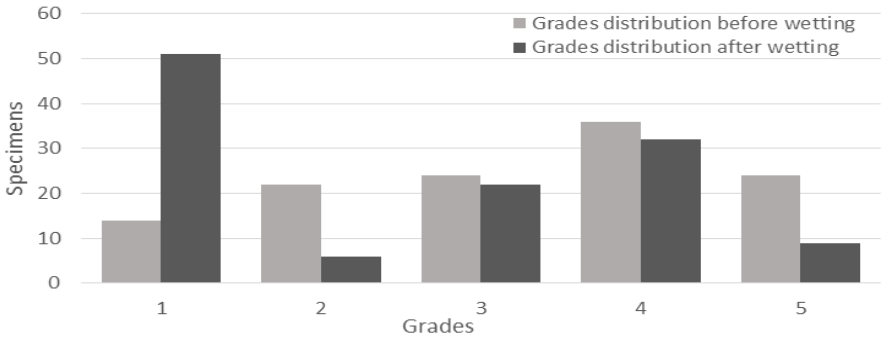

Fig.8 Summarized values of grading variation before and after the wetting processes using the Mechanical Measurement method

Mean values for the two assessment methods including statistical significance are presented in table 2. *ΔGrade* represents the change in grade after the wet planing. *Lower bound* and *upper bound* represents the 95% confidence interval which represents the true mean value of the change of grade after the wetting process.

Table 2. Mean results of the change of grade for both assessment methods

ΔGrade	**Mean**		**Standard deviation**		**Lower bound (95% confidence interval)**		**Upper bound (95% confidence interval)**	
Wetting time [min]	VT	MM	VT	MM	VT	MM	VT	MM
0	0.58	0.9	0.9	1.21	0.25	0.46	0.91	1.33
30	0.24	0.72	1.18	1.22	-0.18	0.28	0.67	1.16
60	0.48	1.03	1.02	1.23	0.11	0.59	0.85	1.47
120	0.06	0.44	0.99	1.05	-0.43	0.06	0.29	0.76

4. Discussion

4.1 Qualitative grading

Mean results of the qualitative grading using the *Visio-Touch* method show slight improvements for *0 min.* and *60 min.* wetting time groups while for *30 min.* and *120 min.* wetting time the differences after treatment were not significant. The reason is not only because of torn grain occurrence but also due to other defects created when planing wood with increased moisture content e.g. fuzzy grain or lifted grain. A general behavior after planing of a wetted surface in relation to defects zones being that the torn occurrence will be substituted by the fuzzy or lifted grain defect which is essentially not a destruction of the surface but rather a deficient processing which can be removed in further processing stages e.g. by sanding and finishing.

The most positive results have been registered with the *0 min.* wetting time, with water spraying of the specimens which can be assessed as very positive with respect to implementation into production. A general behavior of surface quality after wetting processes will be that the number of *1st* and the *5th* graded surfaces will be significantly reduced while "middle" grades will be uniformly increased, Fig.2. The conclusion is that the method should be used only for the lowest grade surfaces.

4.2 Quantitative grading

Differently from qualitative assessment, the results of the *Mechanical measurement* method reflect only the changes in surface quality according to torn grain occurrence. Respectively, the results show slightly more significant improvements in surface quality. All the wetting classes proved to have positive impact on torn grain occurrence, the true mean values of grading parameters changes being positive. Hence, there is no significant difference in parameters change between wetting times, but there is a small tendency towards decreasing quality with increased wetting time.

Surprisingly, the best results with the *Mechanical Measurement* method were obtained with *60 min*. wetting time, the mean increase in surface quality of about 1 grade unit proofing the positive effect of wood wetting in torn grain reduction. Similarly positive impact could be observed on the other side of the same specimens, wetted for *0 min.* It can be concluded that the raw material features parameter has a more important impact on surface quality modification than the wetting time itself.

Cumulative results of grades variation showed different behavior from qualitative assessment in terms that the mean increase in surface quality is due to increase of 1st graded specimens by 364% (Fig.3), the rest of grades frequency was lowered. This indicates that in many cases the torn grain defect was eliminated or reduced to insignificant sizes.

An interesting feature of the torn grain occurrence is that it happened always where grain angle was not parallel to the surface and it was latewood portions where the torn grain occurred. This indicates that denser material – latewood fibers, due to thicker cell walls, need a much higher cutting force and it will produce fiber avulsion. Also, presence of reaction wood close to the knots due to external stresses increases the difference between cutting forces.

5. Conclusions

The wetting process proofed to have slightly positive impact on surface quality when planing Scots pine wood. Softening of the wood surface layer hindered the ripping of fibers from surface, the torn grain defect. The disturbances zones, characteristic with torn grain occurrence, after wet planing gathered a more „wooly" surface due to lifted fibers, fuzzy grain defect. For particular uses, the fuzzy grain defect can be easier to „fix" by further processes e.g. sanding and finishing. Wood wetting for short periods of time appeared to be the most suitable for surface quality increase due to loss in cell walls stiffness in top layers but also, keeping rather low, suitable moisture content in the detachment zones.

The current study covered two grading methods for surface quality in relationship to torn grain occurrence. Especially of interest for planing mills might be the quantitative method which allows measurement and classification of the defects based on distinct criteria. It can be said that despite the good correlation between the two methods, there is need for completion of the *mechanical measurement* method from the fuzzy/raised grain defect assessment perspective.

As a preliminary hypothetical study, current work was focused on torn grain classification and identification of wetting processes influences on the surface quality of wood. Future studies should be focused in detailed studies of the wood properties in the disturbances zones and their surface quality behavior using different machining properties.

References

1. Aguilera A.; Martin P. 2001. Machining qualification of solid wood of Fagus silvatica L. And Picea excesa L.: cutting forces, power requirements and surface roughness. Holz als Roh- und Werkstoff, vol. 59, no.6, pp. 483-488.
2. ASTM D1666-11. Standard Test Methods for Conducting Machining Tests of Wood and Wood-Base Materials, ASTM International, West Conshohocken, PA, 2011
3. Davim J. P., 2011. Wood Machining. ISTE Ltd., London, UK
4. Dinwoodie JM., 2000. Timber; its nature and behavior. Second edition, Taylor&Francis, Abingdom, UK
5. EN 1310:1997. Round and sawn timber – Method of measurement of features. European standard.
6. Garrido N., Martins J., Carvalho L.H., Mendes J.G., Costa C.2007. Method of sawing conditions on the quality of particleboard edges. Proceedings of the 18th International Wood Machining Seminar, p.247-255, Vancouver, Canada.
7. Goli, G.; Fioravanti M.; Marchal R.; Uzielli L.; Busoni S. 2009. Up-milling and down-milling wood with different grain orientations – the cutting forces behavior, Eur. J. Wood Prod. (2010) 68:385-395.

8. Jackson M.R.; Hynek P.; Parkin R.M. 2007. On planing machine engineering characteristics and machined timber surface quality. Mechatronics Research Centre, Loughborough University, Loughborough, Leicestershire, UK. ImecE Vol.221 Part E: J. Process Mechanical Engineering.
9. Krish J., Csiha C. 1999. Analyzing wood surface roughness using an S3P perthometer and computer based data processing. Proceedings of the 13th Sesja Naukowa Badania dla Meblarstwa, Poland, p. 145-154.
10. Lemaster R.L. 1995.The use of an optical profilometer to monitor product quality in wood and wood-based products. Proceedings of the Forest Products Society, p.33-42, Madison, WI.
11. Mothe F., "Essai de comparaison de 3 méthodes de classement de surface bois massif pour leur rugosité; méthodes pneumatique et sensorielle", Annales des Sciences Forestieres, col.42, no.4, p.435-452, 1985.
12. Triboulot P (1984). Réflexion sur les surfaces et mesures des états de surfaces du bois. Annales des Sciences Forestière,vol.41, no.3, p.335-354,
13. Wyeth D.J.; Goli G.; Atkins A.G. 2009. Fracture toughness, chip types and the mechanics of cutting wood. A review COST Action E35 2004-2008: Wood machining – micromechanics and fracture. Holzforschung, Vol.63, pp. 168-180.

Acknowledgements

The first author wants to thank Åforsk foundation for financial support provided in order to present the project results at the International Convention of SWST to be held in Jun 7-12 2015 in Jackson, US (ref. nr 15-277).

Proceedings of the 58th International Convention of Society of Wood Science and Technology
June 7-12, 2015 – Grand Teton National Park, Jackson, Wyoming, USA

Fiber Properties Chain: From Cell Wall to End Products Session
Moderator: *Jean-Michel Leban, INRA, France*

Assessing Timber MOE&MOR in the Forest Resources: What We Have Learnt During the Last Twenty Years

Jean-Michel Leban, leban@nancy.inra.fr

INRA, 4 rue Giradet, Nancy 54000

Abstract

MOE, MOR and to a lesser extend wood density, are the main wood properties used by engineers and architects for the dimensioning of wooden structures.
For a given construction market, it is possible to estimate the amount of timber that is necessary for fulfilling the consumer demand. The question that arises is therefore» how to produce the right raw material for the end users requirements?"
The recent development of non destructive testing technologies permits the low cost measurement of timber MOE-MOR at the stand level in forests, and at the sawmill before and after log conversion in boards and battens. During the same period scientists have produced models that permit to simulate the variations of the timber properties by quantifying the different sources of variability. In this paper we will review the main results published during the last twenty years by considering the different studied tree species and the geographic areas covered. After the identification of the patterns and trends for the studies of the timber MOE-MOR and wood density variations, an attempt will be made for (i) evaluating if today, forest managers know how to produce the right raw material for the construction market and (ii) identifying the new research questions that need now to be answered in the assessment of the timber properties from the present and future forest resources.

Proceedings of the 58th International Convention of Society of Wood Science and Technology
June 7-12, 2015 – Grand Teton National Park, Jackson, Wyoming, USA

Bending Properties of Clear Bamboo Culm Material from Three Species

Patrick Dixon, pdixon7@mit.edu
Arfa Aijazi, anaijazi@gmail.com
Sally Lin, sallylin@mit.edu
Stephanie Chen, stephchen11@gmail.com
Peter Augusciak, peteraug@mit.edu

Massachusetts Institute of Technology, 77 Massachusetts Avenue, Building 8-032, Cambridge, MA 02139

Abstract

Bamboo is a renewable, lingo-cellulosic resource, being studied for use as sustainable construction material. The woody nature and size of timber bamboos, make them appropriate for the fabrication of structural products, analogous to wood products. Here, we compare the bending properties (modulus of elasticity, MOE, and modulus of rupture, MOR) and the microstructure of three species of timber bamboo: Phyllostachys pubescens, referred to as Moso; Guadua angustifolia, referred to as Guadua; and Bambusa stenostachya, referred to as Tre Gai. Bamboo has a fiber-reinforced structure, consisting of vascular bundles embedded in parenchyma cells. The vascular bundle volume fraction increases radially (inside to outside of the culm wall) and longitudinally (up the height of the culm), giving a structure of varying density. Bend specimens are cut from different positions in culm materials to assess the effect of density on the axial MOE and MOR. Initial results show similar MOR-density relationships for all three species, with MORs between 50 MPa to 250 MPa. However, the MOE of the Guadua is higher than the other species' at a given density. The MOE and MOR are related to microstructural models accounting for the varying fiber volume fraction. The understanding of the differences among these species determined here will allow for more informed selection of raw material for bamboo structural products. Sixth author: Lorna Gibson ljgibson@mit.edu

Proceedings of the 58th International Convention of Society of Wood Science and Technology
June 7-12, 2015 – Grand Teton National Park, Jackson, Wyoming, USA

Tannin-Based Foams from the Bark of Coniferous Species

Milan Sernek, milan.sernek@bf.uni-lj.si
Matjaž Čop, matjaz.cop@bf.uni-lj.si
Antonio Pizzi, antonio.pizzi@univ-lorraine.fr
Marie-Pierre Laborie, marie-pierre.laborie@fobawi.uni-freiburg.de

University of Ljubljana, 101 Jamnikarjeva, 1000 Ljubljana

Abstract

The use of renewable resources has a positive impact on the conservation of nature, and thus represents an important aspect of sustainability. The development of new bio-based tannin foams could make a significant contribution to the more efficient use of forest biomass resources. The objectives of this study was to characterize the curing kinetics of tannin-based foams by means of differential scanning calorimetry (DSC), as well as also to determine the influence of the individual components used to make up the foam on the latter's density, the structure of its pores, homogeneity, and compression strength, as well as on the compression modulus of the foam. DSC revealed that increased amounts of tannin slowed down the curing, whereas increased amounts of the catalyst accelerated the curing reaction. The advanced isoconversional method appears to be an appropriate model for the characterization of the curing kinetics of tannin-based foams. The investigation of the foam properties revealed that the amount of cross-linker affected homogeneity, and that the surfactant defined the foam morphology. Partial replacement of pine tannin with spruce tannin led to a decreased compression strength and compression modulus of the foam, but an increased proportion of the closed structure. It was found that the main factor of the foaming reaction was the amount of polyphenols present in the tannin extract.

Proceedings of the 58th International Convention of Society of Wood Science and Technology
June 7-12, 2015 – Grand Teton National Park, Jackson, Wyoming, USA

Comparison of Cost, Sustainability and Ecology for Different Solid Wood Panels

Dietrich Buck, diebuc-3@student.ltu.se
Xiaodong (Alice) Wang, alice.wang@ltu.se
Olle Hagman, olle.hagman@ltu.se
Anders Gustafsson, anders.gustafsson@sp.se

Luleå University of Technology, Forskargatan 1, , Skellefteå 93155

Abstract

Wood is considered as a pure ‘‘sustainable’’ and ‘‘renewable’’ material. The increasing use of wood for construction can have a positive impact on the sustainability of constructions. There are various techniques to join solid wood into prefabricated panels for construction. However, comparative market and economy studies are missing. In this paper, the following techniques for the production of solid wood panels are compared: Laminating, Nailing, Stapling, Screwing, Stress laminating, Doweling, Dovetailing and Wood welding. The production costs, durability and ecological consideration have been presented. This study is based on literatures and the reviews of 27 companies in 6 countries. The study shows that the techniques of solid wood construction are very different. Cross Laminated Timber (CLT) scores the highest in terms of cost and durability. For ecological fact, dovetailing is the best. Taking into account both durability and ecological considerations, doweling is the best. These alternatives give some freedom of choice regarding the visibility of surfaces and the efficient use of lower qualities of timber. CLT is the most cost-effective, not patented and well-established option in the market; the development of more health-friendly adhesives is still going on. Current researches demonstrate an alternative: Wood welding. From the ecological point of view, panels made exclusively of wood; no chemicals or no non-renewable resources are used.

Proceedings of the 58th International Convention of Society of Wood Science and Technology
June 7-12, 2015 – Grand Teton National Park, Jackson, Wyoming, USA

Anatomical, Physical and Mechanical Properties of Transgenic Loblolly Pine

Zachary Miller, zdmiller@ncsu.edu
Ilona Peszlen, impeszle@ncsu.edu
Perry Peralta, pperalta@ncsu.edu

North Carolina State University, 3911 Greenleaf Street, Raleigh, NC 27695

Abstract

The forest industry is moving toward fast-grown plantation timber to keep up with raw material needs and to reduce costs. Trees are being harvested at a younger age, producing wood with a larger portion of juvenile wood, knots and reaction wood, corresponding declines in modulus of elasticity (MOE) and modulus of rupture (MOR), and stability issues associated with the shrinking and swelling differential between juvenile and mature wood. The tree improvement industry utilizes good silvicultural methods along with genetic manipulation and subsequent selection of elite clones as powerful tools with the ultimate goal of enhancing tree growth while maintaining or increasing wood quality. Wood anatomy and physical properties are major factors in the selection process. The objectives of this study were to analyze mechanical, physical and anatomical properties of these transgenics and compare them to the control. This investigation consisted of 55 sample trees from two control groups and three transgenic groups modified for increased density. One elite transgenic group exhibited higher density and mechanical properties and showed thicker tracheid walls with smaller diameter compared with the control.

Proceedings of the 58th International Convention of Society of Wood Science and Technology
June 7-12, 2015 – Grand Teton National Park, Jackson, Wyoming, USA

Hybrids of TEMPO Nanofibrillated Cellulose and Copper Nanoparticles Embedded in Polyvinyl Alcohol for Antimicrobial Applications

Tuhua Zhong[1] *- Gloria S. Oporto*[2*] *- Jacek Jaczynski*[3] *- Changle Jiang*[1]

[1] PhD student, Division of Forestry and Natural Resources,
West Virginia University, Morgantown, WV 26506.

[2] Assistant Professor, Division of Forestry and Natural Resources,
West Virginia University, Morgantown, WV 26506.
* *Corresponding author*
Gloria.oporto@mail.wvu.edu

[3] Associate Professor, Division of Animal and Nutritional Sciences,
West Virginia University, Morgantown, WV 26506.

Abstract

Copper nanoparticles on TEMPO nanofibrillated cellulose (TNFC) and on carboxymethyl cellulose (CMC) templates were successfully synthesized. Polyvinyl alcohol (PVA) films embedded with the resulting hybrids of cellulose-copper nanoparticles were prepared by solvent casting method. Antimicrobial testing demonstrated that both PVA composite films have excellent antimicrobial properties against *E.coli* DH 5α. Approximately 90% less cellulosic material was required when using TNFC as template compared to CMC template to get similar films antimicrobial performance. The maximum thermal decomposition temperature of the films increased 18℃ and 25℃, when TNFC-copper nanoparticles and CMC-copper nanoparticles were incorporated into the films. Likely, compared to pure PVA, the storage modulus at 48℃ resulted enhanced up to 164% and 217% after the incorporation of the hybrid materials. The results shows that both hybrid cellulose-copper nanoparticles materials have potentiality to be used as advanced antimicrobial and reinforcing materials for thermoplastic composite applications.

Keywords: TEMPO nanofibrillated cellulose, Carboxymethyl cellulose, Polyvinyl alcohol, copper nanoparticles, antimicrobial properties, reinforcement material.

Introduction

Cellulosic micro- and nanomaterials have been effectively used to improve mechanical properties of several thermoplastic resins (Chakraborty et al 2006; Lee et al 2009; Liu et al 2014). The feasibility to improve also the antimicrobial properties of those films will open novel opportunities of applications that range from packing, medical, safety, etc. Copper has been used as antimicrobial agent since antiquity; metallic copper and copper oxides have demonstrated effective antimicrobial activities against a broad spectrum of microorganisms, fungi and viruses (Borkow and Gabbay 2009). In contrast to the low sensitivity of human tissue to copper (Hostynek and Maibach 2004), prokaryotes (ie, bacteria) are extremely susceptible to copper. There are a growing number of researches on the synthesis of metallic nanoparticles using cellulose as a stabilizer and nanoreactor (Padalkar et al 2010; Zhong et al 2013). However, little knowledge is reported on the effects of this type of hybrid cellulose-copper nanoparticles materials on thermoplastic resins and films.

The main objective of this work consisted on to evaluate the antimicrobial performance, thermal and mechanical properties of polyvinyl alcohol films after the incorporation of hybrid materials composed of carboxylate cellulose and copper nanoparticles. Because of their unique properties, such as light weight, high strength, biodegradability, biocompatibility and carboxylic group availability, carboxymethyl cellulose (CMC) and 2,2,6,6-tetramethylpiperidine-1-oxyl radical (TEMPO) nanofibrillated cellulose were chosen as template to attach copper nanoparticles.

Materials and Methods

Preparation of the hybrid TNFC-copper nanoparticles

Hybrid TNFC-copper nanoparticles was prepared by introducing copper nanoparticles on TNFC substrate by the chemical reduction of cupric ions (Zhong et al. 2013 modified procedure).

Preparation of the hybrid CMC-copper nanoparticles

The general procedure used for the preparation of the hybrid CMC-copper nanoparticles has been described previously (Zhong et al 2013).

Preparation of PVA/TNFC-copper nanoparticles and PVA/CMC-copper nanoparticles films

Polyvinyl alcohol (99-100% hydrolyzed, approx. M.W. 86000; Sigma Aldrich, St. Louis, MO)/TNFC-copper nanoparticle and PVA/CMC-copper nanoparticles films were prepared by solvent casting method described by Cheng et al (2007). The components of the films are presented in Table 1. Control films of PVA/TNFC and PVA/CMC were also prepared.

Table 1. Weight percentage (wt%) of main element to the total weight of PVA, cellulose and copper.

Sample Code	PVA (wt%)	Cellulose (wt%)	Copper (wt%)
PVA/TNFC-Cu0.6	98.3	1.1	0.6
PVA/CMC-Cu0.6	90.4	9.0	0.6
PVA/TNFC	98.9	1.1	---
PVA/CMC	90.9	9.1	---

Transmission Electron Microscopy (TEM)
The morphology and particle size of copper nanoparticles on TNFC substrate were observed by JEOL TEM-2100 instrument (Tokyo, Japan) operating at 120 kV, the observation of CMC-copper nanoparticles were operated at 200 kV. TEM samples were typically prepared by dropping the hybrid TNFC-copper nanoparticles and CMC-copper nanoparticles solutions on a 200 mesh nickel grid coated with a carbon film.

Antimicrobial activities of PVA/TNFC-Cu and PVA/CMC-Cu films
The *E.coli* DH5□□□Invitrogen Inc., Carlsbad, CA□ culture, with appropriately 10^8 colony-forming units per milliliter (CFU/mL), was used as targeted microorganism to test antimicrobial activities of PVA/TNFC-Cu and PVA/CMC-Cu films. A 2-mL aliquot of such culture was transferred to a surface of PVA/TNFC-Cu0.6 and PVA/CMC-Cu0.6 films and incubated at room temperature for 1 wk. The dilution and enumeration producers developed by (AOAC 1995, method 991.14; Black and Jaczynski 2006; Levanduski and Jaczynski 2008) were followed to enumerate the *E.coli*. All bacterial enumerations were performed in triplicate. Mean values are reported as CFU/mL.

Thermo-gravimetric analyzer (TGA) characterization
The thermal performance of pure PVA and its nanocomposite films was determined by TA Q50 thermo-gravimetric analyzer (New Castle, USA), with temperature ramp-up rate of 10 ℃/min while being purged with nitrogen at a flow rate of 20 mL/min. The sample weight was chosen between 3 mg and 4 mg for all of the samples tested.

Dynamic Mechanical Analysis (DMA)
Samples of 38 mm × 15 mm × 0.35 mm for DMA analysis were prepared. Dynamic mechanical analysis was conducted in a tension-film mode on a TA Q800 DMA instrument (New Castle, USA), temperature scans were run from 30℃ to 150℃ at a heating rate of 2℃ /min with a frequency of 1 Hz and amplitude 30 μm.

Results and Discussion

Characterization of hybrid TNFC-copper nanoparticles and CMC-copper nanoparticles
The transmission electron micrographs of hybrid TNFC-copper nanoparticles and CMC-copper nanoparticles are presented in Fig 1. Copper nanoparticles reveal spherical

morphology for both hybrid materials, the particle size of copper nanoparticles on TNFC template is 9.2±2.0 nm as shown in Fig 1a, nanoparticles with the diameter around 12.5±2.8 nm are observed on CMC template as shown in Fig 1b.

a) b)

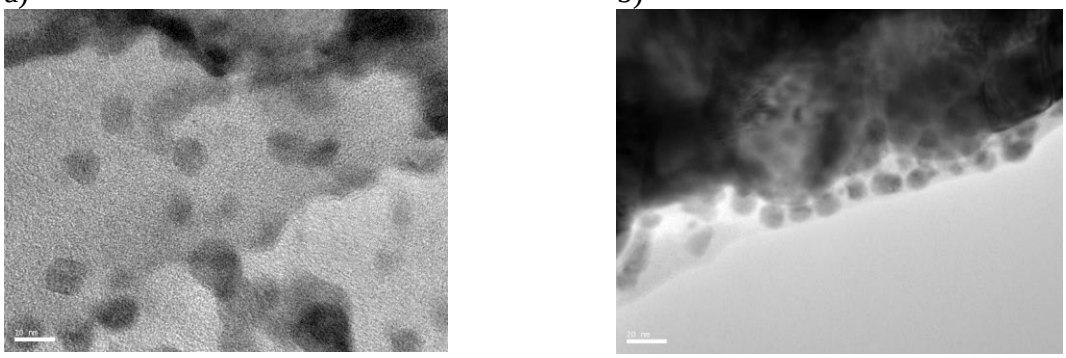

Figure 1. TEM images of (a) TNFC-copper nanoparticles and (b) CMC-copper nanoparticles.

Antimicrobial Activities of PVA/TNFC-Cu0.6 and PVA/CMC-Cu0.6 films

For both PVA composite films, reduction of *E.coli* has gradually increased over time as shown in Fig 2. Both PVA composite films have similar antimicrobial activities, over 99.99 % of *E.coli* were killed after 3-day exposure of *E.coli* to either PVA/TNFC-Cu0.6 film or PVA/CMC-Cu0.6 film. It is important to mention that approximately 90% less cellulosic material was required when using TNFC as template compared to CMC template to get similar films antimicrobial performance (Table 1 and Fig 2).

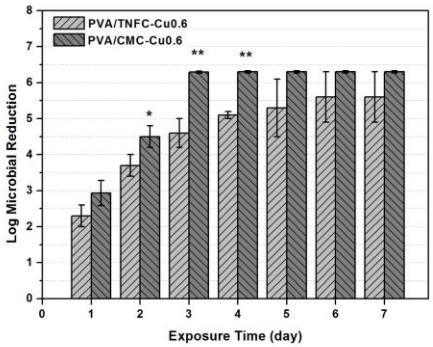

Figure 2. Microbial reduction induced by PVA containing cellulose-copper nanoparticles after various exposure time. The asterisks refer to significant level regarding antimicrobial efficacy of PVA/CMC-Cu0.6 compared to PVA/TNFC-Cu0.6 at the same exposure time: $p < 0.05$ (*), $P < 0.01$ (**).

Thermal analysis

Fig 3a shows typical derivative thermogravimetric (DTG) curves of the PVA composite films. T_{max} is the decomposition temperature corresponding to the maximum weight loss and relates to the maximum decomposition rate. In Fig 3a, we can see that T_{max} of PVA/TNFC-Cu0.6 and PVA/CMC-Cu0.6 films shifted to higher temperature compared to that of pure PVA, an increase of T_{max} was observed from 260 to 278℃ for PVA/TNFC-Cu0.6 composite film. The T_{max} of PVA composite was brought up to 285℃ after being incorporated CMC-copper nanoparticles compared to pure PVA. The major degradation peaks shifting to higher temperature is an indicator of enhanced thermal stability (Lu et al

2008). The thermal decomposition of PVA/TNFC-Cu0.6 and PVA/CMC-Cu0.6 films shifted slightly toward high temperature, suggesting that the composite films had higher thermal stability, which mainly was attributed to the presence of the crystal structure of copper nanoparticles and cellulose that were embedded in PVA matrix.

Dynamic mechanical analysis (DMA)

Fig 3b displays the temperature dependence of storage modulus of PVA and various PVA composite films. All PVA composite films have higher storage modulus than pure PVA, the order of the storage modulus for pure PVA and various PVA composite films on a heating around the glass transition temperature (T_g) at 48℃ was shown: PVA/CMC-Cu0.6 > PVA/TNFC-Cu0.6 > PVA/TNFC > PVA/CMC > PVA, and storage modulus increased by 217%, 164%, 158% and 33% when compared with the storage of PVA, respectively. The increase in storage modulus for PVA composites might be attributed to the synergistic effect of crystalline of cellulose and copper nanoparticles.

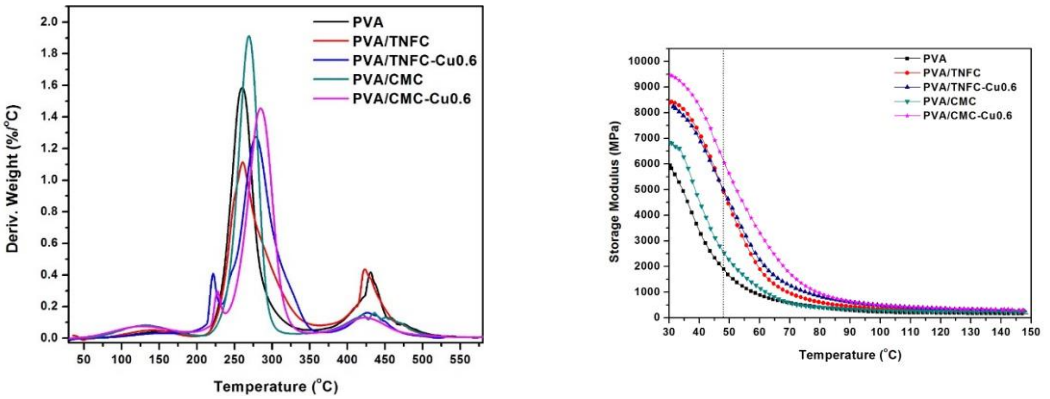

Figure 3. (a) DTG curves (Peak temperature (T_{max}) of PVA, PVA/TNFC, PVA/TNFC-Cu0.6, PVA/CMC, PVA/CMC-Cu0.6 was 260, 263, 278, 269, and 285℃, respectively); (b) Storage modulus as function of temperature for PVA composite films.

Conclusions

- PVA films embedded with two hybrid cellulose-copper nanoparticles (TNFC-copper nanoparticles and CMC-copper nanoparticles) were effectively prepared.
- The antimicrobial analysis demonstrated that one-week exposure of nonpathogenic *Escherichia coli* DH5α to the PVA composite films resulted in up to 5-log *E. coli* reduction after exposure.
- Approximately 90% less cellulosic material was required when using TNFC as template compared to CMC template to get similar films antimicrobial performance.
- The incorporation of TNFC-copper nanoparticles and CMC-copper nanoparticles on the PVA matrix increased the maximum decomposition temperature by 18℃ and 25℃ compared to pure PVA, respectively.

- The storage modulus of the PVA composite films at 48°C increased up to 164% and 217% with the incorporation of TNFC-copper nanoparticles and CMC-copper nanoparticles, respectively.

Acknowledgements

Funding for this work was provided by NIFA-McStennis WVA00098 "Efficient utilization of biomass for biopolymers in central Appalachia" and NIFA-USDA Grant/Contract No. 2013-34638-21481 "Development of novel hybrid cellulose nanocomposite film with potent biocide properties utilizing low quality Appalachian hardwoods".

References

AOAC (1995). Official methods of analysis. 16th ed. Association of Official Analytical Chemists International, Gaithersburg, MD.

Black JL, Jaczynski J (2006) Temperature effect on inactivation kinetics of *Escherichia coli* O157: H7 by electron beam in ground beef, chicken breast meat, and trout fillets. J Food Sci 71(6): M221-M227.

Borkow G, Gabbay J (2009) Copper, an ancient remedy returning to fight microbial, fungal and viral infections. Current Chemical Biology 3(3):272-278.

Chakraborty A, Sain M, Kortschot M (2006) Reinforcing potential of wood pulp-derived microfibres in a PVA matrix. Holzforschung 60(1):53-58.

Cheng Q, Wang S, Rials TG, Lee SH (2007) Physical and mechanical properties of polyvinyl alcohol and polypropylene composite materials reinforced with fibril aggregates isolated from regenerated cellulose fibers. Cellulose 14(6):593-602.

Lee SY, Mohan DJ, Kang IA, Doh GH, Lee S, Han SO (2009) Nanocellulose reinforced PVA composite films: effects of acid treatment and filler loading. Fiber Polym 10(1):77-82.

Levanduski L, Jaczynski J (2008) Increased resistance of *Escherichia coli* O157: H7 to electron beam following repetitive irradiation at sub-lethal doses. Int J Food Microbiol 121(3):328-334.

Liu D, Sun X, Tian H, Maiti S, Ma Z (2013) Effects of cellulose nanofibrils on the structure and properties on PVA nanocomposites. Cellulose 20(6):2981-2989.

Lu J, Wang T, Drzal LT (2008) Preparation and properties of microfibrillated cellulose polyvinyl alcohol composite materials. Composites Part A 39(5):738-746.

Hostynek JJ, Maibach HI (2004) Copper hypersensitivity: dermatologic aspects*. Dermatol Ther 17(4):328-333.

Padalkar S, Capadona JR, Rowan SJ, Weder C, Won YH, Stanciu LA, Moon RJ (2010). Natural biopolymers: novel templates for the synthesis of nanostructures. Langmuir 26(11):8497-8502.

Zhong T, Oporto GS, Jaczynski J, Tesfai AT, Armstrong J (2013) Antimicrobial properties of the hybrid copper nanoparticles-carboxymethyl cellulose. Wood Fiber Sci 45(2):215-222.

Proceedings of the 58th International Convention of Society of Wood Science and Technology
June 7-12, 2015 – Grand Teton National Park, Jackson, Wyoming, USA

Comparison Study of Nondestructive Testing Methods in Visual Grade No.2 Southern Pine Lumber: Bending Stiffness

Bonnie Yang, bonnie.yang@cfr.msstate.edu
Dan Seale, dseale@cfr.msstate.edu
Rubin Shmulsky, rshmulsky@cfr.msstate.edu

Mississippi State University, Box 9820, Mississippi State, MS 39762

Abstract

Bending stiffness (modulus of elasticity, or E) is one of the main indicators in structural lumber stress grading systems. Due to a relatively high amount of variability in contemporary sawn lumber, it is important that nondestructive evaluation technology is developed and employed to better discern potentially high E value pieces from potentially low E value pieces. The research described herein is from a field test of various nondestructive technologies (machine stress rating, transverse vibration and longitudinal stress wave techniques) applied to visually graded No. 2 southern pine lumber. A total of 343 pieces of 2 × 6, 2 × 8, 2 × 10, and 2 × 12 SP lumber were evaluated nondestructively with four commercial tools; static bending E values were then obtained by four-point bending tests. For each of the nondestructive techniques, results are correlated to static bending E. In all cases, the non-destructive techniques successfully predicted E for all lumber sizes, with linear regression R2 values ranging from 0.56 to 0.87. Based on these research findings, further testing and analysis related to strength performance seems appropriate.

Proceedings of the 58th International Convention of Society of Wood Science and Technology
June 7-12, 2015 – Grand Teton National Park, Jackson, Wyoming, USA

Distortion Energy Criterion for Estimating Dowel Bearing Strength of Timber Member Loaded at Angle

Bambang Suryoatmono [1] – Johannes Adhijoso Tjondro[2] - Lie Ting Hwe[3] - Clemen[3]*

[1] Professor, Department of Civil Engineering – Parahyangan Catholic University, Jalan Ciumbuleuit 94, Bandung 40141, Indonesia.
* *Corresponding author*
suryoatm@unpar.ac.id suryoat@yahoo.com

[2] Associate Professor, Departament of Civil Engineering – Parahyangan Catholic University, Jalan Ciumbuleuit 94, Bandung 40141, Indonesia.

[3] Former Student at Departament of Civil Engineering – Parahyangan Catholic University, Jalan Ciumbuleuit 94, Bandung 40141, Indonesia.

Abstract

To estimate the strength of a mechanical timber member connection loaded at an angle, one of the important properties is the dowel bearing strength of the member. Hankinson-type formulas have long been used to predict wood mechanical properties at an angle to the grain, including dowel bearing strength. The most recent wood specification in the USA (ANSI/AWC National Design Specification 2015) is one of the specifications that use Hankinson's type formulas. In this paper, distortion energy criterion (DEC) is used and an alternative equation to the Hankinson's formula is introduced. To verify the formula, dowel bearing tests on two sets of specimens were conducted. The first set of specimens had bolts of various diameter. Wood of various specific gravity in the hardwood category were loaded at an angle of 0º, 30º, 45º, 60º, and 90º to the grain. The second set of specimens were similar to the first set except that the mechanical fastener was lag screw of various diameter. The tests were conducted according to ASTM D5764-97a. It can be concluded that the proposed alternative equation based on distortion energy criterion (DEC) is better than the Hankinson's formula. This is due to the shear strength of the wood that is not considered in the Hankinson's formula.

***Keywords*:** dowel bearing strength at an angle, distortion energy criterion (DEC), Hankinson's formula, hardwood, bolt, lag screw.

Introduction

Dowel bearing strength of wood member is one of the most important parameters that influences the strength of the connections. According to the most recent code in the USA (ANSI/AWC 2015), the empirical formulas for computing dowel bearing strength parallel $F_{e\parallel}$ and perpendicular $F_{e\perp}$ to the grain, after converting to SI, are

for D $\geq$ 6.35 mm,

$$F_{e\parallel} = 77G\ MPa \tag{1}$$

$$F_{e\perp} = 212\frac{G^{1.45}}{\sqrt{D}}\ MPa \tag{2}$$

for D < 6.35 mm,

$$F_{e\perp} = 114G^{1.84}\ MPa \tag{3}$$

where G is specific gravity and D is fastener diameter (mm). In a case where the bearing stress is not parallel to the grain, the dowel bearing strength at an angle θ is computed using Hankinson's formula

$$F_{e\theta} = \frac{F_{e\parallel}F_{e\perp}}{F_{e\parallel}\sin^2\theta + F_{e\perp}\cos^2\theta} \tag{4}$$

Consider a differential element subjected to a uniaxial stress σ as seen in Fig. 1(a). This is a situation where a wood member is subjected to dowel bearing stress at an angle. Using coordinate transformation, it can easily be proven that the uniaxial stress σ causes

$$\begin{aligned}\sigma_1 &= \frac{\sigma}{2} + \frac{\sigma}{2}\cos(2\theta)\\ \sigma_2 &= \frac{\sigma}{2} - \frac{\sigma}{2}\cos(2\theta)\\ \tau_{12} &= -\frac{\sigma}{2}\sin(2\theta)\end{aligned} \tag{5}$$

in the material principal axes (Sadd 2009).

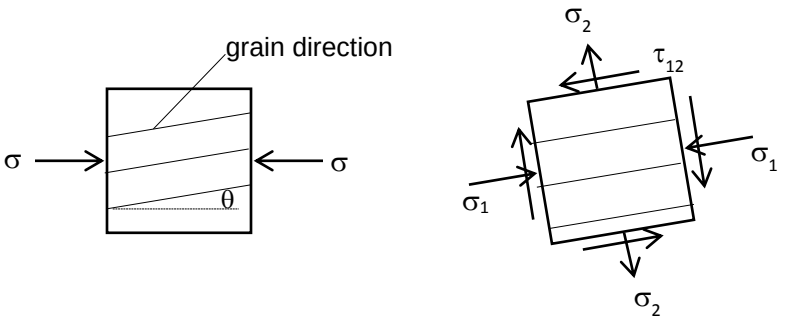

(a) (b)

Figure 1. (a) Differential element of wood material under uniaxial stress at an angle θ to the grain (b) Stress components in principal material axes.

For an orthotropic material such as wood under plane stress, the distortion energy criterion (DEC) of failure can be written as (Chen and Han 2007)

$$\frac{\sigma_1^2}{F_{e\|}^2}+\frac{\sigma_2^2}{F_{e\perp}^2}-\frac{\sigma_1\sigma_2}{F_{e\perp}^2}+\frac{\tau_{12}^2}{F_v^2}=1 \quad (6)$$

This is the extension of Von Mises criterion for the orthotropic case. Eq. 6 is similar to the equations used in Pranata and Suryoatmono (2012) for the tension case, Kharouf et.al (2005) for the compression case. It is seen that Eq. 6 considers the presence of shear stress. On the other hand, the Hankinson's type of equations, as seen in Eq. 4, neglects the presence of shear stress.

In this paper, Hankinson and DEC equations (Eqs 4 and 6) are compared with the test results. To measure the accuracy of the equations, a standard error of the estimate S_e is used (Montgomery and Runger 2014),

$$S_e=\sqrt{\frac{\Sigma(Y_{act}-Y_{pred})^2}{N}} \quad (7)$$

where Y_{act} is the actual (observed) value, in this case the dowel bearing strength obtained from test, Y_{pred} is the predicted value, in this case the dowel bearing strength computed using either Hankinson's equation (Eq. 4) or DEC formula (Eq. 6), and N is the number of data observed. Clearly, the equation that results in smaller standard error of the estimate S_e is the better one.

Materials & Methods

Specimens

The specimen dimensions to obtain dowel bearing strength conform to ASTM D5764-97a (2013). As seen in Eqs (1), (2), and (3), grain angle, specific gravity and diameter of the fastener influence the dowel bearing strength. Therefore, five Indonesian species in hardwood category with various cross grain specimens were tested, namely red meranti (shorea spp.), keruing (dipterocarpus spp.), sengon (paraseriantes falcataria), acacia mangium, and albasia (albizzia falcata). See Fig. 2 for the definition of cross grain (grain angle). A total of 337 specimens were made with cross grain varies from 0° to 90°. Two types of fasteners were used, namely bolt (diameter 11.2 mm, 16.0 mm, and 19.0 mm) and lag screw (diameter 8.1 mm and 9.4 mm).

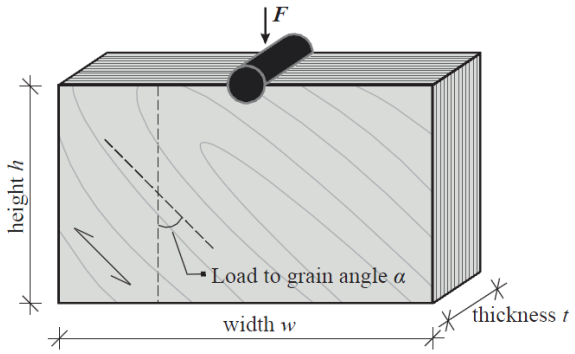

Figure 2. Specimen for evaluating dowel bearing strength at an angle (Franke and Quenneville, 2011)

In order to utilize DEC equation, shear strength F_v needs to be evaluated for each species. This was done in accordance to ASTM D 143-09 (2009).

Dowel bearing testing

A Universal Testing Machine (UTM) was utilized to load each specimen. The typical test setup for dowel bearing testing is shown in Figure 3. The loading was displacement controlled with a displacement rate of 1.5 mm/minute. The rate was so slow that the dynamic effects could be neglected. The loading was terminated when the specimen has shown significant failure. The load-displacement relationship during the test was recorded digitally. According to ASTM D5764-97a (2013), the dowel bearing strength is computed using

$$F_e = \frac{P_{0.05}}{Dt} \tag{8}$$

where $P_{0.05}$ is the load determined using 5% offset of the fastener diameter D and t is the thickness of the specimen (see Fig. 2).

Figure 3. Typical test setup for evaluating dowel bearing strength of wood (Clemen (2013).

Each specimen was weighed as well to obtain its specific gravity. Moisture content of each specimen after being air dried was measured using Lignomat digital moisture tester.

Results and Discussion

Figure 4 shows all dowel bearing strength from the test results (Hwie 2006 and Clemen 2013). Along with the test results, the Hankinson and DEC equations (Eq. 4 and 6, respectively) are also shown. In both the Hankinson's and DEC equations, the dowel bearing strength parallel $F_{e\parallel}$ and perpendicular $F_{e\perp}$ to the grain are the average values of the test results. Furthermore, the shear strength F_v in the Hankinson's formula is the average of the test results.

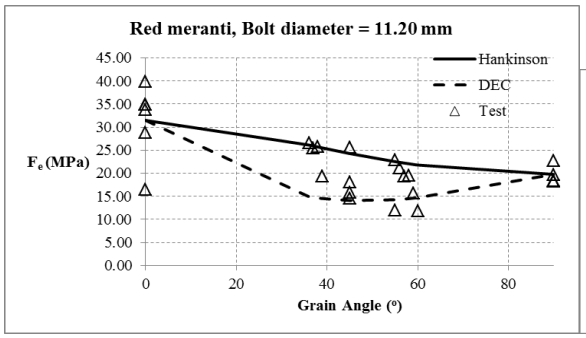
Red meranti, Bolt diameter = 11.20 mm
Hankinson
DEC
Test
F_e (MPa)
Grain Angle (º)

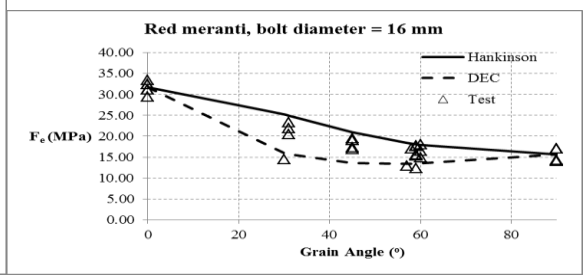
Red meranti, bolt diameter = 16 mm
Hankinson
DEC
Test
F_e (MPa)
Grain Angle (º)

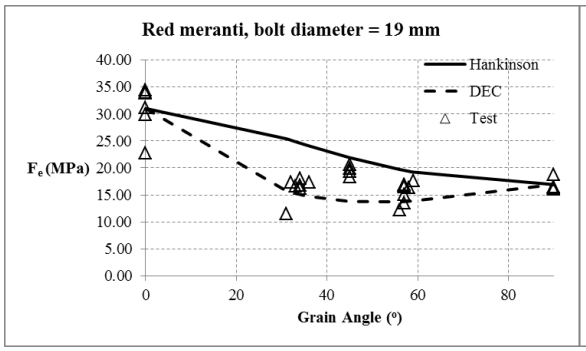
Red meranti, bolt diameter = 19 mm
Hankinson
DEC
Test
F_e (MPa)
Grain Angle (º)

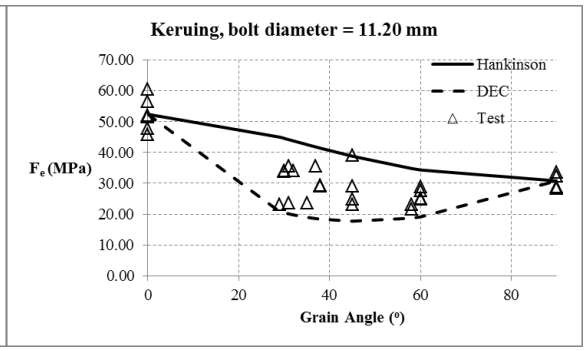
Keruing, bolt diameter = 11.20 mm
Hankinson
DEC
Test
F_e (MPa)
Grain Angle (º)

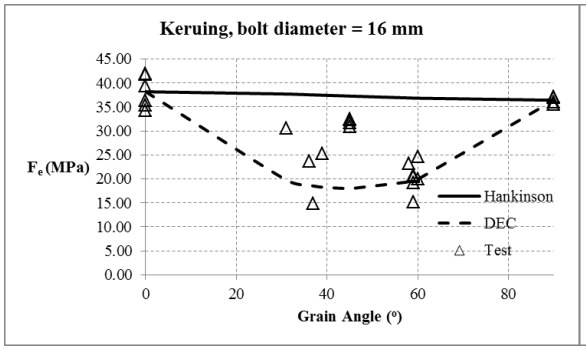
Keruing, bolt diameter = 16 mm
Hankinson
DEC
Test
F_e (MPa)
Grain Angle (º)

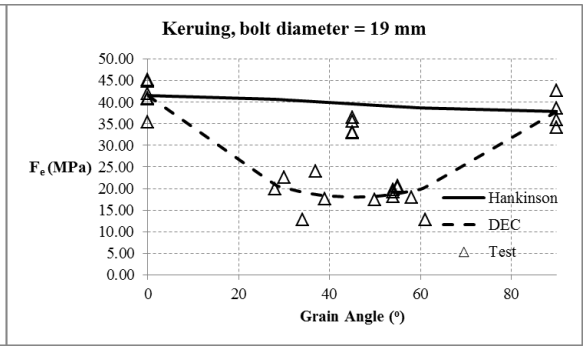
Keruing, bolt diameter = 19 mm
Hankinson
DEC
Test
F_e (MPa)
Grain Angle (º)

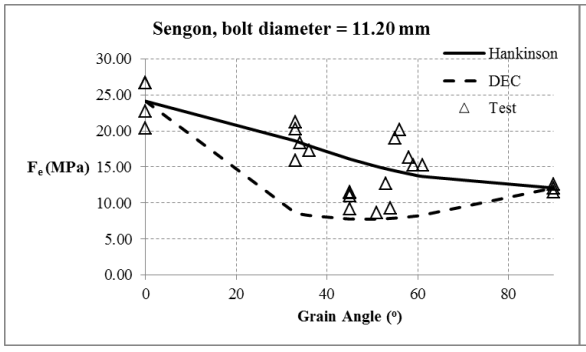
Sengon, bolt diameter = 11.20 mm
Hankinson
DEC
Test
F_e (MPa)
Grain Angle (º)

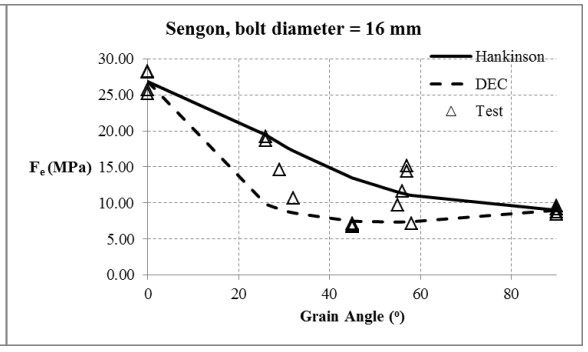
Sengon, bolt diameter = 16 mm
Hankinson
DEC
Test
F_e (MPa)
Grain Angle (º)

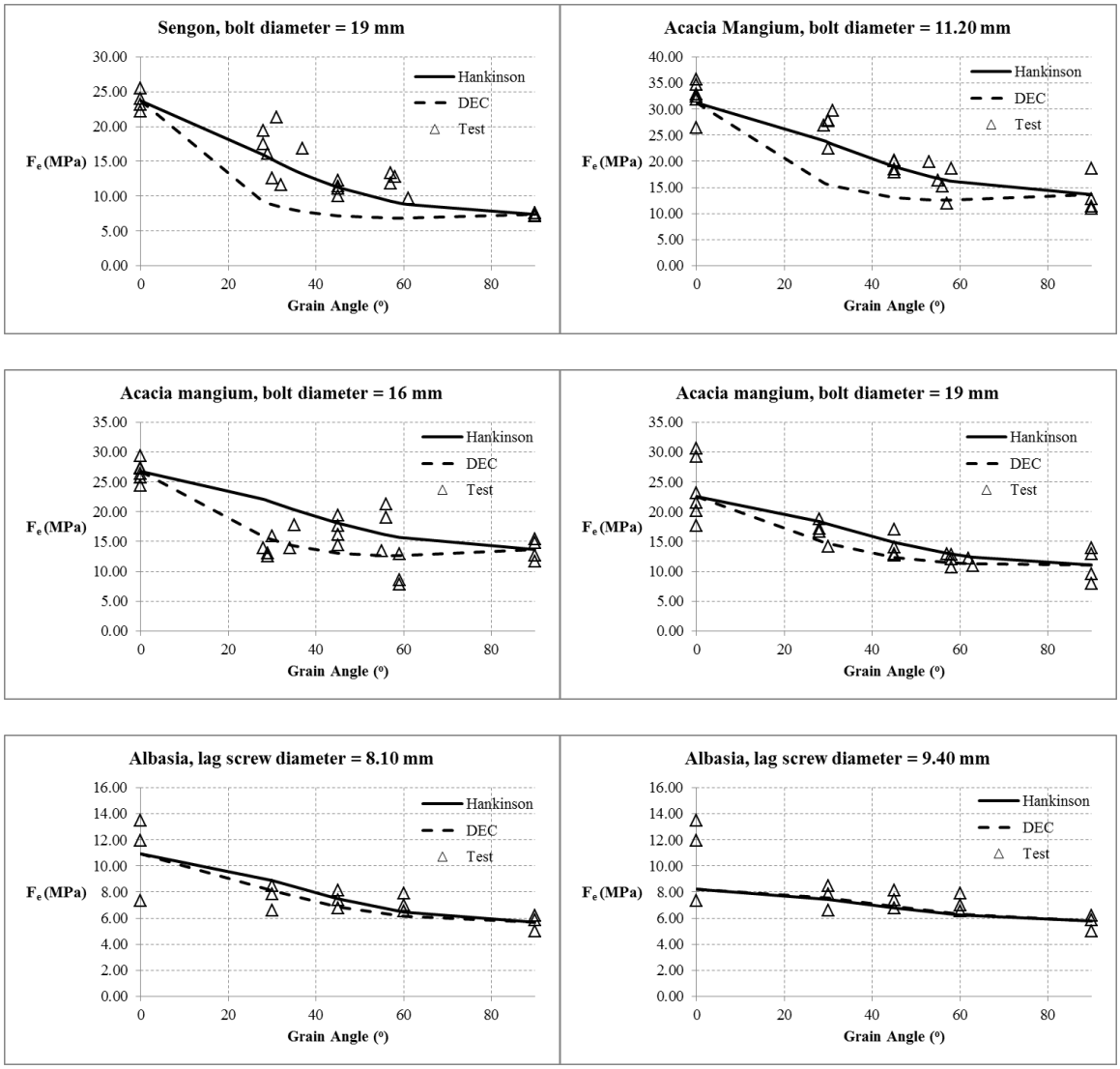

Figure 4. Dowel bearing strength F_e (MPa) for various grain angle (º).

Summary of Fig. 4 along with the standard error of the estimates are shown in Table 1. Out of the 14 categories (rows) in the table, there are six categories where S_e of DEC equation is smaller than that of Hankinson's equation. Although this is not a conclusive evidence, this is an indication that the presence of shear stress in the dowel bearing at an angle should be considered.

Table 1. Standard error of estimates S_e of dowel bearing strength F_e obtained from Hankinson's equation and distortion energy criterion, compared with test results.

Species	Average G	Fastener Type	Fastener Diameter (mm)	Average $F_{e\parallel}$ (MPa)	Average $F_{e\perp}$ (MPa)	Average F_v (MPa)	S_e of Hankinson's Eq'n (MPa)	S_e of DEC Eq'n (MPa)
(1)	(2)	(3)	(4)	(5)	(6)	(7)	(8)	(9)
Red Meranti	0.55	Bolt	11.2	31.46	19.77	7.55	5.83	6.56

Red Meranti	0.55	Bolt	16	31.69	15.65	7.55	3.21	3.38
Red Meranti	0.55	Bolt	19	31.02	16.92	7.55	5.25	3.37
Keruing	0.68	Bolt	11.2	52.40	30.81	9.27	10.38	9.09
Keruing	0.68	Bolt	16	38.18	36.40	9.27	10.95	6.61
Keruing	0.68	Bolt	19	41.53	37.84	9.27	14.85	7.06
Sengon	0.36	Bolt	11.2	24.13	12.08	4.10	3.54	6.66
Sengon	0.36	Bolt	16	26.84	8.99	4.10	3.68	4.05
Sengon	0.36	Bolt	19	23.70	7.38	4.10	2.39	5.43
Acacia Mangium	0.44	Bolt	11.2	26.22	13.64	7.43	3.05	6.57
Acacia Mangium	0.44	Bolt	16	26.77	13.67	7.43	4.47	3.31
Acacia Mangium	0.44	Bolt	19	22.56	11.09	7.43	2.92	3.00
Albasia	0.25	Lag screw	8.1	10.93	5.69	4.30	1.44	1.41
Albasia	0.25	Lag screw	9.4	8.22	5.78	4.30	3.33	3.32

Summary and Conclusions

In order to evaluate dowel bearing strength at an angle to the grain, a failure equation which is based on distortion energy criterion is proposed as an alternative to the Hankinson's formula. As supported by test results, although it is not conclusive, the alternative equation is better because it considers not only the bearing strengths parallel and perpendicular to the grain, but also shear strength of the material.

Acknowledgements

The authors gratefully acknowledge financial support of Parahyangan Catholic University, Indonesia. The authors also gratefully acknowledge the assistance of staffs at the Structural Laboratory at the university.

References

ANSI/AWC (2015) National Design Specification for Wood Construction 2015 Edition. American Wood Council, Leesburg, VA.

ASTM (2013) D5764-97a. Standard test method for evaluating dowel-bearing strength of wood and wood-based products. American Society for Testing and Materials, West Conshohocken, PA.

ASTM (2009) D 143-09. Standard methods for testing small clear specimens of timber. American Society for Testing and Materials, West Conshohocken, PA.

Chen WF, Han DJ (2007) Plasticity for structural engineers. Ross Publishing. Lauderdale, FL. 606 pp.

Clemen (2013) Experimental study on dowel bearing strength of lag screw on Indonesian wood members. Undergraduate thesis, Parahyangan Catholic University, Bandung, Indonesia. 91 pp.

Franke S and Quenneville P (2011). Bolted and dowelled connections in Radiata pine and laminated veneer lumber using the European yield mode. Australian Journal of Structural Engineering 13(1) :13-24.

Hwie LT (2006) Experimental study on dowel bearing strength of bolt loaded at an angle. Undergraduate thesis, Parahyangan Catholic University, Bandung, Indonesia. 156 pp.

Kharouf N, et.al.(2005) Postelastic behavior of single- and double-bolt timber connections. Journal of Structural Engineering 13(1):188-196.

Montgomery DC, Runger GC (2014) Applied statistics and probability for engineers, Sixth edition. McGraw-Hill, New York. 811 pp.

Sadd MH (2009) Elasticity theory, applications, and numerics, 2nd ed. Elsevier Inc, Burlington, MA. 536 pp.

Suryoatmono B, Pranata YA (2012) An alternative to Hankinson's formula for uniaxial tension at an angle to the grain. Pages 217-222 in Pierre Quenneville in Proc World Conference onTimber Engineering, 15-19 July 2012, Auckland, New Zealand.

Proceedings of the 58th International Convention of Society of Wood Science and Technology
June 7-12, 2015 – Grand Teton National Park, Jackson, Wyoming, USA

Comparison of Stranding and Strand Quality of Moso (*Phyllostachys pubescens* Mazel) and Guadua (*Guadua angustifolia* Kunth) Using a CAE 6/36 Disk Flaker.

Kate E Semple[1], Polo K Zhang[2], Gregory D Smith[3*]

**Corresponding author*
[1]Research Scientist, [2]Graduate Research Assistant, and [3]Associate Professor, [1,2,3]Department of Wood Science-Composites Group, University of British Columbia, 2900-2424 Main Mall, Vancouver, BC, Canada, V6T 1Z4. Email: kate.semple@ubc.ca, polo.kq.zhang@gmail.com, greg.smith@ubc.ca.

Abstract

High tensile strength make giant timber bamboos such as Moso and Guadua are potentially suited to the production of engineered strand-based structural composite building materials. Using the right slicing technology and tooling, conversion to strands utilizes a much higher proportion of the culm than the conventional milled, dried strips currently used to fabricate laminated bamboo lumber and boards. It also incorporates the fibre-rich, strongest portion of the culm located at the outer cortex into the composite. Previous studies have found Moso bamboo produces good quality strand-based composites but there is very little information available on strand production, especially from Guadua. Here we compare Moso and Guadua pole characteristics and re-saturation behavior likely to affect strand outcomes, as well as strand size classification and their thickness and width distributions from stranding re-saturated Moso and Guadua quartered culm pieces using a CAE 6/36 single-blade disk flaker. Strand slicing and quality was significantly better for Moso than Guadua, even though Guadua has a larger culm wall and fewer nodes. Setting the blade to cut 0.65 mm thick strands, the frequency distribution of strand thickness for Moso was similar to that found in industrial Aspen mill strands, whereas the thickness distribution was shifted upwards in Guadua due to the propensity for splitting rather than clean slicing. Only 5% of bulk Guadua strands has a smooth sliced surface on both sides, compared with 25% of Moso strands and over 60% of Aspen mill strands. Splitting was caused by the much larger fibre bundles present in Guadua. Node tissue in the culm wall is denser and disrupts its structure, resulting in greater damage and strand breakage; the much larger zone of node tissue in Guadua created a major problem with strand breakage.

Key words: Bamboo; Processing; Disk flaker; Furnish Quality; Surface Roughness; Oriented Strand Board

Introduction

Bamboo is one of the fastest growing renewable woody biomass plants and also one of the world's most widely used building materials. Over one billion people globally live in a mostly primitive dwelling built from bamboo (De Flander and Rovers 2009). Due to deforestation bamboo is emerging as a significant non-wood forest resource to replace wood in construction and other uses where it grows native across the tropical and sub-tropical belt of Asia, Africa and Latin America (Leise 1998). Raw bamboo rounds are unsuitable for modern wood-based construction systems due to longitudinal splitting and flaws, high variation in geometry and mechanical properties both within and across culms which prohibits conformation to the narrow range of properties required for composites used in construction of large, modern structures (Van der Lugt et al. 2003, Correal and Ramirez 2010, Harries et al. 2012). A wide range of reconstituted lumber and panel products has been developed over decades to overcome the natural variability in wood logs to produce building products with the required uniformity and controlled properties (Stark et al. 2010). Yet despite the plethora of laminated bamboo-based composites developed in recent years, relatively little attention has focused on developing similar kinds of modern engineered composite building products from bamboo that would foster modern housing construction from this resource (De Flander and Rovers 2009). OSB is one product which lends itself to automated, economically efficient production and with the appropriate adaptations most wood composite processing technologies can be extended to bamboo. Commercial development of bamboo OSB for housing construction in China is thwarted by a lack of efficient, automated technology for converting culm stock to strands and very few published experiences converting bamboo culms to strands. The aim of this study is provide technical information on converting bamboo culms to strands and compare strand size and quality outcomes between two commercially important bamboos, Moso and Guadua.

Materials and Methods

Culm procurement and characterization

Twenty poles of 5-inch diameter Chinese-gown Moso culms (mean diam. = 101.7 mm) in 8 foot lengths were purchased from Canada's Bamboo World, located in Chilliwack, BC, Canada, which imports seasoned and fumigated (methyl bromide) bamboo poles from Zhejiang Province, China, harvested at four years of age. Ten 19-ft long Guadua culms (mean diameter = 103.7 mm) came from Koolbamboo, Miami, FL ex Columbia and Panama harvested at between 4 and 6 years of age. Node frequency (number per m length of culm), internode length, wall thickness and basic density of wall and node tissue were measured. Each pole was marked into 17 to 19 130-mm-long sections, approximately half of which were node free, and the other half containing a node in or near the middle. This meant some small sections of culm were cut and discarded. Each pole was then cut lengthwise into four quarters, and each quarter then cross cut into the pre-marked 130 mm sections. After cross cutting, the noded and internode sections were kept in separate bins ready for re-saturation and stranding. The node plates from both

species had to be removed prior to re-saturation and stranding; this was done with a hammer in the case of Moso, but in the case of Guadua the node plates were very thick and tough requiring manual removal with a Dremel saw and sanding down the remaining thick portion till flush with the inner wall. This was to enable the pieces to be stacked into the feed drawer of the stranding machine.

Stranding

Details on the flaker equipment and methodology for effectively re-saturating the seasoned bamboo culm tissue to facilitate stranding, and the development of the most effective operating parameters for Moso bamboo are given in Semple et al. (2014). The theoretical basis for maximizing the production of bulk strands from bamboo culm rounds can be found in Semple and Smith (2014). Optimal strand numbers and quality outcomes (total strands per round, average thickness, thickness and width distributions, and surface smoothness were obtained when fully saturated culm pieces were quartered, and stranded vertically at 734 RPM with a knife protrusion of 0.726 mm (nominal strand thickness = 0.65 mm), corresponding feed rate of 7.95 mm/s. Disposable knives were Udderholm Sleipner heat tempered cold work tool steel (HRc 58). Slicing the culm tissue parallel to the fiber direction resulted in a more consistent strand thickness distribution with 85% of strands falling within the thickness range of 0.25 to 0.75 mm. Strand recovery (number of strands per culm round) was increased by over 50% if the culm rounds were converted to quarters and stacked in the feed drawer (Semple and Smith 2014). This slicing configuration also confines the waxy outer cortex layer to one thin edge of each strand. These stranding parameters were used to produce bulk strands from both Moso and Guadua for comparative purposes and for subsequent OSB fabrication. The bulk strands were distributed into large wire baskets and dried down to approx. 4% MC in a walk-in oven over night at a temperature of 85°C. The dried strands were bagged and screened to remove fines and dust on a 56 cm x 117 cm vibrating sieve machine fitted with three screen sizes; 14.3 mm (collects large face strands), 7.8 mm (collects intermediate strands and fragments) and 3.2 mm (collects fines). The material collected on each sieve was bagged separately and weighed to give the weight proportions out of the total weight of bulk strands.

Strand sampling and measurement, strand surface roughness

The full sized stands retained on the 14.3 mm screen were sampled for representative strand thickness and width properties, and surface characteristics. Strand thickness and width at mid-length of a randomly sampled batch of 250 strands each of Moso and Guadua were measured using digital calipers and compared with the same measurements made on 250 industrial Aspen mill strands (face furnish) supplied by the Weyerhauser OSB mill in Edson, AB. Assessment of strands surface quality was done in two ways. First a combination of visual and tactile assessment of each measured strand as made as to whether each strand fell into one of three surface roughness groupings: (1) rough on both sides, (2) smooth on one side and rough on the other, or (3) smooth on both sides. Laser surface topography scanning (Lundberg and Porankiewicz 1995, Hu and Afzal 2005) of examples of the ‘rough’ and ‘smooth’ surfaces of each type of tissue (Aspen, Moso, Guadua strands, and ‘smooth’ reference surface of Moso sliced cabinet makers veneer) was carried out using a LaserScan LT (Solaris, San Francisco, USA) laser surface

profilometer fitted with a Keyence K2000 Series LK-031 sensor head. Profile data was mapped and analyzed using Solar Map Universal 3.2 software. Each scan was 10 mm x 10 mm in area, with a sampling increment of 1 µm in the *x*-direction (i.e. across the grain). The average roughness profile was compiled from a total of 50 cross-grain scans taken at increments of 200 µm along the grain (*y*-direction), a process that took approximately 20 minutes per scan. Reported variables included average roughness (Ra) and average maximum roughness (Rz). Ra is the arithmetic average of all the absolute values for peak height and valley depth from center line, and Rz is the average of the five highest in magnitude peak height and valley depths.

$$\mathrm{Ra} = \frac{1}{n}\sum_{i=1}^{n}|yi| \qquad \text{[eqn 1]}$$

$$\mathrm{Rz} = \frac{1}{5}\sum_{i=1}^{5} Rpi - Rvi \qquad \text{[eqn 2]}$$

where *Rpi* and *Rvi* are the i^{th} highest peak and lowest valley, respectively.
A DX100 Olympus Digital Light Reflection Microscope (5x magnification) was used to examine the sliced transverse cross-sections through the culm wall of Moso and Guadua tissue to visually compare the morphology of the vascular bundles.

Results and Discussion

Pole characteristics and resaturation MC

Average basic density of Moso was 436 kg/m^3 (internode) and 532 kg/m^3 (node plates), an increase of 22% in density for node plates. Average basic density of Guadua was 526 kg/m^3 (internode) and 581 kg/m^3 (node plates), an increase in 14% in density of node plates. Node plates were significantly thicker in Guadua (7.4 mm) than Moso (2.7 mm), and much tougher to remove manually. Guadua poles were also slightly greater in average diameter and wall thickness; (103.7 mm and 12 mm, respectively) than Moso (101.7 mm and 10.9 mm, respectively). The frequency of nodes was less for Guadua (3.3 nodes per m of culm) than Moso (3.8 per m), and spaced further apart (average internode length 30.7 cm compared with 24 cm for Moso). Soaking in cold water for 24 h was insufficient to resaturate either species - Moso tissue was 38.6%, and 38.4% for Guadua; whereas the MC of pieces boiled then steeped in cold water for a further 18 h was 128% for Moso and 114% for Guadua. After 96 h the boiled/steeped Moso pieces reached 142.7% MC, but only 114.4% for Guadua, indicating a lower maximum water holding capacity. Fresh Moso culm stock harvested and stranded by Lee et al. (1994) was 137% MC suggesting full tissue resaturation was reached with the boil/steep method.

Strand size classifications

The proportions of complete strands (remaining on top of the large 14.3 mm screen) was higher for Moso (75.5% for internodes and 67.8% for noded strands) than Guadua (65.4% for internode and 59.4% for noded). The proportion of the stranded material broken up into smaller pieces that fell through large screen was higher for Guadua (34.7% for internode and 40.6% for noded strands) reflecting greater damage and fragmentation of strands during slicing this type of bamboo. Many of the Guadua strands

were very damaged and broken adjacent to embedded node tissue. The percentage of broken strands in the 250 strand sample of Guadua noded strands was 25.2% compared with 7.6% for internode strands. The fraction of smaller strands and fines for Moso was 24.6% for internode and 32.2% for noded strands). The proportion of intermediates and fines from stranding Moso are not dissimilar to the 27% fraction of this material from similarly screening Aspen mill face strands (Semple et al. 2014b). Average strand thickness was 0.67 mm for Aspen, 0.65 mm for Moso and 0.75 mm for Guadua, while average strand width was 18.1 mm for Aspen, 12.9 mm for Moso and 15.0 mm for Guadua. The frequency distributions for strand thickness and width are shown in Figure 1 below. Note the higher proportions of Moso and Aspen mill strands in the smaller thickness class (0.5-0.75 mm) compared with Guadua. Due to its greater average wall thickness, especially in the lower culm Guadua produced more strands in the width class 20-25 mm than Moso, while Aspen mill strands were spread over a greater range of width classes.

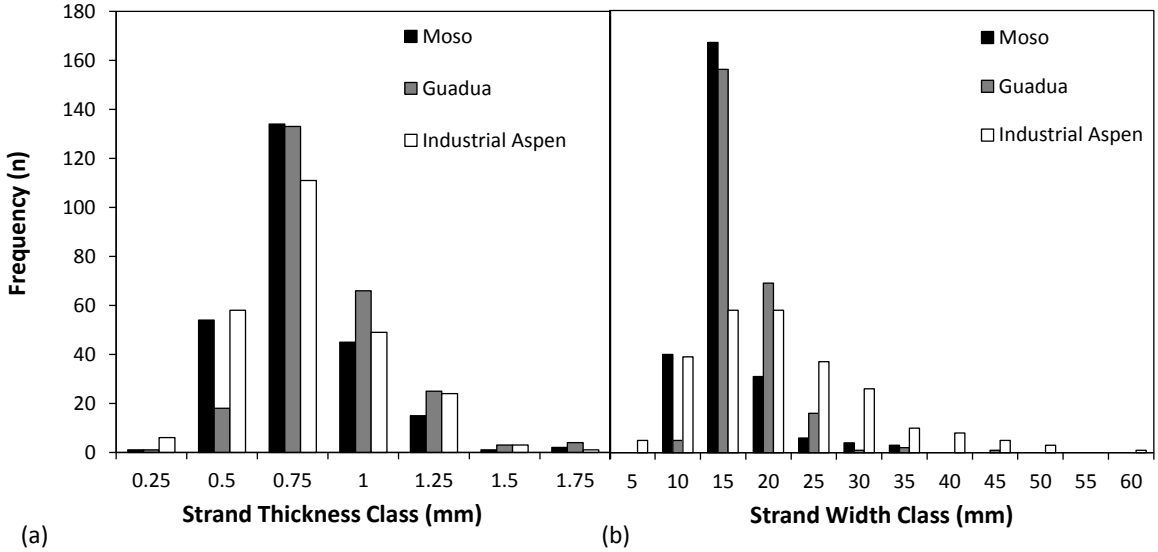

Figure 1 Frequency distributions for (a) strand thickness, and (b) strand width for complete Moso, Guadua and Aspen mill strands.

Strand quality (surface roughness)

The greater proportion (60%) of industrial Aspen strands were classified as ‘smooth’ both sides, and 10% classified as ‘rough’ on both sides. Semple et al. (2014a) found that strand surface quality in Moso (identified as maximum the proportion of strands that were smooth on both sides) was very sensitive to tissue moisture content, knife protrusion setting, material feed rate and whether the pieces were stranded horizontally or vertically. Full tissue saturation to above 130% MC, low knife protrusion setting, slower feed rate, and stranding parallel to the fibre direction were all necessary to maximize the proportion of ‘smooth-both-sides’ strands. Despite these efforts, no more than about 25% of bulk Moso strands were classified as ‘smooth’ on both sides. The strand quality outcome for Guadua was markedly lower than for Moso using the same stranding parameters used to produce the best outcome for Moso. Only 5% of bulk Guadua strands were classified as smooth on both sides. The majority of Guadua strands (65%) were rough on both sides. Node tissue had a much stronger effect on surface quality and propensity for breakage of

Guadua strands. Guadua resulted in the knives dulling very quickly: to strand approximately 115 kg of Guadua pieces required three knife changes. Examples of surface roughness profiles for surfaces classified as 'smooth' and 'rough' to touch are shown in Figure 2 for Moso, and Figure 3 for Guadua. The average Ra and Rz values for each surface types are given in Table 1. Ra values for 'smooth' surfaces were 7.2µm for Moso cabinet-makers veneer, 7.70µm for Moso strands, 10.1µm for Aspen, and 10.7 for Guadua. Corresponding Rz values for 'smooth' Moso and Guadua surfaces were 43.9µm and 57.3µm, respectively. Ra values for 'rough' Aspen, Moso and Guadua were more variable: 17.3µm, 20.9 µm, and 23.4 µm, respectively. However all the strand surfaces classified as 'rough' to the touch were similar in the topographic index that makes them noticeably rough to feel, i.e. the magnitude of the highest peaks and troughs, expressed by Rz. Average Rz values were 113.83µm, 115.43 µm and 115.22 µm for 'rough' Aspen, Moso and Guadua respectively.

	Ra (µm)	COV (%)	Rz (µm)	COV (%)
Aspen smooth	10.11	10.31	57.98	10.66
Aspen rough	17.37	15.91	113.83	38.04
Moso smooth	7.70	7.60	43.97	7.89
Moso rough	20.87	20.18	115.43	37.02
Moso veneer	7.19	10.18	37.63	8.54
Guadua smooth	10.70	26.61	57.33	20.27
Guadua rough	23.38	16.61	115.22	14.91

Table 1 Ra and Rz values for surface types (n = 6).

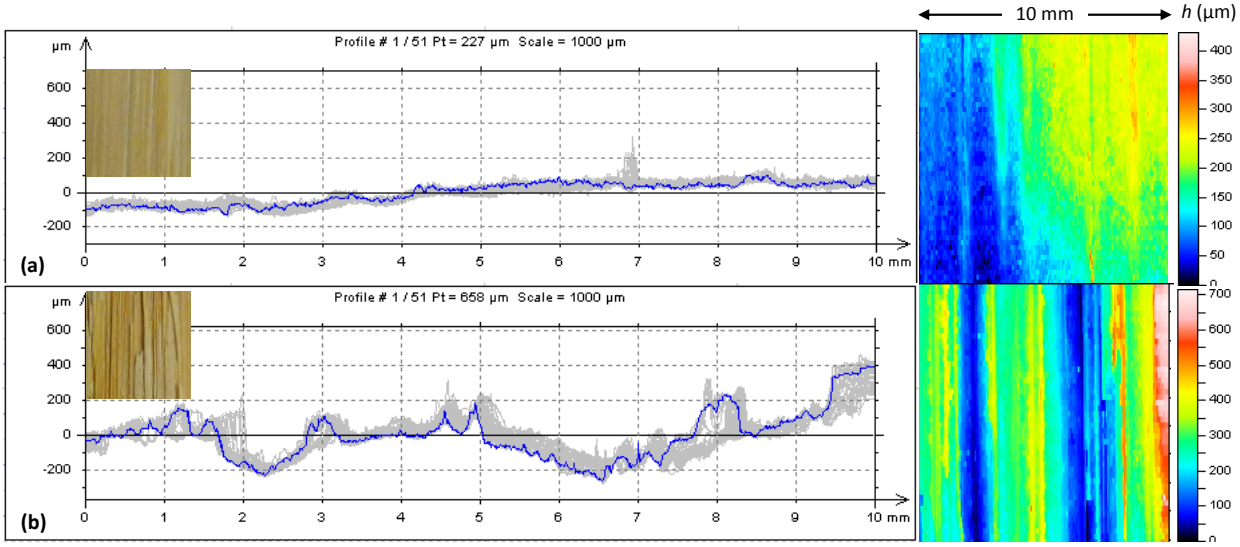

Figure 2 Example of (a) 'smooth' and (b) 'rough' surface of Moso strands.

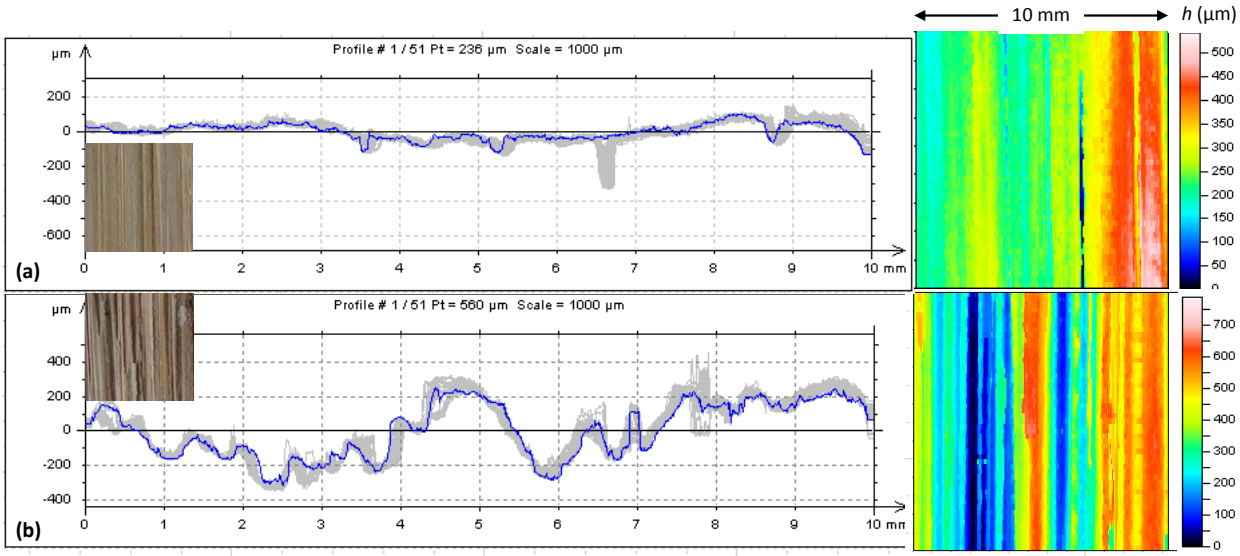

Figure 3 Example of (a) 'smooth' and (b) 'rough' surface of Guadua strands.

Guadua is contains very large, closely spaced solid fibre bundles especially near the outer culm wall, which are in cross-section an average 1.1 mm in length. In contrast Moso contains much smaller, and more discrete fibre bundles, seen in Figure 4 below.

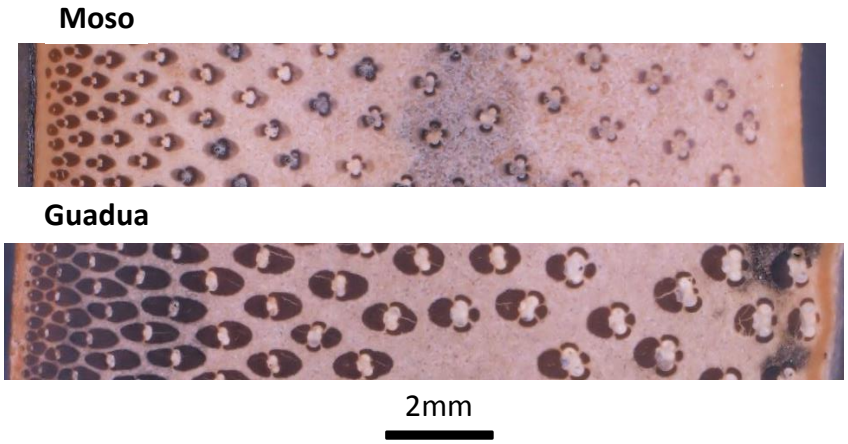

Figure 4 Transverse section through the culm wall of Moso and Guadua bamboo, showing different vascular bundle size and morphology.

Unless the blade was very sharp Guadua had a tendency to tear along the weaker ground tissue surrounding the fibre bundles leaving them as exposed ridges in the surface. In Guadua the strand surface deteriorated even further, accompanied by a higher rate of breakage with slicing through the large zone of embedded node tissue in the culm wall. This zone is where the fibres deviate from parallel and are shortest (Leise and Grosser 1972) and therefore there is considerable variability in the strength of the tissue along the length of a strand that has a node in it. The nodes are largest and most numerous in the bottom portion of each whole culm and so one relatively simple strategy for minimizing the effects of nodes on OSB boards would be to separate the lower third of each culm, and only use the strands from these in the core layers of OSB where consistency of strand length and strength properties is not as critical. Other processing parameters found to

impinge on strand quality in the case of dense, difficult-to-strand hardwoods include slower cutting speed and lower knife angle (De Vallance et al. 2012), and further adjustment of these may improve strand quality from Guadua.

Conclusions

Due to its lower density and smaller, more discrete fibre bundles Moso was less wearing on strander knife blades and strand quality was much higher than Guadua. The proportion of whole strands was 75% for Moso and 65% for Guadua, with many Guadua strands tending to break adjacent to the node tissue. Average strand thickness and coefficient of variation (0.65 mm and 37.7% COV) for Moso was very close to that found in Aspen mill strands (0.67 mm and 35.7% COV). Due to the constrained wall thickness of bamboo culms average Moso strand width was around 13 mm compared with 18 mm for sampled industrial Aspen strands. In contrast Guadua strands were an average of 0.75 mm in thickness, 31.3% COV; and 15.0 mm in width, 27.3% COV; in keeping with its greater average wall thickness. The mean surface roughness index (Ra) for 'smooth' Moso strands was 7.7µm, and 20.9µm for 'rough' strands, and 10.7µm and 23.4µm for 'smooth' and 'rough' Guadua strands, respectively. The maximum roughness index (Rz) for the roughest strand surfaces was similar across tissue types, Moso, Guadua and Aspen, at approx. 115 µm. In contrast to Moso, much further work is needed to find a more effective method of removing Guadua nodes prior to processing and improving the strand quality before the species could be considered suitable for OSB manufacture.

Acknowledgements

This study was funded through an NSERC (National Science and Engineering Research Council) G8 Tri-Council grant. The authors gratefully acknowledge the following personnel at Forest Products Innovations (Western Division): Mr John Hoffman for access to boil tank facilities and operation of the disk flaker, and Dr Zarin Pirouz and Mr John White for access to laser surface profilometry equipment.

References

Correal JF, Ramirez F (2010) Adhesive bond performance in glue line shear and bending for glued laminated Guadua bamboo. J. Trop. For. Sci. 22(4): 433-439.

Dagilis TD (1999) Bamboo composite materials for low cost housing. PhD thesis, Department of Civil Engineering, Queens University, Kingston, ON, 248 pp.

De Flander K, Rovers R (2009) One laminated bamboo-frame house per hectare per year. Construction and Building Materials 23(1): 210-2

De Vallance DB, Gray JD, Grushecky ST (2012) Improving strand quality of upland oaks for use in oriented strand board. Proceedings, 18th Central Hardwoods Forest Conference, G Miller et al. (eds), 26-28 March 2012, West Virginia University, Morgantown, WV. USDA Forest Service Northern Research Station GTR-NRS-P-117: 284-291.

Harries K, Sharma B, Richard M (2012) Structural use of full culm bamboo: the path to standardization. Int J Arch, Eng & Constr 1(2): 66-75.

Hu C, Afzal MT (2005) Automatic measurement of wood surface roughness by laser imaging. Part 1: Development of laser imaging system. Forest Products Journal 55(12): 158-163.

Liese W (1998) The anatomy of bamboo culms. INBAR Technical Report 18, International Network for Bamboo and Rattan, Beijing, pp. 175-191.

Liese W, Grosser D (1972) On the variability of fiber length of bamboo. Holzforschung 26: 202-211.

Lundberg IA, Porankiewicz S (1995) Studies of non-contact methods for roughness measurements on wood surfaces. Holz als Roh- und Werkstoff 53(5): 309-314.

Semple KE, Smola M, Hoffman J, Smith GD (2014a) 'Optimising the stranding of Moso bamboo (*Phyllostachys pubescens* Mazel) culms using a CAE 6/36 disk flaker. In M Barnes and V Herian (eds) Proceedings of the 57th International Convention of Society of Wood Science and Technology, June 23-27, 2014, Zvolen, Slovakia, pp. 257-269.

Semple KE, Xian D, Smith GD (2014b) Reinforced core particleboard for improved screw-holding ability. Wood Fiber Sci 46(1): 48-64.

Semple KE, Smith GD (2014) Theoretical models for bamboo strand recovery and width distribution. Proceedings, Processing Technologies for the Forest and Biobased Products Industries-PTF BPI 2014, A Petutschnigg, MC Barbu (eds), 24-26 September 2014, Salzburg University of Applied Sciences, Kuchl, Austria, pp. 401-408.

Stark N, Cai Z, C Carll (2010) Chapter 11 Wood-Based composite materials, in Wood Hand Book: Wood as an Engineering Material, FPL General Technical Report FPL-GTR-190, USDA Forest Products Laboratory, Madison, Wisconsin, 509 pp.

Van Der Lugt P, Van Der Dobbelsteen A, Abrahams R (2003) Bamboo as a building material alternative for Western Europe? A study of the environmental performance costs and bottlenecks of the use of bamboo (products) in Western Europe. J. Bamboo and Rattan 2(3): 205-223.

Proceedings of the 58th International Convention of Society of Wood Science and Technology
June 7-12, 2015 – Grand Teton National Park, Jackson, Wyoming, USA

Temperature and Humidity Dependent Mechanical Performance of Nanocellulose and its Composites

Mehdi Tajvidi, mehdi.tajvidi@maine.edu
Justin Crouse, <justin.crouse@maine.edu
Douglas Gardner, douglasg@maine.edu
Douglas Bousfield, DBousfield@umche.maine.edu
William Gramlich, william.gramlich@maine.edu

Abstract

The two main forms of cellulose nanomaterials namely, cellulose nanocrystals (CNC) and cellulose nanofibrils (CNF) are known as high strength, high stiffness renewable nanomaterials of the future. Current information on the mechanical performance of these fibers and their composites confirms such understanding. However, these interesting nanomaterials are hydrophilic and viscoelastic in nature and their mechanical properties are highly temperature and moisture dependent. The problem exacerbates when the polymer matrix used in the formulation is also temperature and humidity sensitive. Therefore, there is a need to understand the mechanical and viscoelastic performance of these materials and their composites under service conditions where either or both humidity and temperature are variable. For this purpose, pure films of CNC and CNF as well as their composites with poly vinyl alcohol (PVA) at various concentrations were produced by solution casting. An environmentally controlled dynamic mechanical analyzer (DMA) was used to obtain stress/strain curves at various temperatures and relative humidities. Dynamic mechanical tests were also carried out under different temperature and humidity regimens to establish basic material behavior under service condition. The fundamental behavior of CNF and CNC films and their composites as affected by temperature and relative humidity will be presented and discussed.

Proceedings of the 58th International Convention of Society of Wood Science and Technology
June 7-12, 2015 – Grand Teton National Park, Jackson, Wyoming, USA

IUFRO 5.10 Forest Products and Communities Session
Moderator: *Paul Dargusch, University of Queensland, Australia*

Business Management Research in the Forestry Sector: Past, Present and Future Directions

Rajat Panwar, rajat.panwar@ubc.ca

University of British Columbia, 2424 Main Mall, , Vancouver, BC V6T 1Z4

Abstract

Insofar the forest sector is at a cross-road, business and management scholars in the forest sector have an unprecedented responsibility to address difficult questions that may, at times, involve even explicating why or why not should the forest industry exist. Is globalization of industry a fundamental reason for a number of environmental concerns surrounding us? Could the sub-sectors that developed due to a growth in the bio-economy domain co-exist with the traditional forest industry as spin-offs or would they emerge as the next stage of evolution of an industry.

The forest sector provides a fertile ground for addressing a number of such fundamental questions that have not been considered before in strategy, management, and industry evolution literatures. And indeed forest sector business scholars are better positioned to take lead. How can the current forest sector scholarship take the leap from merely replicating the studies conducted by business school researchers in a forestry context to leveraging the much-professed uniqueness of the forestry in order to contribute to our fundamental knowledge about business and the environment?

Proceedings of the 58th International Convention of Society of Wood Science and Technology
June 7-12, 2015 – Grand Teton National Park, Jackson, Wyoming, USA

Challenges in Communicating Forest Industry Sustainability to the General Public: Results from a Four-Country Comparison in Europe

Toppinen, A.[1], Korhonen, E.[1], Lähtinen, K.[1], Ranacher, L.[2], Werner, A.[2], Stern, T.[2] and Kutnar, A.*

[1] University of Helsinki, Department of Forest Sciences, Latokartanonkaari 7, FI-00014, Helsinki, Finland
* *Corresponding author* anne.toppinen@helsinki.fi
[2] Market Analysis and Innovation Research Team, Kompetenzzentrum Holz (Wood K plus), Feistmantelstraße 4, A-1180 Vienna, Austria
[3] University of Primorska Faculty of Mathematics, Natural Sciences and Information Technologies, Glagojaška 8, SI-6000 Koper, Slovenia,

Abstract

Despite increasing global awareness of environmental issues, little is known regarding how different segments of the European forest industry communicate their sustainability efforts to the general public. Communication is an important tool in maintaining legitimacy and acceptability of company operations, and public expectations are found to be high. Consequently, some key empirical questions emerge such as what is the core content and what challenges exist in forest related communication? This study applies a qualitative content analysis in four forestry-rich European countries (Austria, Finland, Germany, Slovenia). Online communication of 61 companies and 19 industry associations were qualitatively analysed with a focus on eight "core topics of interest" (TOIs) identified as a results from an international stakeholder feedback process. Our results also show high conformity in communication across countries. The most frequently communicated TOI was Forest and the economy particularly within large companies (28 %) and bioenergy producers (30%); Added Value of wood (AVA, 34%) within family businesses and SMEs, and on Forests and global warming (FGW, 22%) within associations. Characteristically, current content focuses on supplying facts or referring to certificates or standards, and lacks feedback mechanisms, pointing towards areas of future development in the forest sector communication.

Introduction

Overall, forests are a rich source of ecological, economic and social benefits. As a material, wood is used for various purposes, such as construction material, energy carrier,

boards, paper, cellulose, fibres and chemicals. Co-products of the wood processing industries are an important raw material for further processing. Chips from sawmilling can be used directly on site, for energy production or pellets, or are sold to a company using the fibers for subordinated processing like pulp or panel production. This reuse of the raw material thus increases the overall wood availability on the market (Steirer, 2005). Even though a lot of by-products are used, there is still room for improvement to further increase efficiency of wood use (Windsperger, 2010). In addition, there is a need for forest sector to renew its product and service portfolio, which calls for increased attention to enhancing added value via intangible product attributes and putting efforts to new forest and wood-based innovations (Hetemäki, 2014). However, the final market demand is determined by consumer acceptance and based on competition between alternative products and services. These are examples of issues that we would like to investigate in this analysis from the forest sector communication perspective.

In the previous studies, public expectations regarding transparency and responsible business conduct of the natural resource based sectors are found to be high (e.g., Ranängen and Zobalt 2014). Communication is an important tool in maintaining legitimacy and acceptability of organizations. When covering sustainability communication in forest products industry, previous studies have mainly been focusing on sustainability reporting (Vidal and Kozak 2008). However, after spread of digitalization the importance of sustainability-related online communication has increased, especially among forest companies and associations. Consequently, an empirical question emerges as "What is the core content in forest related communication when using different dimensions of sustainability as a lens?"

As an analytic lens, eight "topics of interest" (TOIs) were chosen based on written stakeholder feedback and final discussion in a stakeholder workshop (Helsinki 22.9.2014). The topics were chosen to be both of interest for stakeholders from the forest-based sector and also to cover a clear societal relevance towards a bio-based and sustainable economy. They are identified as follows (with acronyms used in the text and figure captions):

1. Wood based innovations (WBI)
2. Multifunctional forestry and forest ecosystem services (FES)
3. Forest conservation by [forest management and] production (CBP)
4. Forests and global warming (FGW)
5. Forests and economy (FEC)
6. Added value of wood (AVA)
7. Building with wood (BWW)
8. Efficient use of wood (EUW)

Our point of departure is that the three-dimensional concept of sustainability (environmental, social and economic) can be implemented at four hierarchical levels, i.e. as societal, sectoral, corporate and product (or service) level (see Figure 1).

Firstly, *societal level sustainability*, as a more extensive level of the sustainability concept, includes strategic decisions, regulations and operations related to sustainable development in a global scale. The societal level has a high impact on other three levels as carried through the implementation of national and international regulations and commitments, which create limitations and incentives for society, governments, companies, organizations and individuals.

Secondly, the main focus of *sectoral level* sustainability, which is a lesser used concept according to Draper (2006), is to maintain or enhance the current legitimacy or solid reputation of a sector in sustainability related matters with the aim to improve competitiveness in relation to other sectors. Thus, the success of improving sustainability performance requires collaboration with other companies, organizations and value-chain members in the same sector.

Thirdly, the sustainability in *corporate level* encompasses communicating the current state and goals of corporate social responsibility, as mentioned above.

Fourthly, the *product level sustainability* is primarily concerned with consumers' perceptions on environmental and social sustainability of products, which has been affected by corporate strategic decisions-making process. Based on e.g. Toppinen et al. (2013) for Finnish consumers of wood products, the safety aspect and health impacts of a product are emphasized. In addition we hypothesize based on workshop discussions that sustainability of forest based ecosystem services, including provisioning of wood based products (Räty et al., 2014), to customers is of potential relevance at this level.

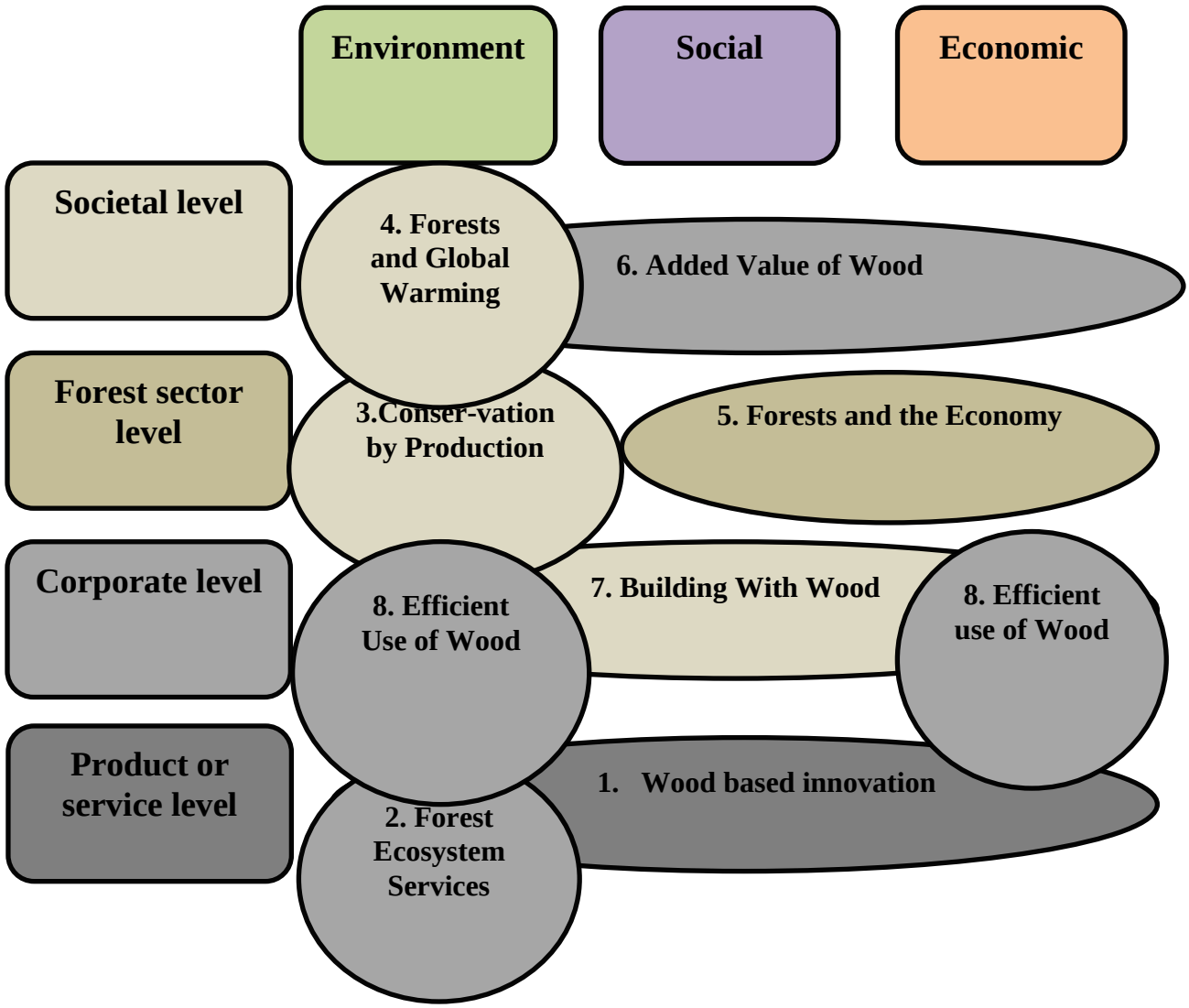

Figure 1. Eight TOIs and their alignment with level of analysis and dimensions of sustainability (environmental, social and economic sustainability).

Materials & Methods

This qualitative content analysis followed aims of the purposive sampling method in a sampling process (Ritchie and Lewis 2003). Firstly, we ensured that all relevant groups or segments from the population are covered. We are including four different segments; *large scale international companies, small and medium sized (mostly family businesses), industry associations* and *bioenergy producers*. Secondly, it is important to ensure that some diversity within each segment is included in order to disengage impacts of the segment's feature and other factors involved. Therefore, each segment contains a comprehensive range of representative organizations, which fulfill the criteria of the segment as well as cover the characteristics of a population. In addition, companies and

organizations are selected for this study based on the coverage of their websites in terms of sustainability matters.

In deductive content analysis, the coding unit consists of either several sentences, a section or a paragraph depending on the context. Predominantly in the study quotations tagged with a code were comprised of sections, which are separated from each other with a section break. Eventually, the length of coded quote has no great significance to the results due to frequency counts were based on number of quotation. The codes, sub-categories, were grouped into code families and TOIs. Only one code from the same code family can be chosen in order to make the coding and results comparable between countries and to avoid the risk of double coding.

Results and Discussion

In total, our data set consist of a count of 7090 observations regarding pre-selected 8 TOIs in the data. We discuss next the results by segments, as differences in communicating TOIs were fairly similar between the four countries across the Europe. The most frequently communicated TOI was *Forest and the economy* (FEC, 28%) particularly within large companies, *Added Value* (AVA, 34%) within family businesses and SMEs, *Forest and global warming* (FGW, 22%) within associations and *Forest and economy* (FEC, 30%) within bioenergy producers. FEC consists of a wide range of sustainability subcategories such as employment, income, energy, local environmental impacts and social impacts covering both economic, environmental and social sustainability dimensions (see figures 1 and 4), which partly explains the high frequency of hits FEC received from the analysis. In contrast, the least commonly communicated topic areas are *Wood Based Innovations* and *Forest Ecosystem Services*.

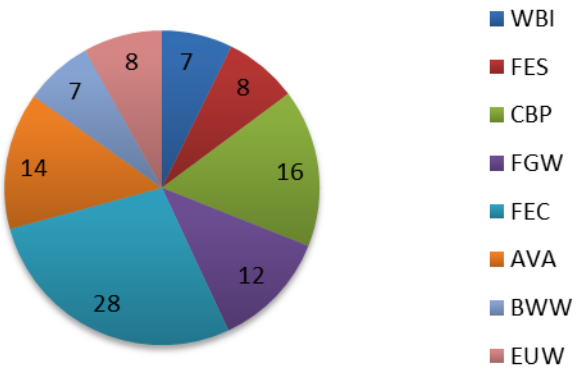

Figure 1. Large companies, in total for four countries (N=25)

Emotional bond and health benefits of wood as well as the eco-labels and forest certifications (FSC, PEFC) from TOI number 6 AVA are highly emphasized within segment of SMEs and family businesses (especially in data from Slovenia, see figure 2). In addition to FEC, regarding sustainability related online-communication, associations

communicate mostly about the positive carbon impacts of wood material as well as forests as a carbon sink, which address to help prevent climate change (figure 3).

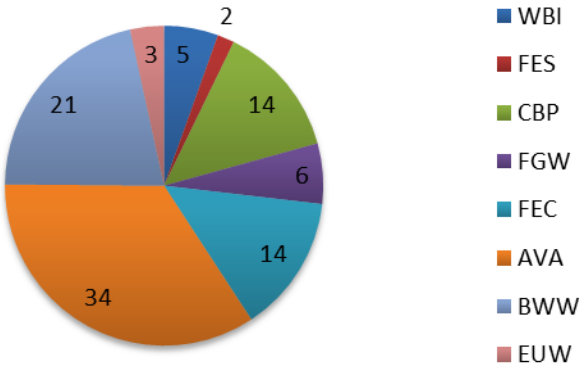

Figure 2. Family businesses and SMEs, in total for four countries (N=34)

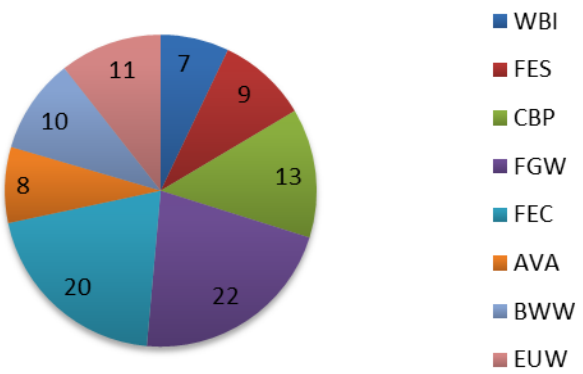

Figure 3. Associations, in total in four countries (N=19)

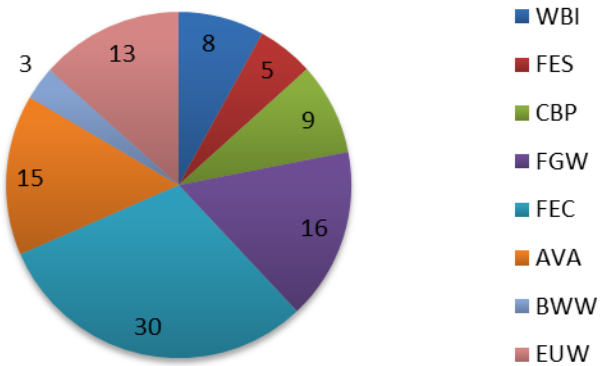

Figure 4. Bioenergy producers, in total for three countries (N=10, but 8 of them already included in the above three segments).

Taken together, the state of communication efforts of the analyzed organizations in four countries strongly focus on distributing information (e.g. supplying facts or by mentioning use of environmental certificates or standards). Formally, the communication in the sector seems to lack feedback mechanisms, especially among smaller sized wood

companies. Furthermore, stakeholder expectations about tailored communication were rarely expressed in explicit terms, making the evaluation of the effectiveness of communication difficult.

Summary and Concluding Remarks

The share of eight pre-selected topics for total data indicates dominance of *Forest and the economy* (FEC). As the second most frequently communicated the TOI is *Added value of Wood* (AVA), despite that its dominance was due mainly to heavy emphasis on this in Slovenian sample. In contrast, among the TOIs, the two future-oriented topics, i.e. WBI of *Wood-based innovations* and FES *Forest ecosystem services* deserved the least weight in the data. Furthermore, stakeholder expectations about tailored communication were rarely expressed in explicit terms, making the evaluation of the communication effectiveness difficult. In addition, the communication efforts of sample organizations heavily focused on distributing information (e.g. supplying facts or by mentioning use of environmental certificates or standards), and lacked feedback mechanisms with targeted stakeholders, especially among the smaller sized wood companies.

In comparison to the corporate level results focusing on sustainability reports by globally leading pulp and paper companies, Vidal and Kozak (2008) found that sustainable forest management was on average the most commonly reported topic. In addition, in Vidal and Kozak (2008) larger sized companies were found to report on a wider range of activities than smaller sized firms, whereas it was not possible to draw such a conclusion from our sample. However, sustainability reporting may be more suitable for communicating with regulators and auditors whereas general communication towards a wide range of stakeholder groups, such as consumers, would require clearer messages that also appeal to the emotional side (see e.g. Joutsenvirta 2009). Such issues would seem to include e.g. forest sector contribution to solving global sustainability challenges or emphasizing safety and health benefits of wood material at individual or societal level.

As a final note, communicators in the forest sector should critically examine their efficacy of communicating in all topic issue areas. For example, is all the economic performance and value added related communication worth it, or should some of it be replaced by other less represented categories? The answers to these questions will be searched for in the surveys and experimental research performed in the frame of this Wood Wisdom Net (W3B) project.

Acknowledgements

Financial support from ERANET WoodWisdom Net W3B partners and financers is gratefully acknowledged. Work of Slovenian author was supported by the Ministry of education, science and sport.

References

Berg B. 2009. Qualitative research methods for the Social Science. Seventh edition. Pearson Education, Inc., published by Ally & Bacon. Chapter 11.

Draper S. 2006. Corporate responsibility and competitiveness at the meso level. Key models for delivering sector-level corporate responsibility. Corporate Governance, 6(4), 409-419.

Hetemäki, L. (editor). 2014. Future of the European Forest-Based Sector: Structural Changes Towards Bioeconomy, What Science Can Tell Us 6, 2014, http://www.efi.int/portal/virtual_library/publications/what_science_can_tell_us/6/

Joutsenvirta, M. 2009. A language perspective to environmental management and corporate responsibility. Business Strategy and the Environment, 18(4), 240-253.

Ranängen, H. & Zobel, T. 2014. Revisiting the 'how' of corporate social responsibility in extractive industries and forestry. Journal of Cleaner Production, 84, 299–312.

Ritchie J. and Lewis J. 2003. Qualitative Research Practice. A Guide for Social Science Students and Researchers. Sage, London.

Räty T., Toppinen A., Roos A., Nyrud A Q. and Riala M. 2014. Environmental Policy in the Nordic Wood Product Industry: Insights Into Firms' Strategies and Communication, Business Strategy and the Environment. Online first version.

Steirer, F. 2005. Current wood resources availability and demands – national and regional wood resource balances EU/EFTA countries. *United Nations Economic Comission for Europe/Food and Agriculture Organization of the United Nations*, Timber Section, Genf, pp. 7f (http://www.unece.org/fileadmin/DAM/timber/publications/DP-51_for_web.pdf)

Toppinen A., Toivonen R., Valkeapää A. and Rämö A-K. 2013. Consumer perceptions of environmental and social sustainability of wood products in the Finnish market. Scandinavian Journal of Forest Research, 28(8), 775-783.

Vidal N. G. and Kozak R. A. 2008. The Recent Evolution of Corporate Responsibility Practices in the Forestry Sector. International Forestry Review, 10(1), 1-13.

Proceedings of the 58th International Convention of Society of Wood Science and Technology
June 7-12, 2015 – Grand Teton National Park, Jackson, Wyoming, USA

Study on 1/F Features of Wood Texture Changes Based on Spectrum Analysis

Jianping Sun, sjp_jpcn@163.com
Long Tao, 497614200@qq.com
Jianju Luo, luojianju@foxmail.com

Guangxi University, College of Forestry, 100 Daxue Road, Nanning, Guangxi 530005

Abstract

There is similarity between the power spectrum of wood texture change and certain physiological rhythms spectrum of the human body, because of which wood can make people feel happy and comfortable. This study focused on exploring the texture change spectrum characteristic parameter of common softwood, hardwood and precious rosewood. Results showed that wood texture change spectrum of the cross section, radial section and tangential section were characterized in 1/f features. And their power spectrum parameters γp were in the range of 0 to 1.5. However, the power spectrum parameters of different sections were different; even there was no significant effect of different microscopic magnification on the 1/f spectrum characteristics. Like hardwood, softwood texture change was also with the characteristics of 1/f spectrum feature, but the parameter γp was smaller than that of hardwood. It was also found that the spectral parameters Lushi black Dalbergia and cocobolo were 0.96 and 0.9 respectively, which were corresponding to the spectrum coefficient of human heart beat signal and a brain wave, that were considered to be close to 1. The results obtained from the study explained the fundamental reason why people like wood, and also provided a new theoretical basis for the reasonable, effective, scientific evaluation and utilization of wood.

Proceedings of the 58th International Convention of Society of Wood Science and Technology
June 7-12, 2015 – Grand Teton National Park, Jackson, Wyoming, USA

Operations Management, Cooperation and Negotiation in the Wood Supply Chain – The Relationship Between Sawmills snd Sawlog Suppliers

Matti Stendahl, matti.stendahl@slu.se
Emanuel Erlandsson, emanuel.erlandsson@slu.se

Swedish University of Agricultural Sciences, Department of Forest Products, PO Box 7008, SE-75007 UPPSALA

Abstract

Recent decades' development of technology in forest inventory, harvesting, logistics, and sawmilling have created new possibilities for better integration of sawmills' and sawlog suppliers' operations. This could largely increase value creation in the wood supply chain. However, industry practitioners indicate that integration still is at a fairly basic level and that the full potential of available technology is not used. The literature does not provide much information about the relationship between sawmills and sawlog suppliers and the reasons for this incongruity are therefore not well known. This study investigates the relationship between sawmills and sawlog suppliers in four Swedish cases. Semi-structured individual interviews and focus group discussions with respondents from a cross-functional sample in each case provided deep insights into operations management, cooperation and negotiation involved in the relationship. Function modeling (IDEF0) was used to map actors, activities and information flows in the negotiation process. The study indicates that managing social relationships is equally important as managing technology in the management of the wood supply chain.

Proceedings of the 58th International Convention of Society of Wood Science and Technology
June 7-12, 2015 – Grand Teton National Park, Jackson, Wyoming, USA

Nanocellulose Market Volume Projections: A Derived Demand Analysis

E.M. (Ted) Bilek, tbilek@fs.fed.us
John Cowie, John Cowie <cowie.john@gmail.com>
Jo Anne Shatkin, Jo Anne Shatkin <jashatkin@gmail.com>
Theodore Wegner, twegner@fs.fed.us

USDA Forest Products Laboratory, One Gifford Pinchot Drive, Madison, WI 53726

Abstract

Nanotechnology has enormous promise to bring about fundamental changes and significant benefit to society and to the forest products industry. This study creates a methodology to estimate the potential volume of nanocellulose that will be used in diverse products and markets in the United States. Published data sources are used to identify research that cites the utility of nanocellulose for particular applications. Eleven potentially high-volume applications are identified along with twelve low-volume applications. In addition, three identified novel applications are considered to be potentially promising, but not developed enough to make nanocellulose market demand projections. Volume projections are made by estimating nanocellulose market penetrations into representative end-product markets. Middle market-penetration estimates are bracketed by both high and low estimates to establish a plausible volume range for nanocellulose demand. When summed, the annual market potential in high-volume applications in the U.S. is approximately 12 million tonnes of nanocellulose with nearly half coming from the combined packaging and paper industries. This estimate is based on current markets and our middle market-penetration estimates. The spread around this middle point is quite wide, ranging from around 45 percent less to around 55 percent more, reflecting the early stage of the technology development

Proceedings of the 58th International Convention of Society of Wood Science and Technology
June 7-12, 2015 – Grand Teton National Park, Jackson, Wyoming, USA

A Demand-pricing Management Approach to Add Value in the U.S. Hardwood Industry

Henry Quesada-Pineda

Virginia Tech, USA

Abstract

It is a common practice for companies to determine their prices based on cost plus a profit markup and or market prices. The hardwood lumber industry usually works in a similar way. The problem with these approaches is that they are usually based on arbitrary decisions and do not account for the risk of either setting prices to high and therefore losing demand, or too low and leaving money on the table. The goal of this study is to test a demand-pricing methodology based on mathematical modeling, that have proved to be successful in increasing profits in other industries, and that may also be valuable in the hardwood lumber industry. There is a particular interested in exporting firms because it is considered that they have to deal with more challenges and complexities at the time of determining prices than those whose focus remain only on the domestic market. In this study, researchers analyzed historic sales data in order to determine optimum pricing values for each product in each geographic region, which will serve the sales and marketing groups in negotiating with customers abroad. It was observed that in specific circumstances, the suggested approach, which is based on statistical modeling and mathematical optimization may lead to higher profits than the traditional pricing method.

Proceedings of the 58th International Convention of Society of Wood Science and Technology
June 7-12, 2015 – Grand Teton National Park, Jackson, Wyoming, USA

Comparing Health, Emotional Wellbeing and Indoor Environment in Solid Wood and Brick Built Student Housing

Kristian Bysheim, kristian.bysheim@treteknisk.no
Maren Grønseth, maren.gronset@nmbu.no

Norwegian Institute of Wood Technology, Po Box 113, Blinder, , Oslo 0314

Abstract

Indoor environment in student housing in solid wood built in the years 2013-2014 were compared with the indoor environment in student residences in brick and concrete construction with non-load bearing timber frame walls built in the years 1964-1975. A survey that measured subjective environmental factors, health problems related to indoor environment and emotional well-being were distributed to residents by email during the fall of 2014. The survey was based on Ørebro model and Russel's circumplex model of Affect. The questionnaire was distributed via email to 990 students twice to measure any changes in indoor environments and emotional wellbeing. The response rate was 42 percent. Temperature and humidity were measured using sensors in the apartments during the same period. Results from Örebro model showed fewer registered complaints among residents of solid wood construction for most environmental factors and symptoms. This was true for both the first and second measurement. Analysis of variance of the factors that measured emotional well-being showed a significant relationship between residence and experience of well-being for several of the self-reported factors

Proceedings of the 58th International Convention of Society of Wood Science and Technology
June 7-12, 2015 – Grand Teton National Park, Jackson, Wyoming, USA

Mapping of Wood Supply Chains, a Case Study.

Magnus Larsson, magnus.larsson.skog@sca.com
Anders Roos, anders.roos@slu.se
Matti Stendahl, matti.stendahl@slu.se

SLU, Forest Products, PO Box 7008, SE-7500 07 Uppsala

Abstract

The aim of the study is to suggest and test a model for mapping the structure and processes and assessing the performance in wood based supply chains. This will describe the performance of the whole supply chain and enable managers to achieve cost effective, customer responsive and resilient product flows. The work includes mapping supply chains (forest-sawmill-customer) and factors that impact the production and flow. This proceeds to identify methods to manage and improve the supply chains. The work is based on qualitative case-studies and comprises the following sub-studies: 1.Mapping of a wood-based SC from raw material production to the customer. 2.Analysis of the conditions and restrictions for achieving an enhanced wood based SC in terms of cost efficiency, customer value and flexibility. 3.Development of performance indicators, models for assessment of efficient resource management, customer value and risk management (uncertainties). A suggested mapping framework draws on the works by Lambert & Cooper, used by Haartveit et al. The mapping is supplemented with qualitative studies, in which costs appearing from sub optimized activities, as well as value creation potential, are detected and defined. The result is intended to be used as a base for decisions on strategy and desired performance by the SC management in charge.

Proceedings of the 58th International Convention of Society of Wood Science and Technology
June 7-12, 2015 – Grand Teton National Park, Jackson, Wyoming, USA

Comparative Analysis of the European Forest Sector Production 2008-2013

Michael D. Burnard[1,2] – Monika Cerinšek[2] – Andreja Kutnar[1,3]– Boris Horvat[1,2]*

[1] Andrej Marušič Insitute, University of Primorska, Koper, Slovenia
[2] Abelium R&D, d.o.o., Ljubljana, Slovenia
[3] Faculty of Mathematics, Natural Sciences and Information Technology
**Corresponding author*
michael.burnard@iam.upr.si
monika@abelium.eu
andreja.kutnar@upr.si
boris@abelium.eu

Abstract

Wood is available in many forms and is present in many products available on the market. In order to analyse Europe's forest sector production, detailed production quantities and values along with labor force data from 2008-2013 made available by the European Commission and the Food and Agriculture Organization of the United Nations were examined with hierarchical clustering using Ward's method. The production data (the Eurostat "Prodcom" dataset) is derived from annual surveys and covers approximately 4000 manufactured products, 205 of which are forest sector products. Labour force data includes employed persons and hours worked in four broad categories including forestry and logging, the manufacture of wood and wood products, the manufacture of paper and paper products, and furniture manufacturing. By using this data it is possible to identify the strengths and weaknesses in forest sector production in many European countries. Furthermore, this analysis provides an opportunity to identify possible areas of expansion for specific countries. This paper will provide an overview of the methods and results from performing the analysis. The combination of labour force and production data will provide an estimate of the relative efficiency of the forest products sector (and sub sectors) in European countries.

Keywords: clustering, Ward's method, policy, industrial development

Introduction

Europe has identified the need to transform their economy into a socially responsible and biobased economy in order to achieve sustainable growth. The EU polices that directly

impact the forest sector include the EU Sustainable Development Strategy (European Commission 2009), the EU Roadmap 2020 (European Commission 2011) and the recycling society directives (European Parliament 2008), amongst others. The European Forest Technology Platform (FTP) is working to position the forest sector as key actors throughout this transition (FTP 2013a, FTP 2013b). As countries and regions across Europe develop and update their smart specialization strategies to focus their innovation efforts, they will seek as much information as they can about relating to market trends in a wide range of areas, including the forest sector. Similarly, businesses and researchers seeking to both follow and shape the market continually search for new information about the forest sector's performance. In each situation, both new and established methods for examining, understanding and making predictions about the market are needed.

In this exploratory study we apply Ward's clustering method on three separate aspects of the forest sector (categorized production quantities, roundwood production, and labour) to look for models of growth and expansion for Slovenia's forest sector. Our clustering method will group countries together that manufacture similar sets of products, that produce similar quantities of roundwood, and that have similarly segmented forest products labor statistics (all relative to their total).

Objective

Our objective is to determine which countries Slovenia may emulate or learn lessons from by examining the successful countries that fall in the same cluster as Slovenia. Similarly, successful countries that fall outside of Slovenia's clusters may also provide insights for reinvigorating the countries forest sector.

Materials and Methods

Data sources and quality

The data analysed in this project comes from three sources. First, the production data is derived from the Eurostat Prodcom database (Eurostat, 2015). We analysed a subset of this dataset that reflects 205 products closely related to the forest products sector. These 205 products were grouped by their 4-digit NACE2 codes and resulted in production quantities for 26 categories of products (Table 1). Additionally, the roundwood production data was retrieved from the Food and Agriculture Organization of the United Nations (FAO) forestry production and trade database for six categories of roundwood (FAO, 2015). Labour statistics were derived from the Eurostat employment database and include four categories of forest sector related jobs. It should be noted that these data include estimates and missing data (which may be missing because survey respondents chose to keep them confidential). We know, for example, that Austria produces a significant amount of particleboard, however the quantity is missing from the Prodcom data.

Dataset	Categories included
Prodcom	1520: Wooden footwear; 162x: Sawmilling, veneer and wood based panels; parquet flooring; builder's carpentry and joinery, containers, other wood products; 171x: Pulp; 172x; Paper products; 2014: Chemicals from/for wood; 2041: soaps, cleansers and related products from wood; 2365: Fibre cements using wood; 2573: Tools made with wood; 2594: Fasteners for wood; 2651: Testing and measurement machines for wood; 2849: Machines for working with wood; 2899: Special purpose machinery for wood; 310x: Furniture made of wood;
FAO Roundwood	1601: Coniferous sawlogs and veneer logs; 1604: Non-coniferous sawlogs and veneer logs; 1602: Coniferous pulpwood, round and split; 1603: Non-coniferous pulpwood, round and split; 1623: Coniferous other industrial roundwood; 1626: Non-coniferous other industrial roundwood
Labour	Wood, Forestry, Paper, Furniture*

Table 19 Categories included in cluster analysis
* This furniture category is not restricted to wood furniture.

Prodcom data is considered on a "unit" basis because the units of measurement for each product vary.

Hierarchical clustering
Clustering methods allow entities (in our case countries) to be grouped based on how similar a set of attributes defining the entities are (Everitt et al. 2011). We performed clustering on three sets of variable separately: relative share of forestry labour categories within the forestry sector by country, relative production of individual wood-related products to overall wood-related production in the PRODCOM data by country, and relative share of six categories of roundwood production to overall roundwood production by country. In each case, the data were analysed yearly from 2008 to 2013. Using roundwood production as an example, the share each category of roundwood production contributed to a country's total roundwood production for each year during the period was considered by the clustering algorithm.

We chose to use Ward's method to determine the hierarchical clusters, which defines the dissimilarity among entities as the squared Euclidean distance between entities (Everitt et al. 2011). This measure can be interpreted as the distance between two points in a Cartesian coordinate system and lends itself to simple interpretation and best reflects the differences between countries. In our data, these points represent countries and their values are equal to their distribution of wood production (Prodcom and FAO Roundwood) or their distribution of labour within the forest sector. Ward's method forms clusters by grouping countries together that have the smallest error sum of squares – the sum of squared distances from each cluster to all others. The clusters are represented in a dendogram (cf. Figs. 1, 3 and 4) with each country occupying a leaf position. Each leaf is an individual cluster with one member (the listed country). Moving away from the leaves each branch merger represents a larger cluster until all clusters are joined at the stem. The

height of a merger (the lengths of the branches) represents the dissimilarity between each two clusters. Longer branches indicate greater dissimilarity. Choosing the number of clusters in this type of analysis is at the discretion of the researcher. In our case, we examined the results with different numbers of clusters to find what appeared to be the most reasonable based on our knowledge of the European market.

Analysis and plotting was carried out in R (R Core Team, 2015).

Results

The cluster analysis effectively identified meaningful groups in each dataset. However, problems with the data, including missing data, estimated values and confidential values limit how meaningful any interpretation of the clustering may be. In each case, there are expected groupings; Countries known to produce large quantities of primary wood products relative to their overall production, such as France, Spain, Italy, Germany, and Turkey were grouped together in the Prodcom clusters. This provides some level of confidence that this initial, exploratory step towards developing a new lens through which we can examine the European forest sector will yield helpful information for researchers, industry members and policy makers.

Wood products manufacturing clustering

We chose to use 10 clusters for our analysis of the Prodcom data (Fig. 1). Slovenia is in the largest cluster, which also includes: Poland, Denmark, Belgium, Croatia, The United Kingdom, Slovenia, and Hungary.

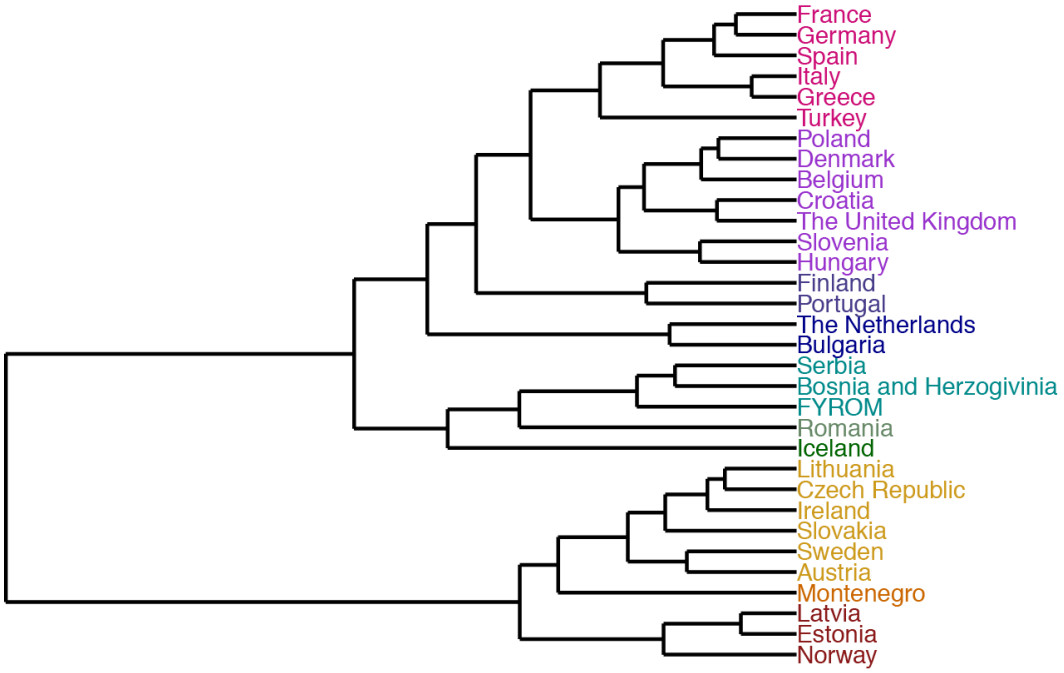

Figure 47 Clustering results for the Eurostat Prodcom data from 2008-2013.

As an example of cluster comparison, contrasting Slovenia's group with Sweden's (also containing Lithuania, Czech Republic, Slovakia, Ireland, and Austria) shows a greater emphasis on paper products in the latter group, while in the former primary wood products are a more significant portion of each countries production (Fig. 2).

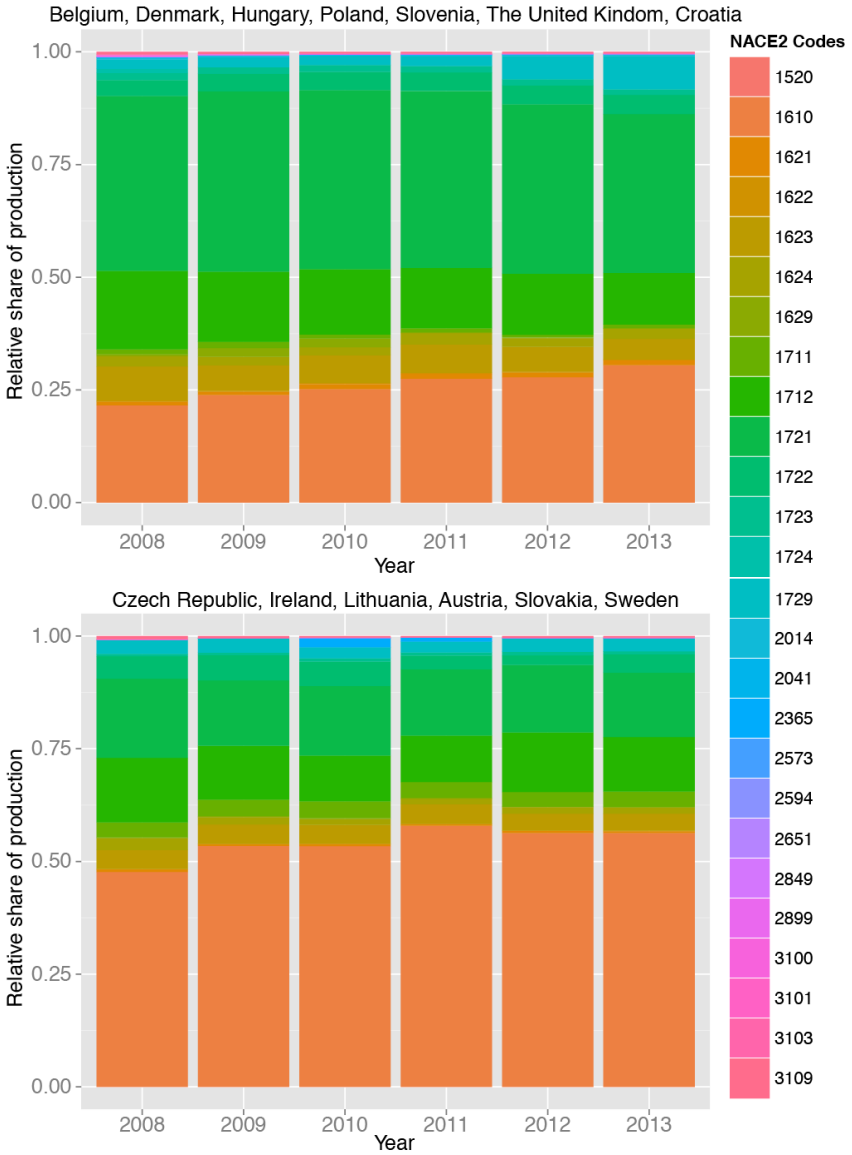

Figure 48 Relative share of wood related products manufacturing for two groups (Slovenia's - top, and Sweden's - bottom). NACE codes are described in Table 1.

Roundwood production clustering

We determined eight to be the most effective number of clusters to produce a meaningful analysis of roundwood production in Europe (Fig. 3). In this case, Slovenia was grouped with Germany, Greece, Switzerland, and Cyprus. Like the group containing Austria, Czech Republic, Ireland, and The United Kingdom, the average coniferous sawlog and veneer log production is approximately 65% of all roundwood production between 2008

and 2013 for Slovenia's group. However, the group containing Austria produces a more significant quantity of coniferous pulpwood (an average of approximately 26%) than Slovenia's group (an average of approximately 8%).

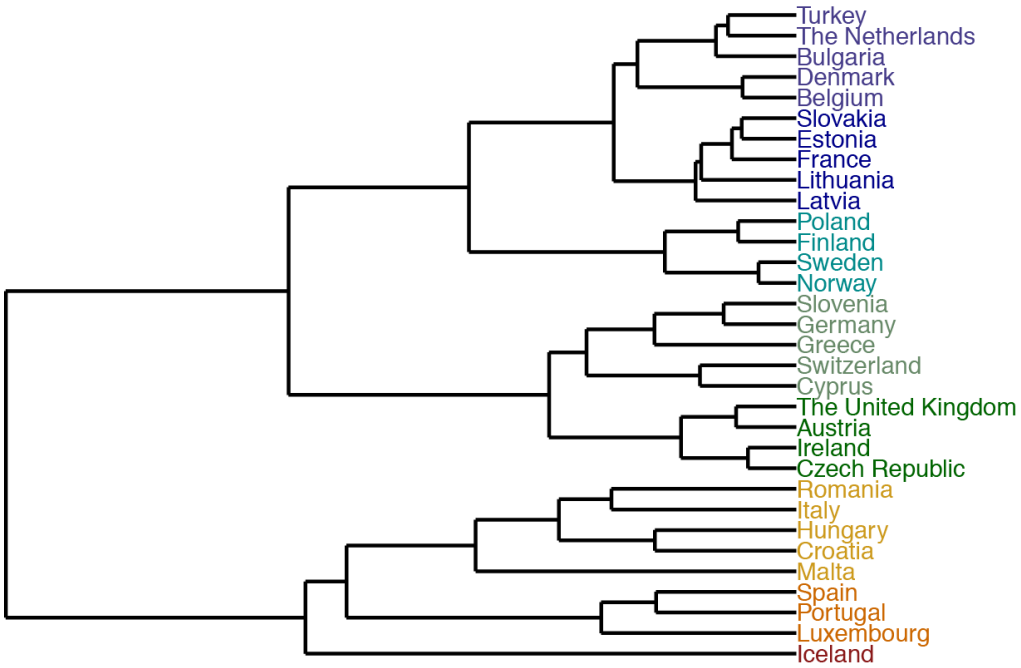

Figure 49 Clustering results for roundwood production data from 2008-2013

Labour clustering

We determined nine clusters adequately segmented the European forest-related labour data into useable groups (Fig. 4).

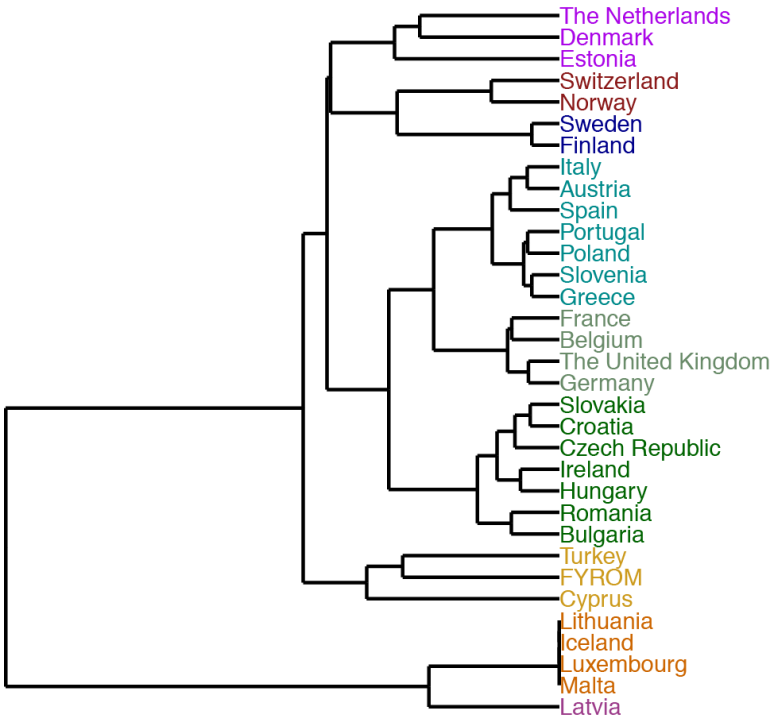

Figure 50 Forest sector labour market clusters using Eurostat data from 2008-2013.

However, the produced clusters have the most significant gaps present. Iceland, Lithuania, Luxembourg, and Malta completely lack data, while only the 2008 data for Latvia is available. Latvia and Lithuania are known to employ many workers in the forest sector. The group containing Cyprus, the Former Yugoslav Republic of Macedonia (FYROM) and Turkey also has significant gaps: no data is available for 2008 and data is missing for all other years except 2011. The group containing Denmark, Estonia, Finland, Sweden, and The Netherlands also has gaps from 2009 through 2012. While these gaps do not necessarily invalidate the clusters, more complete data would improve the accuracy and meaningfulness of the analysis.

Slovenia's cluster (containing Austria, Greece, Italy, Poland, Portugal, and Spain) employs much of their forest related workforce in wood manufacturing and furniture, with only a small portion working in paper or forestry.

Discussion

This exploratory analysis of Europe's forest sector with an emphasis on Slovenia can provide manufacturers who wish to expand their offerings based on existing resource production. By identifying a product category that is underproduced in Slovenia but is manufactured in a country with similar raw wood resources, an industry member may decide to expand their capacity to produce the item. Similarly, researchers and policy makers can identify strengths in the labour market abroad, in resource utilization and

production to focus innovation and provide incentives for smart expansion within the industry.

Slovenia may not produce the raw quantities of products and roundwood, and does not employ the raw number of employees in the sector as larger countries but it uses it's resources similarly to countries with very successful forest sectors. However, there is always room to improve, expand, or to reign in production in the wrong areas. This type of cluster analysis is a useful early step in determining where these opportunities lie.

Conclusion

Clustering methods provide researchers, industry members and policy makers with a relatively easy to understand introduction point to a large amount of data. Although the quality of the data will greatly impact the level of confidence the analysts should have in their conclusions, cluster analysis provides many advantages, especially for exploratory research. In our example of the forest sector, a Slovenian researcher may determine that a product category is produced to great effect in another country and may conduct research to help drive innovation related to that product category at home. Furthermore, these results are derived from interdisciplinary research activities and demonstrate the type of collaborative work needed to continue moving the forest sector forward.

References

Eurostat (2015a) Eurostat Employment Database (lfsa_egan22d, v3.0.3.3-20150102-5511-PROD_EUROBASE) http://ec.europa.eu/eurostat/web/lfs/data/database (8 Jan 2015)

Eurostat (2015a) Eurostat Prodcom Database (DS_066342, v3.0.3.3-20150102-5511-PROD_EUROBASE) http://ec.europa.eu/eurostat/web/prodcom/data/database (8 Jan 2015)

European Commission, 2009. Mainstreaming sustainable development into EU policies: 2009 Review of the European Union Strategy for Sustainable Development. Communication. Brussels: European Commission European Commission. http://eur-lex.europa.eu/LexUriServ/LexUriServ.do?uri=CELEX:52009DC0400:EN:NOT. (15 Sept 2013).

European Commission (2011) A Roadmap for moving to a competitive low carbon economy in 2050. Communication. Brussels: European Commission European Commission. http://eur-lex.europa.eu/LexUriServ/LexUriServ.do?uri=CELEX:52011DC0112:EN:NOT. (15 Sept 2013)

European Parliament (2008) Directive 2008/98/EC of the European Parliament and of the Council of 19 November 2008 on waste and repealing certain Directives. Directive. Brussels: European Parliament http://eur-lex.europa.eu/LexUriServ/LexUriServ.do?uri=CELEX:32008L0098:EN:NOT. (15 Sept 2013)

Everitt BS, Landau S, Leese M, and Stahl D (2011) Cluster Analysis, 5th Edition. John Wiley & Sons, Ltd. West Sussex. 287 pp.

Food and Agriculture Organization of the United Nations, Rome, Italy. FAOSTAT. Forestry (Collection). (http://data.fao.org/ref/4d0e8c4f-abb6-43e0-902f-a1b522a32f09.html?version=1.0 (9 Feb 2015)

Forest Technology Platform (2013a) Horizons – Vision 2030 for the European Forest-based sector. http://www.forestplatform.org/files/FTP_Vision_revision/FTP_Vision_final_Feb_2013.pdf (15 April 2015)

Forest Technology Platform (2013b) Strategic Research and Innovation Agenda for 2020. http://www.forestplatform.org/files/SRA_revision/Renewed_SRA_for_2020.pdf (15 April 2015)

R Core Team (2015). R: A language and environment for statistical computing. R Foundation for Statistical Computing. Version 3.0.1.1. Vienna, Austria. URL http://www.R-project.org/.

Acknowledgments

The authors would like to acknowledge the WoodWisdom-Net+ and the Ministry of Education, Science and Sport of Republic of Slovenia for financial support of the project CaReWood. Furthermore, the authors would like to acknowledge the Slovenian Research Agency for financial support within the frame of the project P1-0294.

Proceedings of the 58th International Convention of Society of Wood Science and Technology
June 7-12, 2015 – Grand Teton National Park, Jackson, Wyoming, USA

Market Appeal of Hawaiian Koa Wood Product Characteristics: A Consumer Preference Study

Eini C. Lowell[1] – Katherine Wilson[2] – J.B. Friday [2] – Jan Wiedenbeck[3] – Catherine Chan[2]*

[1] Research Scientist, USDA Forest Service Pacific Northwest Research Station, Portland OR, USA.* *Corresponding author*
elowell@fs.fed.us
[2] Graduate Student, Extension Specialist, Professor, College of Tropical Agricultural and Human Resources, University of Hawai'i at Mānoa, Honolulu, HI. USA.
kawils65@hawaii.edu, jbfriday@hawaii.edu, chanhalb@hawaii.edu
[3] Research Scientist, USDA Forest Service Northern Research Station, Princeton WV. USA.
jwiedenbeck@fs.fed.us

Abstract

Acacia koa is an endemic Hawaiian tree species whose wood is prized globally. Today, most woodworkers use koa wood from dead and dying old-growth trees. Wood from young-growth koa is thought to be less appealing to consumers because of its lighter color and lack of figure. A conjoint choice experiment was conducted to evaluate consumer preference of these koa characteristics and their willingness-to-pay. This experiment randomly combined different attributes: colors, figure, and prices and used six identically shaped bowls (an item likely to be purchased by Hawaiian residents and visitors) from which respondents selected their preference. The survey was conducted at Hawaii's Woodshow (129 respondents) to canvass consumers likely to be familiar with koa. Results were analyzed using latent class analysis software that separates respondents into distinct classes based upon preferences. The results identified three classes of respondents. Class 1 (32% of respondents) showed significant preference for lower prices and curly figure but not for color. Class 2 (42% of respondents) significantly preferred curly figure and medium or light colored koa bowls. Class 3 (27% of respondents) significantly preferred lower prices, medium color, and bowls with no curly figure. Koa woodworkers can use these results to design and create pieces for different market groups. Through substitution of young-growth koa for the decreasing supply of old-growth wood, the legacy of koa wood can be sustained.

Key words: *Acacia koa*, conjoint choice, Hawai'i, consumer preferences, willingness-to-pay, old-growth, young-growth

Introductiom

Beauty is in the eye of the beholder. This especially holds true when considering wood products. Variation in wood characteristics such as color and figure make each piece unique. The appeal of one piece of furniture or household item made from wood over another is personal. While differences in consumer preference can vary by geographic location, *Acacia koa* is especially prized both in the Hawaiian Islands and globally. Its reputation comes primarily from pieces crafted from old-growth trees.

Many woodworkers and craftspeople in Hawai'i prefer to work with old-growth koa as their raw material for its color and figure (e.g., curl). This resource is dwindling in supply with limited amounts available in the foreseeable future. The koa wood being used now comes from dead and dying trees. Little data are available on second-growth koa wood properties and much anecdotal information as to its inferiority for woodworking is common. The ability to market products made from young-growth koa will promote active management in young-growth stands. Research conducted on genetic variation in wood quality, including color and grain, was reported by Simmons et al. (1991). Work by Dudley and Yamasaki (2000) found indications that figure may be under genetic control. Sun et al. (1996) recommended that more attention be paid to selection and silviculture in koa reforestation programs. Results point to the ability of land managers to select and manage for characteristics that match consumer preferences.

Color and figure have been identified as key attributes in creating and marketing koa products. In fact, it is thought that just the name koa has market recognition and creates desirability. Yet a lack of ability by consumers to identify wood species was documented by Bowe and Bumgardner (2004) and Bumgardner et al. (2007). Consumer preference research on other species has found other attributes that resonate with buyers. Secondary manufacturers using Eastern white pine (*Pinus strobus* L.) found that lumber quality and region of origin had the largest influence on purchasing decisions (Alderman et al. 2007). Consumers were willing to pay more for an end table made in Alaska over one manufactured in China (Donovan and Nicholls 2003). Along with name recognition and origin are appearance attributes such as color and figure. Bumgardner and Bowe (2002) found that consumers thought darker color woods reflected higher value than lighter color woods and the lighter color was perceived to be less expensive. In studying character-marked furniture made from red alder (*Alnus rubra*), Bumgardner et al. (2009) found a disconnect between retailer and consumer cues on willingness-to-pay. These past research studies suggest that there are opportunities for marketing koa products from both young- and old-growth trees.

Conjoint choice analysis is a technique that has the ability to determine how certain product attributes affect whether a consumer is likely to purchase an item and also quantify its significance (Green and Srinivasan 1978). This means of analysis in preference research is widely used for consumer and industrial goods (Green and Srinivasan 1990). Lihra et al. (2012) found that price drove decision when buying

furniture 50% of the time. Wang et al. (2004) used conjoint analysis to assess four attributes of fine furniture: design, price, density of character marks, and guarantee policy. They found that design was more important to consumers with price the second most important attribute.

This project was designed to evaluate purchaser perception of important attributes of koa wood, color and figure, and their willingness to pay, using a product likely to be purchased by a variety of consumers because of its versatility.

Materials & Methods

This study used the conjoint choice experiment method to indirectly obtain consumers' willingness to pay and preference for different attributes of a koa wood bowl. The attributes and levels were chosen based upon typical koa wood characteristics. Darker colors and a higher degree of figure (curl) are typically equated to wood coming from old-growth trees. It is perceived that wood which is darker in color and has more curl is more desirable to consumers. Lighter colored wood with less figure, typically harvested from younger koa trees or from the sapwood of older trees, is thought to be less desirable. This experiment randomly combined three different color levels, two levels of figure (non-curly and curly) and three prices using six identically shaped bowls as examples of each possible combination of color and figure (Figure 1). An 8-in diameter koa bowl was chosen to represent a koa wood product that is an item likely to be purchased by Hawai'i residents for their own home, by visitors as a keepsake of their visit to the Hawaiian Islands, or as a gift. The color, figure, and price are classified as "attributes" and each attribute had different levels. Table 1 depicts the selected attribute levels that were used. Price levels were set by retail market value of similar bowls.

Figure 1. The six koa bowls on display at Hawaii's Woodshow in Honolulu, HI. Photo credit: William Weaver.

Attributes	Price per bowl	Color of bowl	Figure of bowl
Levels	$400	Light	Not Curly
	$500	Medium	Curly
	$600	Dark	
	$700		

Table 51: Attributes and levels used to create the conjoint choice experiment profiles

The discrete choice analysis survey design was created using Sawtooth Software[4] using the three attributes and their associated levels found in Table 1. The survey was comprised of 12 choice tasks each containing a scenario of three different koa bowl attributes. Each choice task consisted of a level from each attribute for a total of 24 possible combinations. Two survey versions were created to cover all possible attribute-level combinations and each respondent was asked to complete one survey containing 12 choice tasks. Respondents chose their preferred bowl from each task. They were also asked to select their favorite bowl and indicate the maximum they would be willing to pay for it.

Figure 2 shows an example choice task that was presented to respondents. This method forces the respondent to make trade-offs among varying product attributes and levels therefore determining which attributes and levels they prefer. From the survey results, estimates on consumers' willingness to pay for one attribute over another can be calculated.

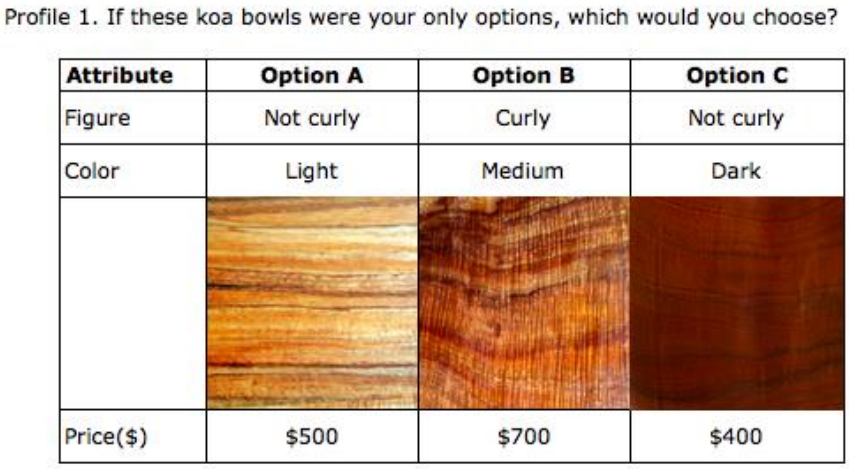

Figure 52. Example choice task created by Sawtooth Software that was presented to respondents. Each respondent must choose only one koa bowl, Option A, B, or C, based upon the attributes they prefer.

The survey also contained demographic questions to see what additional factors, if any, influence preference. Other questions relating to consumer actions were asked such as if they had ever purchased koa products before and where they would prefer to buy the products.

[4] Sawtooth Software, Inc. Orem, UT. http://www.sawtoothsoftware.com/

Surveys were conducted at Hawaii's Woodshow in Honolulu, HI (Labor Day weekend 2014) to capture consumers familiar with koa. The survey was administered to attendees willing to participate. A brief description of the project background was given to respondents prior to their answering the survey. Demographic information was also collected from respondents.

Results were analyzed using latent class analysis that aggregates responses and separates them into classes based upon expressed preferences. Latent GOLD® software[5] was used for the analysis. The criterion used to select the optimal number of preference classes is based on the Bayesian Information Criterion statistic (BIC).

Results and Discussion

Response

There were a total of 129 complete surveys. Response rate was about 80%.

Demographics

Respondents answered questions relating to demographics, their knowledge of koa, and whether they had experience working with koa. Of the 129 respondents from Hawaii's Woodshow, 84% lived in Hawai'i and 16% were visiting. Eighty-five percent of the Hawaiian residents have lived in Hawai'i for more than 5 years. Fifty-one percent of the people surveyed were female and 49% surveyed were male. Figure 3a depicts the age breakdown of respondents. Over one-third of the respondents were between the ages 60 and 69. Almost 50% of respondents had an annual household income of at least $90,000 and only 14% of respondents had an annual household income of below $30,000 (figure 3b).

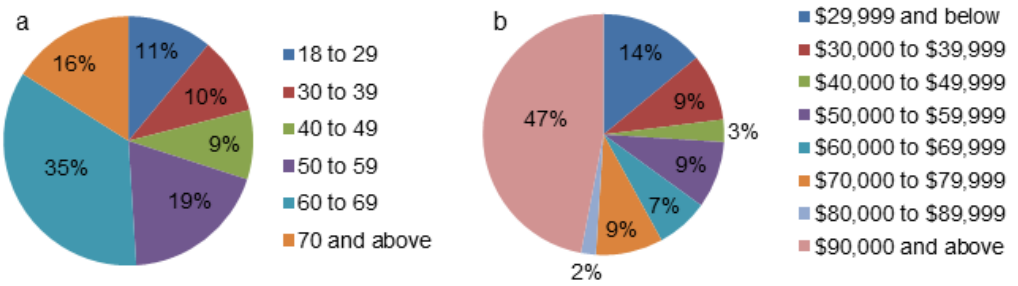

Figure 53. (a) Age distribution and (b) annual household income of respondents from Hawaii's Woodshow.

The majority of respondents, 84%, had graduated with at least a Bachelor of Science degree and within this group, the majority had a higher income and education level, and was older. Also, 73% had purchased a koa wood product in the past. Twenty-eight percent of respondents were woodworkers with 40% selling their work. This respondent group was very familiar with koa wood (95%). None of the respondents' socio-

[5] Statistical Innovations, Belmont, MA. http://www.statisticalinnovations.com/

demographics were found to influence their attribute preference in the survey based on Latent GOLD® software results.

Model results

The software identifies consumer groups or clusters (called classes) based on product attributes preferences. The model containing three classes was chosen as the best for characterizing consumer preferences based upon the Bayesian Information Criterion (BIC) statistic. Table 2 is a summary of which attribute parameters were statistically significant at the 0.05 level as shown by part worth utilities. The negative sign for a part worth utility indicates a non-preference for a certain attribute and in the case of price, a lower price for the bowl.

Attribute (class size)	Class 1 (32%)	Class 2 (42%)	Class 3 (27%)
Price	-0.397*	-0.025	-0.189*
Color			
Light	-0.158	1.458*	-0.144
Medium	0.166	0.561*	0.406*
Dark	-0.009	-2.019*	-0.262*
Figure			
Non-curly	-1.187*	-0.831*	0.243*
Curly	1.187*	0.831*	-0.243*

* significant at the $p<0.05$ level

Table 2. Model estimates for consumer preferences as shown by part worth utilities. (*) is statistically significant at the 0.05 level, (-) symbol indicates a negative preference.

Table 3 lists the attribute importance for each class. Class 1 (with 32% of the respondents) had no significant preference in color but preferred having a lower price and curly figure. This class had a significant non-preference for bowls that were non-curly. While figure was the most important attribute to this class, price still somewhat important accounting for almost a third of their decision and color was the least important. Class 2 accounted for 42% of respondents and color was most important to them; they significantly preferred light or medium colored koa bowls and bowls with curly figure. They significantly did not prefer darker color and non-curly bowls. Color was almost twice as important to them as figure. Price was not a significant factor. The third consumer class was made up of 27% of respondents who significantly preferred lower prices, non-curly bowls, and medium color. Class 3 significantly did not prefer darker color and curly figured bowls. Color was the most important attribute followed closely by price and then figure.

Attribute (class size)	Class 1 (32%)	Class 2 (42%)	Class 3 (27%)
	----------percent----------		
Price	30.6	1.5	33.0
Color	8.3	66.6	38.8
Figure	61.0	31.9	28.2

Table 3. Attribute importance by percent for each class. Highlighted boxes indicate the attribute of highest importance to each class.

Figure 4 shows the maximum price that consumers are willing to pay for a bowl. Just over half of the respondents would pay less than the minimum level set for this study. This could provide market opportunities for using young-growth koa wood for those who are price conscious but would like to own a koa product.

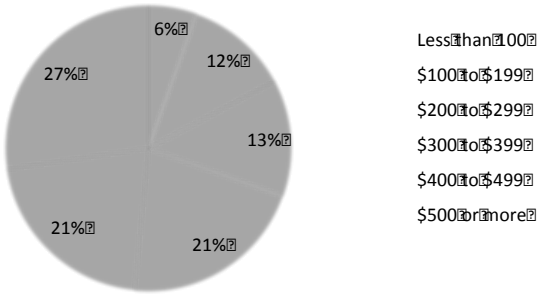

Figure 4. Maximum price respondents would pay for their favorite bowl.

Summary and Conclusions

The study drew from a small, knowledgeable portion of the population. For Class 1 (32% of the sampled population) figure was the most important attribute. Price influenced about one-third of their decision. The largest group represented (42% of respondents) preferred medium and light colored, curly figured koa bowls and had no price preference. They did not prefer dark color. About one quarter of the respondents (27%) preferred bowls with medium color, non-curly figure, and having a lower price. They also did not prefer dark color.

If these results hold for the larger population, stores or woodworkers, depending on which consumer group they market to, would either need to have a competitively priced bowl; or one light or medium in color; and could either be figured (curly) or not (non-curly). The majority of respondents preferred the light or medium color, which is often associated with young-growth koa. The desire to have a piece of Hawaiian culture could be met using materials that are not necessarily reflective of old-growth characteristics.

These results have implications for koa silviculture and harvesting regimes and suggest a change in the paradigm that consumers only want darker wood with either curly or non-curly figure. It appears young-growth koa can be a viable resource option for the manufacture of certain types of koa products (in this case bowls) and there will be consumers to purchase these products.

Koa woodworkers can use these results to design and create pieces for market segments that occupy a similar market niche to these small koa bowls. Through substitution of young-growth koa for the decreasing supply of old-growth wood, the legacy of koa wood can be sustained.

Acknowledgements

The authors would like to thank the Hawai'i Forest Industry Association for allowing us to conduct our survey during their annual Woodshow. We appreciate the assistance of Cassie Zhang and Nicole Evans, graduate students, University of Hawai'i, who aided in conducting the surveys and/or analyzing the data. The bowls were turned by Timothy Allen Shafto.

References

Alderman D, Smith R, Bowe S (2007) Eastern white pine secondary manufacturers: Consumption, markets, and marketing. For Prod J 57(10): 28-35.

Bowe S, Bumgardner M *(*2004) Species selection in secondary wood products: perspectives from different consumers. Wood Fiber Sci 36(3): 319–328.

Bumgardner MS, Bowe SA (2002) Species selection in secondary wood products: Implications for product design and promotion. Wood and Fiber Sci. 34(3): 408-418.

Bumgardner M, Nicholls D, Barber V (2009) Character-marked furniture made from red alder harvested in southeast Alaska: product perspectives from consumers and retailers. Can J For Res 39(12): 2450-2459.

Bumgardner M, Nicholls D, Donovan G (2007) Effects of species information and furniture price on consumer preferences for selected woods. Wood and Fiber Sci 39(1): 71-81.

Donovan GH, Nicholls DL (2003) Estimating consumer willingness to pay a price premium for Alaska secondary wood products. Res. Pap. PNW-RP-553. Portland, OR: U.S. Department of Agriculture, Forest Service, Pacific Northwest Research Station. 7 p.

Dudley NS, Yamasaki J (2000) A Guide to Determining Wood Properties of Acacia koa. HARC Forestry Report 3.

Green PE, Srinivasan V (1978) Conjoint analysis in consumer research: issues and outlook. J Consumer Res: 103-123.

Green PE, Srinivasan V (1990) Conjoint analysis in marketing: new developments with implications for research and practice. The J Marketing: 3-19.

Lihra T, Buehlmann U, Graf R (2012) Customer preferences for customized household furniture. J For Econ 18(2): 94-112.

Simmons P, Winkle E, Conkle T, Willers K, Glover N (1991) Genetic variation of koa. In: Improvement of *Acacia koa*: Resource documents. J.L. Brewbaker, N. Glover, and E. Moore (eds). U.S. Forest Service Institute of Pacific Islands Forestry, State of Hawaii Department of Land and Natural Resource, and Nitrogen Fixing Tree Association, Honolulu, Hawai'i.

Sun W, Brewbaker JL, Austin MT (1996) Genetic variation of Acacia koa seed, seedling, and early growth traits. Pages 33-38 *in* DO Evans and L. Ferentinos, eds. Koa: a decade of growth. Proceedings of the Hawaii Forest Industry Association Annual Symposium. Honolulu, HI.

Wang Q, Shi G, Chan-Halbrendt C (2004) Market potential for fine furniture manufactured from low-grade hardwood: Evidence form a conjoint analysis in the northeastern United States. For Prod J 54(5): 19-25.

Proceedings of the 58th International Convention of Society of Wood Science and Technology
June 7-12, 2015 – Grand Teton National Park, Jackson, Wyoming, USA

To Own Forest or Not? Vertical Integration in Pulp and Paper Sector

Jaana Korhonen, jaana.e.korhonen@helsinki.fi
Yijing Zhang, yijing.zhang@helsinki.fi

University of Helsinki, Department of Forestry, Pl 27, 00014 Helsinki

Abstract

Vertical integration in forest industry refers to firms that provide large portion of wood from their own or controlled forests. Access to resources and competition for cost effective acquisition of industrial raw material are some of the main concerns and advantages for globalized forestry corporations. However, quantitative studies in this topic are still lacking especially at the global scale. This analysis is based on the logistic regression analysis on dichotomous variable whether company owns forest land or not. Data is based on sample of 99 forest companies reported in TOP 100 A Global Forests, Paper & Packaging Industry Survey, and the information provided with regards to corporate forest holdings and corporate financial performance available in corporate sustainability and other reports for year 2012. In results, we see that decision on vertical integration is significantly affected by the firm size, profitability, and product diversification of the company. The influence of location and other relevant factors of firm performance are discussed to the extents that the data allows.

Proceedings of the 58th International Convention of Society of Wood Science and Technology
June 7-12, 2015 – Grand Teton National Park, Jackson, Wyoming, USA

Exploring the Future Use Oo Forests in Finland: Perspectives from Sustainability Oriented Forest Owners

Liina Häyrinen, liina.hayrinen@helsinki.fi
Osmo Mattila, osmo.mattila@helsinki.fi
Sami Berghäll, sami.berghall@helsinki.fi
Markus Närhi,
Anne Toppinen, anne.toppinen@helsinki.fi

University of Helsinki, P.O. Box 27, (Latokartanonkaari 7), Helsinki FI-00014

Abstract

The objective of the study was to explore the views of sustainability oriented non-industrial private forest owners (NIPFs) on the future use of forests in Finland. Findings from the qualitative analysis based on 4 focus group discussions from 17 NIPFs show that generally NIPFs have a strong emotional attachment towards forests and are interested in more diversified opportunities of forest use in the future beyond dominant raw-material driven mindset. They also presented a lot of insight for enhancing intangible value creation based on forest ecosystem services. Even though groups of forest owners also recognized factors that inhibit the more diversified development of the forest-based products and services, they saw the overall future of forests in bringing welfare to society as positive. They identified unused possibilities in e.g. peer-to-peer learning via organized forest owner forums and cross-sectoral co-operation between forestry and nature-based tourism. Finally, results elaborated the high diversity between four groups in NIPF associations to forest use and their inherent service and information needs, which can be considered as a challenge for current service organizations. However, further research is needed beyond these findings to generalize them, as well as to study the business potential in sustainable lifestyle aspects of forestry.

Proceedings of the 58th International Convention of Society of Wood Science and Technology
June 7-12, 2015 – Grand Teton National Park, Jackson, Wyoming, USA

Impacts of Policies to Eliminate Illegal Timber Trade

Ed Pepke[1] – Jim Bowyer[2] – Steve Bratkovich[3] – Kathryn Fernholz[4] – Matt Frank[5] – Harry Groot[6] – Jeff Howe[7]

[1] Associate, Forest Products Marketing and Policies, Dovetail Partners, Minneapolis, MN, USA, ed@dovetailinc.org
[2] Director of Responsible Materials, Dovetail Partners, Minneapolis, MN, USA, jimbowyer@comcast.net
[3] Project Manager for Recycling and Reuse, Dovetail Partners, Minneapolis, MN, USA, sbratkovich@comcast.net
[4] Executive Director, Dovetail Partners, Minneapolis, MN, USA, Katie@dovetailinc.org
[5] Program and Research Associate, Dovetail Partners, Minneapolis, MN, USA, matt@dovetailinc.org
[6] Associate, Dovetail Partners, Minneapolis, MN, USA, harry@dovetailinc.org
[7] Founder and Chairman, Dovetail Partners, Minneapolis, MN, USA, jeff@dovetailinc.org

Abstract

Recognizing the multiple and exorbitant costs of illegal timber trade, governments and trade associations are increasingly implementing policies to ensure the legality of imports and exports. When illegal timber trade stems from illegal logging it has tremendous additional social, economic and environmental consequences—stopping the illegal trade reduces demand for illegally logged timber. The establishment of policies started in the United States (Lacey Act Amendment), then Europe (European Union Timber Regulation), Australia and some other countries, including China. These policies have had positive impacts, e.g. through the successes of wood and paper trade associations in sensitizing the wood chain to the effects of illegal logging and timber trade. Systems for the certification of sustainable timber management made improvements to meet the policies' demands for due diligence. However, at least initially, they have not directly raised demand for timber, including that for tropical timber, on which some government policies are focused. This paper and its presentation will include up-to-date analysis of market effects of the policies' implementation.

Keywords
Illegal timber trade, illegal logging, trade policy, Lacey Act, EU Timber Regulation, Australia Illegal Logging Act,

Executive Summary

Illegal timber trade stemming from illegal logging has tremendous social, economic and environmental consequences. Illegal logging negates the intent of sustainable forest management, often causing or leading to forest degradation and deforestation—outcomes that can devastate forest dependent communities. Such activity is also linked to habitat destruction and species extinction. In addition, illegal logging results in huge losses in assets on, and revenues from, public lands, as well as losses in taxes and royalties within developing countries. The global trade in illegally harvested timber is highly lucrative and comparable to the production value of illegal drugs. Recognizing the multiple and exorbitant costs of illegal timber trade, governments and trade associations are increasingly implementing policies to ensure the legality of imports and exports.

Establishment of policies aimed at stemming international trade in illegally logged timber started in the United States (Lacey Act Amendment) in 2008, followed soon thereafter by Europe (European Union Timber Regulation), Australia and other countries including China. These policies have had positive impacts, in part by sensitizing players in wood and paper supply chains to the effects of illegal logging and timber trade, and also by bringing the force of law specific to timber trade regulation. But without wider participation of governments in the effort to stem the flow of illegal timber, the actions of the United States, European Union, and others are likely to be ineffective. The reality is that if only legal timber goes to Australia, the European Union and the United States, illegal timber will simply flow to innumerable ports where customs agents are inadequately equipped to stop the illegal trade.

Systems for certification of sustainable timber management have laid the groundwork for verification of proof of legality from forest to consumer. The policies to prevent the trade of illegal timber have not yet increased sufficient consumer confidence to raise the demand for wood, including tropical timber. In fact, attention to illegal logging that policy discussions stimulated has led to several unintended consequences. Substitution of temperate species for tropical species has occurred, and worse from the standpoint of the forest sector, substitution of non-wood products for wood.

Introduction

Illegal logging refers to harvesting, transporting, processing, buying or selling timber and timber products in contradiction with national laws. The laws referred to are not only the laws regulating harvest, but may also cover laws regulating access to resources, land tenure, forest management, environmental protection, labor, community welfare, trade and export procedures and also taxes, duties and fees related to timber harvesting and timber trade. Illegal timber trade is the import and export of either illegally logged timber, or if the timber was legally harvested, then of timber linked to some other violation of law during the sequence of processing and trade until the final consumer.

The costs of illegal logging and trade are impossible to accurately quantify, since there are no statistics. However, there are estimates, which vary widely and are difficult to compare. In 2004, a Seneca Creek Associates and Wood Resources International study estimated that the trade of illegal timber causes losses as high as US$ 1 billion a year to the US timber trade. In 2006, the World Bank estimated that illegal logging losses in assets and revenues were over US$ 10 billion on public lands in developing countries. In addition, governments lost US$ 5 billion annually in taxes and royalties according to the World Bank. In 2012, the United Nations Environment Programme (UNEP) and the International Criminal Police Organization (Interpol) estimated that annual losses globally from illegal logging are from US$ 30 to 100 billion, an amount equal to 10 to 30 percent of the total global wood trade. According to UNEP and Interpol, the three major hubs for imports of illegal timber are the US, the EU and China (Fig. 1).

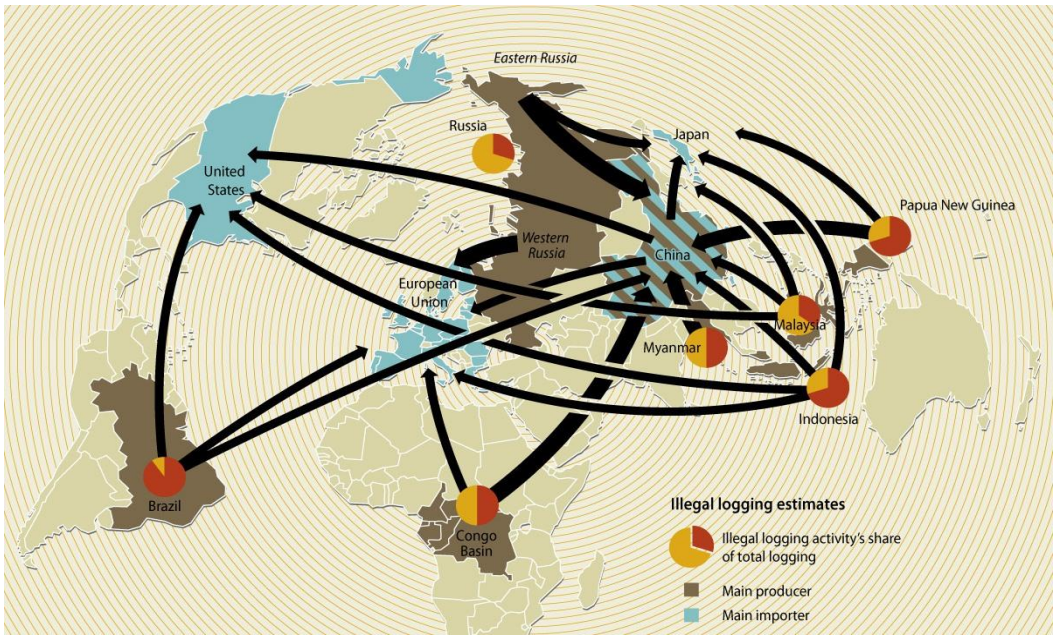

Figure 1. Illegal Trade of Timber and Illegal Logging
Source: UN Environment Programme and Interpol, 2012.

Potentially greater than all of the estimates above are the collective losses to the forest sector due to substitution of non-wood products. Architects, specifiers, builders and consumers appreciate the beauty, function and efficiency of wood products. But, when they confuse deforestation, illegal logging and illegal timber trade with wood products that are produced sustainably and legally, they might choose non-wood options. Numerous studies have demonstrated environmental benefits of using wood rather than alternative materials in building construction.[6]

The world's attention was drawn to the wide-ranging detrimental effects of illegal logging when the G-8 raised the issue in 1998 and launched an Action Programme on Forests. The Programme included recommendations as to steps that countries could take

[6] Dovetail reports on the environmental benefits of using wood appear with other Dovetail reports at http://www.dovetailinc.org/reports

to eliminate illegal logging. In 2005, the G-8 Environment and Development Ministerial Conference prepared a plan of action, subsequently adopted by G-8 leaders, for reducing illegal logging activity and trade of illegally sourced timber.

The first regional Forest Law Enforcement and Governance (FLEG) conference was held in 2001 in Indonesia and resulted in the Bali Declaration, where participating countries committed to strengthening bilateral, regional and multilateral collaboration. Collaboration is recognized as key to fighting illegality in international trade.

In 2003, the European Union (EU) initiated the Forest Law Enforcement Governance and Trade (FLEGT) Action Plan. The key difference from previous processes is the "T" for trade, which puts teeth into the plan. Without tackling the trade aspect, from which illegal logging gains revenues, other parts of the previous plan were weaker. Elimination of demand for illegal timber in international trade is just one aspect of the FLEGT Action Plan. FLEGT goes far beyond policies of individual countries, as it acknowledges shared responsibility between exporters and importers. The cornerstone of the plan is Voluntary Partnership Agreements (VPAs) with tropical timber producing and exporting countries. The VPAs include bilateral processes to establish legislation and its enforcement. As of early 2015, 15 countries had initiated or were implementing VPAs, with another 11 considering participation in them. VPA countries are to produce FLEGT-licensed timber for export to the EU and other destinations, of which the first shipments are forecast for 2016.

A 2004 UN Economic Commission for Europe meeting found that all countries in its region of Europe, North America and the Commonwealth of Independent States have some degree of illegal logging; however, illegality ranges from negligible to considerable (from less than 1 percent to in excess of 35 percent of legal wood volume harvested). The greatest illegal logging occurs in countries suffering from inadequate laws and enforcement. Illegal logging negates the intent of sustainable forest management, often causing or leading to forest degradation and deforestation.

Illegally harvested logs and wood products too often enter into international trade. The majority of illegal harvests are fuelwood for local use in cooking and heating, often tolerated due to poverty and lack of alternative energy sources. However, the more valuable species and sizes are exported.

Interpol states, "Illegal logging and the international trade in illegally harvested timber is a serious, international organized crime responsible for habitat destruction, species extinction and climate change. National legislation in many countries, and numerous international mechanisms, such as the European Union Action Plan named FLEGT and REDD+, the United Nations Collaborative Programme, are diligently working to ensure forest sustainability and manage carbon emissions. The trade in illegally harvested timber is highly lucrative and comparable to the production value of illegal drugs. Environmental criminals are often also involved in acts of corruption, smuggling and violence, with their activities leading to loss of tax revenue, political upheaval and post-

conflict instability. Without strong, coordinated law enforcement, criminals will exploit these invaluable natural resources."

According to Interpol, the consequences of illegal logging on the legal timber trade include an evasion of costs along the supply chain (e.g. taxes, licenses, permits, exploitation of cheap labor, illegal traders' operations, etc.). This results in global price suppression of 7 to 16 percent, meaning that law-abiding timber industry firms are denied US$ 30 billion annually in lost income (ETTF, 2015). Interpol works together through its 190-country members and with organizations such as UNEP, against illegal timber trade. Interpol handles a wide range of illegal trade concerns, including transportation of waste (e.g., dumping of e-waste)[7], wildlife trade[8], ivory sales[9], pharmaceutical crime[10], and stolen goods.[11] In recent years, there has also been growing concern about illegal oil trade[12] and the diamond trade.[13] Efforts to address illegal logging have parallels with many other international trade concerns.

Policies to Eliminate Illegal Timber Trade

Current policies aimed at eliminating the illegal trade of wood and wood products range from specific timber-related laws to weaker public procurement policies. The US, EU and Australia lead with legislation against illegal wood trade, including penalties. Other countries, such as Japan, have policies to promote the import and purchase of legal wood. Yet another tier of countries, such as China, are enacting timber-linked legislation, for which the severity of penalty for violation is not yet known. While most countries have laws against illegal trade of products in general, most lack the specificity to tackle illegal trade of timber products.

US Lacey Act Amendment (LAA)

In 2008, the US Lacey Act of 1900 was amended to include timber and timber products. It became the premier legislation against illegal logging through banning imports of illegal timber and timber products. The LAA imposes uniform requirements throughout the US wood supply chain (timber importers, traders, processors, middlemen, wholesalers and retailers). The amendment resulted from a broad consensus between the timber industry, environmental organizations and the US government – all parties agreed that the law would benefit the legal timber trade.

The LAA prohibits any person from importing, exporting, selling, receiving, acquiring or purchasing any plant or plant product (e.g. wood or paper product), knowing that it was

[7] http://www.solidwastemag.com/recycling/interpol-cracks-down-on-illegal-e-waste-trade/1002753151/
[8] http://voices.nationalgeographic.com/2012/07/26/4000-people-arrested-during-interpols-operation-cage-that-targeted-the-illegal-trade-in-birds/
[9] http://www.huffingtonpost.com/2012/07/26/interpol-operation-worthy_n_1696166.html
[10] http://www.interpol.int/Crime-areas/Pharmaceutical-crime
[11] http://www.insightcrime.org/news-briefs/interpol-highlights-potential-profits-of-transnational-cell-phone-trade
[12] http://www.brookings.edu/research/interviews/2014/09/27-isis-oil-funds-terror-alkhatteeb
[13] http://money.howstuffworks.com/african-diamond-trade2.htm

taken, possessed, transported or sold in violation of existing laws or regulations. The Act extends to operators abroad with the possibility for prosecuting non-US citizens. The LAA also prohibits false labeling of goods.

The LAA suggests that companies which trade, use and/or market timber apply "due care" to ensure compliance. This is different than EU and Australian legislation, where there are specific requirements for a "due diligence" system (explained below). Due care is a concept developed in the US legal system that means the degree of care that a reasonably prudent person would exercise under the circumstances. Therefore, it recognizes varying degrees of knowledge among different operators.

The Act has clear, progressive penalties. The severity of LAA penalties and sanctions vary according to an offender's awareness of the illegality of a given action. The value of the goods also affects the severity of punishment. Sanctions and penalties range from small fines and possible forfeiture of the goods, to a felony level fine of US$ 500,000 (or twice the maximum gain or loss from the transaction), a possible prison sentence of up to five years, and forfeiture of the goods. The amount of the fine is determined based on the type of operator, with larger corporations facing the highest penalties.[14]

European Union Timber Regulation (EUTR)
The EUTR is a regulatory act adopted by the EU in 2010 that prohibits placing illegal timber on the EU market. It entered fully into law in March 2013. The regulation requires "operators" (the companies that first place timber on the EU market, i.e. importers) to exercise due diligence to ensure that the timber is completely legal.

According to the EUTR, the three key elements of a due diligence system are:

- *Information:* The operator must have access to information describing the timber and timber products, country of harvest, species, quantity, details of the supplier, and information on compliance with national legislation.
- *Risk assessment:* The operator should assess the risk of illegal timber in the supply chain involved based on the information identified above and taking into account criteria set out in the regulation.
- *Risk mitigation:* When the assessment shows that there is a risk of illegal timber in the supply chain that risk can be mitigated by requiring additional information and verification from the supplier.

If the information in the three elements above is not sufficient to assess legality, then operators must request additional information or impose additional measures (e.g. certification of sustainable and legal forest management, third party verification of legality, and/or documentation of the harvest site, licensing, transport, processing, etc.).

Companies may create and maintain their own due diligence systems or outsource to a monitoring organization (MO) that is officially recognized by the European Commission. Trade associations, some of which are also MOs, play an important role for small and

[14] For additional discussion of the Lacey Act, see the Dovetail Report, "Understanding the Lacey Act" available at: http://www.dovetailinc.org/report_pdfs/2013/dovetaillaceyact1113_0.pdf

medium-sized enterprises. The MOs are either designated as national or EU-wide. As of April 2015, the European Commission had officially recognized nine MOs. The lack of sufficient MOs has hindered advancement of the EUTR.

In contrast to the LAA, which encompasses a wide variety of plant products as mentioned in the previous section, the EUTR covers main timber products, but excludes some others (e.g. recycled products, printed paper and bamboo). Similar to the LAA, the EUTR can be revised, and other products can subsequently be added. As with the LAA, the EUTR applies to both domestically produced and imported timber products; this not only allows it to coincide with World Trade Organization requirements, but also allows it to apply to illegal timber produced within the EU.

Another difference from the LAA is that the EUTR is less broad. The LAA extends to activities outside of the US and beyond the initial importing. But, the EUTR stops with the initial importer - it only prohibits operators from placing illicit timber or timber products on the EU market and it requires those first-time operators to be able to demonstrate the legality of timber. In contrast, the LAA applies throughout the supply and processing chain, and all entities must be able to show at any time that their timber products are legal.

The EUTR obliges EU member states to determine penalties for failing to comply with the regulation. In contrast, the LAA includes a list of penalties and sanctions. The EUTR requires that the penalties be "effective, proportionate and dissuasive." EU trade associations frequently express concern that EU countries will not have equivalent enforcement, thus allowing illegal timber to enter where weaker enforcement exists. Under the EUTR, each of the 28 EU states has nominated one or two "Competent Authorities." Competent Authorities are responsible for setting penalties and enforcement. They also oversee MOs operating within their country.

Australia Illegal Logging Prohibition Act

Australia's Illegal Logging Prohibition Act of 2012 promotes the trade of legally logged timber and timber products. According to a 2005 study by JP Management Consulting for the Australian Government, Australia is a significant importer of wood products (AUD$ 4.4 billion in 2014) of which up to AUD$ 400 million come from sources with some risk of being illegally logged. As stated on the webpage[15] associated with the Act, Australia needs this legislation "... as a responsible member of the global community. It is in Australia's interests to protect plants and animals and the environment, promote sustainable forest management and reduce the depletion of exhaustible natural resources that are threatened by illegal logging. As a producer of timber products, it is in our interest to promote the trade in legally logged timber. By strengthening our laws, we are making Australia a less attractive destination for cheap illegal timber and timber products that can undercut legitimate Australian businesses. We are also strengthening our reputation in domestic and international markets."

[15] www.daff.gov.au/forestry/policies/illegal-logging

The Act considers "intentionally, knowingly or recklessly" importing or processing illegally logged timber a criminal offense. In order to be in accordance with World Trade Organization rules, like the EUTR, the Australian Act covers timber harvested nationally and internationally. The legislation only places requirements on Australian businesses, and importers are required to practice and prove due diligence. Australian businesses must practice due diligence "to assess and manage the risk that the timber or timber products they are importing for processing has been illegally logged." The Australian Act is designed to complement EUTR and LAA.

Other Countries' Similar and Evolving Legislation

Illegal trade is illegal everywhere by definition. But there is always the question of specificity and enforcement of laws, i.e. the degree of enforcement that can be determined by the will to enforce and the related level of corruption, and often the capability of enforcement. Few countries have timber-specific trade laws such as those presented above.

Some governments – national, regional and local – have procurement regulations that pertain specifically to timber; often these specify that timber must be certified as originating from sustainably managed forests. Sometimes they go further, as for example in Japanese legislation, which specifically address illegal timber trade. The Japanese Government introduced a Green Purchasing Law in 2006 to ensure that domestic companies import legal and sustainably produced timber products. Japanese importers voluntarily certify, according to various methods, the legality and sustainability of wood and wood products (Goho-wood, 2015). Due to their voluntary nature, Japanese rules are viewed as weaker than those of the US, EU and Australia.

Despite progress in addressing illegal logging, illegal trade channels continue to operate in some parts of the world. China, for example, commonly imports illegal timber, often softwood from Russia, and too often tropical timber. The necessity to prove legality for export markets in Australia, the EU and the US has raised the consciousness of the Chinese timber trade and the government. Following enactment of the LAA and preceding the EUTR coming into force, trade associations informed their members that export customers would demand proof of legality for their due care and due diligence systems. Nevertheless, according to an expert familiar with the situation in China, the impact on business practices due to the LAA and EUTR has been quite limited due to weak and uncoordinated enforcement by the authorities.

China is in the process of developing a legal verification policy. Currently, it is in an experimental stage and not yet implemented. Although some local industry associations have started to introduce their own verification programs, they lack resources, credibility, and transparency needed for wide acceptance by the marketplace, especially in international markets.

Comparison of LAA, EUTR and Australia's laws

The EUTR is part of a larger FLEGT Action Plan, which aims to eliminate illegality in the wood trade by attacking supply and demand. On the supply side, the EU has VPAs with tropical timber producing and exporting countries. These agreements are designed to improve legislation and enforcement in the VPA countries. FLEGT-licensed timber will be automatically accepted under the EUTR.

The requirements for timber traders in Australia, EU and the US are similar. The major difference is the process by which traders adhere to the laws. The EU and Australian laws use a prescriptive approach, under which compliance means that the traders and operators must meet the specific requirements of the regulation. By contrast, under the LAA, which is a fact-based law, the individual company alone is responsible for compliance. A table comparing the LAA and the EUTR appears in the annex. The EUTR automatically accepts as legal any timber accompanied by a FLEGT license (expected in 2016) or CITES (Convention on International Trade in Endangered Species of Wild Fauna and Flora) permit. None of the systems accept certification of sustainable forest management as sufficient proof of legality.

Why Certification Alone is Not Sufficient to Ensure Legality

In order for any forest to be certified as sustainably managed, one of the first tenets is legality. This includes legality in land ownership, harvesting rights, employment of forest workers, and so on. But the European Commission, which is responsible for running the EU program, including the EUTR, states that certification alone is not enough to prove legality. Why? Because even if all of the above-mentioned conditions were legal, when logs leave the forest, illegality could occur that would not be identified through certification of the forestland or the tracking of such material.

For example, various aspects of transportation from the log landing to the domestic or overseas buyer may be illegal (e.g. unlicensed drivers, unregistered or illegal vehicles or loads exceeding weight limits). Similarly, illegal activity can occur in conjunction with processing logs, resulting lumber or their value-added products (e.g. undocumented workers or illegal working conditions). Defining illegality in this way makes it difficult for any importing company to be certain of legality. How is a company to know, for instance, that the wood they bought was completely legal from stump until they took possession? One solution available to large enterprises is development of a completely integrated production and distribution system, starting at the forest and continuing through sale of products. One international company that tries to do this is IKEA, and although they often do not own the processing subsidiaries, they have extensive controls in place to ensure legality of their suppliers.

Certification systems have modified their standards to better address the needs for proving legality of due diligence systems. Although the US and EU governments do not

recognize privately certified timber as automatically complying with the law, companies can use certification as a mainstay in their due diligence or due care systems.

For example, according to the Programme for the Endorsement of Forest Certification (PEFC), "the 2013 PEFC Chain of Custody certification has been updated to offer an efficient mechanism for companies to demonstrate alignment with EUTR requirements. The PEFC Due Diligence System (DDS), which is integral to PEFC chain-of-custody, mirrors the EUTR requirements. The main difference between the PEFC DDS and the EUTR is that the PEFC DDS goes further than the EUTR:

- the PEFC DDS applies to all products and not to only a selection of product groups that the EUTR covers, and
- the PEFC DDS is compulsory for every stage of the chain, and not only for the first placer on the EU market as required by the EUTR."

It is important to note that the European Commission has never said that certification is not sufficient to prove legality, but simply that certification is not actual proof of legality. In fact, the European Commission clearly recognizes certification as evidenced by its language regarding the EU timber regulation: "In practice, operators may rate credibly certified or legally verified products as negligible risk of being illegal, i.e. suitable for placing on the market with no further risk mitigation measures" (http://ec.europa.eu/environment/eutr2013/faq/index_en.htm).

There are a number of potential issues that have kept the European Commission from accepting certification as proof of legality – potentially most important is that, different from CITES and FLEGT, certification is a private mechanism. PEFC strongly believes, however, that the European Commission needs to find ways and means to recognize the role of certification, especially since certification goes beyond legality, also promoting sustainable management. As noted by PEFC, the more companies that obtain PEFC chain-of-custody, the more the demand for sustainably sourced material will increase, and the more it will be possible to effectively promote sustainable forest management certification in Asia, Africa and Latin America.

The Forest Stewardship Council (FSC), the other main global certification system, also recognizes the importance of aligning with due diligence systems' needs. According to FSC, "In support of the EUTR (and the US and Australia laws), FSC took measures to accommodate compliance by its certificate holders. It elaborated further its definition of legality, it incorporated trade and customs laws into the chain-of-custody requirements and it ensured that where the FSC definition of 'reclaimed material' is in line with the concept of 'waste' in the EUTR, where due diligence is applied. In a separate decision ('Advice Note') it obliged certificate holders to cooperate in collecting the necessary information about origin, species and legality documents on request of the clients."

Impact to Date on the Timber Trade

Policies to eliminate the trade of illegal timber have had direct, intended impacts, as well as unintended consequences. The following impacts are described below:

- Raising awareness of illegal logging and trade
- Establishment of due diligence systems by traders and industry
- Confiscation of illegal timber and penalties for possession
- Substitution of temperate timber for tropical timber and non-wood for wood.

Awareness of the existence of illegal logging and trade
The political processes cited above, and the major legislation in the US and EU, have raised awareness of the existence of illegal logging and its associated trade. Not only are the forest sector and environmental community aware, but also a much broader audience is now concerned about potential devastation and how forests will be regenerated and subsequently managed.

There is increasing awareness that the best way to foster sustainable forest management is to recognize and capture value from responsible periodic harvests of wood and non-wood products. When forests' greatest value is for their wood and non-wood products, on a sustained yield basis, only then will forests remain forests. Otherwise, if the value of the land that forests occupy is greater for agricultural crops, grazing, mining or urbanization, then land conversion for these purposes can be expected.

One of the most rewarding aspects of the EUTR and the LAA has been the support for these policies by the timber industry. Wood and paper associations and their members have voiced their beliefs that through the elimination of illegality, the legal timber trade will benefit. Some trade associations made members establish due diligence systems as a requirement for membership. Since illegal timber undermines profits of legal timber, it is in the trade's best interest to support legal wood. But beyond that, having confidence in the sustainable and legal source of wood products means potentially higher demand by users and buyers.

Due diligence systems
The necessity for US and EU companies to establish or ameliorate their due care or due diligence systems has also increased awareness of the risks of imports from various countries and regions within countries. Importing certified forest products gives better level of risk minimization than non-certified forest products. When sufficient certified products of a desired species are not available, importers need to seek alternative sources of verification of legality from suppliers.

Confiscation, court cases
The LAA, like many US laws, got additional clarification from courts' interpretations. The first case to draw widespread attention was against Gibson Guitar Corporation for the import of illegal ebony from Madagascar in 2009. In 2011, Gibson had a second

seizure by US Government authorities of ebony and rosewood imported from India. In both cases Gibson claimed that products were improperly classified, and as finished products were legally exported. In August 2012, Gibson settled the case with the US government by paying a US$ 300,000 fine, a US$ 50,000 community payment, and forfeiting the seized rosewood and ebony, which was valued at over US$ 300,000.

While the EUTR is newer than the LAA, it too has seen cases brought against importers that not only have raised consciousness of the law, but also further defined its extent. One of the first cases resulted from NGO whistleblowers (Greenpeace) calling attention to illegal logs shipped from Brazil to the Antwerp, Belgium port. The containers were impounded by the Belgium Competent Authority, Santé Publique, Sécurité de la Chaîne Alimentaire et Environnement (SPF), awaiting proof of legality. The timber was produced and exported by a Brazilian company, Rainbow, which was the focus of an investigation by Greenpeace that showed some of its timber was illegal; this was confirmed by the Brazilian authorities which have fined Rainbow multiple times. The European Timber Trade Federation (ETTF) reported in January 2015 that SPF released the containers following adequate proof of legality; however, the importing companies cancelled further contracts with Rainbow.

In February 2015 the UK National Measurement Office (NMO), which is the UK Competent Authority for the EUTR, investigated Chinese plywood imports. It found that only one of sixteen UK companies fully met their EUTR due diligence obligations. Specifically the companies were informed that they must take further steps in their due diligence systems to minimize the risk of importing illegal material through product and species identification testing. Although these 16 companies were small- to medium-sized enterprises, and accounted for only 10 percent of the UK plywood imports from China, the NMO stated that this sample was an indication that the problem was widespread among UK importers. Some of the plywood had poplar core, which was presumably domestically produced, and is currently a challenge to guarantee legality due to the lack of comprehensive chain-of-custody in China. The NMO Enforcement Project Manager, Mr. Michael Worrell told the *Timber Trade Journal (TTJ)*, "Fundamentally what the report highlights is that a composite product, coming from half way around the world, with a complex chain of custody and containing tropical timber represents a higher level of risk in terms of complying with the legislation and that the material it contains is what the documents say. It may contain one thing one day and something else the next" (TTJ, 2015).

The NMO ordered correction under the threat of sanctions and prosecution. Of added interest was the NMO's intention to work with other EU countries' Competent Authorities on high risk wood products and countries (ETTF, 2015). Of further interest was the response by the UK Timber Trade Federation, which commended the NMO for its investigation, saying that, "the EUTR is a regulation that is being taken seriously by the UK government and that it [the government] wishes to continue playing a leading role in driving illegal timber out of its supply chains." The Federation stated that the challenge is primarily one of procedures and process, and that this development helps address the detail required in due diligence systems. Indeed, a common complaint is that the

European Commission did not offer sufficient guidance in the level of detail required in EU due diligence systems.

It is the continued responsibility of the broader forest sector to root out the causes of illegal logging and illegal trade, and to communicate that through responsible management, trade, and purchasing so that consumers can feel positive in selecting wood and also show support for economic development in the forests and forest sector.

Substitution: temperate for tropical; non-wood for wood
EU imports of timber, both temperate and tropical, have been declining in large part due to the weak construction-related demands for exterior and interior applications (illustrated in the next section). The EUTR did not cause the decline. However, it did influence the decline in tropical timber imports (Giurca, et. al., 2014). Before the onset of the EUTR, in March 2013, some buyers increased their stocks of tropical timber. After the EUTR took effect, some substitution and trade diversion occurred. Some European importers, in doubt about the legality of timber coming from tropical countries, opted for products coming from countries with (perceived) more reliable documentation, such as temperate hardwood or softwood exporters (within the EU or North America). Hence, some EU businesses chose safe sources, which led away from less-documented tropical and temperate timber (both hardwoods and softwoods). Worse, there was substitution of non-wood based commodities for wood. On the other hand, exporters of tropical timber, uncertain about the costs of complying with legal requirements, have the option of trading with partners with less stringent regulatory frameworks (Giurca et al.2013).

Temperate species are often a viable substitute for tropical timber. New temperate softwood and hardwood products have been marketed as an alternative for traditional tropical hardwoods, performing equally in many applications (e.g. for exterior uses exposed to weather). More recently, temperate hardwoods such as oak have consolidated leading market positions in the European flooring and joinery sectors while tropical hardwoods have continued to lose market share (ITTO 2011). Research indicates significant positive cross-price elasticity for oak, implying that oak and tropical lumber are indeed substitutes (Giurca et al. 2013). Substitution of preservative-treated timber occurs at an increasing rate for naturally durable tropical timber species. Engineered wood products have also benefited by efficiently and economically providing an alternative to solid timber. When legality of tropical species cannot be assured, manufacturers have substituted other tropical species (TTJ, 2015). From a forest management standpoint, it is advantageous to have markets for diverse species, as it reduces high-grading of the most valuable and marketable species.

Substitution and trade diversion can thus be seen as causing market effects leakage. Leakage occurs when policy actions in one place indirectly create incentives for third parties to increase activities elsewhere and is caused by a shift in market (e.g. legality verification and certification, reducing the share of illegally sourced timber on the market, and thus increasing prices and pressures on temperate forests (Jonsson et al. 2012).

Effects on the Tropical Timber Trade

Worldwide, the trade of timber declined dramatically between 2007 and 2009 due to the global economic and financial crisis that began in 2006, in part due to the sub-prime mortgage crisis and associated construction collapse in the US (Fig. 2).

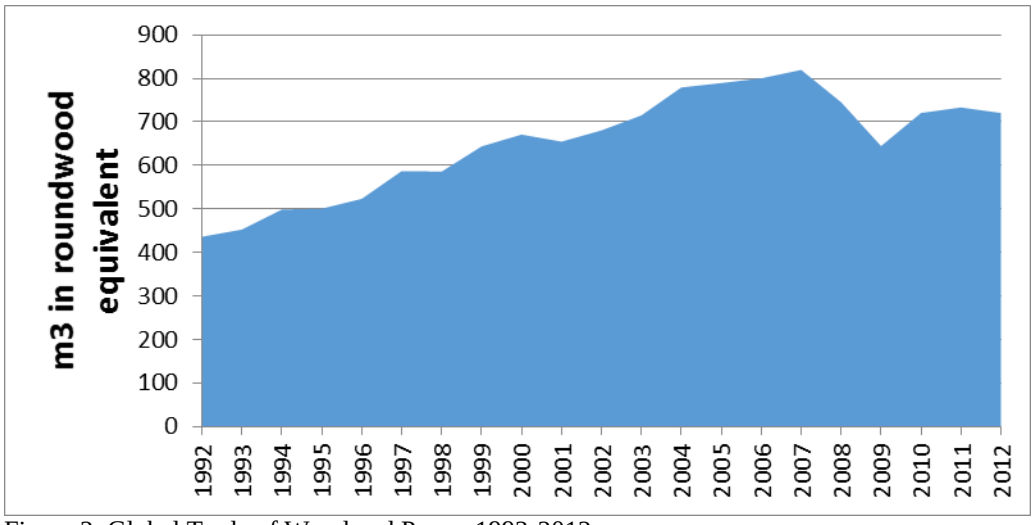

Figure 2: Global Trade of Wood and Paper, 1992-2012
Notes: Wood and paper products converted to roundwood equivalents. Using imports: globally exports = imports.
Source: FAO ForesStat, May 2014.

It was a coincidence that the drop in trade in 2008, following years of growth, occurred when the LAA went into effect. However, from an analysis standpoint, it obscures the direct effects of the LAA.

When considering global trade during the period 2003-2012 of only four primary products, often called the FLEGT primary products (i.e. industrial roundwood, which excludes fuelwood, lumber/sawnwood, plywood and veneer) the share of tropical timber remained relatively stable compared to temperate timber. Tropical timber's market share based on volume was almost consistently 17 percent of global trade. If based on value, for which tropical timber generally has a higher unit value, the share fell slightly from 34 percent in 2003 to 32 percent in 2013 (Fig. 3).

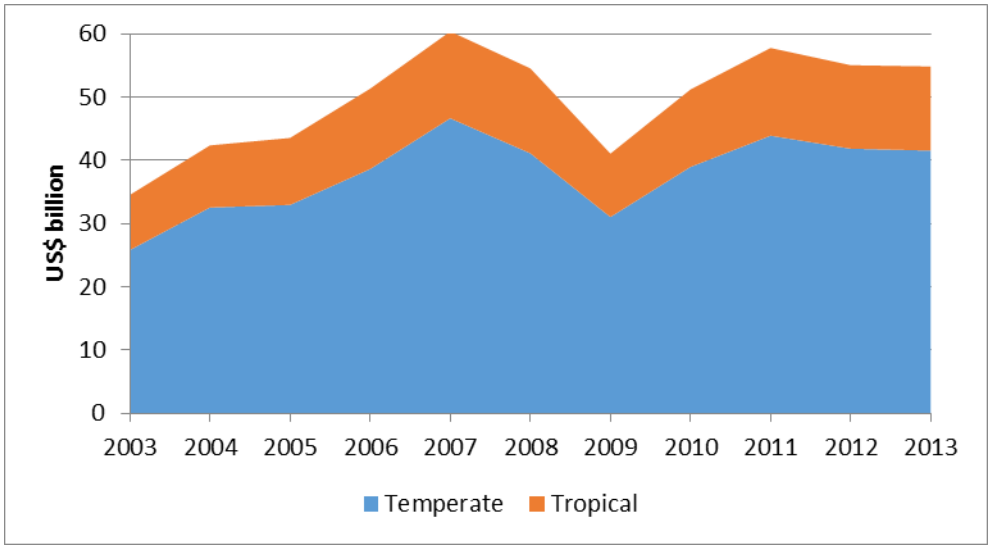

Figure 3: Market Share of Temperate and Tropical Timber in International Trade, 2003-2013
Note: 4 primary products. Source: ITTO, 2015.

In the EU, tropical timber imports accounted for only 3 percent of import volume, and temperate imports accounted for 97 percent in 2012. Tropical timber was twice that ten years earlier, i.e. six percent in 2003. Note that the 97 percent includes trade between EU countries, which constitutes the majority of the EU trade. Again, based on value, the tropical timber share is higher, but it still declined over the past decade, falling from 19 percent in 2003 to 15 percent in 2012. Looking at only the same four FLEGT primary products, EU tropical timber imports have fallen by 66 percent, from a high of nearly 7 million m^3 in 1995 to 2.3 million m^3 in 2012 (Fig. 4).

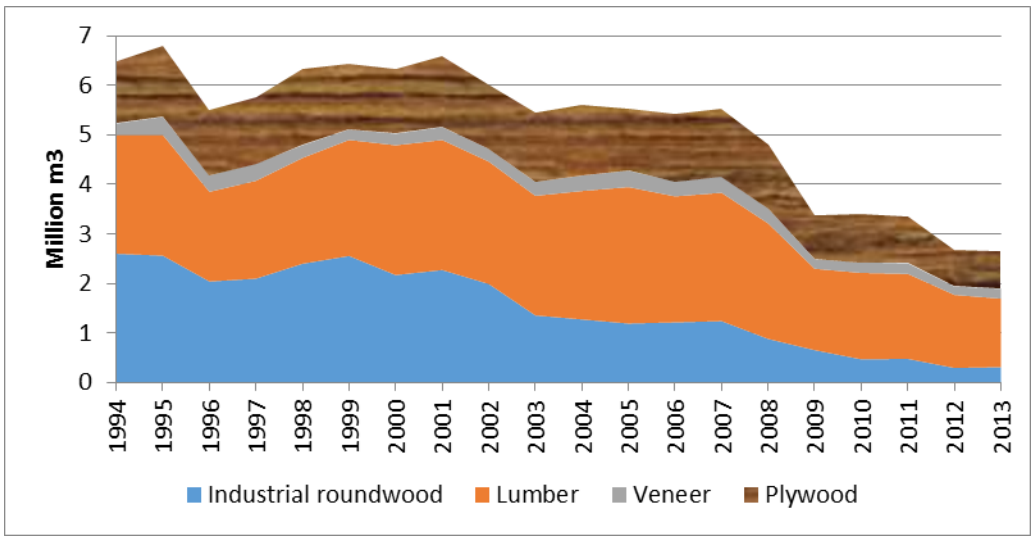

Figure 4: EU Tropical Timber Imports, 1994-2013
Source: ITTO, 2015.

Changing Trade Patterns

It may be too early to see direct effects of the EUTR on European imports since import data does not yet encompass the past two years. Analysis is complicated by the continued decline in tropical and temperate timber shown above (Figure 4). However, it is possible to use secondary information as evidence of changing trade patterns.

In the months before the onset of the EUTR in March 2013, imports of some tropical and temperate wood products rose. For example plywood imports from Brazil and China rose in early 2013, presumably because importers realized it would be difficult if not impossible to provide proof of legality once the regulation went into effect. Now, two years later, the UK Competent Authority is investigating some Chinese plywood imports (mentioned above).

The timing of the LAA enactment, even after accounting for the potentially confounding factors, corresponded with an upward shift in prices and reduction in available quantities (i.e. quantities for which legality could be proven) according to a recent study by the USDA Forest Service (Prestemon, 2015). Presumably in part because of the reduced availability of wood from unknown sources (i.e. potentially illegal), the study found that the LAA generally resulted in a 25 to 50 percent increase in import prices and a 33 to 75 percent reduction in import quantities, depending on the country and product. The US import of timber from natural forests in Bolivia, Brazil, Peru and Indonesia fell substantially. An unpublished report discussing the Forest Service study stated that its findings could not be interpreted as evidence that the LAA reduced illegal logging, but rather that exporters could have directed their goods to other markets.

An open question is, ‘What will happen if countries such as China cannot provide satisfactory evidence of legality for Australian, EU or US importers?’ Will importers simply turn to other sources to minimize the risk of illegal, or at least unproven, imports? And will exporting companies in turn, seek less scrupulous markets, especially domestic? In the latter case, such markets may be less lucrative, providing a disincentive to shifting target markets. In any case, what is desired is that exporters will not abandon markets, but instead realize the need to have assurance of legality, and that they in turn will demand proof from their suppliers.

As previously mentioned, only a few policies against illegal timber imports exist, albeit for two of the major timber trading hubs (i.e. the EU and the US). At this time, this leaves the vast majority of countries without laws specifically prohibiting illegal timber trade. Without wider participation of governments in the effort to stem the flow of illegal timber, the actions of the US, EU, and others are likely to be ineffective. The reality is that if only legal timber goes to Australia, the EU and the US, illegal timber will simply flow to innumerable ports where customs agents are inadequately equipped to stop the illegal trade.

What is Needed to Further Reduce Illegal Trade

Reducing illegal logging and the illegal trade of wood is not easy, and cannot be done unilaterally. More countries need to establish collaboration and uniform legislation that specifically aims at eliminating the illegal timber trade. The LAA is a unilateral measure, aimed at the demand side (US imports) in comparison to the EUTR that establishes bilateral (or multi-lateral considering the 26 EU states) regulations aimed at both the demand side (EU imports) and supply side (VPA exports). In all of the policies cited above, the goal is to reduce incentives for illegal logging and illegal trade. Legislation alone is not enough—it must be accompanied by sufficient enforcement throughout the timber supply chain. Customs agents at the exporting and importing ends of the chain need to be sufficiently trained to know different wood products and species. There must also be enough customs agents with sufficient time available to inspect containers of logs, lumber, plywood and a host of other timber products.

More research is needed to quantify the magnitude of the problem relating to lack of statistics on illegal logging/trade, including both benchmarking the current situation and monitoring change. Only with sufficient information can policies be judged to be either efficient or in need of modification. While accurate and detailed statistics on illegal timber trade may never be available, research on various indicators enables estimations and monitoring trends.

Illegal trade affects many diverse products and sectors – including e-waste, wildlife, endangered species, oil, diamonds, and others. Policies and actions taken to address one form of illegal trade can provide valuable lessons to other sectors facing related challenges. Building on the LAA, efforts to combat illegal logging and the illegal trade of wood in US markets were informed by previous efforts related to wildlife trade. Emerging new understandings from innovative policies to address illegal logging can and should be applied to other trade concerns with the shared objective that responsible trade is a necessary common theme throughout supply chains. Needs for widespread legislation, enforcement, research, and monitoring are not limited to the trade in forest products.

Conclusion

Government policies, backed by the legal timber trade, are tackling the disastrous effects of illegal logging and the trade of illegal timber products. These effects are far-reaching, from loss of forests and their many attributes to undermining the revenues of governments and profits of forest sector companies. Worse is confusion about illegality in timber, and the potential choice of less environmentally sound, non-wood substitutes. When managed sustainably, forests can produce a renewable supply of wood and non-wood products. Through effective, enforced policies to eradicate illegal logging and

illegal trade, confidence can be restored in wood products, while enhancing profitability of the forest sector. An important benefit of both outcomes is that the value of forests, as forests, is enhanced, increasing the likelihood of retention of forested areas even in the face of competitive pressures for conversion to agriculture or other land uses.

References

Australian Government. Illegal Logging Prohibition Act 2012. (2012) www.daff.gov.au/forestry/policies/illegal-logging. Accessed 22 January 2015.

Environmental Investigation Agency (EIA). (2012) The US Lacey Act: Tackling the illegal trade in timber, plants and wood products. Funding for implementation in 2012. http://eia-global.org/images/uploads/The_U.S_Lacey_Act.pdf.

EIA. (2011) EIA statement regarding 24 August 2011 Gibson Guitars raid by US Fish & Wildlife Service. http://eia-global.org/news-media/eia-statement-regarding-24-august-2011-gibson-guitars-raid-by-us-fish-wildl. 2011. Accessed 23 February 2015

European Commission. Independent evaluation of the implementation of the EU Action Plan on Forest Law Enforcement Governance and Trade. (2014) Unpublished overview of evaluation.

European Forest Institute. Literature review: United States Lacey Act Amendment and the European Union Timber Regulation – Focus on their communications. (2012) Unpublished report.

European Timber Trade Federation (ETTF). ETTF news. (2015) Winter 2014/15. www.ettf.info. Accessed 23 February 2015.

ETTF. (2015) Probe uncovers EUTR failings in UK Chinese plywood importing. http://www.ettf.info/node/161. Accessed 23 February 2015.

EU. (2015) Competent authorities. http://ec.europa.eu/environment/forests/pdf/list_competent_authorities_eutr.pdf. Accessed 11 February 2015.

EU Timber Regulation. (2013) http://eur-lex.europa.eu/LexUriServ/LexUriServ.do?uri=OJ:L:2010:295:0023:0034:EN:PDF.

European Union. (2003) FLEGT Action Plan. http://eur-lex.europa.eu/LexUriServ/LexUriServ.do?uri=COM:2003:0251:FIN:EN:PDF.

EU. (2013) EU Timber Regulation. http://ec.europa.eu/environment/forests/timber_regulation.htm

EU. (2015) Monitoring organizations. http://ec.europa.eu/environment/forests/pdf/mos.pdf. Accessed 11 February 2015.

Florian D., Masiero M., Mavsar R., Pettenella D. (2012) How to support the implementation of due diligence systems through the EU Rural Development Programme: problems and potentials. L'Italia Forestale e Montana 67(2): 191–201. doi: 10.4129/ifm.2012.

FSC. Personal communication on 16 February 2015. (2015) FSC website concerning compliance with due diligence systems at https://ic.fsc.org/timber-legality.492.htm.

Giurca, A., Jonsson, R., Lovric, M. and Pepke, E. (2014) EUTR impact on international timber markets. In proceedings for Joint Society of Wood Science and Technology, Wood Structure and Properties and European Hardwood Conference. http://www.swst.org/meetings/AM14/pdfs/proceedings.pdf. 2014.

Goho-wood. (2015) Law concerning the promotion of the procurement of eco-friendly goods and services by the state and other entities. Japan. https://www.goho-wood.jp/world/outline/doc/101126_leaflet.pdf. Accessed 23 February 2015.

Greenpeace. Logging in the Amazon. (2005) http://www.greenpeace.org/international/en/campaigns/forests/amazon/logging-in-the-amazon.

Interpol. (2015) Project Leaf. http://www.interpol.int/Crime-areas/Environmental-crime/Projects/Project-Leaf. Accessed 17 February 2015.

Jonsson, R., Giurca, A. Masiero, M., Pepke, E., Pettenella, D. Prestemon, J., Winkel, G. (2015) Assessement of the EU Timber Regulation and FLEGT Action Plan. EFI Think Forest Policy Brief. http://www.efi.int/files/attachments/thinkforest/efi_thinkforest-brief_eutr.pdf

Jonsson, R., Mbongo, W., Felton, A., Boman, M. (2012) Leakage Implications for European Timber Markets from Reducing Deforestation in Developing Countries. Forests. 3:736-744

JP Management Consulting (Asia Pacific) Pty Ltd. (2005) Overview of illegal logging: A report prepared for the Australian Government. Unpublished.

Oliver, Rupert. (2014) EUTR introduced just as EU economy hits bottom. ETTF News. 2014.

PEFC. (2015) Personal communication on 16 February 2015. PEFC website: www.pefc.org

Pepke, Ed, J. Bowyer, S. Bratkovich, K. Fernholz, M. Frank, H. Groot, J. Howe. (2015) Impacts of policies to eliminate illegal timber trade. Dovetail Partners Inc. http://www.dovetailinc.org/reports/Impacts+of+Policies+to+Eliminate+Illegal+Timber+Trade_n679?prefix=%2Freports. 2015.

Prestemon J.P. (2015) The impacts of the Lacey Act Amendment of 2008 on US hardwood lumber and hardwood plywood imports. Forest Policy and Economics 50: 31–44. http://www.illegal-logging.info/sites/default/files/ja_2014_prestemon_002.pdf.

Seneca Creek Associates, LLC and Wood Resources International, LLC. (2004) Illegal logging and global wood markets: The competitive impacts on the US wood products industry. 2004.

Timber Trade Journal (TTJ). (2015) NMO bears its teeth in Chinese plywood enforcement action. February.

TTJ. (2015) Hardwood health. February.

UNECE/FAO. (2004) Illegal logging and trade of illegally-derived forest products in the UNECE region.http://www.unece.org/fileadmin/DAM/timber/docs/sem/2004-1/summarynote.pdf. 2004.

UK Timber Trade Federation. TTF response to NMO report on Chinese plywood. Issued 23 February 2015.

UN Environment Programme and Interpol. (2012) Green carbon, black trade: Illegal logging, tax fraud and laundering in the world's tropical forests. http://dev.grida.no/logging/layout/RRAlogging_english.pdf.

World Bank. (2006) Strengthening Forest Law Enforcement and Governance. Report N. 36638-GLB. http://www-wds.worldbank.org/external/default/WDSContentServer/WDSP/IB/2006/09/05/000160016_20060905125450/Rendered/PDF/366380REVISED010Forest0Law01PUBLIC1.pdf. 2006

Annex. Comparison of the EUTR and LAA by Florian, et. al, 2012.

Table 2 – Comparison among the requirements of EU-TR and US Lacey Act.

	EU Timber Regulation (EU-TR)	U.S. Lacey Act (LA)
Goal	Prohibition to place on the market (i.e. to "*supply by any means*") illegally harvested timber or products derived from such timber	Prohibition to "*to import, export, transport, sell, Preceive, acquire, or purchase*" illegally sourced plants.
Illegality definition	Focus on "illegally harvested" timber, i.e. timber harvested in contravention of the applicable legislation in the country of harvest.	Focus on any plant that is taken, possessed, transported, or sold in violation of any law or regulation of any State or in violation of any foreign law or Indian tribal law
Scope In geographical terms:	Timber and timber products being placed for the first time on the EU market independently whether they have been harvested from EU forests or imported from outside EU.	It applies to wood and wood products imported by/exported from the U.S., and to those originating from the U.S. and being domestically traded.
In terms of products:	Timber and timber products as classified in the Combined Nomenclature set out in Annex I to the Regulation. Printed products to be included in the next amendment.	It covers fish, wildlife and plants. Due to 2008 amendments it refers to plants as "*any wild member of the plant kingdom, including roots, seeds, parts, and products thereof, and including trees from either natural or planted forest stands*".
Effective date(s)	Regulation entered into force on 2nd December 2010 Secondary legislation expected in March-June 2012 Applicable from 03rd March 2013	Approved in 1900, amended on 22nd March 2008. Effective since 2008.
Approach	System based (and prescriptive) approach	Fact-based (and reactive) approach
Point of control and traceability	Legality verification is done just at "first placing" stage. Basic traceability requirements for traders on the EU market.	Verification can be done at any point in the supply chain. Basic traceability is not explicitly required.
Tools	*Operators:* exercise of DD, including information access, risk assessment, and risk mitigation through use of a system They can be supported by MOs. *Traders:* identification throughout all the supply chain	*Operators:* exercise of due care, including a basic declaration. Due care implies lower sanctions in case of infraction.
Actors	EC, Operators, Traders, Monitoring Organisations and Competent Authorities (at Member State level)	Customs and Border Protection, Animal and Plant Health Inspection Service, U.S. Dep. of Agriculture (APHIS), Dep. of the Interior's Fish and Wildlife Service (FWS), Operators
Penalties	To be defined by Member States. They must be effective, proportionate and dissuasive, and may include fines, seizure of the timber or suspension of trading authorisation.	Civil and criminal penalties defined by the LA itself. They might include civil and criminal fines, forfeiture of products and imprisonment, depending on whether people are knowingly engaged in prohibited conduct.
Green lanes	Timber or timber products with valid FLEGT licenses or CITES permits are considered in compliance with the Regulation	
Exemptions	Timber or timber products that have completed their lifecycle and would otherwise be disposed of as waste, as defined in Article 3(1) of Directive 2008/98/EC of the European Parliamen and of the Council of 19 November 2008 on waste	Plants used exclusively as packaging material, unless the packaging material itself is the imported item. Any plant that is to be used only for laboratory or field research; except for protected or endangered species (by international or national laws)

Source: APHIS, 2008; EC, 2010; EIA, 2011; SCHULMEISTER, 2011; TFT, 2011.

Proceedings of the 58th International Convention of Society of Wood Science and Technology
June 7-12, 2015 – Grand Teton National Park, Jackson, Wyoming, USA

Improving Production Efficiency to Increase the Capacity and Profitability of a Swedish Wooden Single-Family House Producer

Tobias Schauerte[1*] *– Victor Svensson*[2] *– Simon Allhorn*[2]

[1] Assistant professor Industrial Engineering and Marketing, Faculty of Technology, Department of Mechanical Engineering – Linnaeus University, Växjö, Sweden.
* *Corresponding author*
tobias.schauerte@lnu.se
[2] Industrial Engineer, Faculty of Technology, Department of Mechanical Engineering – Linnaeus University, Växjö, Sweden.

Abstract

After the economic downfall and declining orders for wooden single-family houses in the past, order quantities on the Swedish market are turning upwards again. Yet, production costs for the firms are too high, often due to an inefficient production with too long lead-times. Further, a lot of capital is tied up in stock, leading to a relatively low rate of inventory turnover. Many firms face such production-related bottlenecks that affect profitability in a negative way. At the same time, firms want to increase their production capacity since the market is gaining strength.

In this study, principles and methods of the LEAN production philosophy were applied on a case firm, where the value stream was mapped to explore bottlenecks in the production of a wooden single-family house and to calculate production efficiency. By means of the DuPont scheme for economic analysis, the firm's return on assets was analyzed.

Data reveal how stock utilization, production and material flow, capacity and consequently return on capital are affected by a suboptimal facility planning. Changes in the current facility layout are suggested and measurements performed to exploit the direct effects of such changes and show their potential.

Results show that with the suggested changes, stock could be reduced by 37 %, value-adding space increased by 13 % and production capacity by 50 %. By implementing the

suggestions, production efficiency could increase between 10.3 % and 230 % and the firms return on assets could improve from 2.5 % to 37.8 %, which corresponds to an increase of profitability by around 1 506 %.

Keywords: Wooden Single-Family Houses, Lean Production, Production Efficiency, Value Stream Mapping, Production and Material Flow, Return on Assets

Introduction

Background

Todays' competitive business environment places high requirements on the different industries. In that context, the Swedish industry for prefabricated wooden single-family houses is no exception. Since the industry structure is characterized by a high degree of perfect competition, the products, here single-family houses, are highly substitutional in the eye of the consumer and firms mainly compete by prices. (Schauerte *et al.*, 2014). Nevertheless, production costs per m^2 increased by more than 60 % from 2001 to 2013 (SCB, 2015a), which is highly disproportional compared to the consumer price index that increased by 15 % in the same period (SCB, 2015b). This unbalanced development could be explained by different rationales, like e.g. a sales downfall by ca 70 % from 2007 to 2012 due to the economic crisis (Schauerte *et al.*, 2013) or rising direct costs for material or salaries. Yet, as various researchers indicate (a.o. Brege *et al.*, 2004; Eliasson, 2014; Eliasson and Sandberg, 2015; Jonsson and Rudberg, 2014; Meiling *et al.*, 2012), actual ways of working and production facilities do not correspond to the current state of development compared to other industries. Many firms in the Swedish industry for prefabricated wooden single-family houses are lacking behind in efficiency and production development.

Working more efficient and reducing production costs could be achieved by several means. According to Pullan *et al.* (2013), LEAN production offers a number of tools that could help to improve production flow by reducing lead-times, semi-finished products or downsizing stocks and minimizing waste (Sandberg and Bildsten, 2011). This could lead to a decrease of tied up capital and an improvement in the rate of turnover, production efficiency and consequently profitability. Such development would allow for better resource utilization and can free production capacity (Pullan *et al.*, 2013). As mentioned above, the sales quantity on the market declined by ca 70 % from 2007 to 2012, from 12 000 to 4 800 units. However, since 2012, the number of produced houses is raising. In 2014, 7 000 units were produced and for 2015, the Swedish national trade and employers' association of the wood processing and furniture industry forecasted 9 000 units to be produced (TMF, 2014; 2015). As the market is gaining strength, firms in the industry have to adjust their overall strategic conduct to meet that growing demand. Considering the above described situation on production efficiency, especially production related adjustments should be made to successfully be part of the positive market development.

The case firm and research question of this study

The case firm, which wants to stay anonymous due to a high degree of competition in its industry, prefabricates semi-finished modules for wooden single-family houses, row houses and multi-family houses up to 4 floors. Elements are produced off-site and assembled on-site. At the time of the study, the firm employed 16 people and had a production capacity equaling ca 40 single-family houses per year. Yet, this quantity varies depending of the type of house to be produced. Production takes place in a rented factory building that offers no possibility to expand production facilities by extending the existing building. As the demand for the case firm's products steadily increases, it could sell or market approximately 50 % more than actually can be produced today. Thus, the management of the firm decided to map possibilities how to improve and develop its production strategy and facility planning, in order to expand the production capacity. Therefore, the research question of this study is as follows:

How can production efficiency be improved to free production capacity for a firm producing wooden single-family houses?

Lean Thinking and Value Stream Mapping

LEAN is a philosophy originating from Toyota Production System (TPS), aiming at shaping a firm's production in a way that utilizes resources as efficient as possible. One important part of this is constituted by the reduction of waste. By analyzing customer demand, value-adding processes and activities can be identified. According to TPS, all other activities should be eliminated, or reduced as much as possible, in order to reach higher production and value stream efficiency (Liker, 2004).

Value streams include all activities needed to process materials and parts into the finished product. Mapping a value stream, data on e.g. lead time, value adding time, set-up times, stock levels, staffing, delivery frequencies and available capacities have to be gathered. In order to improve a product's value stream efficiency, the existing stream needs to be analyzed, starting with the material- and information flow at the dispatch point of the finished product, i.e. the end of the value stream. This, since delivery frequency is directly linked to quantity of demand and should determine the production and throughput rate. Mapping the value stream then continues upstream and as much relevant primary data as possible should be gathered on the different steps in the process. After mapping the whole process, a desired future state has to be created, depending on the strategic intend of the individual firm (Rother, 2009). In the current study, the case firm was aiming at increasing production capacity by 50 %.

The description above is a simplified depiction of mapping a value stream. Since a detailed description of all steps, including all other related and used methods and theories in this study, would exceed the scope of this paper, the authors refer the interested reader to Allhorn and Svensson (2014). Further, this study is limited to the investigation of

prefabricated wall elements in the case firm; the production of floor or roof elements is not included.

Current value stream efficiency, facility layout and profitability

In production of prefabricated walls, relatively simple butterfly tables are used by the case firm to retain flexibility. Due to this and determined by the product range, value adding activities are not alike from one wall to the other. Lead times can differ to a large extend and below, an attempt was made to measure value stream efficiency in form of an interval, ranging from fastest to slowest process time for certain walls. According to Liker *et al.* (2009), value stream efficiency (VSE) can be measured as in equation (1):

$$VSE = \frac{value\ adding\ time}{lead\ time} \tag{1}$$

Studying the lead time of a wall element, certain value adding operations need to be performed; e.g. cutting raw material, assembly of wooden parts, insulation, windows, etc. Further, waiting and queuing times emerge due to production bottlenecks. All parts to be produced have to pass the same production process. Depending on the design of the parts, lead time and value adding time can differ. For a detailed description of that process read Allhorn and Svensson (2014). The interval for value adding time when producing walls in the case firm ranges from 3.15 to 10.65 hours; lead time from 108.15 to 521.65 hours. Using equation (1), this equals a current VSE ranging between 0.029 (=2.9 %) and 0.02 (=2 %). The corresponding facility layout of that production process is depicted in figure 1, where the red colored objects, numbered from 1 to 19, represent stock areas (=27 % of total area), and the green colored objects, numbered from 20 to 35, are areas for value adding activities (=23% of total area). The remaining 50 % of the total area represent free space to move materials and products safely.

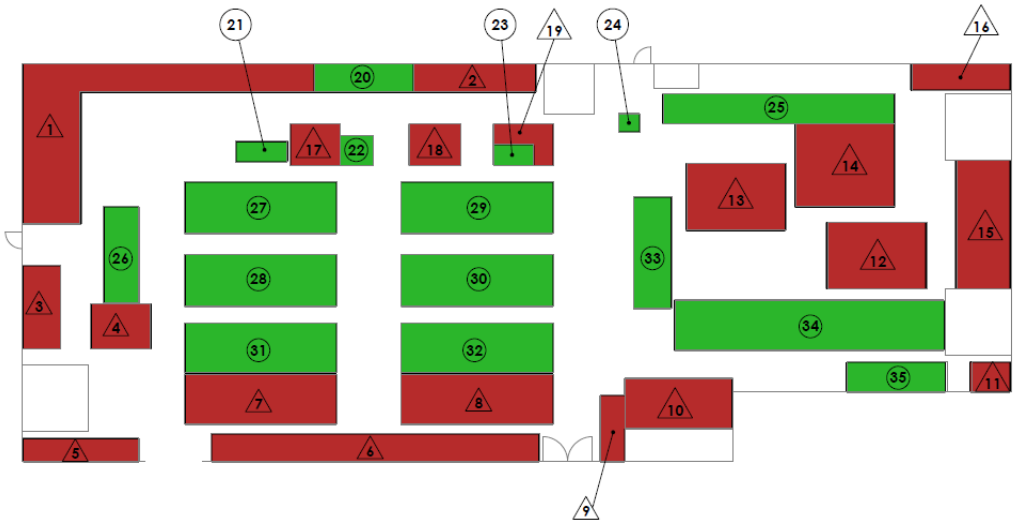

Figure 1: Current facility layout

With the VSE and the production facilities organized as described above, the case firm's profitability can be calculated by means of the DuPont scheme. An advantage of the

DuPont scheme is that it offers a clear and easy overview of a firm's financial key figures and how these are related to and affect each other (Skärvad and Olsson, 2011). Therefore, an increasing turnover, with the probable corresponding increase in costs, can be recalculated into return on assets, i.e. profitability. For the current situation of the case firm, all necessary financial information was provided by the firm's economist and used to generate profitability according to figure 2. The DuPont analysis reveals that the firm's current profitability is 2.51 %.

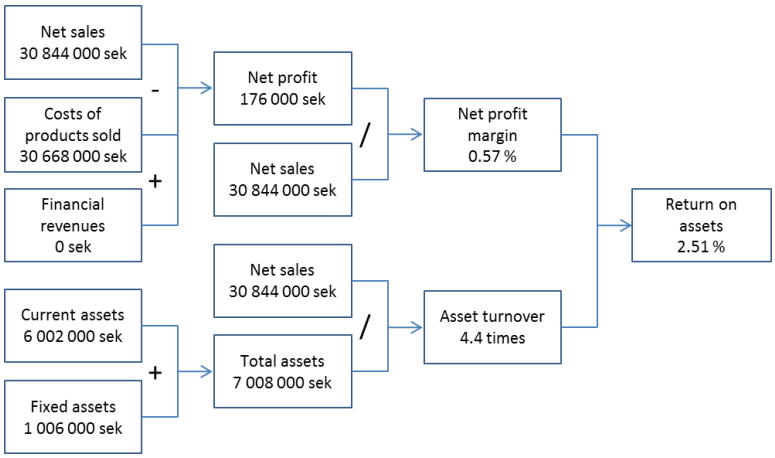

Figure 2: DuPont analysis on the case firm's current profitability

Future state of value stream efficiency, facility layout and profitability

The case firm's current situation exposes some challenges to be mastered. Below follows a short description of three critical areas, i.e. stock space, flexibility in material preparation and outsourcing of the painting station. For a detailed analysis of all steps, the interested reader is referred to Allhorn and Svensson (2014).

To start with, stock areas compete with production areas. Since the firm offers a large variety of houses, a lot of stock is needed to guarantee the adherence of delivery times. To expand production capacity, either the product range has to be limited or purchase strategies and habits to be adjusted by means of e.g. just-in-time deliveries. Since the firm does not want to limit its product variation due to its comprehensive corporate strategy, the firm's purchase habits should be revised. Further, operators cut material for too many walls at a time to avoid set-ups, which are time intensive due to an overaged technology. This however requires a lot of space for interim storage and could be solved by investing in a more flexible saw and implementing a Kanban system. This means that two carts would serve as material supply for each butterfly table. Material from the first cart can be used for assembly, whilst the second cart is being filled. In this vein, products and materials in progress can be limited. Since the existing saw has reached its expected technical lifetime, the case firm wants to replace it shortly and at the same time implement the described Kanban system. In figure 1, object number 34 is the painting station. This station is very resource intensive, since façade boards are handled manually and require too much space for drying, thereby competing with production space. Thus, it

is highly recommended to outsource this work step. The case firm already was aware of this fact and had offers from potential nearby suppliers to perform this operation.

With the described changes, a new value stream was designed and together with the employees, appropriate lead times estimated. The interval for value adding time still is between 3.15 to 10.65 hours, since handling the ready painted boards before assembly demands a similar amount of time compared to the initial situation, where the boards were painted. Lead time, in contrast, gets affected by outsourcing, since drying time can be avoided. The new lead time ranges from ca 100 to 162 hours. Thus, the new value stream efficiency ranges between 0.032 (=3.2 %) and 0.066 (=6.6 %), which is an improvement between 10.3 % and 230 %. The corresponding desired state of facility layout is presented in figure 3.

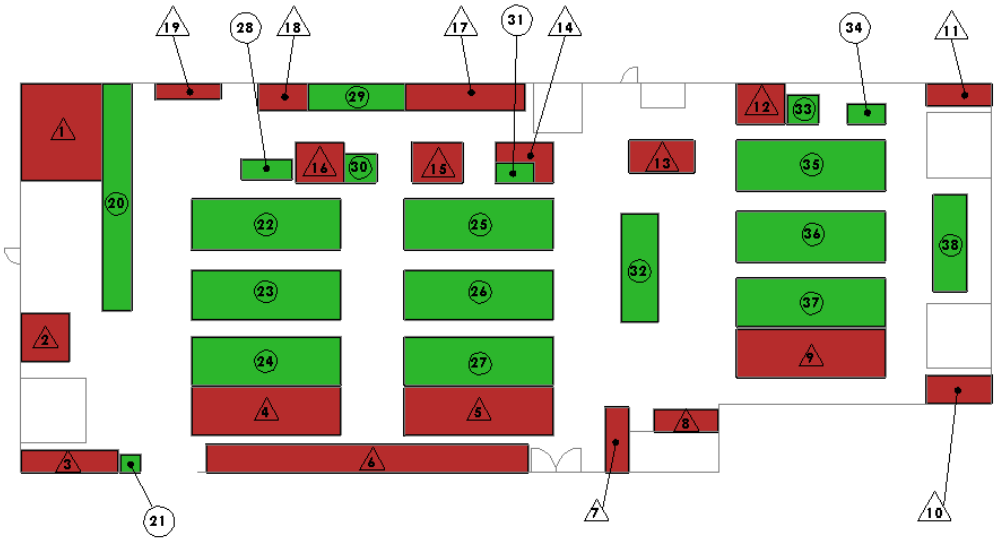

Figure 3: Future facility layout

Here, red colored stock areas account for 17 % of the total area, which is a reduction by 37 %. Green colored objects for value adding activities equal 26 %. This is an increase by 13 %, with the painting station being replaced by a third butterfly table (no. 35 and 36 including window assembly no. 37) and a new saw installed (no. 20). In this way, production capacity could increase by 50 %. Finally, free space accounts for 57 %, i.e. an upgrade with 14 %. With the changes at hand, the case firm's economist recalculated the necessary financial key numbers to generate the new return on assets, compare figure 4.

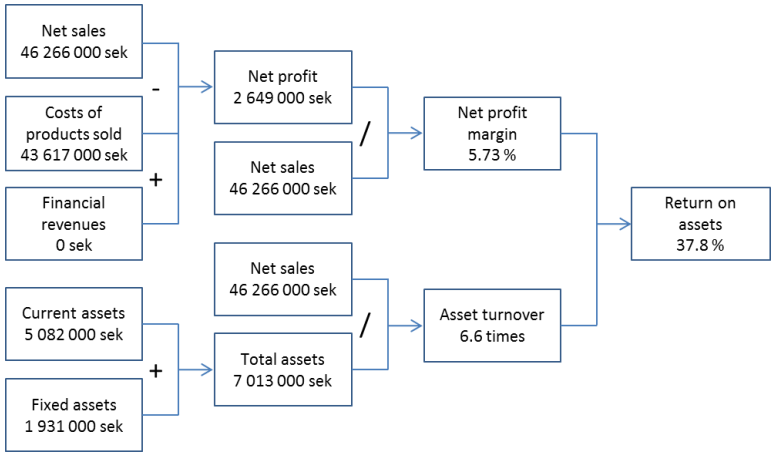

Figure 4: DuPont forecast analysis on the desired state of the firm's profitability

Net sales multiply with 1.5, since output would increase by 50 %. Costs would increase with material expenditures for the extra output and the outsourced painting activities. Employees from the painting station would be job rotated to the new butterfly table and one extra worker would be needed at that table. Fixed assets would increase, since investments for a new saw and the additional butterfly table would apply. Finally, current assets would increase, since the new purchasing strategy would inherit higher depts for goods and transportation. The resulting DuPont forecast analysis shows that the case firm could increase their profitability from 2.51 % to 37.8 %, which is an increase by 1 506 %.

Conclusion and Discussion

In this study it was investigated, how production efficiency for a firm producing wooden single-family houses could be improved to free production capacity. The results show that stock areas play an important role in the facility planning and utilization when having limited space at disposal. By changing purchase behavior, less stock is needed in the future and the firm's stock area could be downsized. Further, obsolete technology let to high set-up costs at a saw; hence machine operators pre-produced too much material at a time that needed to be stored intermediately. By investigating in up-to-date technology, material could be pre-produced according to a Kanban system that could secure material availability with relatively low interim storage. Finally, the resource intensive painting station competed with production area and should be outsourced.

Implementing these changes, the case firm could reduce stock areas by 37 % and increase value-adding space by 13 %. The adjusted production flow could lead to an upgrade of the production efficiency between 10.3 % and 230 % and production capacity could be expanded by 50 %. This, in turn, could lead to an improvement of the firm's return on assets from 2.5 % to 37.8 %, i.e. an increase by 1 506 %. Yet, implementing the suggestions remains to be done, which probably constitutes the most difficult part. Yet, considering the benefit the firm could realize, implementing efforts seem to be relatively

accomplishable. However, follow up efforts should be made to evaluate whether or not implementation succeeded with the calculated numbers above. Since production efficiency is regarded as relatively low in this industry, additional firms could be investigated to see, if industry common production issues exist and could be worked upon.

References

Allhorn S and Svensson V (2014) Capacity expansion in a manufacturing firm. Bachelor thesis in Ind Org and Econ, Dep of Mech Eng, Faculty of Techn, Linnaeus Univ, 79 pp.

Brege S, Johansson H-E, Pihlqvist B (2004) Trämanufaktur – det systembrytande innovationssystemet [Wood manufactury – the system-breaking innovationsytem]. VINNOVA analysis 2004:02, ISBN 91-785084-08-5. In Swedish.

Eliasson L (2014) Some aspects on quality requirements of wood f or use in the industrial manufacture of single-family houses. PhD thesis no. 174/2014, ISBN 978-91-87427-88-6, Dep of For and Wood Techn, Faculty of Techn, Linnaeus Univ.

Eliasson L, Sandberg D (2015) A case-study of single-family timber housing in Sweden and its wood material processing cost. Wood Mat Sc & Eng, ISSN 1748-0272, in press.

Jonsson H and Rudberg M (2014) Classification of production systems for industrialized building: a production strategy perspective. Constr Manag and Econ, 32:53-69.

Liker J K (2004) The Toyota Way: 14 Management Principles from the World's Greatest Manufacturer. New York: McGraw Hill.

Meiling J, Backlund F, Johnsson H (2012) Managing for continous improvement in off-site construction. Eng, Constr and Archit Manag, 19(2):141-158.

Pullan T, Bhasi, M and Madhu, G (2013) Decision support tool for lean product and process development. Prod Planning & Contr, 24:449-464.

Rother M (2009) Toyota Kata: Managing People for Improvement, Adaptiveness and Superior Results. New York: McGraw Hill.

Sandberg E and Bildsten L (2011). Coordination and waste in industrialised housing. Constr Innov, 11(1):77-91.

SCB (2015a) Total production costs for constructed single-family houses. Online at: http://www.statistikdatabasen.scb.se/pxweb/sv/ssd/START__BO__BO0201__BO0201C/KostnaderPerAreorSM2/table/tableViewLayout1/?rxid=391c81a8-fdd5-4d12-8e13-705ede2ab3eb. (26 March 2015). In Swedish.

SCB (2015b) Consumer price index. Online at: http://www.scb.se/sv_/Hitta-statistik/Statistik-efter-amne/Priser-och-konsumtion/Konsumentprisindex/Konsumentprisindex-KPI/33772/33779/Konsumentprisindex-KPI/272151/. (26 March 2015). In Swedish.

Schauerte T, Johansson J and Gustafsson Å (2013) From Customer Values to Production Requirements – Improving the Quality of Wooden Houses. Pro Ligno, 9(4):780-787.

Schauerte T, Lindblad F and Johansson J (2014) Industry Structure and Risk Positions for Wooden Single-Family House Firms in Sweden: Evaluating their Potential to Enter the Multi-Family House Segment. *In* For Prod Soc and World Conf on Tim Engin joint proc, 10-14 August 2014, Québec City, Canada.

Skärvad P-H and Olsson J (2011) Företagsekonomi 100 [Business economics 100]. Malmö: Liber.

TMF (2014) Wooden house barometer. December 2014. Online at: http://www.tmf.se/statistik/statistiska_publikationer/trahusbarometern. (26 March 2015). In Swedish.

TMF (2015) Wooden house barometer. March 2015. Online at: http://www.tmf.se/statistik/statistiska_publikationer/trahusbarometern. (26 March 2015). In Swedish.

Proceedings of the 58th International Convention of Society of Wood Science and Technology
June 7-12, 2015 – Grand Teton National Park, Jackson, Wyoming, USA

Matching Market Signals to the Canadian Wood Products Value Chain: A Disaggregated Trade Flow Analysis

Wei-Yew Chang, changwy@mail.ubc.ca
Chris Gaston, chris.gaston@fpinnovations.ca

University of British Columbia, 4025-2424 Main Mall, , Vancouver, BC V6T 1Z4

Abstract

Forest sector economic models have frequently used by researchers to analyze potential impacts of various policies or forest products market shocks. Most studies, however, typically used aggregated product groups and assumed that each commodity (e.g., logs, lumber, etc.) under investigation was viewed by the consumer as a homogeneous good, which implies that there are no price differences between product grades, sizes, and species. For example, Scots pine lumber from Russia is assumed to be a perfect substitute for old-growth yellow cedar from Canada; however, there is more than a ten-fold price difference between these products. In this study, we develop a dynamic global forest products trade model that considers forest products heterogeneity to examine the competitiveness of Canadian softwood logs and lumber products on the world markets. Factors that may affect global forest products markets such as the mountain pine beetle infestation in western Canada, Russia's log export tariff and WTO accession, the recovery of American housing starts, and the high economic growth in China are simulated to project future global softwood logs and lumber trade flows. Results of this study will not only shed light on the future competitiveness of forest products by region and type but also provide strong market signals for both forest managers and the forest-products industry to link back to the upstream forest products value chain.

Proceedings of the 58th International Convention of Society of Wood Science and Technology
June 7-12, 2015 – Grand Teton National Park, Jackson, Wyoming, USA

Hotspot Markets and Specifier Perception for Wood-Based Materials in Appalachian LEED Building Projects

David DeVallance, david.devallance@mail.wvu.edu
Gregory Estep, gdestep@mix.wvu.edu
Shawn Grushecky, shawn.grushecky@mail.wvu.edu

West Virginia University, PO Box 6125, Division of Forestry & Natural Resources, Morgantown, WV 26506

Abstract

A growth in green building projects within the Appalachian Region of the United States has increased the potential for wood product use. The overall objective of this research was to identify factors that influenced the use of wood products in commercial LEED projects within the Appalachian Region. Through purposeful sampling methods, the study determined wood-based product perceptions of material specifiers that prescribed the use of building materials in the projects. Using spatial analysis techniques, two major geographic areas in the Appalachian Region (surrounding Pittsburgh, PA and Greenville, SC) were identified where wood products have been awarded points towards LEED building certification. Results indicated that material specifiers generally had a positive perception towards wood-based building materials and felt wood offers the environmental and physical attributes needed in green building practices. Specifiers also felt that the main barrier to wood use in commercial green building projects lie in the building type and building code restrictions. However, optimism exists for specifiers in the form of building code acceptance to new and innovative wood-based materials like Cross Laminated Timbers (CLTs). The results of the research are expected to help improve the marketing techniques of wood product manufacturers by indicating the perceptions of those specifying the material used for LEED commercial projects within Hotspot market areas of the Appalachian Region.

Proceedings of the 58th International Convention of Society of Wood Science and Technology
June 7-12, 2015 – Grand Teton National Park, Jackson, Wyoming, USA

The Forest Products in a Digital Age: The Use and Effectiveness of Social Media as a Marketing Tool

Iris Montague, imontague@fs.fed.us
Kathryn Arano-Gazal, Kathryn.Arano@mail.wvu.edu
Jan Wiedenbeck, jwiedenbeck@fs.fed.us
Rajendra Poudel, rpoudel@mix.wvu.edu

USDA Forest Service, 201 Lincoln Green, Starkville, MS 35759

Abstract

The use of social media as a marketing tool has increased significantly in the recent years. While a number of studies regarding the use of social media among Fortune 500 companies and other industries have been conducted, very limited information is available regarding social media use among the U.S. forest products industry. A mail survey was conducted in 2013 to investigate the use social media as a marketing tool and to examine the factors affecting the use of social media in the U.S. forest products industry. Results show that close to 58 percent of respondents currently use some form of social media. Social media adoption was influenced by company age, net sales revenue, product type, the use of online marketing, perceived importance of e-commerce and website quality. About 94 percent of the respondents thought that social media is an effective tool for marketing. While no major concerns were expressed regarding the use of social media there was some concern on generating the return on investment to cover the costs associated with social media use. The information collected from this study can be used in assisting the forest products industry in understanding the social media marketing world and developing an effective social media marketing strategy.

Proceedings of the 58th International Convention of Society of Wood Science and Technology
June 7-12, 2015 – Grand Teton National Park, Jackson, Wyoming, USA

Demographic Changes and Challenges in the Woodworking Industry

Manja Kitek Kuzman, manja.kuzman@bf.uni-lj.si

University of Ljubljana, Biotechnical Faculty Department of Wood Science and Technology, Jamnikarjeva 101 1000 , Ljubljana

Abstract

The woodworking industry is a major employer in many of the Member States of the European Union. It provides jobs to nearly 3 million people in the EU27. The companies within the woodworking industry are mostly small and medium-sized enterprises, with only a few large groups. The woodworking industry, being an important employer in the European Union, faces an enormous challenge in these difficult times of economic crisis. Despite an unemployment rate that has never been higher in the EU, the woodworking industries have difficulties of finding skilled workers and attract them to work in a woodworking company, also the sector is not seen as an attractive sector.
The public tends to imagine jobs in the industry as manual, repetitive and unskilled, poorly paid and without any great career prospects. Young people in particular are put off as they see no scope for exercising their creativity. The woodworking industry is being faced with a relatively 'old' work force. Over the coming years, many workers will reach the retirement age and will leave the sector. Some of the best practices will be presented. Also the Slovenian Initiatives for societal perceptions of the forest-based sector and its products towards a sustainable society will be discussed.

Proceedings of the 58th International Convention of Society of Wood Science and Technology
June 7-12, 2015 – Grand Teton National Park, Jackson, Wyoming, USA

Almaciga Resin and Willd Honey the Backbone of Indigenous Peoples in Palawan, the Philippines

Arsenio Ella, Arsenioella@gmail.com
EMMANUEL DOMINGO
FLORENA SAMIANO

Forest Products Research and Development Institute, FPRDI-DOST, 7456 Sta. Rita, San Antonio, Los Banos, Laguna 4030

Abstract

Almaciga (Agathis philippinensis Warb.) source of almaciga resin grow naturally in almost all of the Philippine forests and mountains like in Palawan. For a period of 10 years (2003-2012) an average of 202,400 kg of Manila copal valued at US$ 188,900 were exported to France, Germany, etc. They are known for their superior quality for the manufacture of varnish, lacquer and paint. Palawan tappers who are mostly Indigenous People (IPs) practice the unscrupulous harvesting methods, e.g., deep tapping, over tapping and frequently rechipping. The situation has prompted FPRDI to improve the traditional methods in order to sustain productivity and save the remaining almaciga trees. Gathering of wild honey in Palawan has been an integral part of IPs existence suffice it to say it is part of their culture and rituals. As an enterprise, it is a very viable activity at the level of the gatherer. The technology offers low capital input, high returns per unit of time spent and low technical requirement needed by the gatherer. An investigation was carried out to determine IPs methods of gathering, trading and marketing for these 2 important non-timber forest products (NTFPs).